POLYMER

*The Chemistry, Physics and Technology of
High Polymers*

Classified Contents

Author Index

Author Index

An Infra-red–Deuteration Study of the Melting and Quenching of Nylon 6.6

R. Jeffries

This paper describes an infra-red (i.r.) and deuteration study of films of nylon 6.6 that have been melted and quenched. The i.r. spectra indicate that the disorder in the quenched film increases with increasing length of time in the molten condition, and with increasing temperature of the melt. This behaviour is confirmed by measurements of the fraction of the amide groups that are readily deuterated with deuterium oxide.

THERE is evidence[1,2] that when an ordered polyamide is melted, some of this order persists in the melt for considerable periods of time. The aim of the work described in this paper is to study with the i.r.–deuteration technique the effect of time in the molten condition, and temperature, on the state of order in the melt. The order in a quenched film is assumed to be related to, if not closely similar to, that of the molten film before quenching.

The structure of nylon needs to be considered at two levels: first, the degree of lateral ordering of the polyamide chains relative to their near neighbours; second, the state of aggregation of the chains to give the larger structural units, e.g. spherulites[1-10]. The i.r.–deuteration technique is a means of studying the first of these. This method provides a measure of the strength and regularity of the amide–amide interactions in the nylon structure; some of these amide–amide linkages, as a result of disorder in the lateral alignment of the nylon chains, are sufficiently weak or strained to allow the access of deuterium oxide to the NH group, and the H $\longrightarrow$ D exchange reaction thus takes place in these parts of the structure. The extent of the deuteration is a measure of the proportion of 'disordered' amide interactions, and is thus a measure of the degree of short-range lateral disorder in the structure. It is not possible at present to be precise as to the nature of this disorder, i.e. it is not known what proportion of the exchangeable NH groups are in the surface of, or at the imperfections within, 'crystalline' regions, and what proportion can be accounted for in terms of any distinct fraction of 'disordered' nylon.

EXPERIMENTAL

Preparation of samples

Films of nylon 6.6 were cast on microscope cover slides from a dilute solution of the pigment-free polymer in 95 parts by volume formic acid, five parts water, and two parts concentrated hydrochloric acid. A few films were cast on calcium fluoride plates. The solvent was evaporated in an oven at 100°C; the temperature of drying has little obvious effect on the glass-cast film, but has a significant effect on the calcium fluoride-cast films (films dried on calcium fluoride at room temperature are distinctly different in structure from those dried at 100°C, and from glass-cast film[11]).

1

The films were freed from any residual formic acid by washing in water at room temperature for one day and drying in air. The dry films (3 to 6μ thick) were coherent but slightly cloudy; this cloudiness is associated with a coarse, grainy structure clearly visible under the polarizing microscope. The films were heat-treated and spectroscopically examined without removing them from the glass or calcium fluoride support.

Melting–quenching treatments

Two techniques for melting the films were employed; both methods gave similar results. In the first technique, the nylon film (plus the glass or calcium fluoride) was mounted in a brass cell which was then evacuated for two to three hours at 100°C, filled with oxygen-free nitrogen, and immersed in silicone oil (MS 550) at the desired temperature. In the second method, the nylon film was immersed directly into degassed silicone oil. This second technique is similar to those used by other workers in crystallization studies[1, 2, 4, 7-9], and has the obvious advantage, compared with the first technique, of a very short heating-up time; thus melting times of only a few seconds could be studied. All samples were quenched by rapidly immersing them in silicone oil at 0°C.

With both methods of melting, the nylon films tended to become a pale yellow-brown in colour during the more prolonged treatments. This scorching may have been the result of traces of oxygen in the system. However, despite considerable efforts to exclude oxygen completely this discoloration was never eliminated, and it may, therefore, be due to direct thermal degradation of the polymer. The 'directly-immersed' samples appeared to be no worse than the 'brass-cell' samples in this respect, which suggests that any chemical effect of the hot silicone oil is not important. The results given below were obtained by the direct-immersion method.

I.r.–deuteration technique

The i.r.–deuteration studies were in general made as soon as practicable after the quenching treatment to eliminate so far as possible any slow increase in the order of the quenched samples; there is some evidence that a gradual crystallization may occur in quenched nylon films in the presence of moisture[1, 10] (this crystallization is discussed further below).

In general, the samples after quenching were rapidly mounted into brass cells (calcium fluoride windows). The i.r. spectra of these samples, after drying by evacuation, were measured on a Grubb–Parsons double beam spectrometer, with either a lithium fluoride or a sodium chloride prism as required. A few quenched samples were allowed to equilibrate with the atmospheric moisture and the spectra measured in this 'air dry' condition. The films, mounted in the brass cells, were deuterated in the absence of air by exposure to the saturated vapour of a reservoir of 99·7 per cent deuterium oxide; the deuterated samples were dried by evacuation before i.r. study.

RESULTS AND DISCUSSION

I.r. spectrum of solvent-cast nylon

The i.r. and deuteration behaviour of nylon film has been discussed elsewhere[6, 12, 13]; the i.r. spectrum and deuteration characteristics of the solvent-

cast films used in the present work are illustrated in *Figures 1* and *3*. The NH-stretching band near 3 300 cm^{-1} is 1·5 to 2 times as intense as the CH band near 2 935 cm^{-1}, and the half-band width varies from about 40 cm^{-1} to 50 cm^{-1}, depending upon the particular film used. The resolution of the doublet near 2 870 cm^{-1}, and the shape of the overtone near 3 070 cm^{-1}, also vary slightly from film to film (the overtone is a two-component band[12] and the change in shape is a result of the variation in the relative intensity of the two components). This slightly variable nature of solvent-cast films must be related to the way in which the solvent is evaporated in the latter stages of the drying, but the nature of this irreproducibility in drying technique has not been investigated. Each of these differences in spectrum can be interpreted in terms of variations in the degree of order of the nylon films; the films with the more intense and narrower NH band, with the best resolved 2 870 cm^{-1} doublet, and with the 3 070 cm^{-1} overtone relatively more intense on the low frequency side, are the more highly ordered. These differences in molecular order seem to be related to the cloudiness of the film; the more ordered films have a more pronounced grainy structure under the polarizing microscope.

I.r. spectra of quenched films

Figure 1 shows typical spectra in the 3μ region of nylon 6.6 after melting for various times at 295°C, and 325°C, followed by quenching. The in-
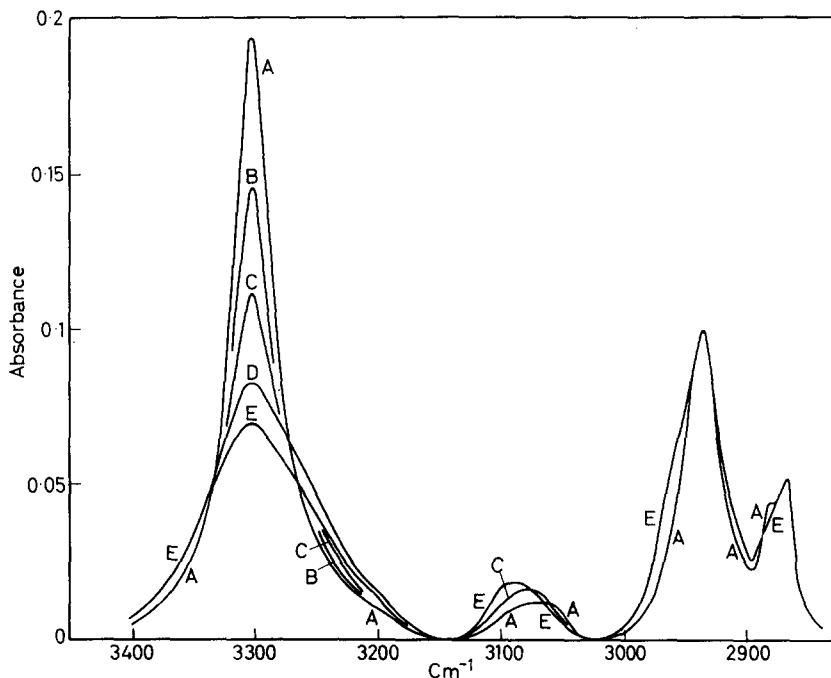
Figure 1—I.r. spectrum of quenched films of nylon 6.6 in 3 to 4μ region: A, untreated film; B, 2 min 325°C or 5 min 295°C, then quenched; C, 6 min 325°C or 20 min 295°C, then quenched; D, 10 min 325°C or 30 min 295°C, then quenched; E, 15 min 325°C or 40 min 295°C, then quenched

tensity of the NH band of the quenched films decreases with increase in the time spent in the molten condition. This decrease in intensity agrees with measurements of the NH intensity of nylons in the molten condition[6, 14, 15]; the slight increase in peak frequency on melting observed in this latter work is not apparent in the spectra of the quenched samples which probably confirms that this frequency shift is the result of thermal expansion increasing the amide–amide distance, as was suggested by Cannon[6]. The decrease in NH intensity in *Figure 1* is accompanied by a marked increase in the half-width of the band. The CH bands also decrease slightly in intensity, and broaden a little, with time of treatment; in *Figure 1* the CH bands are adjusted to the same peak intensity at $2\,935$ cm^{-1} to make the relative changes in the NH band more readily apparent. *Figure 1* also shows that the resolution of the $2\,870$ cm^{-1} doublet in the CH bands of the quenched films decreases rapidly as the length of time in the molten state is increased, and that the amide II overtone at $3\,070$ cm^{-1} becomes relatively more intense on the high-frequency ('disordered') side.

The changes in spectrum of the quenched films occur after shorter times in the melt at 325°C than at 295°C, as would be expected (see legend to *Figure 1*). The changes in the NH band level out after about 15 minutes at 325°C and about 30 to 40 minutes at 295°C. The nature of the various changes is, however, the same at both temperatures.
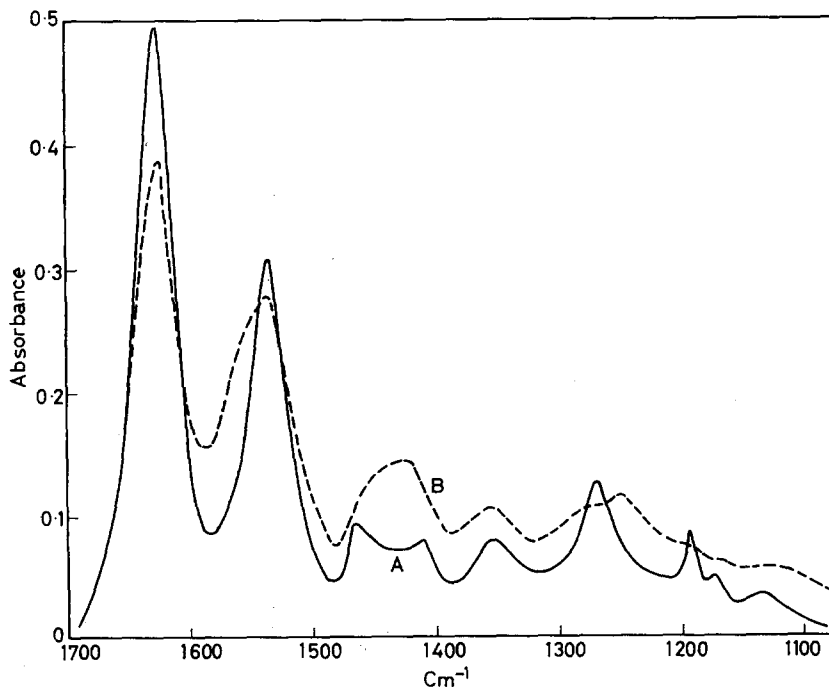
Figure 2—I.r. spectrum of quenched film of nylon 6.6, sodium chloride optics: A, untreated film; B, 20 min 325°C, then quenched. Films approximately the same thickness

Figure 2 shows the spectrum down to about 1 100 cm⁻¹ of untreated (solvent-cast) film and film after 20 minutes at 325°C followed by quenching. The effect of melting–quenching on the relative intensities of various bands and on the general resolution of the spectrum is readily apparent. The spectrum of the quenched film is, in fact, similar to the spectrum of molten nylon 6.6 shown by Cannon[6], except for the peak frequencies of the NH-stretching and amide bands; as pointed out above, these frequency shifts are probably the result of thermal expansion.

All the melted/quenched films are optically clear. This clarification of the film occurs within a few seconds at either temperature of melting and is associated with the disappearance of the coarse, grainy structure of untreated film.

If it is assumed that the molecular order in the quenched film is similar to (or at least directly related to) the order in the melt, then all of the changes in spectrum illustrated in *Figures 1* and *2* are consistent with there being a gradual decrease in the degree of order as the length of time in the molten condition is increased. The changes in the NH-stretching band and the amide II overtone indicate a weakening and disordering of the amide–amide interactions, and the decreasing resolution of the 2 870 cm⁻¹ CH doublet suggests an increase in the disorder of the CH_2 chains in the structure.

The intensity of the shoulder on the high frequency side of the NH band of air-dry films increases as the time in the melt increases. This shoulder is the result of absorbed water and, since water is absorbed mainly in the disordered, accessible regions, its increasing intensity is another indication that the order in the quenched samples decreases with time in the melt. The shoulder of completely accessible samples (i.e. after 15 minutes at 325°C) is about three times as intense as that of the original, solvent-cast film; this is as would be expected from measurements of the accessible fraction of the latter[6, 13].

Deuteration studies

Deuteration of solvent-cast film gradually reduces the intensity of the NH band, this effect levelling-off after several days at room temperatures; for example, the absorbance of the NH band is reduced by 13 per cent after 1·5 h and by 24 per cent after 10 days at 20°C[13]. The NH band width also narrows[6, 13] (i.e. the exchangeable NH groups give a broader NH band than the inaccessible NH groups), and the 3 070 cm⁻¹ overtone becomes relatively more intense on the low frequency side; this latter observation confirms that the high frequency and low frequency components of this overtone are associated with disordered and ordered material, respectively. The 'ND' band resulting from this deuteration of the accessible amide groups is a doublet in the 2 400 cm⁻¹ region (*Figure 3*); this doublet is not a simple ND-stretching mode [6, 16].

Figure 3 illustrates that the longer the time in the melt, i.e. the broader and less intense the NH band, the greater the proportion of exchangeable NH groups in the quenched film. The width of the NH band remaining after deuteration for 30 minutes (resulting from the inaccessible amide groups) is usually about 40 to 50 cm⁻¹, and this resistant band becomes less intense with increased time in the melt. After about 15 minutes at 325°C
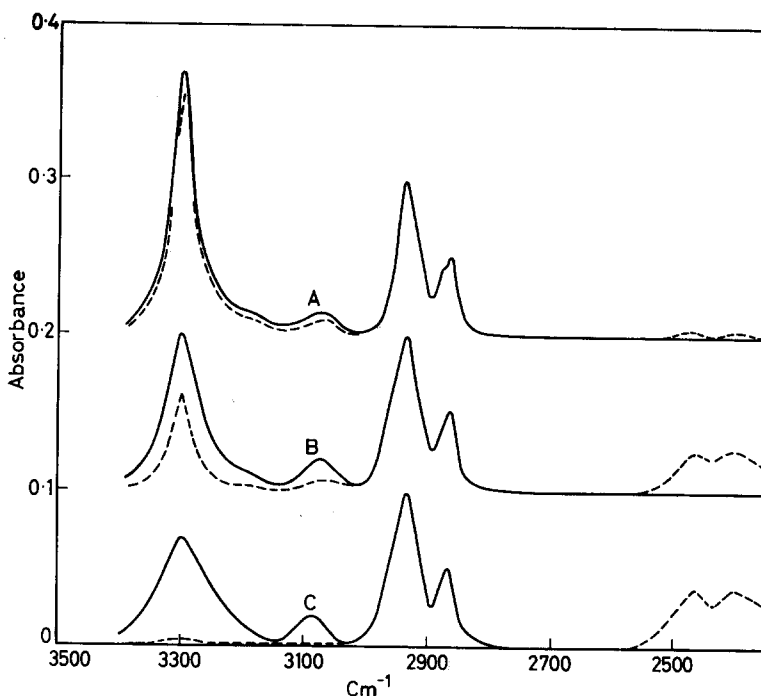
Figure 3—The deuteration of quenched films of nylon 6.6: A, untreated film; B, melted for short time, then quenched; C, melted for long time, then quenched; ———— before deuteration; — — — — deuterated 0·5 h at 20°C

or about 30 to 40 minutes at 295°C (i.e. after the changes in the NH bands have levelled off) the amide groups are completely accessible to deuterium oxide and the NH band is completely removed by deuteration for 30 minutes; the 3 070 cm^{-1} overtone also disappears on complete deuteration of the nylon, as would be expected[6]. Thus the deuteration results substantiate the conclusion that there is a gradual decrease in the degree of order as the length of time in the molten condition is increased.

Crystallization of quenched films

Quenched films in which some 'order' remains (i.e. which contain a deuteration-resistant component) undergo an increase in order upon boiling in water; the NH band becomes more intense and narrower, and the fraction of the NH groups which exchange with deuterium oxide decreases. However, films melted for long enough to give a completely accessible quenched film seem to crystallize only slowly on boiling in water. This may be because samples melted for a long time have fewer small regions of order present to nucleate the recrystallization in water. Quenched films kept in a desiccator over phosphorus pentoxide showed little, if any, change in i.r.-deuteration behaviour during three weeks.

6

GENERAL DISCUSSION

The conclusion that molecular order persists for up to 15 to 30 minutes at temperatures up to 60 deg C higher than the apparent 'melting point' of nylon 6.6 is in good agreement with the results of other workers[1, 2, 5]. McLaren[2] showed that the induction time for the onset of crystallization, and the rate of spherulitic growth, in nylon 6.6 depend upon the length of time spent in the molten condition, up to about 30 minutes at least. Magill[1] showed a similar relation between induction period and time of melting for nylon 6. These time effects were attributed[1, 2] to the relatively slow breakdown of crystalline aggregates in molten nylon. These workers obtained results consistent with a more rapid decrease in order in the melt as the temperature of the latter was increased, again in agreement with the present results. Magill[1] suggested that the order in the melt has its origin in chain folding and coiling, as well as in the alignment of chains in the melt. It may be noted that even after the changes in spectrum have levelled off, e.g. after 15 to 20 minutes in the melt at 325°C, there is still no indication from the i.r. spectra (*Figure 1*) of any significant numbers of free NH groups in the quenched samples, i.e. of any significant i.r. absorption in the 3 420 to 3 460 cm⁻¹ region. If the spectra of the molten nylon are similar in this respect to the spectra of the quenched samples then it must be concluded that the peptide groups are still fully associated, even in the 'disordered' melt.

(*Received July 1966*)

The Cotton, Silk & Man-Made Fibres Research Association,
  Shirley Institute, Manchester

REFERENCES

[1] MAGILL, J. H. *Polymer, Lond.* 1962, **3**, 43
[2] McLAREN, J. V. *Polymer, Lond.* 1963, **4**, 175
[3] MORGAN, L. B. *J. appl. Chem.* 1954, **4**, 160
[4] KHOURY, F. *J. Polym. Sci.* 1958, **33**, 389
[5] SLICHTER, W. A. *J. Polym. Sci.* 1959, **36**, 259
[6] CANNON, C. G. *Spectrochim. Acta*, 1960, **16**, 302
[7] MAGILL, J. H. *Polymer, Lond.* 1961, **2**, 221
[8] MAGILL, J. H. *Polymer, Lond.* 1962, **3**, 655
[9] MANN, J. and ROLDAN-GONZALEZ, L. *J. Polym. Sci.* 1962, **60**, 1
[10] CHAPPEL, F. P., CULPIN, M. F., GOSDEN, R. G. and TRANTER, T. C. *J. appl. Chem.* 1964, **14**, 12
[11] JEFFRIES, R. and HAWORTH, S. *Polymer Lond.* 1966, **7**, 563
[12] CANNON, C. G. *Mikrochim. Acta*, 1955, **2**, 555
[13] JEFFRIES, R. *J. Polym. Sci. A*, 1964, **2**, 5161
[14] HOLLIDAY, P. *Disc. Faraday Soc.* 1950, No. **8–9**, 325
[15] KING, G. and WOOD, F. *Nature, Lond.* 1962, **195**, 1093
[16] CANNON, C. G., STACE, B. C. and JEFFRIES, R. *Nature, Lond.* 1962, **196**, 436

Melting and Annealing of Polyethylene Single Crystals

H. E. BAIR, R. SALOVEY and T. W. HUSEBY

Melting and annealing of irradiated and unirradiated polyethylene single crystals have been studied with a differential scanning calorimeter. Crystals grown at 85°C in xylene exhibited multiple melting peaks. These peaks have been related to the lamellar thickening process. When irradiated, these crystals melted at 127°C with a single peak indicating little change in lamellar morphology during the heating process. Isothermal annealing of 85°C crystals between 118°C and 126°C caused an initial lowering in the apparent heat of fusion followed by a gradual increase approximately linear with log time. In addition, the lamellar thickness (as derived from melting points) at each temperature increased linearly with log time. The annealing process in this temperature region was attributed primarily to lamellar thickening. Above 126°C, annealing occurred also by recrystallization of melted lamellae. At 114°C and below, no changes in apparent heat of fusion or lamellar thickening were noted regardless of annealing time. Annealing of irradiated samples was studied as was the effect of irradiation on the apparent heat of fusion and melting point of recrystallized polyethylene. Under all circumstances the apparent heat of fusion was substantially less than the thermodynamic value for ideal crystals.

HEATING of chain folded polyethylene single crystals from room temperature to above the melting point may involve absorption or liberation of heat. While the fusion process requires heat to be absorbed, it is also possible within this temperature range for molecular segments to reorganize and thereby release heat. The major exothermic processes which can occur are lamellar thickening (reorganization), and recrystallization of earlier melting lamellae. The thickening process has been treated theoretically by Hoffman and Weeks[1]. Experimentally, it is well known that annealing polyethylene single crystals at a temperature near their melting point causes the thickness to increase with annealing time[2]. Indeed, precision adiabatic calorimetry[3, 4] has revealed that polyethylene single crystals begin to evolve heat at annealing temperatures only 10 deg. C above their growth temperature. This exothermic reorganization is therefore partly coincident with the melting process in polyethylene. Thus, the shape of the fusion curve can be influenced by initial crystalline morphology, and the details of reorganization, recrystallization, and melting processes. In an attempt further to elucidate these several processes, we have studied calorimetrically the melting and annealing behaviour of irradiated and unirradiated polyethylene single crystals.

EXPERIMENTAL

Materials

Solutions of polyethylene (Marlex 6000, type 50) in boiling xylene were

poured into a tenfold excess of xylene, thermostatically controlled at a crystallization temperature of 70°C, 77°C, or 85°C, to produce a final concentration of 0·04 g/100 ml[5]. The 70°C crystals precipitated from solution so rapidly that careful adjustment of the bath temperature was required
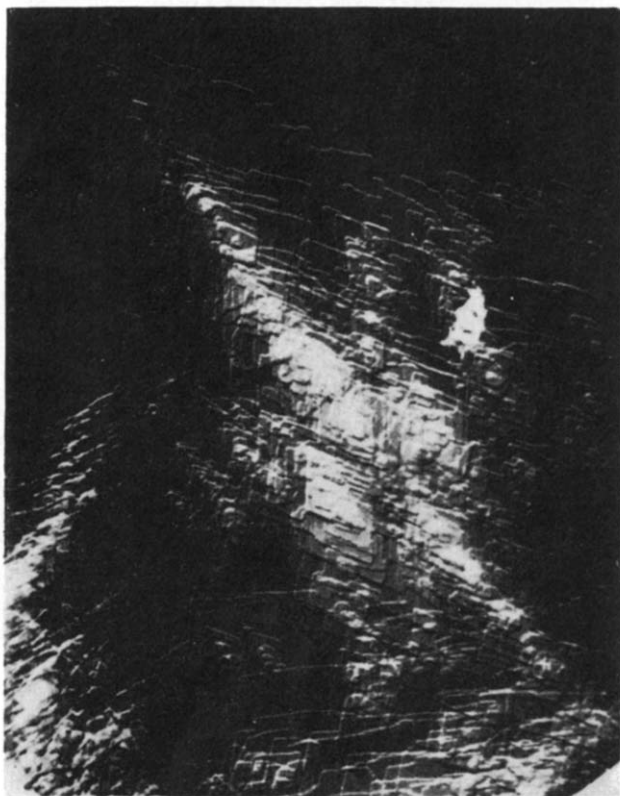
Figure 1—Electron micrograph of isothermally crystallized polyethylene from xylene (0·04 g/100 ml) at 70°C (× 20 000; reproduced without reduction)

to ensure crystallization at that temperature. After several days, hot suspensions were filtered at the growth temperature and crystal aggregates dried in a vacuum. These three separate preparations had different morphologies as revealed by electron and optical microscopy (*Figures 1* to *3*).

Apparent heats of fusion

A Perkin–Elmer differential scanning calorimeter[6], DSC-1, was used to obtain apparent heats of fusion, $\Delta H_f^\star$. Except where indicated, all samples were heated at 10 deg. C/min. Sample weights were typically 1 to 3 mg determined to one per cent accuracy on a Cahn electrobalance. The linear baseline response of the empty calorimeter between 35°C and 145°C was subtracted from the calorimetric curve produced by melting a polyethylene

sample. The area under the melting curve was integrated and expressed in cal/g using a calibration factor determined from melting a known weight of indium. The accuracy of this method was compared with density and X-ray techniques on a polyethylene sample crystallized at 148°C under 826 atm pressure. Density and X-ray measurements of crystallinity gave values of 87 per cent and 93 per cent, respectively[7], as compared to 88 per cent from the calorimeter*. The reproducibility of ΔH_f^* was found to be better than two per cent.

Melting points

The temperature scale was calibrated from the melting points of benzoic acid ($T_m = 122 \cdot 4°C$) and indium ($T_m = 156 \cdot 6°C$). The melting points, T_m, of polyethylene samples were determined by extrapolating the final portion of the melting curve to the instrument baseline.

RESULTS AND DISCUSSION

Melting of polyethylene single crystals

It has been demonstrated that irradiation of polyethylene films produces crosslinks within the structure[9]. It is thought that crosslinking occurs predominantly at the fold surfaces between adjacent lamellae[10]. Provided the irradiation dose is sufficiently low, it is believed such treatment does not influence the heat of fusion or the thermodynamic melting point and that irradiation suppresses the lamellar thickening process.
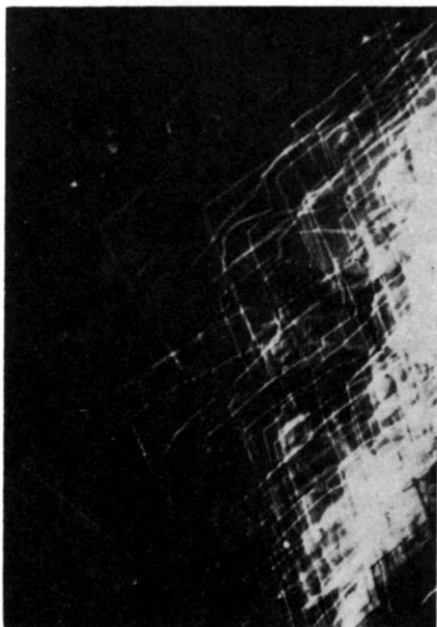
Figure 2—Electron micrograph of crystals grown at 77°C in xylene (×20 000; reproduced without reduction)

*The thermodynamic heat of fusion, ΔH_f, is assumed[8] to be 66 cal/g and the degree of crystallinity is computed from the ratio $\Delta H_f^* / \Delta H_f$.

Prior to irradiation, samples of each morphology were melted and the results are shown in *Figure 4*. The many tiered crystals with a dendritic habit, which had been grown in xylene at 70°C (*Figure 1*), yielded a typically smooth endothermic curve quite similar in shape to the melting
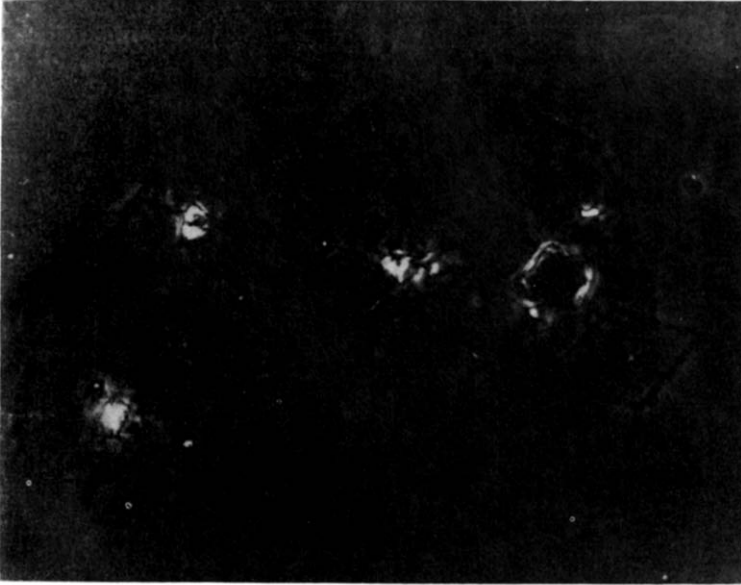
Figure 3—Phase contrast micrograph of crystals grown in xylene at 85°C
(×300; reproduced without reduction)

behaviour of bulk crystallized polyethylene. Melting of 70°C dendrites begins in the vicinity of 98°C (not shown in *Figure 4*) and continues until about 131°C. Stacks of crystals prepared at 77°C (*Figure 2*) possessed smoother crystal edges and, in general, more regular features than 70°C dendrites. This morphology produced a slightly different melting behaviour. The first sign of melting was detected at 103°C. Between 113°C and 127°C two small shoulders were observed. Melting is completed at 132°C. The relatively large monolayered platelets (*Figure 3*), grown and collected at 85°C, resulted in a pronounced multiple peaked melting pattern. Melting is complete by 133°C. The calculated apparent heats of fusion of 70°C, 77°C, and 85°C crystals were 50, 52 and 55 cal/g, respectively, which correspond to 76, 79 and 83 per cent crystallinities. These results support density and X-ray evidence[11-13] which indicates that single crystals have an amorphous content of 15 to 20 per cent. It should be noted that the apparent degree of crystallinity for a linear polyethylene crystallized from the melt by slow cooling (1 deg. C/min) was 84 per cent.

At least two possible explanations for the multiple peaked endotherms of 85°C and 77°C crystals can be suggested: (*1*) the behaviour results from different morphologies within each structure; or (*2*) a single morphology with competing endo- and exo-thermic processes produces the result. For

example, the latter possibility might arise from competition between melting and the exothermic processes of lamellar thickening or recrystallization of melted lamellae. In what follows we wish to argue that the latter explanation more correctly identifies the origin of these multiple peaked endotherms.

Samples of 85°C crystals irradiated to 26 Mrads yielded a single peaked endotherm (*Figure 5*). The single peak between 120°C and 127°C appears in the same temperature range as the two lower melting peaks of the un-irradiated 85°C platelets shown also in *Figure 5*. Furthermore, if the melting point, $T_m = 400 \cdot 3°K$, is substituted into Hoffman and Week's[1] expression for the melting point lowering due to fold surfaces

$$T_m = T_{m_0} [1 - 2\sigma_e / \Delta H_f l] \tag{1}$$

where σ_e denotes end surface free energy[14] $= 60 \text{ erg/cm}^2$, T_{m_0} is the thermodynamic melting temperature[15] $= 414 \cdot 3°K$, $\Delta H_f =$ heat of fusion of polyethylene[8] and $l =$ lamellar thickness, Å, a single crystal thickness of 124 ± 4 Å is obtained. This value agrees closely with the long-period spacing of 128 ± 5 Å obtained by Price[16], Keller[17], and Salovey and Bassett[10] from low angle X-ray scattering for single crystals grown at 85°C in solution. In addition, the apparent heat of fusion was found to be, within experimental error, the same as for unirradiated 85°C crystals, 55 cal/g. Since irradiation caused no detectable lowering of $\Delta H_f^\star$, it appears that the radiation absorbed by the 85°C crystals was insufficient to damage the crystal lattice perceptibly[18].
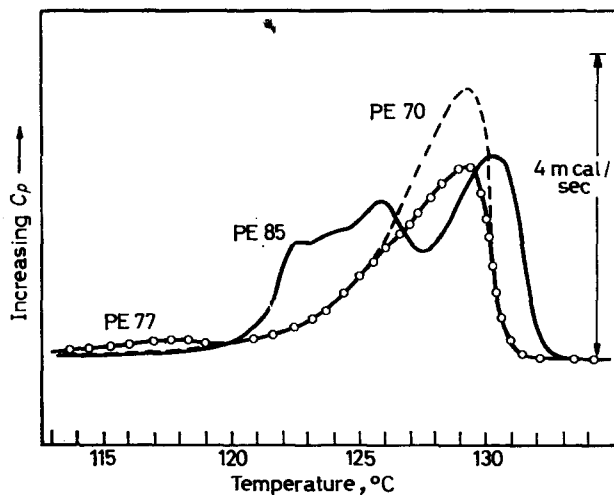
Figure 4—Melting curves for 70°C, 77°C and 85°C crystals at 10 deg. C/min

Analysis of the thermogram for the unirradiated sample in *Figure 5* revealed that about half the lamellae reorganized between 120°C and 127°C into more stable lamellae which subsequently melted between 127°C and 133°C. Thus, in the unirradiated 85°C crystals these lamellae reordered themselves (thickened) within less than sixty seconds to yield the higher

temperature melting peak. The evidence indicates that irradiating 85°C crystals to 26 Mrads suppresses the lamellar thickening process sufficiently so that these crystals are melted without significant reorganization during the heating process. Irradiation to smaller doses may not suppress re-
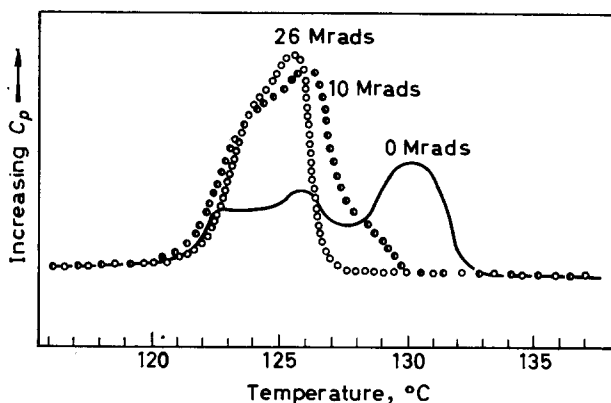
Figure 5—Comparative melting behaviour of unirradiated and irradiated 85°C crystals (10 deg. C/min)

organization entirely but may enable some thickening to occur on heating at 10 deg. C/min. A sample of 85°C crystals irradiated to 10 Mrads exhibited this behaviour as shown in Figure 5. About 24 per cent of the original lamellae increased in thickness and melted at temperatures higher than 127°C. The apparent heat of fusion for this sample was also identical to that of the original 85°C crystals.

The thermograms shown in Figure 6 for thin films of 70°C dendrites also illustrate the efficacy of crosslinking in hindering lamellar reorganization.
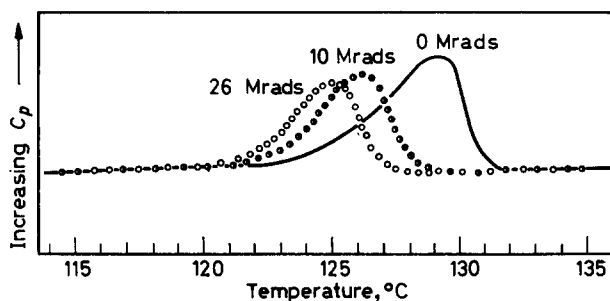
Figure 6—Comparative melting behaviour of unirradiated and irradiated 70°C dendrites (10 deg. C/min)

In this case, a dose of 26 Mrads does not appear completely adequate to retard thickening. Some perfecting of lamellae persists as indicated by the melting point being equal to that for 85°C crystals (26 Mrads). It was expected that crystals grown at lower temperatures would have a lower melting point[19]. Dendritic 70°C crystals irradiated to 52 Mrads melted

another 0·7 deg. C lower at 399·6°K (figure not shown). The final melting of these lamellae at 399·6°K yields a lamellar thickness of 117 Å from equation (1). This thickness is near the expected value for crystals grown at 70°C in xylene[19]. At all doses the apparent heat of fusion for 70°C dendrites was invariant, 50 cal/g.

Figures 5 and *6* indicate that single crystals grown at 70°C reorganize to a greater extent than crystals formed at 85°C. At least two causes can be advanced for this behaviour: (*1*) the reorganization rates are more rapid for 70°C crystals; and (*2*) 70°C crystals reorganize at lower temperatures. Since 70°C crystals appear to melt without multiple peaks the first possibility is more important. This is further strengthened by recent observations of Wunderlich and Hellmuth[20]. Using heating rates in excess of 1 000 deg. C/min, they concluded that 70°C dendrites reorganize faster than single crystals made at 80°C in toluene.

After 85°C single crystals were melted, they were cooled to room temperature at 10 deg. C/min to induce bulk crystallization. The subsequent fusion of these samples is shown in *Figure 7* and reveals a progressive lowering of $\Delta H_f^\star$ and T_m with increasing irradiation dose. The introduction
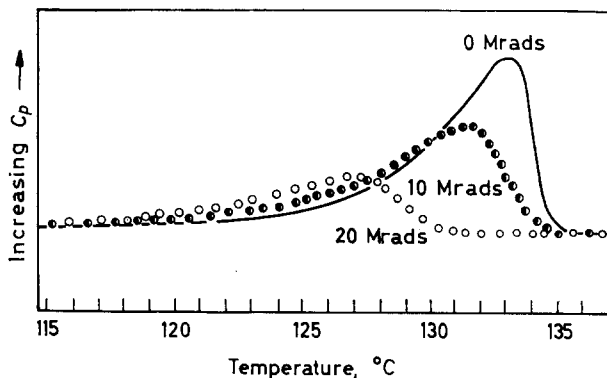
Figure 7—Comparison of the melting of unirradiated and irradiated recrystallized polyethylene (10 deg. C/min)

of roughly four crosslinks per polymer chain (10 Mrads) reduced the apparent heat of fusion by about 20 per cent from 49 cal/g for the unirradiated bulk crystallized sample to 39 cal/g. Increasing the periodicity of crosslinks with a dose of 26 Mrads resulted in a 40 per cent decrease in $\Delta H_f^\star$ to 30 cal/g. Upon bulk recrystallization the incorporation of these relatively few crosslinks within the crystals (rather than at the fold surfaces) may still be insufficient to produce the large observed diminution of $\Delta H_f^\star$ and T_m. However, if two crosslinks are separated by less than the critical chain length, $l^\star$, required for incorporation into a particular lamella, it is conceivable that the entire segment might be rejected from that crystal. The sequence probability for such an occurrence increases as $l^\star$ becomes larger. Thus, thinner crystals with low melting points might result as the frequency of crosslinks increases. Furthermore, the exclusion of entire segments asso-

ciated with crosslinks can explain the large reduction in ΔH_f^* by a comparatively small number of crosslinks[21].

Very rapid heating rates may also, in principle, suppress the thickening process. However, it has been found[22] that superheating of polyethylene crystals may occur at rates in excess of 20 deg. C/min. Nevertheless, two experiments at heating rates above 20 deg. C/min were conducted. Comparison of the double peaked fusion curves in *Figure 8* suggests that as the heating rate is doubled from 40 deg. C/min to 80 deg. C/min, the fraction of crystals associated with the higher melting peak is diminished. These experiments indicate that the more stable crystals melting at the highest
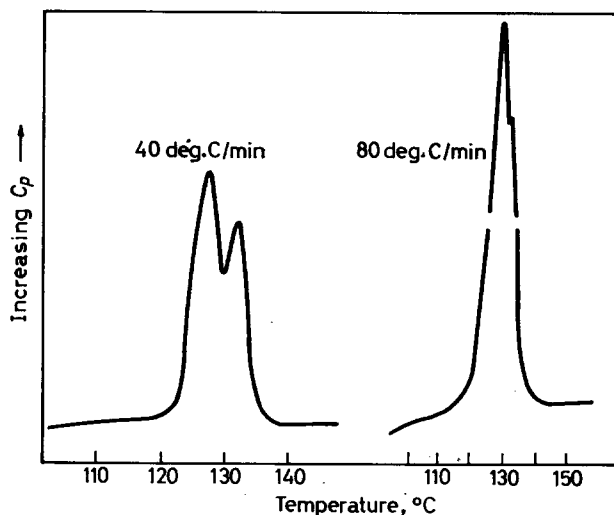
Figure 8—Melting curves of 85°C crystals at 40 deg. C/min and 80 deg. C/min

temperature are perfected through the lower temperature zone. These observations are consistent with the evidence on irradiated crystals.

Annealing of 85°C single crystals

All annealing experiments were performed in the nitrogen atmosphere of the scanning calorimeter. At the end of each annealing period, the sample was cooled to near room temperature at a linear rate from 2·5 deg. C to 10 deg. C/min. During cooling the enthalpic response was monitored for any sign of recrystallization. Less than one per cent could be detected recrystallizing from the melt. All annealed samples were reheated from near room temperature to 147°C. Apparent heats of fusion and melting points were obtained for each annealed sample. The results for ΔH_f^* and lamellar thickness [computed from T_m using equation (1)] are shown in *Figures 9* and *10*.

At 114°C little change in ΔH_f^* of 85°C crystals was observed with annealing time. A sample held at 102°C for 1 000 minutes produced no measur-

16

able change in $\Delta H_f^\star$. However, the shape of the fusion curve was in sharp contrast with the melting pattern of unannealed 85°C crystals*. For annealing temperatures between 118°C and 126°C unirradiated 85°C crystals showed an initial decrease in $\Delta H_f^\star$ followed by a gradual increase, approximately linear with log time, until the original $\Delta H_f^\star$ was reached or surpassed. Density measurements by Fischer and Schmidt[2] on polyethylene single crystals grown at 80°C show similar behaviour.

After annealing for five minutes at 127°C, nearly 50 per cent (27 cal/g) of the lamellae had melted and recrystallized upon cooling. Until the annealing temperature of 127°C had been reached, no detectable amount of recrystallization was observed for the 85°C crystals regardless of annealing time. This existed even though a substantial endotherm up to 126°C in *Figure 4* appears in this dynamic experiment (indicating a melting process). These results indicate that for 85°C crystals: (*1*) relatively insignificant changes occur at annealing temperatures of 114°C or less; (*2*) substantial rearrangement is possible when these crystals are annealed in the temperature interval 118°C to 126°C; and (*3*) annealing at 127°C and above causes lamellae to melt. If annealing times are sufficiently long at these temperatures (127°C and above), melted lamellae recrystallize. Matsuoka[24] has presented dilatometric results on annealed polyethylene single crystals grown from 0·3 per cent xylene solution at 85°C. His data indicate that the annealing kinetics at 130°C are similar to those of bulk polyethylene at the same temperature. The marked difference in annealing behaviour at 127°C suggests that between 118°C and 126°C the 85°C crystals anneal primarily by lamellar thickening. Since we wished to avoid the added variable of recrystallization from the melt in these isothermal annealing experiments, 85°C crystals were not annealed above 127°C. At all temperatures (below 127°C) except 102°C the multiple peaks disappeared on annealing for a sufficient length of time.

The melting points of annealed crystals were used to determine lamellar long periods [equation (1)] and some of the results are shown in *Figure 10*. At 121°C and 125°C the growth was nearly linear with log time. These results are in good agreement with Fischer and Schmidt's[2] X-ray studies of long period.

Irradiated single crystals annealed differently than unirradiated crystals. Samples with a dose of 10 and 26 Mrads were annealed at 121°C for various lengths of time. Apparent heats of fusion for annealed 85°C crystals irradiated to 10 Mrads were four to six per cent below the $\Delta H_f^\star$ values for the originally unirradiated single crystals (*Figure 9*). In addition, the thickening process lagged behind the unirradiated 85°C lamellae by almost 50 Å, although the long period still increased linearly with log time (*Figure 10*). Crystals irradiated to 26 Mrads exhibited more severe alteration; $\Delta H_f^\star$ is reduced by about 16 per cent and appeared to be shifted behind the apparent heats of fusion by about three decades in time (*Figure 9*).

Annealing behaviour for crystals grown at 85°C differ in three tempera-

---

*We have also observed that thermograms for untreated 85°C crystals vary for samples collected in different manners and may be associated with lamellar packing[10, 23].
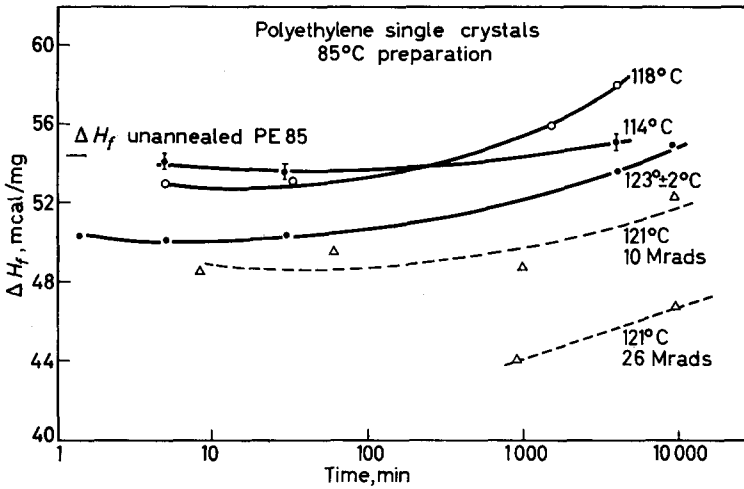
Figure 9—Apparent heats of fusion for 85°C crystals as a function of annealing temperature and time

ture regions[2(c)]. Rationalization for this behaviour may be sought in terms of supercooling. The dissolution temperature, T_s, for the infinitely thick polyethylene crystal in xylene has been extrapolated by Holland[14] to be $106° \pm 2°C$. Thus the platelets crystallized at 85°C ($T_c = 85°C$) may be
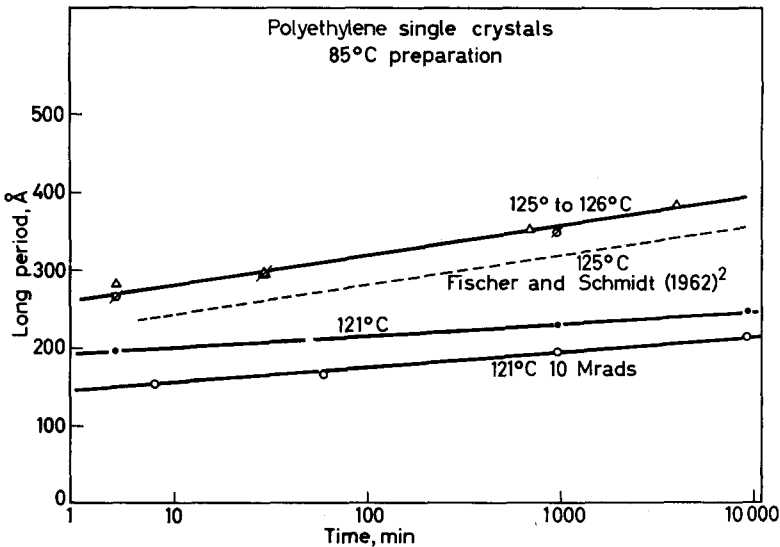
Figure 10—Lamellar thickness of 85°C crystals as a function of annealing temperature and time

assumed to have about $21° \pm 2°C$ supercooling ($T_s - T_c$). Referred to the thermodynamic melting point (T_{m_0}) of 141°C, a comparable supercooling

18

exists at $120° \pm 2°C$. Annealing at a temperature, T_a, such that the condition $T_{m_0} - T_a > T_s - T_c$ is satisfied, crystals do not reorganize. Experimental results for annealing at 114°C and below showed that $\Delta H_f^\star$ and T_m remained constant for times in excess of 4 000 minutes. Annealing between 118°C and 126°C, 85°C crystals apparently reorganize by lamellar thickening. In addition, crystals grown at 70°C, where $T_s - T_c = 36° \pm 2°C$, showed signs of annealing at temperatures too low for 85°C platelets to reorganize significantly. When isothermally annealed at 110°C for 1 200 min, these crystals showed a 10 per cent increase in $\Delta H_f^\star$ to 55 cal/g.

The observation that crystals prepared at 85°C melt at 127°C, provided no reorganization occurs during heating, is sufficient to indicate a change in annealing behaviour for this material at 127°C and above.

CONCLUSIONS

(1) Irradiating polyethylene single crystals provides an effective technique for studying melting and annealing behaviour. We believe that 85°C crystals irradiated to 26 Mrads can be melted (10 deg. C/min) without significant reorganization. Such a melting behaviour is thought to be truly characteristic of the original crystals as prepared from solution. Thus the origin of multiple peaks in thermograms of the unirradiated polyethylene single crystals is due to the process of lamellar thickening.

(2) Annealing chain folded 85°C single crystals between 118°C and 126°C occurs mainly by the process of lamellar thickening. Annealing of these crystals above 127°C is accomplished by melting of lamellae which can recrystallize provided annealing time is sufficiently long. Annealing 85°C crystals at 114°C or below causes no change in thickness or crystallinity.

(3) The approximate degree of crystallinity for polyethylene single crystals prepared at three different solution temperatures ranged from 79 per cent to 84 per cent.

NOTE: After completion of this manuscript we discovered a paper on melting of polyethylene single crystals[25]. It should be noted, however, that this interpretation of melting differs from ours.

Bell Telephone Laboratories Incorporated,
Murray Hill, New Jersey

REFERENCES

[1] HOFFMAN, J. D. and WEEKS, J. J. *J. Res. nat. Bur. Stands.* A, 1962, **66**, 13
[2](a) FISHER, E. W. and SCHMIDT, G. F. *Angew. Chem.* 1962, **74**, 551; (b) STATTON, W. O. and GEIL, P. H. *J. appl. Polym. Sci.* 1960, **3**, 357; (c) TAKAYANAGI, M. and NAGATOSHI, F. *Mem. Fac. Engng Kyushu*, 1965, **24**, 33
[3] KARASZ, F. E. and HAMBLIN, D. J. *Report* of National Physical Laboratory, *BPR 15*, May 1963

[4] RICHARDSON, M. J. *Trans. Faraday Soc.* 1965, **61**, 1876

[5] HOLLAND, V. F. and LINDENMEYER, P. H. *J. Polym. Sci.* 1962, **57**, 589

[6] WATSON, E. S., O'NEILL, M. J., JUSTIN, J. and BRENNER, N. *Analyt. Chem.* 1964, **3**, 1238

[7] MATSUOKA, S. and ALOISIO, C. J. Private communication

[8] DOLE, M. *Fortschr. HochpolymForsch.* 1960, **2**, 221

[9] CHARLESBY, A. *Atomic Radiation and Polymers.* Pergamon: New York, 1960

[10] SALOVEY, R. *J. Polym. Sci.* 1962, **61**, 463; SALOVEY, R. and BASSETT, D. C. *J. appl. Phys.* 1964, **35**, 3216

[11] STATTON, W. O. and GEIL, P. H. *J. appl. Polym. Sci.* 1960, **3**, 357

[12] JACKSON, J. B., FLORY, P. J. and CHIANG, R. *Trans. Faraday Soc.* 1963, **59**, 1906

[13] PETERLIN, A. and MEINEL, G. *Polymer Letters,* 1965, **3**, 1059

[14] HOLLAND, V. F. *J. appl. Phys.* 1964, **35**, 59

[15] BROADHURST, M. G. *J. chem. Phys.* 1962, **36**, 2578

[16] PRICE, F. P. *J. chem. Phys.* 1961, **35**, 1884

[17] KELLER, A. and O'CONNOR, A. *Polymer, Lond.* 1960, **1**, 163

[18] ORTH, H. and FISCHER, E. W. *Makromol. Chem.* 1965, **88**, 188

[19] See, for example, MANDELKERN, L. *Crystallization of Polymers,* McGraw-Hill: New York, 1964

[20] WUNDERLICH, B. and HELLMUTH, E. *J. appl. Phys.* 1965, **36**, 3039

[21] DOLE, M., STOLKI, T. J. and WILLIAMS, T. F. *J. Polym. Sci.* 1961, **48**, 61

[22] WUNDERLICH, B., SULLIVAN, P., ARAKAWA, T., DiCYAN, A. B. and FLOOD, J. F. *J. Polym. Sci.* A, 1963, **1**, 3581

[23] SALOVEY, R., HUSEBY, T. W. and BAIR, H. E. To be published.

[24] MATSUOKA, S. *J. Polym. Sci.* 1962, **57**, 569

[25] MANDELKERN, L. and ALLOU Jr, A. L. *Polymer Letters,* 1966, **4**, 447

Acoustic Birefringence of Polymer Solutions
II—Necklace Model

A. PETERLIN

The necklace model of randomly coiled macromolecule with ideally elastic links but a finite resistance to the rate of shape change (internal viscosity) was used for the calculation of frequency dependence of acoustic birefringence and the phase shift between the latter and the displacement field of acoustic wave. The calculation was performed for a model with 100 links. In contrast with the results for the perfectly soft dumb-bell model, the initial birefringence is much smaller, has a shorter linear range but a much longer transition to saturation, and a limiting value which decreases with increasing internal viscosity. The phase shift is first rather similar to that of the dumb-bell model. Approaching 45° it shows an inflection which grows larger with larger number of segments and smaller internal viscosity. The transition from 0° to 90° extends over a much wider frequency range (between two and three decades more) than for the dumb-bell. A comparison with experimental data on polystyrene solutions indicates that a smaller number of segments (about 40 instead of 100) may give a satisfactory fit.

IN AN acoustic field

$$v_2 = B \cos \omega (t - z^\star/c_a) \tag{1}$$

where B is velocity amplitude, ω is circular frequency and c_a is velocity of sound, the molecules are oriented and deformed so that the liquid becomes birefringent[1-6]. The theory of the effect was first developed for low molecular weight liquids[1,5,7,8] and for suspensions of rather large particles[9]. In the former the molecules get oriented in the oscillating laminar flow with longitudinal (parallel) gradient in a very similar manner as in the steady state flow[10], and in the latter the orientation is due to radiation pressure.

The theory for macromolecular solutions was developed by Peterlin[4] who used the perfectly elastic and soft dumb-bell model. Badoz[5] treated the elastic sphere model of Cerf[11] with consideration of optical internal field according to Böttcher[12]. His results, as far as the frequency and intensity dependence of the effect are concerned, agree with those of Peterlin.

As pointed out by Hilyard and Jerrard[6] the experimental data on polymer solutions cannot be completely reproduced by the existing theories of the effect. Particularly the relaxation times derived from the experiment on polystyrene solution in toluene and chloroform on the basis of Peterlin's dumb-bell model seem to be too small as compared with those obtained from intrinsic viscosity data on the basis of the necklace model. Such a discrepancy is to be expected because the dumb-bell model with only one

21

relaxation time instead of the discrete spectrum of the necklace model has the inherent deficiency of not representing correctly relaxation phenomena.

It seems therefore worthwhile to present a theory of acoustic birefringence based on the necklace model[13] with consideration of hydrodynamic interaction[14] between any two beads and of finite resistance of coil to rapid shape changes[15] (internal viscosity). Such a model turned out to be extremely valuable in explaining the gradient[15] and frequency[16] dependence of intrinsic viscosity and of the orientational effects of streaming birefringence[15]. The replacement of a single relaxation time with a discrete spectrum modifies the frequency dependence. The transition from the initial linear increase of birefringence with the frequency to the final saturation value becomes more gradual and extends over a wider frequency range. The internal viscosity shifts the effect closer to that of rigid particles.

In what follows the data of the ideally flexible dumb-bell model (I) will be summarized first and the so-obtained results extended to the necklace model.

Dumb-bell model

The molecule moves in the oscillating velocity field [equation (1)] which one expands in powers of the relative coordinates r of the macromolecule

$$v_z = B\, e^{i\omega(t-z*/c_a)}_v \; (1 - i\omega z/c_a - \omega^2 z^2/2c_a^2 + \; \ldots) \qquad (2)$$

where $z\star$ is the coordinate of the centre of hydrodynamic resistance of the molecule which in first approximation coincides with the centre of mass and z is the relative coordinate of the free ends of the dumb-bell with the centre of mass in the origin. Due to the smallness of the macromolecule as compared with the wavelength $\lambda = 2\pi c_a/\omega$ one may neglect all the terms beyond the linear so that the relative velocity of the acoustic field which orients and deforms the molecule reads

$$v_z^0 = v_{z,\mathrm{rel.}} = v_z - v_z{}^*_v = Gz$$

$$G = G_0 \exp(-i\omega t) \qquad (3)$$

$$G_0 = -(i\omega B/c_a) \exp(-i\omega z\star/c_a)$$

The product $G_0 z$ is the amplitude of velocity. The parameters G_0 and G play the same role as the velocity gradient in laminar flow with transverse gradient. The flow field in the sound wave is laminar with a longitudinal gradient. Such a field has no rotational component.

According to Peterlin[4] the intrinsic birefringence $\Delta n/nc$ is proportional to the product of a frequency factor $\omega\tau/(1+\omega^2\tau^2)^{1/2}$ and the square root of intensity $I = \frac{1}{2}\rho B^2 c_a$ of the acoustic wave field, i.e. to the actual amplitude G_0, and is out of phase with the displacement wave by an angle ψ which depends on the frequency. The actual gradient G is always so small that the saturation effects are hardly observable. Therefore it makes sense to divide the birefringence by the amplitude G_0 or by $I^{1/2}$. One so obtains the specific Lucas constant

$$
\left.
\begin{aligned}
L_{\text{sp.}} &= (\Delta n / ncl^{1/2})_{c=0, I=0} \\
&= K \left[\omega\tau / (1 + \omega^2\tau^2)^{1/2} \right] \quad \sin \; [\omega \, (t - z^\star / c_a) - \psi] \\
&\qquad\qquad \tan \psi = \omega\tau \\
K &= \frac{4\pi}{5} \left(\frac{n^2 + 2}{3n} \right)^2 \left(\frac{2}{\rho c_a^3} \right)^{1/2} \left(\frac{N}{M_0} \right) (\alpha_1 - \alpha_2) \\
\tau &= 1 / 4\mu_z Z D_z = Z f b_0^2 / 24 kT \\
\mu_z &= 3 / 2 Z b_0^2 \qquad\qquad\qquad D_z = 4kT / Zf
\end{aligned}
\right\} \qquad (4)
$$

where Z is the number of statistically independent segments of the macro-molecule, M_0 is molecular weight, b_0 is the length and f is the frictional coefficient of such a segment. Other symbols have the usual meanings.

Equations (4) contain a great many factors which also occur in the Maxwell constant[17] (streaming birefringence) so that it may be valuable to have $L_{\text{sp.}}$ expressed in terms of $M_{\text{sp.}} = (\Delta n / nc\eta_0 G)_{G=0, c=0}$ where G is the velocity gradient of the linear laminar flow

$$
L_{\text{sp.}} = M_{\text{sp.}} \eta_0 \left(\frac{2}{\rho c_a^3} \right)^{1/2} \times \frac{\omega}{(1 + \omega^2\tau^2)^{1/2}} \; \sin \, [\omega \, (t - z^\star / c_a) - \psi] \qquad (5)
$$

This relationship is valid even when one has a substantial contribution of shape anisotropy to birefringence. This is the consequence of the fact that in the limit $G = 0$ the macromolecule is undeformed so that the optical factor is the same for acoustic and streaming birefringence.

The initial proportionality of $L_{\text{sp.}}$ with the frequency of the acoustic field and the subsequent levelling off or at least the occurrence of saturation effects were well proved by experiments[3, 5, 6].

The necklace model

The necklace model of Rouse[13], Zimm[14], Reinhold–Peterlin[18] and Cerf[15] has $Z + 1$ beads connected by Z statistically independent non-linear elastic links of root mean square length b_0 and maximum length b_∞. The hydrodynamic resistance f is concentrated in the beads. Hydrodynamic interaction is assumed to be proportional to the inverse r.m.s. distance between the two beads under consideration. Due to the already mentioned fact that the flow field is of low intensity, the segment deformations are so small that one may completely neglect the non-linearity of link elasticity. The model resists shape changes with a force proportional to the rate of deformation, the proportionality factor φ being called inner viscosity coefficient. It has the dimension of viscosity time length (g sec^{-1}). The $Z + 1$ vectors $\mathbf{r}_j$ from the centre of mass to the single beads are written as a $3(Z + 1)$ dimensional vector $\mathbf{r}$. In the same manner the relative velocities of the acoustic flow field at the beads are represented by a vector $\mathbf{v}_z = G\mathbf{z}$ in complete analogy to equation (3).

Under consideration of hydrodynamic interaction the equilibrium between the friction force of the liquid and the forces transmitted by the chain

23

(elastic links, inner viscosity, Brownian motion) yields for the velocity of the beads[15]

$$\mathbf{v} = \mathbf{v}^0 - \mathbf{H}\,(2\mu_0 D_0 \mathbf{Ar} + f^{-1}\mathbf{Q}^{-1T}\Phi\mathbf{Q}^{-1}\mathbf{v} + D_0\nabla^T \ln \Psi) \Big\}$$

$$\mu_0 = 3/2b_0^2 \qquad D_0 = kT/f \qquad\qquad\qquad\qquad \Big\} \tag{6}$$

μ_0 and D_0 are the distribution parameter and the diffusion constant of the bead [note the difference in definition between equations (6) and (4)]. $\mathbf{A}$ is the orientational tensor of elastic forces transmitted by the links, $\mathbf{H}$ is the tensor of hydrodynamic interaction, and $\mathbf{Q}$ is the transformation matrix from space coordinates $\mathbf{r}$ to the normal coordinates $\mathbf{u} = (\xi,\ \eta,\ \zeta)$

$$\mathbf{r} = \mathbf{Qu} \tag{7}$$

$$\nabla_r^T = \mathbf{Q}^{-1T}\nabla_u^T$$

The tensor Φ of inner viscosity measuring the resistance of macromolecule to deformation, yielding the force $\mathbf{F}'$ by which the molecule resists the deformation rate $\mathbf{v}_{\text{def.}}$

$$\mathbf{F}'_u = -\Phi\mathbf{v}_{u,\text{def.}} \tag{8}$$

is a diagonal tensor in the space of normal coordinates. Its diagonal values $\varphi_p = p\varphi/Z$ express the resistance F'_p connected with a deformation described by the pth eigenmode. The deformation rate $\mathbf{v}_{\text{def.}}$ is obtained by subtracting the rotational component from the total velocity. In the longitudinal flow field [equation (3)] there is no rotational component so that $\mathbf{v} = \mathbf{v}_{\text{def.}}$.

The continuity equation

$$\partial\Psi/\partial t = -\nabla^T\mathbf{v}\Psi \tag{9}$$

is orthogonalized by transformation to normal coordinates [equation (7)]:

$$\partial\Psi/\partial t = -(1 + f^{-1}\mathbf{N}\Phi)^{-1}\nabla_u\Psi\,[\mathbf{v}^0 - D_0\mathbf{N}\nabla_u \ln \Psi - 2\mu_0 D_0\Lambda\mathbf{u}] \Big\}$$

$$\mathbf{M} = \mathbf{Q}^T\mathbf{AQ} = \mathbf{Q}^{-1}\mathbf{AQ} \qquad\qquad\qquad\qquad \Big\} \tag{10}$$

$$\mathbf{N} = \mathbf{Q}^{-1}\mathbf{HQ}^{-1T} = \mathbf{Q}^{-1}\mathbf{HQ} \qquad \Lambda = \mathbf{Q}^{-1}\mathbf{HAQ} = \mathbf{NM} \Big\}$$

where $\mathbf{Q}^{-1}$ is the inverse and $\mathbf{Q}^T$ the transpose of the Q matrix. Since $\mathbf{HA}$, $\mathbf{H}$ and $\mathbf{A}$ are symmetric the transformation matrix $\mathbf{Q}$ is orthogonal so that $\mathbf{Q}^T = \mathbf{Q}^{-1}$. The eigenvalues of $\mathbf{M}$, $\mathbf{N}$ and Λ are μ_p, ν_p and λ_p with $p = 1, 2, \ldots, Z$.

Optical birefringence

Assuming with Kuhn and Grün[19] that the optical anisotropy of the statistical segment is proportional to the average square of the link length:

$$(\gamma_1 - \gamma_2)_j = (2\mu_0/5)\,(\alpha_1 - \alpha_2)\,b_j^2 = (3/5)\,(\alpha_1 - \alpha_2)\,b_j^2/b_0^2$$

$$b_j^2 = (\mathbf{r}_j - \mathbf{r}_{j-1})^2 \qquad\qquad j = 1, 2, \ldots Z \tag{11}$$

where γ_1 and γ_2 are the polarizability of the segment in the link direction and perpendicular to it and α_1, α_2 are the corresponding quantities for the monomer. By denoting the average polarizability of the macromolecule

in the z and x direction as α_z and α_x respectively one obtains:

$$
\left.
\begin{aligned}
\frac{\Delta n}{n} &= \frac{n_z - n_x}{n} = \left(\frac{n^2+2}{3n}\right)^2 (2\pi)\left(\frac{cN}{M}\right)(\alpha_z - \alpha_x) \\
\alpha_z - \alpha_x &= (2\mu_0/5)(\alpha_1 - \alpha_2)\langle \mathbf{z}^T\mathbf{A}\mathbf{z} - \mathbf{x}^T\mathbf{A}\mathbf{x}\rangle \\
&= (2\mu_0/5)(\alpha_1 - \alpha_2)\langle \boldsymbol{\zeta}^T\mathbf{M}\boldsymbol{\zeta} - \boldsymbol{\xi}^T\mathbf{M}\boldsymbol{\xi}\rangle \\
&= (2\mu_0/5)(\alpha_1 - \alpha_2)\sum_p \mu_p(\langle \zeta_p^2\rangle - \langle \xi_p^2\rangle)
\end{aligned}
\right\} \quad (12)
$$

The last average is directly derivable from the diffusion equation by multiplication of the latter with $\boldsymbol{\zeta}^T\mathbf{M}\boldsymbol{\zeta}$ and $\boldsymbol{\xi}^T\mathbf{M}\boldsymbol{\xi}$ respectively and integrating over the whole space. Neglecting the higher than linear terms in G_0 and the transient terms describing the transition from the initial solution at rest to the final steady state one obtains:

$$
\left.
\begin{aligned}
\langle \mathbf{z}^T\mathbf{A}\mathbf{z} - \mathbf{x}^T\mathbf{A}\mathbf{x}\rangle &= (G/\mu_0)\sum_p [4\mu_0 D_0\lambda_p + i\omega(1 + \nu_p\varphi_p/f]^{-1} \\
&= \frac{B}{\mu_0 c_a}\sum \frac{i\omega\tau_p}{1 + i\omega\tau_p'}\exp[i\omega(t - z^\star/c)] \\
\tau_p &= 1/4\mu_0 D_0\lambda_p \qquad \tau_p' = \tau_p(1 + \nu_p\varphi_p/f)
\end{aligned}
\right\} \quad (13)
$$

After inserting this expression in equation (6) one has for the specific birefringence

$$
L_{\text{sp.}} = \frac{4\pi}{5}\left(\frac{n^2+2}{3n}\right)^2\left(\frac{2}{\rho c_a^3}\right)^{1/2}\left(\frac{N}{M}\right)(\alpha_1 - \alpha_2)\sum_{p=1}^{z}\frac{\omega\tau_p}{(1 + \omega^2\tau_p'^2)^{1/2}}\sin[\omega(t - z^\star/c_a) - \psi_p]
$$

$$
\tan\psi_p = \omega\tau_p' \qquad\qquad (14)
$$

This formula has the same characteristics as that derived for the dumb-bell model. Of course the single frequency-dependent factor of equation (4) is replaced by the sum over Z terms corresponding to the Z eigenvalues. In addition the relaxation time occurring in the denominator is modified by the factor depending on inner viscosity. The same applies to the phase angle.

At $\omega = \infty$ one has $\psi_p = \pi/2$ so that the sine turns into negative cosine. The birefringence is by 180° out of phase with the velocity field of the acoustic wave. At $\omega = 0$ (steady dilatational flow)[20] $\psi_p = 0$ and the birefringence is in phase with the displacement field $(B/\omega)\sin[\omega(t - z^\star/c_a)]$. At finite frequency the observable total shift ψ_a and the effective amplitude, i.e. the r.m.s. average of Lucas constant, is given by:

$$
\left.
\begin{aligned}
L_{\text{sp., eff.}} &= K(I^2 + II^2)^{1/2} \\
\tan\psi_a &= II/I \\
II &= \sum_p \omega^2\tau_p\tau_p'/(1 + \omega^2\tau_p'^2) \\
I &= \sum_p \omega\tau_p/(1 + \omega^2\tau_p'^2)
\end{aligned}
\right\} \quad (15)
$$

The birefringence first linearly increases with frequency and finally approaches a saturation value

$$L_{\text{sp., eff., } \omega = \infty} = (K/Z) \sum_{p=1}^{Z} (1 + \nu_p \varphi_p / f)^{-1} \qquad (16)$$

The phase angle ψ_a by which the birefringence lags behind the displacement goes from $0°$ to $90°$ with increasing frequency.

It is worthwhile here to insert a brief comparison with the more familiar Maxwell constant of streaming birefringence which is derived from the analogue of equation (12):

$$M_{\text{sp.}} \eta_0 G = \left(\frac{\Delta n}{nc} \right)_{\text{str.}} = 2\pi \left(\frac{n^2 + 2}{3n} \right)^2 \left(\frac{N}{M} \right) 2\alpha_{xy}$$

$$\alpha_{xy} = (2\mu_0 / 5)(\alpha_1 - \alpha_2) \langle \mathbf{x}^T \mathbf{A} \mathbf{y} \rangle \qquad (17)$$

From the definition of $L_{\text{sp.}}$ in equation (4) and of $M_{\text{sp.}}$ one derives

$$L_{\text{sp.}} / M_{\text{sp.}} = (\eta_0 G / I^{1/2})_{G=0, I=0} \langle \mathbf{z}^T \mathbf{A} \mathbf{z} - \mathbf{x}^T \mathbf{A} \mathbf{x} \rangle / 2 \langle \mathbf{x}^T \mathbf{A} \mathbf{y} \rangle$$

$$= \eta_0 (2/\rho c_a^3)^{1/2} e^{i\omega(t - z^*/c_a)} \sum_p [-i\omega \tau_p (1 + i\omega \tau_p')^{-1}] / \sum_p \tau_p \qquad (18)$$

The ratio of $L_{\text{sp.}} / M_{\text{sp.}}$ contains explicitly the time factor. Usually one measures only the effective values of birefringence, i.e. the amplitude of $L_{\text{sp.}}$ or $M_{\text{sp.}}$ divided by $2^{1/2}$. For streaming birefringence, however, the observation at constant gradient is the rule, so that the factor $2^{1/2}$ applies merely to $L_{\text{sp.}}$. One so obtains for the ratio between the effective acoustic and static streaming birefringence

$$L_{\text{sp., eff.}} / M_{\text{sp.}} = \eta_0 (\rho c_a^3)^{-1/2} (I^2 + II^2)^{1/2} / \sum_p \tau_p \qquad (19)$$

where I and II were defined in equation (15).

RESULTS AND DISCUSSION

For a calculation of $L_{\text{sp.}}$ and ψ_a one needs the eigenvalues λ_p and ν_p and the coefficient φ of the inner viscosity. The former are:

$$\lambda_p = 4 \sin^2 [\pi p / 2(Z + 1)] \sim \pi^2 p^2 / Z^2$$

$$\nu_p = 1 \qquad (20)$$

for the free draining coil[13] and

$$\left. \begin{array}{l} \lambda_p^\star = (4h/Z^2) \lambda_p' = 2f\lambda_p' / (3\pi^3)^{1/2} Z^{3/2} b_0 \eta_0 \\[4pt] \lambda_p' \sim (\pi^2 p^{3/2})(1 - 1/2\pi p) \\[4pt] h = Zf/(12\pi^3)^{1/2} Z^{1/2} b_0 \eta_0 = Zf/1 \cdot 023 \times 6\pi Z^{1/2} b_0 \eta_0 \\[4pt] \nu_p^\star = \lambda_p^\star / \lambda_p \sim (f/1 \cdot 023 \times 3\pi b_0 \eta_0)(Z/p)^{1/2}(1 - 1/2\pi p) \end{array} \right\} \qquad (21)$$

for the impermeable coil[14, 21]. The parameter h measuring the strength of hydrodynamic interaction is just the ratio of translational frictional resistance of the free draining and completely impermeable coil with a radius very nearly equal to the r.m.s. end-to-end distance $Z^{1/2} b_0$ of the coil. The

eigenvalues λ'_p according to equation (21) are a little too small[22]. The error is largest, about ten per cent, at λ'_1 and drops quickly to a few per cent at higher p. In what follows the uncorrected values of equation (21) have been used.

Convenient dimensionless parameters for consideration of internal viscosity are:

$$a = \varphi / Zf \qquad \text{free draining coil}$$
$$a^\star = h\varphi / Zf = \varphi / 1 \cdot 023 \times 6\pi Z^{1/2} b_0 \eta_0 \qquad (22)$$
$$\text{impermeable coil}$$

They measure the ratio of internal viscosity coefficient φ to the hydrodynamic frictional resistance coefficient of the free draining coil and of an impermeable sphere with a radius $1 \cdot 023 \, Z^{1/2} b_0$, respectively. Values between 0 (ideally flexible coil) and 1 (rather stiff coil) will be considered. One must not, however, forget that one is not permitted to increase the parameter too much because all the derivations were based on the assumption that the coil is not rigid. For the extreme case of rigid coil one has to adopt a slightly different approach as shown by Cerf[15]. We hope soon to report the respective results.

In order not to complicate the matter too much, the data for a free draining and for the impermeable coil only are presented. The number Z of statistically independent segments is 100. In *Figures 1* and *2* the specific birefringence and in *Figures 4* and *5* the phase angle are plotted as functions of $\omega\tau_1$ for different values of a and $a^\star$ respectively. At small $\omega\tau_1$ the birefringence is independent of internal viscosity. The values for the ideally soft coil with no hydrodynamic interaction are slightly below those for the model with complete solvent immobilization. But the slope is very nearly identical through $\omega\tau_1 = 1$, that means in the whole range when the birefringence is proportional to frequency. Thereafter the free draining coil shows a more gradual decrease in slope but also slightly later reaches saturation.

Deviations from the value of the ideally flexible coil become noticeable at $\omega\tau_1 = 1$ and rapidly increase with approach to the saturation value. With increasing internal viscosity they occur earlier and reach the saturation value at lower $\omega\tau_1$. The latter decreases with internal viscosity according to equation (16) as $Z^{-1} \Sigma (1 + \nu_p \varphi_p / f)$. The respective values are plotted in *Figure 3*. The reduction of saturation value plotted over a or $a^\star$ respectively is larger for the free draining case.

There is quite a spectacular difference in birefringence between the necklace and dumb-bell models [equation (4)]. In the latter the linear region extends over a much wider frequency interval. Saturation effects are not noticeable before the birefringence has reached about 70 per cent of the limiting value. That occurs at $\omega\tau_1 = 1$. With the necklace model, deviations from linearity start at slightly smaller values of $\omega\tau_1$ between 0·1 and 1. But 70 per cent of saturation value is reached much later at $\omega\tau_1$ between 20 and 500 for the impermeable coil and between 20 and 4 000 for the free draining case. The dumb-bell curve is shifted to smaller $\omega\tau_1$ values by quite an
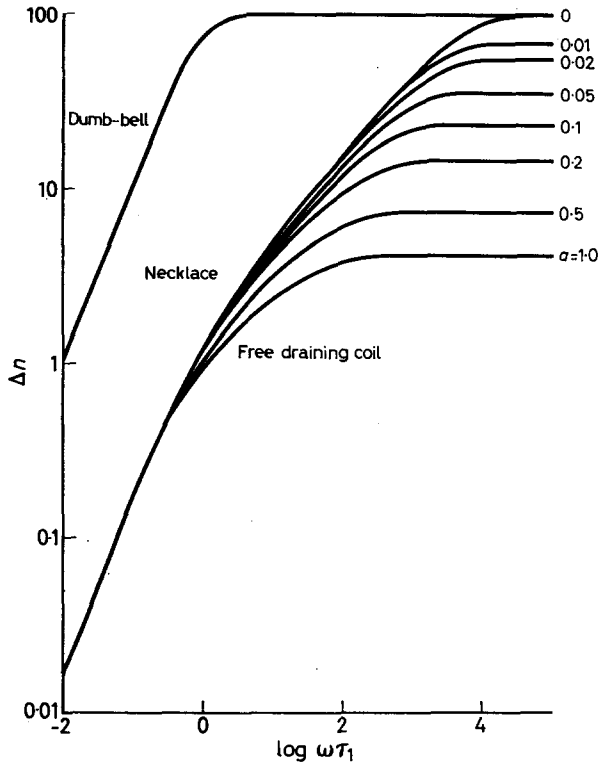
Figure 1—Acoustic birefringence $L_{sp.,eff.}/K$ as function
of $\omega\tau_1$ for the free draining dumb-bell and necklace models
with 100 links. The parameter $a=\varphi/Zf$

appreciable amount which increases with Z. In our case with $Z=100$, the
shift equals a factor between 50 and 60 in the linear range and approaches
values between 500 and 2 000 in the saturation region. The factor is larger
in the free draining case.

The phase angle plotted in *Figures 4* and *5* exhibits a shift to smaller $\omega\tau_1$
with increasing internal viscosity. Concurrently the peculiar inflection at
45° gradually diminishes. It must disappear with $a=a^\star=\infty$ because the
completely rigid coil has only one relaxation time so that the phase angle
dependence on frequency is given by equation (4). The inflection at 45°
characteristic for the perfectly soft coil is becoming more pronounced with
increasing number of segments as was shown by Thurston and Schrag[23] for
oscillatory flow birefringence. The inflection is stronger for the free draining
coil. As a result of this the transition from $\psi=0°$ to $\psi=90°$ extends over
a large frequency range. Partial coil rigidity as measured by the internal
viscosity coefficient φ reduces the inflection and hence the frequency range
of this transition.

The curves for the dumb-bell model are markedly steeper than those for
the necklace and there is, of course, no trace of a step at $\psi=45°$. But the
displacement in the frequency scale is much less than for the birefringence.
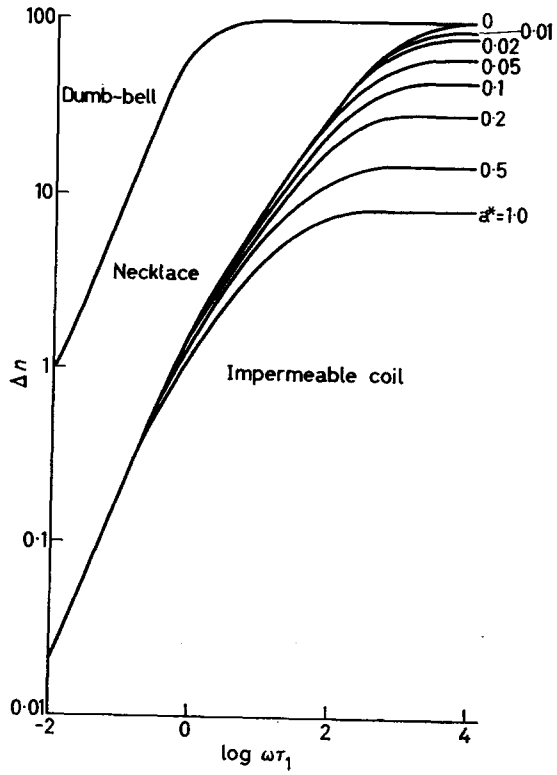
Figure 2—Acoustic birefringence $L_{sp.,eff.}/K$ as function of $\omega\tau_1$ for the dumb-bell and necklace models with complete solvent immobilization. The model has 100 segments. The parameter $a\star = h\varphi/Zf$
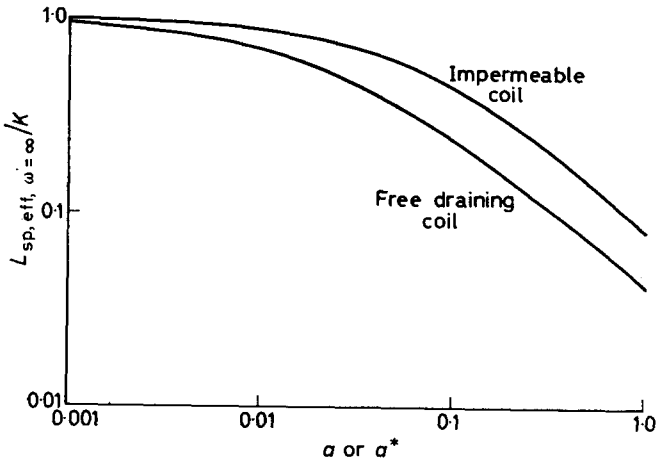
Figure 3—Limiting values of acoustic birefringence $L_{sp.,eff.,\omega=\infty}/K$ according to equation (16) for the free draining dumb-bell and completely impermeable necklace models with 100 segments as a function of a and $a\star$, respectively

29
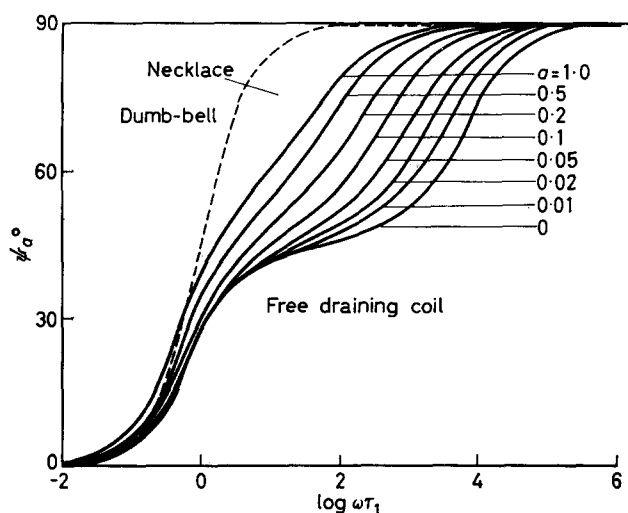
Figure 4—Phase angle ψ as a function of $\omega\tau_1$ for the free draining dumb-bell and necklace models with 100 segments

It is nearly zero at $\psi=0$ and approaches a value between one and two decades at ψ close to 90°. One must not expect that the necklace curves with infinitely large a or $a^\star$ will coincide with the dumb-bell curve because the latter represents a perfectly flexible and the former a rigid coil.

Experimental investigations of acoustic birefringence[1-6] were only concerned with intensity and not with the phase shift. The data on rather concentrated polystyrene solutions in toluene and chloroform ($c = 10$, 8 and $4 \times 10^{-2} \, \text{g cm}^{-3}$) investigated by Hilyard and Jerrard[6] exhibit an extremely rapid transition from linearity to saturation. They are much closer to the results predicted by the dumb-bell than to those of the necklace model. On
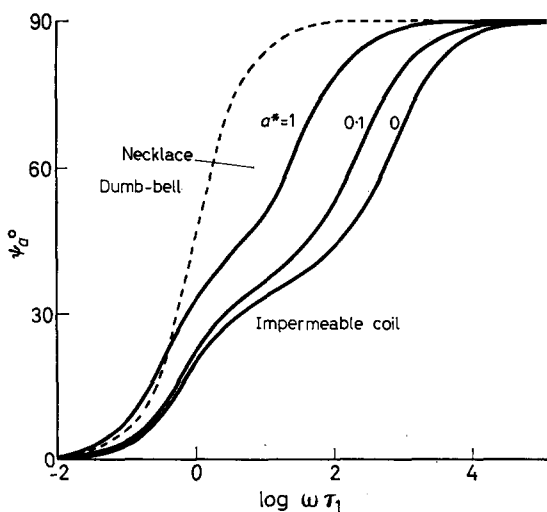
Figure 5—Phase angle ψ as function of $\omega\tau_1$ for the impermeable dumb-bell and necklace models with 100 segments

30

the other side the difference in relaxation time 0.6×10^{-7} sec as observed in acoustic birefringence and 3.6×10^{-6} sec as deduced from intrinsic viscosity on the basis of the impermeable necklace model is most easily explained as a consequence of the large frequency shift between the birefringence curves corresponding to the two models. The ratio 40 between the two relaxation times is less than the shift derived from *Figures 1* or *2* with plots based on $Z = 100$. With smaller Z the shift also decreases and finally disappears with $Z = 1$. Concurrently the transition between the linear and the saturation region becomes sharper. One may therefore hope that with a Z about 40 and a non-vanishing φ one will be able to reproduce the experimentally observed frequency dependence and to achieve a fit between the relaxation time τ_1 from viscosity and birefringence.

Camille Dreyfus Laboratory,
   Research Triangle Institute,
      Research Triangle Park, N.C.27709

REFERENCES

[1] LUCAS, R. *C.R. Acad. Sci., Paris*, 1938, **206**, 827; *J. Phys. Radium*, 1939, (7) **10**, 153; *Rev. Acoust.* 1939, **8**, 121

[2] PETRALIA, S. *Nuovo Cim.* 1940, **17**, 378

[3] ZVETKOV, V., MINDLINA, A. and MAKAROV, C. *Acta phys.-chim. U.R.S.S.* 1946, **21**, 135
ZVETKOV, V. and MARININ, V. *Dokl. Akad. Nauk U.S.S.R.* 1948, **63**, 653
ZVETKOV, V. and ESKIN, V. E. *Zh. eksp. teor. Fiz.* 1948, **18**, 614

[4] PETERLIN, A. *Rec. Trav. chim. Pays-Bas*, 1950, **69**, 14. This is paper I of the series on 'Acoustic birefringence of polymer solutions'

[5] BADOZ, J. *J. Phys. Radium*, 1954, **15**, 777; *Thesis*, University of Paris, 1957

[6] HILYARD, N. C. and JERRARD, H. G. *Nature, Lond.* 1962, **194**, 173; *J. appl. Phys.* 1962, **33**, 3470

[7] PETERLIN, A. *Zbornik prirodoslovnega drustva Ljubljana*, 1941, **2**, 24
PETERLIN, A. and STUART, H. A. *Hand- u. Jahrbuch der Chemischen Physik*, Vol. VIII/1B, pp 54–59. Akademische Verlagsgesellschaft: Leipzig, 1943
PETERLIN, A. *J. Phys. Radium*, 1950, **11**, 45

[8] FRENKEL, J. *Kinetic Theory of Liquids*, p 292. Clarendon Press: Oxford, 1946

[9] OKA, S. *Kolloidzschr.* 1939, **87**, 37; *Z. Phys.* 1940, **116**, 632

[10] ZIABICKI, A. *J. appl. Polym. Sci.* 1959, **2**, 24

[11] CERF, R. *J. Chim. phys.* 1951, **48**, 59, 85; *J. Phys. Radium*, 1954, **15**, 145

[12] BÖTTCHER, C. J. F. *Theory of Dielectric Polarization*. Elsevier: New York, 1952

[13] ROUSE, P. E. *J. chem. Phys.* 1953, **21**, 1272

[14] ZIMM, B. H. *J. chem. Phys.* 1956, **24**, 275

[15] CERF, R. *J. Phys. Radium*, 1958, **19**, 122; *Advanc. Polym. Sci.* 1959, **1**, 382

[16] PETERLIN, A. *Kolloidzschr.* 1966, **209**, 181

[17] See for instance Chap. 14 'Flow birefringence', by V. N. TSVETKOV in B. KE *Newer Methods of Polymer Characterization*. Wiley: New York, 1964

[18] REINHOLD, CHR. and PETERLIN, A. *J. chem. Phys.* 1966, **44**, 4333

[19] KUHN, W. and GRÜN, F. *Kolloidzschr.* 1942, **101**, 248

[20] PETERLIN, A. *J. Polym. Sci. B*, 1966, **4**, 287
TAKSERMAN-KROZER, R. IUPAC International Symposium on Macromolecular Chemistry, Prague, 1965, Preprint P 347 (A297)

[21] ZIMM, B. H., ROE, G. M. and EPSTEIN, L. F. *J. chem. Phys.* 1956, **24**, 229

[22] PYUN, C. W. and FIXMAN, M. *J. chem. Phys.* 1965, **42**, 3838

[23] THURSTON, G. B. and SCHRAG, J. L. *J. chem. Phys.* In press

ABS Mouldings for Electroplating—An Electron Microscope Study

Koichi Kato

A method for preparing replicas of acid-etched ABS surfaces is described. Replicas made in this way are compared with ultra thin stained sections cut from the surfaces of moulded specimens at different stages of the plating process. It is concluded that orientation in the surface of injection-moulded articles is responsible for lowering the peel strength, probably by reducing the penetration of the metal plating layer into the subsurface of the polymer and hence weakening the key between the two materials; orientation also reduces the tear resistance of the ABS surface.

IN BROAD terms, any plastic can be electroplated, but amongst the common materials the one with the best potential adhesion to metals may well be ABS, a rubber-modified two-phase plastic made from acrylonitrile, butadiene and styrene. The present process for plating ABS mouldings comprises the following essential steps: alkaline cleaning, neutralizing, chemical microetching, sensitizing, activating, electroless copper-plating and electroplating. It is clear that the most drastic changes in surface features take place during the chemical microetching step, which cannot be replaced by any mechanical surface roughening procedure. The adhesion between the metal and the ABS moulding depends not only on the type of ABS resin used but also on the moulding conditions. An electron microscope study of the surface features of ABS mouldings, particularly their surface etch patterns, can provide valuable information about various practical aspects of ABS metal-plating.

The present paper deals with the techniques required for such a study. A polyvinyl alcohol (PVA) film replica technique has been developed for examining the microetched surface of ABS mouldings. The osmium tetroxide procedure previously reported by the author[1] has been adapted for preparing ultra thin sections from the surface of ABS mouldings. Representative results show that residual strain in the surface layer is one of the most important factors determining the adhesion between the ABS and the metal coating, and that the strains present in a surface are observable as anisotropic flow patterns.

MATERIALS

Test specimens consisted of 3 mm × 80 mm × 120 mm plaques moulded on laboratory machines from Toyolac 100, an ABS resin marketed by the Toyo Rayon Co. Two types of specimen were used, one injection-moulded under a standard set of conditions, the other compression-moulded under a standard set of conditions. In order to make an accurate comparison the two groups were subjected to all subsequent plating processes side by side.

Peel strength measurements on copper-plated specimens gave results as much as four or five times higher for compression mouldings than for injec-

tion mouldings. Much more marked differences would presumably be shown up by the heat-cycling test, which approximates more closely to service conditions.

PVA REPLICA TECHNIQUE

The choice of a replica material for ABS is greatly limited by the need to avoid any thermal or solvent effects during the replicating step. A pre-shadowed carbon replica technique was employed by Mann, Bird and Rooney[2] in their study on ABS fracture, while methyl cellulose, a water-soluble polymer, was used by Matsuo[3] in a similar study on ABS and high impact polystyrene.

Low molecular weight PVA ($DP = 500$) has been found useful for the present purpose. When an aqueous PVA solution is cast directly on to the microetched ABS surface, it is almost impossible to remove the replica intact because the specimen surface is so rough. A 1 mm thick film is therefore prepared by casting a 20 per cent aqueous solution of the polymer on to a clean glass plate and leaving it to dry slowly. The dried film is cut into pieces about 10 mm square and stored for later use.

A piece of this film is dipped for a moment into distilled water, applied to the surface to be studied, and left to stand overnight at room temperature. The resulting replica is tough enough to be stripped away from the specimen without difficulty. Ordinary two-stage carbon replica techniques can be used in the subsequent preparation of the specimen, the primary PVA film being dissolved away with distilled water.

SECTIONING

The osmium tetroxide procedure for sectioning ABS resins was reported in a previous paper[1]. This reagent selectively fixes and stains the rubber phase so that it becomes possible to cut ultra thin sections without embedding the specimen, and to obtain electron micrographs of excellent contrast and definition. For the purposes of the present study, however, the procedure must be adapted so that sections can be taken from a selected portion of a plated or prepared surface, and in a known direction relative to any orientation introduced during moulding. One edge of each ultra thin section should come from the surface under investigation. Fortunately, this can be achieved by exercising a little care in cutting the specimen block and trimming its tip. For best results, the cutting direction of the ultra-microtome should be set parallel to the surface of the specimen. Using a diamond knife, it is even possible to cut sections from an electroless copper-plated surface.

Owing to the fixing effect of the osmium tetroxide it is also possible to examine the distortion caused in the subsurface layers of the ABS by peeling off the copper plating.

RESULTS AND DISCUSSION

Typical surface replicas of etched injection-moulded and compression-moulded specimens are shown in *Figures 1* and *2* respectively. Since the numerous round-shaped projections on the replica correspond to hollows on

the original ABS surface, there can be no doubt that the chemical etching agent (chromic–sulphuric acid mixture) attacks the dispersed rubber particles in an entirely selective manner without affecting the resin matrix, thus forming a large number of minute etch cavities in the surface of the moulding.
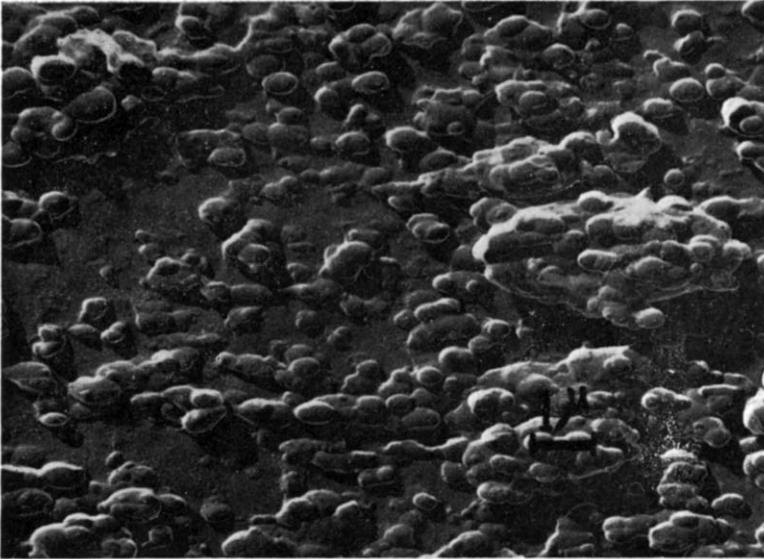
Figure 1—Replica of etched surface of an injection-moulded ABS specimen
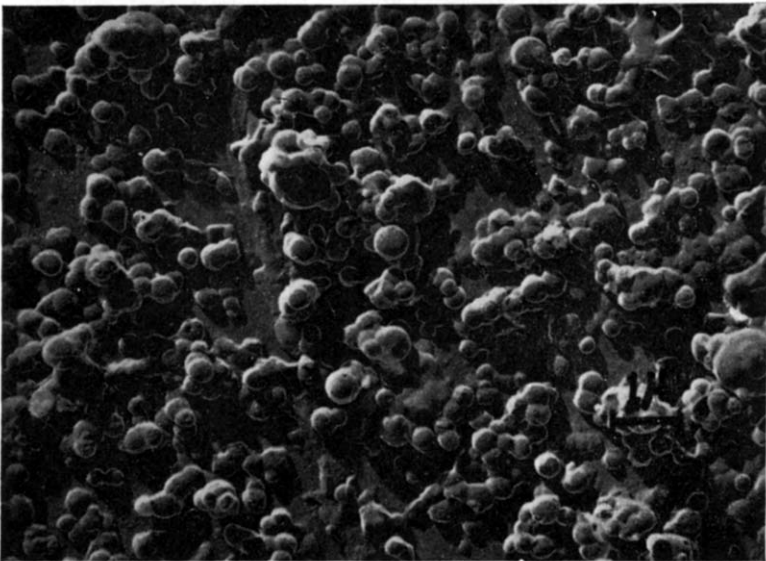
Figure 2—Replica of etched surface of a compression-moulded ABS specimen

35

The etch cavities on the injection moulding (*Figure 1*) are all elongated in the same direction to show a distinct flow pattern, whereas the hollows on the compression moulding (*Figure 2*) are almost perfectly round, and show no evidence of moulding orientation. Furthermore, the hollows on the former are often joined together in the plane of the surface, to form large but rather shallow etch cavities, whereas the hollows on the latter tend to be connected in the direction normal to the surface, to give narrow etch cavities that penetrate deeply into the subsurface of the moulding. These conclusions, based on evidence obtained from replicas, are completely confirmed by the complementary work on sections described below.

An ultra thin section through the surface of an injection moulding is illustrated in *Figure 3*. (In this paper all electron micrographs of sections
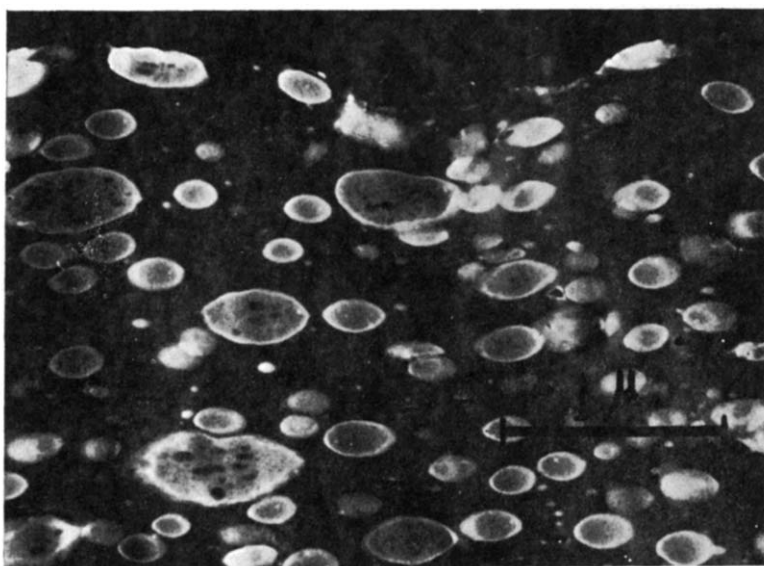
Figure 3—Ultra thin section through surface of an injection-moulded ABS specimen

are negatives, in which the osmium-stained rubber phase appears bright against the darker resin matrix.) The rubber particles in the subsurface are all elongated and aligned parallel to the surface, showing a moulding flow pattern similar to that observed on the replica (*Figure 1*).

The ultra thin section shown in *Figure 4* was cut from a compression moulding that had been subjected to electroless plating. The bright irregular band along the edge of the section is chemically deposited copper metal. In contrast to the structure found in the injection moulding, every rubber particle appears almost perfectly round, and there is no evidence of a flow pattern. It should be noted that the copper is deposited not only on the surface but also at certain points in the interior, indicating that the cavities produced by the chemical etching process penetrate to a considerable depth. No such penetration has been observed in injection mouldings. Since copper
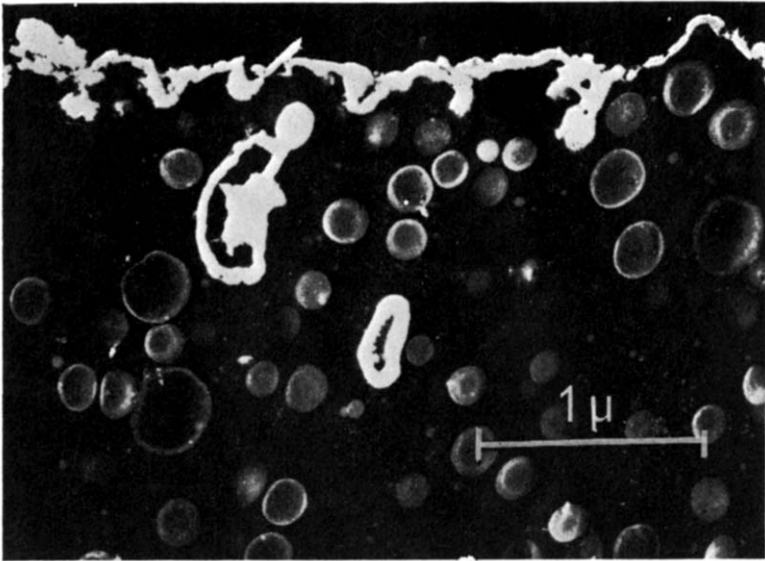
Figure 4—Ultra thin section through electroless copper and subsurface layers
of a compression-moulded ABS specimen

deposited in deep cavities should have an anchoring effect on the main
metal coating, this observation might well account, at least partly, for varia-
tions in peel strength with moulding conditions.
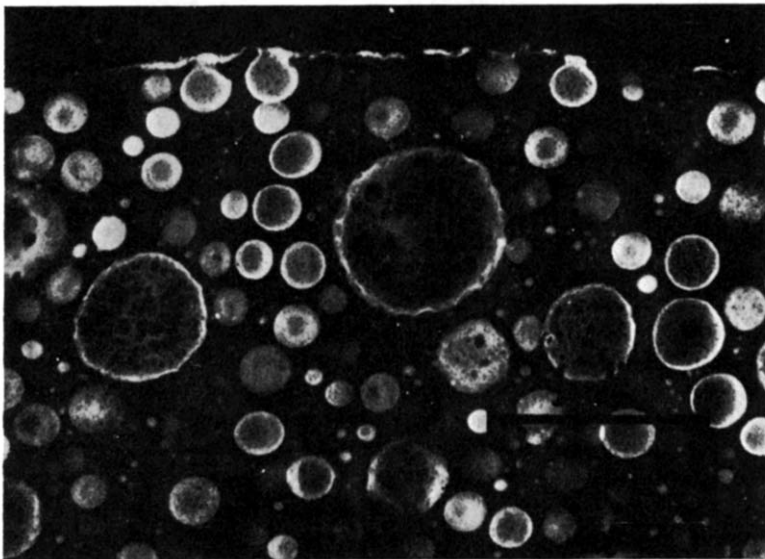
Figure 5—Ultra thin section through acetone-treated surface of an injection-
moulded ABS specimen

Figure 5 shows an ultra thin section through the surface of an injection moulding that had previously been subjected to mild treatment with acetone. The rubber particles are no longer deformed, but restored to a perfectly round shape. The same effect can also be produced by thermal annealing. It is therefore obvious that injection-moulded ABS resins very often solidify with high orientation and internal strains, especially in the surface layer, and that these residual strains are relieved whenever environmental conditions are suitable. This effect may have an important influence on the behaviour of metal-plated specimens in the heat-cycling test.
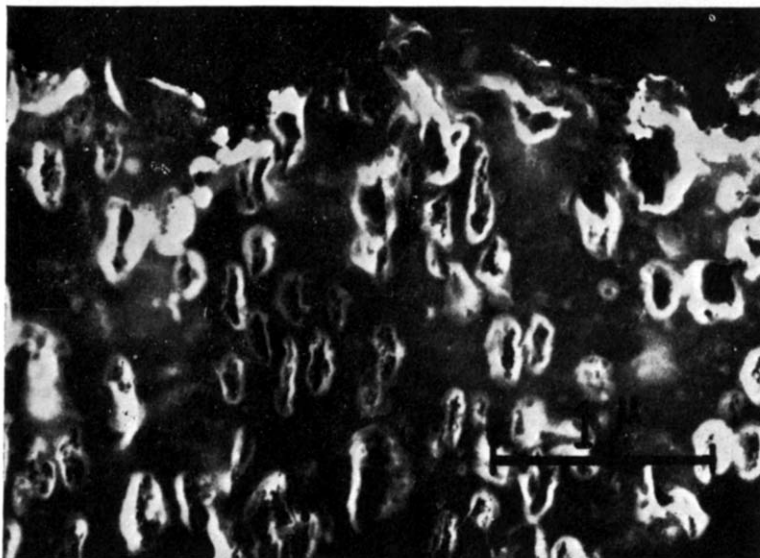
Figure 6—Ultra thin section through peeled surface of an electroplated ABS compression-moulding

The ultra thin section shown in *Figure 6* was cut from the surface of a compression moulding from which the electroplated copper had been pulled away according to the standard peel test procedure. The rubber particles in the subsurface layer are all severely deformed, proving that the whole of the subsurface had responded to the peeling stress, as a result of the strong adhesion between the copper and the ABS. No such deformation was observed in the subsurface layer of an injection-moulding which had given a low peel strength.

Figure 6 also shows a number of faint white bands running through the resin matrix approximately parallel to the surface. These features in the ABS resin matrix appear to correspond to stress-whitening crazes, which will be described elsewhere.

In conclusion it should be pointed out that the osmium tetroxide technique is applicable to various other problems concerning ABS mouldings, including anisotropy, fracture and surface gloss. The technique has two great advantages: the rubber is selectively stained, so that the internal

structure of the specimen is clearly revealed, and also fixed, so that every detail is perfectly preserved throughout the sectioning operation.

Central Research Laboratories,
Toyo Rayon Co. Ltd,
Otsu, Shiga-ken, Japan

REFERENCES

[1] KATO, K. *Polymer Engng Sci.* In press
[2] MANN, J., BIRD, R. J. and ROONEY, G. *Makromol. Chem.* 1966, **90**, 207
[3] MATSUO, M. *Polymer, Lond.* 1966, **7**, 421

The Crosslinking of Polypropylene

J. R. HATTON*, J. B. JACKSON and R. G. J. MILLER

A study has been carried out on the formation of networks in atactic and isotactic polypropylene by the irradiation with u.v. light of samples swollen in a solution of benzophenone in allyl acrylate. Network formation only occurs when allyl acrylate is present and infra-red spectra of the networks suggest that both double bonds have reacted. The concentration of acrylate units in atactic and isotactic polymer networks were measured by infra-red absorption. Swelling measurements, though of doubtful validity due to the high crosslink density, support the view that each molecule of allyl acrylate is associated with one crosslink and the effective link must be the ester linkage since monofunctional compounds such as allyl acetate are ineffective in network production.

POLYPROPYLENE is available in three tactic forms. This study has been restricted mainly to atactic polymer with some preliminary data for isotactic material. When subjected to radiation, the polymer is readily degraded by a radical mechanism and exhibits a scission to linking ratio of 0·8 to 1·0 even *in vacuo*[1]. Consequently, the unmodified polymer may not be crosslinked by conventional means such as the action of peroxides or the use of radiation sources. However, it has been shown[2,3] that the presence of certain additives can improve the crosslinking efficiency of many polymers when using γ-rays and other high energy ionizing radiation. This type of system has been found to work successfully with polypropylene[2,3]. Here we report preliminary results of an examination of the structure of crosslinked polypropylene formed by *u.v. light* in the presence of allyl acrylate using benzophenone as an u.v. sensitizer.

The additives were incorporated in the polymer by swelling to equilibrium in a solution of benzophenone in allyl acrylate prior to irradiation. After irradiation some of the allyl acrylate is known to be incorporated in the network chemically, presumably acting as a bridging molecule between chains or parts of chains. The object of the work was to obtain a better insight into the structure of the crosslinked network and its mode of formation by comparing the i.r. spectra of composite networks so produced with those of unmodified polypropylene.

EXPERIMENTAL

Preparation of crosslinked films

The atactic polypropylene was a solid, rubbery polymer, (R.S.V. = 1·2 corresponding to a molecular weight, M_n, of 70 500) supplied by Imperial Chemical Industries Limited, Plastics Division. The isotactic polypropylene was a standard commercial sample of 'Propathene' (code number H.W.E. 24 from Imperial Chemical Industries Limited). Allyl acrylate was available from Eastman-Kodak Ltd and benzophenone as an 'AnalaR' reagent from British Drug Houses.

---

*Work carried out during tenure of a vacation studentship.

Due to the limits imposed on sample thickness by the requirements of i.r. spectroscopy the atactic polymer was used in the form of a film, thickness $50\,\mu$; the isotactic polymer was used as films varying in thickness between 140 and $270\,\mu$. The isotactic polypropylene films were hot pressed at 190°C and $200\,kg/cm^2$ pressure. Various methods of preparing the films of atactic polypropylene were tried, and it was found that solvent casting over mercury gave the best results.

A solution of atactic polypropylene in heptane (about three per cent) was poured on to mercury contained in a 12 cm Petri dish. The heptane was evaporated slowly at room temperature and a pressure of 100 mm of mercury until a tacky film had been formed; the bulk of the heptane had evaporated at that stage. The vacuum was then increased to less than 1 mm of mercury and the whole left for a further two hours. This procedure ensured complete removal of the heptane and also minimized the chances of bubbles forming in the film. Great care had to be exercized in handling the thin films of atactic polymer as they remained tacky, even after full evacuation of the solvent.

Prior to crosslinking, the films were swollen by immersion overnight at room temperature in allyl acrylate containing benzophenone (12 per cent by weight). Under these conditions the films are swelled to equilibrium, giving an increase in weight of about 13 per cent for the atactic and 5 per cent for the isotactic polymer. Irradiation was carried out by exposing the films (after excess allyl acrylate had been dried off the surface) to the radiation from a mercury lamp (Hanovia type u.v.s. 500 W) for a period of about 30 minutes. Excess allyl acrylate, benzophenone and uncrosslinked polymer were then removed from the atactic film by extraction in a Soxhlet apparatus for four hours with heptane; the isotactic material was extracted overnight with tetralin.

Quantitative spectroscopic analysis

The analysis for the molar ratio of combined allyl acrylate and polypropylene units was made from i.r. measurements. Spectra were recorded on a Grubb–Parsons 'Spectromaster' i.r. spectrometer. Absorbance of the $1\,740\,cm^{-1}$ band (due to the stretching vibration of the carbonyl group of the ester) and the $965\,cm^{-1}$ band (due to a C—C stretching $+$ CH$_3$ rocking vibration of the polypropylene) were measured on the crosslinked films. These absorbances were related to weights of ester and polypropylene by comparison with reference solutions of ester and polypropylene in cyclohexane in a $240\,\mu$ cell. Calibration graphs were plotted of absorbance as a function of concentration and from them the molar ratio of the ester and the atactic polymer was established. For isotactic polypropylene the percentage of allyl acrylate chemically incorporated into the network was measured by the absorbance of the $1\,740\,cm^{-1}$ band in the network, related to a direct measurement of the polypropylene film thickness. The equivalent concentration of allyl acrylate in cyclohexane solution was read off the calibration graph and from the known thickness of cell and film the molar ratio of allyl acrylate and polypropylene (monomer units) was calculated.

Qualitative observations of related experiments

Other experiments giving qualitative results for atactic polypropylene are described below.

(*a*) The possibility of the presence of residual carbon–carbon double bonds originating from the allyl acrylate was investigated by examining the spectra for evidence of bands at $1\,650\ cm^{-1}$ (due to the allyl group) and at $1\,638$ and $1\,622\ cm^{-1}$ (due to the acrylic group). The conclusion reached was that there was a weak band at $1\,650\ cm^{-1}$ remaining in the crosslinked polymer only revealed by the use of ordinate scale expansion. This was ascribed to residual allyl groups and when compared with the absorbance of the carbonyl group at $1\,740\ cm^{-1}$ indicated that not more than ten per cent of the original C—C double bond concentration remained.

(*b*) Under the experimental conditions employed, little crosslinking of polypropylene occurs without the presence of an efficient u.v. absorber such as benzophenone since the polymer–allyl acrylate system is almost transparent to u.v. radiation. A sample of polypropylene swollen by allyl acrylate without benzophenone and irradiated for a period of approximately 30 minutes dissolved completely in heptane indicating that negligible crosslinking had taken place. It should be noted in this context that γ-radiation will produce networks under these conditions, since large numbers of reactive species are produced whereas without an efficient absorber such as benzophenone, u.v. radiation produces very few radical centres.

(*c*) From a further examination of the spectra of the networks it was observed that an absorption band appeared at $695\ cm^{-1}$ which was assigned to a phenyl derivative presumed to have formed from benzophenone. It was incorporated chemically into the structure since samples had been carefully solvent extracted [see (*d*) below]. The incorporated component was estimated from the absorbance of the phenyl band at $695\ cm^{-1}$ to be present at a concentration of approximately 10^{-3} mole/mole of chain unit.

(*d*) As a check on the efficacy of the extraction process three portions of the sample were examined by infra-red, before extraction, after the usual four hours, and after 20 hours. There was found to be no noticeable difference between the two extracted samples. This established that extraction was complete within four hours.

(*e*) Allyl acrylate sensitized by benzophenone does not polymerize to any extent when irradiated with u.v. light. Examination of the spectra of solutions of benzophenone in allyl acrylate before and after irradiation for two hours shows no change in double bond concentration, which would have been seen had any polymerization of the allyl acrylate occurred.

(*f*) When polypropylene containing about two per cent benzophenone (i.e. without allyl acrylate) is irradiated, the polymer degrades rather more rapidly than when irradiated without benzophenone present. However, a small amount of crosslinking may occur.

(*g*) Samples swollen with either allyl acetate or methyl acrylate in place of allyl acrylate in an attempt to produce networks from monofunctional compounds using the experimental method described above were unsuccessful. The polymer remained completely soluble in the extraction pro-

cedure showing that the di-unsaturated compounds are required for network formation.

Volume swelling measurements

The molecular weight between crosslinks was calculated from swelling data. The large dimensions of a rectangular sample of crosslinked atactic polypropylene were measured accurately (to ± 0.001 mm) using a travelling microscope. The sample was then swelled to equilibrium in benzene at room temperature and the increased lengths measured. From the ratio of the two measurements, the molecular weight between crosslinks was calculated. Similarly the networks of isotactic polypropylene were examined; the samples being swollen in tetralin at 207°C and the changes in dimension noted. The value of the molecular weight between crosslinks was computed from the equation presented by Treloar[4]:

$$\ln (1 - v_2) + v_2 + \mu v_2 + \rho V_1 / M_c (v_2^{1/3} - v_2/2) = 0$$

where: v_2 is the swelling ratio which equals the volume ratio of the network unswollen to the network swollen, V_1 is the molar volume of the solvent, μ is the thermodynamic interaction parameter and ρ is the density of the network. The values of the parameter μ used were abstracted from the literature. Kinsinger and Hughes[5] quote a value of 0·492 for atactic polypropylene in benzene and a value of 0·475 has been determined from data[6] for isotactic polymer in tetralin. The densities[7] of the polymer at the appropriate temperature are 0·855 g/cm³ for atactic polymer at 25°C and 0·750 g/cm³ for isotactic polymer at 207°C.

The average number of moles of allyl acrylate per crosslink is then easily calculated from the determined molar ratio of ester to polymer and the average chain length between crosslinks.

RESULTS AND DISCUSSION

From the quantitative experiments described above it is clearly established that:

(1) Benzophenone is necessary for the initiation of the crosslinking reaction with u.v. light;

(2) A derivative of benzophenone is incorporated into the network, therefore it attacks the polypropylene to form a chemical bond;

(3) A difunctional monomer such as allyl acrylate is necessary for network formation and most of the allyl acrylate has reacted at both unsaturated sites;

(4) No polymerization of the allyl acrylate is initiated by activated benzophenone;

(5) Only a small amount of crosslinking can occur not involving allyl acrylate.

It has been shown[3] that monofunctional materials (e.g. allyl acetate) as additives do not lead to network systems at the concentrations involved in non-crosslinking polymers using high energy radiation and here confirmed

for u.v. initiated systems that a difunctional monomer is necessary to induce crosslinking. The effective chemical link between chains is then the ester bond of the allyl acrylate; both the unsaturated parts of the molecule react to form attachments with the chains. Consequently it seems reasonable that each allyl acrylate molecule forms two attachment points to polypropylene chains and therefore the number of chain units to be grouped with a single crosslink is twice the average chain length between crosslinks.

Table 1. Summary of infra-red results

Sample number	Experimental conditions	Absorbance at $1\,740\,cm^{-1}$	Absorbance at $965\,cm^{-1}$	Moles ester per mole polypropylene $\times 10^2$	Sample thickness μ
Atactic					
1	Samples swollen	0·70	0·28	2·7	30
2	overnight:	0·60	0·34	1·9	30
3	irradiated for	0·46	0·33	1·4	30
4	30 min at	0·64	0·38	1·8	30
5	room temp.	0·60	0·38	1·8	30
6	Samples swollen	0·49	0·29	1·7	30
7	for six hours: irradiated for 40 min at room temp.	0·54	0·33	1·7	30
Isotactic					
8	Samples swollen	0·76	—	1·0	145
9	overnight:	0·86	—	1·0	187
10	irradiated for 50 min at room temp.	0·96	—	0·9	267

The results of quantitative measurements are given in *Tables 1* and *2*. The atactic networks were calculated to contain nearly twice as much combined allyl acrylate as the isotactic networks. The swelling measurements on the isotactic networks particularly show considerable variation with the thickness of the samples, an observation which is discussed below. Calculations from the i.r. data suggest that for each mole of allyl acrylate in the atactic networks there were 50 chain units and hence the average chain-length between crosslinks was of the order of 25 units (i.e. 50 atoms). This is a highly crosslinked network formed presumably due to the use of thin film specimens. Bulk (rather than thin film) samples of crosslinked polypropylene available from other experiments[6] and prepared by a similar method to that described above, have given swelling measurements which indicate much larger average chain-length between crosslinks. The swelling data of *Table 2* can only be used as an indication of the extent of crosslinking in such a 'tight' network; the internal agreement is reasonable and the value of moles of ester per crosslink tends to support the proposition that there is of the order of one ester molecule *and not more* for each crosslink. It is possible to postulate a mechanism for the crosslinking reaction

Table 2. Swelling measurements

Sample number	Swelling V_2	Chain length* between cross-links	Mean no. of† chain units per cross-link	Mean no. of ester‡ molecules per crosslink
1	0·552 0·491	12·3	24·6	0·65
2	0·656 0·651	4·96	9·9	0·16
3	0·373 0·618	15·2	30·4	0·57
4	0·528 0·634	8·6	17·2	0·31
6	0·503 0·397	20·5	4·0	0·695
7	0·656 0·414	12·5	25·0	0·43
8	0·661 0·663	6·1	12·2	0·12
9	0·389 0·389	41·9	83·8	0·76
10	0·260 0·291	108·1	216·2	2·12

*From the mean of the swelling ratio.
†Assuming each crosslink is tetrafunctional.
‡Using the ester/polymer ratio from spectroscopic results.

which is consistent with the results of the experiment. Details are attached in the Appendix.

The results for isotactic polymer are sparse. However, the i.r. studies show here again a large concentration of allyl acrylate links although only half that in atactic polymer and approximately 100 propylene units per crosslink, assuming one acrylate unit for each link. The crystalline texture of this polymer must affect the crosslinking reaction in that the polymer can be considered as a two-phase system, amorphous material surrounding the crystal phase. The allyl acrylate penetrates into the amorphous regions and this is where crosslinking will occur. Thus the network must consist of heavily crosslinked regions interspersed with non-crosslinked areas. This has led to variable results obtained from swelling measurements and where the influence of film thickness can also be seen. It is doubtful if a more detailed analysis will be fruitful on crystalline material; nevertheless useful crosslinked networks are produced and the average allyl acrylate content is known.

The work described above is published by the kind permission of the Laboratory Director.

Imperial Chemical Industries Limited,
  Petrochemical and Polymer Laboratory,
    P.O. Box 11, The Heath,
      Runcorn, Cheshire

REFERENCES

[1] CHARLESBY, A. and PINNER, S. H. *Proc. Roy. Soc. A*, 1958, **247,** 367

[2] ODIAN, G. and BERNSTEIN, B. S. *Nucleonics*, 1963, **21,** 80

[3] ODIAN, G. and BERNSTEIN, B. S. *J. Polym. Sci. A*, 1964, **2,** 2835

[4] TRELOAR, L. R. G. *Physics of Rubber Elasticity* p 135. Clarendon Press: Oxford, 1958

[5] KINSINGER, J. B. and HUGHES, R. E. *J. phys. Chem.* 1959, **63,** 2002

[6] PARRINI, P., SABASTIANO, F. and MERSINA, G. *Makromol. Chem.* 1960, **38,** 27

[7] WILSKI, H. *Kunststoffe*, 1964, **54,** 10

[8] JACKSON, J. B. Unpublished results

APPENDIX

Reaction mechanism

The following reactions are postulated:

$$Ph_2C{=}O + h\nu \longrightarrow Ph_2C{=}O\star \text{ (excited)} \qquad (1)$$

$$\text{Polymer (P)} + h\nu \longrightarrow R^{\cdot} + H^{\cdot} \qquad (2)$$

$$Ph_2C^{\cdot}{=}O + P \longrightarrow R^{\cdot} + Ph_2\underset{\underset{\displaystyle OH}{|}}{C} \qquad (3)$$

$$2Ph_2C^{\cdot} \longrightarrow Ph_2\underset{\underset{\displaystyle OH}{|}}{C}{-}\underset{\underset{\displaystyle HO}{|}}{C}{-}\underset{\underset{\displaystyle OH}{|}}{}Ph_2 \qquad (4)$$

$$R^{\cdot} + \text{allyl acrylate (A{-}A)} \longrightarrow R{-}A^{\cdot}{-}A \qquad (5)$$
$$(\text{or } Ph_2C^{\cdot}OH) \qquad (\text{or } Ph_2\underset{\underset{\displaystyle OH}{|}}{C}{-})$$

$$2R{-}A^{\cdot}{-}A \longrightarrow R{-}A{-}A \qquad (6)$$
$$\underset{\underset{\displaystyle A{-}A{-}R}{|}}{\phantom{R{-}A{-}A}}$$

$$R{-}A^{\cdot}{-}A + H^{\cdot} \longrightarrow R{-}A{-}A \qquad (7)$$
$$(\text{or } Ph_2\underset{\underset{\displaystyle OH}{\diagdown}}{C}^{\cdot}\quad) \qquad H\,(\text{or } Ph_2\underset{\underset{\displaystyle OH}{\diagdown}}{C}\quad)$$

$$R{-}\underset{\underset{\displaystyle H}{|}}{A}{-}A + R^{\cdot} \longrightarrow R{-}\underset{\underset{\displaystyle H}{|}}{A}{-}A^{\cdot}{-}R \qquad (8)$$

$$R{-}\underset{\underset{\displaystyle H}{|}}{A}{-}A^{\cdot}{-}R + H^{\cdot} \longrightarrow R{-}\underset{\underset{\displaystyle H}{|}}{A}{-}\underset{\underset{\displaystyle H}{|}}{A}{-}R \qquad (9)$$
$$(\text{or } Ph_2C^{\cdot}{-}OH) \qquad (\text{or } Ph_2\underset{\underset{\displaystyle |}{}}{C}{-}OH)$$
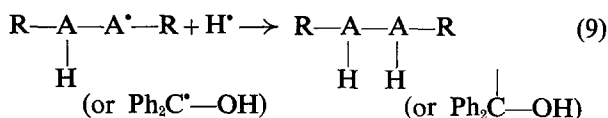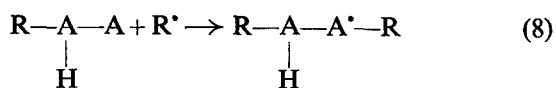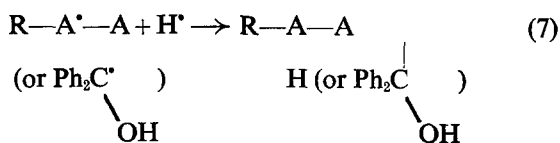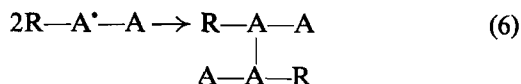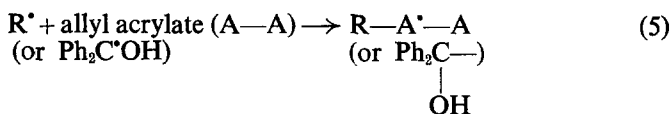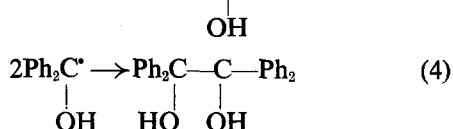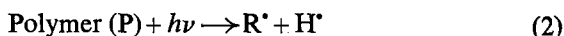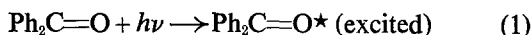
and similar reactions.

Reaction 6 is considered to be unlikely in view of the evidence presented.

Reactions 7, 8 and 9 are the most probable course for the crosslinking reaction occurring in this system. Inclusion of a derivative of benzophenone into the network can occur at various stages but dimerization to benzopinacol has been suggested* as a more likely reaction.

Contributions to Polymer

Papers accepted for future issues of
POLYMER include the following:

*A Method of Thermal Analysis of Polymers by Measurement of Electrical
Conductivity*—M. I. POPE

*Effect of Uranyl Perchlorate on the Kinetics of Polymerization of
Acrylamide*—E. A. S. CAVELL and A. C. MEEKS

Polymer Degradation VI—R. S. PORTER, M. J. R. CANTOW and J. F.
JOHNSON

Thermoelastic Measurements of Some Elastomers—J. A. BARRIE and
J. STANDEN

Melting Characteristics of Isotactic Polypropylene Oxide—W. COOPER,
D. E. EAVES and G. VAUGHAN

*The Hydrodynamic Properties of the System Poly Alpha-methyl Styrene—
Cyclohexane*—J. M. G. COWIE, S. BYWATER and D. J. WORSFOLD

Coil Dimensions of Poly(olefin sulphone)s III—T. W. BATES and K. J. IVIN

Thermal Degradation of Vinyl Polymers I, II, III—D. H. RICHARDS and
D. A. SALTER

The Dilute Solution Properties of Polyacenaphthalene I, II—J. M.
BARRALES-RIENDA and D. C. PEPPER

*The Polymerization of Some Epoxides by Diphenylzinc, Phenylzinc
t-Butoxide and Zinc t-Butoxide*—J. M. BRUCE and F. M. RABAGLIATI

Solution and Diffusion of Gases in Poly(vinyl chloride)—R. M. BARRER,
R. MALLINDER and P. S.-L. WONG

CONTRIBUTIONS should be addressed to the Editors, *Polymer*, c/o Butter-
worths, 125 High Holborn, London, W.C.1.

Authors are solely responsible for the factual accuracy of their papers.
All papers will be read by one or more referees, whose names will not
normally be disclosed to authors. On acceptance for publication papers
are subject to editorial amendment.

If any tables or illustrations have been published elsewhere, the editors
must be informed so that they can obtain the necessary permission from
the original publishers.

All communications should be expressed in clear and direct English,
using the minimum number of words consistent with clarity. Papers in
other languages can only be accepted in very exceptional circumstances.

A leaflet of instructions to contributors is available on application to the
editorial office.

A Method of Thermal Analysis of Polymers by Measurement of Electrical Conductivity*

M. I. POPE

Conventional methods of thermal analysis involve measuring either changes in mass or enthalpy of a substance, which is heated at a constant rate of rise of temperature in a controlled atmosphere. Work on a range of organic polymeric materials has now shown that, if the rate of change in electrical conductivity with temperature is plotted against temperature, then the curve obtained is characteristic of that particular substance. With the aid of information obtainable by a number of other techniques, it has proved possible to ascribe each of the peaks in the various curves to physical or chemical changes occurring in the heated polymer. The utility of this technique is illustrated by its application to a medium rank coal, both before and after chemical treatment, and to a sample of unplasticized polyvinyl chloride.

THE idea that measurement of changes in electrical conductivity during heating could be used to characterize complex organic compounds was first suggested by the results of research into the low temperature carbonization of coals[1].

It had long been known[2] that, at some stage during the carbonization process, coals changed from electrical insulators to relatively good conductors, with properties approaching those of graphite. The object of the research project was originally to investigate the possibility of partially de-volatilizing coals on heating a finely ground powder in a fluidized bed, by means of passing electrical current through the coal. Results soon indicated that this process was impracticable due to the extremely low initial conductivity of the coal; aggravated by the fact that much of the room temperature conductivity was due to adsorbed water[3], which is rapidly lost at temperatures above about 150°C.

However, carbonization studies of a large number of bituminous coals, differing quite widely in rank, indicated that the rise in electrical conductivity with increase in temperature of carbonization was remarkably similar in each case. Measurements were made on compacted samples in an atmosphere of oxygen-free nitrogen, maintaining a constant rate of rise of temperature of 3 deg. C/min by use of an apparatus described elsewhere[1]. A typical graph of conductivity against temperature is shown in *Figure 1* and refers to Markham Black Shale, a coal of rank number 401.

The differences between the behaviour of the individual coals only become apparent where the rate of change in electrical conductivity is plotted against temperature [*Figure 2*(a)]. The resulting curve shows essentially three characteristic peaks, although the peak occurring in the region of 600° to 800°C frequently splits into two distinct maxima. Each of these

49
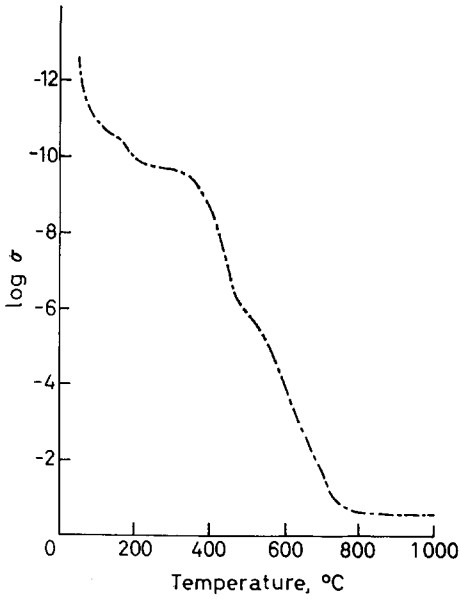
Figure 1—The logarithm of the conductivity of untreated Markham Black Shale, plotted against temperature of carbonization
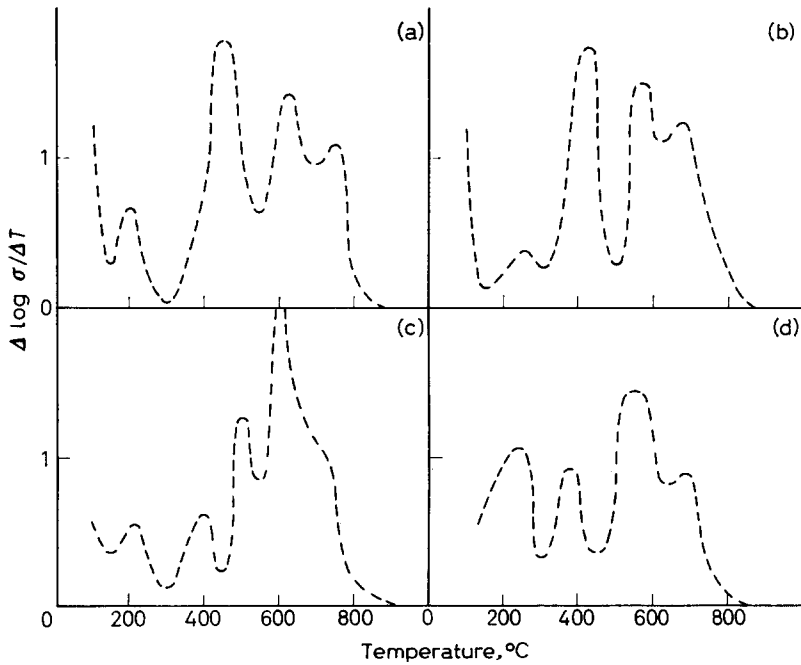
Figure 2—The rate of change of conductivity (in arbitrary units) plotted against temperature of carbonization for Markham Black Shale which was: (a) untreated; (b) methylated; (c) dehydrogenated; and (d) brominated

peaks corresponds to a definite stage in the carbonization process and the reasons for their occurrence are discussed below.

If we consider a hypothetical, intrinsic, organic semi-conductor, which does not decompose on heating, then the rate of increase in conductivity with temperature will fall progressively as the temperature is increased, in accordance with the equation

$$\sigma = A \exp\left(-E/2kT\right)$$

where σ is the electrical conductivity at absolute temperature T, k is Boltzmann's constant, E is the energy of activation for semi-conduction and A is a constant.

The peaks observed in *Figure 2* (a) would therefore be expected to be due to one, or more, of the following factors.

(1) Decomposition of the solid may result in a new mechanism of conduction becoming possible.

(2) Evolution of a decomposition product having a significantly higher conductivity than that of the residue.

(3) Sintering, or partial melting, bringing about an improvement in electrical contact between the particles of the solid.

Factors (1) to (3) would all cause the rate of increase in conductivity to be greater than that expected for our hypothetical semi-conductor. In addition, a fourth factor needs to be considered.

(4) Evolution of non-conducting decomposition products may (a) disrupt the grain structure of the solid, causing a fall in the area of inter-particle contacts, or (b) lead to the formation of a non-conducting film over the surface of the particles.

Factor (4) would cause the rate of increase in conductivity to be less than expected.

Although conductivity results are not sufficient in themselves to give a clear picture of the different decomposition reactions which occur during the carbonization of coals, it has proved possible[4], with the aid of information obtained by a number of other techniques. to put forward a reasonable interpretation of the mechanism of the carbonization process.

It appeared that up to 150°C the loss of physically adsorbed water predominated and little change in the coal structure occurred; then above 150°C and below about 350°C, a small amount of alkyl aromatic material was given off[5] and was presumably due to the evolution of molecules trapped within the coal structure during the coalification process.

Primary carbonization commenced at between 400° and 500°C, and involved the fission of the carbon–carbon bonds between aliphatic bridges which join together the aromatic clusters in the coal. A certain amount of the aromatic material is thereby liberated to form tar, while the hydrogen from the broken aliphatic bonds disproportionates between the residue and the tar, the latter being richer in hydrogen. Where a methylene group is activated by replacement of one or both hydrogen atoms, e.g. by an aromatic group, bond fission would be expected to occur at a lower temperature than with the unsubstituted group. The bulk of the non-aromatic material remaining above 500°C appears to be hydrogen and methyl groups at the

periphery of aromatic clusters. The loss of these methyl groups would be expected to take place at a temperature higher than that required to split methylene bridges, from bond energy considerations. For example, the strength of the methylene bond in $C_6H_5CH_2$—$CH_2C_6H_5$ is quoted[6] as being 47 kcal, as compared with 87 kcal for C_6H_5—CH_3. Secondary carbonization involves the loss of this periphery material, mainly as methane and hydrogen, thus leaving the aromatic groups free to grow into sheets similar to, but much smaller than, those in graphite. The mean layer diameter of these sheets appears to have reached a steady value by about 800°C, and little further structural change seems to take place below 1 000°C.

In accordance with this picture, the free radical concentration in carbonized coals reaches a maximum[7,8] value between 400° and 600°C, due to the bond fission associated with primary and the beginning of secondary carbonization. When aliphatic groups adjacent, or attached, to an aromatic cluster are split off, electron traps are formed; electrons from the aromatic π band can now fall into trapping σ orbitals[9] where bond fission has occurred, leaving conducting holes in the π band. The onset of primary carbonization (at about 400°C) is therefore accompanied by a rapid increase in electrical conductivity.

The free radical concentration begins to fall off sharply[7] above 600°C, as a result of coalescence of the aromatic clusters to form small graphite-like sheets[10]; however, the conductivity continues to increase steeply up to about 800°C due to intrinsic semi-conduction in the aromatic sheets, since the energy of activation for semi-conduction has been shown[11] to be approximately inversely proportional to the area of the aromatic sheet.

It follows that any alteration in the structure of a coal brought about by chemical treatment, which affects the mechanism of the carbonization process, should lead to corresponding changes in the electrical conductivity during carbonization. Measurements have therefore been made[12] on samples of Markham Black Shale (hereafter referred to as MBS) which were (a) untreated, (b) approximately 50 per cent methylated using alkaline dimethyl sulphate, (c) dehydrogenated by heating with sulphur at 190°C and (d) brominated by treating acetylated MBS with N-bromosuccinimide. This particular coal was chosen because a great deal of information concerning its structure and properties was already available through the work of Dicker, Gaines et al.[13,14].

The three main peaks observed with the untreated sample of MBS are illustrated in Figure 2(a) and occur in the ranges of temperature (i) 150° to 350°C, (ii) 300° to 500°C and (iii) 500° to 800°C. Each peak, or group of peaks, is associated with the corresponding stage involved in the carbonization process. Peak (i) has been ascribed[12] to the disruption of the grain structure of the coal when trapped volatile material escapes. Peak (ii) results from the primary carbonization process, and peak (iii) from secondary carbonization.

Methylation of the hydroxyl groups in MBS appears to leave the mechanism of the carbonization process virtually unchanged [cf. Figure 2(a) and 2(b)]. The peak (i) at 250°C is somewhat reduced in size, due probably to

the leaching out of some of the adsorbed organic material from the coal structure during methylation and the subsequent washing.

Dehydrogenation by heating with sulphur has a marked influence on carbonization, as can be seen from *Figure 2*(c). Peak (*i*) at 250°C is again slightly reduced in size, due probably to the pre-heating of the MBS at 190°C during dehydrogenation. The primary carbonization peak (*ii*) occurring in the untreated material at 450°C, is now split into two separate peaks at *ca.* 400° and 500°C. Evidence, discussed elsewhere[12], suggests that the 400° peak is due to loss of hydroxyl groups present in the original coal and also to the evolution of sulphur compounds, resulting from the rupture of bonds formed between the added sulphur and aromatic material in the coal.

The 500°C peak is in the region where it is known that the rupture of methylene bridges occurs and is presumably due to fission of those aliphatic bridges which were not converted to aromatic material during the dehydrogenation process.

The secondary carbonization peak (*iii*) is also much changed in the dehydrogenated sample [*Figure 2*(c)], the rate of increase in conductivity becoming very great at about 600°C. This is not unexpected since the rate of coalescence of aromatic groups is likely to be governed by the rate at which edge groups, mainly CH₃— and hydrogen, are split off. The rapid onset of secondary carbonization thus suggests that dehydrogenation by sulphur has resulted in removal of a proportion of the hydrogen attached directly to the aromatic ring systems, a conclusion also reached by Dicker *et al.*[14].

Bromination of MBS considerably alters peaks (*i*) and (*ii*) but leaves the secondary carbonization peak (*iii*) little changed [*Figure 2*(d)].

The marked increase in the size of the 200° peak was shown by TGA to be associated with the splitting-off of hydrogen bromide, leaving a residue containing a much increased proportion of carbon–carbon double bonds.

The primary carbonization peak appears now to have been displaced towards a lower temperature, relative to untreated MBS; the position now corresponds closely with that of the lower primary carbonization peak of the sulphur dehydrogenated sample. The higher (500°C) peak occurring during primary carbonization of the sulphur dehydrogenated sample is either absent or has merged with the secondary carbonization peak. Absence of this peak would suggest that all the aliphatic bridges in the coal had been converted into aromatic ring systems; such an occurrence is most improbable and should have led to a very large increase in electrical conductivity, which was not observed. It thus appears that the peak must have moved to a higher temperature region, resulting in the apparent broadening of [*Figure 2*(d)] the secondary carbonization peak. Such a movement would be explained by the conversion of the single carbon–carbon bonds in the methylene bridges to double bonds. In polyatomic molecules, the bond energies of —C—C— and —C=C— are 83 kcal and 146 kcal respectively[6], indicating that the latter bonds are thermally more stable and would therefore be expected to break at a higher temperature.

The success achieved by using rising temperature conductivity measure-

ments to study the decomposition of coals (and coal models[6]), suggested that this technique might prove to be of general use in identifying and following the thermal degradation of polymers.

Warfield[15] has already shown that resistivity measurements can be used to study the thermal stability of polymers, in the temperature range 25° to 400°C. The procedure used by Warfield has been restricted to crosslinked polymers and differs markedly from the present work; blocks of polymer weighing about 350g were heated at a range of constant temperatures for 16 h prior to resistivity measurements being made. Although this procedure was termed electrothermal analysis (ETA), it shows little similarity to such techniques as DTA and TGA, both in the amount of sample consumed and in the time required. On the other hand, the technique discussed here is comparable with DTA in both respects and leads to a graph of similar form, suggesting that it might be useful in the routine analysis of polymers.

To illustrate the application of this technique to polymers, polyvinyl chloride has been chosen, because of its relatively simple chemical structure. *Figure 3* illustrates the changes in conductivity of a compact prepared from PVC powder as a function of temperature, while the rate of change in conductivity is plotted against temperature in *Figure 4*. From *Figure 3* it can be seen at once that the thermal decomposition involves two distinct stages: stage I occurs in the region of 250°C and is accompanied by the evolution
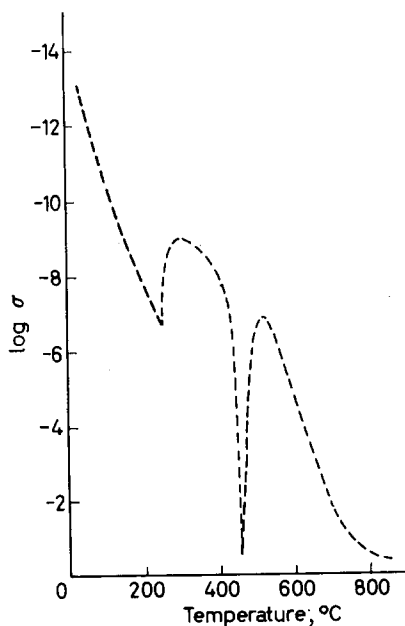
Figure 3—The logarithm of the conductivity of unplasticized polyvinyl chloride plotted against temperature
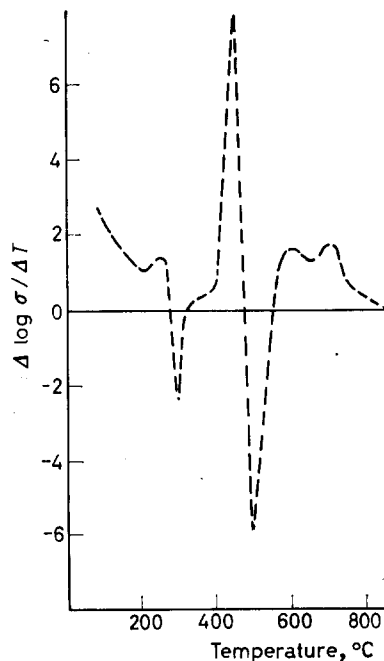
Figure 4—The rate of change of conductivity (in arbitrary units) plotted against temperature for unplasticized polyvinyl chloride

of hydrogen chloride while stage II occurs at 400° to 500°C. The curve shows good reproducibility up to 250°C and above 550°C, but between these limits a certain amount of scatter occurs, due to the disruption of the grain structure of the compact as large quantities of gas are evolved. Differential thermal analysis likewise indicates a two-stage reaction[16], in the same range of temperatures. Kipling and McEnaney[17] have shown by thermogravimetric analysis that stage I involves a 42 per cent loss in weight while the loss for stage II is 17·8 per cent. Up to 250°C, the weight loss is due almost entirely to evolution of hydrogen chloride, without any appreciable loss of carbon or hydrogen[18]; the mechanism of the reaction is

$$(\text{—CH}_2\text{—CHCl—})_n \longrightarrow (\text{—CH}=\text{CH—})_n + n\text{HCl}$$
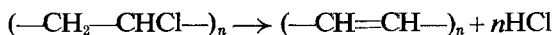
The resulting straight-chain polyene at once undergoes a certain amount of cyclization, with the proportion of aromatic material increasing with temperature.

Stage II occurring at about 400°C, is accompanied by the evolution of simple gaseous hydrocarbons and a rapid fall in the H/C ratio[18]. The presence of polycyclic aromatic regions in PVC chars heated above 400°C has been demonstrated by Winslow et al.[19] and by Kipling[20]. Above 500°C, the predominant decomposition reaction observed by Gilbert and Kipling was the evolution of hydrogen. In accordance with this picture of the decomposition process, Wynne-Jones et al. have shown that the specific surface[21] of the residue passes through a maximum in the region 500° to 550°C and that the free spin concentration[22] passes through a maximum value at 560°C.

The mechanism of carbonization of PVC is thus far closer to that of a coal than might have been expected; this is reflected in the general similarity between *Figures 2*(a) and *4*. The peaks of *Figure 4* can therefore be explained as follows.

(1) Loss of HCl in the region 200° to 250°C initially leads to a rapid increase in conductivity as the polyene is formed; but the sudden evolution of gas disrupts the grain structure of the compacted powder to such an extent that the conductivity shows a subsequent fall.

(2) Primary carbonization occurs in the region 400° to 500°C with the evolution of tar and volatile decomposition products, some of which must be good conductors of electricity.

(3) The double peak at 600° to 700°C appears to result from the evolution of hydrogen and coalescence of the aromatic residue during secondary carbonization, as has been observed with medium and low rank coals.

CONCLUSION

Measurements of electrical conductivity during carbonization have now been carried out on widely differing polymeric, organic compounds. The results indicate that this technique could prove useful in studying both the chemical structure and the mechanism of thermal decomposition of such materials.

Since a plot of the rate of change of electrical conductivity with temperature, against temperature, gives a curve which is characteristic of a particular compound, the technique provides a new method of thermal

analysis. The technique described shows many points of general similarity with such well-established methods of thermal analysis as DTA and TGA. It therefore seems reasonable to suggest that this technique be referred to as 'Electro Thermal Analysis', even though Warfield has used the term in a rather different sense.

Department of Chemistry,
College of Technology,
Portsmouth, Hants

REFERENCES

[1] POPE, M. I. and GREGG, S. J. *Brit. J. appl. Phys.* 1959, **10**, 507
[2] SANDOR, J. *Proceedings of the Conference on the Ultrafine Structure of Coals and Cokes,* p 342. British Coal Utilisation Research Association: London, 1944
[3] GREGG, S. J. and POPE, M. I. *Fuel, Lond.* 1960, **39**, 301
[4] POPE, M. I. *Proceedings of the Second Conference on Industrial Carbon and Graphite,* p 474. Society of Chemical Industry: London, 1965
[5] HOLDEN, M. W. and ROBB, J. C. *Fuel, Lond.* 1960, **39**, 39
[6] COTTRELL, T. L. *The Strengths of Chemical Bonds,* 2nd edition. Butterworths: London, 1958
[7] AUSTEN, D. E. G., INGRAM, D. J. E. and TAPLEY, J. G. *Trans. Faraday Soc.* 1958, **54**, 400
[8] SMIDT, J. and VAN KREVELEN, D. W. *Fuel, Lond.* 1959, **38**, 355
[9] MROZOWSKI, S. Symposium on the Properties of Carbon, p 1. Durham (1956)
[10] DIAMOND, R. and HIRSCH, P. B. *Proceedings of the Conference on Industrial Carbon and Graphite,* p 197. Society of Chemical Industry: London, 1958
[11] SCHUYER, J. and VAN KREVELEN, D. W. *Fuel, Lond.* 1955, **34**, 213
[12] POPE, M. I. 6th International Conference on Coal Science, Münster (1965)
[13] DICKER, P. H., GAINES, A. F. and STANLEY, L. *J. appl. Chem.* 1963, **13**, 455
[14] DICKER, P. H., FLAGG, M. K., GAINES, A. F. and MARTIN, T. G. *J. appl. Chem.* 1963, **13**, 444
[15] WARFIELD, R. W. *Nature, Lond.* 1961, **189**, 1002. See also *Testing of Polymers,* edited by J. V. SCHMITZ, Vol. I, p 292. Interscience: New York, 1965
[16] YOUNG, R. N. 1st International Conference on Thermal Analysis, p 70. Aberdeen (1965)
[17] KIPLING, J. J. and McENANEY, B. *Fuel, Lond.* 1964, **43**, 367
[18] GILBERT, J. B. and KIPLING, J. J. *Fuel, Lond.* 1962, **41**, 493
[19] WINSLOW, F. H., BAKER, W. O. and YAGER, W. A. 2nd Conference on Carbon, p 93. Buffalo (1956)
[20] KIPLING, J. J. and SHOOTER, P. V. *Proceedings of the Second Conference on Industrial Carbon and Graphite,* p 15. Society of Chemical Industry: London. 1965
[21] MARSH, H. and WYNNE-JONES, W. F. K. *Carbon,* 1964, **1**, 269
[22] JACKSON, C. and WYNNE-JONES, W. F. K. *Carbon,* 1964, **2**, 227

Relationships Involving the Densities and Isothermal Compressibilities of Amorphous Polymers

J. C. McGOWAN

A relationship between the isothermal compressibilities and densities of amorphous polymers is discussed and it is shown how, at one temperature, from the density at one pressure, the compressibilities and densities at other pressures can be estimated. A method is suggested for the estimation of the 'constants' of the Tait equation and this method can be used not only for amorphous polymers but for non-associated liquid compounds as well.

ROE[1] has shown that the formula (1) of Sugden[2] for the parachor can be used to calculate the surface tension γ of an amorphous polymer from the density (d_l) and the ratio of the parachor (P) to the molecular weight (M)

$$\gamma = [Pd_l/M]^4 \qquad (1)$$

Moreover, Roe has developed a method for the measurement of surface tensions of highly viscous polymers and the experimental values are close to those calculated using equation (1).

Some time ago, it was pointed out[3] that, for unassociated liquids, the isothermal compressibility κ_T at low pressures was related to the surface tension γ and

$$\kappa_T \gamma^{3/2} = 1\cdot33 \times 10^{-8} \text{ (c.g.s. units)} \qquad (2)$$

$$(d_l - d_g) \kappa_T^{1/6} = M/21P \text{ (c.g.s. units)} \qquad (3)$$

Here M is again the molecular weight, P is the parachor, d_l is the density of the liquid and d_g is the density of the vapour in equilibrium with it. The molecular volume of the liquid V is M/d_l. If d_g can be neglected in comparison with d_l, plots of log κ_T against log V should give straight lines of slope six. Straight lines with slopes close to six have been found experimentally by Reed[4]. From the expression (2) and the values of the surface tension at 20°C deduced by Roe[1] from extrapolation (rather a long extrapolation, in most cases!) of his experimental values, the isothermal compressibilities in *Table 1* were obtained. These values are compared with experimental results of Allen *et al.*[5] which are mostly for 'polymers' of much lower molecular weight than those used by Roe. Thus the compressibility for linear polyethylene is actually that of *n*-tetradecane of density 0·765 while Roe used Alathon 7050 of density 0·855. Since the isothermal compressibility is sensitive to changes in density, close agreement between the values in the two columns of *Table 1* is hardly to be expected. In *Table 2*, some values of $1/(d_l - d_g) \kappa_T^{1/6}$ for hydrocarbons are compared with $21P/M$. The parachors were calculated by the method described previously[6]. The densities were taken from Timmermanns[7] and the isothermal compressibilities for low pressures from the *Handbook of Chemistry*

and Physics[8]. It will be seen that $1/(d_1 - d_g)\kappa_T^{1/6}$ is independent of the temperature and in reasonable agreement with the calculated values of $21P/M$.

Table 1. Isothermal compressibilities of amorphous polymers

	Isothermal compressibility at 20°C (c.g.s. units)	
Polymer	Found[5]	Calculated from surface tension and equation (2)
Poly(ethylene oxide)	$4 \cdot 8 \times 10^{-11}$	$4 \cdot 8 \times 10^{-11}$
Linear polyethylene	$8 \cdot 6 \times 10^{-11}$	$6 \cdot 3 \times 10^{-11}$
Poly(dimethyl siloxane)	$11 \cdot 3 \times 10^{-11}$	$14 \cdot 2 \times 10^{-11}$

For polymers, d_g can be neglected and P' and M' can refer to the repeating unit so that formula (3) can be written

$$21P'/M' = 1/d_1\kappa_T^{1/6} \text{ (c.g.s. units)} \tag{4}$$

In *Table 3*, some values of $21P'/M'$ are compared with values of $1/d_1\kappa_T^{1/6}$ from Moraglia[9] for polypropylene and poly(butene-1), from Heydemann and Guicking[10] for polyvinylchloride and poly(methylmethacrylate) and other values from Allen *et al.*[5]. The agreement is quite good especially in view of the fact that amorphous polymers are very difficult to purify. It is of interest that values of $21P'/M'$ can be calculated readily from the formula of the repeating unit for polymers on which no measurements have been made or for polymers which are unknown at present. For example, for the polymer of formula $[-OC_6H_4-C(CH_3)_2-C_6H_4OC_6H_4SO_2C_6H_4-]_n$ which has recently been described[11,12], $21P'/M'$ comes to 43.7.

If equation (3) is correct, values of $1/(d_1 - d_g)\kappa_T^{1/6}$ for a series of compounds $A(X)_nY$ plotted against $1/M$ should fall on a straight line which when produced to $1/M = 0$ will give $1/d_1\kappa_T^{1/6}$ for the polymer of group X with molecular weight so high that the effect of the end groups is negligible. This type of extrapolation was suggested by Exner[13]. The value of $21P'/M'$ of 59·7 c.g.s. units given in *Table 3* for polyethylene is close to the intercept for $1/M = 0$ of the line obtained by a plot of $1/M$ against the $1/(d_1 - d_g)\kappa_T^{1/6}$ values for normal paraffins from *Table 2*.

Since $\kappa_T = (1/V)(\partial V/\partial p)_T$ and $1/d_1 = V$ where V is the specific volume and p is the pressure, equation (4) can be written

$$\kappa_T = (1/V)(\partial V/\partial p)_T = [M'/21P']^6 V^6 \tag{5}$$

and the solution of this differential equation gives

$$p + L' = (1/6V^6)[21P'/M']^6 \tag{6}$$

where L' is a constant at a given temperature. This equation and (4) will apply under similar conditions, i.e. constant temperature and p small (compared to L'). Equation (6) can be written

$$6(p_1 - p_2)/(d_{11}^6 - d_{12}^6) = [21P'/M']^6 \tag{7}$$

where d_{11} and d_{12} are densities of a liquid at pressures p_1 and p_2 respectively and the same temperature. Equation (7) like equations (2) and (3) will hold

Table 2. Values for normal paraffins

Compound	Temp., °C	$\dfrac{1}{(d_l - d_a)\,\kappa^{1/6}}$	$\dfrac{21P}{M}$	$\dfrac{1\,000}{M}$
n-Hexane	0	65·6		
	25	64·7	65·9	11·60
	40	65·6		
	60	65·7		
n-Heptane	0	64·5		
	25	64·5	65·0	9·98
	40	64·5		
	60	64·6		
n-Octane	0	64·6		
	25	64·5	64·3	8·75
	40	64·5		
	60	64·5		
n-Pentadecane	60	62·5	62·9	4·71

at low pressures. Cutler *et al.*[17] have measured the effects of pressure on the specific volumes of liquid hydrocarbons of fairly high molecular weight. Their results for specific volumes at one atmosphere and at the comparatively low pressure of 344·6 bars have been used in *Table 4*. It will be seen that $d_{11}^6 - d_{12}^6$ is constant with temperature. There is good agreement

Table 3. Tests for equations (4) and (7)

Polymer	$\dfrac{21P'}{M'}$	$\dfrac{1}{d_1\kappa_T^{1/6}}$	$\dfrac{6\,(p_1 - p_2)^{1/6}}{d_{11}^6 - d_{12}^6}$ at $\begin{cases} t\,^{\circ}C \\ p_1\ dyne\ cm^{-2} \end{cases}$
Polyethylene	59·7	62·2	58·0 (t 181·7; p_1 1·22 × 10⁹; made low pressure)
Polyethylene	59·7	—	59·9 (t 174·5; p_1 1·62 × 10⁹; made high pressure)
Polypropylene	59·7	60·0	62·3 (t 250; p_1 6·26 × 10⁸)
Poly(butene-1)	59·7	59·8	—
Polyisobutylene	59·7	59·1	—
Polystyrene	50·9	51·5	50·6 (t 202·8; p_1 2·03 × 10⁹
Poly(propylene-oxide)	49·4	49·8	—
Poly(dimethyl-siloxane)	47·1	46·7	—
Poly(methyl-methacrylate)	46·3	44·4	46·0 (t 139·3; p_1 2·03 × 10⁹
Poly(ethyl-acrylate)	46·3	51·2	—
Poly(ethylene-oxide)	46·0	48·9	—
Poly(methyl-phenylsiloxane)	46·0	46·4	—
Poly(vinyl chloride)	38·5	38·9	—
Poly(trifluoro-chloroethylene)	26·7	25·5	—

between $21P/M$ from the densities (the average value from the previous column has been used) and the calculated values. No value in the last column of *Table 4* exceeds the corresponding value in the previous column and this suggests that it would be more accurate to replace $21P/M$ by $21.06P/M$. In *Table 3*, some values of $21P'/M'$ have been obtained from the data of Hellwege, Knappe and Lehmann[14] (but Foster, Waldman and Griskey[15] for polypropylene) and equation (7). In each case p_2 was one atmosphere, 1.01×10^6 c.g.s. units. It will be seen that these values of $21P'/M'$ are in good agreement with the calculated values given in the same table.

In conclusion, it is of interest to compare the well known Tait equation which in the form used by Wohl[16] is

$$(1/V_0)\,(\partial V/\partial P)_T = C/(p+L) \tag{8}$$

with equation (9) which follows from (5) and (6)

$$(1/V)\,(\partial V/\partial P)_T = 1/6\,(p+L') \tag{9}$$

where V_0 is the specific volume at low pressure (usually one atmosphere), L is a constant at a given temperature and C is a constant for all temperatures. Values of C given[8] for the Tait equation are for most simple compounds nearer a tenth than a sixth suggested by (9). Equation (9) probably only applies when p is small compared with L'. Cutler *et al.*[17], whose measurements were used for *Table 4*, fitted their results to the Tait equation and found the greatest deviations were at low pressures. The Tait equation is usually tested at pressures sufficient to produce a significant change in compressibility from the compressibility at atmospheric pressure, which is usually the standard, and C may well be lower than a sixth at these moderately high pressures (i.e. when p is comparable with L). The integrated form (10) of the Tait equation is

$$V_1 - V_2 = CV_0 \ln\{(L+p_2)/(L+p_1)\} \tag{10}$$

At a very high pressure p_2, $V_1 - V_2$ will tend to V_1, while

$$\ln\{(L+p_2)/(L+p_1)\}$$

will tend to infinity[18] and so, as the pressure goes up, C will have to decrease if the equation is to hold. It is of interest that equation (9) can be used for the estimation of the 'constants' of the Tait equation because this equation is useful even if it is not accurate at pressures of several hundred atmospheres and fails at very high pressures. Equations (8) and (9) can both be used when p is atmospheric pressure

$$\therefore (C/L) = (1/V_0)\,(\partial V_0/\partial P)_T = [MV_0/21P]^6 \tag{11}$$

With $C = 1/6$, a value of $L = L'$ can be obtained and these values can be used if p is small compared with L. As p rises, lower values of C are required, with C about $1/10$ when p is not too different from L. However, unless the pressure is high, the exact value of C is not of great importance

Table 4. Effects of pressure change (344·6 bars) upon the densities of liquid hydrocarbons

Hydrocarbon	$d^6_{11} - d^6_{12}$ at $t°C$						Average $d^6_{11} - d^6_{12}$	$\left[\dfrac{6 \times 344 \cdot 6 \times 10^6}{d^6_{11} - d^6_{12}}\right]^{1/6}$	$\dfrac{21P}{M}$
	37·8	60·0	79·4	98·9	115·0	135·0			
9-n-Octyl heptadecane	0·0386	0·0384	0·0379	0·0382	0·0377	0·0391	0·0383	61·4	61·3
n-Octadecane	—	0·0352	0·0350	0·0365	0·0370	0·0369	0·0361	62·1	61·9
n-Pentadecane	0·0328	0·0328	0·0337	0·0341	0·0339	0·0340	0·0336	62·8	62·4
1-Cyclohexyl-3-(2-cyclohexylethyl) hendecane	0·0499	0·0490	0·0514	0·0508	0·0528	0·0526	0·0511	58·6	58·3
9-(3-Cyclopentylpropyl) heptadecane	0·0448	0·0448	0·0435	0·0451	0·0433	0·0442	0·0443	60·0	59·8
1-Cyclopentyl-4(3-cyclopentylpropyl) dodecane	0·0514	0·0533	0·0523	0·0512	0·0536	0·0505	0·0521	58·4	58·3
1,7-Dicyclopentyl-4(3-cyclopentylpropyl) heptane	0·0563	0·0590	0·0591	0·0622	0·0592	0·0603	0·0592	57·2	56·8
n-Dodecane	0·0336	0·0316	0·0328	0·0324	0·0315	0·0318	0·0323	63·2	62·9
9-(2-Phenylethyl) heptadecane	0·0471	0·0483	0·0496	0·0501	0·0496	0·0534	0·0497	58·8	58·6
9-(2-Cyclohexylethyl) heptadecane	0·0430	0·0427	0·0440	0·0455	0·0454	0·0450	0·0443	60·0	59·8
1-α-Naphthylpentadecane	—	0·0633	0·0626	0·0634	0·0642	0·0628	0·0633	56·5	56·2
1-α-Decalylpentadecane	—	0·0482	0·0490	0·0504	0·0493	0·0499	0·0494	58·9	58·9

because from (11) C/L is constant and changes in C are largely compensated by changes in L. The equation (11) applies to amorphous polymers and other non-volatile liquids. For volatile liquids, it should probably be written

$$(C/L) = [M/21P(d_{l0} - d_{p0})]^6 \tag{12}$$

For ethyl bromide, this equation gives, with values from Timmermanns[7], $C/L = 1.217 \times 10^{-10}$ c.g.s. units at 20°C. If $C = 1/10$, $L = 810.8$ atm and equation (10) with these values, $p_1 = 1$ atm and $p_2 = 1\,000$ atm gives $V_1 - V_2 = 0.0549$ cm³. The value found experimentally[19] for $V_1 - V_2$ is 0.0543 cm³ at 20°C and the same pressures.

Imperial Chemical Industries Limited,
Research Department, Bessemer Road,
Welwyn Garden City, Herts

REFERENCES

[1] ROE, R. *J. phys. Chem.* 1965, **69**, 2809
[2] SUGDEN, S. *J. chem. Soc.* **1924**, 1185
SUGDEN, S. *The Parachor and Valency.* Routledge: London, 1929
[3] McGOWAN, J. C. *Rec. Trav. chim. Pays-Bas*, 1957, **76**, 155
[4] REED, T. M. *Fluorine Chemistry*, Vol. V, p 168. Edited by J. H. SIMONS. Academic Press: London and New York, 1964
[5] ALLEN, G., GEE, G., MANGARAJ, D., SIMS, D. and WILSON, G. J. *Polymer, Lond.* 1960, **1**, 467
[6] McGOWAN, J. C. *Rec. Trav. chim. Pays-Bas*, 1956, **75**, 193
[7] TIMMERMANNS, J. *Physico-Chemical Constants of Pure Organic Compounds*, Elsevier: Amsterdam, Vol. I, 1950; Vol. II, 1965
[8] WEAST, R. C., SELBY, S. M. and HODGMANN, C. D. *Handbook of Chemistry and Physics.* 46th Edition, pp F9-F11, The Chemical Rubber Publishing Co: Ohio, 1965
[9] MORAGLIO, G. *R.C. Accad. Lincei*, 1965, **39**, 277
[10] HEYDEMANN, P. and GUICKING, H. D. *Kolloidzschr. u. Z. Polym.* 1963, **193**, 16
[11] BASSETT, H. D., FAZZARI, A. M. and STAUB, R. B. *Plast. Technol.* September 1965, **11**, 50
[12] KRUMMEL, E. W. *Modern Plastics Encyclopedia 1966*, Vol. 43, p 335. McGraw-Hill: New York
[13] EXNER, O. *Nature, Lond.* 1962, **196**, 890
[14] HELLWEGE, K. H., KNAPPE, W. and LEHMANN, P. *Kolloidzschr. u. Z. Polym.* 1962, **183**, 110
[15] FOSTER, G. N., WALDMAN, N. and GRISKEY, R. G. *Polymer Engineering and Science*, 1966, **6**, 131
[16] WOHL, A. *Z. phys. Chem.* 1921, **99**, 234
[17] CUTLER, W. G., McMICKLE, R. H., WEBB, W. and SCHIESSLER, R. W. *J. chem. Phys.* 1958, **29**, 727
[18] HIRSCHFELDER, J. O., CURTISS, C. F. and BIRD, R. B. *Molecular Theory of Gases and Liquids*, p 261. Wiley: New York, 1954
[19] BRIDGEMAN, P. W. *International Critical Tables*, Edited by E. W. WASHBURN. Vol. III, p 40. McGraw-Hill: London and New York, 1928

Irradiated Polyethylene II—Free Radical Formation[*][†]

I. Auerbach

Allyl free radical formation in Marlex 50 polyethylene at room temperature is correlated with vinyl group disappearance and vinylene group formation. The allyl radicals were generated with 2 MeV electrons from a Van de Graaff accelerator and their concentrations were measured with electron spin resonance techniques. A kinetic analysis of the free radical formation and vinyl disappearance data provides a mechanism for these reactions. The mechanism assumes the formation of a steady state concentration of positive alkyl ions, which are formed initially, followed by charge transfer to vinyl and vinylene groups. A subsequent reaction between the vinyl ion and a neutral vinyl group takes place. The resultant divinyl and vinylene ions form allyl radicals following charge recombination. Kinetic equations derived from this mechanism correlate well with experimental data. The G value for alkyl ion formation calculated from these equations, is the same as that obtained for radical formation in lower molecular weight hydrocarbons and for alkyl radical formation in polyethylene at 77°K and at low doses. This G value also correlates with the G values for the polymerization of olefins. The kinetic data provide evidence that allyl radical formation does not take place through a precursor alkyl radical.

A NUMBER of mechanisms for free radical formation in polyethylene under high energy radiation conditions have been suggested (see also part I of this work[1]). The literature on this subject, and other aspects concerned with the effects of radiation on polyethylene, are reviewed and discussed by Charlesby[2] and Chapiro[3]. In more recent studies of related interest Crook and Lyons[4], Charlesby, Gould and Ledbury[5], and Dole, Fallgatter and Katsuura[6] have considered the formation and decay of unsaturation in polyethylene and their relationships to crosslinking.

The purpose of the present and following studies is to show that vinyl group decay, vinylene group formation, allyl free radical formation, and crosslinking are quantitatively related. In the present study the formation of the allyl free radical possessing the seven line electron spin resonance (e.s.r.) spectrum was investigated. It is shown that the allyl radical is formed as the result of radiation interacting with polyethylene to form an intermediate product which then reacts with existing vinyl and generated vinylene groups. It is assumed that the intermediate is the alkyl positive ion. In the reaction sequence, the positively charged alkyl ion is formed initially and the charge is transferred along the alkyl chain to the points of unsaturation. If a vinyl group traps the charge, the resultant vinyl ion reacts with a neutral vinyl group. Charge recombination for the divinyl and vinylene ions produces excited species and, subsequently, allyl radicals.

A linear polyethylene, Marlex 50, was used in this study. It was irradiated with 2 MeV electrons obtained from a Van de Graaff accelerator.

The conclusions derived from this study are obtained from a kinetic analysis of radical formation, vinylene group formation, and vinyl group decay studies at room temperature. The results from the previous study[1], which are concerned with e.s.r. spectral transformations involving alkyl and allyl free radicals at various temperatures and doses also contribute to these conclusions. The previous study[1] provided evidence for the conclusion that an alkyl–allyl radical transformation does not take place and that the observed products, i.e. alkyl or allyl radicals, may be dependent on the amorphous phase condition in polyethylene at the time of irradiation, i.e. glassy or viscous-elastic.

Data obtained in this study are used in the kinetic interpretation, section 2 of Results and Discussion, to show how a mechanism involving an intermediate existing under steady state conditions accounts for allyl radical formation. The kinetic analysis provides equations which are in agreement with experimental data. Values for the constants in the kinetic expressions correlate with the G values obtained by others for radical formation in polyethylene and in lower molecular weight hydrocarbons, for polymerization, and for vinylene formation.

EXPERIMENTAL METHODS

Linear polyethylene in rod form (3/16 in.) was used for this study. It was prepared from a Marlex 50 stock which has a density of 0·96 and a melt index of 0·9. The rod is supplied by Allied Resinous Products, Inc., and is listed as Resinol Type F polyethylene.

Electrons from a 2 MeV Van de Graaff accelerator were used for generating the free radicals. The 1 cm wide circular beam was expanded vertically with a magnet to 9 cm. The polyethylene rod and a blue cellophane dosimeter were attached to a mechanical horizontal oscillating device. The rod and dosimeter passed through the beam every two seconds providing a uniform incident dose to the sample and dosimeter. The samples were irradiated in air and cooled with an air stream to 20° to 25°C.

DuPont No. 300 MSC blue cellophane was used as a dosimeter. It was calibrated by plotting the calculated delivered dose versus the optical density change. The plot was verified with a calibrated ionization chamber. The dose absorbed by the rods was 67 per cent of the incident dose. This value was determined by integrating over the cylindrical shape using absorbed dose versus thickness data for polyethylene.

Free radical concentrations were measured with a Varian Model 4500 X-band EPR spectrometer. Absolute radical concentrations were not determined. Instead, it was assumed that the concentrations were proportional to the peak-to-peak amplitude of the largest line in the differential form of the spectrum. A coal sample was used as a relative standard. The microwave power supplied to the cavity was 10 mW.

trans-Vinylene formation was measured with a Beckman IR-4 spectrophotometer. Optical densities of samples 0·7 to 1·0 mm thick were determined at $10·35 \mu$ before and after irradiation. These were converted to concentrations with the extinction coefficient value[7] of 169. All infra-red (i.r.) measurements were performed in air.

64

RESULTS AND DISCUSSION

(1) *Radical formation*

A study of the kinetics for allyl radical formation in polyethylene at room temperature provides constants for calculating yields which correlate with vinyl group decay and vinylene group formation data. Radicals were generated by irradiating polyethylene rods with 2 MeV electrons for various time periods at room temperature. The dose rate range was 0·63 to 17.9×10^{20} eV/g min. *Figure 1* shows some representative data.
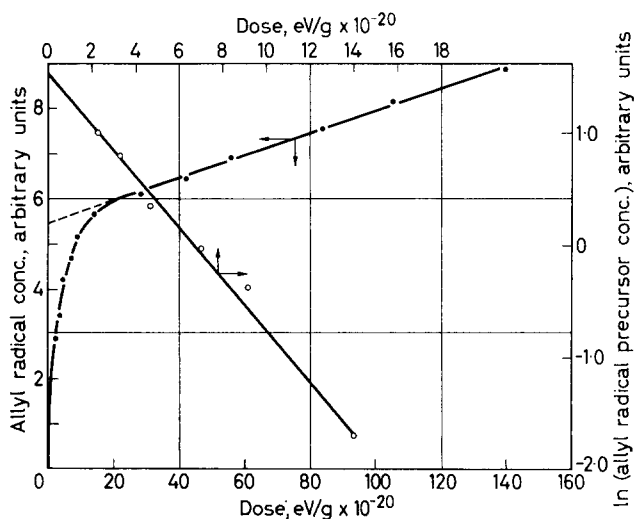
Figure 1—Allyl free radical formation as a function of dose,
●; apparent first order relationship for the radical precursor
disappearance, ○. Incident dose rate 17·9 eV/g min

The results can be interpreted by assuming that radical formation stems from two processes. The initial yield for the process with the higher yields is initially high, but decreases with dose and levels off after approximately 2×10^{21} eV/g have been absorbed. The yield for the second process is constant with dose. The radicals formed in the second process were found to be linear with dose in all experiments covering a series of dose rates. The total absorbed doses extended beyond 6×10^{21} eV/g in a number of experiments.

The data also suggest that the following corollaries can be added to the assumption that two radical formation processes are involved. (*1*) The radical precursor for the non-linear process is limited and becomes depleted with increasing dose. (*2*) The radical precursor for the linear process exists in concentrations greatly in excess to the radicals formed in this process in the dose range studied. (*3*) Both radical formation processes take place simultaneously.

A value for a reaction constant in the non-linear process can be obtained by extrapolating the straight line in *Figure 1* to the vertical axis (dashed line). The intercept provides the initial concentration of the precursor for

the radicals. The differences between the extrapolated and experimental values are the concentrations of the precursor that are available for the non-linear process as a function of dose. The log values of these differences are also plotted against dose in *Figure 1*. The linear plot and others obtained from similar experiments suggest that the non-linear process is a first order reaction. The first order kinetics are only approximate, however. A consideration of the mechanism in the following section will show that the kinetics are more complex. The first order interpretation is presented at this point only to obtain constants for comparison with the data of others.

Most of the irradiations were performed under intermittent, swept-type exposures to provide uniform doses to the samples and dosimeters. Intermittent exposures of this type could provide different data from those obtained under continuous exposure if the decay rates of the generated radicals were comparable in magnitude to the formation rates. Experiments were therefore performed in which the samples were continuously irradiated. Dosimeters and polyethylene rods were irradiated separately for equivalent time periods.

The effect of dose rate on these constants was also examined. This effect was studied by varying the Van de Graaff beam current. The zero order constants, k_0 (equivalent to the yields for the linear process) and the first order constants, k_1', are presented in *Table 1*. The values show the absence of a dose rate and an intermittent irradiation effect indicating that the radicals are relatively stable at room temperature.

Table 1. Reaction constants for radical formation

Incident dose rate (eV/g min)	Radiation delivery method	k_0 Radicals (arb. units)/eV	k_1' (g/eV)
0.630×10^{20}	Intermittent	404	1.50×10^{-21}
0.72	Intermittent	494	1.73
1.09	Intermittent	706	1.70
1.19	Intermittent	591	1.73
1.57	Intermittent	526	2.16
2.52	Intermittent	591	1.73
3.64	Intermittent	537	1.95
2.49	Continuous	409	1.76
17.9	Continuous	503	1.74
Mean		529	1.77

Of particular interest to this study is a comparison of the values for the constants realized in this study with those obtained for vinyl decay. Dole, Milner and Williams[8] and Charlesby et al.[5] measured the decay of vinyl groups in Marlex 50 with i.r. techniques. They reported first order reactions with decay constant values of 1.61×10^{-21} and 1.5×10^{-21} g/eV, respectively. These values are sufficiently close to the average value of 1.77×10^{-21} g/eV obtained in this study to suggest that the free radical

formation reaction is related to the decay of vinyl unsaturation. This relationship will be discussed in the following section.

(2) *Kinetics*

Consideration of the kinetics for the reactions taking place in irradiated polyethylene provides relationships which are confirmed by the experimental data for radical formation, vinyl decay and vinylene formation. The relationships also provide G values for intermediate radiation products which compare well with the data of others, thereby linking together the radiation induced reactions in this study with those taking place in similar compounds. The kinetic expressions also account for the deviation from first order kinetics for vinyl decay which were noted by Dole et al.[8], Crook and Lyons[4], and Sears[9]. In the present study, a first order deviation in the radical formation data was apparent in the calculated reaction constant values. These decreased with increasing dose.

A mechanism which accounts for this deviation and for other observations is based on the reactions given below. In these reactions, the constants φ, k_1, k_2, etc., which provide the yields for specific reactions will be used in a subsequent mathematical treatment. $(CH_2)_n$ represents the n methylene units in the polyethylene molecular chain, Vi represents the vinyl group in a polyethylene molecule, Vi^+ is the ionized form of this group, Vl represents a vinylene group in a polyethylene molecule, and R represents the alkyl radical $CH_3(CH_2)_n^-$.

$$CH_3(CH_2)_nCH{=}CH_2 \xrightarrow{\varphi} CH_3(CH_2)_n^+CH{=}CH_2 \xrightarrow{k_1} CH_3(CH_2)_n\,CH{\overset{+}{=}}CH_2$$
$$\text{(RVi)} \qquad\qquad \text{(R}^+\text{Vi)} \qquad\qquad \text{(RVi}^+) \qquad (1)$$

$$RVi^+ + RVi \xrightarrow{k_5} R(CH)^+{-}CH_2{-}CH_2{-}\overset{\cdot}{C}HR \rightarrow$$
$$RCH{=}CH{-}\overset{\cdot}{C}H{-}CH_2R^+ + H\cdot \qquad (2)$$

$$RVi \xrightarrow{k_3} CH_3(CH_2)_mCH_2{-}CH{=}CH(CH_2)_pCH{=}CH_2 + H_2$$
$$\text{(R'VlR''Vi)}$$
$$R' = CH_3(CH_2)_m{-}, \quad R'' = {-}(CH_2)_p{-}, \quad n = m + p + 3 \qquad (3)$$

$$R'CH_2{-}CH{=}CHR''Vi \xrightarrow{\varphi} R'^+CH_2{-}CH{=}CHR''Vi \rightarrow$$

$$R'CH_2{-}CH{\overset{+}{=}}CHR''Vi \xrightarrow{k_2} R'\overset{\cdot}{C}H{-}CH{=}CHR''^+Vi + H\cdot \qquad (4)$$

$$RVi^+ + R'CH_2{-}CH{=}CHR''Vi \xrightarrow{k_6} R'CH_2{-}CH{-}(CH)^+R''Vi$$
$$\Big|$$
$$R\overset{\cdot}{C}H{-}CH_2$$

$$\rightarrow R'CH_2{-}C{-}\overset{\cdot}{C}HR''^+Vi$$
$$\|$$
$$RCH_2{-}CH + H\cdot \qquad (5)$$
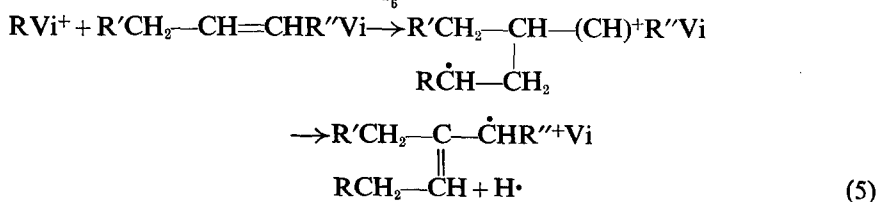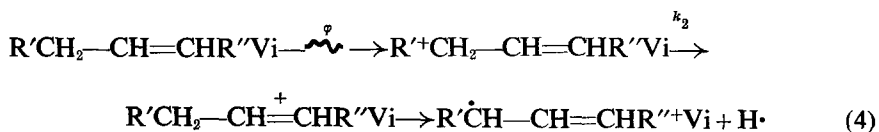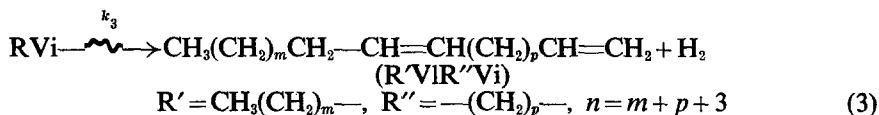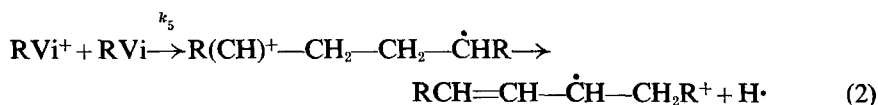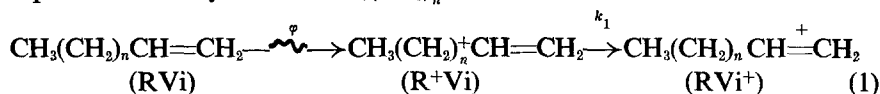
The above mechanism is based on the initial formation of a positive alkyl ion in the polyethylene molecule. Charge transfer occurs along the

chain of —CH_2— groups with eventual capture of the charge by a vinyl or a vinylene group, reaction (1). The resultant vinyl ion subsequently reacts with a neutral vinyl group to form an ion-radical. Following charge neutralization of the ion-radical, an allyl radical is formed, reaction (2). Reaction (3) represents vinylene formation. Vinylene ions, which are formed when vinylene groups capture positive charges, also form allyl radicals following charge neutralization, reaction (4). Reaction (5) represents the possible reaction of Vi^+ with Vl to give a branched allyl radical. The charges which are part of the resultant ion-allyl radicals in reaction sequences (2), (4) and (5) can lead to additional radical formation.

(2.1) *Kinetic equations*

The relationships involved in the above mechanism are presented below. They assume that the alkyl ion exists under steady conditions. An expression for the steady state concentration can be given in the following form

$$d\,[R^+]/dD = \varphi - k_1[R^+]\,[Vi] - k_2\,[R^+]\,[Vl] = 0 \tag{6}$$

where $[R^+]$, $[Vi]$ and $[Vl]$ represent the alkyl ion, vinyl and vinylene group concentrations, and D represents the dose. φ, k_1 and k_2 are reaction constants associated with reactions in the reaction sequences (1) and (4).

Under the assumed steady state conditions, equation (6) can be expressed as

$$[R^+] = \varphi / \{k_1\,[Vi] + k_2\,[Vl]\} \tag{7}$$

and the yield relationship involving allyl radical formation and vinyl group decay can be expressed as

$$\frac{d\,[A]}{dD} = -\frac{d\,[Vi]}{dD} = k_1\,[R^+]\,[Vi] = \frac{\varphi k_1\,[Vi]}{k_1\,[Vi] + k_2\,[Vl]} \tag{8}$$

where $[A]$ is the allyl radical concentration. Integration of equation (8) is possible if it is assumed that vinylene group formation is linearly dependent on dose. Justification for this assumption will be provided in section 5. Thus, $[Vl] = k_3D$ (k_3 is the yield) and

$$d\,[A]/dD = -d\,[Vi]/dD = \varphi k_1\,[Vi]/\{k_1\,[Vi] + k_2k_3D\} \tag{9}$$

Integration of equation (9) for the case of vinyl decay gives

$$-\ln D = \frac{k_2k_3}{\varphi k_1} \ln \frac{[Vi]}{[Vi]_{D=1}} + \ln\left(k_1\frac{[Vi]}{D} + \varphi k_1 + k_2k_3\right) - \ln\,(k_1\,[Vi]_{D=1} + \varphi k_1 + k_2k_3) \tag{10}$$

Evidence that equation (10) applies to the reactions under consideration, i.e. radical formation and vinyl disappearance, is provided in *Figures 2* and *3*. The data from the present study and those from Dole *et al.*[8] are plotted in these figures. When $[Vi]/D$ is sufficiently small, during the latter stages of the reaction, a plot of $\ln D$ versus $\ln [Vi]/[Vi]_{D=1}$, *Figure 2*, is linear with a slope equal to $k_2k_3/\varphi k_1$ and an intercept (I_R or I_{Vi}) of the constant terms in equation (10). The subscripts R and Vi relate the intercepts

to the radical formation and vinyl group decay data, respectively. The substitution of the radical precursor concentration for [Vi] in these equations implies that a radical is formed for each vinyl group which disappears.

The form of equation (9) allows only for the determination of the ratios of the reaction constants associated with [Vi] and D. However, if it is
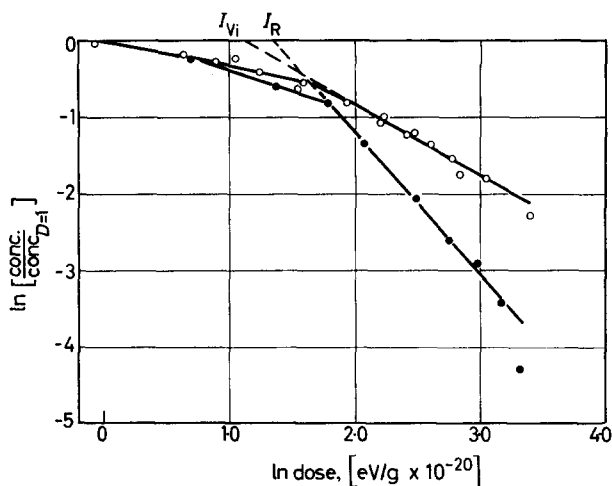
Figure 2—Evaluation of $k_2 k_3 / \varphi k_1$ from equation (10). ●, radicals, data from the present study; ○, vinyl groups, data from Dole et al.[8]

assumed that $\ln (k_1 [Vi]_{D=1} + \varphi k_1 + k_2 k_3) \gg \ln (\varphi k_1 + k_2 k_3)$ (these terms represent the intercept I in Figure 2), or more concisely, that $k_1 [Vi]_{D=1} \gg \varphi k_1 + k_2 k_3$, then equation (10) can be rearranged to give

$$\exp \left(I - \ln D - \frac{k_2 k_3}{\varphi k_1} \ln \frac{[Vi]}{[Vi]_{D=1}} \right) = k_1 \frac{[Vi]}{D} + \varphi k_1 + k_2 k_3 \qquad (11)$$

A plot of the left hand member of equation (11) versus $[Vi]/D$ should provide a straight line of slope k_1 and an intercept of the constant terms. The linear plot was realized from the radical formation data of this study and the data of Dole et al.[8], Figure 3. From the slopes in Figures 2 and 3 and the intercepts in Figure 3, values for φ, k_1 and $k_2 k_3$ were determined.

Charlesby et al.[5] have also measured the decay of vinyl groups in Marlex polyethylene. The lack of low exposure values in their data and the precision of their data did not permit an evaluation of the same constants by the above method. Vinyl group concentrations were calculated as a function of dose however, and these values were used to obtain values for φ, k_1 and $k_2 k_3$.

To obtain a reaction constant for calculating the vinyl concentrations, a second order decay process was assumed. The validity for this assumption will be discussed in section 2.3. Recently, Dole et al.[6] published additional vinyl decay data. A set of constants was not determined from these data, however.
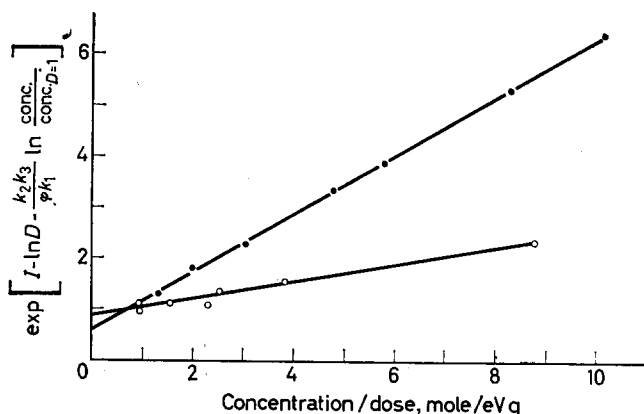
Figure 3—Evaluation of k_1 and $\varphi k_1 + k_2 k_3$ from equation (11).
●, radicals, abscissa $\times 10^{-3}$, data from the present study;
○, vinyl groups, abscissa $\times 10^{25}$, data from Dole *et al.*[8]

Table 2 provides comparative data from the radical formation and the vinyl decay studies. In order to convert the radical concentrations from arbitrary units to moles, it was assumed that the radical concentration at the intercept, *Figure 1*, obtained in arbitrary units, corresponds to the initial vinyl concentration in Marlex 50, 1.08×10^{-4} mole/g[5, 8, 10, 11]. Evidence

Table 2. Values for constants in equation (9)

Constant	From radical formation data (mean values)	From vinyl decay data	
		Dole *et al.*[8]	Charlesby *et al.*[5]
φk_1 (eV)$^{-2}$	0·35	0·37	0·40
k_1 (mole eV)$^{-1}$	3.01×10^{24}	1.70×10^{24}	1.47×10^{24}
φ (mole/eV)	1.15×10^{-25}	2.18×10^{-25}	2.72×10^{-25}
$G(\varphi)$ (molecule/100 eV)	6.9 ± 0.6	13·1	16·4
$k_2 k_3$ (eV)$^{-2}$	0·22	0·51	0·54
k_2 (mole eV)$^{-1}$	7.9×10^{24}	12.8×10^{24}	13.6×10^{24}

for this assumption is provided by the observation that the vinyl group decay and free radical formation reaction constants are sufficiently similar to assume a 1 : 1 correspondence. It was also assumed that the linear radical formation constant, k_0, *Table 1*, is proportional to G (Vl) (vinylene). A G (Vl) value of 1.7_3 was obtained in the present study. This was used to determine k_3 and then k_2 for the radical formation data. A corresponding G (Vl) value[8] of 2·4 was used to obtain k_3 and k_2 for the vinyl group decay data.

The above values from the two types of experiments differ markedly except for the values of φk_1. General agreement in the values for φk_1 is not surprising since they are related to the first order reaction constants for radical formation and vinyl group decay. However, the individual values

70

for φ and k_1 differ approximately by a factor of two. Since φ was determined from k_1, validity for one or the other set of these values was sought elsewhere.

(2.2) Significance of G (φ)

It is significant that the value for the ion yield from the allyl radical formation data, $G(\varphi_A) = 6.9 \pm 0.6$, in polyethylene is the same as the G values for alkyl radical yields, $G(R)$, of the lower molecular weight saturated hydrocarbons. Free radical yields from a variety of hydrocarbons have been determined with the aid of iodine and the diphenylpicrylhydrazyl radical (DPPH). The mean $G(R)$ values for all data collected by Chapiro[12] are $G(I) = 6.9 \pm 1.0$ and $G(DPPH) = 6.5 \pm 0.6$. Branching apparently does not affect the radical formation yield.

Of particular interest is the $G(R)$ value for alkyl radical formation in polyethylene, 6.4, obtained by Ohnishi[13]. This value is in agreement with that for $G(\varphi_A)$, Table 2. The agreement in values shows that most or all of the ions formed initially produce alkyl or allyl radicals. It should be added, however, that the $G(R)$ value for polyethylene was found not to be constant, but decreased with increasing dose. The value of 6.4 represents an initial value obtained from the tangential slope of the non-linear relationship, radicals versus dose. The several values for $G(\varphi_A)$, $G(I)$, $G(DPPH)$ and $G(R)$ make it possible to assign a proper value of 6.9 to $G(\varphi)$.

(2.3) Second order character of the vinyl group decay reaction

The agreement between $G(\varphi_A)$, $G(I)$, $G(DPPH)$ and $G(R)$ indicates that $G(\varphi_{Vi})$ is greater than should be expected from the suggested mechanism. This is also true for k_2 which is the constant for the ion–vinylene group interaction.

The factor of two between $G(\varphi_A)$ and $G(\varphi_{Vi})$ can be explained by assuming that the vinyl groups disappear in pairs. This assumption is proven, in part, from evidence that vinyl decay approximates bimolecular kinetics very closely. One set of second order reaction constants was obtained from the data of Dole et al.[8], using equation 12,

$$1/[Vi] - 1/[Vi_0] = k_4 D \tag{12}$$

where k_4 is the reaction constant. A mean value of $2.67 \pm 0.25 \times 10^{-17}$ (mole eV)$^{-1}$ was obtained when an initial mean vinyl concentration value of 1.08×10^{-4} mole/g[5, 8, 10, 11] was used. This latter value is in agreement with the value of 1.05×10^{-4} mole/g obtained from the data of Dole et al.[8] when a straight line plot of $1/[Vi]$ versus dose is extrapolated to zero dose. The linear requirement for this plot follows from equation (12). Although the mean deviation for the rate constants from their mean value is ± 9.4 per cent, the individual reaction constants show no deviating pattern toward higher or lower values. This observation supports the second order character for this reaction.

In addition to the above vinyl decay data, the data of Lawton, Balwit and Powell[14], Charlesby et al.[5] (γ-irradiations), and Dole et al.[6] also provide

linear second order plots and calculated reaction constants which are constant within experimental error. Reaction constant values of $2 \cdot 40 \times 10^{-17}$, $2 \cdot 21 \pm 0 \cdot 35 \times 10^{-17}$, and $2 \cdot 63 \pm 0 \cdot 14 \times 10^{-17}$ (mole eV)$^{-1}$, respectively, were obtained from the data in the above publications. In none of the above studies did the first order constants approach the degree of correlation realized with the second order constants.

Additional evidence that the factor of two is associated with the decay of vinyl groups in pairs can be obtained directly from equation (8). The evidence assumes that the vinyl group captures the transferred charge associated initially with the alkyl ion to give another ion, Vi^+. This ion then reacts with an additional vinyl group or may possibly interact with a vinylene group. Equation (13) represents the kinetic equation for the formation and decay of the vinyl ion. It is assumed that it exists in a steady state condition.

$$d [Vi^+]/dD = k_1[R^+] [Vi] - k_5[Vi^+] [Vi] - k_6 [Vi^+] [Vl] = 0 \qquad (13)$$

$$[Vi^+] = k_1 [R^+] [Vi]/\{k_5 [Vi] + k_6 [Vl]\} \qquad (14)$$

Substituting an expression for $[R^+]$ from equation (7) and once again assuming that $[Vl] = k_3D$, equation (14) becomes

$$[Vi^+] = \varphi k_1 [Vi]/(k_1 [Vi] + k_2k_3D) (k_5 [Vi] + k_3k_6D) \qquad (15)$$

Equation (9) can now be modified to include the secondary reaction of the vinyl ion.

$$-d [Vi]/dD = \varphi k_1[Vi]/\{k_1 [Vi] + k_2k_3D\} + k_5 [Vi^+] [Vi] + k_3k_6 [Vi^+] [Vl] \qquad (16)$$

Substituting for $[Vi^+]$ from equation (15), and simplifying gives

$$-d [Vi]/dD = 2\varphi k_1 [Vi]/\{k_1 [Vi] + k_2k_3D\} \qquad (17)$$

The factor 2 in equation (17) shows that the yield for the decay of vinyl groups in the secondary reaction is equal to that for the primary reaction in which vinyl ions are formed. The existence of this factor 2 is verified experimentally in the data of *Table 2* where, within experimental error, $G (\varphi_{Vi}) = 2G (\varphi_A)$. Equation (17) also shows that the yield is independent of the values for k_5 and k_6. This result follows from the imposed steady state condition on equation (13) in which vinyl ion formation is the rate controlling step.

Equation (13) includes a term for the reaction of vinyl ions with vinylene groups. The general form of this equation is such that deletion of this term or addition of other possible vinyl ion reactants would not change the character of equation (17). This follows from the condition that the rate determining step is the formation of vinyl ions, rather than the interaction of these ions with other reactive groups. The inclusion of a vinylene term in equations (13) to (16) is motivated by the generalization that most forms of unsaturation act as traps for charges on ions.

The assumption that vinyl groups in polyethylene dimerize by an ionic mechanism is consistent with the behaviour of vinyl groups in lower molecular weight olefins under irradiation conditions. This is seen in the

results of Chang, Yang and Wagner[15], who studied hexene-1 and octene-1, and in the results of Collinson, Dainton and Walker[16] who studied n-hexadecene-1. The correlations in these several studies will be discussed in another publication.

(2.4) Comparison of calculated and experimental data

The adequacy of equation (9) to describe the formation of allyl radicals and the decay of vinyl groups is seen in comparative plots of calculated and experimental values. The calculated values were obtained from equation (9) by the use of the Runge–Kutta numerical method for solving differential equations. *Figure 4* shows the correlation between calculated
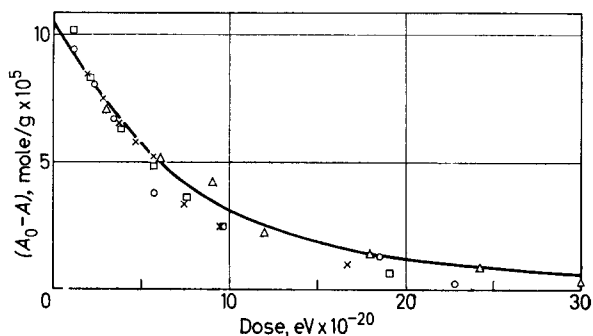
Figure 4—Comparative calculated and experimental radical formation data. (A_0-A), radical precursor concentration. Calculated values (line) are from equation (9). Values for constants are from *Table 2*. Points are experimental data from the following dose rate experiments, $(eV/g \ min \times 10^{-20})$: $\bigcirc$, 0.72; $\times$, 1.09; $\square$, 1.19; $\triangle$, 3.64

(line) and experimental (points) values for radical formation in terms of (A_0-A) which is the allyl radical precursor concentration. The experimental points were obtained from four experiments involving different dose rates. The values for φ, k_1 and k_2k_3, listed in *Table 2* under Radical Formation Constants, were used to obtain the calculated values. Similar calculated plots, *Figure 5*, were prepared for vinyl group decay from constants in *Table 2* for the data of Charlesby et al.[5] (dashed line) and Dole et al.[8] (solid line). The superimposed experimental points follow the calculated values well at low radiation exposures in both figures. At high exposures, however, it appears that the calculated values for vinyl decay for the data of Dole et al.[8] and for radical formation are higher than the observed values, although they are not very far removed from the range enclosing the experimental error.

An alternative equation for obtaining calculated values for radical formation and vinyl decay, and one which adds support to the hypothesis for a second order vinyl decay reaction, is obtained from the following. When equation (12) is rearranged to the following form

$$[Vi] = [Vi_0] / \{k_4 [Vi_0] D + 1\} \tag{18}$$
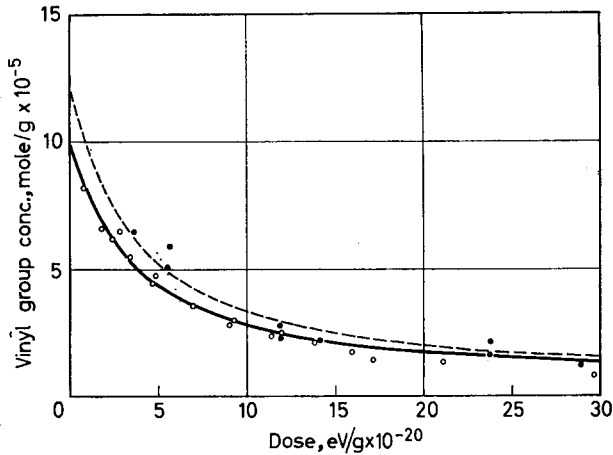
Figure 5—Comparative calculated and experimental vinyl group decay data. Calculated values are from equation (9) and *Table 2*. Data from Dole *et al.*[8]: solid line, calculated values; O, experimental points. Data from Charlesby *et al.*[5]: dashed line, calculated values; ●, experimental values

and when the above expression for [Vi] is substituted into equation (9), the resultant equation obtained is

$$\frac{d[A]}{dD} = -\frac{d[Vi]}{dD} = \frac{\varphi k_1 [Vi_0]}{k_1 [Vi_0] + k_2 k_3 D + k_2 k_3 k_4 [Vi_0] D^2} \tag{19}$$

The substitution has separated the variables and provided an equation which is readily integrated. The integrated form is given below.

$$[A] = [Vi_0 - Vi] = (c/q^{1/2}) \tan^{-1} \{(2cD + b)/q^{1/2}\} \tag{20}$$

where $c = k_2 k_3 k_4 [Vi_0]$, $b = k_2 k_3$, and $q = 4k_1 k_2 k_3 k_4 [Vi_0]^2 - (k_2 k_3)^2$.

Figures 6 and *7* provide comparative data between calculated values for [A] and [Vi_0 − Vi] (lines) and observed values (points), respectively. The correlation between calculated and observed values for vinyl group decay is good; however, some deviation exists in the higher dose range for radical formation.
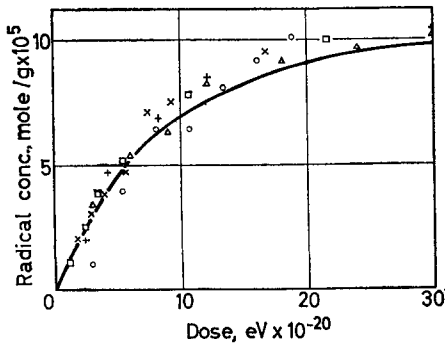
Figure 6—Comparative calculated and experimental radical formation data. Calculated values (line) are from equation (20). Average values for the constants which were used:
$k_4 = 2.43 \times 10^{-17}$ (mole eV)$^{-1}$, [Vi_0] = 1.08×10^{-4} mole/g. The values for the other constants are from *Table 2*. Dose rates for the experimental points, (eV/g min × 10^{-20}: O, 0.63; ×, 1.09; +, 2.52; □, 3.38; △, 3.64

(3) *Correlation between G (φ) and crosslinking*

The G values for crosslinking or polymerization, $G(X)$, obtained for a series of saturated and unsaturated hydrocarbons provides additional evidence that underscores the conclusions in this study (especially the bimolecular character of the vinyl decay reaction) and relates them to crosslinking. For vinyl olefins, $G(X)_{Vi}$ attains a maximum value[17] of 6·0; thus, $G(\varphi_R) \sim G(X)_{Vi}$. Centrally located vinylene group olefins and acetylenes, however, provide an average $G(X)_{Vl}$ value of 3·6, thus
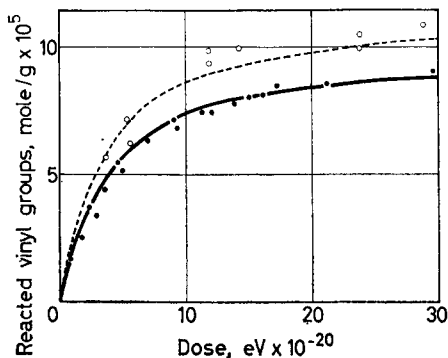
Figure 7—Comparative calculated and experimental data for reacted vinyl groups. Calculated values are from equation (20). Values for φk_1 and $k_2 k_3$ are from *Table 2*. Values for $[Vi_0]$ and k_4 were obtained from the data of the following authors. Dole et al.[8]: solid line, calculated values; ●, experimental data. Charlesby et al.[5]: dashed line, calculated values; ○, experimental data

$G(\varphi_R) \sim 2G(X)_{Vl}$. These results show that one alkyl ion causes vinyl group dimerization to take place as with polyethylene. However, two ions are needed for vinylene group hydrocarbon crosslinking or dimerization, i.e. each vinylene group requires activation by an ion prior to crosslinking. These results and other aspects of crosslinking related to this study will be discussed in greater detail in another publication.

(4) *G value for allyl radical formation*

The mechanism for radical formation which has been presented provides a basis for calculating G values for allyl radical formation, $G(A)$, from vinyl group decay and vinylene group formation data. $G(A)$ will not be constant since its value depends on both the vinyl and vinylene group concentrations and these will vary with dose. A maximum value for $G(A)$ will be realized initially when the vinyl group concentration is a maximum. Since a 1 : 1 correspondence exists between allyl radical formation and vinyl group decay, $G(A)$ can be obtained from the reaction constant for vinyl group decay and the initial vinyl group concentration. These values provide a mean $G(A)$ value of 16. At higher doses after the vinyl groups have reacted, radical formation will be equivalent to vinylene group formation. Since $G(Vl)$ was found to have a value of $1·7_3$ in the present study, this value would represent a limiting value for $G(A)$.

The above range of G values, 16 to $1·7_3$ obtained at room temperature irradiations, is of interest since it can be compared with a G value based on a possible alkyl–allyl radical transformation at lower temperatures. Results from the present study and those from Ohnishi[13] show that $G(M)$ (alkyl radicals) can have values of 6·9 and 6·4, respectively. The previous

publication, Part I, shows that at very low doses a maximum value of 0·039 is obtained for the ratio [A]/[M] where [A] is the allyl radical concentration at room temperature following alkyl radical decay, and [M] is the initial alkyl radical concentration obtained at $-185°C$ for liquid nitrogen irradiations. An alkyl–allyl radical transformation would provide a maximum $G(A)$ value of 0·27 (calculated from the above value of 0·039). This value correlates well with the $G(A)$ value of 0·31 obtained by Ohnishi[13] under similar conditions. Since the calculated $G(A)$ values of (16 to 1·7$_3$) from the present study are so much higher than the value of 0·3 realized when alkyl radicals are formed initially, they provide additional evidence that allyl radical formation at room temperature does not involve an alkyl–allyl radical transformation in any large proportions, if at all.

(5) trans-*Vinylene formation*

It is assumed in the present study that the *trans*-vinylene group formation yield is constant with respect to dose and that these groups contribute to radical formation [equation (8)]. Support for these assumptions has been provided in terms of the correlation between calculated and experimental data for several derived equations. Additional support is provided by showing that the radical yield obtained in this study for the linear radical formation process (*Table 1*) corresponds to the *trans*-vinylene yield.

The *trans*-vinylene formation yield was found to be constant with dose for Marlex 50 polyethylene over a $3·3 \times 10^{21}$ eV/g range covered in the study. However, not all investigators have found the yield to be constant. Charlesby *et al.*[5] have collected the *trans*-vinylene formation data from a number of publications and discussed the effect of dose on this process in the light of their own observations. The extent of the deviation from initial linearity varies with the polyethylene type and with the particular study. Reasons for these differences are also discussed by Sears[9]. It is of particular interest to this study, however, that all investigators consider vinylene formation to be linear with dose and that deviations from linearity are due to secondary reactions.

Infra-red techniques provided a G (Vl) value of 1·7$_3$ in the present study. In addition to the i.r. techniques, it was also possible to determine G (VI) from the reaction constant for radical formation, *Table 1*, which is given in arbitrary units. The determination was made by converting the radical concentration in arbitrary units to conventional units, as before, from a conversion factor relating the maximum radical concentration in the high yield reaction to the vinyl concentration. The conversion factor, therefore, was obtained from a source independent of vinylene formation.

A G (Vl) value of 1·6$_8$ which was obtained by this method is in good agreement with the value of 1·7$_3$ realized by i.r. techniques. The agreement confirms the relationship between the linear radical formation and *trans*-vinylene formation reactions. The agreement also implies that all *trans*-vinylene groups form allyl radicals.

SUMMARY

A kinetic study of allyl-free radical formation in polyethylene by 2 MeV electrons shows that radical formation can be quantitatively related to vinyl

group disappearance and vinylene group formation. A mechanism is formulated and kinetic equations are derived which are based on a positive alkyl ion being formed initially, when radiation interacts with polyethylene, which exist under steady-state conditions. The charge associated with this ion is transferred and trapped by vinyl and vinylene groups. When vinyl groups trap the charge, the resultant vinyl ion reacts with a second vinyl group. The resultant divinyl or vinylene ion forms an allyl radical following charge neutralization. The derived kinetic equations are verified with experimental data from radical formation, vinyl decay and vinylene formation studies. *G* values obtained from this study correlate well with those obtained for lower molecular weight saturated and unsaturated hydrocarbons in radical formation and polymerization studies.

REFERENCES

[1] AUERBACH, I. *Polymer, Lond.* 1966, **7,** 283

[2] CHARLESBY, A. *Atomic Radiation and Polymers,* Chap. 13. Pergamon: New York, 1960

[3] CHAPIRO, A. *Radiation Chemistry of Polymeric Systems,* Chap. IX. Interscience: New York, 1962

[4] CROOK, M. A. and LYONS, B. J. *Trans. Faraday Soc.* 1963, **59,** 2334

[5] CHARLESBY, A., GOULD, A. R. and LEDBURY, K. J. *Proc. Roy. Soc. A,* 1964, **277,** 348

[6] DOLE, M., FALLGATTER, M. B. and KATSUURA, K. *J. phys. Chem.* 1966, **70,** 62

[7] DE KOCK, R. J., HOL, P. A. H. M. and BOS, H. *Z. anal. Chem.* 1966, **205,** 371

[8] DOLE, M., MILNER, D. C. and WILLIAMS, T. F. *J. Amer. chem. Soc.* 1958, **80,** 1580

[9] SEARS, W. C. *J. Polym. Sci. A,* 1964, **2,** 2455

[10] SMITH, D. C. *Industr. Engng Chem. (Industr.),* 1956, **48,** 1161

[11] CERNIA, E., MANCINI, C. and MONTAUDO, G. *Polymer Letters,* 1963, **1,** 371

[12] Ref. 3, p 82

[13] OHNISHI, S. *Bull. chem. Soc. Japan,* 1962, **35,** 254

[14] LAWTON, E. J., BALWIT, J. S. and POWELL, R. S. *J. Polym. Sci.* 1958, **32,** 257

[15] CHANG, P. C., YANG, N. C. and WAGNER, C. D. *J. Amer. chem. Soc.* 1959, **81,** 2060

[16] COLLINSON, E., DAINTON, F. S. and WALKER, D. C. *Trans. Faraday Soc.* 1961, **57,** 1732

[17] Ref. 3, p 87

Effect of Uranyl Perchlorate on the Kinetics of Polymerization of Acrylamide

E. A. S. Cavell and A. C. Meeks

The effect of uranyl perchlorate on the mechanism and kinetics of the radical polymerization of acrylamide has been investigated in aqueous solution over a range of temperatures, employing 4,4'-dicyano-4,4'-azopentanoic acid as initiator. All measurements were made in the complete absence of light.

With no azo-initiator present, uranyl perchlorate has been found to initiate polymerization of acrylamide, the rate of polymerization (R_p^0) observed being approximately proportional to the concentration of the uranyl salt. The overall rate of polymerization (R_p) with the azo-initiator present is directly proportional both to the concentration of monomer and to the concentration of the azo-initiator. Linear termination of polymerization is indicated by the fact that ($R_p - R_p^0$) is approximately inversely proportional to the concentration of uranyl perchlorate.

An electron transfer mechanism has been proposed for the termination reaction and a dimeric ion, produced by the partial hydrolysis of the uranyl salt has been suggested as the entity responsible for initiation.

PHOTOCHEMICAL initiation of radical polymerization by uranyl ions (UO_2^{2+}) has been investigated by several authors[1,2], and has been shown to involve reduction of the uranyl salt to the 4-valent uranous state (UO_2H^+). The present investigation was undertaken in order to determine whether or not in favourable circumstances uranyl ions could also terminate polymerization in an analogous manner. Because of the instability of the 5-valent uranium ions with respect to their disproportion products, the significant oxidation–reduction equilibrium in aqueous acidic solutions is: —

$$UO_2H^+ + H_2O \rightleftharpoons UO_2^{2+} + H_3O^+ + 2e^-$$
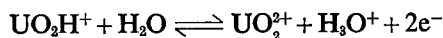
for which the standard oxidation potential[3] (E^0) is $-0.334V$ at 25°C. Now in aqueous acidic solutions, both vanadyl ions[4] ($E^0 = -0.361V$) and cupric ions[5] ($E^0 = -0.153V$) have been found to terminate the radical polymerization of acrylamide, the termination reaction being first-order with respect to the metal salt.

Thermodynamic considerations are not in themselves sufficient to establish the actual occurrence of a reaction since the availability of a suitable mechanism is also an essential requirement. Nevertheless acrylamide was the obvious choice as monomer for the present study. As in previous investigations, the water-soluble azo-compound, 4,4'-dicyano-4,4'-azopentanoic acid (ACV) was used to initiate polymerization. All measurements were necessarily made in the complete absence of light, in order to avoid complications from photochemical initiation by the uranyl salt.

EXPERIMENTAL

Commercial acrylamide was purified by successive crystallizations from benzene, followed by vacuum drying; m.pt 84.5°C. 4,4'-Dicyano-4,4'-

azopentanoic acid was prepared and purified as described previously[6] and water used as solvent was deionized by allowing it to percolate through Amberlite monobed resin MB-1. Ninety per cent perchloric acid (reagent grade) was twice distilled *in vacuo* before use. Uranyl perchlorate was prepared by repeatedly fuming uranyl acetate with perchloric acid until the odour of acetic acid was imperceptible. Stock solutions of uranyl perchlorate were prepared and analysed gravimetrically by precipitating and weighing the uranyl complex formed with 8-hydroxyquinoline[7].

Rates of polymerization were measured by the dilatometric procedure described in an earlier paper[4]. In order to exclude light as far as possible, all measurements were performed in a photographic darkroom. The bulb of the dilatometer was itself housed in an aluminium can, the inner surface of which had been suitably blackened. The can was immersed in a thermostat and allowed to fill with water. The capillary of the dilatometer protruded through a small hole in the top of the can, which was sealed to prevent the ingress of any light. A low powered lamp was used when readings of the meniscus level were actually being taken but this was switched off immediately the reading had been recorded. Satisfactory linear plots of contraction against time were obtained, indicating that the effect of any photo-initiation was negligible. A shrinkage factor of 0·050 millimole of acrylamide polymerized for a contraction of 1 mm in a capillary of 1 mm diameter was used to calculate rates of polymerization.

R E S U L T S

In spite of the complete exclusion of light, uranyl perchlorate in decimolar perchloric acid solutions is still able to initiate the polymerization of acrylamide under our experimental conditions. Rates of polymerization (R_p^0) obtained with no initiator other than uranyl perchlorate present are summarized in *Figure 1*, in which R_p^0 has been plotted against the concen-
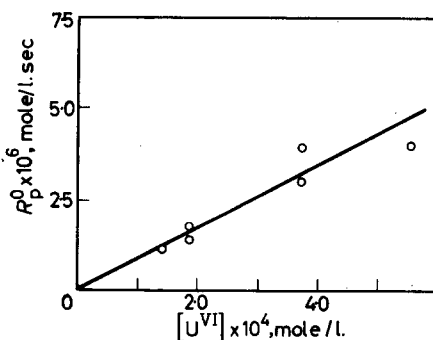
Figure 1—Variation of rate of polymerization (R^0) with concentration of uranyl perchlorate ($[U^{VI}]$) in the absence of azo-initiator. Temperature 25°C; monomer concentration = 1·00M; $[HClO_4] = 0·11$M

tration of the uranyl salt ($[U^{VI}]$). The slope of the linear plot shown is $8·7 \times 10^{-3}$ sec^{-1}. R_p^0 also showed a noticeable tendency to increase when the concentration of perchloric acid was decreased, although the values obtained were not sufficiently reproducible to warrant the formulation of a precise functional relation between rate and hydrogen ion concentration.

The approximate linear dependence of R_p^0 on the concentration of uranyl perchlorate does not in itself provide evidence that the uranyl salt is involved in the termination step of the polymerization reaction. However, when the azo-initiator ACV is also present, the retarding effect of the uranyl salt on the polymerization of acrylamide is immediately apparent, since the total rate of polymerization (R_p) observed is now only between a third and a quarter of the value, which would have been obtained under identical conditions had there been no metal salt present[6]. In the presence of a fixed concentration of uranyl perchlorate, R_p is directly proportional to the concentration of ACV. This is illustrated in *Figure 2*, in which the best
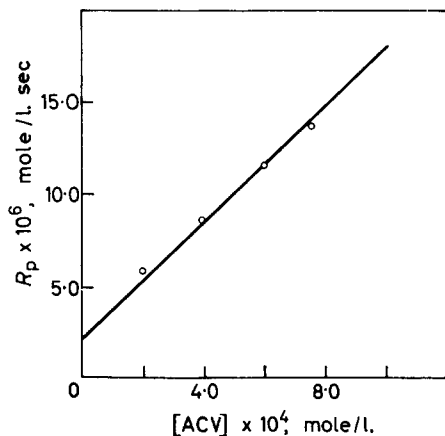
Figure 2—Variation of rate of polymerization (R_p) with concentration of azo-initiator ([ACV]). Temperature 25°C; monomer concentration $= 1.00M$; $[HClO_4] = 0.11M$; $[UO_2(ClO_4)_2] = 1.85 \times 10^{-4}M$

straight line through the experimental points has a slope of 1.57×10^{-2} sec^{-1} and gives a positive intercept on the ordinate axis corresponding to a rate of polymerization of 2.17×10^{-6} mole/l. sec. This value is in fair agreement with the average value of 1.58×10^{-6} mole/l. sec obtained for R_p^0 with the same concentration of uranyl perchlorate present. These observations indicate that termination of polymerization by uranyl perchlorate does occur under our experimental conditions. This conclusion is confirmed by the fact that for a fixed concentration of ACV, $(R_p - R_p^0)$ is approximately inversely proportional to the concentration of the uranyl salt, as shown in *Figure 3*, the straight line drawn having a slope 8.0×10^{-10} mole^2/l.^{2} sec. For the purpose of constructing this plot, R_p^0 has been taken as being directly proportional to the concentration of uranyl perchlorate.

The kinetic results summarized by means of *Figure 4* show that in the presence of fixed concentrations of both ACV and uranyl perchlorate, the total rate of polymerization is also directly proportional to the concentration of acrylamide $[m_1]$. This result demonstrates that the monomer itself is not involved in the rate determining step of either initiation process. The mean value of the ratio $R_p/[m_1]$ for the data illustrated is 5.27×10^{-6} sec^{-1}.

The effect of temperature variation on both R_p^0 and R_p has also been investigated, the initial concentrations of all reactants being kept constant for the various measurements involved. The apparent energy of activation

(E_A) as calculated from the variation of R_p with temperature was found to be $23 \cdot 9 \pm 0 \cdot 6$ kcal/mole. The corresponding value of the apparent energy of activation (E'_A) calculated from the temperature variation of R_p^0 is, however, less certain, although we estimate it to be about 13 kcal/mole.

DISCUSSION

Under our experimental conditions, uranyl perchlorate is evidently able both to initiate and to terminate the polymerization of acrylamide. Within the limits of experimental error, the rate of termination is directly proportional to the concentration of the uranyl salt, which implies that the rate of initiation must be approximately proportional to the square of its concentration. Provided therefore that mutual termination may be neglected, the total rate of polymerization in the presence of ACV may be represented by means of equation (1), in which k'_i and k_t are respectively the specific rate constant for initiation and termination by uranyl perchlorate and the other symbols have their usual significance.

$$R_p = k_p [m_1] \{k_i [ACV] + k'_i [U^{VI}]^2\} / k_t [U^{VI}]$$

$$= R_p^0 + k_p [m_1] k_i [ACV] / k_t [U^{VI}] \tag{1}$$

The propagation constant (k_p) is known[5] to be $1 \cdot 8 \times 10^4$ l./mole sec at 25°C and the rate constant for initiation by ACV (k_i) may be taken as $4 \cdot 62 \times 10^{-7}$ sec^{-1} at the same temperature[6]. The termination constant (k_t) may, therefore, be evaluated from the slopes of the plots shown in *Figures 2* and *3*, a mean value of $(2 \cdot 47 \pm 0 \cdot 39) \times 10^3$ l./mole sec at 25°C being obtained. By means of this value for k_t we estimate from the slope of the linear plot shown in *Figure 1*, that the apparent first order initiation constant (k'_i) is $1 \cdot 19 \times 10^{-3}$ sec^{-1}, and hence by appropriate substitution in equation (1), $R_p / [m_1]$ has been calculated to be $5 \cdot 25 \times 10^{-6}$ sec^{-1}, which is in excellent agreement with the value computed from the linear plot shown in *Figure 4*.

The dependence of the rate of the initiation reaction involving the uranyl salt on the square of the concentration suggests that the agency responsible for initiation is a dimeric entity derived from the uranyl salt. Several such
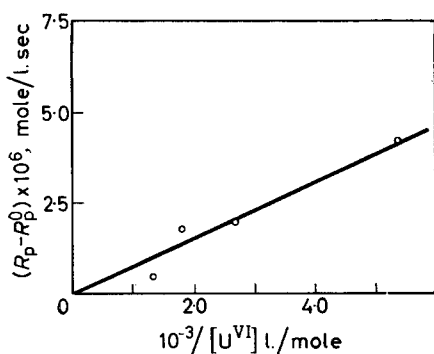
Figure 3—Plot of $(R_p - R_p^0)$ against the reciprocal of the concentration of uranyl perchlorate ([U^{VI}]). Temperature 25°C; [HClO$_4$]=0·11M; [ACV]= $2 \cdot 0 \times 10^{-4}$M; monomer concentration =1·00M

species have in fact been proposed by Sillen *et al.*[9] as partial hydrolysis products of uranyl ions, e.g.

$$2UO_2^{2+} + 2H_2O \rightleftharpoons (UO_2)_2OH^{3+} + H_3O^+$$
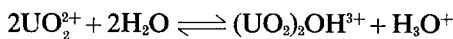
The equilibrium constants for such hydrolyses are usually found to be small, being *ca.* 10^{-4} for the example cited. The true first order initiation constant

Figure 4—Variation of rate of polymerization (R_p) with concentration of acrylamide ([m_1]). Temperature 25°C; [$HClO_4$]=0·11M; [ACV]=2·00×10^{-4}M; [$UO_2(ClO_4)_2$]=1·85×10^{-4}M
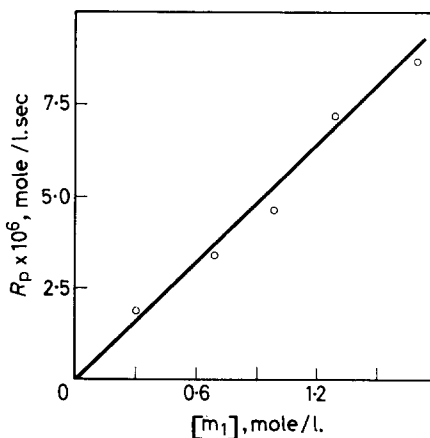
may, therefore, be much larger than the value quoted above for k_i'. In addition, since the concentration of dimer is inversely proportional to the hydrogen ion concentration, the explanation proposed is qualitatively consistent with the observed sensitivity of R_p^0 to the pH of the solution.

Termination of polymerization is probably principally due to oxidation of the polymeric radicals by the uranyl ions themselves, although the dimeric and other ionic species present may also be involved. The experimental data are not sufficiently precise for an unequivocal conclusion to be drawn.

From equation (1) it follows that the temperature variation of the rate of polymerization (R_p) may be represented by means of equation (2).

$$RT^2 \frac{d \ln R_p}{dT} = E_i + E_p - E_t + RT^2 \frac{d \ln}{dT} \left\{ 1 + \frac{k_i' [U^{VI}]^2}{k_i [ACV]} \right\} \qquad (2)$$

The energy of activation of the propagation reaction (E_p) is known[5] to be 1·38 kcal/mole and that for the initiation reaction involving ACV (E_i) may be taken[8] as 26·05 kcal/mole. The temperature coefficient of the logarithmic term on the RHS of equation (2) is numerically negative, because with increasing temperature k_i increases more rapidly than k_i' does, so that E_t probably does not therefore exceed 3·5 kcal/mole. From a plot of log ($R_p - R_p^0$) against the reciprocal of the absolute temperature, E_t has been estimated to be about 2·9 kcal/mole, although the uncertainty involved in this estimate is large because of the difficulty of obtaining reproducible values of R_r^0. However, the low energy of activation obtained for the termination reaction is consistent with an electron transfer mechanism, and is

similar in magnitude to the energies of activation reported for the oxidative termination of the polymerization of acrylamide by other metallic ions of variable valency (*Table 1*).

Table 1. Rate constants (k_t) at 25°C and energies of activation (E_t) for linear termination of polymerization and standard oxidation potentials (E^0) of metal ions[3]

Metal ion	E^0, volts	$k_t \times 10^{-3}$ l./mole sec	E_t kcal/mole	Ref.
Fe^{3+}	-0.771	2.8	2.35	5
$FeOH^{2+}$	—	21.2	0.37	5
VO^{2+}	-0.361	2.8	1.2	4
UO_2^{2+}	-0.334	2.47	~ 2.9	present work
Cu^{2+}	-0.153	1.17	5.4	5

Comparison of the appropriate data summarized in *Table 1* indicates that no obvious relation exists between the standard oxidation potential of a metal ion and the kinetic parameters of the corresponding termination reaction and none perhaps should be expected, since the thermodynamic magnitudes of a chemical reaction are independent of its mechanism. The importance of oxidation potential for investigations of the present type is the indication which it gives of the thermodynamic feasibility of a given termination reaction.

For a radical to be oxidized to the corresponding carbonium ion by means of a metal ion, the oxidation potential of the radical must necessarily be more positive than that of the reduced form of the metal ion concerned. The failure to satisfy this condition may explain the inability of uranyl ions to terminate the polymerizations of acrylonitrile, methyl methacrylate and methyl acrylate, reported by Mahadevan and Santappa[2]. According to Haines and Waters[10] the oxidation potentials of the radicals,

$$\cdot C\,(CH_3)\,(CN)\,CH_2\;CH_2CO_2H \text{ and } \cdot C\,(CH_3)_2CN$$

are approximately $-0.4V$. It seems likely, therefore, that the oxidation potentials of the polymeric radicals derived from all three monomers studied by Mahadevan and Santappa are such as to preclude their oxidation by uranyl ions. The cyano- and carbomethoxy- groups are usually considered to be more powerfully electron-withdrawing substituents than the acid amido-group[11], although the electron attracting characteristics of this last group may be modified considerably in aqueous, acidic solutions as a result of environmental interactions. Nevertheless the greater ease of oxidation of polyacrylamide radicals may well be the result of the weaker electron-withdrawing character of the acid amido-group.

Department of Chemistry,
  The University,
    Southampton

REFERENCES

[1] WHYTE, R. B. and MELVILLE, H. W. *J. Soc. Dy. Col.* 1949, **65**, 703
[2] MAHADEVAN, V. and SANTAPPA, M. *J. Polym. Sci.* 1961, **50**, 361

[3] LATIMER, W. M. *Oxidation Potentials,* 2nd ed., p 340. Prentice Hall: New York, 1952

[4] CAVELL, E. A. S. and MEEKS, A. C. *Makromol. Chem.* 1964, **78**, 178

[5] COLLINSON, E., DAINTON, F. S., SMITH, D. R., TRUDEL, G. J. and TAZUKE, S. *Disc. Faraday Soc.* 1960, No. 29, 188; *Nature, Lond.* 1963, **198**, 26

[6] CAVELL, E. A. S. *Makromol. Chem.* 1962, **54**, 70

[7] RODDEN, C. J. *Analytical Chemistry of the Manhattan Project,* p 51. McGraw-Hill: New York, 1950

[8] CAVELL, E. A. S., GILSON, I. T. and MEEKS, A. C. *Makromol. Chem.* 1964, **73**, 145

[9] HIETANEN, S. and SILLEN, L. G. *Acta chem. scand.* 1959, **13**, 1828

DUNSMORE, H. S., HIETANEN, S. and SILLEN, L. G. *Acta chem. scand.* 1963, **17**, 2644

[10] HAINES, R. M. and WATERS, W. A. *J. chem. Soc.* **1955**, 4256

[11] JAFFE, H. H. *Chem. Rev.* 1953, **53**, 191

Polymer Degradation VI—Distribution Changes on Polyisobutene Degradation in Laminar Flow

R. S. PORTER*, M. J. R. CANTOW and J. F. JOHNSON

Precisely established polymer molecular weight distribution changes with varia-tions in shear degradation history are extensively interpreted. The systems consist of solutions of polyisobutenes degraded in homogeneous, laminar-flow, shear fields. The polymer solutions studied were 9·6 volume per cent in n-hexadecane and 9·7 volume per cent in 1,2,4-trichlorobenzene. The procedure for preparing equilibrium shear degraded systems is described. A new com-puter programme is used to derive integral and differential distributions as well as molecular weight averages from number to Z+1. The programme also computed distribution inhomogeneities and standard deviations from the different molecular weight averages. It is found that the standard deviation, derived from number and weight average, changes linearly with weight average molecular weight. A predominantly random mechanism of degradation in laminar flow shear is postulated to explain the results. The efficiency of bond rupture due to storage of shear energy in polymer bonds is shown to be low. Equivalent results were obtained in the two solvents.

IN THIS laboratory some interesting features have been observed concerning changes in molecular weight distribution on exposure of polyisobutenes to high intensity and homogeneous shear fields in laminar flow. The polymer solutions were sheared at 9·6 and 9·7 volume per cent in n-hexadecane and in 1,2,4-trichlorobenzene. The source and definition of these solutions has been previously described[1]. The interpretation and understanding of in-formation on shear degradation is of practical importance in the processing and use properties of polymers.

Viscosity average molecular weights and complete molecular weight distributions have been determined on the original polymer and on each of the shear degraded polymer solutions. Proton magnetic resonance mea-surements have confirmed that the polymer was essentially pure polyiso-butene. This polymer has advantages for shear degradation studies because it is linear, amorphous, and not prone to crosslink on degradation.

Details of the instrument used to perform the shear degradation experi-ments have been recently published[2]. A special attachment has been developed for this rotational concentric-cylinder viscometer which permits a slow, regular, and controlled flow of test polymer solution through the rotating cylinders where the shear degradation is performed. This new technique provides extrusion of solution from the cylinders after it has been exposed to equilibrium conditions for shear degradation. The new equip-

*University of Massachusetts, Amherst, Mass.

ment for extruding the polymer solution is illustrated in *Figure 1*. It is a motor-driven metal syringe which exposes the test fluid to shear rates only a fraction of those developed between the concentric cylinders. This is also confirmed by measurement on extruded solution which indicates no changes in polymer molecular weight.
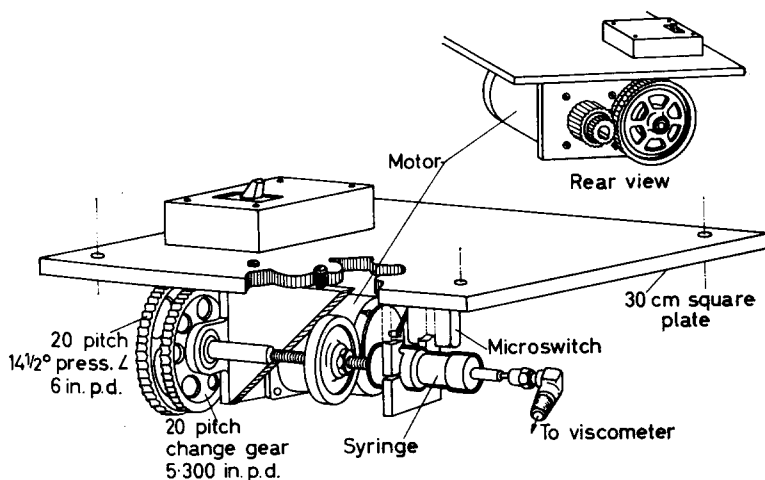
Figure 1—Motor driven syringe for high shear viscometer injection

Table 1 shows clearances between the concentric cylinders in the rotational viscometer which were used in the laminar-flow shear degradation studies. The clearance, and therefore, the shear rate for a given speed of

Table 1. Sample injection conditions for laminar flow shear degradation

Viscometer cylinders		Sample injection rate, cm^3/min			
		0·151	0·0754	0·0302	0·0151
Inner cylinder	*Clearance,* cm*	Viscometer residence time, sec			
A	$7·74 \times 10^{-4}$	1·81	3·63	9·06	18·1
C	$5·01 \times 10^{-4}$	1·74	2·35	5·87	11·7
E	$3·56 \times 10^{-4}$	0·83	1·67	4·16	8·33
3A	$1·32 \times 10^{-4}$	0·31	0·62	1·55	3·1

*Same outer cylinder.

rotation may be varied by choice of inner cylinder. The speed of rotation may also be adjusted continuously from 20 to 2 000 rev/min. The shear volume has nominal dimensions of 1·0 in. in diameter and 1·88 in. in length. The residence time for an element of polymer solution in the shear volume at each of the four possible injection rates is also given in *Table 1*. From this matrix of residence times it was found that a minimum of about two seconds is required for equilibrium shear degradation. Attainment of degradation equilibrium was ascertained by comparison of viscosities measured during continuous injection versus viscosities measured without flow

through the shear volume. These measurements were made *in situ* in the concentric cylinder instrument[2].

The shear degradation data on polyisobutene appear to be the most definitive of any made under conditions of laminar flow in a high and homogeneous shear field[1,3]. The gel permeation chromatographic fractionation method used has been described[4]. The data are interpreted here with the aid of a recently published computer programme[5] which prints out directly complete integral and differential molecular weight distributions. Also computed have been the distribution index, U, and the standard deviation of the molecular weight distribution, σ. These measures of dispersion have been computed for the original and each of the shear degraded samples using molecular weight averages from number to $Z+1$, see equations (1) and (2).

$$U_n = (M_w/M_n) - 1; \qquad U_w = (M_z/M_w) - 1; \qquad U_z = (M_{z+1}/M_z) - 1 \qquad (1)$$

$$\sigma_n = \{M_w M_n - M_n^2\}^{\frac{1}{2}}; \qquad \sigma_w = \{M_z M_w - M_w^2\}^{\frac{1}{2}}; \qquad \sigma_z = \{M_{z+1} M_z - M_z^2\}^{\frac{1}{2}} \qquad (2)$$

The change in distributions due to degradation has been followed in terms of these parameters. Distribution changes have also been evaluated in terms of rate of energy input and reduced variables for laminar-flow shear degradation. The results aid in evaluation of the extent, selectivity, and nature of polymer degradation in laminar flow shear.

RESULTS AND DISCUSSION

Tables 2 and 3 show a compilation of data on the original polymer and on this polymer degraded in a series of successively higher shear fields in laminar flow. The degraded polymers represent the equilibrium molecular weight distribution for shear degradation at the stated shear conditions. It has been previously shown that shear intensity can be successfully ex-
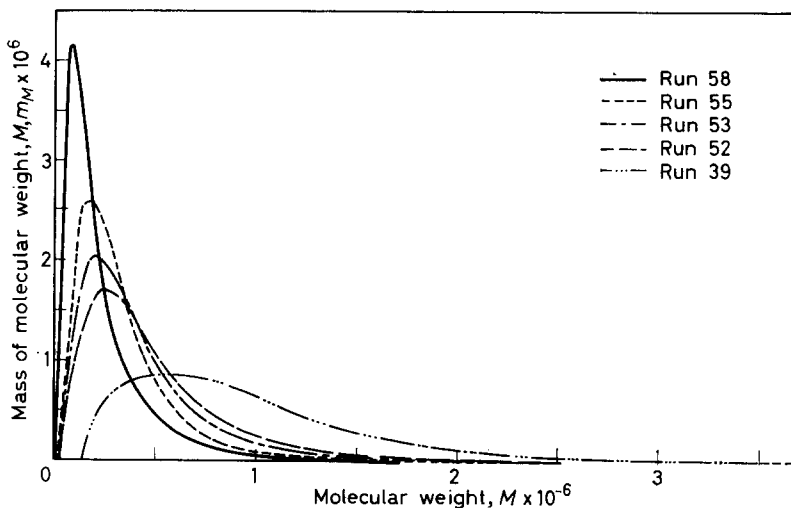
Figure 2—Changes in differential molecular weight distributions with shear intensities

Table 2. Molecular weights computed for shear degraded polyisobutene solutions

Polymer system and shear conditions		GPC run no.	Degrading stress, dyne $\overline{cm^2 \cdot T°K}$	Small peak, wt %	Molecular weight averages, $\times 10^{-3}$:			
					M_n	M_w	M_z	M_{z+1}
Original Run 1		36	—	Nil	609	938	1 300	1 640
Undegraded polyisobutene, M_v 8·0×10⁵ Run 2		39	—	Nil	646	925	1 240	1 560
Solution in 1,2,4-trichlorobenzene (TCB)		54	—	Nil	564	957	1 470	2 050
TCB solution pumped but unsheared		56	—	Nil	583	874	1 200	1 530
Degraded 1·72×10⁵ sec⁻¹ 55°C TCB solution		52	161	Nil	281	481	717	960
Degraded 1·72×10⁵ sec⁻¹ 40°C TCB solution		53	205	Nil	239	413	647	889
Degraded 3·44×10⁵ sec⁻¹ 40°C TCB solution	Main peak	55A	236	13·1	210	341	542	821
Degraded 3·44×10⁵ sec⁻¹ 21°C TCB solution	Main peak	57A	276	7·0	133	254	486	822
Degraded 7·15×10⁵ sec⁻¹ 21°C	Main peak	58A	566	7·4	119	228	397	589
n-Hexadecane solution Degraded 3·44×10⁵ sec⁻¹ 60°C	Main peak	38A	~250	14·5	168	289	447	619

Table 3. Measures of distribution for shear degraded polyisobutene solutions

Polymer system and shear conditions		Dispersion indexes			Standard deviations		
		M_w/M_n	M_z/M_w	M_{z+1}/M_z	$\sigma_n \times 10^{-5}$	$\sigma_w \times 10^{-5}$	$\sigma_z \times 10^{-5}$
Original Undegraded polyisobutene, $M_F\ 8\cdot0\times10^5$	Run 1	1·54	1·38	1·26	4·48	5·81	6·68
Solution in 1,2,4-trichlorobenzene (TCB)	Run 2	1·43	1·34	1·26	4·24	5·43	6·31
		1·69	1·54	1·39	4·71	7·03	9·24
TCB solution pumped, unsheared TCB solution		1·50	1·38	1·27	4·12	5·37	6·27
Degraded $1\cdot72\times10^5\ \text{sec}^{-1}$ 55°C TCB solution		1·71	1·49	1·34	2·37	3·37	4·18
Degraded $1\cdot72\times10^5\ \text{sec}^{-1}$ 40°C TCB solution		1·72	1·54	1·39	2·04	3·05	4·00
Degraded $3\cdot44\times10^5\ \text{sec}^{-1}$ 40°C TCB solution	Main peak	1·62	1·59	1·51	1·66	2·62	3·89
Degraded $3\cdot44\times10^5\ \text{sec}^{-1}$ 21°C TCB solution	Main peak	1·90	1·92	1·69	1·27	2·43	4·04
Degraded $7\cdot15\times10^5\ \text{sec}^{-1}$ 21°C	Main peak	1·91	1·75	1·48	1·14	2·00	2·76
n-Hexadecane solution Degraded $3\cdot44\times10^5\ \text{sec}^{-1}$ 60°C	Main peak	1·72·	1·54	1·39	1·48	2·13	2·78

pressed for these systems in terms of shear stress divided by absolute temperature and polymer volume concentration[1,3]. The general idea for use of standard deviations (see *Table 3*) to express distributions has recently been reintroduced for interpreting both temporary (Newtonian flow) and permanent (polymer degradation) viscosity changes with shear[6].

Figure 2 shows the complete differential molecular weight distributions for the shear degradation series on polyisobutene. It may be seen that the
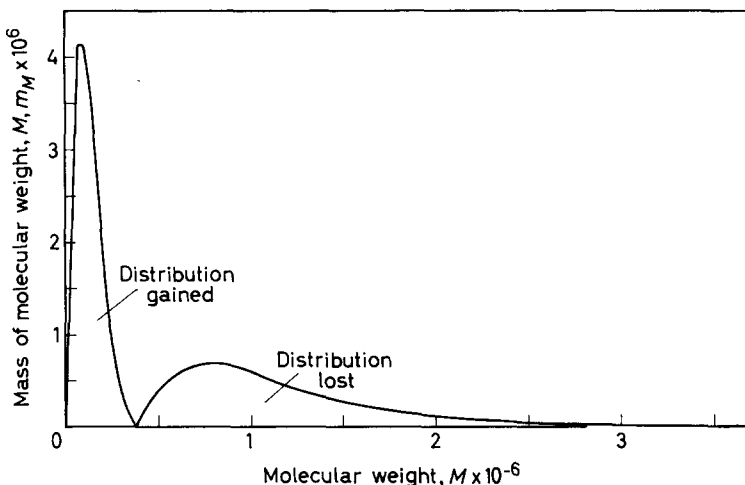
Figure 3—Differences in differential distributions between original (Run 39) and shear degraded polyisobutene (Run 58)

distributions move generally to lower molecular weights. The change in viscosity average molecular weight with the intensity of the shear field for these systems has been quantitatively predicted and correlated by the use of previously developed reduced variables[1,3]. It is the goal of this study to evaluate the change in complete molecular weight distribution for the purpose of establishing the mechanism of degradation and predicting the course of reaction.

Figure 3 represents a further interpretation in terms of distribution changes. This figure shows the distribution of polymer molecular weights which were reacted and the distribution of molecular weights which were formed in the most severe shear degradation experiments. The number of bonds broken to accomplish reaction may be calculated from the number average molecular weight for original and degraded polymer. This equation

is
$$n = w \left(1/M_d - 1/M_0\right) \tag{3}$$

where n is the moles of broken bonds per cm^3 of solution, w is the weight of polymer per cm^3 of polymer solution, and M_d and M_0 represent the number average molecular weights of the degraded and initial polymer, respectively[7,8]. The absolute values and the change in the number of moles of broken bonds with shear intensity are shown in *Table 4*. Also given in *Table 4* are the rates of energy input which provided the degraded solu-

tions. The force transmitted across a unit area perpendicular to the velocity gradient is equal to shear rate, $\dot{S}$, times shear stress, τ, as given in *Table 4*[8]. These results indicate that the number of broken bonds increases regularly with rate of energy input. At the highest rate, however, there is a marked decrease in efficiency and perhaps a limit in the bonds that can be broken in shear for this system. It is important to point out, relative to the degradation mechanism, that the low molecular weight limit corresponds closely with the minimum molecular weight needed to achieve entanglements in these systems, compare M_w 211 000 from shear degradation, with an M_w of 175 000 from entanglement theory[9].

The results indicate that both onset and terminal conditions for shear degradation are indicated by reduced variables[1,3]. A minimum value of 60 dyne/cm$^2 \times T$ [°K] is necessary to achieve shear degradation. It is thus a minimum stress, which increases with shear temperature rather than a minimum shear rate, as frequently stated, which is required to achieve degradation in concentrated polymer systems[10]. The negative temperature coefficient is consistent with a mechanical rather than thermally induced chemical reaction.

From the known rate of energy input required to achieve degradation, a calculation may be made concerning the efficiency of energy input in achieving bond rupture. Since it takes a minimum of two seconds to achieve equilibrium degradation, then in the least and most severe measured shear degradation conditions $1\cdot8 \times 10^{10}$ and $2\cdot4 \times 10^{11}$ erg/cm^3 or 0·43 and 5·7 kcal/cm^3 were introduced. This may be compared with the moles of broken bonds for these experiments given in *Table 3*. The results indicate the inefficiency of bond rupture with over a million times the kcal being required to produce a mole of broken bonds as compared with the activation energy to break a mole of C—C bonds of about 80 kcal. The efficiency is least at the highest temperatures. These results are consistent with the findings of inefficiency in capillary shear degradation experiments on comparable systems[7].

Table 3 provides a variety of parameters for evaluating the change in molecular weight distribution occurring on shear degradation. Traditionally, values of U or just M_w/M_n have been used to express the molecular weight distributions. These data represent a crucial test for the use of M_w/M_n and U for expressing shear degradation because (a) the magnitudes of shear degradation are large and (b) M_n and M_w are determined by an internally consistent manner from the complete distribution curves. In general, however, values of U and of M_w/M_n derived here are found to be an imprecise and insensitive measure of the degradation in shear, see *Table 3*. This effect is due to the mechanism of degradation and the normal distribution of the starting polymer, $M_w/M_n \sim 2\cdot0$. For such polymers, Kotliar has shown from Monte Carlo calculations that this ratio is not expected to change, even with drastic degradation, if the reaction mechanism is entirely random[11,12].

The similarity of shapes of the molecular weight distributions for the original and for shear degraded polymer distributions is indicated by the general trend in every case for a decrease in U and an increase in σ for

comparison at successively higher molecular weight averages. For a normal distribution polymer $M_n:M_w:M_z=1:2:3$. This would mean for a random mechanism that U and σ should indeed change in this order found in *Table 3*. By theory, $M_w/M_n=2$; $M_z/M_w=1\cdot5$ and $\sigma_n=M_n$; and $\sigma_w=0\cdot7M_w=1\cdot4\sigma_n$. These features are demonstrated experimentally by a comparison of the standard deviation of distributions in *Table 3* with the average molecular weight for the original and shear degraded polyisobutenes in *Table 2*. Each of the standard deviations σ_n, σ_w, and σ_z shows a regular trend with individual molecular weight averages M_n, M_w, and M_z. The ratios of σ to M are given in *Table 4*. Each set of ratios is essentially constant, independent of the magnitude of the shear degradation reaction. This means that the σs are linearly dependent on Ms with a zero intercept. This is illustrated particularly using the experimentally most reliable pair, σ_n and M_w, see *Table 4*. The expression relating the standard deviation of molecular weight distributions is

$$\sigma_n=KM_w \tag{4}$$

$K=0\cdot5$, within experimental error with zero intercept for M_w. This is just the ratio and expression expected for random degradation of a normal distribution polymer, compare definition given earlier. For this process $\sigma_n/M_n=1$ and $\sigma_w/M_w=0\cdot7$, which is in the range observed experimentally, see *Table 4*. This is also borne out qualitatively by the approximate values described in *Table 2*. The M_w/M_n ratios in *Table 2* are quite generally within 25 per cent of $2\cdot0$ and becoming closer with degradation.

These results evaluating the distribution with shear degradation, strongly infer an essentially random process of bond breaking within a matrix of
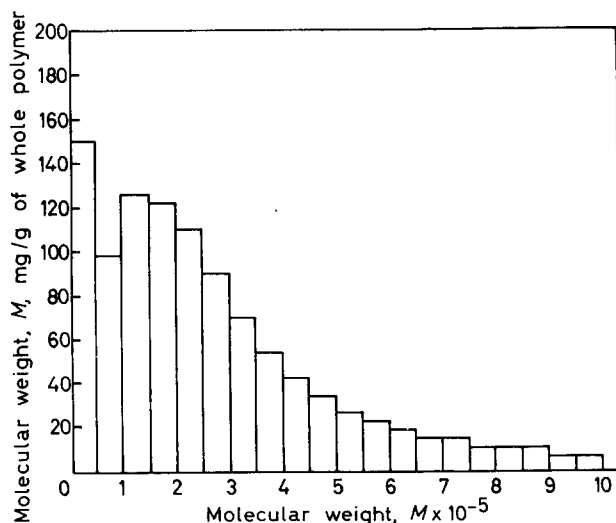
Figure 4—*n*-Hexadecane solution degraded at $3\cdot44\times10^5$ sec^{-1} and 60°C. Run 38, differential histogram of lower 99 per cent of sample

94

Table 4. Energy efficiency and distribution expressions for shear degradation of polyisobutene solutions

Polymer system and shear conditions		$10^{10}\tau_S$ dyne $cm^{-2} sec^{-1}$	Moles of broken bonds/cm^3, $\times 10^9$	$\dfrac{\sigma_n}{M_w}$	$\dfrac{\sigma_n}{M_n}$	$\dfrac{\sigma_w}{M_w}$	$\dfrac{\sigma_z}{M_z}$
Original Undegraded polyisobutene, M_v 8.0×10^5 Solution in 1,2,4-trichlorobenzene (TCB) TCB solution pumped, unsheared	Run 1		0	0·477	0·735	0·619	0·515
	Run 2			0·459	0·657	0·587	0·507
				0·492	0·836	0·734	0·627
				0·471	0·707	0·614	0·521
Degraded TCB solution 1.72×10^5 sec^{-1} 55°C		0·908	1·8	0·493	0·842	0·700	0·583
Degraded TCB solution 1.72×10^5 sec^{-1} 40°C		1·10	2·3	0·495	0·852	0·739	0·628
Degraded TCB solution 3.44×10^5 sec^{-1} 40°C	Main peak	2·54	2·8	0·487	0·790	0·768	0·718
Degraded TCB solution 3.44×10^5 sec^{-1} 21°C	Main peak	2·58	5·2	0·501	0·953	0·899	0·832
Degraded TCB solution 7.15×10^5 sec^{-1} 21°C	Main peak	11·9	6·0	0·500	0·959	0·878	0·695
n-Hexadecane solution Degraded 3.44×10^5 sec^{-1} 60°C	Main peak	2·84	3·8	0·493	0·848	0·737	0·622

entangled polymer chains[13]. Because of statistical cooperation of segments needed to achieve flow, the longer molecules will have longer relaxation times and will be more prone to storage of shear energy and the subsequent higher probability of bond cleavage.

It has been postulated that the preferential rupture of the large molecules in their central portions yields a narrowing of molecular weight distribu-

tion[14, 15]. It has been pointed out that this postulate has not been adequately tested experimentally[16]. The correlations developed here appear to indicate conclusively that the degradation mechanism is random and that there is no narrowing of the distribution in terms of U and in terms of σ/M. Equivalent results were obtained in the two solvents.

Concerning the mechanism of shear reaction, it is well to restate that in some of these experiments bimodal distributions were apparently produced[1]. This took the form of additional small, low molecular weight peaks which represented from 0 to 15 per cent of the total distribution, see *Table 1*. An example of the bimodal distribution is given in *Figure 4*. The tests among which bimodal distributions were formed generally represented the most severe shearing conditions. The small peak had a negligible influence on calculations involving the higher average molecular weights. It markedly influenced calculations involving number average. The small peak, which averages ~ 10 per cent of the polymer, where found, was neglected in the calculations given in the table. High resolution proton magnetic resonance spectra are consistent with the conclusion that the second, small, low molecular weight distribution peak represents short fragments of polyisobutene. If this bimodal distribution is confirmed in subsequent studies, it would be a finding consistent with shear degradation through the stress on a network of entangled chains. The break of short chain ends, which appears possible only at extremely high shear, could explain the second, low molecular weight peak illustrated in *Figure 4*.

Chevron Research Company,
  Richmond, California

REFERENCES

[1] PORTER, R. S., CANTOW, M. J. R. and JOHNSON, J. F. Preprint p 617, Prague IUPAC Meeting, 1965; *J. Polym. Sci. C,* in press
[2] PORTER, R. S., KLAVER, R. F. and JOHNSON, J. F. *Rev. sci. Instrum.* 1965, **36,** 1846
[3] PORTER, R. S. and JOHNSON, J. F. *J. appl. Phys.* 1964, **35,** 3149
[4] CANTOW, M. J. R., PORTER, R. S. and JOHNSON, J. F. Preprint p 618, Prague IUPAC Meeting, 1965. *J. Polym. Sci. C,* in press
[5] PICKETT, H. E., CANTOW, M. J. R. and JOHNSON, J. F. *J. appl. Polym. Sci.* 1966, **10,** 917
[6] PORTER, R. S., CANTOW, M. J. R. and JOHNSON, J. F. Preprint American Chemical Society, Division of Rubber Chemistry, San Francisco, May 1966
[7] BESTUL, A. B. *J. chem. Phys.* 1960, **32,** 350
[8] HARRINGTON, R. E. and ZIMM, B. H. *J. phys. Chem.* 1965, **69,** 161
[9] PORTER, R. S. and JOHNSON, J. F. *Chem. Rev.* 1966, **66,** 1
[10] GROHN, H. and KRAUSE, F. *Plaste und Kautschuk,* 1964, **11,** 2
[11] POLLER, D. and KOTLIAR, A. M. *J. appl. Polym. Sci.* 1965, **9,** 501
[12] KOTLIAR, A. M. *J. Polym. Sci. A,* 1963, **1,** 3179
[13] BOOTH, C. *Polymer, Lond.* 1963, **4,** 471
[14] BRISTOW, G. M. and WATSON, W. F. in *The Chemistry and Physics of Rubberlike Substances,* edited by L. BATEMAN. Wiley: New York, 1963
[15] BUECHE, F. *J. appl. Polym. Sci.* 1960, **4,** 101
[16] CERESA, R. J. and WATSON, W. F. *J. appl. Polym. Sci.* 1959, **1,** 101

Thermoelastic Measurements
on Some Elastomers

J. A. Barrie and J. Standen

Length versus temperature curves at a series of constant loads have been obtained for cis polyisoprene, polydimethylsiloxane and ethylene–propylene elastomers in the temperature range 25° to 100°C. Thermoelastic coefficients for these networks are evaluated and compared with values obtained by more direct procedures. The deviation of the stress/strain data from the simple gaussian theory is discussed briefly in terms of the C_2 constant of the Mooney equation.

RECENT modifications to the elastic theory of the gaussian network have provided a method for the evaluation of the temperature coefficient of the unperturbed end-to-end distance d log $\langle r_c^2 \rangle$/dT from stress/temperature coefficients of the network[1,2]. The departure of real networks from the ideal gaussian behaviour has been the subject of much discussion and on this basis the validity of the analysis has been questioned[3]. In the present investigation stress/temperature coefficients were obtained for several elastomers and the non-ideal behaviour of the networks measured in terms of the Mooney C_2 constant. These results are of interest for comparison with existing literature data in that a less direct method of measurement was used.

EXPERIMENTAL

Materials

Natural rubber (NR) and *cis* polyisoprene (CP) crosslinked with two per cent of dicumylperoxide at 140°C for 60 minutes were supplied by the Natural Rubber Producers Research Association. Silicone rubber (SR) was prepared from a polydimethylsiloxane gum extracted to remove residual catalyst[4] and crosslinked with dibenzoyl peroxide for 30 minutes at 141°C by the Natural Rubber Producers Research Association. A similar gum containing on average one vinyl side group per 100 Si atoms was cross-linked with 0·05 per cent of dicumyl peroxide for 20 minutes at 150°C by Midland Silicones Ltd. An ethylene propylene rubber (EP) was prepared from Enjay 404 gum by crosslinking with dicumyl peroxide for 45 minutes at 153°C by the Rubber and Plastics Research Association.

Sheet thickness varied from 1 mm to 4 mm. Rectangular strips of approximately 3 cm length were cut and then extracted with hot acetone for eight hours under a nitrogen atmosphere and finally outgassed under high vacuum (10^{-6} cm of mercury).

Measurements

For each strip a series of length/temperature measurements was made at constant load and under high vacuum so as to minimize relaxation effects associated with oxidative degradation. The stretching apparatus is shown

97

in *Figure 1*, the temperature in which was controlled to within 0·01 deg. C with a silicone oil bath.
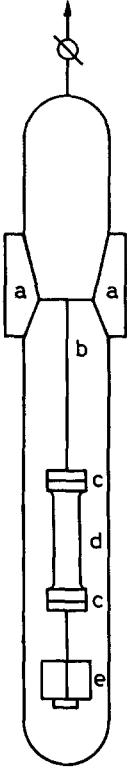
Figure 1—Stretching equipment: a, double B45 socket in brass with water cooled jacket; b, support for upper clamps; c, clamps; d, rubber strip; e, weight

The procedure adopted for all samples was as follows. The cross sectional area of the unstrained strip was obtained from length, weight and density measurements. A load greater than the maximum to be used was applied, the system outgassed and raised slowly to the maximum temperature at which it was held for two hours before cooling slowly to 25°C. This cycle was repeated over a period of several days until the sample length was constant to within 0·01 cm on two successive days. The load was now reduced to the maximum value and after one day the length between the clamps at 25°C recorded with a cathetometer to within ±0·004 cm. In addition for one sample the length was recorded as the distance between ink marks on the rubber but no significant differences in the two methods of measurement were evident. The temperature was then raised to 35°C and the length recorded after a period of 45 minutes. The process was repeated at 10 deg. C intervals up to 75°C, then at 70°C and back in steps of 10 to 30 deg. C and finally 25°C. Above 85°C neither the natural rubber nor the silicone rubber was stable enough by the criterion adopted whereas the ethylene–propylene samples were sufficiently stable for measurements to be made up to 120°C. On completion of a temperature cycle the load was

changed to a smaller value, the system quickly re-evacuated and left over-
night at 25°C. The temperature cycle was repeated and in this way 9 to 15
loads were used per sample, a typical sequence being 111, 86, 61, 36, 11, 21,
46, 71, 96 and finally 100g.

<div align="center">RESULTS</div>

Analysis

The first step was the evaluation of l_0, the length of the unstrained
sample. Each set of length (l) versus temperature (t°C) results at constant
load was fitted with a cubic equation in t computed by the method of least
squares. Points deviating by more than 2·5 times the standard deviation
were culled but at most no more than one point was rejected in any set of
twelve. Some typical curves are shown in *Figure 2* and it is clear that
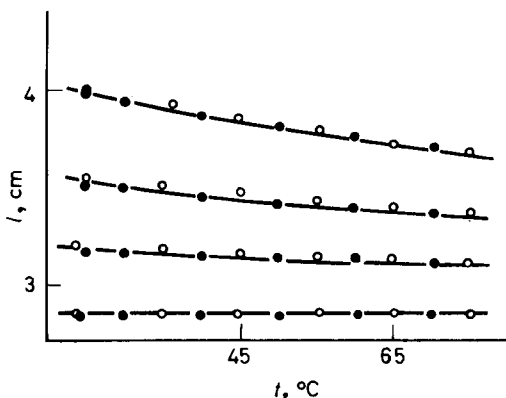
Figure 2—Typical length versus temperature curves at four different loads: ○, temperature increasing; ●, temperature decreasing

within a temperature cycle hysteresis effects are practically negligible. By
interpolation sets of length versus load results were obtained at several
standard temperatures of 25°, 40°, 55°, 70°, ·85° and 100°C. Length
versus load polynomials were then computed which by extrapolation to zero
load yielded l_0 values for each of the standard temperatures. Cubic poly-
nomials of elongation (α) versus load were also evaluated using $\alpha = l \times l_0^{-1}$.
The calculations were carried out on the London University Computer and
details of these and other programmes used are given elsewhere[5].

Stress/temperature coefficients

To facilitate the comparison of samples of different cross section the
load (kg) was divided by the unstrained cross section at 25°C to give
the stress f (kg cm^{-2}). Values of f for α ranging from 1·1 to 2·0 in steps of
0·1 were computed by interpolation from the f versus α polynomials at each
of the standard temperatures to give values of $(\Delta f/\Delta T)_{p\alpha}$. Typical f versus T
plots shown in *Figure 3* indicate that in the temperature range investigated
$(\Delta f/\Delta T)_{pa}$ may be identified with the stress-temperature coefficient $(\partial f/\partial T)_{pa}$.
The constant volume coefficient was then evaluated from

$$\left\{\frac{\partial \ln (f/T)}{\partial T}\right\}_{lV} = -\frac{1}{T} + \frac{1}{f}\left(\frac{\partial f}{\partial T}\right)_{pa} - \lambda \qquad (1)$$

<div align="center">99</div>

where λ is the coefficient of linear expansion[1]. The LHS of equation (1) is equal to $-d \log \langle r_t^2 \rangle / dT$, values of which are given in *Table 1* along with values of $(\partial f / \partial T)_{pa}$ for selected values of α. These values of $d \log \langle r_0^2 \rangle / dT$ are averaged over the whole of the temperature range as there was no significant variation with temperature except for ethylene–propylene where
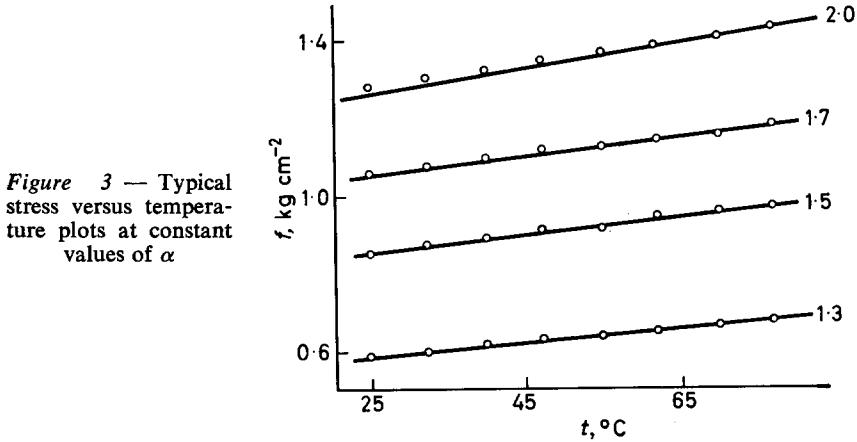
Figure 3 — Typical stress versus temperature plots at constant values of α

the values increased from $\sim -20 \times 10^{-3}$ at 25°C to $\sim -11 \times 10^{-3}$ at 100°C. Averaging was then carried out over the α; the averages in parentheses in *Table 1* were obtained by averaging over the complete set of α values and not just the selected α values. The accuracy of the results is difficult to estimate by this indirect procedure but is in the region of 50 per cent or more. A comparison with other literature values obtained by different experimental techniques as in *Table 2* shows reasonable agreement. No

Table 1. Tension/temperature results (Temperature range 25° to 70°C)

$\left(\frac{\partial f}{\partial T}\right)_{pa} \times 10^3$	$\frac{d \log}{dT}\langle r_0^2 \rangle \times 10^4$	$\left(\frac{\partial f}{\partial T}\right)_{pa} \times 10^3$	$\frac{d \log}{dT}\langle r_0^2 \rangle \times 10^4$	$\left(\frac{\partial f}{\partial T}\right)_{pa} \times 10^3$	$\frac{d \log}{dT}\langle r_0^2 \rangle \times 10^4$
cis *Polyisoprene* (CP); $\lambda = 2\cdot2 \times 10^{-4}$					
α	CP1		CP2		CP3
1·2	4·74	1·6	4·2	6·9	5·2	2·5
1·4	7·35	5·1	6·97	7·5	7·97	5·4
1·6	9·26	6·0	8·86	7·9	10·30	5·5
1·8	11·27	5·3	10·38	8·1	13·92	1·7
		4·5 (3·7)		7·6 (7·6)		3·6 (3·8)
Natural rubber (NR); $\lambda = 2\cdot2 \times 10^{-4}$					
α	NR1		NR2		NR3
1·2	4·06	3·5	4·70	2·5	4·01	4·7
1·4	6·99	4·3	7·22	5·6	6·51	6·5
1·6	8·72	6·1	9·22	6·2	8·22	7·5
1·8	9·23	9·0	12·34	3·1	9·87	7·1
		5·7 (6·7)		4·3 (4·1)		6·4 (6·1)

Silicone rubber with one per cent vinyl groups (SR1, 2), without (SR3, 4); $\lambda=3\cdot2\times10^{-4}$

α	SR1		SR2		SR3	
1·2	0·80	3·5	0·91	1·7	1·54	0·60
1·4	1·30	5·5	1·41	5·1	2·39	3·90
1·6	1·64	6·8	1·72	7·1	2·84	6·8
1·8	1·94	6·9	2·09	6·4	3·16	8·3
		5·7 (5·4)		5·1 (4·5)		4·9 (6·0)

α	SR4	
1·2	1·28	4·9
1·4	2·08	6·9
1·6	2·62	8·1
1·8	3·14	7·9
		7·0 (6·6)

Ethylene–propylene rubber (EPR); $\lambda=1\cdot8\times10^{-4}$

α	EPR1		EPR2		EPR3	
1·2	9·48	−8·8	9·21	−7·8	9·37	−8·1
1·4	13·71	−3·7	14·17	−5·0	14·69	−5·9
1·6	19·02	−6·8	20·39	−9·7	20·72	−9·3
1·8	33·17	−24·0	33·01	−24·0	30·79	−18·0
	−11	(−17)	−12	(−17)	−10	(−14)

Measurements EPR1 and EPR2 are for the same sample using respectively marks on the clamps and on the rubber. EPR3 measurements were made in the range 50° to 100°C.

comparable data were available for ethylene–propylene rubber but a negative coefficient is in line with the results for polyethylene[7,9].

Table 2. Comparison of d log $\langle r_i^2 \rangle / \mathrm{d}T \times 10^3$ values

Sample	This work	Literature data	
Natural rubber	0·56	$0\cdot55\pm0\cdot8$[6];	$0\cdot41\pm0\cdot04$[7]
cis Polyisoprene	0·51	—	
Silicone rubber	0·57	$0\cdot46\pm0\cdot15$[8];	$0\cdot75\pm0\cdot15$[7]
Ethylene–propylene rubber	−1·6	—	
Polyethylene	—	$-0\cdot97\pm0\cdot1$[9];	$-1\cdot2\pm0\cdot15$[7]

Stress/strain isotherms

For these measurements the stress was referred to unit unstrained cross section at $t°C$ by converting the cross section at 25°C for the expansion of the rubber. As expected the results do not conform to the simple gaussian network expression $f/\phi=G$ where ϕ denotes $\alpha-\alpha^{-2}$ and G is a constant. In the range $\alpha=1$ to 2 the reduced stress for all samples decreased with increasing α by about 10 to 20 per cent. In the range $\alpha^{-1}=0\cdot5$ to 0·75 the results were reasonably represented by the Mooney equation

$$f/\phi=2C_1+2C_2\alpha^{-1} \tag{2}$$

101
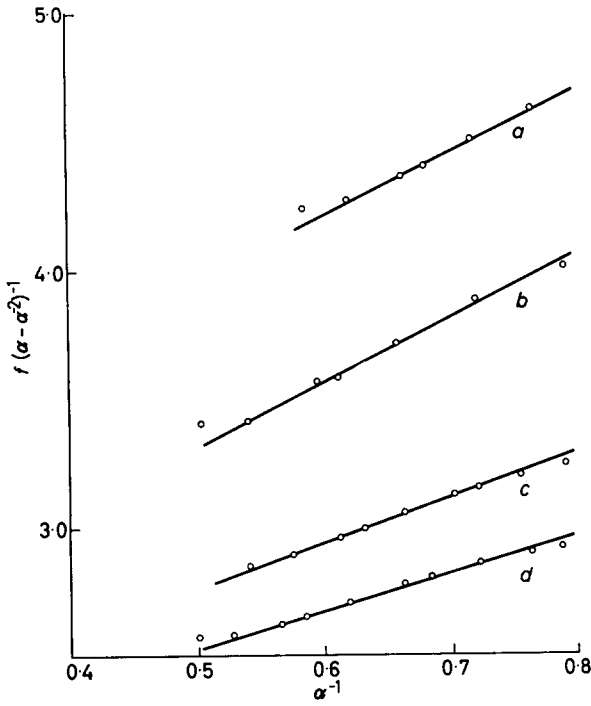
Figure 4 — Typical Mooney plots: a, EPR1 at 70°C; b, EPR1 at 25°C; c, CP2 at 70°C; d, CP2 at 25°C

as shown by some typical examples in *Figure 4*. The values of the constants $2C_1$ and $2C_2$ are compared with existing literature data in *Table 3*.

Due to slight errors in l_0 small but significant residual values of f were obtained with most samples for $\alpha = 1$. Accordingly the values of l_0 were adjusted by progressively altering α in small steps so as to find those values giving the smallest values of f at $\alpha = 1$. For only one sample was the correction factor greater than one per cent and for most samples it was

Table 3. Mooney constants $2C_1$ and $2C_2$

	°C	CP1	CP2	CP3	NR1	NR2	NR3	
$2C_1$	25	1·8	1·8	1·9	1·4	1·9	1·7	
	70	2·0	1·9	2·3	2·1	2·1	1·9	
$2C_2$	25	1·3	1·4	1·5	1·7	1·1	1·3	
	70	1·4	1·7	1·4	1·9	1·2	1·3	
		SR1	SR2	SR3	SR4	EPR1	EPR2	EPR3
$2C_1$	25	0·30	0·34	0·48	0·55	2·1	2·4	2·6 (55°C)
	70	0·32	0·35	0·53	0·61	2·8	2·2	3·1 (100°C)
$2C_2$	25	0·25	0·24	0·50	0·36	2·4	2·9	2·2 (55°C)
	70	0·26	0·25	0·54	0·37	2·4	2·2	2·4 (100°C)
				Selected literature values				
			Natural rubber				*Silicone rubber*	
$2C_1$	30	2·5[10]	1·92[11]	2·6[12]			0·70[11]	
	60	2·73					0·98 (149°C)	
$2C_2$	30	0·86	1·60	1·70 (25°C)			0·60	
	60	0·90					0·62 (149°C)	

less than 0.5 per cent. Even so the linearity of the Mooney plots was much improved particularly in the region $\alpha^{-1} > 0.75$ where the function ϕ becomes increasingly sensitive to changes in α. However, the values of $2C_1$ and $2C_2$ were not substantially altered as a result of these corrections..

DISCUSSION

Although a more indirect procedure has been used in the measurement of stress/temperature coefficients the agreement with data obtained by more direct methods is satisfactory. The correction term λ in equation (1) follows from the use of the simple gaussian theory and its importance can be judged by comparison with the values of $d \log \langle r_0^2 \rangle / dT$ in *Table 1*. The use of the gaussian theory in this fashion is open to criticism as the stress-strain data follow more closely the Mooney equation. Ryong-Joon Roe[3] has shown that with the Mooney equation an additional term appears on the RHS of equation (1) of the form $\lambda (1 - \mu_2) / \{(C_1/C_2) \alpha + 1\}$. From an analysis of volume dilation data on natural rubber he suggested that in the absence of suitable data the coefficient $\mu_2 \approx -1$. From *Table 3* the ratio C_1/C_2 for most of the rubbers is approximately unity and it is clear that the magnitude of this new term is comparable with that of λ itself in the range of α investigated. On the other hand Allen *et al.*[13] by direct measurement of both constant volume and constant pressure coefficients concluded that for natural rubber the correction term of equation (1) was correct within experimental error.

This problem of the correct equation of state for a real network has been the subject of much discussion, in particular the origin of the C_2 term. On the one hand non-equilibrium effects have been held responsible[11, 14, 15] and on the other molecular interpretations have been advanced for the departure of real networks from the simple gaussian theory[16-19]. The C_2 constants of *Table 3* tend to increase slightly with an increase of temperature. However, this in itself cannot be taken as evidence for the absence of non-equilibrium effects as it may be shown that non-equilibrium behaviour can lead to either a decrease or an increase of C_2 with temperature[14]. The force/elongation curves showed little if any sign of hysteresis and in this respect it appears unlikely that non-equilibrium effects are entirely responsible for the departure from the simple theory. The Mooney equation is only of limited applicability as it fails to describe a rubber under unidirectional compression[20]. Even in the limited range of simple extension it is probably not unique as the results of this investigation were equally well fitted by a quadratic of the form $f = a\phi + b\phi^2$. The nature of the deviations from the simple gaussian theory must still be largely regarded as open to question and in this respect the accuracy of the coefficients determined from equation (1) and similar relations will ultimately be governed by the validity of the equation of state used to describe the real network at equilibrium.

Department of Chemistry,
  Imperial College,
    London, S.W.7.

REFERENCES

[1] FLORY, P. J. *Trans. Faraday Soc.* 1961, **57**, 829
[2] TOBOLSKY, A. V., CARLSON, D. W. and INDICTOR, N. *J. Polym. Sci.* 1961, **54**, 175
[3] RYONG-JOON ROE. *Trans. Faraday Soc.* 1966, **62**, 312
[4] OSTHOFF, R. C., BUECHE, A. M. and GRUBB, W. T. *J. Amer. chem. Soc.* 1954, **76**, 4659
[5] STANDEN, J. *Ph.D. Thesis,* London, 1965
[6] CIFERRI, A. *Makromol. Chem.* 1961, **43**, 152
[7] MARK, J. E. and FLORY, P. J. *J. Amer. chem. Soc.* 1964, **86**, 138
[8] CIFERRI, A. *Trans. Faraday Soc.* 1961, **57**, 846
[9] CIFERRI, A., HOEVE, A. J. and FLORY, P. J. *J. Amer. chem. Soc.* 1961, **83**, 1015
[10] RYONG-JOON ROE and KRIGBAUM, W. R. *J. Polym. Sci.* 1962, **61**, 167
[11] CIFERRI, A. and FLORY, P. J. *J. appl. Phys.* 1959, **30**, 1498
[12] GUMBRELL, S. M., MULLINS, L. and RIVLIN, R. S. *Trans. Faraday Soc.* 1953, **49**, 1495
[13] ALLEN, G., UMBERTO BIANCHI and PRICE, C. *Trans. Faraday Soc.* 1963, **59**, 2493
[14] CIFERRI, A. and HERMANS, J. J. *Polymer Letters,* 1964, **2**, 1089
[15] KRAUS, G. and MOCZVGEMBA, G. A. *J. Polym. Sci. A,* 1964, **2**, 277
[16] DiMARZIO, E. A. *J. chem. Phys.* 1962, **36**, 1563
[17] KRIGBAUM, W. R. and KANEKO, M. *J. chem. Phys.* 1962, **36**, 99
[18] DOBSON, G. R. and GORDON, M. *Trans. Instn Rubb. Ind.* 1964, **40**, T262
[19] GEE, G. *Polymer, Lond.* 1966, **7**, 373
[20] MULLINS, L. *The Chemistry and Physics of Rubberlike Substances,* ed. L. BATEMAN, p 182. MacLaren: London, 1963

The Hydrodynamic Properties of the System Poly α-Methyl Styrene– Cyclohexane*

J. M. G. COWIE, S. BYWATER and D. J. WORSFOLD

The theta temperature for the system poly α-methyl styrene–cyclohexane has been determined as 37° ±0·5°C. The samples used in the determination were prepared by anionic polymerization in tetrahydrofuran and have a syndiotactic diad content of 0·68. The dependence of intrinsic viscosity on molecular weight has been measured in cyclohexane at 37°C and was found to be $[\eta]=7\cdot8\times10^{-4}\overline{M}_w^{0\cdot5}$. Examination of the solution properties indicates that the Kurata–Yamakawa theory is valid in the vicinity of the theta temperature, but that in non-ideal solvents the polymer is best represented by either the Peterlin or Ptitsyn–Eizner coil models. The ratio $(\langle\overline{s^2}\rangle_{0z}/\overline{M}_w)^{1/2}$ was found to be $0\cdot281\times10^{-8}$ cm which after correcting for sample heterogeneity gives
$$(\langle\overline{s^2}\rangle_{0w}/\overline{M}_w)^{1/2}=0\cdot269\times10^{-8}\ cm.$$

THE dilute solution properties of polystyrene and poly α-methyl styrene polymers of narrow molecular weight distribution, which were produced by anionic catalysis, have been reported previously[1,2]. These measurements were made in a non-ideal solvent toluene, but for a comprehensive study of the hydrodynamic properties of any polymer molecule, data in a theta solvent are desirable where inter- and intra-molecular interactions have been eliminated and the conformation of the chain is more readily determined. As sample heterogeneity can have a marked effect on the values of the various hydrodynamic parameters obtainable in these studies, the use of polymers with $(\overline{M}_w/\overline{M}_n)<1\cdot10$ helps to minimize these errors and should make the comparison of experimental results with theory much more reliable.

The theta temperature for the system poly α-methyl styrene–cyclohexane has been obtained and the results have been analysed using the more recent polymer solution theories[3,4].

EXPERIMENTAL

Sample preparation

The poly α-methyl styrenes were prepared in tetrahydrofuran (THF) solution at $-78°$, using butyllithium as the initiator, in an all glass apparatus. Polymer Corporation monomer was fractionally distilled, degassed on a vacuum line and then distilled on to butyllithium. When the yellow colour of poly α-methyl styryllithium appeared the residual

monomer was distilled on the vacuum line to an evacuated storage vessel. From here monomer was distilled as required to vessels fitted with a breakseal, which were glassblown on to the reaction vessels. The tetrahydrofuran was purified as described before[5], and distilled on the vacuum system to an evacuated reaction vessel containing a fragile bulb of butyllithium solution. The reaction vessel was then sealed. For molecular weights in excess of 0.5×10^6 the reaction vessel was washed as described elsewhere[5,6]. The monomer side arm breakseal was then broken, the solution cooled to $-78°$, and the initiator bulb was broken open. The reaction mixture was left overnight, and finally precipitated with methanol.

Sample analysis
Molecular weight determinations by both light scattering and osmometry on several samples showed[2] that the technique produced polymers with $\overline{M}_w/\overline{M}_n < 1.10$.

The microstructure of the samples was obtained by measuring the relative amounts of the iso-, syndio- and hetero-tactic forms from the proton resonance spectra, as described previously[7]. A typical analysis showed the relative contents to be: isotactic 0.08, heterotactic 0.48, syndiotactic 0.44.

Solvents
Reagent grade cyclohexane and toluene were fractionally distilled and the middle fractions were used in all physical measurements. The cyclohexane fraction used was analysed by gas chromatography and found to be 99.99 per cent pure; the major impurity was 2,4-dimethylpentane.

Physical measurements
Viscosity and light scattering measurements were carried out as detailed elsewhere[8,9].

Refractive index increment
Measurement of the refractive index increment (dn/dc) was made in a modified Brice–Phoenix differential refractometer[10] at 37°C. A value of 0.199 ml/g was obtained for poly α-methyl styrene in cyclohexane, at $\lambda = 4358$Å.

RESULTS

Determination of the theta temperature
The theta temperature of the system, defined as the temperature at which the second virial coefficient A_2 is zero, can be determined conveniently by light scattering techniques. A sample of $\overline{M}_w = 9.6 \times 10^4$ was used for the initial determination, and data were plotted as (c/I_{90}) against concentration for each temperature, as shown in Figure 1. Two other samples $(\overline{M}_w = 1.25 \times 10^6$ and $1.54 \times 10^6)$ were also examined but A_2 was obtained from the zero angle line of the respective Zimm plots. The second virial coefficient was then plotted against temperature, shown in Figure 2, and the theta temperature obtained was $\theta = 37.0° \pm 0.5°$C. A previous approxi-

mation of 38°C was found to be slightly high[11], but the new value is in reasonably good agreement with values of 36°C and 36·2° ± 1·0°C reported by Kotera *et al.*[12] and Cornet and van Ballegooijen[13] respectively.
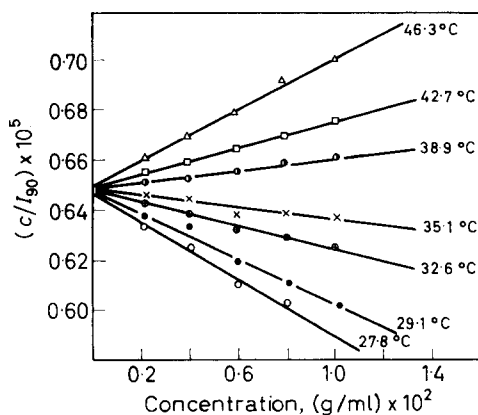
Figure 1—Plot of (c/I_{90}) against concentration for sample αD in cyclohexane at several temperatures

Intrinsic viscosity/molecular weight relations

Weight average molecular weights $(\overline{M}_w)$ were obtained from light scattering measurements in cyclohexane and plotted against the intrinsic viscosity $[\eta]$ measured in both cyclohexane and toluene at 37°C. Detailed results are shown in *Table 1* and the data are best represented by

$$[\eta] = 7\cdot80 \times 10^{-4} \overline{M}_w^{0\cdot5} \tag{1}$$

in cyclohexane and

$$[\eta] = 1\cdot00_5 \times 10^{-4} \overline{M}_w^{0\cdot72} \tag{2}$$

in toluene.
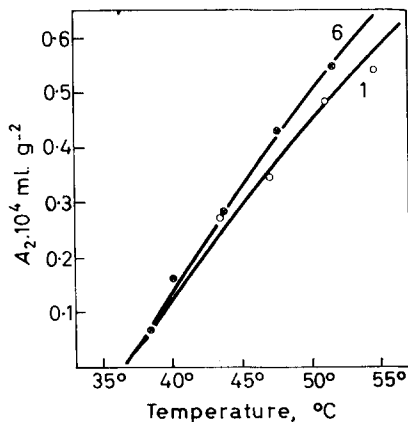
Figure 2—Variation of second virial coefficient with temperature of samples Nos. 1 and 6 in cyclohexane

Molecular parameters

Characteristic hydrodynamic parameters for the polymer–cyclohexane system may be calculated from the familiar Flory–Fox equations[14]

107

$$[\eta] = K\overline{M}_w^{1/2}\alpha^3 \qquad (3)$$

where

$$K = (\Phi_0/q)(\langle\overline{R^2}\rangle_{0z}/\overline{M}_w)^{3/2} \qquad (4)$$

Here, α^3 is the expansion factor, $\langle\overline{R^2}\rangle_{0z}^{1/2}$ is the z-average root mean square unperturbed end to end distance, and Φ_0 is a constant under theta conditions. As the value of Φ_0 is normally calculated from number averages of

Table 1. Molecular weights and intrinsic viscosities in cyclohexane and toluene for poly α-methyl styrene at 37°C

Sample No.	$\overline{M}_w \times 10^{-6}$	$[\eta]$ cyclohexane	$[\eta]$ toluene
7	4·00	1·60	5·40
6	1·54	1·01	2·92
2	1·40	0·93	2·60
1	1·25	0·90	2·45$_4$
8	0·84	0·69$_5$	1·80
3	0·66	0·64$_5$	1·58$_6$
5	0·48	0·52	1·14
αG	0·22	0·36$_2$	0·73$_2$
αD	0·09$_6$	0·23$_3$	0·37$_2$

$(R^2)^{1/2}$ and M, a factor q is introduced to correct for sample heterogeneity when light scattering data are used in equation (4). If a Zimm–Schulz[15] exponential distribution is assumed for each sample, the conversion factor may be defined as

$$q = (h+1)^{-1}\Gamma(h+1)[\Gamma(h+1\cdot5)]^{-1}[\Gamma(h+3)/\Gamma(h+2)]^{3/2} \qquad (5)$$

where the breadth parameter $h = [(\overline{M}_w/\overline{M}_n)-1]^{-1}$. Of course this distribution may not be the most representative one for the samples used here, but should give a reasonable estimate of the order of magnitude of the correction. For anionically polymerized samples one can use $h = 10$ which gives $q = 1\cdot15$. Table 2 contains values of Φ_0 calculated from equations (3) and (4); an average uncorrected Φ_0 of $2\cdot43 \times 10^{21}$ was obtained which after correction became $2\cdot79 \times 10^{21}$.

Table 2. Hydrodynamic parameters for poly α-methyl styrene–cyclohexane at 37°C

Sample No.	$\langle\overline{R^2}\rangle_{0z}^{1/2}, \mathring{A}$	$10^{21} \times \Phi_0$	$10^{21} \times \Phi_{0\,(\text{corr.})}$	$10^8 \times A, cm$
7	1 409	2·29	2·63	0·704
6	848	2·55	2·93	0·683
2	804	2·50	2·87	0·679
1	825	2·07	2·38	0·738
8	608	2·61	3·00	0·662
3	550	2·56	2·94	0·677
5	468	2·44	2·81	0·676

In the Flory–Fox dilute solution theory the polymer was assumed to have a gaussian distribution of chain segments. This was replaced in later

theories[3, 16] by a non-gaussian distribution which resulted in the expression of the intrinsic viscosity[3] as a power series in z, the excluded volume parameter,

$$[\eta] = [\eta]_\theta (1 + p(X) z - \ldots.) \tag{6}$$

where X is the draining parameter and the function $p(X)$ increases with X or M to an asymptotic limit of 1·55. The intrinsic viscosity at the theta temperature was then defined as

$$[\eta]_\theta = (\pi^{3/2} N_A / 100 \times 6^{3/2}) [XF_0(X)] (\langle \overline{R^2} \rangle_0^{3/2} / M) \tag{7}$$

where N_A is Avogadro's number, and $XF_0(X)$ approaches 1·259 at $X = \infty$. Thus

$$\Phi_0 = (\pi^{3/2} N_A / 100 \times 6^{3/2}) [XF_0(X)]_{X=\infty} = 2·87 \times 10^{21} \tag{8}$$

and the data in *Table 2* are in agreement with this value indicating that the polymer behaves as an impermeable coil in cyclohexane.

Consideration of the excluded volume and its effect on the hydrodynamic radius, by Kurata and Yamakawa[17], has resulted in the modification of equation (3) to

$$[\eta] = (\Phi_0 / q) (\langle \overline{R^2} \rangle_{0z}^{3/2} / \overline{M}_w) \alpha^{2·43} \tag{9}$$

where
$$\alpha^{2·43} = \alpha_\eta^3 \tag{10}$$

and
$$\alpha_\eta^3 = [\eta] / [\eta]_\theta \tag{11}$$

Thus equation (10) implies that the hydrodynamic radius of the polymer chain will increase less rapidly than the statistical radius, with increase in the excluded volume. This is confirmed for the present system by plotting log α_η^3 against log α, for sample 6, from the results of *Table 3*. A slope of 2·27 was obtained (see *Figure 3*) which can be corrected for sample heterogeneity by using[17]

$$\text{Slope} = \frac{105}{67} p(X) \frac{(h+1)^2 (h+2) [\Gamma(h+1)]^2}{\Gamma(h+\frac{3}{2}) \Gamma(h+\frac{7}{2})} \tag{12}$$

which for $h = 10$ and $p(X) = 1·55$ gives a slope of 2·30, reasonably close to the value predicted by equation (10).

Table 3. Temperature dependence of hydrodynamic parameters of poly α-methyl styrene No. 6 in cyclohexane

Temp. °C	$\langle \overline{R^2} \rangle_z^{1/2}$, Å	$[\eta]$	$A_2 \times 10^4$ ml g^{-2}
37·0	848	1·00	0·000
38·5	864	1·04	0·068
40·2	870	1·06	0·163
43·7	899	1·15	0·258
47·5	933	1·24	0·416
51·5	965	1·34	0·512

In the final column of *Table 2* are listed values of the parameter A defined by

$$A = [\langle \overline{R^2} \rangle_{0z} / \overline{M}_w]^{1/2} = [K_\theta / \Phi_0]^{1/3} \tag{13}$$

The average was $A = 0.688 \times 10^{-8}$ cm obtained from the experimentally determined coil dimensions. It is also possible to estimate A from K_θ in equation (2), and if the theoretical value of $\Phi_0 = 2.87 \times 10^{21}$ is corrected first for sample heterogeneity, then $A = 0.678 \times 10^{-8}$ cm is obtained. These values are in reasonable agreement with the result of Cornet[18] who estimated $A = 0.667 \times 10^{-8}$ cm from viscosity measurements in concentrated solutions where perturbation of the polymer chain is supposed to be negligible. This value for A is considerably lower than the corresponding value for poly-styrene, indicating that the α-methyl group may play a significant role in deciding the conformation of the polymer chain. However, it should be remembered that the microstructure of the polymers differs from that of the polystyrene, and this problem will be examined in detail in a future publication.

Figure 3—Log-log plot of α_η^3 against α; the observed slope is 2·27
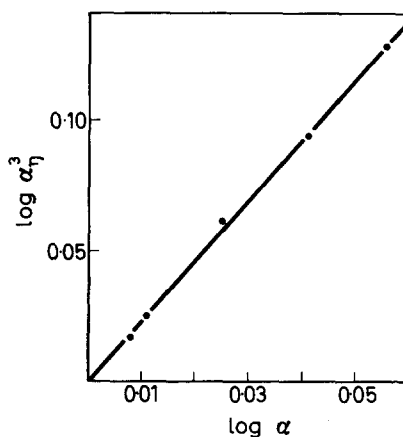
Second virial coefficient (A_2)

The excluded volume z was related directly to the second virial coefficient by Zimm[19], who proposed the equation

$$A_2 = \tfrac{1}{2} N_A B h(z) \tag{14}$$

where

$$h(z) = 1 - 2.865z + 18.51z^2 - \ldots \tag{15}$$

Here N_A is the Avogadro number, B is a parameter related to the Flory interaction parameter χ, and z can be described effectively in terms of the radius of gyration $\langle s^2 \rangle^{1/2}$ by[3]

$$\langle \overline{s^2} \rangle = \langle \overline{s^2} \rangle_0 [1 + 1.276z - 2.077z^2 + \ldots] \tag{16}$$

By combining equations (14), (15) and (16), and neglecting the triple contact terms, it is possible to arrive at an approximate form incorporating the double contact terms viz.

$$\langle \overline{s^2} \rangle = \langle \overline{s^2} \rangle_0 \left\{ 1 + 1.276 \left[\frac{A_2 M^{1/2}}{4\pi^{3/2} N_A} \cdot \left(\frac{M}{\langle \overline{s^2} \rangle_0} \right)^{3/2} \right] + 1.579 \left[\frac{A_2 M^{1/2}}{4\pi^{3/2} N_A} \left(\frac{M}{\langle \overline{s^2} \rangle_0} \right)^{3/2} \right]^2 \right\} \tag{17}$$

110

Substitution of the experimental value for $(\langle \bar{s^2} \rangle_{0z}/M_w)$ obtained here reduces equation (17), after correcting for heterogeneity[4], to

$$\alpha^2 - 1 = 4 \cdot 51 \,(A_2 M^{1/2}) + 18 \cdot 9 \,(A_2 M^{1/2})^2 \qquad (18)$$

which predicts essentially a linear relationship between $\langle \bar{s^2} \rangle$ and A_2 for any given molecular weight in the vicinity of the theta temperature, or low α, with increasing deviation at higher α values. The validity of equation (18) is examined in *Figure 4*, in which the points are calculated from data
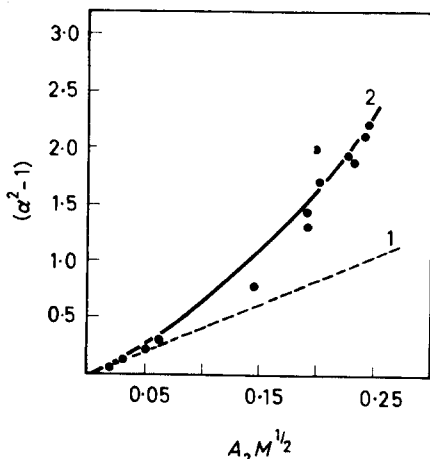
Figure 4—Dependence of α^2 on A_2. Curve 1 theoretical line using single contact approximation, curve 2 constructed using double contact approximation

obtained for sample 6 in cyclohexane and samples 1, 2, 3 and 6 in some non-ideal solvents; details are given in *Table 4*. The broken line, curve 1, was calculated from equation (18) using only the single contact approximation and fits the data only in the low range of α. The theoretical line for equation (18) is denoted as curve 2 and shows remarkably good agreement with the experimental results over the whole range examined.

The Flory parameter Φ

The Flory parameter was originally defined as a universal constant, but examination of equation (10) indicates that

$$\Phi = \Phi_0 \,(\alpha_\eta/\alpha)^3 \qquad (19)$$

which suggests that Φ will be dependent on both molecular weight and solvent power. Equations (10) and (19) predict an unlimited decrease in Φ as the expansion factor approaches infinity[4], i.e.

$$\Phi = \Phi_0 \alpha^{-0 \cdot 57} \qquad (20)$$

whereas a similar relationship proposed by Kurata, Stockmayer and Roig[16]

$$\alpha_\eta^3 - \alpha_\eta = 1 \cdot 10 \, g \,(\alpha_\eta)\, z \qquad (21)$$

predicts Φ should reach an asymptotic limit. Here $g\,(\alpha_\eta) = 8\alpha_\eta^3/(3\alpha_\eta^2 + 1)^{3/2}$.

Ptitsyn and Eizner[20] used a somewhat different approach by generalizing the Kirkwood–Riseman theory and using the factor ϵ to describe the excluded volume effect, where $R^2 = K_R M^{1+\epsilon}$. They arrived at the relation

111

$$\Phi\,(\epsilon)=\Phi_0\,(1-2\cdot63\,\epsilon+2\cdot86\,\epsilon^2) \tag{22}$$

which shows that the decrease in Φ will be limited only by the limiting value of ϵ which is adopted.

In *Table 4* are listed values of (Φ/Φ_0) and α for poly α-methyl styrene in a range of solvents.

Table 4. Molecular parameters for poly α-methyl styrene in various solvents

Sample No.	Measurement temp., °C	Solvent	$\langle \overline{s^2} \rangle^{1/2}$, Å	$A_2 \times 10^4$	α	(Φ/Φ_0)
5	37	Toluene	254	2·07	1·33	0·91
3	37	Toluene	349	2·12	1·55	0·67
2	37	Toluene	588	2·09	1·79	0·50
6	37	Toluene	613	2·00	1·77	0·53
1	37	Toluene	551	2·02	1·64	0·50
1	37	THF	571	2·06	1·70	0·49
1	37	Dioxan	509	1·73	1·51	0·56
1	37	CCl₄	588	1·79	1·75	0·47
1	37	Ethyl benzene	539	1·82	1·60	0·50
6	40·2	Cyclohexane	355	0·16	1·03	0·99
6	43·7	Cyclohexane	367	0·26	1·06	0·97
6	47·5	Cyclohexane	381	0·42	1·10	0·94
6	51·5	Cyclohexane	394	0·51	1·14	0·92

These can be compared with the theoretical relationships if a suitable interconversion of α and ϵ can be made. This can be done in several ways[21]. According to the Flory theory ϵ cannot be greater than one fifth if the coil expansion is due only to the excluded volume effect, thus

$$\epsilon=(\alpha^2-1)/(5\alpha^2-3) \tag{23}$$

but if the Kurata–Yamakawa approach is used $\epsilon=0\cdot5$ is the limiting value and

$$\epsilon=0\cdot5\,(\alpha^2-1)/\alpha^2 \tag{24}$$

By taking these two extreme cases we can plot Φ/Φ_0 against ϵ, as shown in *Figure 5*, where the open circles represent ϵ calculated according to equation (24), while the solid circles are obtained for ϵ using equation (23). These experimental values can now be compared with three theoretical treatments. Recently, computer calculations of the intrinsic viscosity of coiling macromolecules using the Kirkwood–Riseman adaptation of the Oseen approximation have been made by Ullman[22]. He considered a gaussian coil, the Kurata–Yamakawa model, and a coil expansion model proposed by Peterlin. From his tabulated results it is possible to construct the theoretical dependence of Φ/Φ_0 on ϵ for the K–Y approach (dotted line) and the Peterlin coil model (solid line), while the broken line in *Figure 5* was calculated from the P–E equation (22).

Recent views on the dependence of α on z, proposed by Ptitsyn[23] and Stockmayer and Fixman[24], favour a limiting value of $\epsilon=1/3$. Thus Tschoegl[25] has shown that

$$\epsilon=\tfrac{1}{3}\,(1-0\cdot786/\alpha^2)-1/30\cdot3\,\alpha^3\,(1-0\cdot786/\alpha^2)^{1/2} \tag{25}$$

if the Ptitsyn relation is used, and points calculated according to equation (25) are shown as triangles on *Figure 5*.

Figure 5—Variation of (Φ/Φ_0) with ϵ. Solid line is the Peterlin coil model (P), broken line (P–E) the Ptitsyn–Eizner theory, dotted line (K–Y) the Kurata–Yamakawa theory. For limit of $\epsilon = 1/2$ (—○—), limit $\epsilon = 1/3$ (—△—) and limit $\epsilon = 1/5$ (—●—)
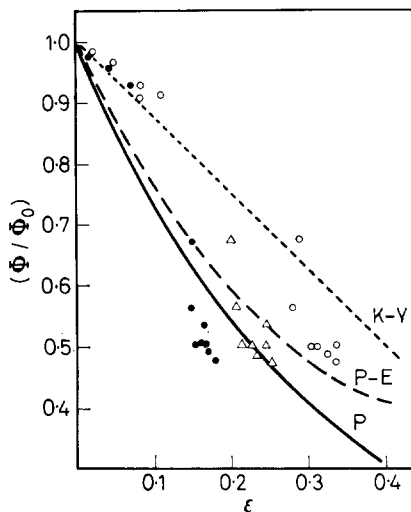
DISCUSSION

The theta temperature of the system poly α-methyl styrene–cyclohexane has been found to be $37^\circ \pm 0.5^\circ C$ which is about one degree higher than other reported values. This slight discrepancy may be due to differences in sample tacticity although this cannot be substantiated as no details of material preparation have been given in the other references[12, 13]. The samples used in this study have approximately 64 per cent syndiotactic placements (diad analysis), whereas the syndiotactic content of cationically prepared samples is considerably higher[7]. By analogy with polymethylmethacrylate, it seems likely that the theta temperature may decrease slightly with increasing syndiotacticity[26].

The Kurata–Yamakawa (K–Y) theory using a single contact approximation has proved adequate in predicting the solution properties of the polymer in the vicinity of the theta temperature. As the solvent power increases, however, the agreement deteriorates somewhat. This is most obvious when examining the dependence of (Φ/Φ_0) on ϵ. The K–Y theory is most suitable at low ϵ, and the agreement is not unreasonable in good solvents if ϵ is allowed to approach one half. Under the same limiting conditions the P–E equation is also a moderately good approximation at high ϵ, and it is interesting to note that a recent treatment by Bloomfield and Zimm[27], who treated the molecule as a 'pearl necklace' with beads connected by Hookean springs, produces a curve which is almost identical with the P–E curve. If a limit of ϵ equal to one fifth is imposed then the K–Y is still a good fit at low ϵ but deviates badly in good solvents, and the Peterlin coil model is now the closest approximation to the experimental points. However, $\epsilon = \frac{1}{5}$ as a limiting value is invalid for the K–Y treatment

and makes any comparison meaningless under these conditions in good solvents. On the other hand if ϵ approaches one third as predicted by more current views[23,24], then the experimental points scatter between the Ptitsyn–Eizner and Peterlin models, while at low ϵ the Kurata–Yamakawa approach remains the best fit.

In the K–Y theory, however, it has been shown that if the double contact terms are used, the agreement between theory and experiment at high α is much better. The dependence of A_2 on $\langle s^2 \rangle$ is predicted well in non-ideal solvents when the double contact approximation is employed. Unfortunately this does not agree with recently reported data on polystyrene[28] where a linear relationship was found to be valid over a wide range of thermodynamic conditions.

It is thus extremely difficult to decide if extrapolation of the K–Y theory beyond the immediate vicinity of the theta temperature is a valid procedure, and whether or not there has been a fortuitous cancellation of errors which has resulted in the apparent experimental coincidence with theory.

The characteristic ratio $(\langle s^2 \rangle_{0z}/\overline{M}_w)^{1/2}$ of the polymer was found to be 0.281×10^{-8} cm which can be corrected for sample heterogeneity ($h = 10$) to give $(\langle s^2 \rangle_{0w}/\overline{M}_w)^{1/2} = 0.269 \times 10^{-8}$ cm. This is lower than the value reported by Berry[28] for polystyrene of 0.276×10^{-8} cm, obtained for very sharp fractions. However, as the microstructure of the polymers may differ no direct comparison may be made at this time.

The authors wish to thank P. M. Toporowski for valuable technical assistance.

Division of Applied Chemistry,
National Research Council,
Ottawa, Ontario, Canada

REFERENCES

[1] COWIE, J. M. G., WORSFOLD, D. J. and BYWATER, S. *Trans. Faraday Soc.* 1961, **57**, 705
[2] SIRIANNI, A. F., WORSFOLD, D. J. and BYWATER, S. *Trans. Faraday Soc.* 1959, **55**, 2124
[3] KURATA, M. and YAMAKAWA, H. *J. chem. Phys.* 1958, **29**, 311
[4] KURATA, M. and STOCKMAYER, W. H. *Fortschr. Hochpolym. Forsch.* 1963, **3**, 196
[5] BYWATER, S. and WORSFOLD, D. J. *J. phys. Chem.* 1966, **70**, 162
[6] WORSFOLD, D. J. and BYWATER, S. *J. chem. Soc.* 1960, 5254
[7] BROWNSTEIN, S., BYWATER, S. and WORSFOLD, D. J. *Makromol. Chem.* 1961, **48**, 127
[8] COWIE, J. M. G. and TOPOROWSKI, P. M. *Polymer, Lond.* 1964, **5**, 601
[9] COWIE, J. M. G. and BYWATER, S. *Polymer, Lond.* 1965, **6**, 197
[10] COWIE, J. M. G. and BYWATER, S. *J. macromol. Chem.* 1966, **1**, 581
[11] COTTAM, B. J., COWIE, J. M. G. and BYWATER, S. *Makromol. Chem.* 1965, **86**, 116
[12] KOTERA, A., SAITO, T. and FUJISAKI, N. *Rep. Progr. Polym. Phys., Japan,* 1963, **6**, 9
[13] CORNET, C. F. and van BALLEGOOIJEN, H. *Polymer, Lond.* 1966, **7**, 293
[14] FLORY, P. J. *Principles of Polymer Chemistry.* Cornell University Press: Ithaca, New York, 1953

[15] SCHULZ, G. V. *Z. phys. Chem. B*, 1939, **43,** 25
ZIMM, B. H. *J. chem. Phys.* 1948, **16,** 1099
[16] KURATA, M., STOCKMAYER, W. H. and ROIG, A. *J. chem. Phys.* 1960, **33,** 151
[17] KURATA, M., YAMAKAWA, H. and UTIYAMA, H. *Makromol. Chem.* 1959, **34,** 139
[18] CORNET, C. F. *Polymer, Lond.* 1965, **6,** 373
[19] ZIMM, B. H. *J. chem. Phys.* 1946, **14,** 164
[20] PTITSYN, O. B. and EIZNER, YU. E. *J. tech. Phys. U.S.S.R.* 1959, **29,** 1117
[21] BURCHARD, W. *Makromol. Chem.* 1961, **50,** 20
[22] ULLMAN, R. *J. chem. Phys.* 1964, **40,** 2193
[23] PTITSYN, O. B. *Vysokomol. Soedineniya,* 1961, **3,** 1673; *Polym. Sci. U.S.S.R.* 1963, **1,** 1061
[24] STOCKMAYER, W. H. and FIXMAN, M. *J. Polym. Sci. C,* 1963, **1,** 137
[25] TSCHOEGL, N. W. *J. chem. Phys.* 1964, **40,** 473
[26] BYWATER, S., COWIE, J. M. G. and WILES, D. M. Paper presented at Twelfth Canadian High Polymer Forum, Ste Marguerite, P.Q., 1964
[27] BLOOMFIELD, V. and ZIMM, B. H. *J. chem. Phys.* 1966, **44,** 315
[28] BERRY, G. C. *J. chem. Phys.* 1966, **44,** 4550

115

ANNOUNCEMENTS

UNIVERSITY OF BRADFORD SCHOOL OF POLYMER SCIENCE

A Symposium on 'Structural Analysis of Polymers' will be held on 24 and 25 February 1967.

Papers will include a general introduction, infra-red and u.v. spectroscopy, n.m.r. spectroscopy, X-ray diffraction, crystallinity in polymers, and DTA with particular reference to transitions in polyamides. Fee for the Symposium £5 0s. 0d.

Further details and forms of application may be obtained from the Registrar, University of Bradford, Bradford, 7.

FOURTEENTH CANADIAN HIGH POLYMER FORUM

The Fourteenth Canadian High Polymer Forum will be held 24 to 26 May 1967 at the Université Laval in Quebec City. The Forum is sponsored by the National Research Council of Canada in cooperation with the Chemical Institute of Canada, and is concerned with all aspects of Polymer Science. The Chairman is Dr H. DAOUST, Department of Chemistry, University of Montreal, Montreal, Quebec.

The Forum Lecturer is to be Professor SEIZO OKAMURA, Department of Polymer Chemistry, Kyoto University, Kyoto, Japan. His subject will be 'Some Aspects of Ionic Polymerization'.

Persons wishing to contribute papers should contact the Program Chairman, Dr D. M. WILES, Division of Applied Chemistry, National Research Council, Ottawa, Ontario. Titles, authors' names, and abstracts of 200 to 300 words should reach Dr WILES no later than 15 February 1967.

Those wishing to attend the Fourteenth Forum will be requested to pre-register and should apply to Dr J. F. HENDERSON, Secretary-Treasurer, 14th Canadian High Polymer Forum, Research and Development Division, Polymer Corporation Limited, Sarnia, Ontario, Canada.

The Crystal–Crystal Transition in Poly[3,3-bis(chloromethyl)-oxacyclobutane]

J. R. COLLIER* and E. BAER

The transformation β to α form 'Penton'† was studied using differential thermal analysis and X-ray techniques. This transformation which starts around 115°C is rapid when accompanied by annealing of the β form, and the amount transformed increases with the annealing temperature. However, the α to β transformation does not occur even after long annealing times. Samples crystallized from the glassy state were predominantly β with a small amount of α, while samples crystallized from the melt were essentially all α form.

POLY[3,3-bis(chloromethyl)oxacyclobutane], trade-name Penton, has previously been shown to exist in two crystalline modifications[1-3]. The α form, which is obtained by crystallization from the molten state[1] and from solution[4], has an orthorhombic unit cell and the symmetry of a P_{nnm} space group[3]. Crystallization from the quenched glassy state[1], or from the melt under pressure[5] yields the β form, which has a monoclinic unit cell and a B_m space group[3]. In both forms the molecular chains have a zig-zag configuration with the same chain axis repeat distance[2,4]. However, the chlorine groups are in a *trans* relationship to the main chain in the β form and are *gauche* in the α form[2]. Sandiford[1] reported that the β form is monoclinic with two molecules per unit cell and calculated a theoretical crystal density of 1·469 g/cm³ which is equivalent to that of the α form[3,4]. However, the lattice parameters of Wasai *et al.*[3] gave a theoretical density of 1·455 g/cm³ for the β form. This density is surprisingly low since the low temperature form usually has the higher density[6].

Imura and Kondo[7] have reported that the β form transforms to α around 130°C. However, the reported diffractometer scans indicate that the transition was not complete at 130°C and that more β had transformed at 150°C. The object of this investigation was a more detailed study of the β to α crystal–crystal transformation in Penton.

EXPERIMENTAL

The samples used in this investigation were extruded pellets of Penton 9215 (lot number 90189) which were generously supplied by the Hercules Powder Company. Using a platen press these pellets were moulded into a film, cooled from the melt to 154°C and then held at this temperature for 16 hours to ensure complete crystallization. Selected samples were remelted at 230°C for one hour and then quenched to the amorphous glassy state in ice water. The quenched samples were then crystallized isothermally at predetermined temperatures above their glass transition temperature. Unless otherwise specified in the text, crystallization from the glassy state was performed at 25°C.

*Present address: Dept. of Chemical Engineering, Ohio University, Athens, Ohio.
†Registered trademark Hercules Powder Company.

X-ray scans and differential thermal analysis (DTA) thermograms were obtained using a General Electric XRD-6 Diffractometer and a DuPont 900 Differential Thermal Analyzer respectively. Unless the effect of heating rate was being considered, the DTA thermograms were run at a heating rate of 10 deg. C per minute. The reported DTA curves were normalized but no correction for heating rate was introduced.

RESULTS AND DISCUSSION
Evidence for α and β crystallographic forms

Discrimination between the α and β crystallographic forms of Penton can be achieved with a reflecting X-ray diffractometer. In *Figure 1* are shown three normalized X-ray patterns of samples which have been subjected to different thermal histories. Curve I is typical for a sample crystallized from the amorphous glassy state at 25°C. The first peak at $2\theta = 14\cdot4°$, is due to the (210) reflections of the α form; and the two stronger peaks at $2\theta = 15\cdot0°$ and $15\cdot6°$ are assigned respectively to the (020) and (110) reflections of the β form using the lattice constants of Sandiford[1]. In this sample, the X-ray pattern indicated that the polymer went predominantly into the monoclinic β form. However, a detectable amount of the orthorhombic α form was also observed. Curve II was obtained after annealing the glass crystallized sample of curve I. That some of the β material originally present is transformed to α during annealing at 150°C was evidenced by the more intense α peak. Since the intensity of and area under the β peaks on the original scans decreased relative to the amorphous scattering and the α peaks, the α material was not due to additional crystallization from amorphous polymer. Samples crystallized from the melt exhibit strong α peaks as shown by curve III. Whether small amounts of the β form were also present cannot be resolved due to experimental limitations.

The same samples were used for both the X-ray scans of *Figure 1* and
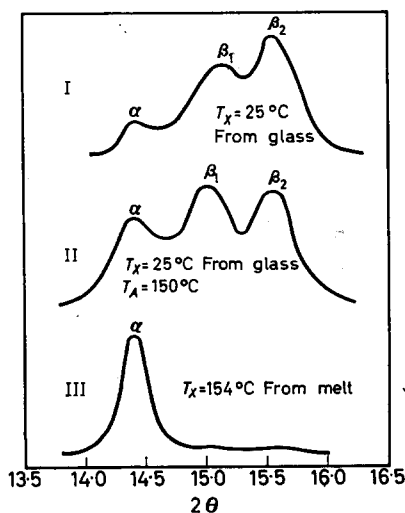
Figure 1—Effect of crystallization and annealing temperatures on the X-ray patterns of Penton. T_x is the crystallization temperature, T_A is the annealing temperature

118

the normalized DTA thermograms of *Figure 2*. Samples isothermally crystallized from the melt, which according to X-ray analysis are essentially α, exhibited only one DTA melting peak at $167.5\,^{\circ}$C as is shown in curve III, *Figure 2*. However, when crystallized from the glassy state (curve I) two definite peaks at $159.0\,^{\circ}$ and $164.5\,^{\circ}$C were present. By annealing at $150\,^{\circ}$C (curve II) the first of the two peaks decreased in relative intensity and the shoulder around $149\,^{\circ}$C, believed to be due to the β to α trans-

Figure 2—Effect of crystallization and annealing temperatures on the DTA scans
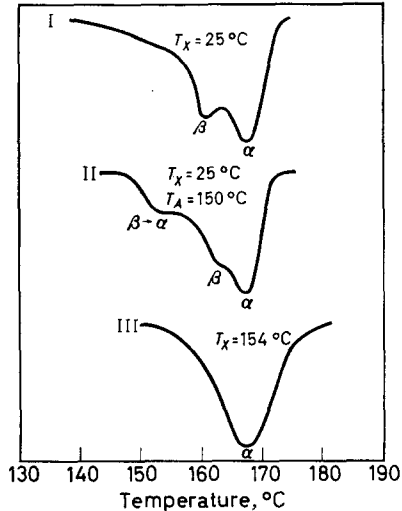
formation, became more pronounced. The X-ray scans of the same annealed sample indicated that some of the β form had transformed to α during annealing. It appears that the first peak is due to the melting of the β form; consequently, the higher temperature peak must be due to the melting of α material.

These assignments are validated by the heating rate studies shown in *Figures 3* and *4* of unannealed and annealed glass crystallized samples respectively. In both of these figures the intensity of the β peak relative to the α peak increases with increasing heating rate. This is in agreement with the above mentioned assignment since the amount of the β material transformed to α should decrease as the heating rate increases thereby giving a stronger β melting peak. Further confirmation of the β peak assignment was achieved by heating a sample in the DTA unit at 10 deg. C per minute through this peak and then cooling back to room temperature before reaching the α peak. The subsequent DTA scan for this sample showed only the higher temperature peak indicating that the β material, which had not transformed, did melt during the initial heating and upon cooling recrystallized into the α form.

The shoulder observed around $155\,^{\circ}$C especially in the annealed samples was attributed to the β to α transformation. Annealing produces an increase in surface area[8] and according to McCrone[6] this in turn accelerates

119
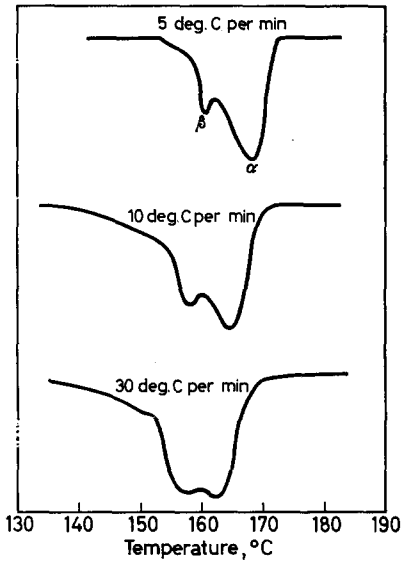
Figure 3—Effect of heating rate on the DTA thermograms of Penton crystallized from the glass at 25°C

the rate of transformation. At faster heating rates the β to α shoulder is less evident since there is insufficient time for the transformation. This is consistent with the observation of a relatively intense β peak at fast heating rates. Further confirmation of this assignment was obtained by heating a glass crystallized sample in the DTA apparatus through this shoulder at 10 deg. C per minute and then, before reaching the β melting peak, cooling to room temperature. The DTA thermogram which was then obtained at 50 deg. C per minute exhibited a strong α melting peak and only a slight indication of a β peak. This implies that during the initial heating and
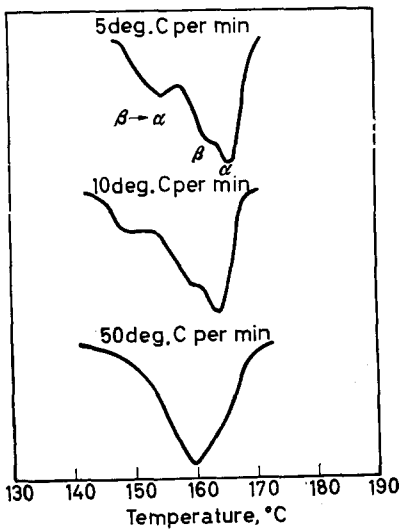
Figure 4—Effect of heating rate on the DTA scans of Penton crystallized from the glass at 25°C and annealed at 150°C for two hours

120

cooling step, most of the β material transformed to α while the sample was in the temperature region in which transformation is quite rapid.

The effect of annealing temperature on the α to β concentration ratio
Figure 5 illustrates the time dependence of the β to α transition at two annealing temperatures. In this and succeeding figures the relative extent
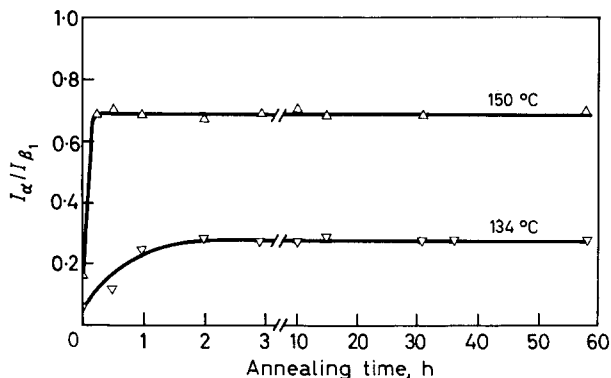
Figure 5—Effect of annealing time on the ratio of α
to β forms. Samples were crystallized from the glassy state
at 25°C and sequentially annealed for the time specified

of transformation is represented by the ratio of the (210) α peak intensity, I_α, divided by the intensity of the (020) β peak, $I_{\beta 1}$. The atomic positions assigned by Wasai *et al.*[3] are questionable since they catalogued only one reflection in the 15·0° to 15·6°, 2θ region. Two peaks were observed in
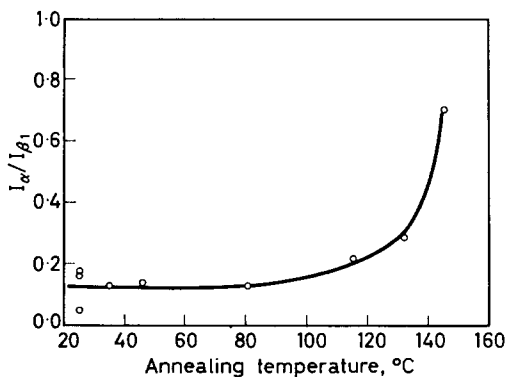
Figure 6—Effect of annealing temperature on the α to β
intensity ratio. Samples crystallized from the glassy state
and annealed for 36 h at various temperatures

this region of diffractometer scans but due to their proximity and intensity they appear as one ring in an unoriented pattern and one spot in a fibre pattern. Consequently, the atomic positions which were assigned on the

121

basis of a fibre pattern do not account for the 15·6° peak and predict a zero intensity for such a peak. Therefore, an intensity ratio of two strong peaks, one from each crystal form cannot be converted to an exact concentration ratio because the theoretical intensities are not available. Since X-ray peak intensities are directly proportional to the actual amount of material present, and the magnitude of the proportionality constant is dependent on the particular crystal form, the intensity ratio is directly proportional to a molar concentration ratio but not equal to it. Consequently, even when a concentration ratio cannot be calculated due to a lack of crystallographic data, an intensity ratio can be used to observe the extent of a crystal–crystal transformation. Satisfactory results were obtained using this technique to investigate the β to α crystal–crystal transformation in polypropylene[9].

As is shown in *Figure 5*, the β to α transformation in Penton proceeds to a constant $I_\alpha/I_{\beta 1}$ value which is dependent upon the annealing temperature. A similar result was observed in the transformation of β to α form polypropylene[9], and the transformation of form III to form I' of polybutene-1[10, 11]. As would be expected, the time required to reach this value decreased as the annealing temperature was increased. Two hours were necessary at 134°C and only 14 minutes at 150°C. In order to obtain constant concentrations at temperatures lower than 134°C an annealing time of 36 hours was used, and for temperature above 150°C samples were annealed for 30 minutes.

Figures 6 and *7* show the effect of annealing temperature on the $I_\alpha/I_{\beta 1}$ ratio for samples which had been sufficiently annealed to assure a constant concentration ratio. It appears from these data that a gradual onset of the β to α transformation probably occurs between 81° and 115°C and that the amount of β form transformed to α is a strong function of the annealing temperature.

The DTA scans in *Figure 2* showed that when sufficient time for transformation was not allowed at a heating rate of 10 deg. C per minute, some of the β material would melt before it could transform to α. For this reason, the investigation of the transformation at annealing temperatures greater than 154°C was carried out by successive annealing treatments on the same sample. After annealing a glass crystallized sample at 157°C for half an hour this sample was removed for X-ray measurements at room temperature. Since α material does not transform to β, cooling the sample to room temperature does not change the relative concentration. After removing a small amount of material for DTA thermograms, the sample was again placed in an oven which had been preset to a temperature two degrees higher than the previous annealing temperature and the identical procedure was repeated. The results of these sequential experiments shown in *Figure 7* indicate that the limiting ratio continues to increase up to an annealing temperature of 173°C at which point complete conversion β to α was effected.

Mechanism of crystal–crystal transformation

As was mentioned earlier the β to α transformation in Penton is quite
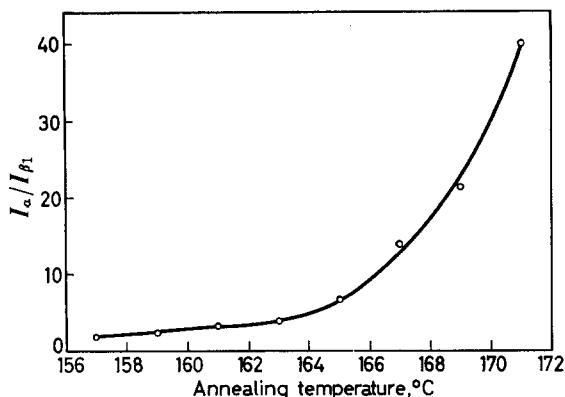
Figure 7—Effect of annealing temperature on the α to β intensity ratio. Samples crystallized from the glassy state and sequentially annealed for 30 min at various temperatures

similar to the β to α transformation in polypropylene[9] and the form III to form I′ transformation in polybutene-1[10, 11]. The amount of material transformation in all three cases proceeds to a limiting value which is controlled by the annealing temperature. However, some polymer crystal–crystal transitions proceed kinetically to complete conversion at all allowed temperatures as does the form II to form I transition in polybutene-1[11, 13]. Therefore, there is more than one mechanism for polymer crystal–crystal transformation.

The observed transformation in Penton probably proceeds by a crystal–crystal mechanism and not by a crystal–melt–recrystallization mechanism since the rate increases with annealing temperature (*Figure 5*), and no observable exothermic DTA peak occurs between the β and α melting peaks (*Figures 2* and *3*). Also, as temperature increases, the rate of crystallization has been noted to pass through a maximum below 140°C and then decrease with any further increase in temperature[14]. However, the rate of transformation was observed continually to increase with temperature. Furthermore, this transformation begins in the same temperature region as the onset of annealing of the β form (*Figure 8*), which suggests that segmental chain mobility may be necessary before the transformation is energetically favourable. If this annealing motion is required for the forward transformation of β to α, then a sample crystallized from the melt, which is predominantly α, would not be expected to transform partially to β.

Effect of annealing on the melting of α and β forms

The melting of the α and β forms was also studied by using the same annealed samples. The onset of annealing of the β material occurred near 115°C as was evidenced by the increasing β melting peak temperature (*Figure 8*). However, the last trace of the β form as detected by DTA did

not disappear until annealing at 167°C. This DTA measurement of the annealing temperature necessary for complete conversion is slightly lower than the 173°C revealed by X-ray analysis. This disagreement results from the fact that as the annealing temperature increased, the β peak decreased in relative intensity but increased in peak temperature, while the α peak temperature remained essentially constant. Therefore, a small peak corresponding to the trace of β material which remained after annealing at 167°C was effectively masked by the intense α peak.

The α melting peak temperature increased with annealing temperature between 165° and 185°C. Since samples crystallized from the melt into the α form usually melt around 165°C, the sequential annealing technique allowed an increase in the perfection of the polymer morphology as has been observed in other crystalline polymers[8].
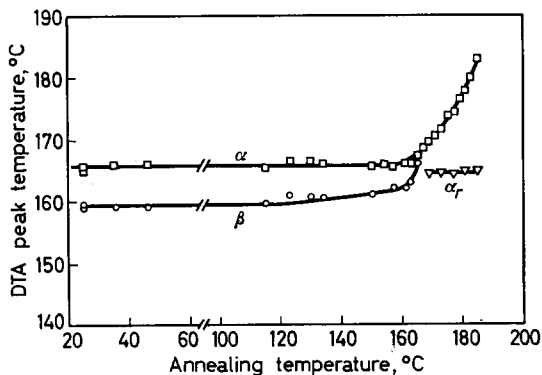
Figure 8—Effect of annealing on the DTA peaks of Penton samples crystallized from the glassy state and annealed. α_r, recrystallized α material

Theoretically the melting point should increase with annealing temperature up to the equilibrium melting point which was estimated to be 191°C[15]. However, as expected due to experimental limitations, the highest melting peak observed was 185°C. The appearance of an additional peak at 164°C corresponds to some material which was melted during annealing at temperatures greater than 165°C and recrystallized into the α form while cooling to room temperature. The intensity corresponding to the annealed α peak continually decreased while that of the recrystallized α peak increased with annealing temperature indicating that an increasing amount of the material melted at progressively higher annealing temperatures.

CONCLUSIONS

Crystallization of Penton from the glassy state yielded predominantly the β form with a detectable amount of α material also present. However, crystallization from the melt gave essentially all α material. When a glass crystallized sample is annealed the β form transforms to α by a crystal–crystal transformation mechanism. The reverse transformation α to β was not observed in either melt or glass crystallized samples.

The amount of material converted from β to α form during annealing of glass crystallized samples, was strongly dependent on the annealing temperature. As expected, the time required to reach the conversion characteristic of the particular annealing temperature decreased with increasing temperature.

The β to α transformation began slightly below 115°C and continued as a result of sequential annealing to complete conversion at 173°C. This transformation appears to proceed by a crystal–crystal mechanism which is energetically favourable only when accompanied by concurrent annealing of the polymer to a more perfect morphology.

Sequential annealing of glass crystallized samples showed that the melting point of α material increased significantly with annealing temperature. The highest melting point observed by this technique was 185°C which is only a few degrees lower than the predicted equilibrium melting point of 191°C.

Polymer Science and Engineering,
  Case Institute of Technology,
    Cleveland, Ohio 44106

REFERENCES

[1] SANDIFORD, D. J. H. *J. appl. Chem.* 1958, **8**, 188
[2] ENOMOTO, S., OPASKAR, C. G. and KRIMM, S. Paper presented .at International Symposium on Macromolecular Chemistry, Prague, Summer 1965, A396
[3] WASAI, GO, SAEGUSA, TAKEO and FURUKAWA, JUNI. *Kogyo Kwagaku Zasshi,* 1964, **67**, 1428
[4] HEBER, I. and LEHMANN, J. *Kolloidzschr.* 1964. **200**, 7
[5] KARDOS, J. L. *Ph.D. Thesis,* Case Institute of Technology, 1965
[6] McCRONE, W. C. *Physics and Chemistry of the Organic Solid State,* Ed. D. FOX, M. M. LABES and A. WEISSBERGER. Interscience: New York, 1965
[7] IMURA, K. and KONDO, S. *J. appl. Polym. Sci.* 1962, **6**, S52
[8] GEIL, P. H. *Polymer Single Crystals.* Interscience: New York, 1963
[9] TURNER JONES, A., AIZLEWOOD, JEAN M. and BECKETT, D. R. *Makromol. Chem.* 1964, **75**, 134
[10] GEACINTOV, C. Paper presented at Polymer Science Colloquia, Case Institute of Technology, 1965
[11] DANUSSO, F., GIANOTTI, G. and POLIZZOTTI, G. *Makromol. Chem.* 1964, **80**, 13
[12] POWERS, J., HOFFMAN, J. D., WEEKS, J. J. and QUINN JR, F. A. *J. res. Nat. Bur. Stand. A,* 1965, **69**, 335
[13] TURNER JONES, A. *J. Polym. Sci. B,* 1965, **3**, 591
[14] COLLIER, J. R. and BAER, E. To be published
[15] BAER, E., COLLIER, J. R. and CARTER, D. R. *S.P.E. Trans.* 1965, **4**, 22

Thermal Degradation of Vinyl Polymers
I—Thermal Degradation of Polystyrene–
Poly(α-methylstyrene) Mixtures

D. H. Richards and D. A. Salter

Thermal degradation of polystyrene (PS) has been induced at temperatures at which it is normally stable (260° to 287°C) by using poly(α-methylstyrene) (PMS) as a radical producing agent. PMS degrades at these temperatures in a kinetically simple manner. The decompositions were followed by measuring the monomers evolved from the mixtures by gas–liquid chromatography.

Experiments where the PMS molecular weight was varied over a wide range established that, whereas the degradation of PMS was unaffected by the presence of PS, the PS degradation varied as an inverse function of PMS molecular weight. These observations were taken to mean that the system was heterogeneous, consisting of micelles of PMS embedded in a PS matrix. The PMS could then only initiate PS by completely unzipping to produce monomer radicals which could diffuse into the PS matrix. The heterogeneity of the system was confirmed kinetically. It was found that the rate constant of primary scission of PMS was given by the expression $5 \times 10^{18} \exp(-65\,000/RT)$ and that the degradation of the polymer was unaffected by the type of catalyst used in its synthesis. The depropagation of PS was found to be described by the equation $k_d/k_t^{\frac{1}{2}} = 65 \exp(-10\,500/RT)$ where k_d and k_t are the rate constants of depropagation and termination respectively. This equation was shown to hold from 5 000 up to 100 000 molecular weight of PS.

THE thermal degradation of polystyrene has been studied by a number of authors and the results have recently been reviewed by Wall and Flynn[1] who point out that many important questions remain unanswered. It is uncertain whether the initial rapid decrease in molecular weight is caused by scission of weak bonds, intermolecular chain transfer or both. Strong support for chain transfer is obtained from work on poly(α-deuterostyrene)[2], but evidence for the presence of thermally active weak links[3-5] is equally convincing. Gordon[6] interpreted the results of Grassie and Kerr[7] by assuming the initial scission to be terminal, but had also to postulate some random or weak link scission and/or chain transfer. Later work[8] indicates that, at medium molecular weights, terminal scission predominates with very short zip lengths but that, at high molecular weights, random initiation becomes significant.

One of the main factors preventing the quantitative analysis of the degradation kinetics is the uncertainty of the position and nature of the initial scission. We have adopted a fresh approach to try to overcome this difficulty, viz. to induce decomposition of polystyrene at temperatures at which it is normally stable. Three methods have been used: the first introduces into the system a radical producing agent which initiates the polystyrene by hydrogen abstraction. The second and third methods (see succeeding papers) involve the synthesis of polystyrene with weak terminal bonds and with weak bonds at specific points along the polymer backbone

127

respectively. The last two methods thus enable the position of initial scission to be established.

Poly(α-methylstyrene) was found suitable for the first method and also, as a block copolymer with polystyrene, for the second[9]. The third approach involves the reaction of low molecular weight 'living' polystyrene with iodine—a process which we have found to result in a Wurtz type of condensation with the formation of weak links at the coupling points[10]. This paper is confined to a detailed discussion of the first method.

Poly(α-methylstyrene) (PMS) was chosen because it degrades at temperatures about 50 deg. C lower than polystyrene (PS) and in an apparently simple manner. Low temperature studies (220° to 240°C) by Bywater et al.[11, 12] and high temperature studies (270° to 290°C) by Madorsky[13, 14] and Wall[15], indicate random initiation and extremely large zip length (1 340 monomer units at 270° to 290°C), with negligible chain transfer. Thus PMS with low degrees of polymerization should exhibit proportionality between their molecular weights and initial rates of monomer evolution. If, however, chain transfer to PS takes place, this linearity will be affected so that measurement of α-methylstyrene evolution should allow the evaluation of the rate of production of PS radicals. Simultaneous measurement of the styrene evolved would then enable the behaviour of these radicals to be studied.

<div align="center">EXPERIMENTAL</div>

Synthesis of polymers

All polymers were prepared by the 'living' polymer technique[16]. Sodium naphthalene was catalyst for PS, and cumyl potassium[17] or disodium α-methylstyrene tetramer[18] was used for PMS. The polymerizations were carried out in a vacuum with tetrahydrofuran as solvent.

Polystyrene—Polymers were prepared with molecular weights up to 92 000 as measured by viscometry[19]. They were 'killed' with methanol to produce —CH$_2$ ϕ end groups.

Poly(α-methylstyrene)—Polymerizations were performed at $-78°C$ (when the equilibrium monomer concentration[20] is less than 0·005M) for times greater than five half-lives[21] after which methanol was added to produce —CH (CH$_3$) ϕ end groups. Polymers were prepared with viscosity molecular weights[22] ranging from 7 000 to 1 210 000.

Degradation experiments

Degradations were performed in modified U-tubes based on Jellinek's design[23]. The appropriate volumes of 5 per cent w/v benzene solutions of PMS and PS were introduced into one of the arms so that the total weight added was 0·1 g. Preliminary experiments showed that this weight was in the range where the rate of monomer evolution was proportonal to the weight of the sample. The polymer mixture was freeze-dried under vacuum and then slowly heated to 180°C when a pressure of 10^{-5} mm of mercury was obtained before sealing. This procedure was carried out simultaneously on up to fifteen U-tubes. Each U-tube was placed with the arm containing the sample in a salt bath at the required temperature and the other arm immersed in liquid nitrogen. At the required time the cold

fingers were sealed and the styrene and α-methylstyrene monomer contents analysed by gas–liquid chromatography using a Perkin–Elmer model 451 fractometer.

Jellinek's system has been criticised by Atherton[24] on the ground that loss of polymer from the reaction zone occurs by sputtering. This has now been avoided by blowing an inch diameter thin-walled glass bulb in the U-tube arm containing the polymer.

Degradation experiments were performed between 260° and 290°C to study the effect of molecular weight changes of PMS on the breakdown pattern of the mixtures. Fifteen U-tubes, each containing 0·086 g of PS of 60 000 molecular weight and 0·014 g of PMS of differing molecular weights ranging from 7 400 to 1 210 000, were degraded at each temperature. The reaction times were arranged so that less than five per cent of the lowest molecular weight PMS was decomposed. The PMS samples used were prepared using 'tetramer' as catalyst.

Two experiments were carried out at 270°C to determine the effect of concentration on the breakdown. In the first, PMS of 1 210 000 molecular weight was mixed with 400 000 molecular weight PS in all proportions, and in the second, the molecular weights of PMS and PS were 195 000 and 44 000 respectively.

To discover whether the degradation was affected by the nature of the PMS catalyst, comparative measurements were made on mixtures where the PMS component had been prepared using either 'tetramer' or cumyl potassium as initiator.

Degradation measurements were performed on mixtures containing PMS of 7 400 molecular weight, but with PS of molecular weights up to 92 000 to evaluate the effect of the viscosity of the medium on the rate of termination of polystyryl radicals.

RESULTS

The quantities of monomers resulting from typical degradations between 260° and 287°C are given in *Table 1*. The styrene produced must have resulted from interaction of PS with the degrading PMS as no styrene was obtained from pure PS under these conditions. The α-methylstyrene evolved increases initially with PMS molecular weight and then levels off at high values whilst the styrene decreases to extremely low values at medium and high molecular weights. These trends will be discussed later.

Figure 1 shows the amounts of α-methylstyrene evolved in an hour at 270°C against the weight fraction of PMS present. The two graphs refer to differing molecular weights of the components but both exhibit linearity.

Table 2 compares the α-methylstyrene evolution from polymer mixtures with PMS prepared using either 'tetramer' or cumyl potassium as catalyst. The rate is seen to depend only on the molecular weight, and not on its mode of synthesis.

The results in *Table 5* indicate that the rate of styrene evolution at constant PMS molecular weight is independent of the molecular weight of PS used as diluent.

129

Table 1. Weights of monomers evolved from polystyrene–poly(α-methylstyrene) mixtures as a function of poly(α-methylstyrene) molecular weight $(M\alpha)$ and temperature

Temp., °C	260		268		270		274		280		287	
Time, h.	7·5		5·33		3·25		2·08		1·25		1·0	
Mol. wt α (mg monomer)	S	α	S	α	S	α	S	α	S	α	S	α
7 400	0·326	0·28	0·55	0·533	0·36	0·42	0·39	0·43	0·23	0·40	—	—
12 300	0·340	0·440	0·515	0·856	0·39	0·70	0·35	0·88	—	—	0·40	1·65
16 600	0·377	0·85	0·44	1·57	0·31	1·09	0·30	1·14	0·27	1·11	0·26	2·02
23 000	0·353	1·11	0·49	2·20	0·31	1·70	0·37	1·81	0·178	1·49	0·354	2·95
31 600	0·297	1·56	0·26	2·56	0·31	2·04	0·26	1·97	0·159	2·18	0·24	4·30
42 200	0·220	1·82	0·26	3·92	0·25	2·62	0·087	3·56	0·106	2·88	0·22	5·64
65 000	0·125	2·44	0·186	4·48	0·185	2·94	0·178	3·40	0·107	3·56	0·21	7·28
73 000	0·053	2·15	0·175	4·36	0·12	2·72	0·149	3·51	0·050	2·71	—	—
82 000	0·041	2·47	0·131	4·16	—	—	0·088	3·17	0·073	3·47	—	—
105 000	0·007	2·96	0·070	5·40	0·058	3·56	—	—	0·067	4·58	0·073	7·00
144 000	0·036	2·75	0·062	6·16	0·045	3·98	0·075	4·50	0·031	6·4	—	—
195 000	0·008	3·43	0·035	6·12	0·044	5·38	0·041	6·80	0·063	6·95	—	—
332 000	0·00	4·30	0·028	6·80	0·051	6·20	0·030	5·84	0·043	6·88	0·00	9·04
860 000	0·00	4·68	0·006	7·84	0·034	5·96	0·030	6·04	0·030	7·76	0·016	8·56
1 210 000	0·00	5·28	0·016	8·08	0·021	6·04	0·028	7·44	0·036	9·36	0·00	10·92
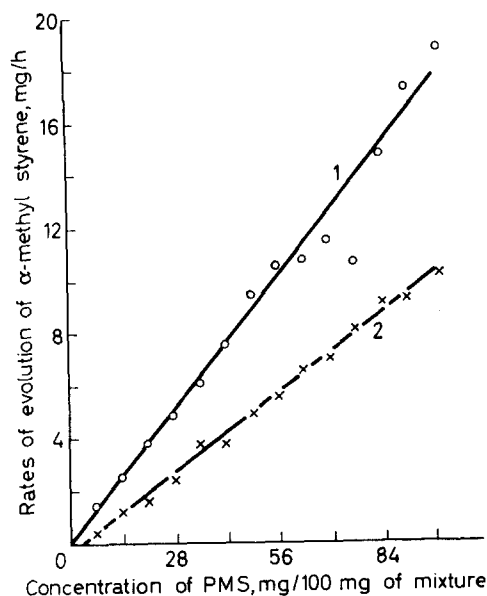
Figure 1—Rate of α-methylstyrene evolution against concentration of PMS in PMS–PS mixtures at $T=270°C$. 1, PMS$=1\,210\,000$ and PS$=400\,000$; 2, PMS$=195\,000$ and PS$=44\,000$

DISCUSSION

It is convenient to discuss the degradation behaviours of the two polymer components separately and to consider the PMS degradation first.

Poly(α-methylstyrene) degradation

A simple picture of the kinetics of degradation of PMS can be obtained with the following assumptions: (*a*) the initial scission is random and produces two polymer radicals which subsequently depropagate, (*b*) no chain transfer to another PMS chain occurs, (*c*) the degree of polymerization is sufficiently small to assume that each chain unzips completely after scission, (*d*) monomer radicals left after unzipping diffuse out of the system.

The total number of inter-unit bonds in W_a g of PMS is

$$(W_a/M_a)\ \{(2M_a/m_a)-2\}\ \text{moles}$$

where M_a denotes polymer molecular weight and m_a is the monomer mole-

Table 2. Comparison of rates of monomer evolution from PMS prepared with 'tetramer' and cumyl potassium as catalyst, $T=260°C$, $t=5$ h

Cumyl potassium		'Tetramer'	
Mol. wt	α mg	Mol. wt	α mg
26 700	0·585	23 000	0·54
56 200	1·17	65 000	1·13
87 000	1·37	82 000	0·93
87 000	1·21	82 000	0·95
186 000	1·95	195 000	1·87

cular weight. Therefore at normal polymer molecular weights, the number of inter-unit bonds must be

$$2W_\alpha / m_\alpha \text{ moles}$$

If k_i is the rate constant of initiation, then the rate of chain scission is $2k_i W_\alpha / m_\alpha$ moles/sec [from (a)] and the rate of monomer evolution is given by

$$-dW_\alpha / dt = 2k_i W_\alpha M_\alpha / m_\alpha \quad [\text{assuming } (c)].$$

Whence by integration,

$$\ln (W_\alpha^0 / W_\alpha) = 2k_i M_\alpha t / m_\alpha$$

or

$$\log (W_\alpha^0 / W_\alpha) = 7 \cdot 36 \times 10^{-3} k_i t M_\alpha$$

At unit value of t, a plot of $\log (W_\alpha^0 / W_\alpha)$ against M_α should be linear with a gradient of $7 \cdot 36 \times 10^{-3} k_i$ passing through the origin.

At sufficiently high molecular weights, condition (c) no longer holds and the residue contains increasing amounts of low molecular weight polymer. The kinetic picture then becomes much more complex although a general theoretical analysis has been developed by Simha, Wall and Blatz[25–27].

Much information can be obtained from the simple picture above, however, and *Figures 2* and *3* show the curves obtained when $\log (W_z^0 / W_\alpha)$ is plotted against M for a time of one hour. *Figure 2* shows that at high
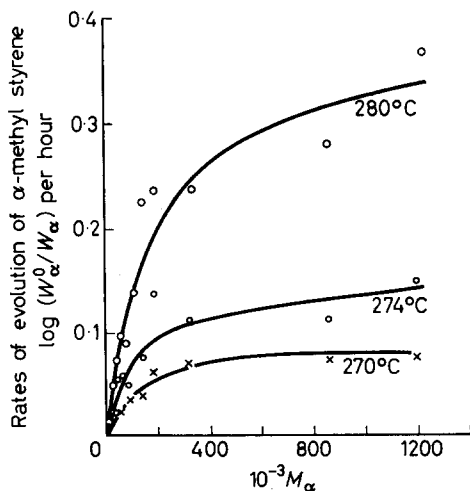
Figure 2—Rates of evolution of α-methylstyrene against molecular weight of PMS in PMS–PS mixtures at various temperatures. Complete molecular weight range

molecular weights the curves become parallel to the abscissa indicating a zip length much smaller than the polymer chain lengths. A linearity exists up to 60 000 molecular weight (*Figure 3*) for all temperatures studied (the complete graph at 287°C is not shown), and the rate constants for primary scission were calculated from the slope (*Table 3*). An Arrhenius plot (*Figure 4*) of these results gives an activation energy of 65 kcal, and a frequency factor of 5×10^{18} sec^{-1}.
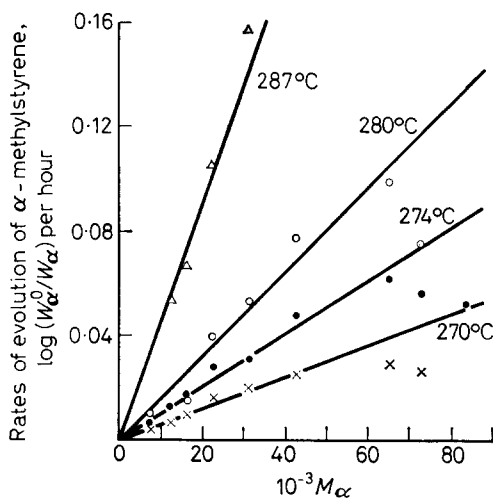
Figure 3—Rates of evolution of α-methylstyrene against molecular weight of PMS in PMS–PS mixtures at various temperatures. Low molecular weight range

Table 3. Values of k_i determined as a function of temperature

$T°C$	260	268	270	274	280	287
$10^8 k_i$ (sec^{-1})	0·767	2·07	2·25,2·18,2·18	3·96	5·87,5·80,5·20	17·3

Brown and Wall[15] examined the degradation of pure PMS (sodium initiated) at these temperatures using a different experimental technique. They used material between 79 000 and 480 000 molecular weight, and so did not cover the linear portion of the rate versus molecular weight curve. They analysed their results using the theory of Simha, Wall and Blatz[25] and also obtained Arrhenius plots of the initial rates of a number of different molecular weight samples. These showed the activation energy to be molecular weight independent and equal to 65 kcal, and the frequency factor to be approximately 10^{18} which is in excellent agreement with our results.

The degradation of PMS is therefore unaffected by the presence of PS, although decomposition of PS is induced by PMS, especially at low DPs.

Figure 4—Arrhenius plot to determine activation energy of primary scission of PMS chains
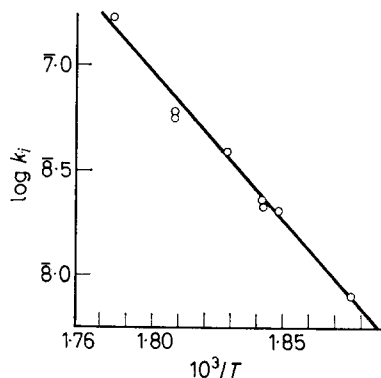
These observations may be reconciled if only the monomer radical produced after complete unzipping can initiate PS decomposition. Then the rate of PS initiation would decrease with increasing PMS molecular weight, as is observed.

PS is said to exhibit chain transfer on degradation due to the susceptibility of the tertiary hydrogens to radical attack[1] and the absence of hydrogen abstraction by the degrading PMS radicals can therefore be most reasonably explained if the system were heterogeneous and consisted of micelles of PMS in a matrix of PS. Degradation of PMS would take place within the micelles until the monomer radicals were produced. These could then diffuse out into the matrix (they should have about the same diffusion constant as the monomer) and attack the PS.

Microscopic examination of castings of PMS and PS mixtures showed no heterogeneities, but the sensitivity of this method is governed by the difference in refractive indices of the components, which is probably very small. Baer[28] has recently observed that mouldings of PMS–PS mixtures are cloudy whereas similar block copolymers are transparent. Furthermore, the mixtures exhibit two damping maxima whereas the block copolymers exhibit only one. This is strong evidence of heterogeneity at room temperature.

No reported information on the heterogeneity of the system under melt conditions has been found, but experiments where mixtures of a given PMS and PS, with compositions varying between the extremes, were degraded (*Figure 1*) shed some light on this problem. Molecular weights of PMS were chosen at which bimolecular radical termination predominates (*Figure 2*) and so, in a homogeneous system, an increase in PMS concentration should result in a decrease in the zip length and give a plot of monomer evolution against PMS concentration which curves toward the abscissa. In a heterogeneous system increase in PMS concentration would merely increase the size and/or number of micelles present and leave the zip length unaffected. The rate of monomer evolution would then be proportional to the PMS concentration, as it is.

The good agreement with Brown and Wall[15] confirms their analysis of the PMS degradation process at high molecular weights. Thus, in the absence of chain transfer and assuming all depropagating radicals terminate bimolecularly, the initial rate of monomer production is given by $dm/dt = (W_a k_2/m_a)(2k_i/k_4)^{\frac{1}{2}}$ where k_2 and k_4 are rate constants of depropagation and termination respectively. The overall activation energy is then $E = \frac{1}{2}E_i + E_2 - \frac{1}{2}E_4$, compared with $E = E_i$ at low molecular weights. In the intermediate range E should vary between these values, and Brown and Wall have interpreted its observed invariance to mean that $\frac{1}{2}E_i = E_2 - \frac{1}{2}E_4$. This is confirmed by our direct measurement of E_i.

Assuming the termination step to be diffusion controlled and its activation energy to be that of viscous flow, i.e. about 20 kcal as has been found for poly(methylmethacrylate)[29], the value of $E_2 \simeq 43$ kcal is obtained. Further, as $E_2 = E_p - \Delta H_p$ (subscript p refers to the propagation reaction) and $\Delta H_p = 9$ kcal[30], E_p is approximately 34 kcal.

Recently, Wall[31, 32] briefly referred to preliminary experiments on the

photo-initiated thermal decomposition of PMS where he obtained the relation $E_2 - \frac{1}{2}E_4 \simeq 25$ kcal. Substitution in the above energy equation with $E = 65$ kcal gives $E_i = 80$ kcal. This is in disagreement with our result and Wall[33] has suggested that at low molecular weights the cage effect, i.e. the activation energy of viscous flow, may be absent. This seems unlikely and his latest findings are inconsistent with his observed invariance of E with molecular weight. A more detailed discussion on these points must, however, await publication of the experimental evidence on which the recent results are based.

The PMS used in the experiments so far discussed was prepared using 'tetramer' as catalyst. This has the structure[18] $Na^{+-}C (CH_3) \phi$—CH_2—CH_2—C—$(CH_3) \phi$—$C (CH_3) \phi$—CH_2—CH_2—$C (CH_3) \phi^- Na^+$ and is present in the middle of each polymer chain. The degradation behaviour of the polymers could be influenced by the presence of head–head linkages as we have recently found that PMS consisting almost entirely of head–head bonds degrades to produce less than one per cent of monomer[34]. Thus, polymers initiated with cumyl potassium, possessing only head–tail bonds, could exhibit different degradation characteristics. *Table 2* compares the degradation rates of these two types of polymers. It is evident that the catalyst has little influence and, although no explanation can be given, this is in line with previous results obtained[11] at 230°C.

Polystyrene degradation

If it is assumed that *all* α-methylstyrene monomer radicals formed within the micelles emerge and chain transfer to PS, then quantitative information can be obtained about PS degradation. The zip length of PS is said to be very small (about five monomer units at 330°C[35]) and so the termination step with 60 000 molecular weight material may be assumed to be exclusively bimolecular. Indeed, we have confirmed this directly in studies on PMS–PS block polymers of similar composition[9]. The degradation scheme may therefore be written as:

$$\alpha \cdot + P_N \longrightarrow P_n^\cdot + P_{(N-n)} + \alpha H$$

$$P_n \cdot \xrightarrow{k_d} P_{(n-1)}^\cdot + S$$

$$P_{(n-x)}^\cdot + P_N \xrightarrow{k_{tr}} P_k^\cdot + P_{(N-k)} + P_{(n-x)} H$$

$$P_k^\cdot + P_l^\cdot \xrightarrow{k_t} Polymer$$
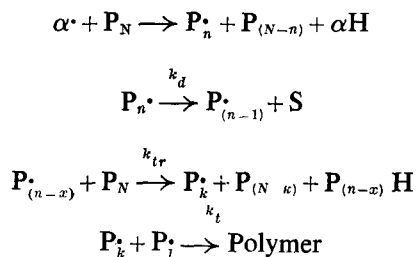
where $\alpha \cdot$ denotes α-methylstyrene monomer radical, S is styrene monomer, P is polystyrene or its radical, and k_{tr} is a chain transfer constant.

Under conditions where PMS radicals unzip completely, the rate of formation of PS radicals equals the rate of formation of PMS radicals, viz. twice the rate of scission of PMS, and it may be readily shown that rate of production of styrene (g/sec) from sample (g) is given by

$$r_s^0 \text{ (sec}^{-1}) = k_d (2W_s W_a m_s k_i / m_a k_t)^{\frac{1}{2}}$$

135

where W_a is weight of PMS$=0.014$ g and W_s is weight of PS$=0.086$ g. Substituting these values and the monomer molecular weights into the above equation, we get $r_s^0 (h^{-1}) = 166 \ k_d (k_i/k_t)^{\frac{1}{2}}$. Here r_s^0 is the initial rate of styrene evolution, whereas *Table 1* gives styrene rates averaged over the experimental time. However, as less than about five per cent of the PMS of lowest molecular weight is decomposed in this period, the error involved is quite small.

Table 1 indicates that the rate of evolution of styrene decreases with increase in PMS molecular weight even in the range where the α-methyl-styrene rate increases linearly. The assumption that all the monomer radicals attack the PS is therefore incorrect and some termination by dimerization takes place. Any significant reaction between the monomer radicals and the degrading PMS radicals would result in deviations from proportionality of α-methylstyrene evolution with molecular weight. They must therefore terminate by mutual reaction or by hydrogen abstraction from PS and it is apparent that the proportion which recombines increases with PMS molecular weight. This is explicable if the micelle size increased with molecular weight. Further, increase in chain length, by lowering the mobility of the monomer radical by increased viscosity, would lessen its probability of escape from the micelle. Whatever the explanation it is reasonable to suppose that the maximum probability of hydrogen abstraction is obtained by extrapolating to zero PMS molecular weight.

It is found that plots of log r_s against molecular weight are approximately linear up to 100 000 (*Figure 5*) and the rates at zero molecular weight (r_s^0) are listed in *Table 4*. There is some evidence to support the assumption that r_s^0 represents the condition where *all* the monomer radicals chain transfer from preliminary work on the degradation of block polymers of the

Table 4. Extrapolated rates of styrene evolution as a function of temperature

$T°C$	260	268	270	274	280	287
$10^5 r_s/h$	5·6	10·5	12·6, 13·0	16·5	20, 22	40
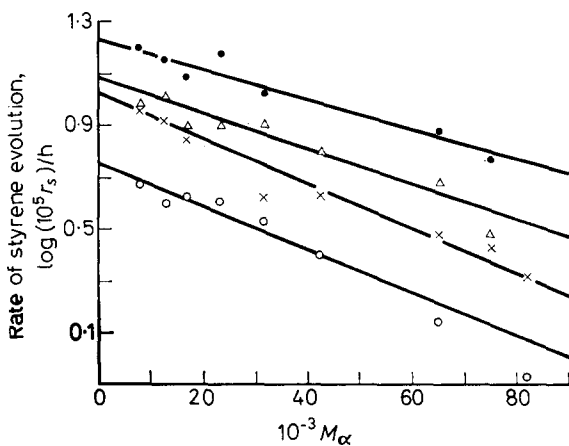
Figure 5—Rate of styrene evolution as a function of PMS molecular weight. $\bigcirc$, 260°C; $\times$, 268°C; $\triangle$, 270°C; $\bullet$, 274°C

136

type PS—PMS—PS[9]. Here problems of heterogeneity and monomer radical transfer do not arise, and similar rates of styrene evolution to those obtained by extrapolation have been found. Experiments with PS with backbone weak links also give similar values[10].

The overall activation energy for styrene evolution is given by $E = E_d + \frac{1}{2}E_i - \frac{1}{2}E_t$ and, with $E_i = 65$ kcal/mole and E_t again taken as 20 kcal/mole the equation becomes $E = E_d + 22 \cdot 5$ kcal. An Arrhenius plot of r_s^0 is shown in *Figure 6* and E was found to be 43 kcal/mole so that
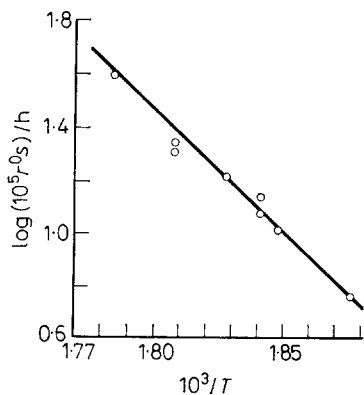
Figure 6—Arrhenius plot to determine activation energy of depropagation of polystyryl radicals

$E_d \simeq 20 \cdot 5$ kcal/mole, which is in reasonable accord with the published figure of 24 kcal/mole.

The depropagation and termination rate constants for PS degradation are then related by the expression

$$k_d / k_t^{\frac{1}{2}} = 65 \exp\left(- 10\ 500 / RT\right)$$

Finally, it is necessary to determine whether this relation is independent of PS molecular weight. *Table 5* shows that between 5 000 and 100 000

Table 5. Variation of styrene evolution as a function of PS molecular weight $MW_a = 7\ 400$, $T = 278°C$, $t = 2 \cdot 5$ h, wt of PS = 0·086 g, wt of PMS = 0·014 g

Mol. wt PS	S mg	α mg	S/α
4 730	1·96	1·87	1·04
8 900	1·72	1·78	0·96
15 850	1·68	1·82	0·92
40 800	1·61	1·73	0·93
69 300	2·09	1·85	1·12
76 700	1·85	1·81	1·02
92 000	1·54	1·70	0·91

molecular weight approximately, the amounts of α-methylstyrene and styrene monomers evolved and hence their ratios are independent of PS molecular weight. Therefore, the equation evaluated above is valid within this molecular weight range. Fox and Loshaek[36] have shown that the isothermal viscosity/molecular weight dependence of polystyrene is $\log \eta = 3 \cdot 4 \log Z + K$ when the molecular weight $(Z) > 1\ 000$. Thus if the

termination step involved gross polymer chain motion, k_t should be an inverse function of Z. The depropagation step is unlikely to be affected by the medium viscosity, and so $k_d/k_t^{\frac{1}{2}}$ should increase with the molecular weight. This is not observed and so the termination step must be determined principally by the segmental jump frequency J which is molecular weight independent at constant temperature and density.

Crown Copyright, reproduced with permission of the Controller, Her Majesty's Stationery Office.

Explosives Research and Development Establishment,
  Ministry of Aviation,
    Waltham Abbey, Essex

(Received September 1966)

REFERENCES

[1] WALL, L. A. and FLYNN, J. H. 'Rubber reviews for 1962', *Rubb. Chem. Technol.* 1962, **5**, 1157
[2] WALL, L. A. and FLORIN, R. E. *J. Res. Nat. Bur. Stand.* 1961, **60**, 451
[3] GRASSIE, N. and KERR, W. W. *Trans. Faraday Soc.* 1959, **55**, 1050
[4] CAMERON, G. G. and GRASSIE, N. *Polymer, Lond.* 1961, **2**, 367
[5] CAMERON, G. G. and GRASSIE, N. *Makromol. Chem.* 1962, **53**, 72
[6] GORDON, M. *Trans. Faraday Soc.* 1957, **53**, 1462
[7] GRASSIE, N. and KERR, W. W. *Trans. Faraday Soc.* 1957, **53**, 234
[8] MADORSKY, S. L., McINTYRE, D., O'HARA, J. H. and STRAUS, S. *J. Res. Nat. Bur. Stand.* 1962, **66A**, 307
[9] RICHARDS, D. H. and SALTER, D. Unpublished results
[10] RICHARDS, D. H. and SALTER, D. Part II, *Polymer, Lond.* 1967, **8**, 139
[11] GRANT, D. H., VANCE, E. and BYWATER, S. *Trans. Faraday Soc.* 1960, **56**, 1697
[12] COWIE, J. M. G. and BYWATER, S. *J. Polym. Sci.* 1961, **54**, 221
[13] MADORSKY, S. L. *J. Polym. Sci.* 1952, **9**, 133
[14] MADORSKY, S. L. *J. Polym. Sci.* 1953, **11**, 491
[15] BROWN, D. W. and WALL, L. A. *J. phys. Chem.* 1958, **62**, 848
[16] SZWARC, M., LEVY, M. and MILKOVITCH, R. *J. Amer. chem. Soc.* 1956, **78**, 2656
[17] ZIEGLER, K. and DISLICH, H. *Ber. dtsch. chem. Ges.* 1957, **90**, 1107
[18] SZWARC, M. *Makromol. Chem.* 1960, **35**, 142
[19] WAACK, R., REMBAUM, A., COOMBES, J. and SZWARC, M. *J. Amer. chem. Soc.* 1957, **79**, 2026
[20] McCORMICK, H. W. *J. Polym. Sci.* 1957, **25**, 488
[21] WORSFOLD, D. J. and BYWATER, S. *Canad. chem. J.* 1958, **36**, 1141
[22] SIRIANNI, A. F., WORSFOLD, D. J. and BYWATER, S. *Trans. Faraday Soc.* 1959, **55**, 2124
[23] JELLINEK, H. H. G. *J. Polym. Sci.* 1948, **3**, 850
[24] ATHERTON, E. *J. Polym. Sci.* 1950, **5**, 378
[25] SIMHA, R., WALL, L. A. and BLATZ, P. J. *J. Polym. Sci.* 1950, **5**, 615
[26] SIMHA, R. and WALL, L. A. *J. phys. Chem.* 1952, **56**, 707
[27] SIMHA, R. and WALL, L. A. *J. Polym. Sci.* 1951, **6**, 39
[28] BAER, M. *J. Polym. Sci. A*, 1964, **2**, 417
[29] COWLEY, P. R. E. J. and MELVILLE, H. W. *Proc. Roy. Soc. A*, 1951, **210**, 461
[30] ROBERTS, D. E. *J. Res. Nat. Bur. Stand.* 1950, **44**, 221
[31] WALL, L. A. *S.P.E. J.* 1960, **16**, No. 8, 1
[32] WALL, L. A. *S.P.E. J.* 1960, **16**, No. 9, 1
[33] WALL, L. A. Private communication
[34] RICHARDS, D. H., SALTER, D. A. and WILLIAMS, R. L. *Chem. Comm.* **1966**, 38
[35] SIMHA, R. *Trans. N.Y. Acad. Sci. Ser. II*, 1952, **14**, 151
[36] FOX, T. G. and LOSHAEK, S. *J. appl. Phys.* 1955, **26**, No. 9, 1080

Thermal Degradation of Vinyl Polymers II—The Synthesis and Degradation of Polystyrene Containing Thermally Weak Bonds

D. H. RICHARDS and D. A. SALTER

By reacting 'living' polystyrene with iodine, polystyrenes have been synthesized which possess thermally weak links at known positions along the polymer chain. The thermal rupture of these links produces radicals which depropagate to give monomer. Diluting the system with 'normal' polystyrene showed that cage recombination plays a significant role in the radical termination step. Measurements of the rates of monomer evolution agree with the theoretical analysis of the degradation mechanisms involved. Rate constant ratios were obtained which, although complicated by the complexity of the termination process, are in reasonable agreement with those from previous work on polystyrene-poly(α-methylstyrene) mixtures. The nature of the links formed in the iodine coupling reaction is discussed.

IN THE previous paper[1] it was pointed out that the quantitative analysis of the kinetics of thermal degradation of polystyrene was hampered by uncertainty of the position and nature of the initial scission. Three methods were outlined for overcoming this difficulty, all based on inducing decomposition of polystyrene at temperatures at which it is normally stable. The first of these, in which a radical producing agent [poly(α-methylstyrene)] was introduced into the polystyrene melt was described in detail. The present paper is concerned with the second method which involves the synthesis and subsequent thermal degradation of polystyrene with weak bonds at specific points along the polymer backbone.

The synthesis of these 'weak link' polystyrenes (PS_0) was based on the observation that reaction of the 'living' polymer with iodine resulted in chain extension. It seemed reasonable that the following reaction sequences are involved.

$$\sim CH_2-CH\phi-CH_2-CH\phi^- Na^+ + I_2 \rightarrow \sim CH_2-CH\phi-CH_2-CH\phi I + N$$

$$+ \sim CH\phi-CH_2-CH\phi$$

$$\cdot CH_2-CH\phi-CH_2-CH\phi-CH\phi-CH_2-CH\phi-CH_2 \sim \longleftarrow$$
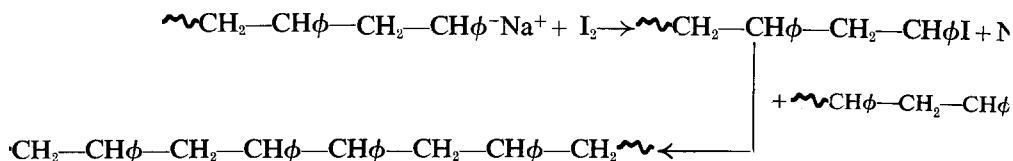
For living polystyrenes with two active ends per chain the degree of chain extension is unlimited under controlled conditions. The new bonds formed differ from the head–tail links of the polymer backbone and should therefore have different thermal properties. Since the C—C bond dissocia-

tion energies in the molecules ϕCH_2—$CH_2\phi$ and ϕCH_2—CH_3 are 47 and 63 kcal/mole respectively[2], the head–head coupling points should be relatively thermally unstable. The polymer should consequently exhibit low temperature degradation and initiation should occur at well defined sites. Under these circumstances the kinetic analysis is much simplified.

This approach has the further advantage that 'normal' polystyrene (PS) may be used as a diluent, because degradation studies can be conducted at temperatures at which it is stable. Thus problems of inhomogeneity are eliminated and, moreover, the use of PS with the same molecular weight as the 'weak link' material (PS_0) enables the effect of radical concentration changes to be studied at approximately constant bulk viscosity. Previous studies[3, 4] where diluents such as naphthalene and tetralin were used are suspect because of the unconsidered effect of the large drop in viscosity on reactions which are undoubtedly diffusion controlled.

<div align="center">EXPERIMENTAL</div>

Preparation of 'weak link' polystyrene (PS_0)

All the polystyrene samples used in this investigation were prepared by the 'living' polymer technique[5] using sodium naphthalene as catalyst. The living polymer solution in tetrahydrofuran was divided into two portions and the first terminated with methanol to produce —$CH_2\phi$ end groups (normal polystyrene). The second portion was reacted with a solution of iodine in tetrahydrofuran using the apparatus shown in *Figure 1*. The
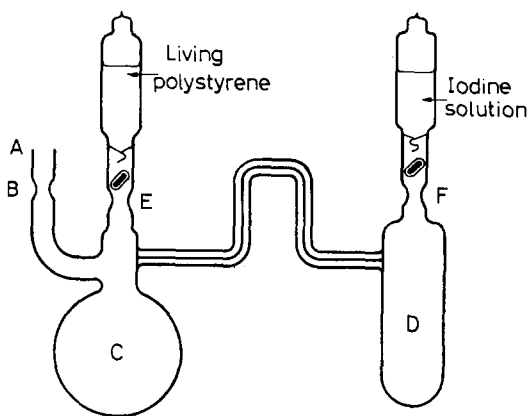
Figure 1—Apparatus for titration of 'living' polymer with iodine solution under high vacuum conditions

apparatus was evacuated through A and flamed before sealing at B. The living polystyrene and iodine solutions were introduced into flasks C and D respectively and the constrictions at E and F sealed off after 'cleaning' by refluxing solvent through them. Small aliquots of iodine solution were added to the polymer solution via the capillary tube by slowly tilting the apparatus, and after each addition the flask C was shaken vigorously. The whole operation took about one hour and, as the reaction neared completion, the characteristic red colour of the living polymer decreased until the solution became colourless at the end point. This polymer, and

<div align="center">140</div>

the sample killed with methanol, was precipitated three times with methanol and dried overnight in a vacuum oven.

Analysis of polymer

Molecular weights were determined viscometrically at 25°C with toluene as solvent and using the equation of Waack *et al.*[5].

The residual iodine content of polystyrene was determined by oxygen flask combustion and subsequent titration of iodine with thiosulphate.

Polymer degradation experiments

The apparatus for these experiments consisted essentially of modified U-tubes. They have been described previously, as have the methods of introducing and then degassing the polymer samples[1]. One arm of the evacuated tube held a known weight of polymer (10 mg) and was immersed in a salt bath at the required temperature, whilst the second arm was immersed in liquid nitrogen. On completion of the experiment, the second arm was sealed off and the contents analysed.

Experiments were designed either to determine the effect of dilution on the monomer evolution or to study the rate of monomer evolution with time. In the former case up to fifteen U-tubes were used per experiment and each tube contained a mixture of PS_0 and PS which ranged between the two extremes of concentration. The molecular weights of the polystyrenes were 17 000 and 19 000 respectively. Complete homogeneity of the samples was ensured by shaking the benzene solutions of the mixtures for four days before freeze drying. All tubes were removed simultaneously from the salt bath after the required degradation time and the amount of distillate determined. The study of the rate of monomer evolution against time was conducted at different temperatures and again fifteen U-tubes were used per experiment. Ten tubes contained PS_0 and the other five contained PS to act as blanks. Samples and blanks were removed from the bath at convenient time intervals and the distillates analysed.

Analysis of degradation products

The main product in the thermal degradation of polystyrene is monomer ($\sim$42 per cent) although significant quantities of dimer, trimer, etc., are also formed. However, as the fraction of monomer is insensitive to changes in degradation conditions, its determination gives a reliable measure of the polymer degradation.

Styrene monomer was measured by dissolving the distillate in a suitable solvent and determining the optical density at the absorption peak ($\sim$254 mμ) with a Perkin–Elmer 137 U.V. spectrometer. The most suitable solvent was spectroscopically pure methanol, but some measurements were made with chloroform. Polystyrene also absorbs in this range, but it has an extinction coefficient one tenth of that of monomer and has a broader absorption curve. It is estimated from the peaks obtained that less than two per cent of the absorption is due to polymer fragments.

Molecular weights of the residual polystyrene in preliminary experiments were estimated by viscometry[5] although the equation used was derived for polymers with Poisson distribution.

141

THEORY
Monomer evolution as a function of time
  Assume the following degradation mechanism

$$\text{Polymer} \xrightarrow{k_i} 2\text{P·}$$

$$\text{P}_n\text{·} \xrightarrow{k_d} \text{P}_{n-1}\text{·} + m$$

$$\text{P}_k\text{·} + \text{P}_l\text{·} \xrightarrow{k_t} \text{Polymer}$$

$$[\text{P}_k\text{·} + \text{P}_l\text{·}] \xrightarrow{k_c} \text{Polymer}$$
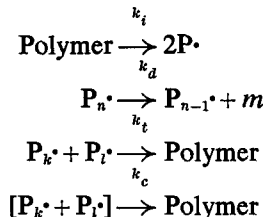
where P· is a polymeric radical and m is the amount of styrene monomer.

  The two termination steps are the normal bimolecular reaction (k_t) and a 'cage' termination step (k_c). This latter reaction is the recombination of radicals originating from the same polymer molecule and is consequently first order (pseudo-unimolecular).

  If the initiation step is due to scission of weak bonds (concentration $= x_0$) then, with short zip lengths, and under steady state conditions it may be shown that the amount of monomer (m) evolved after time t is given by

$$m = \frac{k_c k_d}{k_i k_t} \left\{ \ln \left[\frac{(1 + \{4k_i k_t x_0 / k_c^2\} \exp\{-k_i t\})^{1/2} + 1}{(1 + \{4k_i k_t x_0 / k_c^2\})^{1/2} + 1} \right] \right.$$
$$\left. + (1 + \{4k_i k_t x_0 / k_c^2\})^{1/2} - (1 + \{4k_i k_t x_0 / k_c^2\} \exp\{-k_2 t\})^{1/2} \right\} \qquad (3)$$

  The derivation of this expression, and of others below, is given in the Appendix. The equation is too complex to be of great computational value, and so two extreme cases are considered.

Bimolecular termination predominating $(k_c \rightarrow 0)$
  Equation (3) can be reduced to

$$m = 2k_d (x_0 / k_i k_t)^{1/2} (1 - \exp\{-k_i t / 2\}) \qquad (4)$$

Total monomer evolved (m_∞) is given by

$$m_\infty = 2k_d (x_0 / k_i k_t)^{1/2} \qquad (5)$$

and the rate constant of initiation may be expressed in terms of the half-life of the reaction, for which

$$1 - \exp\{-\tfrac{1}{2}k_i t_{\frac{1}{2}}\} = \tfrac{1}{2}$$

so that

$$k_i = (2 \ln 2)/t_{\frac{1}{2}} = 1 \cdot 386 / t_{\frac{1}{2}} \qquad (6)$$

Cage termination predominating $(k_t \rightarrow 0)$
  Equation (3) can be reduced to

$$m = (k_d x_0 / k_c)(1 - \exp\{-k_i t\}) \qquad (7)$$

Total monomer evolved

$$m_\infty = k_d x_0 / k_c \qquad (8)$$

and

$$k_i = 0 \cdot 693 / t_{\frac{1}{2}} \qquad (9)$$

The effect of dilution

Both equation (4) and equation (7) can be expressed as

$$m = m_\infty (1 - \exp\{-0.693 t/t_{\frac{1}{2}}\}) \qquad (10)$$

Thus, under these conditions, the nature of the termination step cannot be established by studying monomer evolution with time. However, if the initial weak bond concentration, x_0, is varied, then at constant degradation time equation (4) gives $m \propto x_0^{\frac{1}{2}}$ whereas equation (7) gives $m \propto x_0$. The termination step may therefore be determined by measuring monomer evolution as a function of dilution.

RESULTS AND DISCUSSION

Synthesis of weak link polystyrene (PS₀)

Comparison of the molecular weights of methanol and iodine terminated 'living' polystyrenes from the same batch gives the degree of chain extension obtained. If each coupling point constitutes a thermally weak bond, the number of weak links per molecule, or per gramme of material, may be readily determined. The relevant data for a number of polystyrenes are given in *Table 1*. Polymers B and C were analysed for iodine after three precipitations from methanol and the results, *Table 2*, establish that the

Table 1. Molecular weight increases obtained by reacting 'living' polystyrene with iodine

Living polymer batch no.	Mol. wt MeOH killed M_0	Mol. wt I_2 killed M	Fractional increase M/M_0	No. of weak links	
				per chain $M/M_0 - 1$	per gramme $\dfrac{M - M_0}{MM_0}$
A	15 850	27 600	1·74	0·74	$2·68 \times 10^{-5}$
B	7 260	17 400	2·40	1·4	$8·05 \times 10^{-5}$
C	4 730	20 900	4·42	3·42	$16·4 \times 10^{-5}$
D	109 000	280 000	2·56	1·56	$0·56 \times 10^{-5}$

Table 2. Iodine analysis of iodine killed 'living' polystyrenes

Batch no.	I_2 found g atom/g polymer	No. of weak links mole/g	No. of polymer ends, mole/g
B	$0·39 \times 10^{-5}$	$8·05 \times 10^{-5}$	$11·5 \times 10^{-5}$
C	$0·56 \times 10^{-5}$	$16·4 \times 10^{-5}$	$9·6 \times 10^{-5}$

iodine contents are far less than the number of weak links created so that the coupling reaction involves carbon–carbon bond formation. The residual iodine concentration is also much less than the number of polymer ends and so the terminal groups are not alkyl iodides. This discrepancy is probably due to termination by impurities, perhaps water, introduced from the iodine solution, and methods of drying this material further are at present being investigated.

Thermal degradation of weak link polystyrene (PS₀)

Preliminary experiments, *Table 3*, showed that PS₀ samples were less thermally stable than PS although, at the temperatures used, both polymers

Table 3. Comparison of degradation of iodine killed and methanol killed polystyrenes of similar molecular weights. $T = 329°C$, wt of sample $= 100$ mg, $S =$ styrene monomer distillate (mg) and $M =$ molecular weight of residue

Time (h)	0·0		0·5		1·0		3·1		4·3		5·3	
Polymer	S	M	S	M	S	M	S	M	S	M	S	M
MeOH killed	0·0	20 000	0·6	18 800	1·3	16 200	6·2	—	12·7	—	17·5	—
I_2 killed (B)	0·0	17 400	5·6	7 260	7·6	5 000	14·7	4 650	22·7	—	28·8	—

exhibited appreciable styrene evolution. Furthermore, the molecular weight of the PS_0 decreased very much more rapidly and levelled off at a value equivalent to the chain length between the coupling points. These facts prompted a detailed study of the degradation of these polymers at lower temperatures where decomposition of the control is relatively much less.

Effect of dilution

Dilution experiments were conducted between 276° and 289°C using PS_0 'B' (*Table 1*) with PS of 19 000 molecular weight as diluent. Some of the results are given in *Table 4* and the 'normalized' values have been

Table 4. Monomer evolution at constant temperatures and times as a function of weak link concentration. Total weight of polymer $= 10$ mg, $F =$ fraction of weak link polymer B present

276°C		285°C		289°C	
2·0 h		0·92 h		0·67 h	
F	S (mg)	F	S (mg)	F	S (mg)
0·00	0·007	0·00	0·005	0·00	0·008
0·07	0·032	0·09	0·031	0·07	0·028
0·14	0·045	0·16	0·041	0·14	0·049
0·21	0·053	0·23	0·065	0·21	0·050
0·28	0·051	0·30	0·079	0·28	0·071
0·35	0·078	0·37	0·081	0·35	0·062
0·42	0·089	0·44	0·088	0·42	0·094
0·49	0·084	0·51	0·089	0·49	0·110
0·56	0·086	0·58	0·118	0·56	0·118
0·63	0·124	0·65	—	0·63	0·128
0·70	0·141	0·72	0·133	0·70	0·138
0·77	0·150	0·79	—	0·77	0·113
0·84	0·156	0·86	0·139	0·84	0·141
0·91	—	0·93	0·131	0·91	—
1·00	0·169	1·00	0·133	1·00	0·145

plotted in *Figure 2* against initial weak bond concentration. This plot should be linear when the cage reaction predominates and curved towards the abscissa when the bimolecular termination step is significant. Apparently cage recombination is predominant in this system at low weak bond concentrations, but at high concentrations bimolecular termination becomes increasingly important. This trend is explicable if at low weak link concentration the average distance between radical pairs produced by

Figure 2—Effect of weak link concentration on styrene evolution
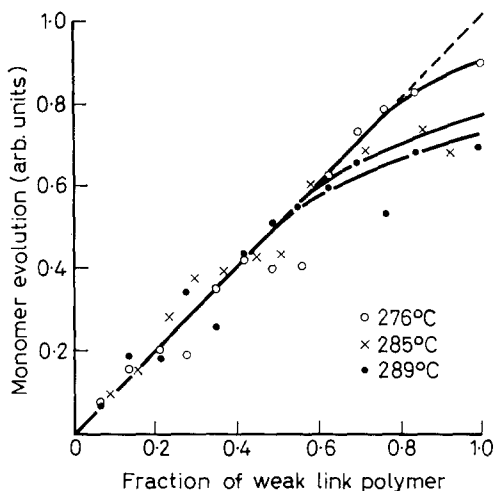
weak link scission is much greater than the average distance between the two radicals composing each pair. The probability of recombination of radicals originating from the same molecule is then much greater than the random recombination assumed in the 'normal' bimolecular process. An increase in weak link concentration, by increasing the equilibrium radical concentration, reduces the average distance between radical pairs and hence the probability of cage recombination. Similarly an increase in the reaction temperature should also increase the probability of bimolecular termination. Both these effects are observable in *Figure 2* although the experimental points exhibit considerable scatter.

These trends would also occur if the first order termination step were a unimolecular process of the type:

$$\sim\!\!\text{CH}_2\!-\!\text{CH}\!-\!\text{CH}_2\!-\!\text{CH}\!\cdot \longrightarrow \sim\!\!\text{CH}\!=\!\text{CH} + \text{CH}_3\!-\!\text{CH}\!\cdot \uparrow$$
$$\phi \qquad\quad \phi \qquad\qquad \phi \qquad\quad \phi$$
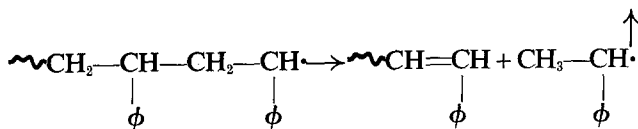
This is kinetically identical to the cage reaction and its significance cannot be determined in the present work. However, in the degradation of polystyrene–poly(α-methylstyrene) block polymers of the type PMS–PS–PMS[6], polystyryl radicals are produced by the complete unzipping of the PMS of molecular weight 6 000 and so no cage reaction can take place. Under similar temperature conditions (290°C), where the rate of polystyryl radical formation is in the range in which the weak link system produces principally first order termination, the termination step was found to be second order. This is explicable only if unimolecular reactions of the kind given above are absent.

The presence of a cage reaction does not exclude the possibility of an intermolecular chain transfer occurring. The cage reaction concept has merely to be extended to include recombination of radicals produced from

145

the primary macroradical pairs. Because PS is used as solvent, the dilution process leaves the probability of intermolecular chain transfer unchanged[7].

The cage effect in polymer thermal degradation has not been generally considered and the present work appears to be the first direct demonstration of its significance, although a cage reaction was recently postulated in the thermal degradation of poly(tetrafluorethylene)[8]. Normal polystyrene degrades predominantly by terminal scission up to medium molecular weights, although at higher values random initiation becomes important[9]. With terminal scission one of the radicals is either a monomeric or a polymeric radical of very low molecular weight which can diffuse away from its partner very easily. Therefore, cage effects would be much less important in this case and Grassie and Kerr[10] have suggested that terminal initiation might be favoured principally because the presence of a cage effect would facilitate recombination of internally formed macroradicals.

Monomer evolution with time

If either of the termination steps predominates then the rate of monomer evolution against time is given by equation (10) and the intermediate case [equation (3)], although more complex, should approximate to this curve. Examples of runs at various temperatures are given in *Figure 3*. The solid
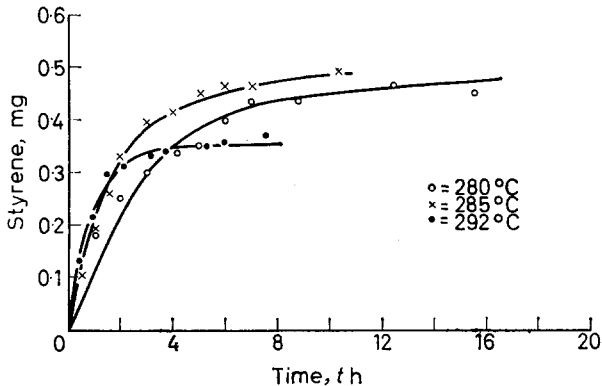
Figure 3—Evolution of styrene from weak link polymer as a function of time

lines represent curves calculated from equation (10); m_∞ was taken as the value of m for which the experimental points are asymptotic, and $t_{\frac{1}{2}}$ was then found as the time taken to evolve $\frac{1}{2}m_\infty$ monomer. The experimental points corresponded closely to the calculated curve in all cases and the hypothesis of weak bond scission is supported for the following reasons: (*a*) scission is restricted to specific bonds because only about five per cent of the polymer appears as monomer after degradation is complete, (*b*) the fact that each weak link produces on average about six monomer units supports the view that the scission involves a free radical mechanism, (*c*) the assumption of a small zip length is justified and is in accord with Wall's assessment[11] rather than Grassie's figure of about 1 000.

The evaluation of m_∞ and $t_{\frac{1}{2}}$ enables the various rate constants to be

determined although the interpretation of these terms depends on the nature of the predominating termination step. *Table 5* lists the rate constants

Table 5. Rate constant evaluations based on the predominance of (*a*) cage termination and (*b*) bimolecular termination

			Cage		Bimolecular		Ref. (*1*)
$T°C$	m_∞ (*mg*)	$t_{\frac{1}{2}}$ (*h*)	$k_i \times 10^4$	k_d/k_c	$k_i \times 10^4$	$k_d/k_t^{\frac{1}{2}} \times 10^3$	$k_d/k_t^{\frac{1}{2}} \times 10^3$
280	0·47	2·0	0·97	5·4	1·93	3·5	
285	0·48	1·3	1·48	5·5	2·96	4·4	5·5
286	0·41	1·5	1·28	4·7	2·56	3·5	
287	0·40	1·4	1·37	4·6	2·74	3·6	5·8
292	0·35	0·7	2·75	4·0	5·50	4·9	6·1

calculated assuming first that the cage reaction and secondly that the bimolecular reaction predominates. The last column gives values obtained from previously reported work[1]. The units are base moles–seconds.

If the cage reaction takes place exclusively at all temperatures then k_d/k_c decreases with temperature, i.e. $E_d < E_c$. If the termination is diffusion controlled, the energy E_c is likely to be that of viscous flow, estimated at about 20 kcal/mole for poly(methylmethacrylate)[12]. However, E_d has been variously estimated as 20·5 and 24 kcal/mole[1] and certainly must exceed the 16·4 kcal/mole given as the heat of polymerization[13]. Cage termination therefore appears not to be predominant at all temperatures studied. If the cage reaction took place by the radical pairs unzipping to each other then $E_d = E_c$ and k_d/k_c would be temperature independent.

The assumption that the bimolecular process is the exclusive termination step gives values of $k_d/k_t^{\frac{1}{2}}$ which increase with temperature, i.e. $E_d > \frac{1}{2}E_t$. Thus taking $E_t = 20$ kcal/mole, $E_d > 10$ kcal/mole. This does not conflict with the values quoted in the previous paragraph.

These observations and the dilution experiments indicate that the termination reaction is complex and so any activation energies calculated from m_∞ would have little kinetic significance. However, bimolecular termination appears to predominate at the higher temperatures and, on this basis, the values for $k_d/k_t^{\frac{1}{2}}$ may be compared with those obtained previously using a mixed polymer system[1]. In this latter work the problem of cage recombination does not arise. The results, *Table 5*, are generally in agreement although the 'weak link' results are lower. This is understandable as cage recombination, becoming more prominent as degradation proceeds, reduces the amount of monomer evolved and hence the value of $k_d/k_t^{\frac{1}{2}}$. This agreement, and similar results from work on styrene–α-methylstyrene block copolymers[6] support the postulated kinetic scheme.

The evaluation of k_i is also affected by the nature of the termination step although if either of the two possibilities predominates, the activation energy is 55 kcal.

The nature of the weak links

The chemical nature of the weak bonds formed by the coupling reaction

has no direct bearing on the degradation kinetics previously discussed unless more than one type of weak link results. It is important, however, in deciding what types of molecular structure to avoid in the synthesis of polymers of maximum thermal stabilities.

Consideration of the three main canonical forms of resonance of the polystyryl anion suggests the following links to be possible.
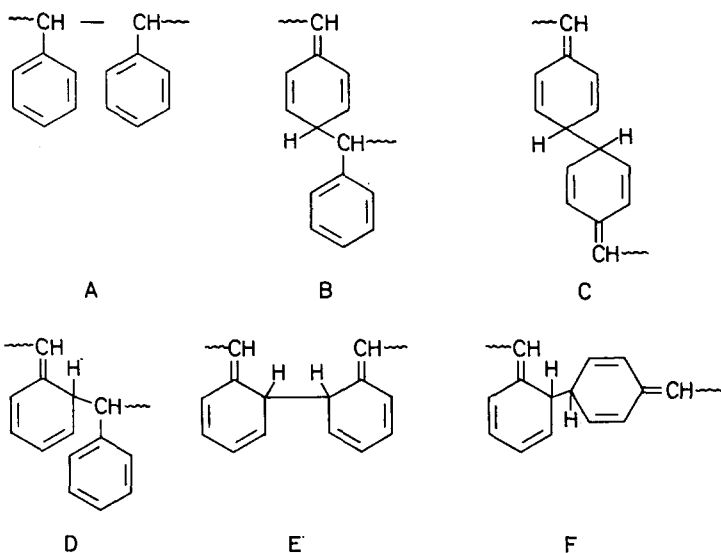
Forms B to F are probably unstable and would quickly rearrange to form the corresponding benzenoid structures. For example, B and D would become
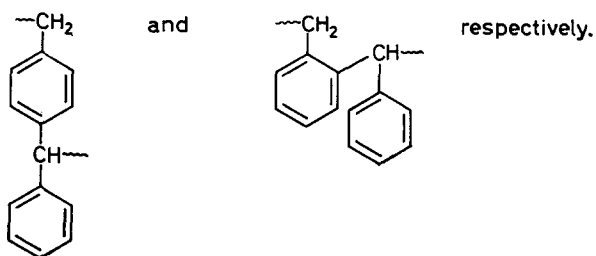
The most probable of these structures appears to be A above, as this is the type of bond produced by the reaction of benzyl–metal compounds with benzylhalides[14]. However, Cameron and Grassie[15] have copolymerized styrene with traces of stilbene to produce polymers with head–head bonds as in A. These were found to degrade in a manner similar to 'normal' polystyrene which suggests that this bonding is not thermally active†.

†There is, however, the possibility that the addition of stilbene to the styryl radical took place via the benzene ring so that head–head bondings were not formed.

Further, polystyrene produced by free radical mechanism should contain one of these bonds per chain (in the absence of chain transfer) and should consequently exhibit low temperature degradation characteristics. This has not been reported.

Cameron and Grassie[16] proposed structures involving ortho- and para-quinonoid groups, similar to B and F above, to account for the 'naturally occurring' weak bonds in thermally polymerized polystyrene, i.e.
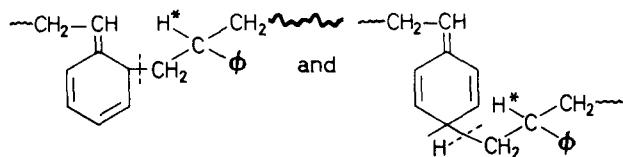
They assumed six-membered rings, involving the starred α-hydrogens, to be formed in the transition state before hydrogen transfer resulted in chain scission at the points indicated. These structures differ from B to F in that the bonding is still essentially head–tail. It is difficult to visualize an equivalent non-radical scission for head–head structures and, as indicated earlier, the six monomer units produced per scission require a radical mechanism.

Investigations involving n.m.r and i.r. analysis of polymers of this type to identify the linkage have been inconclusive, although no i.r. bands corresponding to disubstituted phenyls could be detected. Similar experiments conducted on poly(α-methylstyrene) produced from the disodium tetramer[17] by the iodine reaction and which should have predominantly head–head links confirm that the concentration of disubstituted phenyls is below the detection limits of the methods and the spectra have been interpreted on the basis of head–head bonding[18]. Some u.v. absorption measurements on this material, however, indicate a factor of three increase in the base-mole extinction coefficient at maximum compared with 'normal' poly(α-methylstyrene). As the shapes of the absorption curves are very similar this suggests the presence of substituted diphenyl linkages. Ramart-Lucas[19] has investigated the spectra of the series ϕ—$(CH_2)_n$—ϕ and shown that when $n > 0$, $\epsilon_{max.}$ values are very similar, but that when $n = 0$, $\epsilon_{max.}$ increases by a factor of 100. The position of the maximum is moved only slightly and the absorption curve is of similar shape to the others in the series. It is therefore calculated that less than one sixteenth of the linkages created by the iodine reaction with the tetramer produces substituted diphenyls. It seems likely that the polystyrene–iodine reaction would behave similarly.

Explosives Research and Development Establishment, Ministry of Aviation, Waltham Abbey, Essex

APPENDIX

Monomer evolution as a function of time
Let us assume the following degradation scheme

$$\text{Polymer} \xrightarrow{k_i} 2P\cdot$$

$$P_n\cdot \xrightarrow{k_d} P^\cdot_{n-1} + m$$

$$P_k\cdot + P_l\cdot \xrightarrow{k_t} \text{Polymer}$$

$$\boxed{P_k\cdot + P_l\cdot} \xrightarrow{k_c} \text{Polymer}$$
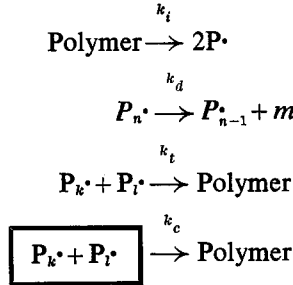
where the symbols have been previously explained. If the concentration of weak bonds present at time $t=x$ then, under steady state conditions,

$$dP\cdot/dt = 2k_i x - 2k_t P^2\cdot - 2k_c P\cdot = 0$$

$$\therefore \quad P\cdot = \frac{k_c}{2k_t}\left\{\left(1 + \frac{4k_i k_t x}{k_c^2}\right)^{\frac{1}{2}} - 1\right\} \text{ for real values of } P\cdot \tag{1}$$

$$\text{Now } \frac{dm}{dt} = k_d P\cdot = \frac{k_c k_d}{2k_t}\left\{\left(1 + \frac{4k_i k_t x}{k_c^2}\right)^{\frac{1}{2}} - 1\right\} \tag{2}$$

Again, $-dx/dt = k_i x$ so that, if $x_0 =$ weak bond concentration at $t=0$, then

$$x = x_0 \exp\{-k_i t\} \tag{3}$$

Substituting (3) in (2) $\dfrac{dm}{dt} = \dfrac{k_c k_d}{2k_t}\left\{\left(1 + \dfrac{4k_i k_t x_0}{k_c^2}\exp[-k_i t]\right)^{\frac{1}{2}} - 1\right\}$

If, then, $m =$ total monomer evolved in time t

$$m = \frac{k_c k_d}{2k_t}\int_0^t \left\{\left(1 + \frac{4k_i k_t x_0}{k_c^2}\exp\{-k_i t\}\right)^{\frac{1}{2}} - 1\right\}dt$$

$$= \frac{k_c k_d}{2k_t}\left\{\int_0^t\left(1 + \frac{4k_i k_t x_0}{k_c^2}\exp\{-k_i t\}\right)^{\frac{1}{2}}dt - t\right\} \tag{4}$$

Now

$$\int\left(1 + \frac{4k_i k_t}{k_c^2}\exp\{-k_i t\}\right)^{\frac{1}{2}}dt = \int(1 + ae^{-bx})^{\frac{1}{2}}\,dx = A$$

and, if we substitute $ae^{-bx} = y^2 - 1$,

then $\quad -bae^{-bx}\,dx = 2y\,dy$

i.e. $\qquad\qquad\qquad dx = \{-2y/b\,(y^2-1)\}\,dy$

so that $\qquad\qquad A = -\frac{2}{b}\int\frac{y^2}{y^2-1}\,dy = -\frac{2y}{b} - \int\frac{dy}{y^2-1}$

This last integral may be evaluated readily using partial fractions to give

$$A = -(1/b)\{2y + \ln[(y-1)/(y+1)]\}$$

$$= \frac{1}{b}\left\{\ln\frac{(1+ae^{-bx})^{\frac{1}{2}}+1}{(1+ae^{-bx})^{\frac{1}{2}}-1} - 2(1+ae^{-bx})^{\frac{1}{2}}\right\}$$

Re-introducing limits and substituting for a and b

$$m = \frac{k_c k_d}{2k_i k_t}\left\{\ln\left[\frac{\left(1+\frac{4k_i k_t}{k_c^2}x_0 e^{-k_i t}\right)^{\frac{1}{2}}+1}{\left(1+\frac{4k_i k_t}{k_c^2}x_0 e^{-k_i t}\right)^{\frac{1}{2}}-1} \cdot \frac{\left(1+\frac{4k_i k_t}{k_c^2}x_0\right)^{\frac{1}{2}}-1}{\left(1+\frac{4k_i k_t}{k_c^2}x_0\right)^{\frac{1}{2}}+1}\right] \right.$$

$$\left. -2\left(1+\frac{4k_i k_t}{k_c^2}x_0 e^{-k_i t}\right)^{\frac{1}{2}} + 2\left(1+\frac{4k_i k_t}{k_c^2}\right)^{\frac{1}{2}} - k_i t\right\}$$

which can be simplified to

$$m = \frac{k_c k_d}{k_i k_t}\left\{\ln\left[\frac{\left(1+\frac{4k_i k_t}{k_c^2}x_0 e^{-k_i t}\right)^{\frac{1}{2}}+1}{\left(1+\frac{4k_i k_t}{k_c^2}x_0\right)^{\frac{1}{2}}+1}\right]\right.$$

$$\left. + \left(1+\frac{4k_i k_t x_0}{k_c^2}\right)^{\frac{1}{2}} - \left(1+\frac{4k_i k_t}{k_c^2}x_0 e^{-k_i t}\right)^{\frac{1}{2}}\right\} \qquad (5)$$

Bimolecular termination predominating $(k_c \longrightarrow 0)$
From equation (5) with this restriction

$$m = \frac{k_c k_d}{k_i k_t}\left\{-\frac{k_i t}{2} + \left(\frac{4k_i k_t x_0}{k_c^2}\right)\left(1-e^{\frac{-k_i t}{2}}\right)\right\}$$

$$= 2k_d\left(\frac{x_0}{k_i k_t}\right)^{\frac{1}{2}}\left(1-e^{\frac{-k_i t}{2}}\right) - \frac{k_c k_d t}{2k_i k_t}$$

$$= 2k_d\left(\frac{x_0}{k_i k_t}\right)^{\frac{1}{2}}\left(1-e^{\frac{-k_i t}{2}}\right)$$

Cage termination predominating $(k_t \longrightarrow 0)$
From equation (5) with this restriction

$$m = \frac{k_c k_d}{k_i k_t}\left\{\ln\left[\frac{1+\frac{k_i k_t x_0}{k_c^2}e^{-k_i t}}{1+\frac{k_i k_t x_0}{k_c^2}}\right] + \frac{2k_i k_t x_0}{k_c^2}(1-e^{-k_i t})\right\}$$

and expanding the logarithm to one term

$$m = \frac{k_c k_d}{k_i k_t}\left\{\frac{k_i k_t x_0}{k_c^2}(e^{-k_i t}-1) + \frac{2k_i k_t x_0}{k_c^2}(1-e^{-k_i t})\right\}$$

$$= \frac{k_d x_0}{k_c}(1-e^{-k_i t})$$

151

REFERENCES

[1] RICHARDS, D. H. and SALTER, D. A. *Part I. Polymer, Lond.* 1967, **8**, 127

[2] COTTRELL, T. L. *The Strength of Chemical Bonds,* 2nd ed., p 274. Butterworths: London, 1958

[3] CAMERON, G. G. and GRASSIE, N. *Polymer, Lond.* 1961, **2**, 367

[4] JELLINEK, H. H. G. and SPENCER, L. B. *J. Polym. Sci.* 1952, **8**, 273

[5] WAACK, R., REMBAUM, A., COOMBES, J. and SZWARC, M. *J. Amer. chem. Soc.* 1957, **79**, 2026

[6] RICHARDS, D. H. and SALTER, D. A. Unpublished work

[7] RICHARDS, D. H. and SALTER, D. A. *Polymer, Lond.* 1967, **8**, 153

[8] PENSKI, E. C. and GOLDFARB, I. J. *Polymer Letters,* 1964, **2**, 55

[9] MADORSKY, S. L., McINTYRE, D., O'HARA, J. H. and STRAUS, S. *J. Res. Nat. Bur. Stand.,* 1962, **66A**, 307

[10] GRASSIE, N. and KERR, W. W. *Trans. Faraday Soc.* 1957, **53**, 234

[11] WALL, L. A., STRAUS, S., FLYNN, J. H., McINTYRE, D. and SIMHA, R. In press

[12] COWLEY, P. R. E. J. and MELVILLE, H. W. *Proc. Roy. Soc. A,* 1951, **210**, 461

[13] BEVINGTON, J. C. *Radical Polymerization,* p 57. Academic Press: New York, 1958

[14] SCHLOSSER, M. *Angew. Chem., Internat. Ed.* 1964, **3**, 298

[15] CAMERON, G. G. and GRASSIE, N. *Makromol. Chem.* 1962, **51**, 130

[16] CAMERON, G. G. and GRASSIE, N. *Makromol. Chem.* 1962, **53**, 72

[17] SZWARC, M. *Makromol. Chem.* 1960, **35**, 142

[18] RICHARDS, D. H., SALTER, D. A. and WILLIAMS, R. L. *Chem. Comm.* 1966, **2**, 38

[19] RAMART-LUCAS, M. *Bull. Soc. chim. Fr.* 1942, **9**, 850

Thermal Degradation of Vinyl Polymers III—A Radiochemical Study of Intermolecular Chain Transfer in the Thermal Degradation of Polystyrene

D. H. RICHARDS and D. A. SALTER

The importance of an intermolecular chain transfer reaction in the thermal degradation of polystyrene has been established by a radiochemical method. A polystyrene containing a specific number of thermally weak links at known points along the polymer chain was prepared by an adaptation of the Szwarc 'living' polymer technique. It was thermally degraded at moderate temperatures (280° to 285°C) in the presence of carbon-14 labelled 'normal' polystyrene as diluent. Measurement of the activity of the monomer in the distillate showed that, with a kinetic chain length of about three monomer units, 1·2 chain transfers occurred per radical. Some evidence is also given to indicate that weak link scission plays a significant role in the early stages of polystyrene degradation.

THE mechanism of thermal decomposition of polystyrene has been discussed in previous papers[1,2]. The existence of intermolecular chain transfer in the degradation process has not as yet been established, although often postulated. This paper describes a direct measurement of intermolecular chain transfer in this system.

The chain transfer step is thought to take place via the tertiary hydrogens of the polymer by the following mechanism:

$$(1)$$

$$(2)$$
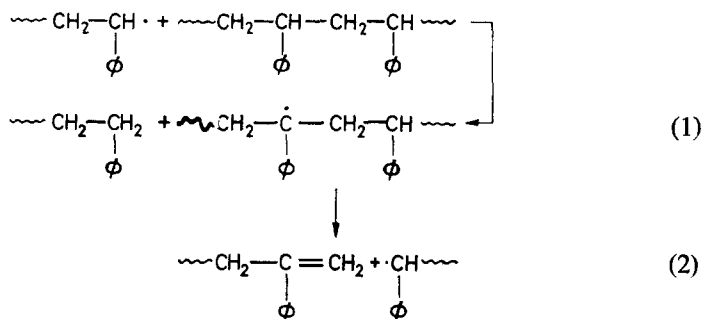
Thus a transfer reaction results in the splitting of a polymer chain and the regeneration of a macroradical. Wall has invoked this step to account for the observed very rapid decrease in molecular weight of polystyrene in the initial stages of degradation[3] and has obtained strong evidence of its existence by showing that in the degradation of poly(α-deuterostyrene) this decrease is halved and a higher monomer yield is obtained (70 per cent)[4]. The replacement of the tertiary C—H bond by the stronger C—D bond has apparently largely inhibited both inter- and intra-molecular transfer.

This view is challenged by Grassie *et al.* who believe that the initial

molecular weight decrease is primarily due to the decomposition of weak bonds in the polymer molecule. These weak links are assumed to be formed during the polymerization process, and these workers have produced evidence correlating the initial rate of molecular weight decrease with the temperature of polymerization[5]. They further argue that the chain transfer step cannot account for the relatively high value at which the molecular weight of residual polystyrene levels off in the later stages of the reaction[6]. Dilution experiments to resolve these different points of view have produced conflicting results[7,8] and suffer from the disadvantage that the naphthalene and tetralin used as solvents drastically reduce the bulk viscosity of the system. Since it has been shown[2] that bulk viscosity is an important factor in determining the degradation pattern where diffusion processes are involved, direct inferences from the dilution experiments therefore cannot easily be drawn.

These problems have now been overcome and a method has been devised to estimate the extent of chain transfer based on the following argument. Consider a system consisting of polystyrene possessing thermally weak bonds (PS_0) mixed with carbon-14 labelled polystyrene without weak links (PS). At a temperature at which only PS_0 degrades significantly, inactive styrene will be produced in the distillate in the absence of chain transfer. If, however, chain transfer is appreciable, both types of polymer molecules will be susceptible to random attack by the primary, inactive, macroradicals resulting in the production of some radioactive monomer. The specific activity of the distillate compared with the original specific activity of the mixed polymer system will then be a direct measure of the degree of chain transfer.

EXPERIMENTAL

Polymer synthesis

Synthesis of weak link polystyrene (PS_0)—The synthetic method has been described in detail previously[2]. It consists of slowly titrating iodine into 'living' polystyrene[9], both being dissolved in tetrahydrofuran. Chain extension occurs with the formation of thermally weak links at the coupling points. The number of weak links may be determined by knowing the degree of chain extension, and their relative positions along the chain is deducible from the chain length of the original living polystyrene. These polymers degrade in the temperature range 260° to 290°C where normal polystyrene is relatively stable[2]. The details of the weak link polymer used are given in *Table 1*. The molecular weights were determined viscometrically[10].

Table 1. Analytical data on weak link polystyrene (PS_0)

Mol. wt living PS $= 7\,260$	Residual $I_2 = 0.39 \times 10^{-5}$ mole/g
Mol. wt weak link PS $= 17\,400$	No. of polymer ends $= 11.5 \times 10^{-5}$ mole/g
No. of weak links $= 8.05 \times 10^{-5}$ mole/g	

Synthesis of β-^{14}C-styrene—The synthesis is based on the reaction of benzaldehyde with ^{14}C-methyl magnesium iodide followed by hydrolysis of the product to yield β-phenyl ethanol. On dehydration with potassium bisulphate β-^{14}C-styrene is formed in about 60 per cent overall yield.

Polymerization of β-^{14}C-styrene—The radioactive styrene was dried overnight with crushed calcium hydride in a vacuum, distilled into an ampoule, and sealed *in vacuo*. Thermal polymerization of the monomer at 182°C produced a polymer which, after being precipitated three times from methanol, was shown viscometrically[10] to have a molecular weight of 42 300.

Mixing and degradation techniques—A solution of 5 mg of polymer per ml of benzene was made of each of the two polystyrenes and the required amounts were introduced into a glass tube with a thin walled bulb at one end such that the total weight of added polymer was 10 mg. For any experiment up to eleven tubes were used with varying proportions of the two components. The solutions were cooled and the tubes evacuated and sealed before being shaken for two days to ensure complete mixing of the polymers. Each tube was then cut open and the contents frozen in liquid nitrogen before being sealed on to a vacuum line and freeze dried. Oil baths were placed around the tubes and the temperature raised to 180°C over about an hour, when a pressure of 1×10^{-5} mm of mercury was recorded. The tubes were sealed, removed, and after cooling were again opened and each joined to shaped glass tubes to form the second arms of U-tubes. These completed U-tubes were re-evacuated and the polymers again taken up to 180°C before removal from the vacuum line.

The degradation technique has been fully described previously[1]. The polymer arm was immersed in a salt bath at the required temperature and the other dipped in liquid nitrogen to collect distillate. After the required time the second arm was sealed off and removed for product analysis.

Product analysis—The contents of the ampoules were washed out with chloroform into weighed stoppered bottles and the total weight determined. 0·5 ml of the solution was then diluted with scintillator solution and counted and the remainder weighed before being diluted to 10 ml with more chloroform for spectroscopic analysis.

Measurement of total styrene—Total styrene was determined from the ultra-violet absorptions of the chloroform solutions using a Perkin–Elmer 137 u.v. spectrometer. The peak heights were measured at 254 mμ and compared with a standard styrene solution. Polystyrene also absorbs in this range, but with an extinction coefficient one tenth that of monomer and with a broader absorption curve. From the shapes of the peaks obtained it is estimated that the contribution due to the distilled polymer fragments are negligible ($<$ 2 per cent).

Measurement of radioactive styrene—Carbon-14 activities of the distillate and polymer were measured using a Tritium Scintillation Counter Type 6012A (comprising a liquid measuring head and a coincidence control unit) and a 1700 scaler, both supplied by Isotope Development Ltd. The scintillator solution was the hydrocarbon based NE 211 supplied by Nuclear Enterprises Ltd. The counting efficiencies for polymer and monomer were shown to be the same by experiments which indicated that the addition of small amounts of polystyrene to a scintillation solution containing active styrene left the counts unchanged, as did the converse procedure. The activity of the ^{14}C-labelled polystyrene was found to be 1 800 counts/sec mg.

It is obvious that the activity is not specific to monomer and that small polymeric fragments in the distillate will be counted with equal efficiency. This may be corrected for, however, by a method described under *Table 2(b)*.

Table 2. Degradation of mixtures of weak link polystyrene (PS$_0$) and ^{14}C-labelled polystyrene (PS); $T = 288°C$

(a) Spectroscopic analysis

Sample no.	a Wt fraction PS (f)	b Opt. dens.	c Diln, ml	d Wt soln (g)	e Total wt (g)	g W_s	h ΔW_s
1	1·0	1·07	10	1·2776	2·0424	0·122	0
2	1·0	1·10	25	1·0622	1·8267	0·134	0
3	1·0	0·99	25	0·9705	1·7230	0·125	0
4	0·875	1·33	25	1·1998	1·9498	0·154	0·043
5	0·750	0·96	25	1·1421	1·9131	0·293	0·197
6	0·625	0·94	25	0·8406	1·5988	0·319	0·239
7	0·500	1·22	25	0·9873	1·7313	0·380	0·316
8	0·375	1·28	25	1·0278	1·7779	0·393	0·345
9	0·250	1·42	25	1·0152	1·7564	0·438	0·406
10	0·125	1·40	25	1·0254	1·7600	0·424	0·408
11	0·0	1·37	25	1·0374	1·8098	0·426	0·426

Standard (7·125 mg styrene/l) 0·99 O.D.

Column *a* gives the weight fractions of active polystyrene present in the mixtures (*f* in theory) and *b* gives the optical densities in 1 cm silica cells of chloroform solutions of distillate of total volumes as listed in *c*. Column *e* tabulates the weights of chloroform containing the total distillate and *d* gives the weights of these solutions diluted to perform the spectroscopic measurements. Thus the optical densities which would have been obtained from the total distillates may be calculated and converted into weights of monomer by comparison with the standard (column *g*). Finally, the blank due to 'normal' thermal decomposition of the ^{14}C-polystyrene is subtracted from the total styrene evolution by averaging the results obtained from samples 1, 2 and 3 ($W^°_s$) and subtracting $f \times W^°_s$ from column *g* to give column *h*. This last column then represents the amounts of styrene monomer evolved as a direct consequence of weak link scission.

(b) Radiochemical analysis

Sample no.	a Cts/sec	b Wt soln (g)	c Total wt (g)	d C^0/S	e $\Delta C/S$	g ΔW^* (g)	h $W(g)$	i $\dfrac{\Delta W^*_s}{\Delta W_s}$	j n
1	96·7	0·765	2·0424	262	0				
2	117	0·765	1·8267	279	0		0·172		
3	118	0·763	1·7230	266	0				
4	111	0·750	1·9498	288	49	0·031		0·466	1·14
5	173	0·771	1·9131	428	223	0·142		0·462	1·60
6	189	0·758	1·5988	399	228	0·146		0·392	1·68
7	157	0·744	1·7313	365	227	0·145		0·292	1·40
8	125	0·750	1·7779	297	193	0·123		0·229	1·57
9	94	0·741	1·7564	222	152	0·097		0·155	1·63
10	44	0·735	1·7600	105	68	0·043		0·067	1·16
11	1·3	0·772	1·8098	3·1	0	0			

Standard 8 310 cts/sec=4·6 mg styrene.

Column *a* gives the counts per second obtained from those fractions of total distillate calculated from the ratios of results in columns *b* and *c*. Column *d* gives the counting rates for the total distillates. The activities from the distillates produced directly by weak link scission (column *e*) are calculated by averaging the C^0/S obtained from the first three samples (*c*) and subtracting *fc* from the remaining values in column *d*. Reference to the activity of the standard polystyrene sample enables the weights of radioactive distillates to be calculated (column *g*). Similarly, column *h* shows the average weight of distillate obtained from the active sample only, i.e. the blank, and this is significantly higher than the figure obtained by spectroscopic measurements [*Table 2(a)* column *g*]. As explained in the text, this discrepancy is due to the radiochemical method not being specific for monomeric styrene. and the ratio of the two values obtained (0·74) may be used as a correction factor to convert the active distillate weights (ΔW^*) to active monomer weights (ΔW). The ratios of these results with total monomer weights are given in column *i*.

Finally, use is made of equation (4) to convert these figures into values of n which are listed in column *j*.

THEORY

Two important parameters which characterize the degradation patterns of polymers are the zip length and the kinetic chain length. The former gives the average number of monomer units which unzip from a macroradical before it is removed either by termination or by chain transfer. The kinetic chain length gives the average number of monomer units produced by the primary and secondary macroradicals before termination by interaction with another radical. Thus, if no transfer occurs then the zip length and kinetic chain length are equal. Similarly, the relative values of these parameters give a direct measure of the degree of intermolecular chain transfer.

Let x denote zip length, and y the kinetic chain length, then, if the average number of chain transfers per radical is n,

$$y = (n+1)x \qquad (3)$$

Let f be the weight fraction of ^{14}C-labelled polymer in the mixture.

Then average number of active monomer units produced in the kinetic lifetime of a radical

$$y^1 = fnx \qquad (4)$$

Therefore, the fraction of monomer units evolved which derive from radioactive polymer is given by

$$y^1/y = fn/(n+1) \qquad (5)$$

The ratio y^1/y can be determined as the ratio of the specific activity of the monomer evolved to that of the ^{14}C-labelled polymer. In the nomenclature of *Table 2*, this is obtained experimentally as the ratio of the weight of labelled styrene evolved (ΔW_s^*) to the total weight of styrene evolved, i.e.

$$\Delta W_s^* / \Delta W_s = fn/(n+1) \qquad (6)$$

RESULTS AND DISCUSSION

The results of a typical degradation experiment are given in *Tables 2(a)* and *(b)*. Detailed explanations of the derivations of the columns are given under each table. *Table 3* lists the values of n obtained from a number of experiments, and the results indicate significant chain transfer with n having an average value of 1·2.

Table 3. Values of n obtained at various temperatures

f \ $T°C$	284	286	288	288
0·875	—	1·31	—	1·14
0·750	1·52	1·50	0·95	1·60
0·625	—	1·27	0·97	1·68
0·500	1·58	1·40	0·98	1·40
0·375	—	1·07	1·25	1·57
0·250	1·78	0·97	—	1·63
0·125	—	1·07	1·07	1·16

The main factor determining the sensitivity of this method is the size of the radioactive polymer blank, i.e. the amount of styrene directly produced from the PS at the experimental temperature. *Table 2(a)* shows that this lies between a quarter and a third of the styrene evolved from the PS_0, and so is a severe limitation on the sensitivity, as comparatively large correction factors have to be applied. Polystyrenes of similar molecular weights synthesized by the 'living' anionic technique produce a blank about one twenty fifth of the present blank at the same temperature. It appears that the mode of synthesis is of prime importance in producing thermostable polymers. The polymerization temperatures of the thermal and anionic polymerizations were 184°C and 0°C respectively and so the probability of forming weak links in the former case is greatly enhanced. This fact, therefore, supports the weak link theories of Grassie and Kerr[5].

Despite the high blank, a reasonably consistent value of n is obtained of about 1·2. Thus with a kinetic chain length of about three units[2] a zip length of about 1·4 units is obtained. The fact that a radical cage termination reaction[2] plays a significant role in these systems does not affect the analysis and the results are equally applicable to polystyrene even if only one macroradical is produced in the primary scission, i.e. in terminal scission.

Wall et al.[11] have analysed the results of polystyrene degradation at 353°C by computer using the theory of Simha, Wall and Blatz[12]. They find it necessary to introduce a chain transfer constant such that one transfer step occurs for every seven radicals produced. As the zip length under these conditions is assessed at about three units, the degree of chain transfer they assume is considerably less than in the present work. If both results are valid then the activation energy of depropagation (E_d) must be about 17 kcal/mole greater than that of chain transfer (E_{tr}). E_d has been estimated as 20·5 and 24 kcal/mole[13] so that E_{tr} could not exceed about 7 kcal/mole. This result is improbably low and casts doubts on the accuracies of the chain transfer estimates. It is perhaps significant that Wall et al. could obtain reasonable agreement with experiment only over the first fifty per cent decomposition and over a very limited initial molecular weight range.

No data for the thermodynamics of the chain transfer reaction have been reported although the bond dissociation energy of Leigh and Szwarc[14] indicates that the analogous model system

$$CH_3-\overset{|}{\underset{\phi}{C}}H\cdot + CH_3-\overset{|}{\underset{\phi}{C}}H-CH_3 \rightleftharpoons CH_3-\overset{|}{\underset{\phi}{C}}H_2 + CH_3-\overset{\cdot}{\underset{\phi}{C}}-CH_3$$
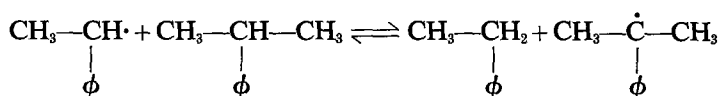
should be exothermic with a value of 1·0 kcal/mole. Thus the stabilities of the two radicals are similar, but in the polymer chain transfer reaction the splitting of the polymer chain causes the process to be irreversible. It is possible that the activation energy of chain transfer might be significantly lowered if the transition state involves the polymer scission process and

the polymer radical $\sim\!\!\overset{\cdot}{\underset{\phi}{C}}\!\!\sim$ has no independent existence [cf. reactions

158

(1) and (2)], i.e.
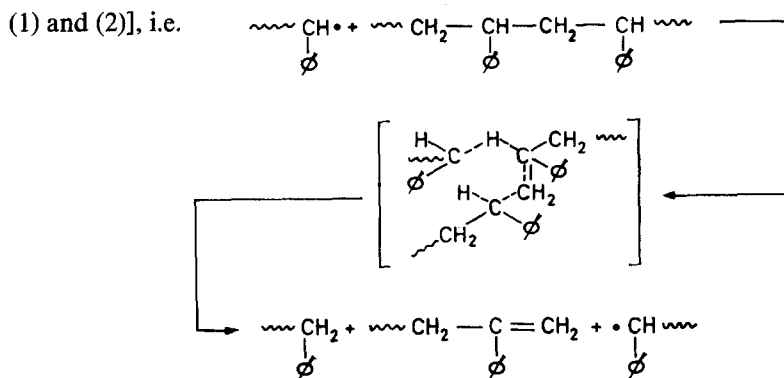
Despite this difficulty in quantitative correlation with other workers the present work establishes that the chain transfer step plays an important role in the thermal degradation of polystyrene. The indications obtained of 'naturally occurring' weak link scission suggest that this mechanism also contributes to the characteristics of the early stages of the degradation process.

Crown Copyright, reproduced with permission of the Controller, Her Majesty's Stationery Office.

Explosives Research and Development Establishment,
  Ministry of Aviation,
    Waltham Abbey, Essex

REFERENCES

[1] RICHARDS, D. H. and SALTER, D. A. *Polymer, Lond.* 1967, **8**, 127
[2] RICHARDS, D. H. and SALTER, D. A. *Polymer, Lond.* 1967, **8**, 139
[3] WALL, L. A. and FLYNN, J. H. 'Rubber reviews for 1962', *Rubb. Chem. Technol.* 1962, **5**, 1157
[4] WALL, L. A. and FLORIN, P. E. *J. Res. Nat. Bur. Stand.* 1958, **60**, 451
[5] GRASSIE, N. and KERR, W. W. *Trans. Faraday Soc.* 1959, **55**, 1050
[6] GRASSIE, N. and KERR, W. W. *Trans. Faraday Soc.* 1957, **53**, 234
[7] CAMERON, G. G. and GRASSIE, N. *Polymer, Lond.* 1961, **2**, 367
[8] JELLINEK, H. H. G. and SPENCER, L. B. *J. Polym. Sci.* 1952, **8**, 273
[9] SZWARC, M., LEVY, M. and MILKOVITCH, R. *J. Amer. chem. Soc.* 1956, **78**, 2656
[10] WAACK, R., REMBAUM, A., COOMBES, J. and SZWARC, M. *J. Amer. chem. Soc.* 1957, **79**, 2026
[11] WALL, L. A., STRAUS, S., FLYNN, J. H., McINTYRE, D. H. and SIMHA, R. In press
[12] SIMHA, R., WALL, L. A. and BLATZ, P. J. *J. Polym. Sci.* 1950, **5**, 615
[13] BROWN, D. W. and WALL, L. A. *J. phys. Chem.* 1958, **62**, 848
[14] LEIGH, C. H. and SZWARC, M. *J. chem. Phys.* 1952, **20**, 844

Contributions to Polymer

A Complex Plane Representation of Dielectric and Mechanical Relaxation Processes in Some Polymers

S. HAVRILIAK and S. NEGAMI

In a previous paper it was shown that the complex dielectric constant data of polymers can be represented by an empirical dispersion function. In the present work it is shown that the complex polarization of the same data can be represented by a function of the same form but with different values for the constants. This means that a quantitative evaluation of Scaife's remarks can be made. The dispersion parameters for eighteen polymers were determined for the $\epsilon^*(\omega)$ or the $\rho^*(\omega)$ data. In general, as the ratio $\epsilon_0/\epsilon_\infty$ increases, the $\rho^*(\omega)$ data become broader and faster than the $\epsilon^*(\omega)$ data, thus $1-\alpha$, β and τ_0 decrease. The normalized loss maximum was found to be temperature dependent [$\epsilon^*(\omega)$ data] for eleven polymers where $\epsilon_0/\epsilon_\infty \approx 2.0$. However, the normalized loss maximum [$\epsilon^*(\omega)$ data] for the two acetates was found to be independent of temperature while the normalized loss maximum for the $\rho^*(\omega)$ behaved in a way similar to the other polymers. This observation can be traced to a fortuitous compensation of effects encountered with large dispersions. For those cases where the method of reduced variables is applicable $\epsilon^*(\omega)$ calculated from the dispersion function is in good agreement with the shifted values of $\epsilon^*(\omega)$. The two parameters α and β are shown to be uniquely related to distribution of relaxation times. The agreement between the distribution function calculated from the dispersion function is in good agreement with the approximate methods used to calculate the function from the shifted data. A complex plane plot of the complex compliance is not at all similar to the dielectric dispersions. An empirical transformation procedure is constructed by analogy with the one used to calculate the complex polarization in order to normalize the mechanical data. The locus of this complex deformation resembles the dielectric dispersion with nearly the same values of α, β and τ_0. At very low frequencies, deviations from the assumed behaviour were observed. With polyisobutylene and poly(n-octyl methacrylate) the deviations were in terms of another dispersion. With poly(vinyl acetate) and poly(methyl acrylate) the deviations could be attributed to another low frequency dispersion. The similarity between the dielectric and mechanical dispersions suggests that the following mechanical model can be considered: a spherical inclusion containing the specimen of interest is perfectly bonded to an otherwise continuous homogeneous elastic continuum. Under these conditions the complex distortion of the sphere subjected to a periodic tensile field at infinity is very nearly the empirical complex deformation with Poisson's ratio of $\frac{1}{2}$ for both media. It can also be shown for this model that if the distortion of the sphere is time dependent, then there will be in-phase and out-of-phase components to the distortion in a periodic field. In other words it is not necessary to postulate an internal viscosity to account for a macroscopic viscosity. The equilibrium distortion of the sphere is shown to be related to the square of the asymmetry of the orienting segments. The decay of the distortion with time of the removal of stress field is interpreted in terms of transition probabilities.

I. INTRODUCTION

A COMPLEX plane plot of either a dielectric or mechanical dispersion (relaxation process) is an isothermal plot of the real part of the experimental quantities against their imaginary counterparts for each frequency of measurement. In the dielectric case one such plot is constructed for each

temperature of measurement. In the mechanical case the data from different temperatures are first superimposed in such a way as to obtain a single master curve for the frequency dependence of the real and imaginary parts of the experimental quantities. It is possible to construct a complex plane plot of the data at this single or reference temperature. The shape of the dielectric relaxation process for simple inorganic or organic systems may take either one of two forms; a circular arc[1], which is the most common shape, or a skewed semi-circle[2], which is observed infrequently. Cole and co-workers[1,2] have been able to represent these two dispersions with two empirical dispersion functions which represent the data with high accuracy. A complex plane plot of polymeric dielectric dispersions is neither of the two simple shapes observed in the case of small molecules but rather a combination of the two shapes. In other words, the loci of polymeric dispersions are circular arcs at low frequencies and linear at high frequencies. A complex plane plot of the complex compliance for most polymeric dispersions is not any of these three shapes. Generally[3] the locus appears to be approximately linear at high frequencies, then at some lower frequency the locus passes through a maximum in the loss compliance and almost invariably terminates at some finite value of the loss when the equilibrium value of the real compliance has been reached.

The authors[4] have studied the shapes of dielectric dispersions for twenty one polymers and found that they all have approximately the same shape, i.e. linear at high frequencies and a circular arc at low frequencies. In order to represent this behaviour quantitatively the authors postulated an empirical relaxation function of the form

$$\frac{\epsilon^*(\omega) - \epsilon_\infty}{\epsilon_0 - \epsilon_\infty} = [1 + (i\omega\tau_0)^{(1-\alpha)}]^{-\beta} \tag{1}$$

This relaxation function has two intriguing features associated with it. First, and most importantly, it represents the experimental quantities almost within their reliability. Secondly, this function could be considered as a generalized way of writing the two known and well documented dispersion functions of Cole[1,2]. For example, when $\beta = 1$ and $0 \leqslant \alpha \leqslant 1$ in equation (1), the circular arc expression is obtained and when $\alpha = 0$ and $0 \leqslant \beta \leqslant 1$, the skewed semi-circle is obtained. In addition it was shown[4] that the five parameters in equation (1) have the same counterpart as they do in Cole's dispersion functions. This latter feature implies that as the kinetics of the relaxation process for small molecular systems become known because the three dimensional details of local structure are known, then it should be possible to transfer this kinetic scheme to polymeric behaviour.

Recently criticism has been made concerning the use of the complex dielectric constant to represent the relaxation behaviour of simple systems. It was proposed by Scaife[5] that the customary method of representing the dielectric data be replaced by the use of a polarizability plot, in which the imaginary coordinate of the complex polarizability of a dielectric sphere of unit radius is plotted against its real counterpart. This quantity is chosen because, in a sphere, long-range dipole-dipole coupling vanishes and, therefore, the complex polarizability will be a good measure of the intrinsic

properties of a substance. According to Scaife, this method gives proper weight to all polarization mechanisms and provides a ready means of comparing the dielectric behaviour of different substances.

There are several objects to this work. The first of these is to study the changes in the shape of the relaxation curve when the data are treated in the manner suggested by Scaife. The second object is to construct empirically an analogous transformation procedure for mechanical dispersions and assess its influence on the shape of these mechanisms. Finally, dielectric theory should be adapted to mechanical behaviour consistent with the extent to which these mechanisms are analogous.

II. DIELECTRIC RELAXATION

(A) General background

Before reporting the experimental data in detail, a discussion of some of the features of the complex plane method of representing dielectric data seems to be worthwhile because this method is rarely used to treat polymeric dispersion data. First of all, based on some very fundamental assumptions regarding cause and effect, linearity and superposition, it can be shown that[6]

$$\epsilon^*(\omega) - \epsilon_\infty = \int_0^\infty B(t) \exp(-i\omega t)\, dt \qquad (2)$$

The function $B(t)$ which must contain the instantaneous and equilibrium responses of the system is only a function of time and has been interpreted in two ways. The earliest and most commonly accepted interpretation is that it is related to the distribution of relaxation times. In other words, the equilibrium and instantaneous responses of all of the elements of the system (assuming a single relaxation process) are the same but they take different times to come to equilibrium. The more recent interpretation of $B(t)$ is that it represents the interaction of the moving species with its environment; i.e. a time dependent correlation function. In the former interpretation it can readily be shown that[6]

$$\epsilon_n'(\omega) = \frac{\epsilon'(\omega) - \epsilon_\infty}{\epsilon_0 - \epsilon_\infty} = \int_{-\infty}^{+\infty} F(\tau/\tau_0) \times \frac{1}{1 + \omega^2\tau^2}\, d\ln(\tau/\tau_0) \qquad (3a)$$

and

$$\epsilon_n''(\omega) = \frac{\epsilon''(\omega)}{\epsilon_0 - \epsilon_\infty} = \int_{-\infty}^{+\infty} F(\tau/\tau_0) \times \frac{\omega\tau}{1 + \omega^2\tau^2}\, d\ln(\tau/\tau_0) \qquad (3b)$$

In equations (3a) and (3b) $F(\tau/\tau_0)$ is only a function of relaxation time and is referred to as the distribution of relaxation times. We see from these equations that both the reduced real and imaginary parts are uniquely determined by functions of time alone. If, as it is customary to assume, $F(\tau/\tau_0)$ is independent of temperature while τ_0 varies with temperature, then a complex plane plot of all of the reduced experimental data from different temperatures must fall on to a single line. It is important to note the difference between this construction and the one used in the Time Temperature Superposition Method (TTSM). In that method the data must be shifted on to an unknown curve so that any changes in shape may be

compensated for by overshifting or undershifting the data. In the present method, the data either fall on to a single line or they do not.

A second distinguishing feature of the complex plane method is that the frequency dependence of the real and imaginary parts is not lost as might be supposed. This point has been studied in some detail by Mopsik[7], who showed that a semicircular locus in a complex plane must originate from a Debye relaxation process. This point has also recently been shown by Fang[8]. Therefore, according to Mopsik, any analytic function that can represent the shape of the relaxation data in a complex plane must be uniquely related to the distribution of relaxation times because the relationship between $\epsilon^*(\omega)$ and $F(\tau/\tau_0)$ is unique. This is so because the relationship between any function and its Laplace transform is unique. Therefore the relationship between real and imaginary parts with $F(\tau/\tau_0)$ must also be unique.

The foregoing discussion implies that one need only check the shape of the data in a complex plane plot against one that has been calculated for a particular relaxation function in order to test its validity. In general this is true; however, a much more quantitative check can be made by calculating $\epsilon^*(\omega)$ with the aid of the assumed dispersion function and comparing it to the experimental value. This procedure, if repeated for each frequency of measurement, can provide a quantitative statement for the accuracy of representation. In this way an assumption basic to the understanding of polymers, i.e. whether or not the distribution of relaxation times is independent of temperature, may be studied. One may question the wisdom of studying such a tenaciously held hypothesis by means of an empirical function. This question is of no concern so long as the accuracy of representation is constantly checked.

(B) *Isothermal data*

In *Figure 1* we have represented the frequency dependence of the complex dielectric constants for three systems as black circles; in *Figure 1*(a) it is the poly(carbonate of bisphenol), in *Figure 1*(b) it is poly(vinyl acetate) and in *Figure 1*(c) it is glycerol. These systems were chosen, not because they are the best examples of the dispersion functions, but because they represent a large range of equilibrium values of the dielectric constant. The temperatures shown were chosen because the relaxation process was centred in the available frequency range, which minimizes errors due to extrapolations in order to obtain some of the dispersion parameters. Equation (1) is tested for accuracy of representation by comparing calculated and experimental values of $\epsilon^*(\omega)$ for the entire experimental frequency range. The $\epsilon^*(\omega)$ were calculated by the method described in Appendix A and the results for the three polymers are represented as open circles in *Figures 1*(a)–(c). As can be seen from these figures the differences between experimental and calculated results are small. The parameters for these three polymers, together with the parameters used to describe the relaxation behaviour of sixteen other polymers, are given in *Table 1*. The accuracy of representation for these other systems is equally good.

The complex dielectric constant can be transformed into the complex
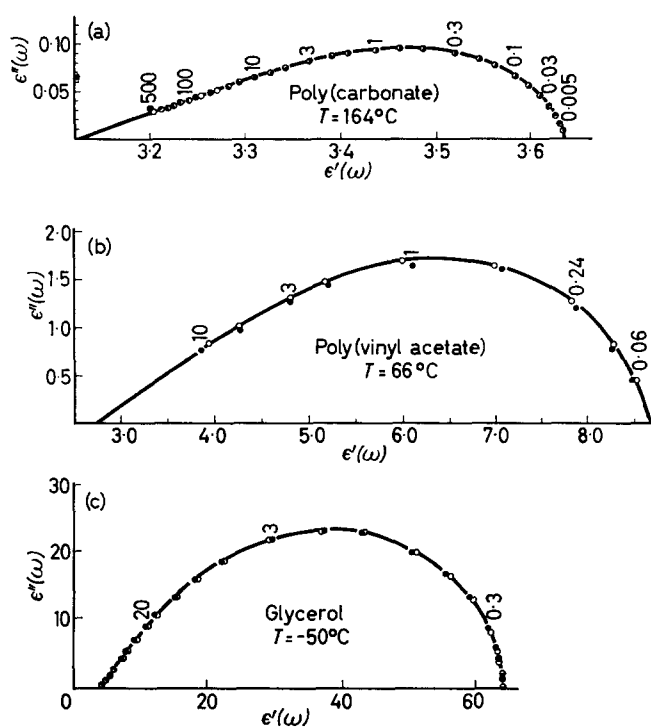
Figure 1—Complex plane plot of dielectric constant for three materials: (a) poly(carbonate of bisphenol) at 164°C; (b) poly(vinyl acetate) at 66°C; and (c) is glycerol at −50°C. Numerals on curves denote frequencies in kc/s

Table 1. Dispersion parameters used to represent dielectric data as ε^* (ω) or ρ^* (ω)

Polymer	Method	Equil.	Instan.	β	$1-\alpha$	$2\pi\tau_0 \times 10^3$ (sec)	$T\,°C$
poly(nonyl methacrylate)[9]	ϵ^*	3·510	2·44	0·520	0·790	2·5	42·8
	ρ^*	0·454	0·322	0·475	0·820	2·0	
poly (carbonate)[4]	ϵ^*	3·637	3·128	0·285	0·795	6·9	164·0
	ρ^*	0·468	0·416	0·290	0·780	6·0	
poly (m-chlorostyrene)[10]	ϵ^*	3·695	2·355	0·422	0·368	1400	74.7
	ρ^*	0·4725	0·3420	0·548	0·30	250	
poly (vinyl laurate)[11]	ϵ^*	3·80	2·34	0·413	0·862	0·67	6.2
	ρ^*	0·483	0·310	0·437	0·790	0·40	

Table 1—continued

Polymer	Method	Equil.	Instan.	β	$1-\alpha$	$2\pi\tau_0 \times$ $2\ 10^3$ (sec)	$T\,^\circ C$
poly(n-octyl methacrylate)[12]	ϵ^*	3·86	2·58	0·455	0·843	0·715	21
	ρ^*	0·488	0·343	0·408	0·859	0·10	
poly(isobutyl methacrylate)[9]	ϵ^*	3·97	2·38	0·489	0·724	1·6	102·8
	ρ^*	0·498	0·313	0·425	0·732	1·15	
poly(n-hexyl methacrylate)[12]	ϵ^*	4·03	2·45	0·468	0·796	1·1	40·0
	ρ^*	0·504	0·325	0·447	0·747	1·0	
poly(cycloheyxl methacrylate)[9]	ϵ^*	4·24	2·46	0·247	0·842	30	121
	ρ^*	0·521	0·323	0·231	0·77	20	
poly(vinyl decanoate)[11]	ϵ^*	4·24	2·515	0·528	0·796	1·43	−2·2
	ρ^*	0·521	0·325	0·426	0·797	1·1	
poly(n-butyl methacrylate)[9]	ϵ^*	4·28	2·41	0·526	0·676	4·2	59·0
	ρ^*	0·521	0·318	0·509	0·651	2·5	
poly(vinyl octanoate)[11]	ϵ^*	4·61	2·51	0·488	0·869	3·3	−6·1
	ρ^*	0·549	0·334	0·532	0·753	1·6	
poly chloroprene[13]	ϵ^*	5·96	2·44	0·470	0·540	5·0	−26
	ρ^*	0·617	0·310	0·254	0·63	3·33	
poly(vinyl formal)[14]	ϵ^*	6·45	3·00	0·458	0·584	0·285	130·0
	ρ^*	0·641	0·404	0·461	0·555	0·083	
poly(methyl acrylate)[4]	ϵ^*	6·480	3·705	0·392	0·655	13	30·0
	ρ^*	0·646	0·466	0·336	0·630	7·5	
poly(trifluoro mono-chloroethylene)[15]	ϵ^*	6 7	2·5	0·48	1·0	—	−30
	ρ^*	0·653	0·290	0·291	0·956	—	
poly(vinyl acetate)[16]	ϵ^*	8·62	2·74	0·45	0·910	6·7	66
	ρ^*	0·722	0·431	0·395	0·827	2·2	
copolymer[4]	ϵ^*	12·30	4·0	0·331	0·940	3·23	145
	ρ^*	0·793	0·480	0·300	0·730	0·9	
glycerol[17]	ϵ^*	63·9	4·10	0·603	1·000	0·78	−50
	ρ^*	0·955	0·465	0·443	0·810	0·05	

polarization $[\rho^*(\omega)]$ of a unit sphere imbedded in a vacuum (i.e. $\epsilon_\infty = 1$) by means of the following expression[5]

$$\rho^*(\omega) = \frac{\epsilon^*(\omega) - 1}{\epsilon^*(\omega) + 2} \qquad (4)$$

which becomes after separating real and imaginary parts

$$\rho'(\omega) = \frac{[\epsilon'(\omega) - 1][\epsilon'(\omega) + 2] + \epsilon''(\omega)^2}{[\epsilon'(\omega) + 2]^2 + \epsilon''(\omega)^2} \qquad (4a)$$

$$\rho''(\omega) = \frac{3\epsilon''(\omega)}{[\epsilon'(\omega) + 2]^2 + \epsilon''(\omega)^2} \qquad (4b)$$

The experimental quantities in *Figures 1*(a)–(c) were transformed into $\rho^*(\omega)$ by using equations (4a) and (4b). The results of this transformation are shown in *Figures 2*(a)–(c) and are represented by the full black circles. To measure the extent to which the curves have been modified it is necessary to rewrite equation (1) in the form

$$\frac{\rho^*(\omega) - \rho_\infty}{\rho_0 - \rho_\infty} = [1 + (i\omega\tau_0)^{(1-\alpha)}]^{-\beta} \qquad (5)$$

The five dispersion parameters have the same significance in the polarization plot as they did in the dielectric constant plot. Equation (5) can be
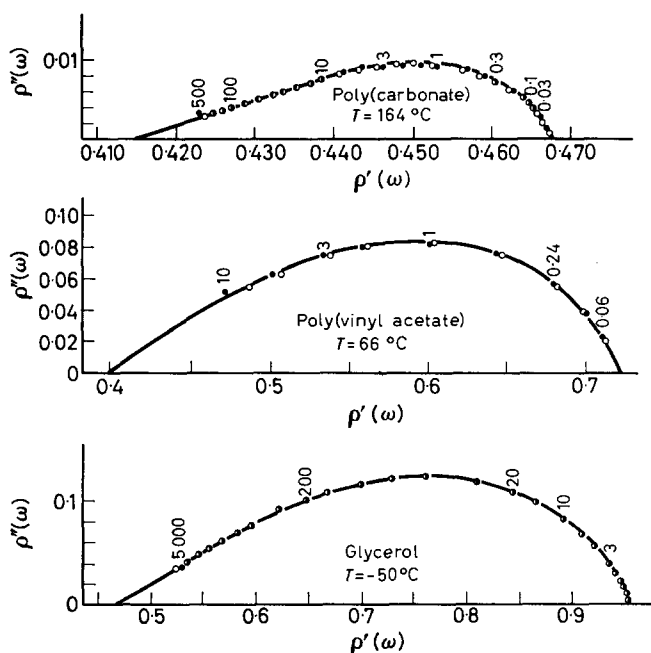
Figure 2—Complex plane plot of polarization for the same three materials as in *Figure 1:* (a) poly(carbonate of bisphenol) at 165°C; (b) is poly(vinyl acetate) at 66°C; and (c) is glycerol at −50°C. Frequencies in kc/s

separated into real and imaginary parts obtaining equations that are analogous to equations (60) to (63). The differences are that $\rho^*(\omega)$ replaces $\epsilon^*(\omega)$, ρ_0 replaces ϵ_0, and ρ_∞ replaces ϵ_∞. The graphical significance of the five dispersion parameters is the same as before and is determined in the same way. These parameters, which are listed in *Table 1*, together with equation (5) are used to calculate the complex polarization. The results are shown as the open circles in *Figure 2*. As can be seen from that figure the agreement between calculated and transformed results is as good as the agreement between the calculated and experimental values in the complex dielectric constant case provided of course the appropriate dispersion parameters are used. The parameters that were used to represent the dielectric constant and polarization data are not the same (see *Table 1*). As the dispersion becomes larger, i.e. as $\epsilon_0/\epsilon_\infty$ increases, the differences between $1 - \alpha$ or τ_0 become larger. For the polycarbonate where $\epsilon_0/\epsilon_\infty = 1 \cdot 161$ the time parameters are almost the same, while for glycerol where $\epsilon_0/\epsilon_\infty = 15 \cdot 34$ the time parameters are quite different. The effects for other systems are intermediate to these two extremes.

(C) Variable temperature data

The temperature dependence of five dispersion parameters used to repre-
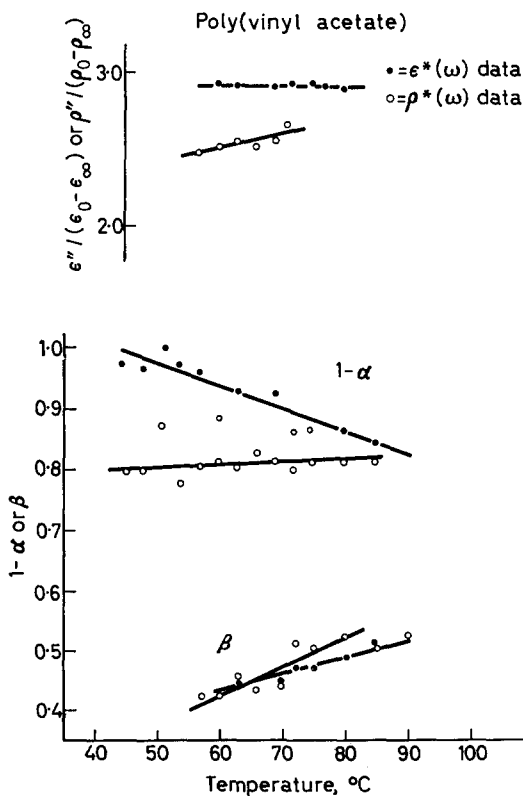
Figure 3—The dispersion parameters used to represent $\epsilon^*(\omega)$ and $\rho^*(\omega)$ data for poly(vinyl acetate) are plotted as functions of temperature in degrees Centigrade

168

sent $\epsilon^*(\omega)$ data for poly(vinyl acetate)[16] was determined by the method described in Appendix B. The temperature dependence of ϵ_0 and ϵ_∞ is essentially linear and is given by, where T is in degrees Centigrade,

$$\epsilon_0 = 11\cdot56 - 0\cdot043\ T$$

and

$$\epsilon_\infty = 4\cdot02 - 0\cdot017\ T$$

The temperature dependence of $1 - \alpha$ and β is given in *Figure 3*, where it can be seen that they depend on temperature in the opposite sense. The parameter φ_L is essentially independent of temperature. The normalized loss maximum was found to be independent of temperature over the temperature range where it can be determined directly. The temperature dependence of τ_0 is given in *Figure 4*, where the usual curvature is observed.
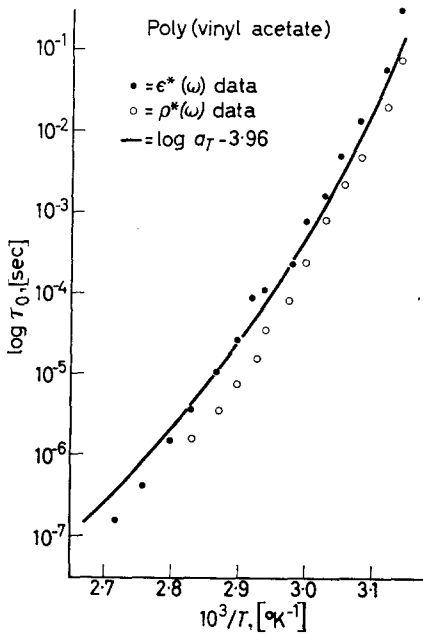
Figure 4—The relaxation time (sec) for the $\epsilon^*(\omega)$ and $\rho^*(\omega)$ data for poly(vinyl acetate) is plotted as a function of reciprocal temperature (degrees absolute). The solid line represents the relaxation time calculated from the shift factors

The temperature dependence of the five dispersion parameters used to represent $\rho^*(\omega)$ data for poly(vinyl acetate) was determined by the method described in Appendix B. The temperature dependence of ρ_0 and ρ_∞ is essentially linear and is given by, where T is degrees Centigrade,

$$\rho_0 = 0\cdot804 - 0\cdot00124\ T$$

and

$$\rho_\infty = 0\cdot459 - 0\cdot000945\ T$$

The parameter φ_L is temperature dependent and can be represented by

$$\varphi_L = 26 + 0\cdot089\ T$$

The temperature dependence of $1 - \alpha$ and β is given in *Figure 3* where it

169

can be seen that they depend on temperature in the same sense. The normalized loss for the complex polarization decreases with decreasing temperature. These differences in the temperature dependence of φ_L, $1-\alpha$, β and the normalized loss maximum are very important to the understanding of polymer behaviour because of the nature of certain assumptions that are used to describe their behaviour.

Figure 5—The relaxation time (sec) for the $\epsilon^*(\omega)$ data for poly(vinyl acetal is plotted as a function of reciprocal temperature (degrees absolute). The solid line is the relaxation time calculated from the shift factors while the broken line represents the time at maximum loss
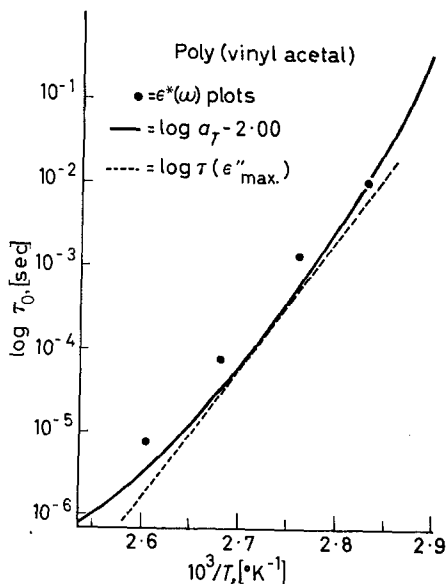
The temperature dependence of the five dispersion parameters used to represent $\epsilon^*(\omega)$ data for poly(vinyl acetal)[14] was determined by the Appendix B method and is listed in *Table 2*. The parameters φ_L, β and the reduced loss maximum decreased with decreasing temperature, while ϵ_0 and ϵ_∞ varied linearly with temperature. A rate plot (i.e. log τ_0 versus $10^3/T$) of the relaxation time is linear and can be represented by, see *Figure 5*,

$$\log \tau_0 = 13 \cdot 77 \times 10^3 / T - 40 \cdot 895$$

The activation energy for the τ_0 plot is slightly lower (63·0 kcal) than the value obtained by Funt and Sutherland (71·2 kcal) who used the loss

Table 2. Dispersion parameters used to represent $\epsilon^*(\omega)$ data for poly(vinyl acetal)

$T, °C$	φ_L	$1-\alpha$	β	$\tau_0 \times 10^4$ sec	ϵ_0	ϵ_∞	$\epsilon''_{max.}$ $\epsilon_0-\epsilon_\infty$
120	31·3	0·79	0·440	0·0159	6·50	—	0·248
110	30·7	0·81	0·420	0·0796	6·55	2·60	0·243
100	26·8	0·78	0·378	0·763	6·63	2·63	0·230
90	25·5	0·81	0·350	15·9	6·70	2·65	0·222
80	24·6	0·79	0·345	111·0	6·80	2·67	0·214
40	—	0·58	1·00	0·03	2·925	2·600	—
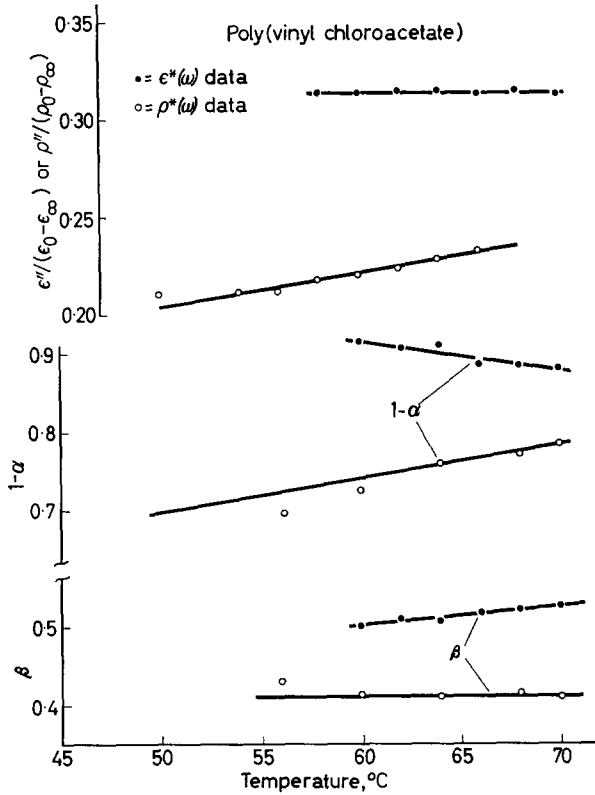
Figure 6—The dispersion parameters used to represent $\epsilon^*(\omega)$ data and $\rho^*(\omega)$ data for poly(vinyl chloroacetate) are plotted as functions of temperature in degrees Centigrade

maximum frequency to represent the relaxation time. The ratio of the relaxation time to the loss maximum frequency depends on specific values of $1 - \alpha$ and β, see Appendix A. Inasmuch as β is temperature dependent, the ratio of the two times will also vary. In other words the temperature dependence of the frequency at which the loss becomes a maximum includes changes in the shape of the relaxation curve which make the activation energy higher.

At temperatures above 100°C and at low frequencies deviations from the assumed behaviour were observed. These deviations are readily attributed to d.c. conductivity and are also observed as the so-called d.c.-tail when the loss factor is plotted as a function of temperature. At temperatures below 70°C deviations from the linear high frequency plot in a complex plane were observed. At 40°C a maximum in the complex plane is observed. The data can be represented approximately by a circular arc with the parameters in *Table 2*.

171

The temperature dependence of the five dispersion parameters used to represent $\epsilon^*(\omega)$ and $\rho^*(\omega)$ data for poly(vinyl chloroacetate)[16] was determined by the Appendix B method. The variation of $1 - \alpha$ and β (*Figure 6*) with temperature for the $\epsilon^*(\omega)$ data is in the opposite sense, while the normalized loss maximum is independent of temperature. For the $\rho^*(\omega)$ data, β is independent of temperature while $1 - \alpha$ and the normalized loss maximum decrease with decreasing temperature, see *Figure 6*. These observations are similar to those observed for poly(vinyl acetate). A plot of the relaxation time versus $10^3/T$ (*Figure 7*) for the $\epsilon^*(\omega)$ and $\rho^*(\omega)$ data exhibit the usual curvature. In addition the relaxation time for the $\rho^*(\omega)$ data is shorter than those from the $\epsilon^*(\omega)$ data.

(D) Comparison of the CPM with TTSM

Before a comparison of the complex plane method (CPM) and the TTSM can be made, their respective inherent assumptions must be carefully examined. In the previous sections we have described the extent to which the proposed dispersion function represents the dispersion data and have found that it does so almost within experimental error. The assumption basic to the TTSM can be formulated in various ways. One such formulation is to assume that the shapes of the normalized real and imaginary parts are independent of temperature. In terms of the CPM this means that $1 - \alpha$ and β must be independent of temperature, a fact which is not verified for either the $\rho^*(\omega)$ or the ϵ^* (ω) data. However, for poly(vinyl acetate and chloroacetate) the changes of $1 - \alpha$ and β are in opposite
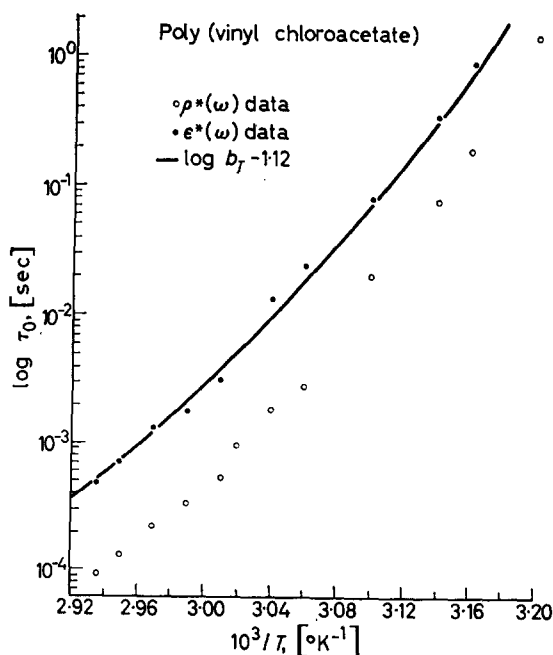
Figure 7—The relaxation time (sec) for the $\epsilon^*(\omega)$ data and $\rho^*(\omega)$ data for poly-(vinyl chloroacetate) is plotted as a function of reciprocal temperature (degrees absolute). The solid line represents the relaxation time calculated from the shift factors

directions so that their effects might be partially compensated. In the poly(vinyl acetal) polymer both $1 - \alpha$ and β change in the same direction so that we would expect this polymer to be the worst example.

A second method for formulating the assumption basic to the TTSM is to state that the distribution of relaxation times is independent of temperature. A single point on the distribution of relaxation times is readily examined from the approximate methods that exist to compute this function from the experimental data. Williams and Ferry[18] have shown that the distribution of relaxation times is related to the variation of the $\log \epsilon''(\omega)$ with $\log \omega$ by means of

$$F_{(\tau=1/\omega)} = B\epsilon''(\omega)[1 - |d\{\log \epsilon''(\omega)\} / d\{\log \omega\}|] \qquad (6)$$

If we examine the distribution of relaxation times at the condition of maximum loss then the distribution function is given by

$$F_{(\tau=1/\omega)} = B\epsilon''_{(\text{max.})} \text{ for } d \log \epsilon''_{(\text{max.})}/d \log \omega = 0$$

In other words a plot of the normalized loss maximum against temperature
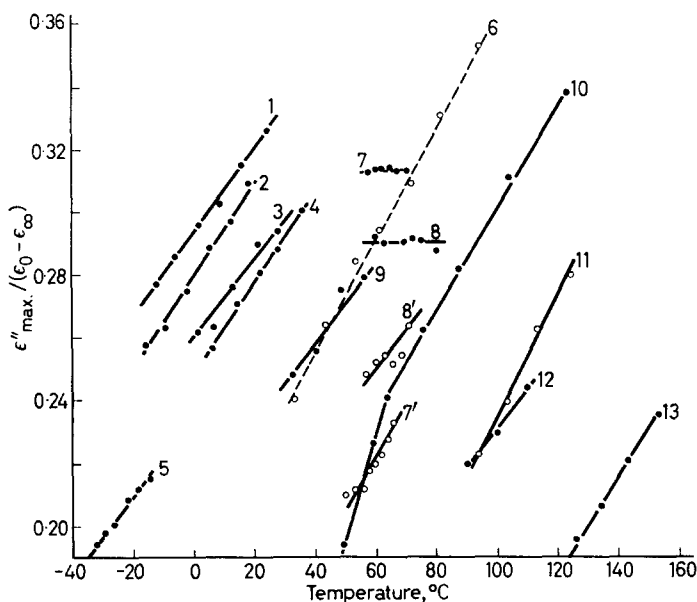
Figure 8—The normalized loss maximum for a number of polymers is plotted as a function of temperature (degrees Centigrade). The broken and solid lines as well as the open and filled circles have no meaning other than to resolve closely spaced points. The numerals refer to the following polymers: 1. poly(vinyl octanoate); 2. poly(vinyl decanoate); 3. poly(vinyl laurate); 4. poly(n-octyl methacrylate); 5. polychloroprene; 6. poly(nonyl methacrylate); 7. poly(vinyl chloroacetate) $\epsilon^*(\omega)$ data; 7'. poly(vinyl chloroacetate) $\rho^*(\omega)$ data; 8. poly(vinyl acetate) $\epsilon^*(\omega)$ data; 8'. poly(vinyl acetate) $\rho^*(\omega)$ data; 9. poly(n-hexyl methacrylate); 10. poly(butyl methacrylate); 11. poly(isobutyl methacrylate); 12 poly(vinyl acetal); 13. poly(cyclohexyl methacrylate)

is essentially a temperature plot of the distribution function at the most probable relaxation time. For poly(vinyl acetate and chloroacetate) the normalized loss maximum is independent of temperature (see *Figures 3* and *6*) while for poly(vinyl acetal) the reduced loss maximum varies with temperature. Again we see that poly(vinyl acetal) is probably the poorest of the three examples. A plot of the reduced loss maximum for some of the polymers in *Table 1* is given in *Figure 8*. From that figure it can be seen that for eleven polymers the reduced loss maximum varies with temperature. Furthermore the temperature dependence of the reduced loss maximum for these polymers (including the vinyl acetal) is the same. This observation implies that the behaviour of the acetate and chloroacetate is not at all typical of polymers but rather that they are exceptions. It is of interest to note that all of the polymers in *Figure 8* except that of the acetals have ϵ_0s less than about five. Based on the results of the previous section we may tentatively conclude that when ϵ_0 is small the $\rho^*(\omega)$ dispersion parameters are similar to $\epsilon^*(\omega)$ parameters so that the normalized loss maximum for the $\rho^*(\omega)$ data will behave similarly to the normalized loss maximum for the $\epsilon^*(\omega)$ data. For polymers whose ϵ_0s are large this assumption is not valid. A plot of the reduced loss maximum for poly-(vinyl acetate and chloroacetate) using the $\rho^*(\omega)$ data is given in *Figure 8*. We can see from this graph that $\rho^*(\omega)$ data for the two acetates behave
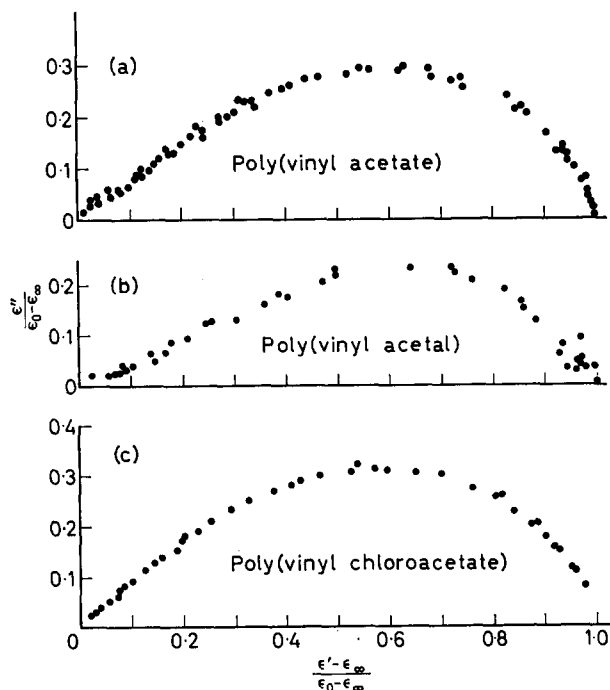
Figure 9—A normalized complex plane plot utilizing all the data: (a) poly(vinyl acetate), (b) poly(vinyl acetal) and (c) poly(vinyl chloroacetate)

174

similarly to $\rho^*(\omega)$ for all the other polymers. We can conclude, therefore, that the reason why the normalized loss maximum for the two acetates is independent of temperature is that although the dispersion would become broader with decreasing temperature, this effect is compensated for by ϵ_0 increasing with temperature.

A third way of formulating the basic assumption to the TTSM was considered earlier in this section, i.e. to construct a complex plane plot of the normalized loss and real parts of the complex dielectric constants for all of the temperatures where measurements were made. A plot of these normalized data is given in *Figure 9* where it can be seen that the data for the chloroacetate fall on to a single line, the band for the acetate data is somewhat larger while the acetal is the poorest (if allowance is made for fewer experimental points). If we compare these results with those obtained for other polymers we find that the scatter for these polymers is trivial. For example with poly(ethyl, butyl, hexyl or octyl methacrylate)[19] the band associated with the $\epsilon_n^*(\omega)$ data in the complex plane fills nearly half the available area.

We may conclude, therefore, that for the present three polymers the
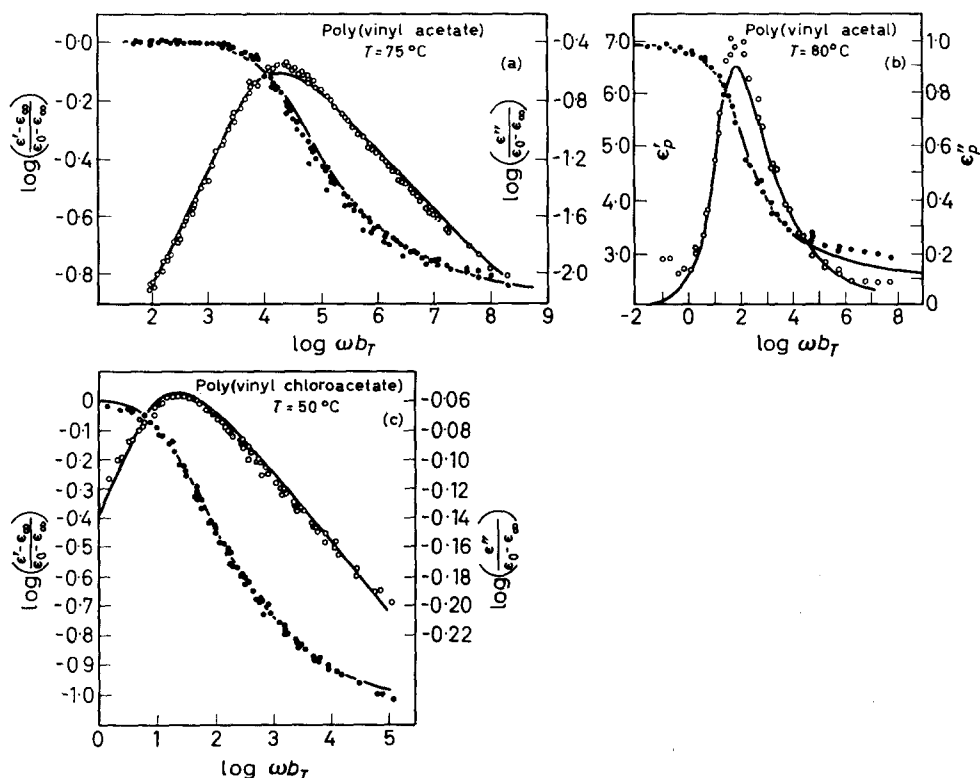
Figure 10—The real ($\bullet$) and imaginary ($\circ$) parts of the dielectric constant are calculated from the dispersion function at the reference temperature and are compared to the shifted values for: (a) poly(vinyl acetate) at 75°C, (b) poly(vinyl acetal) at 80°C and (c) poly(vinyl chloroacetate) at 50°C

inherent TTSM assumption is approximately correct. The reason for this behaviour is a fortuitous compensation of effects due to changes of ϵ_0 with temperature.

The real and imaginary parts of the complex dielectric constant can now be calculated at these reference temperatures using smooth values of ϵ_0, ϵ_∞, $1 - \alpha$, β and τ_0 for the entire shifted (i.e. ωa_T) frequency range which is about six decades in time. The result of such a calculation is given in *Figure 10*. From that figure it can be seen that the agreement between calculated and shifted values for the chloroacetate[20] is excellent. With the acetate[20] small and probably insignificant deviations are observed near the loss maximum and the low frequency side of the real dielectric constant. The deviations with the poly(vinyl acetal)[20] are significant only near the loss maximum and are due to the variation of $1 - \alpha$ and β with temperature. The deviations between the calculated and shifted data in all cases are no greater than the extent of the scatter in the shifted data.

A second comparison between the two methods of data reduction is made by comparing the response times of the system as a function of temperature. Ferry[3] has shown that the shift factor is proportional to the relaxation time, i.e.

$$\log \tau_0 = \log K + \log a_T$$

The proportionality constant K can be evaluated at the reference temperature by measuring the difference between $\log \tau_0$ and $\log a_T$. The shifted relaxation time may then be calculated at all the other temperatures and compared to the present relaxation time. The shifted relaxation time is represented by the solid line for the acetate in *Figure 4*, for the chloroacetate in *Figure 7* and for the acetal in *Figure 5*. In the chloroacetate the agreement between the two relaxation times is excellent over the entire scale. In the acetate some deviations are observed at elevated temperatures, which account for the discrepancy between the calculated and shifted normalized dielectric constants. The agreement between the two times for the acetal is poor. The agreement would have been better had one of the other temperatures been chosen for the evaluation of $\log K$.

III. INTERPRETATION OF THE DISPERSION PARAMETERS

(A) *General remarks*

An interpretation of three of the five dispersion parameters is straightforward. It is shown in Appendix A that ϵ_0 is the low frequency (i.e. $\omega \tau_0 \rightarrow 0$) limiting value of the dielectric constant. For that reason it represents the equilibrium behaviour of the polymer. The parameter ϵ_∞ is the high frequency (i.e. $\omega \tau_0 \rightarrow \infty$) limiting value of the dielectric constant. In the present case this value would intersect the real axis at the square of the refractive index plus some allowance made for atomic polarization (*ca.* 5 to 10 per cent). The quantity $\epsilon_0 - \epsilon_\infty$ is then related to the effective moment of the unit that orients with respect to the applied field. Calculation of the dipole moment of this unit indicates that it is seldom, if ever, the moment of a free gaseous monomer unit. In other words Kirkwood's[21]

176

correlation factor is different from unity. Although it is, in principle, possible to interpret this equilibrium correlation factor in terms of discrete local structure, it is seldom done because of a lack of such information. What is needed and not available is information concerning the relative positions of the dipole moments along the polymer chain. The parameter τ_0, which has the units of time, is readily interpreted along the lines of Kauzmann[22] as the time between segmental jumps. In other words when the field is applied to the specimen, equilibrium is approached by means of a series of jumps, the parameter τ_0 is a measure of these jumps. An interpretation of α and β amounts to a discussion of why dispersions are broader than the simple Debye process. This subject has not yet been completely analysed in terms of molecular details, although three models, which will now be considered, currently exist.

(B) Distribution of relaxation times

The first such model for interpreting broad dispersions is to consider the broadening to be due to a distribution of relaxation times, $F(\tau/\tau_0)$, i.e.

$$\frac{\epsilon^*(i\omega\tau_0) - \epsilon_\infty}{\epsilon_0 - \epsilon_\infty} = \int_{-\infty}^{+\infty} \frac{F(\tau/\tau_0)}{1 + i\omega\tau} \ d \ln (\tau/\tau_0) \tag{7}$$

Davidson and Cole[17] solved this equation for $F(\tau/\tau_0)$ in terms of $\epsilon^*(i\omega\tau_0)$

$$F(y) = \frac{1}{2\pi i (\epsilon_0 - \epsilon_\infty)} \left[\ \epsilon^* \left(\frac{1}{ye^{i\pi}} \right) \ - \epsilon^* \left(\frac{1}{ye^{-i\pi}} \right) \right] \tag{8}$$

where $y = \tau/\tau_0$. Gross[23] has also discussed the solution to this integral equation and pointed out that one merely replaces $i\omega$ by $\omega \exp (\pm i\pi)$ in the formula for $\epsilon^*(\omega)$. For our applications we need only to substitute into the present dispersion function $ye^{\pm i\pi}$ for iy. This substitution leads to

$$\epsilon^* \left(\frac{1}{ye^{\pm i\pi}} \right) = \epsilon_\infty + \frac{\epsilon_0 - \epsilon_\infty}{[1 + (1/\{ye^{\pm i\pi}\})^{(1-\alpha)}]^\beta}$$

The solution for $F(y)$ becomes

$$F(y) = (1/\pi)y^{(1-\alpha)\beta} \sin \beta\theta [y^{2(1-\alpha)} + 2y^{(1-\alpha)} \cos \pi(1-\alpha) + 1]^{-\beta/2} \tag{9}$$

where $y = \tau/\tau_0$ and $\theta = \arc \tan \left\{ \dfrac{\sin \pi (1-\alpha)}{y^{(1-\alpha)} + \cos \pi(1-\alpha)} \right\}$.

It is of interest to examine this function for the various extremes in $1-\alpha$ or β. When $\alpha = 0$, i.e. Davidson and Cole's skewed semi-circle[17], this equation becomes

$$F(y) = (1/\pi)y^\beta \sin \beta\theta [y^2 - 2y + 1]^{-\beta/2}$$

with $\theta = 0, \pi$. When $\theta = 0$, $F(y) = 0$, which is a trivial solution. When $\theta = \pi$,

$$F(y) = (1/\pi) \ y^\beta \sin \pi\beta \ (1-y)^{-\beta} \tag{10}$$

Inasmuch as $F(y)$ must be real, then $y < 1$, so that

$$F(\tau/\tau_0) = (1/\pi) \ \sin \beta\pi \{\tau/(\tau - \tau_0)\}^\beta \quad \text{for } \tau < \tau_0 \tag{10a}$$

$$F(\tau/\tau_0) = 0 \qquad\qquad\qquad \text{for } \tau > \tau_0 \tag{10b}$$

We see that in the limit of $\alpha = 0$ equation (9) converges to those of Davidson and Cole[17], which is of course to be expected.

The other extreme of interest is when $\beta = 1$, which is the Cole and Cole circular arc. Substitution of this condition into equation (9) leads, after some manipulation, to

$$F(y) = (1/2\pi) \sin \alpha\pi \{\cosh [(1-\alpha) \ln y] - \cos \alpha\pi\}^{-1} \qquad (11)$$

with $y = \tau/\tau_0$, which is the exact form recorded by Cole and Cole[1].

Therefore, the two parameters α and β uniquely represent the distribution of relaxation times. The parameter α appears to represent the breadth while β represents the skewness of the distribution of relaxation times. A very simple test exists (which is necessary but not sufficient) to determine if the distribution function is temperature dependent. This test is based on the relationship between φ_L, $1 - \alpha$ and β

$$\varphi_L = (1-\alpha)\beta\pi/2 \qquad (12)$$

Therefore, if φ_L is temperature dependent, then either $(1-\alpha)$ or β or both must be temperature dependent which makes $F(\tau/\tau_0)$ temperature dependent. On the other hand if φ_L is independent of temperature then $(1-\alpha)$ and β may be independent of temperature so that $F(\tau/\tau_0)$ is independent of temperature. It is possible, however, that the temperature dependences of $(1-\alpha)$ and β are in opposite senses so as partially to annihilate their effects. The two acetates studied in the previous section are two such examples.

The determination of $1 - \alpha$ and β, as well as their temperature dependences, is a simple matter as noted in Appendix B. It is a simpler matter to determine the distribution function $F(\tau/\tau_0)$ from $1 - \alpha$ and β. Equation (9) is readily programmed on any digital computer (such as the IBM 1620) to compute $F(\tau/\tau_0)$ over any range of τ/τ_0 for a given set of values for $1 - \alpha$ and β.

Davidson and Cole[17] considered the distribution of relaxation times for glycerol at $-50°C$, see *Figure 11*. The function $F(\tau/\tau_0)$ increases without limit as τ/τ_0 ranges from zero to unity. The function is then zero for all values of τ/τ_0 greater than one. Although $F(\tau/\tau_0)$ has a singularity at $\tau/\tau_0 = 1$, the distribution function is still normalized because Davidson and Cole were able to show that

$$\int_{-\infty}^{+\infty} F(\tau/\tau_0) \, \mathrm{d} \ln \tau/\tau_0 = 1$$

The parameter β was found to be temperature dependent over the region where it could be measured. In *Figure 11* we have included $F(\tau/\tau_0)$ for $1 - \alpha = 1.0$ and $\beta = 0.550$ which are the dispersion parameters for glycerol at $-70°C$. The general features of the distribution function are the same except that the curve is slightly broader at the lower temperature.

When the $\epsilon^*(\omega)$ data are transformed into $\rho^*(\omega)$ data the parameters used to represent the dispersion are no longer the same or even similar because the shape of the curve has markedly changed. The curve for glycerol is no longer a skewed semi-circle but rather one that is typical of many
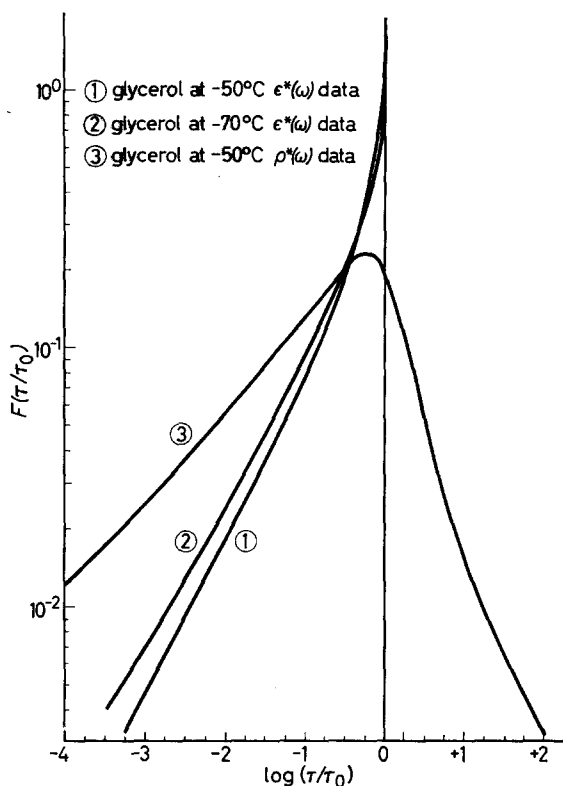
Figure 11—The distribution function $F(\tau/\tau_0)$ is plotted as a function of τ/τ_0 for glycerol at two temperatures

polymers. The distribution function is readily calculated from the dispersion parameters $1-\alpha$ and β used to represent the $\rho^*(\omega)$ data for glycerol at $-50°C$. The distribution function $F(\tau/\tau_0)$ is finite everywhere, see *Figure 11*, having a maximum slightly to the short time side of $\tau/\tau_0=1$. Furthermore the distribution function is no longer zero for $\tau/\tau_0 > 1$ and exhibits a shape that is similar to polymeric functions obtained from shifted data.

The distribution of relaxation times for the three polymers described in Section II is readily calculated from the appropriate values of $1-\alpha$ and β. In each case the parameters were chosen at the reference temperature. The results of the calculation are recorded in *Figure 12*. Although the distribution function was calculated for the $\epsilon^*(\omega)$ data the differences between the $\rho^*(\omega)$ and $\epsilon^*(\omega)$ distribution functions at the reference temperatures are too small to be seen because of the scale size. In general the $\rho^*(\omega)$ distribution function is slightly broader than that for $\epsilon^*(\omega)$.

It is of interest to compare the distribution functions calculated from the relaxation function to those calculated by the approximate methods described by Ferry *et al.*[20]. Before describing the comparison, once again several points must be emphasized. First, the relaxation function is empirical but accurate. The calculation of $F(\tau/\tau_0)$ from the relaxation function is exact. Therefore the reliability of $F(\tau/\tau_0)$ is as good as the reliability of the relaxa-

179
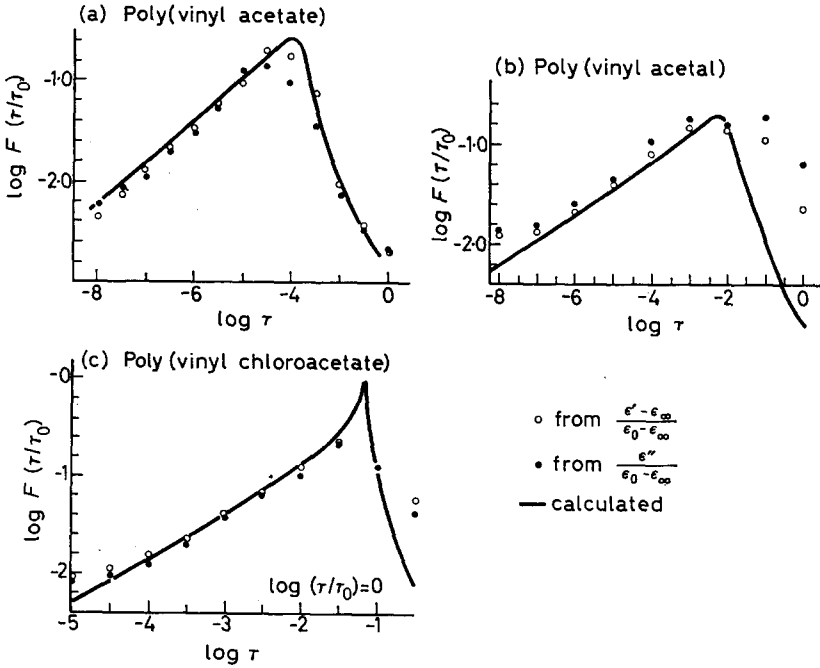
Figure 12—The distribution function $F(\tau/\tau_0)$ is plotted as a function of t(sec) for three polymers. In all cases $\bigcirc$ represents the function calculated from the real data while $\bullet$ represents the function from imaginary data while the solid line is calculated using equation (9): (a) poly(vinyl acetate), (b) poly(vinyl acetal) and (c) poly(vinyl chloroacetate)

tion function. Second, the basic assumption in TTSM is not precisely maintained (*Figure 9*) except, perhaps for the chloroacetate. Third, the method used by Ferry *et al.*[20] to calculate $F(\tau/\tau_0)$ is approximate. The magnitude of the error is at least as large as the differences between $F(\tau/\tau_0)$ calculated from real and imaginary data. Finally the real and imaginary parts calculated from equation (1) are in good agreement with the shifted data of Ferry *et al.*[20] (*Figure 10*).

Keeping these approximations and assumptions in mind, we can now compare the two calculated $F(\tau/\tau_0)$s. In *Figure 12*(a) we have represented the two $F(\tau/\tau_0)$s for poly(vinyl acetate) where it can be seen that the agreement between the two distribution functions is as good as the internal agreement of Ferry's approximate method. In *Figure 12*(b) we have represented the two $F(\tau/\tau_0)$s for poly(vinyl acetal) where it can be seen that the agreement at very short and very long times is poor. These discrepancies are no doubt due to those factors considered in Section II (C). In *Figure 12*(c) we have represented the two $F(\tau/\tau_0)$s for poly(vinyl chloroacetate). The agreement at times greater than $\tau/\tau_0 > 1$ is poor, although the agreement between the calculated and shifted $\epsilon^*(\omega)$s was excellent. We conclude, therefore, that the discrepancies are due to Ferry's approximate methods.

(C) Fluctuations in free energy

A second model for interpreting broad dispersions, and hence giving meaning to α and β, has been given by Scaife[24] who related the average fluctuation in free energy associated with the moment of the sphere imbedded in a vacuum to the following expression

$$\langle F(\mathbf{M}^2) - F(0) \rangle = \frac{3kT}{\pi} \int_0^\infty \frac{\rho'(\omega)\rho''(\omega)}{\rho^*(\omega)\overline{\rho^*(\omega)}} \frac{d\omega}{\omega} \tag{13}$$

In this expression $F(\mathbf{M}^2)$ is the free energy of the sphere with moment $\mathbf{M}$ while $F(0)$ is the condition of zero moment. Scaife has defined the integrand

$$(3/\beta)\,(\rho'\rho''/\rho^*\overline{\rho}\,^*)\,(d\omega/\omega) = \Psi(\omega) \tag{14}$$

as the spectral distribution of free energy associated with the fluctuations. The function $\Psi(\omega)$ can be rearranged to read, remembering that $\rho^*\overline{\rho}^*$ are complex conjugates

$$\Psi(\omega) = \frac{1}{\{\rho'(\omega)/\rho''(\omega)\} + \{\rho''(\omega)/\rho'(\omega)\}} \tag{15}$$

The function $\rho''(\omega)/\rho'(\omega)$ is the loss tangent, whose value rarely exceeds 0·3, so that $\Psi(\omega)$ becomes

$$\Psi(\omega) = \rho''(\omega)/\rho'(\omega)$$

and the integral becomes

$$\langle F(\mathbf{M}^2) - F(0) \rangle = \frac{3kT}{\pi} \int_0^\infty \frac{\rho''(\omega)}{\rho'(\omega)} \frac{d\omega}{\omega} \tag{16}$$

In other words the spectral free energy associated with the fluctuation is essentially the integral of the loss tangent versus log ω curve. The parameters α and β then describe the shape of the loss curve leaving us with little or no molecular picture.

(D) Correlation function

A third approach to the problem of broad dispersions has been made by R. H. Cole[25] who considered the response of a macroscopic sample in terms of a time-dependent correlation of the electric moment of the sample including all moments, i.e. permanent and induced. The result of his analysis is given by

$$\frac{\epsilon^*(\omega)-1}{\epsilon^*(\omega)+2} = \frac{\epsilon_\infty-1}{\epsilon_\infty+2} + 4\pi N \frac{\langle \mu(0)\cdot\mathbf{M}(0)f^0\rangle}{9kTV} \mathcal{L}\,[-\Psi(t)] \tag{17}$$

where

$$(\epsilon_\infty - 1)/(\epsilon_\infty + 2) = 4\pi N\alpha/3V$$

and

$$\Psi(t) = \langle \mu(0)\cdot\mathbf{M}(t)f^0\rangle / \langle \mu(0)\cdot\mathbf{M}(0)f^0\rangle \tag{18}$$

with $\mathcal{L}$ representing the Laplace transform. The first term on the left, i.e. $[\epsilon^*(\omega)-1]/[\epsilon^*(\omega)+2]$, is of course the polarization of the sphere under consideration which is suspended in a vacuum. The first term on the right,

$(\epsilon_\infty - 1)/(\epsilon_\infty + 2)$, represents the instantaneous polarization of the sphere. The term $\langle \mu(0) \cdot M(0) f^0 \rangle$ represents the equilibrium effective induced moment of the sphere. The term $\mathcal{L}[-\Psi(t)]$ has the effect of a macroscopic decay function for the spherical sample and represents the average moment at time t with respect to the equilibrium value. Unfortunately not much can be achieved with this approach at this time because of the scarcity of structural data and the absence of information leading to the nature of interactions. However, one point can be made and that is to combine equation (17) with Cole's equations (9) and the one following (12) together with the empirical equation (5) to give

$$\frac{\rho^*(\omega) - \rho_\infty}{\rho_0 - \rho_\infty} = \{1 + (i\omega\tau_0)^{(1-a)}\}^{-\beta} = \mathcal{L}[-\dot{\Psi}(t)] \qquad (19)$$

In other words, the curly brackets $\{\ \}^{-\beta}$ describe the relationship between the central dipole and its environment as it moves to offset the effects of the applied field.

IV. MECHANICAL DISPERSIONS

(A) *Poly(vinyl acetate)*

The results of a complex plane plot using the shifted complex compliance data of Williams and Ferry[26] for poly(vinyl acetate) are given in *Figure 13*(a). The shape of this curve, typical of some polymers, is not similar to any dielectric dispersions reported in the previous section. The limiting angle $\varphi_L = 74°$ is twice that observed for the dielectric dispersion. Examination of the complex plane plot at very high frequencies [see *Figure 13*(b)] reveals a curvature not seen in the corresponding dielectric dispersion. A bisector of φ_L and extrapolated to the experimental locus intersects it at a
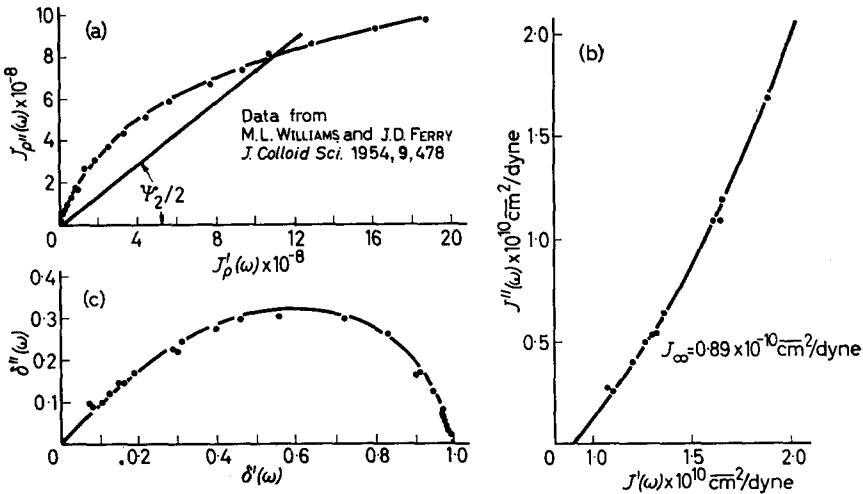
Figure 13—(a) Complex plane plot of poly(acetate) at the reference temperature using shifted data[26] in units of $\overline{cm^2}$/dyne. (b) Extreme high frequency end of plot. (c) Complex plane plot of transformed data for poly(vinyl acetate)

frequency that is 2·5 decades slower than the corresponding dielectric dispersion. This intersection point takes place at the high frequency side of the loss maximum, a phenomenon not observed in dielectric dispersions. Finally there is no loss maximum but this may be due to incomplete experimental data rather than a basic shape of mechanical dispersions. Based on these observations the relaxation processes are not similar despite the fact that Williams and Ferry[26] found the temperature dependence of the dielectric and mechanical shift factors to be the same. This correlation implies that the activation energy associated with each relaxation process is the same.

In view of the results in Section II, i.e. that different methods of representing dielectric data lead to slightly different conclusions because of changes in the shape of the relaxation curve, one should not be surprised that no comparison is observed at this point. The discussion in the previous section was among systems with ratio of $\epsilon_0/\epsilon_\infty$ less than 15; here J_0/J_∞ is approximately one thousand. For these reasons a suitable transformation† procedure must be devised. This can be done by noting that equation (4) is the specific case (where $\epsilon_\infty = 1$) of the following generalization[27],

$$\rho^*(\omega) = \{\epsilon^*(\omega) - \epsilon_\infty\} / \{\epsilon^*(\omega) + 2\epsilon_\infty\} \tag{20}$$

If we can replace ϵ_∞ by J_∞ and $\epsilon^*(\omega)$ by $J^*(\omega)$ and refer to the resulting transformed quantity as $\delta^*(\omega)$ [complex deformation] we obtain

$$\delta^*(\omega) = \{J^*(\omega) - J_\infty\} / \{J^*(\omega) + 2J_\infty\} \tag{21}$$

It is important to note that $\delta^*(\omega)$, like its dielectric counterpart, will contain all of the deforming mechanisms that can contribute to the complex compliance [$J^*(\omega)$] at frequency ω, i.e. all elastic and viscoelastic mechanisms will be present. The range of these observables will be limited to the interval $0 \leqslant \delta^*(\omega) \leqslant 1$ as is the case for the complex polarization. The real and imaginary parts can be separated quite readily to yield

$$\delta'(\omega) = \frac{[J'(\omega) - J_\infty][J'(\omega) + 2J_\infty] + J''(\omega)^2}{[J'(\omega) + 2J_\infty]^2 + J''(\omega)^2} \tag{21a}$$

and

$$\delta''(\omega) = \frac{3J_\infty \cdot J''(\omega)}{[J'(\omega) + 2J_\infty]^2 + J''(\omega)^2} \tag{21b}$$

Inasmuch as J_∞ will play the counterpart of ϵ_∞, this parameter may be obtained by extrapolating a complex plane plot of the compliance to the real axis, where $J''(\omega) = 0$. For poly(vinyl acetate) a complex plane plot at very high frequencies is given in *Figure 13*(b) where J_∞ is determined to be $0·89 \times 10^{-10}$ $cm^{+2}/dyne$. This value of J_∞ together with equations (21) and the data of Ferry[26] can be used to calculate $\delta^*(\omega)$. The results of this transformation are recorded in *Figure 13*(c) where it can be seen that the experimental locus has been drastically altered. The locus is now similar to the corresponding dielectric dispersions. It is possible to test for a quan-

†We refer to the following procedure as a transformation, following the nomenclature of Scaife. This procedure is in reality a normalization but this term like the term reduced has been widely used to denote specific operations on experimental quantities.

Table 3. Comparison of dispersion parameters for dielectric and mechanical dispersions

Parameter	Poly (vinyl acetate)	Poly (methyl acrylate)	Poly (n-octyl methacrylate)
$1-\alpha$			
$\rho^*(\omega)$	0·80	0·75	0·80
$\delta^*(\omega)$	0·94	0·92	0·92
β			
$\rho^*(\omega)$	0·51	0·33	0·49
$\delta^*(\omega)$	0·50	0·33	0·37
$2\pi\tau_0$ (sec)			
$\rho^*(\omega)$	$0·73 \times 10^{-5}$	10×10^{-1}	—
$\delta^*(\omega)$	$3·66 \times 10^{-5}$	$2·86 \times 10^{-1}$	2×10^{-8}
δ_0	0·993	0·995	0·995
δ_∞	0	0	0
$T, °C$	70	25	100

titative agreement between the shapes of dielectric and mechanical dispersions by assuming the mechanical dispersion to take the form

$$\{\delta^*(\omega) - \delta_\infty\} / \{\delta_0 - \delta_\infty\} = [1 + (i\omega\tau_0)^{(1-a)}]^{-\beta} \qquad (22)$$

The deformation parameters are calculated by the methods outlined in Appendix A and are listed in *Table 3*. The instantaneous and equilibrium values (ρ_∞ versus δ_∞ and ρ_0 versus δ_0) are quite different as is to be expected. However, the dynamic parameters (τ_0, φ_L, $1-\alpha$ and β) are very similar. In fact the differences are readily attributed to differences in molecular weight (but see intrinsic viscosities listed in original reference[26]) because we have found that the dispersions of lower molecular weight polymers tend to be faster and narrower. The reliability of equation (22) in terms of representing the experimental quantities is shown in *Figure 14* where the real
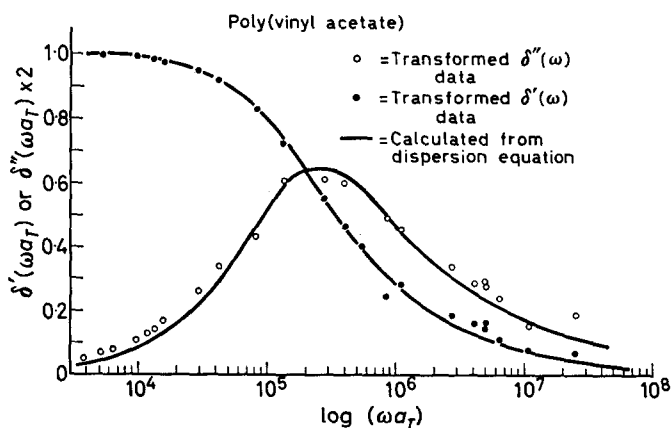
Figure 14—Comparison of calculated real (●) and imaginary (○) parts of transformed compliance (represented by solid line)
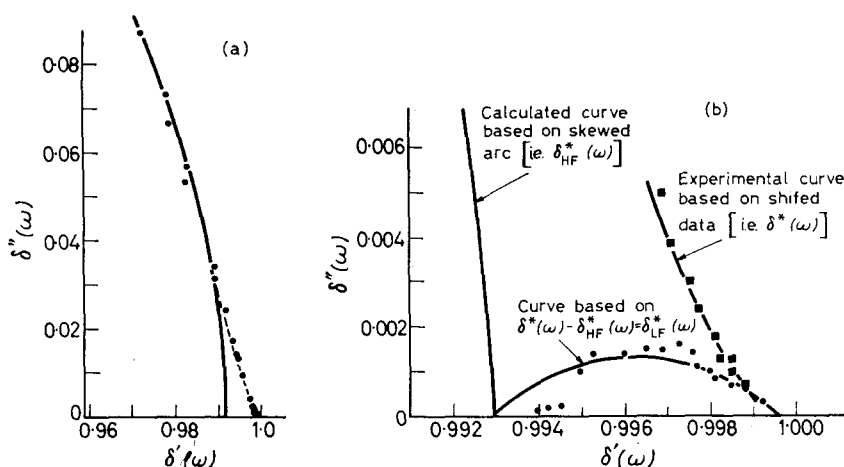
Figure 15—(a) Experimental deviations (●) for poly(vinyl acetate) from assumed behaviour which is represented by the solid line. (b) Decomposition of deviations in terms of another process. The solid line represents the assumed behaviour, filled circles represent the deviations and filled squares represent the experimental data

and imaginary parts of $\delta^*(\omega)$ both observed and calculated are plotted against log ωa_T. The agreement between calculated and observed $\delta^*(\omega)$ is fair but not as good as was observed in the electrical case. At very low frequencies the deviations become pronounced, see *Figure 15*, not only in terms of scatter between calculated and observed values of $\delta^*(\omega)$ but the locus of the experimental curve deviates from the calculated curve. These deviations can be represented in terms of a second dispersion by assuming the deformation of the two processes to be additive, i.e.

$$\delta^*(\omega) = \delta^*_{LF}(\omega) + \delta^*_{HF}(\omega) \qquad (23)$$

In this equation $\delta^*_{HF}(\omega)$ is the high frequency dispersion which has been described by the parameters in *Table 3* while $\delta^*_{LF}(\omega)$ is the low frequency dispersion in which the deviations described in *Figure 15*(a) will be represented. The parameters $\delta^*_{HF}(\omega)$ are calculated for the necessary ωs and then subtracted from the experimental values of $\delta^*(\omega)$. The difference is plotted in *Figure 15*(b) after the addition of δ_0 which is the equilibrium value of the high frequency process. As can be seen in *Figure 15*(b) the results may be represented by a circular arc.

The transformation equation can be rearranged to read

$$J^*(\omega) = J_\infty \{1 + 2\delta^*(\omega)\} / \{1 - \delta^*(\omega)\} \qquad (24)$$

which can be separated into real and imaginary parts to read

$$J'(\omega) = J_\infty \frac{[1 + 2\delta'(\omega)][1 - \delta'(\omega)] - 2(\delta'')^2}{[1 - \delta'(\omega)]^2 + (\delta'')^2} \qquad (24a)$$

and

$$J''(\omega) = J_\infty \frac{3\delta''(\omega)}{[1 - \delta'(\omega)]^2 + (\delta'')^2} \qquad (24b)$$

185
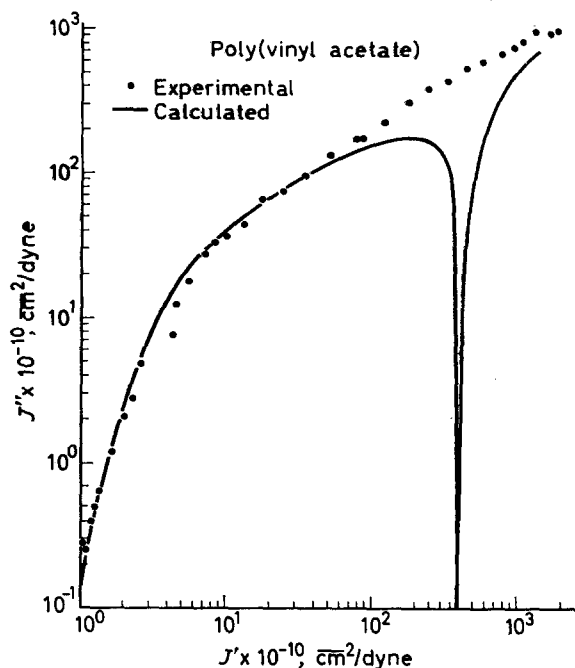
Figure 16—Complex plane plot of compliance in
$cm^2/dyne$ for poly(vinyl acetate). The filled circles
are experimental values while the two solid lines
represent the calculated values of the low and high
frequency processes

Inasmuch as $\delta'(\omega)$ and $\delta''(\omega)$ can be calculated from the dispersion equations and parameters as functions of frequency then $J'(\omega)$ and $J''(\omega)$ can also be calculated as functions of frequency. A complex plane plot of $J'(\omega)$ and $J''(\omega)$ is given in *Figure 16* using the high frequency dispersion parameters. The agreement is quite good except for that region where the low frequency dispersion exists. This contribution to $J^*(\omega)$ is calculated from the above equations together with the dispersion parameters obtained from the deviations in the complex deformation case.

(B) *Poly(methyl acrylate)*

A complex plane plot of the complex compliance is readily constructed using the shifted data of Williams and Ferry[28] for poly(methyl acrylate). The result of this complex plane plot is given in *Figure 17*(a) where it can be seen that the locus goes through a maximum and appears to be a distorted arc. As with poly(vinyl acetate) the complex compliance can be transformed into the complex deformation using equation (21). The parameter J_∞ was obtained from a complex plane plot and was found to be $1 \cdot 0 \times 10^{-10}$ $cm^{+2}/dyne$. The results of this transformation are recorded in *Figure 17*(b). The skewed arc parameters are listed in *Table 3*. Calculation of $\delta^*(\omega)$ from the skewed arc parameters in comparison with the experimental values led

to deviations similar to those encountered in the poly(vinyl acetate) case. At very low frequencies the deviations become significant (see *Figure 18*) but it is possible to represent these deviations in terms of a low frequency dispersion.

Poly(methyl acrylate)
$T = 25\,^{\circ}\mathrm{C}$
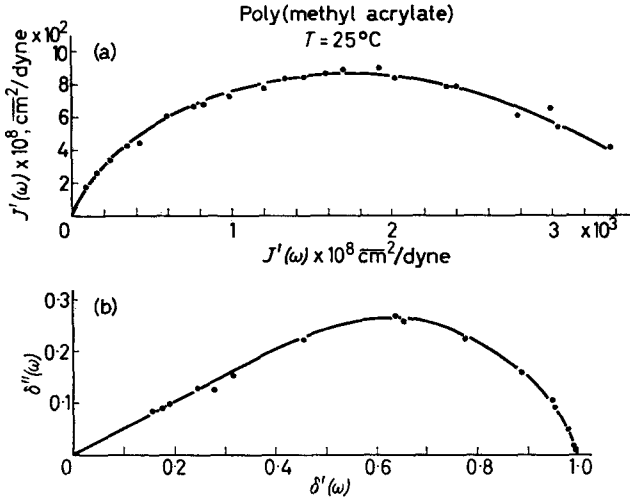
Figure 17—(a) Complex plane plot of compliance (in $cm^2/dyne$) for poly(methyl acrylate) at $25\,^{\circ}C$. (b) The transformed complex compliance, i.e. complex deformation for poly(methyl acrylate) at $25\,^{\circ}C$

Figure 18—Complex plane plot of deformation for poly(methyl acrylate) at $25\,^{\circ}C$. The solid line represents the calculated behaviour, the filled circles are experimental quantities while the open circles represent the deviations at constant frequency

Poly(methyl acrylate)
$T = 25\,^{\circ}C$

Calculated curve based on skewed arc [i.e. $\delta_{HF}^{*}(\omega)$]

Experimental curve based on shifted data [i.e. $\delta_{e}^{*}(\omega)$]

Curve based on $\delta^{*}(\omega) - \delta_{HF}^{*}(\omega) = \delta_{LF}^{*}(\omega)$

187
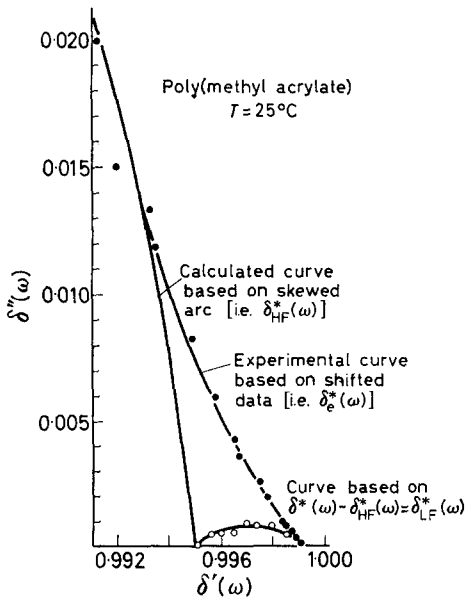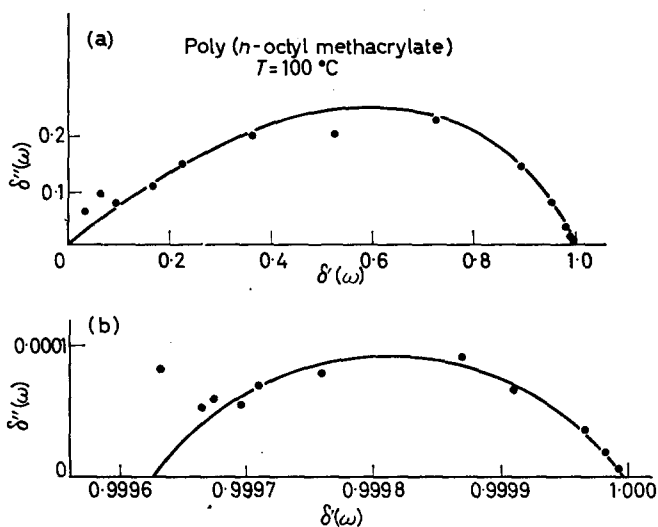
Figure 19—(a) Complex deformation of poly(n-octyl meth-
acrylate) at 100°C. (b) Extreme low frequency behaviour

(C) *Poly*(n-*octyl methacrylate*)

A complex plane plot of the complex compliance is readily constructed
using the shifted data listed by Ferry[3] in Appendix D. The parameter J_∞
was found to be 2×10^{-10} cm^{+2}/dyne. This parameter together with equation
(21) was used to transform $J^*(\omega)$ to $\delta^*(\omega)$. The results of this transformation
are listed in *Figure 19*(a) where it can be seen that the now familiar skewed
arc is obtained. The dispersion parameters associated with this mechanism
are listed in *Table 3* along with the appropriate electrical parameters.
Calculation of $\delta^*(\omega)$ from the dispersion parameters and equation (21) led
to discrepancies similar to those for poly(vinyl acetate). At very low
frequencies significant deviations were encountered, except that for this
polymer it was not necessary to postulate the existence of two dispersions
because they were found to be resolved, see *Figure 19*(b).

(D) *Polyisobutylene*

A complex plane plot of the complex compliance is readily constructed
using the shifted data listed by Ferry[3] in Appendix D. The parameter J_∞
was found to be 0.9×10^{-20} cm^{+2}/dyne. This parameter together with
equation (21) was used to transform $J^*(\omega)$ to $\delta^*(\omega)$. The results of this
transformation are listed in *Figure 20*(a) where it can be seen that the
relaxation process for this polymer is a circular arc, i.e. $\beta = 1$. As in the
other cases the deviations become significant at very low frequencies where
a second or low frequency dispersion is readily seen, *Figure 20*(b).

V. A SIMPLE LINEAR MECHANICAL MODEL
(A) *Preliminary remarks*

In the previous section a correlation was described between the dielectric

188
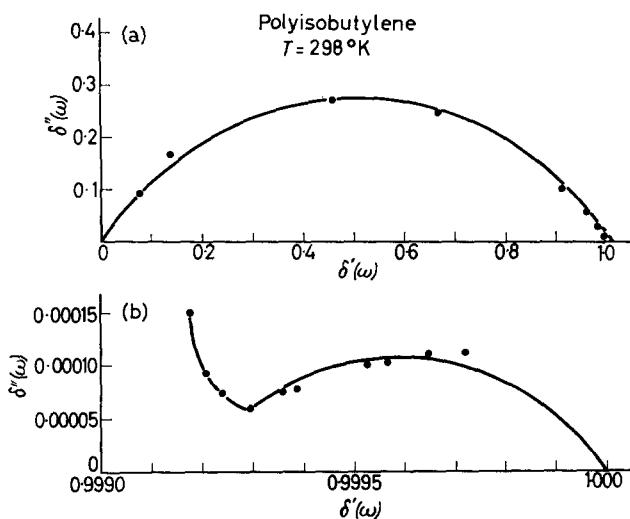
Figure 20—(a) Complex deformation of polyisobutylene at 25°C. (b) Extreme low frequency behaviour

and mechanical dispersions when these mechanisms were transformed in a particular way. The dielectric transformation is quite clear, it is the polarization of a unit sphere imbedded in a vacuum. The meaning of the mechanical transformation is not quite as clear but probably represents an analogous transformation. The correlations that were observed were only between the dynamic parameters α, β and τ_0 and not between the equilibrium and instantaneous parameters. This means that the mechanism by which the systems approach equilibrium after they have been disturbed must be the same. These correlations suggest that a mechanical analogue of current dielectric model should be studied.

In the mechanical analogue of this dielectric model we need to replace the vacuum by an isotropic elastic continuum (material constant J_∞) because a vacuum cannot support a mechanical stress field. Furthermore we shall take J_∞ to represent the higher frequency limiting behaviour of the specimen. The origin of a right-handed coordinate system is located at the centre of the continuum. A spherical inclusion, centred at the origin of the coordinate system shall take the place of the dielectric specimen and become the object of study. The adhesion between the surface of the specimen and the continuum is considered to be perfect. This specimen is small enough so that there is no spatial variation in the stress field, while the field may or may not vary with time. On the other hand this specimen is large enough to contain enough polymer chains so that statistical averaging is possible.

Consider the behaviour of this specimen when it is subjected to an external stress field applied to the continuum in the usual way. Let this stress field, represented by $\mathbf{T}U(t)$, be applied in the direction of the z axis and have the form of a step function, see *Figure 21*(a). $\mathbf{T}$ is a constant and
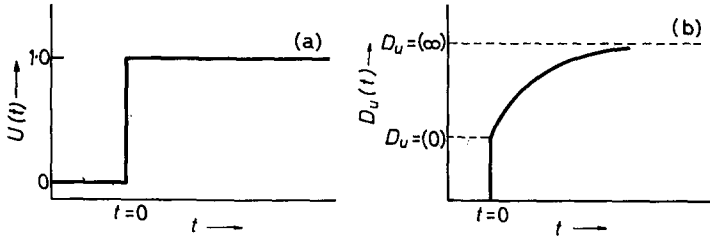
Figure 21—(a) Plot of unit step function $U(t)$ versus t. (b) Plot of distortion of sphere $Du(t)$ as a function of time

determines the magnitude of the stress while $U(t)$ is a unit step function such that at times $t < 0$, $U(t) = 0$ and at times $t > 0$, $U(t) = 1$. In general this stress field will distort the spherical specimen in the following way. First there will be an instantaneous distortion $Du(0)$ corresponding to the instantaneous response of the system. Actually, the response cannot be instantaneous because of inertial effects; however, we shall take as instantaneous any time interval that is small compared to the times associated with the measurements. Following this initial distortion there will be one that is time dependent. Eventually the system will cease to be distorted and come to some equilibrium value $Du(\infty)$, see *Figure 21*(b). Inasmuch as we have assumed the specimen to be isotropic in its properties, the distortion $Du(\infty)$ will be co-linear with the applied stress field $TU(t)$. At this point we can define linearity as the condition where the equilibrium distortion of the specimen, i.e. $Du(\infty)$, depends only on the field intensity T, in other words

$$\lim_{t \to \infty} Du(t) = D_s T \tag{25}$$

In this expression D_s (s implies static or equilibrium conditions) is the equilibrium distortion of the sphere.

At this point it is convenient to divide the discussion into three parts. First, we need to discuss the relationship between the distortion of this sphere and its gross mechanical properties in terms of classical continuum mechanics. Next we need to discuss some properties of the sphere itself. Finally the distortion of the sphere needs to be related to some aspect of polymer molecules using classical statistical mechanics.

(B) *Spherical inclusion problem*

The solution for the equilibrium distortion (D_s) of the inclusion subjected to body forces in terms of the gross mechanical properties of the sphere and its surrounding medium may be obtained from elasticity theory[29]. Uemura and Takayanagi[30] have recently considered such a problem, i.e. a spherical isotropic inclusion with known elastic constants. When the medium is stretched in simple tension T, they calculated the displacement and the stress in the vicinity of the particle. The distortion (U) and stress

190

(σ) in the $\theta = 0$ direction (see Appendix C) is given as:

$$U_{(\theta=0)} = -TA_2J_2 \quad \text{and} \quad \sigma_{(\theta=0)} = T\{4\nu_2B_2 - 2A_2\} \tag{26}$$

where

$$A_2 = \frac{3(1-\nu_1)[2(3-\nu_2+5\nu_1\nu_2)+(9+5\nu_1)(1-2\nu_2)J_2/J_1]}{2(1+\nu_1)[2(4-5\nu_1)+(7-5\nu_1)J_2/J_1][1+\nu_2+2(1-2\nu_2)J_2/J_1]}$$

and

$$B_2 = \frac{3(1-\nu_1)}{4(1+\nu_1)[1+\nu_2+2(1-2\nu_2)J_2/J_1]}$$

In these equations subscript 1 refers to the continuum while 2 refers to the sphere. The quantity $U_{(\theta=0)}$ is the distortion at the surface of the sphere of unit radius, ν is Poisson's ratio and J is the equilibrium compliance of the medium.

If we consider the case of $\nu_1 = \nu_2 = \frac{1}{2}$, then the distortion in the direction of the stress field becomes

$$U_{(\theta=0)} = (5/3)TJ_2J_1/(3J_2+2J_1) \tag{27}$$

If we subtract from this quantity the distortion of the continuum at the surface of the sphere, had the spherical specimen not been there, we have

$$D = U_{(\theta=0, J_2 \neq J_1)} - U_{(\theta=0, J_2=J_1)} = \tfrac{2}{3}TJ_1(J_2-J_1)/(3J_2+2J_1) \tag{28}$$

Now if we set $J_1 = J_\infty$, and invoke the principle of correspondence in the same way as did Uemura and Takayanagi by letting $J_2 = J^*(\omega)$ and $D = D^*(\omega)$ we have after some rearrangement

$$\Lambda^*(\omega) = \frac{9D^*(\omega)}{2T(\omega)J_\infty} = \frac{J^*(\omega)-J_\infty}{J^*(\omega)+\tfrac{2}{3}J_\infty} \tag{29}$$

We conclude from these arguments that the empirical transformation [i.e. equation (21)] resulted, very nearly, in the complex distortability of a sphere with unit radius, complex compliance $J^*(\omega)$ and Poisson's ratio of one half suspended in an otherwise continuous elastic medium of compliance J_∞ and Poisson's ratio of one half. The differences between 2/3 and 2 in equations (29) and (21) are readily compensated for by the errors that exist in the determination of J_∞ and ν_2.

(C) *Properties of the sphere†*

Let us now consider the distortion of the sphere as the stress varies arbitrarily with time. We define the quantity

$$D(t)/T \equiv Au(t) \tag{30}$$

as the unit step function response of the sphere. In other words, we shall assume a knowledge of the way the system responds in time to the application of a unit stress field. The arbitrary stress field $T(t)$ (*Figure 22*) can be

†This section is essentially an adaptation of dielectric theory to the present mechanical model. The dielectric discussion can be found in refs. 6 or 24. In the following discussion, the moment of the sphere $m(t)$ is replaced by this distortion $D(t)$, the electric field E by the tensile field T and the complex polarization $\alpha^*(\omega)$ by the complex distortability $\Lambda^*(\omega)$. The mathematical arguments are the same for both cases because the following discussion is essentially in macroscopic terms.
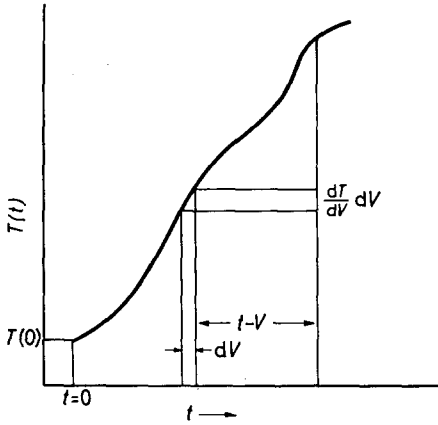
Figure 22—Variation of an arbitrary tensile stress field with time can be represented as a sum of incremental values to which the response of the sphere is known

thought of as arising from a succession of unit step functions of magnitude $dT(t)$ for which the response of the sphere is assumed to be known. The total response of the sphere $D(t)$, at some time t, is given as the summation of the individual responses to the succession of unit step functions (Boltzman's Superposition Principle[3]). This response is given by

$$D(t) = T(0)Au(t) + \int_{0^+}^{t} Au(t-v)[dT(v)/dv] \tag{31}$$

The lower limit of integration is not allowed to become zero because the derivative of $Au(t-v)$ may become infinite if part of the response is instantaneous. This equation can be rewritten with zero as the lower limit provided the integrand is changed by subtraction of the initial response. The equation can be further rearranged by partial integration and a change in variables (i.e. $v = t - x$). For the case of periodic fields, i.e.

$$T(t-x) = T_0 \cos(\omega t - \omega x)$$

Equation (31) becomes

$$D(t) = \Lambda'(\omega)T_0 \cos \omega t + \Lambda''(\omega)T_0 \sin \omega t \tag{32}$$

In these equations the following substitutions were made:

$$\Lambda'(\omega) - \Lambda_\infty = \int_0^\infty B(t) \cos \omega t \, dt \tag{32a}$$

$$\Lambda''(\omega) = \int_0^\infty B(t) \sin \omega t \, dt \tag{32b}$$

$$B(t) = d[Au(t) - Au(0)]/dt \tag{32c}$$

$$\overline{A}u(t) = Au(t) - Au(0) \tag{32d}$$

$$\Lambda^*(\omega) = \Lambda'(\omega) - i\Lambda''(\omega) \tag{32e}$$

$$\Lambda'(0) = [Au(\infty)] = \Lambda_0 \tag{32f}$$

$$\Lambda'(\infty) = [Au(0)] = \Lambda_\infty \tag{32g}$$

We deduce from equations (32a) and (32b) that $\Lambda'(\omega) - \Lambda_\infty$ is an even function of ω while $\Lambda''(\omega)$ is an odd function or that $\overline{\Lambda'}(\omega) = \Lambda'(-\omega)$ and $\Lambda''(\omega) = -\Lambda''(-\omega)$ so that $\Lambda^*(\omega) = -\overline{\Lambda^*}(-\omega)$. Equations (32a) and (32b) have an inverse Fourier transform so that

$$B(t) = (2/\pi) \int_0^\infty [\Lambda'(\omega) - \Lambda_\infty] \cos \omega t \, d\omega \qquad (33a)$$

$$B(t) = (2/\pi) \int_0^\infty \Lambda''(\omega) \sin \omega t \, d\omega \qquad (33b)$$

Equations (32a) and (32b) may be added to yield the following equation

$$\Lambda^*(\omega) - \Lambda_\infty = \int_{-\infty}^{+\infty} B(t) \exp(-i\omega t) \, dt \qquad (34)$$

Equations (33a) and (33b) may be added to yield the following equation

$$B(t) = (1/2\pi) \int_{-\infty}^\infty [\Lambda^*(\omega) - \Lambda_\infty] \exp(i\omega t) \, d\omega \qquad (35)$$

The lower limits of integration can be extended from zero to minus infinity because $B(t) \equiv 0$ for $t < 0$ on the basis of causality. In other words no response can occur in anticipation of a stimulus. Finally it can be shown by a suitable combination of equations (32a) with (33b) or (32b) with (33a) that

$$\Lambda'(\omega) - \Lambda_\infty = (2/\pi)P \int_0^\infty \frac{\Lambda''(\omega)V \, dV}{V^2 - \omega^2}$$

$$\Lambda''(\omega) = (2/\pi)P \int_0^\infty \frac{[\Lambda'(\omega) - \Lambda_\infty]\omega \, dV}{\omega^2 - V^2} \qquad (36)$$

where $P \int_0^\infty$ represents the Cauchy principal value of the integral.

These results lead to two important findings. The first of these is that the in-phase and out-of-phase responses of the system come about because of a delayed response to a periodic stress field. Therefore, it is not necessary to postulate an internal viscosity to account for an out-of-phase component of the response. Any mechanism which delays the response of the system will give rise to a 'macroscopic' viscosity term. The second finding is that the real and imaginary parts of the response are not independent quantities but rather are closely related terms. Any knowledge of one response over the entire time scale uniquely determines the other response.

(D) *Molecular potential and elongation terms*

In this section we shall relate some aspect of molecular structure to the complex distortability $\Lambda^*(\omega)$ of the sphere. In order to meet this aim we need to discuss two important aspects of the problem. The first one is that some form of interaction potential is needed to describe the potential energy of the molecule in the stress field as a function of its position co-

ordinates. The second aspect is to assume some mechanism by which the changes in the shape of the spherical inclusion occur as the molecule orients to offset the effects of the stress field.

For the interaction potential we note that each bond in the molecule will experience a torque[31] tending to orient the polymer in the direction of the stress field. However, each bond cannot move independently of its surrounding bonds so that the orientation process must be a cooperative one. We assume that each of the bonds l_i (l_i represents the difference between the length and width of each bond) in the polymer chain may interact with the applied stress field σ in such a way that the potential energy of the interaction is given by $-\sigma z_i$, where z_i is the component of l_i in the direction of the stress field. In vector notation this becomes $-\boldsymbol{\sigma} \cdot \mathbf{l}_i$. Inasmuch as the neighbouring bonds will be rigidly connected to one another in the unit that orients, hereafter referred to as the segment, we may write for the potential energy of this segment in the stress field

$$\cdot V_s = -\boldsymbol{\sigma} \cdot \sum_{i=1}^{n} \mathbf{l}_i = -\boldsymbol{\sigma} \cdot \boldsymbol{\lambda}_s \qquad (37)$$

where n is the number of bonds $\mathbf{l}_i$ in the segment of the polymer chain. The quantity $\boldsymbol{\lambda}_s$ represents the asymmetry of the polymer segment. It can be seen from this quantity that for spherical segments or for cylindrical segments constrained to move about their long axis there is no potential energy of interaction, much like the equivalent dipole case.

The change in shape of the spherical inclusion is due to the orientation of the segment with the applied stress field. As this segment changes its direction with respect to the applied field its projection in the field direction also changes and is given by

$$\sum_{i=1}^{n} l_i \cos \theta_i = \sum_{i=1}^{n} \cos \theta_i = \lambda_s \cos \theta = \lambda_s(z) \qquad (38)$$

As this segment moves to alleviate the effects of the applied stress field, we shall assume that the average molecular packing about this segment does not change. In other words as the segment orients, elements of the polymer molecule must move out of its way while still other elements must move into the void left by the segment. So long as this orientation process continues without any change in the average packing about the segment in question, this process is an isometric one so that Poisson's ratio is one half.

It is of interest to note at this time that the model under consideration is amenable to the same analysis as used by Cole for dielectric relaxation. Two separate correlations or sets of interactions have been assumed although a single relaxation process is considered. The first correlation is between a single bond and its immediate surroundings to form what we have called a segment. The second correlation is between this segment and its surroundings. This latter set of interactions can give rise to a time-dependent correlation function which could make the orientation time dependent. Although it is possible to develop the analysis along the lines used by Cole at this point we shall proceed along simpler analytical lines because this leads to a much clearer physical picture.

(E) *Equilibrium deformation*†

The time dependent distortion of the sphere at equilibrium, exclusive of the instantaneous deformation, is related to its gross mechanical properties and the tensile field by the following variation of equation (29)

$$(9\mathbf{D}_0/2J_\infty) = \{(J_0 - J_\infty)(J_0 + \tfrac{2}{3}J_\infty)\}\mathbf{T}_0 \tag{39}$$

The problem on hand is to relate $\mathbf{D}_0$ in terms of the asymmetry $\lambda_s(z)$, the tensile field $\mathbf{T}_0$ and the potential energy of interaction V_s. These quantities are related by classical statistical mechanics[32] in the form

$$D_0 = \int \int f(p, q, \mathbf{T}_0) D_z(q) \, dp \, dq \tag{40}$$

where p and q are the conjugate moments and coordinates of the segment, so that $f(p, q, \mathbf{T}_0) \, dp \, dq$ is the equilibrium distribution function of the segments and $D_z(q)$ represents the sum of the z components of the individual segments. The equilibrium distribution function is proportional to

$$f(p, q, \mathbf{T}_0) \approx \exp\left[-H(p, q, \mathbf{T}_0)/kT\right] \tag{41}$$

where H is the Hamiltonian of the system and is given by

$$H(p, q, \mathbf{T}_0) = H^0(p, q) - D_z(z, q)T_0 \tag{42}$$

The quantity $H^0(p, q)$ is the unperturbed Hamiltonian of the system in the absence of external fields while the second term in equation (42) represents the interaction energy of the segment with the field. Inasmuch as we are concerned only with weak tensile fields, the perturbing term may be made arbitrarily small so that

$$f(p, q, \mathbf{T}_0) = f^0(p, q)[1 + (T_0/kT)D_z(q)] \tag{43}$$

where $f^0(p, q)$ is the unperturbed distribution function of the system.

The equation for the equilibrium deformation becomes

$$D_0 = \langle D_z \rangle_0 + (T_0/kT)\langle D_z^2(q) \rangle_0 \tag{44}$$

where the angle brackets $\langle\ \rangle_0$ indicate an averaging using $f^0(p, q)$ as a weighting factor. The quantity $\langle D_z \rangle_0$ vanishes because for the present case there is no net deformation in the absence of any external field. The term $\langle D_z^2 \rangle_0$ may be written as

$$\langle D_z^2 \rangle_0 = \tfrac{1}{3}\langle \mathbf{D}\cdot\mathbf{D} \rangle_0 = \tfrac{1}{3}\langle \sum_{i,y}^{N_0, N_0} \lambda i \cdot \lambda y \rangle_0 \tag{45}$$

If we combine this equation with equations (39) and (44) we have

$$\frac{J_0 - J_\infty}{J_0 + \tfrac{2}{3}J_\infty} = \frac{3}{2kT\,J_\infty}\langle \sum_{i,y}^{N_0, N_0} \lambda i \cdot \lambda y \rangle_0 \tag{46}$$

This equation, which is of fundamental importance to the present work, relates the gross equilibrium compliance of the medium in terms of shape asymmetry of the segments that move to alleviate the effects of the applied field. This equation can be simplified one step further if we assume no

---

†As in the previous section, this discussion is an adoption of Dielectric Theory, see particularly Chapter 11 of ref. 6.

correlation between segments. Under these circumstances we have

$$(J_0 - J_\infty)/(J_0 + \tfrac{2}{3}J_\infty) = (3N_0/2kTJ_\infty)\lambda^2 \tag{47}$$

because

$$\lambda i \cdot \lambda y = 0 \text{ for } i \neq y \tag{47a}$$

and

$$\lambda i \cdot \lambda y = \lambda^2 \text{ for } i = y \tag{47b}$$

(F) *Decay of the deformation*†

Thus far the equilibrium deformation of the sphere has been related to the shape asymmetry of the segments with a simple non-periodic stress field applied to the system. Now consider the case when the stress field is suddenly removed. Under these conditions there will be an excessive number of segments (partially) pointing in the z direction. The problem is to relate the decay of the deformation with time to the change in the number of segments with time. In other words assume that the new equilibrium comes about because the segments move from one position to another and this process is controlled by the number of segments that can move per unit time. On these grounds equation (47) may be written as

$$\frac{J(t) - J_\infty}{J(t) + \tfrac{2}{3}J_\infty} = \frac{3\lambda^2}{2kT J_\infty} \ N_0(t) \tag{48}$$

When the stress field is suddenly removed, these N_0 (at $t=0$) segments cannot move instantaneously, there being a probability that only a certain number of segments can move in any time interval dt. Suppose that one of these segments has an orientation θ,φ. The probability that it will move to a new position θ',φ' with a solid angle $d\Omega'$ in the interval of time dt is given by

$$k(\theta,\varphi, \longrightarrow \theta',\varphi') \ dt \ d\Omega' \tag{49}$$

The number of such segments having an orientation θ,φ in $d\Omega$ is given by

$$N(\theta,\varphi,t) \ d\Omega \tag{50}$$

The function N is normalized such that

$$N_0(t) = \int N(\theta,\varphi,t) \ d\Omega \tag{51}$$

Inspection of the rates of decay for a large number of polymer systems shows that this process is very strongly temperature dependent. This observation may be interpreted to mean that the transition probability k is governed by the rate at which these segments may be thermally activated. That is, the rate of reorientation is proportional to the Boltzmann factor $\exp(-E/kT)$, where E is the energy that must be supplied for the segments to overcome the surrounding interactions which hold them in one position and re-establish themselves in another position. For many polymeric dispersions, these activation energies are of the order of 50 kcal so that E must be of the order of 100 kT. This fact indicates that the segments cannot

---

† As in the previous cases, this section is an adoption of dielectric theory. In particular see ref. 33.

change their position continuously but rather as a series of sudden jumps. The transition probability $k(\theta,\varphi \longrightarrow \theta',\varphi')$ dt dΩ', may then be regarded as the probability that a jump will occur in an interval of time dt resulting in the indicated change of orientation.

The total number of segments in a solid angle dΩ about θ,φ which leave that direction in an interval dt will be

$$A \, \mathrm{d}\Omega \, \mathrm{d}t = \int_{\Omega'} N(\theta,\varphi,t) \, k(\theta,\varphi \longrightarrow \theta',\varphi') \, \mathrm{d}\Omega \, \mathrm{d}\Omega \, \mathrm{d}t \tag{52}$$

where the integration is over Ω', the directions into which the segments jump. Similarly, the number of segments entering the same solid angle dΩ from the other directions will be

$$A \, \mathrm{d}\Omega \, \mathrm{d}t = \int_{\Omega'} N(\theta',\varphi't) \, k(\theta',\varphi' \longrightarrow \theta,\varphi) \, \mathrm{d}\Omega' \, \mathrm{d}\Omega \, \mathrm{d}t \tag{53}$$

The net rate of change in the probability function N is

$$\mathrm{d}N(\theta,\varphi,t) \, \mathrm{d}\Omega / \mathrm{d}t = (B - A) \, \mathrm{d}\Omega = \int_{\Omega'} [N(\theta',\varphi',t) \, k(\theta',\varphi' \longrightarrow \theta,\varphi)$$
$$- N(\theta,\varphi,t) \, k(\theta,\varphi \longrightarrow \theta',\varphi')] \, \mathrm{d}\Omega' \, \mathrm{d}\Omega \tag{54}$$

If the integration is over all space the total number of segments leaving their positions in order to establish the new equilibrium is therefore

$$\mathrm{d}N_0(t) / \mathrm{d}t = \int_{\Omega} \int_{\Omega'} [N(\theta',\varphi',t) \, k(\theta',\varphi' \longrightarrow \theta,\varphi)$$
$$- N(\theta,\varphi,t) \, k(\theta,\varphi \longrightarrow \theta',\varphi')] \, \mathrm{d}\Omega \, \mathrm{d}\Omega' \tag{55}$$

These equations may be further simplified not only by assuming that k is independent of the direction of jump, but that there is only one size of jump. Under these conditions we have

$$\mathrm{d}N_0(t) / \mathrm{d}t = - k_0 N_0(t) \tag{56}$$

because

$$k_0 \int_{\Omega'} N(\theta',\varphi',t) \, \mathrm{d}\Omega' = 0 \tag{57}$$

otherwise there would be a build-up in the deformation with time due to the fact that some jumps would tend to maintain the original deformation. This differential equation leads to

$$N_0(t) = N_0 e^{-k_0 t} \tag{58}$$

Combining this with equation (48) leads to

$$\frac{J(t) - J_\infty}{J(t) + \frac{2}{3} J_\infty} = \frac{3\lambda^2}{2kT \, J_\infty} \, N_0 e^{-k_0 t} \tag{59}$$

At $t = 0$, the exponent in equation (59) is unity so that the deformation of the sphere is given by the equilibrium equation as required. As t increases the term $\exp(-k_0 t)$ becomes smaller so that the deformation becomes smaller. In fact the decay in the deformation is exponential with time. Finally as t becomes very large the exponent approaches zero so that the deformation approaches zero.

VI. DISCUSSION

The present relaxation function, although not theoretically justified, has one single important feature. It represents the relaxation behaviour of twenty polymers either as the complex dielectric constant or as the complex polarization. The relaxation behaviour of small organic or inorganic molecules which may be represented as a skewed semi-circle or as a circular arc may be added to this list of polymers because these are limiting forms of the present relaxation function. This list of materials becomes larger because at least in four cases the mechanical relaxation behaviour may be represented by this function. Although the relaxation function is empirical, the number of systems whose relaxation behaviour may be represented is large and for that reason the function has meaning.

The procedure outlined in Appendix B to determine the temperature dependences of the dispersion parameters is similar to the procedure referred to as the TTSM with a single important exception. In both methods a knowledge of ϵ_0 and ϵ_∞ are required at temperatures where direct determinations are not possible. For this reason extrapolations must be used. The differences in the two methods are their basic assumptions. In the TTSM, the shape of the normalized relaxation mechanism is assumed to be independent of temperature, a behaviour that has little experimental support (*Figure 8*), although one that may be argued from simple molecular theory[34]. In the present method an empirical relaxation function is assumed which has no theoretical verification but one that can represent experimental data accurately and, therefore, can represent the variation of the normalized loss curve with temperature.

Mead and Fuoss[16] considered the shape of the relaxation process for the acetates when viewed in a complex plane and postulated three possible interpretations: an unsymmetrical relaxation process, simultaneous presence of two dispersions, or a distribution parameter which is a function of time. Although it must be admitted that the skewed behaviour observed in poly(vinyl acetate) can be represented as the sum of two symmetrical dispersions as was done for the polycarbonate[4], we believe the simplest interpretation is to represent this process as a single mechanism using the proposed relaxation function. Although their third mechanism is feasible, we believe that this interpretation leads to an unnecessary complication of the picture.

Mead and Fuoss[16] compared the square of the refractive index (n^2) to ϵ_∞, actually one should make some allowance for atomic polarization. If a nominal five per cent of n is allowed to represent this contribution then one calculates a value for ϵ_∞ as 2·38, which agrees quite well with the experimental value at 100°C. It is possible that the deviations observed at lower temperatures could come about from one per cent or less water as an impurity.

Mead and Fuoss[16] interpreted the breadth of the dispersion in poly(vinyl acetate) to be due to the flexible linkage connecting the side chain dipole moment to the main chain. Based on the results obtained in this paper it is seen that the breadth of the dispersion is due in part to the method of representation. The polarization parameters for poly(vinyl acetate) are

similar to the dispersion parameters used to describe the polycarbonate where the dipole is part of the backbone of the polymer chain. These authors interpreted the side chain motion to be independent of the polymer chain conformation. Ferry *et al.*[26] have shown that the electrical and mechanical shift factors for this polymer are the same. In addition we have shown that the initial response of the system to the mechanical stress field is the same as the response to the electrical field because the dispersion parameters are so much alike. Inasmuch as this response must involve the polymer backbone because of the large value of the compliance associated with this process then independent side chain rotation is not a suitable mechanism for this response. There is no doubt, based on the large value of the dielectric constant, that the side chain is involved with this mechanism but the motion of the side chain must be rigidly coupled through the backbone in an unknown fashion. In other words the segment that moves to offset the effects of either a mechanical or an electrical stress field must involve several monomer units rigidly coupled together.

By analogy with dielectric theory it is possible to construct a set of transformation equations for mechanical dispersions. These transformation equations were used to transform experimental values of the complex compliance to the complex deformation. The locus in a complex plane for $\delta^*(\omega)$ is very similar to the corresponding complex dielectric dispersion. The comparison of dispersion parameters must be taken as being qualitative at this point because the mechanical and electrical measurements were not made on the same polymer. Calculated values of $\delta^*(\omega)$ from the dispersion parameters and equations were in agreement with transformed values to the same extent as is the band that is almost always associated with the shifted values. In other words the reliability of representing $\delta^*(\omega)$ by equation (22) is the same as that of the band associated with the shifted values. Clearly, what needs to be done is to evaluate the dispersion parameters for measurements made on the same polymer. The systems studied by Strella and Zand[35], who measured dielectric properties of some polymers, and by Child Jr and Ferry[36], who measured the complex compliance of the same polymer, provide such an opportunity. Such a comparison is presently under way and preliminary results indicate the mechanisms to be the same.

At very low frequencies significant deviations from the assumed behaviour were observed. In two of these [poly(*n*-octyl methacrylate) and polyisobutylene] the deviations were in terms of another lower frequency dispersion. In the other two polymers [poly(vinyl acetate) and poly(methyl acrylate)] the deviations could be interpreted in terms of another lower frequency relaxation process. In the latter two systems it is not known whether the actual behaviour is as observed or whether two overlapping dispersions actually exist. The initial response of the polymer to the stress field is virtually the same as it is to the electric field. Otherwise the three time parameters, α, β and τ_0 would not be so similar. This means that the initial response of the polymer to the applied field must be a segmental orientation mechanism or there would be no net polarization and the dielectric constant associated with the dielectric dispersion would be zero. Later on the deformation of the polymeric systems may be due to segmental

199

translations where there would be no equivalent low frequency dielectric process. This assessment of the deforming mechanism is identical with what has been proposed by Tobolsky and Aklonis[37] for the stress relaxation behaviour of polyisobutylene. In this work we are extending their deformation mechanism (segmental orientation followed by segmental translation) to three more polymers.

Three experimental facts described in the previous sections appear to support Scaife's[5] theoretical contentions, i.e. that one ought to compare complex polarization data rather than complex dielectric constant data for different systems. The strongest of these arguments comes from the analogy of dielectric and mechanical dispersions. It should be pointed out that although one is tempted to compare the time dependent polarization and deformation responses of a unit sphere suspended in a medium whose response is instantaneous, an equally good analogy would have been made by comparing $\delta^*(\omega)$ with $\epsilon^*(\omega)$. At this point the data are not sufficient to prove which is the better correlation. What needs to be done is to make comparisons of dielectric and mechanical data obtained on polymers with large dielectric constants to maximize the differences between the constants used to represent $\epsilon^*(\omega)$ and $\rho^*(\omega)$ data.

The second piece of evidence, which was acually considered by Scaife, is that the relaxation behaviour of glycerol is simpler in the $\rho^*(\omega)$ case. In the $\epsilon^*(\omega)$ case deviations from assumed behaviour were interpreted in terms of another dispersion, an interpretation which is consistent with the behaviour of other alcohols. In the $\rho^*(\omega)$ case there are no deviations so that the dispersion appears to be dependent on the method of representation. At this point one could argue that either the existence of a dispersion ought to be independent of the method of representation or that the data ought to be represented in such a way as to exaggerate these deviations.

Finally the behaviour of $\epsilon^*(\omega)$ for the two acetates is not at all typical of polymers. The normalized loss maximum is independent of temperature while for other systems this quantity depends strongly on temperature. Furthermore the temperature dependences of $1-\alpha$ and β for the two acetates are in opposite senses leaving one with the interpretation that the distribution of relaxation times is becoming narrower, at times longer, than τ_0 while becoming broader, at times shorter, than τ_0 as the temperature decreases. The complex polarization parameters, as well as the reduced loss maximum, depend on temperature in a way that is similar to eleven other polymers. One could argue that the complex dielectric constant is the better representation because the behaviour of the two acetates becomes almost an ideal example of the TTSM. However, we believe that representation of data as $\rho^*(\omega)$ systematizes the behaviour of polymers.

If one can rightfully conclude that one ought to compare dispersion data in terms of the complex polarization rather than the complex dielectric constant, then one is left with some radically different conclusions concerning mechanical data. The dispersion parameters used to represent the dielectric behaviour of the polycarbonate, poly(vinyl acetate) and glycerol are very similar. This observation may be interpreted to mean that the mechanism of the three relaxation processes must be the same or at least

very similar. The significant difference is that their respective temperatures are about 200 degrees apart. However, in these three systems there is an example of a polymer with the dipole group in the backbone, another polymer with the dipole group on the side chain and finally a hydrogen bonded liquid which is, of course, not a polymer at all. Add to this, the fact that, initially at least, the dielectric and mechanical dispersions of poly(vinyl acetate) are one in the same dynamic process. The correlation would be even more astounding if the deviations from assumed behaviour at long times are due to a varying Poisson's ratio. If this were so, then the two mechanisms might be the same over the entire ωa_T scale. At any rate, the correlations observed so far lead one to question precisely what is the role of chain statistics in polymeric dispersion? Although one might be tempted to postulate a polymer-like structure for glycerol due to the hydrogen bonding at low temperature, the recent results of Denney and Ring[38] refute this hypothesis. In that work they studied the dielectric relaxation behaviour of mixtures of i-amyl bromide and 2-methylpentane. The shapes of their relaxation curves are very similar to the present ones. Inasmuch as hydrogen bonding to form chains would be absent from that system, then a chainlike structure with normal modes of vibration need not be the mechanism giving rise to broad dispersions.

In a paper by Ferry, Williams and Fitzgerald[20], the point was made that dielectric data ought to be interpreted in terms of polymer viscoelastic theory. We wish to take exception to that statement for the following reasons.

First of all, methods have existed for representing dielectric relaxation data in terms of simple empirical expressions containing one or two parameters. This means that large quantities of data can be represented in terms of a few parameters and comparative studies be put on a quantitative basis. No such technique exists for mechanical dispersions and for this reason one of the most basic assumptions to the TTSM has never been thoroughly experimentally studied.

Another point is that the shape of the dielectric specimen under theoretical consideration must be a sphere, as pointed out by VanVleck[39] in 1932. Inasmuch as many of the materials under consideration for mechanical studies are polar, one would expect analogous arguments to exist for any mechanical model. In fact, this point we believe to be amply demonstrated in the present work.

In addition, Kirkwood has shown[21] in 1938 that the unit that equilibrates with the electric field is seldom the single dipole unit but rather one has to take into account the dipole moment originating from discrete local structure. No such sophistication exists in viscoelasticity theory, the mechanical theory is equivalent to a simple dielectric theory because correlations in time and space are neglected. This point is very important because this simple mechanical theory is used to reduce mechanical dispersion data.

Furthermore, the delayed response in the mechanical behaviour is assumed to arise from a local viscosity. The concept of a local viscosity to impede the movement of a polymer chain has been widely studied by a number of people[3]. The usual model for deformation is a treatment of the

normal modes of vibration of a polymer chain which is impeded by a local viscosity. The viscosity acting to damp the made of vibration is proportional to segment length. At best this concept is an artefact. Macroscopically a viscosity, or rather a dissipation of energy, is observed but on a microscopic level molecules simply do not rub together to dissipate energy.

Finally, and perhaps most importantly, the recent work of Cole[25] is a generalization of dielectric behaviour which does not have any parallel in mechanical theory. In that work he was able to combine the nature of broad dispersion and the dissipation of energy in terms of a time dependent correlation function. In addition, the equilibrium behaviour of his model converges to that of Kirkwood which takes into account specific short range correlations.

Based on these reasons, we believe that a mechanical analogue of recent dielectric theory should be the starting point for a mechanical model rather than the other way round. We start by considering a spherical inclusion containing the sample in an otherwise continuous elastic medium. We know that as the individual polar groups undergo their random gyrations, the effects of their fields will be cancelled out for every point inside that sphere except for the small number of systems along the boundary[40]. Since we are considering the surrounding medium to be continuous and structureless, there is no adverse contribution to the field inside the sphere. Under these conditions the tensile field, when applied to the inclusion, truly acts as a perturbation term. Under these conditions the Hamiltonian of the system can be written as the equilibrium term plus an interaction potential term similar to equation (42). Based on the analogy between the two dispersions observed so far, one would expect that if one followed the arguments of Cole one would obtain a set of mechanical equations similar to his dielectric equations [equation (17)]. Presumably one would obtain the complex distortion of the sphere as the sum of two terms. The first of these would be the instantaneous distortion while the second would contain the time dependent distortion terms. Furthermore, it would appear that the form of the second term would be similar to the dielectric expression in that it would contain the equilibrium distortion containing all equilibrium corre-lations which is modified by a time dependent correlation function which describes the interaction of the moving species with its environment. In other words, it would seem possible to obtain an expression which contains a macroscopic dissipation term (viscosity) without the assumption of a local viscosity in addition to having a broad dispersion without the assump-tion of a distribution of relaxation times. Before this analysis is possible a number of technical problems must be solved.

A study of the molecular model for mechanical properties described in the preceding paragraph was initiated but not completed. In some cases a simple, perhaps even a primitive, solution to the problem was discussed. Although incomplete and simple the solutions obtained to the problem have several important facets. First of all, the empirical equation (21) was shown nearly to represent the complex distortability of a unit sphere in a con-tinuous homogeneous medium when Poisson's ratios for both media are one-half [equation (29)]. The difference between the two equations is a

numerical constant in the denominator of one of the terms. Inasmuch as J_∞ is not precisely known and Poisson's ratio is not one-half in the glass phase then these factors may tend to compensate for each other so that equation (21) may be very nearly correct. An alternative interpretation of the deviations from assumed behaviour [*Figure 15*(a)] is that Poisson's ratio is variable throughout the experiment. In other words, at low temperatures (or large ωa_T) Poisson's ratio might be approximately 0·35 while at high temperatures (or low ωa_T) the ratio might be 0·50. The transition from glass to rubberlike behaviour involves a change in Poisson's ratio which might be spread out over several decades of time and compliance.

The second step in the study of the proposed model, which is soundly based, was to show that if one is concerned with time dependent systems then for a periodic tensile field one will always observe an in-phase (elastic) and an out-of-phase (dissipative) response. In other words, a necessary and sufficient condition for the dissipation of energy and hence the observation of a macroscopic viscosity is to assume the system to be time dependent in its approach to equilibrium.

The third step in this study is to postulate a potential energy of interaction for one of the polymer bonds in the tensile field as well as to describe the elongation of the specimen in terms of bond orientation. Once these quantities are defined they are immediately related to the average distortion of the sphere by means of classical statistical mechanics, i.e. equation (46) which is exact. In the event that no correlations between segments are assumed then the averaging becomes simple and the distortability of the sphere is proportional to the square of the shape asymmetry of the segments, i.e. equation (47). The dielectric counterpart of this derivation is Debye's theory which relates the polarizability of the sphere to the square of the dipole moment which is, of course, a measure of the electrical asymmetry. This is a very important result because it shows that the distortability of the sphere is directly related to the shape of the segment of the polymer chain.

However, this result, like Debye's, has an anomalous temperature dependence of the distortability with temperature. From equation (47) we see that although the LHS cannot exceed unity the RHS can increase without limit. This conclusion is obviously wrong and probably for the same reason that Debye's theory is wrong. The averaging cannot be treated by assuming there is no correlation between the segments. In the dielectric case both Onsager and Kirkwood (see ref. 6) were able to show the existence of a depolarization term which demutes the effects of the dipole moment. Such a factor must be acting in the present case for the following reasons. In the construction of the asymmetry of the orienting unit all of the bonds in the segment were taken to be equal. Consider a polymer such as poly(vinyl acetate) and ignore the C—H bonds. The remaining bonds, which are C—C, C—O and C=O are probably similar with respect to their shape, but one important feature was ignored, namely the dipole moment associated with the C=O group. In other words, allowance was made for an orientation of the segments in such a way that the effects of oriented dipoles were ignored. Inasmuch as the dipole moment is rigidly

attached to the carbonyl group and it is incorporated into the segment, then one must take into account the effects of long-range couplings at equilibrium. If this effect were taken into account equation (47) might be modified by a term which demutes the effects of the shape asymmetry of the orienting segment.

The last step in the analysis of this model was to investigate the decay in the distortion of the sphere after removal of the tensile field. In this case the number of segments that could move to eliminate the distortion was considered to depend on time. The transition probabilities were treated as a rate process, i.e. equilibrium positions were separated by an energy barrier. Under these conditions the initial distortion decayed exponentially with time after removal of the stress field. Assumption of N to be dependent on time had the effect of a simple time dependent correlation function. In other words, a viscous response was obtained without postulating a local viscosity. The advantage of treating the transition probability as a rate process is that it is exponentially related to temperature while at constant temperature the rate is a function of stress. This latter feature may serve as a basis for interpreting non-linear behaviour in polymers, particularly the results of Payne[41].

VII. CONCLUSIONS

We wish to conclude this work by making the following statements. Mechanical and dielectric dispersions are analogous mechanisms when appropriately normalized. These processes may be identical if studies were conducted on the same polymers and a variable Poisson's ratio is taken into account. In addition, both relaxation mechanisms can be represented by the proposed relaxation function. These correlations suggest that the mechanical properties of a sphere should be investigated in a way that is similar to the methods used in current dielectric theory. In addition it is not necessary to postulate a monomer friction coefficient in order to describe macroscopic viscous behaviour.

Finally, before any development of polymeric viscoelastic behaviour of dilute solutions can be extended to the bulk behaviour of polymers the following information is of utmost importance. First, a quantitative comparative study of the dielectric behaviour of polymers and small organic molecules is needed to ascertain the extent of similarity between these dispersions. Any differences, if they should exist, would then be attributed to chain statistics while the similarities would have to be attributed to discrete local structures similar to those of small organic molecules. Secondly a quantitative comparative study of the dielectric and mechanical behaviour, including the variation of Poisson's ratio with stress or strain, is needed to determine to what extent segmental orientation of local three-dimensional structures can account for the viscoelastic dispersions observed in the bulk phase of polymers in the vicinity of their glass transition temperature. Any differences between dielectric and mechanical dispersions would be due to segmental translation effects as well as chain statistics.

and especially to Professor J. D. Ferry who supplied them with much of the viscoelastic data as well as reduced dielectric data.

Rohm and Haas Company,
  Research Laboratories,
    Bristol, Pa.

REFERENCES

1 COLE, K. S. and COLE, R. H. *J. phys. Chem.* 1941, **9**, 341
2 COLE, R. H. *J. phys. Chem.* 1955, **23**, 493
3 FERRY, J. D. *Viscoelastic Properties of Polymers.* Wiley: New York, 1961
4 HAVRILIAK, Jr, S. and NEGAMI, S. *J. Polym. Sci.,* Part C, 1966, No. 14, 99
5 SCAIFE, B. K. P. *Proc. phys. Soc., Lond.* 1963, **81**, 124
6 FRÖHLICH, H. *Theory of Dielectrics.* Clarendon Press: Oxford, 1958
7 MOPSIK, F. I. *Ph.D. Thesis.* Brown University, 1964
8 FANG, P. H. *J. chem. Phys.* 1965, **42**, 3411
9 ISHIDA, Y. and YAMAFUGI, K. *Kolloidzschr.* 1961, **177**, 7
10 CURTIS, H. *SPE Trans.* 1962, **2**, 82
11 BUR, A. J. *Ph.D. Thesis.* Pennsylvania State University, 1962
12 STRELLA, S. and CHINAI, S. N. *J. Polym. Sci.* 1958, **31**, 45
13 MATSUO, M., ISHIDA, Y., YAMATUJI, K., TAKAYANAGI, M. and IRIE, F. *Kolloidzschr.* 1965, **201**, 89
14 FUNT, B. L. and SUTHERLAND, T. H. *Canad. J. Chem.* 1952, **30**, 940
15 REYNOLDS, S. I., THOMAS, U. G. and FUOSS, R. M. *J. Amer. chem. Soc.* 1951, **73**, 3716
16 MEAD, D. J. and FUOSS, R. M. *J. Amer. chem. Soc.* 1941, **63**, 2832
17 DAVIDSON, D. W. and COLE, R. H. *J. chem. Phys.* 1951, **19**, 1484
18 WILLIAMS, M. L. and FERRY, J. D. *J. Polym. Sci.* 1953, **11**, 169
19 FERRY, J. D. and STRELLA, S. *J. Colloid Sci.* 1958, **13**, 459
20 FERRY, J. D., WILLIAMS, M. L. and FITZGERALD, E. R. *J. phys. Chem.* 1955, **59**, 403
21 KIRKWOOD, J. G. *J. chem. Phys.* 1939, **7**, 911
22 KAUZMANN, W. *Rev. mod. Phys.* 1942, **14**, 12
23 GROSS, B. *Mathematical Structure of the Theories of Viscoelasticity.* Hermann: Paris, 1953
24 SCAIFE, B. K. P. *Progress in Dielectrics.* Heywood: London, 1963
25 COLE, R. H. *J. chem. Phys.* 1965, **42**, 637
26 WILLIAMS, M. L. and FERRY, J. D. *J. Colloid Sci.* 1954, **9**, 478
27 BÖTTCHER, C. J. F. *Theory of Electric Polarization.* Elsevier: New York, 1952
28 WILLIAMS, M. L. and FERRY, J. D. *J. Colloid Sci.* 1955, **10**, 474
29 LOVE, A. E. A. *A Treatise on the Mathematical Theory of Elasticity.* Dover: New York, 1944
30 UEMURA, S. and TAKAYANAGI, M. *J. appl. Polym. Sci.* 1966, **10**, 113
31 FLORY, P. J. *Principles of Polymer Chemistry.* Cornell University Press: Ithaca, N.Y., 1953
32 TOLMAN, R. C. *The Principles of Statistical Mechanics.* Oxford University Press: London, 1938
33 KAUZMANN, W. *Rev. mod. Phys.* 1942, **14**, 12
34 FERRY, J. D. and STRELLA, S. *J. Colloid. Sci.* 1958, **13**, 459
35 STRELLA, S. and ZAND, R. *J. Polym. Sci.* 1957, **25**, 97
36 CHILD, Jr, W. C. and FERRY, J. D. *J. Colloid Sci.* 1957, **12**, 389
37 TOBOLSKY, A. V. and AKLONIS, J. J. *J. phys. Chem.* 1964, **68**, 1970
38 DENNEY, D. J. and RING, J. W. *J. chem. Phys.* 1966, **44**, 4621
39 VANVLECK, J. H. *Theory of Electric and Magnetic Susceptibilities.* Clarendon: Oxford, 1932
40 COLE, R. H. *Progress in Dielectrics.* Wiley: New York, 1961
41 PAYNE, A. R. *J. appl. Polym. Sci.* 1965, **8**, 2661

APPENDIX A

Successive applications of DeMoivre's theorem to equation (1) followed by separation of real and imaginary parts leads to the following equations:

$$\epsilon'(\omega) - \epsilon_\infty = r^{-\beta/2}(\epsilon_0 - \epsilon_\infty) \cos \beta\theta \tag{60}$$

$$\epsilon''(\omega) = r^{-\beta/2}(\epsilon_0 - \epsilon_\infty) \sin \theta\beta \tag{61}$$

$$r = \{1 + (\omega\tau_0)^{(1-\alpha)} \sin \alpha\pi/2\}^2 + \{(\omega\tau_0)^{(1-\alpha)} \cos \alpha\pi/2\}^2 \tag{62}$$

$$\theta = \arctan \frac{(\omega\tau_0)^{(1-\alpha)} \cos \alpha\pi/2}{1 + (\omega\tau_0)^{(1-\alpha)} \sin \alpha\pi/2} \tag{63}$$

If one substitutes zero for α, Cole's skewed semi-circle equations are obtained while if unity is substituted for β Cole's circular arc equations are obtained. At this point it is convenient to substitute numerical values for the parameters α, β, ϵ_0 and ϵ_∞ and calculate $\epsilon^*(\omega)$ for a range of $\omega\tau_0$s. The results of this numerical computation are recorded in *Figure 23*.
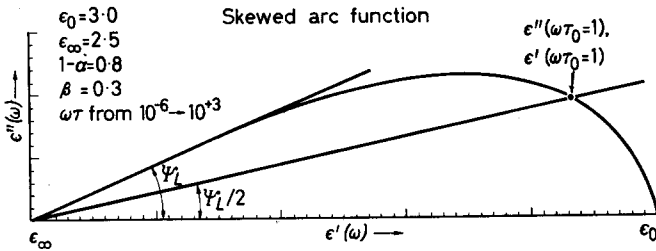
Figure 23—Complex dielectric constant calculated for a range of $\omega\tau$ and the parameters listed above using equations (60) to (63)

The graphical significance of ϵ_0 is obtained by examining the four equations under the conditions of $\omega\tau_0 \longrightarrow 0$. Under these conditions $\tan \theta \longrightarrow 0$, so that $\beta\theta \longrightarrow 0$, at the same time $r \longrightarrow 1$, so that $\epsilon^*(\omega\tau_0 \longrightarrow 0) \longrightarrow \epsilon_0$ because $\sin \beta\theta \longrightarrow 0$. The graphical significance of ϵ_∞ is obtained by examining the four equations as $\omega\tau_0 \longrightarrow \infty$. Under these conditions r increases without limit so that $r^{-\beta/2} \longrightarrow 0$. Therefore $\epsilon''(\omega) \longrightarrow 0$ and $\epsilon^*(\omega\tau_0 \longrightarrow \infty) \longrightarrow \epsilon_\infty$. In words the high and low frequency intercepts of the locus with the real axis are ϵ_∞ and ϵ_0, respectively.

The limiting angle (φ_L) that the high frequency locus makes with the real axis relates α and β. From *Figure 23* we note that the angle φ from ϵ_∞ to any point $\epsilon^*(\omega)$ is given by

$$\tan \varphi = \epsilon''(\omega) / \{\epsilon'(\omega) - \epsilon_\infty\} = \tan \beta\theta$$

so that $\varphi = \beta\theta$. Substituting this definition of θ into equation (63) we have, when $\omega\tau_0 \gg 1$,

$$\tan (\varphi_L/\beta) = \cot (\alpha\pi/2) \tag{64}$$

so that $\varphi_L = (1 - \alpha)\beta\pi/2$.

If we define the relaxation time as the condition $\omega\tau_0 \equiv 1$, and introduce

it into equations (62) and (63) which are then substituted into equations (60) and (61), we have, after taking the ratio of equations (61) and (60),

$$\frac{\epsilon''_{(\omega\tau_0=1)}}{\epsilon'_{(\omega\tau_0=1)} - \epsilon_\infty} = \tan \gamma = \tan \beta \left[\arctan \left\{ \frac{\cos \alpha\pi/2}{1 + \sin \alpha\pi/2} \right\} \right]$$

For this equality to be true it can be shown that $\gamma = \varphi_L/2$. In words the angle bisector of φ_L from ϵ_∞ intersects the locus at τ_0.

The parameter α is given by taking the length R of the line from ϵ_0 to $\epsilon^*_{(\omega\tau_0=1)}$ to be given by

$$R = [\epsilon''^2(\omega\tau_0 = 1) + \{\epsilon'(\omega\tau_0 = 1) - \epsilon_\infty)^2\}]^{\frac{1}{2}}$$

which can be reduced after taking logarithms to

$$\frac{1}{\varphi_L} \log \frac{R}{\Delta\epsilon} = -\frac{1}{\pi(1 - \alpha)} \log (2 + 2 \sin \alpha\pi/2) \qquad (65)$$

This expression is used to calculate α by measuring R, $\Delta\epsilon$ and φ_L. The numerical relationship between the LHS of equation (65) and α is given in *Table 4*.

Table 4. Numerical values of α calculated from the RHS of equation (65)

α	$\frac{1}{\varphi_L} \log \left(\frac{R}{\Delta\epsilon} \right)$	α	$\frac{1}{\varphi_L} \log \left(\frac{R}{\Delta\epsilon} \right)$	α	$\frac{1}{\varphi_L} \log \left(\frac{R}{\Delta\epsilon} \right)$
1	—	0·70	0·0107	0·20	0·00290
0·96	0·0835	0·60	0·00776	0·16	0·00263
0·94	0·0557	0·50	0·00593	0·13	0·00243
0·92	0·0417	0·40	0·00462	0·10	0·00224
0·90	0·0332	0·30	0·00368	0·06	0·00201
0·80	0·0164	0·25	0·00327	0·03	0·00184

The condition for which frequency (ω), $\epsilon''(\omega)$ becomes a maximum either in a complex plane plot or in an $\epsilon''(\omega)$ versus $\log \omega$ diagram is given by

$$\partial\epsilon''(\omega)/\partial\omega = 0$$

Evaluation of this derivative using equations 61, 62 and 63 leads to

$$\beta \arctan \left\{ \frac{(\omega\tau_0)^{(1-\alpha)} \cos \alpha\pi/2}{1 + (\omega\tau_0)^{(1-\alpha)} \sin \alpha\pi/2} \right\} = \arctan \frac{1}{\beta} \left\{ \frac{\cos \alpha\pi/2}{1 + (\omega\tau_0)^{(1-\alpha)} \sin \alpha\pi/2} \right\}$$

In general this equality is not true for $\omega\tau_0 = 1$ except for the particular case of $\beta = 1$ where the equation becomes

$$\arctan \left\{ \frac{\cos \alpha\pi/2}{1 + \sin \alpha\pi/2} \right\} = \arctan \left\{ \frac{\cos \alpha\pi/2}{1 + \sin \alpha\pi/2} \right\} \quad \text{for } \omega\tau_0 = 1$$

which is of course true for all values of α. In words the frequency at which the loss becomes a maximum is not the relaxation time except for the particular case of $\beta = 1$ (i.e. the circular arc). In fact the frequency at which the loss becomes a maximum is not simply related to the relaxation time but rather dependent on explicit values of α and β.

Poly(carbonate of bisphenol)
$T = 164 \cdot 0$ °C
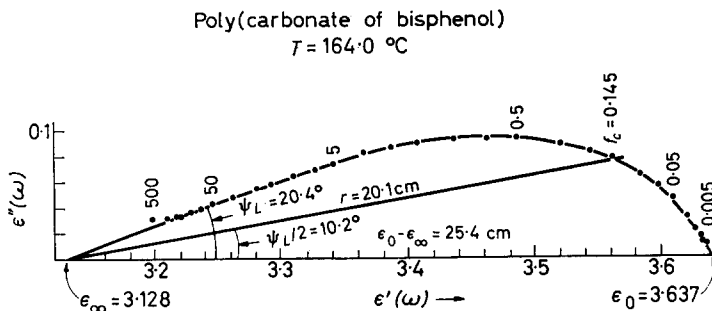
Figure 24—Experimental values of dielectric constant for poly(carbonate of bisphenol) at 160°C. Frequencies along curve in kc/s

The five dispersion parameters are graphically evaluated as follows using the experimental data on the polycarbonate in *Figure 24*. The low frequency end of the dispersion is readily extrapolated to obtain $\epsilon_0 = 3 \cdot 637$. The best straight line is drawn through the high frequency locus to the real axis to obtain a value for $\epsilon_\infty = 3 \cdot 128$. Using this high frequency extrapolation line φ_L was determined to be 20·4°. This angle is bisected (at ϵ_∞) and extended to the experimental locus. The frequency of intersection is determined to be 145 c/s, assuming a linear interpolation. On the original graph R was determined to 22·1 cm while $\epsilon_0 - \epsilon_\infty$ was found to be 25·4 cm. From these two dimensions, and φ_L, the LHS of equation (6) is computed to be 0·00295. This value is then found in *Table 4* and $1 - \alpha$ found to be 0·795. From this value of $1 - \alpha$ and φ_L, β is calculated to be 0·285, using equation (64). These parameters together with equations (60) to (64) inclusive are used to calculate $\epsilon^*(\omega)$ for the same frequencies as the experimental ones. The results of these calculations together with the experimental results are listed in *Figure 1*(a).

APPENDIX B

Most often the experimental data do not define the relaxation process as completely as for the polycarbonate. In addition it may also be important to know the temperature dependence of the dispersion parameters. The dielectric relaxation data of poly(vinyl acetate) is a case in point. There follows a method for determining the temperature dependence of the dispersion parameters when the experimental data do not define the relaxation process. For poly(vinyl acetate) at all temperatures above 66°C [see *Figure 25*(a)] ϵ_0 is readily determined as a low frequency extrapolation to the real axis. A plot of ϵ_0 against T (see *Figure 26*) is seen to be linear. These coefficients were determined from the best straight line thought to represent the data. At temperatures below 69°C, the experimental data are linearly extrapolated to the real axis to obtain ϵ_∞. The same extrapolation line is used to obtain φ_L. A plot of ϵ_∞ or φ_L against T is seen to be linear (see *Figure 26*). The straight line coefficients were determined from the best straight line thought to represent the data. The parameters $1 - \alpha$, β and
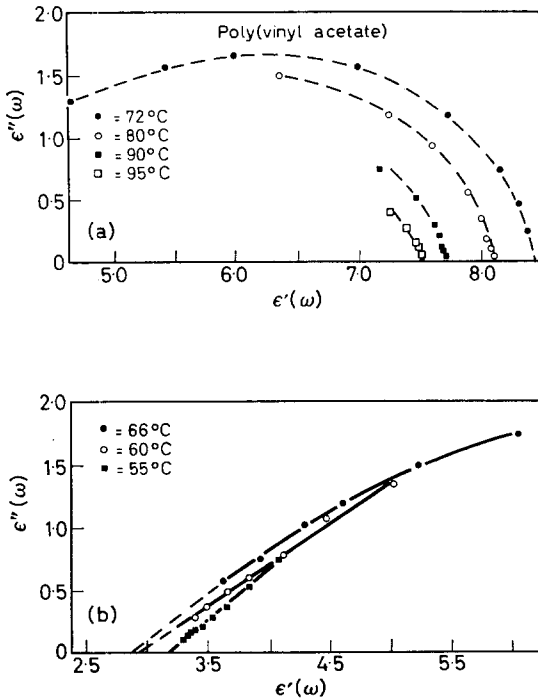
Figure 25 — Experimental values of the complex dielectric constant are represented here at different temperatures to illustrate the extrapolation techniques

τ_0 are now determined at those temperatures where at least one of the highest frequencies is to the short time side of the relaxation time or one of the lowest frequencies is to the long time side of the relaxation time. The points ϵ_0 and ϵ_∞ are marked off on the real axis of the complex plane. A straight line making an angle $\varphi_L/2$ with the real axis at ϵ_∞ is extended to the experimental locus. Interpolation between the two known frequencies gives τ_0. The length of this line together with $\epsilon_0 - \epsilon_\infty$ (in the same units) and φ_L gives $1 - \alpha$ from which β may be calculated.

A similar extrapolation procedure may be constructed to extend the determination of τ_0 to much longer times for those cases when all of the experimental points are to the short time side of τ_0. For this procedure a knowledge of ϵ_0, ϵ_∞ and either $1 - \alpha$ or β is required at the temperature of interest. Usually these parameters exhibit slightly different temperature dependences or experimental scatter. For the polymer under discussion, as an example, β can be extrapolated with greater certainty than $1 - \alpha$ (see *Figure 26*). In the present case β is extrapolated to the required temperature and $1 - \alpha$ is calculated (os in *Figure 4*) from φ_L. A trial value of τ_0 is estimated, $\epsilon^*(\omega)$s are calculated and compared with the experimental values until a minimum deviation is obtained. In this way estimates of τ_0 may be extended two to three decades.

APPENDIX C

Several of the equations listed in ref. 30 have been incorrectly printed. Professor S. Uemura of Kyushu University has been kind enough to
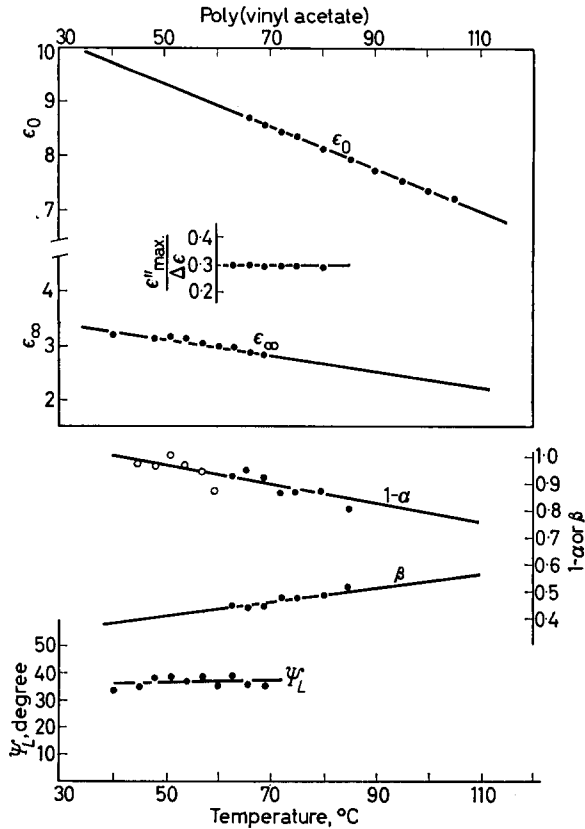
Figure 26—The dispersion parameters for poly(vinyl acetate) are plotted as a function of temperature in degrees Centigrade

supply us with the correct equations; they are listed below. Equation numbers refer to the original reference.

(7)
$$\sigma_{r,1} = T\{ -2A_1/r^3 - 2(5 - 3\nu_1)B_1/r^3 + 4C_1/r^5 \\ + \cos^2\theta[1 + 2(5 - \nu_1)B_1/r^3 - 12C_1/r^5]\}$$

(16)
$$A_1 = -\frac{a^3[(1+\nu_2)(11-7\,\nu_1)+2(4-2\,\nu_1-17\,\nu_2-8\,\nu_1\nu_2+15\,\nu_1^2\nu_2)G_1/G_2 \\ -(1+\nu_1)(19-15\,\nu_1)(1-2\,\nu_2)(G_1/G_2)^2]}{(1+\nu_1)[2(4-5\,\nu_1)+(7-5\,\nu_1)\,G_1/G_2]\,[1+\nu_2+2(1-2\,\nu_2)\,G_1/G_2]}$$

(19)
$$A_2 = \frac{3(1-\nu_1)[2(3-\nu_2+5\,\nu_1\nu_2)+(9+5\,\nu_1)(1-2\,\nu_2)G_1/G_2]}{2(1+\nu_1)[2(4-5\,\nu_1)+(7-5\,\nu_1)G_1/G_2]\,[1+\nu_2+2(1-2\,\nu_2)G_1/G_2]}$$

(20)
$$B_2 = \frac{3(1-\nu_1)}{4(1+\nu_1)[1+\nu_2+2(1-2\,\nu_2)G_1/G_2]}$$

210

The Fractionation of Polypropylene Oxide Polymerized by Ferric Chloride

E. POWELL

Polypropylene oxide prepared with the ferric chloride–propylene oxide complex has been fractionated from isooctane solution by incremental lowering of the temperature. Fractions have been characterized by intrinsic viscosity, melting point and density determinations and the data compared with those for the polymer prepared with the zinc alkyl catalyst. When the difference in crystallinity of the two polymers and the difference in molecular weight of the crystalline fractions of the two polymers are taken into account, the fractionation results may be explained in terms of a polymer similar to that prepared from zinc diethyl, i.e. one having a single distribution of molecular weight and degree of isotacticity.

STUDIES[1-4] of the polymerization of propylene oxide by ferric chloride and by organometallic catalysts (e.g. zinc diethyl) have shown many points of similarity. The polymer obtained using the zinc diethyl–water catalyst has been characterized and fractionated[5, 6]. The polymer prepared with a low mole ratio of water to zinc diethyl (up to 0·5 mole ratio), has been shown to consist of two main fractions (*a*) a low molecular weight oil produced by an initial fast polymerization and (*b*) a high molecular weight polymer produced by a slower secondary reaction which accounts for approximately 80 per cent of the polymerization. This high polymer is polydisperse with respect to both structure and chain length. The fractionation studies show that the molecular weight distribution of the crystalline fractions is the same as that of the amorphous fractions, i.e. all the high molecular weight polymer has the same molecular weight distribution. The polymer is regarded as the product of a single catalyst species.

In this study polypropylene oxide prepared with the ferric chloride catalyst has been fractionated and the results are compared with those for the zinc diethyl–water catalysed polymer.

EXPERIMENTAL AND RESULTS

Polymer

Three samples of polypropylene oxide were prepared using the Price[1] ferric chloride–propylene oxide complex as catalyst. The catalyst was prepared by reacting anhydrous ferric chloride with dry propylene oxide under high vacuum conditions with occasional chilling to control the exothermic reaction. The excess propylene oxide was distilled off leaving a brown oil and a measured volume of monomer was distilled on to this catalyst. In order to ensure the formation of some crystalline polymer[2] a known amount of water was added from an Agla micro syringe through a self sealing serum cap. The amount of water added was such that the molar ratio H_2O/Fe was 0·2. The catalyst concentrations used were for polymer 1, $6·5 \times 10^{-3}$ M and for polymers 2 and 3, $4·0 \times 10^{-3}$ M. Poly-

merization was carried out in sealed tubes for six weeks at 60°C and the polymers were isolated in the manner described by Gee et al.[2]. The polymerizations were found to have attained 100 per cent conversion.

Fractionation

The polymers were fractionated by cooling isooctane solutions as described in previous papers[3,5,6]. Intrinsic viscosities were determined for benzene solutions at 25°C using a Fitzsimmons viscometer. A separation of crystalline and amorphous polymer was carried out from methanol at 0°C and

Table 1. Fractionation data. Polymer 1. ($[\eta]=0\cdot69$)

Fraction No.	Separation temp., °C	Wt %	$[\eta]$ dl g^{-1}
F1	50	2·4	2·81
F2	46	4·9	2·85
F3	42	5·9	2·72
F4	32	5·8	1·89
F5	20	6·8	1·12
F6	0	8·2	0·35
Residue	—	65·2	0·10
$\Sigma\, w_i$	—	99·2	—
$\dfrac{\Sigma\, w_i\,[\eta]_i}{\Sigma\, w_i}$	—	—	0·64

the percentage methanol-insoluble polymer was determined together with the intrinsic viscosity of this fraction. Fractionation data are given in *Tables 1* and 2 and data for the methanol separation at 0°C are given

Table 2. Fractionation data. Polymer 2. ($[\eta]=1\cdot06$)

Fraction No.	Separation temp., °C	Wt %	dl g^{-1}	T_m °C	Density* g cm^{-3}	Crystallinity %
F1	48	11·3	2·72	72–73	1·051	31·6
F2	44	8·2	2·60	65	1·036	21·9
F3	40	5·9	2·70	62	1·033	20·0
F4	32	6·0	2·06	59	1·018	10·3
F5	24	3·7	1·20	—	—	—
F6	0	10·7	0·72	54	—	—
Residue	—	55·5	0·12	—	—	—
$\Sigma\, w_i$	—	101·3	—			
$\dfrac{\Sigma\, w_i\,[\eta]_i}{\Sigma\, w_i}$	—	—	0·98			

*Measured at 20°C.

in *Table 4*. Integral distribution curves for the two polymers are shown in *Figure 1*.

Viscosity average molecular weights $\overline{M}_v$ were computed using the equation $[\eta]=1\cdot12\times10^{-4}\,\overline{M}_v^{0\cdot77}$ for benzene at 25°C[7].

Melting point

Melting points (T_m) of fractions from polymers 2 and 3 were measured on the hot stage of a polarizing microscope as previously described[6]. The

Figure 1—The integral distribution curves for polypropylene oxide polymers prepared with ferric chloride: ⊙ polymer 1, △ polymer 2
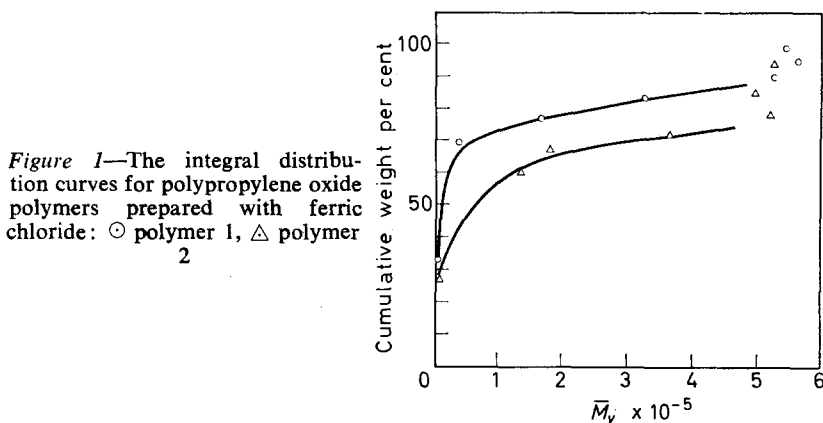
results are shown in *Tables 2* and *3*. Polymer 3 was not fractionated quantitatively but merely to provide fractions for T_m determination as a check on those of polymer 2.

Density

An assessment of the degree of crystallinity was obtained by measuring the density of certain fractions. The densities were determined by flotation in copper sulphate solutions. Each fraction was previously annealed by

Table 3. Melting points of fractions from polymer 3

Fraction No.	Separation temp., °C	T_m °C
F1	46	70
F2	43	67
F3	41	64
F4	37	60
F5	24	58

heating on a Koeffler hot plate to 100°C, holding the polymer at this temperature for fifteen minutes and then allowing it to cool slowly to 40°C (cooling rate approximately 15°/h). The polymer was kept at 40°C for twelve hours and then cooled to room temperature.

Table 4. Separation from methanol at °C

Polymer	$[\eta]$	% Insol. at 0°C	Insoluble polymer			
			$[\eta]$ $dl\ g^{-1}$	T_m °C	Density $g\ cm^{-3}$	Crystallinity %
1	0·69	18·2	2·51	—	—	—
2	1·06	23·1	2.57	69·5	1·049	30·3

It was assumed that there is a linear relation between the weight per cent crystallinity (x) and volume. The densities of crystalline and amorphous

213

polymer were taken to be $\rho_c = 1\cdot157$ g cm^{-3} (X-ray crystal density[8]) and $\rho_a = 1\cdot002$[9] respectively.

The weight per cent crystallinity was computed using the equation

$$x = 100 \, (1 - \rho_a/\rho_c) \, [\rho_c/(\rho_c - \rho_a)]$$

Infra-red spectra

The infra-red spectra of films cast from benzene solution were recorded using a Grubb–Parsons DM3 double beam recording spectrophotometer over the range 650 cm^{-1} to 5 000 cm^{-1}. Using the assignments due to Kawasaki *et al.*[10] certain bands are attributable to crystalline and amorphous regions in the polymer. It was observed with polymers 1 and 2 that strong absorptions at 1 481, 1 387, 1 339 and 1 307 cm^{-1} attributed to crystallinity in the polymer decreased in intensity from fractions F1 $\longrightarrow$ F7.

DISCUSSION

The first three fractions which precipitate as solid phases above 40°C are separated on the basis of decreasing degree of isotacticity. Melting point, density and infra-red data are in accord with this. The subsequent four fractions separate as liquid–liquid phases and are fractionated mainly with respect to molecular weight. The results show a wide distribution of molecular weights. Included in the lower molecular weight polymer is a high proportion (60 per cent of the whole polymer) of very low molecular weight polymer.

It is observed that the average molecular weight of the more crystalline fractions is very much greater than that of the amorphous fractions (even when F7, the low molecular weight oil is excluded). This is found to be so in the methanol separation as well as in the isooctane fraction.

At first sight there is an apparent difference between the ferric chloride catalysed polymer and the zinc diethyl catalysed polymer*. In the latter case fractionation studies have shown that the crystalline fractions have the same average molecular weight as the more amorphous polymer (excluding the very low molecular weight oil). There are, however, the following points which require consideration.

(a) The ferric chloride catalysed high molecular weight polymer contains a much higher percentage of crystalline polymer than that prepared with zinc diethyl, i.e. polymer separating from isooctane above 40°C. For example polymer 2 consists of 45 per cent high polymer and 55 per cent of this polymer is crystalline. A typical zinc diethyl catalysed polymer (polymer 62, ref. 3) contains 80 per cent high polymer and only 25 per cent of this polymer is crystalline.

(b) The molecular weight of the crystalline polymer prepared with zinc diethyl is very much greater than that of the polymer prepared using the ferric chloride catalyst ($[\eta] = 8\cdot3$ compared with $[\eta] = 2\cdot7$).

It has been shown[6] that the precipitation of isotactic polypropylene oxide from isooctane above 40°C is independent of the molecular weight when

*The polymer referred to here and later is that produced with a low mole ratio of water to zinc diethyl.

the molecular weight is high. There is, however, an effect of molecular weight on crystallization at low molecular weights. Crystalline chains of low molecular weight will tend to separate in liquid–liquid phase separation with the more atactic chains instead of crystallizing with the higher molecular weight fractions separating as solid phases above 40°C.

Removal of the crystalline fraction from the zinc diethyl catalysed polymer will result in the molecular weight distribution of the residue being only slightly biased towards the low molecular weight end after separation compared with the initial distribution. This will be so since the average molecular weight of the crystalline fraction is very high and the amount of crystalline polymer separated is small. Only a small amount of low molecular weight crystalline polymer will separate with the more amorphous fractions.

In the case of ferric chloride polymer 55 per cent of the high polymer is removed as a crystalline fraction of very much lower molecular weight than that of the crystalline fraction of the zinc alkyl catalysed polymer. This will leave a residue in which a larger amount of low molecular weight crystalline polymer will be present than in the former case. The average molecular weight of the fraction separating below 40°C will therefore be lowered. It follows that the melting points of fractions separating below 40°C should be greater for the ferric chloride catalysed polymer than for the corresponding fractions separating from the zinc diethyl catalysed polymer. This is expected since with a lower molecular weight crystalline fraction only the highly crystalline chains of the polymer prepared with ferric chloride separate above 40°C. The melting point data in *Table 5* are in agreement with this.

Table 5

*Polymer 44[6] ZnEt–H$_2$O		Polymer 2 FeCl$_3$		Polymer 3 FeCl$_3$	
Separation temp., °C	T_m °C	Separation temp., °C	T_m °C	Separation temp., °C	T_m °C
50	71				
		48	72–73		
46	68			46	70
		44	65		
				43	67
42	68			41	64
		40	62		
39	62				
				37	60
36	56				
		32	59	24	58
0	48	0	54		

*This polymer yielded crystalline fractions upon fractionation with [η] = 5·4 in benzene at 25°C.

The fractionation data may be interpreted in terms of a polymer similar to that produced using the zinc diethyl catalyst, i.e. consisting of (*a*) a very low molecular weight oil and (*b*) a high polymer which has a single distribution of molecular weight and degree of isotacticity.

Chemistry Department,
Leicester College of Technology

REFERENCES

[1] PRICE, G. C. and OSGAN, M. J. *J. Amer. chem. Soc.* 1956, **78,** 4787

[2] GEE, G., HIGGINSON, W. C. E. and JACKSON, J. B. *Polymer, Lond.* 1962, **3,** 231

[3] BOOTH, C., HIGGINSON, W. C. E. and POWELL, E. *Polymer, Lond.* 1964, **5,** 479

[4] COLCLOUGH, R. O. and WILKINSON, K. *J. Polym. Sci. C,* 1964, **4,** 311

[5] BOOTH, C., JONES, M. N. and POWELL, E. *Nature, Lond.* 1962, **196,** 772

[6] ALLEN, G., BOOTH, C. and JONES, M. N. *Polymer, Lond.* 1964, **5,** 257

[7] ALLEN, G., BOOTH, C. and JONES, M. N. *Polymer, Lond.* 1964, **5,** 195

[8] NATTA, G., CORRADINI, P. and DALL'ASTA, G. *Atti Accad. Lincei (Cl. sci. fis. mat. e nat.),* 1956, **20,** 408

[9] ALLEN, G., BOOTH, C., JONES, M. N., MARKS, D. J. and TAYLOR, W. D. *Polymer, Lond.* 1964, **5,** 547

[10] KAWASAKI, A., FURUKAWA, J., TSURUTA, T., SAEGUSA, T., KAKAGAWA, C. and SAKATA, T. *Polymer, Lond.* 1960, **1,** 315

An Electron Microscopical Study
of Polyacrylamide

D. V. QUAYLE

The stages leading to the deposition by spray technique of individual molecules of polyacrylamide have been studied using the electron microscope. The weight and number average molecular weights together with the molecular weight distribution for a fraction of polyacrylamide have been obtained. Good agreement with the viscosity average molecular weight has been found.

IT IS possible with most glassy amorphous polymers to observe single spherical molecules in the electron microscope, if very dilute solutions in a solvent–precipitant mixture are sprayed on to a thin substrate[1,2].

Polymers which are rubbery at the preparation temperature do not deposit as single spherical molecules, but collapse on to the substrate or form a film even at very low concentrations. It is not possible to obtain single spherical molecules from solutions of crystalline polymers.

Polyacrylamide behaves differently from the above, in that a filamentous structure is prevalent when the polymer is sprayed at room temperature from solvent–precipitant mixtures[3]. The extent of the filamentous structure depends on the temperature at which the solvents evaporate on the substrate and on the ratio of solvent to precipitant. After spraying on to a heated substrate, no filaments are seen and single molecules are formed if the polymer concentration and solvent/precipitant ratio are favourable. An unusual feature, however, has been reported by Richardson[2]. Single molecules of polyacrylamide collapse to a shapeless mass even in a weak electron beam in the manner of rubbery polymers even though the glass transition temperature is about 130°C. Experiments have shown that this phenomenon is most likely to be due to the formation of intramolecular bonds on irradiation by the electron beam in the microscope[4].

The filamentous structure is interesting as the finest strands are likely to consist of single molecular chains.

The purpose of this work was to confirm previous observations and attempt to observe and record the various stages in the development of single isolated molecules of polycrylamide as the solvent/precipitant ratio is gradually decreased. Investigations of the possibility of determining the number and weight average molecular weights, together with the molecular weight distribution, for high molecular weight fractions of polyacrylamide were made.

EXPERIMENTAL

Very dilute solutions of polyacrylamide in water–*n*-propanol mixtures were sprayed at room temperature on to evaporated carbon films of thickness

about 100Å, backed with freshly cleaved mica. The films were then shadowed with a 50 per cent platinum–carbon mixture, floated off on to distilled water and picked up on copper microscope grids. Electron micrographs were taken in an A.E.I. EM6G electron microscope at a magnification of 20 000 times. The solutions used in the investigation were:

Solution No.	Percentage of polyacrylamide	in percentage of water–n-propanol mixture
1	10^{-3}	50
2	10^{-3}	45
3	10^{-3}	40
4	10^{-3}	30
5	10^{-4}	20

A Vaponefrin nebulizer, which could produce droplet sizes in the range 2 to 5 μm, was used to disperse the polymer on the carbon films.

DISCUSSION OF RESULTS

Figures 1 to 5 show the effect of a gradual change from good to poor solvent conditions on the way in which polyacrylamide is deposited from solution.

Figure 1 shows the filamentous structure which is prevalent when polyacrylamide is deposited from a solution in a good solvent. The structure, which is very branched, represents bundles of molecular chains lying on
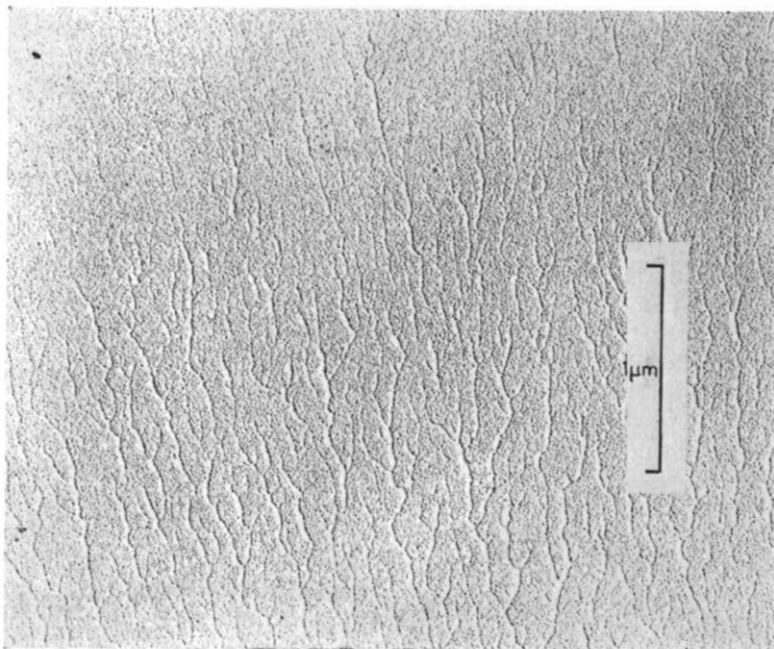
Figure 1—Polyacrylamide from water(50%)–n-propanol

Figures 1 to 5—Polyacrylamide deposited by spraying on to a thin carbon film, 10^{-3} per cent solutions in water–n-propanol mixtures of decreasing water content

the substrate. Richardson[2] has shown that intermolecular hydrogen bonding is not responsible for this behaviour. He observed no change in the structure on spraying from hot aqueous solutions to reduce the number of hydrogen bonds, or on using a less strongly hydrogen-bonding solvent such as ethylene glycol. Indeed, Eliassaf and Silberberg[5] have shown that aqueous solutions of polyacrylamide are not strongly hydrogen-bonded. The intrinsic viscosities of such solutions were unaffected by the addition of salts known to be efficient hydrogen bond breakers. The phenomenon seems to be due to some specific property of the polymer itself. In addition, its formation is time dependent. The strands disappear when solutions are sprayed on to a heated substrate and 'islands' of polymer are formed.

The finest filaments are probably single molecular chains, but this cannot be shown with certainty owing to the reduction in resolution caused by the shadowing material. *Figure 6* is typical of the finest strands which are observable and as it is very well defined, with no strands smaller than this ever having been seen, it is probable that it represents a single molecular chain. The shadow cast by the strand is between 50 Å and 120 Å in length, the shadowing angle being $\cot^{-1} 4 \cdot 2$. This suggests that the strand has a diameter of between 12 Å and 29Å. However, a piling up of shadowing material behind the strand (a snowdrift effect), may have resulted in a longer shadow than would have been cast by the strand alone.

As the precipitant concentration is increased, agglomerates are formed at the junctions of the branches as in *Figure 2*. Further addition of precipi-
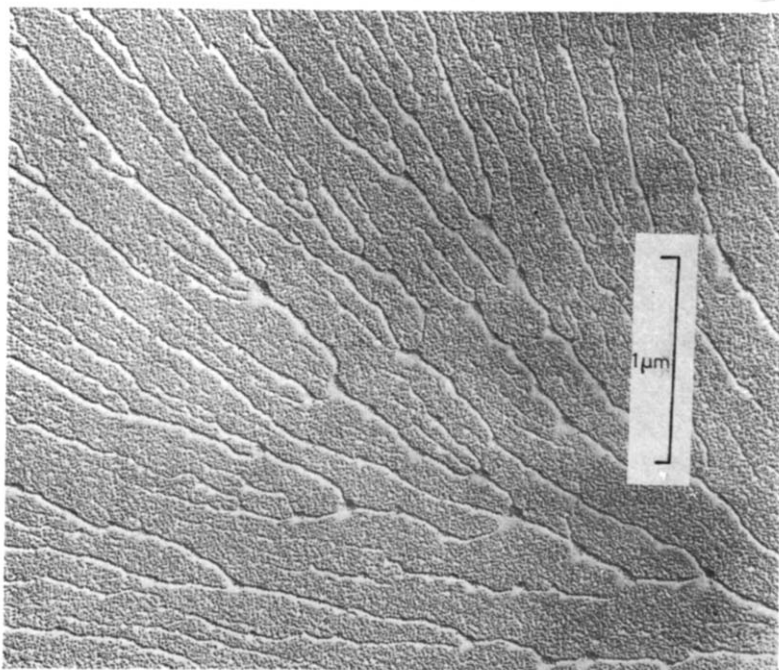
Figure 2—Polyacrylamide from water(45%)-*n*-propanol
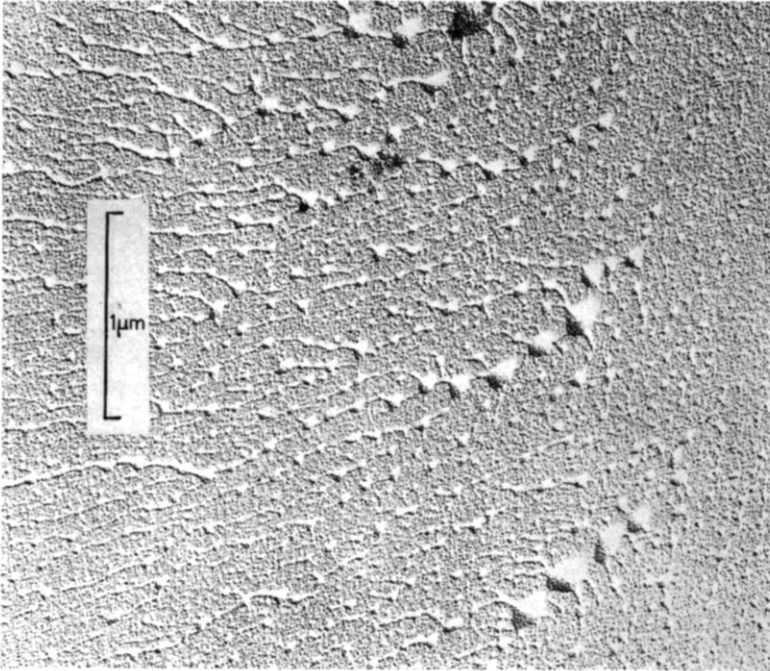
Figure 3—Polyacrylamide from water(40%)–*n*-propanol
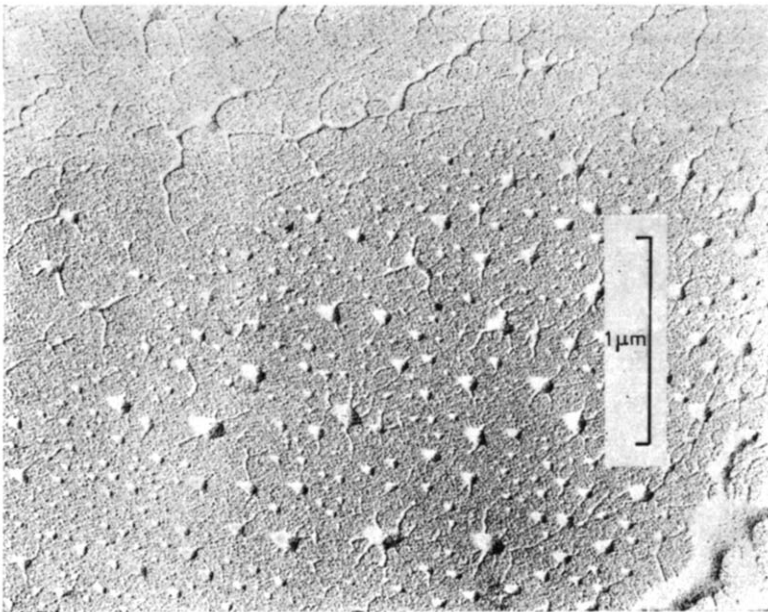
Figure 4—Polyacrylamide from water(30%)–*n*-propanol

220

tant results in more pronounced agglomeration (*Figure 3*), and eventually the filamentous structure is broken up almost completely (*Figure 4*). The agglomerates at this stage may consist of very many molecules but, on further addition of precipitant, they break up to form individual molecules (*Figure 5*) (this is demonstrated later) which, from the shape of the shadows they cast, are spherical.
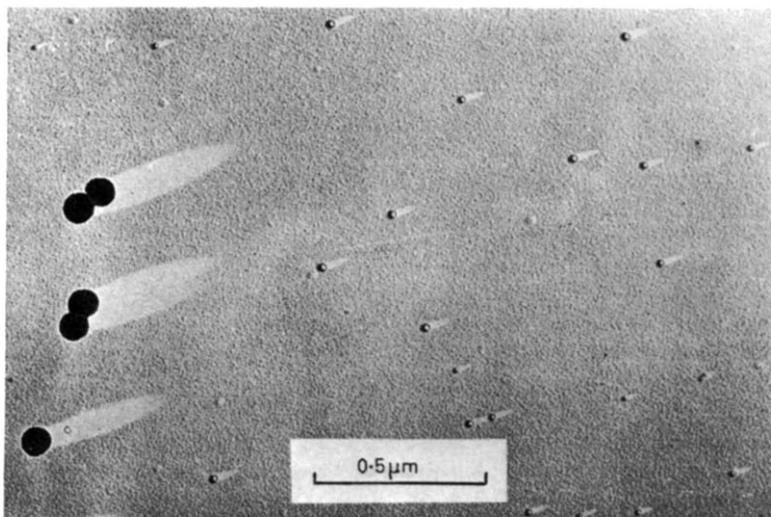
Figure 5—Polyacrylamide from water(20%)-*n*-propanol. The large spheres are polystyrene latex particles of nominal diameter 880 Å

Richardson[2] observed that polyacrylamide molecules appeared to collapse into a shapeless mass, even in a weak electron beam. The molecules in *Figure 3* appear to have collapsed, and recent work[4] has shown that this is most likely to be due to radiation-induced intramolecular bond formation, thus:

$$\begin{array}{c} \text{electrons} \\ -CH_2-CH------------CH_2-CH-CH_2------ \longrightarrow \\ \quad\quad | \quad\quad\quad\quad\quad\quad\quad\quad\quad\quad\quad | \\ \quad\quad CONH_2 \quad\quad\quad\quad\quad\quad\quad CONH_2 \end{array}$$

$$\begin{array}{c} -CH_2-CH--------CH_2-CH-CH_2-- \\ \quad\quad | \quad\quad\quad\quad\quad\quad\quad\quad\quad | \quad\quad\quad +NH_3 \\ \quad O=C \quad\quad\quad\quad\quad\quad\quad C=O \\ \quad\quad\quad\searrow\quad\quad\quad\quad\swarrow \\ \quad\quad\quad\quad NH \end{array}$$
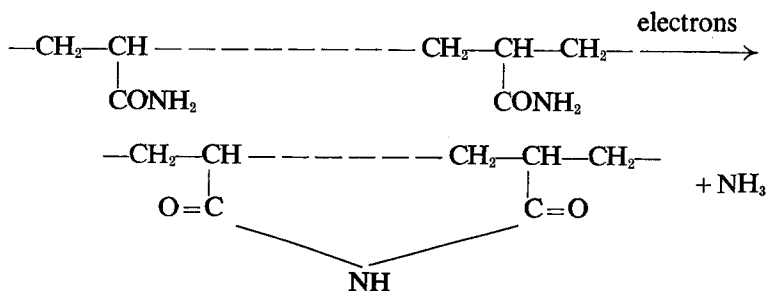
That the spheres observed were in fact individual molecules was demonstrated as follows. Using decreasing concentrations of polyacrylamide in (20 per cent) water–*n*-propanol in the range 10^{-2} to 10^{-5} per cent, particles
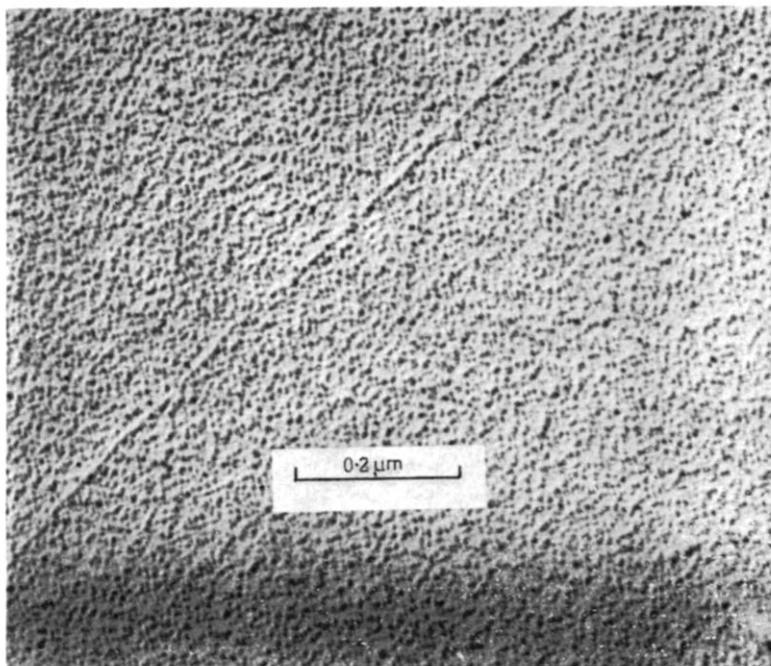
Figure 6—Typical of the finest strands seen, when polyacrylamide is deposited from solution in a good solvent. This may represent a single molecular chain

were prepared as described previously. Polystyrene latex spheres, of nominal diameter 880Å, were sprayed on to the same carbon films and the angle of shadowing was calculated from the lengths of the shadows cast. From a knowledge of the shadowing angle, the heights of the polyacrylamide spheres were determined. Size distributions for about 500 spheres were made for each of the solutions of decreasing polymer concentration and it was found that for concentrations below about 5×10^{-3} per cent the size distributions were virtually identical. This would not be expected if the spheres contained more than one molecule, as a decrease in polymer concentration is accompanied by a decrease in molecular aggregation and hence a pronounced change in the size distributions of the spheres would have been apparent. Also, as will be described later, the value of $\overline{M}_w$ calculated from the distributions was in good agreement with the viscosity average molecular weight.

DETERMINATION OF WEIGHT AND NUMBER
AVERAGE MOLECULAR WEIGHTS, AND THE
MOLECULAR WEIGHT DISTRIBUTION

Experimental

Spherical molecules with molecular weights less than about 5×10^5 are too small to be measured with high accuracy in the electron microscope and therefore a high molecular weight fraction of polyacrylamide was used.

A one per cent solution of the polymer in water was made and about ten per cent by weight was precipitated àt 25°C by the addition of methanol. The precipitate was separated and dried. A 10^{-4} per cent solution of this fraction was made in (20 per cent) water–n-propanol, the alcohol being added slowly to the water while stirring vigorously. The solution was sprayed at room temperature on to a mica-backed carbon film, as previously described. Electron micrographs were taken at a magnification of 20 000 × and measurements of shadow lengths were made on prints having a total magnification of 60 000 × . The shadowing angle was again determined using polystyrene latex spheres of nominal diameter 880Å, an average shadow length being calculated from measurements on about 20 spheres. Electron microscope magnifications were determined from measurements on electron micrographs of a crossed diffraction grating replica having 21 600 lines per centimetre supplied by A.E.I. Ltd.

Although there is distortion of small particles due to the deposition of shadowing materials upon them, it has been demonstrated[2] that the shadow length still provides an accurate estimate of the height of the particle.

More than 200 molecular shadow lengths were measured, using a travelling microscope and measuring to an accuracy of ±0.01 cm. Assuming the molecules to have the same density as the bulk polymer, a molecular weight distribution was built up and the result is shown as a histogram (*Figure 7*). Weight and number average molecular weights were calculated
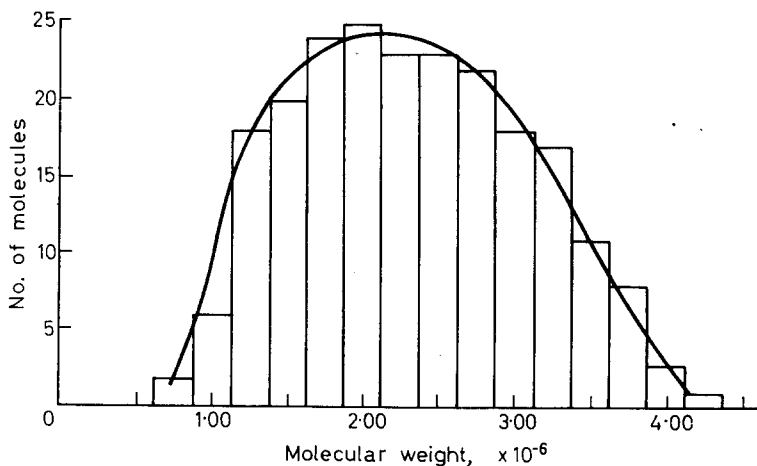
Figure 7—The molecular weight distribution for a polyacrylamide fraction, as determined by electron microscopy. Polymer deposited from 5×10^{-4} per cent solution in water(20%)–n-propanol

from the distribution and compared with the viscosity average calculated from

$$[\eta] = 3.73 \times 10^{-4}\overline{M}_v^{0.66}$$

Discussion of results

The viscosity average molecular weight was found to be 2.71×10^6 while the electron microscope method gave $2.33 \pm 0.3 \times 10^6$ and $2.59 \pm 0.3 \times 10^6$ for the number and weight averages respectively.

In view of the excellent agreement between these values and the good reproducibility obtainable for molecular size distributions, it seems that this electron microscope technique is capable of providing an acurate determination of any molecular weight average together with the complete molecular weight distribution for high molecular weight fractions of polyacrylamide.

It should be emphasized that only the minimum of heavy metal, consistent with clear shadow formation, should be used, and that the shadowing angle should be as small as possible in order to produce shadows of maximum length.

The main source of error occurs in the measurement of the lengths of the shadows cast by the molecules, as the cube of this dimension enters into the calculation of molecular weight. The method of Misra and Das Gupta[7] cannot be used exactly, as the molecules, although deposited as spheres, appear collapsed on the print from which the measurements are taken. It is therefore a matter of some doubt as to where the precise beginning or end of the shadow lies. The accuracy of molecular weight averages obtained by this technique is estimated at ten per cent.

Department of Physics,
Derby and District College of Technology,
Derby

REFERENCES

[1] NASINI, A. G., OSTACOLI, G., SAINI, G., MALDIFASSI, G. and TROSSARELLI, L. Suppl. to *Ric. sci. Mem.* 1955, **25,** 432
[2] RICHARDSON, M. J. *Proc. Roy. Soc. A,* 1964, **279,** 50
[3] ROCHOW, T. G. *Analyt. Chem.* 1961, **33,** 1810
[4] QUAYLE, D. V. *Nature, Lond.* 1966, **209,** 5025
[5] ELIASSAF, J. and SILBERBERG, A. *J. Polym. Sci.* 1959, **41,** 33
[6] American Cyanamid Co. *Publ. No. MDD–9236–5M–6/59*
[7] MISRA, D. N. and DAS GUPTA, N. N. *J. R. micr. Soc.* 1965, **84,** 373

Copolymerization of Styrene and Some α-Olefins Using Ziegler–Natta Catalyst Systems—The Fractionation and Characterization of the Products of Copolymerization

B. BAKER* and P. J. T. TAIT

Styrene has been successfully copolymerized with various α-olefins, using Ziegler–Natta catalyst systems. The products of copolymerization were fractionated with respect to composition using a double-solvent elution technique. The copolymer obtained by the use of the VCl₃–Al (iBu)₃ catalyst was found to be much more heterogeneous than the polymer obtained with the more disperse system, i.e. VOCl₃–Al (iBu)₃. This was considered to be good evidence for the presence of a higher degree of catalytic polyactivity in the more crystalline catalyst with the larger particle size. A series of structural investigations on the copolymer samples was undertaken using X-ray diffraction and infra-red spectroscopic techniques. It was shown that the copolymers of styrene and octadecene-1, and styrene and 4-methylpentene-1, prepared using VOCl₃–Al (iBu)₃ exhibited a high degree of crystallinity. Much evidence is presented for the existence of a stereoblock type of structure. The values of relative reactivity ratios were determined for each of the monomer pairs investigated. A reduction in reactivity ratio values was observed in all cases with the use of the more disperse catalyst system.

THE copolymerization of ethylene and propylene[1-5] and other α-olefins[6-9] and of styrene and substituted styrenes[10], using Ziegler–Natta catalyst systems has been extensively studied by Natta and co-workers. Investigations into the copolymerization of styrene and aliphatic α-olefins have been carried out by Burnett and Tait[11-13], and the work reported in these papers is intended to be an extension of various aspects and problems brought to light by their results.

The catalyst systems most commonly used in Ziegler–Natta polymerization may be classified into two main groups: (i) those catalysts prepared from a finely ground crystalline halide of lower valency (usually a compound of titanium or vanadium) and a metal alkyl, e.g. titanium or vanadium trichloride and aluminium tri-isobutyl and (ii) catalysts prepared by the vigorous reduction of liquid transition metal halides of higher valency by an alkyl of aluminium, e.g. vanadium tetrachloride, or vanadium oxytrichloride and aluminium tri-isobutyl.

The effective catalyst particles in each type differ from each other in several ways. The precipitate from the first type of catalyst is fairly crystalline and in general has a particle size of the order of 5μ[14]; any reduction of the halide is thought to be essentially a surface effect. The precipitate from the second type of catalyst is, however, believed to be

less crystalline, and exists in a much more finely divided suspension with an average particle size approximately equal to one hundredth the size of the first type, and these factors suggest that a more uniform active site is available for polymerization, giving rise to a more homogeneous product in copolymerization.

The investigations described in this paper include the copolymerization of styrene with three different α-olefins, viz. heptene-1, octadecene-1 and 4-methylpentene-1 in the presence of Ziegler–Natta catalyst systems of the aforementioned types, i.e. vanadium trichloride and aluminium tri-isobutyl, and vanadium oxytrichloride and aluminium tri-isobutyl, and an account of the subsequent fractionation of the isolated products, and their characterization.

EXPERIMENTAL

Purification of materials

Styrene—The inhibitor was removed from styrene monomer by extraction with dilute sodium hydroxide solution, followed by washing with distilled water. After drying over sodium sulphate (anhydrous), the monomer was fractionally distilled under reduced pressure. Final traces of water were removed prior to polymerization by treatment with barium oxide under high vacuum.

Heptene-1, octadecene-1 and 4-methylpentene-1—These monomers were supplied by Newton Maine, Rare Chemicals Ltd, Silsoe, England, and were dried over sodium sulphate and purified by fractionation prior to use.

Benzene—Analytical reagent quality benzene was dried over sodium sulphate (anhydrous), purified by fractional distillation and stored over sodium wire.

Vanadium trichloride—The vanadium trichloride as supplied by the Magnesium Elektron Company, Swinton, Lancashire, England, was in the form of a finely divided crystalline powder. Before use, it was washed with sodium-dried benzene and stored in an inert atmosphere.

Vanadium oxytrichloride—The vanadium oxytrichloride as supplied by the Magnesium Elektron Company was purified by distillation under high vacuum, and stored in a tightly stoppered tube in an inert atmosphere of dry nitrogen.

Aluminium tri-isobutyl—The aluminium tri-isobutyl was used as supplied by the Shell Chemical Company, Carrington, England, and stored in an inert atmosphere in a dry box.

Polymerization procedure—As these investigations were carried out in conjunction with a series of copolymerization rate measurements, most of the preparations of copolymer were carried out in dilatometers. The experimental procedure for copolymer preparation and rate determination was similar to that described in an earlier paper[12].

The composition of the copolymer (and fractions thereof) was determined by measurement of the ultra-violet absorption of dilute solutions of the polymer in chloroform. The band used was that at 2 610Å, and the spectrophotometer was first calibrated with standard solutions of each of the appropriate homopolymers.

226

Fractionation technique

Many different fractionation techniques are available which are applicable to polymer fractionation and these have been adequately reviewed in the literature[15, 16]. Most of the techniques involving special apparatus and fractional precipitation methods were considered inappropriate for the current problem, as they do not lend themselves readily to automation, and require relatively large samples. In addition, they are designed primarily to achieve fractionation with respect to molecular weight, whereas the solubility of a copolymer of the type under investigation is a function of molecular weight, composition and tacticity. Thus, as the main purpose of these experiments was to achieve a fractionation with respect to composition, a column elution technique was employed using a double-solvent system rather than the usual solvent–precipitant mixtures. The two solvents were chosen so that ideally, fractions of the copolymer rich in one component would dissolve in solvent A and fractions rich in the second component would dissolve only in solvent B.

The apparatus used was similar to that originally designed by Baker and Williams[17], but the column was enclosed by a simple heating jacket, as recommended by Flowers[18], such that no temperature-gradient device was employed.

The sample of copolymer (1·0 g) was deposited from a concentrated benzene solution on to a small quantity of glass beads (i.e. 'Ballotini' beads, No. 15, diameter 1 mm) which constituted approximately one third of the column. A solvent feed of continuously changing composition obtained by a simple double-solvent-reservoir device was pumped to the top of the column by means of a micro-pump. The various fractions were collected by means of an automatic fraction collector incorporating a syphon-balance delivering a standard volume for each fraction. The fractionations of copolymers of styrene and heptene-1 were carried out at room temperature, but a temperature of 45°C was required for other experiments. The double solvent system used in all cases was hexane–benzene.

Having obtained twenty five to thirty 25 ml fractions, the solvent was evaporated from each fraction in turn, and the polymer reprecipitated from chloroform in cooled methanol. The fractions were bulked so as to give the maximum number of samples containing sufficient polymer for analysis and characterization.

The intrinsic viscosity of solutions of various polymer fractions in benzene was determined using an Ubbelohde dilution viscometer No. 1 at 25°C.

Structural investigations

The isolated products of copolymerization and homopolymerization of the chosen monomers were examined using X-ray diffraction and infra-red (i.r.) spectroscopy techniques.

In order to obtain suitable i.r. spectra, it was found necessary to deposit the sample in the form of a thin film on standard sodium chloride discs.

The sample was then scanned between 15 to 3·5 μ wavelength using a Perkin–Elmer spectrometer.

The X-ray diffraction spectra were obtained by examination of the sample in the form of fine powder and the region scanned was equal to 4° to 30°. The radiation employed was nickel filtered from a copper target operated at 36 kV and 20 mA.

The density of all products of polymerization was determined by a simple flotation method using water and ethyl alcohol. This was also necessary for the calculation of absolute units of polymerization rate.

RESULTS

Styrene has been successfully copolymerized with the three chosen α-olefins, using two different Ziegler–Natta catalyst systems. The typical conditions of polymerization used are listed in *Table 1*.

Table 1. Polymerization conditions

(a) VCl₃–AliBu₃ *catalyst*		(b) VOCl₃–AliBu₃ *catalyst*	
VCl₃ concentration	0·10 mole l⁻¹	VOCl₃ concentration	0·10 mole l⁻¹
AliBu₃ concentration	0·20 mole l⁻¹	AliBu₃ concentration	0·25 mole l⁻¹
Al/V ratio	2·0	Al/V ratio	2·5
Solvent	Benzene	Solvent	Benzene
Temperature	30·0 ± 0·01 deg. C	Temperature	30·0 ± 0·01 deg. C
Total monomer concentration	2·0 mole l⁻¹	Total monomer concentration	2·0 mole l⁻¹

Samples of the copolymer of each of the α-olefins with styrene have been fractionated and the results obtained are shown in *Tables 2 to 7*.

Table 2. Fractionation of products of copolymerization of styrene and heptene-1 using VCl₃–AliBu₃ (F3)

Fraction no.	Solvent	Wt of polymer in fraction, g	Cumulative wt %	Mole % styrene
1	Pure hexane	0·0695	7·6	37·5
2		0·0464	12·7	46·2
3		0·0521	18·5	50·0
4		0·0516	24·1	52·4
5		0·0550	30·2	52·7
6		0·0620	36·9	64·2
7		0·1084	48·8	82·1
8, 9		0·1270	62·8	77·5
10, 11		0·0760	71·3	71·8
12–14		0·1081	83·0	65·0
15–19		0·0993	94·0	59·2
20–26	Pure benzene	0·0459	100·0	66·2

Weight of sample for fractionation = 0·9303 g; weight of polymer recovered = 0·9113 g; per cent recovery of polymer = 97·0; mole per cent of styrene in original sample = 64·6; average mole per cent of styrene in recovered polymer = 62·6.

228

Table 3. Fractionation of products of copolymerization of styrene and heptene-1 using VOCl$_3$–Al*i*Bu$_3$ (F4)

Fraction no.	Solvent	Wt of polymer in fraction, g	Cumulative wt %	Mole % styrene
1	Pure hexane	0·0500	7·2	12·1
2, 3		0·0672	16·8	41·8
4		0·0306	21·1	35·9
5		0·0720	31·4	72·5
6		0·0860	43·7	76·0
7		0·0604	52·4	75·9
8		0·0410	58·4	73·1
9		0·0361	63·5	77·0
10–12		0·0860	75·9	70·6
13–15		0·0506	83·1	72·2
16–20		0·0410	89·2	68·9
21–28	Pure benzene	0·0774	100·0	79·5

Weight of sample for fractionation = 0·7034 g; weight of polymer recovered = 0·6983 g; per cent recovery of polymer = 99·2; mole per cent of styrene in original sample = 67·8; average mole per cent of styrene in recovered polymer = 65·0.

The degree of homogeneity of the samples examined can be assessed by the data in *Table 8,* which is a summary of the results obtained, expressed in terms of the percentage of total recovered material having a styrene content within various limits of an arbitrary mean value (*S*).

It can be seen clearly that copolymerization has taken place and that the products are not merely mixtures of the respective homopolymers.

Table 4. Fractionation of products of copolymerization of styrene and octadecene-1 using VCl$_3$–Al*i*Bu$_3$ (F2)

Fraction no.	Solvent	Wt of polymer in fraction, g	Cumulative wt %	Mole % styrene
1	Hexane	0·0269	2·9	67·8
2		0·0292	6·0	53·5
3		0·0833	14·9	61·4
4		0·1108	26·7	57·8
5		0·2290	52·4	67·7
6		0·1100	63·2	66·7
7		0·0522	68·5	74·5
8		0·0296	71·6	79·3
9		0·0445	76·4	49·2
10		0·0276	79·3	80·0
11		0·0190	81·3	95·3
12		0·0178	83·3	94·0
13		0·0132	84·6	98·9
14		0·0336	88·3	99·3
15		0·0286	91·3	99·8
16, 17		0·0222	93·7	100·0
18–21		0·0308	96·8	100·0
22–25		0·0162	98·6	98·5
26–31	Benzene	0·0132	100·0	98·4

Weight of sample for fractionation = 1·000 g; weight of polymer recovered = 0·9377 g; per cent recovery of polymer = 93·8; mole per cent of styrene in original sample = 73·1; average mole per cent of styrene in recovered polymer = 71·0.

Table 5. Fractionation of products of copolymerization of styrene and octadecene-1 using VOCl$_3$–AliBu$_3$ (F5)

Fraction no.	Solvent	Wt of polymer in fraction, g	Cumulative wt %	Mole % styrene
1–6	Hexane	0·2120	19·7	68·4
7–10		0·0608	25·4	86·3
11–13		0·0772	32·5	37·9
14–15		0·0592	38·0	29·9
16, 17		0·0570	43·4	31·3
18, 19		0·0878	51·5	29·5
20, 21		0·2378	73·6	34·7
22–28	Benzene	0·2855	100·0	34·0

Weight of sample for fractionation = 1·100 g; weight of polymer recovered = 1·0772 g; per cent recovery of polymer 97·9 mole per cent of styrene in original sample = 44·1; average mole per cent of styrene in recovered polymer = 42·7.

Table 6. Fractionation of products of copolymerization of styrene and 4-methylpentene-1 using VCl$_3$–AliBu$_3$ (F6)

Fraction no.	Solvent	Wt of polymer in fraction, g	Cumulative wt %	Mole % styrene
1	Hexane	0·1407	16·1	65·6
2		0·0661	23·6	56·2
3		0·0332	27·4	51·9
4		0·0514	33·2	58·1
5		0·0691	41·2	67·2
6		0·0348	45·2	71·8
7, 8		0·0441	50·2	61·6
9, 10		0·0571	56·7	79·7
11–14		0·1072	68·8	90·6
15–21		0·1225	83·0	22·4
Benzene insoluble	Benzene	0·1495	100·0	38·5

Weight of sample for fractionation = 0·920 g; weight of polymer recovered = 0·8757 g; per cent recovery of polymer = 95·2; mole per cent of styrene in original sample = 56·7; average mole per cent of styrene in recovered polymer = 54·4.

Table 7. Fractionation of products of copolymerization of styrene and 4-methylpentene-1 using VOCl$_3$–AliBu$_3$ (F7)

Fraction no.	Solvent	Wt of polymer in fraction, g	Cumulative wt %	Mole % styrene
1	Hexane	0·0858	13·1	34·8
2		0·0730	24·2	37·7
3, 4		0·0771	36·0	34·1
5, 6		0·0676	46·2	30·6
7, 8		0·0810	58·6	32·3
9, 10		0·0389	64·5	27·7
11, 12		0·0556	73·0	31·3
13–16		0·578	81·8	29·3
17–20		0·0454	88·7	38·8
21–26		0·0336	94·0	74·2
Benzene insoluble	Benzene	0·0410	100·0	59·4

Weight of sample for fractionation = 0·690 g; weight of polymer recovered = 0·6568 g; per cent recovery of polymer = 95·3; mole per cent of styrene in original sample = 39·5; average mole per cent of styrene in recovered polymer = 37·0.

In each experiment, the average mole percentage of styrene in the recovered polymer was less than the styrene content of the original polymer by approximately two per cent. This discrepancy is thought to be well within the limits of experimental error. The variation of increase in styrene

Table 8. Summary of fractionation results

Fractiona- tion no.	Monomer pair	Catalyst system	Percentage of total recovered material having a styrene content within various limits of an arbitrary mean (S)			
			S	$\pm 2 \cdot 5\%$	$\pm 5 \cdot 0\%$	$\pm 10\%$
F3	Styrene–heptene-1	VCl_3	62·5	18·4	35·4	50·0
F4	Styrene–heptene-1	$VOCl_3$	74·0	45·9	63·2	78·9
F2	Styrene–octadecene-1	VCl_3	69·2	39·8	39·8	54·0
F5	Styrene–octadecene-1	$VOCl_3$	32·2	59·4	67·5	74·6
F6	Styrene–4-methylpentene-1	VCl_3	58·0	13·7	18·7	33·9
F7	Styrene–4-methylpentene-1	$VOCl_3$	33·2	43·0	75·9	88·7

content with increase in the enrichment of the solvent feed with benzene is in accordance with the principles governing the choice of solvent system. In most of the fractionations, especially those performed using samples prepared with the vanadium trichloride catalyst, the last few fractions were found to contain less styrene than those preceding them. This phenomenon can be accounted for by the fact that these fractionations take place not only with respect to composition, but to some extent with respect to molecular weight, and that these latter fractions constitute the higher molecular weight material. This was confirmed by the measurement of the intrinsic viscosity of the fractions compared with the viscosity of the appropriate homopolymers.

The fact that fractionation with respect to molecular weight may take place to a limited extent under the conditions of these fractionation experiments in no way invalidates these results, since the object of these fractionation studies is merely to establish the extent of heterogeneity in composition.

The X-ray diffraction spectra of the isolated products of polymerization revealed some interesting and unexpected trends. These can be illustrated by the spectra obtained for the products of copolymerization of various mixtures of styrene and 4-methylpentene-1 using the two different catalyst systems, which are shown in *Figure 1*.

Without exception, the samples of homopolymer prepared using the vanadium oxytrichloride catalyst exhibited a higher degree of crystallinity than those prepared using the vanadium trichloride catalyst system. This trend is not in agreement with the results obtained by some other workers[19], who find that the catalysts prepared using highly crystalline transition-metal halides are more stereospecific than those whose preparation involves the reduction of higher valency halides, which are liquids under normal conditions. Even more surprising is the preparation of highly crystalline copolymers using the vanadium oxytrichloride catalyst system. In the
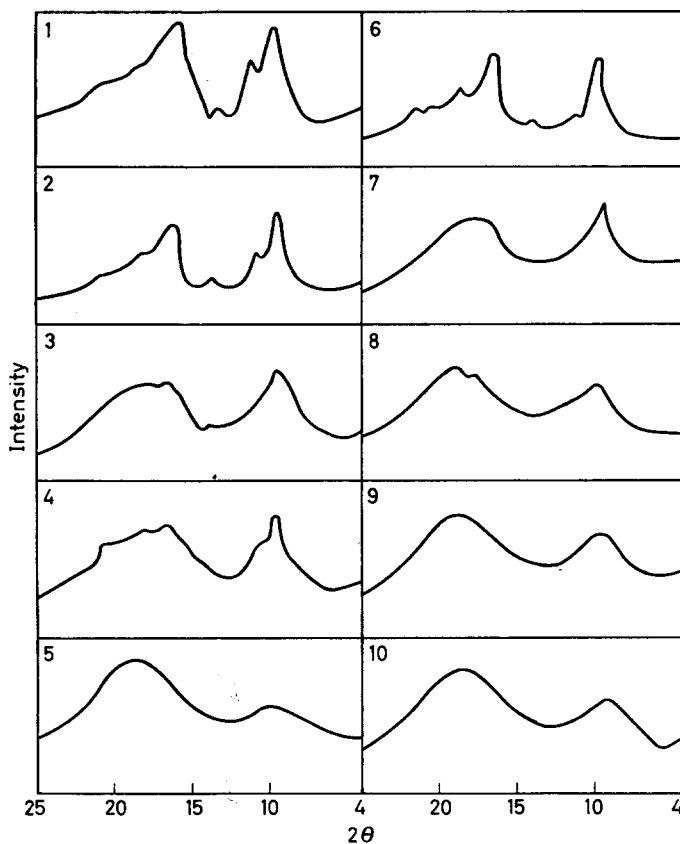
Figure 1—X-ray diffraction patterns of copolymers and homo-
polymers of styrene and 4-methylpentene-1

No.	Mole % styrene	Catalyst	No.	Mole % styrene	Catalyst
1	Poly 4-methyl-pentene-1	VOCl$_3$–AliBu$_3$	6	Poly 4-methyl-pentene-1	VCl$_3$–AliBu$_3$
2	43·0	VOCl$_3$–AliBu$_3$	7	52·3	VCl$_3$–AliBu$_3$
3	67·6	VOCl$_3$–AliBu$_3$	8	70·5	VCl$_3$–AliBu$_3$
4	80·7	VOCl$_3$–AliBu$_3$	9	82·0	VCl$_3$–AliBu$_3$
5	100·0	VOCl$_3$–AliBu$_3$	10	100·0	VCl$_3$–AliBu$_3$

copolymers of 4-methylpentene-1 and styrene the typical X-ray diffraction
pattern for the poly-4-methylpentene-1 persists even for samples of
copolymer containing up to 80 mole percentage of styrene units. This is
definite evidence for the presence of a stereoblock structure.

It is also interesting to note that a further trend of increase in the degree
of crystallinity of the polymer with increase in fraction number was
observed with one set of samples from the fractionation experiments,
proving that fractionation also took place with respect to crystallinity.

Values for the relative reactivity ratios were calculated from the results
obtained for the variations of copolymer composition with monomer feed

composition using the Fineman–Ross and Mayo–Lewis methods, and are shown in *Table 9*.

Table 9. Reactivity ratios
Monomer 1 = Styrene

Catalyst system	Monomer 2	r_1	r_2	r_1r_2
VCl$_3$–Al*i*Bu$_3$	Heptene-1	0·47 ± 0·05	1·34 ± 0·14	0·63
VOCl$_3$–Al*i*Bu$_3$	Heptene-1	0·43 ± 0·05	0·95 ± 0·12	0·41
VCl$_3$–Al*i*Bu$_3$	Octadecene-1	1·94 ± 0·18	0.75 ± 0·10	1·46
VOCl$_3$–Al*i*Bu$_3$	Octadecene-1	1·32 ± 0·14	0·87 ± 0·09	1·15
VCl$_3$–Al*i*Bu$_3$	4-Methylpentene-1	0·55 ± 0·10	1·23 ± 0·15	0·68
VOCl$_3$–Al*i*Bu$_3$	4-Methylpentene-1	0·49 ± 0·06	1·15 ± 0·12	0·56

DISCUSSION

Proof of copolymerization

In these investigations the presence of copolymer in the isolated products has been proved most comprehensively. The calculation of reactivity ratios for each of the monomer pairs with each of the catalyst systems, and the construction of typical copolymer composition curves, can be considered as definite proof. But the most convincing and conclusive evidence is to be found in the results of the fractionation experiments. Although a degree of heterogeneity was observed, especially in polymers prepared using the vanadium trichloride catalyst system, no fraction was obtained with any system which contained appreciable quantities of only one homopolyolefin. The differences observed in the various spectra, i.e. i.r. and X-ray diffraction, of homopolymers and of the products of attempted copolymerization have been used as evidence for the presence of copolymers with several systems[3, 4]. This is not possible in the present investigations, as the results obtained from the structural investigations carried out suggest that most of the copolymers produced are of the stereoblock type of structure, which give rise to spectra which are very similar to those obtainable from mixtures of homopolymers.

Heterogeneity and polyactivity

It can be seen that with material prepared using the vanadium oxytrichloride catalyst system, the first few fractions are of low styrene content, but the majority of the material lies between ±5 per cent of a mean value. With the polymer prepared using the vanadium trichloride catalyst, however, a much wider spread of composition was obtained.

The fairly high degree of heterogeneity observed with products of copolymerization using the vanadium trichloride catalyst system is thought to indicate the presence of catalytic sites having a wide range of activities. It has been suggested[12, 20] that these different activities may be due to the various active sites having different steric environments, which are determined by their positions on the crystal surface. The differences observed in the degree of heterogeneity of the products of copolymerization, using the two chosen catalyst systems, may be considered as evidence in favour of this hypothesis. In every case examined, the polymer prepared using the vanadium oxytrichloride catalyst was markedly more homogeneous

than the corresponding product prepared using the vanadium trichloride catalyst system. Although no work has been undertaken to determine the crystallinity of the various catalyst particles, it is possible that the particles involved in the vanadium trichloride system possess a higher degree of crystallinity than that produced by the reduction of vanadium oxytrichloride. The incidence of heterogeneous products of copolymerization may also be linked with the variation in catalyst particle size. This was established by means of photomicrographs of typical catalyst suspensions. The average particle size of the vanadium trichloride catalyst was of the order of 5 μ, whereas the particles from the vanadium oxytrichloride system were much smaller, and the appearance of the photomicrograph suggested that the majority were approaching colloidal dimensions. Thus it seems reasonable to assume that catalyst particles which are small will have a more uniform surface, which in turn would give rise to active sites having a more uniform steric environment.

The only other work reported in the literature of a similar nature is that of Overberger and Miyamichi[21]. The results obtained by these workers for similar systems are not, however, in agreement with the conclusions of this report. The reasons for these conflicting results may be found in the many differences in the preparation of the samples fractionated, the solvents used, the stirring device employed, and the method of fractionation.

The structure of the copolymers

The presence of highly crystalline copolymers has been confirmed by X-ray diffraction studies.

The presence of large blocks of the same monomer unit, added in a stereoregular manner, and interspersed with smaller groups of the second monomer unit, may give rise to a high degree of crystallinity. There is much evidence for the existence of this type of structure in the copolymers of styrene and α-olefins prepared by Burnett and Tait[11, 12], using the titanium trichloride and aluminium tri-ethyl catalyst system.

The fact that the X-ray diffraction patterns of the copolymers prepared using the vanadium oxytrichloride catalyst contain all the major peaks present in the patterns obtained for the homopolyolefins is conclusive evidence for the existence of stereoblock structures. The i.r. spectra and density determinations may also be considered as supporting evidence for this phenomenon, as these results are similar to those obtainable with mixtures of homopolymers. It is thought that the increased crystallinity observed with the vanadium oxytrichloride catalysed polymers, compared to those prepared using vanadium trichloride, may be correlated in some way with the differences in particle size. With the smaller particle, it has been proved that the types of active site available for polymerization are more uniform in activity and environment.

Reactivity ratios

These results support the conclusions reached from a consideration of the fractionation experiments. The reactivity ratio products were con-

sistently smaller when the vanadium oxytrichloride catalyst was used, indicating copolymers of a more homogeneous composition. It is thought therefore that the reduction in values observed may be correlated with the decrease in particle size as well as with the structure of the copolymer produced.

It will be realized, however, that these values are essentially a mean of the possible values which relate to each possible catalyst site of different activity, and that they cannot be considered to possess exactly the same significance as the values calculated for free-radical initiated systems. It is for this reason that no attempt is made in this paper to compare monomer reactivities in any exact way.

Department of Chemistry,
University of Manchester Institute of Science and Technology,
Manchester 1

REFERENCES

[1] NATTA, G., MAZZANTI, G. and PAJARO, G. *Chim. e Industr.* 1957, **39**, 733

[2] NATTA, G. *Ital. Pat. No.* 554 803, 1955

[3] NATTA, G. *Rubb. Plast. Age,* 1957, **38**, 49

[4] MAZZANTI, G., VALVASSORI, A. and PAJARO, G. *Chim. e Industr.* 1957, **39**, 743

[5] MAZZANTI, G., VALVASSORI, A. and PAJARO, G. *Chim. e Industr.* 1957, **39**, 825

[6] NATTA, G., MAZZANTI, G. VALVASSORI, A. and SARTORI, G. *Chim. e Industr.* 1958, **40**, 717

[7] NATTA, G., MAZZANTI, G. VALVASSORI, A. and SARTORI, G. *Chim. e Industr.* 1958, **40**, 896

[8] NATTA, G., MAZZANTI, G., VALVASSORI, A. and PAJARO, G. *Chim. e Industr.* 1959, **41**, 764

[9] NATTA, G., MAZZANTI, G., VALVASSORI, A., SARTORI, G. and BARBAGALLO, A. *J. Polym. Sci.* 1961, **51**, 429

[10] NATTA, G., DANUSSO, F. and SIANESI, D. *Makromol. Chem.* 1959, **30**, 238

[11] ANDERSON, I. H., BURNETT, G. M. and TAIT, P. J. T. *Proc. chem. Soc. Lond.* **1960**, 225

[12] ANDERSON, I. H., BURNETT, G. M. and TAIT, P. J. T. *J. Polym. Sci.* 1962, **56**, 391

[13] GEDDES, W., BURNETT, G. M. and TAIT, P. J. T. Unpublished work

[14] TAIT, P. J. T. *Ph.D. Thesis,* University of Aberdeen, 1959

[15] HALL, R. W. *Techniques of Polymer Characterization,* Butterworths: London, 1959

[16] GUZMAN, G. M. *Progress in High Polymers,* Vol. I. Heywood: London, 1961

[17] BAKER, C. A. and WILLIAMS, R. J. P. *J. chem. Soc.* **1956**, 235

[18] FLOWERS, D. L., HEWITT, W. A. and MULLINEAUX, R. D. *J. Polym. Sci. A,* 1964, **2**, 2305

[19] GAYLORD, N. G. and MARK, H. F. *Linear and Stereoregular Polymers,* Interscience: New York, 1959

[20] OVERBERGER, C. G. and NOZAKUMA, D. *J. Polym. Sci. A,* 1963, **1**, 1439

[21] OVERBERGER, C. G. and MIYAMICHI, K. *J. Polym. Sci. A,* 1963, **1**, 2021

The Polymerization of N-Vinylcarbazole by Electron Acceptors

Part I. Kinetics, Equilibria and Structure of Oligomers

J. PÁC and P. H. PLESCH

The kinetics of polymerization and the molecular weight of the polymers formed from N-vinylcarbazole (NVC) by (a) chloranil (Ch) in nitrobenzene; (b) tetranitromethane (TNM) in toluene; (c) TNM in nitrobenzene, have been studied. Only system (c) gave simple kinetics and was studied in detail. The structure of oligomers formed in the presence of transfer agents, and the effective formation constants of the relevant charge-transfer complexes were also investigated.

SCOTT et al.[1,2] and Ellinger[3-5] almost simultaneously reported the polymerization of N-vinylcarbazole (NVC) by organic electron acceptors. Subsequent work with these catalysts, with inorganic electron acceptors, and with radical–cation initiators has been mainly concerned with the chemical aspects of the polymerization and there is little kinetic or mechanistic information[6].

Part I of this paper contains results of exploratory work; kinetic and molecular weight information on the systems: NVC–tetranitromethane, (TNM)–toluene, NVC–TNM–nitrobenzene, and NVC–chloranil (Ch)–nitrobenzene (NB); determination of the stoichiometry and equilibrium constants of some of the complexes which are involved; and structural analysis of oligomers made in the presence of transfer agents. Part II contains a discussion of the results and our conclusions concerning the mechanism of these polymerizations.

EXPERIMENTAL

Materials

N-*Vinylcarbazole*—NVC was three times recrystallized from hexane, dried *in vacuo* at 30°C for two days (m.pt = 65·6°C) and finally dried by evacuation in the dilatometer at 10^{-4} torr at room temperature for 3 h. In one series of experiments the monomer was dried in toluene solution over a sodium film under vacuum. The dried solution was tipped into a tipping device[7] which was fused to the drying vessel, and the solvent was then evaporated off under vacuum, leaving the monomer dry in the phials fused to the tipping device.

Tetranitromethane—TNM was dried over barium oxide and distilled *in vacuo* into phials. Only the middle fraction (50 per cent) was collected. From these phials dilute solutions in toluene were prepared by means of a tipping device[7].

Chloranil—Ch was recrystallized from benzene and dried *in vacuo* at 50°C.

Nitrobenzene—NB was three times recrystallized from itself. About 40 per cent of the initial amount was collected, dried over barium oxide powder (24 h), and then dried and distilled under vacuum as follows. The distillation apparatus consisted of three flasks connected by magnetic break-seals and a reservoir with a metal valve. NB was placed into the first flask with alumina, degassed, and dried overnight, then distilled into the second flask containing freshly baked alumina. The first 10 per cent was collected in a third small flask and rejected. The middle 60 per cent was collected in the second flask, dried overnight on alumina, and then distilled into the reservoir fitted with a metal valve. The reservoir was finally sealed to the vacuum line (*Figure 1*). The final product was slightly yellow, $n_D^{20} = 1\cdot5525$ and $\kappa = 8 \times 10^{-7}$ mho cm^{-1}.

Toluene—Toluene was purified conventionally, dried over phosphorus pentoxide, and stored in a reservoir attached to the vacuum line under its own vapour pressure over a drying agent; phosphorus pentoxide and calcium hydride gave indistinguishable results. Before use it was degassed and refluxed for a few days.

Acetonitrile—Acetonitrile containing less than 0·05 per cent of water, was used without further purification.

Methanol—Methanol containing 0·1 per cent of water was used without further purification.

Phenyl acetate—Phenyl acetate was washed with aqueous sodium bicarbonate, dried over potassium carbonate, distilled under reduced pressure, and the middle fraction (50 per cent) was collected, b.pt 108°/48 torr.

Apparatus and technique

Dilatometry—The required amount of solid catalyst [Ch or trinitrobenzene (TNB)] was weighed into a phial which was then sealed to the vacuum line. After 2 h of evacuation at 10^{-4} torr the required volume of toluene was run into the cooled phial from a burette which formed part of the vacuum system. The phial was then sealed off. The phials with water were prepared by the method described[8].

Rate measurements were carried out at 34°C in a dilatometer A whose construction and mode of operation have been described[9-11] (*Figure 1*); in this work, however, dilatometers without electrodes were used. Into the charging arm B of the dilatometer were introduced a phial of catalyst and one of monomer, or the monomer was weighed in and then evacuated for 3 h at 10^{-4} torr. Then the solvent was run into the charging arm from the burette D and the dilatometer assembly was sealed off at C while the solvent was frozen. After temperature equilibration in the thermostat, the catalyst phial was broken magnetically, the solution was mixed rapidly, tipped into the dilatometer bulb, and the whole replaced in the thermostat. Blank experiments showed that the level in the capillary became steady after about 3 min. The change in level of the meniscus in the capillary was followed using a cathetometer. The relation between contraction in millimetres and conversion was established by weighing the polymer formed. The polymer yield and the initial amount of monomer agreed to within two per cent.
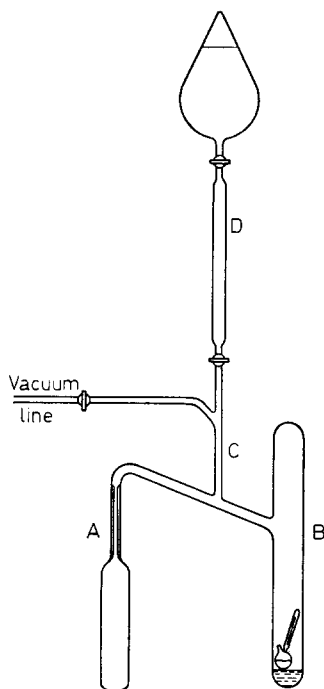
Figure 1—Assembly for filling dilatometer (A), with charging arm (B) and nitrobenzene reservoir and burette (D)

Polymer isolation—The reaction mixture was poured into excess of ethanol, the polymer was filtered off, reprecipitated from toluene solution by ethanol, and dried in a vacuum oven at 40°C.

Molecular weight determination—Molecular weights lower than 20 000 were determined with a Mechrolab vapour pressure osmometer (dioxan solution).

Molecular weights greater than 20 000 were determined from the specific viscosity at four concentrations, measured in benzene solution at 25° with a Craig–Henderson viscometer[12]. The molecular weights were calculated from Ueberreiter and Springer's equation[13] $[\eta] = 3 \cdot 35 \times 10^{-2} M^{0 \cdot 58}$.

Spectroscopy—All i.r. absorption spectra were run by conventional methods on a Perkin–Elmer model 221 spectrophotometer.

Ultra-violet and visible spectra were run on a Beckman DB u.v. spectrophotometer with 1 cm Pyrex or silica cells.

The p.m.r. spectra were run on a Perkin–Elmer model R10 spectrometer. Because of the insolubility of the polymer in carbon tetrachloride, deuterochloroform had to be used as a solvent. Tetramethylsilane was used as internal standard.

N.B. The concentrations of frequently occurring species are denoted by lower-case letters: e.g. $m = $ [NVC], $c = $ [catalyst], subscript $_0$ denotes initial, $_f$ final values.

All concentrations are in mole/litre.

The figures, tables, equations, structures and references are numbered consecutively through the Parts I and II, and the references are given at the end of Part II.

EXPLORATORY EXPERIMENTS

Qualitative work

Ellinger has described a whole range of organic electron acceptors as catalysts for the polymerization of *N*-vinylcarbazole. Polymerizations in toluene solution were generally very slow. Scott used acetonitrile as solvent, in which the polymerizations were fast, but the polymer is not soluble. Thus, for kinetic measurements one problem was to find a catalyst–solvent combination which would give fast and homogeneous polymerization. Several polymerizations in three different solvents and with four different catalysts were carried out.

Table 1 shows the results, on the basis of which the following three systems were chosen for kinetic measurements: (*a*) Ch–NB, (*b*) TNM–toluene, (*c*) TNM–NB.

After some kinetic work systems (*a*) and (*b*) proved to be too intractable, but (*c*) gave simple kinetics and it was therefore studied in greater detail.

Table 1. Data for the qualitative exploratory experiments. Monomer concentration $m_0 = 0.52$ M; temperature 60°C

No.	Solvent	Catalyst	c_0 (M)	Time (min)	Yield (%)
1	Toluene	—	—	100	0
2	Toluene	Ch	4×10^{-3}	240	2
3	Toluene	*Sym.* TNB	1×10^{-2}	160	Traces
4	Toluene	TCE†	4×10^{-2}	90	60
5	Toluene	TNM	5×10^{-2}	150	44
6	Ethylene dichloride	—	—	100	26
7	Ethylene dichloride	—	—	100	Traces*
8	Ethylene dichloride	Ch	3×10^{-3}	70	Traces*
9	Nitrobenzene	—	—	70	0
10	Nitrobenzene	Ch	6×10^{-3}	46	80
11	Nitrobenzene	TNM	5×10^{-3}	50	100

*Ethylene dichloride treated with barium oxide.
†TCE denotes tetracyanoethylene.

POLYMERIZATION IN NB BY CHLORANIL

The rate of polymerization

In order to determine whether there were any catalytic impurities in the solvent or on the walls of the dilatometer, observations were always made for at least 30 min, before the catalyst phial was broken; no noticeable polymerization was found. The results are shown in *Table 2*. All reactions went to completion and the conversion curves gave good first order plots. The rate constants k_1' defined by the equation

$$-dm/dt = k_1' m \qquad (1)$$

are in *Table 2*.

Table 2. Polymerization in NB catalysed by Ch; temperature 34°C

No.	m_0 (M)	$10^3 c_0$ (M)	$10^4 k'_1$ (sec^{-1})	10^3 Mol. wt
82	0·139	3·173	3·56	19·1
81	0·186	3·099	5·71	—
84	0·186	2·970	3·90	22·6
80	0·243	3·020	3·63	24·8
83	0·314	3·010	3·03	26·0
87	0·387	3·130	2·65	26·1
85	0·762	3·110	1·82	29·6
88	0·522	2·950	0·78	—
58	0·064	2·020	1·73	—
56	0·123	1·520	1·76	—
52	0·129	1·534	3·08	18·2
55	0·168	1·505	2·26	—
51	0·263	1·530	1·68	24·0
92	0·149	0·894	2·33	—
91	0·189	0·865	1·92	21·8
93	0·218	0·924	2·30	—

Figure 2 shows the dependence of k'_1 on m_0. The curve has a maximum at $m_0 = 0·18$ to $0·19$. In order to establish the reaction order with respect to catalyst, the dependence of k'_1 on m_0 at different catalyst concentrations was measured. The reason for this was that the position of the maximum of the curve in *Figure 2* might have depended on the catalyst concentration, so that the results obtained at one monomer concentration would have been misleading.

The results in *Table 2* and others not included here indicated that the rate depends approximately on $c_0^{\frac{1}{2}}$. *Figure 3* shows the dependence of $k'_1/c_0^{\frac{1}{2}}$ on m_0 for three different values of c_0. Unfortunately the reproducibility of these measurements was not good and thus the order with respect to catalyst is somewhat uncertain. For the same reason the position of the maxima in *Figure 3* at different catalyst concentrations could not be determined with certainty.

Our many experiments aimed at improving reproducibility had little
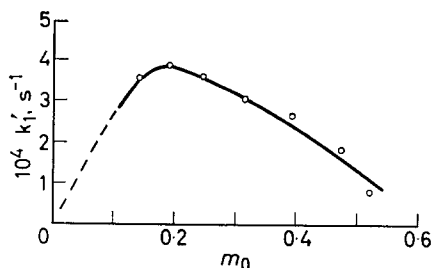
Figure 2—System Ch–NB. Dependence of first order rate constant k'_1 on initial monomer concentration m_0 at $c_0 = 3 \times 10^{-3}$ (*Table 2*)
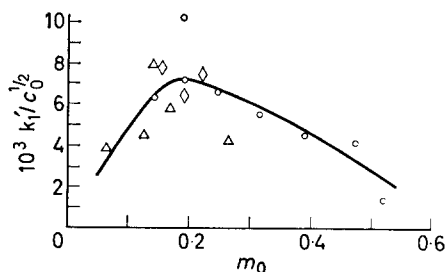
Figure 3—System Ch–NB. Dependence of $k'_1/c_0^{\frac{1}{2}}$ on m_0 at different catalyst concentrations (*Table 2*). $c_0 = 9·0 \times 10^{-4}$ (◇), $1·5 \times 10^{-3}$ (△), $3·0 \times 10^{-3}$ (○)

success. Daylight accelerates the polymerization slightly but the reproducibility was not improved by keeping reaction mixtures dark. A white deposit, possibly boron oxide (B_2O_3), which was occasionally formed when the charging arm was sealed off, had a slight retarding effect. Different methods of drying the monomer, such as drying it in toluene solution with a sodium mirror, or evaporation of the toluene solution and subsequent evacuation for several hours, or drying the solid monomer under vacuum in the dilatometer, had virtually no effect.
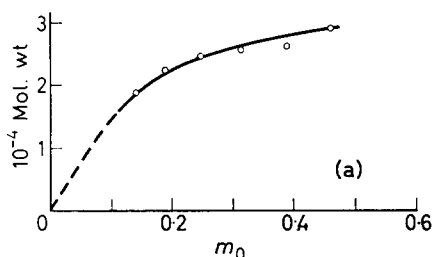
Figure 4(a)—System Ch–NB. Dependence of molecular weight measured at complete conversion on initial monomer concentration (*Table 2*)
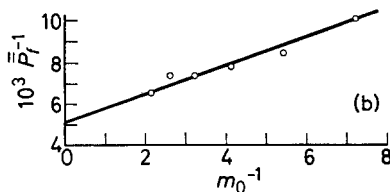
Figure 4(b)—The First Mayo Plot corresponding to *Figure* 4(a)

The molecular weights

Figure 4(a) shows the increase of the molecular weight at complete conversion ($\overline{\overline{P}}_f$) with m_0 at constant $c_0 = 3 \times 10^{-3}$. *Figure* 4(b) shows the First Mayo Plot ($1/\overline{\overline{P}}_f$ versus $1/m_0$) to be a good straight line. This result implies that the propagation is of higher order in monomer than zero and indicates a chain transfer reaction which is of lower order in monomer than the propagation. The catalyst concentration has no effect on the molecular weight (*Table 2*).

POLYMERIZATION IN TOLUENE BY TNM

This system was studied in order to establish the effect of a solvent of low polarity on the polymerization rate and molecular weights. All results are in *Table 3*.

Table 3. Polymerization in toluene catalysed by TNM; temperature 34°C

No.	m_0 (M)	$10^2 c_0$ (M)	$10^3(-dm/dt)_{01}$ (M min^{-1})	$10^3(-dm/dt)_{02}$ (M min^{-1})	$m_0 - m_1$ (M)	$m_0 - m_f$ (M)	Mol. wt
99	0·525	2·25	4·78	0·69	0·019	0·206	1 920
100	0·617	5·13	11·50	2·60	0·052	0·343	1 960
101	0·515	3·76	7·30	1·35	0·035	0·254	1 610
102	0·510	6·12	14·90	3·47	0·057	0·292	1 650
103	0·319	3·81	8·73	0·96	0·052	0·205	1 680
104	0·790	3·55	7·35	2·21	0·025	0·434	1 960
105	0·592	2·75	6·30	1·13	0·027	0·256	—
105a	0·336	3·14	5·60	0·18	0·054	0·083	—

m_1 is the monomer concentration at the end of the first, rapid, phase.
m_f is the monomer concentration when the polymerization has ceased.
Expt 105a is a second polymerization started in reaction mixture 105 when the first polymerization had ceased, by addition of a second dose of catalyst.
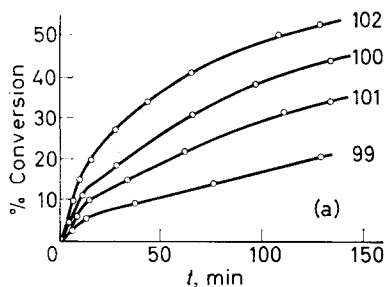
Figure 5(a)—Conversion curves of polymerizations in toluene by TNM at constant m_0 with varying c_0 (*Table 3*)
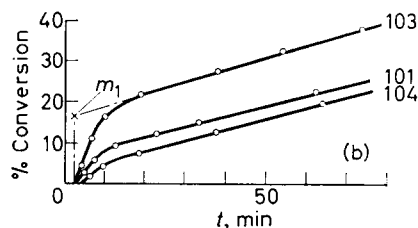
Figure 5(b)—Conversion curves of polymerizations in toluene by TNM at constant c_0 with varying m_0 (*Table 3*)

The originally dark red colour of the polymerizing solution turned bright orange at the end of the incomplete polymerization. This suggests that the catalyst is consumed, i.e. a termination reaction.

Figures 5(a) and (b) show the conversion curves at constant monomer concentration with varying catalyst concentration, and at constant catalyst concentration with varying monomer concentration. These curves are unusual in that the rate is very high during the first few per cent of conversion and then decreases sharply. The polymerizations were always incomplete, which also indicates existence of a termination reaction. The initial rate in the first phase, $-(dm/dt)_{01}$, increases linearly with c_0 and is independent of m_0 (*Figure 6*); therefore the rate of polymerization during the first phase appears to obey the equation

$$-(dm/dt)_{01} = kc_0 \qquad (2)$$

The kinetic analysis of the second phase of the polymerization is uncertain because, since there is a termination reaction, the catalyst concentration is unknown after the start of the polymerization. *Figures 7* and *8* indicate that the reaction is of second order with respect to the initial catalyst concentration and probably of first order in monomer.

Figure 6—System TNM–toluene. Dependence of initial rate $(-dm/dt)_{01}$ in first phase of polymerization on c_0 (*Table 3*)

243
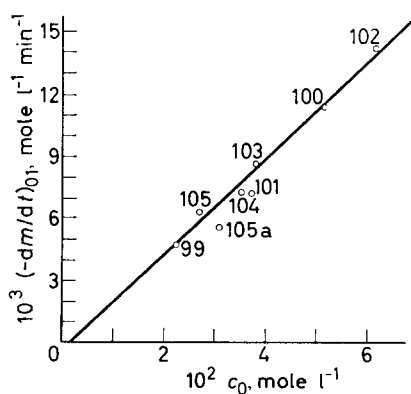
The other parameters which could be employed in kinetic analysis are the conversions during the first and second phases of the polymerization and the total conversion (*Table 3*). The yield in the first phase, $(m_0 - m_1)$, increases with c_0 and decreases with m_0. The latter result suggests the participation of monomer in the termination. The final conversion $(m_0 - m_f)$ increases both with m_0 and c_0. These results show that the polymerization mechanisms in the first and second phases are very different and complex.
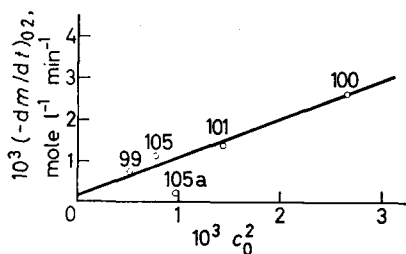
Figure 7—System TNM–toluene. Dependence of initial rate $(-\mathrm{d}m/\mathrm{d}t)_{02}$ in second phase of polymerization on c_0^2

(Table 3)
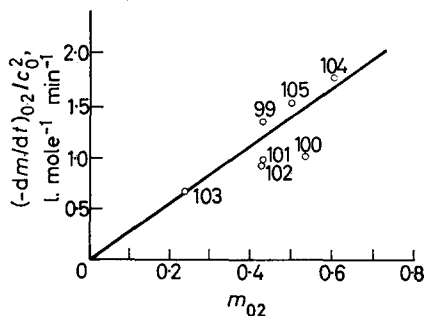
Figure 8—System TNM–toluene. Dependence of $(-\mathrm{d}m/\mathrm{d}t)_{02}/c_0^2$ on m_0 at beginning of second phase of polymerization, when $m = m_{02}$ (*Table 3*)

These reactions are characterized by a dominant termination reaction. In order to find out whether the polymerization stops for lack of catalyst, an experiment with a second addition of catalyst was carried out (*Table 3, expt 105a*). The first phase of the second polymerization is not affected by the polymer from the first polymerization. Both $-(\mathrm{d}m/\mathrm{d}t)_{01}$ and $(m_0 - m_1)$ are consistent with the other experiments. The rate in the second phase is much lower than that in the first polymerization. This experiment confirms that catalyst is consumed during polymerization. Molecular weights are generally very low compared to those obtained with the other systems described here, and they show no obvious dependence on m_0 or c_0 (*Table 3*).

POLYMERIZATION BY TNM IN NB

The rate of polymerization

Preliminary experiments showed that the polymerization of NVC by TNM in NB is reasonably reproducible and obeyed simple kinetics and therefore it was chosen for a detailed study. All the results are in *Table 4*. Typical conversion curves with and without addition of water are shown in *Figure 9*. After a short acceleration period, both reactions are of first order with respect to monomer. The first-order rate constant k_1' defined by equation (1) depends linearly on the initial catalyst concentration (*Figure 10*), so that

$$k_1' = k_1 c_0 \tag{3}$$

From all experiments the average $k_1 = 11 \cdot 0 \pm 1 \mathrm{M}^{-1} \sec^{-1}$.

244

Because k_1 is independent of the initial monomer concentration the rate of the polymerization is given by the following equation

$$-dm/dt = 11c_0 m \quad M^{-1} sec^{-1} \tag{4}$$

Table 4. Polymerization in NB solution catalysed by TNM; temperature 34°C

No.	m_0 (M)	$10^5 c_0$ (M)	$10^3 k_1'$ (sec^{-1})	k_1 ($M^{-1} sec^{-1}$)	10^{-4} Mol. wt	$10^2 [H_2O]$ (M)	$\frac{[H_2O]*}{[P]_f}$
150	0·091	6·28	0·625	9·95	3·34		
142	0·135	5·74	0·634	11·04	4·90		
136	0·162	14·17	1·610	11·36	6·37		
135	0·285	14·17	1·535	10·83	7·70		
144	0·339	5·72	0·609	10·64	8·54		
137	0·442	14·16	1·340	9·46	9·30		
139	0·279	4·39	0·597	13·59	—		
141	0·285	5·73	0·562	9·86	—		
148	0·280	6·20	0·622	10·03	6·86		
138	0·291	7·11	0·900	12·60	7·25		
140	0·274	10·0	1·120	11·14	6·70		
147	0·281	5·75	0·444	7·72	6·80	4·13	5·15
149	0·273	6·27	0·426	6·79	4·91	8·78	8·10

The average $k_1 = 11\cdot0$ M^{-1} sec^{-1}.

*$[P]_f$ is the concentration of macromolecules at the end of the polymerization.
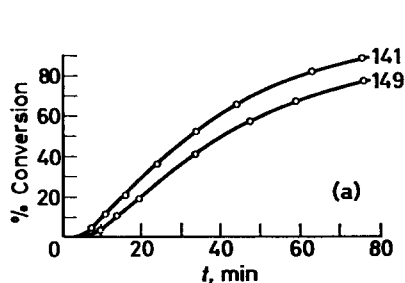
Figure 9(a)—Typical conversion curves of polymerizations in NB by TNM with (149) and without (141) addition of water (*Table 4*)
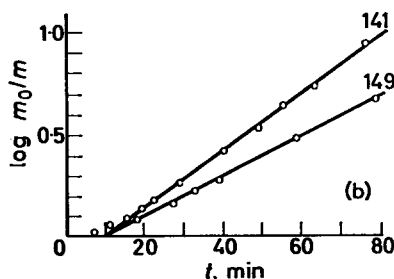
Figure 9(b)—First order plots of polymerization experiments 149 and 141 (*Table 4*)
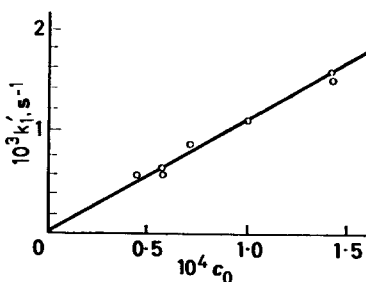
Figure 10—System TNM–NB. Dependence of first order rate constant k_1' on c_0 (*Table 4*)
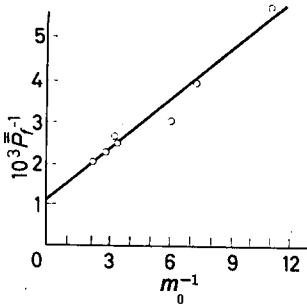
Figure 11—The First Mayo Plot for the DP at complete conversion (Table 4)

The effect of water on k_1 is not very strong (Expts 147 and 149, Table 4). The polymerization rate under these conditions was reduced by half at the concentration ratio of water to catalyst $[H_2O]/c_0 = 160$ (Table 4). This means that the basicity (nucleophilicity) of the monomer and water cannot be much different. .

The molecular weights

The curve relating the molecular weight at complete conversion, $\overline{\overline{P}}_f$, to the monomer concentration is similar to *Figure 4*(a) and it gives a straight First Mayo Plot (*Figure 11*). This means that at least one of the chain-breaking reactions must be of lower order in monomer than the propagation. $\overline{\overline{P}}_f$ is independent of the catalyst concentration (*Table 4*), which means that chain breaking reactions with catalyst or catalyst fragments are unimportant in this system.

Finally, the slight decrease of molecular weight with conversion (*Table 5*) suggests that chain breaking by monomer (transfer and/or termination) is the most important chain-breaking reaction and is of the same order in monomer as the propagation.

Expts 147 and 149 (*Table 4*) show the slight decrease of the molecular weight with water concentration. This fact is in favour of the view that chain breaking with monomer is predominant; in other words, the reactivities of monomer and water towards an active centre are of comparable magnitude.

Second addition of monomer

In order to establish whether there is any termination reaction in this system, two experiments with second addition of monomer (in toluene

Table 5. Change of molecular weight with conversion

No.	m_0 (M)	$10^5 c_0$ (M)	Conversion (%)	10^{-5} Mol. wt
155	0·444	6·30	20	1·41
154	0·444	6·24	33	1·34
153	0·447	6·22	50	1·28
151	0·448	6·24	60	1·30
152	0·442	6·28	79	1·19
157	0·442	14·16	100	0·930

solution) were carried out. The results in *Table 6* show about 50 per cent decrease of k_1 in the second polymerization. Both second polymerizations gave good first order plots. It will be shown below that termination is only partly responsible for the lower rate in the second polymerization and that the formation of the polymer–catalyst and toluene–catalyst complexes plays an important role in this system.

Table 6. Second addition of monomer

No.	m_{01} (M)	m_{02} (M)	$10^5 c_{01}$ (M)	$10^5 c_{02}$ (M)	$(k_1)_1$	$(k_1)_2$
					$(M^{-1}$ $sec^{-1})$	
158	0·260	0·238	5·50	5·22	10·90	5·40
159	0·245	0·240	5·42	5·18	9·85	4·23

The subscripts 01 and 02 denote beginning of first and second polymerizations.

STOICHIOMETRY AND ASSOCIATION CONSTANTS OF COMPLEXES OF CATALYSTS WITH MONOMER AND POLYMER

All the initiation mechanisms which have been put forward for the polymerization of NVC by electron acceptor catalysts involve formation of a charge transfer complex between monomer (M) and catalyst (C). Under favourable conditions this complex might form radical-ion pairs and free radical ions. The following equilibria describe the system:

$$n_1 M + n_2 C \overset{K_1}{\rightleftharpoons} n_3 X_1 \overset{K_{II}}{\rightleftharpoons} n_3 (.M^+.C^-) \overset{K_{III}}{\rightleftharpoons} n_3 (.M^+) + n_3 (\cdot C^-) \qquad (5)$$
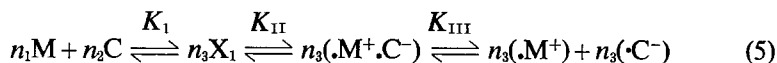
It is known that K_{II} and K_{III} for such complexes are comparable with K_1 only for strong electron acceptors and donors in polar solvents[14]. Inevitably the magnitude of all equilibrium constants would to a great extent determine the initiation mechanism. Moreover, the polymer can also form a charge transfer complex with the catalyst

$$n_4 C + n_5 P \overset{K_2}{\rightleftharpoons} n_6 X_2 \qquad (6)$$

Here, P represents a polymerized monomer unit. If K_2 is comparable with K_1 the complex X_2 must be considered in the reaction mechanism, because it will alter the concentration x_1 of the monomer complex X_1 in the course of polymerization.

Therefore in the first instance the spectroscopic determination of K_1 and K_2 for the systems studied was considered. However, the determination of K_1 was possible only for TNM in toluene and for Ch in NB, for which the rate of polymerization is low and the decrease of monomer concentration during the measurement could be neglected. The charge transfer bands in the visible region were used for the determination of K_1 and K_2. The method described by Moore and Anderson[15] is based on measurements of optical densities of the charge transfer band when one of the components is in excess and altered and the other is kept constant.

If all the stoichiometric coefficients n are equal to one, the mathematical formulation of this method for K_1 is given by the equation (7).

$$\frac{c_0 b}{D} = \frac{1}{K_1 \epsilon m_0} + \frac{1}{\epsilon} \tag{7}$$

where D denotes optical density of X_1 at wavelength λ, ϵ is the extinction coefficient at λ, and b denotes cell length (cm); c_0, m_0, p_0 denote the nominal concentrations of catalyst, monomer and monomeric units in polymer. From the slope and intercept of the straight line plots according to equation (7) K_1 and ϵ can be calculated.

Complexes of TNM with monomer and polymer in toluene

In this system not only the complexes between catalyst and monomer and polymer are formed, but also a complex between catalyst and toluene. Therefore equation (7) for the calculation of K_1 cannot be applied directly, but the method can be extended for a system which involves two 1 : 1 complexes. From the equilibria:

$$M + C \overset{K_1}{\rightleftharpoons} X_1 \tag{8}$$

$$T + C \overset{K_s}{\rightleftharpoons} X_s \tag{9}$$

if $m_0 \gg x_1$ and $[T] \gg m_0$ (T denotes toluene), the expression for x_1 is

$$x_1 = K_1 m_0 c_0 / (1 + K_s' + K_1 m_0) \tag{10}$$

where $K_s' = K_s[T]$. Hence

$$\frac{bc_0}{D} = \frac{1 + K_s'}{K_1 \epsilon m_0} + \frac{1}{\epsilon} \tag{11}$$

A similar treatment for the complex X_2 gives

$$\frac{bp_0}{D} = \frac{1 + K_s'}{K_2 \epsilon c_0} + \frac{1}{\epsilon} \tag{12}$$

because the conditions $m_0 > x_1$ and $c_0 > x_2$ are always achieved by the formation of the strong catalyst–solvent complex, and therefore x_1 and x_2 are always very small. Equations (11) and (12) are similar to equation (7) and allow calculation of $K_1/(1 + K_s')$ and $K_2/(1 + K_s')$. From the first of these and equation (10) the value of x_1 at any monomer and catalyst concentrations can be calculated.

All the measurements were carried out at 20°C by the technique described at constant $c_0 = 1\cdot4 \times 10^{-2}$ and $m_0 = 8 \times 10^{-2}$ to 2×10^{-1}. For the catalyst–polymer system, $p_0 = 3 \times 10^{-2}$ and $c_0 = 10^{-1}$ to 3×10^{-1}. *Figure 12* shows the absorption spectra of the complexes of TNM with monomer, polymer and toluene. The spectra were scanned immediately after mixing in order to avoid the error arising from the slow polymerization. The optical densities of the charge transfer bands were measured at 520 mμ where the absorption of the catalyst–toluene complex was negligible.

The plots according to equations (11) and (12) gave excellent straight lines.
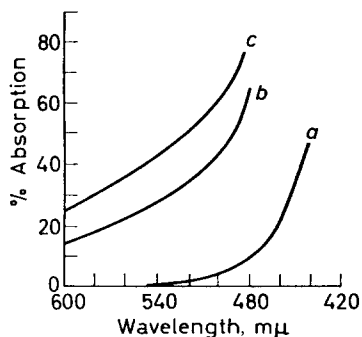
Figure 12—Absorption spectra of complexes of TNM with toluene (*a*); polymer (*b*) and monomer (*c*) in toluene solution: (*a*) $c_0 = 1.4 \times 10^{-2}$, (*b*) $c_0 = 1.4 \times 10^{-2}$; $p_0 = 3.5 \times 10^{-2}$, (*c*) $c_0 = 1.4 \times 10^{-2}$; $m_0 = 2 \times 10^{-1}$

This confirms the supposition that all the stoichiometric coefficients are equal to unity and permits calculation of $K_1/(1 + K'_5)$ and $K_2/(1 + K'_5)$ (*Table 7*). The absorption maxima of X_1 and X_2 could not be determined because they overlapped with the absorption of X_5.

Complexes of Ch *with monomer and polymer and of TNM with polymer in* NB

These systems, like the previous one, involve two equilibria. But this time the second complex is between monomer or polymer and NB (S), because this is a (weak) electron acceptor. That there is an interaction is shown by the broadening of the absorption of NB on addition of monomer or polymer.

A similar mathematical treatment of this system of equilibria:

$$M + C \underset{}{\overset{K_1}{\rightleftharpoons}} X_1 \qquad (8)$$

$$M + S \underset{}{\overset{K_3}{\rightleftharpoons}} X_3 \qquad (13)$$

and

$$P + C \underset{}{\overset{K_2}{\rightleftharpoons}} X_2 \qquad (6)$$

$$P + S \underset{}{\overset{K_4}{\rightleftharpoons}} X_4 \qquad (14)$$

on the supposition that $m_0 \gg x_1$ and $p_0 \gg x_2$, leads again to equation (11).

All the measurements were carried out at 20°C with constant $c_0 = 1.3 \times 10^{-2}$ and variable $m_0 = 4$ to 8×10^{-2}. The equilibrium in the polymer–catalyst system was measured at constant $c_0 = 1.3 \times 10^{-2}$ and variable $p_0 = 6 \times 10^{-2}$ to 10^{-1}M.

Figure 13 shows the absorption spectra of the complexes X_1 and X_2 and the spectrum of Ch. The optical densities of the charge transfer bands were measured at 500 and 540 mμ and corrected for the weak absorption of Ch and of the complexes of NB with monomer and polymer. All the plots gave excellent straight lines and their linearity again confirms the

249
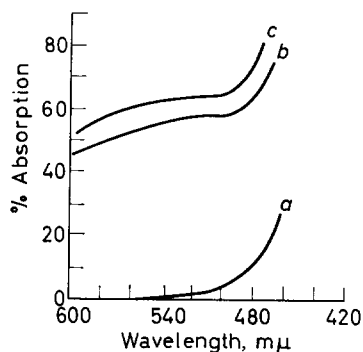
Figure 13—Absorption spectra of Ch and of the complexes of Ch with polymer and monomer in NB: (a) $c_0 = 1 \cdot 3 \times 10^{-2}$, (b) $c_0 = 1 \cdot 3 \times 10^{-2}$; $p_0 = 9 \times 10^{-2}$, (c) $c_0 = 1 \cdot 3 \times 10^{-2}$; $m_0 = 4 \times 10^{-2}$

assumed stoichiometry of the complexes. *Table 7* gives the calculated values of $K_1/(1 + K_3')$ and $K_2/(1 + K_4')$, where $K_3' = K_3[S]$ and $K_4' = K_4[S]$.

The association constant of the complex of TNM with polymer was measured at $c_0 = 3 \cdot 9 \times 10^{-2}$M and $p_0 = 8 \times 10^{-2}$ to $1 \cdot 7 \times 10^{-1}$M. The linearity of the plot confirms that the complex is $1 : 1$.

The absorption maxima of X_1 and X_2 could not be determined because they overlapped with absorptions of X_3 or X_4.

Spectra of charge transfer complex between Ch and monomer in acetonitrile and acetonitrile–water mixtures

It is known that N,N'-tetramethyl-p-phenylenediamine and Ch form a charge transfer complex which in a polar solvent, like acetonitrile, dissociates to radical ions. The absorptions at 422 mμ ($\epsilon = 10^3$) and at 448 mμ ($\epsilon = 1 \cdot 5 \times 10^3$) were attributed to the relatively stable Ch radical anion[14]. The known absorption of the Ch radical anion offered the opportunity to see whether the charge transfer complex of NVC and Ch under the same conditions gives rise to radical ions.

The spectrum showed the absorption of the charge transfer complex ($\lambda_{\text{max.}} = 488$ mμ), but no absorption of radical ions. On the addition of ten

Table 7. The 'effective' association constants of complexes of catalysts with monomer and polymer; temperature 20°C

Donor Acceptor Solvent	TNM monomer T	TNM polymer T	Ch monomer NB	Ch polymer NB	TNM polymer NB
λ (mμ)	520	520	500	540	540
ϵ (l./mole cm)	500	714	330	232	92
$K_1/(1 + K_5')$	0·19				
$K_2/(1 + K_5')$		0·09			
$K_1/(1 + K_3')$			2·52		
$K_2/(1 + K_4')$				1·14	0·45

$K_3' = K_3 [S], \quad K_4' = K_4 [S], \quad K_5' = K_5 [T].$

TNM, Ch, T and NB denote tetranitromethane, chloranil, toluene and nitrobenzene. The values of association constants are expressed in (l./mole).

per cent of water to the acetonitrile, the absorption at 488 mμ was strongly enhanced and a poorly resolved peak at 448 mμ appeared (radical anion). With 20 per cent of water this peak at 448 mμ was quite clear, and after 15 minutes the charge transfer band had decreased and the peak at 448 mμ had become more prominent. This is a very important phenomenon for the initiation reaction because it indicates that if the monomer radical cation is the iniating species, the rate of initiation will be very low. The approximate estimation of the radical anion concentration in the experiments described by means of Foster's value[14] for the extinction coefficient gives a value of 3×10^{-6} to 3×10^{-5} M. These results show that there is a reasonable possibility of radical ion formation in polar solvents like NB but the concentration should be expected to be very low.

PREPARATION AND STRUCTURE OF OLIGOMERS
Oligomers prepared in acetonitrile

Since end group analysis is very useful for the diagnosis of polymerization mechanism, we aimed at preparing oligomers from NVC on which quantitative end group analysis would be possible. After a few polymerizations in NB with TNM in the presence of suitable chain-transfer agents NB had to be abandoned, because oligomers could not be precipitated with ethanol, and precipitation by ethanol–water (1:1) mixture always yielded an intractable emulsion. Therefore we selected acetonitrile as an alternative solvent of high polarity and reasonable water solubility. The next problem was the choice of a transfer agent which would produce easily determinable end groups. After a number of experiments with esters (ethyl, benzyl, phenyl acetates), methanol and water, only the last two compounds were found to be sufficiently reactive at low concentrations to produce oligomers with two to five units. Phenyl acetate was the most reactive of the esters, but very high concentrations had to be used to obtain pentamer.

All the polymerizations with methanol were carried out at room temperature in the dark with $m_0 = 0.43$, [TNM] $= 8 \times 10^{-3}$ to 5×10^{-1}, and [MeOH] $= 0.3$ to 1.0. The oligomers were precipitated and re-precipitated with 50 per cent methanol–water mixture, and dried at room temperature under vacuum for at least five hours. Even after the re-precipitation the oligomers still contained some complexed TNM. 9-(1'-Methoxyethyl)-carbazole, which was required as a reference compound, was prepared by addition of TNM to a solution of NVC in methanol and was isolated by precipitation with water.

A quantitative analysis for CH_3 end groups by p.m.r. spectroscopy, and for OCH_3 end groups by i.r. spectroscopy on oligomers of DP between one and five showed that each molecule contained one end group of each kind, so that they have the expected structure (A)

$$CH_3CHNR_2\text{—}[CH_2CHNR_2]_n\text{—}OCH_3 \qquad (A)$$
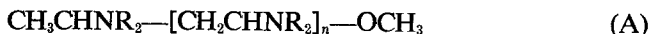
where NR_2 denotes carbazyl. The same end groups, in the same proportions, were found in similarly prepared oligomers when 2×10^{-2} M Ch or 5×10^{-2} M hydrochloric acid were used as catalysts.

Polymerization by TNM in acetonitrile in the presence of phenyl acetate

($m_0 = 0 \cdot 08$, $c_0 = 10^{-2}$, $[PhO_2CCH_3] = 1 \cdot 6$) gave oligomers of $DP = 5$, and p.m.r. analysis showed them to have the structure (B)

$$CH_3 \cdot CO \cdot [CH_2CHNR_2]_n - OPh \qquad \text{(B)}$$
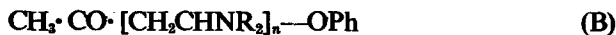
One point common to all polymerizations in the presence of transfer agents should be stressed: that in order to prepare oligomers a very high concentration of transfer agent had to be used, regardless of the type of catalyst studied. This again shows the very high basicity of the monomer.

Oligomers prepared in toluene

Polymerizations in toluene did not go to completion, even at catalyst concentrations as high as 6×10^{-2}. This fact definitely rules out the possibility of termination by impurities which cannot have been present in this range of concentration. Therefore, unless there is a spontaneous decay of the active centre into an inactive form, termination with monomer or polymer should be considered. The aim of this study was to establish the polymer structure, which might give an indication about the termination reaction.

The polymerization was carried out at 33°C at $m_0 = 0 \cdot 42$ and with TNM, $c_0 = 0 \cdot 2$, in toluene solution. The reaction was followed by means of p.m.r. spectroscopy, and at the end of the reaction the p.m.r. spectrum of the oligomers was examined in deuterochloroform (CDCl$_3$) solution. During the reaction the gradual disappearance of the $=CH_2$ group was clearly visible, and concurrently there appeared absorptions, also present in the spectrum of the isolated oligomers, which could only belong to olefinic protons of a vinyl group. One way (probably the only way) in which such a group, giving the observed spectrum, could be formed is by reaction of a growing centre not with the vinyl group, but with the nitrogen of the monomer, giving a quaternary ammonium ion as a stable terminal group, of structure (C)

$$-CH_2 \cdot CHNR_2 \overset{+}{-} NR_2CH : CH_2 \qquad \text{(C)}$$

In fact the p.m.r. spectrum is compatible with structure (C), but not with any other type of unsaturation. The i.r. spectrum also showed the absorptions expected from this structure, at 1 645, 895 and 800 cm^{-1} (vinyl group in monomer 1 640, 963 and 866 cm^{-1}).

Part II. Discussion

J. Pác and P. H. Plesch

The results reported in Part I indicate that the polymerizations in NB are cationic, and they are shown to be incompatible with the theories suggested by others. The molecular weight results show chain-breaking by monomer to be dominant, and by water to be unimportant. The kinetics are explained in detail in terms of a slow initiation by ionogenic dissociation of the charge transfer complex between monomer and catalyst, with a termination by monomer maintaining an (almost) constant, very low, concentration of rapidly growing chains.

MECHANISM

THE phenomenology of the polymerizations set out in Part I suggests that the complex between monomer and catalyst is the primary species involved in the initiation reaction. Consequently one needs to consider whether the propagating species itself is of the same kind, or whether it is a radical-cation formed by dissociation of the complex, or whether it is a radical or a cation. We will show that all our evidence is compatible with a cation being the propagating species and that some of it, at least, is not compatible with any of the alternative theories; this applies particularly to the polymerizations by TNM in NB, to which system the discussion in this section is essentially confined.

The initiation

The concentration x_1 of the complex X_1 between TNM and NVC cannot be calculated precisely because we could not measure $K_1/(1+K_3')$ for this system. However, the information in *Table 7* allows us to estimate that it will be of the order of unity, so that x_1 will be of the order of magnitude of C_0, but smaller.

From the results obtained concerning formation of the Ch radical anion in acetonitrile from Ch and NVC we may infer the formation of radical-cations and -anions also from TNM and NVC in NB. A direct spectroscopic check on this inference was not possible because of the overlapping of spectra. The analogy with the Ch–acetonitrile system also suggests that the ionogenic dissociation of the TNM–NVC complex will be similarly slow. Others[6, 16] have recorded that very similar dissociations are also quite slow, and an explanation of the slowness of these dissociations has been given[17].

The most probable fate of the radical cations thus formed is that possibly before, and certainly after, the first propagation step the radical function becomes inactivated by reaction with excess catalyst, which is a well-known radical trap; *thereafter the cation sets off a normal cationic propagation reaction.* Combination of radicals to give a bi-cation growing by amphibainic* propagation is very unlikely in view of the great excess of catalyst over growing ends. The structures of the oligomers formed in the presence of transfer agents are those which would be expected for propagation by a cation, and it will be shown below that they are not easily, if at all, compatible with other types of propagation. A purely cationic propagation is further supported by the identical results obtained in transfer experiments with the catalysts TNM, Ch and hydrochloric acid. Our view of the initiation is therefore formulated thus (C denotes catalyst):

$$NVC + C \overset{K_1}{\rightleftharpoons} X_1 \quad \text{established rapidly} \qquad (15)$$

$$X_1 \overset{k_i}{\longrightarrow} NVC^{\cdot +} + C^{\cdot -} \quad \text{slow} \qquad (16)$$

$$NVC^{\cdot +} + NVC \longrightarrow {}^{\cdot}(NVC)_2^+ \quad \text{fast} \qquad (17)$$

$${}^{\cdot}(NVC)_2^+ + C \longrightarrow {}^{\cdot}C(NVC)_2^+ \quad \text{fast} \qquad (18)$$

---
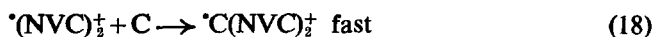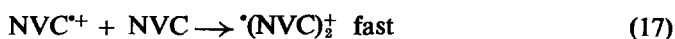
*Amphibainic means going both ways.

Reaction (16) is rate determining; reaction (18) represents the inactivation of the radical function by the excess catalyst.

Propagation and chain breaking reactions

The molecular weight measurements lead to the following conclusions concerning the propagation and chain breaking reactions:

(a) Neither the catalyst, nor any species whose concentration is proportional to that of the catalyst, takes any part in chain breaking reactions.

(b) The chain breaking with monomer is the predominant reaction, and it must be of the same order in monomer as the propagation.

(c) One of the chain breaking reactions must be of lower order in monomer than the propagation.

Because of the manner in which the molecular weight increases with m_0, the propagation cannot be of zero order in monomer[18], and therefore we conclude that propagation is of first order in monomer. It follows from (b) that the transfer and/or termination with monomer must be of the same order. Termination by monomer must be relatively unimportant because all the polymerizations were complete and did not show any noticeable deceleration at higher conversion. On the other hand, under the usual polymerization conditions the concentration of polymer at the end of the reaction is about five times higher than c_0 and therefore monomer transfer must be faster than termination. Also, we will show below that in the experiments with a second addition of monomer only 10 to 20 per cent of the decrease of the rate can be attributed to the loss of catalyst during the first polymerization.

Conclusion (c) suggests some chain breaking reactions other than with monomer, e.g. impurities in the solvent or with water. However, one characteristic feature of these polymerizations is that the monomer seems to be the most basic substance in the system and therefore the transfer even with water is relatively unimportant; as will be shown later, consumption of water is so slow that the water concentration can be considered to be virtually constant throughout the reaction. The chemistry of the propagation and chain breaking reactions can be written as follows (NR_2 denotes carbazyl):

Propagation:

$$\overset{+}{-}CHNR_2 + CH_2{=}CHNR_2 \overset{k_p}{\longrightarrow} -CHNR_2CH\overset{+}{.}CHNR_2 \qquad (19)$$
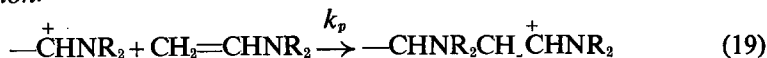
Monomer transfer:
Either:

$$-CHNR_2{-}CH_2{-}\overset{+}{C}HNR_2 + CH_2{=}CHNR_2 \overset{k_m}{\longrightarrow}$$

$$-CHNR_2{-}CH{=}CHNR_2 + CH_3{-}\overset{+}{C}HNR_2 \qquad (20a)$$

Or:

$$-CHNR_2{-}CH_2{-}\overset{+}{C}HNR_2 + CH_2{=}CHNR_2 \overset{k_m}{\longrightarrow}$$

$$-CH_2CHNR_2{-}\overset{+}{C}_{12}H_8{=}N{\cdot}CH{=}CH_2 \overset{M}{\longrightarrow}$$

$$-CH_2CHNR_2{-}C_{12}H_7{=}NCH{=}CH_2 + CH_3CHNR_2 \qquad (20b)$$

Monomer termination:

$$\overset{+}{-}CHNR_2 + CH_2\!\!=\!\!CHNR_2 \xrightarrow{k_{mt}} -CHNR_2\!\!-\!\!\overset{\displaystyle CH=CH_2}{\underset{+}{\overset{|}{N}R_2}}$$ (21)

Transfer with water:

$$-\overset{+}{C}HNR_2 + H_2O \xrightarrow{k_w} \quad -CH(NR_2)\overset{+}{O}H_2 \xrightarrow{\text{M}} -CH(NR_2)OH + CH_3\overset{+}{C}HNR_2$$
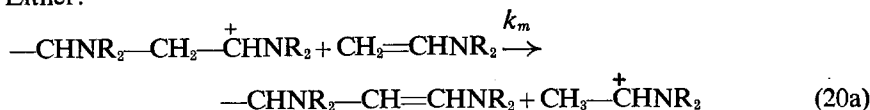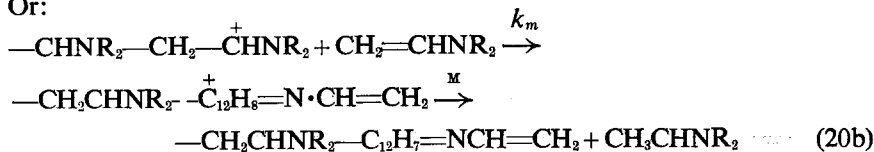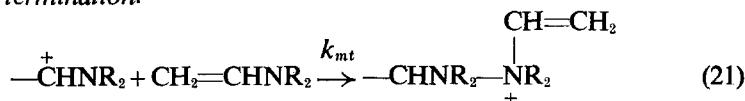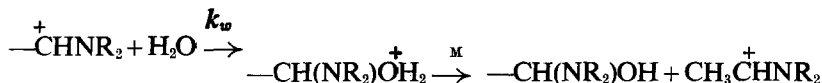
Whatever the actual charge distribution in the species $(-CH_2CHNR_2)^+$ may be, the regular structure of the polymer indicates that it reacts as if the charge were located at C_a.

Because of the high DP of the polymers, we have no evidence to indicate whether monomer transfer takes place by proton transfer from growing ion to monomer (20a), or by ring alkylation and subsequent proton transfer from the alkylated ring to monomer (20b).

The termination by monomer has been written as a quaternization because we found that this does occur in toluene solution and in the absence of evidence to the contrary it seems a reasonable extrapolation to assume its occurrence also in this system.

The mechanism of the transfer with water has been represented conventionally. It must be regarded as tentative, because we were unable to obtain clear evidence on the nature of the end groups formed in the presence of large amounts of water.

THE MOLECULAR WEIGHT

The mathematical formulation will involve the following symbols, in addition to those used previously:

k_p Rate constant of propagation
k_m Rate constant of monomer transfer
k_{mt} Rate constant of monomer termination
k_z Rate constant of transfer with impurities Z
k_w Rate constant of transfer with water
V_p Rate of propagation
V_t Total rate of chain breaking
$\bar{P}$ Degree of polymerization of the polymer formed at time t
$\bar{\bar{P}}$ Degree of polymerization up to the time t
$\bar{\bar{P}}_f$ Degree of polymerization at complete conversion
m^+ Total concentration of growing chains
z Concentration of unknown impurities Z

The rate of the propagation and chain breaking reactions is given by:

$$V_p = k_p m^+ m$$ (22)

$$V_t = (k_m + k_{mt})m^+ m + k_z m^+ z$$ (23)

Therefore

$$\bar{P} = k_p m / [(k_m + k_{mt})m + k_z z]$$ (24)

255

The expression for the measurable $\overline{\overline{P}}$ at time t is given by

$$\overline{\overline{P}} = \int dm / \int dm / \overline{P} \tag{25}$$

If z is constant, the combination of equations (24) and (25) and integration from m_0 to m gives

$$\frac{1}{\overline{\overline{P}}} = \frac{k_m + k_{mt}}{k_m + k_{mt} + k_p} + \frac{k_p k_z z}{(k_m + k_{mt} + k_p)^2} \times \frac{1}{m - m_0} \times \ln \left\{ \frac{k_z z + (k_m + k_{mt} + k_p)m}{k_z z + (k_m + k_{mt} + k_p)m_0} \right\} \tag{26}$$

Equation (26) describes the change of $\overline{\overline{P}}$ with conversion. If $\overline{\overline{P}}$ is high enough and the m at which $\overline{\overline{P}}$ is measured not too low, the following simplifications can be made:

$$k_p \gg k_m + k_{mt} \quad \text{and} \quad k_p m \gg k_z z$$

These conditions prevail in the experiments from which the dependence of molecular weight on conversion was obtained, since $\overline{\overline{P}} \approx 600$ and $m \gg 0.05$.

Therefore equation (26) can be simplified to

$$\frac{1}{\overline{\overline{P}}} = \frac{k_m + k_{mt}}{k_p} + \frac{k_z z}{k_p} \frac{1}{m_0 - m} \ln \frac{m_0}{m} \tag{27}$$

The intercept and slope of the corresponding plot (*Figure 14*) give $(k_m + k_{mt})/k_p = 1.16 \times 10^{-3}$ and $k_z z / k_p = 1.0 \times 10^{-4}$ mole/l., which show that the chain breaking with monomer is dominant. The fact that a straight line was obtained confirms the suggested chain breaking mechanisms. The term $k_z z / k_p$ should be considered as describing a transfer with substances whose concentrations are practically constant throughout the reaction, of which water is an example. Equation (27) also allows determination of the initial degree of polymerization $\overline{\overline{P}}_0 = \overline{P}_0$, because

$$\lim_{m \to m_0} [\ln (m/m_0)/(m - m_0)] = 1/m_0 \tag{28}$$

so that $1/\overline{\overline{P}}_0$ can be determined as indicated in *Figure 14*.

It has been shown that in fact the molecular weights obtained at complete conversion ($\overline{\overline{P}}_f$) give straight line Mayo plots [*Figures 4*(b) and *11*], although such plots are strictly valid only for $1/\overline{\overline{P}}_0$ or $1/\overline{P}$. This can be understood from equation (29) which is derived from equation (26) by means of the assumptions that:

$$k_p \gg k_m + k_{mt} \quad \text{and} \quad k_p m_0 \gg k_z z$$
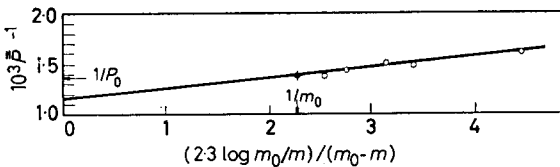
Figure 14—The plot according to equation (27)

and the condition that $m = 0$ (complete conversion).

$$\frac{1}{\overline{\overline{P}}_f} = \frac{k_m + k_{mt}}{k_p} - \frac{k_z z}{k_p}\, \frac{1}{m_0}\, \ln \frac{k_z z}{k_p m_0} \tag{29}$$

The change of $1/m_0$ with m_0 is much greater than the change of its logarithm and therefore the weight of the logarithmic term is small compared to $1/m_0$, so that equation (29) approaches a linear function for moderate changes of m_0.
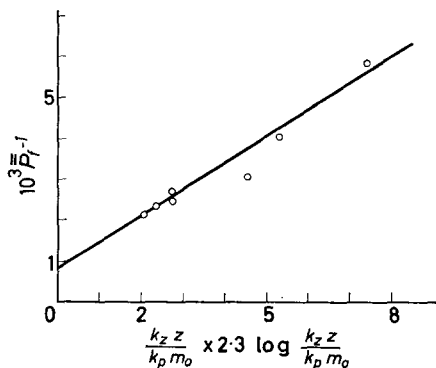
Figure 15—The plot according to equation (29)

Since we know $k_z z/k_p = 10^{-4}$, the logarithmic term in equation (29) can be calculated and so the results obtained from $\overline{\overline{P}}_f$ can be tested. The plot of $1/\overline{\overline{P}}_f$ against $(k_z z/k_p m_0)\ln(k_z z/k_p m_0)$ should give a straight line with slope unity and intercept $(k_m + k_{mt})/k_p = 1{\cdot}16 \times 10^{-3}$. Figure 15 shows that the slope is $0{\cdot}7$ and the intercept is $0{\cdot}88 \times 10^{-3}$. That these values are slightly lower than those given above is easily explained, because viscometric instead of number-average molecular weights were used to calculate $\overline{\overline{P}}_f$. Owing to the fact that the molecular weight decreases only slightly up to 80 per cent conversion, the distribution of the molecular weights up to that point is quite narrow and therefore the viscometric molecular weight is close to the number-average molecular weight. The larger decrease of molecular weight in the last 20 per cent of conversion widens the distribution, so that at complete conversion the viscometric molecular weight is higher than the number-average molecular weight, and so $1/\overline{\overline{P}}_f$ will be lower. Therefore, at lower m_0 lower values of $1/\overline{\overline{P}}_f$ are obtained, which explains the lower values of the intercept and slope in this plot. Thus the chain-breaking coefficients calculated from equation (28) are more accurate.

The assumption that z is constant throughout the reaction can be shown to be valid with the example of transfer by water. The results in Table 4 show that at the end of the polymerization the concentration of macromolecules is at the most one fifth of the initial water concentration and, because the monomer transfer is about ten times faster than any other transfer in the system, the water concentration can be considered to be

constant. The slight decrease in the rate of polymerization at comparatively high concentrations of water (up to 10^{-2} mole/l) can be explained by the formation of less active H_3O^+ ions.

The results of our experiments with transfer agents would, in principle, allow us to calculate transfer coefficients. We have not done this because in our method of isolating the oligomers always some dimer, and possibly trimer, was lost, and thus the $\overline{P}$ values we obtained are not kinetically meaningful.

KINETICS OF POLYMERIZATION IN NB

In the foregoing we concluded that most probably initiation is by radical cations, and therefore the following equilibria (each of which has been discussed before) have to be considered for an analysis of the kinetics:

$$M + C \underset{}{\overset{K_1}{\rightleftharpoons}} X_1 \tag{8}$$

$$P + C \underset{}{\overset{K_2}{\rightleftharpoons}} X_2 \tag{6}$$

$$M + S \underset{}{\overset{K_3}{\rightleftharpoons}} X_3 \tag{13}$$

$$P + S \underset{}{\overset{K_4}{\rightleftharpoons}} X_4 \tag{14}$$

$$T + C \underset{}{\overset{K_5}{\rightleftharpoons}} X_5 \tag{9}$$

where the nomenclature is as in Part I. X_5 is included, because the polymerizations were carried out in mixtures of NB and toluene (9 : 1) and TNM and Ch are known to form complexes with toluene.

From this set of equilibria, supposing that $x_1 \ll m_0$; $x_4 \ll [S]$ and $x_5 \ll [T]$, which are true under polymerizing conditions because $m_0 \gg c_0$, $[S] \gg c_0$ and $[T] \gg c_0$, the concentration x_1 of X_1 can be calculated as

$$x_1 = mc_0K(m) \tag{30}$$

where

$$K(m) = \frac{K_1}{1 + K_3'} \Big/ \left[1 + K_5' + \frac{K_1 m}{1 + K_3'} + \frac{K_2(m_0 - m)}{1 + K_4'} \right]$$

m is the total concentration of complexed and uncomplexed monomer which has not yet polymerized and $K_3' = K_3[S]$, $K_4' = K_4[S]$, $K_5' = K_5[T]$.

The formation of radical cations is given by equation (16). Ion pairs are not considered because of the low concentration of active centres and the high polarity of the solvent. It has been pointed out earlier that reaction (16) is expected to be slow and therefore the concentration of active centres would increase in the course of the polymerization. The result of that would be a non-stationary polymerization, if there were no termination. The experimental results showed that there is indeed always a short acceleration, but that thereafter the overall reaction is described by equation (31).

$$-dm/dt = k_1 c_0 m \tag{31}$$

and the propagation was found to be of first order in monomer, so that

$$- \mathrm{d}m/\mathrm{d}t = k_p m^+ m \qquad (32)$$

These two equations are valid simultaneously only if m^+ is constant and directly proportional to c_0. These conditions would be fulfilled if reaction (16) were:

either finished within the first part of the polymerization which must show an acceleration; then we would have $m^+ = c_0$; and there could be no termination (stationary state of the Second Kind);

or very slow, and a constant m^+ maintained by a termination reaction (stationary state of the First Kind).

According to Scott an equimolar mixture of hydrochloric acid and diethyl hydrogen phosphate at a concentration of 10^{-7} causes noticeable polymerization in a few minutes in acetonitrile. Therefore, the first alternative does not seem to be reasonable, because in this case the concentration of active centres $m^+ = c_0$ would be of the order of 10^{-4} for the experiments with TNM and 10^{-3} for those with Ch, the polymerization would be practically instantaneous, and the rate constants would be the same. Moreover, it has been shown above that the ionogenic dissociation of the NVC–acceptor complexes is very slow, and therefore the first alternative can be ruled out.

Furthermore, from the experiments with a second addition of monomer (*Table 6*) it can be shown that in this system a termination does exist. In both experiments the rate constant $(k_1)_2$ of the second polymerization was about half of the $(k_1)_1$ in the first polymerization. According to equation (16) this means that x_1 must have been reduced by half as well. From equation (30) it would be possible to estimate $(x_1)_1$ and $(x_1)_2$ at the beginning of the first and second polymerizations if all association constants were known. But from the analogy with Ch (*Table 7*) the value of $K_1/(1 + K_3')$ for TNM is expected to be about two. From the literature[19] K_5 is also known to be about two, and $K_2/(1 + K_4')$ was found to be 0·45 l./mole. *Table 8* shows the calculated ratio $(x_1)_2/(x_1)_1 \approx 0 \cdot 7$, i.e. the decrease in rate calculated in this way is much less than was found experimentally (0·43 and 0·49). The most unfavourable case, producing the

Table 8. Polymerizations with second addition of monomer and change of x_1

No.	$10^5 (c_0)_1$ (M)	$10^5 (c_0)_2$ (M)	$(m_0)_1$ (M)	$(m_0)_2$ (M)	$[T]_1$ (M)
158	5·50	5·22	0·260	0·238	0·81
159	5·42	5·18	0·245	0·240	0·80

$[T]_2$ (M)	$10^6 (x_1)_1$ (M)	$10^6 (x_1)_2$ (M)	$\dfrac{(x_1)_2{}^*}{(x_1)_1}$	$\dfrac{(x_1)_2\dagger}{(x_1)_1}$	$\dfrac{(k_1)_2\ddagger}{(k_1)_1}$
1·24	9·11	6·09	0·68	0·57	0·49
1·22	8·58	6·16	0·71	0·62	0·43

*Calculated from equation (30).

†Calculated for the case $K_5 \gg K_1/(1 + K_3') + K_2/(1 + K_4')$.

‡Experimental.

lowest value of this ratio, would be that in which the decrease of x_1 were caused only by the toluene which is added with the monomer in the second addition. In this case K_5 would be much greater than $K_1/(1+K_3')+K_2/(1+K_4')$. The calculation (*Table 8*) shows that then $(x_1)_2/(x_1)_1$ would be about 0·60. Therefore the *ca.* 46 per cent decrease in the rate of the second polymerization cannot be attributed only to the formation of complexes X_2 and X_5 and the difference must be attributed to a termination reaction which can consume about 10 to 20 per cent of the catalyst used. Such a termination reaction is important from the kinetic point of view, but would not have a noticeable effect on the molecular weight, which is largely controlled by monomer transfer.

The equation for the rate of formation of propagating cations can now be written as

$$d[\cdot NVC^+]/dt = dm^+/dt = k_i x_1 - k_{mt} m^+ m \tag{33}$$

Because of the known decrease of c_0 during the polymerization, c_0 in equation (30) has to be replaced by $c_0(1-\beta)$, where β is the relative decrease of c_0. If the steady state assumption is applied to equation (33), and the resultant value for m^+ is combined with the reformulated equation (30) to eliminate x_1, we obtain

$$m^+ = k_i c_0 (1-\beta) K(m)/k_{mt} \tag{34}$$

and therefore the overall rate of polymerization is given by

$$-dm/dt = k_i k_p c_0 m (1-\beta) K(m)/k_{mt} \tag{35}$$

Equation (35) would agree with the experimental equation (31) if the term

$$(1-\beta)K(m) \tag{36}$$

could be proved to be (approximately) constant throughout the reaction. This can be done by estimating the value of this term at the beginning and at the end of the polymerization, because β is known at these points. Taking a 20 per cent loss of catalyst ($\beta = 0·2$) at the end of the reaction, and $m_0 = 0·3$, $K_1/(1+K_3') = K_5 = 2$ and $K_2/(1+K_4') = 0·45$ l./mole, the calculated decrease of the term (36) at the end of the polymerization is eight per cent, so that it can indeed be regarded as constant.

Finally, the comparison of equation (35) with the experimental equation (31) shows that the rate constant k_1 is given by

$$k_1 = k_i k_p (1-\beta) K(m)/k_{mt} \tag{37}$$

and both equations show the same dependence on c_0 and m, which confirms the mechanism suggested for the polymerization by TNM in NB solution.

The polymerization catalysed by Ch showed some similarity with the system discussed. The reaction is internally of first order and gave the same relationship between molecular weight and initial monomer concentration [*Figures 4*(a) and *4*(b)]. But externally (as far as the poor reproducibility permits conclusions) it exhibited a maximum in the dependence of k_1' on m_0 (*Figures 2* and *3*). The reaction order in catalyst is very uncertain and therefore further discussion of the mechanism would not be justified at this stage.

DISCUSSION OF ALTERNATIVE MECHANISMS

Scott *et al.*[1] took the view that the reactions here under discussion are initiated by radical-cations of the Wurster type—with which we agree. However, they regarded the propagating species as of the same type, with no separation of radical and cationic functions—but they did not formulate this suggestion in detail. The only way of representing the chemistry of such a propagation involves a 1–3 hydrogen shift

$$\overset{\cdot}{C}H_2\overset{+}{C}HNR_2 + CH_2:CHNR_2 \longrightarrow CH_3CHNR_2\overset{\cdot}{C}H\overset{+}{C}HNR_2$$
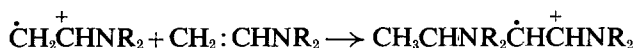
The reaction of the resultant species with a transfer agent such as phenyl acetate would presumably lead to 1,2-addition of the fragments of the transfer agent—which is contrary to our results.

These authors also argued that, because NVC could be polymerized in styrene or acrylonitrile (catalyst not stated!) without these monomers being affected, therefore radicals as such must be absent. However, this is invalid because all the organic catalysts considered in this context are well known radical traps and would sequester the radical function rapidly.

We conclude that propagation by radical-cations is very unlikely in these systems.

The reaction mechanism put forward by Ellinger[4,5] involves the complex between NVC and the electron acceptor as initiating species, and represents the propagation as a reaction of a complexed terminal double bond with a complexed monomer molecule. This scheme, like that of Scott *et al.*, involves a 1–3 hydrogen shift

$$2(CH_2:CHNR_2, C) \longrightarrow CH_3CHNR_2CH{=}CHNR_2, C + C$$

Whilst it is remotely possible that some such mechanism applies in some of the systems studied by Ellinger, it is evidently at variance with the results obtained by us: (*a*) because of our results on transfer by phenyl acetate; (*b*) because it is incompatible with the kinetics which we found.

Nomori *et al.*[6] favour the view that in the polymerization of NVC by Ch in acetonitrile the propagation involves reaction of a terminal complex with uncomplexed monomers. They do not specify details of their theory and it can be ruled out on the same grounds as those of Scott and of Ellinger. Comparison of their so-called calculation of the association constant of carbazole and Ch in toluene and in acetonitrile, with our similar studies, shows that their neglect of the interaction of Ch with toluene, and of NVC with acetonitrile, invalidates their results. Furthermore, their comparison of polymerization rate in toluene and in acetonitrile is of small utility without evidence that the kinetics of the reactions are the same— which, on the basis of our results, seems unlikely.

In conclusion, we maintain that there is no evidence from other workers which is incompatible with our view that in the systems studied by us the propagation is conventionally cationic, and that, at least for the reactions catalysed by TNM in NB, one is dealing with a kinetic situation closely similar to that in conventional radical reactions: slow initiation, balanced by a termination which maintains a (nearly) constant, very small, concentration of rapidly growing centres. However, aware of the dangers

of generalizations in this field, we claim no wide validity for our views at present and advise that each system be investigated fully before mechanistic conclusions are drawn.

Department of Chemistry,
  University of Keele,
    North Staffordshire

REFERENCES

[1] SCOTT, H., MILLER, G. A. and LABES, M. M. *Tetrahedron Letters,* **1963,** 1073
[2] SCOTT, H., KONEN, T. P. and LABES, M. M. *Polymer Letters,* 1964, **2,** 689
[3] ELLINGER, L. P. *Chem. & Ind.* **1963,** 1982
[4] ELLINGER, L. P. *Polymer, Lond.* 1964, **5,** 559
[5] ELLINGER, L. P. *Polymer, Lond.* 1965, **6,** 549
[6] NOMORI, H., HATANO, M. and KAMBARA, S. *Polymer Letters,* 1966, **4,** 261
[7] GANDINI, A. and PLESCH, P. H. *J. chem. Soc.* **1965,** 6019
[8] BIDDULPH, R. H., PLESCH, P. H. and RUTHERFORD, P. P. *J. chem. Soc.* **1965,** 275
[9] GANDINI, A., GIUSTI, P., PLESCH, P. H. and WESTERMANN, P. H. *Chem. & Ind.* **1965,** 1225
[10] GIUSTI, P. *Chim. e Industr.* 1966, **48,** 435
[11] GIUSTI, P. and ANDRUZZI, F. *Chim. e Industr.* 1966, **48,** 442
[12] CRAIG, A. W. and HENDERSON, D. A. *J. Polym. Sci.* 1956, **19,** 215
[13] UEBERREITER, K. and SPRINGER, J. *Z. phys. Chem.* 1963, **36,** 299
[14] FOSTER, R. and THOMSON, T. J. *Trans. Faraday Soc.* 1962, **58,** 860
[15] MOORE, R. L. and ANDERSON, R. C. *J. Amer. chem. Soc.* 1945, **67,** 168
[16] LEDWITH, A. and SAMBHI, M. *Chem. Comm.* **1965,** 64
[17] DAVIES, K. M. C. and SYMONS, M. C. R. *J. chem. Soc.* **1965,** 2079
[18] PLESCH, P. H. Chapter on 'Cationic polymerization' in *Progress in High Polymers,* Vol. II, ed. ROBB, J. C. and PEAKER, M. W. Iliffe-Heywood: London, to be published
[19] HALEVI, E. A. and NUSSIM, M. *J. chem. Soc.* **1963,** 876

The Coil Dimensions of Poly(olefin sulphone)s III—Poly(hexene-1 sulphone) in Dioxan, Benzene and Mixed Solvents

T. W. BATES and K. J. IVIN*

The viscosity/molecular weight relation for poly(hexene-1 sulphone) fractions in a dioxan–n-hexane θ-mixture was found to be $[\eta]_\theta = K_\theta \overline{M}_n^{\frac{1}{2}} = 6 \cdot 5 \times 10^{-2} \overline{M}_n^{\frac{1}{2}}$ ml g^{-1} (θ=20·5°C). Viscosity measurements have also been made in benzene–cyclohexane non-θ-mixtures and in the two good solvents benzene and dioxan at 25°C. For the benzene–cyclohexane mixtures K_θ was found to be $(6 \cdot 6 \pm 0 \cdot 2) \times 10^{-2}$ ml g^{-1} by means of the Flory–Fox–Schaefgen and Stockmayer–Fixman extrapolation methods. The polymer thus has the same unperturbed dimensions in both dioxan–n-hexane and benzene–cyclohexane mixtures, $\langle r_c^2 \rangle / nl^2$ being 6·75 ± 0·14. This is some 15 per cent greater than that found for the θ-mixtures methyl ethyl ketone–isopropanol and methyl ethyl ketone–n-hexane.

THE following abbreviations will be used in this paper:

PHS	poly(hexene-1 sulphone)	IPA	isopropanol
MEK	methyl ethyl ketone	HEX	n-hexane
BENZ	benzene	CHEX	cyclohexane
DIOX	dioxan		

Previous results indicate that $\langle r_c^2 \rangle$, the mean square unperturbed end-to-end distance in PHS, depends on the nature of the θ-solvent[1]. Viscosity measurements show that the chain is rather more extended in the θ-solvent n-hexyl chloride than in either the θ-mixtures MEK–IPA or MEK–HEX[1,2].

In order to investigate this effect further, and at the same time to obtain data for correlation with dipole moment measurements, these investigations have now been extended to the following solvents: DIOX, BENZ, and DIOX–HEX and BENZ–CHEX mixtures. The mixtures were chosen to be non-polar and of low dielectric constant.

EXPERIMENTAL

The fractions were the same as those previously employed[1,2], $\overline{M}_w / \overline{M}_n$ being 1·13 ± 0·02, and limiting viscosity numbers were determined in the usual way.

The θ-temperature for PHS in a 40–60 DIOX–HEX mixture (vol./vol. at 25°) was determined as 20·5° ± 1·0°C from liquid–liquid phase separation temperatures as previously described[1,2]. This method was found to be inapplicable to BENZ–HEX mixtures because solid, not liquid, separated on cooling.

*Department of Chemistry, The Queen's University of Belfast.
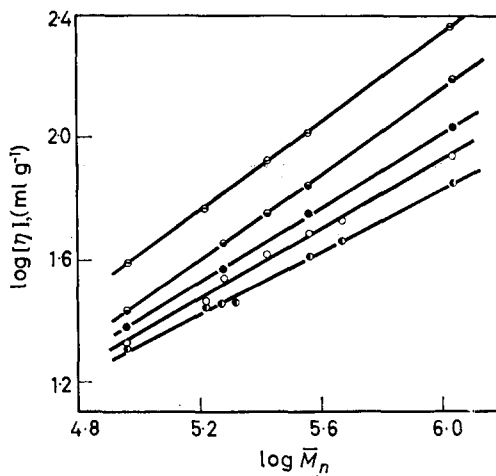
Figure 1—Limiting viscosity numbers of PHS fractions in various solvents: ◔, BENZ 25°; ⊖, DIOX 25°C; ●, 43–57 BENZ–CHEX 25°C; ◑, 40–60 DIOX–HEX 20·5°C; ○, 35–65 BENZ–CHEX 25°C

RESULTS AND DISCUSSION

The viscosity results are shown in *Figure 1* and the parameters in the equation $[\bar{\eta}] = KM^a$ are summarized in *Table 1*, along with the Huggins's

Table 1. Viscosity parameters for PHS in various solvents. Molecular weight range: 92 000 to 1 066 000

Solvent (vol./vol. at 25°)	T, °C	k', mean	10^2K, ml g^{-1}	a
40–60 DIOX–HEX	20·5*	0·57 ± 0·09	6·5	0·50
35–65 BENZ–CHEX	25	1·36 ± 0·15	3·4	0·56
43–57 BENZ–CHEX	25	0·96 ± 0·15	1·7	0·63
BENZ	25	0·39 ± 0·04	0·89	0·70
DIOX	25	0·37 ± 0·05	0·62	0·76

*θ-temperature.

k' values. It will be noted that addition of cyclohexane to benzene causes *a* to fall from 0·70 in pure benzene to 0·56 in 35–65 BENZ–CHEX. However, further decrease in the solvent power, either by lowering the temperature to 13°C or by increasing the proportion of cyclohexane to 66 per cent at 25°C, resulted in phase separation for concentrations greater than about 0·3 per cent. It thus appears that θ conditions are physically unattainable in this mixture, which is probably connected with the separation of solid rather than a second liquid phase on cooling.

K_θ corresponding to $[\eta]_\theta / \bar{M}_n^{\frac{1}{2}}$ for a θ-solvent is given directly for 40–60 DIOX–HEX as $6·5 \times 10^{-2}$ ml g^{-1} (*Table 1*). For the other solvents the extrapolation procedures of Flory, Fox and Schaefgen[4] (FFS) or Stockmayer and Fixman[5, 6] (SF) were tired. These are shown in *Figures 2* and *3* respectively, the intercept at $M = 0$ being K_θ in both cases. The earlier results using other solvents are also included and the K_θ values summarized in *Table 2*. The extrapolation methods appear not to be reliable for benzene and dioxan, but satisfactory for BENZ–CHEX in that both methods give the same answer. The discordant values for *n*-hexyl chloride in *Table 1* are

due to the anomaly previously noted[2] and will be omitted from the present discussion.
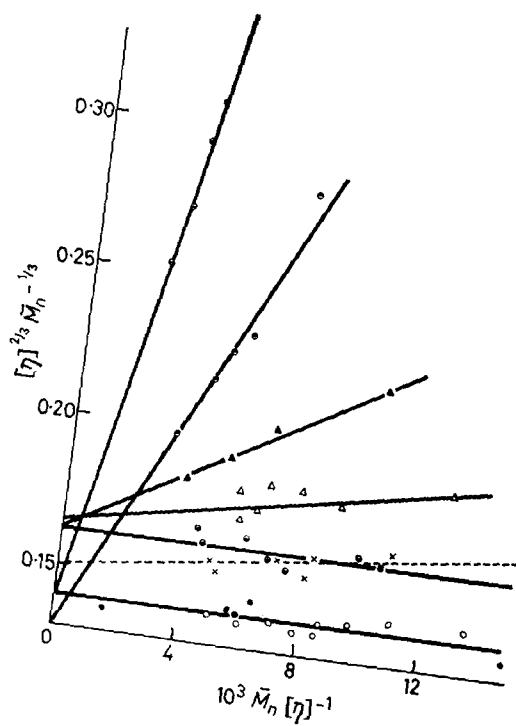
Figure 2 — Flory–Fox–Schaefgen extrapolation of limiting viscosity numbers for PHS fractions: ⊖, DIOX; ⊙, BENZ; ◓, 40–60 DIOX–HEX; ▲, 43–57 BENZ–CHEX; ○, 29·8/70·2 MEK–HEX; △, 35–65 BENZ–CHEX; ●, 37–63 MEK–IPA; ×, *n*-Hexyl chloride
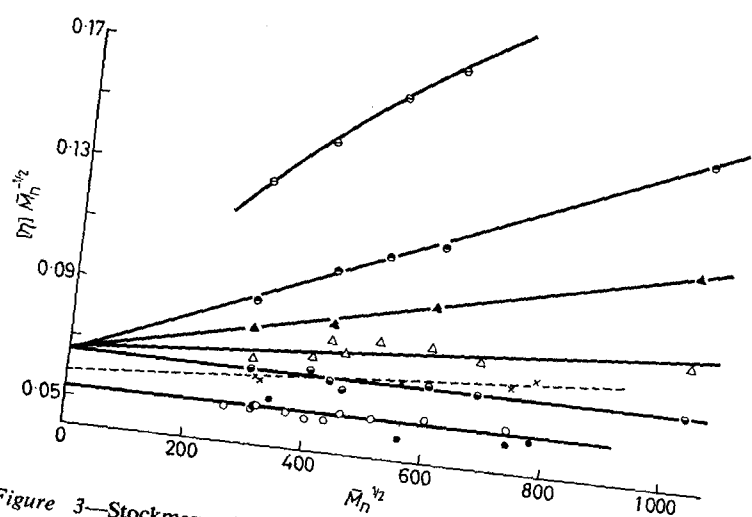
Figure 3—Stockmayer–Fixman extrapolation of limiting viscosity numbers for PHS fractions. Key as in *Figure 2*

Table 2. Unperturbed dimensions of PHS in various solvent media[1,2]

Solvent (1)	Non-solvent (2)	V_1*	T, °C	$10^2 K_\theta$ (ml g⁻¹)				$\langle r_c^2 \rangle / nl^2$	σ	ϵ_1‡
				(i) From $[\eta]_\theta$	(ii) FFS	(iii) SF	Mean			
MEK	IPA	37	27†	5·3	5·3	5·3	5·3±0·2	5·86±0·14	1·71±0·02	18·4
MEK	HEX	29·8	8†							
n-Hexyl chloride		100	13†	6·5±0·3	5·9	5·9	6·5±0·3 / 5·9±0·3	6·71±0·20 / 6·29±0·24	1·83±0·03 / 1·77±0·03	5·92
DIOX	HEX	40	20·5†	6·5	6·5	6·5	6·5±0·2	6·71±0·14	1·83±0·02	2·209
BENZ	CHEX	43 / 35	25 / 25		6·5 / 6·7	6·6 / 6·6	6·6±0·2	6·78±0·14	1·84±0·02	2·274
BENZ		100	25		4·7	6·5				2·274
DIOX		100	25		5·2	Curved				2·209

*Volume per cent of component (1) at 25°C.
†θ-Temperature.
‡From A. A. MARYOTT and E. R. SMITH, Circ. U.S. Nat. Bur. Stand. No. 514 (1957) or measured (25°C).

The so-called characteristic ratio[7], $\langle r_c^2 \rangle / nl^2$, for the polymer chain has been calculated from the Flory[3] relationship, $K_\theta = \Phi (\langle r_c^2 \rangle / M)^{3/2}$, taking Φ as the experimental value[8] $2 \cdot 5 \times 10^{23}$ and nl^2 as $z (l_{C-C}^2 + 2l_{C-S}^2)$ where z is the degree of polymerization, $l_{C-C} = 1 \cdot 54$ Å and $l_{C-S} = 1 \cdot 82$ Å. The results are shown in *Table 2* together with the parameter σ expressing $\langle r_c^2 \rangle^{\frac{1}{2}}$ relative to the value for free rotation, assuming tetrahedral valence angles.

It may be seen that PHS has the same unperturbed dimensions in DIOX–HEX and BENZ–CHEX mixtures, but that in these solvents σ is some seven per cent greater than in MEK–IPA or MEK–HEX mixtures. This difference appears to be well outside the experimental error and supports the suggestion[2] that the conformation in the θ-mixture is determined primarily by the polarity of the solvent component of the mixture as a result of preferential attraction by the polymer molecules. Such effects have recently been established for other polymers[9-12]. It is difficult to relate the magnitude of $\langle r_c^2 \rangle / nl^2$ to some property of the solvent medium, particularly for a ternary system of the type polymer–solvent–non-solvent. The correlation with the dielectric constant ϵ_1 of the solvent component (*Table 2*) may be accidental. However, it is worth noting that models show that rotations from the *trans* conformation about the C—C bond in PHS place adjacent sulphone groups in close proximity, resulting in severe steric and dipolar repulsions. In solvent mixtures containing a polar component the dipolar repulsions will be reduced so that a higher proportion of gauche conformations about the C—C bond may be allowed, hence reducing $\langle r^2 \rangle / nl^2$.

Department of Physical Chemistry,
University of Leeds

REFERENCES

[1] IVIN, K. J., ENDE, H. A. and MEYERHOFF, G. *Polymer, Lond.* 1962, **3**, 129
[2] BATES, T. W., BIGGINS, J. and IVIN, K. J. *Makromol. Chem.* 1965, **87**, 180
[3] FLORY, P. J. *Principles of Polymer Chemistry.* Cornell University Press, 1953
[4] FLORY, P. J. and FOX, T. G. *J. Amer. chem. Soc.* 1951, **73**, 1904
   SCHAEFGEN, J. R. and FLORY, P. J. *J. Amer. chem. Soc.* 1948, **70**, 2709
[5] STOCKMAYER, W. H. and FIXMAN, M. *J. Polym. Sci. C,* 1963, **1**, 137
[6] KURATA, M. and STOCKMAYER, W. H. *Fortschr. HochpolymForsch.* 1963, **3**, 196
[7] MARK, J. E. and FLORY, P. J. *J. Amer. chem. Soc.* 1965, **87**, 1415
[8] McINTYRE, D., WIMS, A., WILLIAMS, L. C. and MANDELKERN, L. *J. phys. Chem.* 1962, **66**, 1932
[9] CRESCENZI, V. and FLORY, P. J. *J. Amer. chem. Soc.* 1964, **86**, 141
[10] BURCHARD, W. *Makromol. Chem.* 1962, **56**, 239
[11] HOEVE, C. A. J. and O'BRIEN, M. K. *J. Polym. Sci. A,* 1963, **1**, 1947
[12] EISENBERG, H. and WOODSIDE, D. *J. chem. Phys.* 1962, **36**, 1844

Communication

A Method for the Determination of Number Average Molecular Weights of Linear Polymers less than 5 000

THE determination of low number average molecular weights of linear polymers in the region 500 to 5 000 presents considerable difficulties. The methods usually employed involve either one or other of the colligative properties of polymer solutions or quantitative assay of the end-group content of the polymer. It has been shown[1] that at constant temperature the density of a linear polymer in the liquid or liquid-like state is determined by the weight fraction of end-groups and in principle, therefore, a determination of the density enables the number average molecular weight to be calculated. The appropriate equation is

$$\overline{M}_n = M_e \frac{\rho \, (\rho_p - \rho_e)}{\rho_e \, (\rho_p - \rho)} \tag{1}$$

where ρ and $\overline{M}_n$ are the density and number average molecular weight of the polymer, ρ_e and M_e are the density and molecular weight of the substance formed by the combination of the two end-groups, and ρ_p is the density of very high molecular weight polymer. It is obvious that the determination of $\overline{M}_n$ requires a knowledge of the end-groups of the polymer and the values of the three densities: ρ_e, ρ and ρ_p.

The measurement of ρ_e is not difficult if the end-group substance is available and exists in the liquid state at the temperature at which the polymer densities are determined; if the end-group substance is a solid, the density it would have in the liquid state at the experimental temperature can be obtained either by extrapolation of the density/temperature relationship established above the melting point to the temperature in question or by measuring its density in solution; this latter method is the more convenient but care must be taken to choose a solvent in which the end-group substance dissolves without deviating from the volume additivity rule. On the other hand, the determination of the two polymer densities, ρ and ρ_p, is not straightforward unless both samples are liquids of fairly low viscosity. In the usual situation where one or both of the polymer samples are solids or liquids of extremely high viscosity, errors in the determination of the polymer densities may arise from: (1) contamination of the polymer sample by air or by solvents; (2) non-equilibrium packing of the polymer molecules. The first source of error can be largely avoided by heating a sample of the polymer under vacuum to drive off all volatile material provided, of course, that the polymer is thermally stable. The second source of error can be minimized by measuring the polymer densities at a temperature greater than the glass transition temperature

269

of the polymer. The combined effect of errors $d\rho_e$, $d\rho$ and $d\rho_p$ in the three densities ρ_e, ρ and ρ_p is to give rise to an error of $d\overline{M}_n$ in $\overline{M}_n$ given by

$$\frac{d\overline{M}_n}{\overline{M}_n} = \frac{\rho_p}{(\rho_p - \rho)(\rho_p - \rho_e)} \left\{ (\rho_p - \rho)^2 \left(\frac{d\rho_e}{\rho_e} \right)^2 + (\rho_p - \rho_e)^2 \left(\frac{d\rho}{\rho} \right)^2 \right.$$
$$\left. + (\rho - \rho_e)^2 \left(\frac{d\rho_p}{\rho_p} \right)^2 \right\}^{1/2} \qquad (2)$$

Equation (2) enables the practical limits of the technique to be estimated. If we assume that the relative errors in the three densities are identical, the relative error in $\overline{M}_n$ becomes

$$\frac{d\overline{M}_n}{\overline{M}_n} = \frac{\sqrt{2}\,d\rho_p}{\rho_p - \rho_e} \cdot \frac{(1 - x + x^2)^{1/2}}{x} \qquad (3)$$

where x is $(\rho_p - \rho)/(\rho_p - \rho_e)$. Since ρ lies between ρ_e and ρ_p, x lies between 1 and 0 and the corresponding relative error in $\overline{M}_n$ between $\sqrt{2}\,d\rho_p/(\rho_p - \rho_e)$ and infinity. The relative error in $\overline{M}_n$ is thus unacceptable unless a substantial difference exists between the density of the high molecular weight polymer and the end-group substance. This is made clear in *Table 1* in which we have estimated the relative errors in $\overline{M}_n$ for a number of values of $(\rho_p - \rho_e)$ and x assuming a value for $|\,d\rho_p\,|$ of 0.0005 g ml^{-1}. This latter value is the result of a number of experiments which we have carried out to test the above arguments. We have also indicated the approximate value of the polymer molecular weight corresponding to the chosen values of x by putting $M_e = 100$ and $\rho_e/\rho = 1$ in equation (1).

Table 1. The relative errors in $\overline{M}_n$ calculated according to equation (3) with $|\,d\rho_p\,| = 0.0005$ g ml^{-1}

Approx. mol. wt polymer	200	1 000	5 000
x $\rho_p - \rho_e$	0·5	0·1	0·02
0·2000	0·006	0·03	0·2
0.1000	0·01	0·07	0·4
0·0500	0·02	0·1	0·7

Obviously, molecular weights much above 5 000 cannot be measured with any accuracy by this technique given that the relative errors in the measurement of the individual densities of end-group substance, polymer and high molecular weight polymer are around ± 0.0005 g ml^{-1}. The lower limit of molecular weight to which the technique might be applied is determined not by the errors discussed above but by the disadvantages of the technique compared to conventional methods of molecular weight determination.

In order to confirm our arguments, we have prepared three samples of syndiotactic polymethyl methacrylate with fluorenyl and hydrogen endgroups of number average molecular weights (1.52 ± 0.05), (6.25 ± 0.25) and $(23.2 \pm 1.1) \times 10^3$; these values were obtained from the absorbance of

the fluorenyl end-group in the ultra-violet[2]. The densities of these three polymers were measured in a density gradient column at 25°. In using this method it is essential to choose a flotation medium to which the polymer is impermeable; in our case a mixture of sodium sulphate and water was selected. Taking ρ_p as the density of the 23.2×10^3 polymer and ρ_e as the density of fluorene in benzene solution, the molecular weights of the first two polymers were calculated as (1.58 ± 0.14) and $(5.0 \pm 0.9) \times 10^3$. These results are in reasonable agreement with the spectroscopic values and suggest that the problems associated with volume equilibration below the glass transition temperature (115°C for high molecular weight syndiotactic polymethyl methacrylate[3]) are not too serious.

Our experience so far indicates that the density method of molecular weight determination is of some utility for polymers. It has the advantages of requiring simple apparatus and only small amounts of material and it is convenient for routine work. Furthermore, its scope and range of applicability for any required degree of precision can be estimated in advance given the densities of the end-group substance and high molecular weight polymer. Its disadvantages are that it is not applicable to polymer samples which are partially crystalline, that the end-groups of the polymers must be known with certainty and that the densities of the end-group substance and high molecular weight polymer must be determined separately. Nevertheless, in the absence of specific information concerning the end-groups, the density method can be employed to arrange a series of polymers in order of molecular weight if all the polymers are otherwise identical.

D. MARGERISON
Miss V. A. NYSS
Mrs E. PULAT

Donnan Laboratories,
 University of Liverpool

REFERENCES

[1] EAST, G. C., MARGERISON, D. and PULAT, E. *Trans. Faraday Soc.* 1966, **62**, 1301
[2] GLUSKER, D. L., STILES, E. and YONCOSKIE, B. *J. Polym. Sci.* 1961, **49**, 297
[3] GOODE, W. E., OWENS, F. H., FELLMAN, R. P., SNYDER, W. H. and MOORE, J. E. *J. Polym. Sci.* 1960, **46**, 317

ANNOUNCEMENTS

MECHANICS OF FIBROUS STRUCTURES

A special course of lectures on the Mechanics of Fibrous Structures has been arranged at the University of Manchester Institute of Science and Technology, Sackville Street, Manchester 1, to be given during 3 to 7 July next. It is hoped the following will be among the lecturers: R. ARRIDGE, S. BACKER, H. CORTE, P. GROSBERG, J. C. HALPIN, J. W. S. HEARLE, M. KONOPASEK, E. SMITH and S. W. TSAI. Subjects for the lectures will include the engineering approach to textiles; general methods of analysis; structural mechanics of fibres, yarns, woven and knitted fabrics, non-woven fabrics, fibre-reinforced materials, paper, and fabricated textiles; use of computer methods and of dynamic modulus measurements. Application forms and details can be obtained from the Registrar, at the address given above.

CONFERENCE ON NON-NEWTONIAN FLOW THROUGH PIPES AND PASSAGES

Papers are invited for a conference to be held at Shrivenham from 19 to 21 September on the flow of non-Newtonian fluids through pipes, ducts, passages and open channels. Further information may be obtained from Dr. M. F. Culpin, 8 Broadway, Pontypool, Mon.

Contributions to Polymer

Papers accepted for future issues of POLYMER include the following:

Copolymerization of Styrene and Some Alpha Olefins using Ziegler–Natta Catalyst Systems 1—The Fractionation and Characterization of the Products of Copolymerization—B. BAKER and P. J. T. TAIT

Conversion Factors in Dilatometry—C. E. M. MORRIS and A. G. PARTS

Macromolecular Polymorphism and Stereoregular Synthetic Polymers— F. DANUSSO

The Dilute Solution Properties of Polyacenaphthalene I, II—J. M. BARRALES-RIENDA and D. C. PEPPER

The Polymerization of Some Epoxides by Diphenylzinc, Phenylzinc t-Butoxide and Zinc t-Butoxide—J. M. BRUCE and F. M. RABAGLIATI

Solution and Diffusion of Gases in Poly(vinyl chloride)—R. M. BARRER, R. MALLINDER and P. S.-L. WONG

Association of Polyacrylonitrile Solutions—R. B. BEEVERS

Temperature Dependence of Association in Polyacrylonitrile Solutions— —R. B. BEEVERS

Mechanical History Effects in the Crystallization of cis-1,4-Polybutadiene —J. C. MITCHELL

Melting Characteristics of Isotactic Polypropylene Oxide

W. Cooper, D. E. Eaves and G. Vaughan

Differential thermal analyses and dilatometric measurements of isotactic poly-propylene oxide have been made. It has been shown that polymers having a thermal history of slow crystallization give curves having two melting transitions, whereas polymers crystallized rapidly have only one. It is suggested that the two transitions result from different modifications of a single crystal struc-ture produced by different nucleation mechanisms during the crystallization process.

The melting behaviour of polymers is known to be markedly dependent upon the thermal history of the sample. Generally imperfections in the crystals are reduced, e.g. the lamellar thickness is increased[1,2], by raising the temperature of crystallization and a higher melting point is observed. In many cases the number of melting transitions which are detected also varies and this has been ascribed either to the existence of different crystalline forms with distinguishable unit cell dimensions[3] or to the presence of more than one morphological form of a single crystal structure[4-7].

With polypropylene oxide, for which only one crystal form has been described[8], the melting point and degree of crystallinity are raised by increased stereoregularity in the polymer[9,10]. Stereoregularity determines mainly the ratio of primary to secondary crystallization but has a relatively minor effect on nucleation and spherulite growth rates—which are governed by crystallization temperature[11]. In this paper the effect of crystallization temperature on the subsequent melting behaviour of the polymer is examined.

EXPERIMENTAL

Polymers A ($[\eta] = 0.38$) and B ($[\eta] = 7.3$) were the isotactic fractions ob-tained by cooling to $-20°C$ acetone solutions of the crude polypropylene oxides prepared using $FeCl_3/H_2O^{12}$ and $ZnEt_2/H_2O^{13}$ respectively as catalyst. Polymer C ($[\eta] = 0.09$) was obtained from B by means of ozone degradation at $20°C$ in chloroform solution and D ($[\eta] = 0.14$) similarly from A.

Differential thermal analysis (DTA)

The apparatus has been described previously[14], and uses thermistors as detectors with a 1.5 g sample. Heating rates of 3 to 6 deg. C/h were used. Samples were melted into the cells and allowed to cool at room temperature before carrying out any thermal treatment.

The start of melting corresponds to an endothermic deviation from the baseline, peaks were measured as the points of maximum deviation, and an indication of the final melting temperature was obtained from the inflection point as the baseline was resumed. Precrystallization (crystallization occur-ring prior to melting) was indicated by an exothermic peak.

Dilatometry

Polymers (approximately 4 g) were loaded into dilatometers under vacuum and mercury was added to fill the bulb to the stem. The heating rate was 15 deg. C/h and the expansion was followed by an automatic recorder[15]. The start of melting, the melting peak and the final melting temperature were taken as the first positive deviation from straight line expansion, the point of maximum slope and the point at which linear expansion was resumed respectively. Precrystallization was indicated by a negative deviation from linear expansion. Crystallinity was calculated from density considerations, taking the amorphous density at 20°C as $1\cdot002$ g/cm³ and calculating the crystalline density at 20°C from X-ray data[8] as $1\cdot155$ g/cm³.

X-Ray

Debye–Scherrer scans were made on 1 mm sheets of polymer using a Cu K_α beam.

RESULTS

DTA results are given in *Tables 1* and *2*. *Table 1* shows the effect of thermal history on various polymer samples, and *Table 2* shows the effect of crystallization temperature. Typical DTA curves are shown in *Figures 1* and *2* where the slight baseline curvature and slope are caused by a small amount of thermistor imbalance. Crystallization on slow cooling as judged by the exothermic peak occurred at 57°C (polymer A). Dilatometric results are shown in *Table 3* and typical curves in *Figure 3*. In *Figure 4* is shown the DTA peak temperature as a function of crystallization temperature.

DISCUSSION

Three features may be observed in the dilatometric and DTA curves—precrystallization, primary melting and, under certain circumstances, a secondary melting transition some 5 to 10 deg. C below the main peak. Precrystallization is observed when the polymers have been crystallized rapidly and it can be eliminated by annealing the polymer. The phenomenon has been observed for other polymers (e.g. in *trans*polyisoprene[3]) and is thought to be caused by crystallization of amorphous polymer during the heating cycle prior to the melting transition. It is likely that this amorphous polymer is 'trapped' as a result of the rapid rate of cooling and crystallizes only when a subsequent temperature rise allows sufficient mobility for orientation of the polymer chain on to existing crystallites to occur. The primary melting transition is as expected. Dilatometric and DTA results agree within experimental error, and are in accord with previous observations[9].

The secondary melting transition, found in all samples which have been crystallized by cooling slowly and continuously from the melt, or, for polymer A, crystallizing at fixed temperatures between 40°C and 60°C, has not previously been reported.

This could arise from several causes.

(*1*) An experimental effect caused by the use of too rapid a rate of heating.

274

Table 1. Differential thermal analysis of polypropylene oxide

Polymer	Thermal treatment	Precrystallization		Shoulder (S) or lower melting peak (P)		Upper melting peak	
		Start °C	Peak °C	Peak °C	Trough °C	Peak °C	Finish °C
A	Cooled to room temp. from melt	47·0	51·6	62·3(S)	64·9	71·5	73·5
A	Slowly cooled from melt	None	—	65·1(P)	67·1	72·2	72·8
B	Cooled to room temp. from melt	None	—	None	—	62·6	65·5
B	Slowly cooled from melt	None	—	Small diffuse peak		63·0	65·9
C	Cooled to room temp. from melt	36·7	39·9	46·9(P)	50·9	55·7	59·4
C	Slowly cooled from melt	None	—	49·0(P)	53·4	57·1	60·1
D	Quenched at −78°C from melt	24·1	35·3	62·8(S)	64·8	67·5	68·8
D	Cooled to room temp. from melt	43·9	51·4	58·1(S)	61·8	67·6	68·7

Table 2. Differential thermal analysis of polypropylene oxide (sample A, recrystallized from acetone at −20°C)

Crystallization temp. °C	Precrystallization		Shoulder (S) or lower melting peak (P)		Upper melting peak	
	Start °C temp.	Peak temp. °C	Peak °C	Trough °C	Peak °C	Finish °C
Slowly cooled from melt	None	None	68·2(P)	70·3	74·8	75·1
−70	33·5	45	None	None	74·7	75·5
0	36·8	47·3	None	None	73·9	74·6
10	42·2	49·2	None	None	74·2	74·9
20	44·7	51·5	62·5(S)	65·2	74·2	75·1
30	50·3	53·8	63·7(S)	67·1	74·3	75·4
40	54·0	57·3	66·7(S)	69·3	72·7	74·9
50	None	None	70·9(S)	71·9	74·5	74·8
55	54·6 (v. small)	57·2	67·5(P)	69·6	75·1	75·2
60	None	None	69·1(P)	71·3	74·6	75·1

275

Table 3. Dilatometric melting transitions of polypropylene oxide

Polymer	Thermal treatment	Precrystallization		Lower melting		Upper melting		Crystallinity
		Start °C	Peak °C	Peak °C	Finish °C	Peak °C	Finish °C	%
A	Cooled slowly from melt	None	—	62·8	65·5	70·3	73·7	40
A	Cooled rapidly from melt to 0°C	47·5	50·7	None	—	70·2	73·7	35
A	Annealed at 65°C for 18 h	60·4	62·8	None	—	70·9	74·8	36
A	Annealed at 60°C for 18 h	51·4	54·9	None	—	71·1	74·2	43
A	Annealed at 55°C for 18 h	57·4	60·0	None	—	70·4	74·0	40
A	Annealed at 44°C for 18 h	47·4	53·3	None	—	70·5	74·0	41
A	Annealed at 30°C for 18 h	54·9	57·1	None	—	70·3	74·0	37
B	Cooled slowly from melt	None	—	None	—	62·6	66·2	14·5
C	Cooled slowly from melt	None	—	45·6	51·1	55·0	61·1	30
C	Cooled rapidly to 0°C from melt	None	—	None	—	56·6	60·2	34

Figure 1—Effect of cooling rate on DTA curves of polypropylene oxides; curve a, Polymer A, cooled to room temperature from melt; curve b, Polymer A, cooled slowly to room temperature from melt; curve c, Polymer D, cooled rapidly to −78°C from melt; curve d, Polymer D, cooled to room temperature from melt; curve e, Polymer D, cooled slowly to room temperature from melt
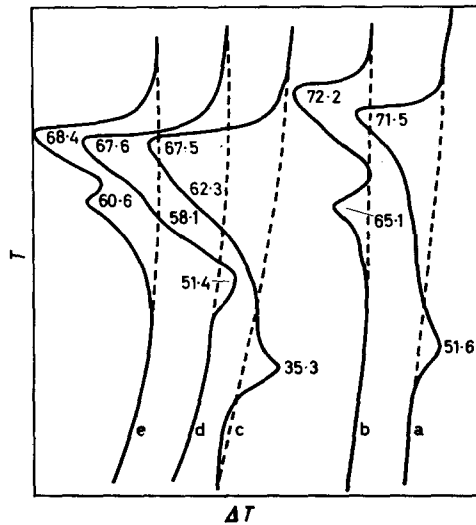
(2) The presence of two crystal forms with distinct lattice structures.

(3) Crystallization occurring during the heating cycle with the resulting trough in a single peak giving the appearance of two peaks. Such a change might occur from the crystallization of amorphous polymer previously trapped by the crystallites and liberated only after some have melted or by the recrystallization of amorphous polymer derived from the melting of the less perfect crystals. [Crystallization of amorphous polymer trapped by
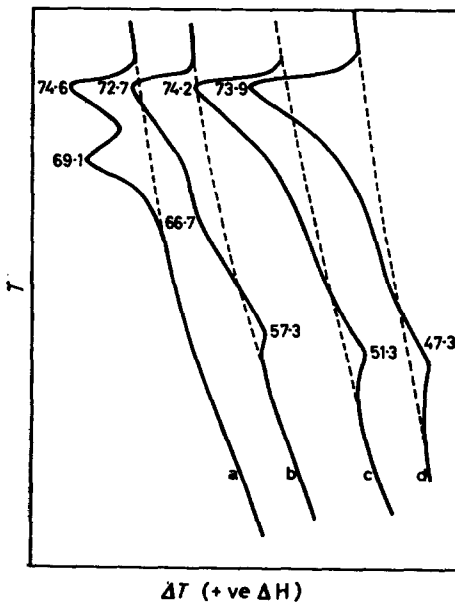
Figure 2—Effect of crystallization temperature on DTA curves of polymer A; curve a, crystallized at 60°C; curve b, crystallized at 40°C; curve c, crystallized at 20°C; curve d, crystallized at 0°C

Figure 3—Effect of thermal treatment on dilatometric curves for Polymer A; curve a, cooled rapidly to 0°C from melt; curve b, cooled slowly to room temperature from melt
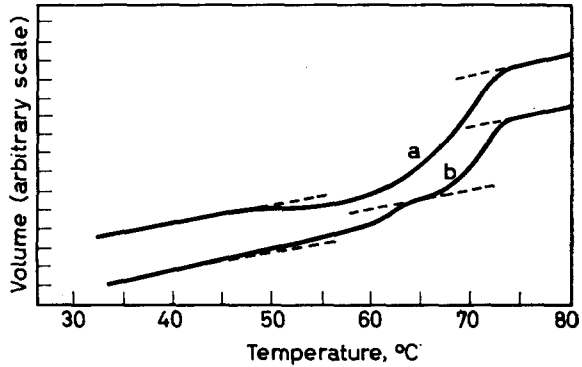
a viscosity effect may also occur (precrystallization) but is generally found at temperatures well below the melting point before any appreciable melting has occurred.]

(4) The presence of one crystal structure in different morphological forms or in crystals of various perfections.

The rates of heating were low (3 to 6 deg. C/h in DTA and 15 deg. C/h in dilatometric experiments) so the possibility that it results from markedly non-equilibrium heating appears to be unlikely. It would be expected that if the existence of two endotherms were adventitious, resulting from the heating rate, apparatus, or the geometry of the sample, then the differential thermograms would depend critically on the experimental conditions. In fact this polymer has been found, independently[16], to exhibit identical behaviour in a Du Pont 900 thermal analyser at a heating rate of 300 deg. C/h. It is apparent that it is the thermal history of the polymer which has the most significant influence.

The occurrence of two distinct crystalline modifications is likewise im-
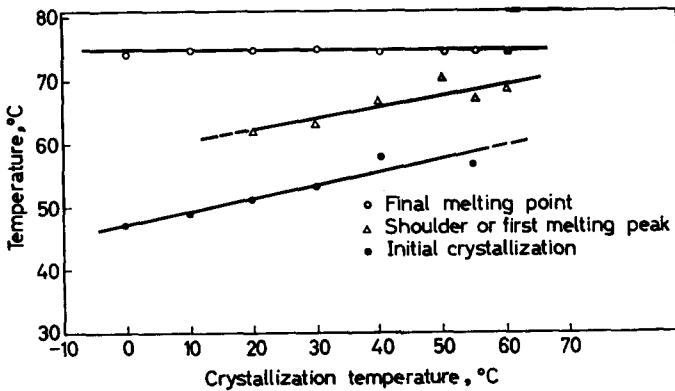
Figure 4—Variation of peak temperature (DTA) with crystallization temperature

278
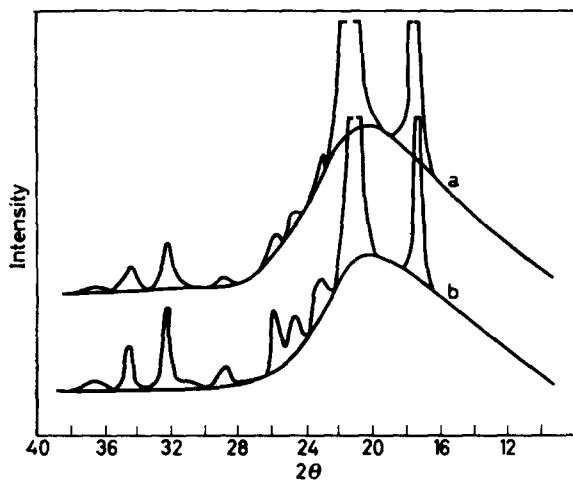
Figure 5—Effect of thermal treatment on X-ray diffraction spectra of polymer A; curve a, cooled rapidly to −20°C from melt (single melting peak); curve b, cooled slowly to room temperature from melt (two melting peaks)

probable although superficially similar DTA and dilatometric melting curves have been observed for *trans*polyisoprene[3], which is known to exist in two modifications with different lattice structures and melting points, readily distinguished by their X-ray diffraction patterns[17]. The X-ray diffraction patterns for polypropylene oxides which show the two transitions (*Figure 5, b*) are similar to those obtained from samples which have only one transition (*Figure 5, a*). The principal peaks, which are seen to be present in both curves, correspond closely with the results of Stanley and Litt[8] and can be acounted for on the basis of a single orthorhombic crystal lattice. However, minor differences in certain normalized peak intensities, particularly those corresponding to spacings of 3·90, 3·65 and 3·48 Å, do indicate some difference in crystal size and perfection between the two types of polymer.

The possibility that recrystallization occurs during melting is unlikely since it would be expected to increase with increased rate of crystallization in preparing the sample, whereas the two peaked melting curves are observed when the polymer is crystallized slowly (at about 55°C). The maximum rate of crystallization occurs at about 30°C and at this temperature there is only a minor second transition.

Multiple melting transitions have been observed with polyethylene[4, 5], polyethylene terephthalate[6] and polybutadiene[7], and have generally been ascribed to the existence of two or more modifications of a single crystalline structure, which would possess definite unit cell dimensions. This explanation would seem to be appropriate to these observations, rather than the alternative that they result from an assembly of more or less disordered crystallites entrapped during crystallization in a metastable condition. The two peaks are most probably the result of multiple independent nucleation as has been proposed by Aggarwal *et al.*[11] for polypropylene oxide and by Holden[5] for polyethylene. It should be observed, however, that in the present instance the two peaks were obtained essentially under conditions giving

slow crystallization, either at a single temperature or over a continuous range of decreasing temperature (in DTA experiments the crystallization exotherm produces a deviation from the natural cooling rate of only 2°C and in dilatometry the effect would be even smaller). In previous work the polymers were generally either partly crystallized and annealed at several distinct temperatures[5] or cooled rapidly from the melt[4].

REFERENCES

[1] KELLER, A. and O'CONNOR, A. *Disc. Faraday Soc.* 1958, **25**, 114
[2] HOFFMAN, J. D. *S.P.E. Trans.* 1964, **4**, 315
[3] COOPER, W. and VAUGHAN, G. *Polymer, Lond.* 1963, **4**, 329
[4] GRAY, A. P. and CASEY, K. *J. Polym. Sci. B,* 1964, **2**, 381
[5] HOLDEN, H. W. *J. Polym. Sci. C,* 1963, **6**, 53
[6] MITSUISHI, Y. and IKEDA, M. *J. Polym. Sci. A,* 1966, **4**, 283
[7] COLLINS, E. A. and CHANDLER, L. A. *Rubb. Chem. Technol.* 1966, **39**, No. 2, 193
[8] STANLEY, E. and LITT, M. *J. Polym. Sci.* 1960, **43**, 453
[9] ALLEN, G., BOOTH, C., JONES, M. N., MARKS, D. J. and TAYLOR, W. D. *Polymer, Lond.* 1964, **5**, 547
[10] AGGARWAL, S. L., MARKER, L., KOLLAR, W. L, and GEROCH, R. *Advanc. Chem. Ser.* 1966, **52**, 88
[11] AGGARWAL, S. L., MARKER, L., KOLLAR, W. L. and GEROCH, R. *J. Polym. Sci. A,* 1966, **4**, 715
[12] COLCOUGH, R. O., GEE, G., HIGGINSON, W. C. E., JACKSON, J. B. and LITT, M. *J. Polym. Sci.* 1959, **34**, 171
[13] BOOTH, C., HIGGINSON, W. C. E. and POWELL, E. *Polymer, Lond.* 1964, **5**, 479
[14] COOPER, W. and SMITH, R. K. *J. Polym. Sci. A,* 1963, **1**, 159
[15] VAUGHAN, G., SEWELL, P. R. and HOLLINS, P. H. *Chem. & Ind.* 1960, 1155
[16] HYBART, F. J. Private communication
[17] FISHER, D. *Proc. phys. Soc., Lond.* 1953, **66**, 7

Macromolecular Polymorphism and Stereoregular Synthetic Polymers*

F. Danusso

Definitions and general concepts on polymorphism are briefly reviewed and specific aspects of the polymorphism of macromolecular substances are emphasized.

A list of synthetic crystallizable polymers for which polymorphism phenomena have been observed to date is presented. For each polymer are briefly reported or discussed: the number of polymorphic forms discovered, the types of unit cell found in the crystallographic research and brief information about thermodynamic stability, kinetic transformations, physical properties and conditions of preparation of single crystalline modifications. Either chain conformation or mode of packing of chains can be responsible for structural differences among crystalline modifications.

More detailed information is then given and a number of experimental results is presented relating to typical cases of enantiotropy and of monotropy found among stereoregular polymers. An extended analysis is made of the enantiotropy of transtactic polybutadiene, which can appear in two crystalline modifications, and shows a reversible solid–solid transition from one form to the other.

The results of a detailed experimental investigation are also reported on the monotropy of isotactic polybutene-1, for which three polymorphic modifications were recognized and thermodynamic and kinetic transformations were examined in different experimental conditions.

A discussion finally deals with the theoretical problem of the prediction of the existence of different polymorphic modifications of given macromolecular chain structures. Satisfactory results have so far been obtained. in the chain conformational polymorphism of isotactic and syndiotactic polypropylene by means of a recent analysis of the energy minima of an isolated chain. This kind of approach appears to be of general application and to be the most convenient for the analysis of even more complicated chains.

SOME GENERAL IDEAS

THE property of a given substance to have more than one characteristic crystalline structure goes under the name of 'polymorphism'.

Two different structures or crystalline modifications of a given substance are today generally accepted to be distinct when they are characterized by atomic or molecular *short-range arrangements* presenting at least some difference in the elements of geometric regularity or symmetry.

Using physical or thermodynamical terms, two crystalline modifications may be said to differ when they form two separate and different phases. This statement, however, implies the concept of phase. This can be expressed in the sense used by Gibbs, but in practice it is known that this concept leads to ambiguities when more subtle differences have to be specified.

It is clear that two different polymorphous modifications must present

appreciable differences in at least some of their macroscopic physical properties, such as the external crystalline habit, solubility, or optical, volumetric, mechanical or electric properties. It is to these differences in properties that we normally refer our experiments when the occurrence of polymorphism is first noticed.

A crystallographic distinction at the atomic or molecular level is, however, considered indispensable for a conclusive judgement on the occurrence of polymorphism. This characteristic is clearly both necessary and sufficient for this purpose, while a distinction based on macroscopic physical properties often appears to be insufficient for a definitive characterization.

It may be of interest to remember that the difficulty of characterizing the polymorphism of a substance, and the attendant ambiguities, arise from various causes. For example two crystals of identical structure from the point of view of geometrical regularity and symmetry can, in certain cases, rotate the plane of polarized light in opposite directions. A well known case of this type is that of the enantiomorphous crystals of quartz which, however, are not two distinct polymorphic forms. The temperature of fusion can sometimes be markedly influenced by imperfections of the crystalline structure and may vary even when the qualitative intrinsic crystalline properties do not vary. Similarly, dynamic isomerism, certain second order transitions and lattice strain effects are all instances of phenomena which cannot be connected with polymorphism but perhaps only with a 'pseudopolymorphism'[1]. Ambiguity can in a certain way arise from 'mesomorphism', which corresponds to partially disordered states of smectic or nematic nature. These are generally not recognized by crystallographers to be polymorphic forms, as they do not imply a three-dimensional arrangement which is considered indispensable for crystallographic definitions.

Polymorphism is a very widespread phenomenon both among the chemical elements and the compounds. In particular it also occurs very frequently among organic compounds[2], even if solid state properties of these are often not investigated in detail.

Synthetic polymers have been extensively studied since about 1930 but, with few exceptions, polymorphism has been thoroughly studied only in the last few years.

The reason is very simple. Until ten years ago, the crystallizable synthetic polymers were relatively few and were studied essentially with a view to immediate application. On the other hand, in the last ten years, research on the crystalline state was specially developed and stimulated by numerous new polymers, which were almost all crystallizable. In particular, the discovery of synthetic stereoregular polymers has considerably improved the study of crystalline macromolecular structures.

The high stereospecificity of some processes of synthesis and the crystallizability to a substantial degree of different polymers obtained with an excellent steric purity, have specially encouraged investigation of the macromolecular solid state. This research appeared more complete and meaningful than that done on previously known polymers.

Thus, until a few years ago, macromolecular polymorphism had been studied only occasionally and was considered relatively uncommon; how-

ever, it now appears to be a widespread phenomenon, exactly as we have seen with low-molecular-weight substances.

Among the first cases of macromolecular polymorphism to be observed is that described in 1930 by Hopff, Von Susich and Hauser for 'gutta-percha'[3] which was later studied in detail by Bunn[4]. Subsequently, before the discovery of synthetic stereoregular polymers (1954), Fuller and co-workers around 1940 presented some data on polyesters[5, 6] and Bunn and Garner[7] reported on the polymorphism of polyamides.

Some discussion has also taken place on the structure of natural pro-teins: thus, some mechanical properties of the filaments of the animal kingdom (hair, fibres) were connected by Astbury with the concept of polymorphism[8]. However, in this respect it must be borne in mind that definitive conclusions have only been reached very recently on the exist-ence and role of real polymorphism[9]. In fact, while both elasticity and extensibility of filaments, or of animal fibrous tissues, must be clearly attributed to changes in the conformation of polymeric chains, it is not equally clear whether real polymorphous phases are present in these cases.

Table 1 lists the polymers for which polymorphism has been clearly

Table 1. Polymorphism of synthetic polymers

*Devoid of stereoisomerism**	*Stereoregular*
Polyethylene	Transtactic polyisoprene
Polytetrafluorcthylene	Transtactic polybutadiene
Polyoxymethylene	Transtactic polypentenamer
Polyselenomethylene	Isotactic polypropylene
Polydimethylketene	Isotactic polybutene-1
Polyvinylidenefluoride	Isotactic polypentene-1
Polyvinylalcohol	Isotactic polyheptene-1
Poly-*p*-xylene	Isotactic polytetradecene-1
Polytrimethylenesebacate	Isotactic polyhexadecene-1
Polyhexamethyleneadipamide	Isotactic polyoctadecene-1
Polyhexamethylenesebacamide	Isotactic polyvinylcyclopropane
Poly-ε-caproamide	(Isotactic polyvinylcyclohexane)
Other polyamides	Crystallizable poly-2-vinylpyridine
	Syndiotactic polypropylene

*Except for polyvinylalcohol which can be crystalline even when not stereoregular.

observed. The polymers without possibility of stereoisomerism are quoted on the left, together with those for which the crystallizability does not require stereoregularity (e.g. in polyvinylalcohol). On the right, the stereo-regular polymers are listed: the first three being transtactic, the following ten isotactic, the last one being syndiotactic.

POLYMORPHISM OF POLYMERS WITHOUT STEREOISOMERISM

A very short survey of the situation of macromolecular polymorphism in polymers for which there is no possibility of stereoirregularity may be of interest (*Table 2*).

The first polymer shown, polyethylene, is the simplest olefin polymer. It usually appears in the well known orthorhombic form, which was the

Table 2. Polymorphism of synthetic polymers for which there is no possibility of stereoirregularity

Polymer and structural unit	Number of polymorphs	Denomination, crystalline class, other information
Polyethylene —CH_2—CH_2—	3	Ortho, Mono, Tri Ortho and Tri have equal chain conformations. Mono under stretching
Polytetrafluorethylene —CF_2—CF_2—	3	Modifs. I, II, III All P.Hex, with chain repeat 2·59Å. Different helix chains. Enantiotropy
Polyoxymethylene —CH_2—O—	2	Hex, Ortho Slightly different helix chains. Ortho transforms to Hex at 70°C
Polyselenomethylene —CH_2—Se—	2	Hex, Ortho Ortho transforms to Hex at about 200°C
Polydimethylketene $\begin{array}{c} CH_3 \\ \vert \\ -C-C- \\ \vert \; \Vert \\ CH_3 \; O \end{array}$	2	Modifs. α (Ortho), β Different helix chain conformations. Modif. α transforms to β at about 250°C. Enantiotropy
Polyvinylidenefluoride —CH_2—CF_2—	3	Modifs. I, II, III Modifs. I and II characterized; different chain conformations. Modif. I by stretching
Polyvinylalcohol $\begin{array}{c} -CH_2-CH- \\ \vert \\ OH \end{array}$	2	Rho, Mono Mono more stable at normal temperatures
Poly-*p*-xylene —CH_2—ϕ—CH_2—	2	Modifs. α (Mono), β (Mono)
Polytrimethylenesebacate —O—$(CH_2)_3$—O—CO—$(CH_2)_8$—CO—	2	Tet, Mono
Polyhexamethyleneadipamide —NH—$(CH_2)_6$—NH—CO—$(CH_2)_4$—CO—	2	Modifs, α (Tri), β (Tri) Equal chain conformations
Polyhexamethylenesebacamide —NH—$(CH_2)_6$—NH—CO—$(CH_2)_8$—CO—	2	Modifs. α (Tri), β (Tri) Equal chain conformations
Poly—ϵ—caproamide —NH—$(CH_2)_5$—CO—	3	Modifs. α (Mono), β (Hex), γ (Mono) Modif. α at high temperature; modif. β at low temperature; modif. γ from special solutions or treatments
Other polyamides	2 (3)	For example: polyamide 7·7; even numbered polyamides *x*; polyamide 11

first macromolecular crystalline structure studied in detail[10]. Extra reflections were occasionally observed by X-rays: in some particular cases, their study led to the detection of the polymorphism. A triclinic modification[11-15], with the same zig-zag planar chain conformation as the orthorhombic one, was found in some cold-worked samples or in some single crystals, having an orthorhombic subcell. It is also formed by subsequent crystallization of part of the polymer below 95°C. Its density being very similar to that of the orthorhombic modification it can hardly be detected by dilatometric methods[13, 15]. The third modification is monoclinic[16-18] and was also observed in substantial amounts in cold-stretched samples; it is transformed into the orthorhombic form when the crystals relax[18].

Polytetrafluorethylene seems to possess at least three modifications[19]: modif. I is stable below 20°, modif. II is stable between 20° and 30°, and modif. III is stable above 30°C. They are all pseudohexagonal, with the same chain repeat of 2·59 Å. However, the chain conformations are different; modif. I corresponds to a 6·5/6 helix (6·5 monomeric units per 6 pitches) and modif. II corresponds to a 7·5/7 helix. By increasing the temperature the helix tends as a limit to relax towards a planar zig-zag. It is interesting to observe that many experimental facts are in favour of an enantiotropic situation, at least between modifs. I and II. This is of great importance, since, as we shall see later on, the macromolecular enantiotropic systems known so far are very few.

Polyoxymethylene, a polymer of formaldehyde, has two modifications of which one is hexagonal, and has been known for a long time[20, 21], and the other is orthorhombic[22, 23]; these have slightly different helix chain conformations (respectively 29/16 and 2/1) being essentially binary helices having a square projection with two monomeric units per pitch. At 75° to 80°C the orthorhombic modification transforms into the hexagonal modification which then remains stable even at low temperature.

The polymorphism of polyselenomethylene is just like that of polyoxymethylene; the orthorhombic modification here transforms into the hexagonal one at about 200°C[24-26].

An interesting case is that of polydimethylketene[27], which seems to be an enantiotropic system. The α and β modifications have chain conformations which in a certain sense are similar and different at the same time.
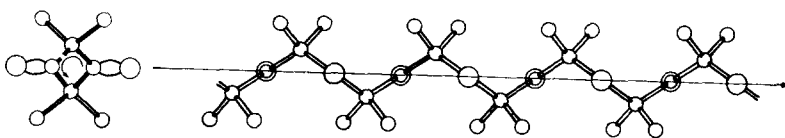
Figure 1—Chain conformation of polydimethylketene in modif. β[27a]

The β modification has a binary helix conformation (*Figure 1*) and is stable above about 250°C. The α modification, on the contrary, has a double twofold helix chain conformation (*Figure 2*) and is stable below 250°C, that is at a lower temperature. The unit cell of this last modification is orthorhombic (*Figure 3*).

O Carbon   ⊘ Methyl group   O Oxygen
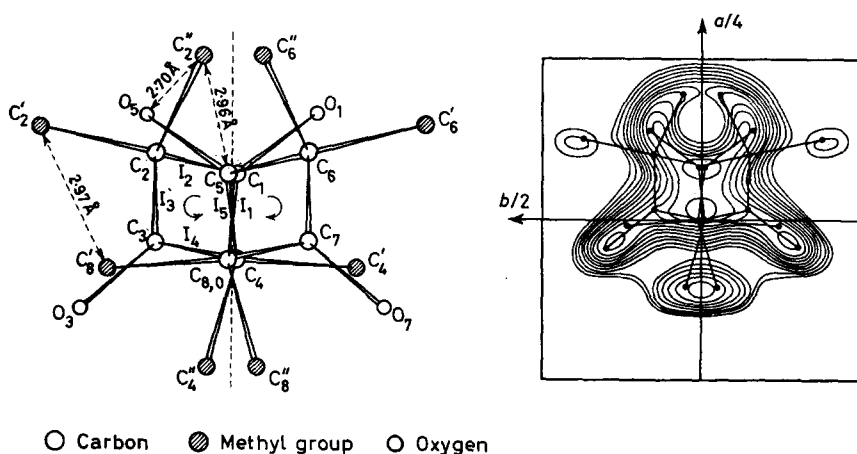
Figure 2—Projection normal to the chain axis of the polydimethylketene in modif. α and its electron density projection on (001)[27c]

Polyvinylidene fluoride has at least three modifications[28]. Modification I is obtained by cold-stretching and shows a very similar structure to that recently determined for polyvinyl fluoride (orthorhombic)[29]; the chain conformation is a planar zig-zag with a repeat of 2·57 Å corresponding to one monomeric unit. Modification II has a chain conformation that is very similar to that of modification I, but with a repeat of 4·66 Å, corresponding to two monomeric units. By melting and cooling modification I, a mixture of modifications II and III is obtained.
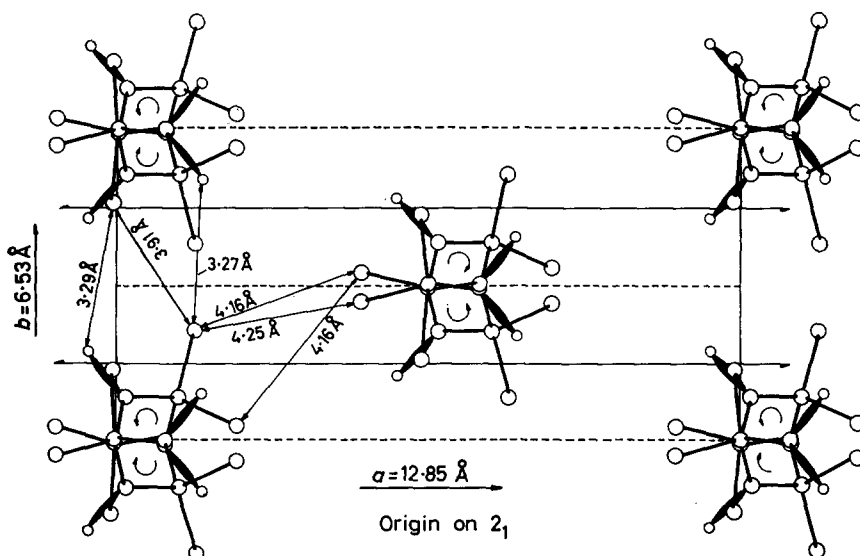
Figure 3—Projection on (001) of the structure of dimethylketene in modif. α[27c]

286

Molten and slowly cooled polyvinylalcohol crystallizes into a monoclinic modification; contrariwise, after quenching it yields a modification with an orthorhombic unit cell[30]. Crystallinity in this polymer does not require a stereoregular molecular structure[31].

Similarly, two crystalline modifications have been observed in the polymers of p-xylene[32].

Among the linear polyesters, two different assignments of crystal structure were suggested for polytrimethylenesebacate, one of tetragonal unit cell[5] and one of monoclinic unit cell[6]. These characterizations can be interpreted in terms of a dimorphism.

Moreover, there is the wide class of polyamides, in which at least dimorphism frequently occurs. Let us recall some examples.

With regard to polyhexamethyleneadipamide and polyhexamethylene-sebacamide (polyamides 6.6 and 6.10), two polymorphous forms were observed long ago[7] which were called α and β; they are both triclinic and differ in the packing of the chains that have the same conformation.

The situation of poly-ε-caproamide (polyamide 6) is more complex; besides the two modifications α and β[33], it presents a third modification γ[34]. The α and β modifications form by crystallization at high and low temperatures respectively. By cold stretching, the α modification transforms into the β one. Modification γ forms by particular processes, e.g. by treating modification α with a solution of potassium iodine–iodide, or sodium thiosulphate.

Polymorphism (commonly dimorphism) has been observed in various other polyamides, such as polyamide 7.7, some polyamides-x with even-numbered x, and polyamide 11[35].

POLYMORPHISM OF STEREOREGULAR POLYMERS

The situation of the polymorphism of stereoregular polymers is summarized in *Table 3*.

The first polymer shown is transtactic polyisoprene which occurs in nature as gutta-percha. Three polymorphous forms were observed for it[3, 4, 36–38] which corresponds to three different chain conformations. *Figure 4* shows the three conformations that were suggested by Natta and Corradini[37], partly modified with respect to the earlier suggestions by Bunn[4]. Modif. α forms under stretching; modif. β is obtained by low-temperature crystallization and shows an orthorhombic structure, which was studied for the first time in detail by Bunn[4]; the γ modification, which is more stable than the β, forms by the transformation of modification β below 64°C or by crystalliz-

Table 3. Polymorphism of synthetic stereoregular polymers

Polymer and structural unit	Number of polymorphs	Denomination, crystalline class, other information
Polyisoprene (transtactic) —CH$_2$—C=CH—CH$_2$— | CH$_3$	3	Modifs. α, β (Ortho), γ Different chain conformations. Modif. α under stretching. Modif. β transforms to modif. γ below 64°C. Monotropy β–γ

Table 3—continued

Polymer and structural unit	Number of polymorphs	Denomination, crystalline class, other information
Polybutadiene (transtactic) —CH₂—CH═CH—CH₂—	2	Modifs. 1 (P. Hex), 2 (P. Hex) Different freedom in chain conformations. Modif. 1 transforms reversibly to modif. 2 (by heating) at 76°C. Enantiotropy
Polypentenamer (transtactic) —CH═CH—CH₂—CH₂—CH₂—	2	Modifs. 1 (Ortho), 2 Different chain conformations. Both modifications under stretching (Rubberlike material; melts at room temperature)
Polypropylene (isotactic) —CH₂—CH— CH₃	3	Modifs. α (Mono), β (P. Hex), γ (Tri) Modif. α by normal cooling or by stretching the other two. Modif. β from certain samples of good stereoregularity. Modif. γ from stereoblock samples, normally with low molecular weight. All ternary helix chains; different packings. One mesomorphous modification in addition (smectic)

Polybutene-1 (isotactic)
—CH₂—CH—
     CH₂
     CH₃
	3	Modifs. 1 (Rho), 2 (Tet), 3 (Ortho) Modifs. 1 and 2 different helix chains. Modif. 1 by transforming the other two; modif. 2 from the melt; modif. 3 from solutions. Modif. 2 easily transforms to modif. 1 far from melting temperature; modif. 3 near melting. Monotropy 2–1 and 3–1

Polypentene-1 (isotactic)
—CH₂—CH—
     (CH₂)₂
     CH₃
	2	Modifs. 1 (Mono), 2 (P. Ortho) Different helix chains. Modif. 2 transforms to modif. 1 below 80°C

Polyheptene-1 (isotactic)
—CH₂—CH—
     (CH₂)₄
     CH₃
	2	Modifs. α, β Modif. α by stretching. Modif. β by cooling

288

Table 3—continued

Polymer and structural unit	Number of polymorphs	Denomination, crystalline class, other information
Polytetradecene-1 (isotactic) —CH$_2$—CH— $\|$ (CH$_2$)$_{11}$ $\|$ CH$_3$	2	
Polyhexadecene-1 (isotactic) —CH$_2$—CH— $\|$ (CH$_2$)$_{13}$ $\|$ CH$_3$	2	Modifs. I, II (Ortho) Modif. I by quenching. Modif. II by cooling the melt or by heating modif. I. One mesomorphous modification in addition
Polyoctadecene-1 (isotactic) —CH$_2$—CH— $\|$ (CH$_2$)$_{15}$ $\|$ CH$_3$	2	
Polyvinylcyclopropane (isotactic) —CH$_2$—CH $\|$ CH HC< $\|$ CH	2	Modifs. 1 and 2 Modif. 2 by cooling the melt. Modif. 1 by suitable quenching; transforms to modif. 2 by heating
Polyvinylcyclohexane (isotactic) —CH$_2$—CH—	(2)	(Tet. 4/1 helix; Tri, 3/1 helix)
Poly-2-vinylpyridine (crystallizable) —CH$_2$—CH—	2	Modifs. 1, 2 Only disclosed
Polypropylene (syndiotactic) —CH$_2$—CH $\|$ CH$_3$	2	Ortho, probably P. Hex Different chain conformations (helix and zig-zag). Ortho more stable. P. Hex by stretching quenched polymer; transforms to Ortho by heating

ation from the melt above about 60°C. The β and γ modifications are clearly in a monotropic relationship, as found by Mandelkern[38].

Transtactic polybutadiene shows two polymorphous modifications[39-43]. Modif. 1 has a pseudohexagonal unit cell and is stable at low temperature; at 76°C it transforms into modif. 2 with a transition that was shown by us to be enantiotropic, as we will see better later. Modif. 1 has a crystal structure very similar to that of β gutta-percha; its chain conformation is shown in *Figure 5*. When modif. 1 transforms into modif. 2, which is stable above 76°C and melts at 145°C, the chains still have a pseudohexagonal mode of

Figure 4—Chain conformations in the three polymorphs of transtactic polyisoprene (as suggested by Natta and Corradini)[37]

β $\qquad$ γ $\qquad$ α
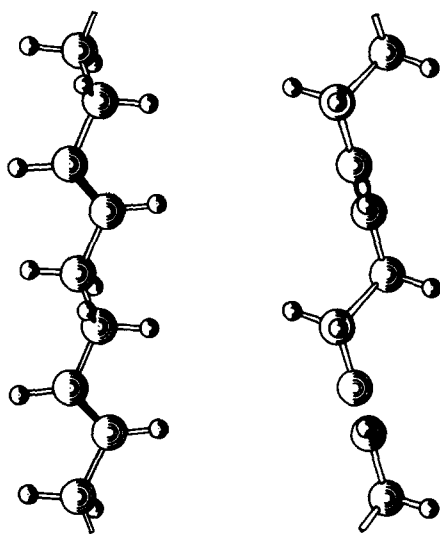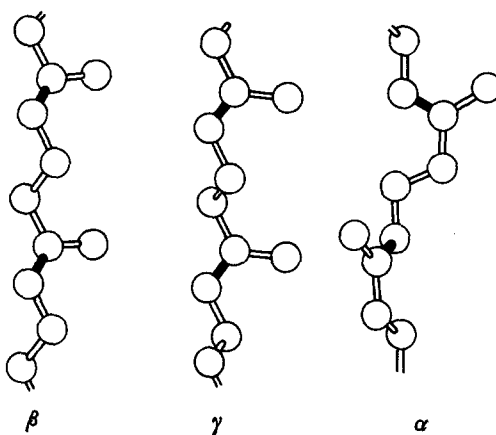
Figure 5—Model of chain of transtactic polybutadiene in modification 1[40]
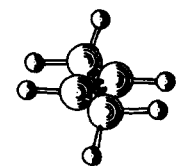
Polybutadiene 1-4 trans

C
H

290
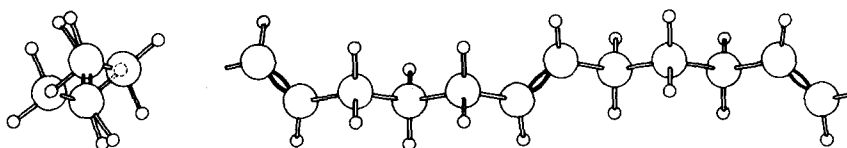
Figure 6—Model of chain of transtactic polypentenamer in modification 1[45]

packing, with parallel axes, but they are more free to move and to rotate along the chain axes, at least for long segments.

The phase change is accompanied by a decrease in density which can be estimated to be about ten per cent and the chain repeat shortens by about five per cent. Consequently, by the transition, an oriented fibre of this polymer undergoes a shrinkage caused by a real phase change which can be carried out reversibly with respect to the temperature (except for a hysteresis cycle: see below, Figure 22).

Transtactic polypentenamer is a new linear polymer of cyclopentene, which was obtained by us in the stereoregular form by stereospecific catalysts[44]. It is a rubberlike material, which is, like rubber, amorphous at room temperature or slightly above. It crystallizes under stretching, and two polymorphous forms can be obtained. Modif. 1 should have an orthorhombic crystalline unit cell[45, 46] with a chain repeat of 11·90 Å, corresponding to two monomeric units. The chain conformation can be seen in Figure 6; it contains segments of five carbon atoms conformed in a planar zig-zag, as in polyethylene, and periodic deviations due to the double
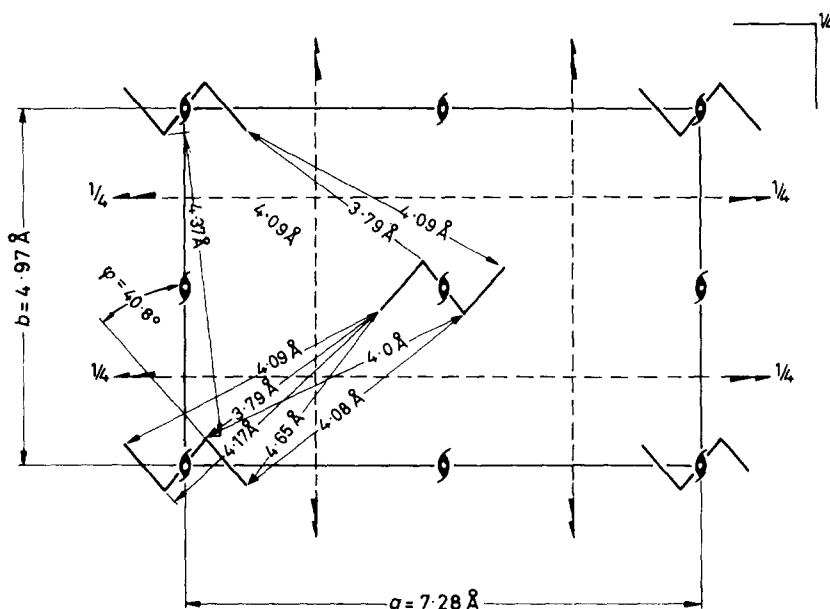
Figure 7—Structure of transtactic polypentenamer in modif. 1 [projection on to (001) plane][45]

bonds. The similarity with the structure of the orthorhombic modification of polyethylene is also seen from the type of arrangement in the unit cell, reported in *Figure 7*. A strict similarity also exists with the orthorhombic structure of the polyesters having an odd number of atoms in the repeating unit[5, 6].

On the other hand, modif. 2, as shown by i.r. analysis on certain samples[47],
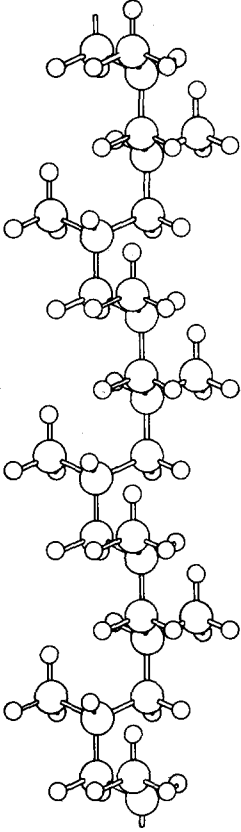
Figure 8—Chain conformation of isotactic poly-propylene[48]
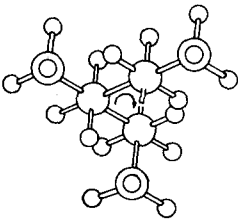
is characterized by a different chain conformation with planar zig-zag segments that are tilted with respect to the chain axis.

Three polymorphous structures have been found so far for isotactic polypropylene: essentially they differ in the mode of packing of the chains,
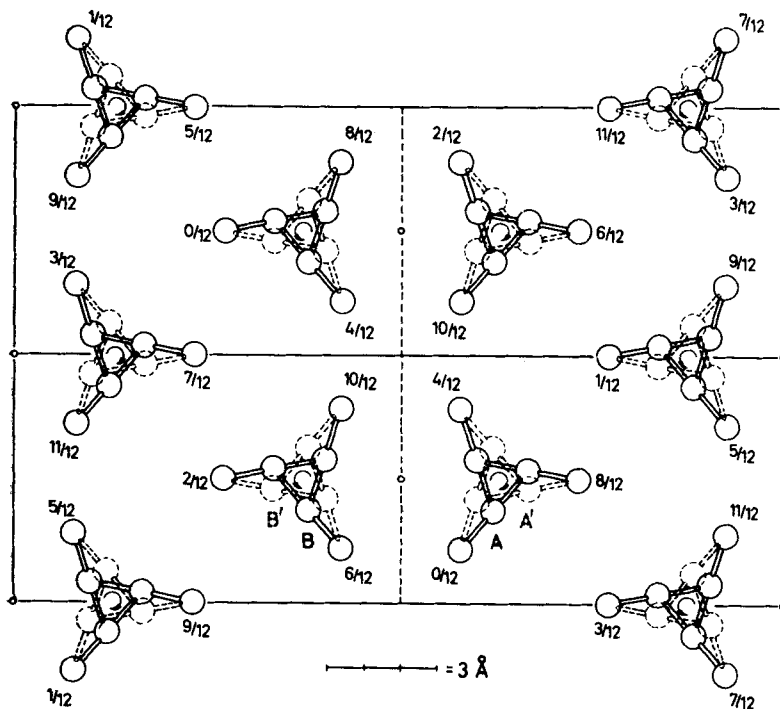
Figure 9—Structure of isotactic polypropylene in modification α [projection on to (001) plane]; dotted lines: possible isomorphous chains[48]

which always have the threefold helix conformation shown in *Figure 8*[48]. The structure of the unit cell of modif. α is reported in *Figure 9* and corresponds to a monoclinic unit cell with facing enantiomorphous helices[48]. The β and γ modifications, which were discovered much later, appear instead to have a pseudohexagonal[49–52] and a triclinic[51,52] structure respectively, *Figure 10* shows the X-ray diagrams of the three modifications[52]. *Figure 11* shows two possible modes of packing for modif. β, as suggested by Turner-Jones *et al.*[52]; according to these, the pseudohexagonal unit cell is particularly large and contains twelve chains arranged in triplets of helices having the same sense. *Figure 12* shows the mode of packing, as discussed by the same authors[52], for the γ modification (bottom), compared with that of the α modification (top). The β modification, at first observed in certain spherulites[49], was then obtained in substantial amounts by crystallizing polymer samples, melted not above 230° and quenched below 130°C. Only some polymeric samples yielded the β modification in substantial amounts; the reason for this has not been elucidated so far[52]. The γ modif. is obtained
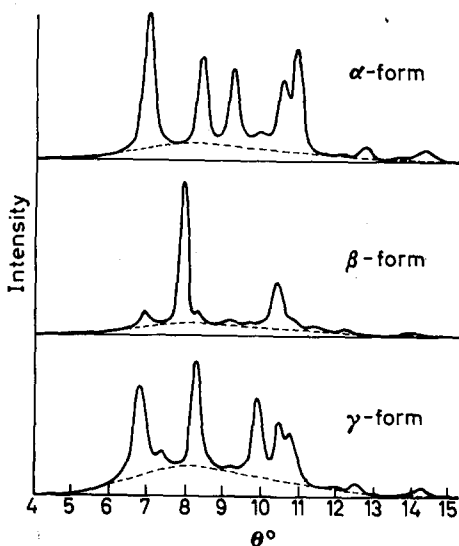
Figure 10—X-Ray diffraction diagrams of isotactic poly-propylene crystalline modifications[52]

by crystallizing under slow cooling only partially stereoregular polymers, of the isotactic stereoblock type, usually having a relatively low molecular weight. Common polypropylenes of good steric purity, cooled at the usual rates, crystallize into the more stable modif. α, which therefore is predominant when handling isotactic polypropylene. This explains why polymorphism in this polymer was observed with some delay.

The polymorphism of the next polymer, isotactic polybutene-1, is more versatile, at least from the phenomenological point of view. Three poly-morphous modifications are known so far, which have been the object of exceptionally intensive studies in these last three years[53-75].

Modif. 1, with threefold helix chains and a rhombohedral unit cell, and modif. 2, with almost fourfold helix chains and a tetragonal unit cell, were discovered since our synthesis of the first isotactic polymers, of which polybutene-1 was an example[53-55]. The crystal structure of modif. 1 is indicated in *Figure 13* (top), where a comparison is also made with the structure of the monoclinic modif. α of isotactic polypropylene (bottom). The structure of modif. 2 was later revised, and a chain conformation 11/3 (with eleven monomeric units every three pitches) was ascertained for it[56]. Modif. 2 is formed by crystallization of the molten polymer and transforms into modif. 1 with a rate which is maximum at practically room temperature. Modif. 1 is in practice obtained only by transformation of modif. 2, except in those very particular cases in which it can be obtained by direct crystallization from solution in a less stable morphological texture[67,68,70], which can also be obtained by solid–solid transformation of the modif. 3[66]. Modif. 3, discovered after the first two[57-66], forms by crystallization from solution and is either mixed with other modifications[67] or pure when prepared under suitable conditions[59,66]. It is supposed to have an ortho-
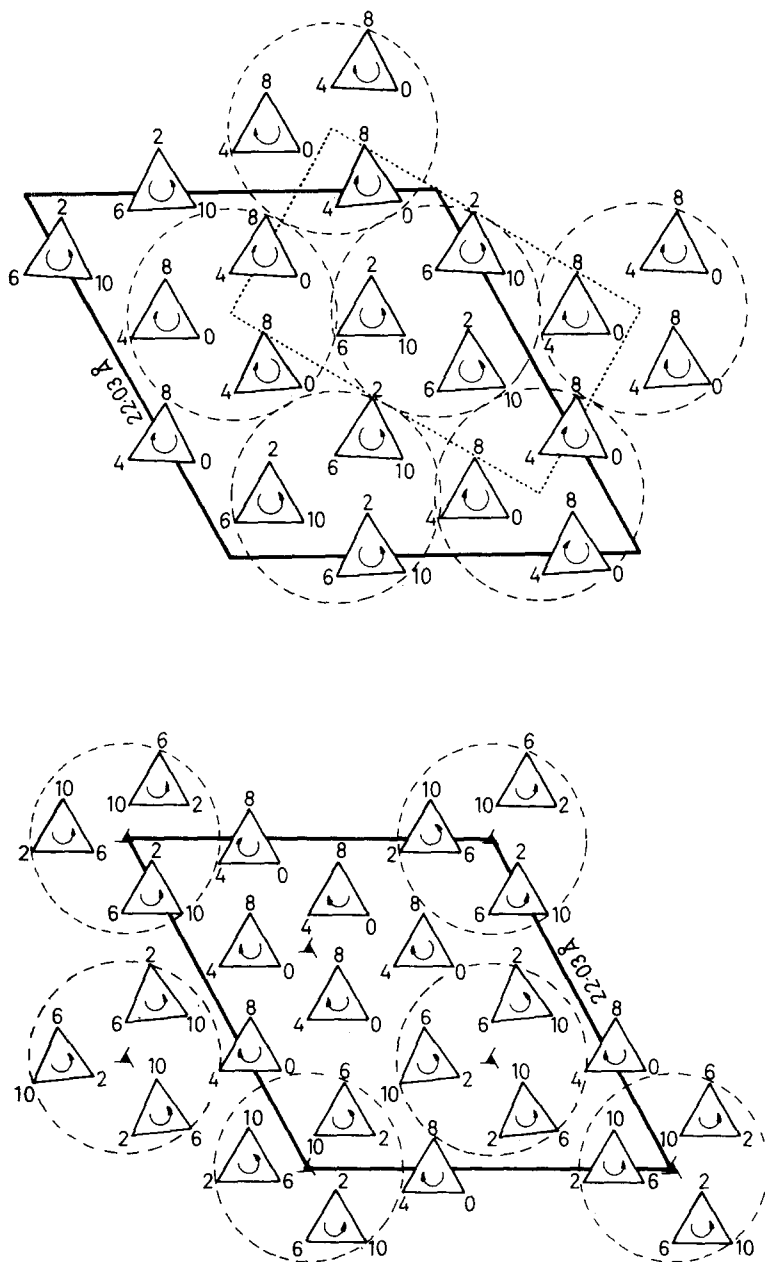
Figure 11—Possible packing of helices in isotactic polypropylene in modification β (numbers denote heights of methyl groups above a plane perpendicular to c, in $c/10$)[52]
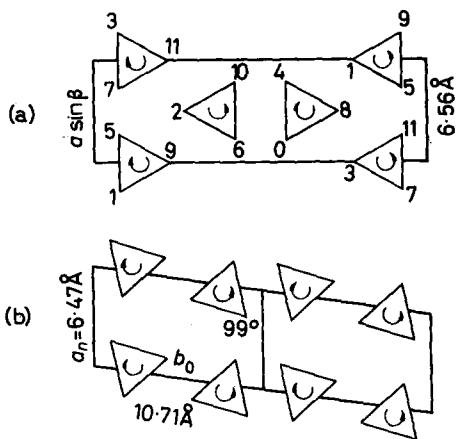
Figure 12—Isotactic poly-
propylene: (a) structure of
modif. α; (b) possible structure
of modif. γ[53]

rhombic unit cell[67, 68]. By thermodynamic investigations we have ascertained[59] that modifs. 2 and 3 are in a monotropic relationship with modif. 1. However, while modif. 3 transforms into modif. 1 practically in its melting interval, modif. 2 easily transforms into modif. 1 only at temperatures about 100 deg. C lower than those of melting[66, 74, 75]. A direct transformation between modif. 2 and 3 has not been observed so far.

The subsequent polymer listed in *Table 3* is isotactic polypentene-1, which appears to be dimorphous. Modif. 2 has been known to us since the synthesis of the first isotactic polymers; its chains have a threefold helix conformation[76], packed in a monoclinic unit cell[77]. Such a modification forms by natural cooling of the molten polymer and melts at 80°C. We have later found[78] that the molten polymer when left to stand for a long time slightly above 80°C, crystallizes very slowly into a new modification, namely modif. 1. The latter melts at very variable temperatures, in practice between 90° and 110°C, depending regularly and to a marked extent on the crystallization temperature, as can be seen from *Figure 14* (melting temperature versus crystallization temperature). The behaviour of this modification of polypentene-1 stimulated our attention to the general concept of 'equilibrium melting temperature'. This led us[65, 79], at the same time as Hoffman and Weeks[79], to the method, later applied to other polymers, of the experimental evaluation of the 'equilibrium melting temperature' by extrapolation of the melting temperatures measured rapidly on the polymer crystallized at various temperatures (in the case of this polymorph, the equilibrium melting temperature should be at about 130°C).

Modif. 1 of polypentene-1 is the more stable, since modif. 2 transforms into it with adequate thermal treatment slightly below the melting temperature. Modif. 1 has fourfold helix chains, packed in a pseudo-orthorhombic unit cell[77].

An interesting case of polymorphism is that found in isotactic polymers of higher olefins of the same normal aliphatic series, and examined in a
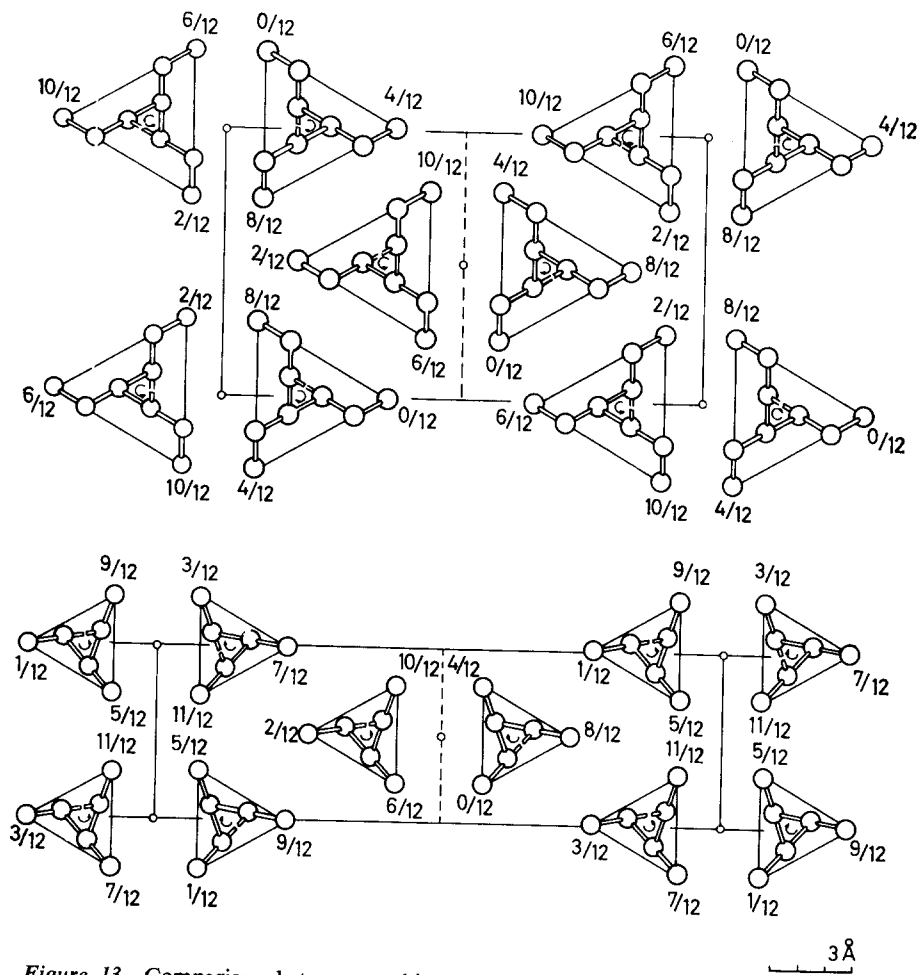
Figure 13—Comparison between packings of isotactic polybutene-1 and of isotactic polypropylene in the most stable polymorphous modifications [respectively: modif. 1 (Rho) and modif. α (Mono)][55]
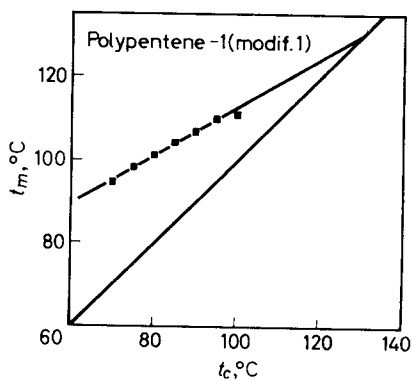
Figure 14—Relationship between melting temperature and crystallization temperature of isotactic polypentene-1 in modification 1[65]

297

recent study by Turner-Jones[80]. Polyheptene-1 crystallizes in two modifications, one of them under stretching, both having a structure which has not been characterized so far. Polytetradecene-1, polyhexadecene-1 and polyoctadecene-1 are dimorphous and the two different modifications of each are correspondingly similar in the series of the three polymers. Modif. I is obtained by quenching melted polymer at 0°C, followed by crystallization between 30°C and a temperature which is about five degrees below that of melting. Modif. II can be obtained by heating modif. I slightly below melting or by slowly cooling the molten polymer. Thus, modif. II is the more stable; it also has a higher degree of crystallinity and an orthorhombic unit cell.

In polymers with such a long side chain in the monomeric unit, some difficulty could have been expected in reaching an ordered conformation of the main chain; that is, it might be supposed that crystallinity would occur only to a reduced extent by packing of the paraffinic side chains, as happens in some atactic polymers with a long side chain (e.g. polyacrylates or polymethacrylates of higher alcohols). It has, however, been proved that a stable packing of macromolecules is nevertheless possible with a regular conformation of both the main chain and the side chains.

The structure of polymers of C_{14}, C_{16} and C_{18} α-olefins was not determined with sufficient accuracy but various elements were pointed out[80]. *Figure 15* shows two structures suggested for the more stable modif. II of such polymers. It can be seen that each polymer chain actually forms a kind of layer which, packed with similar layers in a regular manner, leads to a real three-dimensional crystallinity. In particular, the main chain assumes a regular fourfold helix conformation. This structure of modif. II is essentially orthorhombic like that of paraffins or of polyethylene, and can be considered mainly determined by the strong tendency of the side chains to crystallize.

On the contrary, in modif. I there is only a limited packing of the side chains and it can be assumed that crystallization is governed by the helicoidal form of the main chains. Such a form is, however, less stable in these polymers.

Thus, while in isotactic polypropylene, polybutene or polypentene we cannot think of a stable conformation different from the helicoidal one, in the polymers of higher normal olefins we see that, except for some intermediate and uncertain terms having a low melting temperature, the more stable crystal network becomes that of the orthorhombic packing of chains having a zig-zag planar conformation, these chains being not the main chains, but side chains. To these last, however, the main chains can adapt themselves and equally assume a suitable helicoidal form, so that they too can be inserted in the structure.

Next in our examination we find isotactic polyvinylcyclopropane. Under X-ray examination this polymer has appeared to us to be at least dimorphous; however, the crystal structures have not been thoroughly studied by us[81, 82]. Modif. 2 is formed by normal crystallization from the melt; by contrast, modification 1 forms by suitable quenching and cooling
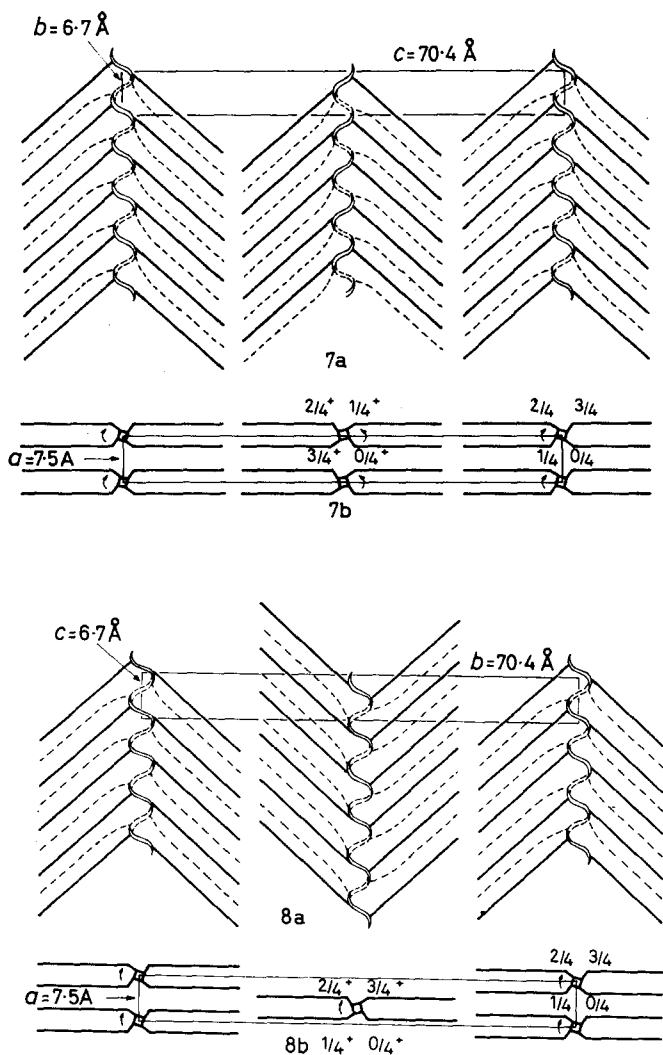
Figure 15—Type of structure envisaged for modification II of isotactic polytetradecene, polyhexadecene and polyoctadecene[80]. Top: 'right' and 'left' helices; side chains all tilted in same direction. Bottom: helices both of same hand; side chains tilted 'up' and 'down'

rates, and is transformed by heating into modif. 2. *Figure 16* shows the diffraction patterns of the two pure modifications, not hitherto published[82].

It is of interest to observe that, while modif. 2 is more dense than the amorphous polymer (density at 30°C, polymer in modif. 2, 0·976 g cm^{-3}; atactic polymer, 0·957 g cm^{-3}), modif. 1 is so little dense, that below about 55°C it is less dense than the amorphous polymer (at 30°C polymer in modif. 1, 0·951 g cm^{-3}). A similar phenomenon has been seen so far also

and only in modif. 2 of isotactic polybutene-1[74, 75] and in isotactic poly-4 methylpentene-1[83].

Isotactic polyvinylcyclohexane seems to have two modifications, in that a fourfold helix tetragonal structure[84] and a threefold helix triclinic one[85] have been independently suggested for it. This polymorphism, however, must be further defined.

With regard to the crystallizable poly-2-vinylpyridine, prepared by stereo-
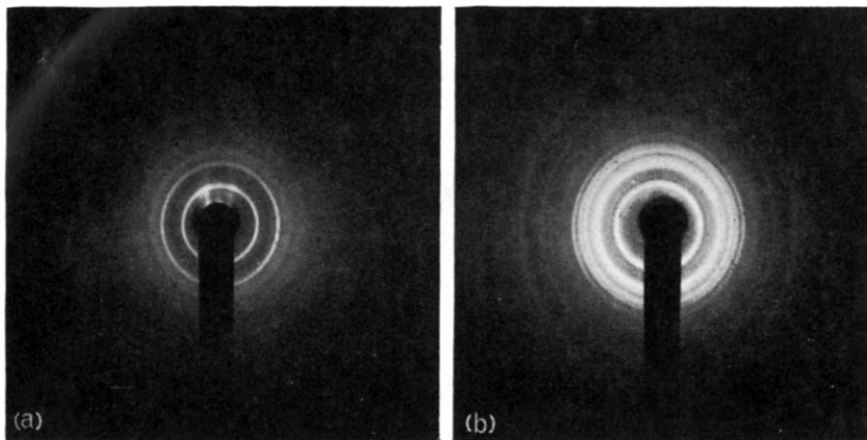
Figure 16—X-ray diagrams of the two modifications of isotactic polyvinylcyclopropane[82]: (a) modif. 1; (b) modif. 2

specific polymerization, we have detected two modifications by X-ray[86], the structures of which, however, have not yet been characterized.

Finally, there is syndiotactic polypropylene, which we deal with as the last case, being the only syndiotactic polymer which has so far shown polymorphism. We have recognized two modifications for it. The orthorhombic modification was found in the first preparation of the polymer[87], and is the more stable; its chains have the well known twofold helix conformation with binary axes perpendicular to the chain axis. Only a year ago[88] we found, by cold stretching of the quenched polymer, a probably pseudohexagonal modification, in which the chains assume a planar zig-zag conformation or nearly so. Such a modification is transformed into the orthorhombic one by heating, e.g. in a few hours at 100°C.

RESULTS ON ENANTIOTROPIC POLYMERIC SYSTEMS
In the course of the preceding examination we have seen that the cases of enantiotropy appear to be very few in the macromolecular field. This does not mean of course that they are necessarily few, but simply that the cases of macromolecular polymorphism sufficiently studied are still few.

We may in general say that a system should be classified as enantiotropic or monotropic only when a complete thermodynamic, and possibly also kinetic, investigation has shown it to be such. Actually, a complete

study is only seldom available and unfortunately it happens that systems not yet recognized for certain to be enantiotropic are frequently reported as monotropic.

It is known that enantiotropy can frequently be recognized by the ascertainment of transitions, from one polymorph to another one, of a 'thermodynamic', and not 'kinetic', character. At constant pressure, such a transformation is endothermal when caused by increasing the temperature, and exothermal when decreasing the temperature. It should be 'reversible', that is easily taking place in both directions. As a matter of fact, it is very seldom that a transformation of this type is 'prompt'. It is mostly 'suspended', in a more or less wide range, towards either high or low temperatures, or in both directions. Consequently, a hysteresis band is to be expected, which, if not entirely revealed by the investigation, may simulate monotropic behaviour.

Among the few cases of enantiotropy so far known with certainty for the polymers, the clearest is that of transtactic polybutadiene; it will be briefly illustrated here, insofar as it has been experimentally studied in its essential features[39-43].
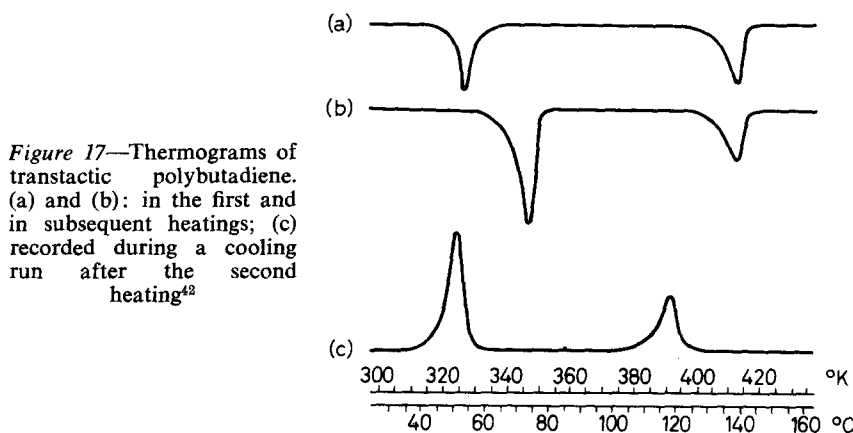
Figure 17—Thermograms of transtactic polybutadiene. (a) and (b): in the first and in subsequent heatings; (c) recorded during a cooling run after the second heating[42]

From *Figure 17* we may see the behaviour of the polymer as revealed by differential thermal analysis of the calorimetric type[42]. Thermogram (a) is that of the first heating of the polymer as prepared from polymerization and not previously melted: the first peak is that of the transformation of modif. 1 to modif. 2 and the second is that of the subsequent melting of modif. 2. Thermogram (b) is common to a number of heating runs performed after the first on the same polymer sample. Thermogram (c) was on the contrary recorded during a controlled cooling run.

In the first run the transition takes place at a lower temperature and with a smaller thermal intensity. In the subsequent runs it settles at 76°C, with about twice the thermal intensity. The melting, on the contrary, appears to take place every time at 145°C. This means that the sample, initially in modif. 1 with a defective crystalline texture, in the polymorphous transition of the first run is already transformed in a well crystallized modif. 2. By

301

cooling the sample, modif. 2 crystallizes first, and then its exothermal transformation to modif. 1 takes place. In both polymorphous and melting transitions an undercooling suspension is apparent. In particular, the polymorphous transformation proves to be substantially reversible, with features which are strictly similar to those of the melting.
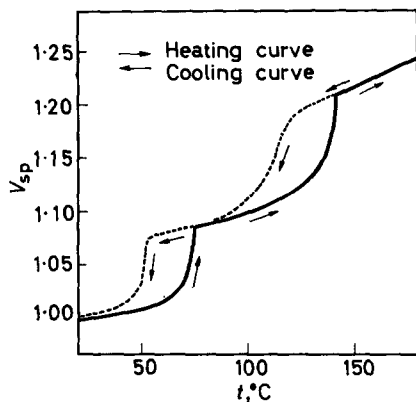
Figure 18—Dilatometric curves of transtactic polybutadiene. Full curve: heating at a rate of 6 deg. C/h; dashed curve: cooling at a rate of 4 deg. C/h[42]

In *Figure 18* dilatometric curves are reported of a heating and a subsequent cooling run of a similar sample[42] in conditions not too different from those of the preceding figure: here the similarity between the two phase transitions is in a sense even more evident. Both the transitions are clearly of a 'diffuse' kind.

Particularly interesting are the results relative to the same polymorphous transition effected in the presence of a solvent or with a polymer chemically modified by introduction of various amounts of comonomeric units of another diolefin in the chain[89].

Figure 19 shows qualitatively two typical sets of results. The upper curve is a horizontal straight line: it indicates that the transition temperature (on the ordinates) is not affected by the presence of a solvent, as is to be

Figure 19—Enantiotropic transition temperature of transtactic polybutadiene versus composition in the presence of a solvent and with the polymer chemically modified by introduction in the chain of isomorphous comonomeric units of another diolefin[89]
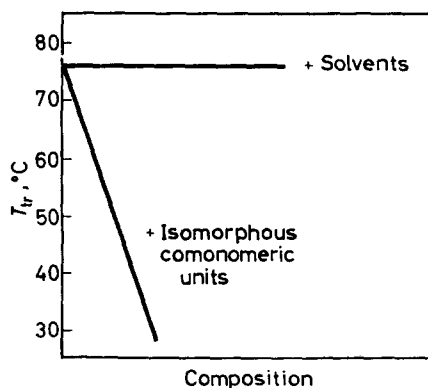
expected for a solid–solid transition. The lower curve, on the contrary, indicates a remarkable depression of the transition temperature when an increasing amount of isomorphous comonomeric units is introduced into the polybutadiene transtactic chain, a fact which again is according to expectation.

Table 4. Thermodynamic properties of transtactic polybutadiene

	ΔH_u (cal/struct. unit)	ΔS_u (e.u./struct. unit)	T (°C)
Fusion			
Mod. 1	3 300	8·95	96
Mod. 2	1 100	2·7	145
Transition 1 $\longrightarrow$ 2	2 200	6·3	76

A thermodynamic analysis was also carried out by determining the fusion quantities of both modifications[42]. The measure of melting temperature depressions in the presence of benzophenone or α-chloronaphthalene, in addition to differential calorimetric determinations, enabled us to calculate the data of *Table 4*[42].

It is apparent that both enthalpy and entropy of fusion have high values for the low melting modif. 1 and comparatively low values for the high melting modif. 2. This means that, by heating the polymer, in the polymorphous transformation there is an increase of enthalpy and a great gain of entropy. This appears to be also in agreement with the structural change from a pseudohexagonal unit cell with a close packing of comparatively rigid macromolecules to a similar unit cell which is shorter along the c axis and broader along the other two axes; this may probably be due to a rotational freedom acquired by the chains around the bonds between monomeric units.

This remarkable gain of entropy, in addition to the low fusion entropy of the high temperature polymorph, is also consistent with the observed similarity between the features of the polymorphous transition and those of the melting; and we may conclude that the transition should be prompt towards the high temperatures, just as for the melting.
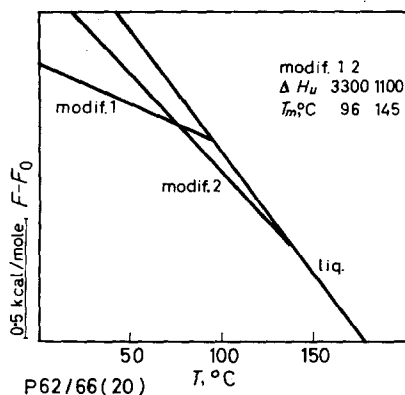
Figure 20—Phase diagram of the enantiotropic polymorphism of transtactic polybutadiene (from the data of *Table 4*)

From the thermodynamic data, the phase diagram of free energy versus temperature should be approximately as reported in *Figure 20*. For simplicity, the functions were chosen as straight lines; those of the solid phases are those of the best crystalline elements actually present in the polymer sample. The transition points, corresponding to the intersections between the straight lines, have consequently to be understood as ultimate transition temperatures, as is usual for thermodynamic considerations on the solid state of polymers.

It is interesting to note that from the thermodynamic and dilatometric data found it is possible to calculate, by means of the Clausius–Clapeyron equation, the value of the derivative of the pressure with respect to the temperature for the polymorphous transition. It results in $dp/dt = 60$ atm/$°K$, which is exactly the value indicated as a rule by Bridgman[90] for a number of polymorphous transitions of low molecular weight compounds.

The enantiotropic transition of transtactic polybutadiene was also studied by mechanical measurements on oriented samples of polymer[43].

Figure 21—Length of an initially oriented sample of transtactic polybutadiene versus temperature, without applied stress; (a) heating; (b) subsequent cooling[43]
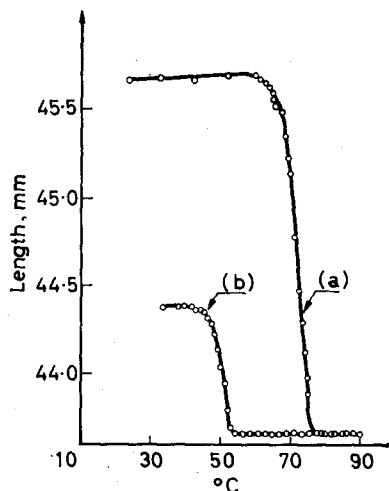
If a ribbon of polymer in modif. 1 is oriented by stretching and then heated without applied stress, the length of the ribbon shrinks through the transition, as reported in *Figure 21*. By cooling the sample, the length increases by coming back from modif. 2 to modif. 1, but the initial orientation is lost. If the same experiment is carried out under a suitable constant stress, as in *Figure 22*, the initial length can be perfectly recovered and the transition is reversible, save for a hysteresis cycle. This means that, at least in principle, the polymer under consideration could be used as a working substance of a thermal machine fit for transforming heat into mechanical work, by utilizing the polymorphous transition.

RESULTS ON MONOTROPIC POLYMERIC SYSTEMS

The monotropic polymeric systems seem to be more frequent than the enantiotropic ones. But only in two cases, gutta-percha and isotactic poly-
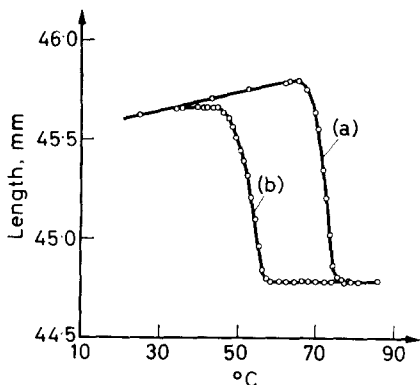
Figure 22—Length of an oriented sample of transtactic polybutadiene versus temperature, with a suitable stress applied; (a) heating; (b) subsequent cooling[43]

butene-1, has a thermodynamic analysis ascertained that the system was really monotropic.

The polymorphism of polybutene-1 has been studied in the last three or four years with exceptional intensity. At least 35 authors have been interested in its investigation[53-75], which implies not only fundamental, but also practical aims.

We will now illustrate the essential results we have obtained for this system, in substantial agreement with the results of other authors.

It may be remembered that the three modifications of polybutene-1 can be normally obtained in the following ways: modif. 2 by crystallization from the melt; modif. 1 by transforming modif. 2 or modif. 3; and modif. 3 by crystallizing the polymer from solutions. In these ways, modif. 2 is normally obtained in a spherulitic or hedritic morphology[60]; modif. 3, by contrast, has so far been obtained in a lamellar or single-crystal morphology, because it is better prepared from dilute solutions. As a consequence, modif. 1 can be obtained either in spherulites and hedrites, or in lamellar and single-crystal form, in that it can be prepared only by transformation either of modif. 2 or of modif. 3, and both these transformations proved to be of the solid–solid type, endowed with morphological memory[65, 66]. In a sense, modif. 1 is in general pseudomorphic, at least for the microscopic external habit.

All three modifications were obtained by Miller and Holland in lamellar or single-crystal form by suitable thermal treatments starting from polymer solutions[67, 68] and separating single morphological elements.

These morphological considerations are important also because they clarify the fact that so far modifs. 1 and 2 have also been prepared with a comparatively more thermodynamically stable texture, whereas modif. 3 has so far been prepared only in a thermodynamically defective morphological texture.

On this ground, we succeeded in evaluating the equilibrium melting temperature of modifs. 1 and 2 by extrapolation of the melting temperature versus crystallization temperature plot[65]. *Figure 23* reports the evaluation for modif. 2 with an equilibrium melting temperature at about 130°C. *Figure 24*

Figure 23—Melting temperature versus crystallization temperature for isotactic polybutene-1 in modification 2[65]
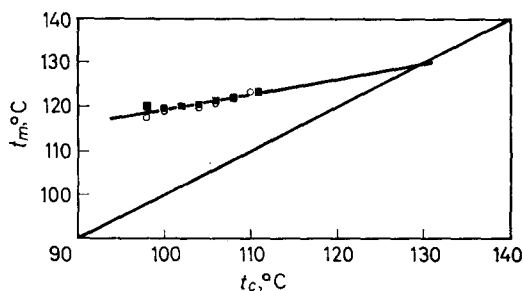
reports the same evaluation for modif. 1. On the abscissa are in this case the crystallization temperatures of the parent modif. 2, then transformed to modif. 1 at the constant temperature of 40°C. It is evident that the morphological memory in modif. 1 allows extrapolation of the data. The equilibrium melting temperature of modif. 1 can be evaluated at about 138°C.

A detailed thermodynamic analysis, based on the depression of the melting temperature in the presence of diluents, allowed us[59] to conclude that the system was monotropic with regard to modif. 1, the fusion enthalpies being about the same for the three polymorphs (around 1·5 kcal/mole with different accuracies for the three modifications). For modif. 2, owing
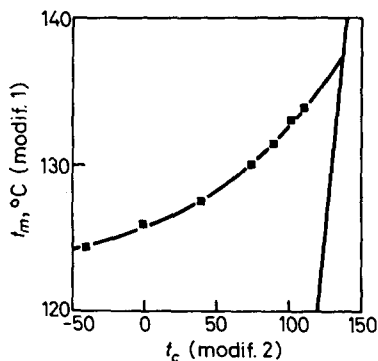
Figure 24—Relationship between melting temperature of polybutene-1 in modification 1 and crystallization temperature of modification 2 from which modif. 1 was prepared by polymorphic transformation at 40°C[65]

to experimental difficulties, the fusion enthalpy was roughly estimated; however, with the present better kinetic knowledge of the transitions between pairs of modifications, the doubt can exist that the assumed and not X-ray controlled modif. 2 considered in that paper[59] could have been in reality a defective modif. 1. Our subsequent differential calorimetric data[91] indicated for modif. 2 a fusion enthalpy of about 1·0 kcal/mole, in reasonable agreement with evaluations published in the meantime by other authors[69, 71, 72].

The results of the thermodynamic analysis can be summarized here as in Figure 25, showing a free energy versus temperature phase diagram drawn on the basis of the data chosen as indicated. The monotropic relationship of modif. 2 with regard to modif. 1 appears to be definitive. The monotropic relationship of modif. 3 with regard to modif. 1 is also

sufficiently clear. On the contrary, some doubts exist on the relationship between the two metastable modifs. 2 and 3, mainly as a consequence of the uncertainty about the equilibrium melting temperature of modif. 3. The free energy of modif. 3 is here indicated with two dotted curves: the upper curve is experimental, but for a modif. 3 with defective morphological texture; the lower dotted curve is only hypothetical and estimated in analogy

Figure 25—Free energy versus temperature phase diagram of isotactic polybutene-1 [59, 65]
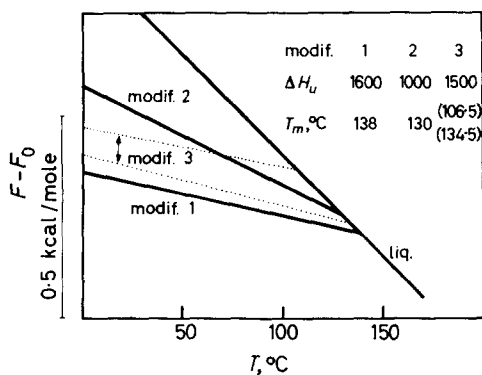
with what is known to occur for modif. 1. Actually, the modif. 1 prepared by solid–solid transformation of the defective modif. 3 melts at about 110°C, that is about 28°C under the equilibrium melting. By transferring this difference of temperature to modif. 3, the presumed value of the equilibrium melting of this last modification could be about 134°C. We may see that the band of free energy values so established can admit either an enantiotropic or a monotropic relationship between (metastable) modifs. 2 and 3. On the other hand a direct transition between these two modifications has never been observed so far in experiment.

An interesting phenomenon of thermodynamic stability inversion was observed in polybutene-1. In order to describe it, we may examine first the kinetic transformation which takes place by heating modif. 3[66].

Figure 26 shows a dilatometric curve recorded during a slow heating of modif. 3 : we can recognize a transformation of modif. 3, during the fusion
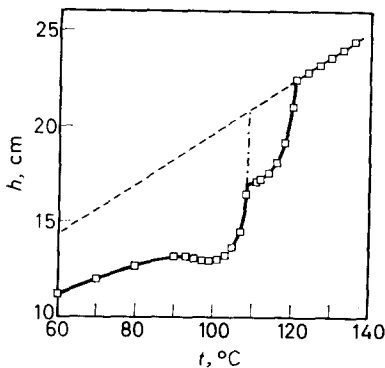
Figure 26—Dilatometric curve of a sample of isotactic polybutene-1, originally in modif. 3, heated slowly to 111°C (1 reading/12 h) and then rapidly to 140°C (2 deg. C/15 min)[66]

interval, in a more dense polymorph and that this last melts at about 110°C, leaving another polymorph which melts just above 120°C.

By repeating an equivalent heating experiment in the X-ray apparatus, the diffraction diagrams of *Figure 27* were obtained at different steps of the
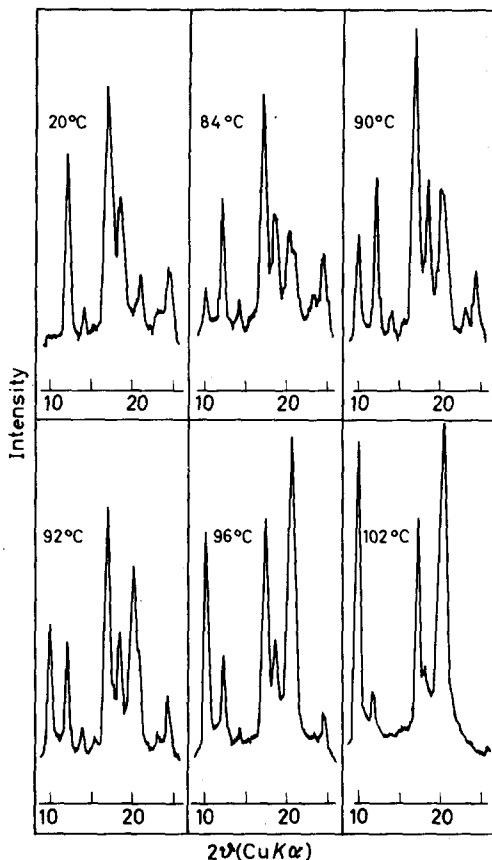
Figure 27—X-Ray diagrams showing the transformation of modif. 3 of isotactic poly-butene-1 to modif. 1 by slow heating to 102°C[66]

heating run. They show that modif. 3 gradually transforms to modif. 1 before melting without the presence of any amount of modif. 2. The transition proved to be of the solid–solid type.

A similar experiment was done by rapid heating and its results are those of *Figure 28*. In this case modif. 3 has insufficient time to be transformed to modif. 1 and, when it is melted, modif. 2 appears and crystallizes to a high degree. This proves that modif. 2 is formed by crystallization of melted polymer which becomes available during the fusion of the other polymorph.

In substantial agreement with this finding is the differential thermogram of *Figure 29*, recorded by Geacintov, Schotland and Miles[63], clearly showing an exothermal peak between the two endothermal peaks of the meltings of the two modifications, and thus supporting a solid–liquid–solid passage from modif. 3 to modif. 2.
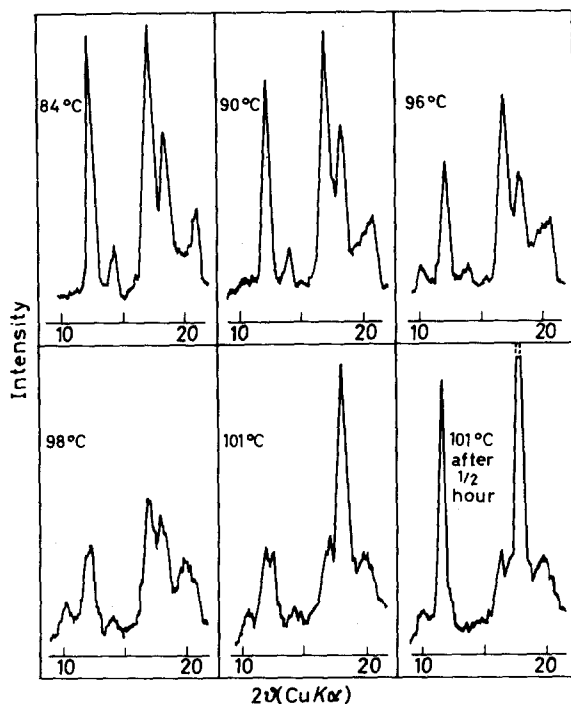
Figure 28—X-Ray diagrams recorded during a rapid heating
of polybutene-1 in modif. 3[66]

Turning back to the phenomenon of stability inversion, we have noticed that in the slow heating of modif. 3, a modif. 1 was formed which melted surprisingly low, at 110°C, that is at a temperature lower than the usual melting temperature of modif. 2. This means that the morphological texture of modif. 1 obtained from modif. 3 was so defective that the free energy
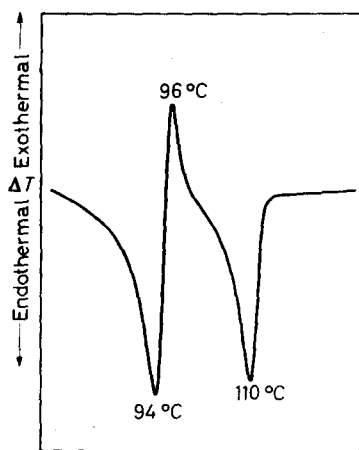
Figure 29—DTA thermogram showing the melting of modif. 3 of polybutene-1 and the subsequent formation of modif. 2[63]

309

of modif. 1 prepared by this particular route happens to be greater than that of the usual modif. 2.

Some interesting results of quantitative kinetics of the polymorphous transformation of modif. 2 to modif. 1 have been obtained by us[75]. However, before presenting this, it is useful for comparison to consider the quantitative kinetic results we have obtained for the crystallization of modif. 2 from the melt[75].

Figure 30 shows the dilatometric isotherms relative to the crystallization

Figure 30—Dilatometric isotherms of crystallization of isotactic polybutene-1 in modif. 2[75]
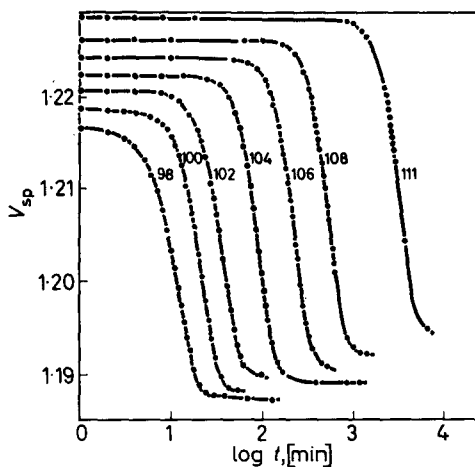
of modif. 2 from the melt at different temperatures, as indicated. These isotherms can be well analysed in terms of Avrami's equation. The value of Avrami's exponent is 3·1, in complete agreement with the values found in good kinetic determinations with other crystallizable polymers.

Now, *Figure 31* shows the dilatometric isotherms relative to the poly-
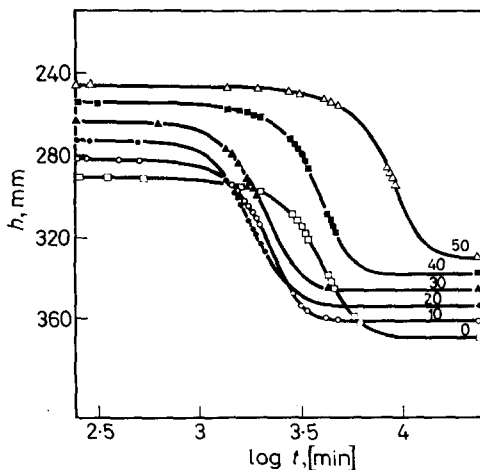
Figure 31—Dilatometric isotherms of solid–solid transformation of modif. 2 to modif. 1 of isotactic polybutene-1[75]

310

morphous transformation of modif. 2 to modif. 1, performed on the same sample crystallized at 102°C, then isothermally transformed at different temperatures, as indicated[75]. We may note that the transformation apparently proceeds with features completely similar to those of a crystallization from the melt, like those we have seen in *Figure 30*. These isotherms can equally be analysed in terms of Avrami's equation and give an exponent of 3·3.

Thus, we may think that the mechanism of the solid–solid transformation may be interpreted by extending the model used in the derivation of Avrami's equation. In other words a mechanism of nucleation can be envisaged, followed by propagation of the new solid phase in the parent phase, at the expense of the latter.

The half-times of the transformation are reported in *Figure 32* as a
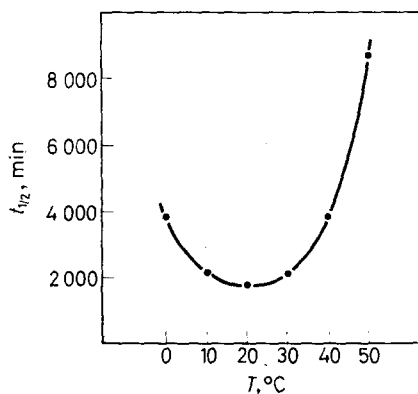
Figure 32—Half-times of the polymorphous transformation of modif. 2 to modif. 1 of isotactic polybutene-1[75]

function of the temperature. The minimum half-time is practically at room temperature.

It seems that the value and the temperature of the minimum half-time can vary slightly depending on the purity of the sample. For instance, Boor and Mitchell[58] found a slight decrease of the minimum value, and a slight increase of the corresponding temperature, by seeding the polymer with a small amount of another suitable crystalline substance, as reported in *Figure 33* (e.g. isotactic polypropylene and stearic acid). They found also[61] an influence of the thickness of film-formed samples, as did Clampitt and Hughes[72], who also observed a difference between samples having different amounts of ash.

Equally, we have found a clear dependence of the transformation on the temperature at which the modif. 2 was crystallized[75]. *Figure 34* shows the relationship for a transformation performed at 30°C. The half-times are lower when the crystallization temperatures are higher, in other words, the better the morphological texture, the easier the transformation. This might be considered to be in agreement with the fact observed in some low molecular weight compounds, that a given polymorph is kinetically more stable when stored in small rather than large crystals.

A peculiar property we have observed[74, 75] in isotactic polybutene-1 which is conditioned by the polymorphism, is a dilatometric isophasic transition that takes place only in the polymer in modif. 2, at about 65°C. In
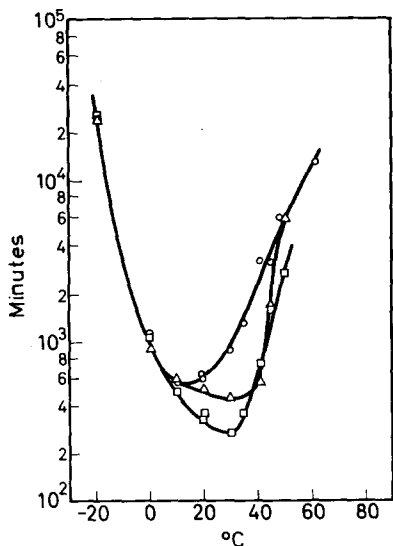
Figure 33—Times required to attain a given dilatometric contraction in modif. 2 (to modif. 1) of isotactic polybutene-1: ○ parent sample; □ seeded with 5% wt isotactic polypropylene; △ seeded with 5% wt stearic acid[58]

Figure 34—Half-times of the polymorphous transformation at 30°C of modif. 2 to modif. 1 of isotactic polybutene-1 as a function of the crystallization temperature of modif. 2[75]
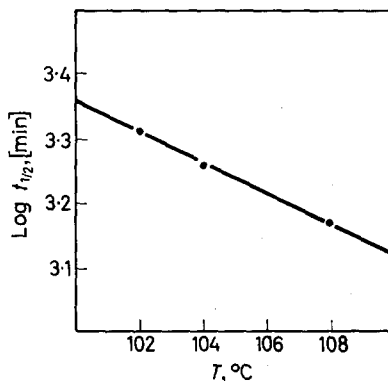
Figure 35, showing dilatometric curves of the three polymorphs, we may see that only for modif. 2 (the highest curve) there is a 'knee' typical of isophasic transitions. The abrupt change at 65°C of the expansion co-efficient in modif. 2 may be better appreciated in *Figure 36*. Such is the change that at low temperature, about 5°C, the density of modif. 2 becomes lower than that which can be foreseen for the amorphous or atactic polymer.

The isophasic transition can be particularly interesting in that it is specific not, as usual, of the amorphous part of the polymer but of the crystalline structure of modif. 2. It is very difficult today to understand the nature of such a transition. A certain analogy might be seen with the not so clear change which occurs in polyethylene at about 90°C[92].

312

Another aspect which could be in some way related to the isophasic transition of modif. 2, is that the temperature range in which modif. 2 can in practice be transformed to modif. 1 is far from the melting tempera-
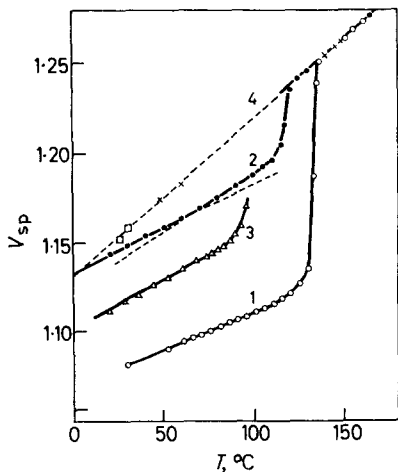
Figure 35—Comparison among dilatometric behaviour of the three modifications of isotactic polybutene-1 (curves 1, 2, 3: modifs. 1, 2, 3; curve 4: atactic polymer)[74]

ture of both polymorphs and it is actually below the transition temperature. In general, a monotropic transformation takes place easily only near to, and not far from, the melting temperature of the less stable polymorph.

A typical monotropic transformation is, for example, that we have seen in *Figure 26* of modif. 3 to modif. 1 of isotactic polybutene-1, or that which was dilatometrically observed in isotactic polypentene-1[78], on the right
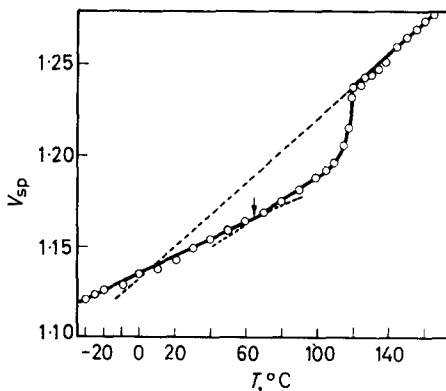
Figure 36—Dilatometric curve of isotactic polybutene-1 in modif. 2[74]

hand diagram of *Figure 37*. These transformations take place during the fusion interval of the low melting modification, which leaves, once melted, a part of the polymer in the high melting modification.

Another interesting feature of macromolecular polymorphism can be seen in *Figure 37* by comparing the two diagrams: the polymorphous
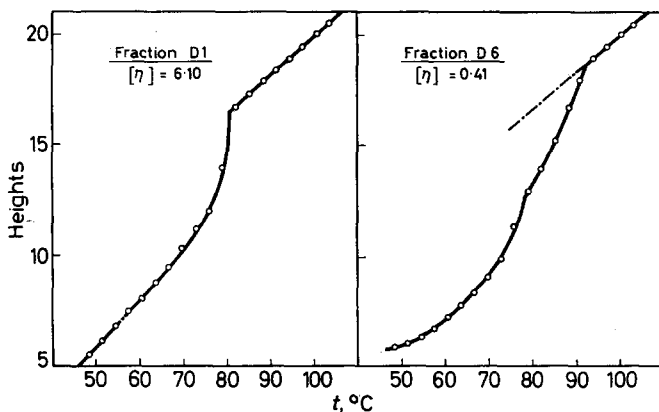
Figure 37—Dilatometric curves of two fractions of different mole-
cular weight of isotactic polypentene-1 in modif. 2 (rapid
heatings)[78]

transition takes place only in the right hand diagram, which refers to a
low molecular weight sample. On the contrary, in the left hand diagram no
polymorphic transformation occurs, the polymer sample being of very high
molecular weight.

The interesting more general conclusion from this fact is that in macro-
molecular polymorphism metastable states are increasingly possible when
the molecular weight increases. This condition can be such that a poly-
morphism could thermodynamically exist without being in practice kinetic-
ally effective. This statement is on the other hand in agreement with our
general knowledge of the relaxation and physical behaviour specific of
high polymeric substances.

THEORETICAL PREDICTION OF POLYMORPHISM

Any prediction concerning polymorphism in general has to be based on
the theory of crystal stability.

It is known that the stability of rare-gas crystals as well as that of simple
ionic solids (especially alkali halides) has been studied in great detail, on the
basis of pair interactions between atoms or ions and looking for a geo-
metrical situation which minimizes the lattice energy.

For metals a similar type of analysis can be undertaken[93], following
the 'electronic gas' theory. A different approach to this problem is based
on the Pauling theory of the metallic bond[94].

The calculated differences in energy between different structures are,
however, in several cases very small, so that definite conclusions concerning
the stable structures do not seem to be justified.

An important improvement in this field appears to be that recently intro-
duced by Jansen[95] for rare-gas crystals and by Lombardi and Jansen[96] for
alkali-halide polymorphism. Their calculations are based on three-body
interactions[97], and it has been shown that, by introducing simultaneous
interactions between triplets of atoms or ions in the solid, discrepancies
between predictions and experiments of previous theories were removed.

314

Also with organic macromolecular substances, the problem of polymorphism falls under the more general question of finding the most probable crystalline arrangements of a given polymer having a known chemical structure (real or hypothetical).

An *a priori* calculation is, however, very difficult if relative to the mode of packing of given macromolecules, even if these are assumed already to have a regular conformation. Today, a packing efficiency can be only empirically considered in terms of a good filling of the space and of suitable distances between atoms or groups of atoms.

Easier to be treated theoretically is, on the contrary, the regular conformation which can be reached by a given chain, assumed to be completely known from the point of view of its chemical structure and geometry (bond distances, valence angles, etc.).

Different approaches were attempted by some authors in this direction. Bunn was the first[4, 98] who applied geometric restrictions deriving from the knowledge of the chemical structure to the selection of trial crystalline structures, and an energetic criterion through the so-called 'principle of staggered bonds'. Fordham[99], and Shimanouchi and Tasumi[100], also derived possible chain conformations through restrictions imposed by electrostatic and steric effects.

A very interesting approach, again from the formal point of view, is that introduced by Natta, Corradini and Ganis[101] and by Liquori *et al.*[102]. It is mainly based on two postulates.

The first postulate is that all the structural units are in geometrically equivalent positions with regard to an axis, and is called 'equivalence postulate'. In other words any unit can be superimposed on the next one along the chain by means of such appropriate symmetry operations as rotation and translation with regard to the axis.

The second postulate is that the regular conformation actually attained in the crystal lattice by the chain should correspond to the same energy minimum which would be reached by the chain when isolated and in no way influenced by external forces. This is called the 'minimum energy postulate', which essentially states that the influence of the packing in the stability of the chain conformation should be negligible.

By means of these postulates, and taking into account the van der Waals repulsion between atoms separated from each other by up to four bonds, the values of the internal energy of the chain can be calculated as a function, for example, of the internal rotation angles which characterize the conformation assumed by every unit inserted in the chain.

Figure 38 shows the energy contour map that was thus obtained for isotactic polypropylene: here two rotation angles are sufficient as conformational variables[101]. It is interesting to see that two minima are formed, for which the rotation angles correspond respectively to a left-hand and to a right-hand helix conformation. The helix symmetry may be that of the threefold helix.

From the point of view of polymorphism, we have seen that in reality in isotactic polypropylene all the three modifications are formed by threefold

shaped helices with differences due only to mode of packing (which is not considered in this theory).

In *Figure 39* the results are shown of a similar calculation for syndiotactic polypropylene[101]. Here three different minima are present: two of them correspond again to left-hand and right-hand helices; the third, on the contrary, to a zig-zag planar conformation. In fact, we have seen that up to now, for that polymer two polymorphous modifications were discovered, having respectively a binary helix and a zig-zag planar conformation.
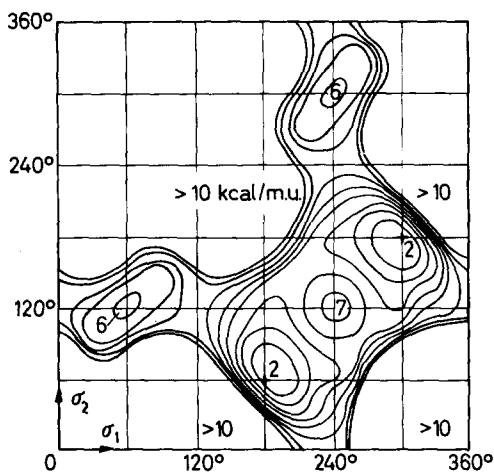
Figure 38—Internal energy of an isotactic polypropylene chain for different axial conformations as a function of the two internal rotation angles[101]

Figure 39—Internal energy of a syndiotactic polypropylene chain for different axial conformations as a function of the two internal rotation angles[101]
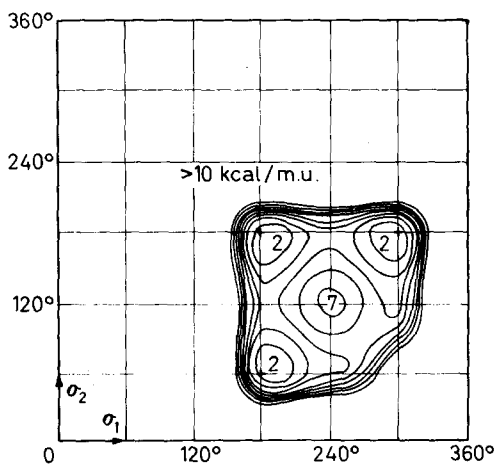
Recently Furukawa *et al.*[103] have calculated the energy of differently helix conformed isotactic polybutene-1 chains, and have found that the ternary helix should be the preferred one, as found in fact for the more stable polymorphous modification of polybutene-1.

Of course, not all the requirements introduced into the theory are actually satisfied and some deviations have to be expected in a more detailed investi-

gation. For example, the 'equivalence postulate', though it often holds, is not expected to be obeyed always. Just as chemically identical molecules can sometimes occupy non-equivalent positions in micromolecular crystals, so identical structural units in polymers may occupy non-equivalent sites. An instance of this kind is under discussion for the crystal structure of polydimethylketene[27]. Similarly, the 'minimum energy postulate' may also be compromised when particular intermolecular forces may distort free macromolecule conformations (polar groups, hydrogen bonding, etc.). It is known that the situation, not considered here, of polypeptide chain conformations is more complex in this respect.

In spite of these difficulties, the above analysis is to be considered as a valuable approach in many simple cases of synthetic polymers.

From all the experimental data illustrated in the preceding paragraphs it is possible to conclude that the macromolecular polymorphism can be theoretically thought of as a consequence either of differences in the packing of chains with equal conformations, and/or of differences in the chain conformations. The chain conformation analysis can evidently solve only problems relative to conformational polymorphism.

It can, however, be noted that, if different types of potential minima are found theoretically, the difference between the foreseen chain conformations can be reasonably clear; if on the contrary only minima corresponding to helices are found, as for example those corresponding to two enantiomorphous helix chain conformations, inaccuracies of both theory and calculation can leave some uncertainty about the real symmetry of the helix. The remark is very recent[104] that helices of types $3/1$, $7/2$ or $11/3$ have such small differences in internal rotation angles that they apparently fall into the same potential energy minimum.

Though it is clear that further refinements are to be introduced, we may conclude that this theoretical way of prediction of the macromolecular polymorphism is highly interesting and has already given very encouraging results.

Istituto di Chimica Industriale del Politecnico,
    Milano, Italy

REFERENCES

[1] McCRONE, W. C. *Physics and Chemistry of the Organic Solid State*, Vol. II, Chap. 8. Interscience: New York, 1965
[2] See, for example, DEFFET, L. *Repertoire des Composés Organiques Polymorphes.* De Soer: Liège, 1942
[3] HOPFF, H. and VON SUSICH, G. *Kautschuk*, 1930, **6**, 234; HAUSER, E. A. and VON SUSICH, G. *Kautschuk*, 1931, **7**, 120, 125 and 145
[4] BUNN, C. W. *Proc. Roy. Soc. A*, 1942, **180**, 40; *Rubb. Chem. Technol.* 1942, **15**, 709
[5] FULLER, C. S. and ERICKSON, C. L. *J. Amer. chem. Soc.* 1937, **59**, 344
[6] FULLER, C. S., FROSCH, J. and PAPE, N. R. *J. Amer. chem. Soc.* 1942, **64**, 154
[7] BUNN, C. W. and GARNER, E. V. *Proc. Roy. Soc. A*, 1947, **189**, 39
[8] See, for example, ASTBURY, W. T. and WOODS, H. J. *Phil. Trans. A*, 1933, **232**, 336; ASTBURY, W. T. *Chem. & Ind.* 1941, **60**, 41 and 491
[9] See, for example, CIFERRI, A. *Trans. Faraday Soc.* 1963, **59**, 562

[10] BUNN, C. W. *Trans. Faraday Soc.* 1939, **35**, 482

[11] TEARE, P. W. and HOLMES, D. R. *J. Polym. Sci.* 1957, **24**, 496

[12] NIEGISCH, W. D. and SWAN, P. R. *J. appl. Phys.* 1960, **31**, 1906

[13] TURNER-JONES, A. *J. Polym. Sci. S,* 1962, **62**, 53

[14] POLLACK, S. S., ROBINSON, W. H., CHIANG, R. and FLORY, P. J. *J. appl. Phys.* 1962, **33**, 237

[15] FATOU, J. G., BAKER, C. H. and MANDELKERN, L. *Polymer, Lond.* 1965, **6**, 243

[16] FUJII, K., MOCHIZUKI, T., IMOTO, S., OKIDA, J. and MATSUMOTO, M. *Makromol. Chem.* 1962, **51**, 225

[17] TANAKA, K., SETO, T. and HARA, T. *Progr. Polym. Phys. Japan,* 1963, **6**, 292; *J. phys. Soc. Japan,* 1962, **17**, 873

[18] KIHO, H., PETERLIN, A. and GEIL, P. H. *J. Polym. Sci. B,* 1965, **3**, 157; *J. appl. Phys.* 1964, **35**, 1599

[19] See, for example, CLARK, E. S. and MUUS, L. T. *Z. Kristallogr.* 1962, **117**, 119

[20] See, for example, TADOKORO, H., YASUMOTO, T., MURAHASI, S. and NITTA, I. *J. Polym. Sci.* 1960, **44**, 266

[21] CARAZZOLO, G. A. *J. Polym. Sci. A,* 1963, **1**, 1573

[22] CARAZZOLO, G. A. and MAMMI, H. *J. Polym. Sci. A,* 1963, **1**, 965

[23] ZAMBONI, V. and ZERBI, G. *J. Polym. Sci. C,* 1964, **7**, 153

[24] MORTILLARO, L., CREDALI, L., MAMMI, M. and VALLE, G. *J. chem. Soc.* **1965**, 807; MORTILLARO, L., CREDALI, L., RUSSO, M. and DE CHECCHI, C. *J. Polym. Sci. B,* 1965, **3**, 581

[25] CARAZZOLO, G. and MAMMI, M. Paper presented to International Symposium of Macromolecular Chemistry, Prague, August 1965

[26] CARAZZOLO, G., MORTILLARO, L., CREDALI, L. and BEZZI, S. *J. Polym. Sci. A.* In press

[27] PREGAGLIA, G., PERALDO, M. and BINAGHI, M. *Gazz. chim. ital.* 1962, **92**, 488; GANIS, P. and TEMUSSI, P. A. *Ric. sci.* In press (Paper presented to the Sections Meeting of the 'Centro Nazionale di Chimica delle Macromolecole' of C.N.R. Varenna, September 1964); BASSI, I. W., GANIS, P. and TEMUSSI, P. A. Paper presented to International Symposium of Macromolecular Chemistry, Prague, August 1965

[28] NATTA, G., ALLEGRA, G., BASSI, I. W. and TORTI, E. *R.C. Accad. Lincei.* In press

[29] NATTA, G., BASSI, I. W. and ALLEGRA, G. *R.C. Accad. Lincei.* 1961, **31**, 350

[30] BECKER, L. *Plaste und Kautschuk,* 1961, **8**, 557

[31] BUNN, C. W. *Nature, Lond.* 1948, **161**, 929

[32] BROWN, C. J. and FARTHING, A. C. *J. chem. Soc.* **1953**, 3270; KAUFMAN, M. H., MARK, H. F. and MESROBIAN, R. B. *J. Polym. Sci.* 1954, **13**, 3

[33] OKADA, A. and HUTINO, K. *Chemy. high Polym.* 1950, **7**, 122

[34] UEDA, A. and KIMURA, T. *Chemy. high Polym.* 1958, **15**, 243; TSURUTA, M., ARIMOTO, H. and ISHIBASHI, M. *Kobunshi Kagaku,* 1958, **15**, 619; KINOSHITA, Y. *Makromol. Chem.* 1959, **33**, 1 and 21; OGAWA, M., OTA, T., YOSHIZAKI, O. and NAGAI, E. *J. Polym. Sci. B,* 1963, **1**, 57; ARIMOTO, H., ISHIBASHI, M., HIRAI, M. and CHATANI, Y. *J. Polym. Sci. A,* 1965, **3**, 317

[35] See, for example, SASAKI, T. *J. Polym. Sci. B,* 1965, **3**, 557

[36] FISHER, D. *Proc. phys. Soc. B,* 1953, **66**, 7

[37] NATTA, G., CORRADINI, P. and PORRI, L. *R.C. Accad. Lincei,* 1956, **20**, 728

[38] MANDELKERN, L., QUINN, F. A. and ROBERTS, D. E. *J. Amer. chem. Soc.* 1956, **78**, 926

[39] NATTA, G., CORRADINI, P. and PORRI, L. *R.C. Accad. Lincei,* 1956, **20**, 728; NATTA, G., CORRADINI, P., PORRI, L. and MORERO, D. *Chim. e Industr.* 1958, **40**, 362

[40] NATTA, G. and CORRADINI, P. *Nuovo Cim. Suppl.* 1960, **15**, 9

[41] NATTA, G. and MORAGLIO, G. *Rubber Plastics Age,* 1963, **44**, 42

[42] MORAGLIO, G., POLIZZOTTI, G. and DANUSSO, F. *Eur. Polym. J.* 1965, **1**, 183

[43] NATTA, G., PEGORARO, M., CREMONESI, P. and PAVAN, A. *Chim. e Industr.* 1965, **47**, 716; NATTA, G., PEGORARO, M. and CREMONESI, P. *Chim. e Industr.* 1965, **47**, 722

[44] NATTA, G., DALL'ASTA, G. and MAZZANTI, G. *Angew. Chem.* 1964, **76**, 765; *Angew. Chem. Internat. Ed.* 1964, **3**, 723

[45] NATTA, G. and BASSI, I. W. *R.C. Accad. Lincei,* 1965, **38**, 315

[46] NATTA, G. and BASSI, I. W. Paper presented to International Symposium of Macromolecular Chemistry, Prague, August 1965

[47] NATTA, G., DALL'ASTA, G. and PERALDO, M. Unpublished results

[48] NATTA, G., CORRADINI, P. and CESARI, M. *R.C. Accad. Lincei,* 1956, **21**, 365; NATTA, G. and CORRADINI, P. *Nuovo Cim. Suppl.* 1960, **15**, 40

[49] KEITH, H. D., PADDEN, F. J., WALTER, N. M. and WYCKOFF, H. W. *J. appl. Phys.* 1959, **30**, 1485; SOBUE, H. and TABATA, Y. *J. Polym. Sci.* 1959, **39**, 427

[50] GEIL, P. H. *J. appl. Phys.* 1962, **33**, 642

[51] ADDINK, E. J. and BEINTEMA, J. *Polymer, Lond.* 1961, **2**, 185

[52] TURNER-JONES, A., AIZLEWOOD, J. M. and BECKETT, D. R. *Makromol. Chem.* 1964, **75**, 134

[53] NATTA, G., PINO, P., CORRADINI, P., DANUSSO, F., MANTICA, E., MAZZANTI, G. and MORAGLIO, G. *J. Amer. chem. Soc.* 1955, **77**, 1708

[54] NATTA, G., CORRADINI, P. and BASSI, I. W. *R.C. Accad. Lincei,* 1955, **19**, 404

[55] NATTA, G., CORRADINI, P. and BASSI, I. W. *Makromol. Chem.* 1956, **21**, 240; *Nuovo Cim. Suppl.* 1960, **15**, 52

[56] TURNER-JONES, A. *J. Polym. Sci. B,* 1963, **1**, 455

[57] ZANNETTI, R., MANARESI, P. and BUZZONI, G. C. *Chim. e Industr.* 1961, **43**, 735

[58] BOOR, J. and MITCHELL, J. C. *J. Polym. Sci.* 1962, **62**, 174

[59] DANUSSO, F. and GIANOTTI, G. *Makromol. Chem.* 1963, **61**, 139

[60] POLIZZOTTI, G. and GIANOTTI, G. Results reported in: POLIZZOTTI, G. *Mater. plast.* 1963, **29**, 1358; LEUGERING, H. J. *Makromol. Chem.* 1963, **68**, 223; SASAGURI, K., RHODES, M. B. and STEIN, H. S. *J. Polym. Sci. B,* 1963, **1**, 571

[61] BOOR, J. and MITCHELL, J. C. *J. Polym. Sci. A,* 1963, **1**, 59

[62] GEACINTOV, C., SCHOTLAND, R. S. and MILES, R. B. *J. Polym. Sci. B,* 1963, **1**, 587

[63] GEACINTOV, C., SCHOTLAND, R. S. and MILES, R. B. *J. Polym. Sci. C,* 1963, **6**, 197

[64] HOLDEN, H. W. *J. Polym. Sci. C,* 1963, **6**, 209

[65] DANUSSO, F. and GIANOTTI, G. *Makromol. Chem.* 1964, **80**, 1

[66] DANUSSO, F., GIANOTTI, G. and POLIZZOTTI, G. *Makromol. Chem.* 1964, **80**, 13

[67] HOLLAND, V. F. and MILLER, R. L. *J. appl. Phys.* 1964, **35**, 3241

[68] MILLER, R. L. and HOLLAND, V. F. *J. Polym. Sci. B,* 1964, **2**, 519

[69] RUBIN, J. D. *J. Polym. Sci. B,* 1964, **2**, 747

[70] BOOR, J. and YOUNGMAN, E. A. *J. Polym. Sci. B,* 1964, **2**, 903

[71] WILSKI, H. and GREWER, T. *J. Polym. Sci. C,* 1964, **6**, 33

[72] CLAMPITT, B. H. and HUGHES, R. H. *J. Polym. Sci. C,* 1964, **6**, 43

[73] LUONGO, J. P. and SALOVEY, R. *J. Polym. Sci. B,* 1965, **3**, 513

[74] DANUSSO, F. and GIANOTTI, G. *J. Polym. Sci. B,* 1965, **3**, 537

[75] DANUSSO, F. and GIANOTTI, G. *Makromol. Chem.* In press

[76] NATTA, G. *Makromol. Chem.* 1955, **16**, 213; NATTA, G. *Angew. Chem.* 1956, **68**, 393

[77] TURNER-JONES, A. *J. Polym. Sci. B,* 1963, **1**, 471

[78] DANUSSO, F. and GIANOTTI, G. *Makromol. Chem.* 1963, **61**, 164

[79] HOFFMAN, J. D. and WEEKS, J. J. *J. Res. Nat. Bur. Stand. A,* 1962, **66**, 13; DANUSSO, F. Lecture to the Summer Course of Chemistry of Macromolecules, Varenna, September 1961, published in *Chemistry of Macromolecules,* National Council of Research, Rome, 1963, p 239

[80] TURNER-JONES, A. *Makromol. Chem.* 1964, **71**, 1

[81] NATTA, G., SIANESI, D., MORERO, D., BASSI, I. W. and CAPORICCIO, G. *R.C. Accad. Lincei,* 1960, **28**, 551

[82] DANUSSO, F. and FASSI, R. Unpublished results; FASSI, R. *M.S. Thesis,* University of Milan, 1960

[83] GRIFFITH, J. H. and RÅNBY, B. G. *J. Polym. Sci.* 1960, **44**, 369

[84] NATTA, G., CORRADINI, P. and BASSI, I. W. *Makromol. Chem.* 1959, **33**, 247

[85] OVERBERGER, C. G., BORCHERT, A. E. and KATCHMAN, A. *J. Polym. Sci.* 1960, **44**, 491

[86] NATTA, G., MAZZANTI, G., LONGI, P., DALL'ASTA, G. and BERNADINI, F. *J. Polym. Sci.* 1961, **51**, 487

[87] NATTA, G. *Makromol. Chem.* 1960, **35**, 93; NATTA, G., PASQUON, I., CORRADINI, P., PERALDO, M., PEGORARO, M. and ZAMBELLI, A. *R.C. Accad. Lincei,* 1960, **28**, 539; NATTA, G., CORRADINI, P., GANIS, P. and TEMUSSI, P. A. Paper presented to International Symposium of Macromolecular Chemistry, Prague, August 1965, A689

[88] NATTA, G., PERALDO, M. and ALLEGRA, G. *Makromol. Chem.* 1964, **75**, 215

[89] DANUSSO, F. and MORAGLIO, G. Unpublished results

[90] BRIDGMAN, P. W. *Proc. Amer. Acad. Arts Sci.* 1937, **72**, 45, p 129

[91] DANUSSO, F., GIANOTTI, G. and BACILIERI, F. Unpublished results; BACILIERI, F. *M.S. Thesis,* Polytechnic School of Milan, July 1963

[92] See, for example, the discussion in ref. 10, p 248

[93] BARDEEN, J. *J. chem. Phys.* 1938, **6**, 367 and 372

[94] PAULING, L. *Phys. Rev.* 1938, **54**, 899; *Proc. Roy. Soc. A,* 1949, **196**, 343

[95] JANSEN, L. *Phys. Rev.* 1962, **125**, 1798; *Phys. Rev. A,* 1964, **135**, 1292

[96] LOMBARDI, E. and JANSEN, L. *Phys. Rev. A,* 1964, **136**, 1011

[97] See, for example, JANSEN, L. and LOMBARDI, E. 'Three-atom and three-ion interactions and crystal stability', *Disc. Faraday Soc.* To be published; JANSEN, L. 'Quantum Chemistry and Crystal Physics. Stability of crystals of rare-gas atoms and alkali halides in terms of three-atom and three-ion interactions' in *Advances in Quantum Chemistry,* Vol. II. Ed. P. O. LÖWDIN, Academic Press: New York, 1965; JANSEN, L. 'Many atom forces and and crystal stability' in *Modern Quantum Chemistry,* Vol. II. Ed. O. SINANOGLU. Academic Press: New York, 1965

[98] BUNN, C. W. and HOLMES, D. R. *Disc. Faraday Soc.* 1958, **25**, 95

[99] FORDHAM, J. W. L. *J. Polym. Sci.* 1959, **39**, 321

[100] SHIMANOUCHI, T. S. and TASUMI, M. *Bull. chem. Soc. Japan,* 1961, **34**, 359

[101] NATTA, G., CORRADINI, P. and GANIS, P. *Makromol. Chem.* 1960, **34**, 238; *J. Polym. Sci.* 1962, **58**, 1191; CORRADINI, P. *On the crystalline structure of stereoregular polymers,* Summer Course Macromolecular Chemistry, Varenna, Italy, September 1961. Ed. by National Council of Research, Rome, 1963

[102] DE SANTIS, P., GIAGLIO, E. and LIQUORI, A. M. *J. Polym. Sci. A,* 1963, **1**, 13 and 1383; LIQUORI, A. M. *Conformational analysis of linear macromolecules in the solid state,* Summer Course Macromolecular Chemistry, Varenna, Italy, September 1961. Ed. by National Council of Research, Rome, 1963; LIQUORI, A. M. Lecture at Summer School Advanced Inorganic Chemistry, Varenna, Italy, 1959. Ed. by Accademia Nazionale Lincei, Rome

[103] WASAI, G., SAEGUSA, T. and FURUKAWA, J. *Makromol. Chem.* 1965, **86**, 1

[104] BORISOVA, N. P. and BIRSHTEIN, T. M. *J. Polym. Sci. USSR,* 1963, 907

Solution and Diffusion of Gases in Poly(vinylchloride)

R. M. Barrer, R. Mallinder and (in part) P. S-L. Wong

Diffusion and solubility coefficients have been measured by several different methods for hydrogen and neon in plasticized and unplasticized poly(vinyl-chloride) sheet, above and below the glass transition temperatures. In unannealed, unplasticized sheet, diffusion was history dependent but after annealing reproducible results were obtained. The plasticizer (tricresylphos-phate) reduced the glass transition temperatures, estimated from permeability/ temperature relations, progressively and in accord with the Free Volume Theory. It also increased the diffusion coefficients but decreased the solubility of the gases in the sheet.

POLY(VINYLCHLORIDE) is an internally viscous, amorphous plastic for which glass transition temperatures, T_g, have been variously quoted in the range $70°$ to $85°C^{1-3}$. The differences in T_g for the unplasticized polymer are likely to reflect differences in purity, micro-structure and molecular weight. In internally viscous polymers, diffusion of penetrants is often partially non-Fickian in character[1-6]. If the probe molecules are permanent gases their diffusion coefficients, D, should not depend on concentration of diffusant in so dilute a solution. Other factors, such as variations of D with distance in the membrane or with time, may occur, as may micro-heterogeneity, which is likely to be most significant below T_g. It was considered of interest to investigate the diffusion and solution of permanent gases in poly(vinylchloride) above and below T_g and in presence and absence of plasticizer, both to examine diffusion anomalies and to evaluate the role of plasticizer.

THEORY

Diffusion coefficients can be evaluated in three different ways by measuring the flow of gas through a membrane of the polymer[5,7]. The first of these, which has been called the early time procedure, gives diffusion coefficients, D_E, which correspond with the situation in the membrane at very small times. The second, the time-lag method, gives diffusion coefficients, D_L, appropriate for a period comparable with the time lag, L, while finally the steady-state method gives diffusion coefficients, D_S, for the membrane for times after the steady state has been established.

The appropriate relations for diffusion in the x direction, when the simple Fick equation

$$\partial c / \partial t = D \partial^2 c / \partial x^2 \tag{1}$$

is valid are as follows. The membrane is bounded by the yz planes at $x = 0$ and $x = l$ respectively. The membrane is free of penetrant at time $t = 0$. For

321

$t > 0$ a pressure p_1 of penetrant is established and maintained constant at $x = 0$. The pressure p_2 of penetrant on the outgoing side is then plotted against time, the membrane permeability being small enough so that $p_2 \ll p_1$ for the duration of the experiment. D_E is then obtained from a plot of $\ln(t^{1/2} \, dp_2/dt)$ versus $1/t$ since it has been shown that initially[8, 9]

$$\ln(t^{1/2} \, dp_2/dt) = \ln\{(2A/V) \, \sigma_E p_1)(D_E/\pi)^{1/2}\} - l^2/4 D_E t \qquad (2)$$

In this expression, A is the area of the membrane of thickness l through which diffusion occurs into a reservoir of volume V, and σ_E denotes the solubility coefficient. Thus, $\sigma_E p_1$ is the concentration in the membrane at $x = 0$. The slope, S, of this line is accordingly

$$S = -l^2/4 D_E \qquad (3)$$

The diffusion coefficient, D_L, is also readily obtained from the time-lag, L, from the relation

$$L = l^2/6 D_L \qquad (4)$$

while the diffusion coefficient, D_S, can be determined from the permeability, P, and the solubility, σ_S, measured directly

$$P = D_S \sigma_S \qquad (5)$$

Then for the ideal diffusion obeying equation (1), and for which equations (2), (3), (4) and (5) are therefore all valid:

$$D_E = D_L = D_S \qquad (6)$$

This equality may then be regarded as a test of equation (1). An equivalent test based on equations (3) and (4) is that

$$-2S = 3L \qquad (6a)$$

The intercept obtained by extrapolation of the line of equation (2) to cut the axis of $\ln(t^{1/2} \, dp_2/dt)$ at $1/t = 0$ may be termed $\ln I$, where

$$I = (2A/V)(\sigma_{E,1} p_1)(D_E/\pi)^{1/2} \qquad (7)$$

and so, combining equations (7) and (3),

$$\sigma_{E,1} = (IV/lAp_1)(-\pi S)^{1/2} \qquad (8)$$

It is also possible to set $P = D_E \sigma_{E,2} = D_L \sigma_L$, and for ideal diffusions obeying equation (1) all the solubility coefficients should be the same, and so

$$\sigma_L = \sigma_{E,2} = \sigma_{E,1} = \sigma_S$$

so that

$$\frac{6LP}{l^2} = -\frac{4SP}{l^2} = \frac{IV}{lAp_1}(-\pi S)^{1/2} = \sigma_S \qquad (9)$$

On the other hand, if the equalities in equations (6), (6a) or (9) are not found, it should be possible to obtain information on the extent and perhaps on the causes of deviations from the ideal behaviour.

The permanent gases, neon and hydrogen, were supplied in the pure state by the British Oxygen Co.

Poly(vinylchloride) sheets of known plasticizer content were supplied by the Plastics Division of I.C.I. Ltd. They were all prepared from the same polymer, Corvic D65/6, which was obtained by suspension polymerization. The polymer, as powder, was reported as at least 99 per cent pure. It was well mixed with appropriate constant amounts of stabilizers (cadmium stearate and stearic acid) and with tricresylphosphate plasticizer as required. The sheets were prepared in their final form by calendering at $\sim 120°$C. The compositions in parts by weight were:

Corvic	100
Cadmium stearate	2
Stearic acid	0·2
Tricresylphosphate	as in *Table 1*.

Further characteristics of the membranes are indicated in *Table 1*. When different membranes, cut from the same sheet, were used they are designated by subscripts (e.g. J_1, J_2, J_3, J_4).

Table 1. The poly(vinylchloride) membranes

Designation	Parts by weight of tricresylphosphate	Vol. fraction of tricresylphosphate	Average thickness $(cm \times 10^2)$
J	0	0	3·4
H	10	0·107	$8·5_7$
G	20	0.194	3·2
F	40	0·325	$7·9_5$
E	60	0·419	7·6

The diffusion cell has been described elsewhere[10]. The more brittle membranes J, H and G were held in the cell between thin rubber washers, the whole being clamped between the steel jaws of the cell. The more highly plasticized membranes F and E were clamped without the need for rubber washers. The exposed area of each poly(vinylchloride) membrane was ~ 2.9 cm². Before each run the membrane was maintained at the experimental temperatures for not less than 12 hours, with appropriate outgassing. Permeation and time-lag experiments were also conducted with membrane J in an all-glass cell without rubber gaskets. The membrane was in this case mounted using Araldite. The membranes of *Table 1* were stored in sealed containers when not in use, to minimize loss of plasticizer. Diffusion of plasticizers in poly(vinylchloride) depends strongly on the plasticizer concentration[11-14], which could result in a tendency to self-sealing at the faces $x = 0$ and $x = l$ from which any evaporation of plasticizer must occur. The vapour pressure of tricresylphosphate is very small and from the reproducibility of the permeability measurements over long time intervals it is considered that the loss of plasticizer during the course of

the work must have been small. Nevertheless the initial plasticizer contents in *Table 1* are to be considered as maximum values.

Measurements of the static solubilities were made by first equilibrating a membrane with the gas under consideration, and then sweeping away the ambient gas phase with mercury which was raised to surround and seal the sample. After evacuating the displaced gas, the mercury was lowered and again raised to sweep away any residual adhering bubbles. The gas desorbed from the polymer samples on finally lowering the mercury was measured from the pressures developed in an attached McLeod gauge. The second sweeping of the membrane with mercury was timed between half coverage of the membrane with mercury descending and rising. A correction was then applied for the quantity desorbed during this interval by using the $\sqrt{t}$ diffusion equation. The correction thus obtained was about five per cent of the total amount desorbed. The method described above has been used successfully by Meares[15] and by Draisbach et al.[16].

The linear relation predicted by equation (2) was tested, as shown for example for hydrogen in *Figure 1* in membrane E at 0°C, and for neon in membrane F_1 at 19·1°C. The continued recording of the outgoing pressure as a function of time served also to evaluate the time lag L, and the steady-state permeability, P, by standard procedures.
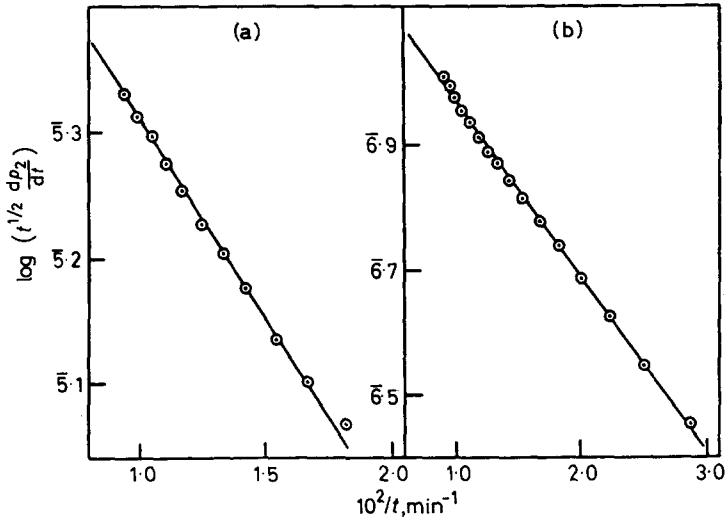
Figure 1—Linear plots of $\log(t^{1/2}\,dp_2/dt)$ versus $1/t$ for (a) hydrogen through membrane E at 0°C and (b) neon through membrane F_1 at 19·1°C

RESULTS FOR UNPLASTICIZED POLY(VINYLCHLORIDE)

Permeation and diffusion

Permeation through unplasticized, unannealed poly(vinylchloride) was history dependent. The first series of measurements were made at a
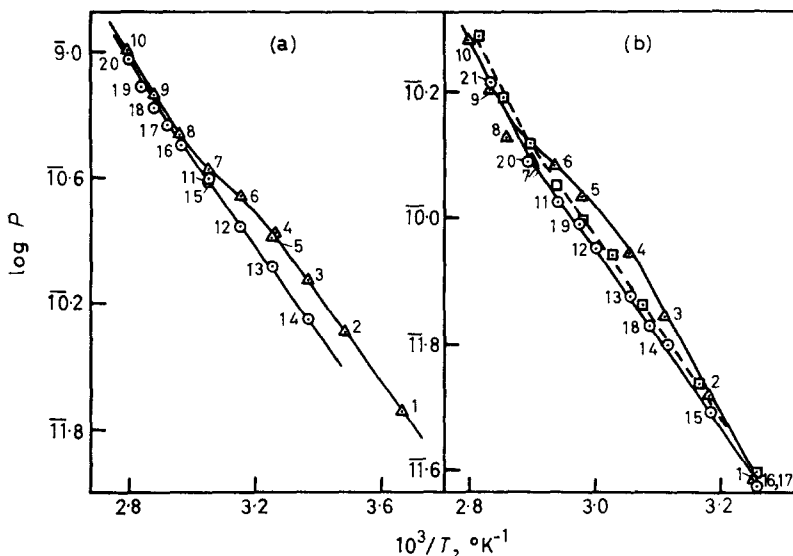
Figure 2—Plots of log P, determined in the metal cell[10], versus $1/T$ for hydrogen and neon diffusing in unplasticized PVC: (a) P for hydrogen in membrane J_1; $\triangle$, unannealed, with T rising in steps from $0°C$ to $84\cdot2°C$; $\bigcirc$, after annealing at $87°C$; (b) P for neon in membranes J_1 and J_2; $\triangle$, J_1 unannealed and T raised in steps from $34°C$; $\bigcirc$, J_1 annealed at $85°C$; $\square$, J_2 annealed at $86°C$, T raised in steps from $34°C$ (therefore points not numbered)

sequence of temperatures raised in steps from either $0°C$ or $34°C$ to $84°–86°C$, without prior annealing. Subsequent series of measurements were then made in the same way, but only after annealing at $86°$ to $87°C$. Some of the results obtained using the metal diffusion cell are shown in *Figure 2*, and more detailed comments may be made as follows.

(i) The values of P first obtained for hydrogen in the range $0°$ to $54°C$ were not reproducible in subsequent runs [points 1 to 7 in *Figure 2*(a)].

(ii) After annealing the membrane at $87°C$ for 12 hours, cooling it slowly, and then repeating the runs between $54°$ and $24\cdot1°C$ (points 11 to 14) P was reduced by as much as 20 per cent. A further repeat run at $54°C$ (point 15) was, however, in good agreement with that of point 11.

(iii) Between $69°$ and $84°C$ (points 17 to 20) the annealed membrane gave values of P in reasonable agreement with the original points 8, 9 and 10.

(iv) Measurements [*Figure 2*(b)] for neon were made in two membranes J_1 and J_2. Membrane J_1 was used five weeks after the hydrogen series referred to in (i), (ii) and (iii). Membrane J_2 was annealed at $86°C$ for 12 hours and was then cooled slowly to $34\cdot1°C$ before commencing the runs. The values of P were one to eight per cent above those for J_1 in its reproducible range (points 7 to 21). Thus the measurements in annealed, unplasticized poly(vinylchloride) were reasonably repeatable.

Subsequently a comparison was made between time lags and permea-

325

bilities measured for neon and hydrogen in the cells with and without rubber gaskets. This comparison established that time lags were several times larger in the metal cell with gaskets than in the glass one with no gaskets, but that the permeabilities were not very different, being 20 to 40 per cent larger in the cell with gaskets.

This behaviour was attributed to an edge effect when rubber gaskets were present associated with diffusion and permeability coefficients in rubber which are much larger than those in poly(vinylchloride). Therefore some gas passes through the membrane by entry into the rubber gaskets, passage through the poly(vinylchloride) membrane, and out through the other gasket. These long flow paths add only a small amount to the permeability but delay the final establishment of the steady state by a large factor. This effect will only be significant for the thin poly(vinyl-cloride) membranes when gaskets are present. Therefore it will affect measurements of L and P in the metal cell when membranes J, G and H are used, but not when membranes E and F are employed (see Experimental). Even so, the effect on P will remain small. In what follows time lags and derived diffusion coefficients are not considered for J, G and H in the metal cell, but permeabilities are.

Solubility and diffusion coefficients

Values of some diffusion and solubility coefficients in annealed unplasticized poly(vinylchloride) are given in *Table 2*. Values of D_L determined from the time lags for neon in membrane J_4 in the glass cell with no gaskets have values similar to, although not identical with, values of D_S derived for membrane J_3 using equation (5) ($P = \sigma_s D_s$). For neon, desorption kinetics were also measured from J_4 in the apparatus used for determining solubility. The kinetics conformed with Fick's equation and led to values of the diffusion coefficient, D_D, close to those of D_L (*Table 2*).

From these results, and those of the previous section, it appears that in annealed poly(vinylchloride) the diffusion of such weakly sorbed gases as neon and hydrogen is not appreciably non-Fickian in character, and thus that solubility coefficients could, in the absence of edge effects, be measured dynamically ($\sigma_L = P/D_L$). One should, in comparing the solubility and diffusion coefficients of *Table 2*, keep in mind that although membranes J_3 and J_4 came from the same sheet, the measurements on J_4 were made about six months after those on J_3. An ageing effect cannot be ruled out as a cause of differences between D_S and D_L, but the data show that such an effect if present at all must be rather small.

RESULTS FOR PLASTICIZED POLY(VINYLCHLORIDE)

Permeability and time lag

In plasticized poly(vinylchloride) the permeability coefficients and time lags no longer showed appreciable history dependence. For example, the permeation of hydrogen through membrane E was re-measured after the lapse of a year and P and L were found to be in reasonable agreement with their original values. When series of measurements were repeated they were adequately reproducible without annealing. Log P is shown as

Table 2. Smoothed diffusion and solubility coefficients in unplasticized poly(vinylchloride)

(a) *Hydrogen*

T, °C	26·0	36·1	46·0	56·0	66·0
$D_S \times 10^7$ (J₃) (cm² sec⁻¹) (metal cell)	3·3	5·0	7·3	10₄	14₃
$\sigma_S \times 10^4$ (J₃) (cm³ at s.t.p. per cm³ per cm of mercury)	4·6₀	4·4₂	4·0₄	3·8₄	3·7₀

(b) *Neon*

T, °C	26·1	36·1	46·0	56·0	66·1
$D_S \times 10^7$ (J₃) (cm² sec⁻¹) (metal cell)	1·2₉	2·0	2·9	4·2	5·8
$D_L \times 10^7$ (J₄) (cm² sec⁻¹) (glass cell)		3·0 (35°)	4·7 (50°)		6·3 (60°)
$D_E \times 10^7$ (J₁) (cm² sec⁻¹)	2·5 (30°)	3·5 (40°)			
$\sigma_S \times 10^4$ (J₃) (cm³ at s.t.p. per cm³ per cm of mercury)	2·2₃	2·1₃	2·0₂	1·8₇	1·8₂

a function of $1/T$ in *Figure 3*(a), (b) and (c). As with unplasticized poly(vinylchloride) the relations were not usually to be represented as a single straight line. This was also true of graphs of $\log D_L$ and $\log D_E$ versus $1/T$ [*Figure 4*(a) and (b)]. Wherever both D_L and D_E were measured their numerical values were very similar, as can be seen from the figure.

Permeabilities increase with the amount of plasticizer, the behaviour being shown semi-logarithmically in *Figure 5*(a) and (b). The trend of the results is similar to those obtained by Brubaker *et al.*[17] for the permeability of carbon dioxide in relation to the amount of dioctylphthalate plasticizer in poly(vinylchloride).

Although their permeability is not large, poly(vinylchloride) membranes show considerable selectivity towards hydrogen as compared with neon (*Table 3*). Among the group of membranes referred to in the table the absolute rates of transmission vary considerably, silicone rubbers and 'Vycor' porous glass being most permeable.

Intersection temperatures

Attention has been drawn in *Figures 2, 3* and *4* to the tendency of each graph of $\log P$ or of $\log D_L$ versus $1/T$ to consist of at least two lines of different slope. The intersection temperatures T_1 of these sections correlate with the volume fraction of plasticizer, as shown in *Figure 6*. With neon in unplasticized poly(vinylchloride) two intersections T_1 and T_2 occurred and only the upper one, T_1, is included in the figure. The intersection temperatures were similar for hydrogen and neon when each was diffused through the same membrane. It is therefore reasonable to regard these
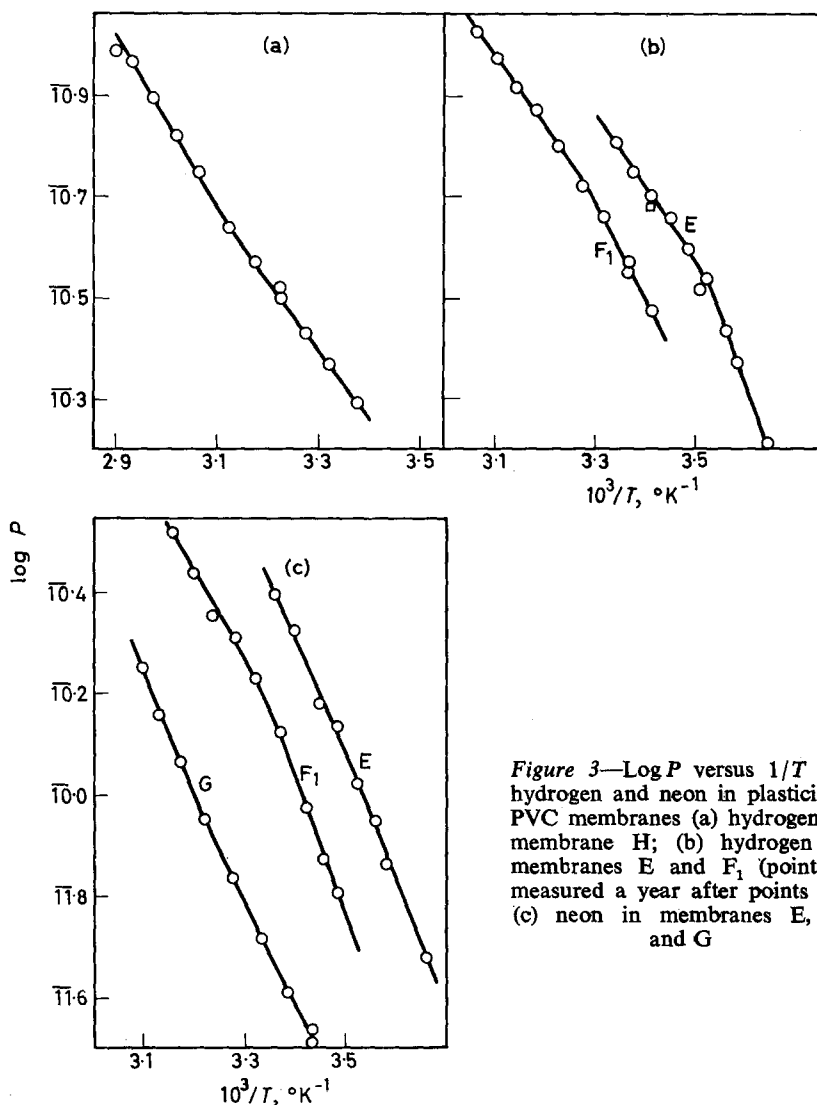
Figure 3—Log P versus $1/T$ for hydrogen and neon in plasticized PVC membranes (a) hydrogen in membrane H; (b) hydrogen in membranes E and F_1 (point $\square$ measured a year after points $\bigcirc$); (c) neon in membranes E, F_1 and G

temperatures as the glass transition temperatures, T_g, of the various plasticizer–poly(vinylchloride) compositions.

Correlations of the kind shown in Figure 6 have been observed in other plasticized polymers[18-20]. According to the Free Volume Theory[20]

$$T_g = \frac{v_2 T_{g,2} \Delta\alpha_2 + v_1 T_{g,1}\alpha_1}{v_2 \Delta\alpha_2 + v_1\alpha_1} \qquad (10)$$

In equation (10) $T_{g,2}$ and $T_{g,1}$ are the glass transition temperatures of the polymer and of its diluent respectively, $\Delta\alpha_2$ is the difference between the coefficients of thermal expansion of unplasticized polymer above and below
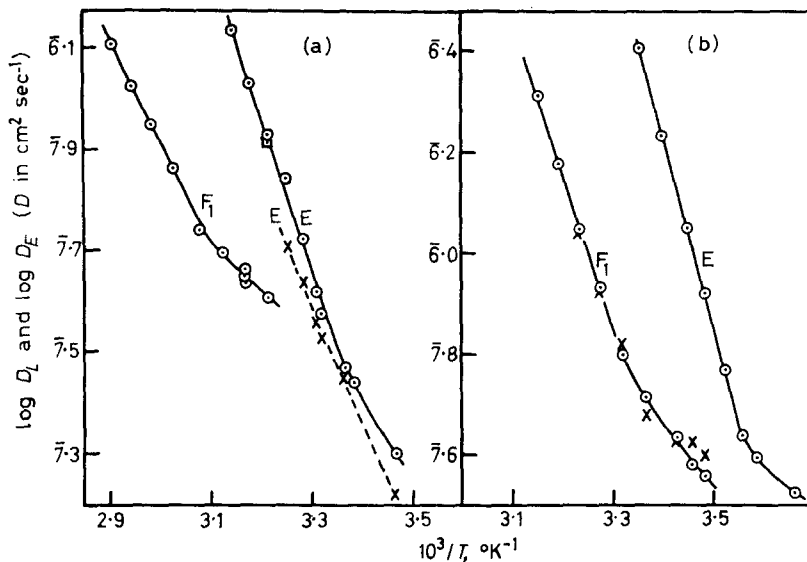
Figure 4—Log D_L and log D_E for hydrogen and neon in plasticized PVC membranes: (a) hydrogen in membranes E and F_1: ○, □, log D_L in both; x, log D_E in E only; (b) neon in E and F_1: ○, log D_L in both; , log D_E in F_1 only. The point □ was measured a year later than points ○
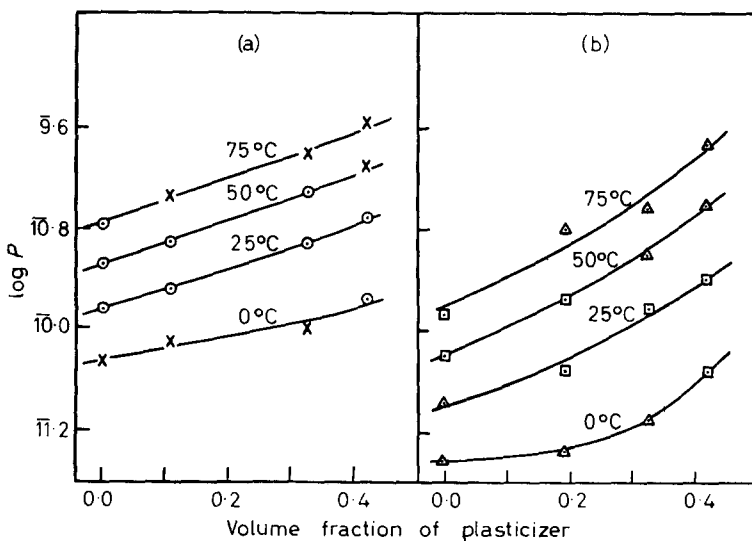
Figure 5—The influence of plasticizer upon P for hydrogen and neon in plasticized PVC: (a) and (b) effect on permeability for hydrogen and neon respectively. For hydrogen, ⊙ and × denote interpolated and extrapolated values and for neon, ⊡ and △ denote interpolated and extrapolated values, respectively

329

Table 3. Permeability ratios for hydrogen and neon

(a) *In plasticized and unplasticized polyvinylchloride*

Vol. fraction of tricresylphosphate	Ratio P_{H_2}/P_{Ne}			
	0°C	25°C	50°C	75°C
0·0	6	5	5·1	5·1
0·107	8	5	4	4
0·194	8	5	4	3
0·325	5	3·3	3	3
0·419	3·7	3·0	2	2

(b) *In various membranes*

Membrane	T°C	P_{H_2}/P_{Ne}
Unplasticized PVC	50	5·1
Plasticized PVC (vol. fraction TCP = 0·419)	25	3·0
Filled silicone rubber tube[21]	0	2·3_6
Filled silicone rubber tube[21]	−78	3·2_0
Poly(vinylacetate)[22]	10	3·5
Poly(vinylacetate)[22]	40	3·7
'Vycor' porous glass[23]	400	2·8
'Vycor' porous glass[23]	450	3·6

T_g and α_1 is this coefficient for the diluent. v_2 and v_1 denote volume fractions of polymer and of diluent. Heydemann and Guicking[3] determined α_2 for unplasticized poly(vinylchloride) over the glass transition and from their data $\Delta\alpha_2$ is taken as $3·8 \times 10^{-4}$ deg^{-1}. $T_{g,1}$ for tricresylphosphate is $-50°C$[19], and if one takes $\alpha_1 \sim 5 \times 10^{-4}$ deg^{-1}, a value which is reasonable according to data of Mellan[18], then the full curve in *Figure 6* is found, when $T_{g,2}$ is 70°C.
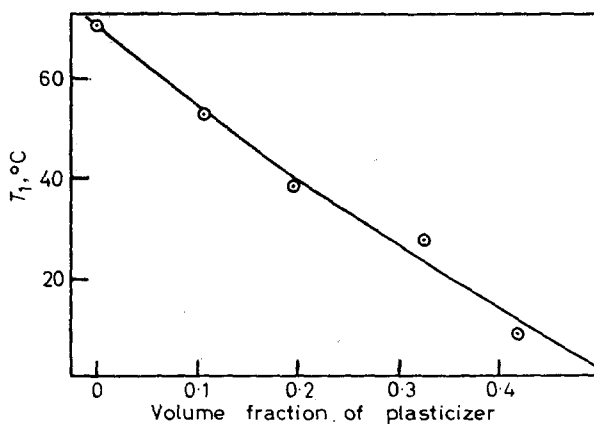
Figure 6—The observed (○) and calculated (full line) relationships between the intersection temperatures, T_1, and the volume fraction of plasticizer

Solubility coefficients

In flow measurements involving membranes E and Ap_1l F the metal cell was used, but without gaskets and therefore without the edge effect referred to above in 'permeation and diffusion'. IV $(-\pi S)^{1/2}/Ap_1l$, $6LP/l^2$ and σ_S [cf. equation (9)] are plotted against $1/T$ in *Figure 7*(a) and (b) for hydrogen and neon. Curves of $6LP/l^2$ show maxima; also, values of $IVl\,(-\pi S)^{1/2}/Ap_1$ and $6LP/l^2$ are numerically in agreement but differ somewhat from those of σ_S. This is particularly true of the temperature dependences as can be seen from the figure. Values of D_L, D_S, $6LP/l^2$ and σ_S in membrane F_1 are given in *Table 4*. Compared with σ_S in unplasticized poly(vinylchloride), (*Table 2*), the values of σ_S in the plasticized polymer, F, are reduced. On the other hand, values of D_S and of $P\,(P=D_S\sigma_S)$ are considerably increased.
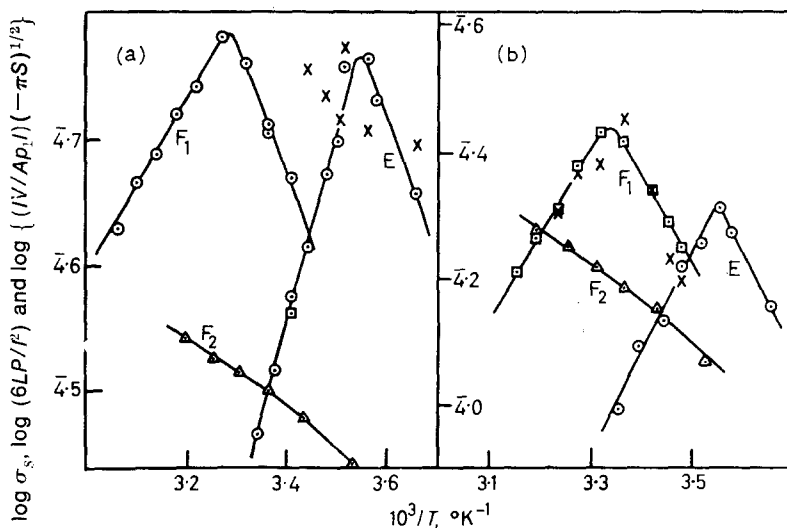
Figure 7—Curves of $\log\sigma$, $\log[6LP/l^2]$ and $\log[IV\,(-\pi S)^{1/2}/Ap_1l]$ versus $1/T$ for plasticized PVC membranes: (a) hydrogen in membranes E, F_1 and F_2; $\odot$, $\log[6LP/l^2]$ in both ($\square$ denotes this quotient measured again a year later); $\times$, $\log[-IV(-\pi S)^{1/2}/Ap_1l]$ in E only; $\triangle$, $\log\sigma_S$ in F_2; (b) neon in membranes E, F_1 and F_2: $\odot$, $\log[6LP/l^2]$ in E; $\boxdot$, $\log[6LP/l^2]$ in F_1; $\times$, $\log[IV(-\pi S)^{1/2}/Ap_1l]$ in F_1; $\triangle$, $\log\sigma_S$ in F_2

DISCUSSION

Solubility

The reduction in solubility in plasticized as compared with unplasticized polymer below its glass transition temperature can be interpreted on the basis of the free volume. In unplasticized polymer some low density micro-regions may constitute the equivalent of pre-existing sorption sites for hydrogen or neon, and effectively simulate the sites postulated by Langmuir, but distributed throughout the polymer matrix. In the plasticized polymer the greater chain mobility and the presence of plasticizer molecules result

Table 4. Smoothed diffusion and solubility coefficients in plasticized PVC with 0·325 volume fraction of plasticizer

(a) *Hydrogen*

T, °C	10·1	17·9	23·9	29·0	33·9	39·1
$D_S \times 10^6$ (F_2) (cm² sec⁻¹)	0·77	1·1$_1$	1·4$_6$	1·8$_3$	2·1$_4$	2·4$_8$
$D_L \times 10^6$ (F_1) (cm² sec⁻¹)	0·61	0·76	0·89	1·0$_2$	1·2$_5$	1·6$_2$
$\sigma_S \times 10^4$ (F_2) (cm³ at s.t.p. per cm³ per cm of mercury)	2·7$_7$	3·0$_2$	3·1$_8$	3·2$_9$	3·3$_8$	3·5$_0$
$6LP/l^2 \times 10^4$ (F_1) (cm³ at s.t.p. per cm³ per cm of mercury)	3·5$_2$	4·4$_1$	5·2	5·9	5·8	5·4

(b) *Neon*

T, °C	10·0	18·0	23·8	28·7	33·9	40·0
$D_S \times 10^7$ (F_2) (cm² sec⁻¹)	3·9$_6$	6·2	8·7	10·7	12·5	14 8
$D_L \times 10^7$ (F_1) (cm² sec⁻¹)	3·1$_1$	4·2$_1$	5·2	6·7	10·0	15·4
$\sigma_S \times 10^4$ (F_2) (cm³ at s.t.p. per cm³ per cm of mercury)	1·18	1·43	1·5$_5$	1·6$_6$	1·7$_9$	1·9$_1$
$6LP/l^2 \times 10^4$ (F_1) (cm³ at s.t.p. per cm³ per cm of mercury)	1·5$_4$	2·1$_0$	2·6$_1$	2·6$_4$	2·2$_1$	1·8$_3$

in the disappearance of these sites, so that only substitutional solution is possible.

If such micro-gaps or sites occur in unplasticized polymer, the insertion of molecules of hydrogen or neon in them would be an exothermal process, whereas substitutional solution involves the expenditure of energy in making holes for the hydrogen or neon and should be endothermal. This behaviour is observed from the values of the standard heats in *Table 5*. These have been obtained from the bunsen solubility coefficients, $\sigma_S^\star = 76\,\sigma_S$, using the relation

$$\partial \ln \sigma_S^\star / \partial T = \Delta H^0 / RT^2$$

Similarly, $-RT \ln \sigma_S^\star = \Delta G^0$, and $R \ln \sigma_S^\star + RT \partial \ln \sigma_S^\star / \partial T = \Delta S^0$. These quantities, and the coefficient σ_0 in the expression $\sigma_S^\star = \sigma_0 \exp - \Delta H^0 / RT$ are also given in *Table 5*. From the table one notes not only exothermal heats but considerable negative values of standard entropies for solution in unplasticized polymer (J_3). σ_0 increases strongly in the plasticized (F_2) as compared with the unplasticized poly(vinylchloride).

If the picture of micro-gaps in polymer J_3 below its glass transition temperature, T_g, is correct, then as the temperature is raised towards T_g the number of gaps may decrease, as well as their dimensions. This behaviour may well contribute in J_3 to the temperature coefficient of $\sigma_S^\star$ and so to the values of ΔH^0 and of ΔS^0. That is, changes in the polymer may contribute to these quantities. The analysis in *Table 5* may also be taken, in comparison with results shown in *Table 6* for hydrogen and neon dissolved in paraffins, to indicate that the plasticized membrane, F_2, behaves more as a liquid-like solvent medium than does J_3. The heats of solution

332

Table 5. Thermodynamic analysis of solubility constants in J_3 and F_2

Membrane and temperature (°C)	J_3 26 to 66		F_2 10 to 40	
Gas	H_2	Ne	H_2	Ne
$\sigma_0 \times 10^4$	0·65	0·36	32	166
ΔH^0 (cal mole^{-1})	−1 170	−1 080	1 370	2 770
ΔG^0 at 30°C (cal mole^{-1})	2 030	2 470	2 220	2 620
ΔS^0 at 30°C (cal mole^{-1} deg^{-1})	−10·6	−11·7	−2·8	0·50

in the paraffins are endothermic and the entropies have small numerical values, just as in F_2.

For the membrane F_2, assuming free rotation of dissolved hydrogen (for neon, rotation is not involved), one may write[26]

$$\frac{v_1}{C_g (1 - 2v_2/Z)^{Z/2}} = \left(\frac{kT}{2\pi m}\right)^{3/2} \frac{1}{\bar{v}^3} \exp \frac{(-\Delta H^0 + \tfrac{1}{2}RT)}{RT}$$

where v_1 and v_2 are volume fractions of sorbed gas and of polymer in equilibrium with gas-phase concentration C_g (in molecules per cm^3 at 1 atm), Z is the coordination number of a dissolved molecule of mass m

Table 6. Standard thermodynamic quantities for hydrogen and neon in paraffins

Gas and ref.	Solvent	$\sigma\star \times 10^2$ (25°C)	ΔG^0 (cal mole^{-1})	ΔH^0 (cal mole^{-1})	ΔS^0 (cal mole^{-1} deg^{-1})
H_2[24]	Nonane	8·6$_4$	1 450	580	−2·9$_2$
Ne[25]	Heptane	5·2$_9$	1 740	1 220	−1·7$_6$
Ne[25]	Octane	4·9$_1$	1 790	1 530	−0·8$_8$

and $\bar{v}$ its mean vibration frequency relative to its environment. This formula is not fully appropriate because of the· small size of the solute molecules relative to ambient polymer segments or plasticizer molecules. However, when one calculates the values of $\bar{v}$ on the RHS which yield the correct values of v_1, one obtains:

$$\bar{v}_{H2} \ (sec^{-1}) = 1\cdot4_2 \times 10^{12} \ (Z=4); \quad 1\cdot5_0 \times 10^{12} \ (Z=6)$$

$$\bar{v}_{Ne} \ (sec^{-1}) = 3\cdot0_8 \times 10^{11} \ (Z=4); \quad 3\cdot2_6 \times 10^{11} \ (Z=6)$$

These are infra-red frequencies of the right order.

Diffusion

The apparent energies of activation, E_S and E_L for D_S and D_L respectively, can be obtained from the Arrhenius equation $D = D_0 \exp - E/RT$. The coefficients D_0 and E are summarized in *Table 7*. E_L changes by a large amount above and below the intersection temperatures T_1 (see above 'Intersection temperatures'), and the changes in E_L are reflected in changes in D_0.

In membranes E and F, *Table 4* shows that there are some differences, although not large ones, between D_L and D_S or between $6LP/l^2$ and σ_S.

In these membranes, since the solubilities of hydrogen and neon are very low, concentration dependence of the diffusion coefficient will not be perceptible and so cannot account for the differences.

Although such differences may be comparable with experimental uncertainties it is worth considering skin effects as a possible additional cause. Skin effects might arise in membranes E and F either from a tendency of plasticizer to evaporate from the faces $x=0$ and $x=l$ or from a tendency of the stabilizer (see Experimental) to segregate at these faces. For a continuous x-dependence of D in which $D=D_0[1+f(x)]$ one can show that[27]

$$D_S = lD_0 / \int_0^l [1+f(x)]^{-1} \, dx \qquad (11)$$

and[28]

$$D_L = \frac{l^2 D_0}{6} \cdot \frac{\int_0^l [1+f(x)]^{-1} \, dx}{\int_0^l [1+f(x)]^{-1} \int_x^l \int_x^l [1+f(x)]^{-1} \, dx \, dx \, dx} \qquad (12)$$

so that D_S/D_L is not unity. This membrane can be approximated by another in which two identical thin skins each of thickness l_1 cover both sides of a central layer of thickness l_2. In the skins the diffusion coefficient is D_1 and in the central lamina it is D_2. Then it can be shown that, when $2l_1 \ll l_2$,

$$D_S = k_1 l_2 D_1 D_2 / (2l_1 D_2 + l_2 D_1 k_1) \qquad (13)$$

where k_1 is the ratio of solubility coefficient in the skin to that in the central lamina. Similarly[29, 30]

$$D_L = \frac{\dfrac{l^2}{6}\left(\dfrac{2l_1}{D_1} + \dfrac{k_1 l_2}{D_2}\right)}{\dfrac{l_1^2}{D_1}\left(\dfrac{4l_1}{3D_1} + \dfrac{k_1 l_2}{D_2}\right) + \dfrac{l_2^2}{D_2}\left(\dfrac{l_1}{D_1} + \dfrac{k_1 l_2}{6D_2}\right) + \dfrac{1}{k_1}\dfrac{l_1^2 l_2}{D_1^2}} \qquad (14)$$

where $l=(2l_1+l_2)$. Since $l_2 \gg 2l_1$, l_2 may be equated with the total thickness of the membrane, l. Two limiting situations are:

(i) $\quad 2l_1 D_2 \gg lD_1 k_1$

and

(ii) $\quad 2l_1 D_2 \ll lD_1 k_1$

The first of these cases gives $D_S \longrightarrow k_1 lD_1 / 2l_1$

and

$$\frac{D_S}{D_L} \longrightarrow \left(\frac{2l_1 k_1}{l} + \frac{3}{2}\right) \geqslant \frac{3}{2}.$$

In the second both D_S and $D_L \longrightarrow D_2$, so that their ratio approaches unity. In terms of this model, a contribution to the differences recorded in *Table 4* between D_S and D_L is nevertheless possible for case (i).

Table 7. Constants D_0 and E from $D = D_0 \exp -E/RT$, for D_L and D_S

(a) *Hydrogen*

Membrane	Intersection temp., T_1 (°C)	Below T_1*		Above T_1	
		E (cal mole⁻¹)	D_0 (cm² sec⁻¹)	E (cal mole⁻¹)	D_0 (cm² sec⁻¹)
J	70	7 700 (D_S)	$1 \cdot 31 \times 10^{-1}$ (D_S)		
F	28	4 500	$1 \cdot 92 \times 10^{-3}$	9 700	9·9
		7 500 (D_S)	0·44 (D_S)		
E	9	7 950	0·92	14 300	$7 \cdot 8 \times 10^4$

(b) *Neon*

J	70 (T_1); 54 (T_2)	7 800 ($<T_2$, D_S)	$6 \cdot 2 \times 10^{-2}$ ($<T_2$, D_S)		
F	28	6 300	$2 \cdot 11 \times 10^{-3}$	13 900	$7 \cdot 4 \times 10^3$
		9 100 (D_S)	3·79 (D_S)		
E	9	4 800	$2 \cdot 31 \times 10^{-3}$	17 500	$1 \cdot 58 \times 10^7$

*Values of E and D_0 are for D_L unless otherwise indicated by (D_S). T_1 and T_2 are the intersection temperatures referred to in the section above on 'Intersection temperatures'.

CONCLUSION

In this study of the permeation of gases through poly(vinylchloride) history dependence has been observed for unannealed, unplasticized polymer, which in part arises from slow relaxation of polymer. This history dependence is not appreciable when the polymer is annealed or is plasticized, but small deviations between D_S and D_L may still persist. These for neon and hydrogen cannot be ascribed to concentration dependence of the diffusion coefficient. Introduction of controlled amounts of tricresyl-phosphate as plasticizer reduces the static solubility and increases the diffusion coefficients and permeabilities.

By increasing the number of quantities measured (in this work P, L, S and σ_S (*see* Theory)) one can obtain considerable information regarding the diffusion behaviour of membranes, and in particular regarding diffusion anomalies. Although for many purposes it is essential to examine technical membranes, from the viewpoint of the basic properties of polymeric diffusion media it would be desirable to minimize the impurities in them, introduced industrially as stabilizers, accelerators or fillers.

Physical Chemistry Laboratories,
  Chemistry Department,
    Imperial College, London, S.W.7

REFERENCES

[1] TOBOLSKY, A. V. *Properties and Structures of Polymers,* p 70, Wiley: New York, 1960

[2] NIELSEN, L. E. *Mechanical Properties of High Polymers*, p 16, Reinhold: New York, 1962

[3] HEYDEMANN, P. and GUICKING, H. D. *Kolloidzschr.* 1963, **193**, 16

[4] KISHIMOTO, A. and MATSUMOTO, K. *J. Polym. Sci. A*, 1964, **2**, 679

[5] MEARES, P. *J. appl. Polym. Sci.* 1965, **9**, 917

[6] FUJITA, H. *Advanc. Polym. Sci.* 1961, **3**, 1, and refs. cited therein

[7] BARRER, R. M. and CHIO, H. T. *J. Polym. Sci. C*, 1965, **10**, 111

[8] ROGERS, W. A., BURITZ, R. S. and ALPERT, D. *J appl. Phys.* 1954, **25**, 868

[9] ALTEMOSE, V. O. *J. appl. Phys.* 1961, **32**, 1309

[10] BARRER, R. M., BARRIE, J. A. and RAMAN, N. K. *Polymer, Lond.* 1962, **3**, 595

[11] HELLWEGE, K. H., KNAPPE, W. and LOHE, P. *Kolloidzschr.* 1961, **179**, 40

[12] LUTHER, H. and MEYER, H. *Z. Elektrochem.* 1960, **64**, 681

[13] HEINE, K., HELLWEGE, K. H. and KNAPPE, W. *Z. angew. Phys.* 1958, **10**, 162

[14] KNAPPE, W. *Z. angew. Phys.* 1954, **6**, 97

[15] MEARES, P. *Trans. Faraday Soc.* 1958, **54**, 40

[16] DRAISBACH, H., JESCHKE, D. and STUART, H. A. *Z. Naturf.* 1962, **17a**, 447

[17] BRUBAKER, D. W. and KAMMERMEYER, K. *Industr. Engng Chem. (Industr.)*, 1953, **44**, 1465

[18] MELLAN, I. *The Behaviour of Plasticizers*, p 103, Pergamon: Oxford, 1961

[19] BOYER, R. F. and SPENCER, R. S. *J. Polym. Sci.* 1947, **2**, 157

[20] KELLEY, F. N. and BUECHE, F. *J. Polym. Sci.* 1961, **50**, 549

[21] CHIO, H. T. *Thesis*, University of London, 1964

[22] MEARES, P. *J. Amer. chem. Soc.* 1954, **76**, 3415

[23] LEIBY, C. C. and CHEN, C. L. *J. appl. Phys.* 1960, **31**, 268

[24] THOMSEN, E. S. and GJALDBACK, J. C. *Acta chem. scand.* 1963, **17**, 127

[25] CLEVER, H. L., BATTINO, R., SAYLOR, J. H. and GROSS, P. M. *J. phys. Chem.* 1957, **61**, 1078

[26] BARRER, R. M. *Trans. Faraday Soc.* 1947, **43**, 3

[27] BARRER, R. M. *Proc. phys. Soc. Lond.* 1946, **58**, 321

[28] ASH, R. In preparation

[29] BARRIE, J. A., LEVINE, J. D., MICHAELS, A. S. and WONG, P. S-L. *Trans. Faraday Soc.* 1963, **59**, 869

[30] ASH, R., BARRER, R. M. and PALMER, D. G. *Brit. J. appl. Phys.* 1965, **16**, 873

The Dilute Solution Properties of Polyacenaphthylene
I—Light Scattering, Osmotic Pressure and Viscosity Measurements

J. M. Barrales-Rienda and D. C. Pepper

Sixteen fractions prepared from thermally polymerized polyacenaphthylene and one polymerized by boron trifluoride–etherate have been measured by light scattering, osmotic pressure and viscometric techniques. Gyration radii, related dimensions, and second virial coefficients have been determined in toluene at 25°C. Viscosities in other solvents lead to the following Mark–Houwink relationships at 25°C.

$$[\eta], \ \mathrm{ml/g} = 21 \cdot 2 \times 10^{-3} \overline{M}_v^{0 \cdot 54} \ \text{in ethylene dichloride}$$

$$= 11 \cdot 6 \times 10^{-3} \overline{M}_v^{0 \cdot 61} \ \text{in dioxan}$$

$$= 7 \cdot 00 \times 10^{-3} \overline{M}_v^{0 \cdot 66} \ \text{in methylene dichloride}$$

$$= 6 \cdot 83 \times 10^{-3} \overline{M}_v^{0 \cdot 66} \ \text{in toluene}$$

$$= 2 \cdot 94 \times 10^{-3} \overline{M}_v^{0 \cdot 74} \ \text{in benzene}$$

The Flory theta-temperature in ethylene dichloride is found to be $20° \pm 2°C$, i.e. lower than the value ($35°$) reported by Moacanin et al.[1]

POLYACENAPHTHYLENE (PAcN) (*Figure 1*) is of interest in that even in its
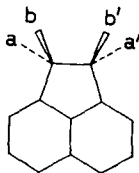
Figure 1—Polyacenaphthylene repeating unit: chain backbone aa′ or bb′, erythro; ab′ or ba′, threo

atactic form its chain might be expected to be rather inflexible, since as well as having a bulky substituent it has alternate bonds 'locked' into the perinaphthylene ring.

This latter feature imposes a characteristic stereochemistry. The stereoregular forms (*di-iso* and *di-syndio* because of the double substitution) are further subdivided into *erythro* and *threo* forms (more easily if less strictly visualized as having the adjacent units *cis* and *trans* to the plane of the ring).

Stereoregular placements are expected to have widely different probabilities because of the hindrance to *cis* placements[2,3] caused by the bulky sub-

337

stituent. Thus three such placements in di-isotactic configuration would bend the backbone into a ring (and a cyclic trimer is known[4]) and three in di-syndiotactic configuration would lead to gross overlap of rings. *Trans* (threo) additions are on the other hand relatively unhindered. Regular sequences would produce a helix (*trans* di-isotactic) or a 'stepped chain' (*trans* di-syndiotactic).

Story and Canty[3] have offered evidence (from spectra) of the existence of the two latter forms in low molecular weight polymers initiated by boron trifluoride–etherate. The original object of this work was to prepare and study the solution properties of such regular polymers, there being grounds for hope that boron trifluoride and its complexes could produce sufficiently high molecular weight polymers (reports of mol. wt $\sim$ 150 000[5,6]). However, many attempts in this laboratory[7] yielded only low molecular weight polymers, whose highest fractions had mol. wt $<$ 50 000. Other authors[3,8] have been similarly unsuccessful and it seems likely that the original reports were unjustified.

Attempts at anionic polymerization (sodium naphthalene in tetrahydrofuran) likewise gave only low molecular weight material[7,9]. This is now understandable in the light of the observation by Rembaum and Moacanin[10] that polyacenaphthylenes are rapidly degraded by this catalyst. Ziegler–Natta catalysts have also been found[6b] to give low molecular weight products.

With the exception then of one low molecular weight 'cationic' fraction, the samples examined here were prepared by the well established[4,11-14] thermal polymerization. They are presumed to be completely atactic, but with a predominance of the *trans* forms and only relatively infrequent *cis* placements.

Previous studies of PAcN are limited to a brief report by Mohorcic[13] of the $[\eta]/\overline{M}_n$ relationship in tetrahydrofuran and recent papers by Moacanin et al.[1,15] describing similar relationships in benzene and ethylene dichloride with the molecular dimensions of three fractions. More recently still, another relationship in benzene has been reported[27].

EXPERIMENTAL

Monomer purification

Acenaphthylene (BDH reagent grade) was recrystallized first from ethanol with charcoal, and then from pure ethanol and stored in the dark (m.pt 93°C; single GLC peak).

Solvents

All solvents were given appropriate chemical purification (usually sulphuric acid, caustic soda, water), dried over calcium hydride and fractionally distilled (10 to 30 in. columns packed with glass helices).

Polymerization conditions

The three samples investigated were prepared as follows:

(A) Acenaphthylene (0·66 M) in benzene with boron trifluoride–etherate (1·64 × 10⁻⁴ M) 80°C; 50 h; yield $\sim$ 100 per cent.

(B)   Bulk polymerization 120°C; 24 h; yield 83 per cent.
(C)   As B but 100°C; 18 h; yield 56 per cent.
The products were dissolved in benzene and the polymer isolated by precipitation with excess methanol, washing with hot methanol, and drying *in vacuo* at 40°C. The resulting polymer samples were fine white powders.

Fractionation
The polymer samples were fractionated from benzene solution (*ca.* 0·3% w/v) as follows:

Sample A (cationic). One fraction only (highest ten per cent) precipitated by methanol,
   B   Precipitant methanol (19 to 45% v/v); 15 fractions, recovery 94·2 per cent,
   C   Precipitant *n*-hexane (18 to 52 per cent); 12 fractions, recovery 94·5 per cent.

Each precipitated fraction was redissolved at 40°C and allowed to separate by slow cooling to and maintenance at 20°C for 24 to 36 h. The precipitated phase was then separated, precipitated completely with methanol, isolated and dried as above.

Viscosity measurements
Viscosities were measured at 25°C in toluene and other solvents, using a suspended-level dilution viscometer of flow time 137·2 sec at 25°C for toluene. Kinetic energy corrections were found to be negligible. No systematic investigation was made of the effect of shear rate, but all viscosities measured are believed to be Newtonian (the highest molecular weight fraction, which should show the greatest deviation, was found to give the same intrinsic viscosity when measured in two viscometers having a sixfold ratio of flow rates).
Intrinsic viscosities (ml/g) were derived using both the Huggins equation[16]

$$\eta_{sp}/c = [\eta]_H + k_H[\eta]_H^2 \cdot c \tag{1}$$

and the Schulz–Blaschke equation[17]

$$\eta_{sp}/c = [\eta]_{SB} + k_{SB}[\eta]_{SB} \cdot \eta_{sp} \tag{2}$$

The two equations appear to fit the data equally well, but the values of $[\eta]_H$ are all slightly (about five per cent) lower than those of $[\eta]_{SB}$ and the slope coefficients $k_H > k_{SB}$ (see *Table 1*). The latter increases as $[\eta]$ falls, and the various constants are interrelated by

$$k_{SB}[\eta]_{SB}^2 = 80 + 0·61 k_H[\eta]_H^2 \tag{3}$$

Similar differences between $[\eta]_H$ and $[\eta]_{SB}$ have been found with other polymers by Ibrahim[18] who argues that the Schulz–Blaschke parameters are the more significant, because of an inadequate approximation in the theoretical justification of equation (1). The differences found here are not

Table 1. Viscosity data for polyacenaphthylene in various solvents at 25°C

Sample	Toluene				Ethylene dichloride		Dioxan		Methylene dichloride		Benzene	
	$[\eta]_H$	k_H	$[\eta]_{SB}$	k_{SB}	$[\eta]_H$	k_H	$[\eta]_H$	k_H	$[\eta]_H$	k_H	$[\eta]_H$	k_H
C I	80·0	0·63	83·5	0·36			67·5	0·49	80·0	0·55		
C II	77·5	0·64	82·0	0·36					71·5	0·45		
C III	74·5	0·65	79·5	0·36							74·0	0·39
C IV	70·5	0·67	75·0	0·38								
B I	56·0	0·64	59·0	0·48	38·5	1·10	52·5	0·48	48·5	0·63		
C V	53·0	0·70	55·0	0·42			47·0	0·51				
C VI	50·0	0·75	53·0	0·43	29·0	1·30	42·5	0·95				
C VII	40·5	0·76	42·5	0·43			35·5	0·80				
C VIII	35·0	0·78	37·0	0·46	24·0	1·11						
C IX	30·5	0·81	31·0	0·49			27·0	0·70	26·0	0·71		
C X	25·0	0·83	26·0	0·58	16·5	0·98						
C XI	18·0	0·93	18·5	0·62	13·5	1·12						
B X	16·0	0·90	16·5	0·66							16·5	0·55
B XI	13·0	0·92	13·0	0·90							12·5	0·53
C XII	10·0	1·00	10·5	0·83	8·0	1·00	10·0	0·76	10·0	0·80		
B XIII	7·5	1·00	7·5	0·98							7·5	0·58
A I	6·0	1·00	6·0	0·97								

much greater than experimental errors and it has not seemed worthwhile to resolve them. The correlations with molecular weight are in terms of the Huggins parameter $[\eta]_H$, in accordance with majority practice. All $[\eta]$ values quoted are the common intercepts of Huggins plots with the corresponding $\ln \eta_r/c$ plots.

Light scattering measurements

A Brice–Phoenix universal light scattering photometer (1000 series) was used, fitted with a cooling coil capable of maintaining the cell compartment temperature at $25° \pm 1°$.

Anomalies were found in the scattering envelope when cylindrical cells (BPC 101) were used, with the narrow beam (4 mm) optics. They were eliminated by fitting a further collimating slit close in front of the cell and blackening its rear surface. The cells themselves were found to be optically symmetrical (fluorescence intensity with sodium fluorescein independent of angle).

Absolute values of the reduced intensity were derived by calibration with Ludox HS (Dupont) and yielded a value for the Rayleigh ratio for toluene (25°C 546 mμ) of $R_{90} = 20 \cdot 0 \pm 0 \cdot 2 \times 10^6$ cm^{-1} in agreement with many recent values[19, 20].

With PAcN there is some reason to fear fluorescence if blue light is used. All measurements were therefore made with the green mercury line at 546 mμ and are believed to be free from error from this source.

Solutions were first clarified by centrifuging at 15 000 rev/min for two hours, and then filtered through a Millipore $0 \cdot 8 \, \mu$ filter directly into the optical cell. Concentrations were determined subsequently by evaporation of the solvent.

A value for the refractive index increment of PAcN in toluene

$$dn/dc = 0 \cdot 190 \text{ ml/g} \quad (25° \quad 546 \text{ m}\mu)$$

was determined in a Brice–Phoenix differential refractometer calibrated with sucrose solutions[21]. This value was found for five different fractions ranging in molecular weight from 250 000 to 800 000.

The Rayleigh ratios, R_θ, were calculated in the usual manner[22] but using the modified values of residual refraction and reflection corrections suggested by Tomimatsu and Palmer[23].

Weight average molecular weights $\overline{M}_w$ and second virial coefficients (A_2) were determined from the zero-angle line in Zimm plots[24] using

$$(Kc/R_\theta) = 1/\{M_w P(\theta)\} + 2A_2c \tag{4}$$

where $P(\theta) \longrightarrow 1$ at $c = 0$; $\theta = 0$ and the constant K has its usual significance

$$K = 2\pi^2 n_0^2 (dn/dc)^2 / N\lambda^4 \tag{5}$$

where n_0 denotes solvent refractive index, N is Avogadro's number, and λ is the wavelength.

The root-mean-square radius of gyration $(\overline{S_z^2})^{\frac{1}{2}}$ was similarly determined from the gradient of the zero concentration lines of the Zimm plots

$$(\overline{S_z^2})^{\frac{1}{2}} = \left[\frac{3\lambda_0^2}{16\pi^2} \times \frac{\text{Slope}}{\text{Intercept}}\right]^{1/2} \text{Å} \qquad (6)$$

where λ_0 is the wavelength of light *in the solution*, i.e. λ/n_0.

A typical Zimm plot is shown in *Figure 2*. No curvature of the lines was
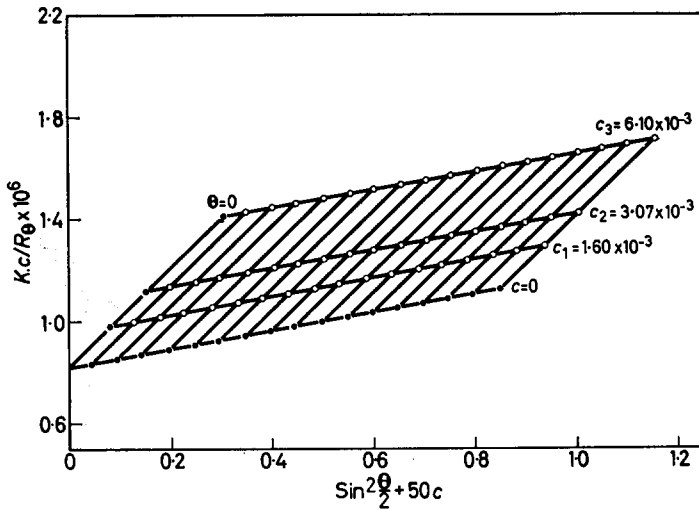
Figure 2—Zimm plot for PAcN (fraction C IV) in toluene, 25°C

encountered with any of the fractions studied, but the angular dependence of the reduced scattering intensity became very small for the lowest molecular weight fractions.

The derived values of $\overline{M}_w$, $A_{2(\text{LS})}$ and $(\overline{S_z^2})^{\frac{1}{2}}$ are given in *Table 2*. Their internal consistency can be judged from the log-log plots shown in *Figures 3* and *4*. *Figure 3* shows also the values of $\log A_{2(\text{OP})}$ derived from osmotic pressure measurements, which on the whole agree very satisfactorily. The slope of the line is, however, unusually high (-0.5); only if the extreme values were to be disregarded could the results be described by a line of 'normal' gradient (0.1 to 0.3). *Figure 4* shows, not $(\overline{S_z^2})^{\frac{1}{2}}$, but the related values of the r.m.s. end-to-end distances (weight average).

Osmotic pressure measurements

Measurements were made at 25°C, at concentrations 2 to 10 g/l in toluene, using a Mechrolab model 501 osmometer with gel cellophane membrane (Dupont type 300). With some solutions there was evidence of slight diffusion of polymer, in that differences could be detected in the solvent readings before and after measurement of the solution. To mini-

Table 2. Light scattering and osmotic pressure data for polyacenaphthylene in toluene at 25°C

Sample	Light scattering			Osmotic pressure	
	$\overline{M}_w$	$(\overline{S^2})^{\frac{1}{2}}_z$ $(\mathring{A})$	$A_{2\,(LS)} \times 10^4$ (mole cm³ g⁻²)	$\overline{M}_n$	$A_{2\,(OP)} \times 10^4$ (mole cm³ g⁻²)
C I	1 720 000	440	0·26	1 140 000	0·28
C II	1 450 000	379	0·29	1 110 000	0·29
C III	1 350 000	369	0·42	1 090 000	0·60
C IV	1 220 000	336	0·49	1 000 000	0·50
B I	962 000	285	0·51	690 000	0·85
C V	826 000	225	0·53	656 000	0·70
C VI	694 000	216	0·52	574 000	0·52
C VII	473 000	179	0·69	405 000	0·71
C VIII	454 000	158	0·83	344 000	0·90
C IX	324 000	148	0·80	273 000	1·00
C X	247 000	120	0·96	206 000	1·10
C XI	169 000	103	1·20	126 000	1·20
B X	119 000	81	1·13	100 000	1·15
B XI	85 000	80	0·90	72 000	1·20
C XII	66 000		2·00	52 000	2·10
B XIII	43 000		2·50	33 000	2·50
A I	33 000		2·42	23 000	2·10

mize this effect the solution pressure was measured as soon as it reached its apparent equilibrium (about 8 min) and was always followed by a re-determination of the solvent value. The maximum uncertainty was two to three per cent of the value of the osmotic pressure, Π.

Satisfactorily linear $(\Pi/c)/c$ plots were obtained in all cases. The derived values of M_n and second virial coefficient $(A_{2\,(OP)})$ are given in *Table 2*.
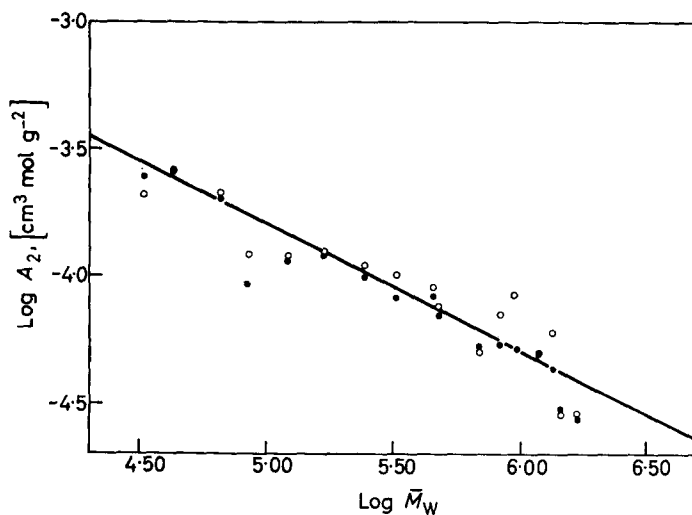
Figure 3—$A_2/\overline{M}_w$ relationship for PAcN in toluene, 25°C; ●, light scattering; ○, osmotic pressure
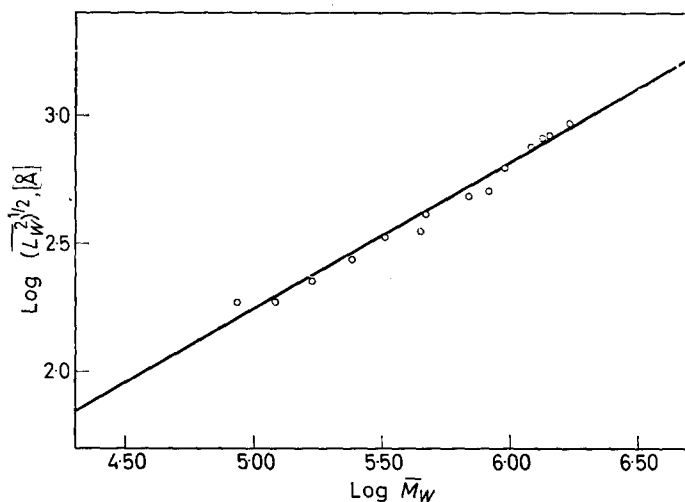
Figure 4—Root mean square end-to-end lengths for PAcN in toluene, 25°C

Heterogeneity corrections

The 'breadth of distribution' within the fractions, and the relationships between the various averages of their properties are most conveniently expressed by the Schulz–Zimm[24, 25] parameter, h. On the most usual assumption that the distribution has the form

$$W(M) = y^{h+1} M^h e^{-yM} / \Gamma(h+1) \qquad (7)$$

the different molecular weight averages are related by

$$y = h/\overline{M}_n = (h+1)/\overline{M}_w = (h+2)/\overline{M}_z$$

and

$$\overline{M}_w/\overline{M}_n = (\overline{S}_w^2)/(\overline{S}_n^2) = (\overline{L}_w^2)/(\overline{L}_n^2) = (h+1)/h$$

$$\overline{M}_w/\overline{M}_z = (\overline{S}_w^2)/(\overline{S}_z^2) = (\overline{L}_w^2)/(\overline{L}_z^2) = (h+1)/(h+2) \qquad (8)$$

The molecular dimensions

Table 3 collects the values of h derived from the experimental values of $\overline{M}_w$ and $\overline{M}_n$, and the weight average r.m.s. end-to-end distances $(\overline{L}_w^2)^{\frac{1}{2}}$ calculated from the experimental (Zimm plot) values of the radii of gyration $(\overline{S}_z^2)^{\frac{1}{2}}$, with the normal assumption[26] that for random coils $(\overline{L}^2) = 6(\overline{S}^2)$. A plot of $\log(\overline{L}_w^2)^{\frac{1}{2}}$ versus $\log \overline{M}_w$ (*Figure 4*) can be represented by

$$(\overline{L}_w^2)^{\frac{1}{2}} = 2.95 \times 10^{-1} \overline{M}_w^{0.55 \pm 0.04}, \qquad \text{Å} \qquad (9)$$

344

Table 3. Characteristics of the fractions in toluene at 25°C

Sample	$\overline{M}_v$	$\overline{M}_w/\overline{M}_n$	h	$(\overline{L^2_w})^{\frac{1}{2}}$
C I	1 620 000	1·51	1·96	932
C II	1 340 000	1·31	3·22	835
C III	1 310 000	1·24	4·16	828
C IV	1 180 000	1·22	4·54	757
B I	916 000	1·39	2·56	615
C V	798 000	1·26	3·84	501
C VI	674 000	1·21	4·76	489
C VII	461 000	1·17	5·88	409
C VIII	436 000	1·32	3·12	348
C IV	315 000	1·19	5·26	337
C V	240 000	1·20	5·00	272
C XI	162 000	1·34	2·94	226
B X	116 000	1·19	5·26	184
B XI	83 000	1·18	5·56	183
C XII	64 000	1·27	3·70	
B XIII	41 000	1·30	3·33	
A I	31 000	1·44	2·27	

Molecular weight/viscosity relationships

Figure 5, where $\log \overline{M}_w$ is plotted against $\log [\eta]$, shows that in toluene at 25°C the Mark–Houwink equation is obeyed by all fractions and gives a slope $\nu = 0·66 \pm 0·02$ which enables values of their viscosity average molecular weight to be calculated from

$$\overline{M}_v = 0·5\,(\nu + 1)\,\overline{M}_w - 0·5\,(\nu - 1)\,\overline{M}_n \qquad (10)$$

The intrinsic viscosities in other solvents (*Table 1*) also give linear relationships of similar 'goodness of fit' with $\overline{M}_w$ and with their corresponding values of $\overline{M}_v$. The constants for the two sets of relationships, defined by

$$[\eta] = K_w\overline{M}^{\nu}_w = K_v\overline{M}^{\nu}_v \qquad (11)$$

are collected in *Table 4*, together with previously reported values.

With the exception of the first value (in ethylene dichloride at 35°) the results for all solvents fit closely on a linear plot of $\log K_v/\nu$, permitting

Table 4. Mark–Houwink constants for polyacenaphthylene, $[\eta]$ in ml/g, 25°C

Solvent	$10^3 \times K_w$	$\nu\ (\pm 0·02)$	$10^3 \times K_v$	Source
Ethylene dichloride	45·6	0·50		30° (ref. 1)
	20·0	0·54	21·2	This work
Dioxan	11·5	0·61	11·6	This work
Methylene chloride	6·92	0·66	7·00	This work
Toluene	6·76	0·66	6·83	This work
Benzene	5·3	0·68		25°C (ref. 1)
	2·82	0·74	2·94	This work
Tetrahydrofuran	0·93	0·87		
	$(K_n)\,20°$			(ref. 13)
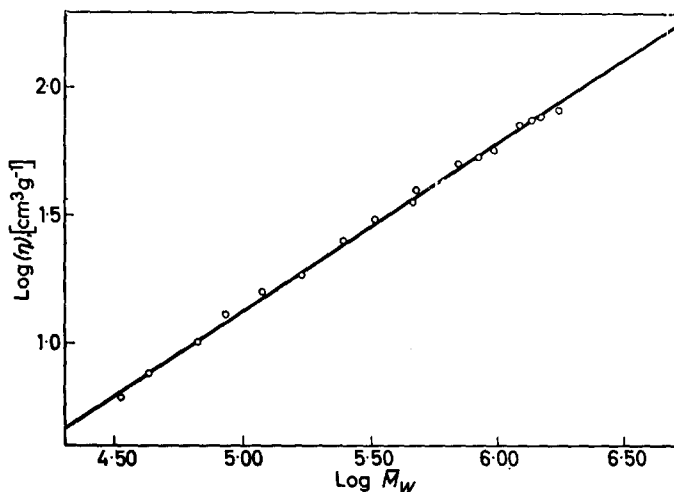
Figure 5—Viscosity/molecular weight relationship for PAcN in
toluene, 25°C

an empirical but rather convincing extrapolation to the value of
$K_{v(\theta)} = 3\cdot 4 \times 10^{-2}$ at $v = 0\cdot 5$.

Theta temperature for PAcN in ethylene dichloride

The value of $v = 0\cdot 54$ at 25°C in ethylene dichloride suggests that its
theta-temperature is about room temperature, in disagreement with Rem-
baum's finding of 35°. Measurements were therefore made of the critical
solution temperature (T_c) of four fractions (mol. wt 206 000 to 10^6). The
results are shown in Figure 6. The Flory extrapolation plot of $1/T_c$ versus
$1/\overline{M}_n^{\frac{1}{2}}$ (Figure 7) yields a value of

$$T\,(\theta) = 20° \pm 2°C$$

DISCUSSION OF RESULTS

Calculation of the unperturbed dimensions of the PAcN chains and discus-
sion of their characteristics is reserved for the following paper, but some
comment is necessary on the experimental results and systems.

The uncertainty in the values of $[\eta]$, arising from different extrapolations
according to the Huggins and the Schulz–Blaschke equations, are presum-
ably shared by most of the data in the literature. The possible errors are,
however, hardly significant, being no more than those in the molecular
weight measurements and much less than the uncertainties involved in the
extrapolation procedures to obtain K and unperturbed dimensions.

The Mark–Houwink relationships found in different solvents show satis-
factory consistency within themselves and with the results of Mohorcic[13]
(linear log K versus v), but appear to differ appreciably from those of
Moacanin, Rembaum and Laudenslager[1]. Thus their reported values in

346
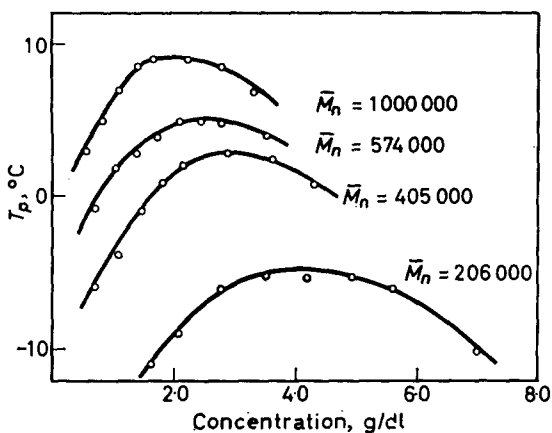
Figure 6—Critical solution temperatures for PAcN fractions in ethylene dichloride

benzene fit in the linear relationship found here, but our plotting of their $\bar{M}_w$ and $[\eta]$ data gives a line with higher K and lower exponent, consistent with their results in ethylene dichloride which they found to be a theta-solvent at 35°C giving K_θ some 30 per cent higher than the (extrapolated) value found here.

Possible differences in the PAcN samples which might explain these discrepancies would seem to be different proportions of the possible *trans isotactic* and *trans syndiotactic* sequences, or different degrees of branching. The proportion of branched chains in the present samples is unknown but is believed to be small, since fractions prepared at different temperatures (and the cationically prepared fraction) all lie on the same Mark–Houwink relationship. It seems very unlikely that if the chains were appreciably branched they would all be so to the same degree.

Another less fundamental source of discrepancy cannot be entirely excluded—possible chemical differences caused by oxidation of the polymer. It was found that samples on long standing or repeated isolation and re-
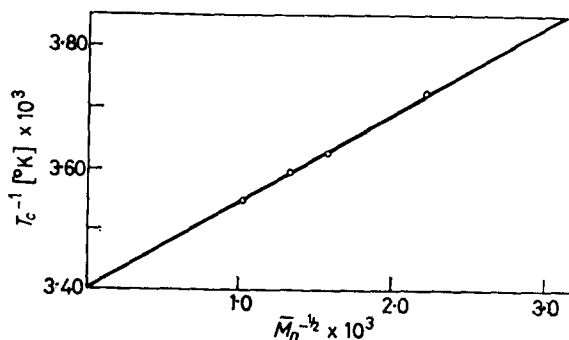
Figure 7—Extrapolation plot for T_c of PAcN in ethylene dichloride

347

measurement fell in intrinsic viscosity, became discoloured and eventually showed i.r. evidence of ketone groups.

Physical Chemistry Laboratory,
Trinity College,
Dublin, Ireland

SUBSEQUENT NOTE

Since this paper was written, a study by Springer, Ueberreiter and Wenzel[27] has been published whose result

$$[\eta]\ ml/g = 3\cdot04 \times 10^{-2}\overline{M}_n^{0\cdot594}\ \text{in benzene}$$

is at variance with the values of the constants found here ($2\cdot82 \times 10^{-3}$ and $0\cdot74$).

These authors also noted that PAcN samples were sensitive to degradation by light, so it is possible that the discrepancy has a chemical origin.

Another possibility is that the breadth of distribution of these authors' fractions (not reported) was greater in their lower than in their higher molecular weight fractions. Since their molecular weights are number averages, they would be displaced ($< \overline{M}_v$) to a greater extent at the lower molecular weights. The Mark–Houwink line would therefore have not only a lower slope but a (much) higher value of K, as found.

REFERENCES

[1] MOACANIN, J., REMBAUM, A. and LAUDENSLAGER, R. K. *Amer. chem. Soc. Polymer Preprints,* 1963, **4**, 179
[2] YAMADA, A., YANAGITA, M. and KOBAYASHI, E. *J. Polym. Sci.* 1962, **61**, S14
[3] STORY, V. M. and CANTY, G. *J. Res. Nat. Bur. Stand. A,* 1964, **68**, 165
[4] DZIEWONSKI, K. and LYLSO, Z. *Ber. dtsch. chem. Ges.* 1914, **47**, 1769 and DZIEWONSKI, K. and STOLYLUWO, T. *Ber. dtsch. chem. Ges.* 1924, **57**, 1531
[5] FLOWERS, R. G. and MILLER, H. F. *J. Amer. chem. Soc.* 1947, **69**, 1388
[6a] IMOTO, M. and TAKEMOTO, K. *J. Polym. Sci.* 1955, **15**, 271
[6b] IMOTO, M. and SOMATSU, I. *Bull. chem. Soc. Japan,* 1961, **34**, 26
[7] BARRALES-RIENDA, J. M. and PEPPER, D. C. Unpublished results
[8] PANTON, M. E. and PLESCH, P. H. Unpublished results: quoted by P. H. PLESCH, *Chemistry of Cationic Polymerization,* p 343. Pergamon: Oxford, 1963
[9] MOACANIN, J., REMBAUM, A. and ADLER, R. *Space Programme Summary* (Jet Propulsion Laboratory) 1963, *IV*, 94
MOACANIN, J. and REMBAUM, A. *J. Polym. Sci. B,* 1964, **2**, 979
[10] REMBAUM, A. *J. Polym. Sci. B,* 1964, **2**, 117
[11] JONES, J. I. *J. appl. Chem.* 1951, **1**, 568
[12] KAUFMAN, M. and WILLIAMS, A. F. *J. appl. Chem.* 1951, **1**, 589
[13] MOHORCIC, G. *Bull. sci. Yougoslavie,* 1957, **3**, 105
[14] MANECKE, G. and DANHÄUSER, J. *Makromol. Chem.* 1962, **56**, 208
[15] MOACANIN, J., REMBAUM, A. and LAUDENSLAGER, R. American Chemical Society Western Regional Meeting, Los Angeles, 1965
[16] HUGGINS, M. L. *J. Amer. chem. Soc.* 1942, **64**, 2716
[17] SCHULZ, G. V. and BLASCHKE, F. *J. prakt. Chem.* 1941, **158**, 130
[18] IBRAHIM, F. W. *J. Polym. Sci. A,* 1965, 3, 469

[19] KRATOHVIL, J. P., DEZELIC, B., KERKER, M. and MATIJEVIC, E. *J. Polym. Sci.* 1962, **57,** 59

[20] JENNINGS, B. R. and JERRARD, H. G. *J. Polym. Sci. A,* 1964, **2,** 2025

[21] NORBER, P. H. and SUNDALÖF, L. O. *Makromol. Chem.* 1964, **73,** 77

[22] BERKOWITZ, J., YAMIN, M. and FUOSS, R. M. *J. Polym. Sci.* 1958, **28,** 69

[23] TOMIMATSU, Y. and PALMER, K. J. *J. Polym. Sci.* 1959, **35,** 549; 1961, **54,** S21

[24] ZIMM, B. H. *J. chem. Phys.* 1948, **16,** 1093; 1948, **16,** 1099

[25] SCHULZ, G. V. *Z. phys. Chem. B,* 1939, **43,** 25

[26] DEBYE, P. *J. chem. Phys.* 1948, **14,** 636; 1948, **16,** 573

[27] SPRINGER, J., UEBERREITER, K. and WENZEL, R. *Makromol. Chem.* 1966, **96,** 1

The Dilute Solution Properties of Polyacenaphthylene
II—Unperturbed Dimensions and Conformation of Chains in Solution

J. M. BARRALES-RIENDA and D. C. PEPPER

The light scattering, osmotic and viscometric measurements reported in the preceding paper are used to derive the unperturbed dimensions of the poly-acenaphthylene chain in solution and estimate the steric hindrances to rotation. The value of $A = [(\overline{L_w^2})_0 / \overline{M_w}]^{\frac{1}{2}}$ is concluded to be $520 \pm 10 \times 10^{-11}$ cm $mol^{\frac{1}{2}}$ $g^{-\frac{1}{2}}$. The values A_f calculated for alternate bonds freely rotating and completely restricted (to either erythro or threo conformation) are 177 and 354, with a weighted average for chains having equal proportions of the two types of 250—all $\times 10^{-11}$. For such equally mixed chains the value of the steric factor $\sigma = A/A_f$ would be $2 \cdot 08$ (cf. $\sigma = 2 \cdot 2$ for polystyrene). Since there is reason to expect a smaller proportion of erythro placements, σ must be even smaller. The anticipated 'stiffening effect' of the bulky substituent is therefore much less than expected.

EVALUATION OF UNPERTURBED DIMENSIONS

THE values of r.m.s. end-to-end distances, $(\overline{L_w^2})^{\frac{1}{2}}$, listed in Part I[1], give the dimensions of the various fractions in toluene solution at 25°C, i.e. with chain coils expanded by the excluded volume effect and the solvent interactions. The unperturbed average dimension $A = [(\overline{L_w^2})_0 / \overline{M_w}]^{\frac{1}{2}}$, needed for comparison with theoretical models, can be obtained directly, by extrapolation, or by combination with values of the expansion factor $\alpha = [(\overline{L^2})/(\overline{L^2})_0]^{\frac{1}{2}}$, if this can be derived independently.

Alternatively, A may be derived indirectly from viscosity measurement, using the equations of Kurata and Stockmayer[2] and of Stockmayer and Fixman[3]. The direct evaluation is theoretically preferable but less accurate because of the insensitivity of the determination of $(\overline{S^2})^{\frac{1}{2}}$ from light scattering. The viscosity measurements are more precise but the compensating disadvantage is some uncertainty in the applicability of the various extrapolated functions and in the relationship expected to hold between viscosity and dimensions. In the hope of avoiding the many possible pitfalls we have analysed the data by several variants of both methods.

(I) From light scattering
(i) By extrapolation—Figure 1 shows the data plotted according to the equation of Kurata and Stockmayer[2]

$$(\overline{L_w^2}) / \overline{M_w} = A^2 + 0 \cdot 421 B \left[g(\alpha) \overline{M_w} / (\overline{L_w^2})^{\frac{1}{2}} \right] \tag{1}$$

where g (α) is a function of the expansion factor $(= 8\alpha^3 / (3\alpha^2 + 1)^{3/2})$ and is obtained by successive approximations [i.e. first plotting with g$(\alpha) = 1$].
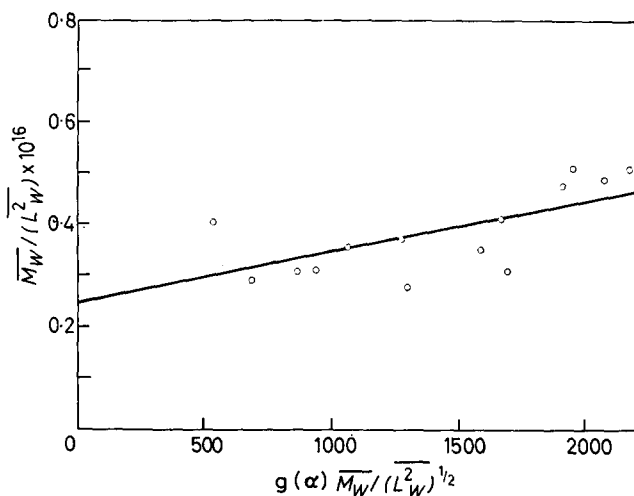
Figure 1—Kurata–Stockmayer plot of dimensions in toluene, 25°C

This refinement moved the values to the right by at most 20 per cent on the uppermost points and 5 to 10 per cent on the lowest, and seems hardly worth while in view of the scatter. The 'best straight' line is hard to locate, but various plausible lines give intercepts between $0.25 \pm 0.02 \times 10^{-16}$ (cm^2 mol g^{-1}), corresponding to values of A between $500 \pm 20 \times 10^{-11}$ (cm mol$^{\frac{1}{2}}$ g$^{-\frac{1}{2}}$), and $B = 0.24 \pm 0.03 \times 10^{-27}$ (cm^3 mol^2 g^{-2}).

Another equation, found by Baumann[4] to give a linear extrapolation, may be obtained by transposing the Stockmayer and Fixman[3] equation for intrinsic viscosities. In the symbols used here Baumann's equation becomes

$$[(\overline{L_w^2})/\overline{M_w}]^{3/2} = A^{3/2} + 0.66B\overline{M_w^{\frac{1}{2}}} \tag{2}$$

and is functionally the equivalent of the unrefined [g $(\alpha) = 1$] Kurata and Stockmayer's plot (1). It is shown in *Figure 2*, and yields values of the parameters $A = 500 \pm 30 \times 10^{-11}$ (cm mol$^{\frac{1}{2}}$ g$^{-\frac{1}{2}}$) and $B = 0.20 \pm 0.03 \times 10^{-27}$ (cm^3 mol^2 g^{-2}).

(*ii*) *From values of* $(\overline{L_w^2})^{\frac{1}{2}}$ *and* α—The expansion factor α may in principle be obtained: (a) from the measured second virial coefficients, A_2, radii of gyration $(\overline{S_n^2})^{\frac{1}{2}}$, and number-average molecular weight, $\overline{M_n}$, using the equation of Orofino and Flory[5],

$$A^2 = [16\pi N_0 (\overline{S_n^2})^{3/2}/3^{3/2}\overline{M_n^2}] \ln [1 + \pi^{\frac{1}{2}} (\alpha^2 - 1)/2]* \tag{3}$$

and (b) from the intrinsic viscosities using $\alpha^{2.43} = [\eta]/[\eta]_\theta$ (Kurata–Yamakawa[20]). Method (a) involves three experimentally measured quantities and proves unreliable with the present data. The calculated α values scatter widely and are abnormally high at low molecular weights, showing an apparent downward trend from 1·4 at the lowest to 1·1 at the highest

*N_0 is Avogadro's number.
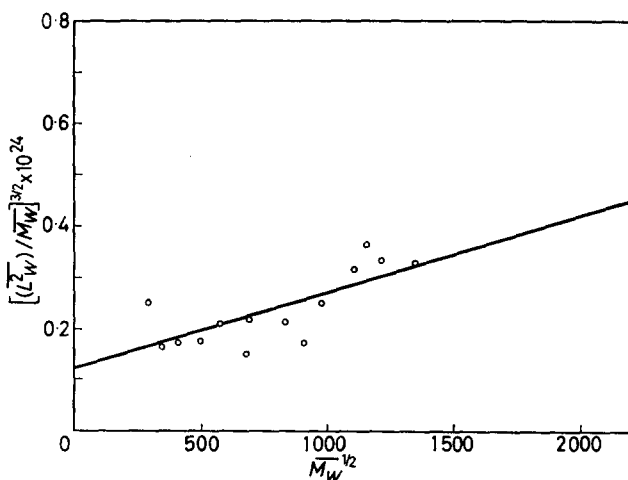
Figure 2—Baumann–Stockmayer–Fixman plot for dimensions, 25°C

molecular weight. The derived values of $A = [(\overline{L_w^2})/\overline{M_w}]^{\frac{1}{2}}/\alpha$ show an apparent upward trend from 380 to 450×10^{-11}. This is to be associated with the anomalous dependence of A_2 on molecular weight noted in Part I.

Values of α derived by method (b) are shown in *Figure 3*(a), compared with a theoretical curve based on the Kurata, Stockmayer and Roig[6] relationship, fitted at $\alpha = 1.21$ when $\overline{M_w} = 10^6$. The corresponding values of A, shown in *Figure 3*(b), scatter between 460 and 580×10^{-11} but a reasonable mean seems about 520×10^{-11}. Use of α values from the smoothed curve
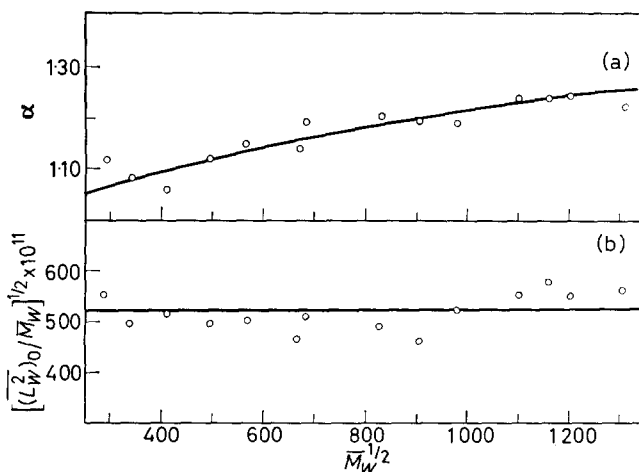
Figure 3(a)—Expansion factor α in toluene at 25°C: O, experimental from $\alpha = ([\eta]/[\eta]_\theta)$; full line, K–S–R theory with $\alpha = 1.21$ at $\overline{M_w} = 10^6$; *Figure 3*(b)—Unperturbed dimension in toluene at 25°C from $[(\overline{L_w^2})/M]^{\frac{1}{2}}/\alpha$

makes no significant difference, indicating that the scatter is dominated by the uncertainties in the measurements of gyration radius.

The failure to obtain corroboration from the Orofino–Flory calculations is disappointing and this method must obviously be applied with great care. Within its limitations, however, it has yielded the same values for the unperturbed dimensions as the extrapolation procedures and lends confidence to what might otherwise be thought somewhat subjective extrapolations.

(II) From intrinsic viscosities

The coil dimension may also be calculated from the intrinsic viscosity by use of the Fox and Flory equation[7]

$$[\eta] = \Phi \, (\overline{L^2})^{3/2} / M \tag{4}$$

or its equivalent for the unperturbed dimensions

$$K_\theta = [\eta]_\theta / M^{\frac{1}{2}} = \Phi \, [(\overline{L^2})_0 / M]^{3/2} \tag{5}$$

The value of Φ, originally thought to be constant at $2 \cdot 1 \times 10^{23}$ (for $[\eta]$ in ml/g), is now expected to tend slowly with molecular weight to a limit

$$\Phi_0 = 2 \cdot 87 \times 10^{23} \quad \text{(Kirkwood–Riseman[8])}$$

The measured viscosities in the various solvents may be extrapolated to obtain K_θ by several procedures. In *Figures 4* and *5* the results in toluene and in ethylene dichloride are plotted according to the equations of Kurata and Stockmayer[2] and Stockmayer–Fixman–Burchard[3, 9] respectively.

K–S
$$[\eta]^{2/3} / \overline{M}_v^{1/3} = K_\theta^{2/3} + 0 \cdot 363 \Phi_0 B \, [g \, (\alpha_\eta) \, \overline{M}_v^{2/3} / [\eta]^{1/3}] \tag{6}$$

S–F–B
$$[\eta] / \overline{M}_v^{\frac{1}{2}} = K_\theta + 0 \cdot 51 \Phi_0 B \overline{M}_v^{\frac{1}{2}} \tag{7}$$

The more refined Kurata–Stockmayer equation (6) shows no advantage over the simple S–F–B plot (7). In both plots the results in ethylene dichloride give good lines of near-zero slope confirming the near-ideal
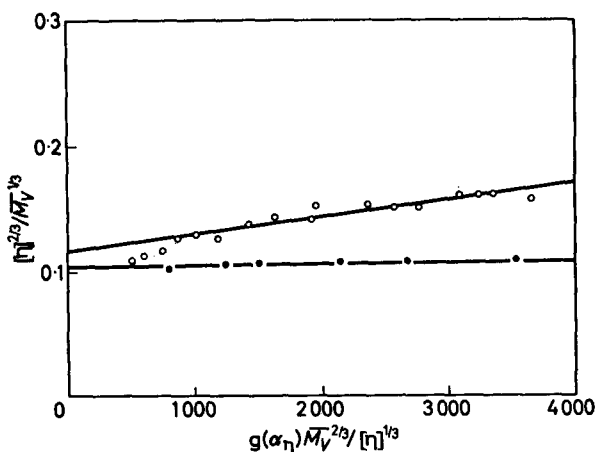
Figure 4—K–S viscosity plot at 25°C; ●, in ethylene dichloride; ○, in toluene

Figure 5—S–F–B viscosity plot at 25°C: ●, in ethylene dichloride; ○, in toluene
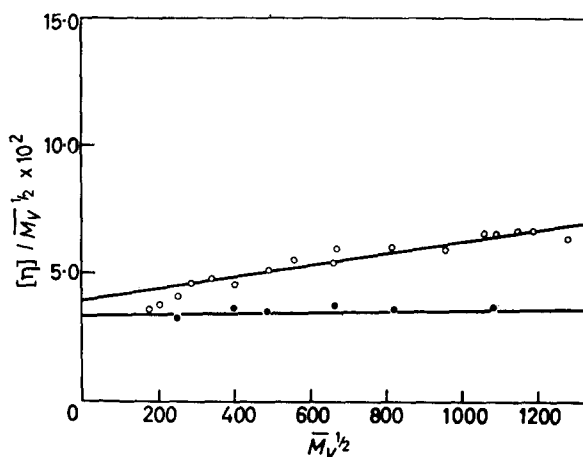
character of this solvent for PAcN. The results in toluene behave similarly in both plots and appear to indicate a slightly higher value of K_θ, but this conclusion is weakened by deviations from linearity at the lowest molecular weights. Similar deviations are found in this region in plots for the other good solvents. They must have their origin partly in applicability of the functions (since no exact fits can be expected from any set of $[\eta]/\overline{M}_v$ values which strictly obey a Mark–Houwink relationship and the deviations become pronounced at $M < 10^5$ when $\nu \geqslant 0.6$).

For this reason, while it can be said that the plots for all solvents converge to approximately the same intercept (values of K_θ collected in *Table 1*), it cannot be decided whether there are small specific solvent effects on K_θ such as have been demonstrated with polymethylmethacrylate[10].

Tests of the data by the equations of Fox–Flory–Schaefgen[12] and of Bohdanecky[13] also give similar results—deviations at the lowest molecular weights, and higher points extrapolating to give K_θ values within the range listed in *Table 1*.

The values of K_θ, combined with the ideal value of $\Phi_0 = 2.87 \times 10^{23}$, yield results for the dimension $A = [(\overline{L^2})_0/M]^{\frac{1}{2}}$ which all lie within the range $500 \pm 30 \times 10^{11}$ derived from light scattering. However, if the calculation is reversed, and values of Φ are calculated for assumed values of A in this range, it is seen (*Table 1*) that all the Φ values based on $A = 480$, and many of those based on $A = 500$ are abnormally high ($> 3 \times 10^{23}$) which is presumably impossible without some very special interactions. It seems best to conclude that the viscosity results favour an A value at the upper end of the range, e.g. $520 \pm 10 \times 10^{-11}$.

Such a value is consistent with our light scattering measurements but is smaller than the result $A \sim 600 \times 10^{-11}$ (derived from light-scattering measurements on three fractions of higher molecular weight[14]). Deductions from our own highest fractions only would similarly have led to a high value, but this seems excluded by the arguments of Section II and the viscosity results. A value as low as 520 is at first unexpected for a chain

355

Table 1. Parameters derived from intrinsic viscosities

Solvent	Method	$10^2 \times K_\theta$*	$10^{27}B$†‡	$10^{11}A$‡	$10^{23}\Phi$		
					$A=480$	$A=500$	$A=520$
	Empirical (Part I)	3·47					
Ethylene dichloride	K–S	3·35	0·01	489	3·02	2·68	2·37
	S–F–B	3·35	0·03	489	3·02	2·68	2·37
Dioxan	K–S	3·65	0·12	503	3·30	2·98	2·59
	S–F–B	3·90	0·11	514	3·52	3·13	2·77
Toluene	K–S	3·94	0·13	515	3·56	3·16	2·80
	S–F–B	3·75	0·18	505	3·31	3·00	2·66
Methylene dichloride	K–S	4·04	0·14	520	3·65	3·23	2·87
	S–F–B	3·90	0·17	514	3·52	3·13	2·77
Benzene	K–S	3·35	0·27	489	3·02	2·68	2·37
	S–F–B	3·50	0·31	496	3·16	3·80	2·48

* $\pm 0\cdot20$ (ml g$^{-1/2}$ mol$^{1/2}$)
† $\pm 0\cdot02$ (ml g^{-2} mol^2)
‡ for $\Phi \simeq \Phi_0 = 2\cdot87 \times 10^{21}$

apparently so heavily hindered as that of PAcN (e.g. $A = 670 \pm 15$ for polystyrene). The considerations of the next section show, however, that it is quite plausible.

SHORT-RANGE INTERACTIONS—THE STERIC FACTOR $\sigma = A/A_f$

With no restrictions on bond-rotation, a chain of N bonds of length l, joined at a valence angle θ ($= \pi - \alpha$) has a mean square end-to-end distance[15]

$$\overline{L^2_{0f}} = Nl^2 (1 + \cos \alpha)/(1 - \cos \alpha) \tag{8}$$

and if the bond rotation is restricted within a range whose mean angle is ϕ (between the bond and the plane defined by the two preceding bonds)[21]

$$\overline{L^2_0} = Nl^2 (1 + \cos \alpha)(1 + \eta)/(1 - \cos \alpha)(1 - \eta) \tag{9}$$

where $\eta = \overline{\cos \phi}$. For 'vinyl type' chains where all bonds are equivalent (and $l = 1\cdot54$ Å, $\theta = 109\cdot5°$, $\cos \alpha = 1/3$), $\overline{L^2_{0f}} = 2Nl^2$, and since there are two bonds per monomer unit

$$A_f = [\overline{L^2_{0f}}/\overline{M}]^{\frac{1}{2}} = 3\cdot08/\overline{M}^{\frac{1}{2}}_\mu \tag{10}$$

where M_μ is the monomer molecular weight.

The influence of chain structure (steric hindrance of substituent groups, etc.) is then revealed by $\sigma = A/A_f > 1$ and can be expressed equivalently in terms of η or ϕ.

For PAcN chains the expected value of A_f will be different since alternate

bonds must have different values of η. Volkenstein[16] has given a general expression for such a type, i.e.

$$\overline{L_0^2} = Nl^2 (1 + \cos \alpha)(1 - \eta_1 \eta_2)/(1 - \cos \alpha)(1 - \eta_1)(1 - \eta_2) + \text{second order terms} \tag{11}$$

which Moacanin *et al.*[14] have applied to PAcN by setting $\eta_2 = 0$ (for free rotation about the intermonomer bond). There are two cases, corresponding to the two conformations possible for the intramonomer bond (erythro; $\phi = 180°, \eta = -1$, and threo; $\phi = 60°, \eta = 0.5$) hence

$$\overline{L_0^2} = 2Nl^2/(1 - \eta_1) = Nl^2 \quad \text{(erythro)} \tag{12}$$

$$= 4Nl^2 \quad \text{(threo)} \tag{13}$$

confirming the subjective expectation that a *cis* chain (erythro) should be more tightly coiled than a *trans* chain (threo).

The dimensions of chains of mixed proportions of *cis* and *trans* placements can be calculated by making use of Volkenstein's[16] concept of the 'effective average cosine of the restriction angle', $\eta_{eff.}$, defined by

$$\overline{L_0^2} = Nl^2 (1 + \cos \alpha)(1 + \eta_{eff.})/(1 - \cos \alpha)(1 - \eta_{eff.}) \tag{14}$$

Combination with equations (12) and (13) gives

$$\eta_{eff.} \text{ (erythro)} = -1/3 \tag{15}$$

$$\eta_{eff.} \text{ (threo)} = 1/3 \tag{16}$$

The average $\eta_{eff.}$ for a chain of fraction p of *cis* placements is then

$$\overline{\eta_{eff.}} = -p/3 + (1-p)/3 = 1/3 - 2p/3 \tag{17}$$

The expected free rotation dimension $A_f = [L_{0f}^2/\overline{M}]^{\frac{1}{2}}$ can be calculated for various values of p, taking $l = 1.54$ Å and $N = 2M/152$ for PAcN. They are shown in *Table 2* with the corresponding values of σ.

The values of A_f show in a formal way how the 'tightening' effect of *cis* (erythro) placements compensates for the loosening effect of *trans* placements, so that equal proportions would produce exactly the dimension expected, 250×10^{-11}, for a chain coil having no restrictions on bond orientation.

If this were true for the polymer samples measured here, then the corresponding σ value, 2.08, would be similar to (slightly less than) that found for polystyrene (2.2). In Part I a general consideration of the stereochemistry led to the (subjective) expectation that the fraction of *cis* placements should be <0.5 and perhaps very small. If so, our value of $A = 520 \pm 20$ indicates a lower σ, e.g. perhaps ~ 1.5, lower than has yet been found for a —C—C— bond. Similar low values are found with polyisoprene (*cis*, 1.67; *trans*, 1.38; ref. 17) whose chains show an analogous pattern of (three) free bonds followed by a fixed bond.

This is at first sight a surprising conclusion for a chain with so large a substituent group. The explanation may perhaps be found in terms of Volkenstein's[16] interpretation of the steric factor, that it arises not so much

Table 2. Effective average cosine of the restriction angle and steric factors for various values of p

p	0	0·2	0·4	0·6	0·8	1·0
$\overline{\eta_{\text{eff.}}}$	0·33	0·20	0·067	−0·067	−0·20	−0·33
$\left[\dfrac{1+\overline{\eta_{\text{eff.}}}}{1-\overline{\eta_{\text{eff.}}}}\right]^{\frac{1}{2}}$	1·414	1·225	1·07	0·935	0·807	0·707
$10^{11} \times A_f$	354	306	267	234	204	177
$\sigma = 520/A_f$	1·47	1·70	1·95	2·22	2·55	2·94

from the resistance to complete rotation of links but from the energy requirements of relatively small amplitude rotations about the potential minima associated with the rotational isomeric positions. In a PAcN chain with a majority of *trans* placements, the large substituent group is held away from the chain backbone (or axis of helix) and might well not be brought into mutual interference if rotations are fairly small.

THE EXCLUDED VOLUME EFFECT

From the applicability of the K–S equation in *Figure 5*, one expects that the expansion factors should correlate with molecular weight according to the equation of Kurata–Stockmayer–Roig[6].

$$(\alpha^3 - \alpha)(3\alpha^2 + 1)^{3/2}/8\alpha^3 = 0\cdot421 B A^{-3}\overline{M_v^{\frac{1}{2}}} \tag{18}$$

This is found to apply (c.f. *Figure 3*(a), but because of the experimental scatter, the fit is no better than that given by the earlier Flory equation[18]

$$(\alpha^5 - \alpha^3) = 0\cdot859 B A^{-3}\overline{M_v^{\frac{1}{2}}} \tag{19}$$

Indeed a much simpler function

$$(\alpha^3 - 1) = B A^{-3/2}\overline{M_v^{\frac{1}{2}}} \tag{20}$$

which is implied by the Stockmayer–Fixman equation[3], gives apparently a slightly better fit than either.

The reason is, of course, that for the relatively low values of α encountered here ($<1\cdot3$) the various functions deviate from each other by hardly more than the experimental uncertainty in α. To decide which is the best form of the excluded volume effect in these solutions would need either much more precise data or a wider range of molecular weights.

COIL PERMEABILITY

Ullman's recent theory[19] of intrinsic viscosity in terms of coil dimensions and permeability to solvent permits an estimate of this latter from the results in toluene. The viscosity is expressed in terms of functions $G(\lambda)$, of a permeability parameter λ, for various chain models, e.g. the

$$\text{Random Gaussian coil: } [\eta] = [(2\pi^3)^{\frac{1}{2}} \cdot N_0\, (\overline{S^2})^{3/2}/M] \times G\,(\lambda) \tag{21}$$

(which strictly applies only to solution in the theta-condition), and for an expanded coil the Kurata–Yamakawa coil[20]

$$[\eta] = [(2\pi^3)^{\frac{1}{2}} N_0\, (\overline{S^2})^{3/2}/M]\,[1 + 134\xi/105]^{-3/2} G\,(\lambda) \tag{22}$$

where ξ is the Kurata–Yamakawa excluded volume parameter related to α by $\alpha^2 = (1 + 134\xi/105)$, and N_0 is Avogadro's number.

For completely impermeable coils $G(\lambda) \rightarrow G(\lambda)_\infty$ which is 0·870 for the random Gaussian coil, and for the Kurata–Yamakawa coil can be calculated for various α.

The value of $G(\lambda)$ can be calculated from the experimental quantities, and hence the impermeability of each fraction expressed as the ratio $G(\lambda)/G(\lambda_\infty)$.

Calculating on the random Gaussian model, the ratios for the various fractions vary between 1·09 and 0·78 with mean value 0·96. For the Kurata–Yamakawa coil, the variation is between 1·22 and 0·90 with mean 1·03. Within these variations the values show no trend to lower values at the lower molecular weights; there is thus no evidence for appreciable coil permeability in any of these fractions.

GENERAL CONCLUSIONS

The main conclusion of these studies is clear, that these samples of PAcN give solution properties that are quite 'normal', and the large substituent and the 'locked' alternate bonds in the chain do not impose abnormally large coil dimensions or appreciably 'stiff' chains with 'free-draining' character.

On the contrary, the unperturbed coil dimension is smaller than that for polystyrene, an unexpected result which appears to be explained by a particular consequence of the structure of the monomer unit. The restriction of alternate bonds, by the ring substituent, into erythro (cis) or threo (trans) conformations should cause a corresponding shortening and lengthening respectively of the contribution of a monomer unit to the average coil dimension. While there is reason to expect a higher proportion of threo placements, and hence a larger coil dimension than for a 'genuine' vinyl-type chain, it seems that this effect is counteracted by a slightly greater than normal freedom of rotation about the inter-monomer bonds.

Abnormal coil dimensions may still be anticipated in stereoregular chains, but only if they contain long regular sequences, since every placement in an opposite stereochemical sense must cause reversal of the sense of helices (di-isotactic) or direction of any 'stepped' chains (di-syndiotactic)[1].

Physical Chemistry Laboratory,
  Trinity College,
    Dublin, Ireland.

REFERENCES

[1] BARRALES-RIENDA, J. M. and PEPPER, D. C. *Polymer, Lond.* 1967, **8**, 337
[2] KURATA, M. and STOCKMAYER, W. H. *Fortschr. HochpolymForsch.* 1963, 3, 196
[3] STOCKMAYER, W. H. and FIXMAN, M. *J. Polym. Sci. C,* 1963, **1**, 137
[4] BAUMANN, H. *J. Polym. Sci. B,* 1965, **3**, 1069
[5] OROFINO, T. A. and FLORY, P. J. *J. chem. Phys.* 1957, **26**, 1067
[6] KURATA, M., STOCKMAYER, W. H. and ROIG, A. *J. chem. Phys.* 1960, 33, 151
[7] FOX, T. G and FLORY, P. J. *J. phys. Colloid Chem.* 1949, **53**, 197

[8] KIRKWOOD, J. G. and RISEMAN, J. *J. chem. Phys.* 1948, **16**, 565

[9] BURCHARD, W. *Makromol. Chem.* 1961, **50**, 20

[10] Ref. 2, p 244, quoting data of ref. 11

[11] SCHULZ, G. V., CANTOW, H.-J. and MEYERHOFF, G. *J. Polym. Sci.* 1953, **10**, 79; CANTOW, H.-J. and SCHULZ, G. V. *Z. phys. Chem.* (*N.F.*), 1954, **1**, 365; BISCHOFF, J. and DESREUX, V. *Bull. Soc. chim. Belg*, 1952, **61**, 10; CASASSA, E. F. and STOCK-MAYER, W. H. *Polymer, Lond.* 1962, **3**, 53

[12] FLORY, P. J. and FOX, T. G. *J. Amer. chem. Soc.* 1951, **73**, 1904

[13] BOHDANECKÝ, M. *J. Polym. Sci. B*, 1965, **3**, 201

[14] MOACANIN, J., REMBAUM, A. and LAUDENSLAGER, R. American Chemical Society, Western Regional Meeting, Los Angeles, 1965

[15] FLORY, P. J. *Principles of Polymer Chemistry*, p 415. Cornell University Press: Ithaca, New York, 1953

[16] VOLKENSTEIN, M. V. *Configurational Statistics of Polymeric Chains*, Interscience: New York, 1962

[17] WAGNER, H. L. and FLORY, P. J. *J. Amer. chem. Soc.* 1952, **74**, 195

[18] FLORY, P. J. *J. chem. Phys.* 1949, **17**, 303

[19] ULLMAN, R. *J. chem. Phys.* 1964, **40**, 2193

[20] KURATA, M. and YAMAKAWA, H. *J. chem. Phys.* 1958, **29**, 311

[21] TAYLOR, W. J. *J. chem. Phys.* 1948, **16**, 257; BENOIT, H. *J. chem. Phys.* 1947, **44**, 18; KUHN, H. *J. chem. Phys.* 1947, **15**, 843

The Polymerization of Some Epoxides by Diphenylzinc, Phenylzinc t-Butoxide, and Zinc t-Butoxide

J. Malcolm Bruce and F. M. Rabagliati

Ethylene oxide is polymerized by diphenylzinc to give polymers with viscosity-average molecular weights of up to 3×10^6. Similar polymers are formed when phenylzinc t-butoxide is used as catalyst, but the reaction is faster; the viscosity-average molecular weight of the product increases in parallel with the degree of conversion of the monomer, and there is a broad distribution of molecular weights.

Zinc t-butoxide, which is insoluble, is more active than either of the above systems, and readily gives high yields of poly(ethylene oxide) with viscosity-average molecular weights of up to 9×10^6. Solvents such as cyclohexane and benzene have little effect on the polymerization, but t-butyl alcohol markedly reduces the rate, and gives a product of comparatively low molecular weight.

Propylene oxide is polymerized by zinc t-butoxide much less rapidly than ethylene oxide, and the product has a lower degree of polymerization; approximately 12 per cent is 'crystalline'. The proportion of 'crystalline' material is somewhat decreased, but its melting point is raised, when tetrahydropyran is used as solvent.

ETHYLENE oxide can be polymerized by soluble organozinc alkoxides, but the greatest catalytic activity is shown by insoluble zinc dialkoxides[1]. The present paper describes some further results obtained for the initially homogeneous polymerization of ethylene oxide by diphenylzinc and phenylzinc t-butoxide, and for the heterogeneous polymerization of ethylene oxide and propylene oxide by zinc t-butoxide.

EXPERIMENTAL

Monomers and solvents were dried over calcium oxide, fractionally distilled, and stored over calcium oxide. Phenylzinc t-butoxide was prepared by treatment of diphenylzinc[2] with 1 mol. of t-butyl alcohol in benzene, followed by removal of the solvent, finally at $90°C/10^{-5}$ mm of mercury for three hours. Zinc t-butoxide[3] was obtained by treating a benzene solution of diphenylzinc with an excess of t-butyl alcohol at 70° to 80°C for 24 hours, and then removing the volatile materials, finally at $180°C/10^{-5}$ mm of mercury for three hours. All materials were handled by the vacuum-line techniques previously described[2-4].

The alkoxide catalysts were prepared in cylindrical ampoules to which the monomer and solvent were subsequently added; the ampoules were then fusion sealed. Preliminary experiments with zinc t-butoxide were carried out without agitation, but for later polymerizations the ampoule was mounted horizontally in the thermostat and rocked so that the contents were continuously transferred from end to end; a glass-encased iron rod present in the ampoule simultaneously scraped the lower wall, preventing build-up of solid catalyst. Effective agitation ceased when the reaction mixture

gelled. Dilatometric experiments were carried out as previously described[5].

Polymerizations were terminated by addition of benzene and a small excess of methanol over that required to precipitate the catalyst; a hindered phenol antioxidant (Antioxidant 2246, Anchor Chemical Co. Ltd, 1 to 3 per cent w/w of monomer used) was also added in all cases except those for which number-average molecular weights and proton magnetic resonance spectra of the polymers were to be determined. Catalyst residues were removed centrifugally, and the polymers were isolated by freeze-drying[5]. Intrinsic viscosities, $[\eta]$, were measured at $25° \pm 0 \cdot 01°C$ in benzene containing the above antioxidant ($0 \cdot 1$ per cent w/v). Viscosity-average molecular weights ($\bar{M}_v$) were calculated for poly(ethylene oxide) using the equation[6] $[\eta] = 3 \cdot 97 \times 10^{-4} (\bar{M}_v)^{0 \cdot 686}$, and for poly(propylene oxide) from the relationship[7] $[\eta] = 1 \cdot 12 \times 10^{-4} (\bar{M}_v)^{0 \cdot 77}$. Number-average molecular weights ($\bar{M}_n$) were determined for benzene solutions using a Mechrolab vapour pressure osmometer, and proton magnetic resonance spectra were measured at $40°C$ with a Varian A-60 spectrometer using tetramethylsilane as an internal standard.

Poly(ethylene oxide) was fractionated according to molecular weight by progressive cooling of solutions in benzene–isooctane[6]. The 'crystalline' content of poly(propylene oxide) samples was determined[8] from the amount of material which separated when a solution, initially $2 \cdot 7$ g l^{-1} at $40°C$, of the polymer in methanol was maintained at $0°C$ for two days; further fractionation[8] of the methanol-soluble material was achieved by cooling its solution, initially 1 g l^{-1} at $60°C$, in isooctane at $0°C$ for 24 hours. Melting points were determined with a Köfler hot stage mounted on a polarizing microscope; for poly(propylene oxide) the sample was first melted and kept at $100°C$ for 20 min, then maintained at $35°$ to $40°C$ for one hour, and the temperature was finally raised at the rate of 12 deg. C/hour.

RESULTS AND DISCUSSION

The following abbreviations are used: $[M_0]$ denotes initial concentration of monomer; $[C_0]$ is the initial concentration of catalyst calculated as if it were monomeric (the t-butoxides are aggregates[3]); M_0 denotes initial volume of monomer; S is the volume of solvent; C_6H_{12} is cyclohexane; THP is tetrahydropyran.

Diphenzylzinc

The results of typical experiments carried out in benzene solution are shown in *Table 1*. Attempts to follow the polymerization dilatometrically gave erratic results, possibly due to the separation of solid material at an early stage; the region immediately surrounding the precipitate became much more viscous than the rest of the solution.

The yield of polymer increased in proportion to the initial concentration of diphenylzinc, but at a fixed concentration the yields were similar after either 288 or 1 080 hours, although the viscosity-average molecular weights of the polymers had increased considerably, suggesting that there may have been an initial fairly rapid production of a comparatively large number of chains of low molecular weight by a reaction which terminated at a fairly

362

early stage, accompanied by a slower reaction, which did not terminate, leading to fewer chains of much higher molecular weight. Two catalyst systems may be involved, a comparatively simple homogeneous one producing the low-molecular weight polymer, and a more complex heterogeneous one (the precipitate which formed during the reaction) giving the material of high molecular weight.

Table 1. Polymerization of ethylene oxide by diphenylzinc in benzene at 60°C $(M_0/S=0\cdot1)$

$\dfrac{[M_0]}{[C_0]}$	Time, h	Yield, %	$[\eta]$ dl g^{-1}	$10^{-6}\overline{M}_v$
15	288	25	1·47	0·16
16	1080	24	1·76	0·21
22	288	15	1·25	0·13
22	1080	19	3·26	0·51
31	288	17	2·03	0·25
31	1080	15	4·52	0·82

Diphenylzinc forms a dietherate[2] with ethylene oxide, and the initial step in the polymerization thus probably involves the production of PhZnOCH$_2$CH$_2$Ph from which, as indicated[1] by proton magnetic resonance spectroscopy, polymer of the form PhZn(OCH$_2$CH$_2$)$_n$Ph can be built up by insertion, with ring-opening, of monomer units at the Zn—O bond. The efficiency of this process is likely to decrease as the concentration of PhZn(OCH$_2$CH$_2$)$_n$Ph increases, since aggregation[1,3,4] of these species to give less active products will become more significant, and, further, as the value of n increases, back-coordination from the oxygen atoms of the growing chain to the zinc atom will decrease the ease of coordination of monomer molecules, which is essential for the propagation steps. This would account for the fall-off in the production of low-molecular weight polymer. If insertion also occurred, even to a small extent, at the Ph—Zn bond of the species PhZn(OCH$_2$CH$_2$)$_n$Ph a zinc alkoxide Ph(CH$_2$CH$_2$O)$_m$Zn(OCH$_2$CH$_2$)$_n$Ph would be formed, and this, like the other zinc alkoxides previously studied[3,4], would be expected to form insoluble aggregates from which high-molecular weight polymer could be produced, probably by a process which would terminate only when all the monomer had been consumed; the high activity of insoluble zinc alkoxides has been noted previously[1].

Phenylzinc t-*butoxide*

Polymerization of ethylene oxide with phenylzinc *t*-butoxide ([M$_0$]/[C$_0$] = 117) for 63 hours at 5°C followed by 24 hours at 70°C gave a 73 per cent yield of polymer with $\overline{M}_v = 2\cdot5 \times 10^6$. Attempts to follow the polymerization dilatometrically at 25°C using [M$_0$]/[C$_0$] = 770 gave irreproducible results, possibly due to separation of solid material during the polymerization; the molecular weight of the product increased in parallel with the conversion (e.g. after 10h, yield 0·6 per cent, $\overline{M}_v = 0\cdot24 \times 10^6$; after 240h, yield 2·7 per cent, $\overline{M}_v = 1\cdot2 \times 10^6$). Subsequent polymerizations were therefore carried out at higher temperatures in order to achieve more rapid conversion, and kinetic studies were not attempted; representative results are shown in

Table 2. They indicate that almost quantitative polymerization can be achieved, and that the viscosity-average molecular weight usually increases with conversion. For benzene solutions, the rate of conversion and the molecular weight are both higher than those obtained with diphenylzinc. There are no striking solvent effects.

Table 2. Polymerization of ethylene oxide by phenylzinc *t*-butoxide

Solvent	$\dfrac{[M_0]}{[C_0]}$	$\dfrac{M_0}{S}$	Temp., °C	Time, h	Yield, %	$[\eta]$ dl g^{-1}	$10^{-6}\overline{M}_v$
None	778	—	70	90	15	5·01	0·95
None	778	—	70	768	99	10·58	2·83
Dioxan	227	0·2	70	90	24	7·45	1·70
Dioxan	227	0·2	70	768	77	16·60	5·45
CH$_2$Cl$_2$	307	0·1	60	63	3	4·39	0·79
CH$_2$Cl$_2$	309	0·1	60	528	13	13·20	3·91
PhH	15	0·1	60	29	6	11·10	3·03
PhH	22	0·1	60	29	7	15·74	5·05
PhH	31	0·1	60	29	8	12·37	3·17
None	770	—	60	48	7	4·72	0·87
None	770	—	60	97	11	4·87	0·91
None	770	—	60	336	37	7·73	1·79

Fractionation of the polymer from the first experiment quoted in *Table 2* gave the results shown in *Table 3*, which indicate the presence of a large proportion of material of comparatively low molecular weight; fraction 4 was the material remaining in solution at 19°C.

Table 3. Fractionation of poly(ethylene oxide)

Fraction	Precipitation point, °C	Yield of fraction, %	$[\eta]$ dl g^{-1}
1	36	44	8·75
2	26	34	2·02
3	19	11	0·93
4	—	11	—

The initial step in the polymerization could involve insertion of an ethylene oxide unit into either the Zn—O or the Ph—Zn bond of the catalyst, for simplicity now represented as the monomer PhZnOBu^t. If the former occurs, and is successively repeated, a polymer PhZn(OCH$_2$CH$_2$)$_n$OBu^t will be produced, and, as the chain grows, the influence of the *t*-butoxyl group on the environment of the zinc will progressively decrease. It would therefore be expected that after a few monomer units had been inserted the species would become catalytically comparable with the compound PhZn(OCH$_2$CH$_2$)$_n$Ph postulated as an intermediate in the polymerization induced by diphenylzinc. This is not so: phenylzinc *t*-butoxide is considerably more effective[1] than diphenylzinc. Insertion at the Ph—Zn bond to give the mixed alkoxide PhCH$_2$CH$_2$OZnOBu^t might therefore be significant. This species may aggregate, or disproportionate to aggregates of the corresponding simple alkoxides: all would be heterogeneous catalysts, but of

different activities, and this could account for the broad distribution of molecular weights found for the high polymer, although transfer reactions may also be involved. Support for the presence of at least some chains containing phenyl end-groups was obtained from the proton magnetic resonance spectrum of a low-molecular weight fraction of the first polymer listed in *Table 2* which showed, for a 12 per cent solution in hexadeuterobenzene, a weak absorption at τ 2·54.

In view of the large number of potentially catalytic species which may be formed in reactions of this type, it is unwise to draw from the evidence so far available firm conclusions about the mechanism of polymerization induced by diphenylzinc and phenylzinc t-butoxide, but it may be significant that both catalysts soon yield heterogeneous systems which could be responsible for the production of high polymer, and which may be related to the dialkoxide discussed in the following section.

Zinc t-*butoxide*

This catalyst is insoluble in all the systems used. Polymerization of undiluted ethylene oxide occurred more rapidly than with phenylzinc t-butoxide, and gave products with $\bar{M}_v$ in the range 4×10^6 to 9×10^6; the polymer appeared to grow from the surface of the catalyst. Typical results for agitated systems are given in *Table 4*; for experiment 7 the catalyst was soaked in THP for 40 hours before addition of the monomer.

Table 4. Polymerization of ethylene oxide by zinc t-butoxide at 60°C ($[M_0]/[C_0]=200$)

Expt no.	Solvent	$\dfrac{M_0}{S}$	Time, h	Yield %	$[\eta]$ $dl\ g^{-1}$	$10^{-6}\,\bar{M}_v$
1	None	—	8	5	10·26	2·7
2	None	—	24	17	19·70	7·0
3	PhH	0·1	8	2	5·17	1·0
4	PhH	1·0	24	23	19·40	6·9
5	C_6H_{12}	1·0	24	27	15·65	5·0
6	THP	1·0	24	18	13·63	4·1
7	THP	1·0	24	10	16·40	5·4
8	Bu^{t}OH	1·0	24	3	0·23	0·01
9	Bu^{t}OH	1·0	720	41	0·33	0·03

Polymerizations in benzene and cyclohexane gave higher yields than those obtained with the undiluted monomer, possibly because in the absence of diluents the mixture soon gelled, whereas in their presence it remained mobile for a longer time. The reaction may involve adsorption of monomer at active sites (e.g. defects in the t-butoxide lattice) on the catalyst, followed by ring-opening with concomitant transfer of a t-butoxyl group to give a new alkoxide system, $-ZnOCH_2CH_2OBu^t$, from which polymer can be produced by repetitive insertion of monomer at Zn—O bonds. An alternative mechanism would involve oxonium ions[5], and may occur together with the insertion mechanism. The yield from experiment 6, in which THP and ethylene oxide were added to the catalyst at almost the same time, is similar to that obtained from the undiluted monomer, but the yield from experiment 7, in which the catalyst was first soaked in THP, is lower, possibly

due to slow solvation of some of the more active sites on the catalyst to give 'complexes' from which the THP is not subsequently readily displaced by ethylene oxide; the remaining sites may produce higher-molecular weight polymer (a similar, but more pronounced effect has been observed[9] for polymerizations catalysed by zinc methoxide). The proton magnetic resonance spectrum of the polymer did not indicate the incorporation of THP residues.

The effect of t-butyl alcohol was more striking, causing significant reduction in both yield and molecular weight, possibly due to solvation of active sites, and to termination reactions which regenerate the catalyst, e.g.

$$Bu^t-O \cdots Zn \cdots O-Bu^t \;/\; Bu^t-O \cdots Zn \cdots (OCH_2CH_2)_nOBu^t,\, H \longrightarrow Bu^t-O \cdots Zn \cdots O-Bu^t \;/\; Bu^t-O \cdots Zn + H(OCH_2CH_2)_nOBu^t$$
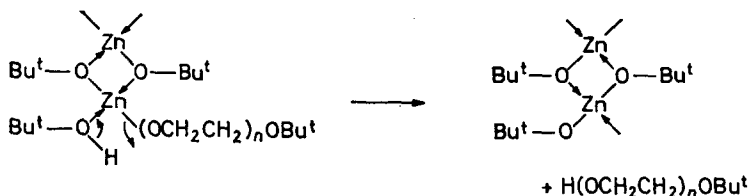
Such a process is supported by the proton magnetic resonance spectra of the products which, for five per cent solutions in benzene, both showed a singlet at τ 8·85 due to t-butoxyl groups, and a strong singlet at τ 6·45 accompanied by two minor ones at 6·53 and 6·59 attributable to the polymer backbone; for the products from experiments 8 and 9 the ratios of the intensities of the resonances at τ 8·85 to the total intensities of the resonances in the τ 6·4 to 6·6 region were, respectively, 1:3·0 and 1:3·4. The latter ratio implies a number-average degree of polymerization of 7·6, in good agreement with the value of 7·4 calculated from the number-average molecular weight (401) of the polymer.

A similar series of experiments was carried out with propylene oxide, giving the results shown in *Table 5*.

Table 5. Polymerization of propylene oxide by zinc t-butoxide at 60°C
($[M_0]/[C_0]=200$; $M_0/S=1\cdot0$)

Expt. no.	Solvent	Time, h	Yield %	$[\eta]$ dl/g^{-1}	$10^{-6}\overline{M}_v$	Fraction of total product insoluble in MeOH at 0°C Yield %	M. pt °C
1	None	120	4	6·50	1·7	10	65·0
2	None	480	12	6·35	1·5	12	68·5
3	PhH	120	4	9·55	2·5	12	65·5
4	C_8H_{12}	120	5	10·32	2·8	12	65·0
5	C_8H_{12}	480	10	6·35	1·5	11	66·5
6	THP	120	4	8·07	2·0	8	71·5
7	Bu*t*OH	120	0·1	—	—	—	—
8	Bu*t*OH	720	1·2	0·31	0·03	—	—

Polymerization was slower than for ethylene oxide, and the polymers had lower molecular weights. The solvent had little effect except with t-butyl

alcohol when, as with ethylene oxide, there was a signficant lowering of both yield and molecular weight; the proton magnetic resonance spectrum of a solution (five per cent in carbon tetrachloride) of the poly(propylene oxide) from experiment 8 showed a singlet at τ 8·86 due to t-butoxyl groups, a doublet ($J = 6$ c/sec) centred at τ 8·86 due to the methyl groups of the repeating unit, and a multiplet at τ 6·63 arising from the protons in the polymer backbone, with relative intensities indicating a number-average degree of polymerization of 6·0.

Fractionations from methanol of the poly(propylene oxide) samples obtained from experiments 1 to 6 indicated that they contained 8 to 12 per cent of 'crystalline' polymer. Further fractionation[8], from isooctane, of the methanol-soluble portions from experiments 2 and 5 revealed a large proportion of low polymer similar to that obtained[8] with the diethylzinc–water system. The 'crystalline' material with the highest melting point (*Table 5*) was obtained when THP was the solvent, possibly because the most stereoregular polymer[10] is formed, probably by an insertion mechanism, at sites on the catalyst which are the least susceptible to solvation by THP (cf. the effect of THP on the polymerization of ethylene oxide). This observation suggests the possibility of controlling the stereoregularity of poly(propylene oxide) by selective solvation of heterogeneous catalysts; further studies are in progress.

Isobutylene oxide gave only one to two per cent yields of polymer when treated with zinc t-butoxide ($[M_0]/[C_0] = 200$ or 100, 960 hours at 60°C). Steric factors in the monomer thus probably play a dominant role in governing the overall rate of polymerization: propylene oxide is polymerized less rapidly than ethylene oxide, and isobutylene oxide much less rapidly than propylene oxide. A similar, but, for ethylene oxide and propylene oxide, less marked, effect has been observed[5] for polymerizations catalysed by the diethylzinc–water system.

Department of Chemistry,
  The University, Manchester 13

REFERENCES

[1] BRUCE, J. M. and FARREN, D. W. *Polymer, Lond.* 1965, **6,** 509

[2] ALLEN, G., BRUCE, J. M. and HUTCHINSON, F. G. *J. chem. Soc.* **1965,** 5476

[3] BRUCE, J. M., CUTSFORTH, B. C., FARREN, D. W., HUTCHINSON, F. G., RABAGLIATI, F. M. and REED, D. R. *J. chem. Soc. (B),* **1966,** 1020

[4] ALLEN, G., BRUCE, J. M., FARREN, D. W. and HUTCHINSON, F. G. *J. chem. Soc. (B),* **1966,** 799

[5] BRUCE, J. M. and HURST, S. J. *Polymer, Lond.* 1966, **7,** 1, and references therein

[6] BOOTH, C. and PRICE, C. *Polymer, Lond.* 1966, **7,** 85

[7] ALLEN, G., BOOTH, C. and JONES, M. N. *Polymer, Lond.* 1964, **5,** 195

[8] BOOTH, C., HIGGINSON, W. C. E. and POWELL, E. *Polymer, Lond.* 1964, **5,** 479

[9] BRUCE, J. M. and CUTSFORTH, B. C. Unpublished work

[10] ALLEN, G., BOOTH, C., JONES, M. N., MARKS, D. J. and TAYLOR, W. D. *Polymer, Lond.* 1964, **5,** 547

Mechanical History Effects in the Crystallization of cis-1,4-Polybutadiene

J. C. MITCHELL

Dilatometric studies have revealed alterations in the crystallization kinetics of cis-1,4-polybutadiene subjected to the shearing action of a laboratory mill. Reduction in the Avrami exponent by more than one unit suggests that, in addition to a change from pseudo-homogeneous to instantaneous nucleation, a change in the growth mechanism of the new phase is involved. These changes are presumed to be brought about either by sub-optical microscopic ordering of the amorphous polymer (e.g. the 'quasi-indestructible' clusters proposed by Rabesiaka and Kovacs) or by shear effects on impurity constituents, with either effect leading to row orientation.

DILATOMETRIC measurement of the volume contraction during isothermal crystallization of *cis*-1,4-polybutadiene has shown that the crystallization kinetics are sensitive to the mechanical history of the sample. These results are similar to the observations of Rabesiaka and Kovacs[1] on polyethylene. These authors postulated that mechanical forces can generate 'quasi-indestructible' clusters in the polymer which survive well above the melting point and serve as especially active heterogeneous nuclei in the crystallization process.

EXPERIMENTAL

The studies reported here were all carried out on one particular experimental sample of *cis*-1,4-polybutadiene. This sample is typical of a series of such polymers prepared at the Shell Development Company Emeryville Research Center using cobaltous chloride/aluminium alkyl catalysis. Infra-red (i.r.) spectra showed these polymers to contain approximately 97 to 98 per cent *cis*-1,4 structural units. Their number and weight average molecular weights were around 100 000 and 220 000, respectively. Similar mechanical history effects were also observed in the crystallization kinetics of other samples of this type.

Standard mercury-filled glass dilatometers were used with a Hallikainen Industrial Calibration bath* which provided temperature regulation to ± 0.02 deg. C. Unless otherwise noted, immediately prior to crystallization kinetics determination, the samples (degassed and under mercury) were heated to 100°C for 40 minutes, then allowed to cool to room temperature.

Analysis of dilatometric data

Crystallization kinetics curves were characterized in terms of half-times, $t_{1/2}$, and Avrami exponents, n. Because of a relatively large extent of secondary crystallization in this polymer, half-times for the primary crystallization process have been estimated by the following somewhat arbitrary expedient. The extent of contraction reached on attainment of an

---

*Hallikainen Instruments, Berkeley, California, U.S.A.

arbitrary slow rate of secondary crystallization was taken as corresponding to the completion of primary crystallization. Having observed that this quantity showed a variation of only a few per cent in 40 different samples of the present type, the average value of 6.36×10^{-2} ml/g was taken as a 'standard' contraction for primary crystallization at $-16°C$. Half-times were taken as the time required for the attainment of one-half of this standard contraction. The Avrami exponent, n, is the exponent of time in the equation[2, 3]

$$\ln \theta = - Kt^n \qquad (1)$$

where θ is the weight fraction[3] of the polymer untransformed at time t, and K is a rate constant. It was evaluated from the experimental data according to the following equation

$$n = 0.718 / \log (t_{1/2}/t_{1/8}) \qquad (2)$$

where $t_{1/8}$ is the time required for one-eighth of the standard contraction defined above. This relationship follows directly from the Avrami equation (1) on substituting $\theta = 1/2$ at $t = t_{1/2}$ and $\theta = 7/8$ at $t = t_{1/8}$. Avrami exponents evaluated in this simple manner were found to agree with those calculated using a curve-fitting computer programme to within a few tenths of a unit. This agreement is within the experimental reproducibility. Considering the complications inherent in the application of the Avrami theory to crystallizing polymers[4–13], this uncertainty is probably also well within the limits of straightforward interpretation.

In melting experiments, dilatometer data were converted to specific volumes following the general procedure given by Bekkedahl[14]. This calls for additional measurements: sample density (gradient column used), dilatometer capillary level at the temperature of density determination, and weight of mercury confining liquid. An IBM 7040 programme was written for making the calculations and plotting specific volume versus temperature. A similar programme was used to convert some of the crystallization kinetics data to specific volume versus time plots.

GENERATION OF MECHANICAL HISTORY

The crystallization kinetics of *cis*-1,4-polybutadiene are sensitive to shear forces. While such effects have been seen in samples subjected to extrusion, the present experiments involve the use of a laboratory rubber mill. In this mill the rubber is passed between two 6-in. rollers rotating at 39.8 and 55.6 ft/min, respectively. In one set of experiments the effect of varying the roller separation was studied. With the rollers heated by water at $70°C$, portions of the baled but previously unmilled *cis*-1,4-polybutadiene sample were passed continuously through the mill in the same direction for five minutes, then subjected to ten individual passes in alternate 90° directions. In *Figure 1* the half-time and Avrami exponents for crystallization at $-16°C$ are plotted against roller separation. Both of these quantities are seen to decrease continuously as roller separation decreases or as shearing stresses increase.

The effect of variations in milling technique was then studied using a roller separation of 0·020 in. The previous procedure was separated into its two parts, continuous passage in the same direction ('banding') and individual passes. It was found that either of these alone had the same effectiveness in reducing half-times. Five minutes of continuous passage reduced the half-time at −16°C from 50 min to 28 min. Ten separate passes through the mill had the same effect whether or not the material was rotated 90° between passes (half-times of 26 and 28 min, respectively).
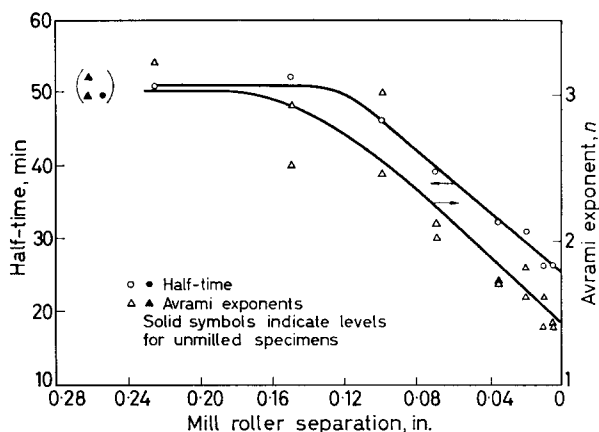
Figure 1—Crystallization half-times and Avrami exponents as a function of mill roller separation

On varying the temperature of the mill a peculiar but reproducible temperature dependence of mechanical history generation was observed. This is shown in *Figure 2* where the ratio of the half-time to the one-eighth time
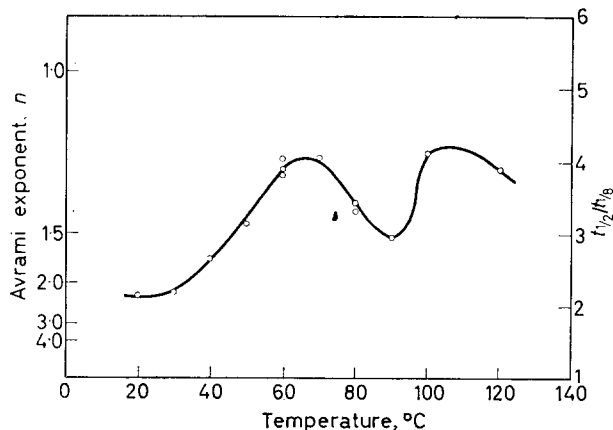
Figure 2—Effect of milling temperature on Avrami exponent for samples milled with a roller separation of 0·020 inch

371

for samples milled with a roller separation of 0·020 in. is plotted against mill temperature. The complicated temperature dependence presumably originates in the interaction of the temperature dependences of chain mobility and stress-induced crystallization, and the occurrence of a known transition affecting rheological behaviour[15-18]. The dip in the mechanical history/temperature curve starts in the region of the transition.

PERSISTENCE OF MECHANICAL HISTORY

Inasmuch as the mechanical history apparently survives our customary heat treatment of 40 minutes at 100°C prior to crystallization kinetics studies, it may be termed 'quasi-indestructible'. The results of studies of higher temperature 40-minute preheating treatments are shown in *Figure 3*. Here
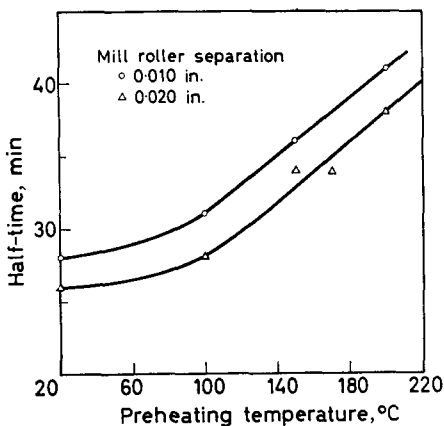
Figure 3—Effect of preheating temperature on crystallization half-time of milled specimens

the crystallization half-times of the samples milled with roller separation 0·020 in. and 0·010 in. referred to in *Figure 1* are plotted as a function of preheating temperature. It can be seen that temperatures well above 200°C would be required to restore half-time values to the 50-minute level characteristic of this sample in the absence of milling. While some of the observed decrease in crystallization rate may be caused by deterioration of the chain microstructure, it would appear that some mechanical history erasure takes place in higher temperature treatments inasmuch as increases in the Avrami exponent have also been observed in these samples.

The mechanical history generated by shearing is even less sensitive to storage at room temperature. Only slight relaxation has been observed after storage at room temperature for several months. Pertinent half-times and Avrami exponents are presented in *Table 1*.

Whatever the nature of the order generated by stress, one would expect it to be eliminated by solution of the polymer. The following technique has, correspondingly, been found to erase mechanical history.

The polymers were dissolved to six per cent concentration in aluminium foil-covered bottles which were gently agitated overnight. The solvent was usually benzene. The solutions were vacuum evaporated for two to three days at room temperature on sheet Teflon. A dry nitrogen bleed was used

during the last few hours to complete the drying. The resulting films were gently rolled off the Teflon. The rubber's adhesion to Teflon is sufficiently low that no large stresses were required to separate the samples from the Teflon. The resulting films ranged from one-half to three millimetres in

Table 1. Effect of room temperature storage on mechanical history effect

Mill roller separation, in.	Initial values		After 2 months		After 6 months	
	Half-time −16°C, min	n	Half-time −16°C, min	n	Half-time −16°C, min	n
(unmilled)	50	3·1	49	3·2	53	3·5
0·225	51	3·2	56	2·9	54	3·2
0·150	52	2·5	49	2·3	49	3·3
0·100	46	2·4	44	2·7	45	2·1
0·070	39	2·0	40	2·0	41	1·9
0·035	32	1·7	32	1·5	36	1·6
0·020	31	1·6	34	1·8	34	1·7
0·010	27	1·6	36	2·1	34	1·8
0·005	27	1·4	32	—	29	1·7

thickness. Chromatographic analysis of samples so prepared showed them to contain less than 0·01 per cent residual benzene.

In *Table 2* half-times and Avrami exponents, n, are presented for polymers of various mechanical history following their recovery from solution in the manner discussed above. The half-times are slightly higher than that of the original unmilled specimen and the Avrami exponents run from somewhat below 4 to the anomalous value of 5. Current evaluations[6–13] of the application of Avrami's analysis of phase change to polymer crystallization predict lowering of the exponent to non-integer values below 4. Higher values would require a nucleation or growth rate increasing with time. The fact that the unmilled specimen showed an Avrami exponent close to 3 before solution and recovery suggests that it had mechanical history as received—presumably from the baling operation.

ADDITIONAL COMPARISONS

With the above work as background, three specimens of *cis*-1,4-polybutadiene were taken as representative of their type for detailed comparisons as presented below. They are designated C, M and MD, referring, respectively, to the untreated control, a milled portion, and a portion recovered by solvent evaporation from benzene solution after milling. The milling was carried out with a water temperature of 70°C. There were six passes at roller separation 0·005 in., four at 0·010 in., and two at 0·0075 in.

Crystallization process

Isothermal crystallization kinetics were studied dilatometrically over the range of temperatures from −29·9° to −10·1°C. Changes in specific volume were plotted against the logarithm of time. For this purpose extrapolated values from the liquidus curves determined for the polymers in melting point experiments were taken as the equilibrium specific volumes

Table 2. Effect of solution and recovery on crystallization kinetics

History			Half-time, min	n
As received			50	3·1
Dissolved and recovered				
	Unmilled specimens		57	4·2
			61	4·7
			60	4·9
			55	3·9
			56	4·9
	Milled specimens			
	Mill temp., °C	Roller separation, in.		
	70	0·150	57	3·7
	70	0·100	59	3·6
	70	0·070	60	—
	70	0·035	64	3·7
	70	0·020	66	4·1
	70	0·010	63	4·2
	20	0·020	65	5·1
	40	0·020	67	5·3
	60	0·020	64	4·5
	60	0·020	59	3·7
	80	0·020	66	3·9
	100	0·020	65	4·2
	120	0·020	61	5·0

before any crystallization took place. This procedure bypasses some of the difficulty associated with the lack of thermal equilibration of the dilatometer during the early portions of the faster crystallizations. Thus while early points can still be in error from this source, later points are still referenced to the correct starting value.

It was found that the kinetics curves so determined were superposable by shifts in log time as is commonly observed[3]. *Figure 4* shows the superposition of kinetics curves obtained at $-24\cdot0°$, $-21\cdot5°$, $-18\cdot0°$, $-16\cdot0°$, $-13\cdot9°$ and $-12\cdot0°C$. Such superposition, while a necessary consequence of the Avrami equation, is a more general phenomenon inasmuch as it still occurs where the Avrami equation does not describe the kinetics data. It is especially interesting to note that the same shift factor 'a', where log a is the shift in log time required to superpose one curve on another, is applicable to the three samples. This is shown in *Figure 5* where a for superposition on the $-16°C$ curves is plotted against temperature. These shifts correspond to a spread of half-times from two minutes at the lowest temperature to 700 minutes at the highest temperature. In any case, the temperature dependence of the primary crystallization rate appears to be unaffected by mechanical history.

Also unaffected by mechanical history are the extent of primary crystallization as measured by the level of the kinetics curve in the region of secondary crystallization (where the volume change has become linear in log t) and the rate of secondary crystallization as measured by the slope
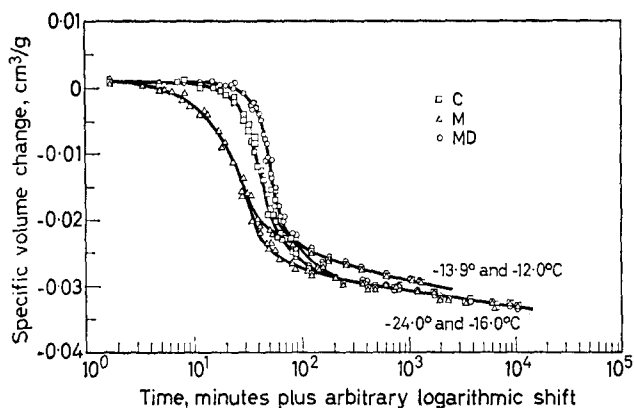
Figure 4—Superposed crystallization kinetics data, −24·0°C to −12·0°C

in this region. The only change in these properties observed over the whole series is that the specific volume changes above −16°C are somewhat less than those at −16°C and below. If the thermal expansion coefficient for the crystalline phase is lower than that of the amorphous phase, this indicates a decrease in extent of crystallization at higher temperatures.

Melting behaviour

Identical melting points have been observed[19] in a series of three samples with mechanical history essentially the same as that of the present series (i.e. control, milled, and milled and then recovered from solution). Melting
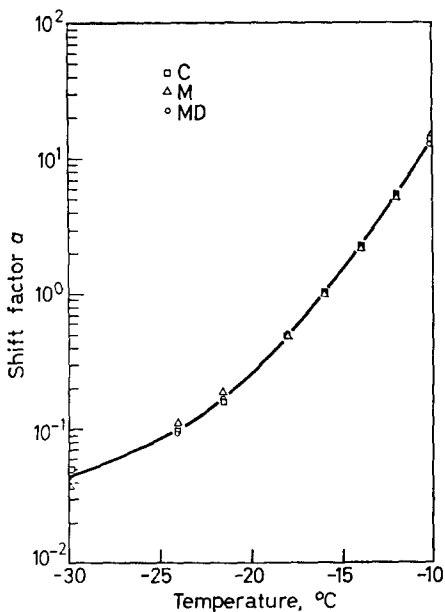
Figure 5—Temperature dependence of shift factor for superposition of crys-tallization kinetics data on −16°C curves

curves for the present series are shown in *Figures 6* and *7*. In these experiments a smooth temperature rise over the 24-hour day was brought about
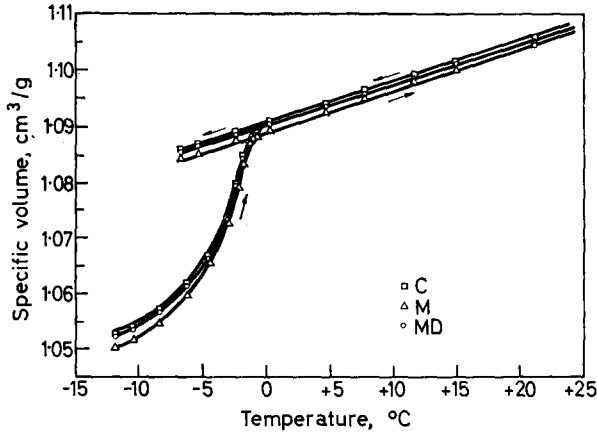
Figure 6—Melting curves for samples of varying mechanical
history—fast heating

through the use of a clock motor drive on the thermostat bath temperature controller. In *Figure 6* the heating rate was 7 deg. C/h throughout. Cooling was at 4·4 deg. C/h. In *Figure 7* the heating rate was 7 deg. C/h from −16° to −14·5°, then 2·1 deg. C/day from −14·5° to −8·0°, 1·2 deg. C/day from −8·0° to +8·0°, and finally 7 deg. C/h. Subsequently, the two experiments will be referred to as 'fast heating' (7 deg. C/h) and 'slow heating' (1·2 deg. C/day).

In both cases it will be noted that not only are the melting points the same for the three samples in each experiment, −0·2° in fast heating and +6·0° in slow heating (±0·2 deg. in both cases), but the melting curves are parallel. Their slight relative displacements originate in the density deter-
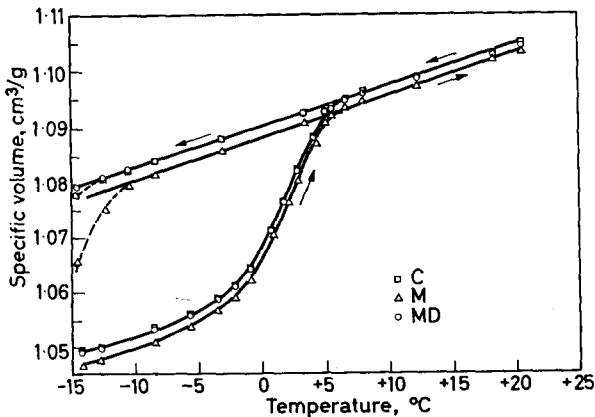
Figure 7—Melting curves for samples of varying mechanical
history—slow heating

minations at 25 °C. The sample is apparently slightly more dense after milling.

Microscope investigations

Microtome sections of the three samples, C, M and MD, were prepared at liquid nitrogen temperature. These were examined at room temperature under both polarizing and phase contrast optics. Neither technique revealed any organization of the 'amorphous' polymer on the optical microscope scale for all three samples.

DISCUSSION

The exponent n in the Avrami equation is determined by the time dependence of the nucleation and growth processes applicable to the phase transformation under study. The differences in n values observed in these studies between solution cast samples and those subjected to shear forces was often greater than one. A simple change from nuclei appearing at a constant rate in time (pseudohomogeneous nucleation) to nuclei essentially preformed by the shearing forces would cause a lowering in n of only one unit. Thus it seems necessary to assume that the time exponent describing the growth process is lowered as well. This could conceivably come about for any of the following reasons: (1) any deviation from isotropic (i.e. spherulitic) growth, (2) a change in the density decrease of spherulites during their growth, (3) an increase in the relative importance of secondary crystallization proceeding simultaneously with the primary process[10-12], and (4) a greater slowing down of the growth rate due to increased competition for inter-spherulitic amorphous material[9]. Of these, the first, directed growth, seems most likely. The decrease in density referred to in case (2) is expected on the basis of Keith and Padden's[20] model for spherulite growth, according to which impurities excluded from the crystalline phase would accumulate, restricting the conversion of amorphous material in the later stages of a spherulite's growth. This effect would lead to fractional Avrami exponents, but it would not seem a likely cause of a change in the exponent on shearing as this would require a change in the amount or nature of material being excluded by the growing crystalline phase. Such a change appears highly unlikely in view of the return to high n values after solution and recovery of the polymer. Furthermore, such changes might lead to structural differences on the lamellar level. Such differences would be quite likely for case (3). However, in the melting experiments, both slow and fast heating rates showed parallel changes in specific volume with the temperature throughout the melting range for the three types of specimens, indicating no large differences in crystalline structure at the level of lamellar dimensions. Case (3) also seems unlikely as the relationship of primary and secondary crystallization does not seem greatly altered as evidenced by the coincidence of the later regions of the crystallization kinetics curves. The secondary process observed after completion of the primary process appears unaffected, as does the extent of primary crystallization. The competitive effect (4) should not be noticeable at the beginning of the transformation, whereas the low n value is evident very early in the experimental curves.

Directed growth would be expected in material oriented in the manner of

377

a stretched elastomeric network. Gent[21] has observed decreases of n from 3 to 1 for crystallization in natural rubber as the elongation was increased. The increased orientation was presumed to change the growth morphology from spherulitic to needle-like. The present microscope observations show no regions of orientation in sheared polybutadiene samples on an optical scale.

Even in the absence of such overall orientation, directed growth and enhanced nucleation would go hand-in-hand if centres for rapid nucleation generated by the shear field were at the same time densely distributed along lines (presumably in the shear direction). If these nucleation sites are sufficiently active, primary nuclei (growth centres) would appear to be present in large numbers at the beginning of the transformation, leading to a unit decrease in the Avrami exponent. An additional decrease would then result from row orientation[22-24] as the large numbers of spherulites originating along lines would soon merge into cylindrical objects ('cylindralites') capable of further growth in only two dimensions.

The active nucleation sites distributed along lines could result from polymer ordering or from sheared impurities. While no overall orientation has been observed in our samples, this does not preclude organization on the electron microscope scale. Kargin et al.[25,26] have reported electron microscope observations of organization of 'amorphous' polymer into bundles. On the other hand, the experiments of Cormia, Price and Turnbull[27] suggest that most polymer crystal nucleation is heterogeneous. (It should be noted that heterogeneous nuclei can readily lead to nucleation proportional to time—in Avrami's terminology, 'germ' nuclei can be converted to 'growth' nuclei at a constant rate. Such a process is commonly referred to as pseudo-homogeneous nucleation.) It is conceivable that shear forces transmitted by the polymer to impurity particles serving as heterogeneous nuclei lead to the exposure of new surfaces and hence to increased nucleating activity. This sheared heterogeneous nuclei explanation seems more attractive than the ordered polymer explanation in view of the quasi-indestructible nature of the mechanical history effect.

Shell Development Company,
A Division of Shell Oil Company,
Emeryville, California

REFERENCES

[1] RABESIAKA, J. and KOVACS, A. J. *J. appl. Phys.* 1961, **32**, 2314
[2] AVRAMI, M. *J. chem. Phys.* 1939, **7**, 1103; 1940, **8**, 212
[3] MANDELKERN, L. in *Growth and Perfection of Crystals*, DOREMUS, R. H., ROBERTS, B. W. and TURNBULL, D. (eds.). Wiley: New York, 1958
[4] SHARPLES, A. and SWINTON, F. L. *Polymer, Lond.* 1963, **4**, 119

[5] BANKS, W., GORDON, M., ROE, R.-J. and SHARPLES, A. *Polymer, Lond.* 1963, **4,** 61

[6] BANKS, W. and SHARPLES, A. *Makromol. Chem.* 1963, **59,** 233

[7] GORDON, M. and HILLIER, I. H. *Trans. Faraday Soc.* 1964, **60,** 763

[8] GORDON, M. and HILLIER, I. H. *Polymer, Lond.* 1965, **6,** 213

[9] ROE, R.-J. and KRIGBAUM, W. R. *Polymer, Lond.* 1965, **6,** 231

[10] HOSHINO, S., MEINECKE, E., POWERS, J., STEIN, R. S. and NEWMAN, S. *J. Polym. Sci. A,* 1965, **3,** 3041

[11] HILLIER, I. H. *J. Polym. Sci. A,* 1965, **3,** 3067

[12] PRICE, F. P. *J. Polym. Sci. A,* 1965, **3,** 3079

[13] PRICE, F. P. *J. appl. Phys.* 1965, **36,** 3014

[14] BEKKEDAHL, N. *J. Res. Nat. Bur. Stand.* 1949, **42,** 145

[15] BULGIN, D. Paper presented at International Synthetic Rubber Symposium, Westminster, October 1960; Abstract in *Rubber and Plastics Age,* 1960, **41,** 1360

[16] GARLANDA, T. *Chim. e Industr.* 1961, **43,** 368

[17] BIANCHI, U. and BIANCHI, E. *Chim. e Industr.* 1963, **45,** 657

[18] PEDEMONTE, E. and BIANCHI, U. *Chim. e Industr.* 1964, **46,** 1455

[19] MITCHELL, J. C. *J. Polym. Sci. B,* 1963, **1,** 285 (also appeared in *Rubb. Chem. Technol.* 1965, **38,** 921)

[20] KEITH, H. D. and PADDEN, F. J. *J. appl. Phys.* 1963, **34,** 2409

[21] GENT, A. N. *Trans. Faraday Soc.* 1954, **50,** 521

[22] VONK, C. G. *Kolloidzschr.* 1965, **206,** 121

[23] MAXWELL, B., GOGOS, C. G., BLYLER Jr, L. L. and MINEO, R. M. *S.P.E. Jnl,* 1964, **4,** 3

MAXWELL, B. *J. Polym. Sci. C,* 1965, **9,** 43

[24] BINSBERGEN, F. L. *Nature, Lond.* In press

[25] KARGIN, V. A., KITAIGORODSKII, A. I. and SLONIMSKII, G. L. *Kolloid Zh.* 1957, **19,** 133

[26] KARGIN, V. A., BAKEEV, N. F. and VERGIN, K. H. *Proc. Acad. Sci., U.S.S.R., Phys. Chem. Sect.* 1958, **122,** 627

[27] CORMIA, R. L., PRICE, F. P. and TURNBULL, D. *J. chem. Phys.* 1962, **37,** 1333

Communication

A Table of Fikentscher K Values versus Relative Viscosities for a Concentration of 1·0

IN WORKING with poly(vinylchloride), correlation of our solution viscosity measurements with Fikentscher K values which are used by European manufacturers has been useful. The tedium involved in the calculations and the lack of readily available tables inspired the writing of a computer programme to supply a list of such values. The data in *Table 1* are solutions to the Fikentscher equation [FIKENTSCHER, H. *Cellulose Chemie*, 1932, **13**, 58]

$$\log \eta_{rel} = \{75k^2/(1+1\cdot5\,kc)+k\}\,c$$

where $K = 1\,000\,k$ for a concentration of $1\cdot0\,g/100\,ml$ of solution. Such a listing is general in the sense that it may be applied regardless of the polymer, solvent or temperature used; it is important, however, that data on the solvent, temperature and concentration used for the measurements in question be included when reporting results.

Table 1. Calculation of relative viscosities from Fikentscher K values for a given concentration

Concentration: $1\cdot0\,g/100\,ml$

K	Rel. visc.	K	Rel. visc.	K	Rel. visc.	K	Rel. visc.	K	Rel. visc.
0·1	1·000	3·5	1·010	6·9	1·024	10·3	1·043	13·7	1·065
0·2	1·000	3·6	1·011	7·0	1·025	10·4	1·043	13·8	1·066
0·3	1·001	3·7	1·011	7·1	1·025	10·5	1·044	13·9	1·067
0·4	1·001	3·8	1·011	7·2	1·026	10·6	1·044	14·0	1·068
0·5	1·001	3·9	1·012	7·3	1·026	10·7	1·045	14·1	1·068
0·6	1·001	4·0	1·012	7·4	1·027	10·8	1·046	14·2	1·069
0·7	1·002	4·1	1·012	7·5	1·027	10·9	1·046	14·3	1·070
0·8	1·002	4·2	1·013	7·6	1·028	11·0	1·047	14·4	1·071
0·9	1·002	4·3	1·013	7·7	1·028	11·1	1·048	14·5	1·071
1·0	1·002	4·4	1·014	7·8	1·029	11·2	1·048	14·6	1·072
1·1	1·003	4·5	1·014	7·9	1·029	11·3	1·049	14·7	1·073
1·2	1·003	4·6	1·014	8·0	1·030	11·4	1·050	14·8	1·074
1·3	1·003	4·7	1·015	8·1	1·030	11·5	1·050	14·9	1·074
1·4	1·004	4·8	1·015	8·2	1·031	11·6	1·051	15·0	1·075
1·5	1·004	4·9	1·016	8·3	1·031	11·7	1·051	15·1	1·076
1·6	1·004	5·0	1·016	8·4	1·032	11·8	1·052	15·2	1·077
1·7	1·004	5·1	1·016	8·5	1·032	11·9	1·053	15·3	1·078
1·8	1·005	5·2	1·017	8·6	1·033	12·0	1·053	15·4	1·078
1·9	1·005	5·3	1·017	8·7	1·033	12·1	1·054	15·5	1·079
2·0	1·005	5·4	1·018	8·8	1·034	12·2	1·055	15·6	1·080
2·1	1·006	5·5	1·018	8·9	1·035	12·3	1·055	15·7	1·081
2·2	1·006	5·6	1·018	9·0	1·035	12·4	1·056	15·8	1·082
2·3	1·006	5·7	1·019	9·1	1·036	12·5	1·057	15·9	1·082
2·4	1·007	5·8	1·019	9·2	1·036	12·6	1·058	16·0	1·083
2·5	1·007	5·9	1·020	9·3	1·037	12·7	1·058	16·1	1·084
2·6	1·007	6·0	1·020	9·4	1·037	12·8	1·059	16·2	1·085
2·7	1·008	6·1	1·021	9·5	1·038	12·9	1·060	16·3	1·086
2·8	1·008	6·2	1·021	9·6	1·039	13·0	1·060	16·4	1·087
2·9	1·008	6·3	1·022	9·7	1·039	13·1	1·061	16·5	1·088
3·0	1·008	6·4	1·022	9·8	1·040	13·2	1·062	16·6	1·088
3·1	1·009	6·5	1·022	9·9	1·040	13·3	1·062	16·7	1·089
3·2	1·009	6·6	1·023	10·0	1·041	13·4	1·063	16·8	1·090
3·3	1·010	6·7	1·023	10·1	1·041	13·5	1·064	16·9	1·091
3·4	1·010	6·8	1·024	10·2	1·042	13·6	1·065	17·0	1·092

K	Rel. visc.	K	Rel. visc.	K	Rel. visc.	K	Rel. visc.	K	Rel. visc.
17·1	1·093	25·6	1·183	34·1	1·309	42·6	1·481	51·1	1·710
17·2	1·094	25·7	1·184	34·2	1·311	42·7	1·483	51·2	1·713
17·3	1·094	25·8	1·185	34·3	1·313	42·8	1·486	51·3	1·716
17·4	1·095	25·9	1·187	34·4	1·315	42·9	1·488	51·4	1·720
17·5	1·096	26·0	1·188	34·5	1·316	43·0	1·490	51·5	1·723
17·6	1·097	26·1	1·189	34·6	1·318	43·1	1·493	51·6	1·726
17·7	1·098	26·2	1·191	34·7	1·320	43·2	1·495	51·7	1·729
17·8	1·099	26·3	1·192	34·8	1·322	43·3	1·498	51·8	1·732
17·9	1·100	26·4	1·193	34·9	1·324	43·4	1·500	51·9	1·735
18·0	1·101	26·5	1·194	35·0	1·325	43·5	1·502	52·0	1·738
18·1	1·102	26·6	1·196	35·1	1·327	43·6	1·505	52·1	1·742
18·2	1·103	26·7	1·197	35·2	1·329	43·7	1·507	52·2	1·745
18·3	1·103	26·8	1·198	35·3	1·331	43·8	1·510	52·3	1·748
18·4	1·104	26·9	1·200	35·4	1·333	43·9	1·512	52·4	1·751
18·5	1·105	27·0	1·201	35·5	1·334	44·0	1·514	52·5	1·755
18·6	1·106	27·1	1·202	35·6	1·336	44·1	1·517	52·6	1·758
18·7	1·107	27·2	1·204	35·7	1·338	44·2	1·519	52·7	1·761
18·8	1·108	27·3	1·205	35·8	1·340	44·3	1·522	52·8	1·764
18·9	1·109	27·4	1·206	35·9	1·342	44·4	1·524	52·9	1·768
19·0	1·110	27·5	1·208	36·0	1·344	44·5	1·527	53·0	1·771
19·1	1·111	27·6	1·209	36·1	1·345	44·6	1·529	53·1	1·774
19·2	1·112	27·7	1·211	36·2	1·347	44·7	1·532	53·2	1·778
19·3	1·113	27·8	1·212	36·3	1·349	44·8	1·534	53·3	1·781
19·4	1·114	27·9	1·213	36·4	1·351	44·9	1·537	53·4	1·784
19·5	1·115	28·0	1·215	36·5	1·353	45·0	1·539	53·5	1·788
19·6	1·116	28·1	1·216	36·6	1·355	45·1	1·542	53·6	1·791
19·7	1·117	28·2	1·217	36·7	1·357	45·2	1·544	53·7	1·794
19·8	1·118	28·3	1·219	36·8	1·359	45·3	1·547	53·8	1·798
19·9	1·119	28·4	1·220	36·9	1·360	45·4	1·549	53·9	1·801
20·0	1·120	28·5	1·222	37·0	1·362	45·5	1·552	54·0	1·805
20·1	1·121	28·6	1·223	37·1	1·364	45·6	1·555	54·1	1·808
20·2	1·122	28·7	1·224	37·2	1·366	45·7	1·557	54·2	1·811
20·3	1·123	28·8	1·226	37·3	1·368	45·8	1·560	54·3	1·815
20·4	1·124	28·9	1·227	37·4	1·370	45·9	1·562	54·4	1·818
20·5	1·125	29·0	1·229	37·5	1·372	46·0	1·565	54·5	1·822
20·6	1·126	29·1	1·230	37·6	1·374	46·1	1·568	54·6	1·825
20·7	1·127	29·2	1·232	37·7	1·376	46·2	1·570	54·7	1·829
20·8	1·128	29·3	1·233	37·8	1·378	46·3	1·573	54·8	1·832
20·9	1·129	29·4	1·235	37·9	1·380	46·4	1·575	54·9	1·836
21·0	1·130	29·5	1·236	38·0	1·382	46·5	1·578	55·0	1·839
21·1	1·131	29·6	1·237	38·1	1·384	46·6	1·581	55·1	1·843
21·2	1·132	29·7	1·239	38·2	1·386	46·7	1·583	55·2	1·846
21·3	1·133	29·8	1·240	38·3	1·388	46·8	1·586	55·3	1·850
21·4	1·134	29·9	1·242	38·4	1·390	46·9	1·589	55·4	1·853
21·5	1·135	30·0	1·243	38·5	1·392	47·0	1·591	55·5	1·857
21·6	1·136	30·1	1·245	38·6	1·394	47·1	1·594	55·6	1·861
21·7	1·137	30·2	1·246	38·7	1·396	47·2	1·597	55·7	1·864
21·8	1·138	30·3	1·248	38·8	1·398	47·3	1·600	55·8	1·868
21·9	1·140	30·4	1·249	38·9	1·400	47·4	1·602	55·9	1·871
22·0	1·141	30·5	1·251	39·0	1·402	47·5	1·605	56·0	1·875
22·1	1·142	30·6	1·252	39·1	1·404	47·6	1·608	56·1	1·879
22·2	1·143	30·7	1·254	39·2	1·406	47·7	1·611	56·2	1·882
22·3	1·144	30·8	1·256	39·3	1·408	47·8	1·613	56·3	1·886
22·4	1·145	30·9	1·257	39·4	1·410	47·9	1·616	56·4	1·890
22·5	1·146	31·0	1·259	39·5	1·413	48·0	1·619	56·5	1·893
22·6	1·147	31·1	1·260	39·6	1·415	48·1	1·622	56·6	1·897
22·7	1·148	31·2	1·262	39·7	1·417	48·2	1·625	56·7	1·901
22·8	1·150	31·3	1·263	39·8	1·419	48·3	1·627	56·8	1·905
22·9	1·151	31·4	1·265	39·9	1·421	48·4	1·630	56·9	1·908
23·0	1·152	31·5	1·266	40·0	1·423	48·5	1·633	57·0	1·912
23·1	1·153	31·6	1·268	40·1	1·425	48·6	1·636	57·1	1·916
23·2	1·154	31·7	1·270	40·2	1·427	48·7	1·639	57·2	1·920
23·3	1·155	31·8	1·271	40·3	1·430	48·8	1·642	57·3	1·924
23·4	1·156	31·9	1·273	40·4	1·432	48·9	1·644	57·4	1·927
23·5	1·157	32·0	1·274	40·5	1·434	49·0	1·647	57·5	1·931
23·6	1·159	32·1	1·276	40·6	1·436	49·1	1·650	57·6	1·935
23·7	1·160	32·2	1·278	40·7	1·438	49·2	1·653	57·7	1·939
23·8	1·161	32·3	1·279	40·8	1·440	49·3	1·656	57·8	1·943
23·9	1·162	32·4	1·281	40·9	1·443	49·4	1·659	57·9	1·947
24·0	1·163	32·5	1·282	41·0	1·445	49·5	1·662	58·0	1·951
24·1	1·165	32·6	1·284	41·1	1·447	49·6	1·665	58·1	1·954
24·2	1·166	32·7	1·286	41·2	1·449	49·7	1·668	58·2	1·958
24·3	1·167	32·8	1·287	41·3	1·451	49·8	1·671	58·3	1·962
24·4	1·168	32·9	1·289	41·4	1·454	49·9	1·674	58·4	1·966
24·5	1·169	33·0	1·291	41·5	1·456	50·0	1·677	58·5	1·970
24·6	1·171	33·1	1·292	41·6	1·458	50·1	1·680	58·6	1·974
24·7	1·172	33·2	1·294	41·7	1·460	50·2	1·683	58·7	1·978
24·8	1·173	33·3	1·296	41·8	1·463	50·3	1·686	58·8	1·982
24·9	1·174	33·4	1·297	41·9	1·465	50·4	1·689	58·9	1·986
25·0	1·175	33·5	1·299	42·0	1·467	50·5	1·692	59·0	1·990
25·1	1·177	33·6	1·301	42·1	1·469	50·6	1·695	59·1	1·994
25·2	1·178	33·7	1·303	42·2	1·472	50·7	1·698	59·2	1·998
25·3	1·179	33·8	1·304	42·3	1·474	50·8	1·701	59·3	2·002
25·4	1·180	33·9	1·306	42·4	1·476	50·9	1·704	59·4	2·006
25·5	1·182	34·0	1·308	42·5	1·479	51·0	1·707	59·5	2·011

382

K	Rel. visc.	K	Rel. visc.	K	Rel. visc.	K	Rel. visc.	K	Rel. visc.
59·6	2·015	67·7	2·398	75·8	2·903	83·9	3·572	92·0	4·466
59·7	2·019	67·8	2·403	75·9	2·910	84·0	3·582	92·1	4·479
59·8	2·023	67·9	2·409	76·0	2·917	84·1	3·591	92·2	4·492
59·9	2·027	68·0	2·414	76·1	2·924	84·2	3·601	92·3	4·505
60·0	2·031	68·1	2·420	76·2	2·932	84·3	3·610	92·4	4·518
60·1	2·035	68·2	2·425	76·3	2·939	84·4	3·620	92·5	4·531
60·2	2·040	68·3	2·431	76·4	2·946	84·5	3·630	92·6	4·544
60·3	2·044	68·4	2·436	76·5	2·953	84·6	3·639	92·7	4·557
60·4	2·048	68·5	2·442	76·6	2·961	84·7	3·649	92·8	4·570
60·5	2·052	68·6	2·447	76·7	2·968	84·8	3·659	92·9	4·583
60·6	2·057	68·7	2·453	76·8	2·975	84·9	3·669	93·0	4·596
60·7	2·061	68·8	2·458	76·9	2·983	85·0	3·679	93·1	4·609
60·8	2·065	68·9	2·464	77·0	2·990	85·1	3·689	93·2	4·623
60·9	2·069	69·0	2·470	77·1	2·998	85·2	3·699	93·3	4·636
61·0	2·074	69·1	2·475	77·2	3·005	85·3	3·709	93·4	4·649
61·1	2·078	69·2	2·481	77·3	3·013	85·4	3·719	93·5	4·663
61·2	2·082	69·3	2·487	77·4	3·020	85·5	3·729	93·6	4·676
61·3	2·087	69·4	2·493	77·5	3·028	85·6	3·739	93·7	4·690
61·4	2·091	69·5	2·498	77·6	3·035	85·7	3·749	93·8	4·703
61·5	2·095	69·6	2·504	77·7	3·043	85·8	3·759	93·9	4·717
61·6	2·100	69·7	2·510	77·8	3·051	85·9	3·769	94·0	4·731
61·7	2·104	69·8	2·516	77·9	3·058	86·0	3·779	94·1	4·744
61·8	2·109	69·9	2·521	78·0	3·066	86·1	3·790	94·2	4·758
61·9	2·113	70·0	2·527	78·1	3·074	86·2	3·800	94·3	4·772
62·0	2·118	70·1	2·533	78·2	3·082	86·3	3·810	94·4	4·786
62·1	2·122	70·2	2·539	78·3	3·089	86·4	3·821	94·5	4·800
62·2	2·126	70·3	2·545	78·4	3·097	86·5	3·831	94·6	4·814
62·3	2·131	70·4	2·551	78·5	3·105	86·6	3·842	94·7	4·828
62·4	2·135	70·5	2·557	78·6	3·113	86·7	3·852	94·8	4·842
62·5	2·140	70·6	2·563	78·7	3·121	86·8	3·863	94·9	4·856
62·6	2·145	70·7	2·569	78·8	3·129	86·9	3·873	95·0	4·871
62·7	2·149	70·8	2·575	78·9	3·137	87·0	3·884	95·1	4·885
62·8	2·154	70·9	2·581	79·0	3·145	87·1	3·894	95·2	4·899
62·9	2·158	71·0	2·587	79·1	3·153	87·2	3·905	95·3	4·913
63·0	2·163	71·1	2·593	79·2	3·161	87·3	3·916	95·4	4·928
63·1	2·168	71·2	2·599	79·3	3·169	87·4	3·927	95·5	4·942
63·2	2·172	71·3	2·605	79·4	3·177	87·5	3·937	95·6	4·957
63·3	2·177	71·4	2·611	79·5	3·185	87·6	3·948	95·7	4·971
63·4	2·181	71·5	2·617	79·6	3·193	87·7	3·959	95·8	4·986
63·5	2·186	71·6	2·623	79·7	3·201	87·8	3·970	95·9	5·001
63·6	2·191	71·7	2·630	79·8	3·209	87·9	3·981	96·0	5·016
63·7	2·196	71·8	2·636	79·9	3·218	88·0	3·992	96·1	5·030
63·8	2·200	71·9	2·642	80·0	3·226	88·1	4·003	96·2	5·045
63·9	2·205	72·0	2·648	80·1	3·234	88·2	4·014	96·3	5·060
64·0	2·210	72·1	2·655	80·2	3·243	88·3	4·025	96·4	5·075
64·1	2·215	72·2	2·661	80·3	3·251	88·4	4·036	96·5	5·090
64·2	2·219	72·3	2·667	80·4	3·259	88·5	4·048	96·6	5·105
64·3	2·224	72·4	2·674	80·5	3·268	88·6	4·059	96·7	5·120
64·4	2·229	72·5	2·680	80·6	3·276	88·7	4·070	96·8	5·136
64·5	2·234	72·6	2·686	80·7	3·285	88·8	4·081	96·9	5·151
64·6	2·239	72·7	2·693	80·8	3·293	88·9	4·093	97·0	5·166
64·7	2·244	72·8	2·699	80·9	3·302	89·0	4·104	97·1	5·182
64·8	2·248	72·9	2·706	81·0	3·310	89·1	4·116	97·2	5·197
64·9	2·253	73·0	2·712	81·1	3·319	89·2	4·127	97·3	5·212
65·0	2·258	73·1	2·719	81·2	3·327	89·3	4·139	97·4	5·228
65·1	2·263	73·2	2·725	81·3	3·336	89·4	4·150	97·5	5·244
65·2	2·268	73·3	2·732	81·4	3·345	89·5	4·162	97·6	5·259
65·3	2·273	73·4	2·738	81·5	3·353	89·6	4·173	97·7	5·275
65·4	2·278	73·5	2·745	81·6	3·362	89·7	4·185	97·8	5·291
65·5	2·283	73·6	2·751	81·7	3·371	89·8	4·197	97·9	5·307
65·6	2·288	73·7	2·758	81·8	3·380	89·9	4·209	98·0	5·323
65·7	2·293	73·8	2·765	81·9	3·389	90·0	4·220	98·1	5·338
65·8	2·298	73·9	2·771	82·0	3·398	90·1	4·232	98·2	5·354
65·9	2·303	74·0	2·778	82·1	3·406	90·2	4·244	98·3	5·371
66·0	2·309	74·1	2·785	82·2	3·415	90·3	4·256	98·4	5·387
66·1	2·314	74·2	2·792	82·3	3·424	90·4	4·268	98·5	5·403
66·2	2·319	74·3	2·798	82·4	3·433	90·5	4·280	98·6	5·419
66·3	2·324	74·4	2·805	82·5	3·442	90·6	4·292	98·7	5·435
66·4	2·329	74·5	2·812	82·6	3·451	90·7	4·304	98·8	5·452
66·5	2·334	74·6	2·819	82·7	3·460	90·8	4·317	98·9	5·468
66·6	2·339	74·7	2·826	82·8	3·470	90·9	4·329	99·0	5·485
66·7	2·345	74·8	2·833	82·9	3·479	91·0	4·341	99·1	5·501
66·8	2·350	74·9	2·839	83·0	3·488	91·1	4·353	99·2	5·518
66·9	2·355	75·0	2·846	83·1	3·497	91·2	4·366	99·3	5·535
67·0	2·360	75·1	2·853	83·2	3·506	91·3	4·378	99·4	5·551
67·1	2·366	75·2	2·860	83·3	3·516	91·4	4·391	99·5	5·568
67·2	2·371	75·3	2·867	83·4	3·525	91·5	4·403	99·6	5·585
67·3	2·376	75·4	2·874	83·5	3·534	91·6	4·416	99·7	5·602
67·4	2·382	75·5	2·881	83·6	3·544	91·7	4·428	99·8	5·619
67·5	2·387	75·6	2·889	83·7	3·553	91·8	4·441	99·9	5·636
67·6	2·392	75·7	2·896	83·8	3·563	91·9	4·453	100·0	5·653

Values of relative viscosity for K in one-tenth unit increments from zero to one hundred are supplied. Since concentration was entered as a variable in the programme, a table of values at different concentrations can be obtained easily.

Tables of values of K at other concentrations or the computer programme in Algol 60 language can be supplied by the author on request.

P. E. HINKAMP

Plastics Production Research Service,
  Bldg 734, Dow Chemical Company,
    Midland, Mich. 48640, U.S.A.

The Effect of the Side Group upon the Properties of the Poly(epoxides)

The work described in this series of papers forms part of an investigation of polyethers of general formula [CHR—CH$_2$—O]$_n$, *which was initiated in the Chemistry Department of the University of Manchester by Professor G. Gee. Early work, principally that of D. J. Marks, showed that polymers with* R=H, CH$_3$, CH:CH$_2$ *or* n-C$_{10}$H$_{21}$ *had similar melting points ca. 70° to 80°C and glass transition temperatures ca. −70°C. Here we report detailed investigations of the properties of two poly(epoxides) with much larger side groups, namely poly(t-butyl ethylene oxide) and poly(styrene oxide). We also report some useful properties of other poly(epoxides) which were not measured earlier.*

I—The Preparation and Characterization of Poly(t-butyl ethylene oxide) and Poly(styrene oxide)

G. ALLEN, C. BOOTH and S. J. HURST*

In this paper the preparation and characterization of polymers of t-butyl ethylene oxide and styrene oxide are described. Mixtures of water and zinc diethyl, having mole ratios approaching unity, were used as catalysts, and dioxan was used as solvent. The poly(t-butyl ethylene oxide) was highly crystalline and had narrow distributions of both molecular weights and degrees of stereoregularity. The poly(styrene oxide) was slightly crystalline, had a wide molecular weight distribution, and contained molecules of widely different degrees of stereoregularity.

POLY(*t*-BUTYL ETHYLENE OXIDE)

THE polymerization of *t*-butyl ethylene oxide (*t*BEO) was recently reported[1]. Zinc diethyl and water (mole ratio 1:0·4) were used to initiate the polymerization and evidence was presented which showed that *t*BEO, in common with other alkyl substituted ethylene oxides, polymerized by a mechanism similar to that described for propylene oxide[2]. Accordingly, in order to prepare high-molecular-weight crystalline poly(*t*BEO), we chose conditions similar to those which were used to produce corresponding samples of poly(propylene oxide)[3], i.e. a mole ratio of zinc diethyl to water approaching unity.

PREPARATION

The polymerization was carried out at 60°C in dioxan solution, by use of the high vacuum technique described earlier[2]. The following concentrations of reagents were used: *t*BEO, 3·27 M; zinc diethyl, 0·28 M; water, 0·252 M. A slight precipitate was formed when the reagents were mixed; in the light of previous experience it was assumed that this would not seriously influence the course of polymerization[2]. Poly(*t*BEO) was precipitated during the reaction. Later it was found that poly(*t*BEO) was not completely soluble in dioxan at 80°C.

*Present address: Stockport College for Further Education.

The reaction was terminated by dissolving the products in benzene at 80°C and adding enough methanol to precipitate the catalyst. A hindered phenol antioxidant (1 wt % of polymer) was added and the products were dried under vacuum. Catalyst residues were removed before using the polymer. The results of the polymerization were as follows: conversion, 83 per cent in 310 h; intrinsic viscosity in toluene at 75°C, 19·2 dl g^{-1}; viscosity average molecular weight (estimated), 7×10^7.

CHARACTERIZATION

Viscometry

Dilute solution viscosities were determined in toluene at 75°C, by use of a Desreux–Bischoff viscometer[4] modified according to Kaufman and Solomon[5]. The maximum shear stress was 1·8 g cm^{-1} sec^{-2}. The intrinsic viscosity/molecular weight relationship was not determined (though some fragmentary molecular weight data are presented in part II of this work).

Fractionation

The poly(*t*BEO) separated from the reaction mixture was incompletely soluble at 25°C in every solvent tried, including a representative selection of paraffins, aliphatic ethers, chlorinated hydrocarbons, aromatic hydrocarbons, ketones and alcohols. At 80°C it was completely soluble in solvents which had solubility parameters in the range 8·6 to 9·5 (cal cm^{-3})$^{\frac{1}{2}}$ at 25°C; e.g. toluene, benzene, carbon tetrachloride.

Fractionation was achieved by dissolving the polymer in benzene at 80°C (concentration 2 g/l.) and cooling the resulting solution. Precipitation of crystalline polymer occurred at a temperature just below 70°C; such fractions were allowed to grow for a day or two before separating the precipitate by filtering the solution through a hot funnel packed with glass wool. Below 60°C liquid phases precipitated, and these were separated in the usual way by allowing them to settle overnight and syphoning off the dilute phase. All fractions were dissolved in benzene and subsequently dried under vacuum for several days.

RESULTS

Typical fractionation data are given in *Table 1*. The melting points (T_m) quoted for the fractions were obtained by methods discussed in ref. 10. Some degradation of the polymer occurred; the weight-average intrinsic

Table 1. Fractionation of poly(*t*-butyl ethylene oxide) from benzene

Fraction No.	Precipitation temperature °C	Nature of precipitate	Wt %	[η] (dl g^{-1})	T_m °C
1	67·4	Crystalline	28·4	17·1	149
2	65·0	Crystalline	11·2	17·9	149
3	62·5	Crystalline	11·6	20·3	149
4	49·9	Liquid	27·0	17·0	150
5	40·5	Liquid	3·6	12·5	—
6	24·3	Liquid	8·3	10·3	149
7	Residue	—	10·0	6·1	149

viscosity of the fractions is some 18 per cent lower than the intrinsic viscosity of the original polymer. Nevertheless the reduction in $[\eta]$ is remarkably small when one considers the high temperatures used and the very high molecular weights involved, and it reflects the stability of poly(tBEO) towards oxidative degradation.

DISCUSSION

All the fractions have the same melting point: $149° \pm 1$ deg. C. It can be assumed that fractional crystallization would separate species of differing stereoregularity[3], and we conclude that our specimen of poly(tBEO) is highly stereoregular with a narrow distribution of sequence lengths among the individual chains.

The molecular weight distribution is more difficult to define from the limited data to hand; only the few fractions obtained by liquid phase separation are pertinent. However, it is clear that the distribution is fairly narrow, e.g. if we assume that the exponent of the Mark–Houwink equation for toluene at $75°C$ (a good solvent) is > 0.7, then the ratio $\bar{M}_w/\bar{M}_n$ calculated from the fractionation data is < 1.4. Taking into account the degradation which occurred before and during the fractionation, we conclude that the original reaction product had a narrow molecular weight distribution, possibly monodisperse, but certainly very much narrower than those of poly(styrene oxide) and poly(propylene oxide)[2] produced under similar conditions.

As far as we can tell, the course of the polymerization of tBEO seems to be parallel to that of propylene oxide[1]. Nevertheless the polymers produced are quite different: poly(propylene oxide) prepared with the same zinc diethyl/water catalyst (mole ratio of $1:0.9$) would consist of many stereoisomers and have a wide molecular weight distribution[2,3]. Of the reactions proposed[2] to explain the polymerization of propylene oxide, it seems that two do not occur with tBEO, i.e. the propagation reaction which results in the occurrence of syndiotactic or perhaps head to head placements, and the transfer reaction with polymer which results in random scission of the chain and causes the wide molecular weight distribution.

These conclusions are understandable in terms of the severe steric interactions which occur in the poly(tBEO) chain due to the large bulk of the t-butyl substituent group. For example it is impossible to construct a model of the syndiotactic poly(tBEO) chain (or indeed a syndiotactic, dld, triad) without distorting bond angles and bond lengths. Thus we also conclude that our product is a polymer with an extremely high probability of isotactic placements. Furthermore, the reduced rate of the propagation reaction is readily explained in terms of these severe steric restrictions[1]. The narrow molecular weight distribution, rationalized in terms of a drastic reduction in the rate of the chain transfer reaction with polymer, also could be a direct consequence of steric factors. However, the insolubility of poly(tBEO) in the solvent used provides a possible alternative mechanism for producing a narrow molecular weight distribution.

POLY(STYRENE OXIDE)

Several accounts of the polymerization of styrene oxide have appeared[1,6,7], including polymerization by the zinc diethyl–water catalyst system[1,7]. It is clear from earlier work[1] that no direct analogy can be drawn between the polymerizations of styrene oxide and those of the alkyl substituted ethylene oxides. Accordingly we have investigated, to a limited extent, the effect of changing the water to zinc diethyl mole ratio.

Polymerizations have been carried out by use of 'dry' zinc diethyl, and by use of a mole ratio of water to zinc diethyl of 0·8:1. Polymerizations at a mole ratio of 0·4:1 have been reported earlier[1]. Attempts to carry out a dry reaction at 50°C resulted in a very slow reaction; the rate decreased as the drying technique was improved, e.g. a conversion of 23 per cent was obtained in 956 hours with styrene oxide (0·84 M) and zinc diethyl (0·093 M) in toluene at 50°C. A similar, though somewhat faster, reaction (67 per cent conversion in 1 100 h) gave poly(styrene oxide) with an intrinsic viscosity in toluene at 25°C of 3·8 dl/g, and a number-average molecular weight of 950[8].

Reactions carried out with a mole ratio of 0·8:1 were extremely rapid at 60°C. Eventually we followed the reaction by dilatometry at lower temperatures: e.g. a conversion of 63 per cent was obtained in 72 h with styrene oxide (1·09 M), zinc diethyl (0·142 M) and water (0·113 M) in dioxan at 40°C.

Representative data for differing water concentrations are compared in *Figure 1*. No attempt has been made to formulate a reaction mechanism consistent with these curves because of the few results available. They merely illustrate that the kinetics of polymerization are very different from
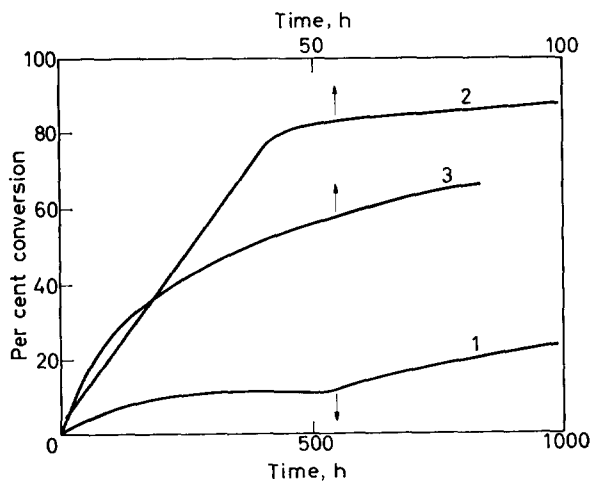
Figure 1—Polymerization of styrene oxide. Conversion versus time for: 1, 'dry' zinc diethyl in toluene at 50°C; 2, mole ratio of water to zinc diethyl of 0·4 in dioxan at 60°C; 3, mole ratio of water to zinc diethyl of 0·8 in dioxan at 40°C

the kinetics of the propylene oxide system and so we have no useful guide to the best conditions for production of high-molecular-weight crystalline polymer.

PREPARATION

Styrene oxide was polymerized in dioxan at 60°C under high vacuum, with the following reagent concentrations: styrene oxide, 4·31 M, zinc diethyl 0·143 M, water 0·114 M. A slight precipitate formed when the reagents were mixed. The reaction was terminated by dissolving the products in benzene and adding sufficient methanol to precipitate the catalyst. Insoluble residues were removed by centrifugation, a hindered phenol antioxidant (1 wt % of polymer) was added, and the polymer was recovered by freeze drying.

The results of the polymerization were as follows: conversion, 91 per cent in 288 h; intrinsic viscosity in toluene at 25°C, 1·94 dl/g; number-average molecular weight, 1 450⁸.

CHARACTERIZATION

Viscometry

Dilute solution viscosities were measured in toluene at 25°C by use of modified Desreux–Bischoff viscometers[4]. Maximum shear stress was 3·0 g cm⁻¹ sec⁻². Viscosity-average molecular weights were calculated by means of the relationship[9]

$$[\eta] = 6·79 \times 10^{-5} \bar{M}_v^{0·766}$$

Fractionation

The poly(styrene oxide) was very soluble at room temperature in such solvents as benzene, toluene, chloroform and carbon tetrachloride but largely insoluble in paraffins, acetone, methanol and methyl ethyl ketone. Fractionation was achieved by adding isooctane to a dilute solution of the polymer in benzene at 25°C: isooctane was added until the solution became turbid, the temperature was raised until the precipitate dissolved, and the solution was then cooled slowly to 25°C. Precipitates were separated by syphoning off the dilute phase through a glass wool plug. Early precipitates were crystalline solids, later ones were liquid gels. Fractions were recovered by dissolving in benzene and freeze drying. Maximum concentration of polymer during fractionation was 2 g l⁻¹.

RESULTS

Typical fractionation data are given in *Table 2*. Some degradation of the polymer occurred even at this low temperature and relatively low molecular weight; the weight-average intrinsic viscosity of the fractions is some 21 per cent lower than the intrinsic viscosity of the original polymer. The stability of poly(styrene oxide) is therefore much lower than that of poly(*t*BEO) towards oxidative degradation. No melting points are available for these fractions. However, subsequent work[10] showed that similar high molecular weight fractions had melting points in the range 150° to 160°C, and that some separation into species of differing melting point occurred

Table 2. Fractionation of poly(styrene oxide) from benzene–isooctane
mixtures at 25°C

Fraction No.	Nature of precipitate	Wt %	$[\eta]$ $(dl\ g^{-1})$	T_m °C
1	Crystalline	1·8	5·54	(162)
2	Crystalline	24·3	4·13	(152)
3	Translucent liquid	18·2	1·35	(150)
4	Liquid	9·6	0·528	—
5	Liquid	5·7	0·347	—
6	Liquid	4·4	0·272	—
7	Liquid	6·0	0·195	—
8	Liquid	4·1	0·151	—
9	Liquid	3·6	0·109	—
10	Residue	22·2	0·051	—

during the fractional crystallization. The data in *Table 2* are the melting
points of corresponding fractions taken from ref. 10.

DISCUSSION

Some separation of species differing in crystallizability takes place during
the fractional crystallization. In contrast to the fractional crystallization
of poly(propylene oxide)[2,3] the molecular weight varies between the
fractions. This may reflect the fact that polymer of high molecular weight
has a higher degree of structural regularity; or it may be due to a hybrid
fractionation of the type discussed elsewhere[11].

The molecular weight distribution of the poly(styrene oxide) is very
wide

$$\bar{M}_v / \bar{M}_n > 450$$

If the effects of crystallization are neglected, all the data of *Table 2* can
be used to construct a molecular weight distribution in the conventional
way. This distribution is shown in reduced form in *Figure 2*, where it is
compared with similar curves calculated for high molecular weight
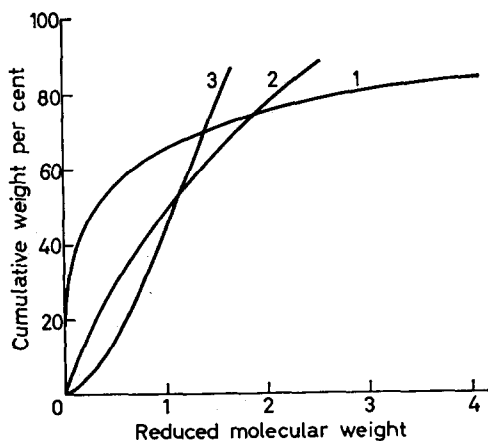
Figure 2—Representative molecular weight distribution of poly-(epoxides) prepared using a mole ratio of water to zinc diethyl approaching unity. Cumulative weight per cent versus reduced weight ($\bar{M}_v$ of fraction divided by $\bar{M}_v$ of whole polymer) for: 1, poly(styrene oxide); 2, poly-(propylene oxide); 3, poly(*t*-butyl ethylene oxide)

poly(propylene oxide)[2,3] and poly(tBEO) (*Table 1*). The distribution of molecular weights of poly(styrene oxide) is seen to be much wider than that of poly(propylene oxide), which in turn is wider than that of poly(tBEO). Unfortunately use of these results to discuss the mechanism of polymerization of styrene oxide is precluded by the fragmentary nature of the data which are available. The primary aim of the work was to produce polymer fractions for studies of physical properties.

Department of Chemistry,
  University of Manchester

REFERENCES

[1] BRUCE, J. M. and HURST, S. J. *Polymer, Lond.* 1966, **7**, 1

[2] BOOTH, C., HIGGINSON, W. C. E. and POWELL, E. *Polymer, Lond.* 1964, **5**, 479

[3] ALLEN, G., BOOTH, C. and JONES, M. N. *Polymer, Lond.* 1964, **5**, 257

[4] DESREUX, V. and BISCHOFF, J. *Bull. Soc. chim. Belg.* 1950, **59**, 93

[5] KAUFMAN, H. S. and SOLOMON, E. *Industr. Engng Chem.* (*Industr.*) 1953, **45**, 1779

[6] See, for example, COLCLOUGH, R. O., GEE, G., HIGGINSON, W. C. E., JACKSON, J. B. and LITT, M. *J. Polym. Sci.* 1959, **34**, 171; VANDENBERG, E. J. *J. Polym. Sci.* 1960, **41**, 486; KAMBARA, S. and TAKAHASHI, A. *Makromol. Chem.* 1963, **63**, 89

[7] See, for example, KERN, R. J. *Makromol. Chem.* 1965, **81**, 261

[8] Model 301A Vapour Pressure Osmometer, Mechrolab. Inc.

[9] ALLEN, G., BOOTH, C., HURST, S. J., JONES, M. N. and PRICE, C. *Polymer, Lond.* 1967, **8**, 391

[10] ALLEN, G., BOOTH, C., HURST, S. J., PRICE, C., VERNON, F. and WARREN, R. F. *Polymer, Lond.* 1967, **8**, 406

[11] BOOTH, C. and PRICE, C. *Polymer, Lond.* 1966, **7**, 167

II—Intrinsic Viscosity and Light Scattering Measurements on Poly(ethylene oxide), Poly(styrene oxide) and Poly(t-butyl ethylene oxide)

G. ALLEN, C. BOOTH, S. J. HURST*, M. N. JONES and C. PRICE

Intrinsic viscosity and light scattering data are reported for fractions of the poly(styrene oxide) and for fractions of a commercial sample of poly(ethylene oxide). A few results obtained for fractions of the poly(t-butyl ethylene oxide) are also included. The following intrinsic viscosity/molecular weight relationships are obtained:

poly(ethylene oxide) $[\eta]$ (benzene at 25°C)$=3 \cdot 97 \times 10^{-4} \, \overline{M}_v^{0 \cdot 686}$

poly(styrene oxide) $[\eta]$ (toluene at 25°C)$=6 \cdot 79 \times 10^{-5} \, \overline{M}_v^{0 \cdot 766}$

*Present address: John Dalton College of Technology, Manchester 1.

poly(propylene oxide)[2,3] and poly(tBEO) (*Table 1*). The distribution of molecular weights of poly(styrene oxide) is seen to be much wider than that of poly(propylene oxide), which in turn is wider than that of poly(tBEO). Unfortunately use of these results to discuss the mechanism of polymerization of styrene oxide is precluded by the fragmentary nature of the data which are available. The primary aim of the work was to produce polymer fractions for studies of physical properties.

Department of Chemistry,
  University of Manchester

REFERENCES

[1] BRUCE, J. M. and HURST, S. J. *Polymer, Lond.* 1966, **7**, 1
[2] BOOTH, C., HIGGINSON, W. C. E. and POWELL, E. *Polymer, Lond.* 1964, **5**, 479
[3] ALLEN, G., BOOTH, C. and JONES, M. N. *Polymer, Lond.* 1964, **5**, 257
[4] DESREUX, V. and BISCHOFF, J. *Bull. Soc. chim. Belg.* 1950, **59**, 93
[5] KAUFMAN, H. S. and SOLOMON, E. *Industr. Engng Chem. (Industr.)* 1953, **45**, 1779
[6] See, for example, COLCLOUGH, R. O., GEE, G., HIGGINSON, W. C. E., JACKSON, J. B. and LITT, M. *J. Polym. Sci.* 1959, **34**, 171; VANDENBERG, E. J. *J. Polym. Sci.* 1960, **41**, 486; KAMBARA, S. and TAKAHASHI, A. *Makromol. Chem.* 1963, **63**, 89
[7] See, for example, KERN, R. J. *Makromol. Chem.* 1965, **81**, 261
[8] Model 301A Vapour Pressure Osmometer, Mechrolab. Inc.
[9] ALLEN, G., BOOTH, C., HURST, S. J., JONES, M. N. and PRICE, C. *Polymer, Lond.* 1967, **8**, 391
[10] ALLEN, G., BOOTH, C., HURST, S. J., PRICE, C., VERNON, F. and WARREN, R. F. *Polymer, Lond.* 1967, **8**, 406
[11] BOOTH, C. and PRICE, C. *Polymer, Lond.* 1966, **7**, 167

II—Intrinsic Viscosity and Light Scattering Measurements on Poly(ethylene oxide), Poly(styrene oxide) and Poly(t-butyl ethylene oxide)

G. ALLEN, C. BOOTH, S. J. HURST*, M. N. JONES and C. PRICE

Intrinsic viscosity and light scattering data are reported for fractions of the poly(styrene oxide) and for fractions of a commercial sample of poly(ethylene oxide). A few results obtained for fractions of the poly(t-butyl ethylene oxide) are also included. The following intrinsic viscosity/molecular weight relationships are obtained:

poly(ethylene oxide) $[\eta]$ (benzene at 25 °C) $= 3 \cdot 97 \times 10^{-4} \overline{M}_v^{0 \cdot 686}$

poly(styrene oxide) $[\eta]$ (toluene at 25 °C) $= 6 \cdot 79 \times 10^{-5} \overline{M}_v^{0 \cdot 766}$

*Present address: John Dalton College of Technology, Manchester 1.

Estimates of the unperturbed dimensions of these polymers yield values of $(\bar{r}_0^2/M)^{\frac{1}{2}}$ of 0·93 Å for poly(ethylene oxide) and of 0·64 Å for poly(styrene oxide).

A USEFUL step in the characterization of a polymer is the determination of an intrinsic viscosity/molecular weight relationship. In this paper results are presented which yield such relationships for poly(ethylene oxide) and poly(styrene oxide), together with an indication of a relationship for poly(*t*-butyl ethylene oxide). These results are used to estimate the unperturbed dimensions of the polymers.

EXPERIMENTAL

Fractionation

Fractions of poly(ethylene oxide) were obtained from a sample of Polyox WSR-205 resin (code number FC2075) prepared by Union Carbide Ltd, Chemical Division. The fractionation methods involved liquid–liquid phase separation, and are described elsewhere[1]. Fractions of poly(styrene oxide) and poly(*t*BEO) were obtained from the samples, and by the methods, described in part I[2]. Only fractions obtained by liquid–liquid phase separation have been used to establish intrinsic viscosity/molecular weight relationships.

Intrinsic viscosity

Relative viscosities of dilute solutions of polymers were measured by use of a modified Desreux–Bischoff viscometer[3,4] of low shear stress (about 2 to 3 g cm^{-1} sec^{-2}). Temperatures were controlled to $\pm 0\cdot01$ deg. C. Both Huggins and Kraemer plots were used to determine the intrinsic viscosities ([η]) from the experimental data.

Molecular weight

Weight-average molecular weights ($\overline{M}_w$) were determined by the light scattering method. The polymer solutions and the solvents were clarified by centrifugation in a number 30 rotor of a Spinco model L preparative ultracentrifuge for at least three hours at 20 000 rev/min. Light scattering measurements were made with a Sofica photometer standardized against benzene. Measurements were made with light of wavelength 5 460 Å at ten angles between 30° and 150° for four solutions of different concentration. Temperatures were controlled to $\pm 0\cdot03$ deg. C. Weight-average molecular weights were determined from the measured intensities of scattered light by the double extrapolation method of Zimm; second virial coefficients (A_2) and z-average root mean square radii of gyration $(\overline{S^2})_z^{\frac{1}{2}}$ were obtained from the concentration or angular dependence of the extrapolations in the normal way[5].

A Brice–Phoenix differential refractometer was used to measure refractive index increments. Temperatures were controlled to $\pm 0\cdot03$ deg. C by means of the water jacket at temperatures below 50°C[6] or by means of an aluminium block thermostat at temperatures above 50°C. The refractometer was calibrated with sucrose solutions, and checked against potassium chloride solutions.

RESULTS

Poly(ethylene oxide)

Intrinsic viscosities were determined for benzene solutions at 25°C. Light scattering measurements were made on methanol solutions at 45°C. The refractive index increment for light of wavelength 5 460 Å was 0·152 cm³ g⁻¹ at 45°C in methanol.

Intrinsic viscosity and light scattering data are given in *Table 1*. The

Table 1. Intrinsic viscosities and light scattering data for fractions of poly(ethylene oxide)

$[\eta]$ $(dl\,g^{-1})$ (benzene at 25°C)	$\overline{M}_w \times 10^{-6}$	$A_2 \times 10^{-4}$ $(cm^3 g^{-1}\,mole)$	$(\overline{S^2})^{\frac{1}{2}}_z\,(\mathring{A})$
		(methanol at 45°C)	
15·8	5·2	2·1	1 880
11·5	3·30	3·8	1 382
7·51	1·56	5·2	1 100
5·20	1·07	3·5	725
3·65	0·56	4·3	672
3·09	0·452	5·9	532
2·03	0·277	6·5	—
1·78	0·204	8·1	—
0·913	0·080	9·8	—

method of least squares has been used to define the best straight line through the log–log plot of intrinsic viscosity versus weight-average molecular weight, and the intrinsic viscosity/molecular weight relationship so obtained is

$$[\eta] = 3\cdot97 \times 10^{-4}\,\overline{M}_v^{0\cdot686}$$

Poly(styrene oxide)

Intrinsic viscosities were determined for toluene solutions at 25°C, and for benzene solutions at 30°C. Light scattering measurements were made on benzene solutions at 30°C. The refractive index increment at 5 460 Å and 30°C in benzene was 0·085 cm³ g⁻¹.

Intrinsic viscosity and light scattering data are given in *Tables 2* and *3*.

Table 2. Intrinsic viscosities and light scattering data for fractions of poly(styrene oxide)

$[\eta]$ $(dl\,g^{-1})$ (toluene at 25°C)	$\overline{M}_w \times 10^{-5}$	$A_2 \times 10^{-4}$ $(cm^3 g^{-2}\,mole)$ (benzene at 30°C)	$[\eta]$ $(dl\,g^{-1})$ (toluene at 25°C)	$\overline{M}_w \times 10^{-5}$	$A_2 \times 10^{-4}$ $(cm^3 g^{-2}\,mole)$ (benzene at 30°C)
2·37	8·08	2·83	0·288	0·546	5·80
1·66	4·95	3·23	0·202	0·265	6·94
1·07	2·80	3·69	0·158	0·222	7·20
0·670	2·00	4·22	0·120	0·174	7·31
0·448	1·38	4·24	0·097	0·144	7·36

The method of least squares has been used to define the best straight line through the log-log plot of intrinsic viscosity in toluene at 25°C versus

Table 3. Intrinsic viscosities of fractions of poly(styrene oxide) in toluene at 25°C and benzene at 30°C

$[\eta]$ $(dl\ g^{-1})$ (toluene at 25°C)	$[\eta]$ $(dl\ g^{-1})$ (benzene at 30°C)	$[\eta]$ $(dl\ g^{-1})$ (toluene at 25°C)	$[\eta]$ $(dl\ g^{-1})$ (benzene at 30°C)
2·36	2·89	0·690	0·870
1·77	2·20	0·371	0·431

weight-average molecular weight, and the intrinsic viscosity/molecular weight relationship so obtained is

$$[\eta] = 6 \cdot 79 \times 10^{-5} \overline{M}_v^{0 \cdot 766} \text{ (toluene at 25°C)}$$

The corresponding relationship for benzene was obtained by combining the above equation with the data of *Table 3* and is

$$[\eta] = 9 \cdot 22 \times 10^{-5} \overline{M}_v^{0 \cdot 758} \text{ (benzene at 30°C)}$$

Poly(t-butyl ethylene oxide)

Intrinsic viscosities were determined for toluene solutions at 75°C. It proved difficult to find a solvent for poly(tBEO) which had a refractive index sufficiently different from that of the polymer to permit accurate determination of molecular weight by the light scattering method. Isooctane at 75°C was used eventually (the refractive index increment at 5 460 Å was 0·114 cm^3 g^{-1}), but the high molecular weight fractions were not com-

Table 4. Intrinsic viscosities and light scattering data for fractions of poly(t-butyl ethylene oxide)

Fraction*	$[\eta]$ $(dl\ g^{-1})$ (toluene at 75°C)	$\overline{M}_w \times 10^{-6}$	A_2 $(cm^3\ g^{-2}\ mole)$	$(\overline{S^2})_z^{\frac{1}{2}}$ $(\mathring{A})$
			(isooctane at 75°C)	
4	4·04	0·73	3·97	520
5	4·62	1·52	3·82	690
6	6·53	1·80	3·74	760
7	4·03	0·73	3·97	530

*Portions of fractions (*Table 1*, ref. 2) soluble in isooctane at 75°.

pletely soluble at this temperature. Measurements were made on samples which had been used for determination of melting point and glass transition temperature by dilatometry (Part V) and which had degraded a little in the process. The few results we obtained are given in *Table 4*; they serve only as an indication of the relationship between intrinsic viscosity and molecular weight for poly(tBEO).

DISCUSSION

No intrinsic viscosity/molecular weight relationship has been published for poly(styrene oxide) prior to this investigation. Several relationships are available for poly(ethylene oxide) including one in our solvent system, benzene at 25°C, due to Rossi and Cuniberti[7], i.e.

$$[\eta] = 12 \cdot 9 \times 10^{-4} \overline{M}_v^{0 \cdot 50}$$

Except for the relationships obtained in aqueous solvents[8], the molecular weight range studied previously has been that of the commercial poly-ethylene gycols, i.e. 100 to 20 000. The difference in the exponent of the Mark–Houwink relationships for the high and the low polymers is very much that expected for a good solvent system.

The intrinsic viscosity and light scattering data can be used to define the coil dimensions of the polymers. There is every indication in our data that the poly(epoxides) under examination have dilute solution properties similar to those of other polymers and in keeping with dilute solution theories, e.g. the second virial coefficients of poly(ethylene oxide) and poly(styrene oxide) fit equations of the form

$$A_2 = CM^{-\epsilon}$$

with ϵ in the region 0·25 to 0·30.

Hence, we are able to treat our data in the conventional way and estimate unperturbed dimensions from the intrinsic viscosity and molecular weight data by the method of Kurata, Stockmayer and Roig[9] or by the method of Stockmayer and Fixman[10]. Both methods give similar results; we have chosen to use the first mentioned in order to be consistent with the most accessible literature[11, 12]. The appropriate equations are:

$$[\eta]_w^{2/3}\overline{M}_w^{-1/3} = K^{2/3} + \text{const. } g(\alpha) \cdot \overline{M}_w^{2/3} [\eta]^{-1/3} \tag{1}$$

$$K = \Phi (\overline{r_0^2}/M)^{3/2} (\overline{M^{\frac{1}{2}}})_w / (\overline{M}_w)^{\frac{1}{2}} \tag{2}$$

$$\Phi = 2·87 \times 10^{23} \, g^{-1} \tag{3}$$
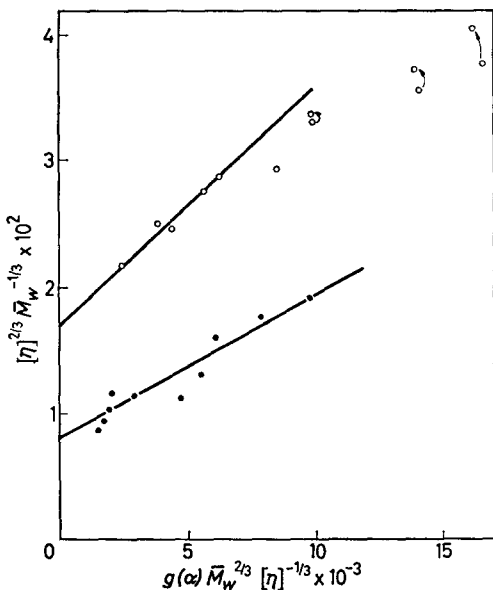
Figure 1—Kurata–Stockmayer–Roig plot for poly(ethylene oxide), O, and poly(styrene oxide), ●

where $\overline{r_0^2}$ is the mean square unperturbed end to end distance of the chain, and $g(\alpha) = 8\alpha^3 (3\alpha^2 + 1)^{-3/2}$ where α is the hydrodynamic expansion factor, which is found by a method of successive approximations.

In *Figure 1* the data are plotted after the manner of Kurata, Stockmayer and Roig. The curvature of the plot for poly(ethylene oxide) is due in some part to the effect of the non-zero shear stress in the viscometers. A correction (indicated in *Figure 1*) can be estimated by analogy with other polymer–solvent systems, and applies to molecular weights in excess of 10^6. In view of this uncertainty, and also in view of the results of Baumann[13] who has found similar curves for very high molecular weight polymers, we have considered only the five lower molecular weight fractions in arriving at a value of K of $0 \cdot 22$ cm^3 g^{-1}. The data for poly(styrene oxide) are more in accord with equation (1) and yield a value of K of $0 \cdot 071$ cm^3 g^{-1}. Assuming that $(\overline{M^{\frac{1}{2}}})_w/(M_w)^{\frac{1}{2}}$ is $1 \cdot 1$ for our fractions, we calculate the following values for $(\overline{r_0^2}/M)^{\frac{1}{2}}$:

$$\text{poly(ethylene oxide)} \quad (\overline{r_0^2}/M)^{\frac{1}{2}} = 0 \cdot 93 \text{ Å}$$

$$\text{poly(styrene oxide)} \quad (\overline{r_0^2}/M)^{\frac{1}{2}} = 0 \cdot 64 \text{ Å}$$

A value of K of $\sim 0 \cdot 12$ cm^3 g^{-1} has been obtained[8] for commercial high molecular weight poly(ethylene oxide) samples (Polyox Resins) from intrinsic viscosity and molecular weight measurements in two θ-solvents ($0 \cdot 45$M aqueous potassium sulphate at $35°$C and $0 \cdot 39$M aqueous magnesium sulphate at $45°$C). These samples probably have rather wide molecular weight distributions; we have reported[1] data for one such sample of poly(ethylene oxide) which yields a value of $\overline{M}_w/\overline{M}_n$ greater than three even when the very low molecular weight fraction, which may be an additive, is ignored. By use of equations (2) and (3), with $K = 0 \cdot 12$ cm^3 g^{-1} and $(\overline{M^{\frac{1}{2}}})_w/(\overline{M}_w)^{\frac{1}{2}} = 2$, we obtain a value of $(\overline{r_0^2}/M)^{\frac{1}{2}}$ of $0 \cdot 84$ Å. The value of $0 \cdot 75$ Å obtained by Kurata and Stockmayer[11, 12] from intrinsic viscosity and molecular weight data[14] for low molecular weight polyethylene glycols does not seem tenable in the light of this discussion; presumably the excluded volume theory upon which the extrapolation methods are based does not extend to the very low molecular weight poly(ethylene oxides) ($M < 10^4$), which are unlikely to be random coils.

It is possible, as suggested by Hughes *et al.*[15], that the unperturbed dimensions estimated from data obtained in good solvents depend upon the nature of the solvent. However, the agreement with the θ-solvent data already noted for poly(ethylene oxide) [and a further comparison made for poly(propylene oxide) in part III][16] leads one to suppose that this effect is not large with the poly(epoxides).

Department of Chemistry,
University of Manchester

REFERENCES

[1] BOOTH, C. and PRICE, C. *Polymer, Lond.* 1966, **7**, 87

[2] ALLEN, G., BOOTH, C. and HURST, S. J. *Polymer, Lond.* 1967, **8**, 385

[3] DESREUX, V. and BISCHOFF, J. *Bull. Soc. chim. Belg.* 1950, **59**, 93

[4] KAUFMAN, H. S. and SOLOMON, E. *Industr. Engng Chem. (Industr.)* 1953, **45**, 1779

[5] See, for example, PEAKER, F. W. *Techniques of Polymer Characterization,* ALLEN, D. W., Ed. Butterworths: London, 1959

[6] ALLEN, G., BOOTH, C. and JONES, M. N. *Polymer, Lond.* 1964, **5**, 195

[7] ROSSI, C. and CUNIBERTI, C. *J. Polym. Sci. B,* 1964, **2**, 681

[8] BAILEY, F. E. and CALLARD, R. W. *J. appl. Polym. Sci.* 1959, **1**, 56; BAILEY, F. E., KUCERA, J. L. and IMHOF, L. G. *J. Polym. Sci.* 1958, **32**, 517

[9] KURATA, M., STOCKMAYER, W. H. and ROIG, A. J. *J. chem. Phys.* 1960, **33**, 151

[10] STOCKMAYER, W. H. and FIXMAN, M. *J. Polym. Sci. C,* 1963, **1**, 137

[11] KURATA, M. and STOCKMAYER, W. H. *Fortschr. Hochpolym.-Forsch.* 1963, **3**, 196

[12] KURATA, M., IWAMA, M. and KAMADA, K. *Polymer Handbook,* BRANDRUP, J. and IMMERGUT, E. H., Editors. Interscience Publishers: New York, 1965

[13] BAUMANN, H. *J. Polym. Sci. B,* 1965, **3**, 1069

[14] SADRON, C. and REMPP, P. *J. Polym. Sci.* 1958, **29**, 127

[15] HAMORI, E., PRUSINOWSKI, L. R., SPARKS, P. G. and HUGHES, R. E. *J. phys. Chem.* 1965, **69**, 1101

[16] ALLEN, G., BOOTH, C. and PRICE, C. *Polymer, Lond.* 1967, **8**, 397

III—The Unperturbed Dimensions of Poly(propylene oxide)

G. ALLEN, C. BOOTH and C. PRICE

Intrinsic viscosity and light scattering data are reported for fractions of poly(propylene oxide) in a theta solvent, isooctane at 50°C. These results are used to obtain a value for the unperturbed dimensions of poly(propylene oxide), i.e. $(\overline{r^2}/M)^{\frac{1}{2}} = 0 \cdot 80$ *Å.*

NUMEROUS methods have been developed for the determination of the unperturbed dimensions of polymer coils and these have been the subject of a recent review[1]. Measurement of the chain dimensions in a theta solvent using the light scattering technique is the most direct method and is reliable provided well characterized fractions of fairly narrow molecular weight distribution are used. Another useful method of estimation involves the measurement of the intrinsic viscosity, $[\eta]$, in a theta solvent and the use of the relationship[2],

$$[\eta] = \Phi \, (\overline{r_0^2})^{3/2}/M$$

where $\overline{r_0^2}$ is the unperturbed mean square end-to-end distance of the polymer coils, M is the molecular weight, and Φ is a parameter which may be calculated from theory. If a theta solvent is not available unperturbed dimensions can still be obtained from intrinsic viscosity and molecular weight measurements in good solvents, e.g. by means of the method of Kurata, Stockmayer and Roig[3].

In order to apply these methods successfully to a polymer it is necessary to define a theta solvent in which light scattering measurements can be made, and also to develop a method of fractionation which yields fractions

REFERENCES

[1] BOOTH, C. and PRICE, C. *Polymer, Lond.* 1966, **7**, 87
[2] ALLEN, G., BOOTH, C. and HURST, S. J. *Polymer, Lond.* 1967, **8**, 385
[3] DESREUX, V. and BISCHOFF, J. *Bull. Soc. chim. Belg.* 1950, **59**, 93
[4] KAUFMAN, H. S. and SOLOMON, E. *Industr. Engng Chem. (Industr.)* 1953, **45**, 1779
[5] See, for example, PEAKER, F. W. *Techniques of Polymer Characterization*, ALLEN, D. W., Ed. Butterworths: London, 1959
[6] ALLEN, G., BOOTH, C. and JONES, M. N. *Polymer, Lond.* 1964, **5**, 195
[7] ROSSI, C. and CUNIBERTI, C. *J. Polym. Sci. B*, 1964, **2**, 681
[8] BAILEY, F. E. and CALLARD, R. W. *J. appl. Polym. Sci.* 1959, **1**, 56; BAILEY, F. E., KUCERA, J. L. and IMHOF, L. G. *J. Polym. Sci.* 1958, **32**, 517
[9] KURATA, M., STOCKMAYER, W. H. and ROIG, A. J. *J. chem. Phys.* 1960, **33**, 151
[10] STOCKMAYER, W. H. and FIXMAN, M. *J. Polym. Sci. C*, 1963, **1**, 137
[11] KURATA, M. and STOCKMAYER, W. H. *Fortschr. Hochpolym.-Forsch.* 1963, **3**, 196
[12] KURATA, M., IWAMA, M. and KAMADA, K. *Polymer Handbook*, BRANDRUP, J. and IMMERGUT, E. H., Editors. Interscience Publishers: New York, 1965
[13] BAUMANN, H. *J. Polym. Sci. B*, 1965, **3**, 1069
[14] SADRON, C. and REMPP, P. *J. Polym. Sci.* 1958, **29**, 127
[15] HAMORI, E., PRUSINOWSKI, L. R., SPARKS, P. G. and HUGHES, R. E. *J. phys. Chem.* 1965, **69**, 1101
[16] ALLEN, G., BOOTH, C. and PRICE, C. *Polymer, Lond.* 1967, **8**, 397

III—The Unperturbed Dimensions of Poly(propylene oxide)

G. ALLEN, C. BOOTH and C. PRICE

Intrinsic viscosity and light scattering data are reported for fractions of poly(propylene oxide) in a theta solvent, isooctane at 50°C. These results are used to obtain a value for the unperturbed dimensions of poly(propylene oxide), i.e. $(\overline{r^2}/M)^{\frac{1}{2}} = 0.80$ Å.

NUMEROUS methods have been developed for the determination of the unperturbed dimensions of polymer coils and these have been the subject of a recent review[1]. Measurement of the chain dimensions in a theta solvent using the light scattering technique is the most direct method and is reliable provided well characterized fractions of fairly narrow molecular weight distribution are used. Another useful method of estimation involves the measurement of the intrinsic viscosity, $[\eta]$, in a theta solvent and the use of the relationship[2],

$$[\eta] = \Phi \, (\overline{r_0^2})^{3/2}/M$$

where $\overline{r_0^2}$ is the unperturbed mean square end-to-end distance of the polymer coils, M is the molecular weight, and Φ is a parameter which may be calculated from theory. If a theta solvent is not available unperturbed dimensions can still be obtained from intrinsic viscosity and molecular weight measurements in good solvents, e.g. by means of the method of Kurata, Stockmayer and Roig[3].

In order to apply these methods successfully to a polymer it is necessary to define a theta solvent in which light scattering measurements can be made, and also to develop a method of fractionation which yields fractions

of fairly narrow molecular weight distribution. We have already des-
cribed[4] a suitable theta solvent for poly(propylene oxide), i.e. isooctance at
50°C. It has also been shown[5] that high molecular weight poly(propylene
oxide), prepared by means of the zinc diethyl and water catalyst, can be
separated on the basis of its solubility in isooctane into fractions which are
identical in average molecular weight and molecular weight distribution,
but which differ in degree of stereoregularity. The more crystalline frac·
tions are known[6] to consist of polymer with a high degree of isotacticity.
The nature of the irregularities in the less crystalline fraction is unclear:
head to head linkages are common in low molecular weight poly(propylene
oxide)[7], but there is no direct evidence that this is true for the high polymer
which is produced by a different propagation reaction[8]. Data published
earlier[4] pertain to fractions crystallized from isooctane and so of molecular
weight distribution similar to that of the whole polymer. However, one
sample had been prepared by mechanical degradation of a very high mole-
cular weight polymer in solution, and was probably of fairly narrow
molecular weight distribution: we estimate that $\bar{M}_w/\bar{M}_n$ for these fractions
was 1·5. Rather than base our study wholly on fractions of this type, we
have also isolated fractions in the conventional manner by liquid–liquid
phase separation of partially crystalline poly(propylene oxide) above its
melting point.

EXPERIMENTAL

Preparation

The polymer was prepared in dioxan solution using a zinc diethyl–water
catalyst[8]. Briefly, propylene oxide (6·8 mole l^{-1}), zinc diethyl (0·52 mole
l^{-1}) and water (0·48 mole l^{-1}) were mixed under high vacuum conditions
and allowed to polymerize at 25°C for one week. The resulting mixture
was dissolved in benzene to which had been added a little methanol, and the
catalyst residues were removed by centrifugation. The partially crystalline
product was finally isolated by freeze drying.

Fractionation

A sample of the whole polymer (identical to that originally[4] designated
part A) was separated into two fractions, crystallizable and non-crystal-
lizable, by precipitation from isooctane at 40°C; similar separations have
been discussed in detail earlier[5]. The crystallizable fraction was then frac-
tionated with respect to molecular weight by liquid–liquid phase separation
at a temperature above the melting point of the polymer. This was achieved
by the successive addition of quantities of octamethyltetrasiloxane, a non-
solvent, to a dilute solution (1 g l^{-1}) of the polymer in isooctane at 75°C.
Following each addition of non-solvent the temperature was raised to
~90°C and then lowered slowly to 75°C in order to ensure an equilibrium
phase separation. Each precipitate was isolated by syphoning off the
dilute phase, washing in isooctane at room temperature in order to remove
the octamethyltetrasiloxane, and finally freeze drying from benzene
solution.

Intrinsic viscosity and light scattering

The experimental methods we adopted in performing these measure-
ments are described in earlier papers[4,9].

RESULTS AND DISCUSSION

We have measured dilute solution properties of three kinds of fractions of the poly(propylene oxide).

(A) Fractions obtained by successive crystallization from isooctane of the whole polymer. The methods used and data obtained have been reported earlier[4]. These fractions have wide molecular weight distributions and our measurements of their properties are not pertinent here.

(B) Fractions obtained by fractional crystallization from isooctane of a sample of the polymer which had been mechanically degraded in solution. The methods used and the fractionation data obtained have been reported earlier[4]: in this discussion the designation (B) and the numbering of the fractions are identical with those used earlier[4].

(C) Fractions obtained by successive precipitation of liquid phases from dilute solution of the crystallizable part of the polymer. These fractions are designated C. The fraction data are recorded in *Table 1*; they are not complete because the method of isolating the fractions was perfected by use of fraction C1, and the work led to excessive degradation of this fraction.

Table 1. Fractionation of poly(propylene oxide) (sample C) from isooctane–octamethyltetrasiloxane mixtures at 75°C

Fraction No.	Weight %	$[\eta]$ (benzene at 25°C) (dl g^{-1})	Fraction No.	Weight %	$[\eta]$ (benzene at 25°C) (dl g^{-1})
C1	20·3	—	C4	32·5	5·0
C2	11·4	9·5	C5	10·0	2·4
C3	12·5	6·4	residue	13·3	—

In *Table 2* we have listed results of interest for fractions B and C. The data include intrinsic viscosities, in isooctane at 50°C and in benzene at

Table 2. Light scattering and intrinsic viscosity data for fractions of poly(propylene oxide)

Fraction No.	$[\eta]$ (dl g^{-1}) Benzene at 25°C	$\overline{M}_v \times 10^{-6}$	$[\eta]$ (dl g^{-1}) Isooctane at 50°C	$(\overline{S^2})^{\frac{1}{2}}_z$ (Å)	$\overline{M}_w \times 10^{-6}$
B1	3·77	0·76	1·13	358	0·78
B5	4·03	0·83	—	339	0·88
B6	3·86	0·78	1·11	—	—
B8	4·04	0·83	1·25	340	0·90
C2	9·5	2·51	2·39	—	—
C3	6·9	1·51	1·74	—	—
C4	5·0	1·10	1·41	—	—
C5	2·40	0·421	0·94	—	—

25°C, weight-average molecular weight ($\overline{M}_w$), and z-average root-mean-square radii of gyration $(\overline{S^2})^{\frac{1}{2}}_z$, measured by light scattering in isooctane at 50°C. The viscosity-average molecular weights, also listed, were calculated from $[\eta]$ in benzene at 25°C by means of the relation[9],

$$[\eta] = 1·12 \times 10^{-4} (\overline{M}_v)^{0·77}$$

Table 3. Values of the ratio $(\overline{(r_0^2)}/M)^{\frac{1}{2}}$ for poly(propylene oxide) fractions

Fraction No.	$(\overline{(r_0^2)}/M)^{\frac{1}{2}} \times 10^3$ from $[\eta]$ (Å)	$(\overline{(r_0^2)}/M)^{\frac{1}{2}} \times 10^3$ from $\overline{(S_0^2)}_z$ (Å)	Fraction No.	$(\overline{(r_0^2)}/M)^{\frac{1}{2}} \times 10^3$ from $[\eta]$ (Å)
B1	789	865	C2	840
B5	—	770	C3	804
B6	785	—	C4	791
B8	796	765	C5	809

The log–log plot of intrinsic viscosity in isooctane at 50°C against viscosity-average molecular weight has, within experimental error, a slope of 0·5. The finding lends support to the value $\theta = 50°C$ determined earlier[4] from the intercepts of the plots of second virial coefficient (A_2) versus temperature upon the $A_2 = 0$ axis.

In *Table 3* we list values of the parameter $(\overline{r_0^2}/M)^{\frac{1}{2}}$. These were calculated from the data of *Table 2* by means of the equations given below, with values of $\overline{M}_w/\overline{M}_n$ ($\sim \overline{M}_v/\overline{M}_n$) of 1·2 for the fractions C obtained by liquid–liquid phase separation and 1·5 for the fractions B obtained by fractional crystallization of the whole polymer.

For the light scattering data (fractions B) we used the equations:

$$(\overline{r_0^2})_z^{\frac{1}{2}} = 6^{\frac{1}{2}} (\overline{s_0^2})_z^{\frac{1}{2}}$$

$$(\overline{r_0^2})_w^{\frac{1}{2}} = 0·88 (\overline{r_0^2})_z^{\frac{1}{2}} \quad (\text{ref. } 10)$$

and

$$(\overline{r_0^2}/M)^{\frac{1}{2}} = [(\overline{r_0^2})_w/\overline{M}_w]^{\frac{1}{2}}$$

For the intrinsic viscosity data we used the equations:

$$[\eta] = \Phi [(\overline{r_0^2})/M](\overline{M}_w)^{\frac{1}{2}} [(\overline{M^{\frac{1}{2}}})_w/(\overline{M}_w)^{\frac{1}{2}}] \quad (\text{ref. } 11)$$

where

$$\Phi = 2·87 \times 10^{23} \text{ g}^{-1}$$

Within experimental error the values of $(\overline{r_0^2}/M)^{\frac{1}{2}}$ are identical for the fractions which crystallize from isooctane at 40°C (average value 810×10^{-3} Å) and the fraction B8 which remained soluble (780×10^{-3} Å). This insensitivity of unperturbed dimensions to degree of isotacticity is consistent with results for other polymers[12]. In itself, however, this result is difficult to interpret since it may well be that the fractions we have studied cover only a small range of degrees of isotacticity.

Intrinsic viscosities in hexane at 46°C and weight-average molecular weights have been reported earlier[9] for four narrow fractions of poly(propylene oxide). Using the method of Kurata, Stockmayer and Roig, together with these data, we obtain a value of 750×10^{-3} Å for $(\overline{r_0^2}/M)$. This value compares well with those listed above, and also with the value obtained by Kurata and Stockmayer[1] from the data of Moacanin[13] for polyurethanes. This agreement is most satisfactory and lends support to the unperturbed dimensions evaluated in part II[14].

400

REFERENCES

[1] KURATA, M. and STOCKMAYER, W. H. *Fortschr. Hochpolym.-Forsch.* 1963, **3**, 196
[2] FLORY, P. J. and FOX, T. G. *J. Amer. chem. Soc.* 1951, **73**, 1904
[3] KURATA, M., STOCKMAYER, W. H. and ROIG, A. *J. chem. Phys.* 1960, **33**, 151
[4] ALLEN, G., BOOTH, C. and PRICE, C. *Polymer, Lond.* 1966, **7**, 167
[5] ALLEN, G., BOOTH, C. and JONES, M. N. *Polymer, Lond.* 1964, **5**, 257
[6] STANLEY, E. and LITT, M. *J. Polym. Sci.* 1960, **43**, 453
[7] PRICE, C. C. and SPECTOR, R. *J. Amer. chem. Soc.* 1965, **87**, 2069
[8] BOOTH, C., HIGGINSON, W. C. E. and POWELL, E. *Polymer, Lond.* 1964, **5**, 479
[9] ALLEN, G., BOOTH, C. and JONES, M. N. *Polymer, Lond.* 1964, **5**, 195
[10] BEATTIE, W. H. and BOOTH, C. *J. Polym. Sci.* 1960, **44**, 81
[11] NEWMAN, S., KRIGBAUM, W. R., LANGIER, C. and FLORY, P. J. *J. Polym. Sci.* 1954, **14**, 451
[12] KRIGBAUM, W. R. *Newer Methods of Polymer Characterization*, edited by B. KE. Interscience: New York, 1964
[13] MOACANIN, J. *J. appl. Polym. Sci.* 1959, **1**, 272
[14] ALLEN, G., BOOTH, C., HURST, S. J., JONES, M. N. and PRICE, C. *Polymer, Lond.* 1967, **8**, 391

IV—Proton Spin-Lattice Relaxation in Poly(styrene oxide) and Poly(t-butyl ethylene oxide)

G. ALLEN, D. J. BLEARS* and T. M. CONNOR

Proton spin–lattice relaxation times (T_1) within the temperature range $-155°$ to $+175°C$ are reported for fractions of the poly(tBEO) and the poly(styrene oxide). Two T_1 minima were observed (at 30 Mc/s) for each polymer: $102°C$ and $-112°C$ for poly(tBEO); $127°C$ and $-130°C$ for poly(styrene oxide). The high temperature minima are associated with chain backbone motions, the low temperature minima with side group motions. Activation energies for both processes are derived and compared.

THE proton spin–lattice relaxation time, T_1, has been studied as a function of temperature for high molecular weight poly(styrene oxide) and poly(t-butyl ethylene oxide). For these polymers two distinct types of molecular motion are possible[1-6], one involving the chain backbone, the other the side group. The T_1 measurements were made in order to study these motions. Activation energies are derived from the slopes of $\log T_1$ versus $1/T°K$ (giving $\overset{+}{Q}$) and from areas under curves of $1/T_1$ versus $1/T \times 10^3$ °K (giving $\langle Q \rangle$). Also for poly(tBEO) for the low temperature methyl group rotation an activation energy is derived by utilizing Stejskal and Gutowsky's quantum mechanical tunnelling calculations.

EXPERIMENTAL

The methods of isolation of the fractions of poly(styrene oxide) and

---

*Present address: Argonne National Laboratory, Chicago, Illinois, U.S.A.

Department of Chemistry,
   University of Manchester   (Received November 1966)

REFERENCES

[1] KURATA, M. and STOCKMAYER, W. H. *Fortschr. Hochpolym.-Forsch.* 1963, **3**, 196

[2] FLORY, P. J. and FOX, T. G. *J. Amer. chem. Soc.* 1951, **73**, 1904

[3] KURATA, M., STOCKMAYER, W. H. and ROIG, A. *J. chem. Phys.* 1960, **33**, 151

[4] ALLEN, G., BOOTH, C. and PRICE, C. *Polymer, Lond.* 1966, **7**, 167

[5] ALLEN, G., BOOTH, C. and JONES, M. N. *Polymer, Lond.* 1964, **5**, 257

[6] STANLEY, E. and LITT, M. *J. Polym. Sci.* 1960, **43**, 453

[7] PRICE, C. C. and SPECTOR, R. *J. Amer. chem. Soc.* 1965, **87**, 2069

[8] BOOTH, C., HIGGINSON, W. C. E. and POWELL, E. *Polymer, Lond.* 1964, **5**, 479

[9] ALLEN, G., BOOTH, C. and JONES, M. N. *Polymer, Lond.* 1964, **5**, 195

[10] BEATTIE, W. H. and BOOTH, C. *J. Polym. Sci.* 1960, **44**, 81

[11] NEWMAN, S., KRIGBAUM, W. R., LANGIER, C. and FLORY, P. J. *J. Polym. Sci.* 1954, **14**, 451

[12] KRIGBAUM, W. R. *Newer Methods of Polymer Characterization*, edited by B. KE. Interscience: New York, 1964

[13] MOACANIN, J. *J. appl. Polym. Sci.* 1959, **1**, 272

[14] ALLEN, G., BOOTH, C., HURST, S. J., JONES, M. N. and PRICE, C. *Polymer, Lond.* 1967, **8**, 391

IV—Proton Spin-Lattice Relaxation in Poly(styrene oxide) and Poly(t-butyl ethylene oxide)

G. ALLEN, D. J. BLEARS* and T. M. CONNOR

Proton spin–lattice relaxation times (T_1) within the temperature range $-155°$ to $+175°C$ are reported for fractions of the poly(tBEO) and the poly(styrene oxide). Two T_1 minima were observed (at 30 Mc/s) for each polymer: $102°C$ and $-112°C$ for poly(tBEO); $127°C$ and $-130°C$ for poly(styrene oxide). The high temperature minima are associated with chain backbone motions, the low temperature minima with side group motions. Activation energies for both processes are derived and compared.

THE proton spin–lattice relaxation time, T_1, has been studied as a function of temperature for high molecular weight poly(styrene oxide) and poly(t-butyl ethylene oxide). For these polymers two distinct types of molecular motion are possible[1-6], one involving the chain backbone, the other the side group. The T_1 measurements were made in order to study these motions. Activation energies are derived from the slopes of $\log T_1$ versus $1/T°K$ (giving $\overset{+}{Q}$) and from areas under curves of $1/T_1$ versus $1/T \times 10^3$ °K (giving $\langle Q \rangle$). Also for poly(tBEO) for the low temperature methyl group rotation an activation energy is derived by utilizing Stejskal and Gutowsky's quantum mechanical tunnelling calculations.

EXPERIMENTAL

The methods of isolation of the fractions of poly(styrene oxide) and

---

*Present address: Argonne National Laboratory, Chicago, Illinois, U.S.A.

poly(tBEO) used in this work are described in ref. 7. The poly(styrene oxide) was fraction 1 of *Table 1*, ref. 8 and had $\overline{M}_v$ $2 \cdot 5 \times 10^6$, $T_m = 162°C$; the poly(tBEO) was fraction 2 of *Table 1*, ref. 7 and had $\overline{M}_v$ 5×10^6, $T_m = 150°C$.

The proton spin–lattice relaxation times were measured within the temperature range $+175°C$ to $-155°C$, using pulse techniques[9, 10], a π, $\pi/2$ pulse train being employed[11]. The spectrometer operating frequency was 30 Mc/s, the $\pi/2$ pulse being of $\sim 1 \cdot 5$ μsec duration with a subsequent receiver recovery time of 5 μsec. The relaxation time is given by the expression

$$h(t) = h_0 [1 - 2 \exp(-t/T_1)]$$

where $h(t)$ is the length of the induction decay signal after the $\pi/2$ pulse, h_0 is the height of the decay in the absence of the π pulse and t is the time between the π and $\pi/2$ pulses. Temperature variation at the samples was achieved by the use of a gas flow cryostat[12]. Non-exponential decays of the induction signal following the $\pi/2$ pulse were not observed although the low signal-to-noise ratio of poly(styrene oxide) and poly(tBEO) would cause T_1s differing by a small factor to go undetected.

RESULTS AND DISCUSSION

The experimental results are shown in *Figure 1* for poly(styrene oxide) and poly(tBEO). The plots in *Figure 1* show two minima corresponding to the
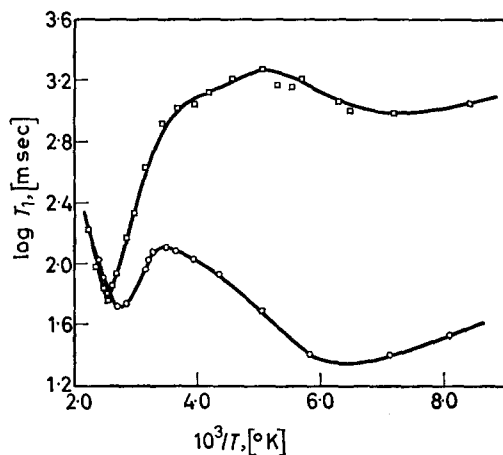
Figure 1—Experimental log T_1 against $(1/T) \times 10^3$ for poly(styrene oxide) □, and poly(t-butyl ethylene oxide) ○

two types of motion mentioned previously. Confirmation of the association of the high temperature minimum with backbone motions and the low temperature minimum with side-group motions has been shown by numerous studies on other polymers[1, 3, 4, 6, 11] and particularly from deuteration and dilution experiments[3, 5, 13]. Results quoted briefly for these polymers in a previous communication[13] differ slightly from those reported in this paper due to the higher purity of the samples used in the present instance.

The temperatures of the high and low temperature minima are shown in *Table 1*, together with the corresponding values of $(T_1)_{min}$.

The temperature at which the high temperature $(T_1)_{\text{min.}}$ occurs rises as the size of the side group increases in the order $Ph \geqslant Bu^t > H^{13}$. Although chain configuration can be expected to influence the temperature of $(T_1)_{\text{min.}}$

Table 1. High and low temperature minima for poly(styrene oxide) and poly(*t*-butyl ethylene oxide)

Sample	M.pt °C	$(T_1)_{\text{min.}}$ msec	High temp. minimum °C	$(T_1)_{\text{min.}}$ msec	Low temp. minimum °C
Poly(styrene oxide)	162	58	127	950	−130
Poly(*t*BEO)	150	50	102	23	−112

it is most likely that the above trend reflects the fact that the ease of backbone motion of the polymers is strongly influenced by the substituent side group. The Ph group, combining bulk and strong dispersion forces, is the most efficient in restricting the motional freedom of the skeleton. The $(T_1)_{\text{min.}}$ occurs in each polymer at a temperature well below its melting point and hence there is no direct correlation between the two phenomena.

The temperatures at which the low temperature minima occur are in the order poly(*t*BEO) > poly(styrene oxide) and hence at temperatures when reorientational motions of the methyl groups on poly(*t*BEO) have been frozen out, motional effects in poly(styrene oxide) are still manifest. In view of the size and planar geometry of the Ph group it is likely that motions of this side group are of a cooperative nature and are so restricted that rotation is absent, the motion being confined to oscillations of small amplitude. This hypothesis is also supported by the unusually large value of $(T_1)_{\text{min.}}$ in poly(styrene oxide) (950 msec) compared to that in poly(*t*BEO) (23 msec), although this in part can be attributed to the larger interproton distance in Ph as compared with Bu^t.

Previous work on poly(propylene oxides)[5] and poly(1-butene oxides)[13] indicated the approximate validity of the Kubo and Tomita equation[14] describing relaxation times in which intramolecular processes are the dominant cause of the relaxation. For the intramolecular contribution,

$$\frac{1}{T_1} = A \left[\frac{\tau}{1 + \omega^2 \tau^2} + \frac{4\tau}{1 + 4\omega^2 \tau^2} \right] \tag{1}$$

where $A = 3\gamma^4 h^2 / 10r^6$, $\omega = 30$ Mc/s and τ is a molecular correlation time. Equation (1) is derived on the basis of a single correlation time applied to a two-spin system. It is thus not strictly applicable to poly(styrene oxide) and poly(*t*BEO). Agreement between experimental relaxation times and those derived from equation (1) can often be improved by introduction of a distribution of correlation times derived from dielectric data[11, 15].

Activation parameters have been derived from the T_1 measurements by a variety of methods. The slopes of the curves of $\log T_1$ against $1/T \times 10^3$ give (assuming a single correlation time) activation energies, $\overset{\pm}{Q}$ for both the high and low temperature minima. On the high temperature side of the minima in the limit $\omega\tau \ll 0\cdot616$, the slope is $-\overset{+}{Q}/2\cdot303R$, whilst on the low temperature side of the minima ($\omega \gg 0\cdot616$) the slope is $+\overline{Q}/2\cdot303R$[15].

Activation energies $\langle Q \rangle$ can be derived from the expression[15]

$$\frac{1}{\langle Q \rangle} = \frac{2\omega}{3\pi AR} \int_0^\infty \left(\frac{1}{T_1}\right) d\left(\frac{1}{T}\right) \tag{2}$$

where the integral represents the area (a) under the $1/T_1$ versus $1/T \times 10^3$ curve and $\langle Q \rangle$ is a mean activation energy over the distribution. A can be derived from equation (1) using the value of T_1 at the minimum, where $\omega\tau = 0.616$. In this case equation (1) gives

$$1/(T_1)_{\min.} = A\,[7.558 \times 10^{-9}] \tag{3}$$

The activation energy evaluated using (2) and (3) is $\langle Q \rangle'$. Since A in equation (1) is equal to $3\gamma^4 h^2/10r^6$, it can be determined by assuming a CH bond distance of 1.091 Å and a tetrahedral angle, giving $A = 5.39 \times 10^9$. The activation energy derived from this value of A and (2) is $\langle Q \rangle''$.

For the rotation of methyl groups, as in the low temperature minimum of poly(tBEO), equation (1) can be modified[6] so that $A = 9\gamma^4 h^2/40r^6 = 4.04 \times 10^9$. Combination of this A value and equation (2) gives $\langle Q \rangle'''$. In addition, a further quantity E can be associated with the low temperature reorientation of the methyl groups in poly(tBEO). The quantity E is the barrier height for methyl group rotation derived from Stejskal and Gutowsky's calculations[16] relating relaxation times to the temperature dependence of the CH_3 reorientation frequency assuming a sinusoidal barrier[17]. The reorientational correlation frequency ν_r (in c/s) corresponding to the low temperature minimum in T_1 is given by[6, 16]

$$\tau = 1/3\pi\nu_r$$

with $\omega\tau = 0.616$ and $\nu_r = 3.25 \times 10^7$ c/s. By interpolation on the diagram given by Stejskal and Gutowsky[16] for different values of barrier height V_0, a value of E corresponding to the position of the low temperature minimum can be deduced.

The experimental activation energies derived as above are given in *Table 2*.

Table 2. Activation energies for poly(styrene oxide) and poly(t-butyl ethylene oxide)

High temperature minimum

Sample	a sec^{-1}	A $\times 10^{-9}$	$\langle Q \rangle'$ kcal/ mole	A $\times 10^{-9}$	$\langle Q \rangle''$ kcal/ mole	$+$ $Q(\omega\tau \leqslant 0.616)$ kcal/mole	$-$ $Q(\omega\tau \geqslant 0.616)$ kcal/mole
Poly(styrene oxide)	0.013	2.30	9.0	5.39	21.1	9.2	7.8
Poly(tBEO)	0.024	2.6	(5.4)*	5.39	11.3	4.8	(2.8)*

Low temperature minimum

Sample	a sec^{-1}	A $\times 10^{-9}$	$\langle Q \rangle'$ kcal/ mole	A $\times 10^{-9}$	$\langle Q \rangle'''$ kcal/ mole	V_0 cm^{-1}	E kcal/ mole	$+$ $Q(\omega\tau \leqslant 0.616)$ kcal/mole	$-$ $Q(\omega\tau \geqslant 0.616)$ kcal/mole
Poly(styrene oxide)	0.018	0.14	(0.4)†					0.9	0.8
Poly(tBEO)	0.138	6.13	(2.2)†	4.04	1.5	1 416	4.1	(1.7)†	1.1

*Difficult to estimate due to overlap with low temperature minimum.
†Difficult to assess due to shallow curve.
‡Overestimate due to overlap with high temperature minimum.

For the purpose of comparison the assumption is made that the activation energies $\overset{\pm}{Q}$ do not vary with temperature. This may be a considerable approximation for motions causing the high temperature minimum[15] in poly(styrene oxide) and poly(tBEO). However, for measurements at 30 Mc/s the temperature at which the T_1 minimum occurs is normally sufficiently greater than the glass transition temperature, T_g, for Q not to be varying very rapidly with temperature. The effect on Q of the melting point, which in both cases lies considerably above the T_1 minimum temperature, is not so clear although no discontinuities appear in the T_1 curves when melting occurs. For each polymer, $\overset{\pm}{Q}$ (calculated from the limiting slope, $\omega\tau \ll 0.616$) is greater than $\overset{-}{Q}$ (calculated from the limiting slope, $\omega\tau \gg 0.616$), neither including the effects of a distribution. The mean of these is always less than the activation energy derived from equation (2) which includes a distribution. Hence, although $\overset{+}{Q}$ is not varying appreciably with temperature, the indication is that the polymers do show some distribution in the energies of activation of the relaxation process. On other grounds, however, it seems unreasonable that $\overset{+}{Q} > \overset{-}{Q}$ for the high temperature minimum, since it is well known from dielectric studies that the apparent Q for the molecular motion commencing at T_g decreases with increase in temperature, as would be expected for a cooperative motion, the molecular correlation time being given by an expression[15] such as $\tau = \tau_0 \exp [B/(T - T_\infty)]$, where $T_\infty \sim T_g$. The larger Q at low temperatures is probably due to overlap with the low temperature minimum in the case of poly(tBEO). Likely contributing causes are a diminution of T_1 at low temperatures due to relaxation mechanisms not described by equation (1), such as spin-diffusion to paramagnetic impurities or lattice defect centres.

There are large differences between $\langle Q \rangle'$, derived from an experimental A based on a $(T_1)_{min.}$ value and (3) and $\langle Q \rangle''$, derived from a calculated A and (3). The closer agreement of the former with values of $\overset{\pm}{Q}$ and its more realistic derivation makes this activation energy more reliable.

For the high temperature minima of poly(styrene oxide) and poly(tBEO), the activation energies are in the order $Ph > Bu^t$. As expected from a consideration of T_1 minimum temperatures the Ph group restricts chain backbone motion more effectively than does Bu^t.

For the low temperature minimum in poly(tBEO) the experimental and calculated values of A are again only in fair agreement. These result in values of $\langle Q \rangle' = 2.2$ kcal/mole and $\langle Q \rangle''' = 1.5$ kcal/mole respectively for the barrier hindering the methyl group rotation. The former value is in good agreement with that in polyacetaldehyde[6] where $\langle Q \rangle'$ is also 2.2 kcal/mole. The value of E for poly(tBEO) is 4.1 kcal/mole also in good agreement with $E = 4.55$ kcal/mole in polyacetaldehyde[6], and greater than other values of the activation energy given. The agreement between the classical activation energy $\langle Q \rangle'$ and E is not good, which may be due to the unsatisfactory assumptions made in calculating the reorientation frequency[16], the theory having been found unsatisfactory in other cases[6, 18, 19].

For poly(styrene oxide) the shallow low temperature minimum indicated, as mentioned previously, that little relaxation occurs due to reorientational effects of the phenyl group. A similar result has been found for polystyrene[4]. It is likely that the bulky phenyl groups are packed in the partially crystalline polymer in such a way as effectively to prevent independent reorientational motions[20], the small minimum being caused by phenyl group oscillations[4]. However, at the present time the nature of the molecular motions responsible for these shallow relaxation minima is not clear.

This work was carried out in part while D.J.B. was a guest scientist in the Basic Physics Division of the National Physical Laboratory, Teddington.

Department of Chemistry,
  University of Manchester

National Physical Laboratory,
  Teddington, Middlesex

REFERENCES

[1] KAWAI, T. *J. phys. Soc. Japan,* 1961, **16**, 1220
[2] HIRAI, A. and KAWAI, T. *Mem. Coll. Sci. Univ. Tokyo,* 1961, **29**, No. 3
[3] POWLES, J. G. and MANSFIELD, P. *Polymer, Lond.* 1962, **3**, 336 and 339
[4] HUNT, B. I., POWLES, J. G. and WOODWARD, A. E. *Polymer, Lond.* 1964, **5**, 323
[5] CONNOR, T. M., BLEARS, D. J. and ALLEN, G. *Trans. Faraday Soc.* 1965, **61**, 1097
[6] CONNOR, T. M. *Polymer, Lond.* 1964, **5**, 265
[7] ALLEN, G., BOOTH, C. and HURST, S. J. *Polymer, Lond.* 1967, **8**, 385
[8] ALLEN, G., BOOTH, C., HURST, S. J., PRICE, C., VERNON, F. and WARREN, R. F. *Polymer, Lond.* 1967, **8**, 406
[9] HAHN, E. L. *Phys. Rev.* 1950, **80**, 580
[10] CARR, H. Y. and PURCELL, E. M. *Phys. Rev.* 1954, **94**, 630
[11] ALLEN, G., CONNOR, T. M. and PURSEY, H. *Trans. Faraday Soc.* 1963, **59**, 1525
[12] CONNOR, T. M. *Brit. J. appl. Phys.* 1963, **14**, 396
[13] CONNOR, T. M. and BLEARS, D. J. *Polymer, Lond.* 1965, **6**, 385
[14] KUBO, R. and TOMITA, K. *J. phys. Soc. Japan,* 1954, **9**, 888
[15] CONNOR, T. M. *Trans. Faraday Soc.* 1964, **60**, 1574
[16] STEJSKAL, E. O. and GUTOWSKY, H. S. *J. chem. Phys.* 1958, **28**, 388
[17] POWLES, J. G. and GUTOWSKY, H. S. *J. chem. Phys.* 1962, **23**, 1955
[18] RUSHWORTH, F. A. 13th Ampère Colloquium, Leuven, 1964
[19] STEJSKAL, E. O., WOESSNER, E. E., FARRAR, T. C. and GUTOWSKY, H. S. *J. chem. Phys.* 1959, **31**, 55
[20] POWLES, J. G., HUNT, B. I. and SANDIFORD, D. J. H. *Polymer, Lond.* 1964, **5**, 505

V—Melting Points, Glass Transition Temperatures and Dynamic Mechanical Properties of Poly(t-butyl ethylene oxide) and Poly(styrene oxide)

G. ALLEN, C. BOOTH, S. J. HURST*, C. PRICE, F. VERNON†
and R. F. WARREN

Melting points and glass transition temperatures, measured under pseudo-equilibrium conditions, are reported for fractions of poly(tBEO) and poly(styrene oxide). For all fractions of poly(tBEO) T_g was 35° ±1 deg. C

*Present address: John Dalton College of Technology, Manchester 1.
†Present address: Sheffield College of Technology.

and T_m was 149° ±1 deg. C. For the high molecular weight fractions of poly(styrene oxide) T_g was 40° ±2 deg. C. For the most crystalline fraction of poly(styrene oxide) T_m was 162°C. Mechanical loss spectra, within the temperature range −130° to +100°C and a frequency range 1 to 1 000 c/s, are given for a fraction of each polymer. In each spectrum a prominent loss peak (β dispersion) is associated with the glass transition. Other smaller loss peaks are also observed; one for poly(tBEO) and three for poly(styrene oxide). The frequency dependence of the temperature of location of the β dispersion is consistent with n.m.r. data. Activation energies for the β-process are calculated.

GLASS transitions, melting points, and dynamic mechanical properties of partially crystalline fractions of poly(t-butyl ethylene oxide) and poly(styrene oxide) have been studied. Additional information on molecular mobility in the amorphous regions of the specimens has been obtained from a comparison of the mechanical data with spin–lattice relaxation measurements[1] made on the same specimens.

<center>EXPERIMENTAL</center>

Materials

Poly(tBEO) fractions were those described in *Table 1* of ref. 2, obtained by precipitation from benzene. Six fractions were used in dilatometric studies, the small fifth fraction was omitted. All fractions were tough, fibrous and partially crystalline. Fraction 2, collected at 65°C by solid–liquid phase separation, was used in the dynamic mechanical measurements.

Poly(styrene oxide) fractions were obtained by dissolving 28 g of the polymer[2] in 2·5 l. of benzene. 7·3 g of the high molecular weight more crystalline polymer were precipitated by adding 1·9 l. of isooctane; this fraction was then redissolved in benzene and refractionated in the manner described[2]. The fractionation data are given in *Table 1*.

Table 1. Fractionation of the high molecular weight portion of poly(styrene oxide)

Fraction No.	Nature of precipitate	Wt %	[η] in toluene at 25°C (dl g⁻¹)
1	Crystalline	27·7	5·46
2	Translucent liquid	17·0	3·94
3	Translucent liquid	23·7	2·99
4	Liquid	12·2	2·33
5	Liquid	10·6	1·35
6	Residue	8·8	—

A fraction (II-10), obtained from a complete fractionation of the polymer carried out for the light scattering measurements, was also used: it was of low molecular weight ([η] = 0·065 dl g⁻¹ in toluene at 25°C). The fraction used for dynamic mechanical measurements was a portion of the amorphous residue from the initial separation. It was obtained by adding excess isooctane to a benzene solution of the residue, and it corresponds in molecular weight to fraction II-10.

Dilatometry

Transition temperatures were determined in conventional glass dilatometers with mercury as the containing fluid. Samples were degassed at

180°C for at least one day. At this temperature poly(styrene oxide) flowed readily and cylindrical samples were formed by using glass tubing as a mould. On the other hand poly(tBEO) would not flow and so the polymer was pressed at 90°C before being degassed again. The storage of samples before determination of transition temperatures, the severe treatment during preparation and the subsequent studies of the transition all contributed to the degradation of the polymer. This was very severe with poly(styrene oxide) (the intrinsic viscosity of fraction 2 fell from 3·94 to 0·33 dl g^{-1} during the course of our experiments) but much less so for poly(tBEO) for which [η] fell only 30 to 40 per cent. It is clear, however, that in neither case were we measuring the properties of fractions with very narrow molecular weight distributions.

For the glass transition measurements, the samples were held overnight at a temperature 15 deg. below T_g and then raised to $T_g + 15$°C at a rate of five degrees per hour. After standing overnight once more the temperature was lowered every hour in decrements of one degree and the meniscus reading made when the reading became constant. On reaching $T_g - 15$°C the procedure was reversed. The glass transition temperature was estimated from the readings taken on the cooling and the two heating cycles. There was no significant effect of rate of heating on the results.

Prior to the determination of T_m samples of both polymers were heated to 170°C and then annealed at 125°C. Poly(styrene oxide) crystallized slowly under these conditions and so the specimen was usually cooled to 70°C before annealing again at 125°C. For the determination of T_m the temperature was raised in increments of two to three degrees, and at each point approximately twelve hours were required for the attainment of an equilibrium meniscus reading.

Density measurements

The measurements on poly(styrene oxide) were made by flotation in aqueous solutions of copper sulphate. A specific gravity bottle was used for density measurements on poly(tBEO) because the values were < 1·0 g cm^{-3}; an attempt to use a flotation method employing methanol–water mixture was frustrated by absorption.

Dynamic mechanical measurements

The in-phase and out-of-phase components of the rigidity modulus were measured on the apparatus described by Wetton and Allen[3]. The specimen in the form of a small cylindrical rod was clamped vertically in a rigid support at its lower end. The upper end was clamped to a coil suspended between the poles of a strong permanent magnet and oscillated torsionally at the frequency of alternating current passing through the coil. A capacitance transducer recorded the response of the sample. Some modifications were made at the outset of the present work:

(1) The pin chuck previously used to clamp the lower end of the sample was replaced by a cup containing 'Araldite'; the cup was clamped to the rigid support and the sample was then set in the cup. This new technique reduced the distortion of the specimen.

(2) The driving current was fed to the coil through fine looped wire instead of through the pivots of the coil.

(3) Only one of the four vanes of the capacitance transducer was used because this improved the alignment of the oscillating system.

(4) The Attree capacitance meter was replaced by an M.700 L gauge oscillator and a frequency modulated gauge amplifier manufactured by Southern Instruments Ltd. The original instrument had an appreciable inherent phase lag which has been removed by this modification.

(5) A new thermostat housing was constructed to allow the vanes to be re-aligned and the sensitivity to be adjusted at low temperature by remote control. This avoided the necessity of dismantling the apparatus on occasions when the alignment was disturbed by thermal contraction of the supports.

<div align="center">RESULTS AND DISCUSSION</div>

Melting points and glass transition temperatures

All six fractions of poly(tBEO) have sufficiently high molecular weights to assume that the glass transition temperature has attained its upper limit. It is not surprising therefore that there is a spread of only three degrees in the results reported in *Table 2*. The actual measurements were reproducible to ± 1 deg. and so the most reliable limiting value for poly(tBEO) is $35° \pm 1$ deg. C. The melting points show no variation outside the probable limits of experimental error (again ± 1 deg.) and in this respect the results are very different from those reported in a similar study[4] of poly(propylene oxide) where T_m for the polymer fractions decreased from 73° to 58°C as fractionation proceeded. It will also be observed (*Table 2*) that the densities of the crystalline materials do not vary in a systematic manner; they all lie within the range 0.96 ± 0.01 g cm^{-3} and are all greater than the density of the amorphous polymer (0.93 ± 0.01 g cm^{-3}). Since all fractions probably

Table 2. Melting points (T_m), glass transition temperatures (T_g) and densities of fractions of poly(t-butyl ethylene oxide)

Fraction*	T_g	T_m	Density at 25°C, g cm^{-3}	
No.	°C	°C	Quenched	Annealed
1	36·1	149	0·92$_6$	0·95$_8$
2	35·2	149	0·93$_2$	0·96$_9$
3	35·4	149	0·94$_3$	0·96$_6$
4	35·0	150	0·92$_4$	0·95$_7$
6	33·9	149	0·92$_6$	0·96$_4$
7	33·0	149	0·93$_0$	0·95$_0$

*Numbers correspond to those in *Table 1* of ref. 2.

contain highly stereoregular polymer molecules, the variation in density is a combination of experimental error and variation in the degree of crystallinity caused by minor variations in thermal history.

For fractions of poly(styrene oxide) the limiting value for T_g is $40° \pm 2$ deg. C (*Table 3*). The range of melting points suggests that the first fraction is more crystalline than the remainder. However, its melting point, 162°C, is intermediate between that reported for poly(styrene oxide) isolated from a ferric chloride–water catalysed reaction (179°C)[5] and that reported for polymer isolated from an aluminium alkyl–water–chelate catalysed reaction (149°C)[6]. It is probable therefore that our first fraction has shorter stereoregular sequences than polymer isolated from the ferric

chloride catalyst system. None of the fractions was highly crystalline and the densities of the partially crystalline samples were only slightly higher than those of the corresponding amorphous quenched glass $(1 \cdot 148 \pm 0 \cdot 003$ g cm^{-3}). Accurate melting point determinations were hampered by the onset of severe degradation at temperatures $> 140°$C.

Dynamic mechanical properties

The results of the mechanical measurements are reported in terms of the in-phase (G') and out-of-phase (G'') components of the complex rigidity modulus $(G\star)$.

$$G\star = G' + iG''$$

The absolute accuracy of G' is ± 10 per cent, but relative values are

Table 3. Melting points (T_m), glass transition temperatures (T_g) and densities of fractions of poly(styrene oxide)

Fraction No.	T_g °C	T_m °C	Density at 25°C, g cm^{-3} Quenched
1	38·1	162	1·151
2	36·8	152	1·149
3	42·3	150	1·147
4	38·9	150	1·148
5	38·0	150	1·147
II-10	33·4	—	1·148

obtained with much higher precision. The error in G'' is ± 5 per cent for values greater than $0 \cdot 1$ G'.

The melting temperatures of both polymers lie outside the range of our instrument. Consequently no α-relaxation processes are observed in the mechanical measurements which are summarized in *Figures 1* and *2*. The figures show that each polymer has a strong dispersion in the region of 50°C, and these are assigned as the β-relaxation process corresponding to the glass transition temperature.

Poly(t-*butyl ethylene oxide*)

The β dispersion is located at 46°C at 1 c/s which compares satisfactorily with the dilatometric glass transition (35°C). As a consequence of the high degree of crystallinity of the sample G' falls only to 5×10^9 dyne cm^{-2} at temperatures above this transition region. There is an indication of a secondary (γ) dispersion centred at $-10°$C but its existence is uncertain since the strength of this loss peak (tan $\delta < 0 \cdot 01$) is well below the limiting sensitivity of the instrument[3].

Poly(*styrene oxide*)

The only sample studied was amorphous. Because the sample is un-crosslinked and non-crystalline the results are complicated by the onset of viscous flow at 60°C. The dilatometric glass transition for a similar sample (fraction II-10) is 33°C which compares with the location of the β-peak at 38°C at 1 c/s. In addition the polymer exhibits three weak subsidiary dispersions which will be termed γ_1, γ_2 and γ_3 respectively located at 20°, $-20°$ and $-85°$C at 1 c/s.

Figure 1—Dynamic mechanical measurements for poly(t-butyl ethylene oxide). The in-phase (G') and out-of-phase (G") rigidity moduli are plotted as functions of temperature
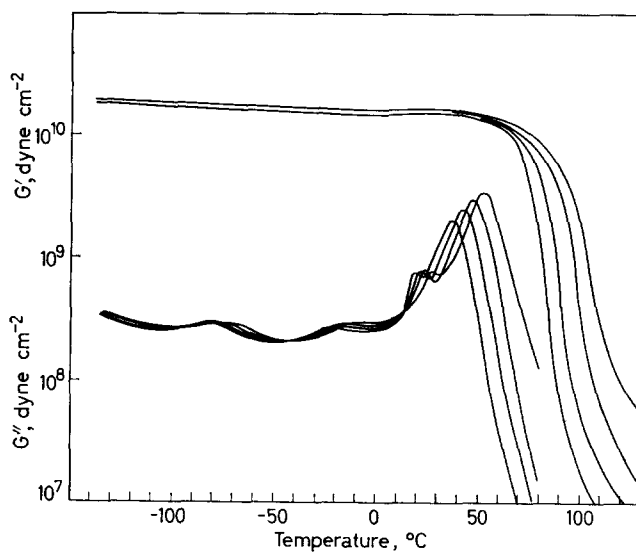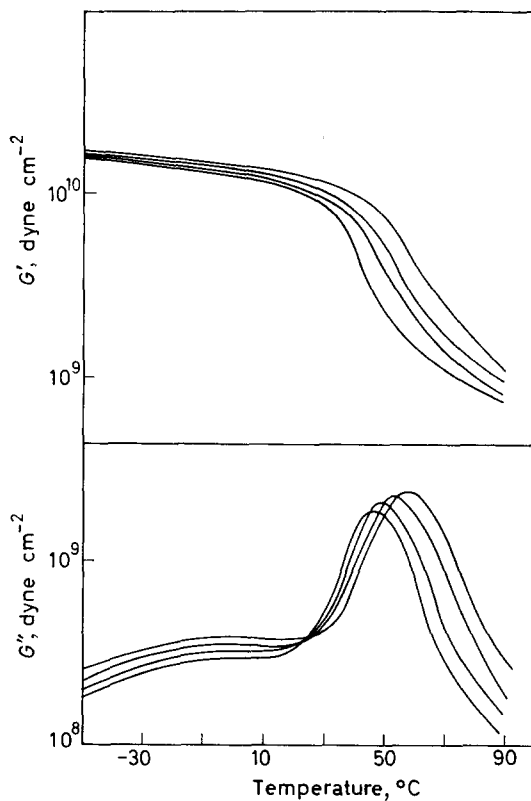
Figure 2—Dynamic mechanical measurements for poly(styrene oxide)

The γ_1 dispersion overlaps the low temperature wing of the β peak in G'' and it is particularly interesting because a very similar subsidiary dispersion is located on the side of the β-peak of polystyrene. *Figure 3* shows results
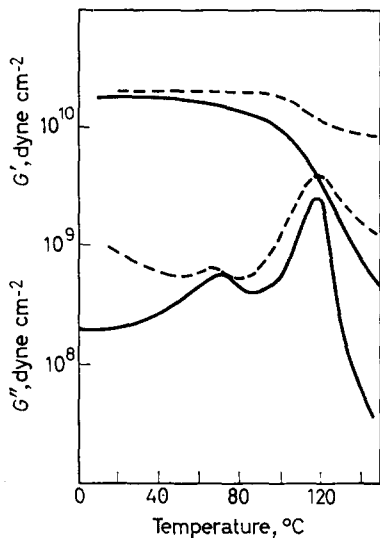
Figure 3—Dynamic mechanical measurements for atactic (full lines) and isotactic (broken lines) polystyrene

which we have obtained on a sample of amorphous polystyrene and also on an isotactic specimen which was approximately 50 per cent crystalline (estimated by density measurements). The strengths of both the γ_1 and β dispersions in polystyrene are reduced in the crystalline specimen and we conclude therefore that both loss mechanisms are located in the amorphous regions. The origin of the γ_1 peak in polystyrene has been attributed by Odajima[7] to rotation of the benzene rings. Kosfield[8] concludes from an n.m.r. study that it arises from a cooperative restricted turning motion of the benzene rings and this is endorsed by n.m.r. measurements[9] on polystyrene solutions. The relative strengths of the γ_1 and β dispersions are similar for both polystyrene and poly(styrene oxide) and the mechanism is likely to be the same in both materials.

Comparison of n.m.r. and mechanical measurements

The temperature dependence of the maxima in G'' is plotted as a function of frequency (f_m) in *Figure 4* for poly(tBEO) and the low molecular weight poly(styrene oxide). The location of the high temperature minima in T_1 measured at 30 Mc/s[1] are also shown for poly(tBEO) and high molecular weight poly(styrene oxide). The plot for poly(tBEO) confirms the assignment of the high temperature minimum in T_1 to the glass transition phenomenon. From the measurements of G'' as a function of temperature and frequency, and also from the area under the loss peak[10], we calculate the activation energies (ΔH) for the β processes to be:

$$\Delta H \quad \text{(kcal mole}^{-1})$$

poly(tBEO), β-relaxation   100 (from log f_m versus T^{-1})

     110 (from area under peak)
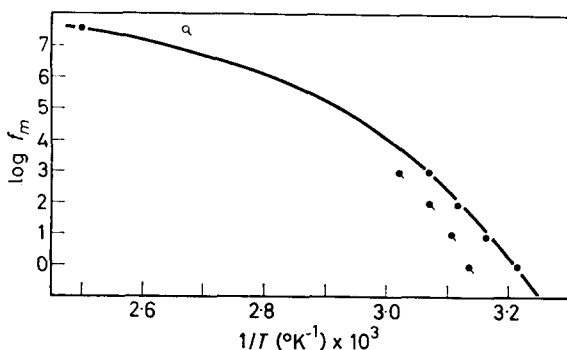
Figure 4—The location of the loss maxima of mechanical measurements ●, and the T_1 minimum of n.m.r. measurements ○, for poly(*t*-butyl ethylene oxide). Tagged points refer to poly(styrene oxide)

poly(styrene oxide), β-relaxation   80 (from log f_m versus T^{-1})
                                                     100 (from area under peak)

The accuracy of these activation energies is not particularly good because of the narrow temperature range over which they are estimated. However, the measurements on polystyrene samples summarized in *Figure 3* yield activation energies of 100 kcal mole^{-1} for both the γ_1 and β peaks in good agreement with results published elsewhere[7].

Finally it is interesting to note that the γ_1 dispersion is not observed in the results of spin–lattice relaxation time measurements on either poly(styrene oxide)[1] or polystyrene[11]. The low temperature T_1 minimum reported in ref. 1 for poly(styrene oxide) cannot be related to either the γ_1, γ_2 or γ_3 relaxations since it is observed at $-128°C$ at 30 Mc/s and the corresponding mechanical dispersion would lie at even lower temperatures at 1 000 to 1 c/s. On the other hand n.m.r. results[11] show that spin–lattice relaxation effects associated with the reorientation of benzene rings are weak and it is probable that the γ_1 relaxation would be difficult to detect owing to its proximity to the β dispersion.

Department of Chemistry,
University of Manchester

REFERENCES

[1] ALLEN, G., BLEARS, D. J. and CONNOR, T. M. *Polymer, Lond.* 1967, **8**, 401
[2] ALLEN, G., BOOTH, C. and HURST, S. J. *Polymer, Lond.* 1967, **8**, 385
[3] WETTON, R. E. and ALLEN, G. *Polymer, Lond.* 1966, **7**, 331
[4] ALLEN, G., BOOTH, C. and JONES, M. N. *Polymer, Lond.* 1964, **5**, 257
[5] BLANCHETTE, J. A. *U.S. Pat. No. 2 916 463* (1960)
[6] VANDENBORG, E. J. *J. Polym. Sci.* 1960, **42**, 486
[7] ODAJIMA, A., SOHMA, J. and KOIKE, J. *J. phys. Soc. Japan,* 1957, **12**, 272
[8] KOSFIELD, R. *Kolloidzschr.* 1960, **172**, 182
[9] KANG-JEN LIN and ULLMAN, R. *Polymer, Lond.* 1965, **6**, 100
[10] READ, B. E. and WILLIAMS, G. *Trans. Faraday Soc.* 1961, **57**, 1979
[11] HUNT, B. I., POWLES, J. G. and WOODWARD, A. E. *Polymer, Lond.* 1964, **5**, 323

VI—The Physical Properties of Poly(epoxides)

G. ALLEN, C. BOOTH and C. PRICE

The physical properties of the poly(epoxides) are summarized, and compared with each other and also with the properties of the corresponding poly(olefins). The nature of the side group has little effect upon the dynamic and equilibrium flexibilities of the poly(epoxides) unless the side group is bulky, e.g. t-butyl and phenyl.

THE data reported in parts I to V[1-5], together with data obtained in earlier investigations, enable us to compare the physical properties of some high molecular weight poly(epoxides) having the structural formula [CHR—CH$_2$—O]$_n$. Most of our data refer to polymers prepared by means of the zinc diethyl–water catalyst system with a mole ratio of water to zinc diethyl of, or approaching, unity. The one exception is poly(ethylene oxide) which was obtained from commercial sources[6]; this inconsistency is not important since poly(ethylene oxide) does not exhibit optical isomerism. Here we review the results, and also take the opportunity to compare the physical properties of the poly(epoxides) with those of the corresponding poly(olefins).

PROPERTIES OF THE POLY(EPOXIDES)

General features of the bulk state

The crystallinity of the poly(epoxides) varied with the group R. Poly(ethylene oxide), poly(*t*-butyl ethylene oxide) and poly(dodecene-1 oxide) were all crystalline. Poly(dodecene-1 oxide) crystallized to waxy products and it seems probable that crystallization occurred on the side chain rather than on the main chain. Poly(propylene oxide), poly(butene-1 oxide), poly(butadiene monoxide) and poly(styrene oxide) were all of low degree of crystallinity as prepared, although it was possible in some cases[7] to isolate highly crystalline fractions by use of suitable fractionation techniques. With the exception of poly(styrene oxide) which was a glass, the amorphous poly(epoxides) were rubbers at room temperature. Poly(butadiene monoxide) crosslinked spontaneously through the pendant vinyl groups; this feature was turned to good account by preparing vulcanizable co-polymers with propylene oxide[8].

Melting and glass transition temperatures

In all our work the transition temperatures were determined by dilatometry using low heating rates (less than five degrees per hour). In determining melting points annealing processes were used which produced

Table 1. Transition temperatures of high molecular weight poly(epoxides)

Poly(epoxide)	T_m, °C	T_g, °C	Poly(epoxide)	T_m, °C	T_g, °C
Poly(ethylene oxide)*	68†	−67‡	Poly(*t*BEO)	149	−35
Poly(propylene oxide)	73§	−75§	Poly(dodecene-1 oxide)	79‡	−41‡
Poly(butene-1 oxide)	—	−83‡	Poly(styrene oxide)	162	40
Poly(butadiene monoxide)	74‡	−75‡			

*Commercial sample; †C. J. DEVOY: unpublished data for fraction; ‡D. J. MARKS: data[9] for whole polymers; §W. D. TAYLOR[10]: data for fraction.

optimum crystallinity in the specimen; in determining glass transition points specimens were cooled rapidly so as to avoid crystallization. The results are collected in *Table 1*. Where polymers have been fractionated the transition temperatures of the most easily crystallized fraction are quoted. In our detailed studies of some of these poly(epoxides)[10] we showed that T_g was not affected appreciably by changes in crystallizability, but that T_m might be 10 to 20 deg. C lower than the value which could be achieved by careful fractionation. In addition, in assessing these data we remember the evidence that poly(epoxides) prepared by the ferric chloride–water catalyst system have higher melting points than those prepared by the zinc diethyl–water catalyst system, e.g. melting points of 75°C for poly(propylene oxide)[11] and 179°C for poly(styrene oxide)[12] have been obtained.

Dynamic mechanical and n.m.r. properties

All the polymers investigated were partially crystalline and so quantitative treatment of the dynamic mechanical and n.m.r. properties was even less successful than usual. Nevertheless these techniques provided useful qualitative information on molecular mobility over a wide range of temperature.

In *Table 2* we list the locations of the β and γ dispersions observed at 1 c/s by dynamic mechanical methods, and the activation energies (ΔH)

Table 2. The dynamic mechanical properties of high molecular weight poly(epoxides): location of the β and γ dispersions at 1 c/s and the activation energies (ΔH) for the β process

Poly(epoxide)	Location of β dispersion °C	ΔH* kcal mole^{-1}	Location of γ dispersion °C
Poly(ethylene oxide)	−60†	65†	—
Poly(propylene oxide)	−55‡	70‡	−150§
Poly(*t*BEO)	46	110	(−10?)
Poly(styrene oxide)	38‖	100‖	20, −20, −85‖

*Calculated from area under loss peak by the method of Read and Williams[13]; †Wetton: data for whole polymer[14]; ‡Wetton: data for fraction[14]; §Reported by Woodward *et al.*[15]; syndiotactic sample; ‖low molecular weight sample (similar to sample II-10 of Table 2, ref. 14).

for the β process estimated by the method of Read and Williams[16]. In *Table 3* we list the locations of the high and low temperature minima in the proton spin–lattice relaxation time versus temperature curves, and the activation energies ($\langle Q \rangle'$) for the high temperature process calculated by

Table 3. The n.m.r. properties of high molecular weight poly(epoxides): location of the high and low temperature minima and activation energies ($\langle Q \rangle'$) for the high temperature process

Poly(epoxide)	High temp. min. °C	$\langle Q \rangle'$* (kcal mole^{-1})	Low temp. min. °C
Poly(ethylene oxide)†	0	5	—
Poly(propylene oxide)‡	1	7	−140
Poly(butene-1 oxide)§	15	6	−140
Poly(*t*BEO)	95	5	−110
Poly(styrene oxide)	127	9	−130

*Calculated by the method of Connor[16] (see ref. 3); †T. M. CONNOR: data for whole polymers[17]; ‡D. J. BLEARS: data for fraction[18]; §D. J. BLEARS: data for fraction[19].

the method of Connor[16]. The β process in the dynamic mechanical loss spectrum and the high temperature minimum in the spin–lattice relaxation spectrum are both associated with the glass transition[5]. The low temperature minima in the spin–lattice relaxation spectra of poly(propylene oxide) and poly(tBEO) are associated with methyl group rotation[4, 18]. The low temperature minimum in the spectrum of poly(styrene oxide) is associated with oscillation of the phenyl group[5]. The subsidiary loss peaks in the dynamic mechanical spectra are less easily assigned. The γ peaks in poly(tBEO) and poly(propylene oxide) are very weak and are probably due to rotation of the side group. The γ_1 peak in poly(styrene oxide) is more intense and is assigned to rotation of the phenyl group[5], and the proximity of this peak [and that in poly(tBEO)] to the main transition is evidence of the high steric hindrance experienced by bulky groups.

Unperturbed dimensions of the coil

In *Table 4* we have listed values of the ratio $(\overline{r_0^2}/\overline{r_f^2})^{\frac{1}{2}}$, where $(\overline{r_0^2})^{\frac{1}{2}}$ is the

Table 4. Values of $(\overline{r_0^2}/\overline{r_f^2})^{\frac{1}{2}}$ for poly(epoxides)

Poly(epoxide)	$(\overline{r_0^2}/\overline{r_f^2})^{\frac{1}{2}}$
Poly(ethylene oxide)	163*
Poly(propylene oxide)	162†
Poly(styrene oxide)	185*

*From intrinsic viscosity/molecular weight relationship in a good solvent; †From intrinsic viscosity and light scattering measurements in good solvents and in theta solvents.

unperturbed root-mean-square end-to-end distance of the poly(epoxide) chain and $(\overline{r_f^2})^{\frac{1}{2}}$ is the corresponding dimension calculated assuming free rotation of the bonds in the chain. We have taken $(\overline{r_f^2}/M)^{\frac{1}{2}}$ equal to $3\cdot77/M_u^{\frac{1}{2}}$ Å for the poly(epoxide) chain), where M_u is the molar weight of the repeating unit.

DISCUSSION

The glass transition and chain flexibility

It is now generally accepted that the glass transition is associated with the loss of internal rotation, and of translational motion of the chain segments. Thus chains having high barriers to internal rotation will lose their dynamic flexibility at a high temperature and have a high glass transition temperature. Considering the polyethers [CHR—CH$_2$—O]$_n$, when R is a bulky group such as t-butyl or phenyl, one would expect high barriers

Table 5. Properties of poly(olefins)*

	T_m^0, °C	T_g, °C	$(\overline{r_0^2}/\overline{r_f^2})^{\frac{1}{2}}$		T_m^0 °C	T_g, °C	$(\overline{r_0^2}/\overline{r_f^2})^{\frac{1}{2}}$
Poly(ethylene)	141	−125	1·6	Poly(3,3-dimethyl			
Poly(propylene)	180	−10	1·6	butene-1)	260	64	—
Poly(butene-1)	140	−24	—	Poly(dodecene-1)	49	−6	—
1,2-Poly(butadiene)	125	−4	—	Poly(styrene)	250	100	2·2

*The values in this table are taken from the *Polymer Handbook*[20]; they have not been chosen critically and are included only for purposes of comparison. The location of T_g in polyethylene is still controversial.

to internal rotation. This effect can be seen in *Tables 1, 2* and *3*, where the glass transition temperatures of the polymers with bulky side groups are some 100 deg. C higher than those of the other poly(epoxides). It is also clear that the introduction of a methyl group, or a linear group such as ethyl or vinyl, has little effect upon T_g when comparison is made with poly(ethylene oxide). This is in marked contrast to the effects noted in the corresponding series of poly(olefins), representative properties of which are listed in *Table 5*, and provides an illustration of the minor steric effects attributable to small linear side groups when they are separated by two unsubstituted main chain atoms.

A second important factor influencing the glass transition temperature is the molecular cohesion of the polymer. Internal rearrangement of the polymer chains in the bulk state must involve the cooperative movement of the segments of several molecules; polymers having low molecular cohesion should therefore tend to have low glass transition temperatures. This is illustrated by comparing the poly(epoxides) with the poly(olefins) in *Table 5*. Compared to that of the poly(olefin) the flexibility of the poly(epoxide) chain should be enhanced by the wider separation of the side groups, and by the presence of the ether linkages. However, the molecular cohesion of the poly(epoxide) should be greater than that of the poly(olefin) because of the polarity of the ether linkages. Thus there are opposing effects to be considered.

Comparison of the glass transition temperature of polyethylene ($-125°C$) and poly(ethylene oxide) ($-67°C$) suggests that in this particular case, the increased molecular cohesion of the polyether is the more important factor. Comparison of the substituted polymers shows clearly the importance of the spacing of the side groups; the substitution of a hydrogen atom by a methyl group raises T_g of the poly(olefin) by ~ 100 deg. C, but affects T_g of the poly(epoxide) very little. Indeed with the poly(epoxides) an elevation of T_g by 100 deg. C or so is achieved only by substitution of a group as bulky as *t*-butyl or phenyl.

The activation energies listed in *Tables 2* and *3* are subject to considerable uncertainty, both in estimation and interpretation. It has been held[14, 19] that a high value of ΔH, or $\langle Q \rangle'$, implies a high impedance to molecular motion in the polymer. This interpretation is supported by the ΔH values of *Table 2*, while the evidence of *Table 3* is equivocal. However, it seems unlikely that these activation energies can be used with much profit until there is a better understanding of the nature of molecular motions in the neighbourhood of the glass transition.

Taken together the data presented here show that the dynamic flexibility of the poly(epoxide) chain is reduced considerably by the presence of a bulky side group.

We also conclude that the low glass transition temperatures of the substituted poly(epoxides) relative to the poly(α-olefins) are due to the greater internal dynamic flexibility of the poly(epoxide) chain, which in turn arises principally from the greater spacing of the substituted groups.

It remains to examine whether the equilibrium flexibility of the chain is also affected by the nature of the side groups. The equilibrium flexibility depends upon the energy differences between rotational states whereas the

dynamic flexibility depends upon the cohesive forces and the heights of energy barriers. *A priori* there is no reason to suppose that there will be any direct correlation between the two properties. The equilibrium flexibility may be described in terms of the ratios $(\overline{r_f^2}/\overline{r_0^2})^{\frac{1}{2}}$ which are presented for the poly(epoxides) in *Table 4*. The larger the ratio, the less flexible is the chain. While the values we present are subject to considerable uncertainty, they indicate sufficiently well that substitution on the poly(epoxide) chain has little effect upon the unperturbed dimensions of the chain when the side group is small (—Me), but increases the dimensions markedly when the side group is large (—Ph). A fortuitous parallel between the dynamic and the equilibrium flexibility seems to exist for the poly(epoxides). No such parallel is found for the poly(olefins) (see *Table 5*).

Melting point

A cursory examination of *Tables 1* and *5* reveals a striking parallel between the variation of melting point and of glass transition temperature in these series of polymers. Unfortunately we have insufficient subsidiary information[21] to permit us to examine this parallel in detail. Moreover variations in degree of stereoregularity from one polymer to another introduce an experimental variable which we are not equipped to deal with in a quantitative way. For these reasons we shall not attempt to discuss the relationship between melting point and chemical structure for these poly(epoxides) at this time.

Department of Chemistry,
University of Manchester

REFERENCES

[1] ALLEN, G., BOOTH, C. and HURST, S. J. *Polymer, Lond.* 1967, **8**, 385

[2] ALLEN, G., BOOTH, C., HURST, S. J., JONES, M. N. and PRICE, C. *Polymer, Lond.* 1967, **8**, 391

[3] ALLEN, G., BOOTH, C. and PRICE, C. *Polymer, Lond.* 1967, **8**, 397

[4] ALLEN, G., BLEARS, D. J. and CONNOR, T. M. *Polymer, Lond.* 1967, **8**, 401

[5] ALLEN, G., BOOTH, C., HURST, S. J., PRICE, C., VERNON, F. and WARREN, R. F. *Polymer, Lond.* 1967, **8**, 406

[6] Union Carbide Ltd, Chemicals Division

[7] See, for example, BOOTH, C., HIGGINSON, W. C. E. and POWELL, E. *Polymer, Lond.* 1964, **5**, 479

[8] ALLEN, G. and CROSSLEY, H. G. *Polymer. Lond.* 1964, **5**, 553

[9] MARKS, D. J. *Ph.D. Thesis*, University of Manchester, 1961

[10] ALLEN, G., BOOTH, C., JONES, M. N., MARKS, D. J. and TAYLOR, W. D. *Polymer, Lond.* 1964, **5**, 547

[11] CHU, N. S. and PRICE, C. C. *J. Polym. Sci. A*, 1964, **1**, 1984

[12] BLANCHETTE, J. A. *U.S. Pat. No. 2 916 463*, 1960

[13] READ, B. E. and WILLIAMS, G. *Trans. Faraday Soc.* 1961, **57**, 1979

[14] WETTON, R. E. and ALLEN, G. *Polymer, Lond.* 1966, **7**, 331

[15] SEBA, R. G., SAUER, J. A. and WOODWARD, A. E. *J. Polym. Sci. A*, 1963, **1**, 1483

[16] CONNOR, T. M. *Trans. Faraday Soc.* 1964, **60**, 1574

[17] ALLEN, G., CONNOR, T. M. and PURSEY, H. *Trans. Faraday Soc.* 1963, **59**, 1525

[18] CONNOR, T. M., BLEARS, D. J. and ALLEN, G. *Trans. Faraday Soc.* 1965, **61**, 1097

[19] CONNOR, T. M. and BLEARS, D. J. *Polymer, Lond.* 1965, **6**, 385

[20] *Polymer Handbook*, BRANDRUP, J. and IMMERGUT, E. H., Editors. Interscience: New York, 1966

[21] ALLEN, G. *J. appl. Chem.* 1964, **14**, 1

Association of Polyacrylonitrile Solutions

R. B. BEEVERS

Kinetic aspects of the association of polyacrylonitrile molecules in dimethyl-formamide solutions containing between 30 and 40 volume per cent benzene have been examined viscometrically. Addition of benzene affects the rate but not the extent of association, with the result that the non-solvent acts as an inert diluent in this system. Rate constants, corrected to zero polymer concentration, were found to be $5\cdot2\times10^{-7}\,sec^{-1}$ at $32\cdot0$ per cent and $8\cdot2\times10^{-4}\,sec^{-1}$ at $37\cdot0$ per cent benzene. Osmometric and sedimentation measurements on these solutions with the same benzene concentrations gave $M_n=3\cdot5\times10^4$, $8\cdot4\times10^4$; $M_{sd}=3\cdot2\times10^5$, $7\cdot0\times10^9$ respectively. The values indicate the presence of a few very large aggregates in the polymer solution. Values of the second virial coefficient are in satisfactory agreement with those obtained by Krigbaum and Kotliar.

THE occurrence of aggregates in dilute polymer solutions through molecular association[1] is quite common and association in polymers containing carboxyl groups is particularly well known[2]. Whenever large numbers of polar substituents are attached to a polymer these groups will interact both intra- and inter-molecularly to form an aggregate. Chang and Morawetz[2] were able to distinguish between these types of bond formation for styrene plus methacrylic acid copolymers using a combination of infra-red and osmotic measurements. Only a few carboxyl groups were found to participate intermolecularly; the majority either acted intramolecularly or were hidden in the interior of the polymer coil. Polyvinylchloride can become associated in dilute solution[3]. Association interferes with molecular weight determinations on this polymer unless the aggregates are previously broken down by heating the solution[4]. Menčík[5] has shown that both polyvinylchloride and polyacrylonitrile are difficult to fractionate by addition of non-solvent.

Evidence of association in polyacrylonitrile solutions has been provided by light scattering and electron microscopy. Heyn[6] has found evidence of microgel, microfibrils and free molecular threads together with macrogel in solutions of the polymer previously examined by Peebles[7]. Both Nicolas[8] and Peebles[7] have shown that strong Zimm plot distortion in light-scattering studies of polymer solutions can be correlated with the presence of microgel since it is possible to correct the distortion by ultracentrifugation of the solutions. Electron micrographs given by Thomas[9], particularly of polyacrylonitrile prepared in aqueous suspension with a redox initiator, show two groups of particles of noticeably different size distributions.

Shashoua and Beaman[10] have prepared well-characterized microgel by addition of small quantities of N,N'-methylene bisacrylamide as cross-linking agent to the emulsion polymerization of acrylonitrile. The purity of the microgel was determined by ultracentrifugation[11]. It is now well established that microgel is a common feature of polymer solutions and

intermediate in solution properties between the linear chain molecule and the macrogel particle. Microgel is soluble in solvents of intermediate solvent power to form a macrosol[12] and can, for example, be characterized by intrinsic viscosity measurements[10].

Climie and White[13] reported on a study of association in solutions of acrylonitrile copolymers in N,N'-dimethylformamide brought about by addition of non-solvent. Solutions of polyacrylonitrile in this solvent become associated on addition of about 35 per cent by volume of benzene—a concentration well below that required to cause precipitation of the polymer. Climie and White[13] further showed that the arrangement of the acrylonitrile residues along the chain affected the volume of benzene required to cause association and it was possible, in this way, to distinguish between block and random copolymers. Investigation[14] of several random copolymers containing a large proportion of acrylonitrile further showed that the nature of the comonomer was unimportant in this respect. Clearly association occurred in these solutions through interaction of the CN groups.

This paper carries the investigation further but devotes attention to the homopolymer. Although association can be brought about by many non-solvents[15] benzene has been used to give continuity with the work of Climie and White[13] and more particularly because of its lack of participation in hydrogen bond formation.

EXPERIMENTAL

Materials

Polyacrylonitrile (sample W12) was prepared according to a redox recipe, details of which have been given previously[16]. Analytical reagent grade benzene was dried over silica gel before distillation. N,N'-dimethylformamide was dried with eight changes of phosphorus pentoxide before vacuum distillation at room temperature. All benzene concentrations were determined by volume, and solution concentrations (g dl^{-1}) make allowance for dilution of the stock polymer solution by benzene.

Viscometry

Viscosities were determined at 25·00°C in suspended level dilution viscometers (Polymer Consultants Ltd), the usual viscometric procedures being followed[17]. Values of the time of flow (t_0) for the solvent–non-solvent mixture were not determined prior to each measurement. Instead t_0 was obtained for each viscometer and at each temperature using six standard solvent–non-solvent mixtures covering the range 20 to 40 per cent benzene. Values of t_0 were found to fit closely to a linear dependence on benzene composition. The equations fitting these data were determined and subsequently used to evaluate t_0 for any particular experiment.

(a) *Limiting viscosity number*—Values of the viscosity number η_{sp}/c were determined for solutions of the polymer in dimethylformamide and dimethylformamide–benzene mixtures up to 60 per cent benzene. Additional measurements of t_0 were made in this case. Lower concentrations of polymer were obtained by dilution using stock dimethylformamide–benzene mixtures. Except for the 60 per cent benzene results, linear plots were

obtained for the dependence of η_{sp}/c on concentration to give values of the limiting viscosity number $[\eta]$ reliable to one per cent. Values of the Huggins parameter k' given by

$$\eta_{sp}/c = [\eta] + k'[\eta]^2 c \qquad (1)$$

were also determined.

(b) *Time dependence of the viscosity number*—Preliminary examination showed that time-dependent viscosity changes occurred between a concentration of 30 and 40 per cent benzene. In order to make measurements of these changes the following procedure was adopted.

The required volume of polymer solution was added to the viscometer by burette (calibrated to 0·01 ml) and a short period allowed for further slight thermal equilibration. Benzene was then added using controlled nitrogen bubbling to effect mixing. This took approximately 50 sec for the addition of 3 to 4 ml benzene. Once mixed the polymer and liquid mixture appeared to be completely free from optical inhomogeneities indicative of precipitation or macrogel formation.

Timing of the experiment commenced with the start of addition of non-solvent and the time recorded for the viscometric determination was taken at the start of flow of the polymer solution from the upper bulb of the viscometer. These measurements were continued at suitable intervals up to one week depending upon the concentration of benzene. During the early stages of an experiment, and particularly at high benzene concentrations, only single determinations of a flow time could be made. Later, the time of flow in the viscometer became negligible as compared with the duration of the experiment and reproducible flow times could then be obtained.

Osmometry

Measurements were made at $25 \cdot 00 \pm 0 \cdot 01$ deg. C using Pinner–Stabin type osmometers (Polymer Consultants Ltd) following the usual procedures[17]. Pecel 600 undried cellophane membranes were used and equilibrium osmotic heights ($\pm 0 \cdot 001$ cm) obtained after 48 hours. The membranes initially in a 60 per cent acetone + water environment were progressively conditioned through 100 per cent acetone to 100 per cent dimethylformamide and subsequently to a dimethylformamide + 35 per cent benzene mixture.

Osmotic measurements were made on solutions of the polymer in dimethylformamide using a stock solution and obtaining lower polymer concentrations by dilution.

Osmotic measurements in mixed liquids

Among the difficulties of osmometry is the possibility when using mixed solvents of an uneven distribution of the two liquids on either side of the membrane. Gee[18] found no evidence of this with benzene–methylalcohol mixtures and obtained the same limiting value of the reduced osmotic pressure (π/c) as for a single liquid.

(i) *Osmotic measurements in 30 per cent and 37 per cent benzene mixtures*—Measurements were made at benzene concentrations on either side of the time-dependent viscosity range. Solutions at each polymer concentration were prepared directly in dilution viscometers. Appropriate quantities of stock solution and dimethylformamide were added to the viscometer followed by the calculated amount of benzene. Viscosity measurements were then carried out for 24 hours as described above to ensure (1) that at 30·0 per cent benzene no time-dependent viscosity changes had occurred, (2) at 37·0 per cent benzene the viscosity number had become independent of time. These solutions, prepared in sufficient quantity, were used for rinsing and filling the osmometers in the usual way.

(ii) *Osmotic measurements at 32 per cent benzene*—At benzene concentrations between 31 and 33 per cent the rate of change of viscosity number with time is small so that, in principle, it is possible to prepare partly associated solutions which can be examined osmometrically. These experiments met with only limited success. Solutions of the required polymer concentration were prepared viscometrically as detailed above. Changes in viscosity were then followed for about three days. Part of the solutions was then removed for rinsing and filling the osmometer whilst viscometric observations were carried on with the remainder. In this way, allowing sufficient time for equilibration in the osmometer, reduced osmotic pressures could be determined at a time when the solutions had shown the same fractional change in viscosity number, i.e. the same extent of association.

Sedimentation

Two exploratory runs were made using a Spinco model E ultracentrifuge operated at 59 780 rev/min and fitted with schlieren optics. Examination of polyacrylonitrile solutions with the ultracentrifuge have previously been made by Bisschops[19], Krigbaum and Kotliar[20] and Shashoua and van Holde[11]. The purpose of these experiments was to compare solutions in different states of association and to examine their sedimentation profiles. Doty, Wagner and Singer[3] have made similar observations with associated solutions of polyvinylchloride in dioxan. No attempt was therefore made to correct the observations for concentration or pressure. Sedimentation constants (s) were evaluated from the relation

$$s = (1/\omega^2 r)(dr/dt) \tag{2}$$

where r is the distance of the boundary from the centre of rotation at time t and ω is the angular velocity in radians/sec.

Solutions to be used for sedimentation were prepared viscometrically as described above with benzene concentrations of 30·0 and 37·0 per cent. Initial polymer concentrations were adjusted to give a final concentration in each case of 0·500 g dl^{-1}. This value was chosen to obtain the maximum peak visibility of the sedimentating species without excessive increase in solution viscosity. Viscosity measurements were made for $1·1 \times 10^5$ sec and the sedimentation experiments then were commenced at about $1·8 \times 10^5$

sec. During the preparative stage the viscosity number of the 37·0 per cent benzene solution fell from 1·88 dl g^{-1} to a constant value of 0·42 dl g^{-1}.

RESULTS AND DISCUSSION
Dependence of viscosity on benzene concentration

Typical changes in the value of η_{sp}/c for a solution of polyacrylonitrile in dimethylformamide (initial concentration 0·529 g dl^{-1}) are shown in *Figure 1*. Benzene has been added in small increments and sufficient time
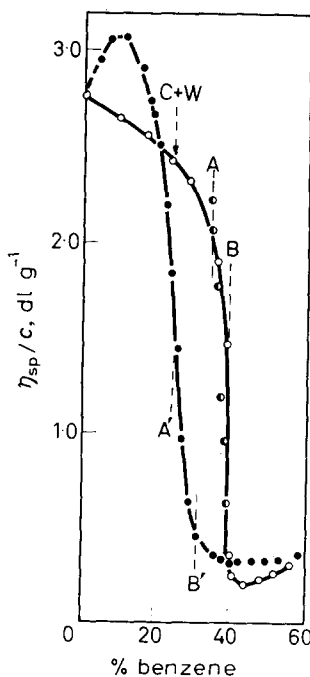
Figure 1—Dependence of η_{sp}/c for a solution of polyacrylonitrile in dimethylformamide on volume per cent of added benzene. AB, A'B' denote regions of time-dependent viscosity. The critical point obtained by Climie and White is indicated by C+W; O, addition of benzene; ●, addition of dimethylformamide; ◑, values of obtained after 10^3 sec in kinetic runs

allowed for thermal equilibrium to be re-established. At low benzene concentrations the weakening solvent power causes a reduction in the dimensions of the random coil and so reduces the viscosity of the polymer solution. Between 30 per cent and 40 per cent benzene the value of η_{sp}/c changes by a large factor as association takes place.

Reduction of the benzene concentration by addition of dimethylformamide brings about dissociation with a marked hysteresis effect. Over the regions AB and A'B' indicated in *Figure 1* values of η_{sp}/c are time-dependent and the points plotted are only indicative of the nature of the changes taking place. These results substantially confirm those reported[13] for acrylonitrile copolymers apart from some disagreement concerning the amount of benzene required to cause association. Climie and White[13] adopted an arbitrary procedure in this respect and the value of 23 ± 1 per cent benzene indicated in *Figure 1* as C+W has been averaged from their tabular data. Measurements similar to those reported in *Figure 1* were

carried out with polymer (sample W 11)[16] prepared by free radical initiation using diethylamine as transfer agent. In this case a much more satisfactory agreement was obtained with Climie and White[13] indicating that the nature of the polymerization reaction is of some significance.

Chiang[21] has also been able to differentiate between methods of polymerization in respect of the crystallization and dissolution temperatures of polyacrylonitrile. Osmometric measurements on polyacrylonitrile in dimethylformamide obtained by Krigbaum and Kotliar[20] are clearly affected by the onset of association. They report, however, that whilst these effects are observed for redox polymer, they are absent in the case of polymer prepared in dimethylformamide with azobisisobutyronitrile as initiator. Such distinction has not been observed here.

Measurements of $[\eta]$ and k' from equation (1) in a series of solvent–non-solvent mixtures are given in *Figure 2*. In a poor solvent the molecule
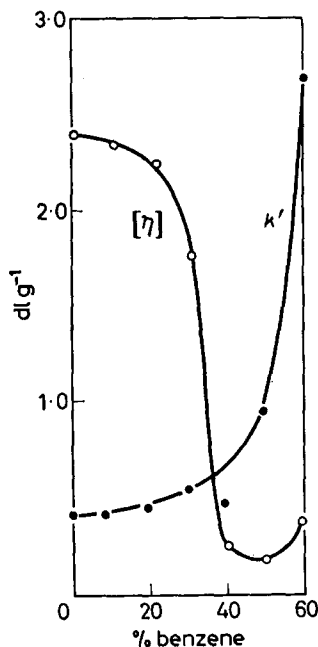
Figure 2—Values of $[\eta]$ and the Huggins constant k' in polyacrylonitrile plus dimethylformamide plus benzene solutions. ○, values of $[\eta]$; ●, values of k'

is more highly coiled and acts hydrodynamically like a sphere. In general this leads to a lower value of $[\eta]$ and higher k'. Measurements by Climie[14] of the dissymmetry of light scattering in the range 60° to 135° show little change suggesting that the aggregate must consist of a tight cluster of molecules. Doty, Wagner and Singer[3] drew similar conclusions in respect of polyvinylchloride solutions. It is then not surprising that the Einstein equation[10]

$$[\eta] = 0.025 \mid \rho \qquad (3)$$

for a dispersion of hard spheres of density ρ appears to be applicable to styrene plus divinylbenzene microgels. In this case the results show that $[\eta]$ falls rapidly for small amounts of crosslinking[10].

Only very tenuous conclusions can be drawn concerning the value of k', and especially in associating systems. Katayama and Ogoshi[22] for example have found that the value of the Huggins parameter for polyacrylonitrile polymerized in a redox system depends on the conditions of polymerization. Nicolas[8] obtained similar results to those given in *Figure 2* for polyethylene (Alkathene) in tetralin plus methylphthalate mixtures, which were correlated with the existence of microgel.

Kinetic viscosity effects at constant benzene composition

The nature of the time-dependent viscosity changes observed in the regions AB and A'B' of *Figure 1* are more clearly demonstrated in *Figure 3*.
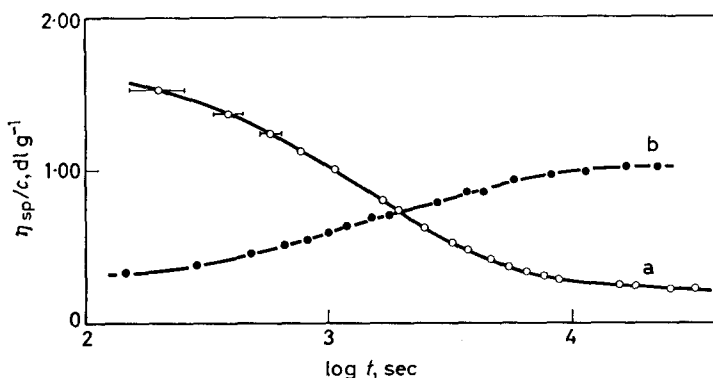
Figure 3—Time dependence of η_{sp}/c for solutions of polyacrylonitrile in dimethylformamide: (a) addition of 38 per cent benzene, $c=0.291$ g dl^{-1} followed by, (b) addition of dimethylformamide to give 27 per cent benzene, $c=0.207$ g dl^{-1}

In this experiment non-solvent was added to the polymer solution at 20°C to give a concentration of 38·0 per cent benzene ($c=0.291$ g dl^{-1}). Viscosity of the solution then decreased (curve a) during several decades of logarithmic time, ultimately reaching a constant value. Horizontal lines drawn through some of the points indicate the uncertainty arising from the time of flow of solution in the viscometer; this has a relatively small effect on the shape of the curve. After the lapse of two days an aliquot portion of solution was removed and returned to the cleaned viscometer. Dimethylformamide was then added to reduce the benzene concentration to 27·0 per cent ($c=0.207$ g dl^{-1}); that is to a point in the region A'B'. Viscosity then increased with time as shown by curve b, ultimately reaching a constant value of 1·03 dl g^{-1}. Calculation of η_{sp}/c corresponding to the conditions pertaining to curve b using equation (1) with values of $[\eta]$ and k' taken from *Figure 2*, gives 2·52 dl g^{-1}. This suggests that the association–dissociation reaction is not completely reversible, at least for the conditions used here. Boedtker and Doty[23] similarly found evidence of irreversibility in dilute gelatin solutions.

Exploration of the effect of polymer concentration reveals two types of

behaviour as shown in *Figure 4* where the benzene concentration is kept constant at 37·0 per cent. Polymer concentration was varied from 0·18 to 1·30 g dl⁻¹ as indicated on each curve.

At low polymer concentrations the curves are qualitatively similar to curve a in *Figure 3*. Increase in concentration to above 1·0 g dl⁻¹ produces a marked change in the time dependence of η_{sp}/c. After about 1 000 sec
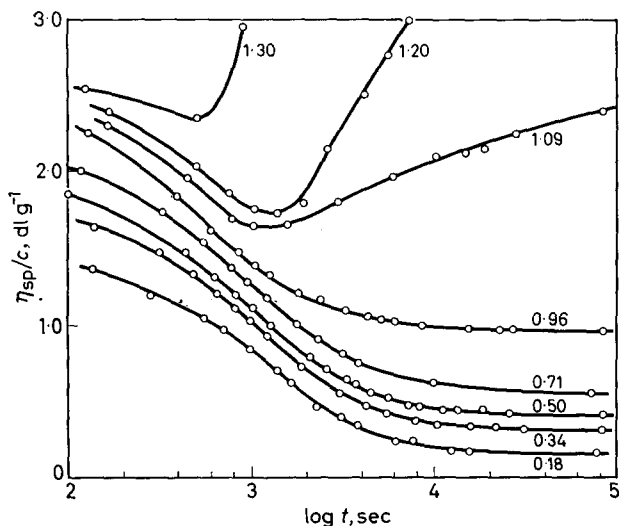
Figure 4—Effect of polymer concentration on the time-dependent viscosity of polyacrylonitrile solutions with 37·0 per cent benzene. Figures on the curves denote polymer concentration in g dl⁻¹

viscosity begins to increase and this is accompanied by visible gel formation in the effluxing liquid of the viscometer. The results given in *Figure 4* now make it possible to delineate between gel and microgel. For this benzene concentration critical polymer concentration is $1·02\pm0·06$ g dl⁻¹, and is in accord with similar measurements by Boedtker and Doty[28] on gelatin in 0·15M sodium chloride at 18°C. They found the critical concentration separating the gel and aggregated forms (microgel) to be about 0·8 g dl⁻¹ for gelatin of similar molecular weight to that of the polyacrylonitrile sample used here.

Effect of variation of benzene concentration

Measurements shown by curve a in *Figure 3* were extended to cover the range 30·0 to 40·0 per cent benzene, corresponding with the points A and B of *Figure 1*. These results given in *Figure 5* reveal the nature of the kinetic effects at 25·00°C. Initial polymer concentration in dimethylformamide was $0·467\pm0·002$ g dl⁻¹ resulting in a variation from 0·327 to 0·280 g dl⁻¹ over the range of benzene concentrations examined. Polymer concentration was sufficiently low and so avoided complications arising from macrogel formation.

426

With increase in benzene concentration the rate of change of η_{sp}/c increases rapidly so that at 40·0 per cent benzene most of the kinetic effects have occurred before viscometric measurements could be made. Only part of the curves are shown in *Figure 5*. Extension to 10^6 and 10^7 sec shows that all curves have a similar sigmoid shape ultimately reaching a constant low value of η_{sp}/c. Small variations in this final value arise from small variations in polymer concentration, and in this section these have been considered to be of the second order. If we consider the magnitude of the change in η_{sp}/c to give a measure of the extent of association, then the curves demonstrate that the effect of benzene is to control the rate and not the degree of association. Benzene must then be considered to act as an inert diluent preventing polymer–dimethylformamide interactions and so allow polymer–polymer interactions to take place.

Values of η_{sp}/c from *Figure 5*, taken after 10^3 sec have been plotted in *Figure 1* where they are indicated by half-closed circles. These show good
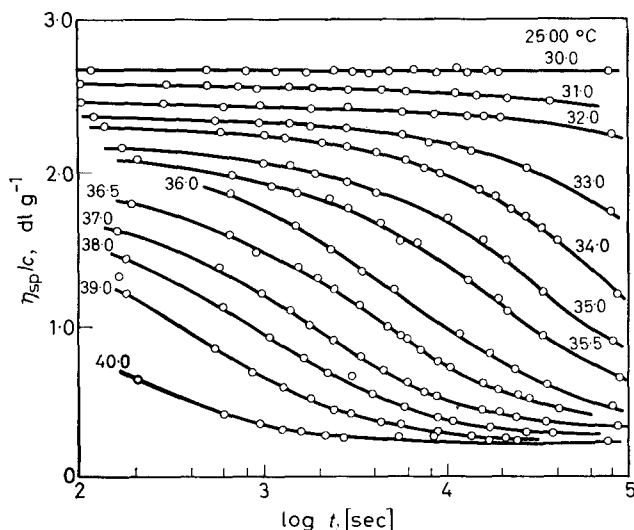
Figure 5—The dependence of η_{sp}/c on log time for poly-acrylonitrile plus dimethylformamide solutions. Numbers on the curves indicate the volume per cent of benzene added at the start of the experiment

agreement with the other data and give further definition to the rapidly changing section of the graph. A time of 10^3 sec was chosen arbitrarily and corresponded roughly with the time interval between readings taken in deriving *Figure 1*.

With the exception of results at high benzene concentrations, plots of $\ln (\eta_{sp}/c)$ depend linearly on time to a reasonable approximation. Thus,

$$\ln (\Phi/\Phi_0) = -kt \qquad (4)$$

where for convenience $\Phi = \eta_{sp}/c$, Φ_0 is the value of Φ at $t = 0$, and k is the rate constant. The association–dissociation process can be considered to be a reaction of the form

$$nP \underset{k_2}{\overset{k_1}{\rightleftharpoons}} P_n \qquad (5)$$

where k_1 and k_2 are the respective rate constants and n the degree of association of the polymer P. Consideration of *Figure 1* shows the hysteresis loop to be very wide so that the association and dissociation reactions do not overlap, i.e. $k_1 \gg k_2$ over the composition range 30 to 40 per cent benzene, and we can consider $k_1 = k$ in equation (4). Values of k_1 determined from *Figure 5* and numerous repeat measurements are given in *Figure 6*.
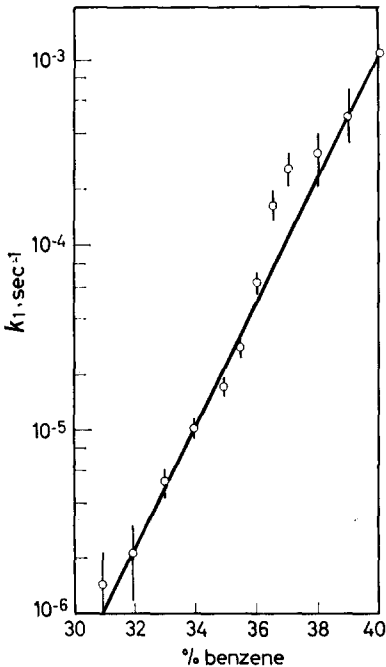
Figure 6—Values of k_1 determined for poly-acrylonitrile plus dimethylformamide solutions at various benzene concentrations

These results are, however, complicated by the dependence of k_1 on polymer concentration. Values of k_1 derived from *Figure 4* at 37·0 per cent benzene and for $c < 1·0$ g dl^{-1} are given by

$$\ln (k_1/k_0) = Ac \qquad (6)$$

where c is the polymer concentration and the constants here take values, $k_0 = 8·2 \times 10^{-4}$ sec^{-1}, $A = -0·38$ dl g^{-1}. Similar measurements for 32·0 per cent benzene yield $k_0 = 5·2 \times 10^{-7}$ sec^{-1}, $A = 1·82$ dl g^{-1}.

Determination of the degree of association
    (a) *Sedimentation*—Doty, Wagner and Singer[3] examined associated

solutions of polyvinylchloride in the ultracentrifuge and observed two distinct peaks whose sedimentation velocities corresponded with the associated and non-associated polymer species previously deduced. Ultra-centrifuge analyses on acrylonitrile plus ethylene bismethacrylate microsols have also been carried out, in this case to determine their purity[10,11]. Shashoua and Beaman[10] report that the microgel sedimentated between 20 and 100 times as fast as the linear polymer.

Experiments were here carried out with solutions containing 30·0 and 37·0 per cent benzene. In each case a well defined peak was observed super-imposed upon evidence of a second component. Sedimentation constants were determined from equation (2) and are given in *Table 1*. Estimation of

Table 1. Ultracentrifuge results on solutions of polyacrylonitrile in dimethylforma-mide with added benzene; room temperature; 59 780 rev/min

% benzene	S sec	S_0 sec	M_{sd}
30·0	1·44	3·08	$3·2 \times 10^5$
37·0	64·7	138	$7·0 \times 10^9$

the limiting values of the sedimentation constants at zero polymer con-centration have been made using data obtained by Krigbaum and Kotliar[20] for a polyacrylonitrile fraction (A-111-8) in dimethylformamide and un-corrected for the effect of hydrostatic pressure. In this case,

$$\ln (S_0/S) = 1·52c \qquad (7)$$

where $S = s \times 10^{-13}$ sec. The sedimentation data of Bisschops[19], which were uncorrected for hydrostatic pressure, were then used to derive a relation between the sedimentation constant and molecular weight M_{sd} and which is given by

$$S_0 = 0·025(M_{sd})^{0·38} \qquad (8)$$

Values calculated from this equation are reported in *Table 1*. They can only be regarded as approximate since equation (8) was derived from measure-ments on four polymer samples covering the molecular weight range 48 000 to 270 000. The degree of association n given by the ratio of molecular weights, is approximately 2×10^4.

Extrapolated values of the turbidity from Zimm plots for solutions of an acrylonitrile plus methyl methacrylate block copolymer (70·6 mole per cent acrylonitrile) in dimethylformamide and in dimethylformamide plus 40 per cent benzene gave molecular weights $\bar{M}_w = 3·5 \times 10^5$ and $\bar{M}_w = 1·5 \times 10^7$ respectively[14]. In this case approximately forty molecules associated to form the aggregate. The higher value observed here would appear com-parable with the observations of Shashoua and Beaman[10] as judged by the ratio of their sedimentation velocities.

(b) *Osmometry*—The results of osmotic measurements on these solutions are shown in *Figure 7* where the reduced osmotic pressure (π/c) is shown plotted against polymer concentration. The non-linearity observed
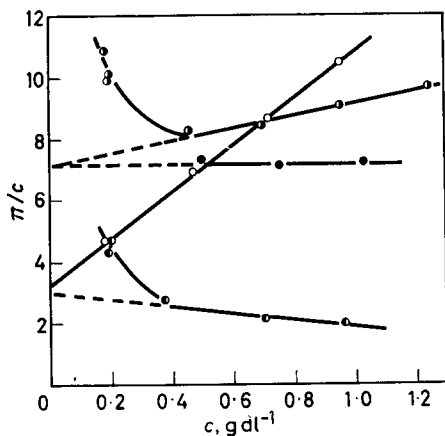
Figure 7—Dependence of reduced osmotic pressure on concentration in polyacrylonitrile solutions. ○ dimethylformamide; ◑, dimethylformamide plus 30·0 per cent benzene; ●, dimethylformamide plus 32·0 per cent benzene; ◐, dimethylformamide plus 37·0 per cent benzene

at low polymer concentrations is reduced if $(\pi/c)^{\frac{1}{2}}$ is taken as ordinate in the manner adopted by Krigbaum and Kotliar[20]. Values of the number average molecular weight $\bar{M}_n$ and the second virial coefficient A_2 obtained from

$$\pi/c = RT[A_1 + A_2c + A_3c^2 + \ \ldots .] \tag{9}$$

where R is the gas constant and T the absolute temperature, are given in *Table 2*. Corresponding values obtained from Krigbaum and Kotliar[20]

Table 2. Osmotic data for polyacrylonitrile

Source	$\bar{M}_n$	$10^4 \times A_2$
Present results at 25°C		
DMF*	75 900	30
+30·0 per cent benzene	35 000	8
+32·0 per cent benzene	35 000	0
+37·0 per cent benzene	83 900	−4
Krigbaum and Kotliar[20] at 30°C		
DMF†	45 900	29
+0·15 per cent water	43 200	15
+0·65 per cent water	43 500	10

*N,N'-dimethylformamide.
†Deionized solution.

(Figure 2 of ref. 20) which show the effect of traces of water on the osmotic behaviour of polyacrylonitrile in dimethylformamide solution at 30°C are also included for comparison. Values in the table are rounded and probably only reliable to $\pm 2\,000$ in $\bar{M}_n$ and $\pm 2 \times 10^{-4}$ in A_2. The result for the second virial coefficient determined in dimethylformamide solution agrees well with Krigbaum and Kotliar[20]. The reduction in A_2 with solvent quality is typical of polymeric behaviour. Marked non-linearity at low concentrations and a slightly negative value of A_2 are features observed in other associating systems, the aggregates dissociating on dilution[24].

Over the range of benzene concentrations of interest $\bar{M}_n$ increased from 35 000 to 83 900 giving $n = 2\cdot4$. The large difference in values of n obtained by sedimentation and osmometry indicates that the majority of associating molecules have combined to form a few very large aggregates in contrast to the observations of Boedtker and Doty on gelatin aggregates[23]. A similar situation was also observed by Newman, Krigbaum and Carpenter[25] with the reversible association of cellulose nitrate solutions in ethanol. It was found that whilst $\bar{M}_n$ changed by two times, the value of $\bar{M}_w$ increased by 800 times for identical conditions of the solutions. The value of $\bar{M}_w$ is sensitive to the presence of a few large aggregates but that of $\bar{M}_n$ is not.

An unexplained feature of *Figure 7* is the reduction in $\bar{M}_n$ on addition of up to 30 per cent benzene. Inspection of the results of Krigbaum and Kotliar[20] reveals a similar effect on addition of water; changes which are undoubtedly connected with the additional hysteresis effects shown in *Figure 1*. These observations together with those of Krigbaum and Kotliar[20] on the deionization of the polymer solutions emphasize the particular difficulties of molecular weight measurements in polyacrylonitrile solutions.

University of Bradford,
Bradford 7

REFERENCES
[1] FRISCH, H. L. *J. Polym. Sci.* 1955, **18**, 299
[2] CHANG, S-Y. and MORAWETZ, H. *J. phys. Chem.* 1956, **60**, 782
[3] DOTY, P., WAGNER, H. and SINGER, S. *J. phys. Chem.* 1947, **51**, 32
[4] MOORE, W. R. and HUTCHINSON, R. J. *Nature, Lond.* 1963, **200**, 1095
[5] MENČIK, Z. *J. Polym. Sci.* 1955, **17**, 147; *Coll. Czech. chem. Commun.* 1955, **20**, 940
[6] HEYN, A. N. J. *J. Polym. Sci.* 1959, **41**, 23
[7] PEEBLES, L. H. *J. Amer. chem. Soc.* 1958, **80**, 5603
[8] NICOLAS, L. *J. Polym. Sci.* 1958, **29**, 191
[9] THOMAS, W. M. *Fortschr. HochpolymForsch.* 1961, **2**, 401
[10] SHASHOUA, V. E. and BEAMAN, R. G. *J. Polym. Sci.* 1958, **33**, 101
[11] SHASHOUA, V. E. and VAN HOLDE, K. E. *J. Polym. Sci.* 1958, **28**, 395
[12] MEDALIA, A. I. *J. Polym. Sci.* 1951, **6**, 423
[13] CLIMIE, I. E. and WHITE, E. F. T. *J. Polym. Sci.* 1960, **47**, 149
[14] CLIMIE, I. E. Unpublished results, 1960
[15] BEEVERS, R. B. *J. appl. Polym. Sci.* 1965, **9**, 1499
[16] BEEVERS, R. B. *J. Polym. Sci. A*, 1964, **2**, 5257
[17] ALLEN, P. W. (Ed.) *Techniques of Polymer Characterization.* Butterworths: London, 1959
[18] GEE, G. *Trans. Faraday Soc.* 1944, **40**, 463
[19] BISSCHOPS, J. *J. Polym. Sci.* 1955, **17**, 81
[20] KRIGBAUM, W. R. and KOTLIAR, A. M. *J. Polym. Sci.* 1958, **32**, 323
[21] CHIANG, R. *J. Polym. Sci. A*, 1965, **3**, 2019
[22] KATAYAMA, M. and OGOSHI, T. *Kobunshi Kagaku*, 1956, **13**, 14
[23] BOEDTKER, H. and DOTY, P. *J. phys. Chem.* 1954, **58**, 968
[24] MORAWETZ, H. and GOBRAN, I. *J. Polym. Sci.* 1954, **12**, 133, 455
[25] NEWMAN, S., KRIGBAUM, W. R. and CARPENTER, D Y. *J. phys. Chem.* 1956, **60**, 648

The Effect of Network Breakdown and Re-formation on the Swelling of Rubbers in Compression

L. R. G. TRELOAR

The effect of changes in network structure on the equilibrium swelling of a crosslinked rubber subjected to uniaxial compressive stress is calculated on the basis of the 'two-network' hypothesis. Equations are also derived for the compressive force and the amount of elastic recovery after removal of the stress. Numerical examples are given to illustrate the effects predicted by the theory for the case of a rubber in a good swelling agent.

THE equilibrium degree of swelling in organic liquids of a crosslinked rubber subjected to any type of stress has been derived theoretically[1], on the basis of the Flory–Huggins treatment[2,3] of the free energy of mixing of polymer and liquid molecules. Experiments involving various types of stress, including uniaxial compressive stress[4-6], have confirmed the theoretical predictions for liquids producing a high degree of swelling.

In an unswollen rubber, the effects of network breakdown and crosslinking reactions taking place in the strained state may be dealt with on the basis of the so-called two-network hypothesis[7]. This hypothesis rests on the assumption that chains which have broken away from the network make no contribution to the stress, while those which become re-attached do so in the relaxed state. The latter likewise make no contribution to the stress so long as the state of strain remains unchanged, but if the strain is changed they behave as if they formed an independent network.

In the present paper the effects of structural changes in a swollen rubber subjected to uniaxial compressive strain are considered on the basis of the two-network hypothesis. It is assumed that the equilibrium swelling in the compressed state is achieved initially before any breakdown occurs. Thereafter either breakdown only, or breakdown plus re-formation (crosslinking) are assumed to occur, at constant compressed length. Both breakdown and crosslinking reactions modify the swelling equilibrium, and this in turn affects the compressive stress. The problem is to calculate the resultant swelling and compressive stress, for given amounts of network breakdown and re-formation.

The analysis of this problem is relevant to many uses of rubber under compression in the presence of swelling liquids, particularly in sealing applications.

Whereas in an unswollen rubber held at a fixed compressed length the changes in network structure occur at a constant state of strain, this is no longer true for a rubber in contact with a swelling liquid. In this case, if the compressed length is held constant, the swelling will continually increase with increasing amount of breakdown, and if crosslinking subse-

quently occurs, the newly-formed network will be formed at varying degrees of swelling and therefore at varying degrees of strain. To treat this problem exactly would appear to be possible in principle, but very difficult in practice, and no attempt has been made to do so. Instead, the difficulty has been evaded by considering the whole process of re-formation to occur at a single state of swelling, which in deriving the formulae need not be further specified. In calculating numerical results, however, some value must be assigned to this parameter. Since the appropriate value, for specified amounts of network breakdown and re-formation, is not known, two extreme values have been chosen, the first corresponding to the initial state of swelling, and the second to the final state of swelling. The practical case necessarily lies somewhere between these two extremes.

DERIVATION OF SWELLING EQUILIBRIUM
The following principal symbols will be used:

N_0 Number of chains per unit volume of original unswollen rubber

N_1 Number of chains remaining unbroken, per unit volume of unswollen rubber

N_2 Number of chains re-formed, per unit volume of unswollen rubber

ρ Density of unswollen rubber

M_c Original mean chain molecular weight

n_0 Number of moles of swelling liquid per unit volume of dry rubber

V_0 Molar volume of swelling liquid

v_2 Volume fraction of rubber in swollen state

l_1, l_2, l_3 Principal extension ratios, referred to unstrained unswollen rubber

General case

The treatment follows the same lines as in the author's earlier work on the problem of swelling under strain[1]. The total change in Helmholtz free energy A, in passing from the unstrained unswollen state to the strained swollen state is expressed as the sum of two terms, ΔA_m and ΔA_e, the first representing the free energy of mixing of polymer and liquid molecules (assumed independent of network formation) and the second the free energy of elastic deformation. The corresponding molar free energies of *dilution* A_{0m}, A_{0e}, are obtained by differentiation with respect to liquid content n_0, hence

$$\frac{\partial A}{\partial n_0} = A_{0m} + A_{0e} = \frac{\partial \Delta A_m}{\partial n_0} + \frac{\partial \Delta A_e}{\partial n_0} \tag{1}$$

For the first component the approximate form of the Flory–Huggins equation

$$A_{0m} = RT \left[\ln (1-v_2) + v_2 + \chi v_2^2\right] \tag{2}$$

will be used. In this expression R and T are the gas constant and absolute temperature, while χ is an experimentally-derived parameter whose value depends on the particular polymer–liquid system considered. The second

component, the free energy of network deformation, for a single unmodified network, is given by the statistical theory in the form*

$$\Delta A_e = \tfrac{1}{2} N_0 kT \, (l_1^2 + l_2^2 + l_3^2 - 3) = (\rho RT / 2M_c) \, (l_1^2 + l_2^2 + l_3^2 - 3) \tag{3}$$

k being Boltzmann's constant. This represents the most general type of strain (including swelling) in which the three principal extension ratios l_1, l_2 and l_3 are unrelated.

We now have to consider a process of network breakdown followed by re-formation or crosslinking at some specified state of swelling and strain. The state at which the breakdown occurs is not involved directly, but only through its influence on the subsequent swelling; it is therefore sufficient to specify the conditions under which the re-formation process occurs. We therefore specify this state by the principal extension ratios l_{11}, l_{21}, l_{31}, and corresponding volume fraction v_{21} of polymer. The system is then allowed to attain a new equilibrium, which will be represented by the extension ratios l_1, l_2, l_3, and volume fraction v_2. According to the two-network hypothesis the elastic free energy in the final state is given by

$$\frac{2\Delta A_e}{kT} = N_1 (l_1^2 + l_2^2 + l_3^2 - 3) + N_2 \left(\frac{l_1^2}{l_{11}^2} + \frac{l_2^2}{l_{21}^2} + \frac{l_3^2}{l_{31}^2} - 3 \right) \tag{4}$$

where N_1 and N_2 are the respective numbers of chains in the original and newly-formed networks.

Assuming additivity of volumes of polymer and liquid, we have the general relation

$$l_1 l_2 l_3 = 1/v_2 = 1 + n_0 V_0 \tag{5}$$

while for the particular case of uniaxial compression (or extension) in the direction l_1 the two transverse dimensions are equal, and are given by

$$l_2^2 = l_3^2 = 1/l_1 v_2 \tag{6}$$

For uniaxial compression equation (4) thus becomes

$$\frac{2\Delta A_e}{kT} = N_1 \left(l_1^2 + \frac{2}{l_1 v_2} - 3 \right) + N_2 \left(\frac{l_1^2}{l_{11}^2} + \frac{2l_{11} v_{21}}{l_1 v_2} - 3 \right) \tag{7}$$

To obtain the equilibrium swelling at a fixed value of compressed length l_1 we require the quantity $(\partial \Delta A_e / \partial n_0)$. Making use of (5) we have

$$\left(\frac{\partial \Delta A_e}{\partial n_0} \right)_{l_1} = \left(\frac{\partial \Delta A_e}{\partial v_2} \right)_{l_1} \cdot \frac{dv_2}{dn_0} = \left(\frac{\partial \Delta A_e}{\partial v_2} \right)_{l_1} (-V_0 v_2^2) \tag{8}$$

Differentiation of (7) with respect to v_2 then gives

$$\frac{2}{kT} \left(\frac{\partial \Delta A_e}{\partial n_0} \right)_{l_1} = \left[N_1 \left(-\frac{2}{l_1 v_2^2} \right) + N_2 \left(-\frac{2l_{11} v_{21}}{l_1 v_2^2} \right) \right] (-V_0 v_2^2)$$

An alternative formula for the network free energy has been derived by Flory. This is
$$\Delta A_g = (\rho RT / M_c) \, (l_1^2 + l_2^2 + l_3^2 - 3 - \ln l_1 l_2 l_3)$$
The use of this in place of equation (3) would lead to a slight modification of the equations derived in the present paper, but would not introduce any difference in principle.

or

$$\left(\frac{\partial \Delta A_e}{\partial n_0}\right)_{l_1} = \frac{kTV_0}{l_1} \quad (N_1 + N_2 l_{11} v_{21}) \tag{9}$$

In the present case it is further assumed that the compressed length is held constant throughout, so that $l_1 = l_{11}$. Introducing this condition, we obtain finally

$$\left(\frac{\partial \Delta A_e}{\partial n_0}\right)_{l_1 = l_{11}} = kTV_0 \left(\frac{N_1}{l_{11}} + N_2 v_{21}\right) = \frac{\rho RTV_0}{M_c} \left(\frac{N_1}{N_0} \cdot \frac{1}{l_{11}} + \frac{N_2}{N_0} v_{21}\right) \tag{10}$$

since

$$N_0 kT = \rho RT / M_c \tag{11}$$

The condition for equilibrium swelling is

$$\frac{\partial A}{\partial n_0} = A_{0m} + A_{0e} = 0 \tag{12}$$

Making use of (2) and (10) this gives the result

$$\frac{\rho V_0}{M_c} \left(\frac{N_1}{N_0} \cdot \frac{1}{l_{11}} + \frac{N_2}{N_0} v_{21}\right) = -\frac{A_{0m}}{RT} = -[\ln (1 - v_2) + v_2 + \chi v_2^2] \tag{13}$$

Special cases

Case 1—Breakdown without re-formation of junction points.
For this simple case $N_2 = 0$, and equation (13) can be reduced to

$$\frac{\rho V_0}{M_c} \cdot \frac{N_1}{N_0} \cdot \frac{1}{l_{11}} = -[\ln (1 - v_2) + v_2 + \chi v_2^2] \tag{14}$$

which may be solved for v_2, the volume fraction of polymer at the equilibrium swelling.

Case 2(a)—Breakdown together with re-formation of junction points at the *initial* state of swelling.
In this case the parameter v_{21} represents the state of swelling of the compressed material before any breakdown or crosslinking reactions have occurred. Its value is obtained by putting $N_1 = N_0$ and $N_2 = 0$ in equation (13), and solving for v_{21}, i.e.

$$\frac{\rho V_0}{M_c} \cdot \frac{1}{l_{11}} = -[\ln (1 - v_{21}) + v_{21} + \chi v_{21}^2] \tag{15}$$

Insertion of this value of v_{21} into equation (13) gives an equation which may be solved for v_2, the final equilibrium volume fraction of polymer.

Case 2(b)—Breakdown together with re-formation of junction points at the *final* state of swelling.
In this case v_{21} is not predetermined, but is equal to the final volume fraction v_2. We therefore put $v_{21} = v_2$ in equation (13), and obtain an equation containing only the variable v_2, i.e.

$$\frac{\rho V_0}{M_c} \left(\frac{N_1}{N_0} \cdot \frac{1}{l_{11}} + \frac{N_2}{N_0} v_2\right) = -[\ln (1 - v_2) + v_2 + \chi v_2^2] \tag{16}$$

COMPRESSIVE FORCE

To obtain the compressive force F, we consider the work δW performed in a reversible increase of length δl_1, at constant v_2. If we consider the material in the unstrained unswollen state to have the form of a unit cube, we have

$$\delta W = -F\, \delta l_1$$

Making the usual assumption of incompressibility with respect to total volume no work is done against the atmospheric pressure and therefore $\delta W = \delta A$. Hence we may write

$$F = -(\partial A / \partial l_1)_{v_2} \tag{17}$$

Furthermore, since the free energy of mixing is a function of v_2 only, we have

$$\left(\frac{\partial A}{\partial l_1}\right)_{v_2} = \left(\frac{\partial \Delta A_m}{\partial l_1}\right)_{v_2} + \left(\frac{\partial \Delta A_e}{\partial l_1}\right)_{v_2} = \left(\frac{\partial \Delta A_e}{\partial l_1}\right)_{v_2} \tag{18}$$

Hence

$$F = -(\partial \Delta A_e / \partial l_1)_{v_2} \tag{19}$$

Differentiation of equation (7) with respect to l_1 gives

$$-\frac{F}{kT} = \frac{1}{kT}\left(\frac{\partial \Delta A_e}{\partial l_1}\right)_{v_2} = N_1\left(l_1 - \frac{1}{l_1^2 v_2}\right) + N_2\left(\frac{l_1}{l_{11}^2} - \frac{l_{11} v_{21}}{l_1^2 v_2}\right) \tag{20}$$

Letting $l_1 = l_{11}$ (the fixed compressed length) and introducing the relation (11) we obtain finally

$$F = \frac{\rho RT}{M_c}\left[\frac{N_1}{N_0}\left(\frac{1}{l_{11}^2 v_2} - l_{11}\right) + \frac{N_2}{N_0}\left(\frac{v_{21}}{l_{11} v_2} - \frac{1}{l_{11}}\right)\right] \tag{21}$$

Special cases

In applying equation (16) to the special cases considered in the preceding section, the values of v_{21} and v_2 obtained as therein described are to be employed. It may be noted here that for Case 1 (no re-formation of junction points) $N_2 = 0$ and the second term in (21) vanishes. For Case 2(b) (re-formation at final state of swelling) $v_{21} = v_2$, and again the second term vanishes. In this case the second network, having been formed at the final state of swelling, is not subjected to any further strain, and hence does not contribute to the stress (though its presence does affect the equilibrium swelling, and therefore, indirectly, the stress).

ELASTIC RECOVERY AND COMPRESSION SET

In certain practical situations, while it may not be possible or convenient to measure the compressive force, it may nevertheless be possible to measure the elastic recovery, i.e. the final length attained after removal of the stress. In discussing the calculation of this recovery, it is necessary to distinguish between the *instantaneous* recovery which takes place on removal of the stress, without change in the state of swelling (v_2), and the *ultimate* recovery, which corresponds to the final equilibrium attained if the

437

rubber is left in contact with the liquid after removal of the stress. In this final state the state of swelling will differ from that existing prior to removal of the stress.

Finally, we consider the final length in the stress-free state *after removal of the swelling liquid.*

Instantaneous recovery

In considering the elastic recovery on removal of the compressive stress, it may be assumed that the state of symmetry existing in the stressed state will be retained, i.e. that the recovery will correspond to an extension along the axis, with equal contractions in the two transverse dimensions. Under these conditions the network free energy may still be represented by equation (7), in which l_{11} and v_{21} are respectively the length and volume fraction of polymer at which the second network was formed, and v_2, in the present context, is the equilibrium volume fraction prior to removal of the stress. The criterion for equilibrium in the stress-free state (with v_2 constant) is that the network free energy shall be a minimum with respect to changes in l_1, or alternatively, that the compressive force F given by (20) shall be zero. Thus if l_1 is the instantaneously-recovered length we have, from (20),

$$N_1 \left(l_1 - \frac{1}{l_1^2 v_2} \right) = N_2 \left(\frac{l_1}{l_{11}^2} - \frac{l_{11} v_{21}}{l_1^2 v_2} \right)$$

or

$$l_1^3 = \frac{1}{v_2} \cdot \frac{N_1 + N_2 l_{11} v_{21}}{N_1 + N_2 / b_{11}^2} \tag{22}$$

Ultimate recovery

In applying equation (22) to the instantaneous recovery, v_2 is given the value corresponding to the state of swelling prior to removal of the stress. However, equation (22) expresses the relation between the stress-free length l_1 and the volume fraction of polymer v_2, whatever the value of v_2. To obtain the final value of v_2 in the stress-free state, a second relation between l_1 and v_2, representing the equilibrium with respect to liquid content, must be introduced. The relevant relation is obtained by combining equations (9) and (12), but without the restriction $l_1 = l_{11}$ previously introduced. Introducing N_0 via (11), the result becomes

$$\frac{\rho V_0}{M_c} \cdot \frac{1}{l_1} \left(\frac{N_1}{N_0} + \frac{N_2}{N_0} l_{11} v_{21} \right) = - \frac{A_{0m}}{RT} = - [\ln(1 - v_2) + v_2 + \chi v_2^2] \tag{23}$$

Equations (22) and (23) now form a pair of simultaneous equations in the two variables l_1 and v_2. They may be solved by successive approximation.

Compression set in unswollen state

If, after network breakdown and re-formation, the compressive stress is removed and the rubber is allowed to dry, the final length l_1 in the stress-free dry state will be given by equation (22), with $v_2 = 1$, i.e.

$$l_1^3 = \frac{N_1 + N_2 l_{11} v_{21}}{N_1 + N_2 / l_{11}^2} \tag{22a}$$

In the case when v_{21} is also unity, this result is in agreement with that obtained by previous workers[9].

The quantity $1 - l_1$ may be called the 'compression set'.

An examination of equation (22) leads to the conclusion that the compression set is independent of the state of swelling, i.e. for uniaxial stresses the material in its final state swells isotropically. In particular, this ratio is the same for the instantaneously recovered state, for the ultimate state of equilibrium in contact with liquid, and for the final dry state.

The result may be proved by putting

$$\frac{N_1 + N_2 l_{11} v_{21}}{N_1 + N_2 / l_{11}^2} = a = \text{const.}$$

so that equation (22) becomes

$$l_1^2 v_2 = a$$

From (6) we then have

$$l_2^2 = 1 / l_1 v_2 = l_1^2 / a$$

or

$$l_2^2 / l_1^2 = 1 / a = \text{const.}$$
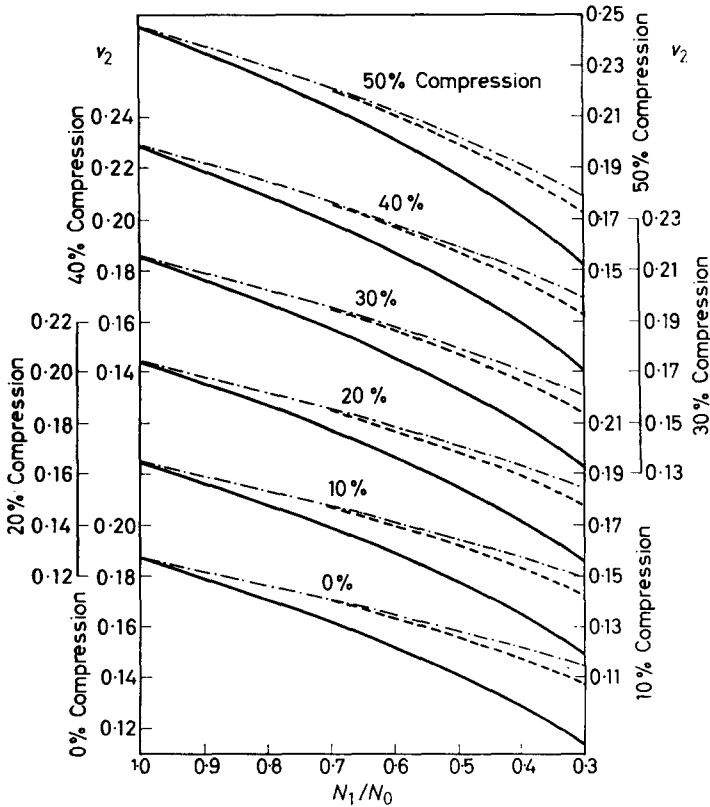
Figure 1—Volume fraction v_2 at equilibrium swelling:
—— Case 1; — · — · — Case 2(a); — — — — Case 2(b)
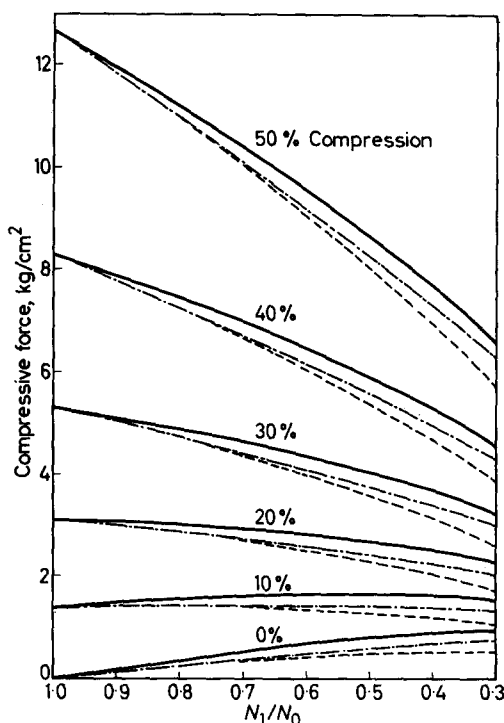
Figure 2—Compressive force per unit unstrained unswollen area:
—— Case 1; — · — · Case 2(*a*); — — — Case 2(*b*)

The isotropy of the network with respect to swelling is analogous to the isotropy of *any* Gaussian network with respect to mechanical strains, which has been proved by Lodge[10].

NUMERICAL CALCULATIONS AND CONCLUSIONS

For the purpose of illustrating the general features of the above results, values of equilibrium swelling, compressive force and final dry length have been calculated for each of the three special cases considered. To avoid over-elaboration the number of chains re-formed, in Cases 2(a) and 2(b), has been put equal to the number broken down, i.e. $N_1 + N_2 = N_0$.

The numerical values of the parameters occurring in the equations were chosen to correspond to the system natural rubber plus benzene, i.e.

$$\rho = 0.95 \text{ g/cm}^3, \qquad V_0 = 89.4 \text{ cm}^3/\text{mole}, \qquad \chi = 0.41$$

Taking $M_c = 8\,490$ we then have $\rho V_0 / M_c = 1/100$. For a temperature of 298°K, taking $R = 84.78$ k cm/deg., this gives $\rho RT / M_c = 2.827$ kg/cm².

The percentage compression is specified with respect to the initial linear dimensions in the swollen stress-free state. Thus, using the above values, one obtains for the initial stress-free state

$$v_2 = 0.1874_7, \qquad l_1 = v_2^{-1/3} = 1.747_3$$

440

A 40 per cent compression, for example, would thus correspond to a length ratio l_{11} of $1\cdot048_4$. Calculations were made for six values of compression, and for values of N_1/N_0 from $1\cdot0$ to $0\cdot3$ at intervals of $0\cdot1$. The results are presented in the accompanying *Figures 1, 2* and *3*.

The most significant feature of the data is the relatively slight difference in swelling between Case 2(a) and Case 2(b). This implies that either of these cases may be taken as a fairly close approximation to the more complex case in which the process of re-formation occurs continuously between the initial and final states of swelling.
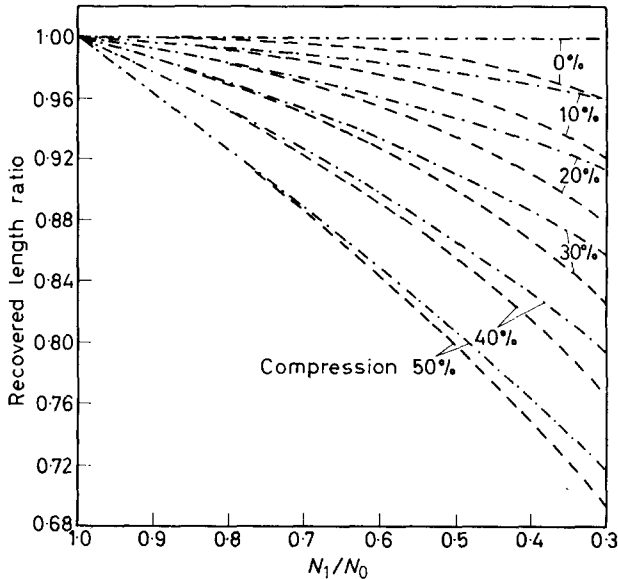
Figure 3—Recovered length ratio in dry state:
———— Case 1; — · — · — Case 2(a); — — — Case 2(b)

It is seen from *Figure 2* that for high initial compressions the force decreases with increasing breakdown (whether or not this is accompanied by re-formation), while for zero or small initial compressions it increases. In the latter case the increase in swelling arising from network breakdown has the effect of increasing the compressive force, and thus tends to compensate for the reduction which would otherwise occur.

In *Figure 3*, data for recovered length are given only for Case 2(a) and 2(b). In Case 1, a second network is not formed, and the recovered length is therefore always unity.

It is perhaps worth noting that Case 2(b) gives a finite compression set even for the case of zero initial compression.

type of theoretical analysis given in this paper, and for a number of discussions on its subject-matter.

Department of Polymer and Fibre Science,
   University of Manchester Institute of Science and Technology,
      Manchester, 1

REFERENCES

[1] TRELOAR, L. R. G. *Proc. Roy. Soc. A,* 1950, **200,** 176
[2] FLORY, P. J. *J. chem. Phys.* 1942, **10,** 51
[3] HUGGINS, M. L. *Ann. N. Y. Acad. Sci.* 1942, **43,** 1
[4] FLORY, P. J. and REHNER, J. Jr. *J. chem. Phys.* 1944, **12,** 412
[5] GEE, G. *Trans. Faraday Soc.* 1946, **42,** 33
[6] TRELOAR, L. R. G. *Trans. Faraday Soc.* 1950, **46,** 783
[7] TOBOLSKY, A. V., ANDREWS, R. D. and HANSON, R. M. *J. appl. Phys.* 1946, **17,** 352
[8] FLORY, P. J. *J. chem. Phys.* 1950, **18,** 108
[9] NEUBERT, D. and SAUNDERS, D. W. *Rheol. acta,* 1958, **1,** 151
[10] LODGE, A. S. *Kolloidzschr.* 1960, **171,** 46

Conversion Factors in Dilatometry

C. E. M. MORRIS and A. G. PARTS

In dilatometric determinations of the extent of polymerization reactions the difference between the partial specific volumes of the reactants and the products determines the volume contraction. The partial specific volumes cannot be assumed to be equal to the specific volumes of the respective pure compounds.

ONE OF the most convenient methods of following the progress of a polymerization reaction is by dilatometry. As many readings as desired can be taken, with considerable precision, of the height contraction of the capillary liquid column (and hence volume contraction) as the reaction proceeds. The difficulty, which is not recognized by many workers, comes in relating the observed volume contraction to the extent of reaction, e.g. the percentage conversion in the case of polymerization. While it is a relatively simple matter to calibrate the dilatometric method for a given system by some absolute technique (e.g. gravimetric determinations) large numbers of workers do not do this but rely instead on a calculation from the densities of the pure components of the system. The validity of such calculations is extremely doubtful and often gives conversion factors greatly in error.

A warning along these lines was given by Treloar[1]. As he said 'frequently the method of calibration (of dilatometry) is to assume ideal mixing of both monomer and polymer with the solvent used and to calculate the expected volume contraction for 100 per cent conversion from a knowledge of the density of both the monomer and the polymer. The percentage conversion is then assumed to be directly proportional to the volume contraction'. However, in the subsequent discussion he assumes linearity of the density of homogeneous mixtures with concentration, which relationship is not fulfilled when volumes are additive.

The main objection to the calculation of the volume contraction accompanying polymerization lies in the assumption that this volume change can be calculated from the bulk densities of the monomer and polymer, since this assumes that the partial specific volumes of the components are the same in bulk as in solution. This is generally not true; see, for example, the investigation of the partial molal volumes of alcohols in water by Nakanishi[2]. Calculation of the volume contraction from the densities of the pure monomer and polymer may be valid for the bulk polymerization of a monomer immiscible with its polymer. In any system which contains a solvent for the monomer or the polymer, or both, or in which monomer and polymer are miscible, the volume contraction accompanying polymerization cannot be calculated from the bulk densities of the monomer and polymer.

The difference in the value of the specific contraction between that determined experimentally and that calculated on the density basis can

be very considerable. *Table 1* summarizes for various systems values of the specific contraction determined experimentally and calculated from the bulk monomer and polymer densities. These examples have been selected at random from the literature.

Table 1

Monomer	Solvent or dispersing medium	Specific contraction on polymerization, experimental, cm^3/g	Ref.	Specific contraction on polymerization, calculated, cm^3/g	Ref. (density data)	T $°C$
Methyl acrylate	H_2O	0·150	3	0·250	4	40·0
Vinyl acetate	H_2O	0·156	5	0·253	6	40·0
Acrylonitrile	H_2O	0·283	7	0·403*	8,9	40·0
Styrene	—	0·175	10	0·159†	11	25·0
Styrene	H_2O	0·188	12	0·182†	11	50·0
Styrene	ethylene dichloride	0·170	13	0·172†	13	25·0
Styrene	50/50 nitrobenzene/ carbon tetrachloride	0.152	14	0·168†	14	0

*Calculated from densities at 25·0°C.
†Various values can be calculated because of the range of density data which is available for the monomer and polymer.

The temperature dependence of the specific contraction has been shown experimentally to be small[10].

It is obvious that calculation of the specific contraction from the bulk densities can give results greatly in error, especially in aqueous systems. In principle, it should be possible to calculate the specific contraction from the partial specific volumes of the components of the mixture. However, lack of suitable data on the density of monomer–polymer–solvent mixtures in general prevents this calculation. Some data are available[9] for mixtures of acrylonitrile in water up to a concentration of 1·20 M. Since neither water nor the monomer is a solvent for polyacrylonitrile, this is potentially a suitable system for calculation of the specific contraction from the partial specific volume of the monomer in water. Unfortunately, the solubility of the monomer in water is limited (up to about seven per cent) so that the mole fraction of monomer in water is very small—up to about 0·023. For calculation of the partial specific volume, the smallness of the monomer mole fraction necessitates extremely accurate measurements of the density of the monomer–water mixtures—probably to greater accuracy than is readily obtainable experimentally. From the density data available (25·0°C) the partial specific volume of acrylonitrile in water was calculated to be 1·106 cm³/g in the mole fraction range 0 to 0·0228, whilst the partial specific volume of water was calculated to be 1·003 cm³/g.

Taking the density[9] of polyacrylonitrile as $1.182 \, g/cm^3$, the specific contraction is thus $0.260 \, cm^3/g$. Gravimetric determinations[7] gave a value of $0.283 \, cm^3/g$. Taking into account the accuracy of the density data from which the partial specific volume was calculated the agreement can be considered satisfactory. These values may be compared with that calculated from the bulk densities of the monomer and polymer, $0.403 \, cm^3/g$ ($25.0°C$).

A further consideration is the dependence of the partial specific volume on concentration, a marked variation being observed in some cases, for example, the alcohols in water[2]. In the calculation reported above, the change in partial specific volume with concentration over the narrow monomer mole fraction range examined is extremely small. It should be noted, however, that the partial specific volume of acrylonitrile alone is $1.249 \, cm^3/g$ at $25.0°C$, which may be compared with the mean value obtained above, $1.106 \, cm^3/g$. Applied to polymerization, this means that where a concentrated monomer solution is used, the conversion factor in dilatometry is not in fact a constant but a variable whose value depends on the composition of the mixture, i.e. on the extent of polymerization. This conclusion is not confined to aqueous acrylonitrile solutions but applies in general to all systems. Without more extensive data on the partial specific volume at various concentrations it is impossible to say at what concentrations such effects become significant as far as the calculation of the extent of reaction from the observed volume contraction is concerned.

It is obvious that to obtain the specific contraction for a particular system one must determine by some absolute method (such as gravimetrically) the amount of formed polymer which corresponds to a given volume change, and not rely on any calculation from the bulk densities of the monomer and polymer.

Department of Physical Chemistry,
  University of Sydney,
    Sydney, N.S.W., Australia

REFERENCES

[1] TRELOAR, F. E. *Polymer, Lond.* 1960, **1**, 513
[2] NAKANISHI, K. *Bull. chem. Soc. Japan,* 1960, **33**, 793
[3] MORRIS, C. E. M., ALEXANDER, A. E. and PARTS, A. G. *J. Polym. Sci. A,* 1966, **4**, 985
[4] MATHESON, M. S., AUER, E. E., BEVILACQUA, E. B. and HART, E. J. *J. Amer. chem. Soc.* 1951, **73**, 5395
[5] NAPPER, D. H. and PARTS, A. G. *J. Polym. Sci.* 1962, **61**, 113
[6] MATHESON, M. S., AUER, E. E., BEVILACQUA, E. B. and HART, E. J. *J. Amer. chem. Soc.* 1949, **71**, 2610
[7] MORRIS, C. E. M. *Ph.D. Thesis,* University of Sydney, 1966
[8] DAVIS, H. S. and WIEDEMAN, O. F. *Industr. Engng Chem. (Industr.),* 1945, **37**, 482
[9] MOORE, D. E. *M.Sc. Thesis,* University of Sydney, 1960
[10] COOPER, W. and SMITH, R. J. *J. Polym. Sci.* 1952, **9**, 463
[11] PATNODE, W. and SCHEIBER, W. J. *J. Amer. chem. Soc.* 1939, **61**, 3449
[12] BARTHOLOMÉ, E., GERRENS, H., HERBECK, R. and WEITZ, H. M. *Z. Elektrochem.* 1956, **60**, 334
[13] PEPPER, D. C. *Trans. Faraday Soc.* 1949, **45**, 404
[14] OVERBERGER, C. G., EHRIG, R. J. and MARCUS, R. A. *J. Amer. chem. Soc.* 1958, **80**, 2456

Note

Aromatic Polyester

THE aromatic polyesters were prepared as a hard segment for an elastomeric polyester. The molecular chain of the flexible rubbery segments is considered to be randomly coiled in a state of tangled disorder so that orientation by the application of an external force will be counteracted by the tendency of the molecules to return to their most likely random configuration. The resistance of the elastomeric polyesters to viscous flow is attributed to the presence of the rigid crystallites of the hard segments in the matrix of the mobile polymer chains. It is felt that the rigid crystallites contribute to producing high tensile strength and elastic recovery. The hard segment must also have a high melting point to counteract the low melting point of the soft segment. The high melting, crystalline segments were best prepared by using symmetrical aromatic acid esters and symmetrical aromatic diols. For this purpose, aromatic diols,

$$HO-(CH_2)_n-\!\!\!\diagup\!\!\!\!\!\diagdown\!\!\!\!\!\bigcirc\!\!\!\!\!\diagdown\!\!\!-(CH_2)_n-OH \quad (n=1-5)$$
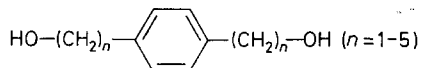
were synthesized to be polycondensed with dimethylterephthalate.

Polymerization

6·99 g (0·036 mole) of dimethylterephthalate, 0·072 mole of aromatic diol and 0·5 cm³ of 20 per cent n-butanol solution of metal butoxide catalyst were placed in a 100 ml flask equipped with a stirrer and nitrogen inlet. The mixture was heated at 200° to 210°C to take methanol out of the system, then the pressure was gradually reduced to the vicinity of 0·3 mm of mercury by raising temperature at the same time up to 270° to 280°C. In two hours the condensation was complete to give a high molecular weight polyester. The intrinsic viscosity was measured by dissolving polymers in phenol–tetrachlorethane (6: 4).

Thus, the essential feature of these aromatic polyesters is high melting, good symmetry and packing to compensate the low melting point of a soft segment.

In *Table 1*, the physical properties of the resulting polyesters are shown. In *Figure 1*, the observed melting points were plotted against the numbers of methylene groups (n). It was found that the series with even numbers of (n) have higher melting points than those with odd numbers. This phenomenon has already been found in polyamides and discussed in terms of hydrogen bonding[1-2] or of pleated structure[3]. The observed densities are plotted for series of aromatic polyester homologues in *Figure 2*. It is to be noticed that the relation between density and number of methylene groups (n) has a close resemblance to the relation between melting point and (n)*. This phenomenon has a feature of significance in itself by the fact that the relation between density and methylene number (n) indicates the characteristics of molecular packing, the molecule with an even number of (n) being

*(n) refers to numbers of carbon atoms between benzene ring and hydroxyl end group in the aromatic diols.
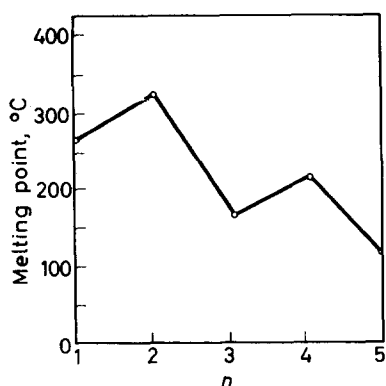
Figure 1—Melting points of aromatic polyesters
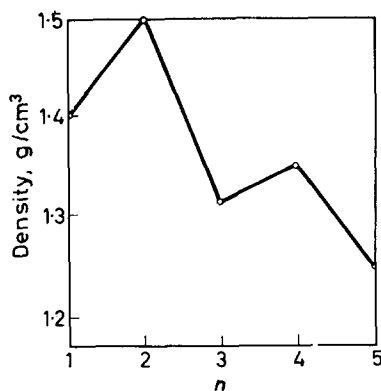
Figure 2—Densities of aromatic polyesters.

expected to pack together much more closely than the molecule with an odd number of (n).

Fibres spun from an aromatic polyester, particularly when $n = 2$, showed high melting point (330°C) and an excellent dimensional stability.
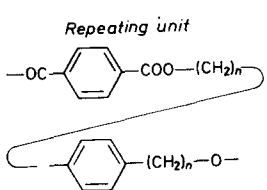
Dimensional stability was measured by immersing each sample which was melt spun and stretched $5 \times$, in a water bath at 100°C for 20 seconds. Disorientation in the amorphous regions usually proceeds rapidly with the longitudinal shrinkage of a fibre.

The shrinkage of a fibre was determined by measuring its length under standard conditions (24°C, 65% RH) before and after a specified exposure.

Fibres from an aromatic polyester ($n = 2$) showed a shrinkage of 2·5 per cent, whereas the commercially available polyethylene terephthalate which was subjected to the same test showed a shrinkage of 10·4 per cent.

In conclusion, it was found that there is a striking difference in melting point depending upon the number of methylene groups (n) attached to diols. This phenomenon was related to a molecular packing of the polymer. High

Table 1. Physical properties of aromatic polyesters

Polymer No.	Repeating unit	M.pt (°C)	[η]*	Density (g/cm³)
1	$n = 1$	265–267	0·71	1·40
2	$n = 2$	327–330	0·82	1·51
3	$n = 3$	159–162	0·91	1·31
4	$n = 4$	214–217	0·80	1·35
5	$n = 5$	113–116	0·75	1·24

*Measured in phenol·tetrachlorethane (6:4) solution at 30°C.

molecular weight aromatic polyester was successfully obtained by using metal double alkoxide such as: $Mg[H Ti(OBu)_6]_2$ as a catalyst.

A. A. NISHIMURA

Research Department,
  Dow Badische Co.,
    Williamsburg, Va 23185

(Received November 1966)

REFERENCES

[1] BUNN, C. W. and GARNER, E. V. *Proc. Roy. Soc. A,* 1941, **189,** 39
[2] CHAMPETIER, G. and AÉLION, R. *Bull. Soc. Chim. Fr.* **1948,** 683
[3] PAULING, L. and COREY, R. B. *Proc. Nat. Acad. Sci. Wash.* 1953, **39,** 253

Thermooxidative Stability of Polypropylene with Regard to the Concentration of Hydroperoxides in the Presence of Phenolic Stabilizer

D. Ryšavý

The inhibited oxidation of atactic polypropylene containing different initial concentrations of hydroperoxidic groups has been studied at 120°C and in the temperature range 160° to 170°C. The mathematical expressions for the dependence of the length of the induction period on concentrations of phenolic stabilizer and hydroperoxidic groups have been derived. It follows from the kinetic analysis that the derived equation for 120°C is valid for the concentration range of stabilizer at which the rates of radical termination by stabilizer and by recombination are of the same order. The expression valid for the temperature range 160° to 170°C has been found to be identical with Shlypanikov's equation derived for the temperatures 180° to 210°C. The critical antioxidant concentration and the length of the induction period are both functions of the initial concentration of hydroperoxidic groups. The activation energy of the direct oxidation of antioxidant 2246 has been determined.

POLYPROPYLENE readily undergoes oxidative destruction of its comparatively weak tertiary C—H bonds. The rate of oxidation can be slowed down by the addition of the compounds which can react with radicals in such a way that less active species are formed. The main representatives of this group of stabilizers are substituted phenols. Their effectiveness for the stabilization of polypropylene and its copolymers with regard to the structure of the stabilizer and temperature has been studied by many authors[1-8].

However, very little attention has been paid to the problem of the extent to which the stability of polypropylene articles depends on the concentration of hydroperoxidic groups which were formed during the preparation and storage of the polymer before the addition of stabilizer. The present paper is devoted to this problem.

The measurements were done on atactic polypropylene, in which we can determine accurately the concentration of hydroperoxidic groups and prepare stabilized samples at temperatures at which the rate of decomposition of hydroperoxides is negligible.

The process of the inhibited oxidation at 120°C is slow. In order to speed up the measurements the concentration of stabilizer was reduced by a factor of ten in comparison with the concentrations used for commercial articles.

EXPERIMENTAL

Materials

The atactic polypropylene was obtained by the propan extraction of polymer prepared with the $TiCl_3$–$AlEt_3$ catalytic system. This polymer was

dissolved in ether, the solution was filtered, concentrated by distillation under nitrogen, then precipitated by acetone and dried in the vacuum oven at 40°C. Molecular weight was 6.8×10^4. The concentrations of titanium and aluminium were less than 50 p.p.m.

Antioxidant 2246—a commercial product of American Cyanamid Co.—was repeatedly recrystallized. M.pt 131°C.

4-Hydroxy-3,5-di-tertbutyl-toluene prepared in our Institute was purified by recrystallization. M.pt 68·5°C.

Analytical grade solvents were used without further purification.

Ether was freed from peroxides by shaking with a five per cent solution of ferrous sulphate and water. This product was dried over calcium chloride and sodium and finally distilled under nitrogen.

Methods

The rate of the inhibited oxidation was characterized by the length of the induction period. The induction period is defined by the time taken for 1 g of polymer to absorb 2 ml of oxygen. It means that 0·4 per cent of tertiary C—H bonds are oxidized.

The simple apparatus shown in *Figure 1* was used for the determination of the induction period.
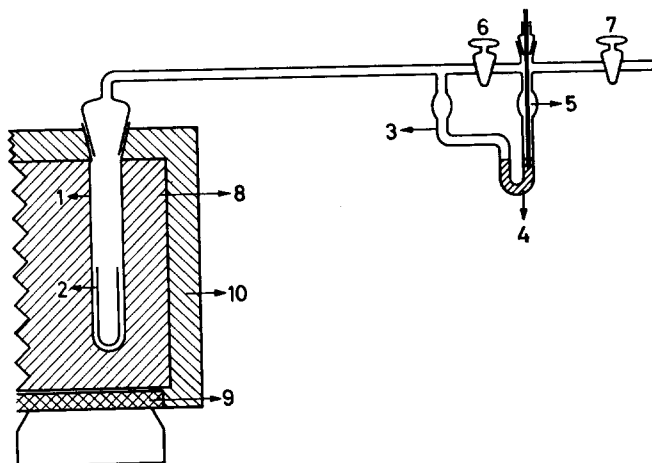
Figure 1—Apparatus for determination of the induction period

The reaction vessel is connected to a pressure gauge which consists of a U-tube with a small bulb on each arm. Both arms are joined by a tube and tap, 6. In the right-hand arm there are two contacts immersed in mercury, 4, and connected to a recorder. Vacuum line and filling assembly are joined to the differential pressure gauge through a tap, 7. The reaction vessel is placed in an aluminium block, 8, which is insulated by glass wool, 10, and heated with a heater, 9. The temperature is kept constant within ± 0.1 deg. C.

A sample (0·05 g) is weighed in tube 2 and placed into the reaction vessel, 1, just before the measurement. Taps 6 and 7 are opened and the

apparatus is evacuated and then filled with oxygen till atmospheric pressure is reached. During the measurement taps 6 and 7 are closed. At the end of the induction period when oxygen is absorbed by a polymer sample, the pressure decreases and subsequently the level of mercury in the right-hand arm goes down till the contacts are disconnected. The disconnection of the electric circuit is recorded.

The two solutions of polymer in heptane and solution of stabilizer in benzene–heptane (3:1) were used for the preparation of samples for the induction period determination.

Polymer solutions—The purified atactic polypropylene was dissolved in pure heptane (6 g atactic polypropylene in 100 g of solvent). The solution was bubbled with argon and stored at −10°C. One part of it was used for the preparation of peroxidic groups on the polymer by the exposure of polymer foils on Petri dishes to oxygen at 120°C. After hydroperoxides were accumulated the foils were again dissolved in heptane. The polymer, with a certain concentration of hydroperoxidic groups, was prepared by mixing these two solutions. The concentration of hydroperoxides was determined analytically. The solution of a known concentration of hydro-peroxides was then mixed with the solution of stabilizer in benzene and the polymer samples were prepared by casting the solution on to Teflon plates. The solvents were removed by a stream of air at 40°C and by drying under vacuum at the same temperature. The foil which was formed on the surface of the plate was pulled off and used for the induction period determination. The foil was easily removed from the Teflon surface.

Determination of hydroperoxidic groups—Dulog's method[9] based on the oxidation of leucomethylene blue by hydroperoxides was used. The photometric determination of the optical density at 643 n.m. was employed for the quantitative measurements.

DISCUSSION

Inhibited oxidation at 120°C

The dependence of the length of the induction period on the concentration of stabilizer 2246 is shown in *Figure 2*. The system behaves as an unstabilized one up to a certain concentration of stabilizer which depends on the concentration of hydroperoxides. When this concentration is reached an induction period is observed. The lower the concentration of hydroperoxides the greater the length of the induction period found.

Each curve (*Figure 2*) can be described by equation (1), as shown in *Figure 3*.

$$\log \tau = m \, [AH]_0 + b \tag{1}$$

The plot of m against concentration of hydroperoxides gives an equi-axed hyperbola (*Figure 4*) which demonstrates the sharp decrease of the effectiveness of the stabilization with increasing concentration of hydroperoxides.

The rectilinear dependence (*Figure 5*) is obtained in $1/m$ versus $[ROOH]_0$ coordinates

$$1/m = a \, [ROOH]_0 \tag{2}$$
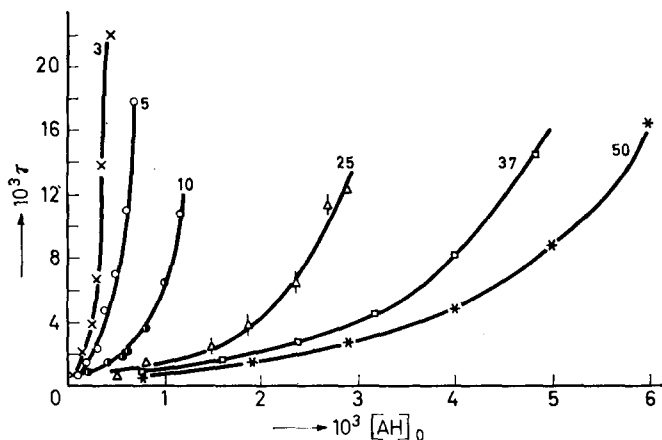
Figure 2—Dependence of length of induction period on initial concentration of antioxidant 2246. Numerals on curves denote initial concentration of hydroperoxidic groups in 10^{-3} mole/l.

The mathematical expression of the dependence of the length of the induction period on the concentration of stabilizer and hydroperoxides can be obtained from equations (1) and (2):

$$\log \tau = m \, [\mathrm{AH}]_0 + b$$

$$\frac{1/m = a \, [\mathrm{ROOH}]_0}{\log \tau = \frac{1}{a} \, \frac{[\mathrm{AH}]_0}{[\mathrm{ROOH}]_0} + b}$$
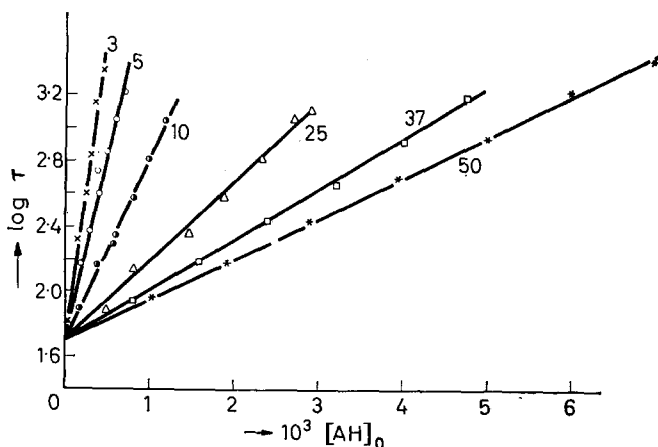
Figure 3—Dependence of logarithm of induction period on initial concentration of antioxidant 2246 at 120°C. Numerals on curves denote initial concentration of hydroperoxidic groups in 10^{-3} mole/l.

452
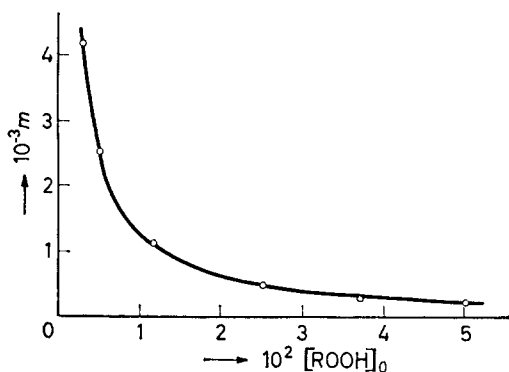
Figure 4—The plot of m versus initial concentration of hydroperoxidic groups

Let

$$b = \log q$$

Then

$$\log \frac{\tau}{q} = \frac{1}{a} \frac{[AH]_0}{[ROOH]_0}$$

or

$$\ln \frac{\tau}{q} = \frac{2\cdot 3}{a} \frac{[AH]_0}{[ROOH]_0}$$

Let

$$k = 2\cdot 3/a$$

Then

$$r = q \exp \{k \, [AH]_0/[ROOH]_0\} \tag{3}$$

The values of q and k characterizing the effectiveness of stabilization of two substituted phenols are given in *Table 1*.

Table 1

Stabilizer	k	q (sec)
Antioxidant 2246	25·75	$2\cdot 87 \times 10^3$
4-Hydroxy-3,5- di-tertbutyltoluene	12·65	$4\cdot 76 \times 10^3$
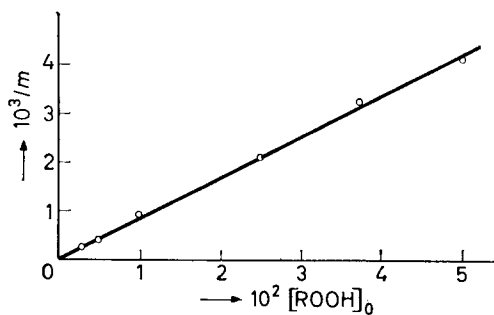
Figure 5—The plot of $1/m$ versus initial concentration of hydroperoxidic groups

453

From the theoretical point of view it is interesting to compare the usual reaction scheme of inhibited oxidation with the experimentally found equation.

The main reactions involved in oxidation of hydrocarbons are as follows:

$$ROOH + ROOH \longrightarrow RO_2^{\cdot} + RO^{\cdot} + H_2O$$

$$k_4 \, [ROOH]^2 \tag{4}$$

$$RO^{\cdot} + RH \longrightarrow ROH + R^{\cdot}$$

$$k_5' \, [RO_5^{\cdot}] \, [RH] \tag{5}$$

$$R^{\cdot} + O_2 \longrightarrow RO_2^{\cdot}$$
$$k_6 \, [R^{\cdot}] \, [O_2] \tag{6}$$

$$RO_2^{\cdot} + RH \longrightarrow ROOH + R^{\cdot}$$

$$k_7 \, [RO_2^{\cdot}] \, [RH] \tag{7}$$

$$RO_2^{\cdot} + AH \longrightarrow ROOH + A^{\cdot}$$
$$k_8 \, [RO_2^{\cdot}] \, [AH] \tag{8}$$

$$RO_2^{\cdot} + RO_2^{\cdot} \longrightarrow \text{inactive products}$$
$$k_9 \, [RO_2^{\cdot}]^2 \tag{9}$$
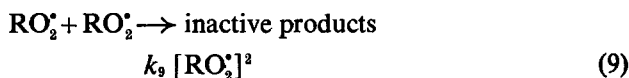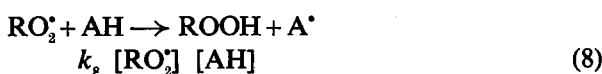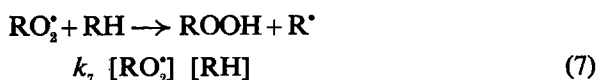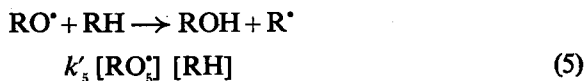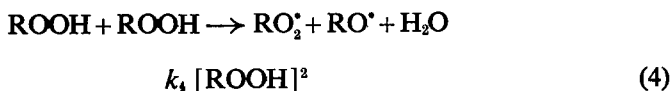
Initiation can proceed by the first or second order decomposition of hydroperoxides. As atactic propylene is involved, the decomposition in the temperature range 120° to 140°C was proved to be of second order. Therefore only this reaction is incorporated in the reaction scheme.

Besides the above-mentioned initiation, the primary initiation reaction

$$RH + O_2 \longrightarrow R^{\cdot} + HO_2^{\cdot} \tag{10}$$
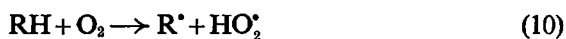
is very often considered.

But this reaction can only be of importance in the oxidation of pure hydrocarbons, because it is known that even at a very low concentration of hydroperoxides the initiation by decomposition of hydroperoxides is dominant. The process of inhibited oxidation, under our experimental conditions, always started at a certain concentration of hydroperoxides, therefore the primary initiation reaction can be neglected.

The system of the above-mentioned reactions has been solved on the assumption that the overall change of radical concentrations is negligible by comparison with the changes of the concentrations of stabilizer and hydroperoxides, and therefore it is assumed to be equal to zero.

Another assumption is that in the presence of stabilizer the radicals disappear mainly by reaction 8, so that

$$k_8 \, [RO_2^{\cdot}] \cdot [AH] \gg k_9 \, [RO_2^{\cdot}]^2 \tag{11}$$

Equations (12) and (13) give the changes of the concentrations of hydroperoxides and antioxidant.

$$\frac{d\,[ROOH]}{dt} = \frac{2k_4k_7\,[RH]\,[ROOH]^2}{k_8\,[AH]} + k_4\,[ROOH]^2 \qquad (12)$$

$$-\frac{d\,[AH]}{dt} = 2k_4\,[ROOH]^2 \qquad (13)$$

The induction period is defined as the time in which the concentration of stabilizer is decreased to a minimum value which is not sufficient to retard the oxidation. The methematical formulation of τ can be derived from equation (13).

$$t = \tau = -\frac{1}{2k_4}\int_{[AH]_0}^{[AH]}\frac{d\,[AH]}{[ROOH]^2} \qquad (14)$$

The relationship between $[ROOH]$ and $[AH]$ can be obtained by division of equations (12) and (13).

$$-\frac{d\,[ROOH]}{d\,[AH]} = \beta\,\frac{1}{[AH]} + \frac{1}{2}$$

$$\qquad\qquad\qquad\qquad\qquad\qquad (15)$$

where
$$\beta = k_7\,[RH]/k_8$$

Therefore

$$[ROOH] = \{[ROOH]_0 + \tfrac{1}{2}\,[AH]_0 + 2\cdot3\beta\,\log\,[AH]_0\}$$

$$- \{\tfrac{1}{2}\,[AH] + 2\cdot3\beta\,\log\,[AH]\} \qquad (16)$$

$[ROOH]$ in equation (14) can be replaced by a term which is a function of $[AH]$ only. But even this simplification is not sufficient for integration. It means that it is not possible to derive a general equation for the induction period and compare it with an experimentally determined equation.

If the values of reaction constants are substituted in equation (16), it is possible, by means of numerical calculation of integrals, to calculate the dependence of τ on $[AH]_0$ and compare the shape of calculated and experimentally found curves.

Constant k_4 was taken from Manásek's data[10] obtained on atactic polypropylene, k_7 and k_8 are from Buchachenko's data[11] obtained on trimethylheptane and k_9 is an average value obtained on a series of hydrocarbons[12],

The following values of constants were used:

$$k_4 = 2 \times 10^{-3}\ \text{l./mol. sec}$$

$$k_7 = 1 \qquad \text{l./mol. sec}$$

$$k_8 = 4 \times 10^2\ \text{l./mol. sec}$$

$$k_9 = 10^6 \qquad \text{l./mol. sec}$$

The hydrocarbon concentration, expressed in moles of monomeric units per litre of polypropylene, was taken to be 2×10 mole/l.

The plot of calculated values against initial concentration of stabilizer is shown in *Figure 6*. It seems that experimental results are inconsistent with our kinetic assumptions.

What is the cause of this contradiction? The calculation was made supposing that $RO_2^{\cdot}$ radicals mostly disappear by the reaction with stabilizer and not by recombination. This assumption, which is common in the systems with dominant retardation of oxidation by stabilizer, is obviously incorrect here.
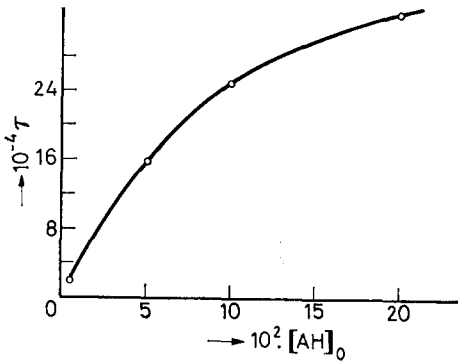
Figure 6—Dependence of calculated values of induction periods on initial concentration of stabilizer

The initial concentration of stabilizer used in the experiments was so low that probably the rates of both types of termination were of the same magnitude.

A mathematical verification of this hypothesis is practically impossible. Therefore we have tried to compare the theoretical equation valid for the boundary of the region in which the rate of termination by radical recombination is predominant and the region in which reaction (8) is predominant with the experimentally found equation. The boundary is defined by the state when the rate of uninhibited termination is n times higher than the rate of the inhibited one.

$$\frac{k_9 [RO_2^{\cdot}]_0^2}{k_7 [RO_2^{\cdot}]_0 [AH]_0} = n$$

$$[RO_2^{\cdot}]_0 = \frac{n k_7 [AH]}{k_9}$$

By the substitution of $RO_2^{\cdot}$ in equation (11) we obtain

$$\frac{[AH]_0}{[ROOH]_0} = \frac{2}{(2n+1)^{1/2}} \frac{k_4^{1/2} \cdot k_9^{1/2}}{k_7} = \text{const.} \tag{17}$$

Experimentally, by the boundary is meant that concentration of stabilizer at which the first increase of induction period, in comparison with uninhibited oxidation, is noticeable. For example, if $\tau_{\text{instab.}} = 60$ min, then all concentrations of $[AH]_0$ at which $\tau_{\text{stab.}} = 70$ min are taken as the boundary state.

456

The validity of the following equation has been experimentally confirmed

$$\tau = q \, \exp \, k \, [AH]_0/[ROOH]_0$$

If $\tau = 70$ min, then the following equations for two different concentrations of hydroperoxides must be valid:

$$\tau = 70 = q \, \exp \, k \, [AH]_1/[ROOH]_1$$

$$\tau = 70 = q \, \exp \, k \, [AH]_2/[ROOH]_2$$

This means that

$$\frac{[AH]_1}{[ROOH]_1} = \frac{[AH]_2}{[ROOH]_2} = \text{constant}$$

Therefore at the boundary value of τ the ratio of the concentrations of stabilizer and hydroperoxides must be constant. This agrees well with the conclusions resulting from the theoretical analysis. Finally, we can say that there is good reason to assume that the experimentally found equation is valid for the region where the rates of radical termination by stabilizer and by recombination are of the same order.

Inhibited oxidation in the temperature range 160° to 170°C

The curves of the dependence of the induction period on concentration of antioxidant 2246 at different concentrations of hydroperoxidic groups are given in *Figure 7*. These curves are S-shaped in comparison with those obtained at 120°C. The first short part of the curve turns to the left and the main second part turns to the right. The rate of growth of the induction period decreases sharply with increasing concentration of stabilizer. The induction period and the rate of growth of τ with $[AH]_0$ both decrease with increasing concentration of hydroperoxidic groups.

The plots of $\log [AH]_0$ versus τ give the curves shown in *Figure 8*. The linear part of the curve starts from a certain concentration of stabilizer which is denoted by $[AH]_k$. The length of the induction period is given by equation (18)

$$\tau - \tau_k = k \log \{[AH]_0/[AH]_k\} \qquad (18)$$

where τ_k is the induction period at the point of inflection (see *Figure 8*). τ_k and $[AH]_k$ are functions of the initial concentration of hydroperoxides. The following equation is valid for $[AH]_k$ (see *Figure 9*).

$$[AH]_k = c \log [ROOH]_0 + d$$

The values of constants c, d for the stabilizer used, at a temperature of 160°C, are as follows:

$$c = 2 \cdot 23 \times 10^{-3} \, \text{mole/l}.$$

$$d = 8 \cdot 5 \times 10^{-4} \, \text{mole/l}.$$

The values of τ_k were found to be reversibly proportional to the initial concentration of hydroperoxides. The dependence of τ_k on $[ROOH]_0$ could
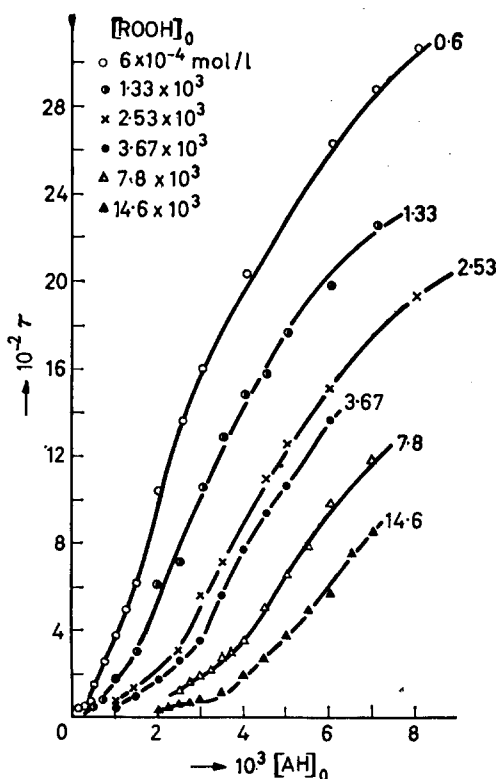
Figure 7—Dependence of induction period on concentration of antioxidant 2246 at 160°C. $[AH]_0$—mole/l., τ—min, $[ROOH]_0$—mole/l. Numerals on curves denote initial concentration of hydroperoxidic groups in 10^{-3} mole/l.

not be expressed by a simple equation because τ_k in fact is a complicated function of a set of competitive reactions.

Two basic reactions can be considered to be responsible for the consumption of antioxidant in the course of inhibited oxidation:

the reaction of stabilizer with peroxy radicals

$$RO_2^* + AH \longrightarrow ROOH + A^* \tag{8}$$
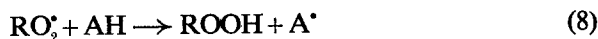
the reaction of stabilizer with oxygen

$$AH + O_2 \longrightarrow A^* + HO_2^* \tag{19}$$
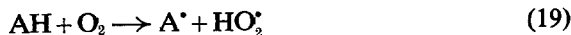
It is reasonable to assume that reaction (19) has a higher energy of activation than reaction (8), therefore the reaction of AH with radicals would be dominant at low temperatures and the reaction of AH with oxygen dominant at high temperatures.

Having assumed that reaction (8) is dominant, the equation for the length of the induction period (14) was derived.

No modification of equation (14) led to an expression which would be in agreement with that found experimentally at 160°C.
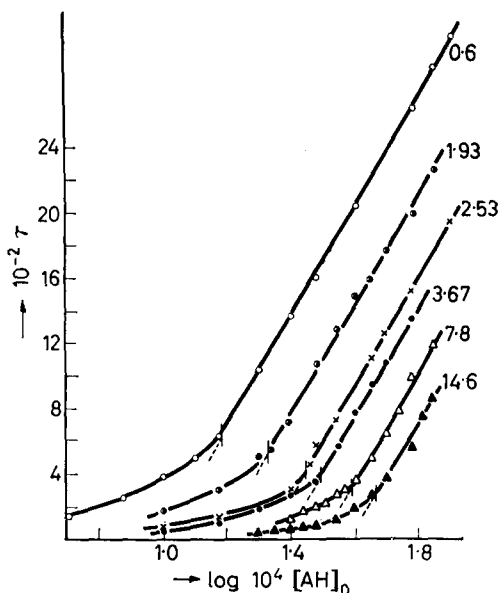
Figure 8—Dependence of τ on log $[AH]_0$ at 160°. $[AH]_0$—initial concentration of antioxidant 2246; τ—induction period (min). Numerals on curves denote initial concentration of hydroperoxidic groups in 10^{-3} mole/l.

Assuming that reaction (19) is dominant we can write

$$- \, d\,[AH]/dt = k_{19}\,[O_2]\,[AH] \tag{20}$$

Solution of (20) leads to

$$t = \frac{2 \cdot 3}{k_{19}\,[O]_2} \cdot \log \frac{[AH]_0}{[AH]} \tag{21}$$

Experimentally, it has been found that

$$\tau - \tau_k = k \log \{[AH]_0/[AH]_k\} \tag{18}$$

From this it follows that if $[AH]_0 > [AH]_k$, the rate of consumption of stabilizer in the concentration range from $[AH]_0$ to $[AH]_k$ is determined by reaction (19), which under these conditions prevails over reaction (8).
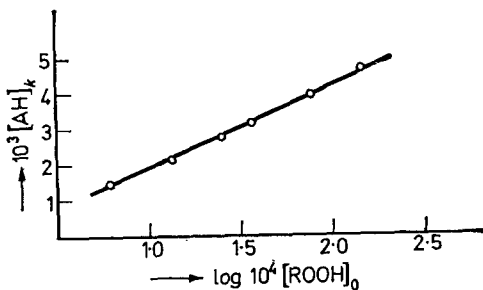
Figure 9—Dependence of $[AH]_k$ on initial concentration of ROOH. $[ROOH]_0$—mole/l.; $[AH]_k$—mole/l.

From the comparison of equations (21) and (8) it follows that the experimentally found constant, k, is given by

$$k = 2 \cdot 3 / k_{19} [O_2]$$

This expression enables us to calculate $k_{19}[O_2]$. Knowing the value of $k_{19}[O_2]$ at several different temperatures, the activation energy of reaction (19) can be calculated (*Figure 10*). $E = 49 \cdot 5$ kcal/mole was found.
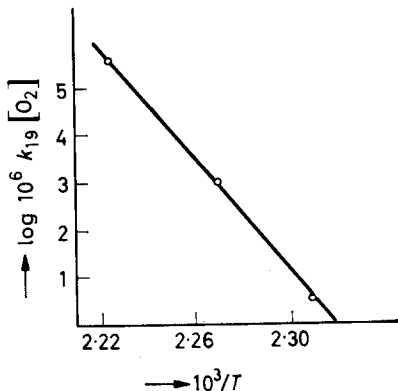
Figure 10—Dependence of $k_{19}[O_2]$ on $1/T$. $k_{19}[O_2]$—(sec^{-1}); T—°K

Our result that stabilizer at higher temperatures is consumed by direct oxidation is in agreement with the findings of Shlyapnikov *et al.*[1,3,6,7] obtained at 180° to 210°C. Our present studies have extended their results to cover the sphere of lower temperatures and the effect of the initial concentration of hydroperoxides has been established.

CONCLUSIONS

Results obtained at 120°C and at 160° to 176°C give a general picture of the dependence of the induction period on the concentration of antioxidant at different temperatures.

Up to a certain concentration the stabilizer has no effect on the rate of oxidation. Inhibition by the stabilizer starts when this concentration is exceeded. The critical concentration depends on the rate of reaction AH with RO$_2$ and initiation. The later one is determined by the concentration of hydroperoxides and temperature. The induction period is an exponential function of the concentration of antioxidant; the curve τ versus $[AH]_0$ turns to the left. In this concentration range the rate of termination is governed by the following reactions :

$$RO_2^{\bullet} + AH \longrightarrow \text{less active products} \tag{8}$$

$$RO_2^{\bullet} + RO_2^{\bullet} \longrightarrow \text{less active products} \tag{9}$$
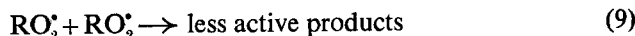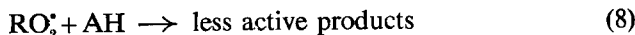
The induction period is given by

$$\tau = q \ \exp \ k \ [AH]_0 / [ROOH]_0 \tag{3}$$

The contribution of reaction (9) to termination decreases with increasing concentration of the antioxidant. The rate of termination by reaction (8)

becomes dominant. The curve of τ versus $[AH]_0$ should exhibit an inflection point and then turn to the right. The length of the induction period should be given by equation (14):

$$\tau = \frac{1}{2k_4} \int\limits_{[AH]_0}^{[AH]} \frac{d[AH]}{[ROOH]_0 + \frac{1}{2}[AH]_0 + 2 \cdot 3\beta \log [AH]_0 - \frac{1}{2}[AH] - 2\,3\beta \log [AH]}$$

where

$$\beta = k_7 [RH]/k_8$$

Unfortunately no measurements intended to confirm the validity of equation (14) could be made at higher concentrations of antioxidant because the induction periods were too long. The induction period could be shortened by working at higher temperatures. But the temperature at which the induction period would be shorter than 2 000 min would be so high that the rate of direct oxidation of antioxidant would strongly influence the relationship of τ versus $[AH]_0$.

The length of the induction period is given by

$$\tau = \tau_k + \frac{2 \cdot 3}{k_7 [O_2]} \ \log \ \frac{[AH]_0}{[AH]_k} \tag{22}$$

where τ_k and $[AH]_k$ are functions of $[ROOH]_0$.

Reaction (19) has a higher energy of activation in comparison with reaction (8). Assuming that the activation energy of reaction (8) measured on polypropylene would have the same value as that determined on the structurally similar compound, trimethylheptane[11], then

$$E_{19}/E_8 \approx 14$$

Therefore, we can suppose that at lower temperatures the consumption of stabilizer is negligible and that the length of the induction period is determined by equations (3) and (14).

At elevated temperatures we must distinguish several concentration ranges of stabilizer (they are arranged with increasing concentration):

(1)   the concentration range in which the shape of curve of τ versus $[AH]_0$ is given by equation (3);

(2)   the range where the shape of the curve of τ versus $[AH]_0$ is given by equation (14);

(3)   the range where the shape of the curve of τ versus $[AH]_0$ is a result of competitive reactions involving $RO_2^{\cdot} + AH$ and $O_2 + AH$;

(4)   the range at which the shape of the curve of τ versus $[AH]_0$ is given by equation (22) and the value of π_k is a considerable part of the total value of τ.

461

At high temperatures the shape of the curve of τ versus $[AH]_0$ is determined by the data stated under 3 and 4. The value of τ_k at 180°C and higher is very small and its proportion of the total value of τ is negligible.

Research Institute of Macromolecular Chemistry,
Brno, Czechoslovakia

REFERENCES

[1] SHLYAPNIKOV, JU. A., MILLER, V. B. and TORSUEVA, E. S. *Izvest. Akad. Nauk S.S.S.R., Otdel Khim. Nauk,* **1961,** 1966

[2] RYSAVY, D. *Chem. prům.* 1961, **11,** 553

[3] SHLYAPNIKOV, JU. A., MILLER, V. B., NEIMAN, M. B. and TORSUEVA, E. S. *Vysokomol. Soedineniya,* 1962, **4,** 1228

[4] RACHINSKI, F. I., SLAVACHEVSKAJA, N. M., POTAPENKO, T. G., KREMEN, M. Z. and MATVEEVA, E. N. *Plast. Massy,* 1963, No. 7, 48

[5] MICHAYLOV, N. V., TOKAREVA, L. G. and POPOV, A. G. *Vysokomol. Soedineniya,* 1963, **5,** 188

[6] GROMOV, B. A., MILLER, V. B., NEIMAN, M. B., TORSUEVA, E. S. and SHLYAPNIKOV, JU. A. *Vysokomol. Soedineniya,* 1964, **6,** 1895

[7] SHLYAPNIKOV, JU. A., MILLER, V. B., NEIMAN, M. B. and TORSUEVA, E. S. *Vysokomol. Soedineniya, Khim. Svoistva i Modifikatsia Polimerov, Sb. Statei,* p 106. Moskva (1964)

[8] GELEJI, F., HOLLY, Z., OCAHAY, G. and WEIN, T. Paper presented at International Symposium on Macromolecular Chemistry, Prague (September 1965)

[9] DULOG, L. *Z. anal. Chem.* 1964, **202,** 192

[10] MANASEK, Z., BEREK, D., MICKO, M., LAZAR, M. and PAVLINEC, J. *Vysokomol. Soedineniya,* 1961, **3,** 1104

[11] BUCHACHENKO, A. L., NEIMAN, M. B. and KAGANSKAJA, K. J. *Trudy po Khimii i khim. Technologii,* 1961, **1,** 31

[12] BATEMAN, L. *Quart. Rev. chem. Soc., Lond.* 1954, **8,** 147

The Thermal Degradation of Poly(benzyl acrylate)

G. G. CAMERON* and D. R. KANE†

The thermal degradation of poly(benzyl acrylate) at 260° to 300° C has been studied. The main products of degradation are carbon dioxide, benzyl alcohol and low polymer. The main polymer chain backbone decomposes in an essentially random manner. In the light of spectroscopic data on the polymeric residue reaction mechanisms to explain the breakdown are considered. The pyrolysis of poly(benzyl acrylate) appears to follow a pattern similar to that of poly(methyl acrylate).

AMONG the common addition polymers whose thermal degradations have been studied the polyacrylates stand out as a group which has received comparatively little attention. This is undoubtedly due in part to their relatively complex mode of breakdown. Recently poly(methyl acrylate) (PMA) has been the subject of a fairly exhaustive study[1-3] which has elucidated the main features of the degradation, with the exception of the precise mechanism of methanol formation.

The object of the work on poly(benzyl acrylate) (PBA) described here was twofold. First, it was carried out as part of a programme, being conducted in these laboratories and elsewhere, to establish the general pattern of polyacrylate pyrolysis, and secondly to complement the work on PMA, particularly to clarify the reactions which lead to methanol formation.

EXPERIMENTAL

(a) Preparation of monomer

Benzyl acrylate was prepared by the method of Rehberg by trans-esterification of methyl acrylate with benzyl alcohol[4]. The crude product was found to be contaminated by a carboxylic acid which was removed by washing with caustic soda solution. Analysis of the purified product gave C, 73·9; H, 6·2; O, 19·9 per cent; calculated for $C_{10}H_{10}O_2$, C, 74·1; H, 6·2; O, 19·7 per cent. Pure monomer was stored under nitrogen in a refrigerator until required.

(b) Preparation of the polymer

Two samples of polymer were prepared at 60°C, one (PBA1) using methyl acetate and the other (PBA2) toluene, as diluent. The volume ratio of monomer to diluent was 0·5. In each case polymerization was conducted in a vacuum-sealed dilatometer using benzoyl peroxide (conc. $\sim 5 \times 10^{-4}$ g mole l^{-1}) as initiator and conversion was taken to approximately 25 per cent. The polymer sample was purified by repeated precipitation in methanol from acetone solution. Since the polymer is a tough rubbery material it could not be powdered and before final vacuum drying at 40° to 60°C it was cut into small (*ca.* 5 mg) pieces.

*Present address: Department of Chemistry, The University of Aberdeen, Old Aberdeen.
†Present address: The Polymer Corp., Sarnia, Ontario, Canada.

(c) *Polymer pyrolysis*

The division of pyrolysis products into fractions is not so clear-cut for PBA as it was for PMA. Collection of the products was most conveniently accomplished using the apparatus shown in *Figure 1*. The glassware was sealed to the main vacuum line at J, and was connected to a calibrated vacustat gauge, M, through T8. Access to a Toepler pump, for collecting gaseous products, was through T9. The whole apparatus could be pumped down to a vacuum better than 10^{-4} mm of mercury, and the arrangement of taps T7, T10, T11, and T12, made it possible for each section to be kept under high vacuum, if necessary, when the adjacent section was not.
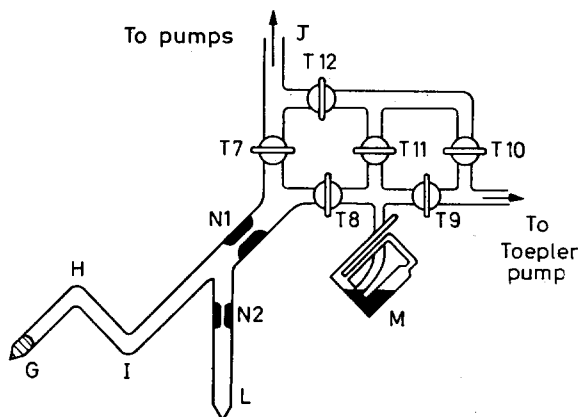
Figure 1—All-glass apparatus for pyrolysis of PBA

The polymer sample was placed at the foot of G which was immersed in a Wood's metal bath controlled to the desired temperature (± 3 deg. C) with a variable transformer. The bend H minimized the return of liquid condensate to the heated zone.

Prior to each run the apparatus was evacuated and the polymer sample heated to 130°C for two hours to remove any contaminating volatiles. At the same time the vessel walls were flamed thoroughly. After this treatment the apparatus was sealed off at N1, the temperature raised to the required level, and the trap L immersed in liquid nitrogen. At the end of a run the heating bath was removed and the liquid in I was distilled into L by gently flaming. L was then sealed off at N2 and the contents analysed. When non-condensable gases were examined this procedure was modified by leaving N1 intact and T7 and T8 closed. The pressure of these gases was measured by M and they were then pumped into a suitable vessel for mass spectrometric analysis. A knowledge of the volume of the system then allowed the absolute weights of the components of this fraction to be calculated.

(d) *Viscosities*

The Mark–Houwink constants for PBA are not known, and the viscosity data (in benzene at 30°C) could not be converted to average molecular weights.

(e) *Spectroscopic measurements*

Some i.r. spectra were recorded using a Perkin–Elmer 621 spectrophoto-
meter and for u.v. spectra a Unicam UP 700 spectrophotometer was em-
ployed. In each case the polymer was in the form of a film, on sodium
chloride and quartz plates for i.r. and u.v. respectively. As degraded resi-
dues contained appreciable amounts of insoluble material the films were
most conveniently prepared by smearing the plate surface with a polymer–
chloroform gel. The chloroform was removed in a vacuum oven at 100°C.

The n.m.r. spectra were measured in deuterochloroform (about five per
cent solution) with a Perkin–Elmer R10 60 Mc/sec instrument.

Mass spectrometric measurements were made by Dr G. R. Woolley to
whom we wish to record our thanks.

RESULTS

(a) *Qualitative and quantitative analysis of fractions of pyrolysis products*

The pyrolysis products from PBA are most conveniently divided into
the following four fractions.

Fraction I—This was the polymeric residue remaining in G. Its nature
will be discussed in detail later. The total weight loss was obtained by
weighing Fraction I, which was slightly discoloured and contained some
insoluble gel.

Fractions II and III—These fractions, which collected together in L, were
separated by cooling the arm L in a solid carbon dioxide cooling mixture at
−76°C. The materials volatile at this temperature (Fraction III) were
pumped via the Toepler pump to a suitable vessel and later examined by
mass spectrometry. Carbon dioxide proved to be the only component and
was analysed quantitatively using the molecular still with a calibrated con-
stant volume manometer as described previously[3]. *Figure 2* shows that the
amount of carbon dioxide liberated increases linearly with weight loss, and
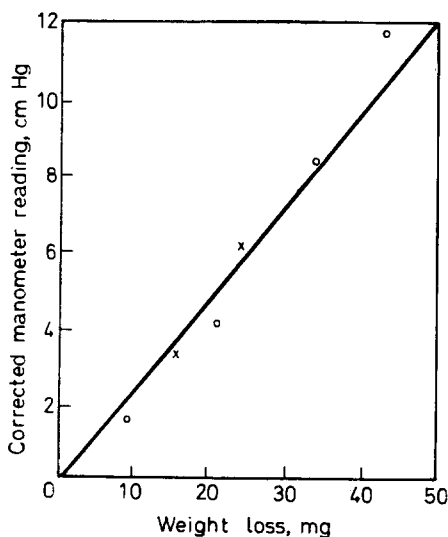
Figure 2—Pressure of carbon dioxide
as a function of weight loss for PBA.
× 260°C; ○ 270°C

represents 4·7 per cent of the total weight loss between 10 and 50 per cent volatilization.

The material involatile at $-76°C$ (Fraction II) was analysed qualitatively by means of gas–liquid chromatography (GLC), i.r., and n.m.r. spectroscopy, which showed it to consist of benzyl alcohol and low polymer, along with traces of six or seven other substances, the only one of which to be positively identified being toluene.

Quantitative analysis of Fraction II was achieved by GLC using a ten per cent silicone oil–celite column at 110°C. As this fraction contained low polymer which remained on the column a known weight of marker, phenyl methyl acetate, was added to permit estimation of the absolute amounts of benzyl alcohol and the other materials. The mean weight per cent of benzyl alcohol was calculated from four or more consistent analyses. The results obtained are summarized in *Table 1*, which shows that the proportion of benzyl alcohol, and possibly other components in the products, diminishes with progressive volatilization of polymer.

Table 1. GLC analysis of liquid products (Fraction II) from the pyrolysis of PBA1 at 300°C

% Conversion to volatiles	Mean wt % benzyl alcohol (based on total conversion)	Mean wt % other components
51·9	32·0	2·4
45·9	38·5	2·5
43·8	40·0	2·9
40·3	40·5	3·9
36·8	44·2	—

No monomer was detected.

Fraction IV—This fraction was collected as described earlier. Mass spectrometry revealed that components were carbon monoxide, methane, and hydrogen, in the molar ratio 7:2:1. The amount of Fraction IV in relation to the total weight loss was approximately one per cent.

The results of these analyses are summarized in *Table 2*.

Table 2. Pyrolysis products from PBA at temperatures below 305°C

Fraction	Components	% of total wt loss	Comments
I—Pyrolysis residue	Long chain PBA	Residue	Yellow in colour: contains some insol. gel
II—Liquid products	Short chain PBA Benzyl alcohol Toluene and others	~50 ~40 ~3	Exact proportions depend on percentage conversion to volatiles
III—Condensable gases	Carbon dioxide	4·7	—
IV—Non-condensable gases	CO, CH_4 and H_2 in molar ratio 7:2:1	~1	—
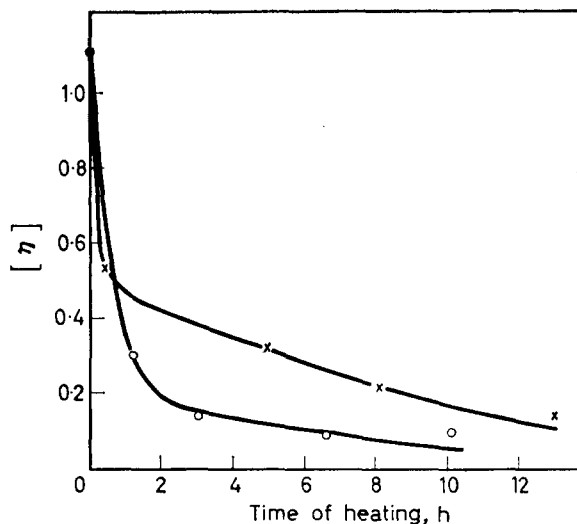
Figure 3—Limiting viscosity number [η] of soluble portions of PBA1 residues versus time of heating.
× 260°C; ○ 270°C

(b) *Examination of the polymeric residue (Fraction I)*

Intrinsic viscosities—Two series of experiments at 260° and 270°C were conducted in the molecular still[2] to obtain viscosity data on the polymeric residues. Plots of limiting viscosity number of the soluble portion of the residue versus time of heating and percentage conversion to volatiles are shown in *Figures 3* and *4*. These graphs show behaviour consistent with a random type of breakdown of the main chain. *Figure 5* is a plot of
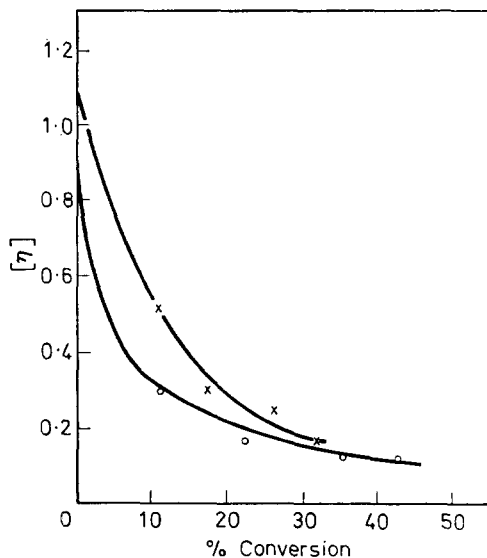
Figure 4—Limiting viscosity number [η] versus percentage conversion to volatiles of PBA1.
× 260°C; ○ 270°C

465
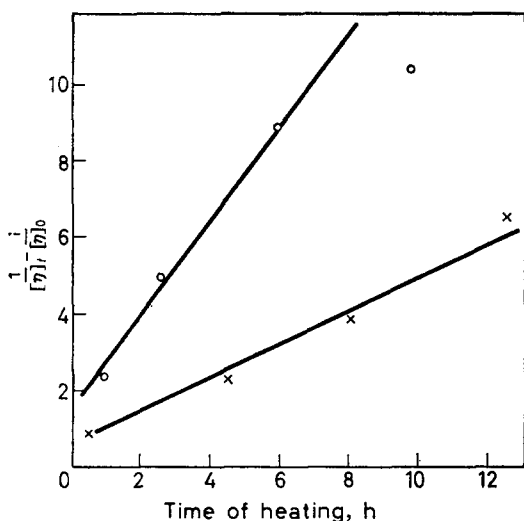
Figure 5—Plot of $1/[\eta]_t - 1/[\eta]_0$ of soluble portions of PBA1 residues versus time of heating. × 260°C; ○ 270°C

$1/[\eta]_t - 1/[\eta]_0$ versus time of heating and the linear nature of the curves supports an essentially random mechanism.

Infra-red spectra—Sections of the infra-red spectra between 2 000 and 900 cm⁻¹ of undegraded and degraded samples of PBA1 are shown in *Figure 6*. Some small but significant differences between the spectra are apparent.

The only increases in absorption in this region occur between 1 700 and 1 500 cm⁻¹ and are attributed to conjugated double bond structures[5]. The carbonyl absorption at 1 725 cm⁻¹ broadens markedly with degradation. The reduction in the peaks at 1 500, 1 450 and 1 028 cm⁻¹ reflects the
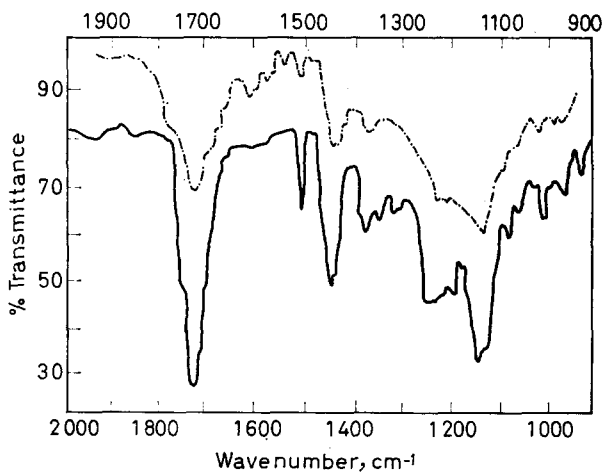
Figure 6—The i.r. spectra of undegraded PBA1 and pyrolysed residues. Undegraded ————; 67·5 per cent volatilized · — · — · — · —

466

diminishing concentration of aromatic rings, while the evolution of benzyl alcohol reduces the main ester C—O peak[6] at 1 155 cm^{-1}.

In the region 4 000 to 2 000 cm^{-1} (not shown) the only changes observed were the reduction in aromatic absorption at 3 100 and 3 000 cm^{-1}, and the appearance of a broad hydroxyl peak which was found to be due to benzyl alcohol remaining in the polymer residue.

The n.m.r. measurements—The spectrum of undegraded PBA has peaks at 2·72, 5·03, 7·6, and 8·2τ, corresponding to phenyl, side chain methylene, methine, and main chain methylene protons respectively. The integral evaluation of these peaks was as required by the formula.
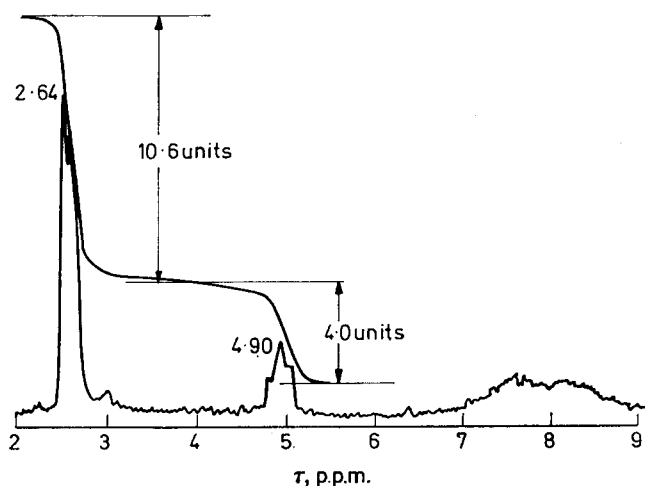
Figure 7—The n.m.r. spectrum of pyrolysed residue of PBA1.
44·5 per cent conversion to volatiles

In *Figure 7* the n.m.r. spectrum of PBA1 pyrolysed to 44·5 per cent volatilization is shown. The absorption of the side chain methylene protons has shifted largely from 5·03τ to about 4·89τ indicating a change of environment on pyrolysis. Since the corresponding protons in the monomer absorb at 4·85τ it is possible that a proportion of the ester groups remaining in the pyrolysed residue are attached to ethylenic carbon atoms. The peak position of the phenyl protons has also changed to a slightly lower value. If it is assumed that benzyl alcohol constitutes 40 per cent by weight of the total volatiles evolved then at 44·5 per cent volatilization two out of seven ester groups should be decomposed and the ratio for phenyl : side chain : main chain protons should be 2·5 : 1·0 : 2·1. The value obtained from *Figure 7* is 2·65 : 1·0 : 2·0. At 67·5 per cent conversion to volatiles three out of five ester groups should be decomposed, giving the above proton ratio of 2·2 : 1·0 : 3·7. The experimental value is 2·2 : 1·0 : 2·5 which may indicate that at higher extents of conversion hydrogen atoms are stripped from the main chain giving rise to main chain unsaturation and the conjugated systems indicated in the i.r. spectra. The same effect, though less pronounced, was observed in the spectra of degraded PMA[3].

DISCUSSION

The foregoing results show that the pyrolysis of PBA follows the same basic pattern as that of PMA, but there are some differences in detail. From both polymers low polymer, carbon dioxide and an alcohol account for the bulk of the degradation products, though in differing proportions for the two systems. Moreover, the viscosity and molecular weight data for the degraded residues are consistent with a random chain breaking process in each case. The chain breaking process in PMA is known to be part of a free radical chain reaction[2], and there is no reason to suppose it is different in PBA. For PMA, however, it was found that plots of molecular weight or intrinsic viscosities versus conversion fell on the same curve, regardless of temperature. As *Figure 5* shows, this is not so for PBA. The different curves followed at 260° and 270°C in *Figure 5* may result from a greater increase in PBA in the relative amounts of intermolecular to intramolecular transfer at higher temperatures.

The spectroscopic information from the degradation of PBA is broadly in line with that obtained from PMA. The n.m.r. spectrum of pyrolysed PBA does show, however, a change in environment of the ester methylene protons, a change which was not apparent in PMA. Also from the i.r. and n.m.r. spectra of PBA residues the evidence for ethylenic unsaturation is stronger, though the reactions leading to it are not entirely clear. In previous papers[2,3] on the degradation of PMA it was suggested that the radical

$$\text{\textasciitilde\textasciitilde}-CH_2-\overset{\displaystyle .}{C}-CH_2-\text{\textasciitilde\textasciitilde}$$
$$|$$
$$CO$$
$$|$$
$$OCH_3$$
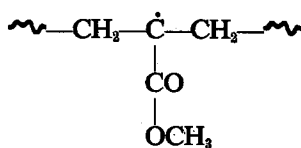
is the precursor of most of the volatile products of degradation. Elimination of a neighbouring methylenic proton would produce an internal double bond. The appearance of hydrogen in the products from PBA confirms that such a process can occur though obviously rather infrequently.

As in the case of PMA identification by i.r. analysis of new carbonyl structures formed was hindered by existing ester absorptions. As before, however, there is no evidence in the i.r. or n.m.r. spectra of carboxyl or aldehyde groupings and it seems most likely that a ketone is formed in the process of alcohol formation. The most satisfactory mechanism therefore to account for alcohol formation is as follows:

468
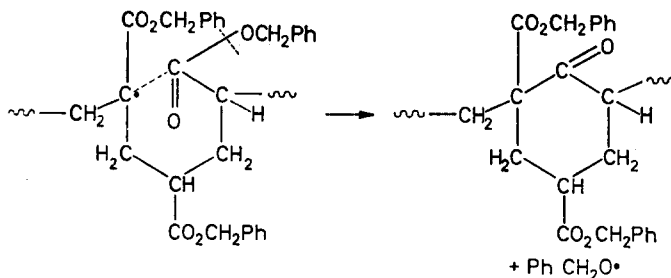
though other possibilities can never be entirely excluded. The same type of reaction occurring intermolecularly would produce a crosslink:
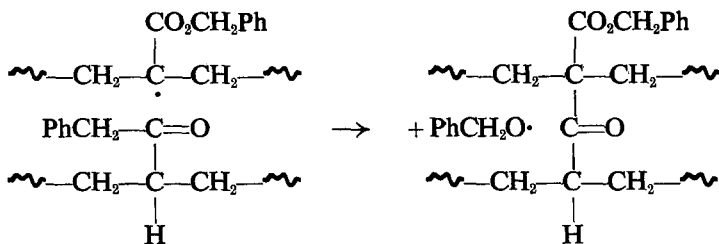
This is consistent with the observation that both PMA and PBA produce some insoluble gel on pyrolysis.

For carbon dioxide formation from PMA a reasonably satisfactory mechanism has already been suggested. The analogous reaction route for PBA is:
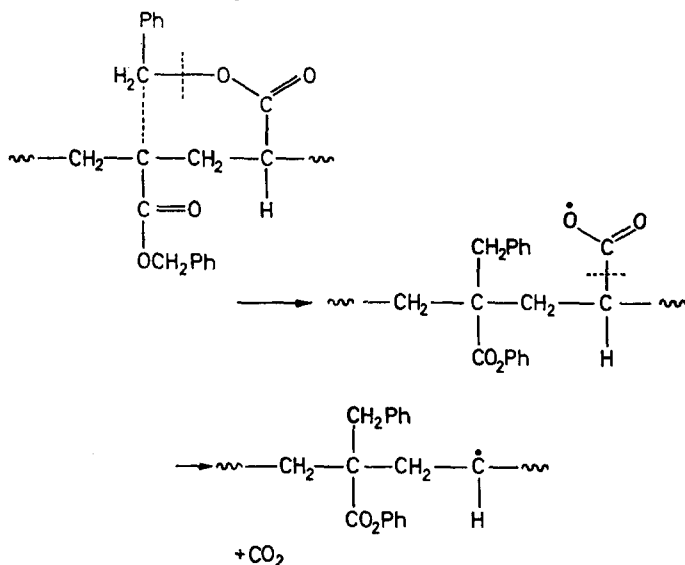
While the occurrence of these reactions cannot be unequivocally proved they are consistent with the experimental results, and molecular models show that there is no serious steric objection.

PBA appears to be less stable thermally than PMA. It was found that PBA volatilizes as rapidly at 270°C as does PMA at 290°C. The source of instability is apparently the ester side group which decomposes to alcohol more readily with PBA than PMA. Thus, for PBA the molar ratio of monomer (as low polymer) to alcohol in the degradation products is approximately 0·8 while the corresponding ratio for PMA is about nine.

Department of Chemistry, St Salvator's College,
The University, St Andrews, Fife.

REFERENCES

[1] CAMERON, G. G. and KANE, D. R. *Polymer Letters*, 1964, **2**, 693
[2] CAMERON, G. G. and KANE, D. R. *Makromol. Chem.* 1967, **109**, 194
[3] CAMERON, G. G. and KANE, D. R. *Makromol. Chem.* 1968, **113**, 75
[4] REHBERG, C. E. *Organic Synthesis*, 1946, **26**, 18
[5] BLOUT, E. R., FIELDS, M. and KARPLUS, R. *J. Amer. chem. Soc.* 1948, **70**, 189 and 194
[6] BELLAMY, L. J. *The Infra-red Spectra of Complex Molecules.* Methuen: London, 1958

Temperature Dependence of Association in Polyacrylonitrile Solutions

R. B. BEEVERS

Rate constants for association in solutions of polyacrylonitrile in dimethyl-formamide containing 35·0 per cent by volume benzene have been determined viscometrically. Two rate processes are observed with constants $k_a = (2·7 \pm 0·3) \times 10^{-4}\,sec^{-1}$, and having no observable temperature dependence, and $k_b = (1·11 \pm 0·14) \times 10^{-5}\,sec^{-1}$ at 15·00°C. Measurements of k_b at temperatures between 8·40° and 27·50°C gave an activation energy of $8·5 \pm 1·0$ kcal mole^{-1} assuming two intermolecular bonds per molecule. This value confirms that association in these solutions is mainly brought about by formation of CN dipole-pair bonds.

SOLUTIONS of polyacrylonitrile in dimethylformamide become associated on addition of about 35 volume per cent benzene. In a previous paper[1] the general kinetic features of this system were examined extending earlier work by Climie and White[2]. It was shown that the rate of association, determined viscometrically, depended on both the benzene and polymer concentrations. The nature of the time-dependent viscosity changes strongly indicated that benzene acts as an inert diluent restricting polymer–solvent interactions so allowing polymer–polymer interactions to take place. Measurement of the temperature dependence of the association in these solutions should permit some understanding of the types of intermolecular bonds formed.

Polyacrylonitrile is an unusual polymer possessing a high degree of lateral order[3] or 'directional crystallization' in the solid state[4]. Previously[5, 6] intermolecular bonds in polyacrylonitrile have been considered to be hydrogen bonds (I). The extensive association in the liquid low molecular weight nitriles and isonitriles, however, indicates the formation of a strong bond comparable to the hydrogen bond in the carboxylic acids. This has led Saum[6] to suggest that association occurs in these liquids through formation of a CN dipole-pair bond (II). With the dipoles on neighbouring molecules placed antiparallel and at their closest distance of approach, the energy of interaction has been calculated to be at least 7 kcal mole^{-1}. It is of course most probable that both hydrogen and CN dipole-pair bonds form between the polymer molecules. Unusual results obtained for the glass transition temperature in acrylonitrile–styrene copolymers[7] have for example been ascribed[8] to the combined effect of both types of bond formation.
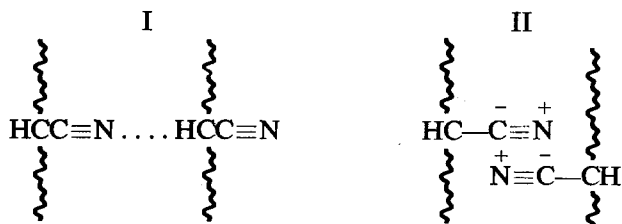
Materials

The same sample of polyacrylonitrile (W12) was used as previously[1]. Analytical reagent grade benzene and N,N'-dimethylformamide were used after careful drying and distillation.

Procedure

The procedure was identical with that described previously[1]. All viscometric measurements were carried out with stock solutions having an initial polymer concentration of $0 \cdot 470$ g dl^{-1}. Temperature variation ($\pm 0 \cdot 01$ deg. C) was restricted to the range 8° to 30°C at which temperature slight losses of benzene occurred through evaporation and made the results irreproducible. To minimize thermal effects when adding benzene, experiments were carried out when the ambient temperature was approximately equal to that of the thermostat.

Although extensive sets of data were obtained showing the effect of benzene concentration at the various temperatures, only results for $35 \cdot 0$ per cent benzene have been taken for analysis. At this concentration viscometer errors and the effect of time of flow in the viscometer on the kinetic data were minimized.

Analysis of data

It was found earlier[1] that the change in the solution viscosity number with time was approximately given by

$$\ln (\Phi_1/\Phi_0) = -k_1 t \tag{1}$$

where $\Phi_1 = \eta_{sp}/c$ at time t and $\Phi_1 = \Phi_0$ when $t = 0$, c being the polymer concentration in g dl^{-1}. A small amount of curvature in plots of equation (1) for low values of t had been neglected. To take account of this non-linearity two association reactions have been assumed, characterized by specific rate constants k_a and k_b, so that now

$$\Phi_1/\Phi_0 = A \exp (-k_a t) + B \exp (-k_b t) \tag{2}$$

where A and B are constants. This procedure assumes that both hydrogen and CN dipolar bonds are formed. For convenience let $\Phi_1/\Phi_0 = \beta$. At large t the term involving k_a will be small provided $k_a \geqslant k_b$. If values of β are obtained for which $t_1 \ll t_2 < t_3$, then to a reasonable approximation:

$$\left. \begin{array}{l} \beta_1 = A \exp (-k_a t_1) + B \exp (-k_b t_1) \\ \beta_2 = \qquad\qquad\quad\; B \exp (-k_b t_2) \\ \beta_3 = \qquad\qquad\quad\; B \exp (-k_b t_3) \end{array} \right\} \tag{3}$$

which are readily solved to give:

$$\ln B = (t_3 \ln \beta_2 - t_2 \ln \beta_3)/(t_3 - t_2) \tag{4}$$

$$k_a = -\ln [(\beta_1 - B \exp (-k_b t_1)]/A]/t_1 \tag{5}$$

$$k_b = \ln (\beta_2/\beta_3)/(t_3 - t_2) \tag{6}$$

In order to simplify computation, the value of β for $t=0$ was obtained by linear extrapolation of the first few results and the data then normalized so that $\beta_n=1$ at $t=0$ for which $A+B=1$. Large scale plots of β_n as a function of time were then prepared and the best curve drawn through the data. Values of β_n and t were taken from the tabular data using points which lay on this line and substituted into equations (4) to (6) to yield B, k_a and k_b. These values were then substituted into equation (2) to give a plot of β_n as a function of time and so check against the arbitrary curve drawn.

RESULTS AND DISCUSSION

Effect of benzene concentration

Results obtained at $8 \cdot 40°$ and $30 \cdot 00°$C are given in *Figure 1* and show a significant shift over this temperature range by about two orders of magnitude in time. Results at $8 \cdot 40°$C for $38 \cdot 0$ per cent benzene for example
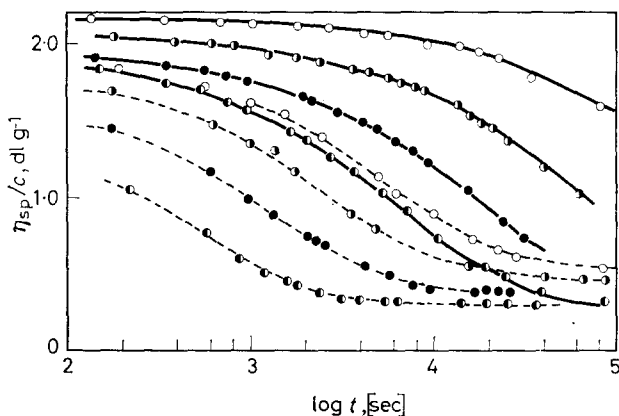
Figure 1—The time-dependence of η_{sp}/c for solutions of polyacrylonitrile in dimethylformamide with added benzene: —— $8 \cdot 40°$C; ———— $30 \cdot 0°$C; $\bigcirc$, $35 \cdot 0$ per cent; $\pmb{\mathbb{O}}$, $36 \cdot 0$ per cent; $\bullet$, $37 \cdot 0$ per cent; $\mathbb{O}$ $38 \cdot 0$ per cent benzene

almost coincide with data at $30 \cdot 00°$C for $35 \cdot 0$ per cent benzene. Increase in temperature causes a lowering of the initial viscosity number as would be expected. At constant benzene concentration the total change in η_{sp}/c decreases with increase in temperature. For example, at $35 \cdot 0$ per cent benzene, $8 \cdot 40°$C, η_{sp}/c decreases from $2 \cdot 17$ to $0 \cdot 52$ dl g^{-1} (not shown) whereas at $30 \cdot 00°$C comparable values are $1 \cdot 83$ and $0 \cdot 50$ dl g^{-1}, a reduction of about 25 per cent. Thus the extent of association decreases with increase in temperature. This is normally to be expected since the solvent power of the liquid mixture will improve with increase in temperature. Frisch and Simha (see ref. 9), however, point out that the temperature coefficient of the state of aggregation could be positive or negative depending upon the nature of the aggregates and the state of the solvation shell around the particles.

465
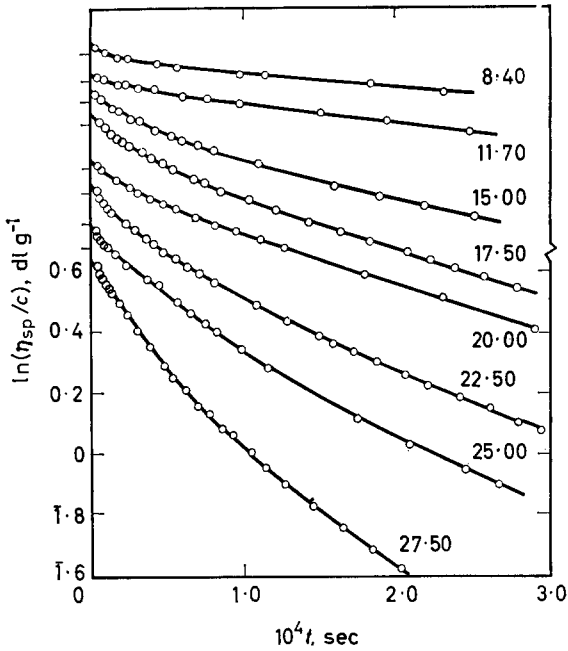
Figure 2—Showing effect of temperature on time-dependent viscosity changes in solutions of polyacrylonitrile in dimethylformamide with 35·0 per cent benzene. Temperature (°C) is indicated against each curve

Temperature dependence of rate of association at 35·0 per cent benzene

At a constant benzene composition of 35·0 per cent the nature of the time-dependent changes observed in $\ln(\eta_{sp}/c)$ are given in *Figure 2* for temperatures between 8·40° and 27·50°C. Data at 30·00°C given in *Figure 1* have not been included on account of the slight changes in benzene composition which were noticed. A shift has been made along the ordinate for greater clarity the unmarked index being at 0·700 dl g^{-1}. For $t > 10^4$ sec the plots are linear except at 25·00° and 27·50°C where the curvature is more pronounced.

Measurements were invariably continued for 8×10^4 sec so that values chosen for t_2 and t_3 were on the linear section of the graph. Analysis of the curves was carried out as described using equations (4) to (6) to yield the values for k_a, k_b and B given in *Table 1*. Lines drawn in *Figure 2* have been calculated from the parameters derived. Analysis of the errors involved shows that values of k_a are particularly unreliable. Error in β is about $\pm 0·005$ which yields an error in the various parameters of k_a, $\pm 1·1 \times 10^4$ sec^{-1}; k_b, $\pm 0·14 \times 10^{-5}$ sec^{-1}; B, $\pm 0·02$.

Table 1. Values of k_a, k_b and B at various temperatures determined from measurements on solutions of polyacrylonitrile in dimethylformamide with 35 per cent benzene

$T,$ °C	B	$k_a \times 10^4$ sec^{-1}	$k_b \times 10^5$ sec^{-1}	$T,$ °C	B	$k_a \times 10^4$ sec^{-1}	$k_b \times 10^5$ sec^{-1}
8·40	0·94	4·3	0·50	20·00	0·89	3·2	1·41
11·70	0·96	6·0	0·63	22·50	0·82	2·2	2·10
·15·00	0·88	2·7	1·11	25·00	0·82	2·5	2·52
17·50	0·88	2·6	1·56	27·50	0·72	2·8	3·65

The temperature dependence of k_b is well defined in *Table 1* whereas k_a shows no significant dependence. With the exception of values at 8·40° and 11·70°C, k_a has a mean value of $(2·7 \pm 0·3) \times 10^{-4}$ sec^{-1} and is well within the error limits calculated.

Temperature dependence of k_b

Values of k_b are shown plotted as log $(10^6 k_b)$ against 1 000/T, where T is the absolute temperature, in *Figure 3*. Vertical lines indicate the error associated with k_b as determined above. The straight line, determined by least squares analysis, fits the data satisfactorily. Assuming an Arrhenius expression for the temperature dependence of k_b

$$k_b = A \exp(-E/RT) \tag{7}$$

where A is a constant and R the gas constant, gives for the activation energy $E = 17 \pm 2$ kcal mole^{-1}.

Evidence has already been given[1], based on osmometric and sedimentation studies of these solutions, to show that large aggregates of polymer molecules form on association. On average each molecule must form two intermolecular bonds, either of the CN dipole-pair or hydrogen bond type.
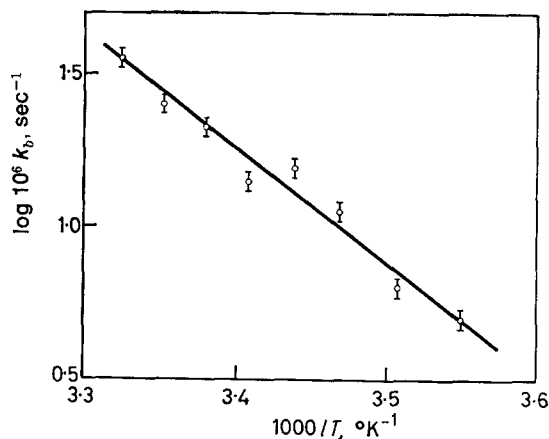
Figure 3—An Arrhenius plot of log $(10^6 k_b)$ as a function of 1 000/T in °K^{-1} for solutions of polyacrylonitrile in dimethylformamide containing 35·0 per cent benzene

It would then follow that the energy per bond is half that found or $8·5 \pm 1·0$ kcal mole^{-1}. This is a value close to that calculated by Saum[6] and strongly indicates that association in these solutions is predominantly brought about by formation of CN-dipolar bonds. As shown by Frisch and Simha[9] the temperature dependence of the association process is undoubtedly complex. There must be contributions to k_b arising from the temperature dependence of the dimethylformamide–CN dipole dissociation coefficient and of the relative diffusion coefficient of benzene and dimethylformamide which remain unknown.

Kobayashi[10] has also detected the association of polyacrylonitrile molecules on addition of nonsolvent. He found the aggregates to be thermally stable and carry a negative charge. His interpretation of the process of

association was in terms of hydrogen bond formation between polymer

and dimethylformamide ($>$ C$=$O .... H—CCN or $>$ C—H .... NCCH)
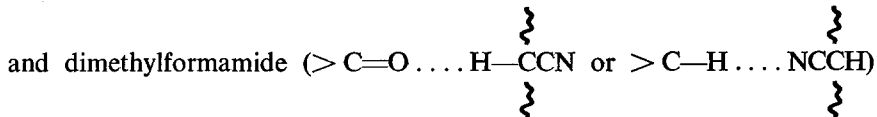
and subsequently between polymer molecules. This has since been considered by Suzuki[11] to be invalid as a result of infra-red and Raman spectroscopic measurements. These indicate that dimethylformamide is strongly polarized in the liquid state. The observed dipole moment is much higher than that calculated from group assignments and is attributed to the strongly polar character of the amide group ($> \overset{+}{N}=C-\overset{-}{O}$). Solution is therefore more likely to be brought about by dipole interaction than by hydrogen bond formation and subsequently association will occur through these interactions.

A note concerning k_a

The experimental error in the measurement of k_a is such that few conclusions can be drawn concerning its temperature dependence or the origin of this rate process. If, for purposes of discussion, this is considered to originate in hydrogen bond formation, two comments may be made.

(1) Hydrogen bond formation usually involves an energy of activation[12] of from 1 to 2 kcal mole^{-1}. To make significant measurements the error in k_a needs to be much less than $\pm 0.1 \times 10^{-4}$ sec^{-1}.

(2) It is almost impossible to determine the properties of weak intermolecular bonds viscometrically. Viscosity results obtained by Gordon *et al.*[13], in a study of the polymerization of water in benzene through hydrogen bond formation, were of little value on account of the disruptive effect of the shear gradient in the viscometer capillary even for shear rates as low as 1.5 sec^{-1}. In the suspended level viscometers used here[1] the shear rate was much higher at about 1 500 sec^{-1}.

University of Bradford,
   Bradford, 7

REFERENCES

[1] BEEVERS, R. B. *Polymer, Lond.* 1967, **8**, 419
[2] CLIMIE, I. E. and WHITE, E. F. T. *J. Polym. Sci.* 1960, **47**, 149
[3] BOHN, C. R., SCHAEFGEN, J. R. and STATTON, W. O. *J. Polym. Sci.* 1961, **55**, 531
[4] STATTON, W. O. *Ann. N.Y. Acad. Sci.* 1959, **83**, 27
[5] FORDYCE, R. G. and HAM, G. E. *J. Amer. chem. Soc.* 1951, **73**, 1186
[6] SAUM, A. M. *J. Polym. Sci.* 1960, **42**, 57
[7] BEEVERS, R. B. and WHITE, E. F. T. *J. Polym. Sci. B,* 1963, **1**, 171
[8] ANDREWS, R. D. and KIMMEL, R. M. *J. Polym. Sci. B,* 1965, **3**, 167
[9] EIRICH, F. R. (Ed.) *Rheology,* Vol. I, p 608. Academic Press: New York, 1956
[10] KOBAYASHI, H. *J. Jap. Chem.* 1953, **23**, 315
[11] SUZUKI, S. *J. Jap. Chem.* 1953, **23**, 535; *Kobunshi Kagaku,* 1954, **11**, 41, 46, 378
[12] PIMENTEL, G. C. and McCLELLAN, A. L. *The Hydrogen Bond,* p 348. Freeman: San Francisco, 1960
[13] GORDON, M., HOPE, C. S., LOAN, L. D. and ROE, RYONG-JOON. *Proc. Roy. Soc. A,* 1960, **258**, 215

Oligomers and Polymers of Thioformaldehyde

L. CREDALI and M. RUSSO

In this paper the results of investigations on thiomethylenic oligomers and polymers are reported and correlated with literature data in this field.

RESEARCH in the field of oligomers, co-oligomers, polymers and copolymers of thioformaldehyde has been developed only recently, though the reaction between hydrogen sulphide and aqueous formaldehyde was carried out in 1868 by Hofmann[1].

Research by Hofmann and other workers in this field had been exclusively developed on the CH_2O—H_2O—H_2S system[2-7] and up to 1959 the following results had been achieved.

(a) Strongly acidic conditions give rise to formation of the cyclic trimer of thioformaldehyde, 1,3,5-trithiane[1, 5, 6].

(b) In basic media unidentified products with variable sulphur contents (depending on the reaction conditions) are obtained.

(c) In weakly acidic or alkaline media a product is obtained which after crystallization shows a melting point of 80°C and a sulphur content of 51·5 per cent[4].

(d) By working under a pressure of 30 atm it is possible to prepare methanedithiol[7].

Since 1959 study in the field of polymers of thioformaldehyde has been intensely developed. These researches have made clear many reactions which take place between formaldehyde and hydrogen sulphide; moreover, they have led to many interesting methods of preparing polymers, oligomers, copolymers and co-oligomers. The crystalline structures of some oligomers and polymers have been elucidated.

The present state of knowledge leads us to classify in the following two ways the reactions which lead to thiomethylenic polymers and oligomers:

(1) Polymerization by condensation: (a) from aqueous formaldehyde and hydrogen sulphide; (b) from different monomers.

(2) Polymerization by addition of cyclic oligomers: (a) by cationic initiators; (b) by radiation.

In this paper the results obtained by research in this field are reported and correlated with literature data.

POLYMERIZATION BY CONDENSATION

(a) Polycondensation of aqueous formaldehyde and hydrogen sulphide

Since thioformaldehyde is unknown in the free state, Bauman[5] proposed

that the absorption of hydrogen sulphide by aqueous formaldehyde occurs by formation of mercaptomethanol; this intermediate by self-condensation (in the presence of a strong acid) gives trithiane. Because of this the nature of the product obtained (the yield in trithiane is almost quantitative[6]) and which occurs in strongly acidic media is well known. It is not known what occurs at a higher pH, particularly in relation to the products yielded by the system.

We have carried out research in this field[8] and have studied the behaviour of hydrogen sulphide uptake by aqueous formaldehyde solutions at their normal pH. By this method it was ascertained that the solution absorbs hydrogen sulphide in an amount proportional to the formaldehyde present, up to a maximum value of the ratio $CH_2O/H_2S = 2$ (by mole). In connection with this ratio a separation takes place of a solid product already described in literature (melting point $80°C$, $S = 51·5$ per cent).

Physical and chemical investigations showed that the first solid product of the system is 1-hydroxy-2-oxa-4,6-dithioheptane-7-thiol (I),

$$HO—CH_2—O—CH_2—S—CH_2—S—CH_2—SH$$
$$(I)$$
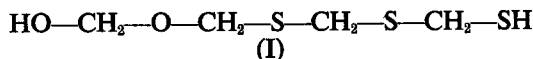
linear formaldehyde-thioformaldehyde co-oligomer.

On the basis of the CH_2O/H_2S ratio in solution when (I) separates, it is proposed that the absorption of hydrogen sulphide in the liquid phase (in which formaldehyde is usually in the form of gem-diol) goes with formation of 1-hydroxy-2-oxapropan-3-thiol* (II),

$$H_2S + 2CH_2(OH)_2 \rightleftharpoons HO—CH_2—O—CH_2—SH + 2H_2O$$
$$(II)$$
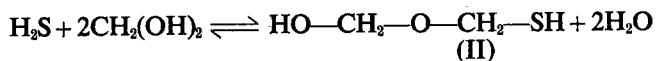
When all the formaldehyde has been consumed in the formation of (II), the further absorption of hydrogen sulphide gives rise to mercaptomethanol (III). This intermediate reacts immediately by a very fast reaction with (II), elongating the chain and giving (I), which is insoluble and precipitates from the solution.

$$HO—CH_2—O—CH_2—SH + H_2S \rightleftharpoons 2HS—CH_2—OH$$
$$(II) \qquad\qquad\qquad\qquad (III)$$

$$HO—CH_2—O—CH_2—SH + HO—CH_2—SH \rightleftharpoons$$

$$HO—CH_2—O—CH_2—S—CH_2—SH + H_2O$$
$$HO—CH_2—O—CH_2—S—CH_2—SH + HO—CH_2—SH \rightarrow$$
$$HO—CH_2—O—CH_2—S—CH_2—S—CH_2—SH + H_2O$$
$$(I)$$
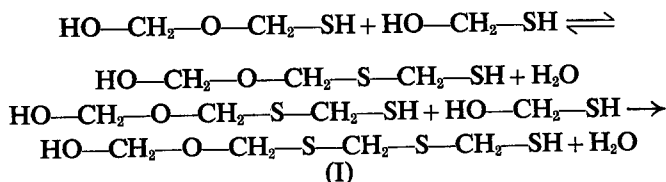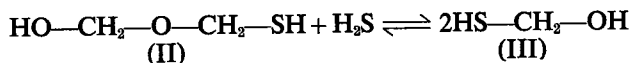
Having ascertained what occurs in neutral or weakly acidic systems, the authors investigated the behaviour of the reaction in the presence of a

---

*It is thought that hydrogen sulphide may react directly with the hydrated dimer of formaldehyde, HO—CH₂—O—CH₂—OH, present in the aqueous solution in equilibrium with the homologous series of polyoxymethylene glycols', from which it may be continually reformed.

catalytic amount of sulphuric acid[10, 11]. It was discovered that in these conditions there is separation of (I) as first solid product, which in the presence of hydrogen sulphide, changes in products (IV) with a higher sulphur content (56·5 to 60 per cent) and higher melting temperatures (220° to 250°C). The progressive rearrangement of (I) in these last products is shown in *Figure 1*, where powder patterns of (I) (a), of an intermediate product (b) and of a final product (IV) (c) are reported.

Figure 1—Powder patterns obtained by high-angle spectrometer with Cu Kα radiation: (a) first solid product (I) of the system; (b) intermediate product; (c) final product (IV)[8]
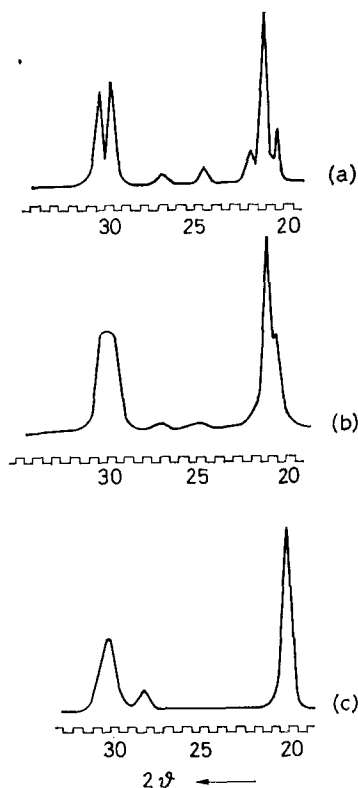
The final product (IV) shows a pattern (c) with diffraction peaks corresponding to interplanar spacings reported in 1961 by Lal[12] for polythiomethylene. The polythiomethylenic nature of (c) is proved because by an annealing process the product undergoes a limited weight loss, its melting range narrows to 240° to 255°C and its sulphur content rises to values of more than 66 per cent, very near the theoretical value for polythiomethylene (69·56 per cent).

Polythiomethylene is a white solid, highly crystalline, insoluble even at high temperatures in the usual organic solvents. The crystalline structure of polythiomethylene has been resolved[11, 13] and appeared to be a hexagonal unit cell like one of the two crystalline forms of isologous polyoxymethylene[14]. The crystalline data for polythiomethylene are reported in *Table 1*[13].

Table 1. Structural parameters of hexagonal polythiomethylene

Unit cell	hexagonal	No. of monomer units in unit cell	17
a (Å)	5·07	Turns of the helix in the period of 36·52 Å	9
c (Å)	36·52		
Observed density (g/cm³)	1·52	Radius of helix, Å	0·99
Calculated density (g/cm³)	1·60	Internal rotation angle	65° 59'
		Bond length for C—S bond, Å	1·815

As shown, in sulphuric acid media (I) changes substantially to polythiomethylene: this reaction was considered by the present authors to be a topochemical reaction of addition of mercaptomethanol present in solution to the chain of (I)[10]

$$HO—CH_2—O—CH_2—S—CH_2—S—CH_2—SH + nHO—CH_2—SH \rightarrow$$
$$nH_2O + HO—CH_2—O(CH_2S)_{n+3}H$$

(IV)
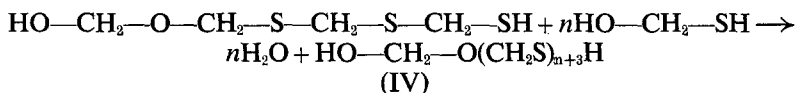
It is known that sulphuric acid is also a catalyst in the formation of 1,3,5-trithiane, yet it has been shown by kinetic data that this reaction is increased by high acid concentration and low formaldehyde concentration[15]. In fact it was ascertained[10] that the formation of trithiane may be avoided by working at a high ratio of CH_2O/H_2SO_4.

The topochemical growing of the thiomethylenic chain by mercaptomethanol over (I) and over the successive terms, is analogous to the growing of the oxymethylenic chain by methyleneglycol during the polymerization of formaldehyde in aqueous solution in the presence of solid polymer[16, 17].

The 1-hydrox-2-oxa-4,6-dithioheptane-7-thiol (I) may be directly converted into polythiomethylene by melting under vacuum; by this process the degradation of the oxymethylenic groups takes place with a contemporaneous condensation of the oligothiomethylenic residues[10]:

$$\overset{heat}{nHS(CH_2S)_2 (CH_2O)_2H \rightarrow 2nCH_2O + (n-1)H_2S + HS(CH_2S)_{2n}H}$$

For example, by heating (I) at 210°C for 6 h polythiomethylene is obtained with a melting temperature of 227° to 237°C and a sulphur content of 67·7 per cent[10].

To complete the study of $CH_2O–H_2O–H_2S$ system the authors have taken into consideration the reaction in alkaline media, and have carried out a reaction between formaldehyde and sodium sulphide. In a first group of experiments the work was carried out below the 'solubility limit' of the aqueous solution of formaldehyde[16], to avoid the homopolymerization of formaldehyde to polyoxymethylene, and with different Na_2S/CH_2O ratios. Results and characteristics of the products obtained are reported in *Table 2*.

X-ray powder spectra of the products of *Table 2* showed that they approach a polythiomethylenic structure when the ratio of sulphide/aldehyde increases.

From all the data it may be postulated that these compounds are formaldehyde-thioformaldehyde copolymers; moreover, by working at a

Table 2. Characteristics of experiments and of the products obtained from the $CH_2O-H_2O-Na_2S$ system below the 'solubility limit'. $T=35°C$, starting formaldehyde concentration in the system$=12$ wt %

Starting ratio $Na_2S \cdot 9H_2O/CH_2O$ *by weight*	*Starting pH*	*Characteristics of the product*	
		S *wt %*	*Melting range,* *°C*
0·03	10·5	50·9	124–129
0·09	11·5	51·3	122–127
0·44	11·5	55·5	123–132
1·00	11·5	55·7	125–132
1·66	11·5	58·9	145–152
2·93	12·5	66·5	170–180

very low ratio of Na_2S/CH_2O (in this case three to four days are needed for the separation of a solid product) the content of sulphur in the copolymer is always more than 50 per cent. By increasing this ratio, the sulphur content rises to values near the theoretical value for polythiomethylene.

As happens for polymers obtained in acidic media, copolymers of *Table 2* approach polythiomethylene by heating at melting temperature.

A second group of experiments was carried out over the 'solubility limit' of the system, that is, in the field in which formaldehyde undergoes polymerization in alkaline media[16, 17]. The experiments were carried out at different Na_2S/CH_2O ratios: results are reported in *Table 3.*

Table 3. Characteristics of experiments and of the products obtained from $CH_2O-H_2O-Na_2S$ system over the 'solubility limit': $T=35°C$, starting formaldehyde concentration in the system$=36$ wt %

Starting ratio $Na_2S \cdot 9H_2O/$ CH_2O *by weight*	*Starting pH*	*Time of reaction, h*	CH_2O *conc. in solution at the product drawing,* *wt.%*	*Product obtained**
0·083	11·5	23	27	Hexagonal POM†+ orthorhombic POM +copolymer S content 50 wt %
0·167	11·5	23	25	Hexagonal POM + orthorhombic POM (few)+copolymer S content 50 wt %
0·250	11·5	8	26	Hexagonal POM + copolymer S content 50 wt %

*Determined by x-ray powder spectra.
†Polyoxymethylene, POM.

The results reported in *Table 3* confirm that it is impossible to obtain, from this system, CH_2O—CH_2S copolymers with a sulphur content below 50 per cent. In fact, the homopolymerization of formaldehyde takes place preferentially in addition to formation of the copolymer described.

(b) Polycondensation from different monomers

The first synthesis of polythiomethylene in 1959 by Schmidt[18] by condensation between alkaline sulphides or hydrosulphides and methylene chloride was reported in the literature. However, no characteristics of the polymer are given.

We[19] have examined again in detail the reaction between sodium hydrosulphide and methylene chloride as follows

$$2n\text{NaSH} + n\text{CH}_2\text{Cl}_2 \longrightarrow (\text{CH}_2\text{S})n + 2n\text{NaCl} + n\text{H}_2\text{S}$$
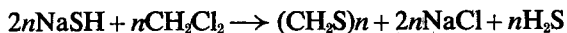
The yield of the process was found to be more than 90 per cent. The melting temperature of the polymer ranges from 160° to 205°C, that is below that of polythiomethylene from aqueous solution. The lower melting temperature is a consequence of a low molecular weight; this is confirmed because this polymer presents a soluble fraction in hot benzene: also the insoluble residue does not show a melting temperature above 230°C.

It is very interesting that this polythiomethylene shows a new crystalline structure (not resolved) rather than the known hexagonal form. This new crystalline structure is metastable and at 153°C irreversibly turns into the normal hexagonal form. In *Figure 2* the X-ray powder pattern of the new
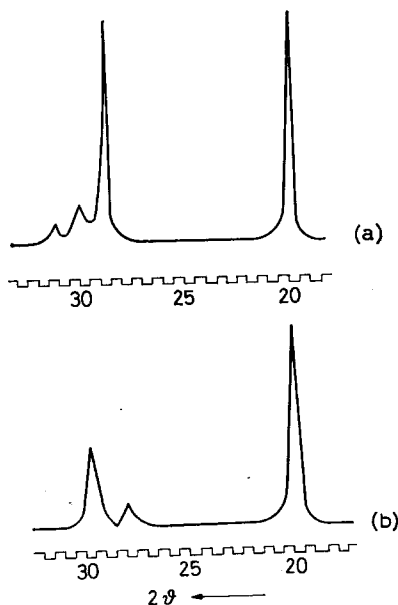
Figure 2—Powder patterns obtained by high-angle spectrometer with Cu Kα radiation: (a) polythiomethylene, new crystalline form; (b) hexagonal polythiomethylene[19]

crystalline form of polythiomethylene (a) and of hexagonal polythiomethylene (b) are reported. The new polymer was acetylated at its end groups; after this treatment the polymer is stable at a temperature of 250° to 260°C, while it is known that polythiomethylene is unstable at the melting temperature (240° to 260°C) owing to thermal degradation of its end groups.

If the condensation reaction is carried out between methylene chloride and alkaline sulphide (in water–alcohol media) cyclic oligomers together with hexagonal polythiomethylene are obtained.

Schmidt separates from the reaction mixture the cyclic trimer (1,3,5-trithiane), tetramer (1,3,5,7-tetrathiocane) and the polymer. Under the same conditions we have isolated the cylic pentamer, 1,3,5,7,9,-penta-thiacyclodecane[20].

Therefore, while trithiane was obtained in different ways (in water solution, by heating the polymer following Lal[12], by reaction between hydrogen sulphide and trioxan following Maura and Tulli[21]), this method is the only one described in the literature for the preparation of tetrathiocane and pentathiacyclodecane.

In *Table 4* some characteristics of the cyclic *sym*-thioformals are reported.

Table 4. Characteristics of cyclic *sym*-thioformals

$(CH_2S)_n$	$n=3$	$n=4$	$n=5$
Melting point, °C	215–218	49–50	120–121
Crystalline system	Orthorhombic	Monoclinic	Monoclinic
Solubility at room temperature in C_6H_6	Low	High	High

A different method of preparing hexagonal polythiomethylene is described by Lal[12], by condensation of bis(chloromethyl) sulphide and sodium sulphide. The polymer shows a high melting point (220° to 245°C) and an intrinsic viscosity value of about 0·05 dl/g at 230°C in mixed tetrachlorobiphenyl. However, this value is not very significant because at this temperature the polymer end groups are not protected against thermal degradation.

Polythiomethylene was also obtained by polycondensation of methanedithiol or mercaptomethylsulphide (with elimination of hydrogen sulphide) in the presence of a basic catalyst[22]. The polymer melts above 240°C and the reported X-ray analysis data correspond to those of hexagonal polythiomethylene.

sym-Cyclic oligomers of thioformaldehyde containing one oxymethylene group (co-oligomers CH_2O—CH_2S) together with linear copolymers (with a unit CH_2S/CH_2O ratio between one and four) were obtained by us[23], by reaction of bis(chloromethyl)ether and sodium sulphide in water–alcohol media. In this way, 1,3,5,7,9-oxatetrathiacyclodecane (V) and 1,3,5,7,9,11-oxapentathiacyclododecane (VI),

$$\begin{array}{c} \text{—O—CH}_2\text{—} \\ \text{—(CH}_2\text{S)}_4\text{—} \end{array}$$
(V)

$$\begin{array}{c} \text{—O—CH}_2\text{—} \\ \text{—(CH}_2\text{S)}_5\text{—} \end{array}$$
(VI)
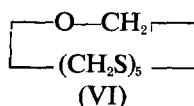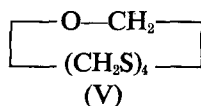
were isolated and characterized, melting respectively at 106° to 108°C and 163° to 165°C, soluble in benzene and insoluble in water.

(2)   *Polymerization by addition of cyclic oligomers*
(a)   *By cationic initiators*

Kern and Jaaks[24] report the mechanism by which trioxan is polymerized in bulk with cationic initiators such as boron trifluoride. The same mechanism is reported by Gipstein *et al.*[25] for the bulk polymerization of trithiane to polythiomethylene. The polymerization of trithiane is also claimed in some patents[26, 27].

We have polymerized in bulk and in solution with boron trifluoride, both tetrathiocane[28] and pentathiacyclodecane[20]. So far, these are the only reported examples of a solution polymerization with cationic initiators of cyclic oligomers of thioformaldehyde. Gipstein *et al.*'s attempt[25] to polymerize trithiane in solution was unsuccessful.

Polythiomethylene obtained by bulk polymerization of cyclic oligomers is presumably of high molecular weight: however, owing to the well known insolubility of the polymer below 190°C, significant viscosity measurements have never been made.

All these polymers show upon X-ray analysis a crystalline structure with a hexagonal unit cell.

Random copolymers with CH_2O and CH_2S units are also obtained by Celanese in the copolymerization of a trioxan–trithiane mixture with a cationic catalyst in bulk, in suspension and in solution[29].

(b)   *Polyaddition by irradiation*

The successful topotactic polymerization of trioxan single crystals induced Lando and Stannet to attempt polymerization of trithiane by the same method[30]. These authors discovered that if trithiane crystals are exposed to gamma radiation, (^{60}Co), a dose of 9·8 Mrads at room temperature and annealed at 195°C for 18·5 h, highly oriented polythiomethylene is obtained. By chloroform extraction the polymer is recovered with a yield of 20 per cent. The polymer presents the usual physical and chemical characteristics of polythiomethylene.

The crystalline structure (which was not hitherto resolved according to the literature) was indicated by the authors as orthorhombic.

However, Carazzolo and Mammi also showed that polythiomethylene obtained by irradiation of trithiane presents the usual hexagonal crystalline structure[31]. Moreover, these authors have indicated in a later paper the possible topotactic polymerization direction of trithiane[32].

It is interesting to note that the monotropic dimorphic system (orthorhombic–hexagonal) described for polyoxymethylene[16, 33, 34] and for polyselenomethylene[35-37], has not been found so far in isologous polythiomethylene.

CONCLUSION

Literature on polythiomethylene has been growing from 1959 till the present time. The polymer has been prepared by different methods, its structure has been resolved and a new crystalline structure (not yet resolved) has been synthesized. Besides trithiane, which has been known for a century, *sym*-cyclic thioformals, tetrathiocane and pentathiacyclodecane have been prepared and characterized.

476

Phenomena taking place in the $CH_2O–H_2O–H_2S$ system at room temperature have been studied and the different reaction products investigated. In detail it was determined that: (a) at strongly acidic pH trithiane is the only product; (b) at normal pH of the formaldehyde solution, or in neutral or alkaline conditions, linear co-oligomers and copolymers CH_2O/CH_2S are obtained. The sulphur content of these products is never less than 50 per cent. With basic or acidic catalysts and with sufficient availability of sulphide, the reaction gives rise to polythiomethylene.

Polythiomethylene, particularly the low molecular weight variety, shows a degree of toxicity which is manifested by skin allergy; fortunately this effect is limited by the low vapour pressure of this compound[38]. The individual sensibility to these manifestations is variable, as was observed in the authors' laboratory.

Besides copolymers trithiane–trioxan, copolymers thioformaldehyde-formaldehyde with ratios ranging between one and four have been synthesized. Moreover, sym-cyclic co-oligomers with one oxymethylenic and either four or five thiomethylenic groups have been isolated.

The authors are indebted to Dr L. Mortillaro for his interest and valuable assistance in this work.

Montecatini-Edison Co.,
  Donegani Research Institute,
    Novara, Italy

REFERENCES

[1] HOFMANN, A. W. *Liebigs Ann.* 1868, **145**, 360
[2] Zeppelin-Chemie, *Ger. Pat. No. 820 000*, 8 November 1951
[3] Degussa, *Ger. Pat. No. 911 544*, 17 May 1954
[4] Du Pont, *U.S. Pat. No. 1 991 765*, 19 February 1935
[5] BAUMAN, E. *Ber. dtsch. chem. Ges.* 1890, **23**, 60
[6] BONST, R. W. and CONSTABLE, E. W. *Org. Synth.* 1936, **16**, 81
[7] CAIRNS, T. L., EVANS, G. L., LARCHAR, A. W. and McKUSICK, B. C. *J. Amer. chem. Soc.* 1952, **74**, 3982
[8] CREDALI, L., MORTILLARO, L., GALIAZZO, G., DEL FANTI, N. and CARAZZOLO, G. *J. appl. Polym. Sci.* 1965, **9**, 2895
[9] BEZZI, S. and ILICETO, A. *Chim. e Industr.* 1951, **33**, 212
[10] CREDALI, L., MORTILLARO, L., RUSSO, M. and DE CHECCHI, C. *J. appl. Polym. Sci.* 1966, **10**, 859
[11] CARAZZOLO, G., MORTILLARO, L., CREDALI, L. and BEZZI, S. *Chim. e Industr.* 1964, **46**, 1484
[12] LAL, J. *J. org. Chem.* 1961, **26**, 971
[13] CARAZZOLO, G. and VALLE, G. *Makromol. Chem.* 1966, **90**, 66
[14] CARAZZOLO, G. *J. Polym. Sci. A*, 1963, **1**, 1573
[15] BOGDANSKI, J. and CHRZASZCZEWSKI, J. *Lodz. Towarz. Nauk, Wydzial III*, 1960, **4**, 37
[16] MORTILLARO, L., GALIAZZO, G. and BEZZI, S. *Chim. e Industr.* 1964, **46**, 139
[17] MORTILLARO, L., GALIAZZO, G., BANDEL, A. and BEZZI, S. *Chim. e Industr.* 1964, **46**, 1297
[18] SCHMIDT, M. and BLAETTNER, K. *Angew. Chem.* 1959, **71**, 4078
[19] RUSSO, M., MORTILLARO, L., DE CHECCHI, C. and CREDALI, L. *Gazz. chim. ital.* 1965, **95**, 448
[20] RUSSO, M., MORTILLARO, L., CREDALI, L. and DE CHECCHI, C. *J. Polym. Sci. B*, 1965, **3**, 455

[21] MAURA, G. and TULLI, L. *Ann. Chim., Roma,* 1965, **55,** 892

[22] Du Pont, *U.S. Pat. No. 3 070 580,* 25 December 1962

[23] MORTILLARO, L., RUSSO, M., CREDALI, L. and DE CHECCHI, C. *J. chem. Soc. C,* **1966,** 428

[24] KERN, V. and JAAKS, V. *J. Polym. Sci.* 1960, **48,** 399

[25] GIPSTEIN, E., WELLISCH, E. and SWEETING, O. J. *J. Polym. Sci. B,* 1963, **1,** 239

[26] Hoechst, *Ital. Pat. No. 652 187,* 1961

[27] Asahi Chemical Industry, *Fr. Pat. No. 1 400 828,* 1965

[28] RUSSO, M., MORTILLARO, L., DE CHECCHI, C., VALLE, G. and MAMMI, M. *J. Polym. Sci. B,* 1965, **3,** 501

[29] Celanese, *Brit. Pat. No. 1 024 614,* 30 March 1966

[30] LANDO, J. B. and STANNET, V. *J. Polym. Sci. B,* 1964, **2,** 375

[31] CARAZZOLO, G. and MAMMI, M. *J. Polym. Sci. B,* 1964, **2,** 1057

[32] CARAZZOLO, G., MAMMI, M. and VALLE, G. *J. Polym. Sci. B,* 1965, **3,** 863

[33] CARAZZOLO, G. and MAMMI, M. *J. Polym. Sci. A,* 1963, **1,** 965

[34] BEZZI, S. *Mater. plast. Elast.* 1963, **29,** 472

[35] MORTILLARO, L., CREDALI, L., RUSSO, M. and DE CHECCHI, C. *J. Polym. Sci. B,* 1965, **3,** 581

[36] RUSSO, M., MORTILLARO, L., CREDALI, L. and DE CHECCHI, C. *J. Polym. Sci. A,* 1966, **4,** 248

[37] CARAZZOLO, G. and MAMMI, M. *Paper* presented at the IUPAC *Symposium on Macromolecular Chemistry, Prague, 1965,* Preprint p 191

[38] FABRE, R., VERNE, J., CHAIGNEAU, M. and LEMOAN, G. *C.R. Acad. Sci., Paris,* 1964, **295,** 2545

Book Reviews

THIS addition to the series of collected conference proceedings, Polymer Symposia, contains papers presented at two symposia, 'Analysis of High Polymers' and 'Characterization and Fractionation of Polymers', which formed part of the American Chemical Society meeting held in Chicago in September 1964. Individual papers cover a wide range of topics, and while many articles deal with the results of detailed investigations and developments in technique, some papers constitute reviews of various aspects of the general field, demonstrating the nature of information obtainable by the use of certain techniques.

In the first section papers describe the use of pyrolytic techniques, infra-red and high-resolution nuclear magnetic resonance spectroscopy, broad-line n.m.r. and dielectric relaxation, X-ray diffraction and the use of radio-tracers. Included in this series are three papers on different aspects of the characterization of polyacrolein. The second series of papers deals almost exclusively with the fractionation of high polymers and the characterization of their molecular weight distributions, including reviews by Billmeyer and Schneider on the characterization of distributions and fractionation respectively. Other articles include investigations on elution fractionation and gel permeation chromatography. The remaining papers deal with fractionation on crystallization, sedimentation velocity, ultracentrifugation and light scattering.

Most people who are concerned with the characterization of polymers will find at least one paper of interest in this volume, which is undoubtedly a useful addition to the Polymer Symposia series.

G. C. EASTMOND

THE contents of this volume, which have already been published in *Pure and Applied Chemistry*, Vol. 12, Nos. 1–4 (1966), form a useful collection of what are for the most part well-documented progress summaries of many of the present growth areas in polymer research, contributed by leading authorities.

The first 100 pages of the book are devoted to the six Symposium Lectures: The future pattern of polymer science (Melville); Synthesis of high temperature resistant materials (Mark); Light scattering as a tool (Debye); Structural phenomena in the formation of polymer properties (Kargin); Physicochemical properties of biological macromolecules (Sadron); Synthesis of monodisperse polymers in the laboratory and in Nature (Schulz).

There follow a further 29 invited lectures in which the high standard of presentation is maintained. Although the emphasis is rather more on chemistry than on physics a wide variety of topics is covered. In addition to contributions on kinetics, mechanism, structure and properties of the more familiar systems there are a number of lectures devoted to relatively novel subjects which have not been reviewed previously. Included among the latter are, for example, non-equilibrium polycondensation (Korshak), oriented chain growth · by polymerization in the crystalline state (Morawetz), analogous polymer reactions (Smets), effects of macromolecular compounds in disperse systems (Heller), place interchange theory (Holzmüller), radical induced cationic polymerization (Okamura) and sheet polymers (Huggins).

There is no doubt that polymer chemists with interests ranging beyond their own immediate speciality will wish to acquire this book, if for no other purpose than to use as a source of stimulating ideas for future research.

P. F. ONYON

The Kinetics of Free Radical Polymerization
A. M. NORTH. Pergamon: Oxford, 1966. 42s

ANY polymer chemist working in the early fifties would have been astonished had he been favoured with a preview of Dr North's new book: in a work of little over 100 pages a substantial fraction of the space is devoted to topics which would, at that time, have been worth a paragraph each—or perhaps nothing. Consider: Diffusion-controlled reactions, Primary radical termination, Heterogeneous polymerization, Reversible polymerization and Solid state polymerization. Virtually all the mathematical derivations are concerned with these aspects of radical polymerization, there being very little formal discussion of basic 'simple' solution reactions but any charge of imbalance on these grounds is neutralized by the author's statement that the later chapters deal with matters of special topical research interest, except insofar as the earlier chapters also are pervaded rather extensively by the same influence.

Any reader using this book as an introduction to radical polymerization can skip the details of these special topics and thereby acquire a useful knowledge of the essentials of the subject as a result of applying himself to perhaps 70–80 pages of material. This is a high commendation of a book which also merits praise for its useful discussion of modern developments. For both these reasons its place in the literature would seem to be as a complement to more detailed textbooks on the same subject which are now a few years old.

The writing is clear, the attitude critical, perhaps rather more so than is necessary in an introductory book. One wonders how author and publisher came to accept the appearance of identically the same equation twice on page 47 only two inches apart!

A. D. JENKINS

Heavy Organic Chemicals
A. J. GAIT. Pergamon: Oxford, 1967. xvii+249 pp. 5 in. × 7½ in. 35s

THE chemical industry is an essential part of the national economy and this up-to-date and readable account of the manufacture of heavy organic chemicals is welcome. This monograph is one of a series on the chemical industry designed as teaching manuals for senior students. It is not, however, only of interest to students, and most industrial chemists will find it provides useful and enjoyable reading.

Industrial chemistry receives little prominence in many university curricula, and graduates are often unaware of the fascination of our complex chemical industry. The reviewer hopes that this volume will find widespread use in teaching as it provides a sound introduction to the field in which many university graduates will find employment.

The book concentrates inevitably on the petrochemical industry, and is divided into chapters covering chemicals based on different raw materials—synthesis gas, acetylene, ethylene, propylene, C_4 hydrocarbons, higher hydrocarbons and aromatic hydrocarbons. The entries on the individual chemicals cover historical aspects, a description of the most widely practised industrial processes, an account of U.K. production with names of manufacturers and annual output, and a brief account of the main industrial applications. Amongst the interesting aspects of industrial history which are commented upon, is the adverse effect of the hydrocarbon oil duties on the development of the petrochemical industry in the United Kingdom.

The chemical industry is still developing rapidly and no book of this type can be completely up-to-date when it appears: this volume does, nevertheless, give a remarkably accurate picture of the U.K. chemical industry in October 1965. In order to cover such a wide field in a brief monograph some selection is inevitable and any industrial chemist will think of products which could have been included and would have provided interesting material.

To remain of value, a work of this type requires frequent revision and the reviewer feels that the work should enjoy sufficient success to justify this.

F. J. WEYMOUTH

Berichte der Bunsen Gesellschaft für Physikalische Chemie, **70,** Pt 3 (1966)

THIS volume contains papers (with discussions) which were presented at a meeting on the Preparation, Structure and Properties of Copolymers held in October 1965.

The contents list is enough to convince any polymer scientist with an interest in copolymers that this volume is an essential addition to his library. Copolymerization is discussed with reference to the formation of random copolymers by all types of mechanism (Mayo) and to the formation of block and graft copolymers (Smets). The following properties of copolymers are discussed in separate articles: Structure determination (Cantow); Fractionation (Fuchs); Ultracentrifugation (Hermans); Light scattering (Benoit); Infra-red (Schnell); N.M.R. (Johnsen); Structural ordering (Müller); Glass temperature and related phenomena (Illers) and Mechanical properties (Oberst).

Each chapter presents a critical account of the present state of information and speculation on one particular aspect of copolymers but many readers may be glad to be warned that apart from the contributions of Mayo and Smets (English) and Benoit (French) all the articles are in German.

<div align="right">A. D. JENKINS</div>

The Kinetics of Free Radical Polymerization
A. M. NORTH. Pergamon: Oxford, 1966. 42*s*

ANY polymer chemist working in the early fifties would have been astonished had he been favoured with a preview of Dr North's new book: in a work of little over 100 pages a substantial fraction of the space is devoted to topics which would, at that time, have been worth a paragraph each—or perhaps nothing. Consider: Diffusion-controlled reactions, Primary radical termination, Heterogeneous polymerization, Reversible polymerization and Solid state polymerization. Virtually all the mathematical derivations are concerned with these aspects of radical polymerization, there being very little formal discussion of basic 'simple' solution reactions but any charge of imbalance on these grounds is neutralized by the author's statement that the later chapters deal with matters of special topical research interest, except insofar as the earlier chapters also are pervaded rather extensively by the same influence.

Any reader using this book as an introduction to radical polymerization can skip the details of these special topics and thereby acquire a useful knowledge of the essentials of the subject as a result of applying himself to perhaps 70–80 pages of material. This is a high commendation of a book which also merits praise for its useful discussion of modern developments. For both these reasons its place in the literature would seem to be as a complement to more detailed textbooks on the same subject which are now a few years old.

The writing is clear, the attitude critical, perhaps rather more so than is necessary in an introductory book. One wonders how author and publisher came to accept the appearance of identically the same equation twice on page 47 only two inches apart!

A. D. JENKINS

Heavy Organic Chemicals
A. J. GAIT. Pergamon: Oxford, 1967. xvii+249 pp. 5 in. × 7½ in. 35*s*

THE chemical industry is an essential part of the national economy and this up-to-date and readable account of the manufacture of heavy organic chemicals is welcome. This monograph is one of a series on the chemical industry designed as teaching manuals for senior students. It is not, however, only of interest to students, and most industrial chemists will find it provides useful and enjoyable reading.

Industrial chemistry receives little prominence in many university curricula, and graduates are often unaware of the fascination of our complex chemical industry. The reviewer hopes that this volume will find widespread use in teaching as it provides a sound introduction to the field in which many university graduates will find employment.

The book concentrates inevitably on the petrochemical industry, and is divided into chapters covering chemicals based on different raw materials—synthesis gas, acetylene, ethylene, propylene, C_4 hydrocarbons, higher hydrocarbons and aromatic hydrocarbons. The entries on the individual chemicals cover historical aspects, a description of the most widely practised industrial processes, an account of U.K. production with names of manufacturers and annual output, and a brief account of the main industrial applications. Amongst the interesting aspects of industrial history which are commented upon, is the adverse effect of the hydrocarbon oil duties on the development of the petrochemical industry in the United Kingdom.

The chemical industry is still developing rapidly and no book of this type can be completely up-to-date when it appears: this volume does, nevertheless, give a remarkably accurate picture of the U.K. chemical industry in October 1965. In order to cover such a wide field in a brief monograph some selection is inevitable and any industrial chemist will think of products which could have been included and would have provided interesting material.

To remain of value, a work of this type requires frequent revision and the reviewer feels that the work should enjoy sufficient success to justify this.

F. J. WEYMOUTH

Berichte der Bunsen Gesellschaft für Physikalische Chemie, **70,** Pt 3 (1966)

THIS volume contains papers (with discussions) which were presented at a meeting on the Preparation, Structure and Properties of Copolymers held in October 1965.

Notes and Communications

Melting Point Relationships for Binary Mixtures of Crystalline Polymers

THE purpose of this communication is to point out some features of phase diagrams for a binary mixture of crystalline substances, in which either of two components or both of them are crystalline polymers. The two components shall be designated as 1 and 2. For the sake of simplicity, we first consider the relation of the melting point depression of species 2 caused by the addition of species 1. A schematic diagram is shown in *Figure 1*.
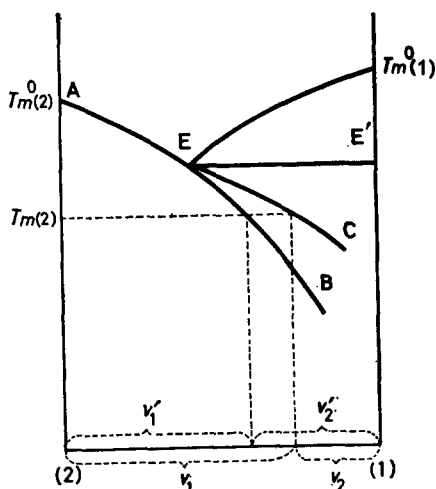
Figure 1—Effect of melting point depression of species 2 caused by addition of species 1

When species 1 is liquid over a given range of composition, the melting point of species 2 decreases along the curve AEB in *Figure 1*. The relationship for this curve can be derived by applying the treatment of phase equilibria. If the thermodynamic properties of a solution surrounding crystals of species 2 are expressed in terms of the Flory–Huggins theory, we have[1]

$$1/T_{m(2)} - 1/T^0_{m(2)} = -(R/\Delta H_2)\{\ln(1 - v_1) + (1 - V_2/V_1)v_1 + \chi_{12}(V_2/V_1)v_1^2\} \tag{1}$$

where $T_{m(2)}$ is the melting point of species 2, $T^0_{m(2)}$ is the value of $T_{m(2)}$ in the absence of species 1, R is the gas constant, ΔH_2 is the heat of fusion of species 2, v_1 is the volume fraction of species 1, V_1 and V_2 are the molar volumes of the respective species and χ_{12} is the Flory–Huggins interaction parameter.

Since we are concerned with polymeric materials, it is convenient to employ the following formulae which can be deduced from equation (1) for each case. Here, H denotes a high polymer and L a low molecular weight substance.

(a) *species 1—L, species 2—H*

$$1/T_{m\,(2)} - 1/T^0_{m\,(2)} = (R/\Delta H_{u\,(2)})\,(V_{u\,(2)}/V_1)\,(v_1 - \chi_{12}v_1^2) \qquad (2)$$

(b) *species 1—H, species 2—L*

$$1/T_{m\,(2)} - 1/T^0_{m\,(2)} = .-(R/\Delta H_2)\,\{\ln(1-v_1) + v_1 + \chi_{12}\,(V_2/x_1 V_{u\,(1)})v_1^2\}$$
$$= -(R/\Delta H_2)\,\{\ln(1-v_1) + v_1 + \chi_{21}v_1^2\}$$
$$= (R/\Delta H_2)\,\{(\tfrac{1}{2} - \chi_{21})\,v_1^2 + (\tfrac{1}{3})\,v_1^3 + \ldots\ldots\} \qquad (3)$$

(c) *species 1—H, species 2—H*

$$1/T_{m\,(2)} - 1/T^0_{m\,(2)} = -(R/\Delta H_{u\,(2)})\,\chi_{12}\,(V_{u\,(2)}/x_1 V_{u\,(1)})\,v_1^2$$
$$= -(R/\Delta H_{u\,(2)})\,\chi_{21}\,(1/x_2)\,v_1^2 \qquad (4)$$

where the subscript u is used to denote a quantity per repeating structural unit, x_1 and x_2 are the numbers of units (not segments) in a polymer molecule of the respective species, and χ_{12} and χ_{21} are the familiar solute–solvent interaction parameters[1].

Next we consider the relation when the diluent of species 1 is a crystalline polymer. In this case, the amount of diluent which is effective for the melting point depression of species 2 will decrease due to the appearance of crystalline phase of species 1. The effective concentration of the diluent v'_1 may be defined as

$$v'_1 = v_1\lambda_1/(1 - v_1 + v_1\lambda_1)$$

where λ_1 is the amorphous fraction of species 1. The degree of crystallinity (percentage) is represented by $(1 - \lambda_1) \times 100$.

The substitution of v_1 by v'_1 in equation (3) or (4) yields

$$(b'): 1/T_{m\,(2)} - 1/T^0_{m\,(2)} = -(R/\Delta H_2)\,\{\ln\,[(1-v_1)/(1 - v_1 + v_1\lambda_1)]$$
$$+ v_1\lambda_1/(1 - v_1 + v_1\lambda_1)$$
$$+ \chi_{21}\,[v_1\lambda_1/(1 - v_1 + v_1\lambda_1)]^2\} \qquad (3')$$

$$(c'): 1/T_{m\,(2)} - 1/T^0_{m\,(2)} \quad -(R/\Delta H_{u\,(2)})\,\chi_{21}\,(1/x_2)$$
$$\times [v_1\lambda_1/(1 - v_1 + v_1\lambda_1)]^2 \qquad (4')$$

The relationship for the curve EC in *Figure 1* can be expressed by equation (3') or (4'). When $\lambda_1 = 1$, equation (3') or (4') can be reduced to equation (3) or (4) respectively. In another limiting case as $\lambda_1 \rightarrow 0$, the curve EC approaches the line EE'. This behaviour that the melting temperature of species 2 is invariant with composition is a consequence of the phase rule of Gibbs, provided the crystalline state of species 1 is perfect.

The relationships for the melting point depression of species 1 caused by the addition of species 2 can be obtained in the same way as mentioned above, by interchanging the suffixes 1 and 2. We therefore come to the

conclusion that there are three types of phase diagram for binary mixtures as shown in *Figure 2*, although the problem of liquid–liquid phase separation is not considered in the present treatment. In the field of simple molecules, there are numerous examples giving the diagram of type (i). On the other hand, so far as the author knows, no systematic investigation has as yet been reported to examine the features of phase diagrams of types (ii) and (iii).

Figure 2—Three types of phrase diagram for binary crystalline mixtures

Although the experimental data for the melting behaviour of crystalline polymers accumulated in this decade were largely due to dilatometric methods[2], the utility of differential thermal analysis (DTA) has been growing in recent years[3], and the latter technique will be more suitable for the purpose of investigating the problems treated here. DTA studies on some binary mixtures involving crystalline polymers are now in progress in our laboratory and the results will be published in a forthcoming paper.

<div align="right">M. HIRAMI</div>

Nylon Department,
  Nippon Rayon Co. Ltd,
    Uji, Kyoto, Japan

<div align="right">*(Received March 1967)*</div>

REFERENCES

[1] FLORY, P. J. *Principles of Polymer Chemistry*, Chap. XIII. Cornell University Press: New York, 1953
[2] MANDELKERN, L. *Crystallization of Polymers*. McGraw-Hill: New York, 1964
[3] KE, B. *Newer Methods of Polymer Characterization*, Chap. IX. Interscience: New York, 1964

Anionic Polymerization in Dimethyl Sulphoxide[1]

IN RECENT years there has been a widespread development in the use of dimethyl sulphoxide (DMSO) as a solvent for promoting base-catalysed reactions[2]. The most common reaction system[3] involves solutions of potassium tert-butoxide in DMSO where enhanced basic character results, in part, from the equilibrium[4]

$$\overset{+}{K}\overset{-}{O}Bu^t + CH_3SOCH_3 \overset{K}{\rightleftharpoons} CH_3SOCH_2^-K^+ + Bu^tOH$$

conclusion that there are three types of phase diagram for binary mixtures as shown in *Figure 2*, although the problem of liquid–liquid phase separation is not considered in the present treatment. In the field of simple molecules, there are numerous examples giving the diagram of type (i). On the other hand, so far as the author knows, no systematic investigation has as yet been reported to examine the features of phase diagrams of types (ii) and (iii).

Figure 2—Three types of phrase diagram for binary crystalline mixtures

Although the experimental data for the melting behaviour of crystalline polymers accumulated in this decade were largely due to dilatometric methods[2], the utility of differential thermal analysis (DTA) has been growing in recent years[3], and the latter technique will be more suitable for the purpose of investigating the problems treated here. DTA studies on some binary mixtures involving crystalline polymers are now in progress in our laboratory and the results will be published in a forthcoming paper.

M. HIRAMI

Nylon Department,
Nippon Rayon Co. Ltd,
Uji, Kyoto, Japan

(Received March 1967)

REFERENCES

[1] FLORY, P. J. *Principles of Polymer Chemistry*, Chap. XIII. Cornell University Press: New York, 1953
[2] MANDELKERN, L. *Crystallization of Polymers*. McGraw-Hill: New York, 1964
[3] KE, B. *Newer Methods of Polymer Characterization*, Chap. IX. Interscience: New York, 1964

Anionic Polymerization in Dimethyl Sulphoxide[1]

IN RECENT years there has been a widespread development in the use of dimethyl sulphoxide (DMSO) as a solvent for promoting base-catalysed reactions[2]. The most common reaction system[3] involves solutions of potassium tert-butoxide in DMSO where enhanced basic character results, in part, from the equilibrium[4]

$$\overset{+}{K}\overset{-}{O}Bu^t + CH_3SOCH_3 \underset{}{\overset{K}{\rightleftharpoons}} CH_3SOCH_2^- K^+ + Bu^t OH$$

Methyl sulphinyl carbanion ($CH_3SOCH_2^-$) has been given the trivial name Dimsyl ion[5] and is involved in the majority of anionic reactions in DMSO, in spite of the fact that the equilibrium lies far to the left[4] ($K = 1·5 \times 10^{-7}$). The most striking feature of DMSO as solvent is the high solvating power for cations and low solvating power for anions[2,6].

Anionic polymerization of unsaturated esters and epoxides is a well established synthetic route to macromolecules and consequently it was decided to investigate anionic polymerizations in DMSO.

Monomers chosen for exploratory studies were ethylene oxide, propylene oxide and methyl methacrylate. These were dried and purified in conventional ways before distillation *in vacuo*. DMSO was dried over barium oxide and fractionated before final distillation *in vacuo*. Polymerizations were carried out and followed by the usual dilatometric technique and typical results are shown in *Table 1*.

Table 1. Polymerization in DMSO catalysed by potassium *t*-butoxide at 25·0°C

Monomer	Concentration (mole/litre)		$10^3 \times$ Rate (mole l.$^{-1}$ sec^{-1})	$10^2 \times k_v^*$ (l. mole^{-1} sec^{-1})	Degree of polmn†	
	[Monomer]	$10^3 \times$ [Initiator]			Calc.	Found
Ethylene oxide	3·22	11·6	2·32	6·2	198	139
	4·25	12·2	8·35	12·4	174	193
	4·31	2·19	1·22	12·8	985	750
	5·50	12·2	8·35	12·4	226	261
Propylene oxide	1·81	6·83	0·25	1·92		Oily liquid
Methyl methacry-late	1·30	5·30	3·40	49	123	281
	1·28	0·26	0·04	13	2 430	1 862
	1·32	1·18	0·52	33	550	355
	1·30	2·73	2·78	78	250	260
	1·58	7·70	7·60	63	100	140
	2·21	7·70	9·60	56	150	132
	1·28	7·64	6·00	61	90	135

*Calculated from the expression: Rate = k_p [Monomer] [Initiator].
†For ethylene oxide, polymerization was taken to completion and yields of polymer recovered were in excess of 80 per cent.
For methyl methacrylate, polymerization was stopped at 50 per cent conversion.
Estimation of DP was from measurements of intrinsic viscosity using the following relationships:
Polyethylene oxide $[\eta] = 1·25 \times 10^{-4} M^{0·74}$ in water at 30°C.
Polymethylmethacrylate $[\eta] = 0·75 \times 10^{-4} M^{0·76}$ in benzene at 25°C.

It was found that ethylene oxide and methyl methacrylate polymerized rapidly and completely at 25·0°C. Molecular weights, at high conversion, were in reasonable agreement with those calculated on the basis of one polymer chain per catalyst molecule. For low molecular weight polymers, elemental analysis established the presence of one sulphur atom per chain. The reaction kinetics were bimolecular in the early stages of the reaction and obeyed the simple expression

Rate of polymerization = k_p [Base] [Monomer]

Beyond a certain chain length (DP $\sim$ 80), however, the polymers were no longer truly soluble in DMSO and the kinetic behaviour became much more complex.

Since the initiation was apparently rapid and complete, and a termination reaction is most unlikely, the measured rates of polymerization represent the propagation reaction and hence values for k_p were estimated and are shown in *Table 1*. The presence of sulphur in the polymers indicates that initiation occurs via reaction of dimsyl ion with monomer, e.g.

$$CH_3SOCH_2^- + CH_2\!\!-\!\!CH_2 \longrightarrow CH_3SOCH_2CH_2CH_2O^-$$
$$\begin{array}{c} \diagdown\!\diagup \\ O \end{array}$$
$$n(CH_2CH_2)$$
$$\begin{array}{c} \diagdown\!\diagup \\ O \end{array}$$

$$CH_3SOCH_2(CH_2CH_2O)_n\!\!-\!\!CH_2CH_2O^-$$
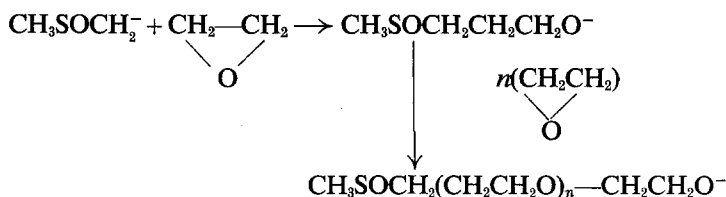
The close agreement between experimental and calculated molecular weights for ethylene oxide indicates that transfer to DMSO occurs at a rate which is many hundreds of times slower than the rate of propagation. Propylene oxide, however, formed only low molecular weight polymers with unsaturated end groups, indicating excessive transfer to solvent or monomer.

Attempts to polymerize styrene with this catalyst system failed unless the ratio styrene/DMSO was greater than unity. Lower values of the styrene/DMSO ratio yielded only a complex mixture of unsaturated molecules formed by rapid reactions of the initial dimsyl ion–styrene adduct, similar to those described by Walling and Bollyky[7].

Since this work was completed[8] there have been several preliminary reports of related polymerizations in DMSO[9, 10] but few kinetic data are available for comparison. However, the value of k_p for propylene oxide in DMSO at 30°, reported by Price and Carmelite[10], is approximately 100 times smaller than that found in the present work. It is clear also that these workers observed very much slower rates of polymerization of ethylene oxide[10, 11] than presently reported. Reasons for these discrepancies, together with experimental details, will be published in a full paper.

It may be concluded that DMSO is a very convenient medium for base-catalysed polymerization of epoxides and olefins with strongly electron-withdrawing substituents.

C. E. H. Bawn
A. Ledwith
N. R. McFarlane*

Donnan Laboratories,
University of Liverpool

(*Received March 1967*)

REFERENCES

[1] Part III. 'Anionic reactivity in DMSO'. For Part II see Ledwith, A. and Yang Shih-Lin, *Chem. & Ind.* **1964,** 1867
[2] Cram, D. J. *Fundamentals of Carbanion Chemistry.* Academic Press: New York, 1965

*Present address: Shell Research, Woodstock Agricultural Centre, Sittingbourne, Kent.

[3] CRAM, D. J., RICKBORN, B. and KNOX, G. R. *J. Amer. chem. Soc.* 1960, **82**, 6412
[4] LEDWITH, A. and MCFARLANE, N. R. *Proc. chem. Soc.* **1964**, 108
[5] PRICE, G. G. and WHITING, M. C. *Chem. & Ind.* **1963**, 775
  COREY, E. J. and CHAYKOVSKY, M. *J. Amer. chem. Soc.* 1962, **84**, 866
[6] PARKER, A. J. *Quart. Rev. chem. Soc., Lond.* 1962, **16**, 163
[7] WALLING, C. and BOLLYKY, L. *J. org. Chem.* 1964, **29**, 2699
[8] MCFARLANE, N. R. *Ph. D. Thesis.* University of Liverpool, January 1964
[9] MULVANEY, J. E. and MARKHAM, R. L. *J. Polym. Sci. B,* 1966, **4**, 343
  TROSSARELLI, L., PRIOLA, A., GUAITA, M. and SAINI, G. *Reprint No. P.578,* I.U.P.A.C. High Polymer Symposium Prague 1965
  MOLAU, G. E. and MASON, J. E. *J. Polym. Sci. A-1,* 1966, **4**, 2336
[10] PRICE, C. C. and CARMELITE, D. D. *J. Amer. chem. Soc.* 1966, **88**, 4039
[11] PRICE, C. C. and SPECTOR, R. *J. Amer. chem. Soc.* 1966, **88**, 4171

Prediction of Gel Permeation Chromatographic Elution Volumes of Silica Gel*

ONE of the earliest reports using gel permeation chromatography (GPC) to separate polymers was presented by Vaughan[1]. He used a silica aerogel, Santocel A, to fractionate polystyrenes in the molecular weight range from 22 000 to 1·2 million. Kohlschütter *et al.*[2] employed silica gel preparations with systematically changed space structure to chromatograph a mixture of two polystyrenes with viscosity average molecular weights 250 000 and 38 000. They found that separation improved with increasing specific pore volume of the gel. Le Page and de Vries[3] used various silica gels with known pore size distributions—as determined by mercury porosimetry—to separate mixtures of polystyrene fractions with weight average molecular weights of 260 000, 125 000, 35 000 and 11 000. The method was extended by MacCallum[4] to fractionate polyvinylchloride, polychloroprene and polyethylene.

The present experiments were carried out with Davison Silica Gel 70, mesh sizes 45–80. A 4 ft stainless steel column with ⅜ in. outer diameter was filled with the dry material, closed off with end plugs described in the

Figure 1—Calculated GPC calibration curve for Silica Gel 70 in toluene at 23°C

[3] CRAM, D. J., RICKBORN, B. and KNOX, G. R. *J. Amer. chem. Soc.* 1960, **82**, 6412

[4] LEDWITH, A. and McFARLANE, N. R. *Proc. chem. Soc.* **1964**, 108

[5] PRICE, G. G. and WHITING, M. C. *Chem. & Ind.* **1963**, 775
 COREY, E. J. and CHAYKOVSKY, M. *J. Amer. chem. Soc.* 1962, **84**, 866

[6] PARKER, A. J. *Quart. Rev. chem. Soc., Lond.* 1962, **16**, 163

[7] WALLING, C. and BOLLYKY, L. *J. org. Chem.* 1964, **29**, 2699

[8] McFARLANE, N. R. *Ph. D. Thesis.* University of Liverpool, January 1964

[9] MULVANEY, J. E. and MARKHAM, R. L. *J. Polym. Sci. B,* 1966, **4**, 343
 TROSSARELLI, L., PRIOLA, A., GUAITA, M. and SAINI, G. *Reprint No. P.578,* I.U.P.A.C. High Polymer Symposium Prague 1965
 MOLAU, G. E. and MASON, J. E. *J. Polym. Sci. A-1,* 1966, **4**, 2336

[10] PRICE, C. C. and CARMELITE, D. D. *J. Amer. chem. Soc.* 1966, **88**, 4039

[11] PRICE, C. C. and SPECTOR, R. *J. Amer. chem. Soc.* 1966, **88**, 4171

Prediction of Gel Permeation Chromatographic Elution Volumes of Silica Gel*

ONE of the earliest reports using gel permeation chromatography (GPC) to separate polymers was presented by Vaughan[1]. He used a silica aerogel, Santocel A, to fractionate polystyrenes in the molecular weight range from 22 000 to 1·2 million. Kohlschütter *et al.*[2] employed silica gel preparations with systematically changed space structure to chromatograph a mixture of two polystyrenes with viscosity average molecular weights 250 000 and 38 000. They found that separation improved with increasing specific pore volume of the gel. Le Page and de Vries[3] used various silica gels with known pore size distributions—as determined by mercury porosimetry—to separate mixtures of polystyrene fractions with weight average molecular weights of 260 000, 125 000, 35 000 and 11 000. The method was extended by MacCallum[4] to fractionate polyvinylchloride, polychloroprene and polyethylene.

The present experiments were carried out with Davison Silica Gel 70, mesh sizes 45–80. A 4 ft stainless steel column with ⅜ in. outer diameter was filled with the dry material, closed off with end plugs described in the

Figure 1—Calculated GPC calibration curve for Silica Gel 70 in toluene at 23°C

literature[5], and filled with toluene. The elution volumes of polystyrene fractions with molecular weights of 51 000, 19 800, 10 300, 4 800 and 3 600 at initial concentrations of 0·1 wt% are indicated by the open circles in *Figure 1*. It was then attempted to calculate an expected calibration curve, as suggested in the literature[6]. For this purpose, the pore size distribution of the silica gel was measured by mercury porosimetry[7]. The average coil sizes of the polystyrene molecules under experimental conditions were calculated by a theory by Ptitsyn and Eizner[8] and a viscosity/molecular weight relation by Outer *et al.*[9]. Both quantities were then matched under the assumption that the cumulative pore volume of the column up to any given pore size is completely accessible to all molecules with end-to-end distances up to one-half of that pore size. The result is indicated by the solid line in *Figure 1*. It is seen that this simple model describes the experimental data to a good approximation.

M. J. R. CANTOW
J. F. JOHNSON

*Chevron Research Company,
Richmond, Calif., U.S.A.*

(Received April 1967)

REFERENCES

[1] VAUGHAN, M. F. *Nature, Lond.* 1962, **195**, 801
[2] KOHLSCHÜTTER, H. W., UNGER, K. and VOGEL, K. *Makromol. Chem.* 1966, **93**, 1
[3] LE PAGE, M. and DE VRIES, A. J. Presented at Third International Seminar on GPC, Geneva, May 1966
[4] MACCALLUM, D. *Makromol. Chem.* 1967, **100**, 117
[5] MALEY, L. E. *J. Polym. Sci. C,* 1965, **8**, 253
[6] DE VRIES, A. J. IUPAC International Symposium on Macromolecular Chemistry, Prague 1965, *Preprint 139*
[7] DRAKE, L. C. and RITTER, M. L. *Industr. Engng Chem. (Anal. Ed.)* 1945, **17**, 786
[8] PTITSYN, O. B. and EIZNER, Y. E. *Tech. Phys. soviet Phys.* 1960, **4**, 1020
[9] OUTER, P., CARR, C. I. and ZIMM, B. H. *J. chem. Phys.* 1950, **18**, 830

Morphology of Annealed Polyethylene Extended Chain Crystals

IN A recent note[1] it was shown that on annealing the fracture surface of polyethylene extended chain crystals at a temperature well below the melting point, the normally sharp ridge-like morphology transformed into ripples aligned transverse to the original fracture striations. It was further suggested that this partial melting and recrystallization of portions of the extended chain crystals could be related to the structure of fibrils pulled out of folded chain single crystals during this deformation and subsequent annealing[2,3]. Similar structures are also seen on the surface and the interior of deformed spherulites[4] and bulk material[5,6] both before and after annealing. Since the impression may have unintentionally been given that folded chain crystals primarily deform into extended chain structures[1], it seems pertinent to report in this note on the morphology of extended chain crystals subjected to identical annealing treatments before and after fracture, and comment briefly on some of the considerable evidence[7,8] in favour of deformation into folded chain structures.

488

literature[5], and filled with toluene. The elution volumes of polystyrene fractions with molecular weights of 51 000, 19 800, 10 300, 4 800 and 3 600 at initial concentrations of 0·1 wt% are indicated by the open circles in *Figure 1*. It was then attempted to calculate an expected calibration curve, as suggested in the literature[6]. For this purpose, the pore size distribution of the silica gel was measured by mercury porosimetry[7]. The average coil sizes of the polystyrene molecules under experimental conditions were calculated by a theory by Ptitsyn and Eizner[8] and a viscosity/molecular weight relation by Outer *et al.*[9]. Both quantities were then matched under the assumption that the cumulative pore volume of the column up to any given pore size is completely accessible to all molecules with end-to-end distances up to one-half of that pore size. The result is indicated by the solid line in *Figure 1*. It is seen that this simple model describes the experimental data to a good approximation.

M. J. R. Cantow
J. F. Johnson

*Chevron Research Company,
Richmond, Calif., U.S.A.*

REFERENCES

[1] Vaughan, M. F. *Nature, Lond.* 1962, **195**, 801
[2] Kohlschütter, H. W., Unger, K. and Vogel, K. *Makromol. Chem.* 1966, **93**, 1
[3] Le Page, M. and de Vries, A. J. Presented at Third International Seminar on GPC, Geneva, May 1966
[4] MacCallum, D. *Makromol. Chem.* 1967, **100**, 117
[5] Maley, L. E. *J. Polym. Sci. C*, 1965, **8**, 253
[6] de Vries, A. J. IUPAC International Symposium on Macromolecular Chemistry, Prague 1965, *Preprint 139*
[7] Drake, L. C. and Ritter, M. L. *Industr. Engng Chem. (Anal. Ed.)* 1945, **17**, 786
[8] Ptitsyn, O. B. and Eizner, Y. E. *Tech. Phys. soviet Phys.* 1960, **4**, 1020
[9] Outer, P., Carr, C. I. and Zimm, B. H. *J. chem. Phys.* 1950, **18**, 830

Morphology of Annealed Polyethylene Extended Chain Crystals

In a recent note[1] it was shown that on annealing the fracture surface of polyethylene extended chain crystals at a temperature well below the melting point, the normally sharp ridge-like morphology transformed into ripples aligned transverse to the original fracture striations. It was further suggested that this partial melting and recrystallization of portions of the extended chain crystals could be related to the structure of fibrils pulled out of folded chain single crystals during this deformation and subsequent annealing[2,3]. Similar structures are also seen on the surface and the interior of deformed spherulites[4] and bulk material[5,6] both before and after annealing. Since the impression may have unintentionally been given that folded chain crystals primarily deform into extended chain structures[1], it seems pertinent to report in this note on the morphology of extended chain crystals subjected to identical annealing treatments before and after fracture, and comment briefly on some of the considerable evidence[7,8] in favour of deformation into folded chain structures.

488

Figure 1—Fracture surface of extended chain crystals of polyethylene as-crystallized. Scale bar represents 0·5 micron in this and subsequent micrographs

Figure 1 shows an electron micrograph of the fracture surface of Marlex 50 polyethylene crystallized at 5 000 atm pressure and between 235° and 250°C followed by slow cooling to room temperature. *Figure 2* is a replica of the fracture surface of the same sample annealed at 120°C for one hour before fracturing. It can be seen to be essentially indentical to the as-grown crystal (the slightly pitted appearance is due to the shadow material and carbon substrate). However, if a fracture *surface* of the same sample is annealed under identical conditions a totally different morphology results as illustrated in *Figure 3* (cf. ref. 1). The ripples or shish-kebabs yield a long period of about 300 Å. Sometimes a larger periodicity than that of these transverse lamellae can be found of the order of 1 000 Å, which has been frequently recorded by workers on drawn (folded chain) bulk polymers[6] and single crystals[10].

Wunderlich and Mellilo[1] compare similar results to the present work on annealing only the fracture surface, to the deformation of single crystals into fibrils. However, together with this, the appearance of the interior of the extended chain crystal must also be compared to the morphology of deformed bulk crystallized polyethylene. It seems very reasonable that the deformation process should be related to that of the single (folded chain) crystals themselves, the main components of the bulk material being folded chain lamellae interconnected by a great many tie molecules[11]. Although the morphology of the surface of drawn bulk material appears to consist of a smooth fibrillar structure before annealing, a clear shish-kebab effect

489

Figure 2—Same as in *Figure 1* but annealed at 120°C for one hour before fracturing
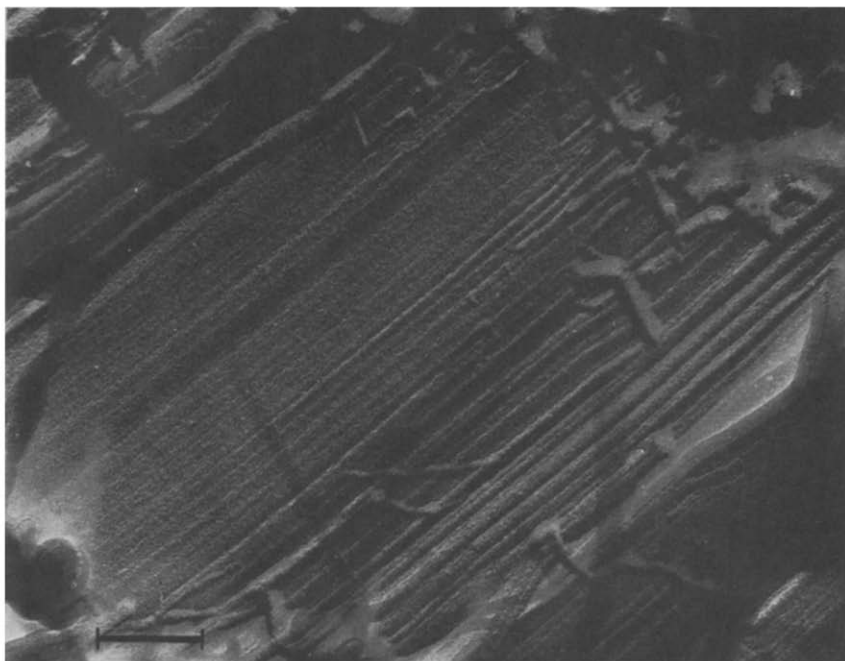
Figure 3—Same as in *Figure 1* but annealed at 120°C for one hour after fracturing

can readily be made manifest by both selective oxidation with fuming nitric acid[5,6], ion etching[9], and by examination of detached replicas or very thin films by dark field (diffraction contrast) electron microscopy[8,9,14]. After annealing, much more pronounced and regular shish-kebabs appear in the interior of the drawn material[6], similar to stress-crystallized material[15].

Dark field electron microscopy has also been successfully applied to the thin fibrils pulled out of single crystals[7]. Once again clear discontinuities in structure are seen before annealing. This must be contrasted to the experiments reported here on extended chain crystals.

Also no periodicity transverse to the chain axis can be observed (in dark field) from extended chain crystals as grown, or after etching with fuming nitric acid, but is a common feature of drawn bulk polyethylene. Furthermore small angle X-ray long periods are observed even at extremely high elongations ($>2\,700$ per cent)[12] although the intensity of the scattering is markedly reduced. (This may be due to the different local draw ratios within the sample[4].) It seems that in these cases as well the fundamental folded chain structure is not appreciably changed. In other words it has to be concluded that although it is very likely that extended chain crystals can serve as nuclei for further folded chain crystallization, for example during flow[13] or on tie molecules[11], the basic internal structure of highly oriented, deformed bulk material at least is largely different from that of extended chain crystals.

P. INGRAM

Camille Dreyfus Laboratory, Research Triangle Institute,
    Research Triangle Park, North Carolina

REFERENCES

[1] WUNDERLICH, B. and MELLILO, L. *Science*, 1966, **154**, 1329
[2] GEIL, P. H. *J. Polym. Sci. A*, 1964, **2**, 3835
[3] INGRAM, P., KIHO, H. and PETERLIN, A. *Polymer, Lond.* 1966, **7**, 135
[4] PETERLIN, A. and SAKAOKU, K. *J. macromol. Sci. (Phys.)*, 1967, **B1**, 103
[5] HAY, I. and KELLER, A. *Nature, Lond.* 1964, **204**, 862
[6] PETERLIN, A. and SAKAOKU, K. *Kolloidzschr.* 1966, **212**, 51
[7] PETERLIN, A., INGRAM, P. and KIHO, H. *Makromol. Chem.* 1965, **86**, 294
[8] PETERLIN, A. *J. Polym. Sci. C*, 1965, **9**, 61; *Kolloidzschr.* 1967, **216**, 129
[9] FISCHER, E. W. and GODDAR, H. IUPAC Symposium on Macromolecules, Prague, 1965
[10] FISCHER, E. W. and SCHMIDT, G. F. *Angew. Chem.* 1962, **74**, 551; see also STUART, H. A. *Ann. N.Y. Acad. Sci.* 1959, **83**, 3
[11] KEITH, H. D., PADDEN, F. S. and VADIMSKY, R. G. *J. appl. Phys.* 1966, **37**, 4027
[12] CORNELIUSSEN, R. Private communication. See also ANDRICHENCO, YU. D., DRUZHININA, T. V., ZUBOV, YU. A., KANKIN, A. A. and TSVANKIN, D. YA. *Vysokomol. Soedineniya*, 1965, **7**, 2126
[13] PENNINGS, A. J. and KIEL, A. M. *Kolloidzschr.* 1965, **205**, 160
[14] SCOTT, R. G. *J. Polym. Sci.* 1962, **57**, 405
[15] KELLER, A. and MACHIN, M. J. *J. macromol. Sci. (Phys.)*, 1967, **B1**, 41

Thermal Degradation of Styrene Polysulphone

IT IS well known[1] that many olefins copolymerize with sulphur dioxide in a strictly alternating manner to give olefin polysulphones of the general structure $-(CH_2-CHR-SO_2)-_n$. Styrene, however, has been reported to give copolymers with sulphur dioxide in which the styrene to sulphur dioxide ratio varies from $1:1^2$ to $2:1^3$ according to the method and conditions of polymerization, and copolymers having intermediate values have also been reported[3,4]. One of the major defects of conventional olefin polysulphones preventing commercial utilization has been their thermal instability. At temperatures above approximately 110° to 120°C many olefin polysulphones begin to depolymerize to the monomers[1], and considerable effort has been devoted industrially in attempts to limit this process[5]. Styrene polysulphones having styrene to sulphur dioxide ratios greater than one show greater thermal stability than do some olefin polysulphones having a 1:1 olefin to sulphur dioxide ratio, and some work has been carried out to investigate the products of their thermal degradation. Typically, it has been found that styrene polysulphones lose less than one per cent by weight when heated in air at 163°C for 3 h, in contrast to weight losses of 10 to 20 per cent usually observed for butene-1 polysulphone under the same conditions.

Styrene polysulphone was prepared by emulsion polymerization of styrene (35 ml) and sulphur dioxide (33 ml) at 37°C for 4 h using ammonium nitrate (0·25g) as catalyst in water (90 ml) containing sodium lauryl sulphate (0·5g) as emulsifying agent. The polymer isolated (31g) after coagulation of the emulsion latex with aqueous magnesium sulphate solution, washing with water and drying, had a styrene to sulphur dioxide ratio of approximately 1·85 to 1 (Found: C,69·0; H,5·5; S,12·3 per cent; theory for this composition requires C,69·2; H,5·8; S,12·45 per cent), and an inherent viscosity of 1·7 (0·5 per cent solution in chloroform at 25·0°C). When this material was heated at 200°C under reduced pressure (*ca.* 20 mm Hg) for 24 to 36 h extensive degradation occurred and oily crystals (approximately 40 per cent yield from a 2·5g polymer sample) collected on a cold finger above the polymer sample. Lower yields were observed when using larger samples. The sublimate (1·0g) was washed with cold petroleum ether (b.pt 80° to 100°C), again sublimed at 120°/0·07 mm Hg, and finally recrystallized from petroleum ether (b.pt 80° to 100°C) to give 0·263g almost colourless plates, m.pt 120° to 120·5°C. (Found: C,81·0; H,5·2; S,13·4. Calc. for $C_{16}H_{12}S$: C,81·4; H,5·1; S,13·6 per cent.) Mass spectrometry indicated a molecular weight of 236 and the mass spectrum, n.m.r. and i.r. spectra were identical in all respects with those of an authentic sample of 2,4-diphenylthiophene (I). The cold petroleum ether washings from the crude sublimate yielded a yellow oil, from which further quantities of 2,4-diphenylthiophene could be isolated. The residual fraction of this oil contained at least eleven other components, which have been partially

separated by gas chromatography. The structures of these other degradation products have not yet been established.

$$-(CH_2-CHC_6H_5-CH_2-CHC_6H_5-SO_2)_n \xrightarrow{200\,^{\circ}C}$$

I

The formation of 2,4-diphenylthiophene from styrene polysulphone can take place formally by the loss of two molecules of water from one repeat unit of the polymer chain. This process, however, is most unlikely since sulphone groups are characteristically resistant to removal of their oxygen atoms; the diphenyl thiophene probably represents the final product in a sequence of polymer degradation steps. Hummel and Schüddemage[6] have recently investigated the pyrolysis of styrene polysulphones in a mass spectrometer. At 350°C samples of styrene polysulphone (styrene : sulphur dioxide ratio = 2 : 1) gave mass spectra which indicated the presence of styrene, styrene dimer and an unidentified material of mass 236. This material, which could be the diphenyl thiophene (mol. wt 236) described above, was not a primary chain decomposition product. The mechanism by which 2,4-diphenyl thiophene is formed in the pyrolysis of styrene polysulphone is not yet understood, but the primary formation of sulphinic acids of the type $-CH_2 \cdot CHC_6H_5 \cdot CH_2 \cdot CHC_6H_5 \cdot SO_2H$ is possible.

D. C. ALLPORT

Imperial Chemical Industries Limited,
 Petrochemical & Polymer Laboratory,
  P.O. Box 11, The Heath,
   Runcorn, Cheshire

REFERENCES

[1] FETTES, E. M. and DAVIS, F. O. *High Polymers,* Volume XIII, Part III, p 225. Interscience: New York, 1962
[2] GLAVIS, F. J., RYDEN, L. L. and MARVEL, C. S. *J. Amer. chem. Soc.* 1937, **59,** 707
[3] BART, W. G. *Proc. Roy. Soc. A,* 1952, **212,** 66
[4] HUMMEL, D. O., and SCHÜDDEMAGE, H-D. R. *Kolloidzschr* 1966, **210,** 97
[5] CROUCH, W. W. and WICKLATZ, J. E. *Industr. Engng Chem. (Industr.),* 1955, **47,** 160
[6] SCHÜDDEMAGE, H-D. R. and HUMMEL, D. O. *Kolloidzschr.* 1966, **210,** 103

Catalysis of the Thermal Decomposition of Azo-Bis-Isobutyronitrile by Silver Perchlorate

THE rate of thermal decomposition of azo-bis-isobutyronitrile (AZO) shows little dependence on the nature of the solvent, and observations made in the presence of some copper[1], lithium[2] and zinc salts[3] indicate that the rate is

separated by gas chromatography. The structures of these other degradation products have not yet been established.

The formation of 2,4-diphenylthiophene from styrene polysulphone can take place formally by the loss of two molecules of water from one repeat unit of the polymer chain. This process, however, is most unlikely since sulphone groups are characteristically resistant to removal of their oxygen atoms; the diphenyl thiophene probably represents the final product in a sequence of polymer degradation steps. Hummel and Schüddemage[6] have recently investigated the pyrolysis of styrene polysulphones in a mass spectrometer. At 350°C samples of styrene polysulphone (styrene : sulphur dioxide ratio = 2 : 1) gave mass spectra which indicated the presence of styrene, styrene dimer and an unidentified material of mass 236. This material, which could be the diphenyl thiophene (mol. wt 236) described above, was not a primary chain decomposition product. The mechanism by which 2,4-diphenyl thiophene is formed in the pyrolysis of styrene polysulphone is not yet understood, but the primary formation of sulphinic acids of the type —CH$_2$·CHC$_6$H$_5$·CH$_2$·CHC$_6$H$_5$·SO$_2$H is possible.

<div align="right">D. C. Allport</div>

Imperial Chemical Industries Limited,
   Petrochemical & Polymer Laboratory,
     P.O. Box 11, The Heath,
       Runcorn, Cheshire

<div align="right"></div>

REFERENCES

[1] FETTES, E. M. and DAVIS, F. O. *High Polymers,* Volume XIII, Part III, p 225. Interscience: New York, 1962
[2] GLAVIS, F. J., RYDEN, L. L. and MARVEL, C. S. *J. Amer. chem. Soc.* 1937, **59**, 707
[3] BART, W. G. *Proc. Roy. Soc. A,* 1952, **212**, 66
[4] HUMMEL, D. O., and SCHÜDDEMAGE, H-D. R. *Kolloidzschr* 1966, **210**, 97
[5] CROUCH, W. W. and WICKLATZ, J. E. *Industr. Engng Chem. (Industr.),* 1955, **47**, 160
[6] SCHÜDDEMAGE, H-D. R. and HUMMEL, D. O. *Kolloidzschr.* 1966, **210**, 103

Catalysis of the Thermal Decomposition of Azo-Bis-Isobutyronitrile by Silver Perchlorate

THE rate of thermal decomposition of azo-bis-isobutyronitrile (AZO) shows little dependence on the nature of the solvent, and observations made in the presence of some copper[1], lithium[2] and zinc salts[3] indicate that the rate is

not significantly changed by the presence of these compounds. We now report that the rate of thermal decomposition may be greatly enhanced by silver perchlorate.

Figure 1 shows the initial rates of free-radical polymerization of methyl methacrylate initiated by AZO at 70°C as a function of the concentration of silver perchlorate. These measurements were made by the dilatometric technique. The rate of polymerization first rises with increasing salt concentration but eventually reaches a plateau value rather more than twice the value obtained in the absence of salt. Silver perchlorate alone initiates the polymerization of methyl methacrylate[4], but at the concentrations employed in the experiments in *Figure 1* the rates are very low and need not be taken into consideration for present purposes.
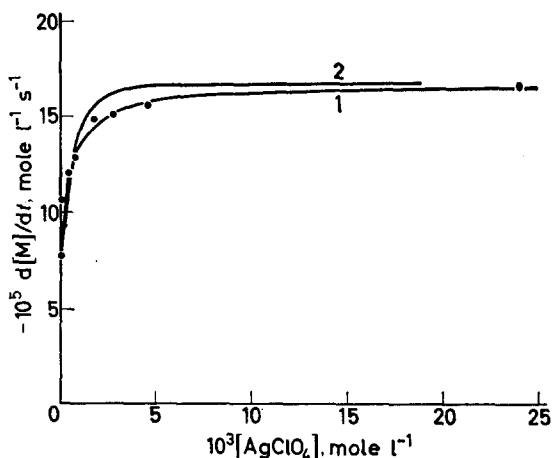
Figure 1—Rates of polymerization of bulk methyl methacrylate (M) at 70°C initiated by azo-bis-isobutyronitrile in the presence of silver perchlorate. [AZO]$= 1 \cdot 15 \times 10^{-4}$ mole 1^{-1}. ● Experimental values. Curve 1: calculated for complex of composition $AgClO_4$: AZO$= 1:1$ with $K = 1\,350$ mole^{-1} l.; Curve 2: calculated for complex of composition $AgClO_4$: AZO$=2:1$ with $K = 2 \cdot 13 \times 10^6$ mole^{-2} l^2

The observations suggest that silver perchlorate either brings about an increase in the rate of initiation, or changes the kinetic parameters so that $k_p k_t^{-\frac{1}{2}}$ is increased (k_p, k_t being the rate constants for chain propagation and termination, respectively). To explore these possibilities the rate of evolution of nitrogen was measured. The apparatus allowed AZO and silver perchlorate to be added to methyl methacrylate preheated to 70°C; after a further period at 70°C the mixture was cooled in liquid nitrogen and the non-condensable gas removed by a Toepler pump. Complete degassing was effected by thawing, freezing and evacuation cycles. The polymer formed was precipitated into methanol and collected, dried and weighed. The number-average molecular weight was then determined viscometrically, with the aid of the relation between intrinsic viscosity and molecular weight given by Fox, Kinsinger, Mason and Schuele[5]. The results set out in *Table 1* indicate that the rate of nitrogen evolution is greatly increased by the presence of silver perchlorate. On the other hand, the parameter $k_p k_t^{-\frac{1}{2}}$, calculated from corresponding rates and degrees of polymerization, is not significantly affected, so that the observed increases in the rate of polymerization apparent from *Figure 1* and *Table 1* arise from increases in the rate of initiation. Mr S. Brumby of this department has confirmed

that at 25°C normal values of $k_p k_t^{-1}$ are also obtained in the presence of silver perchlorate. Values of the first-order velocity constant for decomposition k_d calculated from the nitrogen evolution are given in *Table 1*. The increase in the rate of formation of nitrogen (approximately fourfold) is consistent with the maximum enhancement in the rate of polymerization (approximately twofold).

Table 1. Rates of decomposition and polymerization at 70°C

Reaction time, min	10^4 [AZO] mole l^{-1}	10 [AgClO$_4$] mole l^{-1}	10^5 [N$_2$] evolved, mole l^{-1}	Polymer formed, gl^{-1}	$10^{-5}\,\bar{M}_n$	$k_p k_t^{-1/2}$ mole$^{-1/2}$ $l^{1/2}$ $s^{-1/2}$	$10^5 k_d$ s^{-1}
15	9·45	0	2·48	17·6	8·67	0·15	3·0 ⎫ 3·1
15	9·1	0	2·63	19·1	9·23	0·16	3·2 ⎭
15	10·1	0·89	10·6	36·5	4·01	0·15	12·4 ⎫
15	9·1	0·895	10·1	35·9	3·70	0·15	13·1 ⎪ 12·7
20	9·2	0·915	13·1	48·6	4·10	0·15	12·8 ⎬
25	9·3	0·915	15·9	57·1	3·80	0·14	12·5 ⎭

The catalytic effect of silver perchlorate depends upon the nature of the solvent. Thus we have shown that in ethyl acetate solution, catalysis is much less marked than in methyl methacrylate, the increase in the rate of nitrogen evolution amounting to about 50 per cent for [AgClO$_4$] = 2·3 × 10^{-2} and [AZO] = 9·5 × 10^{-4} mole l^{-1}.

Magnesium perchlorate has only a very small effect on the rate of polymerization initiated by AZO, hence the species responsible for the catalysis by silver perchlorate is the silver ion.

The nature of the dependence of the rate of polymerization on [AgClO$_4$] suggests that a complex is formed between the salt and AZO which decomposes more rapidly than free AZO. The plateau value (*Figure 1*) then corresponds to complete complexing of the AZO. Two types of complex, in which the AgClO$_4$: AZO ratios are 1 : 1 and 2 : 1, respectively, can be envisaged. Calculated rate versus [AgClO$_4$] curves are shown in *Figure 1* for the two types. If the limiting rate is taken to equal the observed plateau value the equilibrium constant for complex formation K is the only remaining adjustable parameter. Curve 1, corresponding to the 1 : 1 complex with $K = 1350$ mole^{-1} l, is a reasonably good fit with experiment. It does not seem possible to obtain such satisfactory agreement on the basis of the 2 : 1 complex; curve 2, with $K = 2·13 × 10^6$ mole^{-2} l.^{2}, illustrates the type of discrepancy. Thus, although not conclusive, the present evidence favours the 1 : 1 complex with an equilibrium constant approximately equal to the value quoted.

The mechanism of decomposition of the complex is not revealed by these experiments; one general type of explanation of the relatively high rate could be that coordination with Ag$^+$ increases the importance of polar contributions to the transition state. The specificity of the catalysis raises interesting problems which are under investigation at present.

Since this work was completed Hirano, Miki and Tsuruta[6] have reported the accelerated decomposition of AZO brought about by organoaluminium compounds. These authors also interpret their findings in terms of complex-formation.

We thank Mr S. Brumby for helpful discussions.

C. H. BAMFORD
R. DENYER
J. HOBBS

Department of Inorganic, Physical and
Industrial Chemistry,
University of Liverpool
I.C.I. Ltd.,
Petrochemical and Polymer Laboratory,
Runcorn, Cheshire

REFERENCES

[1] KOCHI, J. K. and MOG, D. M. *J. Amer. chem. Soc.* 1965, **87**, 522
[2] BAMFORD, C. H., JENKINS, A. D. and JOHNSTON, R. *Proc. Roy. Soc. A*, 1957, **241**, 364
[3] BAMFORD, C. H., BRUMBY, S. and WAYNE, R. P. *Nature, Lond.* 1966, **209**, 292
[4] HERMANS, J. P. and SMETS, G. *J. Polym. Sci. A*, 1965, **3**, 3175
[5] FOX, T. G., KINSINGER, J. B., MASON, H. F. and SCHUELE, E. M. *Polymer, Lond.* 1962, **3**, 71
[6] HIRANO, T., MIKI, T. and TSURUTA, T. *Makromol. Chem.* 1967, **104**, 230

Photodegradation
of Polyphenylvinylketone

C. DAVID, W. DEMARTEAU and G. GEUSKENS

Irradiation of polyphenylvinylketone with 3650 Å ultra-violet light in the solid state or in benzene solution brings about a decrease of the molecular weight. In the presence of isopropanol no photoreduction is observed and naphthalene is not an inhibitor of the photodegradation. These results and the analysis by vapour phase chromatography of volatile products formed suggest that the principal mechanism is the abstraction of a hydrogen in position γ to the carbonyl group followed by breaking of the main polymer chain (Norrish type II mechanism).

ALTHOUGH the photochemistry of simple ketones has been extensively studied in recent years, little is known about the behaviour of polymeric ketone derivatives.

Common organic ketones undergo four principal photochemical reactions[1]:

(*1*) Norrish type I process or cleavage of one bond adjacent to the carbonyl group, which occurs mainly with saturated ketones.

(*2*) Norrish type II process or γ-hydrogen abstraction followed by elimination of an olefin (β-cleavage). This process takes place through the n–π⋆ triplet state in arylalkylketones while triplet and singlet n–π⋆ states participate in the photocycloelimination of di-alkylketones.

(*3*) Intramolecular cyclic alcohol formation. This process also concerns ketones having a γ-hydrogen and often proceeds through the n–π⋆ triplet state.

(*4*) Photoreduction in the presence of hydrogen donors, leading to pinacols through the n–π⋆ triplet state. It concerns arylalkyl- or di-aryl-ketones.

Quenching of the reactive excited state by energy transfer to substances having a lower triplet level demonstrates the occurrence of a triplet state reaction.

Among polymeric ketone derivatives, polymethylvinylketone has been shown to undergo simultaneously Norrish type I and type II processes in solution[2] and in the solid state[3]. The photolysis of polymethylisopropenylketone leads to main chain cleavage[4] followed by depolymerization between 130°C and 180°C[5]; the mechanism of the reaction has not been determined.

This paper is concerned with the photolysis of polyphenylvinylketone. Butyrophenone, which may be considered a model compound for this polymer, has been studied recently: the quantum yield for photocycloelimination is 0·43 at 25°C in benzene solution while the sum of the quantum yields for processes other than the Norrish type II is less than 0·01[5]. It was of interest to see if the same reaction would take place with polyphenylvinylketone.

EXPERIMENTAL

Materials

Benzene (Carlo Erba pro analysi) was used without further purification.

Isopropanol (U.C.B. pro analysi) was dried on sodium carbonate and then on magnesium isopropoxide before distillation.

Naphthalene (U.C.B. technical) was recrystallized twice from alcohol and resublimed twice under vacuum before use.

Phenylvinylketone was prepared according to the method of Mannich and Heilner[6].

Polyphenylvinylketone was obtained by polymerization in bulk at 60°C of the carefully outgassed monomer in the presence of 0·1 weight per cent AIBN, conversion being kept lower than 30 per cent. After dilution with benzene, the polymer was precipitated in heptane, filtered, dissolved in benzene and freeze-dried. The infra-red (i.r.) spectrum of the polymer was identical to that published by other authors[7]. Its ultra-violet (u.v.) spectrum is reproduced in *Figure 1*. The limiting viscosity number of the sample used in the photolysis experiments was 0·55 dl g^{-1} in benzene solution at 25°C.

Figure 1—Ultra-violet spectrum of polyphenylvinylketone in chloroform

Spectra

The u.v. spectra were recorded on a Hitachi–Perkin–Elmer model 139 spectrophotometer and the i.r. spectra on a Perkin–Elmer model 237 spectrophotometer.

Photolysis

Solutions—The light source was a Philips HPW 125 lamp. A parallel beam of light was obtained by a system of lenses. Irradiations were performed in a Pyrex viscometer reproduced in *Figure 2*. It consists of a cylindrical cell, A, (diameter 3 cm, thickness 2 cm) with two parallel windows,
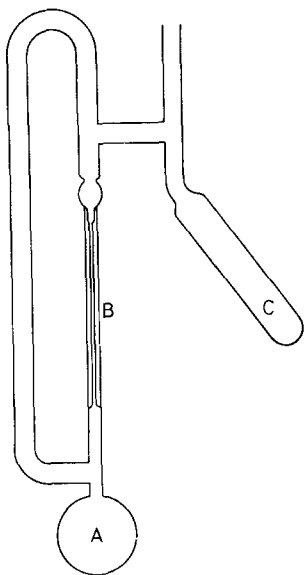
Figure 2—Irradiation apparatus

fitted with a capillary tube, B, and a receiver, C, used to outgas the solution before sealing the viscometer under high vacuum. Lamp intensity was measured using benzophenone–benzhydrol actinometer[8] in a cell identical to the polymer irradiation one, except for the capillary tube. The incident intensity was 5×10^{-7} E min^{-1} on the cell window.

Films—Polymer films 0·01 mm thick were cast from benzene solution in flat Pyrex dishes. They were irradiated under vacuum in a cylindrical Pyrex tube fitted with a trap, kept at liquid nitrogen temperature, for volatile condensable photolysis products and an adaptor to a Toepler pump. The apparatus was surrounded by four lamps and rotated continuously to ensure homogeneous irradiation.

RESULTS AND DISCUSSION

Solution experiments

Polyphenylvinylketone was irradiated in benzene solution. The efflux time of the solution t was measured as a function of the irradiation time. The influence of naphthalene, which is known to inhibit the photoreduction of benzophenone[9] and of isopropanol, a good hydrogen donor in photoreduction reactions, has been investigated. In *Figure 3* $(t - t_0)/t_0$ (t_0 is the efflux time for benzene) was plotted against the irradiation time. It appears that there is no influence either of naphthalene or of isopropanol on the flow behaviour of u.v. irradiated polyphenylvinylketone solutions. A fifty-fold increase in naphthalene concentration does not yield any inhibiting effect on degradation after 30 minutes irradiation. Neither monomer nor acetone could be detected by vapour phase chromatography after irradiation in the presence of isopropanol.

Spectrophotometry at 3 650 Å and gravimetric analysis of the irradiated
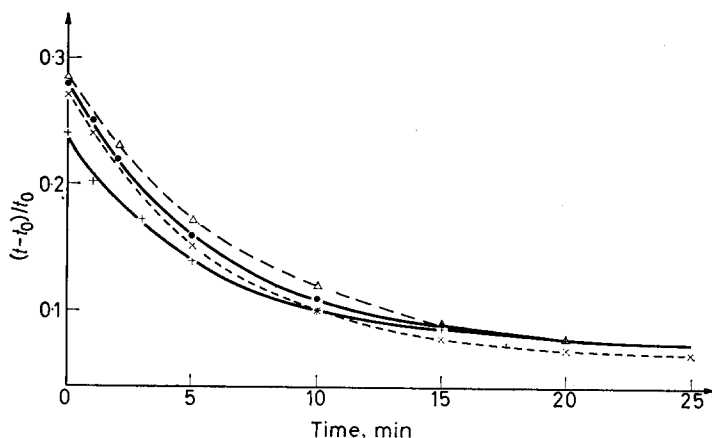
Figure 3—Photodegradation of polyphenylvinylketone: ●, PPVK
(0·035 M in monomeric units) in benzene; ×, PPVK (0·035 M) in
benzene + isopropanol (0·1 M); +, PPVK (0·029 M) in benzene +
naphthalene (0·001 M); △ PPVK (0·035 M) in benzene + isopropanol
(0·1 M) + naphthalene (0·001 M)

solution were performed after centrifugation to separate eventually formed
gel: the initial polymer was recovered complete showing that no insoluble
crosslinked network was formed.

These results show that photoreduction does not occur appreciably. On
the other hand, the Norrish type I mechanism must be excluded since no
benzaldehyde is formed.

Most probably, the decrease of $(t-t_0)/t_0$ for polyphenylvinylketone
solutions as a function of irradiation time is due to main chain scissions by
a Norrish type II mechanism:
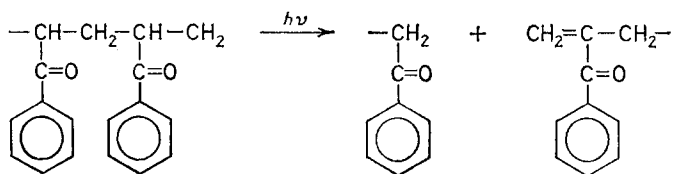
Lack of inhibition by naphthalene cannot be taken as an argument against
a triplet mechanism because the type II process is less sensitive to this than
photoreduction as shown by the results obtained respectively for butyro-
phenone[5] and benzophenone[9].

Furthermore, polymers are less sensitive to quenching of metastable states
than small molecules. This protecting effect occurs by the rearrangement of
the polymer residue in the environment of the excited chromophore[10].

The u.v. spectra of initial and degraded polymer samples are identical.
The i.r. spectra are, however, different for polymers irradiated in the absence
and in the presence of isopropanol (*Figure 4*). The former is identical to that
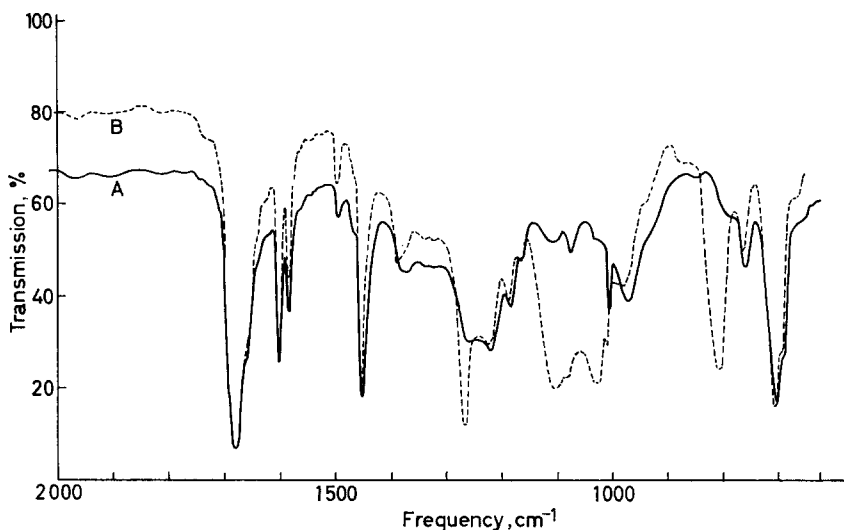
Figure 4—A, infra-red spectrum of polyphenylvinylketone; B, infra-red spectrum of polyphenylvinylketone irradiated for 6 h in benzene–isopropanol (0·1 M) solution

of the initial polymer whereas the latter shows intense new absorption bands at 800, 1 025, 1 100 and 1 270 cm^{-1}. The band at 800 cm^{-1} is characteristic of disubstituted benzene rings but the others cannot be interpreted easily (ethers, alcohols or esters).

For a linear polymer having a number-average molecular weight $\overline{M}_{n0}$ initially and $\overline{M}_n$ after a random cleavage process, the average number of scissions taking place in a polymer chain is given by $(\overline{M}_{n0}/\overline{M}_n) - 1$. If a most probable molecular weight distribution is assumed before and after degradation, the corresponding limiting viscosity numbers can be used to give the number of scissions as $([\eta_0]/[\eta])^{1/a} - 1$, where a is the exponent in the Mark–Houwink relationship $[\eta] = K \overline{M}_v^a$. Although no accurate relationship has been established for polyphenylvinylketone, the initial number-average molecular weight may be estimated to be about 100 000 assuming $K = 10^{-4}$ and $a = 0·7$ in the Mark–Houwink relationship and $\overline{M}_v = \overline{M}_w = \overline{M}_n/2$. $[\eta]$ is extrapolated from the viscosity number at one concentration using the Huggins equation $\eta_{sp}/c = [\eta] + k[\eta]^2 c$ with $k = 0·4 \pm 0·04$. The quantum yield for scissions can then be evaluated from the equation

$$\phi_s = [([\eta_0]/[\eta])^{1/a} - 1]/(I\,t\,\overline{M}_{n0})$$

where I is the rate of absorption of radiation in einstein per gramme of polymer and t is the exposure time. A plot of the number of scissions per molecule against the exposure time is reproduced on *Figure 5*. The quantum yield for chain scissions is estimated to be about 0·3. Quantum yield of the same order of magnitude (0·43) was observed for Norrish type II split in butyrophenone[5].

501
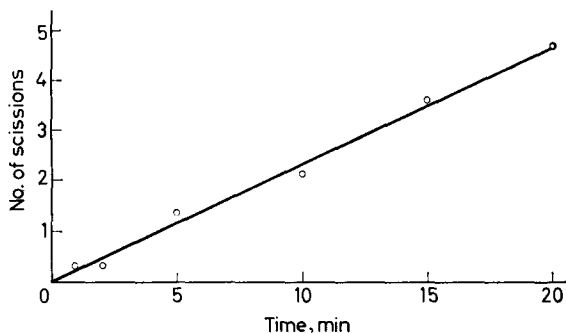
Figure 5—Number of scissions per molecule of poly-
phenylvinylketone versus irradiation time

Film experiments

Decrease in molecular weight without formation of insoluble gel occurs
for solid films. No inhibiting effect of naphthalene was observed with films
saturated with naphthalene vapours for 24 hours at room temperature. The
i.r. and u.v. spectra were unchanged after irradiation. Quantum yield of
carbon monoxide resulting from a Norrish type I radical split is less than
10^{-3} as determined by gas chromatography. No monomer could be detected.
The reaction seems to proceed by the same mechanism as the photo-
degradation in solution.

Our results show that the photochemical behaviour of polyphenylvinyl-
ketone in benzene solution and in the solid state is quite similar to that of
butyrophenone.

*We are very grateful to Professor L. de Brouckère for her interest in this
work.*

Service de Chimie Générale II,
Faculté des Sciences,
Université Libre de Bruxelles

REFERENCES

[1] CALVERT, J. G. and PITTS Jr, J. N. *Photochemistry*, p 379, Wiley: New York,
1966
[2] GUILLET, J. E. and NORRISH, R. G. W. *Proc. Roy. Soc. A*, 1956, **233**, 153
[3] WISSBURN, K. F. *J. Amer. chem. Soc.* 1959, **81**, 58
[4] SCHULTZ, A. R. *J. Polym. Sci.* 1960, **47**, 267
[5] BAUM, E. J., WAN, J. K. S. and PITTS Jr, J. N. *Amer. chem. Soc.* 1966, **88**, 2652
[6] MANNICH, G. and HEILNER, G. *Chem. Ber.* 1922, **55**, 356
[7] TSURUTA, T., FUJIO, R. and FURUKAWA, J. *Makromol. Chem.* 1964, **80**, 172
[8] HAMMOND, G. S., TURRO, N. J. and LEERMAKERS, P. A. *J. phys. Chem.* 1962, **66**,
1148
[9] MOORE, M. W. and KETCHUM, M. *J. Amer. chem. Soc.* 1961, **83**, 2789
[10] OSTER, G. and NISHIJIMA, Y. *Fortschr. Hochpolym.Forsch.* 1964, **3**, 313

A Comparison of Lower Critical Solution Temperatures of Some Polymer Solutions

D. PATTERSON*, G. DELMAS* and T. SOMCYNSKY

The Lower Critical Solution Temperature (LCST) in polymer solutions is discussed in terms of the Prigogine solution theory which predicts an LCST below the vapour–liquid critical temperature of the solvent (T_c). The interval between these two temperatures depends on differences in chain length and 'flexibility' of the polymer and solvent molecules. Predictions are tested for the following series of systems (with some omissions): polyisobutylene with the n-alkanes from C_5 to C_{16}; polydimethylsiloxane–oligomers of dimethylsiloxane from the 'dimer' to the 'pentamer'; polyethylene–C_6 to C_8. The ratio of the LCST to T_c increases with increasing length of the solvent molecule chain; systems with polydimethylsiloxane have their LCST near T_c due to the high flexibility of this polymer. A correlation of the LCST values can be made in terms of the theory.

A NUMBER of experimental investigations[1] have been made of the Lower Critical Solution Temperature (LCST) occurring in a polymer solution under its own vapour pressure as the solvent critical temperature is approached. In their studies of phase relations in systems under pressure, Ehrlich and Kurpen[2] have discussed the LCST and the general critical locus in P, T space. The existence of the LCST can be predicted[3] using a corresponding states theory of polymer solution thermodynamics[4, 5] due essentially to Prigogine *et al.* and which we use here to correlate LCST values found for a number of systems. This theory predicts the LCST through a new temperature dependence of the polymer–solvent interaction parameter χ_1. The pressure dependence of χ_1 can also be obtained and hence phase relations in systems under pressure can be interpreted; here, however, the discussion is limited to the LCST at small, usually negligible, pressures.

The χ_1 parameter is given by[5]

$$\chi_1 = -(U/RT)\,v^2 + (C_p/2R)\,\tau^2 \tag{1}$$

$$\tau = 1 - T_{0,1}/T_{0,2} \tag{2}$$

In equation (1), the first term is due to the interchange energy for forming contacts between polymer and solvent segments and to any difference in the sizes of these segments. This term is the analogue of the usual expression $\chi_1 = zwr_1/kT$ where r_1 is the number of segments in the solvent molecule. The second term gives the new 'structural' contribution arising from changes of free volume on mixing the dense polymer liquid with the expanded solvent. The T_0 are temperature reduction parameters of the solvent, component 1, and the polymer, component 2; v and τ are temperature-independent molecular parameters. The quantities U and C_p are the configurational energy and its temperature derivative, the

configurational heat capacity *of the solvent*. In what follows, all the thermo-dynamic quantities are configurational; no special indication of this is made in the nomenclature. The first term of equation (1) involving $-U/T$ is a positive decreasing function of T, while the structural term in C_p is positive and increasing, going to infinity at the solvent vapour–liquid critical point. Thus, χ_1 first decreases with T, then passes through a minimum and increases toward the LCST. This behaviour of χ_1 is consistent with the variation of polymer dimensions and second virial coefficient which has been observed[6] for two systems.

Two types of phase behaviour can be distinguished. First, if the minimum value of χ_1 is less than the critical value for phase separation, i.e. $\frac{1}{2}[1+(r_1/r_2)^{\frac{1}{2}}]^2$ using the Flory–Huggins combinatorial entropy approxi-mation, both an Upper Critical Solution Temperature (UCST) and an LCST exist, separated by a temperature range of complete miscibility. The struc-tural term of equation (1) is associated with the LCST which occurs at high temperatures, while the usual first term gives the UCST at low temper-atures. The LCST, like the UCST, should be associated with a θ-point at which $\chi_1 = \frac{1}{2}$ and $A_2 = 0$, and where the polymer again attains unperturbed dimensions. This seems to hold for the polyisobutylene (P.B)–*n*-pentane system[6].

The second case occurs if the minimum value of χ_1 is greater than the critical value, as for poor solvents. Then there is no region of complete miscibility, the low and high temperature regions of immiscibility having coalesced. Examples of this behaviour are easily found, e.g. high molecu-lar weight polyproylene oxide–isobutane[10]. For many systems with a solvent of intermediate quality, e.g. PIB–diethyl ether according to our preliminary measurements, a low molecular weight polymer gives the first type of behaviour and a high molecular weight one the second type.

At the LCST both the heat and entropy of dilution are negative. As emphasized by Rice[7] at a Faraday Society Discussion, the peculiarity of the negative $\Delta \overline{S_1}$ condition is such as to limit the occurrence of LCSTs in 'monomer' solutions to certain systems containing hydrogen bonds. This remark immediately followed one[8] calling attention to the present type of LCST, which is due to a negative volume of mixing, and which seems to occur quite generally for polymer solutions as the solvent approaches its vapour–liquid critical temperature. The unexpected negative heats and entropies of dilution have been found in polymer solutions at temperatures even well below the LCST, as for PIB–*n*-pentane[1b] at 32°C. It is evident from the variation of χ_1 in equation (1) that the structural term can give a negative value of $\kappa_1 (\Delta \overline{H_1})$ and $\psi_1 (\Delta \overline{S_1})$ if dC_p/dT is sufficiently positive, i.e. the temperature is sufficiently near the vapour–liquid critical point of the solvent.

COMPARISON OF LCST IN A SERIES OF SOLVENTS

A comparison between the LCSTs for different systems can be made using the law of corresponding states. This gives relations between thermodynamic quantities of all liquids which obey certain assumptions. One of the liquids

may be chosen as a reference liquid; in our case it is heptane, for which there exists a large body of thermodynamic data. Any quantity may also be related to a dimensionless reduced quantity through division by an appropriate reduction parameter. Thus for the molar C_p of the solvent,

$$C_p = Rc_1 C_p^* (T^*)$$ (3)

where

$$T^* = T/T_{0,1}$$ (4)

and a similar relation exists for $-U/T$ which has the same dimension. (Here the asterisk denotes a reduced quantity, this being the original nomenclature of Prigogine *et al.*; it is also used by Hijmans[9] and in our previous work. Refs. 4 and 10, however, use the asterisk to denote *reduction parameters* and a tilde for the reduced quantities.) R is the Gas Constant and and $3c_1$ the number of external degrees of freedom[4b] of the solvent molecule; c_1 increases linearly with r_1, and for different solvents of the same chain length, increases with the 'flexibility' of the molecule. As shown later, to a rather good approximation, T^* may be taken proportional to T/T_c where T_c is the vapour–liquid critical temperature. Equation (1) may be rewritten, using the reduced quantities,

$$\chi_1 = c_1 \left[-\frac{U^*(T^*)}{T^*} \nu^2 + \frac{C_p^*(T^*)}{2} \tau^2 \right]$$ (5)

or, in terms of the reference liquid,

$$\chi_1 = \frac{c_1}{Rc_R} \left[-(U/T)_R \nu^2 + \frac{(C_p)_R}{2} \tau^2 \right]$$ (6)

Here $(-U/T)_R$ and $(C_p)_R$ for the reference liquid must be determined at the same reduced temperature as the solvent, i.e. at a temperature chosen so that T/T_c is the same for the reference liquid as for the solvent, as explained below.

Dependence of parameters on solvent chain length

The parameter ν reflects differences in cohesive energy and size between segments of a chain-molecule solvent and of the polymer. Thus, a single value of ν characterizes a series of systems composed of a polymer and a series of homologous solvents which are chains of identical segments. Since c_1 and $c_1\nu^2$ increase linearly with solvent chain length, the first terms of equations (5) and (6) at constant T should also increase with r_1.

In the second or structural term, the parameter τ, reflecting the difference in reduced temperature between polymer and solvent, depends to some extent on the flexibilities and cohesive energies of polymer and solvent chains; this will be seen later to have an effect on the LCST of systems containing polydimethylsiloxane (PDS). However, τ is mainly a function of the difference in chain lengths between the two component molecules. Thus this parameter rapidly decreases with increasing chain length of the solvent tending to a small value. The product $c_1\tau^2$ should therefore decrease with increasing solvent chain length, but for very long solvent molecules reach

a minimum and then increase. At constant T^*, the structural terms in equations (5) and (6) should show the same behaviour.

Dependence of the critical solution temperatures on solvent chain length

This dependence follows from χ_1 having a constant critical value. Thus, setting a constant value for equation (5),

$$\frac{\mathrm{d}T^*}{\mathrm{d}r_1} = \frac{-(\partial\chi_1/\partial r_1)_{T^*}}{(\partial\chi_1/\partial T^*)_{r_1}} \tag{7}$$

The denominator of this expression is necessarily negative at the UCST and positive at the LCST. At the UCST, at low reduced temperatures, χ_1 is dominated by the first term, and hence from the above discussion, the numerator should be negative at the UCST. However, at the LCST, at high temperatures, the structural term is more important, and the numerator should be positive (except possibly for solvents whose molecules are very long chains). Thus, at both of the critical solution temperatures $\mathrm{d}T^*/\mathrm{d}r_1$ should be positive, or *the ratio of the critical solution temperature to the vapour–liquid critical temperature of the solvent should increase with increasing solvent chain length.* At the UCST this corresponds to the increasing incompatibility of a polymer with an increasingly polymeric solvent. In the Flory–Huggins theory this is expressed by the proportionality of χ_1 with r_1. At the LCST as the solvent chain length is increased, the structural term is decreased. Therefore C_p^* and T^* must be increased for χ_1 to reach the critical value. Hence with increasing r_1 the LCST should approach the vapour–liquid critical temperature, and this behaviour is found for the systems studied here. It is conceivable that for very long solvent molecules the LCST would again draw away from T_c, but the high temperatures involved would probably make observations impracticable.

PREDICTIONS ACCORDING TO A SIMPLE MODEL

LCSTs for a series of systems have been discussed[3] in terms of a simple particular form of the equation for χ_1

$$R\chi_1 = \frac{Ar_1}{T} + \frac{BT}{r_1} \tag{8}$$

and an application was made to the values of the LCST for the series of systems PIB–*n*-pentane to PIB–*n*-octane. In equation (8), A and B are molecular parameters characterizing the whole series of systems. This equation may be derived from equation (5) as follows. According to the smoothed potential cell model for liquids, U^* is a parabolic function of T^* at values of the reduced temperature not too near the critical point. Thus, C_p^* is a linear function of T^*, given by this model to be

$$C_p^* = 21T^* \tag{9}$$

The parameters T_0 for solvent and polymer are given by

$$T_0 = r\epsilon/kc \tag{10}$$

506

where ϵ is an energy characteristic of interactions between segments in the solvent or polymer homologous series. We put

$$3c = r + 3 \qquad (11)$$

This value[4b] of the number of external degrees of freedom assumes free rotation between the segments, and the choice of a segment must be made in consequence. Here a segment is chosen to contain two carbons of the principal chain, i.e. $r = (n+1)/2$. This assumption will be shown below to be remarkably good for the series PIB–n-alkanes. Using equations (2), (10) and (11) and putting $r_2 \longrightarrow \infty$ for the polymer,

$$\tau = 1/c_1 \qquad (12)$$

The structural term in equation (8) is obtained by substituting equations (9) and (12) into equation (5), then converting T^* to T using equation (10). The first term of equation (8) is found assuming $-U^*$ to be approximately independent of T^*, but proportional to the number of segments in the solvent molecule.

Using equation (8) it is predicted that both the UCST and LCST are proportional to the number of segments in the solvent molecule. This held[3] fairly well for the LCSTs[1a] of the series PIB–n-pentane to –n-octane which are much lower than the solvent critical temperatures. However, there appeared to be a trend for the LCST to drop below linearity with r_1 as the length of the alkane increased. The linear dependence of the LCST on r_1 is a consequence of the assumption of C_p^* linear in T^*. In fact, the cell models do predict that at higher T^*, C_p^* curves upward to infinity at a value of T^* corresponding to the solvent critical temperature. This increasingly rapid rise of C_p^* with T^* means that the increase of the LCST with r_1 should be less fast than the linear increase predicted by equation (8). This explanation, and the prediction that with increasing r_1 the LCST must approach T_c, seemed to warrant further experimental investigation.

EXPERIMENTAL AND RESULTS

The following series of systems were studied :
(1)   PIB–n-alkanes from C_5 to C_8, C_{10}, C_{12};
(2)   Polydimethylsiloxane (PDS)–same alkanes, plus C_{16};
(3)   PDS–oligomers of dimethylsiloxane from hexamethyldisiloxane (dimer) to dodecamethylpentasiloxane (pentamer); and
(4)   Polyethylene–n-alkanes from C_6 to C_8.

Materials

Two fractions of Enjay PIB obtained from a double fractionation were donated by Dr H. Daoust. The $\overline{M}_v$ were $7 \cdot 7 \times 10^4$ and $1 \cdot 9 \times 10^6$. Later a third fraction of $\overline{M}_w = 9 \times 10^6$ was obtained. Three fractions of Dow Corning 200 PDS of $\overline{M}_w = 1 \cdot 6$, $2 \cdot 4$ and $3 \cdot 9 \times 10^5$ were obtained following Crescenzi and Flory[11]. A series of fractions of high density polyethylene, GREX–60–

002E, were prepared by Dr R. H. Horowitz and furnished by W. R. Grace and Co. through the courtesy of Dr G. E. Ashby; three fractions of $\bar{M}_v = 4 \times 10^3$, $1 \cdot 2 \times 10^5$ and $4 \cdot 4 \times 10^5$ were used here.

The n-alkane solvents were either dried Phillips 'pure' grade (99 per cent pure) or Fluka materials of comparable purity. The silicone oligomers were given to us by Dr O. K. Johannson of Dow Corning Chemical Co., Midland and were fractionally distilled.

The first series of measurements concerned PIB with the n-alkanes from C_5 to C_{10}. A cell consisting of a ring of Teflon clamped between two glass windows contained about 1 ml of solution. The temperature was controlled using an oil bath for C_5 to C_8 and a small air thermostat for C_{10}. The temperature of phase separation, accompanied by a sharp onset of turbidity, was determined visually for four to six concentrations between 0·5 and 5 per cent for the fractions of $\bar{M}_v = 7 \cdot 7 \times 10^4$ and $1 \cdot 9 \times 10^6$. The precision of the results was $\pm 0 \cdot 2$ deg. C; the coexistence curve for all these systems was very flat varying by only about 2 deg. C throughout the range of concentrations. The LCSTs were taken to be the minima of the curves; they are given in *Table 1*, and are estimated to have an accuracy of ± 1 deg. C. Critical solution temperatures, however, may be sensitive to the molecular weight distribution of the polymer sample, and therefore we place importance only

Table 1. LCST and τ^2 parameters for the systems

No.	PIB–alkanes			PDS–alkanes		
	LCST (°C)	T/T_c	τ^2	LCST (°C)	T/T_c	τ^2
C_5	73	$0 \cdot 73_6$	0·250	180	0·96	0·085
C_6	129	$0 \cdot 79_1$	0·216	220	0·97	0·059
C_7	174	$0 \cdot 82_8$	0·189	255	0·97	0·040
C_8	212	$0 \cdot 85_1$	0·166	280	0·98	0·026
C_{10}	267	$0 \cdot 87_2$	0·135	330	0·98	0·011
C_{12}	312	$0 \cdot 89_5$	0·111	370	0·98	0·003
C_{16}	(±2)			435 (±5°)	0·98	0·00

No.	Polyethylene–alkanes			PDS–oligomers		
C_5				Si_2 221	0·95	0·059
C_6	133	0·79	0·187	Si_3 265	0·96	0·040
C_7	190	0·85	0·161	Si_4 308	0·97	0·028
C_8	209	0·85	0·138	Si_5 340	0·99	0·021
C_{10}	(±3°)			(±5°)		

on the relative values of the LCST. An extrapolation to infinite molecular weight may be made using the familiar plot of the reciprocal of the CST against $M^{-\frac{1}{2}}$. This is of course based upon a linear dependence of χ_1 upon T^{-1} and hence should not be valid if χ_1 is given by equation (1). In fact, assuming that it is the structural term in equation (5) which is important at high temperatures, one might suggest plotting the CST itself against $M^{-\frac{1}{2}}$. However, the CST for $M \longrightarrow \infty$ is independent, within one or two degrees, of the procedure used.

It was apparent that the flatness of the coexistence curves permitted a determination of the critical temperatures using a restricted number of

concentrations. Only two, 1 per cent and 3 per cent, were used for the remaining systems, and the temperatures of phase separation were determined in the following way. The solution, sealed in a glass tube of inner diameter 4 mm, was placed in a small oven whose temperature was read by a chromel–constantan thermocouple and recorded on the X axis of an X/Y potentiometric recorder. The calibration of the thermocouple was checked by determining the melting points of standard substances. The Y axis recorded the intensity of a beam of light traversing the oven and the cell, and whose sudden fall revealed the occurrence of phase separation. The rate of temperature rise in this region was about 0·2 deg. C/min. The tube could also be observed visually. The temperatures of phase separation could be reproduced without a trend toward higher temperature as would be caused by a degradation of the polymer. Degradation of the polyisobutylene and polyethylene was encountered above 320°C and 220°C respectively. Reproducibility with different tubes made up to the same concentration was ± 2 deg. C for the system containing PDS where the LCSTs are close to the solvent critical temperatures, and rather better for the other systems. The LCSTs for the different fractions were extrapolated to infinite molecular weight and the results are presented in *Table 1* together with the estimated accuracies which mainly reflect the difficulty of extrapolating to infinite molecular weight. The critical temperatures of the silicone oligomers were determined by observing the disappearance of the meniscus.

DISCUSSION

The results of *Table 1* confirm the speculation of the introduction. Thus, contrary to the prediction of equation (5), the LCSTs in each series of systems do not increase quite linearly with increase of solvent chain length. This undoubtedly reflects the upward curvature of C_p^* with T^* rather than the purely linear dependence assumed by equation (5). Furthermore, as expected, the ratio of the LCST to T_c increases with increase of solvent chain length.

We now interpret the results more quantitatively using equations (1) to (4) *but keeping only the structural term*. This should be an excellent approximation for all but the PDS–alkanes systems, and even there the LCST are so high as to greatly reduce the importance of the first term in equations (1) to (4). The most direct method would be to calculate τ^2 for each system, and use equation (1) to predict the LCST by setting $\chi_1 = \frac{1}{2}$, whence

$$C_p(\text{LCST})/R = 1/\tau^2 \tag{13}$$

In such a procedure, however, the value of the LCST is very sensitive to errors in the calculation, and poor results are obtained. Instead, we first test the corresponding states principle by using equation (6), keeping only the structural term, and writing

$$R/(C_p)_R = \tau^2 c_1/c_R \tag{14}$$

[The inversion is made since $(C_p)_R$ tends to infinity.] The RHS may be calculated for each system whence values of $R/(C_p)_R$ are found at the

various LCSTs. These LCSTs correspond to reduced temperatures which to a good approximation are proportional to T/T_c as found in *Table 1*. If the corresponding states principle is valid, $R/(C_p)_R$ calculated from equation (14) should give a single curve when plotted against T/T_c.

Determination of T_0 *and* τ

Solvents—We wish to tabulate $T_0/(T_0)_R$ for solvents and polymers whence τ may be obtained through equation (2).

(1) Simha and Havlik[12] have shown that V (T) data for the *n*-alkanes from methane to polyethylene and polymethylene and for the silicones from the trimer to hexamer all obey the corresponding states law. They obtain *absolute values* of T_0 by using various models of the polymeric liquid state. These values therefore depend on the validity of the model chosen; however, the *ratio* $T_0/(T_0)_R$ is purely empirical and independent of the model. Equations (9) and (13) of ref. 12 may be used to obtain values of this ratio for the alkane and silicone solvents, the reference liquid being heptane.

(2) Hijmans[9] has performed a similar analysis for the alkanes leading to values of $T_0/(T_0)_R$.

(3) $T_0/(T_0)_R$ may be obtained as described[5] from a knowledge of αT of polymers and solvents at any temperature and αT of the reference heptane over a wide temperature range. (α is the thermal expansion coefficient $= v^{-1} \, dv/dt$, with v the specific volume.) For αT of heptane, we differentiated a curve of V^* (T^*) established using[13] American Petroleum Institute data for heptane and also V (T) data for other alkanes; some 200 data were reduced to fall on the same curve. For α of the *n*-alkanes C_5 to C_{11}, C_{13} and C_{16} we used new measurements by McGlashan *et al.*[14] at 20°C; for the silicone trimer, tetramer and pentamer V (T) data[15] at 20°C were used. The corresponding datum for the dimer, stated to be inaccurate, gives an α value which is obviously too low compared with those of the other oligomers, while another value[16] of α at 20°C appears too high.

(4) McGlashan has analysed his α and isothermal compressibility (β) data for the above-mentioned alkanes in terms of the corresponding states law obtaining values of $T_0/(T_0)_R$.

All of these four sources give $T_0/(T_0)_R$ to within at most two per cent and in *Table 2* we give the results following source (1), i.e. ref. 12. If equations (10) and (11) are used, one again obtains excellent values of $T_0/(T_0)_R$ which are only one to two per cent different from the others. The choice of an effective segment to contain two principal chain carbons seems to have been very good for the alkanes.

For the silicone trimer to pentamer, sources (1) and (3) were used and give essentially identical results; those given in *Table 2* are from ref. 12 which we also used for the value of the dimer.

Another possible method suggests itself. If the corresponding states theory were to hold rigorously, the vapour–liquid critical temperatures should correspond to the same reduced temperature for all the solvents, and T/T_c of any solvent would thus be proportional to its reduced temperature, or $T_0/(T_0)_R = T_c/(T_c)_R$. *Table 2* also shows the ratios obtained by this method. It is clear that as the solvent chain length increases, the values

obtained at high T, and therefore at low density of the liquid, deviate from those found at lower T and higher density found through the use of V (T). The following argument may explain the discrepancy. The number of external degrees of freedom of any molecule, no matter how long, is 3 for the perfect gas state, as compared with $3c$ for the liquid. The same principle of corresponding states cannot therefore hold for both liquid and gas states; we might expect that at the critical point c will have fallen below its value for a high density liquid and hence T_0, inversely proportional to c, will be

Table 2. Reduction parameters for polymers and solvents

	$T_{0,1}/(T_0)_R$	$T_{0,1}/(T_0)_R$ from T_c	c_1/c_R
C_5	0·89	0·87	0·86
C_6	0·95	0·94	0·92
C_7	1·00	1·00	1·00
C_8	1·05	1·05	1·08
C_{10}	1·12	1·15	1·26
C_{12}	1·18	1·22	1·44
C_{16}	1·27	1·34	1·85
Si_2	0·95	0·97	1·09
Si_3	1·00	1·04	1·54
Si_4	1·04	1·11	1·90
Si_5	1·07	1·15	2·14
PDS	1·23		
Polyethylene	1·67		
PIB	1·77		
Polystyrene	1·98		

larger. The increase must be relatively greater the longer the alkane and hence the larger the c in the liquid state. Nevertheless to a rather good approximation T/T_c is a measure of the reduced temperature of the solvent.

Polymers

PDS—Ref. 16 gives $\alpha = 9 \cdot 0 \times 10^{-4}$/deg. at 20°C for a molecular weight of 15 000. Applying the procedure (3) above we obtain $T_0/(T_0)_R = 1 \cdot 25$, whereas using equation (13) of ref. 12, putting $n \longrightarrow \infty$, gives $T_0/(T_0)_R = 1 \cdot 23$.

Polyethylene—A number of dilatometric studies of polyethylene agree that[17] $dv/dT = 9 \cdot 0 \times 10^{-4}$ ml/g deg. C in the temperature range 115° to 175°C. Taking this value to be valid at 145°C gives $T/(T_0)_R = 1 \cdot 67$. Equation (9) of ref. 12 with $n \longrightarrow \infty$ gives a value of 1·66 for polymethylene.

Polystyrene—Here[18], $dv/dT = 5 \cdot 5 \times 10^{-4}$ ml/g deg. or $\alpha = 5 \cdot 6 \times 10^{-4}$/deg. above the glass transition in a region centred around 130°C. Using procedure (3) above we obtain $T_0/(T_0)_R = 1 \cdot 91$. Using equation (13) of ref. 2 we find $T_0/(T_0)_R = 1 \cdot 98$.

Polyisobutylene—Ref. 18 gives values of dv/dT for a number of low molecular weight homologues of PIB at 30°C. The data extrapolated for an infinite molecular weight give $dv/dT = 6 \cdot 0 \times 10^{-4}$ ml/g deg. and $v = 1 \cdot 131$ ml/g, giving $T_0/(T_0)_R = 1 \cdot 77$. On the other hand a value of 2·0 is found using[19] $dv/dT = 6 \cdot 8 \times 10^{-4}$ ml/g deg. at 217°C. We have discarded this latter value which indicated that PIB is more cohesive and/or less flexible than polystyrene.

Equations (10) and (11) give a value of $T_0/(T_0)_R = 1.75$, which corresponds very closely to the value of 1·77 found above for PIB, but less so to the value for polyethylene with which it might have been expected to agree.

It is of interest that the series of polymers in order of increasing $T_0/(T_0)_R$ values is PDS, polyethylene, PIB and polystyrene. The same series is obtained from a consideration of the polymer chain dimensions placing the polymers in order of increasing values[20] of $\sigma = (\overline{L_0^2}/\overline{L_{0,\,\text{free}}^2})^{\frac{1}{2}}$ as follows: PDS, 1·47; polyethylene, 1·63; PIB, 1·80; polystyrene, 2·22. This seems reasonable since both T_0 and σ should increase with increasing polymer rigidity.

The values of $T_0/(T_0)_R$ of the polymers appear to give a qualitative interpretation of the relative solubilities encountered here. Due to its high flexibility and low cohesive energy, PDS has a value of T_0 close to those of the solvents. Hence the structural terms of systems containing PDS will be relatively small, as indicated by the values of τ^2 shown in *Table 1*. The PDS is therefore soluble in the solvents used here up to a temperature very close to the critical point.

Determination of c_1/c_R

Values of c_1/c_R have been found by McGlashan[14] for C_5 to C_{11}, C_{13} and C_{16}, by applying the corresponding states principle to thermal expansion coefficient and compressibility data obtained from 10° to 50°C. The values are used for *Table 2* together with interpolated values for C_{12} and C_{14}. Hijmans[9] has also determined these quantities using configurational energy data to obtain energy reduction parameters which, coupled with T_0 data, give the required c_1/c_R. These values gradually diverge from those of ref. 14, but even at C_{16} are only 15 per cent below. c_1/c_R may also be determined by a method similar to that used for $T_0/(T_0)_R$. One must have a knowledge of a quantity of dimensions of entropy over a wide temperature range for the reference heptane and at a single temperature for the solvent. A convenient quantity is $C_p - C_v = \alpha^2 VT/\beta$. *Figure 1* (curve a) shows a plot of $R\beta/\alpha^2 VT$ for heptane as a function of T/T_c using data reworked and compiled by Rowlinson[21a]. For the *n*-alkanes C_5 to C_{11}, C_{13} and C_{16}, α and β values at 50°C of McGlashan[14] were used. The ratio of $(R\beta/\alpha^2 VT)_R/(R\beta/\alpha^2 VT)$, obtained at equal values of T/T_c for the two liquids is equal to c_1/c_R. Values obtained in this way were almost identical to those given by McGlashan using the corresponding states principle and the data at all the other temperatures. This method was used to obtain c_1/c_R for the silicones. Compressibility data[22] at 30°C were used, together with data for α from ref. 15 for the trimer to pentamer and for the dimer a value of α calculated from the corresponding states relation of $V(T)$ given by ref. 12.

Correspondence of LCST values

Following equation (14) values of $\tau^2 c_1/c_R$ were calculated from the tabulated data, and are shown in *Figure 1* plotted against the ratio of the LCST to the vapour–liquid critical temperature of the solvent. It seems that the corresponding states principle is obeyed fairly well and that a single curve is found for $R/(C_p)_R$ which goes to zero as $T/T_c \longrightarrow 1$, as required.

Values of C_p for heptane have been calculated from the heat capacities of the gas and liquid phases. They are used here to plot curve b in *Figure 1*. Although the values are limited to lower temperatures, a fair idea of the form of the curve can be obtained since $R/(C_p)_R \rightarrow 0$ as $T/T_c \rightarrow 1$. It
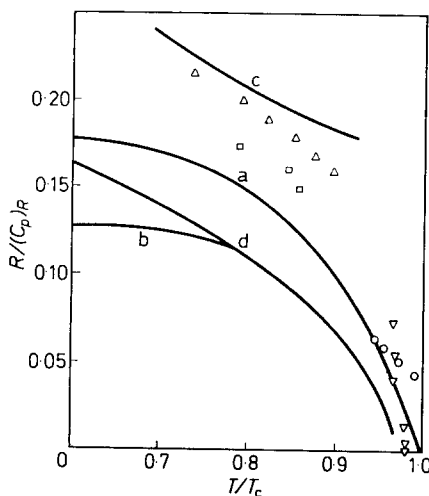
Figure 1—Correlation of LCST values: $\tau^2 c_1/c_R$ against T/T_c for △ PIB–alkanes, ▽ PDS–alkanes, □ polyethylene–alkanes, ○ PDS–oligomers. $R\beta/\alpha^2 VT$ for heptane versus T/T_c, curve a; $R/(c_p)_R$ for heptane using respectively, experimental heat capacities, curve b; equation (9), curve c; and equation (17), curve d

seems that although $\tau^2 c_1/c_R$ has the correct form, the magnitude would have to be decreased by a factor of $\sim 1\cdot5$ to obtain coincidence with the function $R/(C_p)_R$ calculated from the heptane data. This difference could be explained if the critical value of χ_1 were to lie above $\frac{1}{2}$, as indicated by the Huggins–Miller–Guggenheim approximation for the combinatorial free energy. In that approximation[3]

$$\chi_{1c} = \frac{zW}{kT} = \frac{1}{2}\left(\frac{z}{z-2}\right) \tag{15}$$

Making this change, $\tau^2 c_1/c_R (1-2/z)$ would now correspond to $R/(C_p)_R$. By putting $z=6$, instead of letting $z \rightarrow \infty$ with the Flory approximation, the discrepancy would be explained.

On the other hand, a very similar discrepancy was found in calculating excess quantities for mixtures of n-alkanes[13]. A positive 'experimental' value for the non-combinatorial part of the excess free energy was obtained from the experimental values of G^E using the Huggins–Miller–Guggenheim approximation for the combinatorial part of G^E. The theoretical value of the non-combinatorial G^E calculated using C_p and the corresponding states principle is positive but too large by a factor of about two, much as in the present case. However, for the alkane mixtures, if the value of z is lowered the calculated combinatorial G^E which is negative, approaches zero, so that the non-combinatorial part of G^E, obtained by subtraction from the experimental G^E, is even further reduced, increasing the discrepancy. We are inclined to believe that in the present case, as well as for the alkanes, the error does not lie in the combinatorial approximation used, but in the

corresponding states calculation of the non-combinatorial free energy or the parameter χ_1.

We should note in this connection that the assumption of a single average reduced temperature for the mixture corresponds to a completely random mixture. For mixtures of quasi-spherical molecules of different sizes, values of G^E calculated on this basis are usually considerably too large, as discussed by Prigogine, Brown and Scott, who have developed refinements to allow for ordering in the mixture[21b]. We shall return to the question of the discrepancy after discussing the use of models in interpreting the LCST data.

Use of models for the liquid state

The introduction has mentioned the use of a model to obtain equation (8) for χ_1. There, the equations (10) and (11) gave r and c, and the last section shows that this assumption is justified by the remarkably good values of $T_0/(T_0)_R$ and c/c_R obtained. A value of the parameter $B = 8\cdot2 \times 10^{-3}$ cal/deg^2 was found[3] to fit the LCST values for PIB–C$_5$ to C$_8$. Using this value of B and equation (9) for C_p we have drawn $R/(C_p)_R$ for heptane as curve c in *Figure 1*. Since the value of B was chosen for a fit we find good agreement between the curve and $\tau^2 c_1/c_R$ for the above systems. The slight difference is due to ref. 3 taking into account a small value of the parameter A in equation (8); one sees that the parameter A, if small, makes little difference to the LCST results. However, for the longer alkane solvents it is evident that $R/(C_p)_R$ deviates from $\tau^2 c_1/c_R$, as indicated in the introduction, due to the inadequacy of the linear dependence of C_p on T assumed in equation (8).

In our present treatment, we required values of αT, $\alpha^2 VT/\beta$ and C_p for the reference liquid over a wide temperature range. A reliable model of the polymeric liquid could be used to calculate the required thermodynamic properties and thus render the reference liquid unnecessary. Prigogine *et al.* have discussed cell models in the smoothed potential and harmonic potential approximations. They have given particular attention to the simpler smoothed potential model using the well known cell partition function, equal to the free volume, as introduced by Eyring and Hirschfelder[28]. The configurational energy of the liquid is assumed to depend on the volume in a way which is appropriate to the 6–12 intermolecular potential, rather than taking the van der Waals type of dependence of energy on volume as originally used by Eyring and Hirschfelder, i.e.

$$U^* = -(V^*)^{-1} \tag{16}$$

Flory *et al.*[10] have recently developed the Prigogine theory using equation (16) which they suggest compensates for the over-estimation of molecular order inherent in the cell model. They derive an expression (contained in their equation 26), which may be found from the present general equation (3) by putting

$$C_p^* = \left[\frac{4}{3}\left(V^*\right)^{-1/3} - 1 \right]^{-1} \tag{17}$$

514

This is the reduced heat capacity at constant zero pressure in the Eyring–Hirschfelder model.

In the smoothed potential models, the cell partition function depends only on volume and the configurational energy is independent of T at constant volume. Thus, the configurational C_v is zero, so that

$$C_p = \alpha^2 VT / \beta \tag{18}$$

and

$$\chi_1 = \alpha^2 VT\tau^2 / 2\beta R \tag{19}$$

if only the structural term is kept.

Thus, $(C_p)_R$ calculated using such a model should yield the curve a rather than b in *Figure 1*. In *Figure 1* we show $R/(C_p)_R$ calculated from equation (17) with reduction parameters determined at 20°C from values of α, β and V at this temperature, by using the procedure given in ref. 10. Values of $R/(C_p)_R$ at higher temperatures were not calculated since equation (17) requires some modification because of the finite pressure. The model gives quite good agreement with the curve a established from literature values. Ref. 10 allows reduction parameters which vary with the temperature and which are to be calculated from experimental α, β and V data at each temperature. In this case of course $R/(C_p)_R$ would follow curve b exactly and χ_1 would be given by equation (19).

The nearness of $\tau^2\, c_1/c_R$ to $\beta R/\alpha^2 VT$ suggests that equation (19) for χ_1 may be more accurate than using C_p itself. The corresponding states treatment relates changes of thermodynamic functions occurring during the mixing process to changes of reduced temperature and finally to changes with T of thermodynamic quantities of the reference liquid. If the changes of thermodynamic quantities on mixing are only due to changes in reduced volume, then a change of the quantities with T when the volume is constant should possibly be ignored. The better agreement with experiment found by leaving C_v out of C_p and the expression for χ_1 might be justified in this way.

Centre de recherches sur les macromolécules,
  Strasbourg, France
Université de Montréal,
  Montréal, Canada

REFERENCES

[1a] FREEMAN, P. I. and ROWLINSON, J. S. *Polymer, Lond.* 1959, **1**, 20; [b] BAKER, C. H., BROWN, W. B., GEE, G., ROWLINSON, J. S., STUBLEY, D. and YEADON, R. E. *Polymer, Lond.* 1962, **3**, 215; [c] ALLEN, G. and BAKER, C. H. *Polymer, Lond.* 1965, **6**, 181; [d] KINSINGER, J. B. and BALLARD, L. E. *J. Polym. Sci. B,* 1964, **2**, 879

[2] EHRLICH, P. and KURPEN, J. J. *J. Polym. Sci. A,* 1963, **1**, 3217; EHRLICH, P. *J. Polym. Sci. A,* 1965, **3**, 131

[3] DELMAS, G., PATTERSON, D. and SOMCYNSKY, T. *J. Polym. Sci.* 1962, **57**, 79

[4a] PRIGOGINE, I. (with the collaboration of BELLEMANS, A. and MATHOT, V.). *The Molecular Theory of Solutions*, Ch. 16 and 17. North Holland: Amsterdam, 1957; [b] *ibid*, p 328; [c] *ibid*, p 130

[5] PATTERSON, D. *International Symposium on Macromolecular Chemistry, Prague 1965.* Preprint A566. International Union of Pure and Applied Chemistry

[6] DELMAS, G. and PATTERSON, D. *Polymer, Lond.* 1966, **7**, 513

[7] RICE, O. K. *Disc. Faraday Soc.* 1953, **15**, 276

[8] KLINKENBERG, A. *Disc. Faraday Soc.* 1953, **15**, 276

[9] HIJMANS, J. *Physica, 's Grav.* 1962, **27**, 433

[10] FLORY, P. J., ORWOLL, R. A. and VRIJ, A. *J. Amer. chem. Soc.* 1964, **86**, 3515

[11] CRESCENZI, V. and FLORY, P. J. *J. Amer. chem. Soc.* 1964, **86**, 41

[12] SIMHA, R. and HAVLIK, A. J. *J. Amer. chem. Soc.* 1964, **86**, 197

[13] BHATTACHARYYA, S. N., PATTERSON, D. and SOMCYSNKY, T. *Physica, 's Grav.* 1964, **30**, 1276

[14] McGLASHAN, M. L. Unpublished work

[15] HURD, C. B. *J. Amer. chem. Soc.* 1946, **68**, 364

[16] ALLEN, G., GEE, G. and WILSON, G. J. *Polymer, Lond.* 1960, **1**, 456

[17] GUBLER, M. G. and KOVACS, A. J. *J. Polym. Sci.* 1959, **34**, 551

[18] FOX, T. G and LOSHAEK, S. *J. Polym. Sci.* 1955, **15**, 379

[19] FOX, T. G and FLORY, P. J. *J. Polym. Sci.* 1954, **14**, 315

[20] KURATA, M. and STOCKMAYER, W. H. *Fortschr. Hochpolymforsch.* 1963, **3**, 240, 261

[21a] ROWLINSON, J. S. *Liquids and Liquid Mixtures*, p 37. Butterworths: London, 1959; [b] *ibid*. Ch. 9

[22] WEISSLER, A. *J. Amer. chem. Soc.* 1949, **71**, 93

[23] EYRING, H. and HIRSCHFELDER, J. *J. phys. Chem.* 1937, **41**, 249

Limiting Viscosity Number versus Molecular Weight Relations for Polydecamethylene Oxide

Kazuhiko Yamamoto and Hiroshi Fujita

Relations between $[\eta]$ and $\overline{M}_w$ for the tenth member of the series of poly-ethers $[-O-(CH_2)_m-]_n$, i.e. polydecamethylene oxide, were determined in benzene at 35°C and in chloroform at 30°C. Here $[\eta]$ is the limiting viscosity number and $\overline{M}_w$ is the weight-average molecular weight of the polymer. Analysis of the data in terms of the Stockmayer–Fixman plot, with the value of $2 \cdot 5 \times 10^{21}$ being assumed for the Flory constant Φ, yielded a value of $1 \cdot 7_2$ for the conformational parameter σ of this polyether. It was found that this value of σ is well consistent with the linear relation between $[\eta]$ and $(m-1)/(m+1)$ which had been proposed in our previous paper on poly-hexamethylene oxide.

THE present study is concerned with the evaluation of the conformational parameter σ for the tenth member of the series of polyethers having the general structure $[-O-(CH_2)_m-]_n$. It mainly purports to supplement the relation between σ and m that has been derived in our previous paper[1] from the σ values then available for the lower members of this series[2-6] and for polyethylene[7].

EXPERIMENTAL

Polymer

The monomer *n*-decamethylene glycol was extracted by repeated re-crystallization from a commercial product dissolved in a 90 : 10 (by weight) mixture of ethylene dichloride and ethanol, b.pt 72·5°C. Its elemental analysis gave 68·85 per cent for carbon and 12·72 per cent for hydrogen (theoretical, 68·9₁ per cent for carbon and 12·7₃ per cent for hydrogen). Absence of isomers other than the normal form was checked by its i.r. spectrum.

Polymerization was carried out in a reaction tube designed by Lal[8]. About 10 g of the purified monomer, 0·2 to 0·3 g of concentrated sulphuric acid, and 0·1 g of boron-trifluoride ether complex were mixed in the reaction tube and heated for three hours at the boiling point of ethylene glycol under a constant stream of dry nitrogen. The mixture was further heated at the same temperature and for a similar period, this time with the tube being evacuated to a pressure lower than 1 mm of mercury. The product was dissolved in hot ethanol, and precipitated by allowing the solution to stand at room temperature. The dark-brown precipitate was dissolved in hot *n*-butanol, filtered with active charcoal, and the filtrate was cooled to about 20°C. The precipitate formed, now white in colour, was freeze-dried from a benzene solution. The sample of polydecamethylene oxide thus obtained was separated into a number of fractions by successive precipitation with

benzene as solvent and methanol as non-solvent. Eight fractions, numbered 1002, 1003, . . . , 1009 in *Table 1*, were chosen for the present study. No success was achieved in obtaining a polymer sample of a higher molecular weight than those of the fractions indicated in *Table 1*. The trimer tri-decane-1-10 diol, which is numbered 1001 in *Table 1*, was synthesized by the method of Hobin[9]. Its purity was checked by i.r. analysis and by elemental analysis [74·1 per cent for carbon and 12·7 per cent for hydrogen (theoretical, 74·0 per cent for carbon and 12·9 per cent for hydrogen)].

Table 1. Summary of numerical results obtained

Sample No.	$\overline{M}_w \times 10^{-3}$	$A_2' \times 10^3$ (mole ml/g^2) (chloroform, 25°C)	$\overline{M}_n \times 10^{-3}$	$A_2 \times 10^3$ (mole ml/g^2) (chloroform, 37°C)
1001 (trimer)			0·48$_8$	
1002	1·5$_7$		1·5$_5$	2·7
1003	2·0$_9$		1·8$_3$	3·2
1004	2·5$_4$		2·1$_4$	4·5
1005	2·8$_6$		2·3$_9$	5·0
1006	3·3$_6$		2·7$_8$	3·9
1007	3·9$_1$	4·1	3·3$_1$	4·7
1008	6·4$_9$			
1009	8·2$_6$	4·4	3·7$_0$	3·6

Sample No.	$[\eta]$ (dl/g) (chloroform, 30°C)	k'	$[\eta]$ (dl/g) (benzene, 35°C)	k'	$\bar{v}$ (ml/g) (chloroform, 25°C)
1001	0·051$_9$	0·78			
1002	0·11$_8$	0·49	0·099$_6$	0·34	1·082
1003	0·13$_8$	0·41			
1004	0·14$_5$	0·37	0·11$_7$	0·42	1·085
1005	0·15$_1$	0·36	0·13$_5$	0·56	1·084
1006	0·17$_1$	0·34	0·140	0·44	1·082
1007	0·19$_6$	0·38	0·15$_6$	0·38	1·082
1008	0·23$_4$	0·33	0·19$_7$	0·32	1·078
1009	0·29$_7$	0·36	0·25$_0$	0·35	1·078

Solvent

Benzene and chloroform were used as the solvents for viscosity measurements, while the molecular weight determinations were made with chloroform as solvent. These were fractionally distilled before use.

Molecular weight determinations

The number-average molecular weight $\overline{M}_n$ of each sample (including the trimer) was determined osmotically at 37°C by using a Mechrolab 301A vapour pressure osmometer, with chloroform as solvent. The measurements were made on all fractions except fraction 1008. For each sample, the plot of π/RTc versus c was linear and had a positive slope over the range of c examined. Here π is the osmotic pressure, R is the gas constant, T is the absolute temperature, and c is the solute concentration (in g/dl) in a given solution.

The weight-average molecular weights $\overline{M}_w$ for all samples except the trimer were determined by the sedimentation equilibrium method. The measurements were made at 25°C with chloroform as solvent. In this solvent, the polydecamethylene oxide samples studied all floated toward the meniscus of the solution when the cell was rotated in the centrifuge. Thus we actually concerned ourselves with a flotation, rather than sedimentation, equilibrium. The technique and apparatus used for obtaining the necessary data were the same as used in our previous study on polyhexamethylene oxide[1]. The experiments were made at four initial concentrations c_0 for fraction 1009, at two c_0 for fraction 1007, and at one c_0 (0·3 to 0·4 g/dl) for all other fractions. The plots of $1/M_{app}$ versus $\bar{c}$ obtained with fractions 1007 and 1009 are illustrated in *Figure 1*. Here M_{app} denotes the apparent

Figure 1—Sedimentation equilibrium data on polydecamethylene oxide samples 1009, O, and 1007, ●, in chloroform at 25°C; M_{app} is the apparent weight-average molecular weight and $\bar{c}$ is the arithmetic mean of the equilibrium solute concentrations at the ends of the solution column in the cell
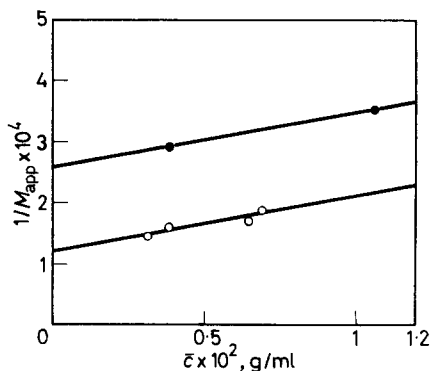
weight-average molecular weight calculated in the usual way[10] from the concentration distribution at sedimentation equilibrium, and $\bar{c}$ is the arithmetic mean of the equilibrium concentrations at the ends of the solution column. When analysed in terms of the well-known equation[10]

$$1/M_{app} = 1/\overline{M}_w + 2A_2'\bar{c} + O(\bar{c}^2) \tag{1}$$

where A_2' is the light-scattering second virial coefficient, these plots yield $4·1 \times 10^{-3}$ (ml mole/g²) for A_2' of fraction 1007 and $4·4 \times 10^{-3}$ (ml mole/g²) for A_2' of fraction 1009. These values are in fair agreement with the values of A_2 (osmotic second virial coefficient) obtained from the osmotic pressure measurements (see *Table 1*). We therefore assumed a constant value $4·1 \times 10^{-3}$ for A_2' of all other fractions in chloroform at 25°C, and calculated their $\overline{M}_w$ by substituting the measured values of M_{app} and $\bar{c}$ into equation (1).

The partial specific volumes $\bar{v}$ of these samples in choloroform at 25°C decreased slightly with increasing $\overline{M}_w$ (see *Table 1*), but the variation was hardly more than the experimental uncertainty, so that a value of 1·082 (ml/g) was chosen as a suitable mean value of the observed data and used for all calculations of M_{app}. The specific refractive index increment, measured on fraction 1007 in chloroform at 25°C, was 0·0357 ml/g, and this value was used for the calculation of M_{app} for all other fractions.
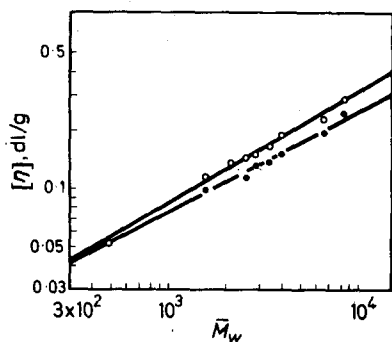
Figure 2—Double logarithmic plots of limiting viscosity number [η] against weight-average molecular weight $\overline{M}_w$ for polydecamethylene oxide in chloroform at 30°C, O, and in benzene at 35°C, ●

Viscosity measurement

The viscosity data were obtained in chloroform at 30°C and in benzene at 35°C, using a capillary viscometer of the Ubbelohde type which had a flow time of 380·0 sec for benzene at 35°C. The limiting viscosity number [η] was determined as a common intercept of the following three plots: η_{sp}/c versus c, η_{sp}/c versus η_{sp}, and (ln η_{rel})/c versus c, where η_{sp} is the specific viscosity, η_{rel} is the relative viscosity, and c is the polymer concentration in g/dl. The Huggins slope parameter k' was evaluated from the slope of the plot for η_{sp}/c as a function of η_{sp}.

RESULTS AND DISCUSSION

Table 1 summarizes all the experimental data obtained. It can be noticed that, except for the highest molecular weight fraction, each fraction was fairly homogeneous with respect to molecular weight when viewed in terms of the ratio of $\overline{M}_w$ to $\overline{M}_n$.

The conventional double logarithmic plot of [η] versus $\overline{M}_w$ constructed from the data given in *Table 1* is shown in *Figure 2*. The solid lines drawn in the figure yield the following Mark–Houwink–Sakurada equations:

$$[\eta] = 1·7_2 \times 10^{-3}\overline{M}_w^{0·56} \text{ (in chloroform at 30°C)} \tag{2}$$

$$[\eta] = 1·9_5 \times 10^{-3}\overline{M}_w^{0·53} \text{ (in benzene at 35°C)} \tag{3}$$

Figure 3—Stockmayer–Fixman plots for polydecamethylene oxide in chloroform at 30°C, O, and in benzene at 35°C, ●
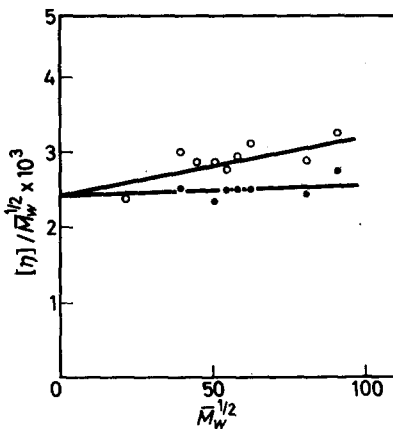
Figure 4—Linear relation between conformational parameter σ and $(m-1)/(m+1)$ for polyethers having the general structure $[\text{—O—(CH}_2)_m\text{—}]_n$
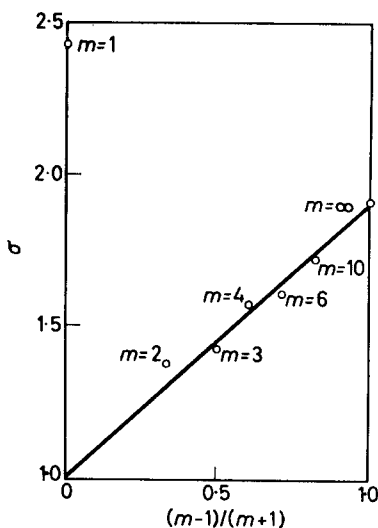
If the data of *Table 1* are treated in terms of the Stockmayer–Fixman method[11], the results shown in *Figure 3* are obtained. Each set of the plotted points may be fitted by a straight line as indicated, and a value of $2.4_0 \times 10^{-3}$ (dl mole/g$^{2/3}$) is deduced for the so-called K value[1] from the common ordinate intercept of the indicated two lines. Assuming as before a value of 2.5×10^{21} for Flory's Φ constant, this K value yields 1.7_2 for the conformational parameter σ of polydecamethylene oxide (at room temperature).

The previously proposed linear relation[1] between σ and $(m-1)/(m+1)$ for polyethers $[\text{—O—(CH}_2)_m\text{—}]_n$ now can be supplemented by this result for $m = 10$, and we obtain *Figure 4*. It is seen that the new datum
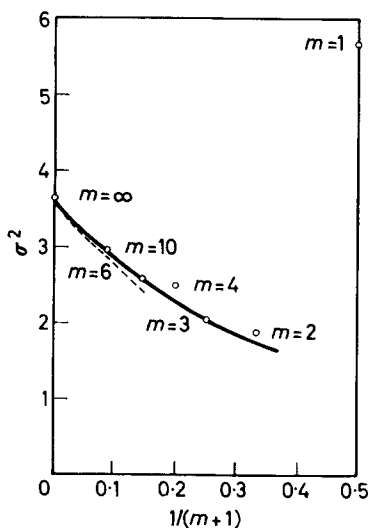
Figure 5—Correlation between σ^2 and $1/(m+1)$ for polyethers having the general structure $[\text{—O—(CH}_2)_m\text{—}]_n$

strengthens the validity of the linear variation of σ with the relative population of CH_2—CH_2 bonds in the polyether chain.

According to the current statistical theory of polymer chains, the quantity that is most directly derived from the theoretical calculation is the statistical average of the square of the end-to-end distance of a polymer chain and hence the square of its conformational parameter σ. This fact implies, in the present case, that a plot of σ^2, not of σ itself, as a function of a suitable structure parameter for the polyether, such as m, is more readily amenable to the theoretical interpretation. *Figure 5* shows one of such plots, where the values of σ^2 are plotted against the relative population of the oxygen atoms in each polyether chain, $1/(m+1)$. We have prepared this plot with the anticipation that the introduction of the ether linkages (at a regular interval) into the polyethylene chain would cause a change in σ^2 proportional to the number density of such linkages in the chain, at least in the region of small values of this density. It is expected that the factor for this proportionality, i.e. the slope of the dashed initial tangent to the solid line shown in *Figure 5*, provides quantitative information on how the internal rotation of the CH_2—CH_2 bond is affected by the presence of the CH_2—O bond in the same chain. Theoretical work concerning this problem is being carried out in this laboratory.

We wish to thank Dr A. Teramoto of this laboratory for his interest in this study.

Department of Polymer Science,
  Osaka University, Toyonaka, Japan

REFERENCES

[1] YAMAMOTO, K. and FUJITA, H. *Polymer, Lond.* 1966, **7**, 557
[2] STOCKMAYER, W. H. and CHAN, L.-L. *J. Polym. Sci. A*, 1966, **2**, 437
[3] SADRON, C. and REMPP, P. *J. Polym. Sci.* 1958, **29**, 127
  ROSSI, C. and MAGNASCO, N. *J. Polym. Sci.* 1962, **58**, 977
[4] KURATA, M. and STOCKMAYER, W. H. *Fortschr. Hochpolym.Forsch.* 1963, **3**, 196
[5] YAMAMOTO, K., TERAMOTO, A. and FUJITA, H. *Polymer, Lond.* 1966, **7**, 267
[6] KURATA, M., UTIYAMA, H. and KAMADA, K. *Makromol. Chem.* 1965, **88**, 281
[7] CHIANG, R. J. *J. phys. Chem.* 1965, **65**, 1645
[8] LAL, J. *J. Polym. Sci.* 1961, **50**, 13
[9] HOBIN, T. P. *Polymer, Lond.* 1965, **6**, 403
[10] FUJITA, H. *Mathematical Theory of Sedimentation Analysis*, Ch. V. Academic Press: New York and London, 1962
[11] STOCKMAYER, W. H. and FIXMAN, M. *J. Polym. Sci. C*, 1963, **1**, 137

Direct Examination of Polymer Degradation by Gas Chromatography II—Development of the Technique for Quantitative Kinetic Studies

A. Barlow*, R. S. Lehrle, J. C. Robb and D. Sunderland†

The following difficulties may be encountered when direct-pyrolysis gas chromatography is aplied to obtain quantitative kinetic measurements: (a) poor reproducibility of the measurements, arising from the method of mounting the sample, (b) time and temperature errors, arising principally from the pre-effect of the temperature/time profile of the filament, and (c) dependence of the observed degradation rate on sample thickness, even for samples in the microgramme range.

The first two problems have been surmounted by depositing the sample within a limited region of a ribbon filament, and supplying an initial current boost to bring the filament to the desired degradation temperature within one second. If in addition the degradation is effected in the carrier-gas stream of a capillary column GLC apparatus incorporating a detector sensitive to better than 10^{-10}g, the pyrolysis may be studied under conditions where the rate becomes independent of sample thickness; i.e. 5×10^{-8}g samples, 200 Å thick.

The requirements of the technique and the choice of operating conditions are described. The principal advantages of the method are that only sub-micro samples are required, and that quantitative kinetic measurements over a wide temperature range may be performed rapidly.

Gas chromatography was first applied to the study of polymer degradation by Davison et al.[1], who condensed the volatile degradation products, and then subjected a sample of the products to gas chromatographic analysis. A single-stage technique, in which the degradation is effected in the gas chromatography flow stream, was developed in these laboratories[2], and initially applied to polymer/copolymer characterization and analysis[3]. In this paper the extension of this technique to quantitative studies of degradation kinetics is discussed. First the special problems of kinetic work and their solution are reviewed, and in the following sections the apparatus, choice of operating conditions, and general technique are described.

DIRECT-PYROLYSIS GAS CHROMATOGRAPHY—THE PROBLEMS IN KINETIC WORK

The general technique

The general technique of direct-pyrolysis gas chromatography has been discussed elsewhere[3]. The apparatus described in ref. 3 employed a spiral pyrolysis filament, on which ca. 1 mg samples were mounted; the GLC detector was a katharometer sensitive to 1 μg. Such apparatus is adequate for characterization and analytical work.

*Present address: U.S. Industrial Chemical Co., Cincinnati Ohio, U.S.A.
†Present address: I.C.I. Ltd., Dyestuffs Division, Huddersfield, England.

Reproducibility of kinetic measurements; sample mounting

In principle the above apparatus can be used to study degradation kinetics by measuring the yields of volatiles from pyrolyses of chosen durations at a specified temperature. However, it is found that a specific rate determined from such results shows considerable scatter[4]; this arises principally because it is impossible to mount samples reproducibly on a spiral filament. The situation is aggravated by the temperature gradient from the ends to the middle of the filament, so that reproducible mounting is all the more desirable.

This problem has been surmounted by constructing ribbon filaments of the type shown in *Figure 1*, and depositing the samples from a solution

Figure 1—Ribbon-filament degradation unit. The sample is deposited from a solution evenly spread between the engraved marks mm'

evenly spread over the area within two marks (m, m') engraved on the surface. A comparison of Figures 4 and 8 in ref. 4 indicates the improvement in reproducibility achieved in this way.

The temperature gradients along such a filament have been measured by observing with a travelling microscope the melting of a standard compound along the length of the ribbon. For example, measurements were made of the filament currents required to just melt potassium dichromate (m.pt 398°C) at different points on a 0·4 ohm Nichrome filament. The results are shown in *Figure 2*. Using a current/temperature calibration
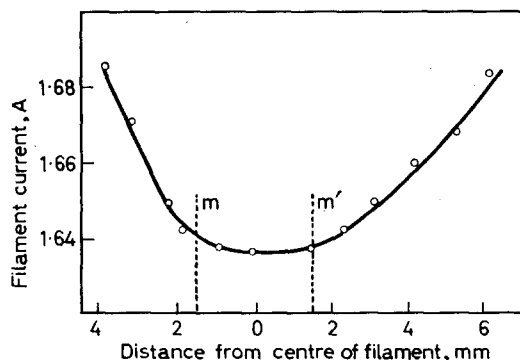
Figure 2—Current required to melt potassium dichromate at various positions along the ribbon filament

similar to that shown later (*Figure 4*), it was calculated that the temperature variation over m, m′ is less than 4 deg. C when the pyrolysis temperature is as high as 400°C.

Time and temperature errors; the filament temperature/time profile

If gas-chromatographic resolution is not to be impaired, the maximum degradation time must not exceed 15 to 20 seconds. The problem is thus to ensure that the sample acquires the specified temperature for the desired time; these conditions are not satisfied by merely switching a filament on and off, since time is required for the filament to attain its equilibrium (i.e. calibrated) temperature. Two temperature/time profiles are shown schematically in *Figure 3*. (These are based on experimental curves deter-
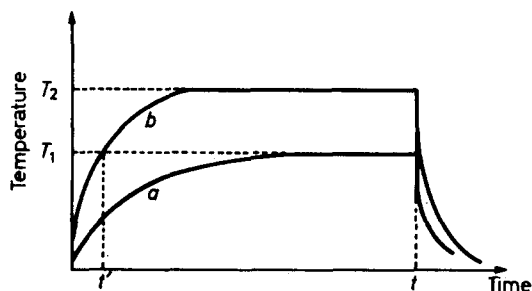
Figure 3—Filament temperature/time profiles shown schematically. (The ordinates cover several hundred degrees, and the abscissae *ca.* 10 sec)

mined with a bridge circuit; some such curves are illustrated in ref. 4.) In both cases the filament is switched on for a nominal duration t, and in both cases the temperature decay is sufficiently rapid to define the end of the degradation. However, the nominal temperatures T_1 and T_2 are attained after a considerable portion of the total degradation time has elapsed, and during this portion the sample has passed through the whole range of intermediate temperatures. This 'pre-effect' can be made insignificant by supplying the current corresponding to curve b for a period $t′$ before supplying current a; this boosts the temperature to T_1 in a relatively short period (0·5 or 1·0 sec has been used in the present work). For each specified filament temperature, corresponding boost currents have been initially chosen on the above basis. Since current b is switched off when the filament temperature is rising steeply, it is desirable to demonstrate that the boost is no more than sufficient under experimental conditions. For this purpose an a.c. bridge with oscilloscope detector has been used[5], and fine adjustments to the boost currents made when necessary. The (1 sec) boost currents (b) required for a range of filament temperatures (a) are shown on the filament calibration plot, *Figure 4*. Filament calibration plots are obtained by the method previously described[3,4], but additional requirements are discussed in a following section.
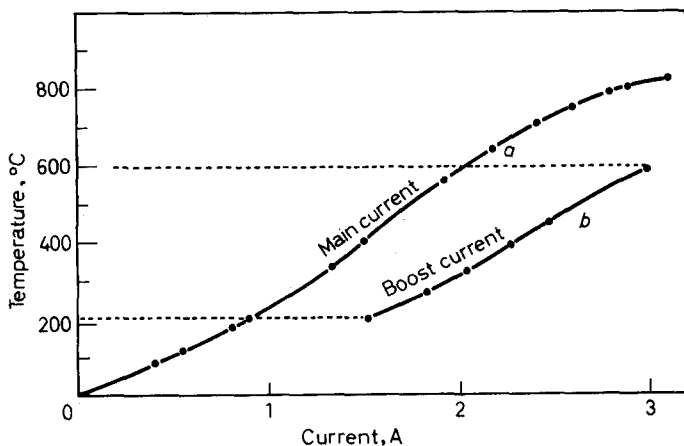
Figure 4—Filament calibration plot (*a*). The corresponding one-second boost currents (*b*) are shown for part of the temperature range

An alternative technique for obtaining a 'square-wave' temperature/time profile has recently been described[6]. This involves raising the filament to its Curie temperature by induction heating, and the choice of filament temperature is dominated by the availability of filament metals or alloys with suitable Curie temperatures. Since each temperature requires a different metal, it is essential to obtain evidence that none of the metals has any catalytic effect on the reaction, otherwise a spurious temperature-dependence will be observed. With this method of heating, it is difficult to demonstrate the absence of such catalytic effects, since modifications to the surface influence the temperature attained. For these reasons the technique has not been utilized in the present apparatus, though the method clearly has potential since pre-effects as short as 20 msec are claimed.

Nichrome ribbon filaments have been used exclusively in the present work; degradation experiments using such filaments which have been sputtered with a thin layer of gold indicate that the filament surface has no specific influence upon the observed rate[4].

In this section only the heat-up of the filament itself has been considered. The additional time required for sample heat-up is considered in a later section.

Dependence of observed degradation rate on sample thickness

Using the apparatus[3] referred to above, the rate of degradation can be studied as a function of sample thickness, over a thickness range down to *ca.* 0·1 mm. Results for polymethylmethacrylate degradations at different temperatures show that the rate is strongly dependent on sample thickness in this range[7].

Unless it can be shown that the rate is independent of sample size, the observed rate cannot correspond to the rate of the chemical process at the specified temperature. If the rate of evolution of volatiles depends on thick-

526

ness, it is probable that one or more of the following is occurring: (a) there is some restriction on the diffusion of volatiles into the gas phase; (b) there is variation in the time taken to raise the sample temperature to the desired value; or (c) there is a pronounced temperature gradient in the sample, so that the temperature of the reaction cannot be accurately specified. Moreover these effects will depend upon thickness to different extents at different temperatures, hence observed activation energies will be in error even if a standard thickness is chosen. The situation is so complex that any experimental solution to the problem becomes attractive; in the present work the sensitivity of the apparatus has been increased by several orders of magnitude and sample sizes chosen in a range where the rate is no longer thickness-dependent.

Thus using a capillary column and an argon triode detector (see next section), the degradation of samples as small as 10^{-8}g can be studied, since *ca.* 10^{-11}g of product can be detected. With this apparatus it has been shown that for sample thicknesses less than 200 Å the specific rates of degradation of polymethylmethacrylate[7] and polystyrene[4] are independent of thickness. In the course of this work, samples as thin as 75 Å were examined[7]. A flame ionization detector of comparable sensitivity has been successfully applied in more recent work[8].

<div align="center">APPARATUS</div>

GLC equipment

Because of the necessity of using small samples in kinetic studies, capillary columns and detectors sensitive to better than 10^{-10}g are essential. However, the actual choices of column, stationary liquid phase, type of detector, and other experimental variables, depend on the system being studied. The apparatus used in these laboratories for two specific problems is briefly listed below for illustrative purposes.

Polymethylmethacrylate degradations[4,5]—50 ft stainless steel capillary column, 0·03 in. bore, coated with squalane, and operated at room temperature. Detector of the argon triode type (constructed to Lovelock's design[9]), containing a 50 millicurie tritium source; anode maintained at $+1$ 200V. The argon carrier gas passes through a BDH type 5A molecular sieve before reaching the apparatus. Carrier gas (argon) flow rate: 4 to 5 cm^3/min, detector scavenger gas flow rate: 3·5 1/h. The detector output current passes through a 10^9 ohm resistor; the potential developed across the latter is amplified by a vibrating reed electrometer, the output from which is displayed on a potentiometric recorder. Output currents from 10^{-9} to 10^{-13} A can be measured.

Polyacrylonitrile degradations[8]—50 ft stainless steel capillary column, 0·015 in. bore, coated with tricresyl phosphate, and operated at 0°C. The flame ionization detector is a modification of that described by Desty[10]; the jet has a platinum tip 0·5 cm long and an orifice of 0·014 in. The jet (anode) is maintained at 90V positive with respect to the cathode, which is a brass cylinder placed 1·0 cm above the jet. The nitrogen carrier gas flows at 0·2 cm^3/min, the hydrogen bleed enters the carrier gas between column and

detector at a rate of 40 cm^3/min. The gases are passed through beds of activated charcoal to remove impurities. Air enters the detector at a rate of 800 cm^3/min through a porous steel disc fitted around the jet. The ion current is passed through a 10^{10} ohm resistor, and the resulting potential measured with an electrometer as above.

To obtain optimum resolution, capillary columns must be coated with care; the procedure described by Dijkstra and Goey[11] has been followed in the present work.

GLC peaks have been characterized by trapping the peak from the column effluent and examining the condensate by mass spectrometry. (Preparative GLC apparatus may be used for such characterization experiments; the results are not then kinetically analysed.) Confirmation of the peak assignments is obtained by injecting the corresponding pure compounds directly into the GLC apparatus through a serum cap, and comparing the retention volumes. A variant of this latter approach is to absorb the compound in the deposited polymer sample on the filament, perform the pyrolysis, and check that the relative area of the peak in question has increased. This method eliminates changes in retention times arising when the 'abnormal' technique of sample introduction (serum cap) is used.

The degradation unit

The degradation unit (*Figure 2*) is inserted into the carrier gas at the head of the column.

The Nichrome ribbon filament is $2 \cdot 2 \times 0 \cdot 08 \times 0 \cdot 008$ (cm), and of nominal resistance 0·4 ohm; it is spot-welded (via nickel intermediate) to the 1 mm diameter tungsten rods. These rods pass through two of the three holes in a glass disc sealed to the end of the B 10 cone.

The degradation chamber, of internal diameter *ca.* 6 mm, tapers down to take a push-fit PTFE adapter which accepts the capillary column. For optimum resolution the degradation chamber should have the minimum convenient size (see below) and the effluent must flow smoothly out of it.

Filaments rarely burn out, but under certain conditions may become bowed after extensive use. This invalidates the temperature calibration since the central part of the filament is now closer to the chamber walls; a new filament must then be fitted and calibrated.

The filament control unit

This unit automatically controls two functions: (*i*) the selected boost current is supplied to the filament for a fixed time (usually 1 sec), and (*ii*) the selected main current is then immediately supplied for the chosen time. Fully automatic control is desirable to remove human errors in timing, and thus to improve reproducibility.

Two types of control unit have been used in the present work. The first of these is essentially the single-cam system (described in ref. 3) modified to include a third microswitch which controls the switching of the boost current. The second type[8] utilizes two synchronous motors, one rotating at 12 rev/min driving cams which operate the boost microswitches, the other rotating at 1 rev/min and controlling the main current. It was initially

considered that the second design would be necessary in order to achieve the required reproducibility of the boost period, but it is now known that adequate boost reproducibility is achieved with the first design. Both types are in current use.

Choice of filament current is effected by switching into the filament circuit one of nine series resistors. These may each be present to provide any sequence of nine temperatures within the range 50° to 1 300°C. The filament is driven with 12V a.c. from a constant voltage transformer. No improvement in reproducibility was observed when this supply was replaced by a 12V 72 A h battery.

<div align="center">TECHNIQUE; OPTIMUM CONDITIONS AND
UNCERTAINTY LIMITS</div>

Mounting of samples and measurement of fractional conversion

A known weight of polymer sample may be deposited between the marks on the filament by using a micropipette containing a solution of known concentration. Sample size is chosen so that the limiting rate, independent of thickness, is measured. (For a film thickness of ca. 200 Å, about 5×10^{-8}g of polymer is required; pipettes of capacity 10^{-4} cm^3 and polymer concentrations in the region of 5×10^{-4} g/cm^3 have been used.)

The filament is first cleared of organic material by heating to 900°C in air for approximately 30 sec. If an inert carbonaceous residue, such as that which may remain after polyacrylonitrile degradation, is present on the filament, some prior mechanical cleaning (lightly scraping the filament) may be desirable. The required volume of solution is then evenly deposited from a Pye micropipette or a Hamilton microsyringe. The bulk of the solvent evaporates away from the filament in a few seconds; any occluded solvent is removed by subjecting the sample to a temperature of e.g. 50°C when the filament is re-mounted in the degradation unit. The absence of any solvent peak in the subsequent degradation chromatogram demonstrates the efficiency of this technique.

The fractional conversion is measured by a method which eliminates pipette reproducibility. The sample is heated for the required time at the desired temperature, and the peak area a_1 of the product of interest is measured. The total available yield of this product from the original sample is then determined as $(a_1 + a_2)$, where a_2 is the peak area obtained when the remainder of this product has been evolved from the residue. For samples such as polymethylmethacrylate a_2 can be determined by totally degrading the residue at 520°C (a period of 15 sec has been shown to be more than adequate) to obtain quantitative yield of monomer; for samples in which the relative yields of degradation products vary with temperature, a_2 must be determined from pyrolyses at the same temperature as that chosen for a_1. Since the sample sizes used are within the linear dynamic range of the detector, which implies a linear dependence of peak area on weight of product, the fractional conversion is given by $x = a_1/(a_1 + a_2)$. The validity of the result may be checked by subjecting the filament to a final temperature pulse; no further yield of the product of interest should be obtained.

For samples which depolymerize quantitatively to give monomer as the

<div align="center">529</div>

sole product, the fractional conversion is clearly based on the total weight of sample. For samples which decompose to give a number of products, x as defined above refers to the ratio (quantity of a product evolved during the chosen degradation period)/(total quantity of this product available from the sample at the chosen temperature). Polyacrylonitrile degradation kinetics have been assessed on this basis[6].

Choice of optimum experimental conditions

(a) *Flow-rate of carrier gas*—The fractional conversion observed for standard conditions with a particular sample has been demonstrated to be independent of carrier gas flow-rate provided that the latter is in the region of 0.5 cm³/min. In certain cases a dependence of conversion on flow-rate has been observed for higher flow-rates, e.g. the conversion decreased by 33 per cent for a polymethylmethacrylate degradation when the flow-rate was changed from 2.6 cm³/min to 4.8 cm³/min. It is considered that this is caused by the influence of high flow-rates upon the filament temperature. When studying any new system it is therefore desirable to check that the results are independent of carrier gas flow-rate. If for any reason it is necessary to work in a region where a dependence is observed, the filament temperature must be calibrated under the flow conditions used.

(b) *Diameter of the degradation chamber*—The filament must be calibrated for a particular degradation chamber, and this calibration does not apply for degradation chambers of different diameter. Two factors may be responsible for this situation: (*i*) if the carrier gas flow-rate is the same for the two different chambers, the linear gas velocity over the filament will be different in each case, and (*ii*) the proximity of the filament to the walls of a narrow chamber may influence the rate of heat loss. Both these factors will be minimized if the chamber has large diameter; on the other hand large chambers have greater dead volume and consequently reduce chromatographic resolution. Chambers of 6 mm diameter have proved to be an acceptable compromise, and this has been chosen as a standard dimension in the present work.

It is interesting to note that when the above situation was neglected and the calibration for a 6 mm chamber was assumed to apply for a 10.5 mm chamber, an apparent increase in the fractional conversion from 15.2 per cent to 20.5 per cent was observed for a particular polymethylmethacrylate degradation.

(c) *Temperature of the degradation chamber walls*—When studying a pyrolysis in which relatively involatile products are evolved, it may be desirable to operate the capillary column at elevated temperature, and moreover to heat the walls of the degradation chamber to discourage condensation of these products (see below). Under these circumstances recalibration of the filament under heated-chamber conditions is essential. To illustrate the importance of this, the following example may be quoted. A polymethylmethacrylate sample, which under standard degradation conditions gave a fractional conversion of 27 per cent when the chamber walls were maintained at 20°C, gave an observed conversion of 88 per cent when the cham-

ber walls were maintained at 80°C. Since measurements of rate of reaction as a function of sample size illustrated that the temperature gradient through the sample was negligible for the sample sizes used in these experiments, the observed change in fractional conversion may be attributed to a change in the temperature attained by the filament.

Since continuous running of the filament itself causes a gradual rise in temperature of the chamber walls, and a consequent change in filament temperature as above, this factor must be taken into acount when calibrating the filament. This rise in temperature of the walls becomes important only when current is passing through the filament for long periods; for calibration it must therefore be specified that the standard compound must melt within a period comparable with the degradation periods to be examined. Since the duration of a degradation experiment does not normally exceed 20 sec, the calibration requirement imposed has been that the standard compound should melt in this period. (The calibration is not sensitive to the value chosen provided it lies in the range of a few tens of seconds; the effect is mentioned here because it is tempting to observe the behaviour of the calibration substance over long periods if incipient melting seems probable.) The boosting arrangements, described earlier, ensure a rapid rise to the chosen temperature, and the constancy of temperature during the degradation period may be demonstrated by the oscilloscope technique mentioned previously.

(d) *Optimization of GLC detector response*—The desirability of using small samples in kinetic work requires that the GLC detector should operate at maximum sensitivity and maximum signal/noise ratio. The following factors may be varied in any attempt to improve sensitivity and reduce noise: (*i*) Purity and flow-stability of the carrier and other gases supplied to the detector. Series columns of molecular sieve or active charcoal, and ballast tanks in the gas lines, may be incorporated. (*ii*) Flow rates of carrier gas, scavenger gas (argon triode detector), and of hydrogen and oxygen bleeds (flame ionization detector). (*iii*) Geometrical factors, such as anode–cathode separation, and siting of the ring electrode (argon triode detector). (*iv*) Electrical factors, such as choice of anode–cathode potential, and minimizing induced currents in the measuring circuit. With respect to the latter, the cable connecting the detector to the impedance converter must be as short as possible, and must be rigidly mounted.

The values of these parameters quoted earlier are optimum values determined as above for the apparatus in use; they can be taken only as indicating orders of magnitude for apparatus of different design.

(e) *Sample size effects*—The importance of demonstrating that kinetic results are independent of sample size has already been discussed. At this stage it must be stressed that it is not sufficient merely to show that the fractional conversion obtained for a chosen degradation period and temperature is independent of sample size. Studies of polyacrylonitrile degradation[8] have shown that this condition is satisfied over a wide range of sample thicknesses (at least up to 3 000 Å), but when fractional conversion is

studied as a function of time, sigmoid plots are obtained for the thicker samples. Only if sample thickness is less than 750 Å does the fractional conversion rise logarithmically with time, i.e. in a manner corresponding to a first-order process.

For insoluble samples it is difficult to determine the effect of sample size on degradation rate, because the grinding or milling of polymer samples may itself cause degradation. In such cases the only safe procedure is to prepare a series of thin samples *in situ* on the filament.

(f) *Solvent effects*—Since traces of solvent may remain in a sample which has been deposited from solution, it is desirable to demonstrate that this solvent is not influencing the rate of degradation in any way. Evidence of this kind may be obtained by two methods: (*i*) by allowing increasing concentrations of the solvent to remain in the sample, and observing no change in rate of degradation for specified conditions, and (*ii*) by employing a series of different solvents and observing an identical rate for all acceptable solvents. Thus benzene, toluene, chloroform and acetone have been used as solvents for polymethylmethacrylate degradation studies; the trace amounts of these solvents remaining in the films during the pyrolyses had no detectable influence on the rate. Whenever possible, it is clearly desirable to avoid solvents which are known to be good chain transfer agents, especially when the reactivity of the depropagating radical is expected to be high.

Reproducibility and uncertainty

(a) *Reproducibility of the time and temperature of reaction*—By the oscilloscope technique it was shown that the reproducibility of the reaction timing was better than 0·03 sec (i.e. within the error of estimation by this technique). Since the shortest reaction times were never less than 5 sec, the timing errors are insignificant. By contrast, the variations in boost and main current have a larger effect. The maximum variations in boost and main current were ±0·01 and ±0·005 A respectively, corresponding to an uncertainty in temperature of ±2 deg. C. With temperature reproducibility of this order, the overall observed uncertainty in polymethylmethacrylate degradations ranged from ±3 per cent (standard deviation of five measurements) at conversions of about 0·80 (5 sec reaction at 460°C), to ±10 per cent at conversions of about 0·08 (20 sec reaction at 340°C). Other possible contributions to this uncertainty are considered in paragraphs (b) and (c) below.

(b) *Product losses*—Since the walls of the degradation chamber are at a lower temperature than that of the filament, the possibility of product condensation or adsorption on these walls must be taken into account. Two kinds of experiment have been performed to assess the importance of such product losses: (*i*) for a sequence of pyrolyses performed in a degradation chamber which is initially cleaned but not cleaned between pyrolyses, the losses in the first pyrolysis are expected to be greater since the walls are not 'conditioned', (*ii*) a series of pyrolyses at different chamber temperatures (the filament being re-calibrated for each wall temperature—see above)

may be performed; if product condensation is occurring the apparent yields should be higher for higher wall temperatures. For polymethylmethacrylate degradations, the fractional conversion was found to be independent of chamber temperature over the range 24° to 110°C; it was therefore concluded that the effects of adsorption were insignificant.

(c) *Measurement of GLC peaks*—The principal uncertainty in measurement of peak area usually lies in the choice of baseline. It is therefore desirable to choose GLC operating conditions (especially carrier gas flow rate, column temperature and stationary liquid phase) so that sharp symmetrical peaks are obtained, and baseline recovery is good. The areas themselves are usually measured with an optical planimeter (Filotechnia Salmoirghi S.P.A. model 236), though alternative methods such as weighing the paper, or triangulation, are acceptable. Comparative measurements on polymethylmethacrylate degradations have shown that the triangulation formula Area = (Height) × (Width at half-height) gives results of a precision similar to those obtained by paper-weighing, the total uncertainty in any one estimation being less than two per cent.

(d) *Confidence limits*—For specified degradation conditions, the determination of fractional conversion takes approximately 10 to 20 min; it is therefore feasible to perform a number of replicate runs. Five such determinations have usually been made for each point in the present work, and the mean value of fractional conversion calculated. A vertical line through the point represents the 75 per cent confidence limits for each mean fractional conversion; the 75 per cent confidence limits for specific rates are calculated from the corresponding limits for the fractional conversion. Examples will be shown in subsequent publications (see for example the paper following), though *Figure 5* in this paper indicates the orders of magnitude.

Verification of reaction order. Sample heat-up period
Unless complicating factors are present, the evolution of volatiles from a bulk-pyrolysed polymer is expected to follow a first-order rate equation, i.e. $dm/dt = k_{obs} (m_0 - m)$, where m_0 is the initial mass of sample, m is the mass of volatile evolved after time t, and k_{obs} is the observed specific rate. The integrated form of this equation is $-\ln(1-x) = k_{obs} t$, where x is the fractional conversion m/m_0. Thus a plot of $-\ln(1-x)$ against time will be linear over the range for which first-order conditions apply. (Deviations from linearity do not necessarily mean that first-order kinetics do not apply; variation of k_{obs} with conversion is expected for some first-order mechanisms. Examples of this will be discussed in the next paper.)

A first-order plot for the pyrolysis of polymethylmethacrylate (fractionated sample, $\overline{M}_n = 580\,000$) at 370°C is shown in *Figure 5*. The graph is linear up to *ca.* 30 per cent conversion, and k_{obs} can be calculated from this initial gradient. There is a positive intercept of $2 \cdot 0 \pm 0 \cdot 3$ sec on the time axis which corresponds to the sum of the filament boosting time (1 sec) and the time required for the sample itself to attain the temperature of the filament. This illustrates the importance of studying the conversion as a
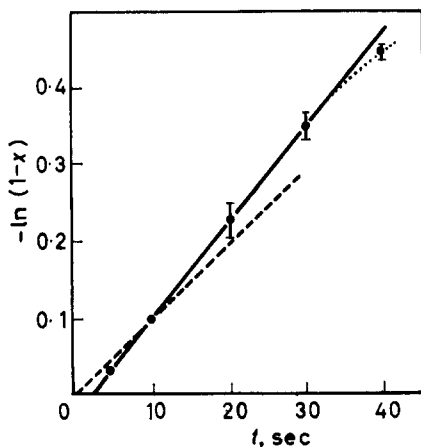
Figure 5—First-order plot for the pyrolysis of a polymethylmethacrylate fraction ($\overline{M}_n = 580\,000$) at 370°C. The broken line through the origin illustrates the erroneous specific rate obtained for a single-point (10 sec) determination (i.e. zero-error neglected)

function of time and plotting as above; a single point determination of conversion at e.g. 10 sec would provide an erroneously low value of k_{obs} (broken line, *Figure 5*) when inserted into the integrated rate equation.

CONCLUSIONS

The pyrolysis–gas-chromatography technique may be applied to study degradation kinetics, and quantitative results are obtained if the experimental variables are controlled more precisely than is required for polymer characterization and analysis. In particular, the effects of sample size, sample mounting, and time and temperature control become important in kinetic work. Modern GLC detectors are, however, sufficiently sensitive to permit measurements to be made on samples in a thickness range where the rate is independent of sample size (*ca.* 200 Å, *ca.* 10^{-8} g), and a range of pyrolysis temperatures in excess of that available with conventional techniques may be rapidly explored.

Chemistry Department,
  University of Birmingham,
    Birmingham, 15

REFERENCES

[1] DAVISON, W. H. T., SLANEY, S. and WRAGG, A. L. *Chem. & Ind.* **1954,** 1356

[2] LEHRLE, R. S. and ROBB, J. C. *Nature, Lond.* 1959, **183,** 1671

[3] BARLOW, A., LEHRLE, R. S. and ROBB, J. C. *Polymer, Lond.* 1961, **2,** 27

[4] BARLOW, A., LEHRLE, R. S. and ROBB, J. C. *S.C.I. Monogr. No. 17,* p 267. Society of Chemical Industry: London, 1963

[5] SUNDERLAND, D. *Ph. D. Thesis,* University of Birmingham, 1965

[6] SIMON, W. and GIACOBBO, H. *Angew. Chem. (Int. Ed.),* 1965, **4,** 938

[7] BARLOW, A., LEHRLE, R. S. and ROBB, J. C. *Makromol. Chem.* 1962, **52,** 230

[8] BELL, F. A. *Ph. D. Thesis,* University of Birmingham, 1966

[9] LOVELOCK, J. *Gas Chromatography 1960,* p 16. Ed. R. P. W. SCOTT. Butterworths: London, 1960

[10] DESTY, D. H., GEACH, G. H. and GOLDUP, A. *Gas Chromatography 1960,* p 46. Ed. R. P. W. SCOTT, Butterworths: London, 1960

[11] DIJKSTRA, C. A. and DE GOEY, J. *Gas Chromatography 1958,* p 56. Ed. D. H. DESTY. Butterworths: London, 1958

Polymethylmethacrylate Degradation— Kinetics and Mechanisms in the Temperature Range 340° to 460°C*

A. BARLOW†, R. S. LEHRLE, J. C. ROBB and D. SUNDERLAND‡

Fractionated samples of polymethylmethacrylate have been degraded at temperatures within the range 340° to 460°C, using the micropyrolysis–GLC technique. The conversion at which deviation from first-order kinetics occurs has been found to vary with the temperature of the degradation. Rate constants for the fractions, calculated from the linear regions of the first-order plots, have been plotted as a function of the initial molecular weight of the fractions. The trends of these plots at different temperatures, and the deviations from first-order kinetics, are consistent with the following changes in mechanism throughout the temperature range. At the lowest temperatures, the depropagation reaction is principally initiated at the ends of the molecules, and termination occurs by bimolecular interaction. At intermediate temperatures, chain scission becomes sufficiently important to account for most of the initiation steps, though bimolecular interaction is still the important termination mechanism. At the highest temperatures, initiation by scission is the predominant initiation process, but the majority of the chains are effectively terminated by the diffusion out of the system of the ultimate radical remaining when a chain has completely depropagated. Temperature coefficients measured over this range cannot therefore be regarded as overall activation energies, but must be interpreted in terms of the change of mechanism with temperature.

THE micropyrolysis–GLC technique involves the degradation of samples on the surface of a filament in the carrier gas stream of a capillary column apparatus. Sample sizes of the order 5×10^{-8} g (thickness 200 Å) must be used, in order to ensure that the specific rate is independent of sample thickness. Experimental details of the method have been presented in the previous paper[1]; this communication considers the results obtained when the technique is applied to study the degradation of fractionated polymethylmethacrylate (PMMA) samples over the temperature range 340° to 460°C.

MATERIALS

Unfractionated sample

Prepared by a high-vacuum technique at 60°C by bulk polymerization to ten per cent conversion, using azobisisobutyronitrile as initiator, $\overline{M}_v = 2.78 \times 10^5$.

Fractionated samples (a) to (e)

Samples of molecular weight (a) 64 850, (b) 167 600, (c) 291 700, (d) 416 900 and (e) 579 500, were fractionated from the unfractionated sample

using a Baker–Williams column (benzene/methanol, 5 deg. C temperature differential, 25 cm³/h flow rate).

All molecular weights were determined viscometrically in methylethyl ketone, using the K and α values for this polymer–solvent system determined by Chinai et al.[2].

RESULTS AND DISCUSSION

Basic kinetics

It has been known for some time[3] that simple depropagation is the basic low-temperature degradation mechanism for PMMA. Direct gas chromatographic analysis of pyrolyses in the temperature range 300° to 550°C[4,5] shows monomer to be the sole degradation product, and this result is of course consistent with a depropagation mechanism. At temperatures above 600° the results[4] indicate that more drastic degradation occurs, but this temperature is outside the scope of the present study. The work described here in fact attempts to elucidate the principal initiation and termination processes of the depropagation chain reaction, and assesses changes in these processes with molecular weight and temperature.

Various possible basic processes are listed below, together with the assumptions made in the present work:

(i) chain-end initiation: $P \longrightarrow R\cdot + X\cdot$ k_i (sec⁻¹)

   R· is the chain radical which will depropagate; X· is a small radical which distils out of the system;

(ii) random scission initiation: $P \longrightarrow 2R\cdot$ k'_i (sec⁻¹);

(iii) depropagation: $R\cdot \longrightarrow R\cdot + M$ k_d (sec⁻¹)

   M is a monomer molecule which distils out of the system;

(iv) termination by bimolecular interaction:

$$R\cdot + R\cdot \longrightarrow P\,[+P] \qquad k_t\,(1.\,\text{mole}^{-1}\,\text{sec}^{-1});$$

(v) 'termination' by depropagation to the end of the polymer molecule, leaving a small radical which distils out of the system. The kinetic chain length will then be equal to the degree of polymerization D, if initiation is by process (i); if initiation is by process (ii) the mean kinetic chain length will be equal to $D/2$.

Equations for the instantaneous rate of monomer evolution at any time t (dm/dt, g/system sec) can be derived by the usual stationary state assumptions, bearing in mind that the system is not at constant volume and the change in volume must be corrected for. The results for various limiting cases are as follows.

(a) Chain-end initiation; depropagation to the end (i, iii, v)

$$dm/dt = k_i\,(m_0 - m) \qquad (1)$$

where m_0 is the initial weight of polymer (g) and m is the weight of monomer evolved after time t.

(b) Chain-end initiation; bimolecular termination (i, iii, iv)

$$dm/dt = (k_i u/2k_t D\rho)^{\frac{1}{2}} k_d\,(m_0 - m) \qquad (2)$$

where u is the molecular weight of a monomer unit, and ρ is the density of polymer in g/l. at the temperature of the experiment.

(c)   Scission initiation; depropagation to the end (ii, iii, v)

$$\mathrm{d}m/\mathrm{d}t = k'_i D\,(m_0 - m) \tag{3}$$

(d)   Scission initiation; bimolecular termination (ii, iii, iv)

$$\mathrm{d}m/\mathrm{d}t = (k'_i u/k_t \rho)^{\frac{1}{2}}\,k_d\,(m_0 - m) \tag{4}$$

These equations may be integrated to obtain relationships between the fractional conversion $(x = m/m_0)$ and time t for each of the cases. Despite the fact that any change in D with conversion affects the situation in cases (b) and (c), for the present, D will be assumed constant and equal to its initial value. This question will be taken up later; at this stage we merely note that the approximation is acceptable provided the fractional conversion is small. The integrated forms are:

case (a): $-\ln(1-x) = k_i t$ (5)

case (b): $-\ln(1-x) = (k_i u/2k_t D\rho)^{\frac{1}{2}}\,k_d t$ (6)

case (c): $-\ln(1-x) = k'_i D t$ (7)

case (d): $-\ln(1-x) = (k'_i u/k_t \rho)^{\frac{1}{2}}\,k_{dt}$ (8)

It will be noted that these equations imply first-order kinetics, and furthermore that in two of the cases the observed first-order specific reaction rate depends on the molecular weight of the sample.

Determination of specific reaction rates

The observed specific reaction rate (k_{obs}) at a chosen temperature for a particular sample is calculated from the mean fractional conversion corresponding to the selected reaction time, assuming a general first-order equation,

$$-\ln(1-x) = k_{obs}t \tag{9}$$

based on equations (5) to (8). The selection of reaction time is restricted by the fact that it must not be too large, otherwise chromatographic peaks of poor shape are obtained, and it must not be too small, for then the temperature 'end-effects' (rise and fall of temperature) give rise to excessive uncertainty. In practice the preferred range is 5 to 20 seconds. Because of the lower limit of 5 seconds it can be appreciated that at high temperatures, where the rate becomes large, degradation to high conversion will occur. For PMMA, reaction times of 20 seconds at 340°C will correspond to approximately seven per cent conversion, but when the temperature is increased to 460°C a reaction time of 5 seconds corresponds to about 80 per cent conversion.

In view of these high conversions, it is desirable to check that the first-order expression applies throughout the conversion range at each temperature. This has been possible for temperatures up to 416°C (see *Table 1*) by varying the reaction time t for each sample and plotting $-\ln(1-x)$ against t. In all cases it was possible to define a conversion range (or maximum reaction time) over which no deviation from linearity could be detected,

Table 1. Data for first-order tests

Expt	Sample	Temp. °C	Conversion range studied, %	Intercept on time axis (sec)
1	(a)	340	17	+0·7±0·7
2	(a)	416	80	+2·8±0·4
3	(e)	340	15	+1·6±0·6
4	(e)	355	84	+2·4±0·7
5	(e)	370	38	+2·0±0·3
6	Unfractionated	330	67	Zero
7	Unfractionated	380	90	Zero
8	(a)	380	90	Zero
9	(e)	330	67	Zero
10	(e)	380	90	Zero

and results within this region were used to calculate k_{obs}. Representative plots covering the temperature range are shown in *Figure 1*, from which it is deduced that linearity is acceptable up to 14 per cent (expt 1, 340°), 30 per cent (expt 5, 370°) and 80 per cent (expt 2, 416°), whereas the approximate conversions used in determinations of k_{obs} at these temperatures were 8 per cent, 28 per cent, and 55 per cent respectively. At the highest temperatures (432° to 463°C) it was not possible to explore a conversion range, and it has been assumed that equation (9) holds for the measured conversions (65 per cent and 80 per cent respectively). The validity of this assumption is considered later.

Reference to *Table 1* shows that experiments 1 to 5 displayed a positive intercept on the time axis, the average value being 1·9 seconds. In these experiments the time values correspond to the sum of the boosting time (i.e. 1 second, see ref. 1) and the time for which the true filament heating current is applied. It is therefore assumed that the filament *and* sample
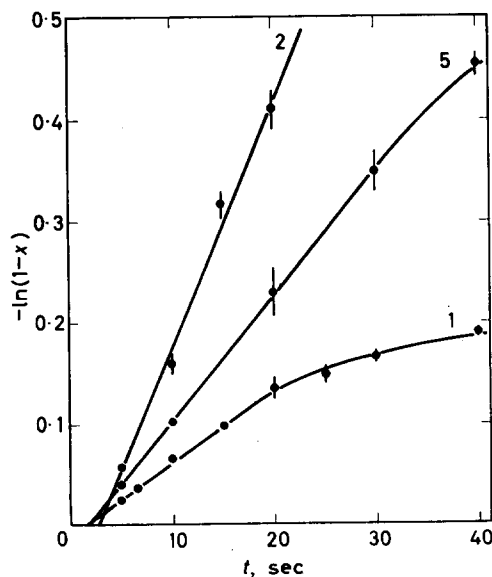
Figure 1—First-order plots for experiments at 340°C (1), 370°C (5), and 416°C (2). The ordinate axis for experiment (2) has been linearly reduced by a factor of four. The key-numbers refer to the experiments listed in *Table 1*. The vertical lines through the points represent 75 per cent confidence limits for each mean fractional conversion (see ref. 1)

540

require a 1·9 second period in order to attain the desired temperature, and values of k_{obs} have been calculated from reaction times corrected on this basis. This assumption is justified by the fact that no intercepts were observed in experiments 6 to 10, where excessive boosting ensured an initial very rapid rise in temperature. (Absolute rate measurements were not made in this way because of the possibility that the sample temperature would initially exceed the desired value.)

Dependence of specific reaction rate on molecular weight and temperature

It has been shown that the proposed kinetic schemes differ in their interpretation of k_{obs}; in particular k_{obs} is independent of D in cases (a) and (d), whereas $k_{obs} \propto D^{-\frac{1}{2}}$ for case (b), and $k_{obs} \propto D$ for case (c). The specific reaction rate for the given PMMA fractions (*a*) to (*e*) is therefore plotted as a function of reciprocal square root degree of polymerization in *Figure 2*,

Figure 2—PMMA degradation over the temperature range 338° to 463°C: dependence of specific rate on molecular weight; 75 per cent confidence limits are shown
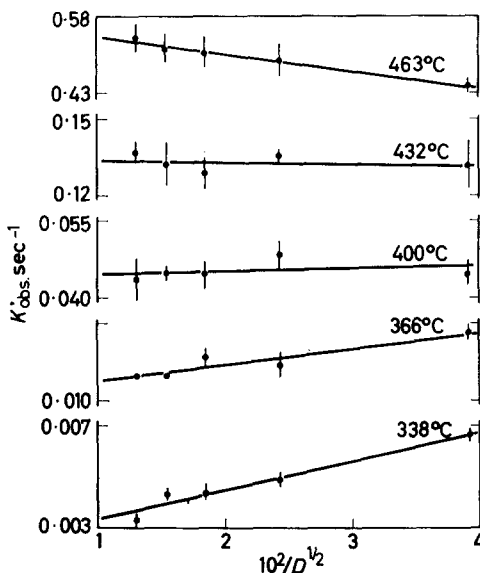
which includes results for five temperatures in the range 338° to 463°. It appears that at the lowest temperatures, 338° and 366°, the specific rate decreases as D increases, whereas at the highest temperature, 463°, this trend is reversed. At the intermediate temperatures, 400° and 432°, the specific rate is independent of the degree of polymerization, or very nearly so.

These results are consistent with the following interpretation of the thermal degradation behaviour of PMMA.

At low temperature the principal mechanism is represented by a rate expression similar to equation (6), which implies that chains are initiated at a terminal link and are terminated principally by bimolecular interaction. Whilst it is statistically inevitable that some chains will effectively terminate by depropagation to the end of the molecule, it appears that at these

temperatures the ratio of k_d to k_t is sufficiently small to make this situation much less probable than bimolecular interaction.

At high temperature both the principal initiation process and the most probable termination process have changed. Here the results are represented by an equation similar to equation (7) which requires that the initiation is principally by random scission, and that bimolecular interaction during depropagation is improbable. Presumably k_d has now become large enough for the majority of chains to depropagate completely before encountering and interacting with another depropagating chain.

At intermediate temperatures (400° to 432°), the results are consistent with either of the following mechanisms: (*i*) initiation at terminal links; effective termination by depropagation to the end of the molecule, (*ii*) initiation by random scission; termination by bimolecular interaction. From the results in *Figure 2* these possibilities cannot be distinguished, but it will be seen in the next section that the first-order plot deviations indicate which is the important mechanism.

Significance of the deviations from first order

Considering first the low temperature mechanism, from equation (6) it is seen that the observed first-order rate constant $k_0 = (k_i u / 2 k_t D \rho)^{\frac{1}{2}} k_d$. Any variation of the parameters in this expression with conversion will lead to an apparent deviation from first-order behaviour. Two such variations are expected.

The first is a gradual reduction of D from its initial value, caused by the accumulation of polymer fragments produced in the bimolecular termination steps. Reduction in D during conversion will lead to a positive deviation from first order, i.e. the first-order plot will display an upward trend.

The other parameter which is expected to vary is k_i. In the derivation of the rate expression, it is assumed that throughout the degradation a constant fraction of the polymer molecules possess ends which are capable of initiation; this implies a constant value for k_i. Accepting the observations of Grassie and Melville[3], Brockhaus and Jenckel[6], and Jellinek and Clarke[7] that terminal double bonds are most readily able to initiate the depropagation, the initial value of the above fraction would be 0·5 if all termination during the polymer synthesis were by disproportionation, and < 0·5 if some combination had occurred. This fraction must decrease during the course of the degradation, since for each pair of depropagating chains which terminate, two double bonds have disappeared in the initiation, whereas in the bimolecular termination process two molecules and one double bond are formed if the mechanism is disproportionation, or one molecule with no double bonds is formed if combination occurs. Thus the effective value of k_t is expected to decrease during the degradation, and this would cause the first-order plot to display a downward trend.

Since the results at 340° and 370° in *Figure 1* show negative deviations from first order, this indicates that variation in k_i with conversion is influencing the plot more than variation in D.

If we now consider the two possible mechanisms at intermediate temperature (400° to 432°C, *Figure 2*; see above), mechanism (*i*) involves end-

initiation whereas (ii) involves initiation by random scission. The first-order plot at 416°C in *Figure 1* indicates no deviation from first-order behaviour even at conversions of 80 per cent. For the above reasons this is inconsistent with a mechanism involving end-initiation, since the effective value of k_i is certainly expected to decrease at conversions exceeding 50 per cent, if not before. On the other hand the rate constant for scission initiation, k'_i is not expected to change during conversion, since scission is assumed to be a random process occurring anywhere within the polymer molecules. This suggests that mechanism (ii) is the principal process occurring in the intermediate temperature region. Thus k_{obs} in this region is interpreted as $(k'_i U/k_t \rho)^{\frac{1}{2}} k_d$; since D does not appear in this expression it can moreover be inferred that any variation in D with conversion, as discussed above, will not cause positive deviations in the first-order plot.

Turning finally to the high-temperature results (463°C, *Figure 2*), it was mentioned previously that because of the rapid rate of reaction it was not possible to explore a sufficiently broad conversion range to demonstrate the first-order relationship (9). It can now be stated that if the foregoing conclusions are accepted, and k_{obs} is interpreted as $k'_i D$ according to equation (7) no deviations from first order are expected. k'_i will be constant for the reasons stated above, and D will be constant at its initial value since virtually all chains which are initiated are completely removed from the system by depropagating to the terminal unit.

Discussion

The kinetic results are therefore consistent with changes in mechanism throughout the temperature range. At the lowest temperatures, depropagation is principally end-initiated, and termination occurs by bimolecular interaction. At intermediate and high temperatures, scission becomes the important initiation process, but the bimolecular termination which occurs at intermediate temperatures is replaced at high temperatures by 'termination' by depropagation to the ends of the molecules.

Grassie and Melville[3] find that PMMA degradation is end-initiated at low temperatures, but their observation of a sharp transition (at $D = 2 \times 10^3$) from exclusively depropagation-to-end termination to bimolecular termination is not confirmed in the present work. Brockhaus and Jenckel[6] have demonstrated that two types of initiation occur in PMMA degradations below 350°C; one of these types involves double bonds at the ends of molecules and is the predominant mechanism at low conversions. The other type is much slower, and accounts for the rates at high conversion when all double bonds have disappeared. Some of their quantitative results are, however, open to criticism. For example, they expect exactly 50 per cent of the molecules to possess double-bonded ends, and ignore any possibility of a combination component[8-10] during synthesis. They also ignore the fact that any termination by disproportionation during degradation will itself create double-bonded ends, and that kinetic chain lengths will not be unique but will have a distribution. Perhaps the most serious criticisms of their work, however, are (a) the shapes of their rate curves were found to depend upon the ambient pressure; and (b) their plots of dm/dt against conversion

(Figure 8 in ref. 6) appear to be rather idealized, and cannot be constructed from the conversion curves presented earlier in their report.

Prior to the present work there have been few studies of PMMA degradation at higher temperatures. An analysis by Gordon and Shenton[11, 12] of low temperature results[3, 6] includes the suggestion that there may be a small scission reaction superimposed on the end-initiation process. It is reasonable to assume that such scission would become more probable at elevated temperatures, and moreover a small proportion of such a reaction is of course very significant in view of the much larger number of normal chain links compared with terminal links. Jellinek and Clarke[7] have studied PMMA degradation at temperatures up to 400°C by measuring with a spoon gauge the monomer pressure developed from a polymer sample coated on the surface of a quartz pot. In more recent work[13] a stainless steel pot has been used in order to minimize heat transfer problems[14]. Evidence was obtained for the participation of two types of mechanism, one of which corresponds to the low-temperature mechanism proposed in the present work. However, no interpretation was suggested by Jellinek for the other mechanism, which would correspond to the high-temperature mechanism in the present work. Jellinek and others have estimated overall activation energies for PMMA degradation; in view of the inversion of mechanism with temperature reported in the present work the values should be interpreted with caution. Such interpretations, together with the results of high-temperature studies of changes in molecular weight with conversion—which provide further evidence for our proposed mechanism—will be presented in a subsequent publication[15].

CONCLUSIONS

The micropyrolysis–GLC technique may be applied to study degradation kinetics, provided that the apparatus is sufficiently sensitive to allow measurements to be made on samples in a thickness range where the rate is independent of sample size.

A temperature range in excess of that available with other techniques has been explored, and predominant mechanisms have been proposed for three temperature ranges. The low-temperature mechanism is in accord with evidence previously reported in the literature, but the high-temperature mechanism has not previously been demonstrated.

Chemistry Department,
University of Birmingham,
Birmingham, 15

REFERENCES

[1] BARLOW, A., LEHRLE, R. S., ROBB, J. C. and SUNDERLAND, D. *Polymer, Lond.* 1967, **8**, 523

[2] CHINAI, S. N., MATLOCK, J. D., RESNICK, A. L. and SAMUELS, R. J. *J. Polym. Sci.* 1955, **17**, 391

[3] GRASSIE, N. and MELVILLE, H. W. *Proc. Roy. Soc. A,* 1949, **199**, 1, 14, 24

[4] BARLOW, A., LEHRLE, R. S. and ROBB, J. C. *Polymer, Lond.* 1961, **2**, 27

[5] LEHMANN, F. A. and BRAUER, G. M. *Analyt. Chem.* 1961, **33**, 673

[6] BROCKHAUS, A. and JENCKEL, E. *Makromol. Chem.* 1956, **18/19**, 262

[7] JELLINEK, H. H. G. and CLARKE, J. E. *Canad. J. Chem.* 1963, **41**, 355; *J. Polym. Sci. A,* 1965, **3**, 1171

[8] BEVINGTON, J. C., MELVILLE, H. W. and TAYLOR, R. P. *J. Polym. Sci.* 1954, **12**, 449, and **14**, 463

[9] AYREY, G. and MOORE, C. G. *J. Polym. Sci.* 1959, **36**, 41

[10] SCHULZ, G. V., HENRICI-OLIVÉ, G. and OLIVÉ, S. *Makromol. Chem.* 1959, **31**, 88

[11] GORDON, M. and SHENTON, L. R. *J. Polym. Sci.* 1939, **38**, 179

[12] GORDON, M. *J. phys. Chem.* 1960, **64**, 19

[13] KACHI, H. and JELLINEK, H. H. G. *J. Polym. Sci. A,* 1965, **3**, 2714

[14] JELLINEK, H. H. G. *J. Polym. Sci. A,* 1966, **4**, 2705

[15] BAGBY, G., LEHRLE, R. S. and ROBB, J. C. To be published

Thermodynamic Properties of
Poly-4-methyl-pentene-1

F. E. KARASZ*, H. E. BAIR† and J. M. O'REILLY

The heat capacity of poly-4-methyl-pentene-1 (P4MP) has been measured from about 77° to 540°K, as a function of the thermal history imparted to the sample. In addition to the glass and the melting transitions ($\sim 305°$ and $522°K$, respectively), an intermediate transition was found at about 445°, and there is some evidence that this is related to the fusion (or solid–solid transformation) of a polymorph of P4MP. The calculated configurational entropy was shown to be unusually low at T_g, and a simple explanation for this, based on differences in the properties of atactic and stereoregular P4MP, is proposed. This could account also for the reported anomaly in the configurational volume.

PREVIOUS studies of poly-4-methyl-pentene-1 (P4MP) have shown that this polymer exhibits at least two comparatively unusual phenomena. First, it has been clearly shown in a number of investigations[1-4] that at room temperature the density of the amorphous polymer exceeds that of the highly crystalline material (by as much as one per cent), a situation unique, in polymers, to P4MP. Secondly, dynamic mechanical[1,5,6] and volumetric studies[1,4] have detected transitions in the polymer at $\sim 400°K$, that is between T_g and T_m, a temperature interval usually devoid of any relaxation.

In the present study, we have examined the properties of P4MP in general, and the above phenomena in particular, through measurements of the heat capacity of samples of P4MP, with differing thermal histories, over a wide temperature range. Such measurements can yield a considerable amount of information, especially relating to transitional behaviour[7], and also provide the basic thermodynamic data required to test various hypotheses concerning, for example, the formation and properties of the amorphous phase.

EXPERIMENTAL

(a) Sample

A crystalline powdered sample of P4MP was obtained from the Union Carbide Co. through the courtesy of Dr F. P. Reding. This sample had a $M_v = 1\cdot4 \times 10^5$ (from viscosity measurements in decalin at 135°C and the data of Goodrich and Porter[8]). The density of a moulded sample at 25°C, measured by hydrostatic weighing, was 0·8325 g ml^{-1}.

(b) Calorimetry

An adiabatic calorimeter was used to measure the heat capacity of P4MP from 77° to 540°K. Full details of the apparatus and technique are given elsewhere[9]. It was necessary to compress the powdered sample to fill the calorimeter with an adequate quantity; 29·004 g was used. The polymer, under 5 cm of mercury pressure of helium, typically was heated

at $\sim$ 15 deg. K h^{-1} in runs of from 2 to 12 deg. K. The precision of the measurements has been estimated to be better than $\pm 0 \cdot 2$ per cent up to about 450°K; at higher temperatures errors may have approached $\pm 0 \cdot 4$ per cent.

(c) Other measurements

Melting point depression measurements were undertaken to obtain the heat of fusion, ΔH_f, of completely crystalline material. Mixtures of P4MP ($\sim$ 1 g) and 1-chloronaphthalene (up to $\sim$ 30 volume per cent) were heated above the melting point in evacuated sealed tubes and then slowly cooled. Sections of about 2 to 5 mg were cut from the resulting plug of polymer and diluent, and the melting point of these determined on a differential scanning calorimeter (Perkin–Elmer DSC-1). The measurements were repeated with samples taken from various parts of the plug to test homogeneity.

X-Ray diffraction patterns were obtained, in reflection, with a General Electric XRD-5 diffractometer, using pressed samples of P4MP powder.

RESULTS

Three series of measurements were made, though two of these extended over only part of the available temperature range. The results are given in *Tables 1* to *3*.

(a) Series I

The heat capacity of the sample, dried under vacuum but otherwise as received, was measured from 77°K to 424°K. The heat capacity versus temperature curve (*Figure 1*) is completely smooth up to about 300°K, at which temperature there is a marked rise in C_p, indicative of the glass transition. Further heating revealed an irregularity in the C_p/T plot between 380° and 410°K, consisting of an anomalous rise in C_p of about 0·7 per cent

Table 1. Heat capacity of P4MP. Series I

T_{av}, °K	C_p, $J\,°K^{-1}g^{-1}$	T_{av}, °K	C_p, $J\,°K^{-1}g^{-1}$	T_{av}, °K	C_p, $J\,°K^{-1}g^{-1}$
79·597	0·560	204·777	1·205	314·511	1·900
84·101	0·582	216·245	1·264	317·985	1·930
91·166	0·624	224·950	1·307	321·763	1·950
100·113	0·677	230·683	1·335	326·425	1·990
108·459	0·726	236·812	1·360	337·900	2·064
115·125	0·764	240·657	1·383	343·344	2·074
119·887	0·791	246·143	1·417	348·754	2·134
124·918	0·818	257·007	1·476	357·312	2·183
131·139	0·849	267·939	1·536	368·086	2·251
138·299	0·887	275·964	1·576	377·302	2·309
145·947	0·925	283·420	1·623	384·468	2·383
154·013	0965	289·610	1·658	391·307	2·425
161·318	1·000	293·474	1·707	395·672	2·456
168·036	1·033	296·403	1·705	400·107	2·468
175·910	1·070	300·028	1·757	406·530	2·504
183·181	1·104	305·983	1·805	413·854	2·539
191·263	1·145	311·226	1·875	420·553	2·573

Table 2. Heat capacity of P4MP. Series II

T_{av}, °K	C_p, J °$K^{-1}g^{-1}$	T_{av}, °K	C_p, J °$K^{-1}g^{-1}$	T_{av}, °K	C_p, J °$K^{-1}g^{-1}$
265·095	1·514	373·169	2·262	470·989	2·814
272·895	1·561	378·482	2·302	477·086	2·867
280·039	1·603	382·896	2·321	482·377	2·918
285·873	1·634	386·536	2·341	487·252	3·016
291·071	1·675	390·306	2·366	492·261	3·138
296·285	1·705	394·856	2·398	496·460	3·119
300·247	1·748	400·939	2·437	500·115	3·262
304·076	1·787	406·791	2·478	503·655	3·463
307·484	1·851	413·416	2·512	506·911	3·557
310·549	1·873	420·610	2·564	510·118	4·015
314·705	1·908	427·530	2·627	513·076	5·057
321·634	1·953	433·863	2·692	515·680	6·881
331·029	2·007	439·123	2·725	518·299	5·142
342·959	2·083	443·365	2·864	521·349	3·234
352·093	2·134	446·808	2·822	524·962	2·99⁚·
357·759	2·182	450·529	2·728	529·057	2·993
363·456	2·189	454·771	2·714	533·087	3·018
367·933	2·243	459·577	2·716	536·725	3·047

relative to the baseline. The anomaly, although very small, was outside experimental error. No unusual temperature drifts were measured during the calorimeter equilibration periods in this temperature region, though such drifts have been frequently encountered just below melting points and sometimes around glass transitions, and are indications of molecular reorganization within a polymer.

To examine the characteristics of the anomaly further, the sample was cooled, at 10 deg. K h⁻¹, to 261°K, and the measurements repeated.

Table 3. Heat capacity of P4MP. Series III

T_{av}, °K	C_p, J °$K^{-1}g^{-1}$	T_{av}, °K	C_p, J °$K^{-1}g^{-1}$	T_{av}, °K	C_p, J °$K^{-1}g^{-1}$
98·204	0·673	316·208	1·935	451·983	2·706
104·290	0·708	321·380	1·968	458·938	2·748
108·310	0·733	326·730	1·992	467·409	2·801
111·653	0·749	333·402	2·028	474·574	2·839
127·764	0·831	346·830	2·104	482·015	2·912
148·929	0·942	365·271	2·207	490·052	3·013
168·882	1·038	376·930	2·278	495·229	3·074
202·054	1·195	382·759	2·307	500·325	3·238
242·224	1·406	387·750	2·337	505·672	3·378
267·233	1·533	394·095	2·369	510·290	3·777
275·163	1·574	401·546	2·409	514·218	5·325
281·264	1·641	408·587	2·454	517·005	7·757
288·133	1·661	415·493	2·477	519·944	3·375
294·910	1·702	423·619	2·548	523·660	2·985
301·868	1·785	430·288	2·586	527·949	2·998
307·743	1·892	436·702	2·618	532·931	3·010
311·536	1·901	444·632	2·665	538·599	3·038
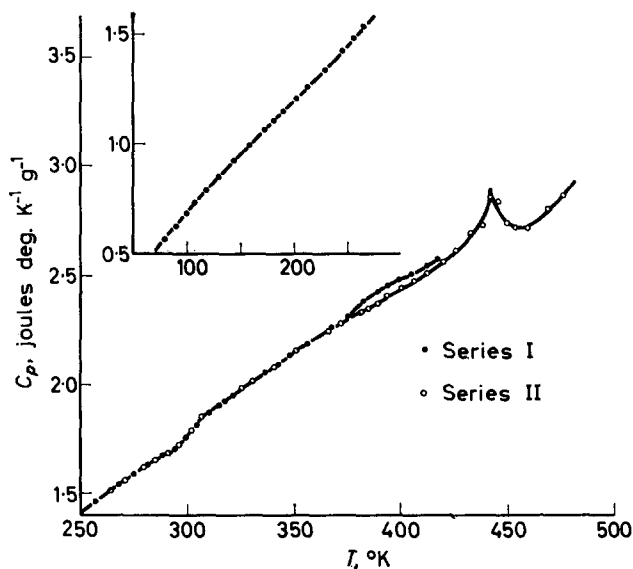
Figure 1—Heat capacity of P4MP at lower temperatures.
For identification of samples, see text

(b) *Series II*

Results up to 380°K were virtually identical to those obtained in the first series of measurements. Particular attention was, of course, paid to the 380° to 410°K region, but the C_p/T plot turned out to be completely smooth (*Figure 1*), with no sign of the previously observed irregularity.

Evidence of a much larger transitional phenomenon was found at about 445°K. This had the qualitative appearance of a polymer melting curve, though the area beneath the peak corresponding to the transition enthalpy, ΔQ_{tr}, was small, about 2·0 joules (J) g^{-1}. Substantial negative temperature drifts equivalent to heat changes of up to 0·5 J h^{-1} g^{-1}) were found on the low-temperature side of the peak.

Above this secondary peak the main melting transition was observed, starting at ∼ 470°K. The maximum melting point was 522°K. The heat of fusion, ΔQ_f, and other thermodynamic data for these measurements, are summarized in *Table 4*.

(c) *Series III*

The molten polymer was cooled, at about 10 deg. K h^{-1}, and the measurements repeated from 95°K.

This annealed sample again showed no substantial difference relative to the previous measurements at low temperatures, but T_g was about 5 deg. K lower. Above T_g the most important difference was the absence of both of the anomalies observed previously. The C_p curve as shown in *Figure 2* rises smoothly into the melting peak, with a maximum melting temperature of 522°K, as before. Above T_m the measurements were in good agreement with those of series II.

550

Table 4. Summary of thermodynamic properties of P4MP

Series	T_g, °K	$\Delta C_p(T_g)$ J °K^{-1} g^{-1}	Intermediate transitions, °K
I (as received)	307	0·055	390
II (cooled from 423°K)	307	0·050	445 ($\Delta Q_{tr} \sim 2$ J/g)
III (cooled from 538°K)	303	0·060	None

	T_m	ΔQ_f, J/g	Crystallinity Calorimetric	X-Ray
II	522	35·8	0·29	0·40
III	522	34·3	0·28	—

Results of the melting point depression experiments, and of the X-ray diffraction studies, are included in the discussion below.

DISCUSSION

(a) *Low temperature behaviour*

In common with many other polymers, P4MP exhibits a dynamic mechanical loss peak at low temperatures. In P4MP this occurs at about 150°K (at frequencies of $1·6 \times 10^3$ c/s[6] and $9·03 \times 10^3$ c/s[10]), and has been attributed to the onset of cooperative rotational or librational side-group motion in the amorphous portions of the polymer. Some n.m.r. data similarly indicate, through second moment and line width decreases between 77° and 100°K, that some internal motion is beginning at these temperatures[11].

The present heat capacity measurements, however, do not show any manifestation of this relaxation in the temperature region of interest, or indeed, at any temperature between 77°K and T_g.
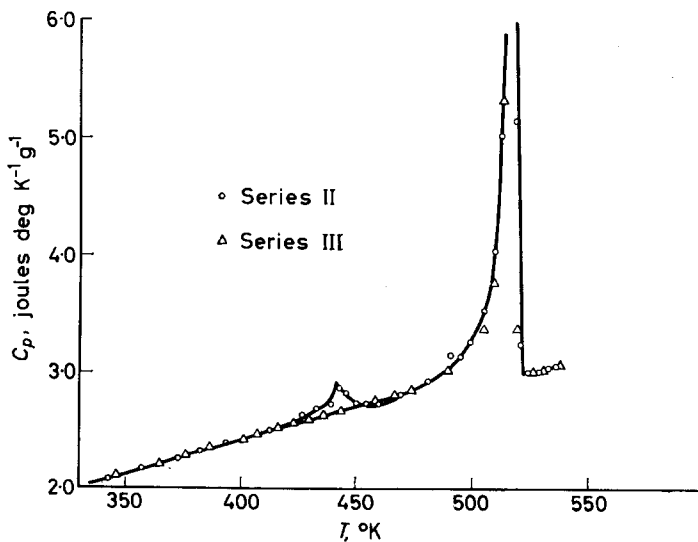
Figure 2—Heat capacity of P4MP, including the melting region

551

In the mechanical measurements, the transition is indicated by a relatively abrupt change in the slope of E', the elastic storage modulus, with temperature, and therefore a corresponding change in the slope of C_p might have been expected. It is possible that this is concealed by the slight curvature in the C_p/T plot which still persists at 150°K, or that, as is suggested by the n.m.r. data, the onset of the motion is relatively diffuse, which again would make the transition more difficult to detect. This absence is not entirely unexpected, in view of similar results for other polymers, for example, atactic polystyrene[12], and poly(4',4'-dioxydiphenyl-2,2-propane carbonate)[13], in which low temperature side-group or backbone motion is postulated, but is not revealed in heat capacity measurements. Possible reasons for the lack of correlation have been discussed elsewhere[7].

(b) T_g region

The glass temperature of P4MP is clearly indicated in all three series by a discontinuous rise in C_p. The centre of the transition lies at about 307°K in the Series I (as received) and Series II (polymer cooled from 420°K) measurements, while in Series III (sample annealed from melt), T_g is slightly lower, the centre lying at 303°K. The shift is probably a result of annealing, and the use of different heating schedules may also have contributed. Rånby et al.[4] have observed values of T_g ranging from 287° to 301°K, and have correlated these to the respective crystallinities.

In the present measurements, the crystallinity of the samples used in Series II and III are essentially the same (see below) and on Rånby's scale would correspond to a T_g of 297°K. The agreement between Rånby's and our results is satisfactory when it is considered that different initial samples, techniques and, in all probability, different crystallinity scales were employed.

(c) Transitions between T_g and T_m

We now consider the two anomalous regions in the heat capacity curve between T_g and T_m, lying at about 390°K and 445°K, respectively. Earlier dilatometric[1], X-ray[4] and dynamic mechanical (but not n.m.r.[14]) measurements[1,4,5] also indicated some anomalous behaviour in this general region, but there is disagreement as to the origin of the phenomena. Thus Griffith and Rånby[1] observed a dynamic mechanical loss peak around 450°K and possibly at 400°K (at $\sim$ 100 c/s), while Penn[5] found a single broad maximum in the compliance at about 400°K (at $\sim$ 1 c/s). Kirschenbaum et al.[15] refer to, but do not discuss, a similar peak in the same temperature region. In dilatometric measurements Griffith and Rånby[1] found a slight change in the slope of the volume/temperature curve at 400°K, which would indicate, therefore, a second-order transition and, in later X-ray measurements of the lattice parameters of P4MP, Rånby et al. observed a change in the slope of the unit cell parameters a and c as a function of temperature at $\sim$ 400°K[4]. However, it should be noted that in the dilatometric measurements the transition becomes more pronounced as the crystallinity is reduced, whereas one would expect the opposite result if the crystalline phase were responsible for the change.

The anomaly observed in our calorimetric measurements at 390°K could be related to one of the transitions previously observed. However, the temperatures are not in very good agreement; furthermore, the effect we observe is very small. It seems more probable that the latter is an artefact, possibly connected with the release of strains in the compacted sample. The irreversibility of the phenomenon, that is the fact that it was completely removed by heating to 420°K, lends some support to this hypothesis.

The transition centred at 445°K is more readily explained. It is a much larger effect, and from the shape of the heat capacity curve, it appears to be almost certainly a smeared-out first-order transition, qualitatively analagous to a polymer melting peak. As already mentioned, the measurements in this region were accompanied by substantial temperature drifts in the calorimeter indicative of relatively slow equilibration, furthering the analogy to a fusion process. We attribute this to the melting (or possibly the solid–solid transformation) of a small quantity of a polymorphic form of P4MP, present in the original sample. To substantiate this postulate, X-ray diffraction patterns of the sample as a function of temperature were obtained (*Figure 3*). This figure shows the scattering diagram obtained at room
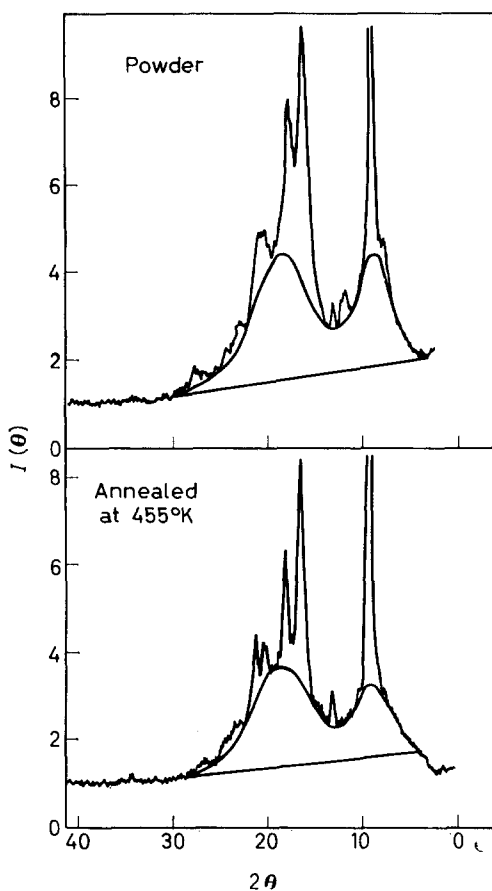
Figure 3—X-Ray diffractometer tracings of P4MP. Division of pattern into amorphous and crystalline scattering areas indicated

temperature and after 30 minutes annealing at 455°K. Apart from some change in relative intensities of the major peaks due to dimensional changes of the sample and possibly to the release of strains, some other differences are observed, including the disappearance of a peak at $2\theta = 12°$. The latter does not reappear on cooling, but cannot be removed by annealing at any lower temperature. We suggest that it is due to a polymorphic component, whose other diffraction maxima are possibly concealed by those of the major component. The relatively small quantity of heat involved in the transition (2 J g^{-1}) suggests that the amount of polymorph present is only a few per cent, especially if the transition is due to melting (as distinct from a solid–solid transformation). Polymorphism is especially prevalent in the higher poly-α-olefins and has been studied in some detail, for example, in polybutene-1[16]. Gallegos[17] has found evidence from optical measurements for the existence of three polymorphic forms in the P4MP isomer, poly-3-methyl-pentene-1. The formation of such metastable crystalline modifications is typically very sensitive to the precise thermal and solvent history, and therefore, as in the present instance, it is not surprising that the minor constituent apparently is not re-formed either on cooling from 455°K or from the melt. Finally, in this connection, we note that the melting of a minor polymorphic component, as suggested above, is at least consistent with the appearance of a loss peak at 450°K in the dynamic mechanical measurements of Griffith and Rånby already noted[1].

(d) Crystallinity

The experimental heats of fusion, ΔQ_f, of the samples in the series II and III measurements were $35\cdot8 \pm 1\cdot5$ J g^{-1} and $34\cdot3 \pm 1\cdot5$ J g^{-1}, respectively. Most of the uncertainty arises from the difficulty of assigning a baseline to the melting peak which represents the true heat capacity of the melting crystal–liquid mixture.

The crystallinity, x, is given by $\Delta Q_f / \Delta H_f$, where ΔH_f is the heat of fusion of the hypothetical completely crystalline material. Results of measurements of the melting-point depression of P4MP–1-chloronaphthalene mixtures are shown in *Figure 4* plotted in the customary manner, $(1/T_m - 1/T_m^0)/v_1$ versus v_1/T_m[18], where T_m^0 is the melting point of pure P4MP, and T_m that of a mixture containing a volume fraction v_1 of diluent. From the intercept we derive $\Delta H_f = 122 \pm 12$ J g^{-1}. This value for ΔH_f of P4MP is in good agreement with one of the two values reported by Isaacson et al.[19], 125 J g^{-1} and 142 J g^{-1}. Although details of the measurements resulting in the former value are not given, it is implied that this is preferred.

The calculated fractional crystallinities of the samples melted in the series II and III measurements are thus 0·29 and 0·28 respectively. It follows that the annealing process in the calorimeter did not materially change the crystallinity of the polymer.

Because of its unusual volumetric behaviour (see below), the crystallinity of P4MP cannot be determined from density measurements at room temperature with any worthwhile accuracy. The X-ray crystallinity was determined from the integrated scattering intensities from $2\theta = 5°$ to $2\theta = 30°$. A smooth amorphous scattering curve was drawn tangentially to the total

scattering at several points between the crystalline peaks (see *Figure 3*). We found it impossible to change the crystallinity of samples significantly by quenching thin films, annealing or solvent treatment, and therefore the crystallinity was calculated simply from the ratio of the crystalline scattering area to total crystalline and amorphous scattering areas. The calorimetric results are only in fair agreement with the X-ray value of 40 per cent
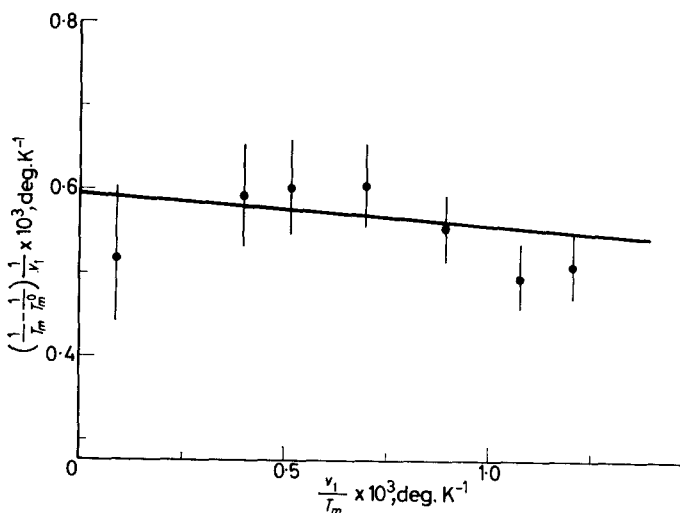
Figure 4—Melting points of P4MP–1-chloronaphthalene mixtures

for the series II sample, but Hermans[20] and co-workers have shown that the actual crystallinity may be less than calculated because the normalized crystalline scattering is usually greater than the normalized amorphous scattering.

The calorimetrically determined melting point of 522°K is in excellent agreement with that observed by Griffith and Rånby[1] (523°K), but is somewhat higher than those of Isaacson *et al.*[19] (511° to 517°K) or of Reding and Walter[21, 22] (508° to 513°K). Earlier measurements have reported much lower melting points, 475° to 479°K[2] and 478°K[23].

(e) *Configurational properties at T_g*

The property of P4MP that has perhaps received the most attention is connected with the abnormal volumetric behaviour. Several studies have shown that around room temperature (i.e. at T_g) the density of the amorphous polymer is greater than that of semicrystalline P4MP[1-4]. Formally this arises simply from the circumstance that

$$V_a(T_g) \int_{T_g}^{T_m} \alpha_a(T)\, \mathrm{d}T > V_c(T_g) \int_{T_g}^{T_m} \alpha_c(T)\, \mathrm{d}T + \Delta V_f$$

where $\alpha_a(T)$ and $\alpha_c(T)$ are the expansion coefficients of the amorphous and crystalline phases, respectively, $V_a(T_g)$ and $V_c(T_g)$ are the specific

volumes at T_g, and ΔV_f is the volume of fusion. Since $\alpha_a(T)$ is always greater than $\alpha_c(T)$ above T_g, this inequality in itself is not implausible, and the phenomenon has been explained morphologically on the basis of an unusual openness of the crystal structure relative to the amorphous phase[2, 24]. In the poly-α-olefin series, considering polymers of ethylene, propylene, 3-methyl-butene-1 and 4-methyl-pentene-1, Pritchard has pointed out that the amorphous densities at room temperature decrease much more slowly with increasing monomer molecular weight than do the crystalline densities, and a 'cross-over' at P4MP is not unexpected from this empirical approach[25].

Thermodynamically, however, the anomaly is less easy to explain, particularly with respect to theories of the glassy state. In the Gibbs–DiMarzio treatments, for example, a positive configurational entropy at T_g, $\Delta S_g(T_g)$, $[\equiv S_{(glass)} - S_{(crystal)}]$, is a principal requirement[12]. Since some parallelism might be expected between the entropy and volume[36], a negative result for the configurational contributions to either of these first-order quantities is surprising. In the theory of Gutzow this point is even more firmly established, because in this theory $\Delta S_g(T_g)$ is an explicit function of the ratio of the glassy and crystalline specific volumes at T_g[27].

As an explanation for the apparent anomaly, we suggest that the properties of two different isomers have been compared. During the course of the present work, it was established that the P4MP used (i.e. a sample of about 30 per cent maximum crystallinity) could not be thermally quenched sufficiently rapidly, using the usual techniques, to attain a completely amorphous sample. It seems likely that this applies generally for this polymer, and that the amorphous samples of P4MP used in the various dilatometric measurements have been extracted from the partially crystalline polymer. (This, in fact, is explicitly stated by Rånby et al.[4].) Hoffman et al.[28] amongst others, have shown the Ziegler polymerization of 4-methyl-pentene-1 produces samples containing atactic as well as stereoregular, presumably isotactic, materials. It may be argued further that the extracted samples are therefore atactic, while the crystallizable P4MP is at least partially stereoregular. If this is so, then the anomalous density behaviour may arise simply from the fact that the bulk properties of two distinct isomers are being compared, and it is not implausible that these are intrinsically different. A well-known example of such divergence is the T_g and density behaviour of the various polymethyl methacrylates[29]. It is suggestive also that the specific volumes of the amorphous and of a highly crystalline P4MP sample *above T_m*, as shown in Figure 2 of ref. 1, differ by about one per cent, a discrepancy which is apparently outside experimental error. This may possibly be considered as some substantiation for the above hypothesis; obviously no difference could be observed if the variation in properties of the two fractions were due solely to crystallinity.

It is of interest, therefore, to examine the temperature dependence of the entropy and enthalpy for this polymer, and to determine whether an anomaly similar to the specific volume behaviour exists. For semicrystalline P4MP, the appropriate heat capacity functions can be integrated directly, using the data obtained in the present study. However, the re-

quired heat capacity data for the amorphous phase are not available (except above T_m), and the temperature dependence of C_p^a, the heat capacity of the totally amorphous polymer, has to be estimated in part.

First, it may be reasonably assumed that the heat capacities of the two forms above T_m and below T_g are equal, and that, at the relatively high temperatures under consideration, C_p^a is a linear function of temperature above T_g. T_g itself for the amorphous material has been well established; therefore the remaining quantity necessary to define C_p^a over the temperature range of interest is the change in heat capacity at T_g, $\Delta C_p^a(T_g)$. There are several possible approaches for estimating the latter: (a) a relatively long extrapolation of the available C_p^a data for the liquid from above the melting point; (b) use of Wunderlich's 'bead' model[30]; or (c) calculating ΔC_p^a from measured ΔC_ps for material of known crystallinity. Using the first method we estimate $\Delta C_p^a(T_g) = 0.4 \pm 0.05$ J $°K^{-1}$ g^{-1}. In the 'bead' model calculation there is difficulty in deciding *a priori* the number of 'beads' per monomer unit; basing the choice on criteria used in other polymers, it is estimated that there are either three or four 'beads', this resulting in $\Delta C_p^a(T_g)$ of 0.40 and 0.53 ± 0.10 J $°K^{-1}$ g^{-1}, respectively. If one uses values of x, the fractional crystallinity obtained from the heat of fusion, and the two-phase model equation, i.e. $\Delta C_p^a(T_g) = \Delta C_p^x(T_g)/(1-x)$, where $\Delta C_p^x(T_g)$ is the observed change in heat capacity at T_g for the partially crystalline samples, then inordinately low values of $\Delta C_p^a(T_g)$ are obtained. This is a reflection of a 'suppressed' ΔC_p^x, a phenomenon encountered in several other polymeric systems, and discussed elsewhere[31].

Through the courtesy of Dr R. S. Porter and the Chevron Research Corp. we obtained a sample of amorphous P4MP (a hexane extract) and were able to measure $\Delta C_p^a(T_g)$ directly using the Perkin–Elmer scanning calorimeter. A value of 0.35 ± 0.06 J $°K^{-1}$ g^{-1} was obtained, though for unknown reasons there were some problems in achieving reproducibility. Taking into account the various estimates, a final value of $\Delta C_p^a(T_g) = 0.4$ J $°K^{-1}$ g^{-1} was adopted.

The resulting enthalpies and entropies for the amorphous and semi-crystalline P4MP are shown in *Figures 5* and *6*. For these calculations, the data acquired in the series III measurements ($x = 0.29$) were used, and the starting temperature of these measurements, $95.563°K$, was taken as the arbitrary zero for the enthalpy and entropy of the semicrystalline polymer. It was initially assumed, also, that the thermodynamic properties for amorphous and crystalline P4MP were the same above T_m. On this basis, it is obvious that the configurational enthalpy and, especially, the entropy, are very small at T_g. This is further demonstrated in *Figure 7* which shows $\Delta S_g(T)$ as a function of temperature. [In these calculations, of course, an error in the assumed $\Delta C_p^a(T_g)$ would affect the results, as is shown in *Figure 7*, but not enough to vitiate the present argument.]

Thus, it may be concluded from *Figure 7* that with the assumptions made above the configurational entropy at (or below) T_g is exceptionally small in comparison, for example, with that of polypropylene[32], polystyrene[12], or
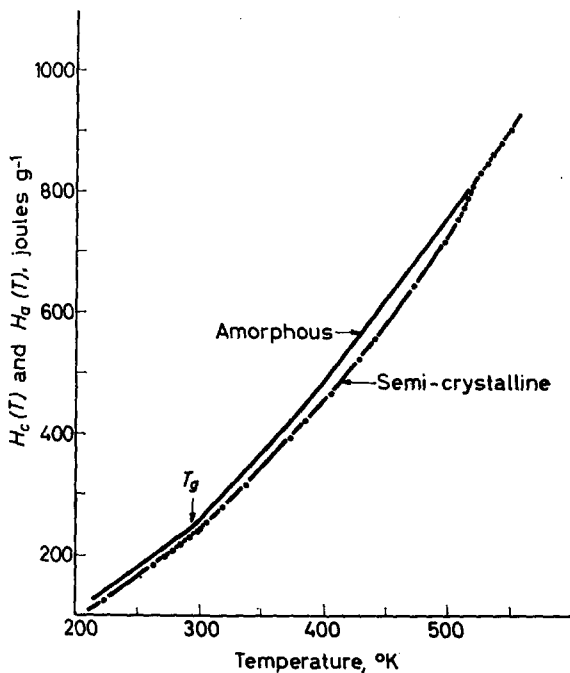
Figure 5—Enthalpies of semicrystalline $[H_c(T)]$ and of amorphous $[H_a(T)]$ P4MP. For assumptions used in calculating $H_a(T)$, see text
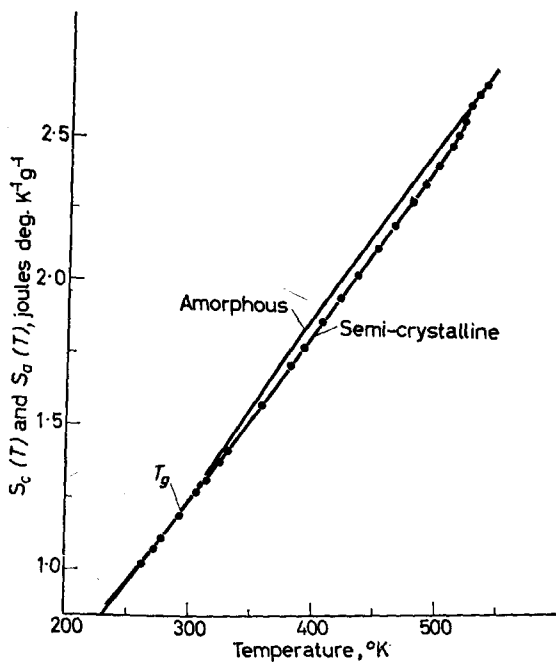
Figure 6—Entropies of semicrystalline $[S_c(T)]$ and of amorphous $[S_a(T)]$ P4MP

558

isotactic polymethyl methacrylate[33]. In these systems $\Delta S_g (T_g)$ is 9 ± 3 J °K^{-1} mole^{-1} of monomer (referred to a wholly crystalline sample), compared to somewhat less than 1 J °K^{-1} (monomer mole)$^{-1}$ for P4MP. The significance of this fact can be expressed in several different ways. In terms of the Gibbs–DiMarzio theory[26], for example, one may use $\Delta S_g (T_g)$ to calculate the difference between the observed glass temperature and T_2, the asymptotic 'thermodynamic' glass temperature, using the approximation

$$T_g - T_2 \sim T_g \, \Delta S_g \, (T_g)/\Delta C_p^a$$

For P4MP an anomalously low value for $T_g - T_2$ is obtained. In other systems values ranging from 30° to 80°K are found[34] in agreement with the Gibbs–DiMarzio theory which suggests about 50°K for the difference [or,
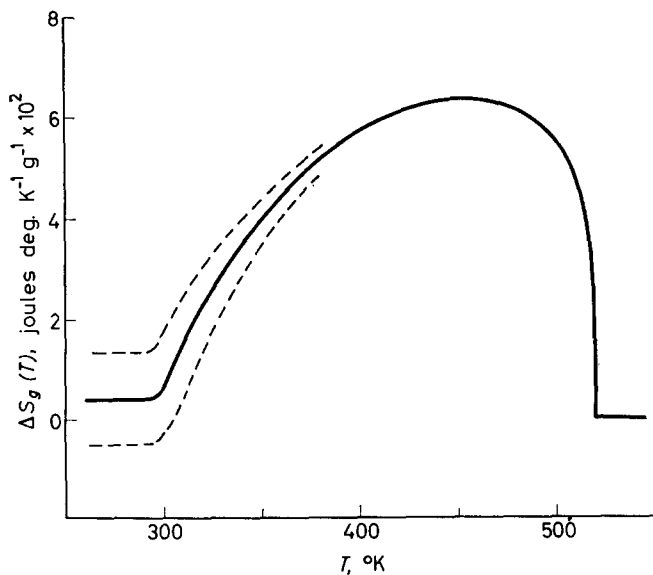
Figure 7—Configurational entropy of P4MP, calculated as difference between entropies of amorphous and semicrystalline samples, and assuming equality above T_m. Dashed lines indicate effect of changing $\Delta C_p^a (T_g)$ by ± 10 per cent

in the Gibbs–Adam[35] kinetic approach, a $T_g/T_2 \sim 1\cdot3$ is predicted; in the temperature range of interest in this study, these predictions are equivalent within the error limits]. As there is no reason to suppose that amorphous P4MP is any closer to thermodynamic equilibrium than other glassy polymers that have been studied, one is led to conclude that the equivalence of the entropies of the crystalline and the amorphous polymer above T_m cannot be assumed. This can only be the case, however, if different isomers are under consideration, and hence supports our contention regarding the origin of the specific volume (and entropy) anomalies.

CONCLUSION

Measurements of the heat capacity have provided new information regarding two unusual aspects of the solid state behaviour of P4MP. There is some evidence for the existence of a polymorphic form of P4MP present, at least in the sample used in this study, in relatively small amounts. The

magnitude of the calculated configurational entropy, taken in conjunction with current theories of glass formation, supports the suggestion that the anomalous volume behaviour is essentially an effect of tacticity. This postulate could be investigated further by additional dilatometric studies of the two isomers. In other respects the thermodynamic properties of P4MP are typical of a semicrystalline polymer.

REFERENCES

[1] GRIFFITH, J. H. and RÅNBY, B. G. *J. Polym. Sci.* 1960, **44**, 369
[2] FRANK, F. C., KELLER, A. and O'CONNOR, A. *Phil. Mag.*, Series VIII, 1959, **4**, 200
[3] LITT, M. *J. Polym. Sci. A*, 1963, **1**, 2219
[4] RÅNBY, B. G., CHAN, K. S. and BRUMBERGER, H. *J. Polym. Sci.* 1962, **58**, 545
[5] PENN, R. W. *J. Polym. Sci. A-2*, 1966, **4**, 559
[6] WOODWARD, A. E., SAUER, J. A. and WALL, R. A. *J. Polym. Sci.* 1961, **50**, 117
[7] O'REILLY, J. M. and KARASZ, F. E. *J. Polym. Sci. C*, 1966, **14**, 49
[8] GOODRICH, J. E. and PORTER, R. S. *J. Polym. Sci. B*, 1964, **2**, 353
[9] KARASZ, F. E. and O'REILLY, J. M. *Rev. sci. Instrum.* 1966, **37**, 255
[10] CRISSMAN, J. M., SAUER, J. A. and WOODWARD, A. E. *J. Polym. Sci. A*, 1964, **2**, 5075
[11] WOODWARD, A. E., ODAJIMA, A. and SAUER, J. A. *J. phys. Chem.* 1961, **65**, 1384
[12] KARASZ, F. E., BAIR, H. E. and O'REILLY, J. M. *J. phys. Chem.* 1965, **69**, 2657
[13] O'REILLY, J. M., KARASZ, F. E. and BAIR, H. E. *J. Polym. Sci. C*, 1964, **6**, 106
[14] CHAN, K. S., RÅNBY, B. G., BRUMBERGER, H. and ODAJIMA, A. *J. Polym. Sci.* 1962, **61**, S29
[15] KIRSCHENBAUM, I., ISAACSON, R. B. and DRUIN, M. *J. Polym. Sci. B*, 1965, **3**, 525
[16] NATTA, G., CORRADINI, P. and BASSI, I. W. *Atti Accad. Lincei, RC, Cl. Sci. Fis. Mat. Nat.* 1955, **19**, 404
[17] GALLEGOS, E. J. *J. Polym. Sci. A*, 1965, **3**, 3982
[18] FLORY, P. J. *Principles of Polymer Chemistry*, p 568. Cornell University Press: Ithaca, N.Y., 1953
[19] ISAACSON, R. B., KIRSCHENBAUM, I. and FEIST, W. C. *J. appl. Polym. Sci.* 1964, **8**, 2789
[20] HERMANS, P. H. *Experientia*, 1963, **19**, 553
[21] REDING, F. P. *J. Polym. Sci.* 1956, **21**, 547
[22] REDING, F. P. and WALTER, E. R. *J. Polym. Sci.* 1959, **37**, 555
[23] NATTA, G., PINO, P., MAZZANTI, G., CORRADINI, P. and GIANNINI, U. *Atti Accad. Lincei, RC, Cl. Sci. Fis. Mat. Nat.* 1955, **19**, 397
[24] CLARK, K. J. and PALMER, R. P. *Symposium on the Chemistry of Polymerization Processes*, Paper 5. Society of the Chemical Industry: London, 1966
[25] PRITCHARD, R. *S.P.E. Trans.* 1964, **4**, 66
[26] GIBBS, J. H. and DiMARZIO, E. A. *J. chem. Phys.* 1958, **28**, 373
[27] GUTZOW, I. *Z. phys. Chem.* 1963, **221**, 153
[28] HOFFMAN, A. S., FRIES, B. A. and CONDIT, P. C. *J. Polym. Sci. C*, 1963, **4**, 109
[29] SHETTER, J. A. *J. Polym. Sci. B*, 1963, **1**, 209
[30] WUNDERLICH, B. *J. phys. Chem.* 1960, **64**, 1052
[31] O'REILLY, J. M. and KARASZ, F. E. Presented at 148th Meeting of the American Chemical Society, Chicago, Ill., August 1964; *Polymer Preprints*, 1964, **5**, 351
[32] PASSAGLIA, E. and KEVORKIAN, H. G. *J. appl. Phys.* 1963, **34**, 90
[33] O'REILLY, J. M., KARASZ, F. E. and BAIR, H. E. *Bull. Amer. phys. Soc.* 1964, **9**, 285
[34] BESTUL, A. B. and CHANG, S. S. *J. chem. Phys.* 1964, **40**, 3731
[35] ADAM, G. and GIBBS, J. H. *J. chem. Phys.* 1965, **43**, 139

Polymerization on Glass-supported Vanadium Trichloride: Morphology of Nascent Polyethylene*

H. CHANZY†, A. DAY and R. H. MARCHESSAULT

A method is described for depositing vanadium trichloride crystals on glass surfaces. Subsequent treatment with aluminium triethyl yields a planar supported catalyst for polymerization of polyethylene. Coherent polyethylene membranes ranging in thickness from a few hundred Ångström units to tens of microns could be polymerized on to the glass surface and examined by physical techniques. As the polyethylene was synthesized in a non-solvent medium (heptane or gas phase) then the resultant crystalline polymer must have been polymerized and crystallized simultaneously. Material from such a process is termed 'nascent' polymer, and its morphology was extensively examined by microscopic and radiation scattering techniques. X-ray and birefringence studies showed a preferred chain orientation in the membranes: chains were parallel to the substrate. The presence of significant anisotropic scattering and a DTA melting point of 141°C lead to the postulate that the nascent polyethylene chains are completely extended. Transmission and replica electron microscopy has led to description of the nascent morphology in terms of a proliferous, polyp-like structure.

RELATIVELY few papers have been published on the morphology of nascent polyolefins, i.e. stereoregular polymers where the growth conditions are such that synthesis and crystallization are nearly simultaneous. When this occurs, one can consider that crystallization is literally part of the overall polymerization mechanism and the free energy contribution could even determine whether or not the reaction takes place. The meagre information in the literature indicates that nascent polyolefins have unusual and somewhat contradictory physical properties[1,2]. If these can be explained, a better understanding of the catalyst mechanism as well as the crystallization process can be expected. Moreover, other systems involving the coordination of a monomer to a crystalline polymer, as is usually postulated in the biological synthesis of macromolecules, can be clarified as their mechanisms involve simultaneous polymerization and crystallization.

During polymerization with a crystalline transition metal catalyst, the chains of growing polymer usually stay adsorbed on the surface of the catalyst crystal[3,4]. If the catalyst crystals are chemisorbed on the surface of a substrate, the growing polymer will still coat the catalyst and under certain conditions, depending on the amount of chemisorbed catalyst, will cover the substrate with a layer of polymer[5]. This phenomenon is operative when flat glass substrates are used as support for a transition metal

catalyst suitable for polymerization of ethylene. This was done in this study, and nascent polyethylene could thus be obtained in the form of films for morphological characterization which was the goal of this investigation.

<div align="center">EXPERIMENTAL</div>

Chemicals and substrates

n-*Heptane*—Reagent grade heptane was washed with sulphuric acid until no further coloration was obtained in the acid layer. It was then stored over anhydrous calcium chloride and distilled through an efficient column. The fraction boiling at 98°C was collected and stored over sodium wire.

Aluminium triethyl—A ten per cent solution of aluminium triethyl in heptane from Ethyl Corporation was used without further purification. Aluminium determination served to establish the reagent concentration.

Vanadium(IV) *chloride*—Fresh vanadium(IV) chloride from K and K Laboratories was used without further purification. On standing for a few months, chemical decomposition occurred as shown by chlorine evolution, and vacuum redistillation was necessary prior to some of the later polymerizations.

Ethylene—Research grade ethylene from Matheson (99·9 per cent pure) was generally used without further purification.

Nitrogen—'High purity dry nitrogen' from Linde was used to create an inert atmosphere in the dry box or polymerization containers.

Glass—Precleaned microscope slides from Fisher Scientific were washed for five minutes with five per cent hydrofluoric acid solutions in water. They were then dried at 120°C in an oven after rinsing in distilled water and acetone. From then on, any contact with the microscope slide surface was carefully avoided and all handling and storage contact was with the edges.

Glass fibres were pulled out of Pyrex rods. Their diameters ranged from 50 to 100 μ. They were cleaned similarly to the microscope slides.

Analysis of solutions

Vanadium was determined by the iron(II) sulphate–persulphate method[6]. Aluminium was precipitated as the hydroxide with ammonium hydroxide at controlled pH6. Chlorine was determined by the Vohlard method.

Polymerization on glass substrate

In a nitrogen filled dry box, 50 to 70 cm³ of 0·001 M vanadium(IV) chloride in heptane were brought to boiling in a 3 cm i.d. test tube fitted with a reflux condenser. A microscope slide was then dropped into the boiling solution and kept in it for a length of time ranging from one to ten minutes. During this period, small crystals of vanadium trichloride were formed and deposited on the surface of the glass slide (substrate) to which they adhered strongly. The substrate was washed thoroughly in dry heptane to remove any trace of vanadium (IV) chloride; it was then immersed in a glass container holding 150 cm³ of 0·006 M solution of aluminium

<div align="center">568</div>

triethyl in heptane, at room temperature. Ethylene was then bubbled through the solution via the fritted glass bottom of the container, and the excess was evacuated. Polymerization started immediately, and in a matter of minutes could be observed as an opalescent coating on the glass slide. Various amounts of polyethylene were thus deposited by controlling the time of monomer bubbling. The polymerization was terminated by cutting the ethylene stream, withdrawing the polyethylene encapsulated slide from the polymerization vessel and washing it in fresh heptane. It was stored edge-on inside the dry box until the end of the planned runs. Then all the encapsulated slides were removed from the dry box and submitted to further washing with dilute hydrochloric acid, water and methanol. They were stored carefully as their surface was rather delicate.

Separation of the polyethylene membranes from the substrates

The polyethylene membranes, still adhering to their glass substrates, were cut into narrow strips with a sharp knife. They were then immersed in a five per cent solution of hydrofluoric acid in water and then in distilled water where the delicate precut strips floated easily without mechanical deformation. In other cases where more coherent membranes could be obtained, the precut strips could be peeled from their glass substrate with a pair of tweezers.

Electron microscopy techniques

For replicating the vanadium trichloride deposit on the slides, a six per cent by weight polystyrene solution in benzene was dried with sodium wire and centrifuged when hydrogen bubbles were no longer evolved. A thin layer of polystyrene solution was spread on the glass slide coated with vanadium trichloride crystals. All operations took place inside the dry box. The benzene was allowed to evaporate leaving a coating of polystyrene holding a replica of the slide surface. The polystyrene coated slide was then removed from the dry box and immersed in a dish of methanol so as to strip off the intermediate replica and dissolve the deposited vanadium trichloride. After conventional chromium shadowing at 30°, a final carbon replica was obtained and examined. Due to the replica technique, resolution was no better than 40 to 50 Å.

Direct transmission electron microscopy could be achieved when polyethylene membranes were sufficiently thin. Thicker membranes were disintegrated in aqueous suspension and deposited on grids, while stretched membranes were observed directly in the electron microscope after germanium shadowing or staining with iodine. The latter method seemed to improve the contrast slightly as compared to an unstained sample.

Electron diffractograms were recorded for unstained, unshadowed material. The area covered in the electron diffraction experiments performed on stretched samples was about 100 square microns.

X-ray study

A Norelco X-ray generator with a vacuum flat film camera capable of wide and small angle resolution was used with $Cu K_a$ radiation. The wide

angle patterns were recorded at a film to sample distance of 2·5 cm, while for small angle patterns the distance was 29 cm. A chromium tube was used on occasion to increase the small angle resolution to 400 Å. Silicone fluid ($n = 1·50$) was generally used as an imbibition fluid to minimize density scattering due to the presence of voids.

Annealing

The samples to be annealed were heated from room temperature to 125°C over a period of 30 min in a nitrogen atmosphere. The final temperature was maintained for 90 min, after which the samples were allowed to cool slowly.

Light scattering measurements

Solid state light scattering was observed by using a Spectra Physics 130 continuous helium–neon gas laser. Records of the scattering patterns were made on polaroid film mounted in a Calumet camera. Two film to sample distances were used: 15·6 and 3·2 cm, which corresponded to scattering angles of 14° and 43°, respectively. The sample preparation was as follows: glass slides encapsulated on one side were prepared by removing the polyethylene from the other side. A drop of silicone fluid ($n = 1·50$) was then added and a clean glass slide pressed on the polyethylene membrane which was thus sandwiched between two glass plates. This sandwich was mounted in the sample holder of the light scattering apparatus and the pattern recorded.

Differential thermal analysis

The differential thermal analysis experiments were performed on a Perkin–Elmer DSC-1 apparatus at Rensselaer Polytechnic Institute. Various heating schedules and 'hold' temperatures were used. The observed melting points were substantiated on a Spex Industries instrument. In both cases, sample size per measurement was in the range of 1 mg. For several runs thermograms were recorded over both the ascending and descending temperature range.

RESULTS

Deposition of vanadium trichloride on glass

Vanadium trichloride was chosen as catalyst since it can be easily obtained by the slow thermal decomposition of vanadium(IV) chloride[7].

$$VCl_4 \longrightarrow VCl_3 + \tfrac{1}{2}Cl_2$$

This reaction has been used[8] to obtain a supported polymerization catalyst, which was in line with the purpose of this study. By controlling the time and the temperature of decomposition, a fine precipitate of crystalline vanadium trichloride was generated, and due to its acidity was chemisorbed on the oxygen-rich glass surface. After extensive washing to remove any loosely bound material, these trichloride coated surfaces were replicated for electron microscopy.

570

Figure 1 has been selected to illustrate the course of vanadium trichloride deposition. A glass surface (microscope slide or coverslip) is refluxed in a boiling 0·001 M solution of vanadium(IV) chloride in heptane. After 3 min of refluxing, tiny irregularities of about 100 Å dimension appear on the glass surface. After a further 2 min, a total decomposition time of 5 min, these irregularities grow into square and rectangular crystals as large as 1 000 Å. There is no doubt that these crystals are also present in the 3 min sample, but due to loss in resolution as a result of the replica technique, their sharp edges are not clearly defined. Other electron micrographs showed how a longer time of refluxing as well as more concentrated vanadium(IV) chloride solutions resulted in a thick and disorganized coating of the trichloride.

It is worth noting that at the start of deposition the vanadium trichloride crystals appear as discontinuous aggregates rather than as continuous
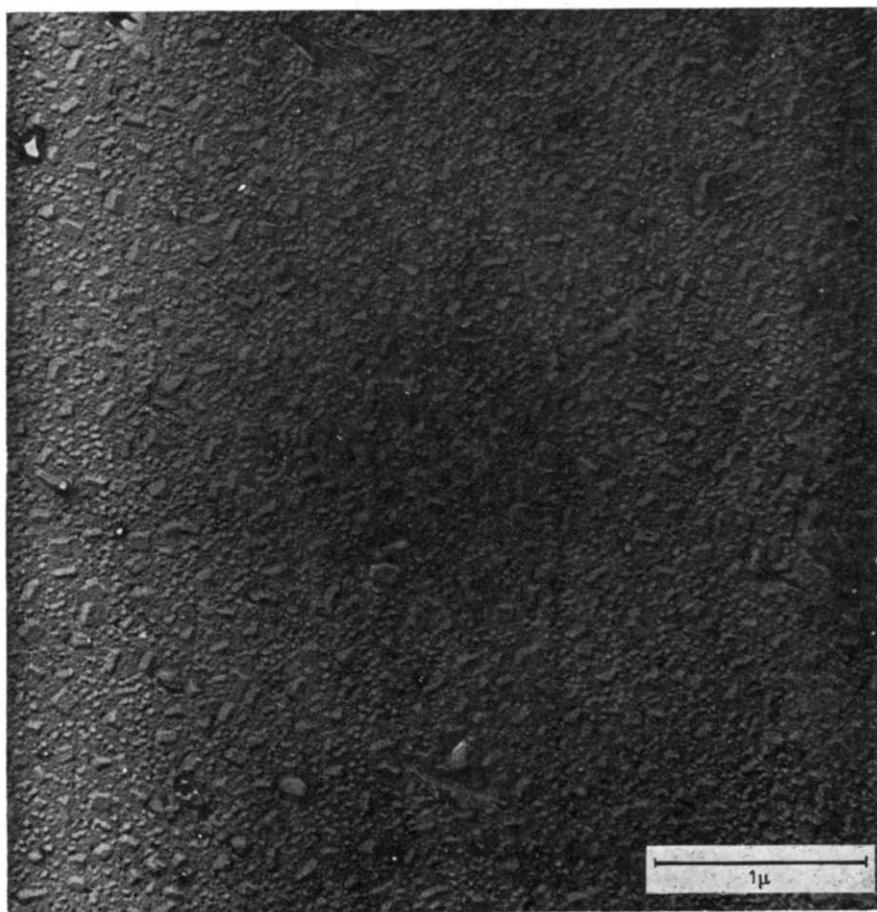
Figure 1—Electron micrograph of replicated surface of a glass slide after refluxing for 5 min in a 0·001 M solution of vanadium (IV) chloride in heptane

films. Since the surface of these crystals rather than their weight is important for subsequent polymerization, the optimum catalyst efficiency will be obtained at the point of maximum external surface for the support catalyst. This optimum will, however, correspond to many layers of trichloride as seen in *Figure 1* and as suggested by Lasky *et al.*[8] who tried to account for catalyst efficiency in a similar supported system. Another interesting fact is that the vanadium trichloride crystals are deposited on the glass as squares or rectangles. Since the trichloride crystalline lattice is hexagonal, this may be due to the growth habit of the trichloride under the experimental conditions or to an epitaxial effect of the glass substrate, a situation not yet clarified.

The crystalline nature of the deposit and its identification as vanadium trichloride could be shown at higher 'add on' levels by depositing the trichloride on pulp fibres that were sealed inside a thin-walled glass capillary. When placed in the X-ray beam, a powder X-ray diagram corresponding to crystalline vanadium trichloride was recorded from this sample[11].

As experience with these systems increased, it became clear that the initial purity of the vanadium(IV) chloride probably has an important influence on the polymer morphology. This particular point was not pursued at this time other than to observe the precaution of freshly distilling the vanadium(IV) chloride prior to its use in some of the later experiments in this study.

Nascent polyethylene films from glass supported vanadium trichloride-aluminium triethyl

Due to its high surface to volume ratio, glass supported vanadium trichloride is expected to be an efficient polymerization catalyst[9-10]. Indeed, when aluminium triethyl cocatalyst was added, polymerization of ethylene was quite rapid. In a matter of minutes, at room temperature, films of nascent polyethylene covered the glass support.

For the rapid production of a coherent polyethylene film, the amount of trichloride on the glass was found to be very critical. On the other hand, the system was insensitive to the amount of aluminium triethyl. If too much vanadium trichloride had been adsorbed on the glass, the films of nascent polyethylene adhered poorly; if insufficient, polymerization was very slow. This is in agreement with quantitative work under similar conditions on cellulose substrates[11]. Typical results are shown in *Table 1*, where only variations in the vanadium trichloride deposit are recorded as the variations in the amount of aluminium triethyl were without marked effect on the morphology of the polymer.

It was also noticed that if aged vanadium(IV) chloride was used for these experiments, poorly coherent films were obtained. This could be explained by the fact that vanadium(IV) chloride decomposes slowly to the trichloride on ageing[12] and consequently the vanadium(IV) chloride solutions prepared for decomposition already contained colloidal vanadium trichloride.

Table 1. Relationship between amount of vanadium trichloride and nascent polyethylene film formation

Deposition conditions of VCl$_3$ catalyst on glass slide	Amount of cocatalyst AlEt$_3$ (0·006 M in n-heptane), cm^3	Polymerization time at room temperature	Condition of resulting polymer
5 min refluxing 75 cm^3 0·001 M VCl$_4$ solution in heptane	150	10 min	No film formation but patches of polymer
3 min refluxing 75 cm^3 0·001 M VCl$_4$ solution in heptane	150	10 min	Film about 10 microns thick covers the glass
2 min refluxing 75 cm^3 0·001 M VCl$_4$ solution in heptane	150	20 min	Thick film obtained
1 min refluxing 75 cm^3 0·001 M VCl$_4$ solution in heptane	150	2 h	Thin film suitable for transmission electron microscopy

The films of nascent polyethylene, once removed from the glass, were white and opaque except where they were unusually thin, when they were transparent. The side that was in contact with the glass was shiny and smooth, whereas the other side had no gloss and gave the impression of a very rough surface. These films could be readily stretched and scratched yielding a fibrous texture. Film thicknesses ranged from 0·1 to 20 microns, but all films were microporous. The bulk density varied over wide limits depending on catalyst and polymerization conditions.

Morphology of the nascent polyethylene film

Light microscopy; birefringence—A typical film of polyethylene grown on a non-birefringent cylindrical glass fibre is shown in *Figure 2.* This film, with a thickness of about 8 microns when viewed between crossed nicols, is birefringent only at the edges of the glass fibre with a maximum occurring when the axis of the glass fibre is at 45° with respect to the crossed nicols.

The explanation of this observation seems to be that the crystallites or, more simply, the chains of polyethylene show preferred orientation in the plane of the film and, therefore, the substrate surface. From the angle of extinction, this direction can be either perpendicular or parallel to the glass surface. The sign of the birefringence was determined according to a Newton's colour method[13] and was found to be positive, which means that the chains of polymer tend to be aligned parallel to the substrate. That the birefringence phenomenon is not due to strain effects is shown by the fact that it is in no way affected by annealing close to the melting point.

Electron microscopy study—The accompanying electron micrographs were chosen to illustrate some of the important characteristics of the nascent polymer membranes observed in this study. *Figure 3* is a transmission micrograph of a shadowed relatively thin membrane (1 000 to 5 000 Å). The salient feature is the extreme particulate heterogeneity, a

characteristic of nearly all the samples examined in this study. This particular membrane was prepared at 80°C via a gas phase polymerization, but it is not unlike membranes prepared at room temperature in a heptane medium. The particulate character in the thinner areas of the membrane
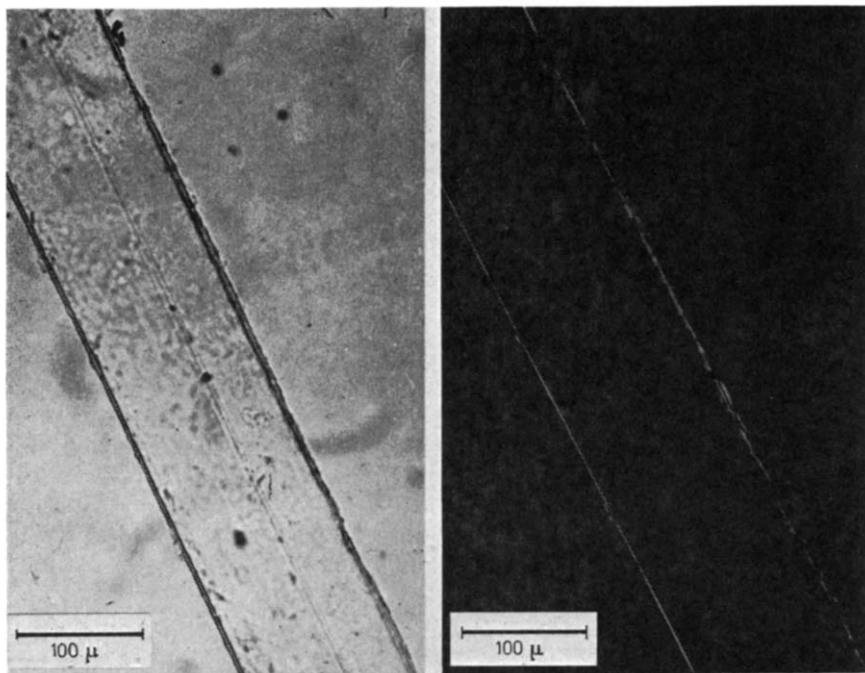
Figure 2—Photomicrograph of a glass rod encapsulated with 15 per cent polyethylene. Left, ordinary light; right, between crossed nicols

is highlighted by what appears to be denser nodules in a less dense matrix. It is tempting to associate these small dense cores with inorganic catalyst, the polymer having literally covered or encapsulated the active centre. In some areas protuberances completely limit transmission but these have irregular shapes seemingly due to agglomeration of smaller irregularly shaped units. These protuberances have been referred to as polyps[5] but it is important to realize that they are composite and can exist over a wide range of sizes intimately connected with the size of the catalyst crystals themselves.

The overall textural heterogeneity is emphasized by the transmission micrograph of the thicker membrane shown in *Figure 4*. Here the grosser density fluctuations due to the polymer are still visible, while anything that might be associated with the catalyst is now lost. The grosser heterogeneity is nevertheless to be associated with a continuity of structure which is a property of these membranes, and is no doubt the result of a prolific growth that causes all areas of the growing mass to be linked with one another.
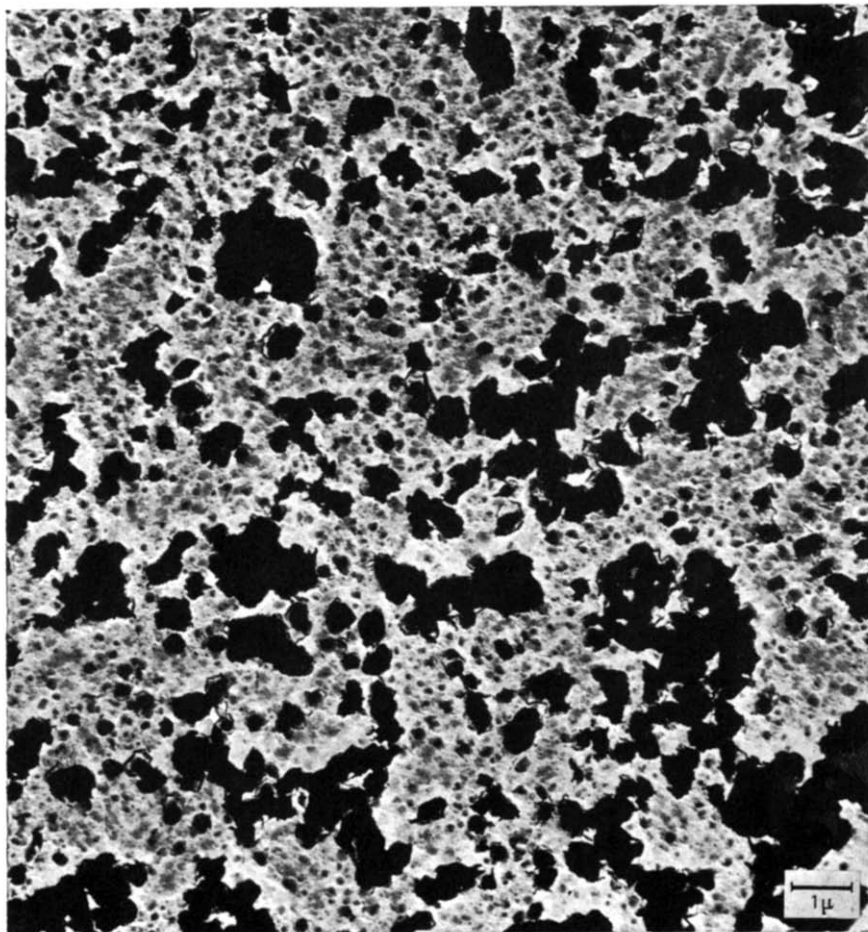
Figure 3—Direct transmission electron micrograph of a thin film of nascent polyethylene prepared at 80°C by gas phase polymerization. Germanium shadowed at an angle of 30°

This property is particularly well illustrated by the appearance of the polymer in *Figure 5*, which is a transmission micrograph of polyethylene grown in heptane at dry ice temperature. The polymerization was significantly slower than at room temperature and the resultant membrane had poor cohesion and high bulk.

On stretching, a strip of nascent polyethylene usually develops multiple fractures which are bridged over by a parallel array of fibrils and microfibrils, together with unstretched polyps which adhere to the fibrils. *Figure 6* is representative of this phenomenon, a stretched membrane where the unstretched areas appear as islands in the middle of the microfibrils. *Figures 7* and *8* show details of the microfibrils and explain how the polyps adhere to these. *Figure 7*, obtained without metal shadowing, reveals the

575
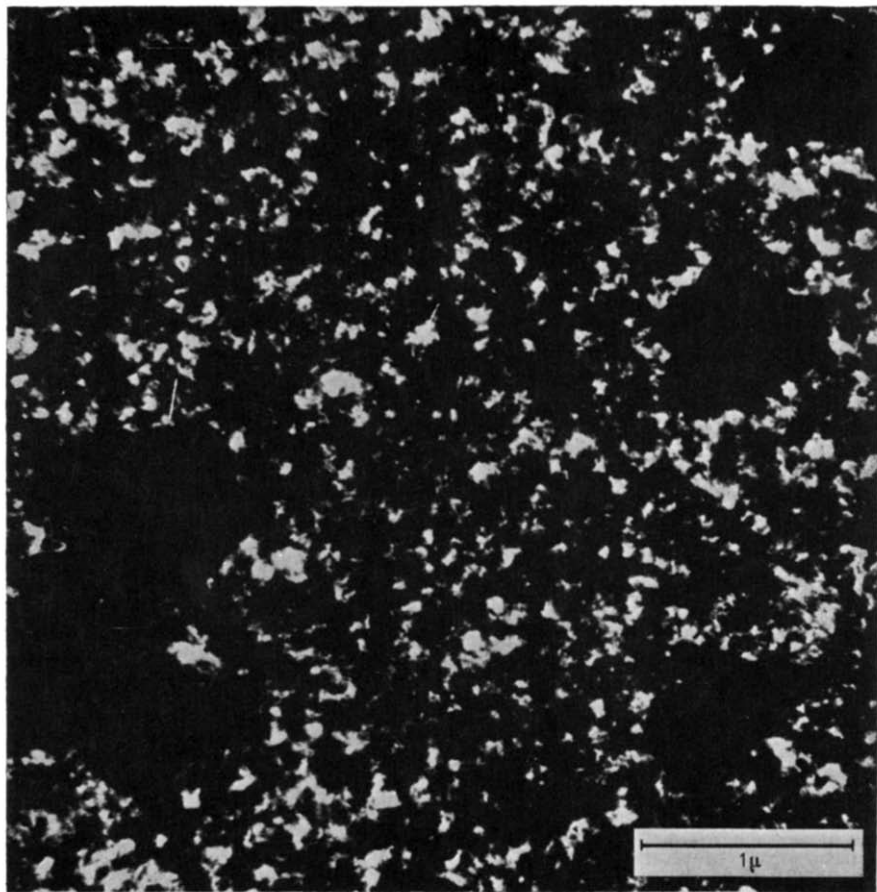
Figure 4—Direct transmission electron micrograph of a nascent polyethylene film thicker than that in *Figure 3*. Film prepared at room temperature and in *n*-heptane. Germanium shadowed at an angle of 30°

structure of some polyps: they consist of a dense core, with rather sharp edges surrounded by a less electron dense shell, without sharp contour. Occasionally the polyp is hollow. The picture is reminiscent of the data reported[3] for α-TiCl$_3$ single crystal catalyst, except that it presents a more advanced stage of polymerization. The hard core is probably a granule of catalyst while the outer shell is the polymer grown around it. The size range of the polyp is comparable to the vanadium trichloride crystal size used in these experiments (cf. *Figure 1*).

The fibrillar aggregates in *Figure 8* were highlighted by shadowing, and their compound nature down to the 100 Å range is brought out. Inclusion of polyps within some of the bundles suggests that the fibrils were created by distension of polyp-like aggregates bridged to one another by inter-polyp links.
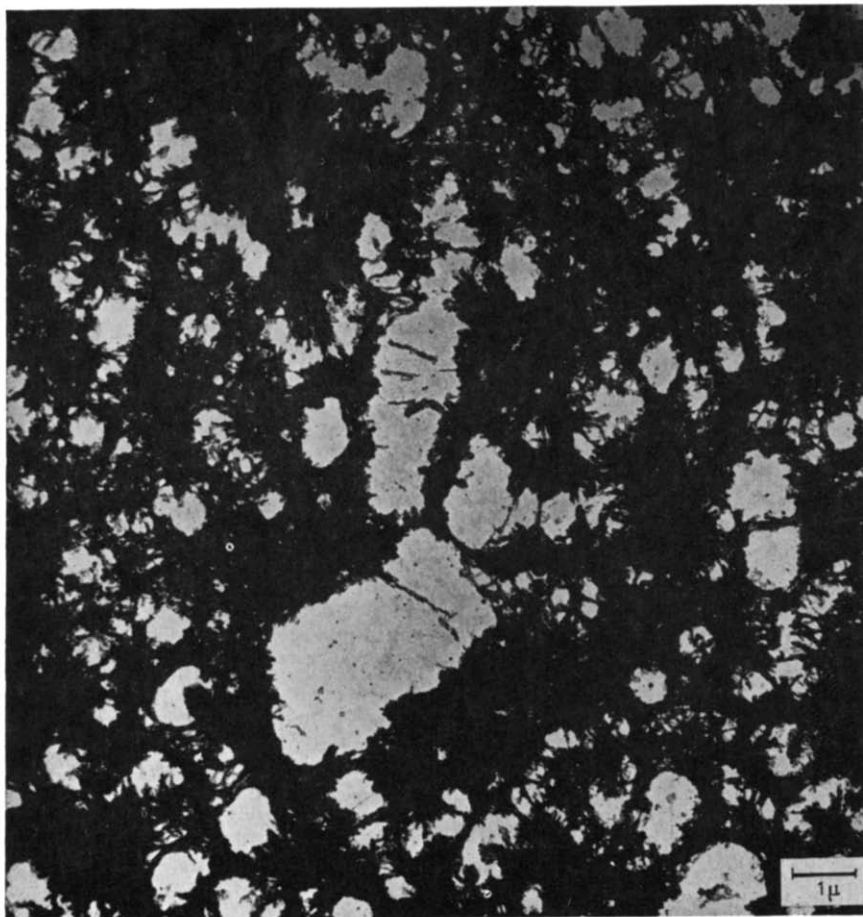
Figure 5—Direct transmission electron micrograph of a nascent polyethylene film prepared at dry–ice temperature and in *n*-heptane. Iodine stained

X-ray examination—Polyethylene encapsulation of glass rods produces birefringent polymer shells, which indicates some preferred orientation in the texture of the polymer encapsulate. Birefringence analysis showed that at least the chains, in the area where they are oriented, are parallel to the support surface. X-ray analysis offers the possibility to confirm this finding and extend the conclusion to include preferred crystallographic orientation. X-ray studies were made by using polyethylene grown on flat glass surfaces.

When a strip of nascent polyethylene film was mounted with the X-ray beam perpendicular to the polymer surface, a conventional polyethylene powder diagram resulted. When the same strip was mounted with the beam parallel to this surface, a pseudo fibre diagram was obtained as seen in *Figure 9*. This pseudo fibre diagram shows poor orientation and each reflection is present as a powder circle, together with discrete intensity

577
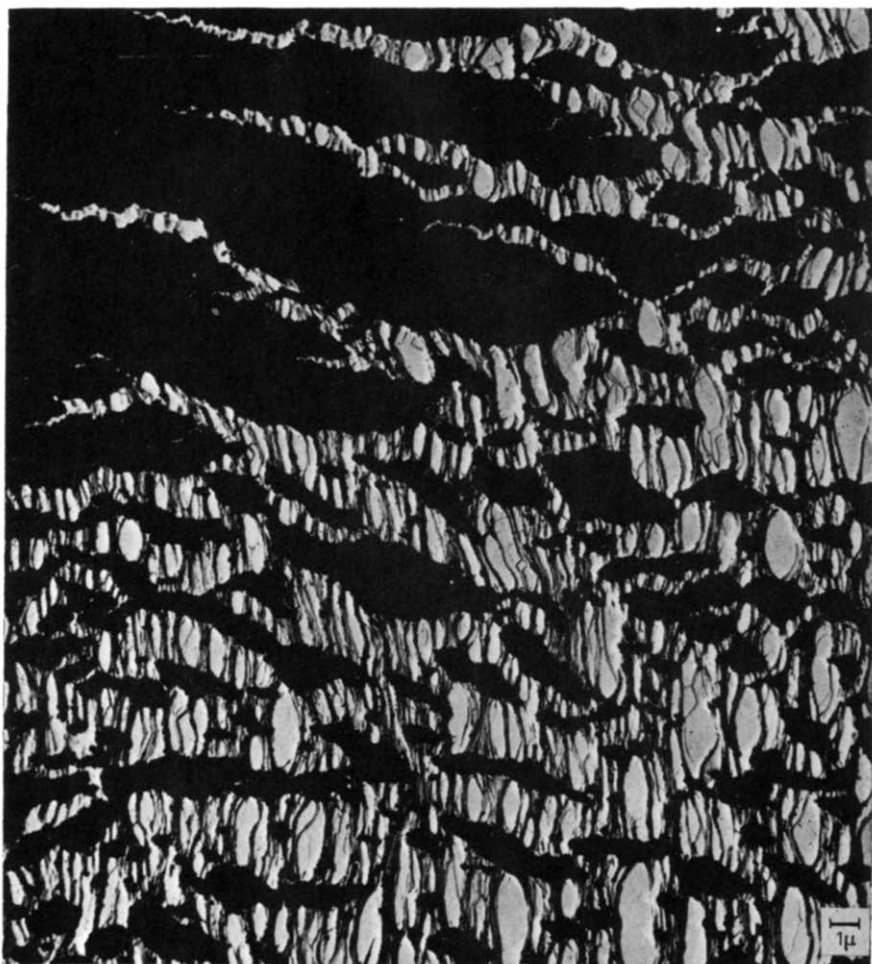
Figure 6—Direct transmission electron micrograph of a stretched area in a thin nascent polyethylene membrane prepared by room temperature polymerization in *n*-heptane. Germanium shadowed at an angle of 30°

maxima. The diagram contains all the reflections of the polyethylene unit cell[14] plus extra reflections that have been already attributed to the triclinic modification of polyethylene[15]. The main feature of the pseudo fibre diagram is the fact that the strongest reflection, corresponding to the 110 planes, presents seven maxima on its powder circle: two maxima are on the equator, one on the meridian and four symmetrically in pairs at an angle from the vertical position. Similarly, the 200 plane, responsible for the second strongest reflection, shows five marked intensity maxima on its circle: one on the meridian, none on the equator and four others symmetrically in pairs at an angle from the meridian. The presence of meridional reflections in the upper part of the diagram is undoubtedly due to non-normality between the rotation axis and the X-ray beam[16]. This non-
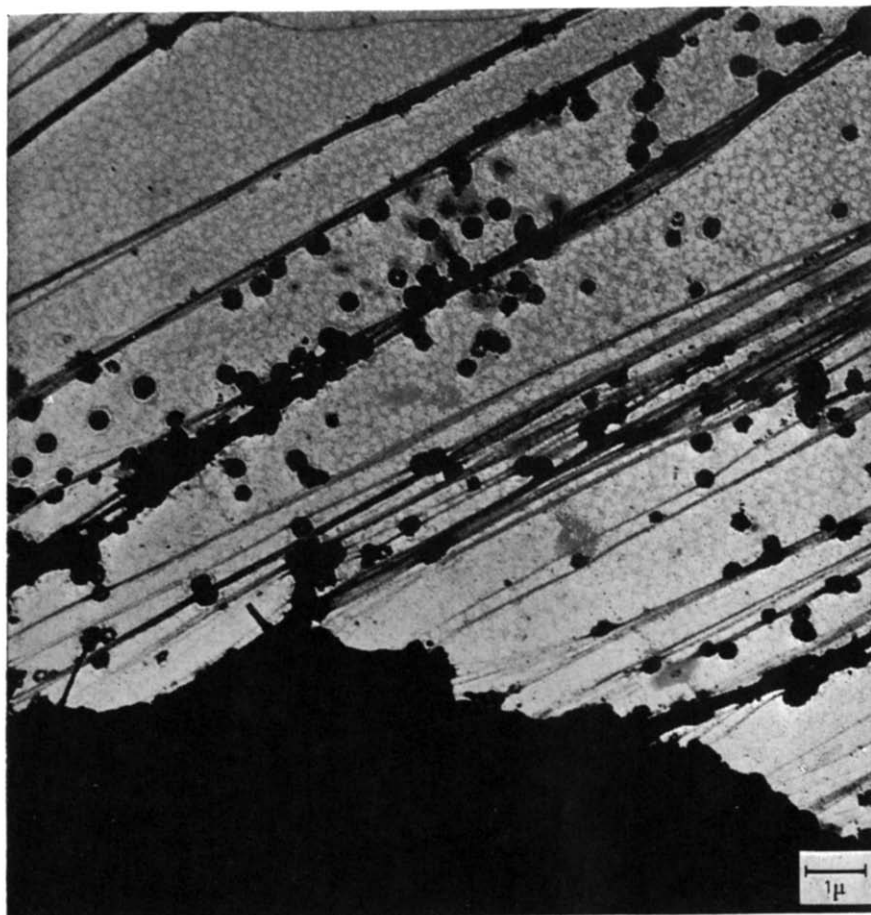
Figure 7—Direct transmission electron micrograph of a stretched area in a thin nascent polyethylene membrane made at 75°C in *n*-heptane. Iodine stained

normality or tilt results also in dissymmetry of the upper and lower parts of the diagram about the equator in *Figure 9*. In this case, the tilt angle can be calculated and amounts to 20°. Reorienting the polymer film to this extent results in the restoration of full symmetry to the fibre diagram about the equator while the meridional reflections are weakened.

The fact that 110 planes present six reflections, if one omits the meridional one, is an indication that the rotation axis of the fibre diagram is parallel to the 110 plane and along the [110] zone axis of the polyethylene unit cell. Indeed, a rotation around this axis directed along the meridian of the diagram, for the orthorhombic cell, gives equatorial reflections for the 110 plane while the $\bar{1}$10 diffracts on four spots, two by two symmetrical about the meridian and the equator. In the same way, 200 planes will give four spots, etc. A theoretical fibre diagram of orthorhombic polyethylene,

579
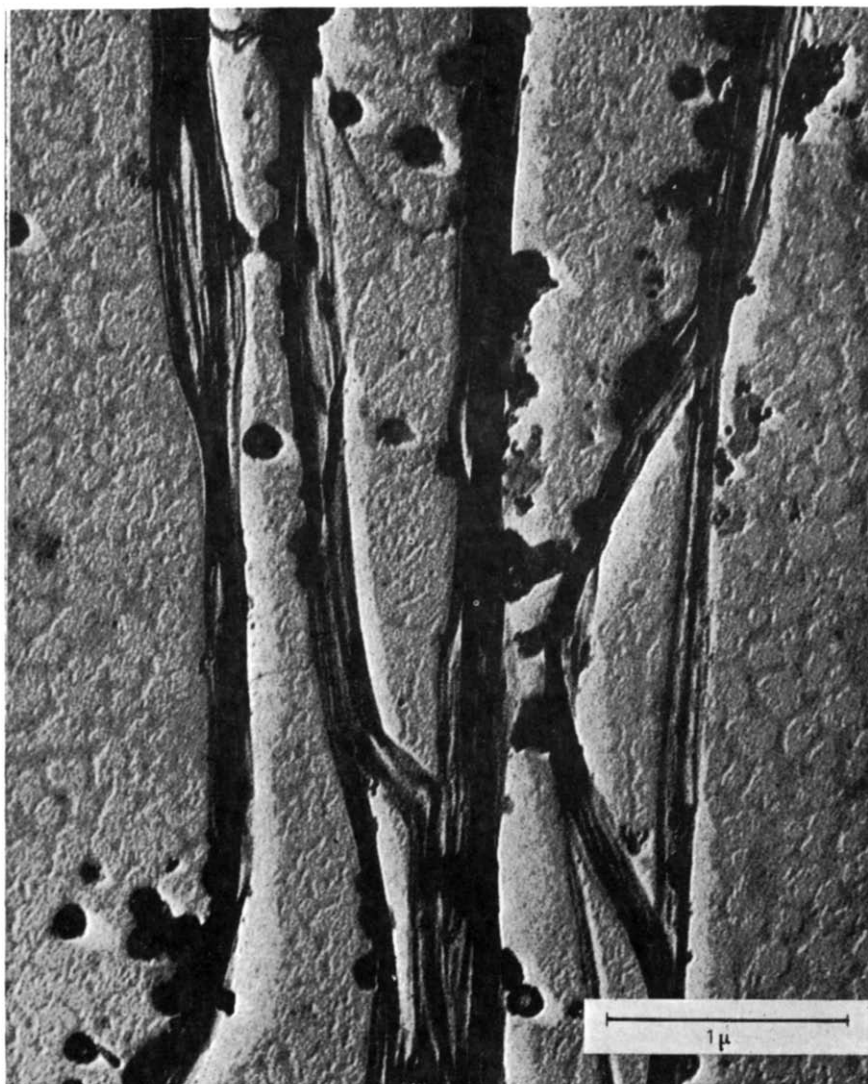
Figure 8—Direct transmission electron micrograph of microfibrils obtained by stretching a nascent polyethylene membrane made at 75°C in *n*-heptane. Germanium shadowed at an angle of 30°

rotated around [110], can thus be constructed. It has a fibre repeat[17] of 8·89 Å and is shown in *Figure 10*. The agreement of such a theoretical diagram with the experimental one is quite good and allows one to conclude that [110] is indeed the rotational axis of the experimental diagram. As the surface of the polyethylene sample was parallel to the equator of the X-ray diagram, it is concluded that the [110] axis is normal to the polymer film surface, while the *c* axis of the unit cell is parallel to it. This

important conclusion proves again that, in areas where the polymer is oriented, the polymeric chains grow parallel to the surface of the support. This is probably due to attraction of the support for the first synthesized molecules of polyethylene which act as a lodestone for subsequent polymer deposition. The fact that in the oriented areas the polymer unit cells all have
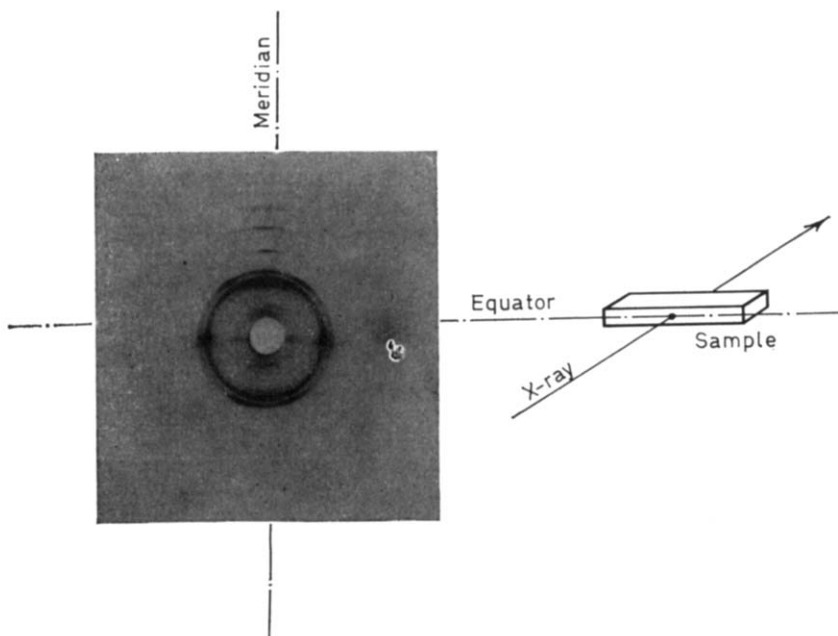
Figure 9—Fibre diagram of a nascent polyethylene film with X-ray beam parallel to the polymer film surface. Normal to polymer film is parallel to the meridian of the X-ray diagram

their [110] axis normal to the polymer film surface has so far not received any explanation. This appears to be a particular growth habit of poly-ethylene, since similar orientation is found in the structure of the wax rods on the stems of the sugar-cane plant[18]. Crystallographically the 110 plane is the one of maximum diffracting intensity for X-rays, and hence contains the most atoms. Its preferred formation can probably be explained in terms of minimum free energy considerations. There is no evidence yet that it is due to a particular catalyst orientation on the glass substrate.

The degree of orientation in the system under study was not established. From the X-ray data of *Figure 9* it seems that most of the polymer is crys-talline, as shown by the absence of any amorphous halo. However, one can say that the orientation is decidely poor, as most of the reflections diffract as a continuous ring together with the discrete intensity maxima.

A typical *small angle* X-ray pattern, recorded with the same sample orientation as for the wide angle region, is shown in *Figure 11*. Distinct maxima are clearly absent and one must conclude that regular folding or

581
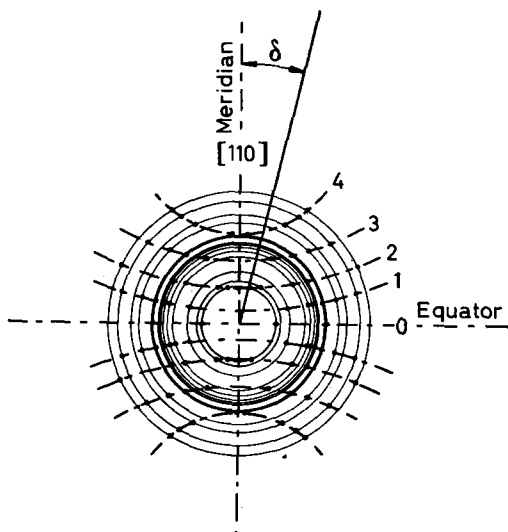
Figure 10—Theoretical fibre diagram of polyethylene with [110] as rotational axis

periodic texture variation smaller than 300 Å is absent. This finding correlates well with the concept that simultaneous synthesis and crystallization of polyethylene yields completely extended chains[2].

The small angle X-ray scattering, as seen from *Figure 11*, has the form of a cross, having a heavy branch on the meridian and a lighter one on the equator. On annealing, this behaviour disappears and the small angle X-ray scattering is quite uniformly distributed around the beam stop. This phenomenon may be explained by assuming that the nascent polymer
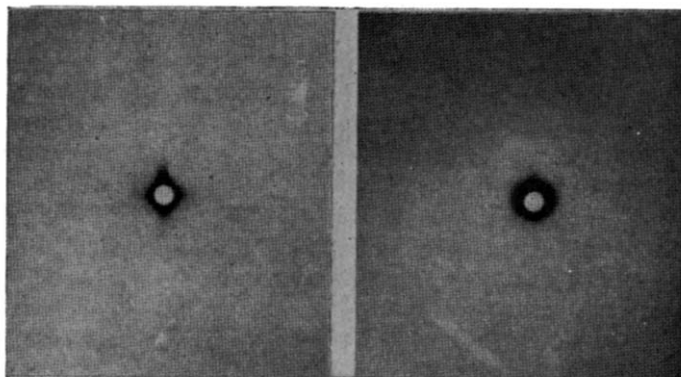
Figure 11—Small angle X-ray diagram of a nascent polyethylene film with X-ray beam parallel to the polymer film surface. The normal to the polymer film is parallel to the meridian of the X-ray film. Photograph taken at 29 cm from sample: left, initial sample; right, annealed sample

films are filled with ribbon-shaped microvoids, these being preferentially laid either in the plane of the film or perpendicular to it. Juxtaposition of polymer and holes results in electron density fluctuations and a cross-like small angle scattering. Annealing, however, tends to compact and reshape most of these holes and to destroy the cross-like pattern.

The stretched nascent polyethylene films were also studied by wide and small angle X-ray and electron diffraction. A conventional polyethylene fibre diagram was obtained in both cases, revealing that in the fibrils the c axis is along the stretch direction and the fibril axis.

The possibility of periodic chain folding in the fibrils was also investigated by small angle X-ray and, as before, sharp maxima could not be observed and the small angle diagram presented only an equatorial streak. This behaviour is in agreement with *Figure 8*, where the fibrils are seen to be composed of bundles of parallel smaller fibrils with no sign of longitudinal periodicity.

Solid state light scattering—As explained above, nascent polyethylene films grown on glass are rather turbid. Interaction with light gives a high degree of scattering, which with thicker samples can lead to total extinction. Scattering of light can, however, be reduced by annealing the sample. As for small angle X-ray scattering, this behaviour can be explained in terms of voids and aggregates in the nascent polymer film. The net result is a wide heterogeneity in the local refractive index of the films. The structures thus show continuous variations in refractive index (n) above and below n_{av}. An additional source of scattering that is operative for visible light but not for X-rays is scattering due to anisotropy fluctuations. This type of scattering can be detected by examining the polarization and angular intensity distribution of a polarized beam scattered by the sample. From the studies by Stein and Rhodes[19], it is known that when polarizer and analyser are crossed, the sample being in between, scattered light passing through the analyser is due solely to anisotropy fluctuations in the material. In this case, the angular distribution of scattered light intensity, called the H_v pattern, can be related to a particular type of supercrystalline organization of the sample. On the other hand, when polarizer and analyser are parallel, V_v pattern, the scattered light passing through the analyser may arise from density as well as from anisotropy fluctuations. If density fluctuations are responsible for most of the scattering, the V_v pattern is a symmetrical halo; if the scattering depends more on anisotropy fluctuations, an asymmetric pattern is recorded.

Such experiments, performed with a nascent polyethylene film, gave the two patterns shown in *Figure 12*. In these, V_v appears as a circular halo of constantly decreasing intensity in the radial direction; the H_v pattern, about 20 times weaker, appears as a cross at 45° from the plane of polarization. No radial intensity maxima can be detected in the arm of this cross and it seems that the intensity of scattered light constantly decreases from the centre toward the outside.

From the intense and non-oriented V_v pattern, one can conclude that

most of the scattering is due to density fluctuations overshadowing the anisotropy scattering. The latter is certainly present, as it is revealed in the H_v pattern, but it is not visible in the V_v patterns due to its weakness compared to density fluctuation scattering. The shape of this H_v pattern is
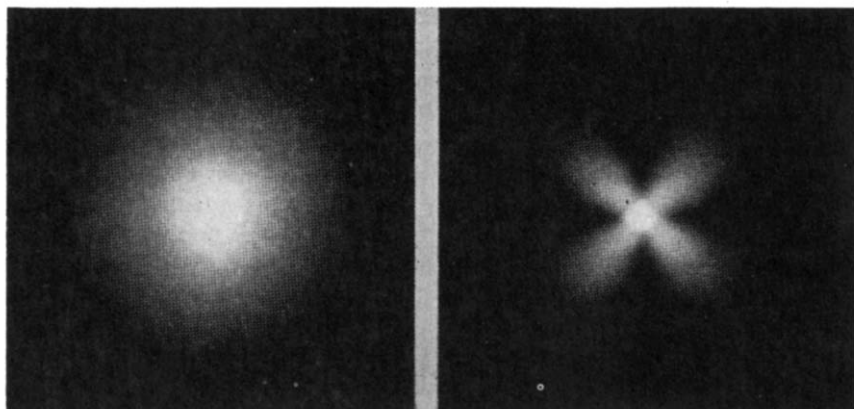
Figure 12—Light scattering patterns from a nascent polyethylene film: left, V_v pattern; right, H_v pattern. Exposure time ratio for V_v/H_v about 20

different from a typical H_v pattern for spherulitic polyethylene, but corresponds exactly to scattering obtained from an anisotropic rodlike structure where the optic axis is also the rod axis[20]. This finding can tentatively be linked to the microscopy and X-ray data and can be explained as follows: the oriented parts of the polyethylene film, which according to *Figures 2* and *3* are parallel to the support surface, are responsible for the H_v pattern just as they were also responsible for the X-ray orientation; on the other hand, the polyp-like parts create density fluctuations, responsible for the opacity of the sample and the shape of the V_v pattern.

Melting point—The melting point of nascent polyethylene is sensitive to the rate of heating of the sample under observation. If the heating is too fast, superheating may take place, which will result in recording too high a melting point[21]. The method used in this melting point determination was a fast heating of the sample to a predetermined temperature. This temperature was then held for a relatively long period of time and was followed by a further increase in temperature. If unmelted polymer was still present after the period at the temperature plateau, it was revealed during the new increase of temperature. Several experiments were conducted, in each of which the plateau temperature varied, starting always with a fresh sample. The maximum melting temperature was thus determined after a series of trials. Such experiments gave in this case a T_m of $141° \pm 1°C$. This value is very high for polyethylene and compares with $141·4°C$ obtained for unfolded linear polymethylene crystals formed by crystallization at a high

temperature and pressure (P. Wunderlich. Private communication). This value compares also with the theoretical value $T_0 = 141 \cdot 1° \pm 2 \cdot 4°C$, which was found as the limiting melting point of n-paraffins (limit as n approaches infinity) with a unit cell similar to that of polyethylene[22].

DISCUSSION

From the foregoing electron microscopy birefringence X-ray and light scattering data one can construct a tentative model of the nascent polyethylene. Initially, polymerization starts from the surface of the vanadium trichloride crystals complexed with a molecular amount of aluminium triethyl. From neighbouring polymerization sites, polyethylene chains undergo two-dimensional crystallization, flowing over whatever surface is present where they crystallize and adsorb because they are insoluble in the polymerization medium. In their outward flow, the growing chains cover the crystals of catalyst as well as the glass support where the former were anchored. Thus a part of the polymer is laid flat on the support as lamellae, and it is believed that this lamellar part is responsible for the
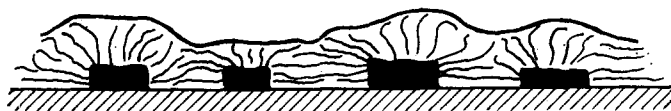
Figure 13—Schematic representation of a nascent polyethylene film grown on glass when the catalyst crystals do not migrate or break during polymerization: ■, catalyst crystal; ≡, polymer orientated parallel to the glass surface

orientation seen in the birefringence, the wide angle X-ray and the light scattering data. If during the polymerization the catalyst is not carried away or cleaved by the forces of polymerization, a thin membrane will result which is depicted schematically in *Figure 13* as suggested by the
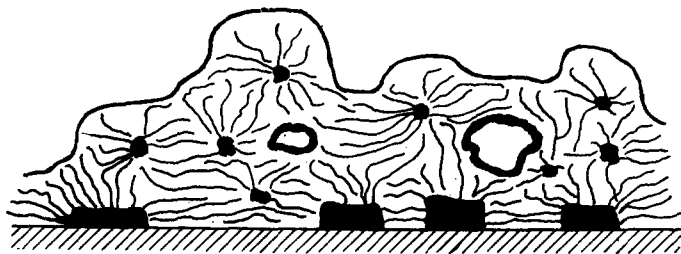
Figure 14—Schematic representation of a nascent polyethylene film grown on glass when the catalyst crystals migrate or break during polymerization

electron micrograph in *Figure 3*. If, however, important catalyst cleavages and displacements occur during polymerization, many polyps can be created and a very porous film is obtained together with lamellae of polyethylene

oriented along the flat substrate. This situation can be represented in *Figure 14* and is illustrated by the electron micrographs, *Figures 4* and *5*.

The orienting effect of the substrate is operative at a considerable distance from it, in fact birefringence can be observed throughout the thickness of a film tens of microns thick. Apparently the polymer is laid down in a layer-like fashion and each preceding layer acts as substrate for the next one.

The two morphological forms, layers and polyps, are closely related and in actual operation overlap to some degree. However, by careful control of polymerization conditions one or the other aspect can be emphasized. Thus the finer the catalyst and the more firm its adherence to the substrate, the more is the lamellar texture emphasized. These conditions are best achieved by a minimum catalyst deposit and very slow polymer growth rate. In fact, the success of the latter condition for producing dense coherent membranes suggests that the nascent texture development is a function of polymeric relaxation phenomena. Rapid growth encourages polyp-like eruptions and catalyst fracture due to 'head on' collisions between growing polymer molecules.

The experimental data support the idea of fully extended polyethylene chains without regular folding. The flow or movement of polymer on the substrate can be depicted as involving ribbons of parallel polymer molecules generated at neighbouring coordination sites. The dynamics of growth cause the ribbons to move about on the surface, collide and perhaps fold accordion style, thereby creating a polypy texture. The randomness of polymerization causes some growing ribbons to merge and form a continuous network, while some polymer sheathed catalyst particles become isolated and are only weakly joined to the network. On stretching, the latter are made visible as distinct entities relative to the network, which is converted to a fibrillar texture. When membranes were disintegrated mechanically by high speed stirring in an aqueous suspension, similar fibrillar textures were revealed but with less directionality and extensively combined with polyps.

The importance of substrate in influencing the chain orientation revealed by the birefringence and X-ray observations cannot be over-emphasized. The growth of polymer under the conditions used could perhaps be described as 'surface seeking' without distinguishing between glass, catalyst or previously formed polymer.

Less clear at this time is the influence of the catalyst itself. Various experiments have established that the finer the particle size, the faster the rate of polymerization. Assuming an affinity between the substrate and the reduced transition metal halide it would seem that a slow generation of the latter offers the best opportunity for adsorption before formation of large crystalline aggregates. The thermal decomposition process used in this study is superior in this respect to the conventional methods for generation of colloidal transition metal polymerization catalysts. The influence of substrate on the catalyst itself is probably morphological only, as the same general phenomena described for glass substrates were observed when

cellulosic fibres were used. In turn, the influence of catalyst morphology on the nascent polymer morphology showed itself most notably in terms of the bulk density and toughness of the generated membranes of polyethylene. A notable factor in this respect was the influence of freshly distilling the vanadium(IV) chloride. This fact suggested that crystalline nuclei tend to develop on storage of vanadium(IV) chloride and that these lead to large catalyst crystals.

CONCLUSIONS

A flat glass surface will be covered by small vanadium trichloride crystals if it is refluxed in a boiling solution of vanadium(IV) chloride in heptane. These adsorbed crystals, activated by aluminium triethyl become catalysts for the coordination polymerization of ethylene. This latter process, performed in heptane, yields a rapid coverage of the support with nascent polymer which grows in the form of a film.

The morphology of these films was studied and two types of structures were considered to occur: a polyp-like and a lamellar texture. The former is crystalline, unoriented and develops around loose crystals of catalysts, while in the latter, the molecular chains are oriented parallel to the support with their [110] axis normal to it.

Observation of a high melting point with superheating as well as absence of discrete small angle maxima suggests that fully extended polymer chains are predominantly present in the polyethylene films. This is consistent with small angle light scattering data which show a rodlike scattering unit to be present.

On stretching, the nascent films generate fibrils and microfibrils to which polyps are found to be attached. In these fibrils, the chains of polyethylene are believed to be similarly extended. This phenomenon is an attractive way to prepare fibrillar polyethylene.

In terms of transition metal polymerization mechanism the present study offers first of all an experimental tool. Catalyst supported at a smooth macroscopic surface and the resultant polymeric film offer a convenient two-dimensional reaction flask. Furthermore, the substrate provides a reference surface for identifying catalyst and product orientational effects. Since present thinking in terms of Ziegler–Natta catalysis focuses on crystalline lattice sites as the active centres, it is clearly of advantage to identify and localize the catalyst orientation. The present investigation still has far to go in this respect, but the clear evidence for local orientation and ribbon- or rod-like texture is most consistent with neighbouring active sites with similar orientation on a catalyst crystal.

REFERENCES

[1] BLAIS, P. and ST JOHN MANLEY, R. *Science*, 1966, **153**, 539

[2] WUNDERLICH, B., HELLMUTH, E., JAFFE, M., LIBERTI, F. and RANKIN, J. *Kolloid Z. u. Z. Polym.* 1965, **204**, 125

[3] RODRIGUEZ, L. A. M. and GABANT, J. A. *J. Polym. Sci.* 1963, **4C**, 125

[4] 'Method for estimation of particle size and distribution of titanium trichloride catalysts', *Application Data Sheet*, Stauffer Chemical Company

[5] HERMAN, D. F., KRUSE, U. and BRANCATO, J. J. *J. Polym. Sci.* 1965, **C11**, 75

[6] HILLEBRAND, W. F. and LUNDELL, G. E. F. *Applied Inorganic Analysis*, 2nd ed. Wiley: New York and Chapman and Hall: London, 1953

[7] EPHRAIM, F. and AMMAN, E. *Helv. chim. Acta*, 1933, **16**, 1273

[8] LASKY, J. S., GARNER, H. K. and EWART, R. H. *Industr. Engng Chem. Prod. Design & Devel.* 1962, **1**, 82

[9] KEII, T. and AKIYAMA, T. *Nature, Lond.* 1964, **203**, 76

[10] NATTA, G. and PASQUON, I. *Advances in Catalysis*, Vol. XI, pp. 1–66. Academic Press: New York, 1959

[11] MARCHESSAULT, R. H. and CHANZY, H. D. To be published

[12] 'Vanadium chloride', *Technical Bulletin*, Stauffer Chemical Company, 1962

[13] OSTER, G. *Physical Techniques in Biological Research*, Vol. I, Chap. 8. Academic Press: New York, 1955

[14] BUNN, C. W. *Trans. Faraday Soc.* 1939, **35**, 482

[15] TURNER JONES, A. *J. Polym. Sci.* 1962, **62**, S53

[16] KLUG, H. P. and ALEXANDER, L. E. *X-ray Diffraction Procedures*, Chap. 10. Wiley: New York, 1954

[17] CHANZY, H. D. *Ph.D. Thesis*, New York State College of Forestry, June 1966

[18] KREGER, D. R. *Selected Topics in X-ray Crystallography*, Part H, p 325. North Holland: Amsterdam, 1951

[19] STEIN, R. S. and RHODES, M. *J. appl. Phys.* 1960, **31**, 1873

[20] STEIN, R. S., ERHARDT, P., VAN AARTSEN, J. J., CLOUGH, S. and RHODES, M. *J. Polym. Sci.* 1966, **C13**, 1

[21] HELLMUTH, E. and WUNDERLICH, B. *J. appl. Phys.* 1965, **36**, 3039

[22] BROADHURST, M. G. *J. chem. Phys.* 1962, **36**, 2578

Polythioacetone

V. C. E. Burnop and K. G. Latham

Polythioacetone was prepared by spontaneous polymerization of the mono-mer in the liquid and solid phases, and in solution. Solid phase polymeriza-tion was initiated by sunlight. Fractionation gave a polymer with 27 000 molecular weight. Unlike trioxan and trithian, trithioacetone did not undergo ring opening polymerization. Thermodynamic calculations confirm that tri-thioacetone is more stable than linear polythioacetone. The polymer was unstable even at room temperature, but was more stable after reacting with ethyl isocyanate. The main decomposition product was trimer. Thermal decomposition began with some chain scission, and was followed by a monomolecular unzipping with an activation energy of 26·6 kcal mole^{-1}. Evidence was obtained suggesting that, during polymerization, about one monomer unit in fifty reacted in the thioenol form, interrupting the carbon-sulphur sequence, and resulting in pendant thiol groups. Some disulphide groups may also occur in the chain.

SEVERAL polythioacetals, with a backbone of alternating carbon and sul-phur atoms, have been reported recently. Thus, polythioformaldehyde has been obtained from bis(chloromethyl) sulphide and sodium sulphide[1]; from hydrogen sulphide and formaldehyde under pressure or from bis(mercapto-methyl) sulphide[2]; from methane dithiol using amine initiators[3]; and from trithian by X-ray initiated solid state polymerization[4,5] or by ring opening polymerization[6,7]. Thiocarbonyl fluoride[8], hexafluorothioacetone[9] and several other perfluorocarbonyl compounds[10] have also been polymerized to linear polythioacetals.

Aliphatic thioketones such as thioacetone normally exist as stable cyclic trimers, e.g. (I), and although some physical properties of the monomers have been given[11-13], the formation of linear polymers has not been recorded. Recent work in these laboratories[15] has shown that substantially pure monomeric thioacetone spontaneously polymerizes to linear polymer (II). Hence these earlier products were of questionable purity. Linear polythio-acetone (II), of molecular weight 2 000 was first reported by Bailey and Chu[14], who found that pyrolysis of allyl isopropyl sulphide gave, among other products, monomeric thioacetone, which polymerized spontaneously. Ettingshausen and Kendrick[15] independently prepared monomeric thioace-tone by pyrolysis of the trimer *in vacuo*, and polymerization in the liquid phase gave polymers of molecular weight up to 14 000.

I   II   III   IV
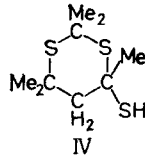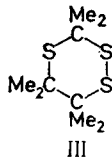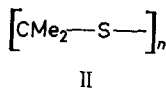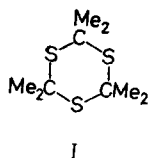
Ettingshausen and Kendrick showed, by mass spectrometry and n.m.r. measurements, that trithioacetone prepared from acetone, hydrogen sulphide and an acid catalyst contained small amounts of isomers (III) and (IV), and that benzoquinone removed the latter. They also showed that trithioacetone did not undergo ring opening polymerization to give (II), thus differing from trioxan and trithian.

EXPERIMENTAL

Special precautions were adopted to avoid disseminating the very offensive and unpopular odours of thioacetone and other products formed during this work. Reactions were carried out in a glove box containing a reservoir of alkaline permanganate for decontaminating apparatus. Small quantities of nitrogen dioxide released into the box destroyed unpleasant vapours presumably by catalysing oxidation.

Polymer molecular weights were determined in benzene solution, using a vapour pressure osmometer (mol. wt $< 20\,000$) or by osmometry (mol. wt $> 20\,000$).

Liquid-phase polymerization of thioacetone

Trithioacetone was purified by partial crystallization, recrystallization from methanol, or treatment with sodium plumbite ('Doctor' solution). The purified product, still unexpectedly containing (III) (see *Table 1*) melted at $21.8°C$. This mixture was used in the following experimental work, and is implied when the term 'trimer' or 'trithioacetone' is used. Bailey and Chu[14] give a melting point of $22°C$ and Fromm and Baumann[16] one of $24°C$. We found that the melting point fell to $17.2°C$ after the trimer was kept at $65°C$ for 3 h, but that it was restored to $21.8°C$ after a further 48 h at room temperature. This phenomenon was not investigated further.

Table 1. Mass spectra of trithioacetone samples. Peak intensities relative to M/e $222 = 100$

M/e	Isomer characterized	Initial product	Crystalline fraction	Methanol recryst.	Na plumbite treated
83	(III)	14·7	20·9	20·1	15·0
138	(III)	91·0	120·2	112·8	90·0
157	(III)	4·5	5·6	5·8	5·0
188	(IV)	1·0	←————— < 0.002 —————→		

Ettingshausen and Kendrick generated thioacetone in a conventional Keten apparatus modified to function at reduced pressure. In the present work this was simplified. A Pyrex reaction tube, 30 cm high 5·5 cm in diameter, contained a loose coil, made from 175 cm s.w.g. 22 Chromel A wire, which extended down two-thirds of the tube [*Figure 1*(a)]. At 17·5 V (31·5 W) very little cracking occurred. At 20 V (40 W) or above, 5 to 6 g of trimer was cracked per hour, but increased voltage led to a decrease in molecular weight of the subsequent polymer. Cracking conditions were therefore standardized at 20 V and 1 mm of mercury pressure. Under these conditions the coil had a long life, and little deposit formed on the walls of

Figure 1—(a) Monomer generator; (b) Reaction tube
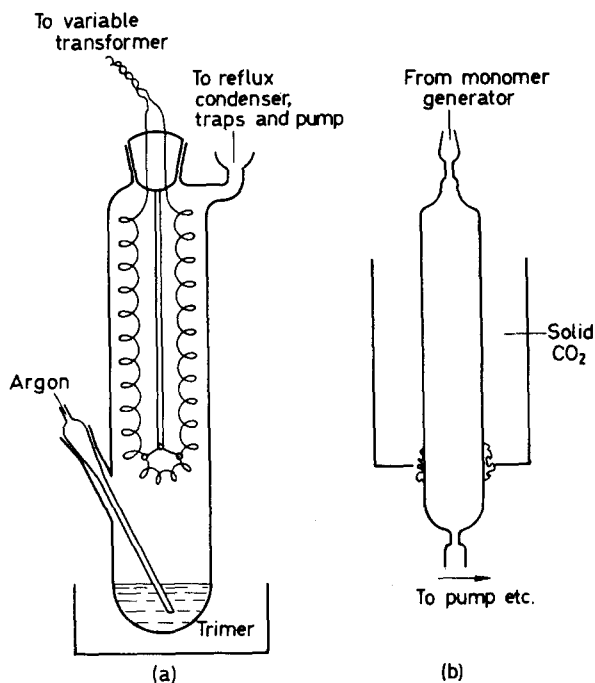
the reaction tube. It was calculated that the residence time in the reaction zone was less than ten seconds.

Thioacetone monomer prepared in this way was collected at $-78°C$ and allowed to polymerize under various conditions. Results are summarized in *Table 2*. Where polymerization temperature is described as 'low', the reaction mixture in the $-78°C$ trap was allowed to warm up undisturbed over two days. The solutions remained clear until the temperature reached $-30°$ to $-25°C$, hence polymerization probably occurred in this tempera-

Table 2. Polymerization of thioacetone

Run No.	Solvent or comonomer*	Initiator	Polymerization temp. °C	Polymer yield, percentage of trimer cracked	M.pt of polymer, °C
1	None	—	low	72	119–120
2	Ether	—	low	81	124–5
3	Ether	BF$_3$ etherate	low	82	101–4
4	Ether	Sodium	low	86	111–6
5	Ether	Ph$_3$N	low	86	122–3
6	Chloroform	—	0°	20	108–9
7	Ethylene oxide	—	0°	86	120–2
8	Ethylene oxide	—	low	90	122–3
9	Epichlorhydrin	—	0°	57	122–3
10	Propylene oxide	—	0°	80	122–3
11	Solid state	Light	−78°	42	122–4

*The monomer was dissolved in an equal volume of solvent or comonomer.

591

ture range. Polymerization in solution was not observed after two days at −78°C in light, contrasting with the solid state polymerization in Run 11, discussed later. No copolymers were isolated, all the products being homopolythioacetone.

Solid-state polymerization of thioacetone

Some of the thioacetone monomer condensed on the wall of the −78°C trap as a thin layer of deep orange fernlike crystals. After a brief exposure to daylight the colour of the crystals slowly faded, and when warmed to room temperature some 24 hours later a film of polymer could be stripped from the wall, retaining the original form of the crystals *(Figure 2)*. The molecular weight of this film could be as high as 33 000, but the polymer was not very stable in solution and results were erratic. The polymer film did not dissolve in benzene below 40°C.
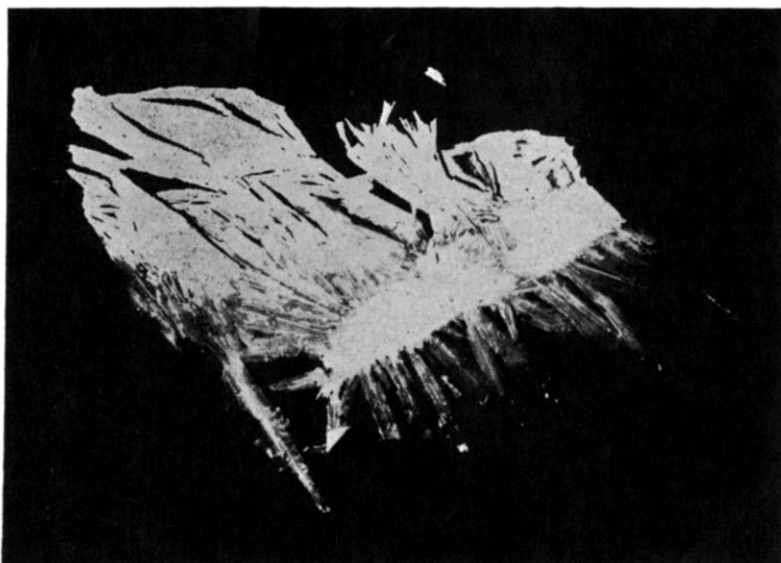
Figure 2—Solid phase polymerization of thioacetone

When the −78°C trap was protected from light by wrapping in aluminium foil, no polymerization of the crystalline monomer occurred in 24 hours. On exposure to light for about a minute, polymerization was initiated. After a further 48 hours at −78°C, acetone was added, and after warming to room temperature 42 per cent of polymer was isolated *(Table 2, Run 11)*, molecular weight 13 700. A second run gave a 45 per cent yield. The distilled acetone washings gave a liquid of b.pt 100° to 115°C at 20 mm of mercury pressure in 39 per cent yield. This liquid was mainly trimer, hence under these conditions approximately equal amounts of polymer and trimer are produced.

This appears to be the first record of solid state polymerization initiated by radiation in the visible region.

Pyrolysis of trithioacetone at atmospheric pressure

The apparatus shown in *Figure 1*(a) was used without the reflux condenser, and 30 V was applied to the coil. Reaction products were collected in two traps, the first at 0°C and the second at −78°C. Argon was passed through the trimer at 175°C to 200°C, giving a trimer evaporation rate of between 2 and 5 g/h. Under these conditions about equal volumes of products collected in each trap. The brown condensate at 0°C, amounting to 43 to 51 per cent of the trimer cracked, contained 35 to 48 per cent of thioacetone as determined by the conventional hydroxylamine hydrochloride method for ketones. The very unpleasant smelling liquid collected at −78°C was not examined further.

The trimer was also pyrolysed, under an argon blanket, by direct heating in a flask fitted with a fractionating column. When the trimer was heated to 200° to 250°C it darkened and after 15 min appeared to boil, giving a brown distillate of b.pt 80° to 90°C. Mayer, Morgenstein and Fabian[11] report thioacetone to boil at 80°C. As distillation continued, the brown colour of the distillate diminished and the boiling point increased. The undistilled trimer was converted to a black tar. Using cracking temperatures of between 200° and 250°C, distillate yields were 60 to 70 per cent and their thioacetone content (hydroxylamine method) 38 to 41 per cent giving an overall yield of 20 to 30 per cent monomeric thioacetone. The results were unchanged when a length of Chromel A wire was immersed in the trimer, showing that the wire exerted no catalytic effect on the cracking.

The brown liquids obtained in these experiments did not deposit crystals at −78°C, although the monomer prepared by the vacuum process melted at −40°C. They reacted with 2,4-dinitrophenylhydrazine, however, with evolution of hydrogen sulphide, to give acetone-2,4-dinitrophenylhydrazone, confirming the presence of monomer. Attempts to prepare pure monomer by redistillation of the brown liquids were not successful. Heating converted monomer to trimer, the colour diminished, and the new distillates contained only 20 to 40 per cent of monomer. The product of one direct distillation pyrolysis at 250°C deposited five per cent of its weight of linear polymer on standing at room temperature. Otherwise none of the above products gave linear polymer, spontaneously or with possible catalysts. Storing at 0° or −78°C with boron trifluoride etherate, tertiary amines, or triphenyl phosphine led to fading of the colour at varying rates ($BF_3 > R_3N > Ph_3P$) but trimerization occurred. The colour was rapidly discharged by u.v. light, less rapidly by daylight.

PROPERTIES OF POLYTHIOACETONE

Polythioacetone, (II), was a white unpleasant-smelling powder of density 1·21. When of high molecular weight (above 10 000) it melted sharply at 124°C to a pink liquid, which on cooling resolidified to a brittle opaque mass. It was soluble in a variety of solvents, being very easily soluble in chloroform and tetrahydrofuran (*Table 3*). The polymer separated as a powder from cooled dioxan solutions.

Films of polythioacteone were prepared by evaporating solutions or by pressing between glass plates above the melting point for a very short time.

Table 3. Solubility of polythioacetone

Solvents at room temperature	Solvents at 50°C	Non-solvents
Chloroform	Trithioacetone	Alcohols
Carbon tetrachloride	Dioxan	Acetone
Ethyl isocyanate	Ethylene chlorhydrin	Ether
Benzene and other aromatics	Dimethylformamide	Ethylene oxide
Tetrahydrofuran		Paraffins
		Dimethyl sulphoxide

The films were glossy, translucent, or almost clear, and had no strength. In some cases they folded without breaking but were usually brittle. Threads drawn from a melt were initially elastic and transparent, but became brittle and opaque in a few minutes.

STABILITY OF TRITHIOACETONE AND POLYTHIOACETONE TO CHEMICAL REAGENTS

Attempts were made to estimate the thiol isomer (IV) in trithioacetone by reacting with mercury(II) chloride and estimating the hydrogen chloride formed[17].

$$RSH + HgCl_2 \longrightarrow RSHgCl + HCl$$
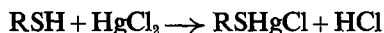
Instead of the expected reaction, cold aqueous mercury(II) chloride slowly hydrolysed the trimer to acetone, identified by its 2,4-dinitrophenylhydrazone, the yellow precipitate formed having a composition approximating to $HgCl_2.HgS$. Acetone-2,4-dinitrophenylhydrazone was isolated in 47 per cent yield from the distillate from the reaction of trimer, mercury(II) chloride and aqueous alcohol.

Following this observation, the effects of other salts were investigated. Aqueous silver nitrate and copper(II) chloride both decomposed trimer in the cold, giving acetone and quantitative yields of metal sulphide. Aqueous iron(II) and iron(III) salts and nickel salts did not react with trimer, but with solid iron(III) or mercury(II) chloride in the absence of water it gave the metal sulphide with evolution of hydrogen chloride and hydrogen sulphide. The trimer was stable to sodium plumbite ('Doctor' solution) even after 24 h at 100°C, the product recovered by steam distilling the reaction mixture being free of thiol (IV).

Solid polythioacetone was less stable to these reagents, whether ground together in the solid state or treated with aqueous reagent. In the latter case, metal sulphide and acetone were formed. Distillation of the polymer with aqueous alcoholic mercury(II) chloride gave a 67 per cent yield of acetone as the 2,4-dinitrophenylhydrazone. Splitting of the sulphide link by metal salts is not unknown[18, 19], but polythioacetone reacted very easily.

The effects of various reagents are summarized in *Table 4.*

Table 4. Stability of thioacetone trimer and polymer to metal salts at room temperature

Reagent	Trimer	Polymer
BF$_3$ etherate	Stable	Unstable
Aq. sodium plumbite ('Doctor' solution)	Stable	Unstable
HgCl$_2$, anhydrous	Unstable	Unstable
HgCl$_2$, aqueous	Unstable	Unstable
FeCl$_3$, anhydrous	Unstable	Unstable
FeCl$_3$, aqueous	Stable	Unstable
CuCl$_2$, hydrate	Unstable	Unstable
CuCl$_2$, aqueous	Unstable	Unstable
NiCl$_2$, hydrate and aqueous	Stable	Stable
FeCl$_2$, hydrate and aqueous	Stable	Stable
AgNO$_3$, aqueous	Unstable	Unstable

Polythioacetone was unstable to hydrochloric acid and hot alcoholic potash. It was more stable to aqueous sodium hydroxide, but probably only because the reagent did not wet the polymer (*Table 5*).

Table 5. Stability of polythioacetone to acids and alkalis. Reaction conditions: 3 h at reflux

Reagent	Polymer decomposed, per cent
1% Hydrochloric acid	50
Conc. hydrochloric acid	(100% in 1 min)
20% aqueous NaOH	10
10% ethanolic KOH	56

ATTEMPTS TO PREPARE POLYTHIOACETONE SULPHONES

Cold alkaline permanganate slowly oxidized trithioacetone to the previously unreported monosulphone, m.pt 102°C (Found: C 42·3, H 7·0, S 38·0 per cent; C$_9$H$_{18}$S$_3$O$_2$ requires C 42·5, H 7·1, S 37·8 per cent). Warm alkaline permanganate (100°C) gives the disulphone, m.pt 209°C, yields in each case being about 80 per cent.

Further oxidation of the disulphone (hydrogen peroxide in acetic acid) gave a poor yield of trisulphone, m.pt 316°C. These sulphones are stable crystalline solids, and unsuccessful attempts were made to convert them to polysulphones by ring opening polymerization, using methods known to function with trithian.

Molten monosulphone, just above its melting point, was decomposed by a trace of boron trifluoride etherate and did not resolidify on cooling, and prolonged heating at 80°C gave no polymeric product. At 120°C, the mixture began to evolve a volatile product and the refluxing vapour was brown, characteristic of monomeric thioacetone. The condensate, on distillation, was unpleasant-smelling and almost colourless, and unexpectedly was shown by infra-red spectroscopy to consist mainly of acetone. This was confirmed by conversion to the 2,4-dinitrophenylhydrazone. The reaction was not continuous, but recommenced each time a drop of boron trifluoride

etherate was added. The mechanism by which the acetone was produced must have involved a ring opening and transfer of oxygen from sulphur to carbon. The monosulphone was unaffected by dimethyl sulphate until the temperature exceeded 175°C, when decomposition set in (cf. ref. 6).

The disulphone was unaffected by cationic catalysts in dimethyl formamide solution up to 170°C and was recovered unchanged. The molten disulphone decomposed above 215°C, and the decomposition was accelerated by boron trifluoride etherate, iron(III) chloride and mercury(II) chloride.

Bailey and Chu[14] claimed that hydrogen peroxide in acetic acid oxidized polythioacetone to a polysulphone, m.pt 295°C (yield unstated). Under the same conditions, our polymer gave a 12 per cent yield of crystalline material, m.pt 300° to 310°C, which recrystallized from acetic acid as needles, m.pt 316°C. These were identical with authentic trithioacetone trisulphone. The polymer not converted to sulphone was found to have been quantitatively oxidized to sulphuric acid. Thus, Bailey and Chu's claim was not confirmed.

Addition of nitrogen dioxide or nitric acid to polythioacetone or trimer gave green complexes, which on heating gave only black tars. Polythioacetone was slowly but completely decomposed by permanganate.

THE THERMAL STABILITY OF POLYTHIOACETONE

Polythioacetone always emitted an unpleasant odour. When placed in the reservoir of a mass spectrometer at room temperature trimer was first desorbed, presumably the accumulated product of decomposition previous to the experiment, and then followed a steady evolution of monomer and trimer. At an inlet temperature of 250°C the products also included hydrogen sulphide, small amounts of $C_3H_6SC_3H_4$ ($M = 114$), $C_6H_{10}SC_3H_4$ ($M = 154$) and $C_3H_6SC_3H_6SC_3H_4$ ($M = 188$) with minor amounts of a series $(C_3H_4)_n$—SC_3H_6.

The main decomposition product of polythioacetone is the relatively non-volatile trimer, b.pt 130°C at 13 mm pressure. In measuring the thermal decomposition of the polymer, it was important to establish that the observed rate of loss of weight was not, in fact, the rate of evaporation of accumulating trimer. To test this, polymer samples (0·2 g) of very different stabilities, and a sample of trimer were heated at 100°C in identical tubes (5 cm high × 1·5 cm diameter). The trimer evaporated steadily at 7 mg/h, while the rates of weight loss of the polymer decreased with time and ranged from 2 to 50 mg/h. If trimer evaporation were the controlling factor, the rates of weight loss of the polymers would have increased until a steady value for trimer was reached, and would then have remained constant. The residues never contained more than one per cent of acetone-soluble material, proving that trimer did not accumulate.

The rate of thermal decomposition of unstabilized polythioacetone does not change appreciably with varying molecular weight. The rate usually increased until about 20 per cent had decomposed, after which there was an apparently first-order decomposition until about 30 per cent remained (*Figure 3*).
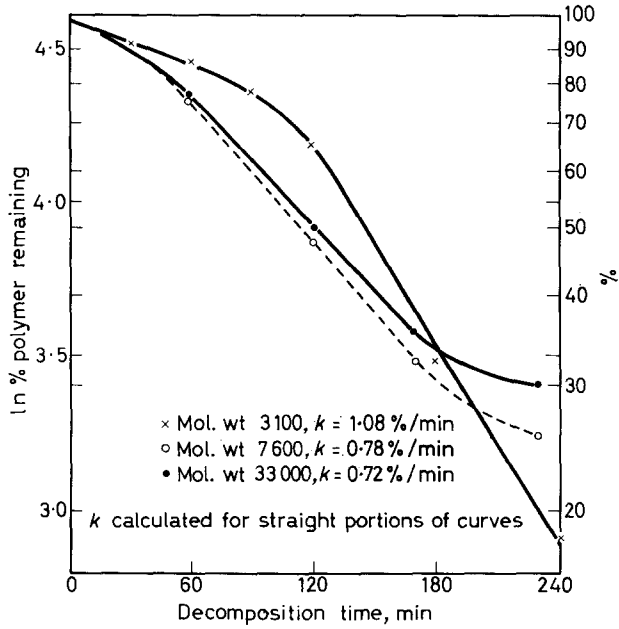
Figure 3—Effect of molecular weight on the thermal decomposition of unstabilized polythioacetone at 100°C in air

As with polyformaldehyde, polythioacetone could be stabilized with suitable end-capping reagents. Refluxing for one hour with acetic anhydride containing one per cent sodium acetate resulted in a 50 per cent loss of polymer. The product, however, had better initial thermal stability than the starting material, but the decomposition rate accelerated until it approached that of the initial polymer. Standing at room temperature with acetic anhydride and benzene had little effect on stability, but ethyl isocyanate (not phenyl isocyanate) gave considerably improved stability over a wide range of decomposition (*Table 6*).

Table 6.   Decomposition rates of stabilized polythioacetone at 100°C

Stabilization procedure	Decomposition rate, per cent/min	Range of decomposition, per cent
None	0·26	0–20
None	1·1	20–80
Refluxing Ac$_2$O, NaOAc	0·05	0–20
Refluxing Ac$_2$O, NaOAc	0·8	20–80
EtNCO in benzene	0·043	10–85

For a more detailed investigation of stability, 100 g of polymer (*Table 2*, Run 2) was reacted with 50 ml of ethyl isocyanate in 200 ml of chloroform for one week at 0°C. The polymer was recovered by acetone precipitation and fractionated at 25°C by extracting with acetone–chloroform mixtures of increasing chloroform content. After extracting more soluble fractions,

17 g of polymer, of molecular weight 20 000, was obtained (which was soluble in a mixture of chloroform and acetone 13:7 v/v, but insoluble in a 12:8 v/v mixture) and 16 g of a higher fraction, molecular weight 27 000, insoluble in the 13:7 v/v mixture.

The polymer of molecular weight 27 000 was heated to between 110° and 115°C in a stream of argon, and was sampled at intervals. Each sample was washed with acetone to remove occluded trimer (the loss in weight in acetone washing proved to be less than one per cent), and finally pumped out for 6 h at 0·1 mm pressure. The molecular weight of the polymer fell rapidly at first, but reached a steady value of about 10 000 (*Figure 4*).
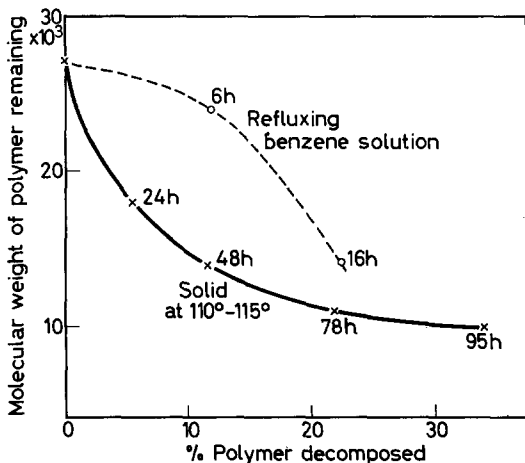
Figure 4—Molecular weight changes in polythioacetone during thermal decomposition at 110°C to 115°C or in refluxing benzene

The molecular weight in refluxing benzene (1 g of polymer to 3 ml of benzene) fell more slowly. The polymer was recovered from the benzene by acetone precipitation. Again the molecular weight was approximately 10 000 (see *Figure 4*).

The thermal decomposition of the polymer of molecular weight 20 000 was studied between 105° and 145°C. At 125°, 135° and 145°C the polymers were liquid and a first-order decomposition rate was followed from 10 to 90 per cent decomposition (*Figure 5*). Below the melting point (125°C) the results were erratic (*Figure 6*). At 118°C initial decomposition was rapid, this corresponding to the chain breaking stage. This was followed by a short first-order decomposition ($k=0·186$ per cent/min), but signs of melting then appeared. The rate of decomposition increased as melting progressed, and when melting was complete a further first-order decomposition was observed ($k=0·55$ per cent/min). Later, the rate decreased ($k=0·37$ per cent/min). At 105°C the polymer did not melt, and the first half of the decomposition, excluding a short initial faster reaction, was first order ($k=0·049$ per cent/min). This increased to about 0·1 per cent/min towards the end of the reaction.

When the logarithms of the rates of decomposition of the liquid polymer at 125°, 135° and 145°C, and those for the early stages of the solid decom-
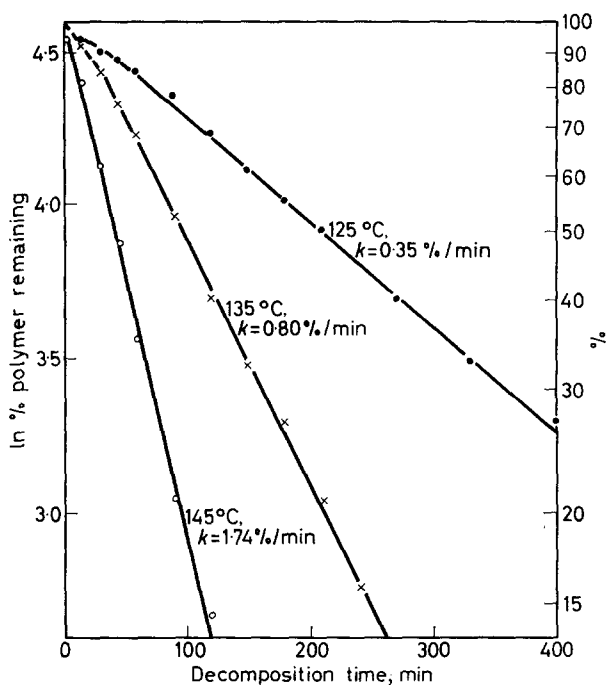
Figure 5—Thermal decomposition of polythioacetone, mol. wt 20 000, ethyl isocyanate stabilized in argon
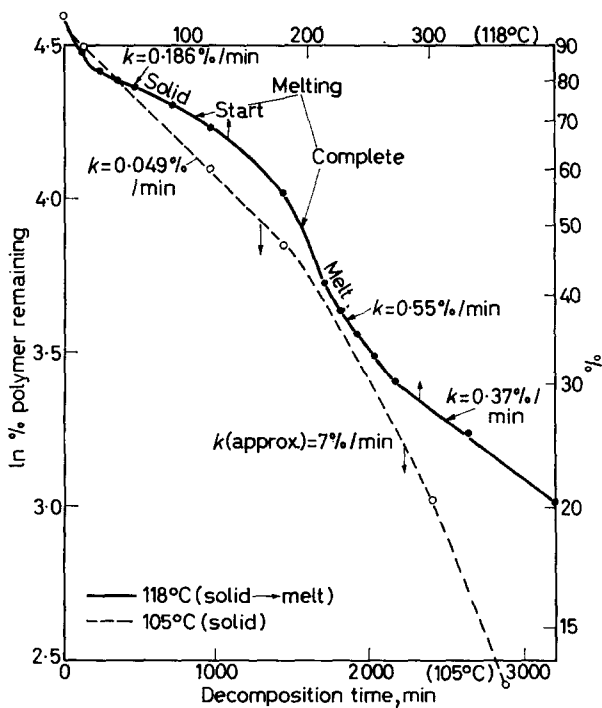
Figure 6—Thermal decomposition of polythioacetone, mol. wt 20 000, ethyl isocyanate stabilized in argon

position at 118° and 105°C, were plotted against the reciprocal of the decomposition temperature, a straight line was obtained corresponding to an activation energy of decomposition of 26·6 cal/mole.

THE STRUCTURE OF POLYTHIOACETONE

The properties of polythioacetone suggest that its structure is mainly that of the polythioacetal (II). Thus it decomposes in a first-order manner to monomer and trimer, has a simple n.m.r. spectrum[15], and the i.r. spectrum is similar to that of the trimer, apart from the expected broadening of the bands (*Figure 7*). Decomposition with desulphurization gives acetone. Other evidence, however, indicates irregularities in the polymer chain.

The improved thermal stability of the polymer after reacting with acetic
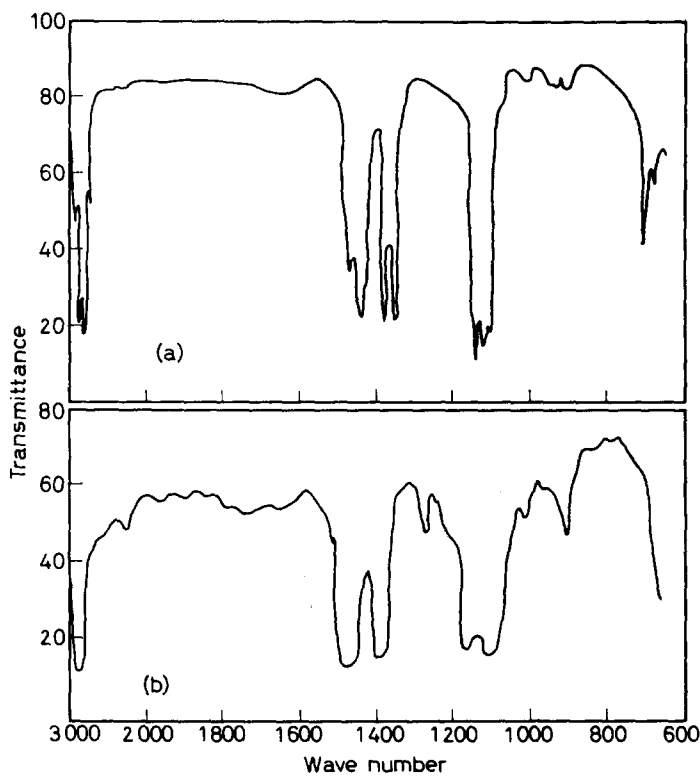
Figure 7—Infra-red spectra of thioacetone trimer and polymer:
(a) trithioacetone (liquid); (b) polythioacetone (film)

anhydride and especially with ethyl isocyanate suggested the presence of esterifiable end groups, possibly —SH. The nitrogen contents of ethyl isocyanate stabilized polymers, however, were not consistent with the presence of two nitrogen atoms per molecule, as shown in *Table 7*.

The nitrogen contents of the polymers prepared by the two methods followed different patterns. For polymers prepared in solution they were

Table 7. Nitrogen contents of ethyl isocyanate stabilized polythioacetones

Polymer mol. wt	Preparative method	Nitrogen found, per cent	Nitrogen calculated for end groups, per cent	% N found minus % N calc.
9×10^3	In ether	0·66	0·31	0·35
20×10^3	In ether	0·55	0·14	0·41
27×10^3	In ether	0·45	0·10	0·35
3×10^3	Solid state	0·35	1·00	(−0·65)
14×10^3	Solid state	0·38	0·21	0·17

about 0·37 per cent in excess of the value required for end groups. The two polymers prepared in the solid state had nitrogen contents of about 0·38 per cent, unrelated to molecular weight or the number of chain ends. A possible explanation is that the solution-prepared polymer has terminal thiol groups whereas these are absent in the solid-state polymerization.

One terminal thiol group may be derived from hydrogen sulphide which is a byproduct of the monomer preparation and therefore available in the solution polymerization but not readily available in the solid phase. The nitrogen content of the stabilized solid-state polymerized product and the excess nitrogen in the stabilized polymer prepared in ether, which are virtually the same, 0·37 per cent, must therefore be due to pendant thiol groups. The poly-acetal sequence of alternating carbon and sulphur atoms is therefore interrupted by an occasional —CH_2—$CMe(SH)$— group (about 1 in 50) derived from the thioenol form of the monomer, CH_2=$CMeSH$. The rapid fall of molecular weight to 10 000 during thermal degradation suggested that the polymer contained a few very unstable links. They may be disulphide links, attached to tertiary carbon atoms: —CMe_2—S—S—CMe_2—. Absence of terminal thiol groups in the polymer would have been expected to give improved thermal stability. This was not observed. The anomalous groups in the polymer may therefore be analogous to the unsymmetrical isomers (III) and (IV) which occur in the trimer.

Unequivocal proof of the presence of these groups in polythioacetone has not been found, probably because their effects are slight and are masked by the preponderance of the main structure. The trimer obtained by decomposing the polymer contained the isomers (III) and (IV) and if the decomposition occurred by a backbiting process, this would constitute a proof. If the primary decomposition product is monomer, however transient its existence, these data are irrelevant to the structure of the polymer. Thermal decomposition of the polymer in the mass spectrometer gave a C_6H_{10}—S—C_3H_4 fragment, but the simultaneous appearance of a series of minor peaks $(C_3H_4)_n$—S—C_3H_6 (which may very well be formed in the apparatus by recombination reactions) introduces the suspicion that the C_6H_{10} group may also be an artefact.

THERMODYNAMIC CONSIDERATIONS

Before postulating a mechanism for thioacetone polymerization, the relevant thermodynamics will be considered.

An interesting fact emerging from this work is that cyclic trithioacetone

is the most stable component of the monomer–trimer–linear polymer system. This contrasts with the formaldehyde system in which linear polymer is the most stable. Theoretical confirmation of this seemed desirable and calculation of the relevant ceiling temperatures has therefore been attempted. Thermodynamic calculations as rigorous as those applied to formaldehyde were not possible, as the necessary bond energy E (C=S) is not accurately known. It was not possible to obtain this by thermochemical measurements on di-t-butylthione. Attempts to prepare this thioketone by published methods[21] did not give a pure stable monomer.

Accordingly, the ceiling temperature has been estimated from the available data. To provide a check, consideration was given to formaldehyde and acetone. The heats of reaction for each system were calculated from estimates of the heats of formation of monomer, cyclic trimer and polymer obtained from additive bond energy relationships and heats of fusion and vaporization. Entropy changes for the polymerizations have been estimated in a similar way.

Enthalpy changes

These were calculated for the C, H, O compounds by using the bond energy scheme of Allen[28] with the revised parameters reported by Skinner and Pilcher[22]. For the thioacetone problem one additional parameter, the bond energy E (C=S) = 110 kcal mole^{-1} bond^{-1} was estimated from a comparison of published heats of formation of CO_2, CS_2, $(NH_2)_2CS$, and Me_2CO. Strain energies introduced by steric hindrance in linear chains or cyclization have been estimated by a method introduced by Skinner[23]. Heats of fusion of the polymers were estimated from literature values for similar polymers. Heats of vaporization were estimated from the cohesive energy densities of similar polymers and cross-checked by calculating the cohesive energy density using Small's additivity relationship[27].

Entropy changes

As far as possible, entropy changes were calculated from absolute values estimated by use of the method of chemical groups introduced by Benson and Buss[24]. In addition, the following approximations have been made:
  (i)   For the change 3 monomer $\longrightarrow$ cyclic trimer ΔS was assumed to be the same as 3 ethylene $\longrightarrow$ cyclohexane.
  (ii) For the polymerization monomer $\longrightarrow$ linear polymer ΔS_p is assumed to be the same as for the corresponding olefin polymerization, as given by Dainton and Ivin[25].

For monomer and trimer the entropy of vaporization is assumed to follow Trouton's rule, i.e. to be 21 cal mole^{-1} (deg. K)$^{-1}$. For the linear polymer we assume from the data for polyethylene given by Dainton and Ivin[25]

$$\Delta S_{c \to g} = 7 \text{ cal mole}^{-1}(\text{deg. K})^{-1} \qquad \Delta S_{l \to g} = 4 \text{ cal mole}^{-1}(\text{deg. K})^{-1}$$

referred to the repeat unit of the polymer. Walden's rule applied to fusion of monomer and trimer gives $\Delta S_{c \to l} = 13$ cal mole^{-1} (deg. K)$^{-1}$ and consideration of the known heats of fusion of polymers suggests for a linear polymer that

$$\Delta S_{c \to l} = 3 \text{ cal mole}^{-1} (\text{deg. K})^{-1}$$

Enthalpy and entropy changes have been estimated and are shown in *Table 8* for the reactions

$$3 \text{ monomer}_{(g)} \longrightarrow \text{polymer}_{(c)} \quad \text{and} \quad 3 \text{ monomer}_{(g)} \longrightarrow \text{trimer}_{(l)}$$
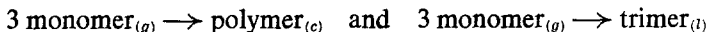
The data for thioacetone in *Table 8* assume that polymerization occurs through the thione form. The ceiling temperature for each reaction is estimated from the relationship

$$T_c = \Delta H / \Delta S$$

This is the temperature above which the free energy change for the reaction becomes positive. If we consider the free energy changes at some lower temperature T, then the higher T_c the more negative will be ΔG in the reaction. Thus comparison of T_c for polymer and trimer formation is a useful guide to their relative stabilities.

Table 8. Comparison of CH_2O and Me_2CS

	Monomer$_{(g)}$ $\longrightarrow$ Polymer$_{(c)}$			Monomer$_{(g)}$ $\longrightarrow$ Trimer$_{(l)}$		
Sample	$-\Delta H$ kcal mole^{-1}	$-\Delta S$ cal mole^{-1} (deg. K)$^{-1}$	T_c °K	$-\Delta H$ kcal mole^{-1}	$-\Delta S$ cal mole^{-1} (deg. K)$^{-1}$	T_c °K
CH_2O	36·6	91·8	400	36·1	111	325
Me_2CS	135·3	144	940	136·6	107	1275

These results are consistent with the known experimental facts that polyformaldehyde may be formed from either the trimer or the monomer because the free energy of the polymer is always lower than that of the trimer. This is not so for thioacetone. Here, the thermodynamic functions show that the trimer is more stable than the polymer, and hence the reaction

$$\text{Trimer}_{(l)} \longrightarrow \text{Polymer}_{(c)}$$
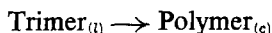
would have a positive free energy change. This supports the observation that polythioacetone cannot be obtained directly from the trimer, but only after it has been converted to monomer.

These results also have some bearing on the comparative stabilities of polyformaldehyde and polythioacetone below the ceiling temperature (monomer$_{(g)}$ $\longrightarrow$ polymer$_{(c)}$). Any decomposition of polyformaldehyde could give monomer or trimer in equilibrium with undecomposed polymer. Decomposition of polythioacetone would not give this equilibrium and trimer would result from an irreversible reaction. In fact, we have observed that unstabilized polythioacetone, on keeping in a sealed tube for 18 months at room temperature, was converted to the trimer in 28 per cent yield. Mass spectrometry showed the main decomposition product to be the trimer containing proportions of (III) and (IV), since its mass spectrum resembled those in *Table 1*.

The ceiling temperature was measured by collecting 1 g portions of thioacetone monomer in thin-walled glass tubes at $-78°$C [*Figure 1*(b)]. The tubes were immediately plunged into constant temperature baths held at various temperatures. After one hour any polymer was washed out and weighed. The results are shown in *Figure 8*. A ceiling temperature of about 370°K is indicated.
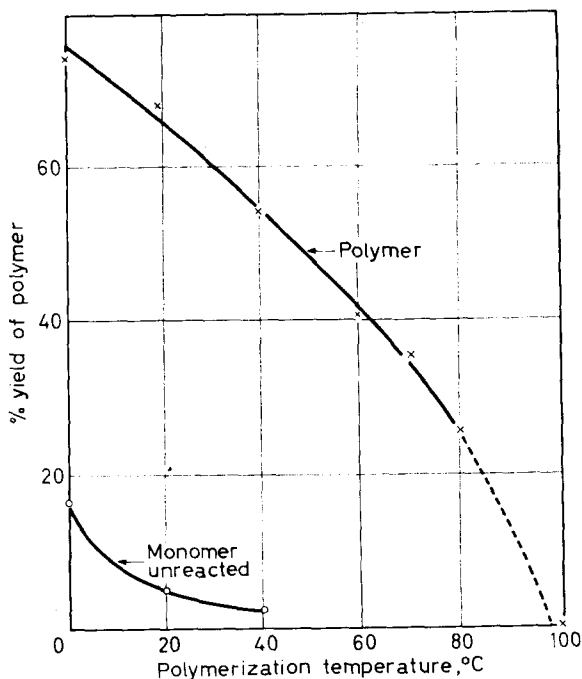
Figure 8—Variations in yield of polythioacetone from
thioacetone monomer at various temperatures.
Reaction duration, 1 h

The predicted ceiling temperatures for formaldehyde are acceptable, but
for thioacetone the calculated 940°K is very high, the experimental esti-
mate being 370°K. The uncertainty in the value of E (C=S) may be the
sole cause of this discrepancy. On the other hand, polymerization may
occur through the thioenol form and this assumption gives a lower estimate
of ceiling temperature, viz. 540°K. If E (C=S) = 110 kcal mole^{-1} bond^{-1}
is correct, the indications are that polymerization proceeds through the
thioenol form.

Table 9. Polymerization of thioacetone–thioenol form

	$-\Delta H$ kcal mole^{-1}	$-\Delta S$ cal mole^{-1} (deg. K)$^{-1}$	$T_c °K$
monomer$_{(g)}$ ——→ polymer$_{(c)}$	81	150	540

The acetone system differs from both thioacetone and formaldehyde.
Reported preparations of polyacetone have been questioned[26] and the only
products isolated were those of a reversible aldol type condensation, namely
diacetone alcohol and triacetone dialcohol. For the reaction

$$n \, Me_2CO_{(g)} \longrightarrow [CMe_2 — O]_{n(c)}$$
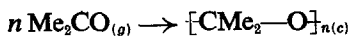
$\Delta H = -7 \cdot 2$ kcal mole^{-1}, $\Delta S = -55$ kcal mole^{-1} (deg. K)$^{-1}$ and $T_c = 120°$K.

For polymerization from liquid monomer, $\Delta H = 0$, hence $T_c = 0°K$, that is polymerization is impossible.

For the observed reactions, the calculated thermodynamic functions are:

$$2\,Me_2CO_{(l)} \longrightarrow Me \cdot CO \cdot CH_2 \cdot CMe_2OH_{(l)}$$
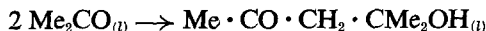
$\Delta H = -9.9$ kcal mole^{-1}, $\Delta S = -20$ cal mole^{-1} (deg. K)$^{-1}$, $T_c = 495°K$.

$$3\,Me_2CO_{(l)} \longrightarrow HO \cdot CMe_2 \cdot CH_2 \cdot CO \cdot CH_2 \cdot CMe_2OH_{(l)}$$
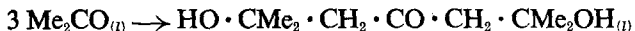
$\Delta H = -18.5$ kcal mole^{-1}, $\Delta S = -36.5$ cal mole^{-1} (deg. K)$^{-1}$, $T_c = 510°K$.

The calculations do not exclude other possible products but they confirm that aldol condensation is more favourable than polyacetal formation.

THE MECHANISM OF THIOACETONE POLYMERIZATION

Theories of the mechanism of thioacetone polymerization must account for the following:

(1)   Addition of boron trifluoride etherate to polymerizing thioacetone reduced the molecular weight relative to that of spontaneously formed polymer without reducing yield (*Table 3*). It may therefore have induced polymerization.

(2)   Boron trifluoride etherate initiates depolymerization of polythioacetone above 12°C.

(3)   The polymer contains pendant thiol groups and a few disulphide linkages.

(4)   Thioacetone would be expected to exist as an equilibrium between thione and substantial amounts of thioenol form[11], but n.m.r. measurements at $-78°C$ in chloroform suggested no more than one per cent enol. Reactions are therefore possible which do not have to be considered in aldehyde polymerizations.

As both forward and reverse reactions are boron trifluoride etherate catalysed, thioacetone polymerization may be cationic. Initiation in the solid phase by light may also be ionic. The colour of monomeric thioketones has been attributed to diradicals, but this is debatable[11, 20].

Whether free radical or ionic, propagation is probably as follows:

Main reaction—P—CMe$_2$—S★ + CMe$_2$=S $\longrightarrow$ P—CMe$_2$—S—CMe$_2$—S★

Subordinate reactions—

(a)   P—CMe$_2$—S★ + S=CMe$_2$ $\longrightarrow$ P—CMe$_2$—S—S—C★Me$_2$

$\longrightarrow$ P—CMe$_2$—S—S—CMe$_2$—CMe$_2$—S★

(b)   P—CMe$_2$—S★ + CH$_2$=CMeSH

$\longrightarrow$ P—CMe$_2$—S—CH$_2$—C★Me
                                    |
                                    SH

$\longrightarrow$ P—CMe$_2$—S—CH$_2$—CMe—CMe$_2$—S★
                                    |
                                    SH

605
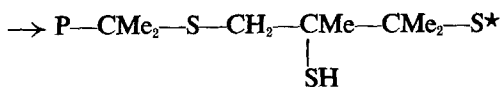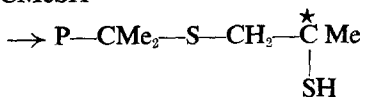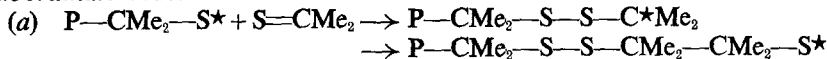
An alternative anionic mechanism can be devised in which the polymer can be derived from the thioenol:

$$P\text{—}CMe_2\text{—}S\ominus + \underset{\underset{Me}{|}}{\overset{\overset{CH_2}{\|}}{C}}\text{—}SH \rightarrow P\text{—}CMe_2\text{—}S\text{—}\underset{\underset{Me}{|}}{\overset{\overset{\ominus CH_2}{|}}{C}}\text{—}SH$$

$$\rightleftharpoons P\text{—}CMe_2\text{—}S\text{—}\underset{\underset{Me}{|}}{\overset{\overset{Me}{|}}{C}}\text{—}S\ominus$$
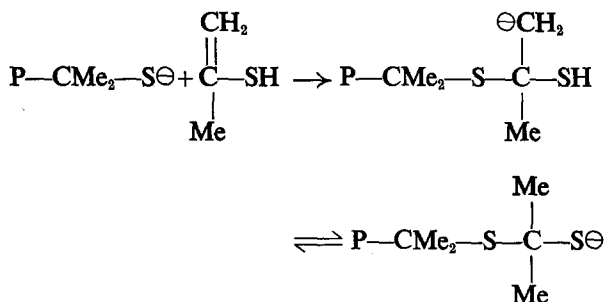
Initiation of anionic polymerization in solution may be similar to that postulated for linear polyformaldehyde, with hydrogen sulphide replacing water as a contributing factor. This would give a polymer terminated at each end by thiol groups.

Initiation—
$$HS\ominus + CMe_2\!\!=\!\!S \rightarrow HS\text{—}CMe_2\text{—}S\ominus$$
Termination—
$$P\text{—}CMe_2\text{—}S\ominus + H_2S \rightarrow P\text{—}CMe_2\text{—}SH + HS\ominus$$
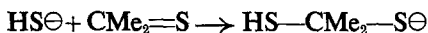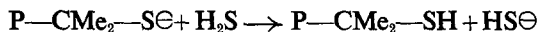
A similar role could be played by the thioenol form to give an isopropylidene end group. This could occur in the solid phase.

$$CH_2\!\!=\!\!CMe\text{—}S\ominus + CMe_2\!\!=\!\!S \rightarrow CH_2\!\!=\!\!CMe\text{—}S\text{—}CMe_2\text{—}S\ominus$$
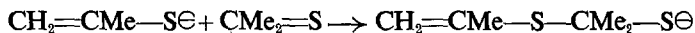
CONCLUSIONS

Liquid thioacetone spontaneously polymerizes. Light induces polymerization in the crystalline phase.

The polymer is linear and comprises $[\text{—}CMe_2\text{—}S\text{—}]_n$. This repeat unit is interrupted by $\text{—}CMe_2\text{—}S\text{—}S\text{—}CMe_2\text{—}$ and by $\text{—}CH_2\text{—}\underset{\underset{SH}{|}}{CMe}\text{—}CMe_2\text{—}S\text{—}$

The polymer irreversibly decomposes to the cyclic trimer.

REFERENCES
[1] LAL, J. *J. org. Chem.* 1961, **26**, 971
[2] Du Pont. *Brit. Pat. No. 981 346* (1965)
[3] Du Pont. *Brit. Pat. No. 932 384* (1959)

[4] LANDO, J. B. and STANNETT, V. *Polymer Letters,* 1964, **2,** 375

[5] CARAZZOLO, G., LEGHISSA, S. and MAMMI, M. *Makromol. Chem.* 1963, **60,** 171

[6] GIPSTEIN, E., WELLISCH, E. and SWEETING, O. J. *Polymer Letters,* 1963, **1,** 237

[7] Hoechst. *Brit. Pat. No. 939 367* (1959)

[8] 145th American Chemical Society National Meeting, *Chem. Engng News,* 1963, **41,** 46

[9] Du Pont. *U.S. Pat. No. 2 970 172* (1961)

[10] MIDDLETON, W. J., HOWARD, E. G. and SHARKEY, W. H. *J. org. Chem.* 1965, **30,** 1375, 1384, 1390, 1395

[11] MAYER, R., MORGENSTEIN, J. and FABIAN, J. *Angew. Chem. (Internat. Ed.),* 1964, **3,** 277

[12] FABIAN, J. and MAYER, R. *Spectrochim. Acta,* 1964, **20,** 299

[13] ROSENGREN, K. J. *Acta Chem. Scand.* 1962, **16,** 2284

[14] BAILEY, W. J. and CHU, H. *Polymer Chemistry,* 149th Meeting of American Chemical Society, Detroit (5 April 1965)

[15] VON ETTINGSHAUSEN, O. G. and KENDRICK, E. *Polymer, Lond.* 1966, **7,** 469

[16] FROMM, E. and BAUMANN, E. *Ber. dtsch. chem. Ges.* 1889, **22,** 1035, 2592

[17] SAMPEY, J. and REID, E. *J. Amer. chem. Soc.* 1932, **54,** 3404

[18] PETERS, R. A. and WAKELIN, R. W. *Biochem. J.* 1947, **41,** 555

[19] FORD-MOORE, A. H., PETERS, R. A. and WAKELIN, R. W. *J. chem. Soc.* **1949,** 1755

[20] LEWIS, G. N. and KASHA, M. *J. Amer. chem. Soc.* 1945, **67,** 994

[21] KRETOV, A. E. and KOMISSOROV, Y. F. *J. gen. Chem., Moscow,* 1935, **5,** 388

[22] SKINNER, H. A. and PILCHER, G. *Quart. Rev. chem. Soc. Lond.* 1963, **17,** 264

[23] SKINNER, H. A. *J. chem. Soc.* **1962,** 4396

[24] BENSON, S. W. and BUSS, J. H. *J. chem. Phys.* 1958, **29,** 546

[25] DAINTON, F. S. and IVIN, K. J. *Quart. Rev. chem. Soc. Lond.* 1958, **12,** 61

[26] BURNOP, V. C. E. *Polymer, Lond.* 1965, **6,** 411

[27] SMALL, P. A. *Trans. Faraday Soc.* 1953, **49,** 441

[28] ALLEN, T. L. *J. chem. Phys.* 1959, **31,** 1039

ANNOUNCEMENT

INTERNATIONAL SYMPOSIUM ON MACROMOLECULAR CHEMISTRY

The International Union of Pure and Applied Chemistry has announced that an International Symposium on *Macromolecular Chemistry* will be held in Toronto, Canada, from 3 to 6 September, 1968. All scientific sessions will be held in the Royal York Hotel.

The major theme will be 'The structure and properties of macromolecular systems' and will embrace synthetic, natural and biological polymers. Topics for discussion include: molecular structure and properties, crystallization and morphology, properties of macromolecular solutions, structure and physical properties of solid macromolecular compounds and systems, structure and function of bio-polymers.

The official languages of the symposium will be English and French. Preprints will be available at the meeting.

Enquiries should be addressed to the Organizing Committee, Box 932, Terminal A, Toronto, Canada.

The Molecular Weight Distribution
of Natural Rubber

G. M. Bristow and B. Westall

A technique for the fractionation of natural rubber by extraction with solvent mixtures has been established. Molecular weight distributions obtained by its application are wider than the normal distribution, ranging from $M = 0.07 \times 10^6$ to $M \curvearrowright 2.50 \times 10^6$, and are positively skew. 15 per cent by weight of the rubber is of molecular weight $\leqslant 0.25 \times 10^6$.

NATURAL rubber has been fractionated by many workers[1-12, 14, 15], and shown to possess a very wide molecular weight distribution ranging between 30 000 and several million[11]; low molecular weight species are associated with high oxygen content and high molecular weight species with high nitrogen content[4]. Viscosity or molecular weight distribution curves have been given by Johnson[8], Madge[12], Schulz[13], Cheng *et al.*[14] and Endo[15].

Johnson observed a maximum in the distribution curve for pale crêpe at an inherent viscosity of seven, whilst Madge reported a maximum intrinsic viscosity of 10 to 12 for unmilled rubber. Such well defined viscosity maxima were not obtained, however, in the fractionations of raw rubber carried out by Cheng *et al.*[14] and by Endo[15]. Schulz and Mula[13] have calculated molecular weight distribution functions from electron microscope particle size determinations of brominated crêpe rubber, and found a distribution curve with a maximum at approximately 1.2×10^6.

The above results do not give an entirely satisfactory picture of the molecular weight distribution of natural rubber. In this paper we report the development of a solvent extraction technique for the fractionation of natural rubber, by means of which molecular weight distributions have been determined for two different types of rubber. The technique consists of the slow precipitation of the rubber on to glass beads, the highest molecular weight material being deposited first and the lowest molecular weight material last. The rubber is then extracted with solvent mixtures of gradually increasing solvent power.

EXPERIMENTAL

Materials

Pale crêpe (No. 1X commercial grade)—This consists of about 95 per cent rubber hydrocarbon (*cis*-1,4-polyisoprene), 2 to 3 per cent proteins, 2 to 3 per cent of various acetone-soluble materials and traces of mineral salts[16].

'Sol' rubber—This rubber was substantially protein-free (N, *ca.* 0.01 per cent), but did contain *ca.* 2 per cent acetone-soluble material. For its preparation, 20 g of pale crêpe was cut into small pieces and placed in a flask with 2 litres of cyclohexane. After storage in the dark at room temperature for one week the resulting solution was filtered through lens tissue

to remove gel rubber, freeze dried, and stored at $-20°C$ to prevent degradation. Approximately 50 per cent recovery was achieved.

Ballotini—No. 15 glass beads, diameter 0·10 mm were used.

Solvents—Analytical reagent grade benzene, methanol and toluene were used throughout. The tetrahydrofuran used for light scattering measurements was treated overnight with about 2% w/v sodium hydroxide pellets and then redistilled to remove peroxides.

Apparatus and method

The apparatus consisted of a water-jacketed glass column 14 in. high and 1 in. in diameter, with a No. 1 porosity sintered glass disc fused into the lower end 2 in. above a tap which was attached to a side arm for water pump, and a B24 cone. A 6 in. × 1 in. diameter solvent reservoir, with water jacket, was fitted into the top of the column. 100 ml B24 conical flasks were used to collect the fractions. Water was circulated around the column and reservoir by means of a pump attached to a low temperature thermostat (temperature control within $\pm 0·1$ deg. C). After collection, the fractions were frozen in a Dewar bowl containing liquid nitrogen, and then dried *in vacuo*.

200 ml of benzene was added to 1 g of rubber and after standing for one week the solution was filtered through a No. 1 porosity sintered glass filter. The concentration of the solution was determined by freeze-drying a 5 ml portion and the gel content, if any, calculated. The intrinsic viscosity of a suitably diluted 2 ml sample of the solution was determined and converted to viscosity in toluene by means of the relationship[17]

$$[\eta]_{\text{toluene}} = 1·076 \, [\eta]_{\text{benzene}} - 0·15 \quad (\text{for } [\eta] \text{ dl g}^{-1})$$

The remaining solution was transferred to a 1 litre conical flask containing 200 g of Ballotini No. 15 beads, with about 20 ml of benzene. The mixture was stirred with a stainless steel paddle stirrer and an equal volume of methanol added, dropwise, over a period of one hour. The rubber-coated Ballotini beads were dried by suction on a water pump for about 15 minutes, using a No. 1 porosity sintered glass funnel, and then transferred to the fractionating column, which contained 50 ml of the solvent mixture with the lowest proportion of benzene. After the extraction period had elapsed the dissolved rubber was collected by suction into a weighed flask, freeze dried, weighed, redissolved in a known volume of toluene and the intrinsic viscosity determined. The second extracting solution, which had been maintained at operating temperature in the solvent reservoir, was then added to the column and the procedure repeated. [The solvent mixtures were prepared by mixing suitable volumes of 75–25 (v/v) and 85–15 (v/v) benzene–methanol stock solutions.]

For a refractionation, 30 ml of a 0·2 per cent solution of the fraction in toluene was precipitated with an equal volume of methanol on to 20 g of Ballotini, packed into a 30 cm × 1 cm diameter fractionating column and extracted for $\frac{1}{2}$ h periods with 10 ml portions of benzene–methanol mixtures in the above manner, at 25°C.

In order to prevent degradation it was necessary throughout the above

work to wrap the apparatus in a black cloth and store solutions in a dark cupboard.

Characterization

Determinations of intrinsic viscosity of the whole rubber and the fractions, and of the osmotic number average molecular weight of the whole rubber, were carried out using the techniques described by Bristow and Westall[17]. Light scattering determinations of the weight average molecular weight of the whole rubber were made on a Brice–Phoenix Series 1000 light scattering photometer, at room temperature (19° to 21°C) and at a wavelength of 4 358 Å, with tetrahydrofuran as solvent, using the technique described by Allen and Bristow[18]. The refractive index increment for rubber in tetrahydrofuran was taken as 0·160 by interpolation of the data of Altgelt, Schulz and Cantow[19].

Calculation

Intrinsic viscosity data were converted to molecular weights using the Carter–Scott–Magat relationship[5] and the results plotted as cumulative weight fraction/molecular weight distribution curves. The expression $(n-1) \Sigma w + \frac{1}{2}\Delta w$, where n is the number of fractions and w the wt %, representing the fraction midpoint, was used as ordinate for the cumulative weight distribution curves (*Figures 1, 2* and *3*). Differential weight/mole-
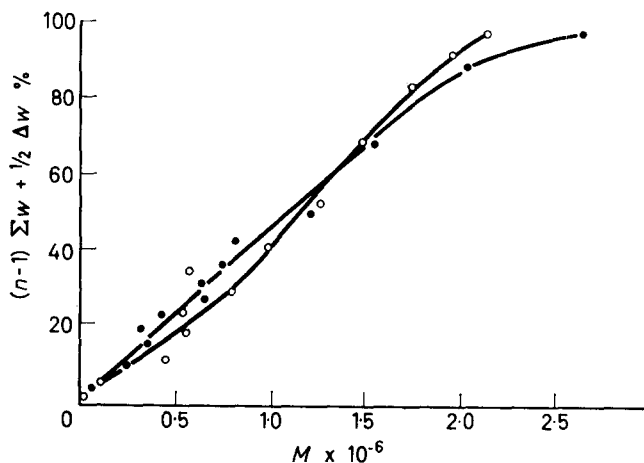
Figure 1—Cumulative weight/molecular weight distributions· of natural rubber. Extraction time 1 h. Temp. 25°C. Solvent composition increment 0·25 per cent. ○ Sol rubber. ● Pale crêpe

cular weight distribution curves are not given because the error in drawing tangents to curves where there is any degree of experimental scatter can often give misleading results.

To check the efficiency of each fractionation the summed viscosities of the fractions $\Sigma w_i [\eta]_i$ were calculated, and compared with the original
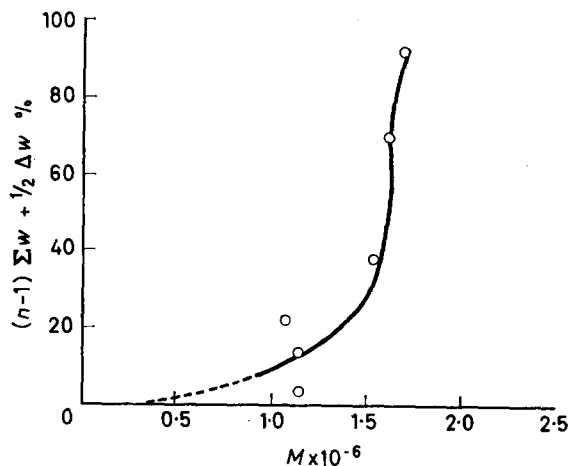
Figure 2—Refractionation of high molecular weight
fraction of sol rubber. Cumulative weight/molecular
weight distribution

viscosity of the sample. M_n and M_w were also calculated from the frac
tionation data using the relationships:

$$M_n = \frac{\Sigma\, w_i}{\Sigma\, (w_i/m_i)} \qquad M_w = \frac{\Sigma\, w_i m_i}{\Sigma\, w_i}$$
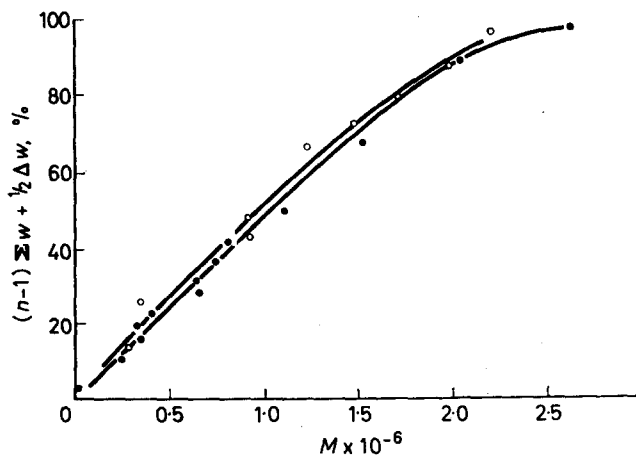
Figure 3—Cumulative weight/molecular weight distributions
of natural rubber by different methods. ● Pale crêpe (solvent
extraction technique). ○ Raw rubber (precipitation fraction-
ation, results of Endo[15])

612

Table 1. Fractionation of natural rubber

Type of rubber	Sol		Sol		Sol		Sol		Sol		Sol		Crêpe	
Extraction time (h)	1		1		½		2		1		1		1	
Temperature (°C)	25		25		25		25		20		13		25	
Vol. % benzene	$\%w_i^*$	$[\eta]_i$	$\%w_i$	$[\eta]_i$	$\%w_i$	$[\eta]_i$	$\%w_i$	$[\eta]_i$	$\%w_i$	$[\eta]_i$	$\%w_i$	$[\eta]_i$	$\%w_i$	$[\eta]_i$
78.00	1.8	0.56	1.3	—	0.5	—	0.4	—	0.6	—	0.5	—	0.5	—
78.25	6.1	1.19											5.6	0.88
78.50	7.0	3.01	5.3	1.46	6.7	1.22	6.7	1.10	3.1	0.70	2.4	0.46	6.8	2.03
78.75	6.7	3.52											4.8	2.54
79.00	4.8	3.41	6.9	2.22	5.1	1.81	7.0	1.57	5.9	1.72	2.8	1.18	3.5	2.40
79.25	6.4	4.22											2.9	2.83
79.50	3.9	3.66	9.2	3.83	7.3	3.45	6.0	2.54	6.2	3.27	1.9	1.51	5.7	3.82
79.75	8.7	5.15											4.2	3.72
80.00	15.1	6.10	10.2	4.31	11.3	3.85	10.8	5.05	7.2	4.35	3.3	2.28	5.1	4.20
80.25	16.9	6.69											5.3	4.45
80.50	12.1	7.49	21.4	6.76	17.4	6.17	29.5	6.28	10.9	5.50	3.9	2.93	9.8	5.44
80.75	5.9	8.16											26.0	6.85
81.00	2.8	8.62	30.7	6.81	22.1	7.75	21.8	6.75	13.1	6.01	2.9	2.44	15.0	8.23
81.25	1.3	6.42											4.0	9.80
81.50			9.4	7.86	16.8	8.15	13.3	7.41	22.9	7.14	7.5	3.92	0.8	—
82.00			2.5	7.80	5.8	8.38	2.4	8.96	20.9	7.61	9.8	4.70		
82.50			2.0	5.42	2.8	7.54	0.9	6.47	8.1	7.95	14.9	5.65		
83.00					2.6	7.24			1.2	7.00	27.3	7.16		
83.50					0.7	—			0.5	4.25	15.3	8.26		
84.00											3.9	6.90		
84.50											2.5	5.70		
85.00											0.6	4.16		
% Recovery	96.3		96.2		91.6		92.8		99.7		99.5		90.3	
% Recession	1.3		2.0		5.4		0.9		1.7		7.0		—	
Initial $[\eta]$	5.44		5.62		5.66		5.66		5.88		5.65		5.65	
$\Sigma\, w_i [\eta]_i$	5.30		5.76		5.83		5.47		5.98		5.59		5.28	
M_n (osm.)	(370 000)		474 000		474 000		474 000		461 000		411 000		486 000	
M_n (calc.)	500 000		<716 000		<646 000		528 000		<586 000		441 000		510 000	
M_w (light scat.)	0.93×10^6		0.93×10^6		0.93×10^6		0.93×10^6		1.06×10^6		0.97×10^6		—	
M_w (calc.)	1.10×10^6		1.21×10^6		1.28×10^6		1.15×10^6		1.29×10^6		1.18×10^6		1.14×10^6	

*w_i is weight fraction.

A summary of the fractionation data is given in *Table 1*.

Effect of solvent concentration increment

An apparently satisfactory fractionation of sol rubber was achieved using benzene–methanol mixtures of composition increasing in steps of 0·25 per cent. benzene content from 78–22 benzene. Extraction time was one hour for each solvent mixture and the operating temperature 25°C. A wide distribution of molecular weight was obtained with fractions ranging from 112 000 to nearly 2×10^6. Approximately two per cent of material of apparent molecular weight 36 000 was obtained but it is doubtful whether this is entirely polyisoprene, because of the abnormally high value of the Huggins constant ($k' = 1·67$) as against an average of about 0·4. There was very little variation in the overall shape of the distribution curve when the solvent concentration increment was changed from 0·25 to 0·5 per cent though more fractions were obtained with the former, with consequent improvement in definition.

Effect of extraction time

The effect of extraction time upon the molecular weight distribution was also studied. The temperature was kept constant at 25°C, and the solvent concentration increment was 0·5 per cent. Up to a molecular weight of about 1×10^6, variation of extraction time from $\frac{1}{2}$ h to 2 h has little effect on the distribution but above this molecular weight, whilst results obtained with 1 h and 2 h extraction times are fairly similar, those obtained with only $\frac{1}{2}$ h extraction time show considerably less weight extracted at a given molecular weight, indicating that extraction of rubber is incomplete. Recession, i.e. a diminution in molecular weight of the final fractions, was also observed under these latter conditions. This effect has frequently been attributed to degradation, e.g. ref. 21, but it has only been found in this work when equilibrium was not complete and when no degradation had been observed. If recession greater than two or three per cent is present, an erroneous molecular weight distribution will be found.

Effect of extraction temperature

An examination was also made of the effect of extraction temperature upon the molecular weight distribution. Fractionations were carried out at 25°C, 20°C and 13°C (extraction time 1 h, solvent composition increment 0·5 per cent). The distributions obtained at the several temperatures were similar, though some recession (7·0 per cent) was found at 13°C.

A typical distribution curve for sol rubber is shown in *Figure 1*.

Refractionation

Figure 2 shows the results of a refractionation of a high molecular weight fraction of sol rubber carried out in order to determine the degree of homogeneity of the sample. Only 70 per cent weight recovery was achieved, but the summed viscosities of the fractions (6·13) showed satisfactory agreement with the original viscosity of the sample (6·32). The molecular weight distribution curve indicates that the sample is about 75 per cent homogeneous.

From the above work it is concluded that a satisfactory fractionation of natural rubber using the solvent extraction technique can be carried out under the optimum conditions described above, i.e. at 25°C with 1 h extraction period, and solvent mixtures of composition changing from 78–22 benzene–methanol by increments of 0·25 per cent benzene to above 81–19 benzene–methanol.

The shape of the cumulative weight/molecular weight distribution curves described above has been shown to be very dependent upon the conditions of extraction, i.e. temperature, time and composition of extracting solvent, and demonstrates the necessity for careful examination of these factors before coming to any firm conclusions about the nature of any molecular weight distribution.

Fractionation of crêpe rubber

The molecular weight distributions for sol and crêpe rubber carried out under the optimum conditions are compared in *Figure 1*. The two curves are very similar and any differences could be due to experimental error. It would appear therefore that the removal of the major part of the nitrogen-containing material from the crêpe rubber has not greatly affected the molecular weight or molecular weight distribution.

It is of interest to note that the samples of sol rubber used contained only *ca.* 50 per cent by weight of the original crêpe, whilst the portion of the crêpe rubber fractionated comprised 97 per cent by weight of the whole rubber. In other words the 'gel' left when the sol rubber was prepared from cyclohexane did not differ appreciably in terms of molecular weight and molecular weight distribution from the benzene-soluble portion of the crêpe. The three per cent of the crêpe which was insoluble in benzene was presumably composed of the small particles discussed by Allen and Bristow[20].

DISCUSSION

In all the above work recovery of the starting material was 90 to 100 per cent by weight, which was considered adequate. Comparison of the summation of individual fraction viscosities with respect to weight, $\Sigma w_i [\eta]_i$, with the intrinsic viscosity of the whole polymer indicates that little if any degradation had taken place.

Values of M_n and M_w were determined by osmotic and light scattering measurements on the samples of rubber before fractionation. Where the calculated values of M_n were appreciably higher than those obtained experimentally, the first fraction had not been characterized due to shortage of material; otherwise agreement was within ±10 per cent. Calculated values of M_w were up to 20 per cent higher than experimental values. It is difficult to say whether this is due to a slight discrepancy in the Carter–Scott–Magat equation used for conversion of viscosity data to molecular weight, or whether the value of 0·160 for the refractive index increment for natural rubber in tetrahydrofuran used for calculation of these results is too small.

In *Figure 3* the fractionation of pale crêpe using the solvent extraction technique is compared with a fractionation of raw rubber (type unspecified)

by Endo[15] using a precipitation technique. Molecular weights are calculated from the viscosity data given by these workers. Agreement between the two methods is very close. It is considered that the solvent extraction method as presented is preferable in that better definition is given to the low molecular weight portion of the curve in that more fractions are obtained; it is also considerably less time-consuming.

Cumulative molecular weight distributions of sol rubber and pale crêpe are given in *Figure 4* on arithmetical probability scales. A good straight line is obtained showing that Gaussian statistics probably apply but the
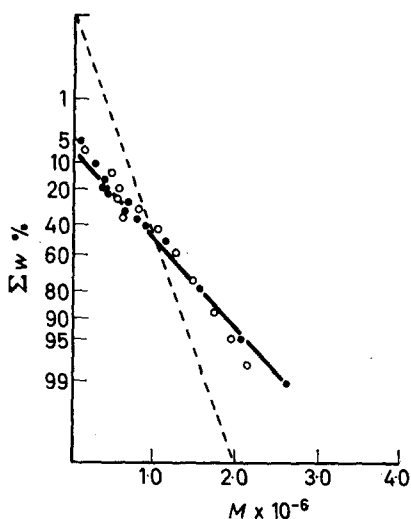
Figure 4—Cumulative weight/molecular weight distributions of natural rubber, plotted on arithmetic probability scales. Extraction time 1 h. Temp. 25°C. Solvent composition increment 0·25 per cent. ○ Sol rubber. ● Pale crêpe. – – – – Normal distribution

slope differs considerably from that shown for a normal distribution of the same weight average molecular weight. Histograms derived from these two straight lines are shown in *Figure 5*. Appreciably higher proportions of low and high molecular weight material are obtained for the natural rubber than for the normal distribution, which is correspondingly
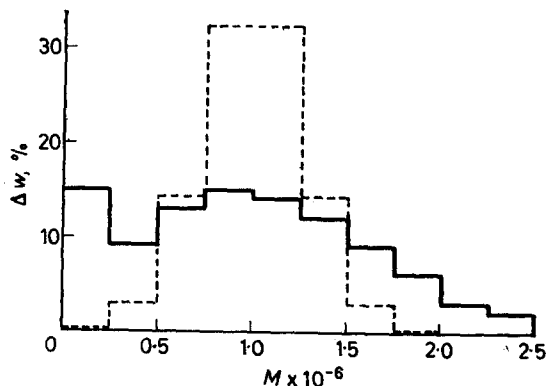
Figure 5—Histograms derived from *Figure 4*.
– – – – Normal distribution. ——— Pale crêpe

deeper in the centre region than is that for natural rubber. The distribution for natural rubber is also markedly positively skew. It would appear possible that there are two overlapping distributions with maxima of the order of $0.07 \times 10^6 < M < 0.25 \times 10^6$ and $0.75 \times 10^6 < M < 1.25 \times 10^6$. The position of the presumed second maximum is in reasonable agreement with the work of Schulz and Mula[13] who obtained a slightly positively skew unimodal distribution with a maximum at $M = 1.2 \times 10^6$ for specially prepared crêpe rubber. It is probable that the electron microscope technique used by these workers is not sufficiently sensitive to detect the first peak. The differential weight intrinsic viscosity distribution for raw rubber given by Madge[12] shows a single well defined maximum of approximately 11. This corresponds to $M = 1.3 \times 10^6$ (using the Carter–Scott–Magat equation), which also agrees reasonably well with the value obtained in this work.

The Natural Rubber Producers' Research Association,
 Welwyn Garden City, Herts.

REFERENCES

[1] MIDGLEY, T., HENNE, A. L. and RENOLL, M. W. *J. Amer. chem. Soc.* 1931, **53**, 2733

[2] MIDGLEY, T., HENNE, A. L. and RENOLL, M. W. *J. Amer. chem. Soc.* 1932, **54**, 3343

[3] KEMP, A. R. and PETERS, H. *J. phys. Chem.* 1939, **43**, 1063

[4] BLOOMFIELD, G. and FARMER, E. H. *I.R.I. Trans.* 1940, **16**, 69

[5] CARTER, W. C., SCOTT, R. L. and MAGAT, M. *J. Amer. chem. Soc.* 1946, **68**, 1480

[6] BATEMAN, L. *J. Polym. Sci.* 1949, **2**, 1

[7] HAUSER, E. A. and LE BEAU, D. S. *Rubber Chem. Technol.* 1947, **20**, 70

[8] JOHNSON, B. L. *Industr. Engng Chem. (Industr.)*, 1948, **40**, 351

[9] BYWATER, S. and JOHNSON, P. *Trans. Faraday Soc.* 1950, **47**, 195

[10] BLOOMFIELD, G. F. and DRAKE, G. W. *J. Rubb. Res. Inst. Malaya*, 1951, *Commun.* No. 272

[11] WAGNER, H. L. and FLORY, P. J. *J. Amer. chem. Soc.* 1952, **74**, 195

[12] MADGE, E. W. *Chem. & Ind.* 1962, **42**, 1806

[13] SCHULZ, G. V. and MULA, A. *Proceedings* of the Natural Rubber Research Conference 1960, pp 602–610. R.R.I. Malaya: Kuala Lumpur, 1961

[14] CHENG, YUNG-SHIH, HO, TSUE-TUAN and CHIEN, JEN-YUAN. *Acta chim. sin.* 1956, **22**, 156

[15] ENDO, RYUICHI. *Chem. High Polymers, Tokyo*, 1961, **18**, 214

[16] BLOOMFIELD, G. F. *The Applied Science of Rubber* (ed. W. J. S. NAUNTON), p 63. Arnold: London, 1961

[17] BRISTOW, G. M. and WESTALL, B. *J. appl. Polym. Sci.* 1965, **9**, 495

[18] ALLEN, P. W. and BRISTOW, G. M. *J. appl. Polym. Sci.* 1960, **4**, 237

[19] SCHULZ, G. V., ALTGELT, K. and CANTOW, H. J. *Makromol. Chem.* 1956, **21**, 13

[20] ALLEN, P. W. and BRISTOW, G. M. *J. appl. Polym. Sci.* 1961, **5**, 510

[21] SHYLUK, S. *J. Polym. Sci.* 1962, **62**, 317

The Electrical Conductivity of Some TCNQ Complexes Derived from 2,2'-Dichlorodiethyl Ether and Poly(epichlorhydrin)

J. Malcolm Bruce and J. R. Herson

The chloromethyl groups of 2,2'-dichlorodiethyl ether and poly(epichlorhydrin) have been used to quaternize pyridine, and the quaternary compounds have been converted into simple and complex salts with TCNQ. The resistivities of these salts have been measured.

COMPARATIVELY high electrical conductivities have been observed for simple organic donor–acceptor systems, especially those involving nitrogenous bases (B) and TCNQ [7,7,8,8-tetracyanoquinodimethane (I)].
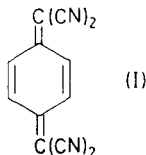
Three types of system have been prepared: complexes B,TCNQ, simple salts RB^+ $TCNQ^-$ in which R is usually alkyl, and complex salts RB^+ $TCNQ^-$ $TCNQ^0$. The simple salts are obtained from quaternary salts RB^+ X^- by metathesis with the lithium salt, Li^+ $TCNQ^-$, of the anion radical of TCNQ, and the complex salts by incorporation of neutral TCNQ into the simple salts. The complex salts show the highest conductivities[1,2].

Attempts have recently been made[3] to prepare conducting polymeric systems by using the pendant pyridyl groups in poly(2- and 4-vinyl-pyridines) as sites for the attachment of TCNQ residues, but the salts obtained had much lower conductivities than those of analogous monomeric systems, and, further, the maximum conductivity of the complex systems occurred when the quotient $[TCNQ^-]/[TCNQ^0]$ was considerably greater than unity.

The present paper describes some studies with poly(epichlorhydrin) in which the chloromethyl groups were used to quaternize pyridine, and the resulting pyridinium chlorides were then converted into simple and complex salts. Ethyl iodide and 2,2'-dichlorodiethyl ether were used as models in order to determine appropriate reaction conditions, and to provide compounds of defined composition for use as spectroscopic standards.

EXPERIMENTAL

Solvents, ethyl iodide, and 2,2'-dichlorodiethyl ether were dried and fractionally distilled; it is important that solvents should not contain readily reducible impurities since these can oxidize $TCNQ^-$ to $TCNQ^0$.

Poly(epichlorhydrin) was prepared using a ferric chloride–propylene oxide catalyst[4], and had $\overline{M_v} \sim 70\,000$. TCNQ was sublimed at $150°/10^{-4}$ mm Hg. Li$^+$ TCNQ$^-$ was prepared[1] from TCNQ and lithium iodide in acetonitrile. Reactions were carried out under nitrogen, and, unless water was involved in the preparation, the products were handled in a dry-box filled with nitrogen.

Ultra-violet–visible spectroscopy was used to differentiate between simple and complex salts, and for the determination[1] of the extent of incorporation of TCNQ$^-$ and TCNQ^0 in the simple and complex salts respectively; carefully purified solvents, usually acetonitrile or dimethyl formamide (DMF), were required in order to obtain reproducible spectra. TCNQ had $\lambda_{max.}$ (in MeCN) 392 mμ (ϵ 39 000), and $\lambda_{max.}$ (in DMF) 338 mμ (ϵ 27 000). Li$^+$ TCNQ$^-$ had $\lambda_{max.}$ (in MeCN) 392 (infl.) 406, 418 mμ (ϵ 21 500, 25 000, 26 000), and $\lambda_{max.}$ (in DMF) 395 (infl.), 408, 420 mμ (ϵ 19 500, 22 000, 23 000). Infra-red spectroscopy of Nujol mulls provided further information: the simple salts had a sharp band at 850 cm^{-1} which was absent from the complex salts.

Resistivity measurements were made using the four-probe method[5] on compressed discs prepared from samples which had been dried at $20°/10^{-2}$ mm Hg over phosphorus pentoxide for 60 hours. The probes were gold-plated. Activation energies were determined from Arrhenius plots obtained by measuring the resistivities at 5° intervals from $-20°$ to $+20°$ inclusive; good straight-line plots of $\log \rho$ versus $10^3/T$ were obtained. All measurements at 20° and those at other temperatures required for the determination of the activation energies quoted in *Table 2* were made *in vacuo*; measurements for the activation energies quoted in *Table 1* were made under a stream of dry nitrogen maintained at the required temperature.

Compounds were prepared as follows, using equimolar proportions of reactants unless stated otherwise:

(a) A boiling solution of N-ethylpyridinium iodide (0·13 g) in ethanol (3 cm^3) was added to a filtered solution of Li$^+$ TCNQ$^-$ (0·11 g) in boiling ethanol (30 cm^3), the mixture was boiled for a few minutes, and allowed to cool to room temperature. The precipitate was collected, and washed with ice-cold ethanol and then with ether to give (N-ethyl pyridinium)$^+$ TCNQ$^-$ (0·065 g, 30 per cent) as purple microcrystals, decomp. 225° to 235° (Found: N, 22·8. C$_{19}$H$_{13}$N$_5$ requires N, 22·5 per cent). It had $\lambda_{max.}$ (in MeCN) 392 (infl.), 406, 418 mμ (ϵ 21 500, 24 500, 25 500), and $\lambda_{max.}$ (in DMF) 395 (infl.), 408, 420 mμ (ϵ 19 000, 21 000, 22 000).

(b) A solution of the foregoing simple salt (0·074 g) in acetonitrile (4 cm^3) was treated with a boiling solution of TCNQ (0·067 g) in acetonitrile (5 cm^3), the mixture was allowed to cool to room temperature, and the precipitate was collected and washed with ether to give (N-ethyl pyridinium)$^+$ TCNQ$^-$, TCNQ^0 (0·078 g, 55 per cent) as deep purple needles, decomp. 195° to 235°. It had $\lambda_{max.}$ (in MeCN) 393 mμ (ϵ 59 000) and $\lambda_{max.}$ (in DMF) 338, 395 (infl.), 408, 420 mμ (ϵ 26 500, 19 500, 20 500, 21 500).

(c) A solution of 2,2′-dichlorodiethyl ether (1·29 g) in pyridine (5 cm³) was refluxed for 12 h, and the excess of pyridine was then removed at 60°/10⁻² mm Hg to leave 2,2′-dipyridiniumdiethyl ether dichloride as a white solid (2·82 g, 100 per cent) (Found: C, 55·6; H, 6·3; Cl, 23·5; N, 9·1. $C_{14}H_{18}Cl_2N_2O$ requires C, 55·8; H, 6·0; Cl, 23·6; N, 9·3 per cent). It had $\lambda_{max.}$ (in EtOH) 261 mμ (ϵ 8 400).

(d) Treatment of the foregoing pyridinium salt with Li⁺ TCNQ⁻ as described under (a) gave (2,2′-dipyridiniumdiethyl ether)²⁺ (TCNQ⁻)₂ (75 per cent yield) as purple microcrystals, decomp. 205° to 225° (Found: N, 21·8. $C_{38}H_{26}N_{10}O$ requires N, 21·9 per cent). It had $\lambda_{max.}$ (in MeCN) 392 (infl.), 406, 418 mμ (ϵ 44 000, 51 000, 53 000), and $\lambda_{max.}$ (in DMF) 395 (infl.), 408, 420 mμ (ϵ 39 000, 44 000, 46 000).

(e) Treatment of the foregoing simple salt with TCNQ as described under (b) gave (2,2′-dipyridiniumdiethyl ether)²⁺ (TCNQ⁻)₂ TCNQ⁰ (80 per cent yield) as deep purple needles, decomp. 230° to 245° (Found: N, 22·9. $C_{50}H_{30}N_{14}O$ requires N, 23·3 per cent). It had $\lambda_{max.}$ (in MeCN) 393 mμ (ϵ 80 500), and $\lambda_{max.}$ (in DMF) 338, 395 (infl.), 408, 420 mμ (ϵ 52 500, 39 500, 41 000, 42 500). An attempt to introduce a further mol. of TCNQ⁰ by using an excess of TCNQ and a reaction time of one hour was unsuccessful.

(f) A solution of poly(epichlorhydrin) (1·58 g) in pyridine (5 cm³) was refluxed for 24 h (a precipitate was formed), and the excess of pyridine was removed at 60°/10⁻² mm Hg to give the polymeric pyridinium compound as a light-brown solid [Found: C, 53·5; H, 6·1; N, 7·7. $(C_8H_{10}ClNO)_n$ requires C, 56·0; H, 5·9; N, 8·2 per cent] which had $\lambda_{max.}$ (in EtOH) 261 mμ (ϵ 3 800). These data indicate that ca. 90 per cent of the chloromethyl groups have reacted with pyridine. Attempts to obtain a higher extent of reaction by prolonging the reflux period led to decomposition, and the use of solvents in attempts to prevent the precipitation of the quaternary compound resulted in lower incorporation of pyridinium groups.

(g) The foregoing quaternary compound (2·55 g) in ethanol (80 cm³) was added to Li⁺ TCNQ⁻ (3·5 g) in DMF (80 cm³), the mixture was refluxed for 2 h, cooled and diluted with water (700 cm³). The precipitate was collected, washed successively with water, ethanol, and ether, and then refluxed with benzene (150 cm³) for 4 h to remove any neutral TCNQ. The polymeric simple salt (3·5 g, 70 per cent) was a purple powder [Found: C, 67·5; H, 4·9; N, 18·3; Cl, 3·5. $(C_{20}H_{14}N_5O)_n$ requires C, 69·5; H, 4·1; N, 20·0 per cent] which decomposed in DMF: the absorption at 420 mμ, characteristic of TCNQ⁻, decayed, and new absorptions, due to a decomposition product, appeared at 330 and 483 mμ, and progressively increased in intensity until, when the peak at 420 mμ had disappeared, that at 483 mμ had ϵ 19 000. The relative intensities of the peaks at 420 and 483 mμ showed an almost linear relationship, and extrapolation back to zero decomposition gave $\lambda_{max.}$ (in DMF) 395 (infl.), 408, 420 mμ (ϵ 15 600, 16 800, 17 600), indicating that 80 per cent of the pyridinium chloride residues had reacted. Solid samples kept in the air decomposed similarly, although much less rapidly.

621

(*h*)   Typically, the foregoing polymeric simple salt (0·46 g) and TCNQ (0·058 g) were dissolved in DMF (25 cm³), and the DMF was removed at 20°/10⁻² mm Hg to leave the polymeric complex salt as a shiny black solid film which had $\lambda_{max.}$ (in DMF) 338, 395 (infl.), 408, 420 mμ (ϵ 10 000, 17 500, 20 000, 22 000 by extrapolation). Like the simple salt, it decomposed in DMF, finally to $\lambda_{max.}$ 347, 418 and 481 mμ. Polymeric complex salts containing various proportions (see *Table 2*) of neutral TCNQ were prepared analogously. When these samples were pressed into discs for resistivity measurements, green patches, suggesting the presence of crystals of neutral TCNQ, appeared on the surface of some of them, and a steady current could not be maintained during the resistivity determinations.

<div align="center">RESULTS AND DISCUSSION</div>

Treatment of 2,2'-dichlorodiethyl ether with pyridine gave the bis-quaternary compound from which the simple salt (II) was obtained, but only one mol. of neutral TCNQ could be introduced into (II) when attempts were made to prepare the complex salt. Interaction of the neutral TCNQ with both TCNQ anion radicals in (II), possibly by formation of a sandwich compound such as (III), may account for this; possibly related compounds, but containing inorganic cations, e.g. $(Cs^+)_2(TCNQ^{\cdot-})_2(TCNQ^0)$, have been observed previously[1].
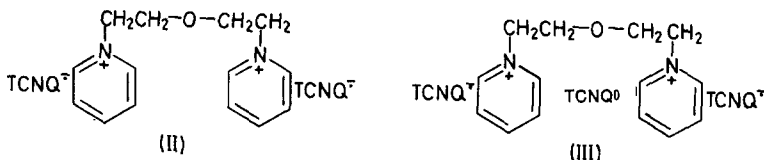
Resistivities and activation energies for the simple (II) and complex (III) salts prepared under different conditions are given in *Table 1*. The resistivities of the samples prepared under nitrogen were higher than those of samples prepared in air, and the resistivities of the samples prepared under nitrogen fell when they were exposed to air, despite subsequent drying prior to the electrical measurements. The decrease in resistivity of the samples exposed to air may be the result of any increase in resistivity due to oxidative decomposition being more than offset by a decrease due to absorption of moisture which could not be removed by drying. The activation energies do not show a parallel trend.

Table 1.   Resistivities and activation energies for compounds (II) and (III)

Compound	Conditions of preparation	ρ (ohm cm at 20°C)	E (eV)
II	a	4.40×10^5	—
II	b	2.52×10^6	0·413
II	c	1.25×10^6	0·385
III	a	2.23×10	—
III	b	1.21×10^2	0·170
III	c·	2.95×10	0·206

(*a*) In air. (*b*) Under nitrogen. (*c*) Under nitrogen, then exposed to air. All samples dried prior to measurement of resistivity.

In view of these observations, the polymer samples were handled entirely under nitrogen. About 90 per cent of the pendant chloromethyl groups in the poly(epichlorhydrin) reacted with pyridine, and about 80 per cent of the resulting pyridinium units underwent metathesis with Li^+ TCNQ $^-$. The resistivities of five polymers (approximately as IV) containing different proportions of $TCNQ^0$ are given in *Table 2*. Activation energies were determined for two of the samples.

(IV)
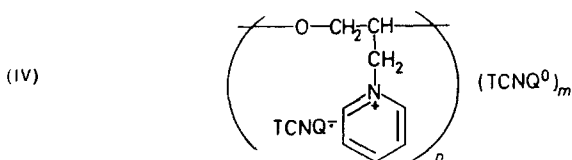
Table 2. Resistivities and activation energies for polymeric complex salts (IV)

$TCNQ^0$ content (% by wt)	$\dfrac{[TCNQ^{-}]}{[TCNQ^0]}$	ρ (ohm cm at 20°C)	E (eV)
0	—	1.5×10^7	0.36
5	10	7.5×10^5	—
15	3.0	3.2×10^4	—
22	1.9	2.6×10^2	—
33	1.1	8.8×10	0.11

As expected, the resistivity falls as the proportion of $TCNQ^0$ is increased, and extrapolation of a plot of $\log \rho$ versus $[TCNQ^-]/[TCNQ^0]$ to $[TCNQ^-]/[TCNQ^0] = 1$ indicates a limiting resistivity of about 60 ohm cm. In contrast to the model simple salt (II), the polymeric simple salt (IV; $m = 0$) is capable of taking up almost the theoretical amount of neutral TCNQ required to yield a normal complex salt. However, the resistivities of (III) and (IV; $n = m$) were not significantly different, indicating that the proximity of potentially conducting groups attached to an essentially insulating chain does not in this case confer conductivity properties which cannot be achieved through the crystal lattice of a system of much lower molecular weight, although a more highly conducting polymer might have resulted had it been possible to cause all the chloromethyl groups to react. These results contrast with those[3] mentioned above for systems based on poly(vinylpyridine).

The polymeric TCNQ compounds decomposed in air, in solution and in the solid state, considerably more rapidly than the model compounds. This may be due to attack of oxygen at the polymer backbone leading to oxidative elimination of cyano groups (cf. ref. 6) from the TCNQ units; such a reaction could be catalysed by traces of iron remaining from the catalyst used for the preparation of the poly(epichlorhydrin). Accelerated decomposition of other polymeric salts has been independently observed[7].

Department of Chemistry,
  The University,
    Manchester, 13

REFERENCES

[1] MELBY, L. R., HARDER, R. J., HERTLER, W. R., MAHLER, W., BENSON, R. E. and MOCHEL, W. E. *J. Amer. chem. Soc.* 1962, **84,** 3374

[2] MELBY, L. R. *Canad. J. Chem.* 1965, **43,** 1448
CHESTNUT, D. B. and PHILLIPS, W. D. *J. chem. Phys.* 1961, **35,** 1002

[3] HATANO, M., NOMORI, H. and KAMBARA, S. *Polymer Preprints, Amer. chem. Soc., Div. of Polymer Chem.,* Sept. 1964, p 849
LUPINSKI, J. H., KOPPLE, K. D. and HERTZ, J. J. *Preprints, I.U.P.A.C. Symposium on Macromolecular Chemistry, Prague,* Aug. 1965, p 196

[4] PRUITT, M. E. and BAGGETT, J. M. *U.S. Pat. No. 2 706 181* (1955)
PRUITT, M. E., BAGGETT, J. M., BLOOMFIELD, R. J. and TEMPLETON, J. H. *U.S. Pat. No. 2 706 182* (1955)

[5] VALDES, L. B. *Proc. Inst. Radio Engrs,* 1954, **42,** 420
UHLIR, A. *Bell Syst. tech. J.* 1955, **32,** 105

[6] HERTLER, W. R., HARTZLER, H. D., ACKER, D. S. and BENSON, R. E. *J. Amer. chem. Soc.* 1962, **84,** 3387

[7] GOODINGS, E. P. and WRIGHT, P. Personal communication

Ionic Polymerizations of α-Methylstyrene Catalysed by Iodine in an Electric Field*

Ichiro Sakurada, Norio Ise and Yoshinobu Tanaka

α-Methylstyrene was polymerized with iodine as a catalyst in nitrobenzene or toluene as the solvent in the presence and absence of an electric field. In nitrobenzene, a large field-accelerating effect was found, while the degree of polymerization was increased, though very slightly, by the application of the electric field. In toluene, no field effects on the polymerization rate and the degree of polymerization were observed.

THE influence of a high intensity electric field on various types of polymerization has been investigated in our laboratory and it has been found that the field can accelerate the polymerization rates of some cationic systems. For α-methylstyrene catalysed by iodine in 1,2-dichlorethane (DCE), the rate has been increased[1] by 30 per cent in the presence of an electric field of 1 kV cm⁻¹. The present paper presents the experimental data of the field effects on the systems α-methylstyrene–iodine–nitrobenzene and α-methylstyrene–iodine–toluene.

EXPERIMENTAL

The monomer was carefully purified by the method previously described[1]. The solvents were fractionally distilled under dry nitrogen. The specific conductivity of the purified nitrobenzene was below 10^{-7} mho cm⁻¹. Iodine (analytical reagent grade of Merck) was used without further purification.

The polymerizations were carried out in a glass vessel fitted with a thermometer and a pair of platinum plate electrodes of 2 cm² in area and 3·7 cm apart. The cell constant was 1·0 cm⁻¹. Details of the polymerization procedures have been described[1]. The polymerization temperatures were 8°C and −78°C for nitrobenzene and toluene, respectively, unless otherwise specified.

The average molecular weight (M) of the polymer produced was determined by viscosity measurement in benzene at 30°C by using the equation

$$[\eta] = 0\cdot0150 + 1\cdot787 \times 10^{-5}M$$

which was obtained by Worsfold and Bywater[2]. Here $[\eta]$ is in units of decilitres per gramme.

RESULTS

I. Nitrobenzene

Polymerization rate and catalyst concentration—The initial rate of polymerization was calculated from the slope of log [M] versus time plots, where [M] represents the monomer concentration. These plots were found to be linear in a conversion range between zero and ten per cent. The rate
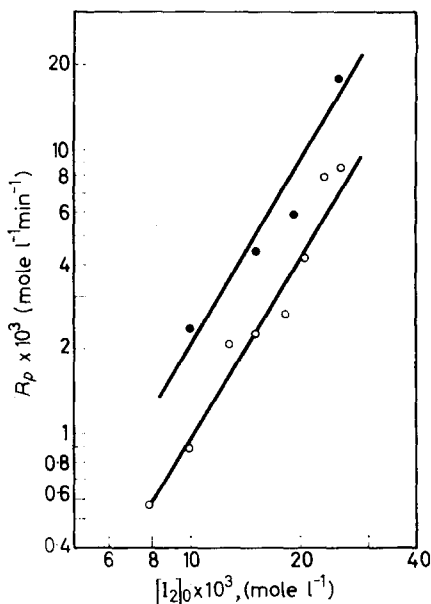
Figure 1—Polymerization rate versus initial catalyst concentration for α-methylstyrene–iodine–nitrobenzene. ($[M]_0 = 0.80$ mole 1^{-1}, $8°C$). $\bullet$, $E = 0.11$ kV cm^{-1}; $\bigcirc$, $E = 0$

of polymerization thus obtained is given as a function of the initial concentration of catalyst in *Figure 1*. The filled circles denote the rates in the presence of an electric field (R_{pE}) and the blank ones the rates with no field (R_{p0}). Clearly, the application of the electric field increases the rates. Furthermore, the relative increase due to the field can be regarded as independent of the initial concentration of catalyst. The independence of the field effects from the catalyst concentration was previously found for other cationic systems such as p-methoxystyrene–iodine–DCE[3], α-methylstyrene–iodine–DCE[1], isobutyl vinyl ether–iodine–DCE[4], and styrene–boron tri-
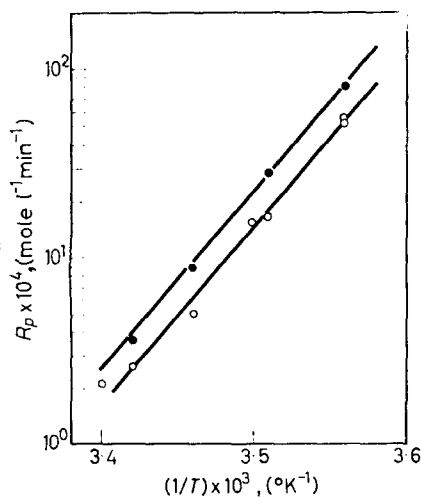
Figure 2—Polymerization rate versus reciprocal polymerization temperature for α-methylstyrene–iodine–nitrobenzene. ($[M]_0 = 0.80$ mole 1^{-1}, $[I_2]_0 = 1.5 \times 10^{-2}$ mole 1^{-1}). $\bullet$, $E = 0.08$ kV cm^{-1}; $\bigcirc$, $E = 0$

fluoride etherate[5]. The rates are seen to be proportional to the second power of the catalyst concentration both in the presence and in the absence of the field.

Polymerization rate and polymerization temperature—The rate of polymerization was determined at various temperatures and the results are given in *Figure 2*. From this figure the apparent overall activation energy is -44 kcal mole^{-1} in the presence and absence of the field. Using this value for the activation energy and observed temperature rise due to the Joule heat, the observed polymerization rate was corrected. R_{pE} and R_{p0} given in this paper are the corrected values.
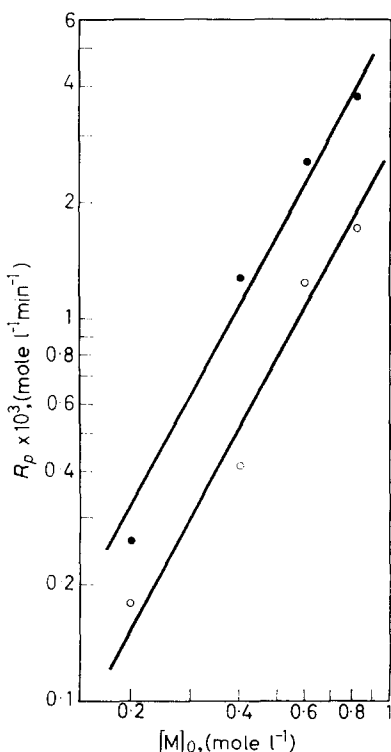
Figure 3—Polymerization rate versus initial monomer concentration for α-methylstyrene–iodine–nitrobenzene. ($[I_2]_0 = 1\cdot5\times10^{-2}$ mole l^{-1}, 8°C). ●, $E=0\cdot11$ kV cm^{-1}; ○, $E=0$

Polymerization rate and monomer concentration—*Figure 3* shows the variation of the initial rate of polymerization with the initial monomer concentration. It should be noted that toluene was used in the present experiments as a substitute for the monomer in order to keep the dielectric constant of the polymerizing solutions of varying monomer compositions practically constant. It is clear from *Figure 3* that the application of an electric field increased the polymerization rate, and that the relative increase was independent of the monomer concentration. These results are in line with our previous observation[1, 3-5]. Furthermore, the R_p value was proportional to the second power of the initial monomer concentration.

627
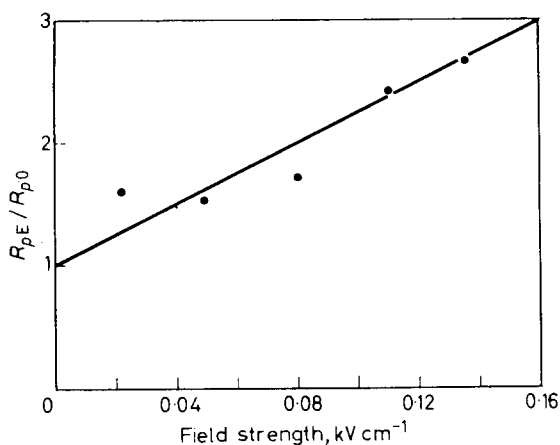
Figure 4—Field effect versus field strength for α-methyl-styrene–iodine–nitrobenzene. ($[M]_0 = 0 \cdot 80$ mole 1^{-1}, $[I_2]_0 = 1 \cdot 5 \times 10^{-2}$ mole 1^{-1}, $8°C$)

Field effect and field strength—The field effect on the polymerization rate is expressed by $R_{pE}/R_{p0}^{\cdot}$ and is given in *Figure 4* as a function of the field strength. A linear relationship appears to hold in the range studied.

Degree of polymerization—In *Table 1* the degrees of polymerization (at zero conversion) of polymers produced under an electric field ($\bar{P}_E$) and in its absence ($\bar{P}_0$) are given. The changes in the degree of polymerization due to the Joule heat were corrected by using the results of control experiments shown in *Figure 5*, which gives the limiting viscosity numbers of polymers

Table 1. Field influence on the degree of polymerization for an α-methylstyrene–iodine–nitrobenzene system.
$[I_2]_0 = 1 \cdot 5 \times 10^{-2}$ mole 1^{-1} at $8°C$.
Field strength $0 \cdot 11$ kV cm^{-1}

Monomer *concn* (mole 1^{-1})	$\bar{P}_0$	$\bar{P}_E$	$\bar{P}_E/\bar{P}_0$
0·80	23	26	1·1
0·59	22	27	1·2
0·29	18	25	1·4
0·21	20	22	1·1
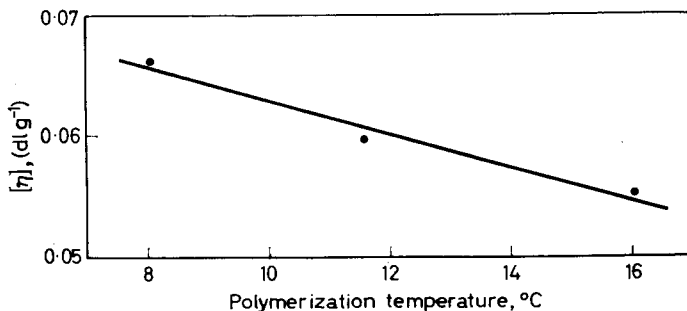
Figure 5—Limiting viscosity number versus polymerization temperature for α-methylstyrene–iodine–nitrobenzene. ($[M]_0 = 0 \cdot 80$ mole 1^{-1}, $[I_2]_0 = 1 \cdot 5 \times 10^{-2}$ mole 1^{-1})

Figure 6—Polymerization rate versus initial catalyst concentration for α-methylstyrene–iodine–toluene. ($[M]_0$ = 0·80 mole 1^{-1}, −78°C). ●, E = 2 kV cm^{-1}; ○, E = 0
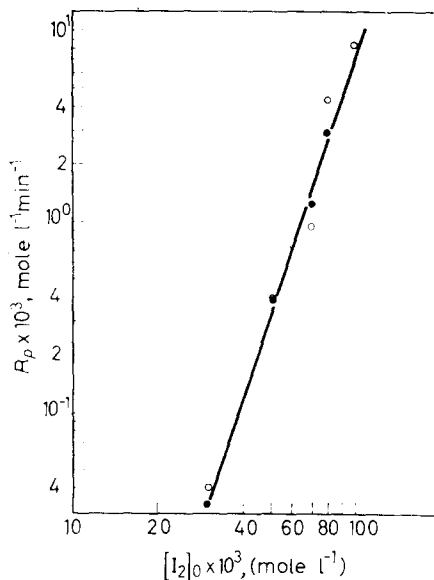
obtained at three different temperatures. *Table 1* shows that the application of an electric field increases, though only slightly, the degree of polymerization. Similar effects have been observed for some other cationic systems for which the field-accelerating effects have been found[1,3,4].
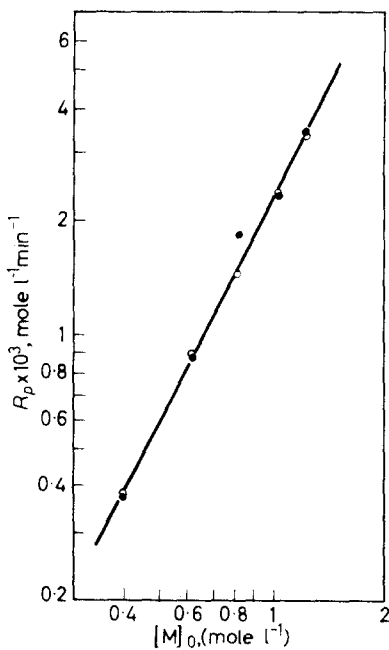
Figure 7—Polymerization rate versus initial monomer concentration for α-methylstyrene–iodine–toluene. ($[I_2]_0$ = 7 × 10^{-2} mole 1^{-1}, −78°C). ●, E = 4 kV cm^{-1}; ○, E = 0

II. Toluene

Polymerization rate and catalyst concentration—The initial rates of polymerization, which were determined in the same way as those for nitrobenzene, are given as a function of the initial concentration of catalyst in *Figure 6*. The rates obtained under an electric field of 2 kV cm^{-1} (denoted by the filled circles) fall on the same straight line as those in the absence of the electric field (given by the blank circles), indicating no field-accelerating effects. The polymerization rate is seen to be proportional to the 4·6th power of the catalyst concentration.

As the current strength was very small in the toluene systems, no temperature rise was observed. In consequence, the Joule heat correction was not needed.

Polymerization rate and monomer concentration—The polymerization rates are given as a function of the initial monomer concentration in *Figure 7*. It is seen that the application of an electric field of 4 kV cm^{-1} does not affect the rates. Furthermore, the rate is seen to be proportional to the second power of the initial monomer concentration.

Field effect and field strength—*Table 2* shows that the rate of polymerization is not influenced by the presence of electric fields below 4 kV cm^{-1}.

Table 2. Polymerization rate and field strength for an α-methylstyrene–iodine–toluene system at $-78°C$.
$[I_2]_0 = 7·0 \times 10^{-2}$ mole l^{-1}. $[M]_0 = 0·80$ mole l^{-1}

Field strength (kV cm^{-1})	0	0·5	1·1	1·8	3·0	3·7	4·2
$R_p \times 10^3$ (mole l^{-1} min^{-1})	1·49	1·47	1·52	1·41	1·45	1·39	1·51

III. Field-accelerating effect and dielectric constant of the solvents

In *Table 3*, the field-accelerating effects on the rates in three different solvents are compared. The rate of the polymerization in toluene above $-20°C$ was too small to measure. Because the freezing point of nitrobenzene is 5·76 degrees below atmospheric, experiments could not be

Table 3. Field-accelerating effects of cationic polymerization of α-methylstyrene catalysed by iodine

Solvent	Dielectric* constant	R_{pE}/R_{p0}	Temperature (°C)
Toluene	2·4	1·0†	$-78 \sim -20$
DCE	10	1·3†	-20
Nitrobenzene	35	2·5‡	$8 \sim 25$

*At 25°C.   †At 1 kV cm^{-1}.   ‡At 0·11 kV cm^{-1}.

carried out below 8°C. The value of R_{pE}/R_{p0} was constant against temperature for polymerization in toluene between $-78°$ and $-20°C$, and in nitrobenzene between 8° and 25°C. It would thus be significant to compare the values of R_{pE}/R_{p0} obtained at various temperatures in various solvents. This experimental fact indicates that the field-accelerating effects that have so far been observed mainly in 1,2-dichlorethane are not due to the specificity of this solvent.

DISCUSSION

As stated above, the initial rate of polymerization, R_v, can be written as follows:

$$R_p \propto [I_2]_0^2 [M]_0^2 \qquad \text{in nitrobenzene} \qquad (1)$$

and

$$R_p \propto [I_2]_0^{4 \cdot 6} [M]^2 \qquad \text{in toluene} \qquad (2)$$

The previous study[1] shows that

$$R_p \propto [I_2]_0^{2 \cdot 4} [M]_0^2 \qquad \text{in DCE} \qquad (3)$$

For the exponent of the catalyst concentration in these equations, we note that it increases in the order nitrobenzene $<$ DCE $<$ toluene, or in the order of decreasing dielectric constant. On the other hand, the exponent of the monomer concentration is independent of the dielectric constant. The change appears to be due to the degree of association of iodine molecules which may become larger with decreasing dielectric constant. This interpretation is substantiated by the specific conductivities of the catalyst solution which are $1 \cdot 0 \times 10^{-7}$, $1 \cdot 5 \times 10^{-10}$, and $<5 \times 10^{-12}$ mho cm^{-1} in nitrobenene at 8°C, DCE at -20°C, and in toluene at -78°C, respectively. The difference in the conductivity seems not to be due to the temperature difference, since the specific conductivity of the nitrobenzene solution of the catalyst increased with decreasing temperature, and that of the DCE solution very slightly decreased with decreasing temperature.

The field effect found in nitrobenzene ($R_{pE}/R_{p0} = 2 \cdot 5$ at $0 \cdot 11$ kV cm^{-1}) is the largest obtained to date. As in the previous papers[1, 3-5] the interpretation for the field-accelerating effect is that the dissociation of the ion pairs at the growing chain ends is enhanced by the presence of the electric field, giving larger populations of free ions which make it possible for the growing chains to grow faster. Furthermore, R_{pE}/R_{p0} increases first with rising degree of dissociation and, through a maximum, decreases to unity for full dissociation. As the degree of dissociation usually increases with increasing dielectric constant, the dielectric constant dependence of the field effects shown in *Table 3* supports in part the interpretation.

Department of Polymer Chemistry,
  Kyoto University,
    Kyoto, Japan

REFERENCES

[1] SAKURADA, I., ISE, N., TANAKA, Y. and HAYASHI, Y. *J. Polym. Sci. A*, 1966, **14**, 2801
[2] WORSFOLD, D. J. and BYWATER, S. *J. Amer. chem. Soc.* 1957, **79**, 4917
[3] SAKURADA, I., ISE, N. and ASHIDA, T. *Makromol. Chem.* 1966, **95**, 1
[4] SAKURADA, I., ISE, N. and HORI, S. *Kobunshi Kagaku.* 1967, **24**, 147
[5] SAKURADA, I., ISE, N. and HAYASHI, Y. *J. makromol. Chem.* 1967, **A1**, 1039

A Light Scattering and Viscosity Study of Polydispersity Changes in the Cellulose of Wood when Subjected to Fungal Attack

D. B. SELLEN and M. P. LEVI*

Light scattering and viscosity measurements were made upon a series of high molecular weight cellulose nitrate samples in acetone. The cellulose nitrate was derived from the α-cellulose of beechwood veneers that had been subjected to various degrees of attack by the soft rot fungus Chaetomium globosum. *This procedure yielded cellulose nitrate samples which, although coming from the same source and having molecular weights of the same order of magnitude, had different degrees and types of polydispersity.*

Z average, weight average and number average molecular weights were calculated from the light scattering data, and the usefulness of the light scattering technique for following changes in degree of polymerization and degree of polydispersity of naturally occurring cellulose is discussed. The relationship between viscosity average molecular weight and molecular weights obtained from light scattering is also discussed. The way in which these types of average vary with the degree of fungal attack seems to indicate that for cellulose nitrate, which has a high degree of polymerization and is highly polydisperse, intrinsic viscosity yields a molecular weight that is somewhat less than the weight average.

IT HAS been shown[1] that, during the attack on beechwood by the soft rot fungus *Chaetomium globosum*, the average degree of polymerization of the α-cellulose remaining rises by about 15 per cent during the first 20 per cent weight loss and then falls again more slowly. The explanation given for this was that the attack along the length of the microfibrils starts at regions of low molecular weight from transverse bore holes. The average molecular weight of the remaining material therefore rises and then falls again when the lengths of those parts of the microfibrils remaining become of the order of one molecular chain length.

The molecular weight variation in the above work was based on viscosity measurements made upon cellulose nitrate in solution. The cellulose nitrate was derived from the α-cellulose which had been obtained from the wood via a holocellulose extraction. As this indirect procedure has a degradative effect upon the α-cellulose, it was decided to repeat the determinations with a more direct extraction procedure and also to make some light scattering measurements.

The analysis of polydisperse samples of cellulose nitrate, however, is of general importance in the study of naturally occurring cellulose, and it is this aspect of the work that is the subject of this paper. In particular the work affords the opportunity of studying the solution properties of a series of cellulose nitrate samples which, although coming from the same source and having molecular weights of the same order of magnitude, have different degrees and types of polydispersity.

*Present address: Hickson & Welch Ltd, Castleford, Yorkshire, England.

The intrinsic viscosity of both fractionated and unfractionated samples of cellulose nitrate has been studied extensively[2], and a number of detailed light scattering investigations has been made[3-6]. Most of the latter have been made upon material derived from cotton or ramie fibres, but Goring and Timell[7] have investigated unfractionated samples from a wide variety of natural sources.

The relationship between intrinsic viscosity and molecular weight has to be obtained empirically by comparing with some other technique (usually light scattering) for a series of fractionated samples. The type of average molecular weight obtained in this way will be discussed later. However, Benoit[8] has shown theoretically that in light scattering the number average, weight average and Z average molecular weights can be obtained, provided that the polymer is of very high molecular weight, unbranched and of Gaussian configuration. This theory has been confirmed for high molecular weight cellulose trinitrate in acetone[9], with measurements upon fractionated samples and their mixtures, and comparison of the measured with the calculated values. The present publication is specifically concerned with the usefulness of this technique in studying the polydispersity of naturally occurring cellulose, and the correlation of the values so obtained with the viscosity data.

PREPARATION OF CELLULOSE NITRATE SOLUTIONS

Beechwood veneers were subjected to attack by the soft rot fungus *Chaetomium globosum* as previously described[1] so as to produce four different weight losses. The resulting samples of wood, together with a sample of the unattacked wood, were dried and ground to pass through a standard 40 mesh sieve. The wood was then nitrated directly at room temperature with the nitration mixture described by Alexander and Mitchell[10] and the cellulose nitrate was obtained as described by Timell[11].

It was decided to use acetone as solvent, partly because most of the previous work on cellulose nitrate has used acetone and comparisons could therefore more easily be made, but also because viscosity measurements require correction for degree of nitration and the empirical equation of Lindsley and Frank[13] used for this purpose was originally obtained by using acetone as solvent.

Stock solutions were made up at concentrations of about 10^{-3} g/cm³. Weighed quantities of cellulose nitrate were dispersed in acetone by slowly agitating for three days. The solutions were then centrifuged for two hours at 30 000 g to remove undissolved material and the concentration determined by weighing the material centrifuged out and measuring the volumes of solution decanted. All the samples were found to be about 80 per cent soluble when treated in this way with the exception of the 68·7 per cent weight loss sample which was only about 60 per cent soluble. Due to the high centrifugal field used, some degree of fractionation must inevitably occur at this stage although it should be roughly the same for each sample. High centrifugal fields have to be used in the clarification procedure before the light scattering measurements, and it was thought better that most of the fractionation should have taken place before obtaining the stock solutions in order to avoid complications in the light scattering measurements.

The nitrogen content for each of the stock solutions was determined by the Kjeldahl method[12]. These are shown in *Table 1*. A higher degree of nitration was attained for the unattacked wood than for the other samples.

Table 1. Intrinsic viscosity data and nitrogen content for cellulose nitrate samples derived from the α-cellulose of beechwood veneers after attack by the soft rot fungus *Chaetomium globosum*

Weight loss, %	Nitrogen, %	$[\eta]_{500}$ dl/g	$[\eta]_{500}$ corrected for % N, dl/g	M_v (10^6)*
0	13·6 ± 0·1	15·0 ± 0·5	17·9 ± 1·1	1·07 ± 0·07
10·5	13·1 ± 0·1	18·1 ± 0·5	25·2 ± 1·5	1·57 ± 0·10
20·5	13·0 ± 0·1	17·3 ± 0·5	24·9 ± 1·5	1·52 ± 0·10
22·5	13·1 ± 0·1	17·3 ± 0·5	24·1 ± 1·4	1·48 ± 0·10
68·7	13·0 ± 0·1	14·4 ± 0·5	20·8 ± 1·2	1·25 ± 0·08

*Calculated using the expression of Huque *et al.*[4].

VISCOSITY MEASUREMENTS

Viscosity measurements were made at 25°C with an Ostwald viscometer, the capillary of which had a mean radius of 0·240 mm. For each sample measurements were made at five concentrations ranging from 4×10^{-5} to 3×10^{-4} g/cm³. Plots were made of $[(t/t_0) - 1]/C$ and $[\ln(t/t_0)]/C$ against C, where t and t_0 are the flow times for solution and solvent respectively and C is concentration. The limiting value of both of these functions as C approaches zero is $[\eta]$, the intrinsic viscosity. The plot of the logarithmic function was somewhat more nearly linear than the other, but both plots gave the same intercept within experimental error. The variation with rate of shear was not investigated, so that the extrapolated values apply to the mean rate of shear of the pure solvent, which was 510 sec⁻¹. The results shown in *Table 1* were adjusted for complete nitration using the empirical expression given by Lindsley and Frank[13], and the viscosity average molecular weight was calculated by means of the expression obtained empirically[6] for approximately the same rate of shear

$$[\eta]_{500} = 5·96 \times 10^{-5} M^{0·91} \tag{1}$$

LIGHT SCATTERING MEASUREMENTS

Testing and calibration of apparatus

Light scattering measurements were made with the Aminco* apparatus.

The system was tested for systematic error with angle of observation relative to the incident beam, θ, by measuring the fluorescence excited by the mercury blue line (4 358 Å) in an aqueous solution of fluorescein. Values constant to within ±0·5 per cent were obtained in the range 40° to 135°. At angles below 40°, lower values were obtained because the field of view of the detecting system was interrupted by the edge of the cell. The appropriate correction factors were calculated and found to be 1·12, 1·08, 1·04 and 1·02 for the angles 20°, 25°, 30° and 35° respectively.

*American Instrument Co. Inc., Silver Spring, Maryland, U.S.A.

The instrument was calibrated for the two strong mercury lines (4 358 Å and 5 461 Å) by comparing the light scattering and turbidity of Ludox (a colloidal dispersion of silica) in the usual way[14]. Turbidity measurements were made with 4 cm cells in a Unicam SP500 spectrophotometer. Linear plots were obtained between optical density and $1/\lambda_0^4$, where λ_0 is the wavelength in a vacuum, provided that the solution and solvent were interchanged between the cells, and the average values of optical density taken. Clarification was achieved by centrifuging for one hour at 15 000 g and filtering through a Millipore filter of pore size $1 \cdot 2\mu$ directly into the light scattering cell. No dissymetry of scatter was observed and the value of R_θ, where R_θ is the Rayleigh ratio divided by $(1 + \cos^2 \theta)$, remained constant to within ± 2 per cent over the entire angular range (20° to 135°), indicating the suitability of the solution for calibration purposes.

The calibration was checked by making measurement upon bovine plasma albumin in 0·2 M sodium chloride. After centrifuging for two hours at 25 000 g and filtering through a $1 \cdot 2\mu$ pore size Millipore filter, a molecular weight of 78 000 was obtained, which is within the accepted range of values. The refractive index increment dn/dC was measured in a Rayleigh differential refractometer and found to be 0·184 cm³ g⁻¹ at 5 461 Å and 0·186 cm³ g⁻¹ at 4 358 Å. The depolarization ratio ρ_u was 0·026.

Cellulose nitrate measurements

The stock solution of each sample was diluted with acetone to give solutions having relative concentrations of one quarter, one half and three quarters. Each of the four solutions was clarified and measured separately.

The only method available for clarification of cellulose nitrate in acetone is centrifugation. Sintered glass filters are ineffective whilst Millipore filters are made of cellulose esters and so dissolve in acetone. Millipore 'solvent resistant' plastic filters, although not visibly affected when placed in acetone for long periods, cause an increase in scatter each time acetone is passed through them. The scattered intensity so caused is somewhat greater than that due to the cellulose nitrate at the concentrations used in this work.

The solutions were each centrifuged for two hours at 35 000 g in a counterbalanced 50 cm³ polypropylene bucket. At the end of this period the centrifuge was stopped without braking. The bucket was left in the centrifuge head and 10 cm³ of solution extracted with a syringe via a hole in the cap. The solution was immediately transferred to the light scattering cell and the low-angle scatter checked for dust by visual observation. This procedure gave a satisfactory degree of clarification about one time in three.

When pure acetone was treated in this way, values of R_θ equal to $4 \cdot 7 \times 10^{-6}$ and $11 \cdot 9 \times 10^{-6}$ cm⁻¹ were obtained for the wavelengths 5 461 Å and 4 358 Å respectively in the range 60° to 135°. At lower angles R_θ rose due to incomplete clarification and the corresponding values at 20° were $10 \cdot 0 \times 10^{-6}$ and $18 \cdot 0 \times 10^{-6}$ cm⁻¹.

Because scattering due to dust is largely independent of wavelength whilst that due to the solute varies inversely as λ_0^4, it is usually preferable to make measurements at 4 358 Å rather than 5 461 Å. However, it was found that the solutions both absorbed and fluoresced at 4 358 Å possibly due to

the presence of some nitrated lignin. The optical density and fluorescence varied between the samples and neither was found to be strictly proportional to concentration. However the optical density was about 0·05 for a concentration of 10^{-3} g/cm^3, whilst the intensity of fluorescence was about one third of the intensity of scatter for $\theta = 90°$. It was decided to make measurements at both wavelengths and to make corrections for the absorption and fluoresence at 4 358 Å. Correction for absorption is merely a matter of allowing for the different optical path lengths of the scattered light and incident beam through the solution. The instrumental readings due to fluorescence were obtained by placing a yellow filter in front of the detecting system. The degree of absorption of the fluorescent light by the yellow filter was determined by assuming that all the horizontally polarized light at $\theta = 90°$ was due to fluorescence and making measurements with and without the yellow filter present. The instrumental readings were corrected for the absorption of the filter and the resulting values subtracted from the instrumental readings without the filter present to obtain the true readings due to scatter.

Analysis of results

The basic light scattering theory as applied to macromolecules[15,16] has been amply reviewed in the literature. Zimm plots[17] were drawn for each sample at the two wavelengths. *Figure 1* shows the Zimm plot at 4 358 Å for cellulose nitrate extracted from unattacked wood. KC/R_θ is plotted against $\sin^2 \frac{1}{2}\theta + fC$, where f is an arbitrary constant chosen so as to spread out the data. K is given by

$$K = 2\pi^2 n^2 \, (dn/dC)^2 / N_0 \lambda_0^4 \tag{2}$$

where N_0 is Avogadro's number and n the refractive index of the solvent. The rate of change of refractive index of the solution with concentration dn/dC was measured using a Rayleigh differential refractometer and found to be 0·101 and 0·102 cm^3 g^{-1} at 5 461 Å and 4 358 Å respectively.

In *Figure 1*, data at given angles are extrapolated to zero concentration and data at given concentrations to zero angle, to give plots of KC/R_θ against $\sin^2 \frac{1}{2}\theta$ for zero concentration and KC/R_θ against C for zero angle. The intercept of both of these plots on the KC/R_θ axis is $1/M_w$ where M_w is the weight average molecular weight. The slope of the plot of KC/R_θ against C is B, the second virial coefficient, while the plot of KC/R_θ against $\sin^2 \frac{1}{2}\theta$ gives information concerning the size, shape and polydispersity of the molecules. The polar radius of gyration ρ is given by

$$\text{initial slope/intercept} = 16\pi^2 \rho^2 / 3\lambda^2 \tag{3}$$

where λ is the wavelength in the solution. The type of average of ρ obtained in this way depends on the shape of the molecule. For Gaussian coils equation (3) becomes

$$\text{initial slope/intercept} = 8\pi^2 \overline{r_z^2} / 9\lambda^2 \tag{4}$$

where $\overline{r_z^2}$ is the Z average of the mean square end to end distance. Benoit[8] has shown that for Gaussian coils of high molecular weight the plot of
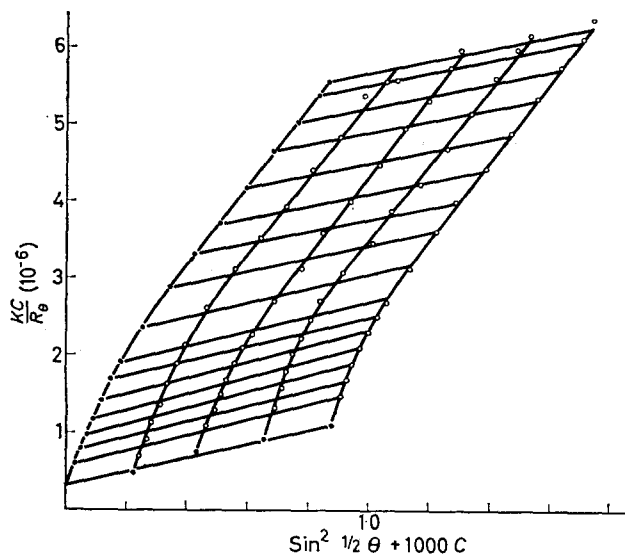
Figure 1—Zimm plot for cellulose nitrate in acetone derived
from the α-cellulose of beechwood veneers

KC/R_θ against $\sin^2 \frac{1}{2}\theta$ approaches a straight line asymptotically at high
angles and, as can be seen from *Figure 1*, this has been confirmed in the
present work. Benoit deduces the following relationships:

$$\text{intercept of asymptote} = 1/2M_N \tag{5}$$

$$\frac{\text{slope of asymptote}}{\text{intercept of asymptote}} = \frac{8\pi^2 \overline{r_N^2}}{3\lambda^2} \tag{6}$$

where M_N and $\overline{r_N^2}$ are the number average values of the molecular weight
and mean square end to end distance respectively. It is customary to define
a statistical quantity b called the 'effective bond length' given by:

$$b^2 = \frac{\overline{r_N^2}}{DP_N} = \frac{\overline{r_w^2}}{DP_w} = \frac{\overline{r_z^2}}{DP_z} \tag{7}$$

where DP denotes the degree of polymerization. It follows that b may be
obtained from the Zimm plot using the relation

$$b = (\lambda/2\pi)(3M_R \times \text{slope of asymptote})^{\frac{1}{2}}$$

where M_R is the molecular weight of the repeat unit. By combining the
above equations the following relationship for M_z is obtained

$$M_z = \frac{3 \times \text{initial slope}}{2 \times \text{slope of asymptote} \times \text{intercept}} \tag{9}$$

Thus M_N, M_w, M_z, B and b may be obtained from the light scattering data,
and the values so obtained for the two wavelengths are shown in *Table 2*.

Table 2. Light scattering data for cellulose nitrate samples derived from the
α-cellulose of beechwood veneers after attack by the soft rot fungus *Chaetomium globosum*

Weight loss, %	Light scattering measurements at 5 461 Å				
	Molecular weight (10^6)			b (Å)	B (10^{-4} cm^3 g^{-2})
	M_N	M_w	M_z		
0	0·53 ± 0·05	3·8 ± 0·7	13 ± 3	32 ± 2	4·3 ± 0·3
10·5	0·54 ± 0·05	4·5 ± 0·5	17 ± 3	32 ± 2	6·0 ± 0·8
20·5	0·63 ± 0·20	5·7 ± 1·3	17 ± 5	37 ± 5	6·0 ± 0·5
22·5	0·45 ± 0·03	5·0 ± 0·8	22 ± 7	33 ± 2	5·6 ± 0·8
68·7	0·32 ± 0·03	5·5 ± 1·0	22 ± 5	30 ± 2	4·6 ± 1·0

Weight loss, %	Light scattering measurements at 4 358 Å				
	Molecular weight (10^6)			b (Å)	B (10^{-4} cm^3 g^{-2})
	M_N	M_w	M_z		
0	0·52 ± 0·04	3·1 ± 0·3	9 ± 2	35 ± 1	4·5 ± 0·2
10·5	0·62 ± 0·12	4·2 ± 0·5	10 ± 4	35 ± 3	7·2 ± 0·4
20·5	0·47 ± 0·05	5·0 ± 0·5	15 ± 3	35 ± 1	8·0 ± 1·5
22·5	0·39 ± 0·06	4·8 ± 1·0	15 ± 4	35 ± 2	6·5 ± 0·2
68·7	0·31 ± 0·05	5·6 ± 1·0	14 ± 4	35 ± 2	6·6 ± 1·0

Figure 2 shows the extrapolated (zero angle) plots of KC/R_θ against $\sin^2 \frac{1}{2}\theta$ at 4 358 Å for unattacked wood and with 68·7 per cent weight loss, and illustrates how a change in polydispersity manifests itself in the Zimm plot. For 68·7 per cent weight loss M_w is higher and M_N lower than for the unattacked wood. The asymptotic slope is related to b and so remains unchanged as it depends only on the molecular configuration and not on the size.

DISCUSSION

Figure 3 shows how the Z, weight, number and viscosity average degrees of polymerization vary as functions of percentage weight loss due to fungal attack. A logarithmic scale has been used so that vertical displacements represent proportional changes, and the broken lines indicate those changes that are experimentally significant.

The form of the variation in the viscosity average degree of polymerization is similar to that reported previously[1] except that the maximum occurs for ten rather than 20 per cent weight loss and the initial rise is considerably larger (about 50 per cent). The absolute values of the degree of polymerization are about three times those previously reported, which is to be expected in view of the less degradative extraction procedure.

Goring and Timell[7] have made light scattering measurements upon cellulose nitrate prepared from a variety of woods using the same extraction procedure as in the present work. They obtained values of DP_w around 8 000. Thus the value of 12 000 obtained here is somewhat higher. However, they did not make measurements below 35° and appear to have assumed a linear extrapolation in their Zimm plots for angles below 60°. The plots of KC/R_θ against $\sin^2 \frac{1}{2}\theta$ in the present work (*Figures 1* and *2*) are somewhat curved in the range 35° to 60° and a linear extrapolation has been assumed only for angles below 35°. If the data below 35° are ignored

and the best straight line drawn in the 35° to 60° range a value for DP_w of about 6 000 is obtained. However, Goring and Timell used a sophisticated clarification technique[18, 19], so that it is not possible to say whether the difference in results arises from a systematic error due to their restricted angular range or from insufficient clarification in the present work.
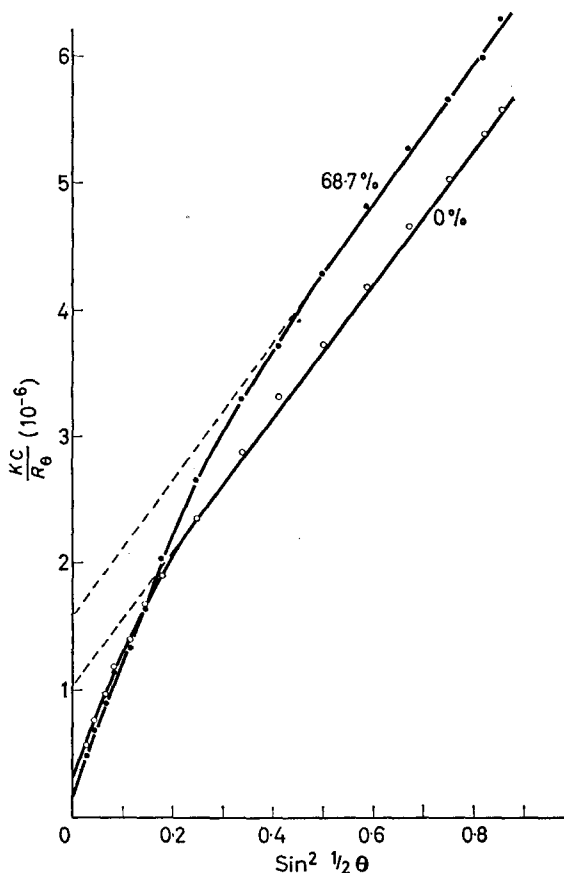
Figure 2—Zero concentration lines of the Zimm plots for cellulose nitrate in acetone derived from the α-cellulose of unattacked beechwood veneers (designated 0 per cent), and beechwood veneers subjected to attack by the soft rot fungus Chaetomium globosum so as to produce 68·7 per cent weight loss

Goring and Timell also obtained reasonable agreement between the viscosity and weight average degrees of polymerization, and the above considerations may also help to explain why this agreement was not obtained here (Figure 3). In the present work not only are the absolute values in disagreement but the form of the variation with weight loss is different as it is not possible to draw the same lines through both sets of data.

The intrinsic viscosity of solutions of flexible polymers is usually correlated with molecular weight by means of the Mark–Houwink empirical equation

$$[\eta] = KM^\alpha \tag{10}$$

This leads to the following expression for M_v

$$M_v = [\sum_i M_i^{\alpha+1} N_i / \sum_i M_i N_i]^{1/\alpha} \tag{11}$$

640

where N_i is the number of molecules having molecular weight M_i. Thus M_v will be less than the weight average if $\alpha < 1$ and greater if $\alpha > 1$. In equation (1), $\alpha = 0\cdot91$. Although this will not make M_v differ significantly from the weight average there is some evidence that α decreases with increasing molecular weight due to the molecule adopting a more coiled configuration[6]. All the weight average molecular weights obtained in the present work are in fact above the range covered by equation (1), and the Z average values indicate that there are molecules present with a degree of polymerization of 50 000 and above. Thus it is possible that molecular weights obtained from viscosity measurements upon solutions of cellulose nitrate which have both a high degree of polymerization and a high degree of polydispersity are significantly less than the weight average.

The values of b given in *Table 2* are in good agreement with each other and with those given by Benoit *et al.*[9]. B, however, seems to vary at random from sample to sample. This has also been observed by other workers[6].

Although the light scattering method has been used here successfully to obtain number, weight and Z average degrees of polymerization, it can hardly be recommended as a routine procedure in work of this kind. Very low concentrations must be used and the scattering due to the cellulose nitrate may be only half that due to the acetone. Also extrapolation depends upon data obtained in the region 20° to 35° so that clarification is crucial. It is quite probable that for high molecular weight cellulose nitrate
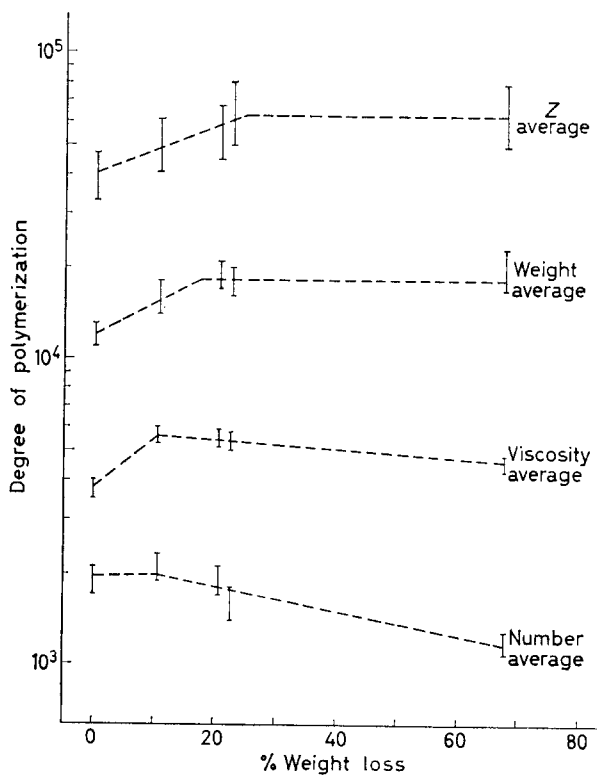
Figure 3 — Variation in the degree of polymerization of cellulose nitrate derived from the α-cellulose of beechwood veneers which had been subjected to various degrees of attack by the soft rot fungus *Chaetomium globosum*

the light scattering technique gives more reliable number average than weight average data.

With these reservations, the pattern that emerges from *Figure 3* is that as one proceeds from the number to the Z average the range of weight loss for which there is an increase in degree of polymerization increases, whilst the proportional magnitude of the fall at higher weight losses decreases. This is consistent with the biological situation and will be discussed fully in a separate publication.

CONCLUSIONS

The light scattering method has been used successfully to investigate how the number, weight and Z average degrees of polymerization of cellulose from wood vary as the wood is subjected to various degrees of fungal attack.

There is some indication that molecular weights calculated from intrinsic viscosity for solutions of cellulose nitrate which have a high degree of polymerization and are highly polydisperse are somewhat less than the weight average. Care must therefore be taken in the interpretation of any experiment in which molecular weight changes of natural cellulose are monitored by means of viscosity measurements.

Astbury Department of Biophysics,
University of Leeds

REFERENCES

[1] LEVI, M. P. and PRESTON, R. D. *Holzforschung,* 1965, **19**, 183
[2] SWENSON, H. A. *Methods in Carbohydrate Chemistry* (Ed. R. L. WHISTLER), Vol. III, p 91. Academic Press: New York, 1963
[3] BADGER, R. M. and BLAKER, R. H. *J. phys. Chem.* 1949, **53**, 1056
[4] HOLTZER, A. M., BENOIT, B. and DOTY, P. *J. phys. Chem.* 1954, **58**, 624
[5] HUNT, M. L., NEWMAN, S., SHERAGA, H. A. and FLORY, P. J. *J. phys. Chem.* 1956, **60**, 1278
[6] HUQUE, M. M., GORING, D. A. I. and MASON, S. G. *Canad. J. Chem.* 1958, **36**, 952
[7] GORING, D. A. I. and TIMELL, T. E. *Tappi,* 1962, **45**, 454
[8] BENOIT, H. *J. Polym. Sci.* 1953, **11**, 507
[9] BENOIT, H., HOLTZER, A. M. and DOTY, P. *J. phys. Chem.* 1954, **58**, 635
[10] ALEXANDER, W. J. and MITCHELL, R. L. *Analyt. Chem.* 1949, **21**, 1497
[11] TIMELL, T. E. *Pulp Pap. (Mag.) Can.* 1955, **56**, 104
[12] GREEN, J. W. *Methods in Carbohydrate Chemistry* (Ed. R. L. WHISTLER), Vol. III, p 229. Academic Press: New York, 1963
[13] LINDSLEY, C. H. and FRANK, M. B. *Industr. Engng Chem. (Industr.),* 1953, **45**, 2491
[14] MOMMAERTS, W. F. H. M. *J. Colloid Sci.* 1954, **58**, 303
[15] DEBYE, P. *J. appl. Phys.* 1944, **15**, 338
[16] DEBYE, P. *J. Phys. Colloid Chem.* 1947, **51**, 18
[17] ZIMM, B. H. *J. chem. Phys.* 1948, **16**, 1099
[18] DANDLIKER, W. B. and KRAUT, J. *J. Amer. chem. Soc.* 1956, **78**, 2380
[19] HUQUE, M. M., JAWORZYN, J. and GORING, D. A. I. *J. Polym. Sci.* 1959, **39**, 9

Some Techniques for the Examination of High Impact Polystyrene by Electron Microscopy

R. J. WILLIAMS and R. W. A. HUDSON

Techniques are described that enable the internal structure of high impact polystyrene to be examined in an electron microscope in such a way that the detail in the structure of the individual rubber particles in the polystyrene matrix is made visible. Techniques described include replication of fractured surfaces and ultra-microtomy, including a novel method of hardening the material for ultra-microtomy by irradiation.

HIGH impact polystyrene (HIPS) consists of a matrix of polystyrene throughout which is dispersed a large number of small particles of a rubbery material, usually polybutadiene. The physical properties of the moulded material depend to a large extent on the amount of rubber dispersed throughout the polystyrene, the size distribution of the rubber particles and the make up of the individual particles.

The techniques to be described have been used to examine HIPS in order to determine:

(*i*)   The size distribution of the rubber particles

(*ii*)   The shape of the rubber particles

(*iii*)   The internal structure of the rubber particles.

Various specimens of different commercial grades of HIPS have been examined by these techniques and the electron micrographs shown have been selected from many examples in order best to illustrate particular points. Three methods were used to obtain the desired information.

METHOD NO. 1

Replication of a fractured surface

The specimen under examination is fractured in an Izod impact tester, first having cooled the specimen to a temperature approaching or below the glass/rubber transition temperature of the rubber phase in the material. This ensures a smooth, glassy surface in the fracture that is fairly easy to replicate.

The replication is carried out by the method outlined in *Figure 1*. This method has the advantages that the replicating medium does not attack the material being examined and leaves the material undamaged and in its original condition after replication. The method is carried out as follows.

Silver is evaporated in a vacuum coating unit on to the surface to be replicated to give an electrically conducting surface. The silver coated specimen is then placed in a copper sulphate bath where the silver is covered with a thick electroplated film of copper. The copper plated silver forms a negative replica of the original surface. The silver/copper replica is then

replaced in the vacuum coating unit and a layer of carbon is evaporated on to the silver surface. The carbon coated replica is then floated, carbon side uppermost, on to the surface of dilute nitric acid where the silver and the copper are dissolved away leaving the carbon film floating on the surface of the acid. The carbon replica, which is a positive replica of the original surface, is washed in distilled water and finally shadowed with palladium before examination in the electron microscope.

Original specimen

Stage 3. Stripped silver/copper replica

Stage 1. Silver deposition by evaporation

Stage 4. Carbon evaporated on silver replica

Stage 2. Copper electroplated on silver

Pd shadowing

Stage 5. Final shadowed carbon replica
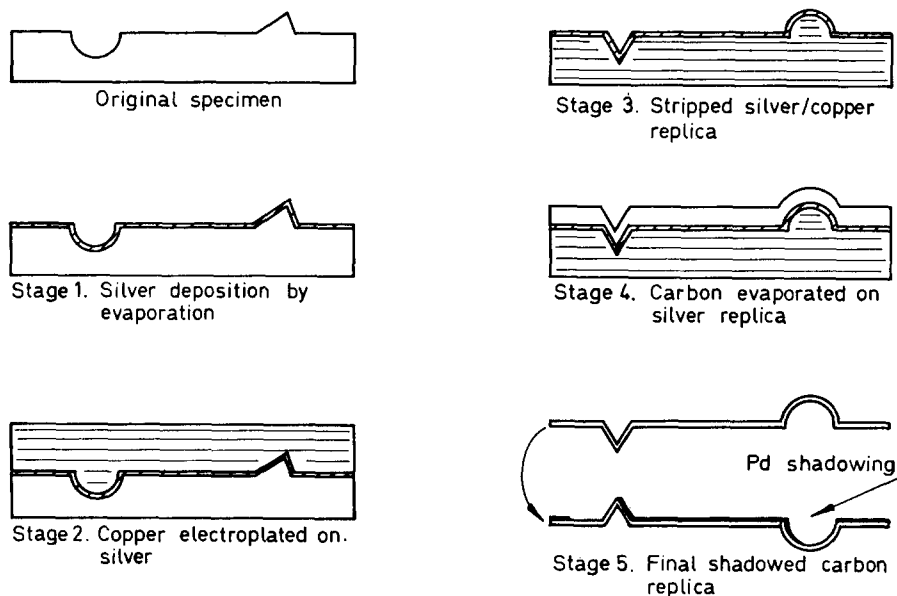
Figure 1—Preparation of silver carbon replica

If the temperature at which the material is fractured is taken to a point below the glass/rubber transition temperature of the rubber particles, the fracture will travel through the rubber particles, resulting in replicas being obtained showing the internal features of the rubber particles. Figure 2 is a typical example of a material fractured after cooling it in a bath of liquid nitrogen.

When the temperature at which the material is fractured is just above the glass/rubber transition temperature of the rubber particles, a fracture will result in which the rubber particles remain intact and where they are embedded in one or other of the fractured surfaces. In this way it is possible to obtain a replica of the outside of the rubber particle and Figure 3 is a typical micrograph of a material that had been cooled to about $-60°C$ in a bath of ethanol–carbon dioxide mixture before being fractured.

It can be seen from both Figures 2 and 3 that the particles in the polystyrene matrix are roughly spherical in shape and that the surface of the particles gives a hint of a formation very similar to that of a blackberry.
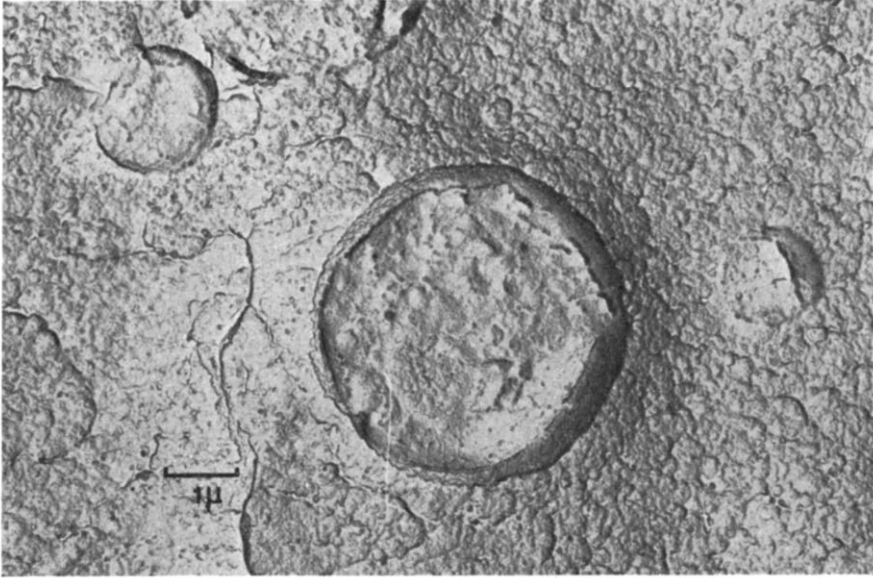
Figure 2—Replica of a fractured surface. Fracture effected after cooling in liquid nitrogen
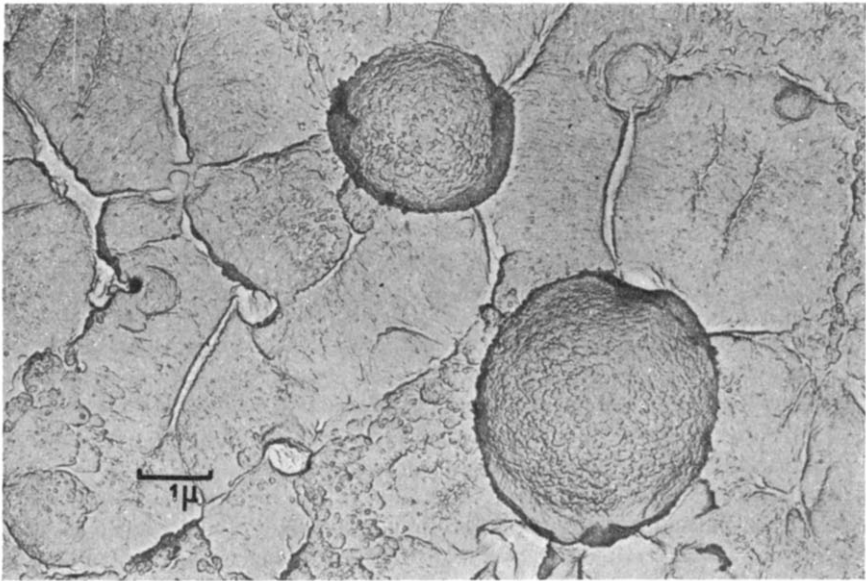
Figure 3—Replica of a fractured surface. Fracture effected after cooling at about −60°C

645

Mainly information regarding particle size and shape is obtained by this method.

METHOD NO. 2

Replication of a polished, etched surface

In this method the specimen is first polished on an ultra-microtome to a depth of about 0·5 mm and the polished surface is etched in the vapours of isopropanol. The etching process dissolves away the polystyrene on the polished surface leaving the rubber in the matrix proud of the surface. It has been found that the most efficient way of etching the surface is to touch the polished surface for about one second on to a drop of isopropanol and then to suspend the polished material approximately one centimetre above a small amount of the solvent in a closed vessel for about four hours at room temperature. It is essential that a freshly cut glass knife be used for the polishing of the material, otherwise knife marks will be apparent in the final replica (see *Figure 4*). Replication of the prepared surface is then carried out by the silver/carbon method already described.
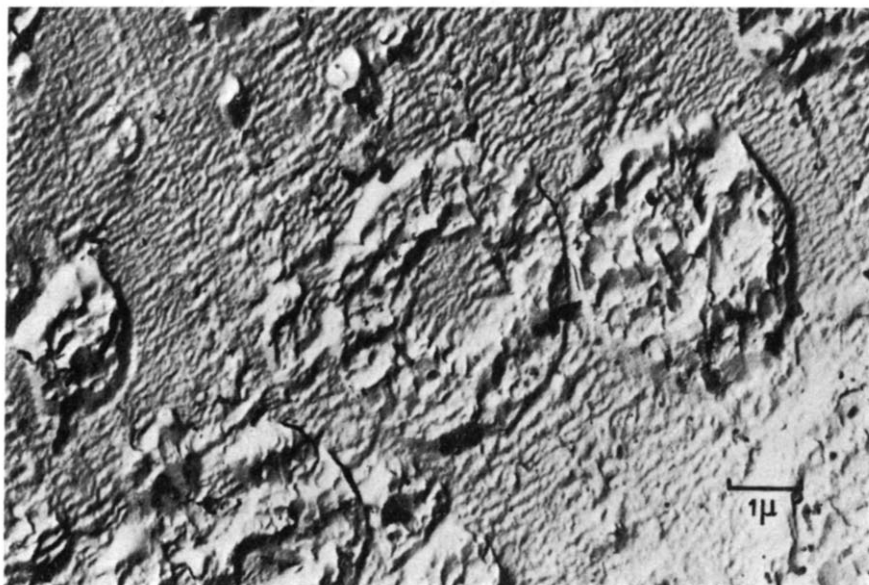
Figure 4—Replica of a polished, etched surface showing knife marks and smeared rubber particles

Figure 4 shows some early results obtained by this method, and apart from the knife marks already referred to, it can be seen that the rubber particles (being much softer than the polystyrene) have been badly smeared by the knife of the ultra-microtome. This smearing also occurs when a freshly cut knife is used.

The work was repeated on material which had first been irradiated by a cobalt-60 source, to a dose in excess of 100 megarads in order to crosslink

the rubber and to harden it. *Figure 5* shows a typical micrograph of the results obtained. It shows clearly that the rubber particles have been cleanly cut through and that each particle is in the form of a 'honeycomb' and that
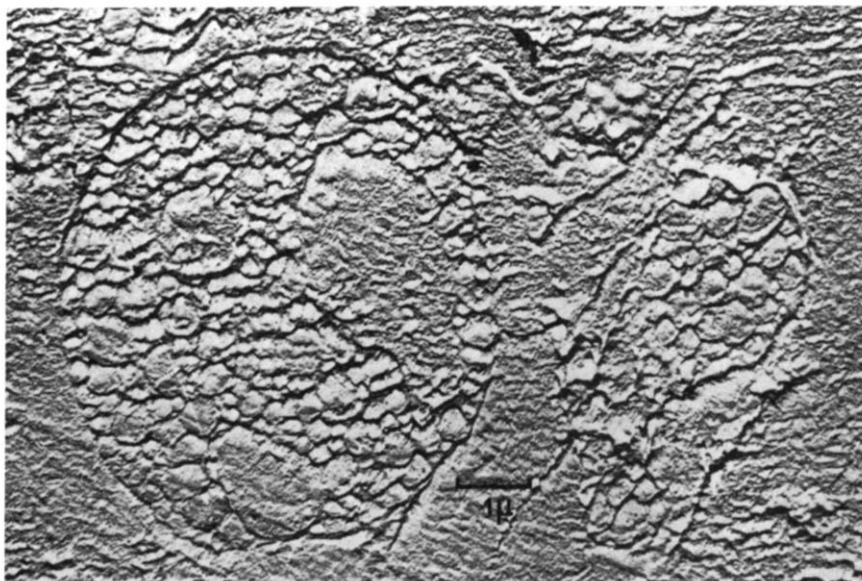
Figure 5—Replica of a polished, etched surface hardened by irradiation before polishing

entrapped in the pockets of the honeycomb are small amounts of (presumably) polystyrene.

METHOD NO. 3

Ultra-microtomy

The ideal way to section elastomers would be to freeze them to below their glass/rubber transition temperature and to keep them at this temperature while being sectioned on the ultra-microtome. At the present time this is not completely feasible (although prototype cooling stages are in course of development) and therefore alternative methods for sectioning this type of material have to be sought.

K. Kato, working in Japan[1], reports that hardening of ABS (acrylonitrile–butadiene–styrene resin) may be effected by soaking the material in a solution of osmium tetroxide. This method was used with HIPS and successful sectioning of the material was found to be possible after the material had been soaked for at least 48 hours at room temperature in a one per cent solution of osmium tetroxide in distilled water. It has been found that in addition to the hardening of the material due to the action of the osmium tetroxide on the rubber, preferential 'staining' of the rubber occurs so that contrast between the rubber and the polystyrene is enhanced in the electron microscope.

Figure 6 shows the results obtained by Kato's method of hardening and it can be seen that the honeycomb formation of the rubber particles observed by method 2 already described, is confirmed. The structure is, however, much clearer in the osmium stained thin section and it can be seen clearly that the sizes of the cells in the honeycombs vary over a wide range of size and shape.

The osmium tetroxide method of hardening, however, is not the complete solution to the problem as the hardening effect produced by this
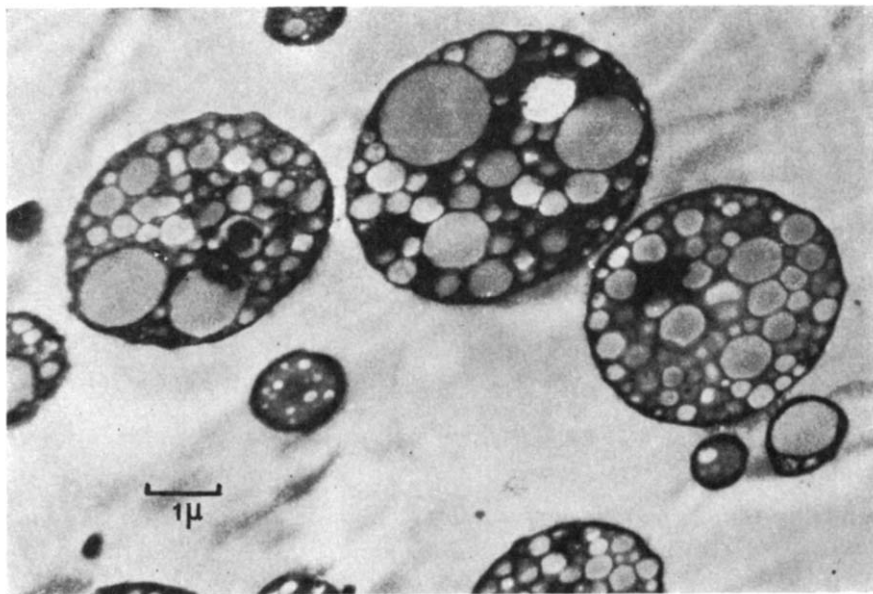
Figure 6—Thin section of osmium tetroxide hardened and stained specimen

method only penetrates to a depth of a few microns into the surface of the material. It is only possible, therefore, to obtain a limited number of sections from each hardening session.

Specimens that have been irradiated can also be successfully sectioned, providing that the specimen is irradiated to about 200 megarads, and *Figure 7* shows a typical micrograph of the results obtained. In this method of hardening, however, the absence of osmium tetroxide in the rubber reduces the contrast obtained in the electron microscope between the images of the rubber and the polystyrene.

In both cases of sectioning of hardened materials, the sections tend to 'concertina' as they come off the knife and two methods of relaxing the sections to something approaching their original dimensions have been used.

The first method for relaxing the sections involves adding a drop of dioxan to the water in the knife trough and waiting for up to 45 minutes for the sections to relax.
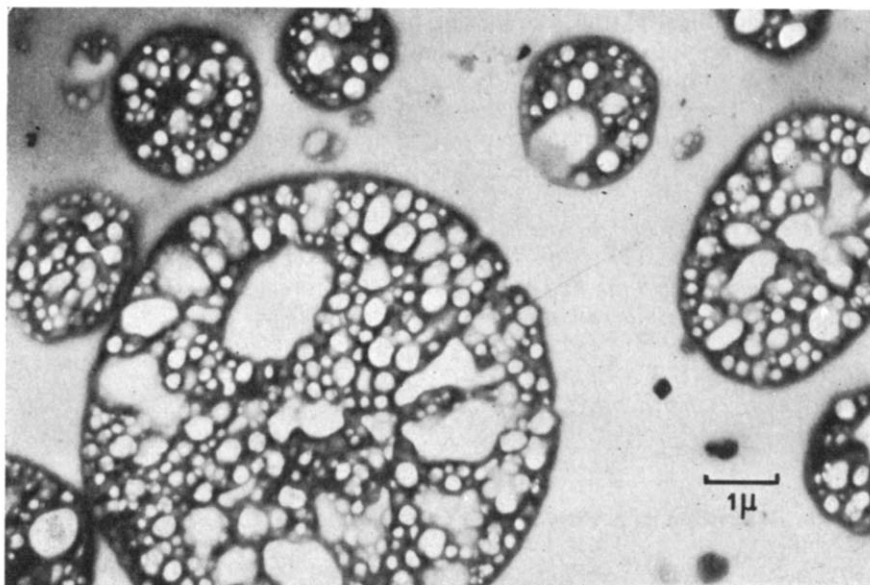
Figure 7—Thin section of irradiation hardened specimen

The second method for relaxing the sections was a modification of the method outlined[2] by Lee D. Peachey in 1958, in which he used a photo-flood lamp as a heat source to relax the sections. The heat source used by the present authors to relax the sections consists of a small coil of fine resistance wire which is heated to cherry red from a low voltage source and held for a few seconds about 2 cm above the sections floating on the water in the knife trough. Sections were obtained from materials hardened by either osmium tetroxide or by irradiation that gave a gold interference colour before relaxation, indicating that the relaxed sections were of the order of about 700 to 800 Ångström units thick. For examination in the electron microscope, sections were supported on a carbon film on a normal 200 mesh 3 mm copper grid.

Apparatus

The work outlined above was carried out with an Edwards vacuum coating unit, a Reichert ultra-microtome using glass knives made on an L.K.B. knifemaker and a Hitachi HS7S electron microscope.

CONCLUSIONS

It is not possible to obtain complete information from any one of the techniques described. Ultra-microtomy gives the best results so far as the internal structure of the rubber particles is concerned, but due to the 'concertina' effect that the knife has on the sections, it is not possible to determine their exact shape. Replication of a polished, etched surface does give information regarding the exact shape of the particles, but gives little or no information about the internal structure of the particles. As micro-

graphs of identical particles cannot be obtained by the three methods outlined, it is not possible to check that each method will give the same information with regard to the actual size of a particle, but results obtained by each of the three methods on a single specimen gave almost identical particle size distribution. Both replication and ultra-microtomy must therefore be employed to obtain the fullest possible information.

BP Chemicals (U.K.) Ltd,
  Research Department, Epsom, Surrey

REFERENCES

[1] KATO, K. 'Electron microscopy of ABS resins'. *J. Electron Microscopy*, 1965, **14** (3), 220–221
KATO, K. 'The osmium tetroxide procedure for light and electron microscopy of ABS plastics'. *Polym. Engng Sci.* 1967, **7** (1), 38–39
[2] PEACHEY, LEE D. 'A study of section thickness and physical distortion produced during microtomy'. *J. Biophys. Biochem. Cytol.* 1958, **4** (3), 233–242

Studies in α-Peptide Formation by Hydrogen Migration Polymerization I—Oligomers from Maleamide, Mesaconic Acid α-Methylester β-Amide* and Mesaconamide

C. H. BAMFORD, G. C. EASTMOND and Y. IMANISHI

The possibility of preparing polymers containing α amino acid residues by the hydrogen migration polymerization of simple olefinic monomers has been explored. Three monomers, viz. maleamide, mesaconic acid α-methyl ester β-amide and mesaconamide, have been subjected to the action of the anionic initiators n-butyl lithium and sodium t-butoxide. In each case oligomers were formed which were shown by hydrolysis and paper chromatography to contain peptide linkages; only with mesaconic acid α-methyl ester β-amide was distinction possible between α- and β-residues present in the polymer; the results showed that both types of residue were incorporated.

An α-peptide residue is considered to arise from addition of the —CONH$^{\ominus}$ anion to the carbon atom of the monomer carrying the amide group [equation (2)], and the structural features favouring this mode of addition are discussed together with the mechanism of chain growth and the conditions necessary for obtaining high molecular weight products. Addition to both carbon atoms of mesaconamide was shown to occur.

IN 1957 Breslow, Hulse and Matlack[1] reported that the anionic polymerization of acrylamide and methacrylamide leads to the incorporation of β-peptide units into polymer chains, possibly by a reaction similar to (1),

$$R^{\ominus} + CH_2 {=} CHCONH_2 \rightarrow RCH_2 {-} \overset{\overset{\displaystyle H}{|}}{\underset{\underset{\displaystyle CONH_2}{|}}{C}}{}^{\ominus} \rightarrow RCH_2 {-} \underset{\underset{\displaystyle CONH}{|}}{CH_2} \quad (1)$$

$$\underset{\ominus}{}$$
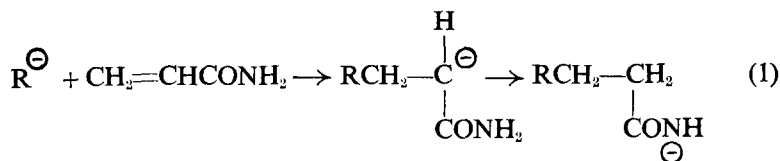
so that the product is effectively a copolymer of β-alanine and acrylamide. This type of reaction, known as hydrogen migration polymerization, has subsequently been studied by a number of workers[2-9]; in all instances, so far as we are aware, peptide residues introduced into the chains, and amino acids produced on hydrolysis of the polymer, were exclusively β in character.

It occurred to us that an α-polypeptide may be formed from an olefinic monomer by hydrogen migration polymerization if the propagating anion could be forced to attack the carbon atom carrying the amide group. To achieve this it would appear to be necessary to use as monomer a 1,2-disubstituted ethylene in which the second substituent X is a stronger

---

*This nomenclature conforms with *Beilstein*.

electron acceptor than the amide group. We number the carbon atoms C(1) and C(2) as shown

$$\underset{\substack{| \\ \text{CONH}_2}}{\overset{\substack{\text{H} \\ |}}{(1)\text{C}}}=\!\!=\!\!=\underset{\substack{| \\ \text{X}}}{\overset{\substack{\text{H} \\ |}}{\text{C}(2)}}$$
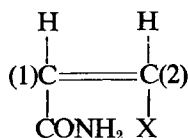
the carbon atom carrying the amide group being denoted C(1). Anionic polymerization of such a monomer can yield an α-polypeptide by repetition of the sequence (2), in which attack of the propagating anion on the double bond at C(1) is encouraged by strong electron withdrawal by X,

$$\text{R}^\ominus + \underset{\substack{| \\ \text{CONH}_2}}{\text{CH}}=\text{CHX} \rightarrow \underset{\substack{| \\ \text{CONH}_2}}{\text{RCH}}\!-\!\!-\!\underset{\substack{| \\ \text{X}}}{\overset{\substack{\text{H} \\ | \\ }}{\text{C}^\ominus}} \rightarrow \underset{\substack{| \\ \text{CONH} \\ \ominus}}{\text{RCH}}\!-\!\text{CH}_2\text{X} \qquad (2)$$
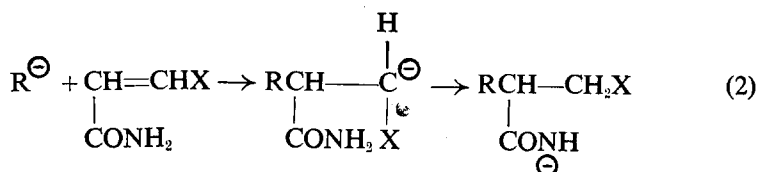
Attack by the anion at C(2) can only lead to the formation of β-peptide units as in (1).

The possibility of synthesizing α-polypeptides by polymerization of olefinic monomers is especially interesting in view of the general lack of methods for preparing high molecular weight polymers of this type. In order to investigate potentialities of the method we have studied the anionic polymerizations of maleamide, mesaconic acid α-methylester β-amide and mesaconamide, initiated by n-butyl lithium and sodium t-butoxide.

EXPERIMENTAL

Materials

Maleamide was synthesized from maleic anhydride by Linstead's method[10], amidation of methyl maleate being effected at about 5°C. The product was recrystallized three times from methanol. Elemental analysis: C 42·25 per cent, H 5·60 per cent, N 24·33 per cent; calc. C 42·10 per cent, H 5·30 per cent, N 24·55 per cent, M.pt 177°C; literature[10-12] 171° to 173°C, 181°C, 180°C.

Methyl mesaconate was synthesized from mesaconic acid as described by Jeffery and Vogel[13], and used in the preparation of mesaconic acid α-methylester β-amide according to the method of van de Straete[14]. The monomer was recrystallized twice from benzene. Elemental analysis: C 49·94 per cent, H 6·30 per cent, N 9·53 per cent; calc. C 50·34 per cent, H 6·34 per cent, N 9·79 per cent. M.pt 103°C; literature[14] 104°C.

Mesaconamide, prepared from the previous monomer as described by van de Straete[14], was recrystallized twice from ethanol. Elemental analysis: C 46·74 per cent, H 6·40 per cent, N 21·68 per cent; calc. C 46·87 per cent, H 6·29 per cent, N 21·87 per cent. M.pt 180°C; literature[14] 179·6°C.

α-Methyl aspartic acid was prepared by hydrolysis with aqueous barium hydroxide of diethyl α-methyl aspartate synthesized by the method of

Pfeiffer and Heinrich[15] (b.pt 118°C/12 mm). After recrystallization from methanol–water the acid gave on analysis: C 40·34 per cent, H 5·87 per cent, N 9·47 per cent (calc. C 40·82 per cent, H 6·17 per cent, N 9·52 per cent). The melting point was 245°C (decomp); literature[15, 16] 234° to 237°C (decomp).

N,N-dimethylformamide (Hopkin and Williams Ltd) (DMF), used as polymerization solvent, was allowed to stand overnight over phosphorus pentoxide, decanted and distilled twice under reduced pressure (b.pt 40·5°C/ 11 mm).

Toluene, also employed as solvent, was washed in turn with concentrated sulphuric acid, water, ten per cent aqueous sodium hydroxide, water, then dried over calcium chloride and distilled over sodium.

n-Butyl lithium (Foote Mineral Co.) was obtained as a 15 per cent solution in n-hexane.

Sodium t-butoxide was prepared from sodium and an excess of sodium-dried t-butyl alcohol. The mixture was warmed and when the sodium had completely disappeared the excess alcohol was distilled off. Finally, the residual material was dried in a vacuum at room temperature.

Techniques

Polymerizations were carried out, in the absence of moisture, without mechanical stirring. A few reactions were carried out in a vacuum and gave similar results. The monomers and the initiator n-butyl lithium are soluble in the diluents employed (50 ml); sodium t-butoxide is insoluble. In all cases the reaction mixture developed a yellow colour as soon as the initiator was added, and often insoluble reaction products were obtained. After a suitable time excess methanol (equivalent to twice the initiator) was added to terminate the reaction.

The methods used to isolate and identify the products are described separately for the three monomers. Hydrolysates were chromatographed on Whatman No. 4 paper without removal of hydrochloric acid. The chromatograms were run either with phenol–water (4 : 1 v/v) (PW) or with n-butanol–acetic acid–water (18 : 2 : 5 v/v) (BAW) mixtures at room temperatures.

Some of the products were submitted to mass spectroscopic examination with an A.E.I.MS9 spectrometer.

RESULTS AND DISCUSSION

1. *Maleamide*

The reaction conditions employed with this monomer are shown in *Table 1*.

Systems containing n-butyl lithium were initially homogeneous, but became heterogeneous during reaction. Precipitates from all reactions were washed thoroughly with DMF at the polymerization temperature to ensure removal of unreacted monomer before drying in a vacuum. The products were extracted successively with boiling methanol, cold water and boiling water. No insoluble residue remained after this treatment. The final fractions, removed by boiling water, gave the data summarized in *Table 2*.

Table 1. Polymerization of maleamide in DMF

Expt No.	[maleamide] mole l^{-1}	[n-BuLi] mole l^{-1}	[t-BuONa] mole l^{-1}	Temperature, °C	Reaction time, h
1	0·175		0·104	90	27
2	0·175	0·0476		90	27
3	0·175		0·104	20	184
4	0·175	0·0476		20	184
25	0·875	0·095		90	6
26	0·875		0·208	90	6
27	0·525	0·190		20	210
28	0·525		0·208	20	168
39	0·875	0·095		90	6

Table 2. Analytical data on products from maleamide

Expt No.	Mass numbers		M.pt °C	Elemental analysis, %		
	Limit scanned	Maximum observed		C	H	N
1	470	305	258	42·02	5·60	24·26
2	270	270	260	42·16	5·52	24·66
3	410	330	266	42·36	5·60	24·30
4	450	430	268	41·85	5·42	24·56

The relevant data for maleamide are m.pt 177°C; mol.wt 114; C 42·10 per cent, H 5·30 per cent, N 24·55 per cent. These results show that these fractions of the reaction products are similar to the monomer in composition, but of higher molecular weight, and therefore suggest the formation of oligomers.

All fractions of polymerizations 1 to 4, and also the monomer, were chromatographed on Whatman No. 4 paper with the aid of methanol–water mixtures. No colours were obtained after spraying with ninhydrin solution, indicating the absence of amino acids. After chlorination and treatment with tolidine, purple-blue spots appeared, as would be expected with compounds containing—$CONH_2$ or —CONHR groups[17]. The presence of these groups was also inferred from observations of the infra-red absorption spectrum. The chromatograms of the polymer fractions showed strong tailing, in contrast to those of the monomer, which gave well-defined spots. This observation is consistent with the presence of oligomers in the fractions. The unfractionated products of expts 25–28, 39 were also ninhydrin-negative.

The latter products were hydrolysed by refluxing with 6N hydrochloric

Table 3. R_f values at room temperatures

Expt No.	PW		BAW	
25	0·24(s)	0·82(m)	0·19(s)	
26	0·25(s)	0·79(m)	0·20(s)	
27	0·24(s)	0·82(m)	0·19(s)	0·30(m)
28	0·25(s)	0·80(w)	0·20(s)	
39	0·26(s)	0·82(w)	0·18(s)	
Aspartic acid	0·24, 0·29		0·20	

acid for 24 hours[18] and the hydrolysate was chromatographed with the aid of PW and BAW mixtures. Strong ninhydrin-positive reactions were always obtained, with the R_f values shown in *Table 3*.

It appears from these findings that two amino acids are produced by hydrolysis, one of which is aspartic acid; the other with $R_f = 0.8$, approximately, in phenol–water, has not yet been identified. Hydrolysis of the monomer under similar conditions gave no product with a ninhydrin-positive reaction.

Further evidence consistent with the incorporation of peptide residues in the polymer was obtained by hydrolysing with 8N sulphuric acid (50 hours)[18]. The excess sulphuric acid was removed by barium hydroxide, and the product (in solution) methylated with dimethyl sulphate and sodium hydroxide[19]. The solid obtained by ether extraction after acidification with sulphuric acid was crystallized from water and identified as fumaric acid. (Found: C 41·33 per cent, H 3·40 per cent; sublimed 290°C. Fumaric acid: C 41·39 per cent, H 3·47 per cent; sublimes[20] 290°C. The two specimens gave identical infra-red absorption spectra.) The reaction occurring under these conditions[19] is

$$
\begin{array}{ccc}
\text{COOH} & \text{CO}\overset{\ominus}{\text{O}} & \text{HOOC—CH} \\
| & | & \| \\
\text{CHNH}_2 + \text{Me}_2\text{SO}_4 \;\rightarrow\; & \text{CH—}\overset{\oplus}{\text{N}}\text{Me}_3 \;\rightarrow\; & \text{HC—COOH} + \text{NMe}_3 \qquad (3) \\
| & | & \\
\text{CH}_2 & \text{CH}_2 & \\
| & | & \\
\text{COOH} & \text{COOH} &
\end{array}
$$
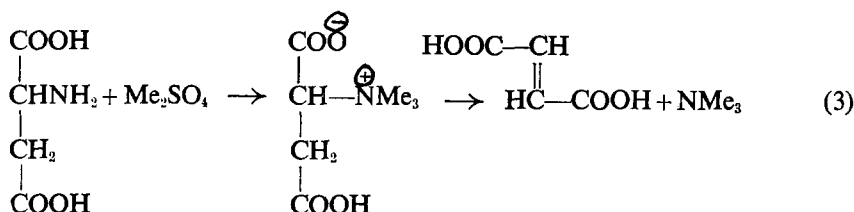
The possibility that some fumaric acid arises from reaction of a terminal group in these experiments cannot be excluded.

Determinations of the ratio (amide N)/(total N) gave the values shown in *Table 4*.

Table 4. (amide N)/(total N)

Expt. No.	25	26	27	28
Ratio	0·91	0·82	0·90	0·67

Polymerization of maleamide without hydrogen migration would give a ratio of unity, while complete migration (i.e. one migration for each addition) would yield a value of 0·5 for long chains. These results are therefore consistent with the formation of peptide residues in the polymer, this process being particularly pronounced in the experiments with sodium *t*-butoxide initiation.

We consider that the evidence presented shows that a portion of the monomer is incorporated into the oligomers in the form of aspartic acid residues, probably by a hydrogen-migration polymerization of the following types:

$$R^{\ominus} + \begin{array}{c} HC—CONH_2 \\ \| \\ HC—CONH_2 \end{array} \quad (a) \quad \longrightarrow \quad \begin{array}{c} R—CH—CONH_2 \\ | \\ CH—CONH_2 \\ \ominus \end{array}$$
$$(I)$$

$$(I) \xrightarrow{(b)} \begin{array}{c} \ominus \\ R—CH—CO\overset{\ominus}{N}H \\ | \\ CH_2—CONH_2 \end{array} \xrightarrow[\text{maleamide}]{(c)} \begin{array}{c} R—CH—CONH—CH—CONH_2 \\ | \quad\quad\quad\quad | \\ CH_2—CONH_2 \;\; CH—CONH_2 \\ \ominus \end{array} \quad (4)$$

$$(I) \xrightarrow{(d)} \begin{array}{c} R—CH—CONH_2 \\ | \\ CH_2—CO\overset{\ominus}{N}H \end{array} \xrightarrow[\text{maleamide}]{(e)} \begin{array}{c} R—CH—CONH_2 \\ | \\ CH_2—CONH—CH—CONH_2 \\ | \\ CH—CONH_2 \\ \ominus \end{array}$$

Repetition of (b–c) would lead to an α-polypeptide, and repetition of (d–e) to a β-polypeptide. We shall call reactions (b), (d), α- and β-migrations, respectively, since they may lead to the inclusion of α- and β-amino acid residues, respectively, in the polymer chain. Thus α-migration involves the shift of a proton from the amide group attached to the carbon atom to which the last anionic addition has taken place. The details of these hydrogen migrations are discussed later. It is, of course, possible that both α- and β-migration may occur in the same molecule. At least two consecutive migration steps, which need not be of the same type, are necessary for aspartic acid to be obtained on hydrolysis, except with terminal groups. Anionic polymerization without isomerization may occur in these systems, but the backbone chain of the polymers so formed would not be hydrolysable, and therefore could not give rise to amino acids. The data in *Table 4* indicate that some vinyl polymerization of this kind is involved.

2. *Mesaconic acid σ-methyl ester β-amide* (MEA)—$CH_3C(CONH_2):CH-(COOCH_3)$

Reaction conditions are given in *Table 5*.

Table 5. Polymerization of MEA

Expt No.	Diluent (50ml)	[MEA] mole l^{-1}	[n-BuLi] mole l^{-1}	[t-BuONa] mole l^{-1}	Temperature, °C	Reaction time, h
17	Toluene	0·14	—	0·104	90	24·5
18	Toluene	0·14	0·0476	—	90	24·5
19	DMF	0·14	—	0·104	20	154
20	DMF	0·14	0·0476	—	20	385
23	DMF	0·70	—	0·520	90	25
24	DMF	0·70	0·238	—	90	25
29	DMF	0·70	0·0476	—	90	6
30	DMF	0·70	—	0·208	90	5·5
31	DMF	0·70	0·095	—	20	119
32	DMF	0·70	—	0·208	20	120
33	Toluene	0·42	0·286	—	90	18·5
34	Toluene	0·42	—	0·416	90	18
40	DMF	0·70	0·095	—	90	6

All reactions involving sodium *t*-butoxide were heterogeneous throughout. Reaction mixtures in which *n*-butyl lithium was used were initially homogeneous, and remained so, except for expts 18 and 33.

The insoluble products from expts 17, 18, 33 and 34 were washed with toluene at 90°C and dried under vacuum. In other cases the reaction liquids were poured into benzene and the products insoluble in hot benzene were collected, washed repeatedly with hot benzene, and dried in a vacuum.

The products of expts 17–20, 23 and 24 were extracted successively with cold and hot methanol and cold and hot water. All fractions were subjected to paper chromatography as described earlier; in no case was a ninhydrin-positive reaction obtained. After chlorination of the chromatograms a tolidine reaction was observed, with strong tailing, showing the absence of amino acids and the presence of amides or monosubstituted amides.

Further evidence for the occurrence of monosubstituted amides was forthcoming from a comparison of the infra-red absorption spectra of MEA and the unfractionated reaction products from expt 33. The latter gave enhanced absorption in the region 1 500–1 700 cm^{-1} as would be expected to arise from peptide groups.

Unfractionated products of expts 29–34, 40 (*Table 5*) were hydrolysed with 6N hydrochloric acid and the hydrolysates chromatographed as described under (1). After treatment with ninhydrin, purple-pink spots were obtained, similar to those reported for glutamic and β-methyl aspartic acids[21]. The R_f values are given in *Table 6*.

Table 6. R_f values at room temperature

Expt No.	PW			BAW		
29	0·33(s)	0·44(m)	0·85(m)	0·29(s)	0·39(m)	0·79(w)
30	0·33(s)	0·42(m)	0·79(m)	0·28(s)	0·37(w)	
31	0·33(s)	0·44(m)	0·85(m)	0·29(s)	0·39(m)	0·97(w)
32	0·33(s)	0·43(m)	0·75(m)	0·28(s)		
33	0·33(s)	0·44(m)	0·85(m)	0·27(s)		
34	0·29———0·50(s)		0·87(w)	0·27(s)		
40	0·36(s)	0·48(m)	0·82(m)	0·24(s)		
α-Me aspartic acid	0·44			0·28		

The amino acid responsible for the spot with $R_f = 0.33$, approximately, is most likely to be β-methyl aspartic, which is reported[61] to give R_f values between aspartic and glutamic acids (0·27 and 0·42, respectively). The hydrolysates are therefore considered to contain a mixture of α- and β-methyl aspartic acids, the latter being in higher concentration. In addition, *Table 6* indicates the presence of a number of hitherto unidentified amino acids. After treatment of the chromatograms with a methanolic solution of cupric nitrate and sodium acetate no ninhydrin reaction was obtainable; this confirms the identification of the products as α-amino acids[22].

Hydrolysis of the original products with 8N sulphuric acid, followed by reaction with dimethyl sulphate as described earlier, would be expected to yield mesaconic acid (from both α- and β-methyl aspartic acids). Unfortunately, only a small quantity of material was obtained, which could not be positively identified as mesaconic acid. However, the ether extract gave crystalline NMe₄ClO₄ on addition of perchloric acid (found C 28·13

per cent, H 7·04 per cent, N 8·18 per cent, Cl 20·14 per cent; calc. C 27·67 per cent, H 6·97 per cent, N 8·07 per cent, Cl 20·42 per cent). This re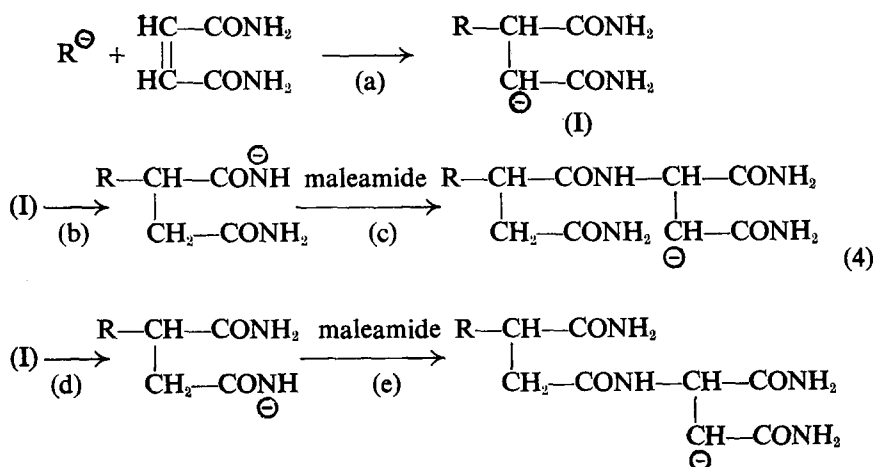sult is consistent with the formation of NMe_3 by a reaction similar to (4)[19]. Determination of the ratio (amide N)/(total N) gave the values in *Table 7*.

Table 7. (amide N)/(total N)

Expt No.	29	30	31	32	33	34
Ratio	0·30	0·33	0·33	0·38	0·49	0·57

Polymerization without hydrogen migration would give a ratio of unity, while complete migration would correspond to a value zero for long chains. Each act of termination by proton transfer must lead to the presence of a terminal amide group in the polymer; since we are probably dealing with short chains in the present system, the results in *Table 7* show that a major portion of the polymerization proceeds through $—CO\overset{\ominus}{N}H$, i.e. involves hydrogen migration.

The types of reaction which could lead to peptide formation are summarized in the following scheme; here it is necessary to distinguish between additions to the different carbon atoms.

Initial 1-addition

(5·1)

Initial 2-addition

$$R^{\ominus} + \underset{\underset{H}{|}}{\overset{\overset{COOMe}{|}}{C}}=\!=\!=\underset{\underset{CONH_2}{|}}{\overset{\overset{Me}{|}}{C}} \longrightarrow \underset{\underset{COOMe}{|}}{RCH}\!-\!-\!-\!-\!\underset{\underset{CONH_2}{|}}{\overset{\overset{Me}{|}}{C}}{}^{\ominus}$$

$$\xrightarrow{\ \beta\text{-migration}\ } \underset{\underset{COOMe}{|}}{RCH}\!-\!-\!-\!-\!\underset{\underset{\underset{\ominus}{CONH}}{}}{CHMe}$$

(III)

(5·2)

$$(III) \xrightarrow{\ 1\text{-addition}\ } \underset{\underset{COOMe}{|}}{RCH}\!-\!-\!-\!-\!\underset{\underset{\underset{\underset{\underset{CONH_2}{|}}{Me\!-\!C}\!-\!-\!-\!-\!\underset{\underset{COOMe}{|}}{CH}{}^{\ominus}}{|}}{CONH}}{CHMe} \xrightarrow{\ \alpha\text{-migration}\ }$$

(III.1)

$$(III) \xrightarrow{\ 2\text{-addition}\ } \underset{\underset{COOMe}{|}}{RCH}\!-\!-\!-\!-\!\underset{\underset{\underset{\underset{\underset{COOMe}{|}}{CH}\!-\!-\!-\!-\!\underset{\underset{CONH_2}{|}}{\overset{\overset{Me}{|}}{C}}{}^{\ominus}}{|}}{CONH}}{CHMe} \xrightarrow{\ \beta\text{-migration}\ }$$

(III.2)
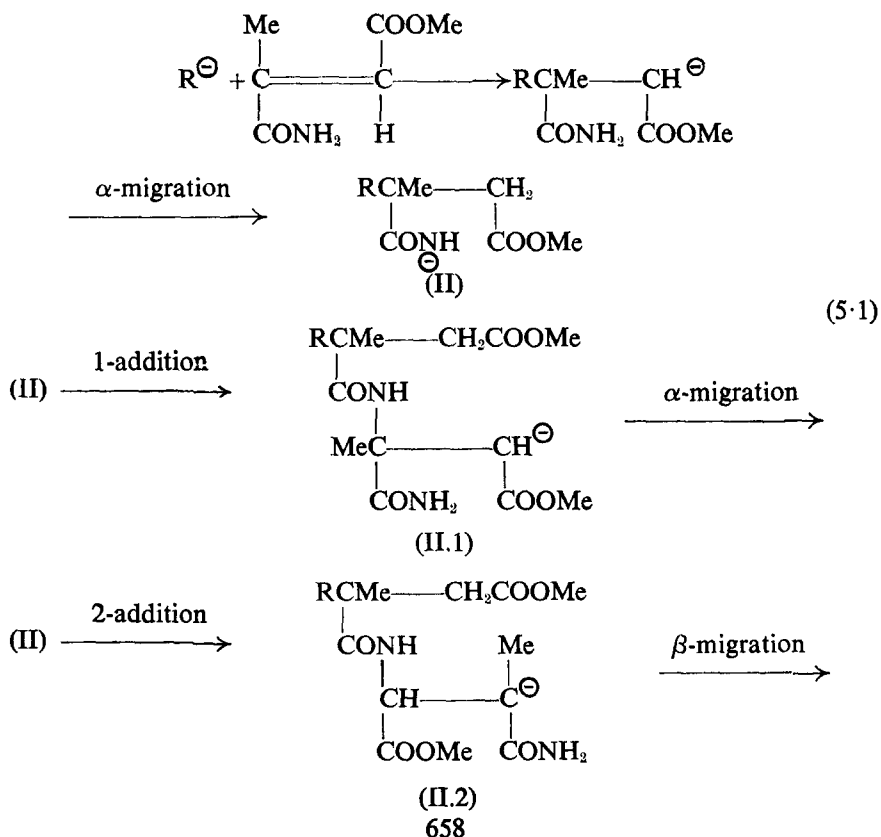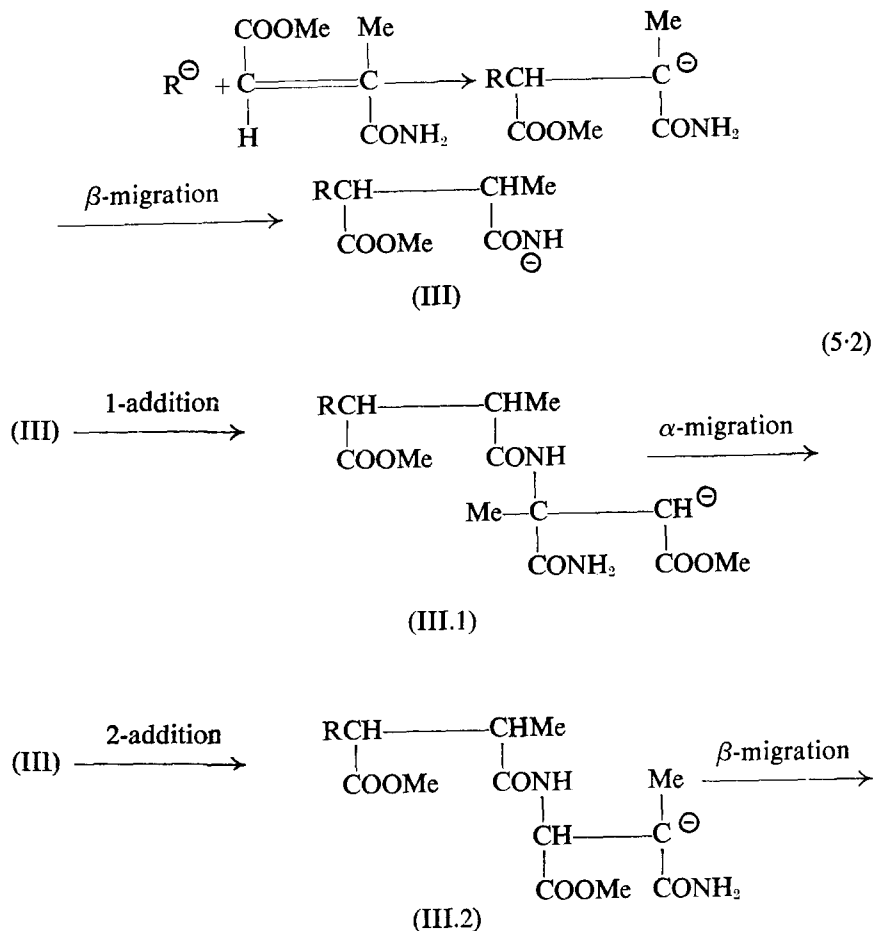
It will be seen that in this case α-migration can only occur after 1-addition, and β-migration only after 2-addition. Further, repetition of the sequence (1α) leads to an α-polypeptide, and repetition of (2β) to a β-polypeptide, which on hydrolysis yield α-methyl and β-methyl aspartic acids, respectively. If, for the moment, we disregard terminal groups, the observed formation of both α- and β-methyl aspartic acids indicates the occurrence of both the sequences (1α), (2β). Inspection shows that hydrolysis of terminal groups formed by proton transfer to structure (II.1), (III.1) would yield α-methyl aspartic acid and those from (II.2), (III.2) β-methyl aspartic acid. Thus the formation of α- and β-methyl aspartic acids proves unambiguously the occurrence of 1-addition and 2-addition, respectively, to an anion of type —$\overset{\ominus}{CONH}$.

Occurrence of the sequence (1α) is the necessary and sufficient condition for the inclusion of α-peptide units in the chain. Termination after

1-addition leads to terminal α-peptide groups which may subsequently be activated by hydrogen migration, equivalent to α-migration.

3. Mesaconamide

$$
\begin{array}{ccc}
 & CONH_2 & Me \\
 & | & | \\
(1) & C\!\!=\!\!\!=\!\!\!=\!\!C & (2) \\
 & | & | \\
 & H & CONH_2
\end{array}
$$
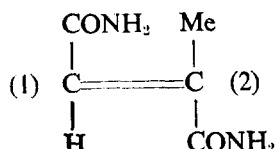
The reaction conditions are shown in *Table 8*.

Table 8. Polymerization of mesaconamide in DMF

Expt No.	[MeDa] mole l^{-1}	[n-BuLi] mole l^{-1}	[t-BuONa] mole l^{-1}	Temperature, °C	Reaction time, h
15	0·156	—	0·104	20	154
16	0·156	0·0476	—	20	385
21	0·780	—	0·520	90	24
22	0·780	0·238	—	90	25
35	0·780	0·095	—	90	11·5
36	0·780	—	0·208	90	27
37	0·625	0·286	—	20	197
38	0·625	—	0·416	20	174
41	0·780	0·095	—	90	5

All systems containing n-butyl lithium were homogeneous.

The insoluble products from expts 15, 21, 36 and 38 were washed with DMF at the polymerization temperature and dried in a vacuum. Reaction mixtures from expts 16, 22, 35, 37 and 41 and the soluble portions from expts 36 and 38 were poured into cold benzene; the resulting precipitates were washed with cold benzene and chloroform, and dried in a vacuum. The products thus obtained were fractionated with methanol and water as described previously. Chromatography of the fractions revealed no ninhydrin-positive material but, after chlorination[17], tolidine-positive substances were observed, the spots showing strong tailing. The presence of —CONHR— groups in the reaction products was confirmed by infra-red spectroscopy.

The soluble and insoluble products of expts 36 and 38 and the whole reaction products of expts 35, 37 and 41 were hydrolysed with 6N hydrochloric acid. Chromatography then showed that ninhydrin-positive materials were present; the R_f values are given in *Table 9*.

These results show that both α- and β-methyl aspartic acids are formed on hydrolysis (cf. *Table 5*). After treatment of the chromatograms with cupric nitrate and sodium acetate in methanol there was no ninhydrin-positive reaction.

Table 9. R_f values at room temperature

Expt No.	PW			BAW	
35	0·30 —— 0·55(s)		0·84(s)		
36 (soluble)	0·40(s)		0·80(s)	0·27(s)	
36 (insol.)	0·31(s)	0·42(s)	0·82(s)	0·31(s)	0·40(w)
37	0·38(s)		0·79(m)	0·25(s)	
38 (soluble)	0·30(s)	0·43(s)	0·87(s)	0·27(s)	
38 (insol.)	0·31(s)	0·43(s)	0·83(m)	0·26(s)	
41	0·40(s)		0·89(m)	0·24(s)	

Hydrolysis with 8N sulphuric acid followed by reaction with dimethyl sulphate and ether extraction yielded mesaconic acid, identified by elemental analysis (found C 45·87 per cent, H 4·61 per cent; calc. C 46·13 per cent, H 4·65 per cent), melting point (found 205°C; literature[20] 204°C) and infra-red absorption spectrum. This is confirmatory evidence for the presence of α- and/or β-methyl aspartic acid in the hydrolysates [equation (3)].

Values of the ratio (amide N)/(total N) are given in *Table 10*. The ratio would be expected to lie between the values 0·5 (total migration) and 1·0 (total vinyl propagation). Clearly a considerable amount of migration must occur.

Reaction sequences leading to the observed products are summarized below. Here again it is necessary to distinguish between the two types of addition; further, both types of hydrogen migration can follow either mode of addition.

Initial 1-addition

$$
R^{\ominus} + \underset{\underset{\text{CONH}_2}{|}}{\overset{\overset{\text{Me}}{|}}{C}} ===== \underset{\underset{\text{H}}{|}}{\overset{\overset{\text{CONH}_2}{|}}{C}} \longrightarrow R\underset{\underset{\text{CONH}_2}{|}}{\overset{\overset{\text{Me}}{|}}{C}} ----- \underset{\underset{\text{CONH}_2}{|}}{\overset{\overset{\text{H}}{|}}{C}}{}^{\ominus}
$$

$$\text{(IV)}$$

$$
\text{(IV)} \xrightarrow{\alpha\text{-migration}} R\underset{\underset{\text{CONH}}{|}}{\overset{\overset{\text{Me}}{|}}{C}} ----- \underset{\underset{\text{CONH}_2}{|}}{\overset{\overset{\text{CH}_2}{|}}{C}} \quad {}^{\ominus}
$$

1-addition

$$
R\underset{\underset{\text{CONH}}{|}}{\overset{\overset{\text{Me}}{|}}{C}} ----- \text{CH}_2\text{CONH}_2
$$
$$
\text{Me}\underset{\underset{\text{CONH}_2}{|}}{\overset{\overset{\text{CONH}}{|}}{C}} ----- \underset{\underset{\text{CONH}_2}{|}}{\overset{\overset{\text{H}}{|}}{C}}{}^{\ominus}
$$

2-addition

$$
R\underset{\underset{\text{CONH}}{|}}{\overset{\overset{\text{Me}}{|}}{C}} ----- \text{CH}_2\text{CONH}_2
$$
$$
H\underset{\underset{\text{CONH}_2}{|}}{\overset{\overset{\text{CONH}}{|}}{C}} ----- \underset{\underset{\text{CONH}_2}{|}}{\overset{\overset{\text{Me}}{|}}{C}}{}^{\ominus}
$$

$$(6.1)$$

(IV) $\xrightarrow{\beta\text{-migration}}$

$$
\begin{array}{cc}
\text{RCMe} & \text{CH}_2 \\
| & | \\
\text{CONH}_2 & \text{CONH} \\
 & \ominus
\end{array}
$$

1-addition   2-addition

$$
\begin{array}{ccc}
\text{RCMe} & \text{CH}_2 & \\
| & | & \text{H} \\
\text{CONH}_2 & \text{CONH} & | \\
 & \text{MeC}\!\!-\!\!\text{C}\ominus \\
 & | \quad | \\
 & \text{CONH}_2 \; \text{CONH}_2
\end{array}
$$

$$
\begin{array}{ccc}
\text{RCMe} & \text{CH}_2 & \\
| & | & \text{Me} \\
\text{CONH}_2 & \text{CONH} & | \\
 & \text{HC}\!\!-\!\!\text{C}\ominus \\
 & | \quad | \\
 & \text{CONH}_2 \; \text{CONH}_2
\end{array}
$$

Initial 2-addition

$$
\text{R}\ominus +
\begin{array}{cc}
\text{CONH}_2 & \text{Me} \\
| & | \\
\text{C}\!\!=\!\!\text{C} \\
| & | \\
\text{H} & \text{CONH}_2
\end{array}
\longrightarrow
\begin{array}{cc}
 & \text{Me} \\
 & | \\
\text{RCH}\!\!-\!\!\text{C}\ominus \\
| & | \\
\text{CONH}_2 & \text{CONH}_2
\end{array}
$$

(V)

(V) $\xrightarrow{\alpha\text{-migration}}$

$$
\begin{array}{cc}
\text{RCH} & \text{CHMe} \\
| & | \\
\text{CONH} & \text{CONH}_2 \\
\ominus &
\end{array}
$$

1-addition   2-addition

$$
\begin{array}{ccc}
\text{RCH} & \text{CHMeCONH}_2 & \\
| & & \text{H} \\
\text{CONH} & & | \\
\text{MeC}\!\!-\!\!\text{C}\ominus \\
| \quad | \\
\text{CONH}_2 \; \text{CONH}_2
\end{array}
$$

$$
\begin{array}{ccc}
\text{RCH} & \text{CHMeCONH}_2 & \\
| & & \text{Me} \\
\text{CONH} & & | \\
\text{HC}\!\!-\!\!\text{C}\ominus \\
| \quad | \\
\text{CONH}_2 \; \text{CONH}_2
\end{array}
$$

(6.2)

(V) $\xrightarrow{\beta\text{-migration}}$

$$
\begin{array}{cc}
\text{RCH} & \text{CHMe} \\
| & | \\
\text{CONH}_2 & \text{CONH} \\
 & \ominus
\end{array}
$$

1-addition   2-addition

$$
\begin{array}{ccc}
\text{RCH} & \text{CHMe} & \\
| & | & \text{H} \\
\text{CONH}_2 & \text{CONH} & | \\
 & \text{MeC}\!\!-\!\!\text{C}\ominus \\
 & | \quad | \\
 & \text{CONH}_2 \; \text{CONH}_2
\end{array}
$$

$$
\begin{array}{ccc}
\text{RCH} & \text{CHMe} & \\
| & | & \text{Me} \\
\text{CONH}_2 & \text{CONH} & | \\
 & \text{HC}\!\!-\!\!\text{C}\ominus \\
 & | \quad | \\
 & \text{CONH}_2 \; \text{CONH}_2
\end{array}
$$

Table 10. (amide N)/(total N)

Expt No.	35	36 (insol.)	37	38 (insol.)
Ratio	0·87	0·57	0·66	0·66

It will be seen that hydrolysis of the reaction products from the succession of steps will lead to methyl aspartic acids. The nature of these is determined only by the mode of addition, 1- and 2-additions giving α- and β-methyl aspartic acids, respectively. On the other hand, the nature of the peptide unit incorporated in the chain depends only on the mode of migration, α-, β-migrations giving α-, β-peptide residues, respectively. The results show, therefore, that both types of addition occur. Nothing can be said about the type of migration since we do not know the detailed structure of the polymer chain.

CONCLUSIONS

Polymerization of maleamide under the conditions described has been shown to give rise to oligomers containing peptide units. On the basis of the present evidence it is not possible to distinguish between α- and β-peptide residues in the products, since both types yield aspartic acid on hydrolysis. However, it is clear that with this kind of monomer hydrogen migration plays an important part in the reaction, although the data in *Table 4* indicate some vinyl polymerization without isomerization. The precise proportion of each mode of reaction cannot be ascertained since the nature of the terminal groups is not known.

With mesaconamide, hydrogen-migration polymerization occurs to a marked extent, but as with maleamide it is not possible to decide from the evidence presented whether the incorporated peptide units are α- or β- in character. Since both α- and β-methyl aspartic acids are formed on hydrolysis it is clear that addition of anions to both carbon atoms can occur.

A distinction between the two types of peptide unit resulting from the polymerization of mesaconic acid α-methyl ester β-amide is, however, possible. Again there is extensive hydrogen migration polymerization; both α- and β-peptide residues are formed, the chromatographic analysis (*Table 6*) indicating some preference for β-peptide incorporation.

The results with these three monomers, therefore, substantiate the expectations we advanced at the outset. By a suitable choice of monomer a higher proportion of α-peptide residues should be obtainable than observed in the present study. The main requirement for a high degree of α-peptide formation is predominant addition to the carbon atom (1) carrying the amide group. The possibility of achieving this will be determined by both electronic and steric factors; groups attached to carbon atom (2) should be as strongly electron-attracting as possible, and should preferably be associated with steric effects reducing the relative probability of addition to C(2). The methyl substituent in MEA is probably favourable electronically and unfavourable sterically. Pearson and Dillon[23] have reported that the methyl hydrogens in $CH_3COOC_2H_5$ are more acidic than those in CH_3CONH_2, so that the carbomethoxy group in MEA should be electronically favourable for addition to C(1). An investigation of monomers

containing more strongly electron-attracting groups such as —CN or nitro-aromatic residues would be of interest in this connection.

We have written the proton-transfer reactions from the amide group as intramolecular processes occurring after addition [equations (4), (5) and (6)]. This may well not represent the course of the reactions; it seems more likely that the migrations are intermolecular, possibly involving the solvent if this is polar. These considerations in no way affect the validity of our conclusions; the equations as written should be understood to represent overall processes in which activation (ionization) of an amide group is not necessarily a result of addition to the same molecule. The system is analogous to a free-radical polymerization in which there is extensive chain-transfer to monomer and polymer. At any stage the protons must be distributed randomly between the different amide sites. As with conventional anionic polymerization, a high value of the ratio [monomer consumed] : [initiator] is necessary to achieve high molecular weights, but it follows from the above discussion that high molecular weights can only be expected after the monomer concentration has been reduced to a very low value, as in a conventional condensation reaction (cf. Breslow, Hulse and Matlack[1]).

The authors are pleased to thank Dr H. Block for helpful discussions.

Department of Inorganic, Physical and Industrial Chemistry,
    Donnan Laboratories,
        University of Liverpool

Department of Polymer Chemistry,
    Kyoto University, Kyoto, Japan

REFERENCES

[1] BRESLOW, D. S., HULSE, G. E. and MATLACK, A. S. *J. Amer. chem. Soc.* 1957, **79**, 3760

[2] OGATA, N. *Bull. chem. Soc., Japan,* 1960, **33**, 906; *Makromol. Chem.* 1960, **44**, 55; *J. Polym. Sci.* 1960, **46**, 271

[3] OKAMURA, S., OISHI, Y., HIGASHIMURA, T. and SENOO, T. *Kobunshi Kagaku,* 1962, **19**, 323

[4] YOKOTA, K., SHIMIDZU, M., YAMASHITA, Y. and ISHII, Y. *Makromol. Chem.* 1964, **77**, 1

[5] TANI, H., OGUNI, N. and ARAKI, T. *Makromol. Chem.* 1964, **76**, 82

[6] YODA, N. and MARVEL, C. S. *J. Polym. Sci. A,* 1965, **3**, 2229

[7] OKAMURA, S., HIGASHIMURA, T. and SENOO, T. *Kobunshi Kagaku,* 1963, **20**, 364

[8] NAKAYAMA, H., HIGASHIMURA, T. and OKAMURA, S. Paper presented to meeting of Japanese High Polymer Society, Nagoya, October 1965

[9] YOKATA, K., SAKAI, Y. and ISHII, Y. *J. Polym. Sci. B,* 1965, **3**, 839

[10] LINSTEAD, R. P. and WHALLEY, M. *J. chem. Soc.* **1952**, 4839

[11] DE WOLF, J. and VAN DE STRAETE, L. *Bull. Acad. Roy. Belg.* 1935, **21**, 216

[12] RINKES, I. J. *Rec. Trav. chim. Pays-Bas.* 1927, **46**, 268

[13] JEFFERY, G. H. and VOGEL, A. I. *J. chem. Soc.* **1948**, 658

[14] VAN DE STRAETE, L. *Bull. Acad. Roy. Belg.* 1935, **21**, 226

[15] PFEIFFER, P. and HEINRICH, E. *J. prakt. Chem.* 1936, **146**, 105

[16] BARKER, H. A., SMYTH, R. D., WAWSZKIEWICZ, E. J., LEE, M. N. and WILSON, R. M. *Arch. Biochem. Biophys.* 1958, **78,** 468

[17] REINDEL, F. and HOPPE, W. *Ber. dtsch. chem. Ges.* 1954, **87,** 1103

[18] WELCHER, F. J., Ed. *Standard Methods of Chemical Analysis,* p 922, Van Nostrand: New York, 1963

[19] DAKIN, H. D. *J. biol. Chem.* 1941, **141,** 945

[20] *Handbook of Chemistry and Physics,* 39th ed. Chemical Rubber Publishing Co.: Cleveland, 1958

[21] INOUE, M. *Bull. chem. Soc. Japan,* 1962, **35,** 1249

[22] Ref. 18, p 932

[23] PEARSON, R. G. and DILLON, R. L. *J. Amer. chem. Soc.* 1953, **75,** 2439

Book Reviews

Strong Solids

A. KELLY. Monographs of the Physics and Chemistry of Materials.

Clarendon Press: Oxford, 1966. xv+212 pp. 6 in. × 9 in. 42s

IN THE search for new materials considerable effort is being devoted to the development of solids exhibiting exceptional strengths, particularly in one dimension. The principal interest of polymer chemists in this connection is the development of fibre-reinforced composites, and Kelly devotes considerable space to this topic within a general treatment of strong solids.

Throughout this book the principles controlling the strengths of solids and theoretical calculations are outlined. References to detailed treatments are given. Methods of estimating the theoretical strengths of various types of crystalline solids are given and where appropriate, these estimates are compared with materials whose strengths are a significant fraction of their theoretical strengths. Defects (e.g. cracks, notches and dislocations) which often reduce the strengths of solids are considered in some detail. The nature of crack tips and their associated stress concentrations, the conditions necessary for crack propagation and the mechanism of brittle fracture are described together with the fracture of strong fibres in which surface defects are absent. Materials which contain mobile dislocations can undergo failure by plastic flow, but in inherently strong solids (potentially good materials for composites) such dislocation motion only occurs at high temperatures; at normal temperatures the strengths of these materials are independent of the presence of dislocations. Essential features of inherently strong solids are enumerated and the mechanism of dislocation motion in such solids at high temperatures is discussed. A general discussion of the principal factors influencing the strengths of metals and of controlling their microstructure to give enhanced strengths is presented. The motion of dislocations in the presence of precipitates is discussed and the principles of fibre reinforcement introduced.

Although a detailed understanding of the behaviour of the fibre/matrix interface in individual composites lags behind present day technology, in the section of this book devoted to fibre-reinforced materials the principles of stress transfer from a matrix to a fibre, the distribution of stress in both fibre and matrix and the stress-strain behaviour and ultimate failure of composites based on metallic and resin matrices are presented. Other factors considered are the dependence of composite strength on fibre length, the mechanism of failure under compression, effects of fibre orientation, a distribution of fibre strengths and the elements of the design of composites. The final chapter deals with the methods of production and mechanical properties of fibre-reinforced polymers, the production of suitable strong fibres, the introduction of fibres into metal matrices, the problems associated with fatigue and creep and possible ways of overcoming these difficulties. Strengths of these new materials are compared with those of present day engineering materials, and in appendices the properties of certain materials are tabulated.

This volume is intended as an introduction to the subject of strong solids and it meets this objective admirably. Very little previous knowledge of the solid state is required to appreciate the arguments and ideas which are presented in a most readable form, and anyone interested in obtaining a grounding in this subject will find this book most useful and extremely good value.

G. C. EASTMOND

Molekülstruktur. Physikalische Methoden zur Bestimmung der Struktur von Molekülen und ihren wichtigsten Ergebnisse

H. A. STUART. 3rd revised edition, in collaboration with E. FUNCK and W. MÜLLER-WARMUTH. Springer: Berlin, Heidelberg, New York: 1967. xvi+562 pp. 154 figs. DM 68.00 or U.S. $17.00

THE first edition of this well known book was published in 1934 with the same title *Molekülstruktur*, but the second edition (1952) was almost entirely rewritten to serve as the first volume of a four volume work, *Die Physik der Hochpolymeren*, edited by the author, and its title was changed to *Die Struktur des freien Moleküls*. The present third edition is once again published as an independent volume without the three polymer volumes and the original title *Molekülstruktur* is restored. This sequence explains some peculiarities of the new edition that may puzzle readers unfamiliar with the second edition.

The author explains that in spite of the enormous literature which has accumulated since 1952 it was decided not to increase the size of the volume so that it might keep its character of a comparatively short general introduction to the subject, but even with this restriction he found it necessary to have the collaboration of colleagues to deal with the mass of new material. There are still only nine chapters, most of which retain the original headings, but the short final chapter of the second edition, on light absorption and constitution, has been dropped, while an entirely new chapter 'The determination of structure parameters by high frequency spectroscopy' by W. Müller-Warmuth, covering nuclear magnetic resonance and electron spin resonance, has been introduced. The chapter 'Eigenschwingungen des Kerngerüstes', dealing with infra-red and Raman spectroscopy, has been rewritten by E. Funck.

This attractively produced new edition with its numerous new references will be welcomed by many, but it must be admitted that the amputation of this work from the polymer volumes of the second edition has left some ugly scars which could have been avoided by more extensive re-writing and more careful checking of the text. Some examples are given below.

Since the subtitle claims that the book contains the most important results obtained by physical methods, the reader will be surprised to find no reference to recent works on proteins, nucleic acids, vitamin B_{12} and (almost none) on modern inorganic chemistry. This is in part explained by the introduction to the second edition (not reprinted in this edition) which states that the volume dealt primarily with small molecules. Similarly the brevity of the section covering X-ray crystal analysis was explained in a sentence saying that the subject was fully treated in Volume III. In the new edition, unaccompanied by Volume III, this sentence is cut out, but the five pages are reproduced unaltered (except for additional references) and no reason is given for the short treatment.

In Chapter 5, 'Dielectric constants, electric moments and molecular structure', there is a final section headed 'Proteins' which contains no referencec to proteins. Reference to the second edition shows that this came about by cutting out the lower half of a table which contained electric moments of several proteins and so leaving only the values for amino acids and peptides, while the accompanying text is reprinted unchanged.

On page 103 the word 'ultrarot' appears in an unaltered paragraph, while elsewhere the more modern 'infrarot' is used.

We should be grateful to the author for the large amount of work which the preparation of this new edition has involved, even though compressing so much new material into the old framework has inevitably produced cracks in the structure.

CONMAR ROBINSON

Proceedings of the Second Tihany Conference on Radiation Chemistry

J. DOBO and P. HEDVIG (Eds.). Akademiai Kiado: Budapest, 1967. xvi+813 pp. 6 in. × 8½ in. 200s

THIS book is the proceedings of a conference held at Tihany in Hungary from 15 to 19 May 1966 and attended by scientists from twenty countries. The general outline is

similar to that of the First Tihany Symposium, held in 1962 [see *Polymer*, **6**, 172 (1965)]. However, there are nearly twice as many contributions (95 compared to 50 previously) which cover the whole field of radiation chemistry, and the average standard is certainly much higher than before.

It is impossible in a review of this nature to give anything like a complete critique of the book; one can only hope to delineate some of the more important areas covered. About half of the papers presented may be of interest to polymer chemists either engaged in or interested in the problems of radiation effects.

The book is divided into four sections as follows (number of papers in parentheses): i. General, Inorganic, Biological (8); ii. Aqueous Solutions (18); iii. Organic (27), and iv. Polymers (42). Several of the papers contain useful short reviews of previous work.

In the first section the papers by Burton on 'Mechanism of energy transfer and localization' and by Pisarevsky *et al.* on 'Radiation protection in biopolymers' are particularly interesting. The second section has several papers dealing with dosimetry problems: most of the others in this section are on work with inorganic solutions.

Studies on the radiolysis of a wide variety of organic compounds are covered in the third section. In many of them, detection of unstable intermediates by low temperature, e.s.r. and pulse radiolytic methods are reported. Other papers in this section are concerned with radiation-induced reactions, such as oxidation, which are of potential technological importance.

The polymer section is divided roughly equally between papers concerned with initiation of polymerization by radiation and those concerned with radiation effects on polymers, particularly grafting. The first two papers discuss the role of ions in initiation, a topic of current interest, and many of the other papers discuss polymerization and copolymerization studies on a variety of monomers. There are about a dozen papers on the solid state polymerization of a variety of monomers, since high energy radiation provides a convenient method of initiation in these systems.

The number of papers concerned with grafting reflects the growing interest in the technological possibilities of these reactions. The papers cover a wide range of theoretical and empirical work. The final two papers deal with luminescence of irradiated polymers.

The book is, on the whole, very well produced. Most of the papers are easily readable even to a non-specialist, and the standard of translation is remarkably high. The editors are to be congratulated on producing the book in a relatively short time. While in no sense comprehensive, parts of the book, particularly the polymer section, do give an indication of the kinds of problems which are being investigated in the field of radiation chemistry.

V. J. ROBINSON

Polyaldehydes

Edited by O. VOGL. Arnold: London; Marcel Dekker: New York, 1967. viii + 137 pp. 70s

THIS book contains the papers which were presented at a Symposium of the American Chemical Society at Phoenix, Arizona, in January 1966. It contains no record of discussions. Prospective purchasers should note the statement at the front of the book that the papers have already been published in the *Journal of Macromolecular Science (Chemistry)*.

Vogl, the editor, opens with a short introductory paper giving an outline of the history of the polyaldehydes. Northrop Brown, also of Dupont, reviews the polymerization of formaldehyde mentioning the many techniques which can lead to the formation of high polymers from the monomer and its solutions; he includes discussion of the making of high polymers from aqueous solutions of the aldehyde, of the new orthorhombic polyoxymethylene and also briefly of the aldol type of condensation. The following article by Price and McAndrew of American Celanese is concerned with conversion of the cyclic trimer, trioxan, to linear high polymer and also with the use of the trimer in the production of copolymers.

Molekülstruktur. Physikalische Methoden zur Bestimmung der Struktur von Molekülen und ihren wichtigsten Ergebnisse

H. A. STUART. 3rd revised edition, in collaboration with E. FUNCK and W. MÜLLER-WARMUTH. Springer: Berlin, Heidelberg, New York: 1967. xvi + 562 pp. 154 figs. DM 68.00 or U.S. $17.00

THE first edition of this well known book was published in 1934 with the same title *Molekülstruktur*, but the second edition (1952) was almost entirely rewritten to serve as the first volume of a four volume work, *Die Physik der Hochpolymeren*, edited by the author, and its title was changed to *Die Struktur des freien Moleküls*. The present third edition is once again published as an independent volume without the three polymer volumes and the original title *Molekülstruktur* is restored. This sequence explains some peculiarities of the new edition that may puzzle readers unfamiliar with the second edition.

The author explains that in spite of the enormous literature which has accumulated since 1952 it was decided not to increase the size of the volume so that it might keep its character of a comparatively short general introduction to the subject, but even with this restriction he found it necessary to have the collaboration of colleagues to deal with the mass of new material. There are still only nine chapters, most of which retain the original headings, but the short final chapter of the second edition, on light absorption and constitution, has been dropped, while an entirely new chapter 'The determination of structure parameters by high frequency spectroscopy' by W. Müller-Warmuth, covering nuclear magnetic resonance and electron spin resonance, has been introduced. The chapter 'Eigenschwingungen des Kerngerüstes', dealing with infra-red and Raman spectroscopy, has been rewritten by E. Funck.

This attractively produced new edition with its numerous new references will be welcomed by many, but it must be admitted that the amputation of this work from the polymer volumes of the second edition has left some ugly scars which could have been avoided by more extensive re-writing and more careful checking of the text. Some examples are given below.

Since the subtitle claims that the book contains the most important results obtained by physical methods, the reader will be surprised to find no reference to recent works on proteins, nucleic acids, vitamin B_{12} and (almost none) on modern inorganic chemistry. This is in part explained by the introduction to the second edition (not reprinted in this edition) which states that the volume dealt primarily with small molecules. Similarly the brevity of the section covering X-ray crystal analysis was explained in a sentence saying that the subject was fully treated in Volume III. In the new edition, unaccompanied by Volume III, this sentence is cut out, but the five pages are reproduced unaltered (except for additional references) and no reason is given for the short treatment.

In Chapter 5, 'Dielectric constants, electric moments and molecular structure', there is a final section headed 'Proteins' which contains no referencec to proteins. Reference to the second edition shows that this came about by cutting out the lower half of a table which contained electric moments of several proteins and so leaving only the values for amino acids and peptides, while the accompanying text is reprinted unchanged.

On page 103 the word 'ultrarot' appears in an unaltered paragraph, while elsewhere the more modern 'infrarot' is used.

We should be grateful to the author for the large amount of work which the preparation of this new edition has involved, even though compressing so much new material into the old framework has inevitably produced cracks in the structure.

CONMAR ROBINSON

Proceedings of the Second Tihany Conference on Radiation Chemistry

J. DOBO and P. HEDVIG (Eds.). Akademiai Kiado: Budapest, 1967. xvi + 813 pp. 6 in. × 8½ in. 200s

THIS book is the proceedings of a conference held at Tihany in Hungary from 15 to 19 May 1966 and attended by scientists from twenty countries. The general outline is

similar to that of the First Tihany Symposium, held in 1962 [see *Polymer*, **6**, 172 (1965)]. However, there are nearly twice as many contributions (95 compared to 50 previously) which cover the whole field of radiation chemistry, and the average standard is certainly much higher than before.

It is impossible in a review of this nature to give anything like a complete critique of the book; one can only hope to delineate some of the more important areas covered. About half of the papers presented may be of interest to polymer chemists either engaged in or interested in the problems of radiation effects.

The book is divided into four sections as follows (number of papers in parentheses): i. General, Inorganic, Biological (8); ii. Aqueous Solutions (18); iii. Organic (27), and iv. Polymers (42). Several of the papers contain useful short reviews of previous work.

In the first section the papers by Burton on 'Mechanism of energy transfer and localization' and by Pisarevsky *et al.* on 'Radiation protection in biopolymers' are particularly interesting. The second section has several papers dealing with dosimetry problems: most of the others in this section are on work with inorganic solutions.

Studies on the radiolysis of a wide variety of organic compounds are covered in the third section. In many of them, detection of unstable intermediates by low temperature, e.s.r. and pulse radiolytic methods are reported. Other papers in this section are concerned with radiation-induced reactions, such as oxidation, which are of potential technological importance.

The polymer section is divided roughly equally between papers concerned with initiation of polymerization by radiation and those concerned with radiation effects on polymers, particularly grafting. The first two papers discuss the role of ions in initiation, a topic of current interest, and many of the other papers discuss polymerization and copolymerization studies on a variety of monomers. There are about a dozen papers on the solid state polymerization of a variety of monomers, since high energy radiation provides a convenient method of initiation in these systems.

The number of papers concerned with grafting reflects the growing interest in the technological possibilities of these reactions. The papers cover a wide range of theoretical and empirical work. The final two papers deal with luminescence of irradiated polymers.

The book is, on the whole, very well produced. Most of the papers are easily readable even to a non-specialist, and the standard of translation is remarkably high. The editors are to be congratulated on producing the book in a relatively short time. While in no sense comprehensive, parts of the book, particularly the polymer section, do give an indication of the kinds of problems which are being investigated in the field of radiation chemistry.

V. J. ROBINSON

Polyaldehydes

Edited by O. VOGL. Arnold: London; Marcel Dekker: New York, 1967.
viii + 137 pp. 70s

THIS book contains the papers which were presented at a Symposium of the American Chemical Society at Phoenix, Arizona, in January 1966. It contains no record of discussions. Prospective purchasers should note the statement at the front of the book that the papers have already been published in the *Journal of Macromolecular Science (Chemistry)*.

Vogl, the editor, opens with a short introductory paper giving an outline of the history of the polyaldehydes. Northrop Brown, also of Dupont, reviews the polymerization of formaldehyde mentioning the many techniques which can lead to the formation of high polymers from the monomer and its solutions; he includes discussion of the making of high polymers from aqueous solutions of the aldehyde, of the new orthorhombic polyoxymethylene and also briefly of the aldol type of condensation. The following article by Price and McAndrew of American Celanese is concerned with conversion of the cyclic trimer, trioxan, to linear high polymer and also with the use of the trimer in the production of copolymers.

Polymerizations of higher aliphatic aldehydes by various mechanisms are reviewed by Vogl. He mentions also polymerizations of some substituted aldehydes but the important topic of the haloaldehydes is considered in another article by Rosen. Vogl deals briefly with polymers derived from certain dialdehydes and with co-polymers of pairs of aldehydes. A contribution from Sharkey deals with fluorothio-carbonyl compounds including $CF_2 : S$.

The remaining three contributions are concerned with structural studies of the polymers rather than their production. Brame and Vogl give an account of n.m.r. studies of polyaldehydes. Corradini explains the crystal structures of various poly-aldehydes. Geil discusses the morphology of polyoxymethylene.

This collection of papers will be of interest to many polymer chemists. There is no claim that it deals with all aspects of polyaldehydes; their solution properties and their mechanical properties might well have formed subjects of other papers. In many places, the problem of instability is mentioned but many who are interested in the polymers would have welcomed a review of this subject.

J. C. BEVINGTON

High-Temperature Polymers

Edited by C. I. SEGAL. Arnold: London; Marcel Dekker: New York, 1967.
viii + 197 pp. 70s

THIS book consists of papers presented at the Symposium on High-Temperature Polymers: Synthesis and Degradation, held at the Western Regional Meeting of the American Chemical Society in Los Angeles in November 1965. Thus, in spite of the title, one should not expect to find a comprehensive account of the subject. Instead, this heterogeneous collection of papers is essentially a progress report in which are recorded the thoughts and activities of some of the prominent workers in the field. Nevertheless the overall balance of material is highly commendable and gives a good representative picture of the state of the subject, as well as its back-ground and motivation, at the end of 1965.

The book opens with what may be regarded as introductory papers on the three themes, organic polymers, inorganic polymers and polymer degradation by C. S. Marvel, J. R. van Wazer and H. L. Friedman respectively. Marvel describes princi-pally his own synthetic work on aromatic and heterocyclic polymers. van Wazer's masterly presentation reviews the basic principles underlying the synthesis of inorganic polymers. Friedman discusses the kinetics of thermal decomposition with particular reference to DTA and TGA techniques and leads on to a consideration of his own contribution to the subject, namely, the combination of thermal analysis with mass spectrometry.

Thermal degradation is further represented by papers by R. T. Conley (Stability of condensation polymers in oxygen-containing atmospheres) and G. P. Shulman (Mass spectrometric thermal analysis of condensation polymers). With particular reference to polyphosphates, A. Eisenberg, S. Saito and T. Sasada describe how viscoelastic relaxation properties are related to ionic forces within molecules. The papers on inorganic polymers are concluded by a description of TGA studies of certain boron-containing polymers by J. Green and N. Mayes.

Representing 'Organic Polymers', A. D. Delman, A. A. Stein and B. B. Simms describe their investigations of the thermal stability of model compounds for aromatic polymers, F. Dobinson and J. Preston demonstrate the improvement in stability which is achieved on progressing from aliphatic to single and multiple ring copolyamides and N. Bilow and L. J. Miller show how tractable and sufficiently stable polyphenylenes may be obtained through branching.

This volume should be regarded as essential to every institutional or industrial polymer library. Unfortunately although not uncommonly, its price will limit its purchase by private collectors to those few who are deeply involved in the field.

N. GRASSIE

Polymerizations of higher aliphatic aldehydes by various mechanisms are reviewed by Vogl. He mentions also polymerizations of some substituted aldehydes but the important topic of the haloaldehydes is considered in another article by Rosen. Vogl deals briefly with polymers derived from certain dialdehydes and with co-polymers of pairs of aldehydes. A contribution from Sharkey deals with fluorothio-carbonyl compounds including $CF_2 : S$.

The remaining three contributions are concerned with structural studies of the polymers rather than their production. Brame and Vogl give an account of n.m.r. studies of polyaldehydes. Corradini explains the crystal structures of various poly-aldehydes. Geil discusses the morphology of polyoxymethylene.

This collection of papers will be of interest to many polymer chemists. There is no claim that it deals with all aspects of polyaldehydes; their solution properties and their mechanical properties might well have formed subjects of other papers. In many places, the problem of instability is mentioned but many who are interested in the polymers would have welcomed a review of this subject.

J. C. BEVINGTON

High-Temperature Polymers

Edited by C. I. SEGAL. Arnold: London; Marcel Dekker: New York, 1967.
viii + 197 pp. 70s

THIS book consists of papers presented at the Symposium on High-Temperature Polymers: Synthesis and Degradation, held at the Western Regional Meeting of the American Chemical Society in Los Angeles in November 1965. Thus, in spite of the title, one should not expect to find a comprehensive account of the subject. Instead, this heterogeneous collection of papers is essentially a progress report in which are recorded the thoughts and activities of some of the prominent workers in the field. Nevertheless the overall balance of material is highly commendable and gives a good representative picture of the state of the subject, as well as its back-ground and motivation, at the end of 1965.

The book opens with what may be regarded as introductory papers on the three themes, organic polymers, inorganic polymers and polymer degradation by C. S. Marvel, J. R. van Wazer and H. L. Friedman respectively. Marvel describes princi-pally his own synthetic work on aromatic and heterocyclic polymers. van Wazer's masterly presentation reviews the basic principles underlying the synthesis of inorganic polymers. Friedman discusses the kinetics of thermal decomposition with particular reference to DTA and TGA techniques and leads on to a consideration of his own contribution to the subject, namely, the combination of thermal analysis with mass spectrometry.

Thermal degradation is further represented by papers by R. T. Conley (Stability of condensation polymers in oxygen-containing atmospheres) and G. P. Shulman (Mass spectrometric thermal analysis of condensation polymers). With particular reference to polyphosphates, A. Eisenberg, S. Saito and T. Sasada describe how viscoelastic relaxation properties are related to ionic forces within molecules. The papers on inorganic polymers are concluded by a description of TGA studies of certain boron-containing polymers by J. Green and N. Mayes.

Representing 'Organic Polymers', A. D. Delman, A. A. Stein and B. B. Simms describe their investigations of the thermal stability of model compounds for aromatic polymers, F. Dobinson and J. Preston demonstrate the improvement in stability which is achieved on progressing from aliphatic to single and multiple ring copolyamides and N. Bilow and L. J. Miller show how tractable and sufficiently stable polyphenylenes may be obtained through branching.

This volume should be regarded as essential to every institutional or industrial polymer library. Unfortunately although not uncommonly, its price will limit its purchase by private collectors to those few who are deeply involved in the field.

N. GRASSIE

Modern Packaging Films

S. H. Pinner. Butterworths: London, 1967. 250 pp. 5 in. × 7½ in. 55s

The book presents a comprehensive account of the rapidly growing use of polymer films in packaging applications. An account of the origins and development of packaging films is followed by detailed discussion of the production, properties and applications of widely used films, in particular polyethylene, polypropylene, polystyrene and poly(vinyl chloride). Some comparative information is also provided about the properties of films of more specialized applications, such as poly(vinylidene chloride) and polyester films. A chapter is devoted to the use of heat-shrinkable films in packaging.

The testing and analysis of polymer films are outlined in some detail; the testing includes a consideration of mechanical properties, permeability, optical and antistatic properties. Printing, bonding and sealing problems associated with packaging films, in particular polyolefins, are discussed. Different printing processes and ink formulations are considered, together with a discussion of different surface treatments.

The final chapter is a discussion of the economics and growth prospects for packaging films although this only extends to 1970.

The book is very readable and should fill a definite gap in the literature. It should prove useful both to those wishing to gain an introduction into the subject of packaging films and also as a reference work for those already working in the area.

A. BUCKLEY

The Production of Polymer and Plastics Intermediates from Petroleum

Edited by R. Long. Butterworths: London, 1967. v + 146 pp. 5½ in. × 8½ in. 45s

Few textbooks on organic chemistry, even those published quite recently, succeed in emphasizing the important changes which have occurred during the last decade or so in the synthesis of polymer intermediates—now dependent almost entirely on petroleum-based sources—nor do they indicate the immense scale on which many types of elastomers and plastics are now produced. This small volume, which brings together a number of papers presented at a recent symposium in London, serves to do both, giving accounts by experts who are in close touch with their particular subjects.

Of the ten chapters, nine are by industry-based authors (from I.C.I., International Synthetic Rubber, B.A.S.F., Shell, Distillers, Courtaulds); the remaining one, dealing with the economics of ethylene versus acetylene as a feedstock, comes from the editorial staff of European Chemical News. The chapters cover a number of intermediates and monomers, four dealing with thermal cracking for olefin production, butadiene, and acetylene. Acetic acid and ethylene and propylene oxides and glycols are dealt with in some detail while there is a comprehensive account of hydroformylation to give OXO alcohols, uses for which are discussed. Other chapters review critically the several manufacturing routes to styrene, phenol and caprolactam.

Throughout, the treatment is such as to present the processes in some detail, discussing the effects of such aspects as reaction conditions and catalysts, while comparison is often made with older-established processes now defunct or unlikely to continue. It is, however, disappointing not to find any review dealing with current routes to vinyl acetate, acrylonitrile, acrylic and methacrylic esters and terephthalic acid, all of which are of very considerable commercial importance. Likewise, nylon 66 intermediates (adipic acid and hexamethylene diamine) get no attention. Such additions would, of course, have made the volume bigger and more expensive, but undoubtedly more comprehensive and informative. Perhaps the publishers would care to remedy this omission, by producing a companion volume.

However, despite this criticism, the present book serves an excellent purpose in reviewing the various processes and in stressing the importance of petroleum to the polymer industry. It will be useful to students who wish to augment their organic chemical reading, in particular from the point of view of industrial practice, and to those involved in research and production in the petroleum and polymer fields.

R. J. W. REYNOLDS

670

Stereoregular Polymers and Stereospecific Polymerizations

The Contributions of Giulio Natta and his school to Polymer Chemistry
Volumes I and II

Edited by G. NATTA and F. DANUSSO. Pergamon: Oxford, 1967.
Vol. I: 466 pp. Vol. II: pp. 467–888. Both vols. 6 in. × 9½ in.
£15 15s per set of two volumes

WHEN Natta and his co-workers announced in 1954 the preparation of crystalline polymers of propylene and 1-butene, their claim that these were stereoregular was received in many quarters with considerable scepticism. It had been recognized for many years that all known synthetic high polymers of asymmetric monomers were stereochemically irregular, and many had assumed that this must always and inevitably be true. Natta's work has by now been so abundantly proved that it is hard to realize how short a time has elapsed from the original discovery. Despite the vast efforts now devoted—especially in industrial laboratories—to the study of stereospecific polymerization, the contribution of Natta's school is massive as well as pioneering.

Many of the original papers were naturally published in Italian journals, and the purpose of the volumes under review is to make available in English a complete record of the work of Natta and his colleagues. Volume I covers the period 1954–58; Volume II, 1958–59; further volumes are promised. The method adopted has been to represent the less important papers by abstracts, but to leave the major papers in their original form (translated if necessary). There is consequently much more repetition than would be acceptable in a specially written text, but by way of compensation the true historical flavour is preserved, and the actual development of ideas and methods remains clearly outlined. Natta's vision and foresight is seen, for example, in a paper written in 1955: 'We believe that the discovery of these new polymerization methods opens a new chapter of stereoisomerism, which should be of considerable practical and theoretical interest . . . . A vast new field of research, which is now only just beginning, is opened to chemists. Our research on block and grafted polymers, and on copolymers, permits one to foresee very important developments. The interest of the new isotactic and syndiotactic polymers is not only theoretical' (p. 73). Prophetic words indeed.

This is an unusual publication, but it will find an honoured place on library shelves. If only it were not so expensive many would like to own it, that they might browse at leisure.

G. GEE

Organic Chemistry of Macromolecules—An Introductory Textbook

A. RAVVE. Arnold: London and Marcel Dekker: New York, 1967. 498 pp. 150s

WHILE polymers are now of such importance that most chemists work with them at some stage in their career, they are still neglected in many university courses. There are, however, many excellent textbooks in this field and these are now joined by Dr Ravve's volume, which has been written as an introduction to the organic chemistry of high polymers for both undergraduates and graduate organic chemists: the work contains only minor excursions into simple physical chemistry. The scope is very broad, ranging from certain aspects of the physical properties of macromolecules, for example crystallinity and transition temperatures, through molecular weight determination to the mechanisms of the principal classes of polymerization reactions and more detailed descriptions of various groups of synthetic and natural polymers. The emphasis is primarily on synthetic macromolecules and some reference is made to most of the known types of organic polymers. There is also some discussion of graft and block copolymers, the chemical modification of polymers and polymer degradation. In a book of such wide scope the treatment of the various topics must be brief, but they are so numerous that those new to polymer chemistry may find it difficult to see the subject in adequate perspective: it will probably be of greater interest to someone with some previous experience of the field.

Despite the technological importance of polymers the text deals almost exclusively with scientific aspects, but where industrial practice is mentioned, the references are often out of date or even misleading. Thus the only reference to the commercial preparation of polystyrene is to bulk polymerization, and it is unlikely that a plant would be installed today to manufacture acrylonitrile by any of the processes quoted. In general little hint is given of the preferred techniques by which various polymers are actually prepared either in the laboratory or on the industrial scale, and it is perhaps unfortunate that the book does not attempt to convey any real picture of the contrasting physical properties of the many types of polymers mentioned.

In a work covering such a wide field, only a selection of literature references can be given but these appear to be well selected and are provided with a good author index. There is an adequate subject index. The number of errors is relatively small but some of these should have been eliminated from the proofs: few organic chemists would expect to make acrylamide by reducing acrylonitrile.

F. J. WEYMOUTH

ANNOUNCEMENT
THE GORDON RESEARCH CONFERENCES

The Winter Gordon Research Conferences will be held from 22 January to 2 February 1968 in Santa Barbara, Calif., U.S.A. Requests for additional information and for application forms for attendance should be addressed to Dr W. GEORGE PARKS, Director, Gordon Research Conferences, University of Rhode Island, Kingston, Rhode Island 02881, U.S.A.

The Polymer Conference, 29 January to 2 February

It is hoped that the following will each present a paper: J. E. Goodrich, H. F. Mark, J. C. W. Chien, F. E. Bailey, F. A. Bovey, W. Heller, J. D. Hoffman, A. Rembaum, R. H. Cole, R. A. Mendelsohn, T. L. Smith, J. C. Halpin, W. R. McDonald, D. J. Meier, J. R. Knox, C. L. Sieglaff, C. C. Prince, C. Job, N. W. Tschoegl, W. J. MacKnight, G. Holden, J. L. Zakin, H. L. Frisch, C. L. Segal, A. P. Gray, W. S. Zimmt.

Other Conferences

Electrochemistry will be discussed during 22 to 26 January, and the Chemistry of Aging Conference is also scheduled for 22 to 26 January. Finally, it is hoped to arrange a Conference on 29 January to 2 February to deal with Science, Technology and Economic Growth.

Stereoregular Polymers and Stereospecific Polymerizations

The Contributions of Giulio Natta and his school to Polymer Chemistry
Volumes I and II

Edited by G. NATTA and F. DANUSSO. Pergamon: Oxford, 1967.
Vol. I: 466 pp. Vol. II: pp. 467–888. Both vols. 6 in. × 9½ in.
£15 15s per set of two volumes

WHEN Natta and his co-workers announced in 1954 the preparation of crystalline polymers of propylene and 1-butene, their claim that these were stereoregular was received in many quarters with considerable scepticism. It had been recognized for many years that all known synthetic high polymers of asymmetric monomers were stereochemically irregular, and many had assumed that this must always and inevitably be true. Natta's work has by now been so abundantly proved that it is hard to realize how short a time has elapsed from the original discovery. Despite the vast efforts now devoted—especially in industrial laboratories—to the study of stereospecific polymerization, the contribution of Natta's school is massive as well as pioneering.

Many of the original papers were naturally published in Italian journals, and the purpose of the volumes under review is to make available in English a complete record of the work of Natta and his colleagues. Volume I covers the period 1954–58; Volume II, 1958–59; further volumes are promised. The method adopted has been to represent the less important papers by abstracts, but to leave the major papers in their original form (translated if necessary). There is consequently much more repetition than would be acceptable in a specially written text, but by way of compensation the true historical flavour is preserved, and the actual development of ideas and methods remains clearly outlined. Natta's vision and foresight is seen, for example, in a paper written in 1955: 'We believe that the discovery of these new polymerization methods opens a new chapter of stereoisomerism, which should be of considerable practical and theoretical interest . . . . A vast new field of research, which is now only just beginning, is opened to chemists. Our research on block and grafted polymers, and on copolymers, permits one to foresee very important developments. The interest of the new isotactic and syndiotactic polymers is not only theoretical' (p. 73). Prophetic words indeed.

This is an unusual publication, but it will find an honoured place on library shelves. If only it were not so expensive many would like to own it, that they might browse at leisure.

G. GEE

Organic Chemistry of Macromolecules—An Introductory Textbook

A. RAVVE. Arnold: London and Marcel Dekker: New York, 1967. 498 pp. 150s

WHILE polymers are now of such importance that most chemists work with them at some stage in their career, they are still neglected in many university courses. There are, however, many excellent textbooks in this field and these are now joined by Dr Ravve's volume, which has been written as an introduction to the organic chemistry of high polymers for both undergraduates and graduate organic chemists: the work contains only minor excursions into simple physical chemistry. The scope is very broad, ranging from certain aspects of the physical properties of macromolecules, for example crystallinity and transition temperatures, through molecular weight determination to the mechanisms of the principal classes of polymerization reactions and more detailed descriptions of various groups of synthetic and natural polymers. The emphasis is primarily on synthetic macromolecules and some reference is made to most of the known types of organic polymers. There is also some discussion of graft and block copolymers, the chemical modification of polymers and polymer degradation. In a book of such wide scope the treatment of the various topics must be brief, but they are so numerous that those new to polymer chemistry may find it difficult to see the subject in adequate perspective: it will probably be of greater interest to someone with some previous experience of the field.

Despite the technological importance of polymers the text deals almost exclusively with scientific aspects, but where industrial practice is mentioned, the references are often out of date or even misleading. Thus the only reference to the commercial preparation of polystyrene is to bulk polymerization, and it is unlikely that a plant would be installed today to manufacture acrylonitrile by any of the processes quoted. In general little hint is given of the preferred techniques by which various polymers are actually prepared either in the laboratory or on the industrial scale, and it is perhaps unfortunate that the book does not attempt to convey any real picture of the contrasting physical properties of the many types of polymers mentioned.

In a work covering such a wide field, only a selection of literature references can be given but these appear to be well selected and are provided with a good author index. There is an adequate subject index. The number of errors is relatively small but some of these should have been eliminated from the proofs: few organic chemists would expect to make acrylamide by reducing acrylonitrile.

F. J. WEYMOUTH

ANNOUNCEMENT
THE GORDON RESEARCH CONFERENCES

The Winter Gordon Research Conferences will be held from 22 January to 2 February 1968 in Santa Barbara, Calif., U.S.A. Requests for additional information and for application forms for attendance should be addressed to Dr W. GEORGE PARKS, Director, Gordon Research Conferences, University of Rhode Island, Kingston, Rhode Island 02881, U.S.A.

The Polymer Conference, 29 January to 2 February

It is hoped that the following will each present a paper: J. E. Goodrich, H. F. Mark, J. C. W. Chien, F. E. Bailey, F. A. Bovey, W. Heller, J. D. Hoffman, A. Rembaum, R. H. Cole, R. A. Mendelsohn, T. L. Smith, J. C. Halpin, W. R. McDonald, D. J. Meier, J. R. Knox, C. L. Sieglaff, C. C. Prince, C. Job, N. W. Tschoegl, W. J. MacKnight, G. Holden, J. L. Zakin, H. L. Frisch, C. L. Segal, A. P. Gray, W. S. Zimmt.

Other Conferences

Electrochemistry will be discussed during 22 to 26 January, and the Chemistry of Aging Conference is also scheduled for 22 to 26 January. Finally, it is hoped to arrange a Conference on 29 January to 2 February to deal with Science, Technology and Economic Growth.